FY16 ANNUAL PROGRESS REPORT

Laboratory Directed Research and Development

Los Alamos National Laboratory

Los Alamos
NATIONAL LABORATORY
EST. 1943

About the Cover

Entropy Engine is a random number generator that addresses a key fundamental flaw in modern crypto systems—predictability. The invention strengthens the foundation of computer security by producing an inexhaustible supply of pure random numbers at speeds of 200 million bits per second. Entropy Engine uses the unique properties of quantum mechanics to generate true entropy (random numbers) in a way that makes it immune from all external influences. Entropy Engine is the winner of a 2016 R&D 100 Award, submitted by Los Alamos as a joint entry with Whitewood Encryption Systems based on technology that Whitewood licensed from the Laboratory. The LDRD program has invested in quantum information science and technology for more than 20 years, playing a critical role in developing capabiltities that have dramatically increased the Laboratory's leadership role in the rapidly-growing area of quantum technologies. Pictured on the cover is Entropy Engine hardware, and a visualization of how the technology uses a macroscopic manifestation of quantum randomness that is directly traceable to the indistinguishability of photons. Read more about Entropy Engine.

Los Alamos
NATIONAL LABORATORY
EST.1943

Disclaimer

Issued March 2017
LA-UR-17-22482

Structure of this Report

In accordance with U.S. Department of Energy Order (DOE) 413.2B, the Laboratory Directed Research and Development (LDRD) annual report for fiscal year 2016 (FY16) provides summaries of each LDRD-funded project for the fiscal year, as well as full final reports on completed projects. The report is organized as follows:

Overview: An introduction to the LDRD Program at Los Alamos National Laboratory (LANL), the program's structure and strategic value, the LDRD portfolio management process, and highlights of outstanding accomplishments by LDRD researchers.

Project Summaries: The project summaries are organized first by Focus Areas: Complex Natural and Engineered Systems, Information Science and Technology, Materials for the Future, Nuclear and Particle Futures, and Science of Signatures. Within each category, summaries are organized by LDRD component in the following order: Directed Research (DR, Exploratory Research (ER), Early Career Research (ECR), and Postdoctoral Research and Development (PRD). Annual reports for ongoing projects appear first, followed by full final reports that ended in FY16.

Projects are listed in numerical order according to their project identification number, which consists of three parts. The first is the fiscal year in which the project began; the second is a unique numerical identifier; and the third identifies the project component.

At Los Alamos, postdocs are hired throughout the fiscal year, and at the time this report was published, some PRD projects did not have significant progress to report due to the fact that the postdoc had just been hired. In the first few weeks of a new PRD project, a postdoc will spend time in general employee training, as well as any additional training required for work in a specialized lab or facility. This was the case for the following PRD projects:

20160643PRD2	20160671PRD3	20160655PRD2	20160679PRD4	20160678PRD4
20160670PRD3	20160672PRD3	20160674PRD3	20160655PRD2	
20160672PRD3	20160680PRD4	20160673PRD3	20160644PRD1	

Acknowledgements

Technical Review
William Priedhorsky
Jeanne Robinson

Publication Designer
Andrea Maestas

Team Contributors
Lisa Lujan
Debora Gage
Stephen Schultz
Epolito Ulibarri
Lydia Herbert

Table of Contents

Information Science and Technology

Materials for the Future

Nuclear and Particle Futures

Science of Signatures

Program Director Retrospective

Dr. William Priedhorsky, Los Alamos Science Resource Office Director

The U.S. Department of Energy has charged the Laboratory Directed Research and Development (LDRD) program with supporting high-risk, potentially high-value research at the national laboratories. A strong LDRD program is important to the success of the Laboratory because it invests to meet three goals: build the science and engineering reputation of the Laboratory, develop new approaches that enable agile responses to critical national security challenges, and recruit, retain, and enhance critical skills for key, long-term mission objectives. By DOE order, only LDRD can make R&D investments under the direct control of the Laboratory, making it a unique and valuable tool in our overall investment strategy.

As New York Times best-selling author and Harvard Business Review contributor Tony Tjan wrote, "there is one quality that trumps all, evident in virtually every great entrepreneur, manager, and leader. That quality is self-awareness. The best thing leaders can to improve their effectiveness is to become more aware of what motivates them and their decision-making." For the Los Alamos LDRD program, fiscal year 2016 was quite introspective, with great effort spent on a program refresh focused on refining the purpose of the program and how to balance our objectives of scientific reputation, mission agility, and talent development. The refresh was chartered by Laboratory Director Charlie McMillian and carried out by a panel composed of Associate Directors and LDRD Program Managers.

I was pleased to hear the refresh panel conclude that much of what we value about LDRD should not change, including its high standards of creativity and innovation. Rather, "balance" was the cornerstone of the recommended changes. LDRD has various modalities to accomplish its diverse objectives, and balance among those modalities is needed to ensure a robust LDRD program. To refine this balance, LDRD will expand its scope to include projects focused on work higher on the technology-readiness-level spectrum. We will continue to emphasize fundamental work, but the portfolio will incorporate a deliberate component of more focused work. Strategic planning is another area where we will aim for more balance – previously a heavily bottom-up process, writing the Strategic Investment Plan will now begin with a top-level statement of priorities written and endorsed by senior line and program management. While we will still have a bottom-up component, not every interest will find a role in the SIP every year. A more detailed summary of conclusions drawn from the refresh can be found on page X of this report.

Leaning toward the future, the Los Alamos LDRD program will continue on a path of self-assessment to measure our success in achieving goals set forth in the new charter for LDRD that resulted from the refresh. In fact, the program is becoming strongly metrics-driven, with a movement toward tracking investments not just while projects are active, but well after completion so that long-term impacts of LDRD can be identified. If we have successfully invested our LDRD resources, Los Alamos will exhibit great agility in growing and evolving the capabilities needed for mission success, with LDRD playing a major role in shaping our R&D workforce, science and engineering capability, and technical reputation.

Overview

Laboratory Directed Research and Development is the most prestigious source of research and development funding at the Los Alamos National Laboratory. It follows a strategic guidance derived from the missions of the U.S. Department of Energy, the National Nuclear Security Administration, and the Laboratory. To execute that strategy, the Los Alamos LDRD program creates a free market for ideas that draws upon the bottom-up creativity of the Laboratory's best and brightest researchers. The combination of strategic guidance and free-market competition provides a continual stream of capabilities that position the Laboratory to accomplish its missions.

The LDRD program provides the Laboratory Director with the opportunity to strategically invest in forward-thinking, potentially high-payoff research that strengthens the Laboratory's capabilities for national problems. Funded in FY16 with approximately 5.5 percent of the Laboratory's overall budget, the LDRD program makes it possible for researchers to pursue cutting-edge research and development. This in turn enables the Laboratory to anticipate, innovate, and deliver world-class science, technology, and engineering.

Program Structure

The Los Alamos LDRD program is organized into four program components with distinct institutional objectives: Directed Research (DR), flagship investments in mission solutions; Exploratory Research (ER), smaller projects that invest in people and skills that underpin key Laboratory capabilities; Early Career Research (ECR), supporting the development of early-career researchers; and Postdoctoral Research and Development (PRD), recruiting bright, qualified, early-career scientists and engineers. In FY16, the LDRD program funded 275 projects with total costs of $116 million. These projects were selected through a rigorous and highly competitive peer review process and are reviewed formally and informally throughout the fiscal year. The LDRD Program Office holds a reserve each year to make modest investments that address new opportunities. In FY16, the reserve budget was approximately $1.0M.

Directed Research

The DR component makes long-range investments in multidisciplinary scientific projects in key competency or technology-development areas vital to LDRD's long-term ability to execute Laboratory missions. In FY16, LDRD funded 47 DR projects, which represents approximately 54% of the program's research funds. Directed Research projects are typically funded up to a maximum of $1.7M per year for three years.

Directed Research is organized around Focus Areas that define key areas of science, technology, and engineering in support of Los Alamos missions and that map directly to the four Los Alamos science pillars, plus an additional multidisciplinary Focus Area that is not captured by the pillars. Between them, they capture the capabilities that are essential to our Laboratory missions in the long term (3-15 years). For each Focus Area, coordinators led a process to engage broadly with the Lab to set investment priorities for the FY16 Strategic Investment Plan, published labwide.

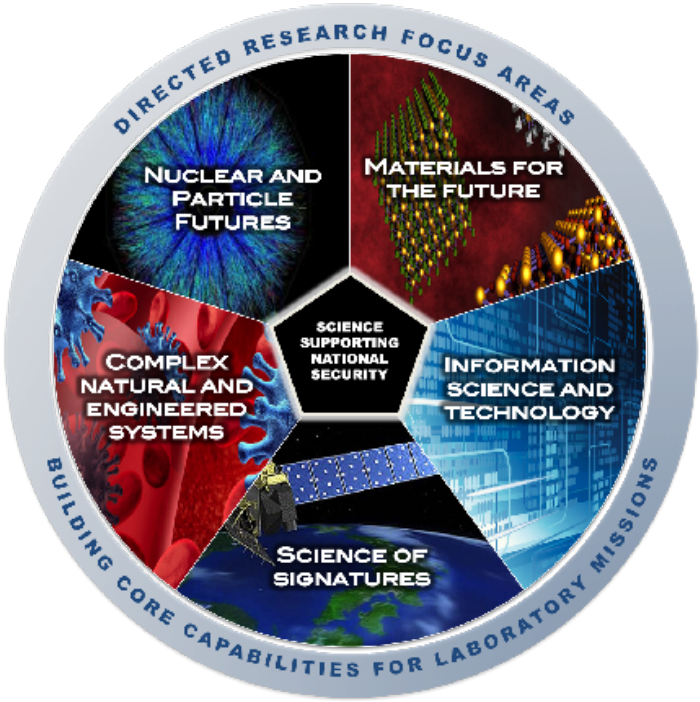

Exploratory Research

The ER component is focused on developing and maintaining technical staff competencies in key strategic disciplines that form the foundation of the Laboratory's readiness for future national missions. Largely focused on a single discipline, ER projects explore highly innovative ideas that underpin Laboratory programs. In FY16, LDRD funded 127 ER projects, which represents approximately 34% of the program's research funds. Exploratory Research projects are funded up to an average maximum of $350K per year for three years.

Unlike DR proposals, division endorsements are not required for ER proposals; instead, this component of the LDRD program is operated as an open and competitive path for every staff member to pursue funding for his/her great idea. The ER component is a critical channel for purely bottom-up creativity at the Laboratory. Nonetheless, it is strongly driven by mission needs via the definition of the 12 ER research categories, and the assignment of investment between them.

Directed Research Focus Areas	Mission Impact
Information Science and Technology	Advance theory, algorithms, and high-performance computing to accelerate the integrative and predictive capability of the scientific method.
Materials for the Future	Rapidly meet mission needs based on a thorough knowledge of materials properties and interactions in relation to composition, structure, and scale.
Science of Signatures	Apply science and technology tools to extremely complex problems in signature, identification, and characterization, understanding, control or mitigation.
Nuclear and Particle Futures	Advance fundamental and applied nuclear science, including accelerator science and technology, in support of all Laboratory missions.
Complex Natural and Engineered Systems	Understand, predict, integrate, design, engineer, and/or control complex systems that significantly impact national security, particularly those involving energy, infrastructure, or societal stainability.

Exploratory Research Technical Categories	Capability Development
Biological, Biochemical, and Cognitive Sciences	Biosciences
Chemistry and Chemical Sciences	Chemistry
Computational and Numerical Methods	Information and knowledge sciences, computer and computational sciences
Computer Science, Mathematics, and Data Science	High-performance computing, data analysis, and data-driven science
Defects and Interfaces in Materials	Theoretical, computation and modeling, and experimental methods to understand defects and interfaces in materials
Earth and Environmental Sciences and Space Physics	Earth and space sciences
Engineering Applications	Weapons science and engineering, advanced manufacturing, sensors, and remote sensing
Emergent Phenomena in Materials Functionality	Theory, computation and modelling, and experimental methods to understand behavior of materials
High-energy Density, Plasma, and Fluid Physics	High-energy density plasmas and fluids and beams
Measurement Science, Instrumentation, and Diagnostics	Measurement methods that enable new scientific discovery
Nuclear and Particle Physics, Astrophysics, and Cosmology	Nuclear physics, astrophysics, and cosmology
Quantum and Optical Science	Fundamental interactions and excitations in atomic, optical, and molecular systems

Early Career Research

The ECR component of the LDRD program is designed to strengthen the Laboratory's scientific workforce by providing support to exceptional staff members during their crucial early career years. The intent is to aid in the sometimes challenging transition from postdoc to full-time staff member, and to stimulate research in disciplines supported by the LDRD program. In FY16, the LDRD program funded 24 ECR projects, which represents approximately 3% of the program's research funds. Early Career Research projects are funded up to $225K per year for two years, and only up to 60% of the project leader's overall funding can be from the LDRD program.

Postdoc Research and Development

The PRD component ensures the vitality of the Laboratory by recruiting outstanding researchers. Through this investment, the LDRD program funds postdoctoral fellows to work under the mentorship of PIs on high-quality projects. The primary criterion for selection of LDRD-supported postdocs is the raw scientific and technical talent of the candidate, with his or her specialty a secondary factor. In FY16, LDRD funded 77 PRD projects, which represents 7% of the program's research funds. These postdocs are supported full-time for two years.

In addition to approximately 64 Director's Postdocs, the LDRD program supported 13 distinguished postdoctoral fellows at a higher salary and for a three-year term. Distinguished postdoctoral fellow candidates typically show evidence of solving a major problem or providing a new approach or insight to a major problem and show evidence of having a major impact in their research field. To recognize their role as future science and technology leaders, these appointments are named after some of the greatest leaders of the Laboratory's past.

More postdocs are hired through DR and ER projects than directly through PRD appointments. Counting both avenues, in FY16 the LDRD program supported 54% of the 501 postdocs who spent at least part of the year at the Laboratory. The average population during the year was 349.

John Yeager

Presidential Early Career Award for Scientists and Engineers

- 2016 Early Career Research project (PI)
- Joined the Lab in 2013 as a technical staff member researching materials science
- Agnew National Security Postdoctoral Fellowship at Los Alamos
- Co-chair of ER "Defects and Interfaces in Materials" review team for FY18 cycle

Jonathan Engle

Early Career Research Program Award Department of Energy Office of Science

- 2015 Early Career Research project (PI)
- Joined the Lab in 2015 as a technical staff member researching radioisotope production
- 2013 Postdoctoral R&D project
- 2013 Los Alamos Frederick Reines Postdoctoral Fellowship working in the DOE Isotope Production Program

Recruiting and Retaining a Word-class Workforce

The LDRD program provides the foundation for Los Alamos' long-term scientific and technological vitality to meet our missions. This program is also a major factor in attracting and retaining talent and launching the early careers of a strong scientific workforce. It enables collaborations with academia that feed our scientific recruitment pipeline. The Laboratory makes strategic LDRD investments based on systematic annual planning and a competitive peer-reviewed selection process. LDRD seeds the Laboratory's capability base and future leadership to prepare for emerging national security challenges within a 3- to 20-year horizon. A recent study of early career R&D staff (within 10 years of earning a PhD) in the Laboratory's Physics Division revealed a strong LDRD influence on their recruitment and retention at Los Alamos. Physics Division was selected for the study because it spans applied and fundamental R&D. Results from 26 interviews are summarized here, along with a few quotes that capture the essence of what staff voluntarily shared about their LDRD experience.

72%
Participated in LDRD projects as postdocs

80%
Said LDRD had a direct or indirect role in recruiting them to Los Alamos

72%
Have made choices to stay at Los Alamos because of LDRD opportunities

Why Los Alamos?

When asked what attracted them to Los Alamos National Laboratory, staff most commonly answered:

The opportunity to do unique science/engineering
People or teams with specific expertise/knowledge
Unique facilities only available at Los Alamos
Multidisciplinary teams/approach to R&D
Location and mountain activities
Interest in doing programmatic work

Has LDRD helped advance your career?

Regarding career advancement, staff most commonly stated that their LDRD experience helped them:

Build scientific reputation (i.e. peer-reviewed publications)
Conduct frontier R&D that resulted in a new capability
Transition to the Weapons Program
Develop a broad view of the Laboratory (networking)
Lead or contribute to innovative, cutting-edge R&D

LDRD allowed me to do interesting science that then let me dip my toe into programmatic work. LDRD tends to fund areas of research that the Lab could possibly do going forward, so the advantage is that you get to do something very interesting and at the same time network with people doing programmatic work.

The project I initially was hired to work on as a postdoc was funded by LDRD. In fact, the only funding available to do that work at the time was through LDRD. Without it, I would not have come to the Lab at all.

LDRD had everything to do with my decision to remain at the Lab after my postdoc appointment...it was exciting to me that a program existed to fund cutting-edge R&D.

My LDRD work has gotten a lot of attention. I've given a lot of talks, received many invitations to join scientific collaborations in my field, and I am currently an advisor to a PhD candidate - all because of the relevance of the LDRD work.

Today I mostly do programmatic work, but my past work on LDRD helped build my technical capabilities.

Project Selection

The LDRD program is the vehicle by which the Laboratory harvests the ideas of some of our best and brightest scientists and engineers to execute DOE/NNSA missions. This bottom-up approach is balanced by a program management strategy in which Senior Laboratory leadership sets science and technology priorities, then opens an LDRD competition for ideas across the breadth of the Laboratory. Panels formed from the Laboratory's intellectual leaders rigorously review proposals. Conflict of interest is carefully regulated, and evaluation criteria include innovation and creativity, potential scientific impact, viability of the research approach, qualifications of the team and leadership, and potential impact on Laboratory missions. The selection processes are modeled on best practices established by the National Science Foundation (NSF) and National Institutes of Health (NIH).

To guarantee fairness and transparency, and to ensure that the strongest proposals are funded, the selection panels include managers and technical staff drawn from the full range of technical divisions. Serving on an LDRD selection panel is often a starting point on the path to leadership roles in the scientific community. Past LDRD panelists have gone on to be Laboratory Fellows, division leaders, program directors, association Fellows, and chief scientists, while others have become leaders in academia.

Benefits of Serving on LDRD Panels

The mission of the Laboratory is to solve the nation's most difficult national security problems. By their nature, these problems lack a well-defined path to solution. In fact, the path is often completely unknown. It is rare that such creative work is done alone; the ideas and results from many colleagues are needed, often drawn out in conferences, hallway conversations, journals, and seminars. LDRD is an internal arena in which Laboratory staff serve as peer reviewers and play a key role of interaction in the scientific process. Proposal selection panelists are chosen for their subject-matter expertise, and the discussions in which they engage are not only critical to the LDRD process, but they also provide an opportunity for panelists to educate themselves on the latest results and practices, and expose themselves to opportunities for collaboration. As noted in an evaluation of peer review conducted by the UK House of Commons, "Peer review is regarded as an integral part of a researcher's professional activity; it helps them become part of the research community."

Annual Project Appraisals

In FY16, the LDRD Program Office reviewed every ongoing project it intends to fund in the next fiscal year. This occurred in various formats, from formal appraisals with external reviewers, to assessments organized by line managers, to informal visits with PIs. The primary objective of the reviews is to assess progress and provide peer input to help PIs maintain the highest quality of work. They also help the LDRD Program Office manage the program portfolio.

Continuing DR projects are appraised in their second and third years, with external reviewers playing an important role in the review that takes place in the second year. The internal-external review is open to all Laboratory staff. Four project appraisers – two internal and two external – are nominated by the PI and approved by the LDRD Program Director. When appropriate, the appraisal is held as part of a broader workshop hosted by the Laboratory. The Chair of the project appraisal panel is responsible for writing a formal report of the review that details how well a project is addressing and meeting its goals, and documents any weaknesses the panel may have observed. The PI is then required to respond to the concerns documented in the report with a revised project plan. The average score for second-year DR projects appraised in FY16 was 4.25, or "excellent."

Written reviews, held in the LDRD archives, address: (1) Brief summary of accomplishments; (2) Assessment of quality of science and technology, relevance to Laboratory and national missions, progress toward goals and milestones, project leadership, and the degree to which the project may establish or sustain a position of scientific leadership for the Laboratory; and (3) Recommendations by the committee for changes in the scope or approach of the project. The criteria for the most important point – number (2) above – are derived from criteria developed by the National Academy of Science to assess all federally sponsored research.

In addition to formal project appraisals, which are conducted annually, the LDRD Program Director and Deputy Program Director meet informally with PIs in their labs at least once a year to discuss their projects. The purpose of these one-on-one meetings is to give PIs individualized assistance and to determine what the LDRD Program Office can do to positively impact the success of the project.

Continuing ER and ECR projects are appraised in their first and second years. The LDRD Deputy Program Director collaborates with the technical divisions to conduct project appraisals. Like DRs, the projects are appraised according to the federal criteria of quality, performance, leadership, and relevance.

LDRD Refresh and New Program Charter

In FY16, Laboratory Director Charlie McMillan charged a panel of Associate Directors, along with LDRD program managers, to carry out a two-stage refresh of the LDRD program. Across the NNSA complex, LDRD resources are limited, and the program carries an increasing burden as other sources of basic research and development remain scarce. As such, it is incumbent upon the Laboratory to determine how to optimize the impact of a finite LDRD resource, as it balances its objectives of scientific reputation, mission agility, and talent development. With unprecedented engagement with applied directorates of the Laboratory and traditional participants, the refresh was an opportunity to think carefully about the future of LDRD.

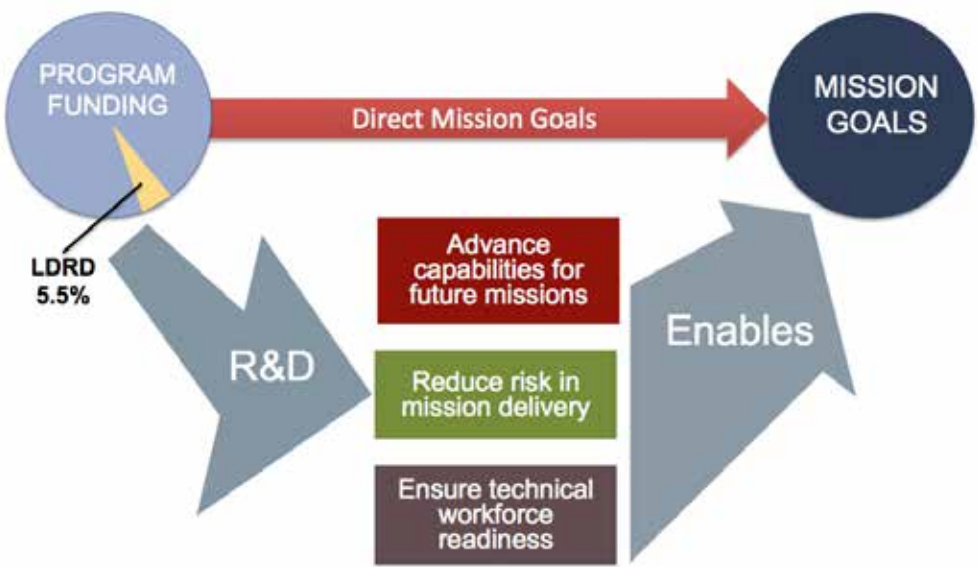

A new charter for LDRD largely reinforces existing program values, including its insistence on the highest standards of innovation and creativity.

In Phase 1 of the refresh, the panel refined LDRD's purpose and top-level objectives, documented in a new charter for LDRD that largely reinforces existing program values, including its insistence on the highest standards of innovation and creativity. The charter also calls for a new level of line-program partnership for LDRD project selection and execution, a rebalanced LDRD portfolio to include higher-risk investments and more applied R&D, and a new Mission Foundations Research (MFR) component of the program. The charter was published on the Laboratory's LDRD website and presented to technical staff in a town-hall style meeting at which the panel solicited ideas about how to implement the charter in Phase 2 of the refresh.

Strategic Investment Planning: Top-down, Bottom-up

Phase 2 resulted in a new approach to line/program partnership in developing the annual Strategic Investment Plan for Directed Research investments. Previously, forming the SIP started with inputs from technical staff from the breadth of the Laboratory, working its way up to senior management for approval; going forward, the process will begin with a top-level statement of priorities written and endorsed by senior line *and* program management. While development of the SIP will still have a bottom-up component, not every interest will find a role in the SIP every year. Directed Research will have a strong flavor of strategic direction focused on mission challenges, and the SIP will be a clear statement of institutional priorities. This new approach will be implemented in the FY18 cycle.

Another significant outcome of Phase 2 was a proposed pilot of an MFR proposal competition. The underlying objective of MFR is to translate discovery into innovative solutions. The MFR pilot, approved by the Director for the FY17 cycle, will fund applied science and engineering in the technology readiness level (TRL) 3-5 range, targeting mission problems defined in advance by mission champions across the Laboratory. Technical readiness levels are a method of estimating technical maturity of a technology used by many federal agencies, such as the U.S. Department of Homeland Security. Proposed work must be at TRL 2 and have a solid scientific foundation.

Leaning Toward the Future

A fresh vision for LDRD has emerged that encompasses three core values: building capabilities for future missions, reducing risk in mission delivery, and ensuring technical workforce readiness. A successful LDRD program will look back 10 or 15 years from now and be able to point to the investments it made to shape the science, technology, engineering, and workforce enabling core missions of the 2030s.

Mission Relevance

Mission relevance is one of the most important criteria in the evaluation of a potential LDRD project; it is carefully considered in project selection and tracked annually through the data sheet process. Many of the technologies that put Los Alamos on the map have deep roots in LDRD and are valuable to DOE/NNSA mission areas of nuclear security, energy security, environmental remediation, and scientific discovery and innovation. LDRD work also benefits the national security missions of the Department of Homeland Security, the Department of Defense, and Other Federal Agencies. As a result, the scientific advances and technology innovations from LDRD provide multiple benefits to all Los Alamos stakeholders, consistent with Congressional intent and the Laboratory's scientific strategy.

Scientific Advances Underscore Integrated, Multidisciplinary Capabilities

From discoveries on Mars to breakthroughs in cancer and solar cell research, as well as shedding new light on the nature of plutonium, Los Alamos National Laboratory's 2016 accomplishments highlighted the Lab's unique capabilities for carrying out its essential national security mission in a broad range of disciplines. Innovations in supercomputing data storage, the use of medical isotopes for cancer treatment, a tissue-engineered artificial lung, and other new technologies rounded out the Lab's year.

Many of the Laboratory's significant achievements in FY16 were made possible by past or current LDRD investments in either the direct technology that was developed, or in the underlying capabilities that enabled it.

Mission Impact of FY16 LDRD Portfolio ($M)

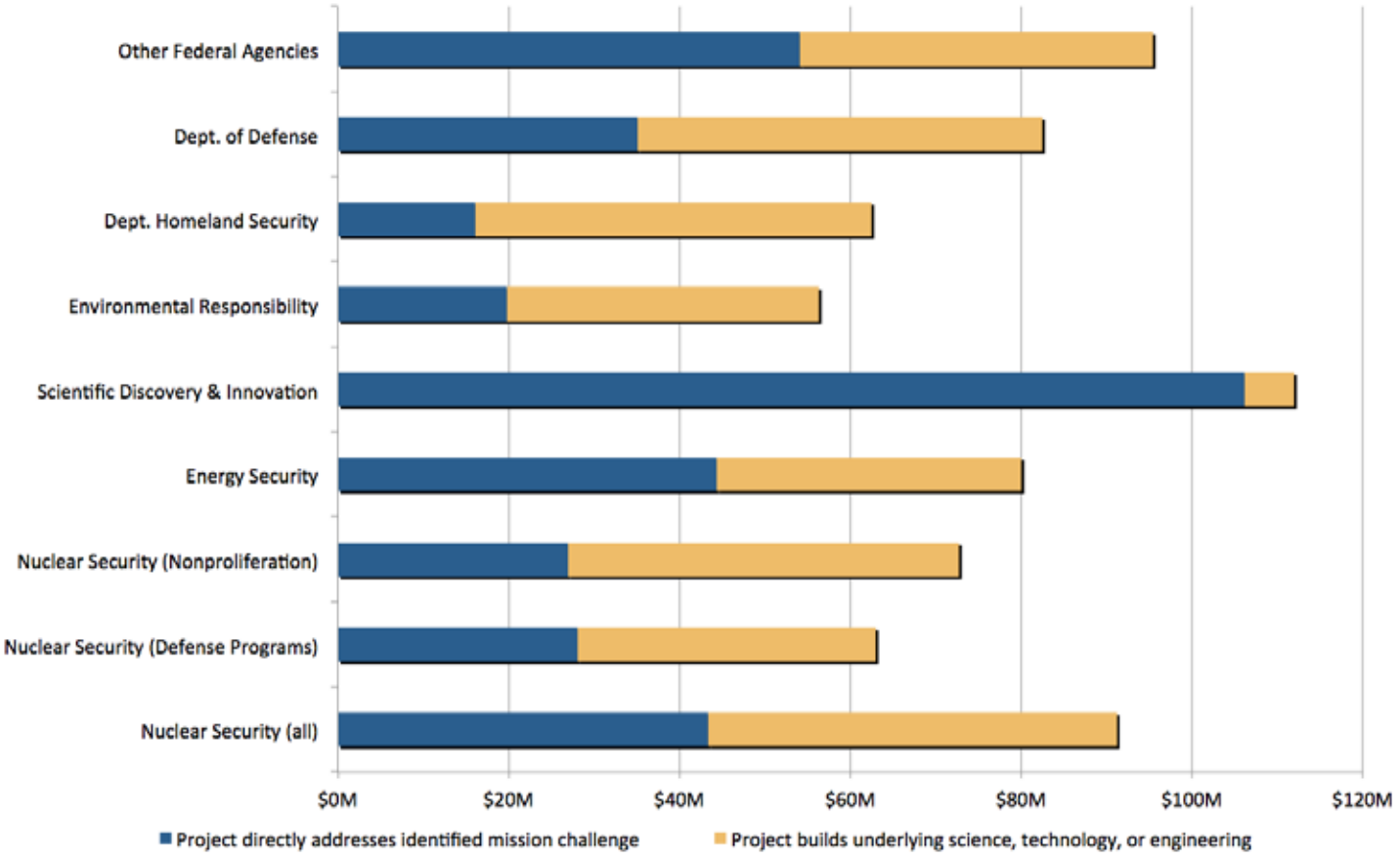

First and foremost, Los Alamos LDRD projects are required to address one or more of the DOE/NNSA mission areas. Due to the nature of basic R&D, the work may also benefit the mission challenges of other federal agencies. The multi-mission impact of LDRD projects is captured in the chart above, which is why the total expected benefit is approximately double actual costs of the program in FY16.

"This year, the Laboratory achieved significant advancements in high-performance computing, materials science, national security and nuclear nonproliferation science, epidemiology and cancer research, space science, earth science, and renewable energy. Taken together, they underscore the Lab's unique multidisciplinary scientific capabilities." **– Alan Bishop, Principal Associate Director for Science, Technology, and Engineering**

Here's a look at just a few of the Laboratory's news and programmatic highlights in 2016, with links to videos or articles about the work. All of the discoveries, advancements, or technologies mentioned here have roots in LDRD—some resulted from investments made 20 years ago, while others reflect LDRD's agility to respond to emerging needs.

Space

Since scientists first began forming a picture of the Van Allen Belts in the 1950s, the understanding of their shape has largely remained unchanged—a small, inner belt, a largely empty space known as the slot region, and then the outer belt, which is dominated by electrons and is larger and more dynamic than the others. But new analysis revealed that the shape varies from a single, continuous belt with no slot region, to a larger inner belt with a smaller outer belt, to no inner belt at all. Many of the differences are accounted for by considering electrons at different energy levels separately. LDRD has made sustained investment in advancing the Laboratory's capabilities for space situational awareness by investing in basic R&D to better understand the shape and size of the belts, which is crucial for protecting our technology in space. YouTube

Materials Science

In a step that could bring perovskite crystals closer to use in the burgeoning solar power industry, researchers have tweaked their crystal production method and developed a new type of two-dimensional layered perovskite with outstanding stability and more than triple the material's previous power-conversion efficiency. LDRD is currently investing in this research, recently published in *Nature*. YouTube

Health

A broad computational study of cancer genome sequences identified telltale mutational signatures associated with smoking tobacco and demonstrates, for the first time, that smoking increases cancer risk by causing somatic mutations in tissues directly and indirectly exposed to tobacco smoke. The study offers fresh insights into how tobacco smoke causes cancer. Dr. Ludmil Alexandrov, Oppenheimer Fellow and Los Alamos lead on the study, is funded by LDRD. He was recognized by Forbes as one of the "30 brightest stars under the age of 30." YouTube

Earth Science

A study of small, deep earthquakes along California's San Andreas Fault reveals depth-dependent frictional behavior that may provide insight into patterns signaling when a major quake could be on the horizon. The study reports that the deepest part of California's 800-mile-long San Andreas Fault is weaker than expected and generates small earthquakes in response to tidal forces. Over the last decade, LDRD has invested in research that advances our ability to identify indicators of fault stress state and identifying new faulting physics. This work has potential for broad application to predicting failure in all systems—both natural and human made—and could have significant impact to Ground Based Explosion Monitoring for developing approaches to identify anomalous sources. YouTube

Cyber Security

Entropy Engine is a random number generator that addresses a key fundamental flaw in modern crypto systems—predictability. The invention strengthens the foundation of computer security by producing an inexhaustible supply of pure random numbers at speeds of 200 million bits per second. Entropy Engine uses the unique properties of quantum mechanics to generate true entropy (random numbers) in a way that makes it immune from all external influences. Over the last 20 years, LDRD has invested in the underlying capability that powers this technology. Entropy Engine was one of four 2016 R&D 100 award-winning technologies developed at Los Alamos.

Other LDRD winners included

- *PathScan*: Security Analytics Software for Network Attack Detection, and
- *Pulmonary Lung Model (PuLMo)*: A Miniature, Tissue-Engineered Lung—Revolutionizing the Screening of New Drugs or Toxic Agents.

Performance Metrics

The LDRD program is a key resource for addressing the long-term science and technology goals of the Laboratory, as well as enhancing the scientific capabilities of Laboratory staff. Through careful investment of LDRD funds, the Laboratory builds its reputation, recruits and retains excellent scientists and engineers, and prepares to meet evolving national needs. The impacts of the LDRD program are particularly evident in the number of publications and citations resulting from LDRD-funded research, the number of postdoctoral candidates supported and converted by the program, and the number of awards LDRD researchers received. The following performance metrics are updated annually to reflect the most current data available as more complete information often becomes available well into the next fiscal year.

Intellectual Property

U.S. Patents Issued				
	FY13	FY14	FY15	FY16
LANL Patents	77	51	50	88
LDRD Supported	32	14	10	19
% due to LDRD	42%	27%	20%	22%

Invention Disclosures				
	FY13	FY14	FY15	FY16
LANL Disclosures	103	71	71	133
LDRD Supported	34	12	16	69
% due to LDRD	33%	17%	23%	52%

Science and Engineering Talent Pipeline

Postdoc Support				
	FY13	FY14	FY15	FY16
LANL Postdocs	596	508	488	501
LDRD Supported	367	266	266	272
% due to LDRD	61%	52%	55%	54%

Postdoc Conversions				
	FY13	FY14	FY15	FY16
LANL Conversions	57	50	55	80
LDRD Supported	26	29	24	47
% due to LDRD	46%	58%	44%	59%

Peer-reviewed Publications and Citations

Publications				
	FY13	FY14	FY15	FY16
LANL Pubs	2082	2215	1872	1968
LDRD Supported	534	475	392	426
% due to LDRD	24%	21%	21%	22%

Citations				
	FY13	FY14	FY15	FY16
LANL Citations	31125	22123	12319	4574
LDRD Supported	10723	5267	4229	1592
% due to LDRD	34%	24%	34%	35%

External Collaborations (FY16)

University of California	New Mexico Universities	International	All
49	38	241	879

On the Cover and Beyond

The numerous publications made possible with LDRD funding help Los Alamos maintain a strong presence and scientific reputation in the broader scientific community. Not only does the program support a significant fraction of the Laboratory's publications, it also supports much of the research featured on the covers of peer-reviewed journals. These are just a few examples from FY16.

The cover of the November 2016 issue of *Applied and Environmental Microbiology* featured a new study by a research team led by Laboratory Fellow Cheryl Kuske. The research compares the ways arid grasslands respond to climate changes and human activities that cause physical disturbance. Alterations in land use, coupled with regional climate changes, may push dryland ecosystems into new ecological states of unknown composition and function. The team conducted multiple long-term field experiments in Utah. Two related papers in *Frontiers in Microbiology* reported the team's work from field experiments in Nevada to examine the effects of additional nitrogen on bacterial and fungal communities in surface soils. Atmospheric deposition of nitrogen could increase as human use of the land for living spaces, recreation, and energy development expands. LDRD supported various aspects of the work.

nature COMMUNICATIONS

Disordered solids such as plastics, window glass and amorphous metals are an important and ubiquitous form of matter with many useful applications. Industrial processing of these materials commonly involves plastic deformation. The physical processes controlling the onset of yield, where a material changes its shape permanently under external deformation, are not yet understood for amorphous solids. The problem is key to understanding how a solid can fail. In findings published in *Nature Communications*, a research team from Los Alamos and their collaborators found strong evidence that the point at which a disordered or amorphous solid begins to yield and flow under an applied stress exhibits features similar to those found in the study of chaos, as well as well as the transition accompanying a change of phase from one state of matter to another.

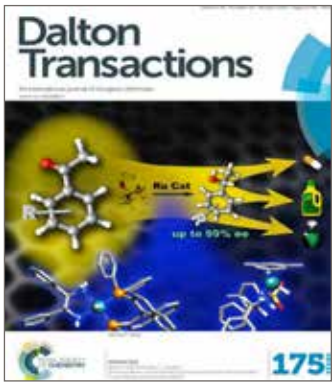

Catalytic hydrogenations represent the largest-volume human-made chemical reactions in the world. Many industrially important processes are based on a homogeneous version of this reaction. Homogeneous catalysis provides convenient properties including: mild reaction conditions, low cost, operational simplicity, high activities and selectivities that can be tuned via electronic and steric effects of the ligand, ease of catalyst structure determination and reaction mechanism analysis that can also be readily probed. In the April 2016 issue of *Dalton Transactions*, Los Alamos researchers John Gordon and Pavel Dub wrote an invited review of the mechanism of one of the most efficient artificial catalytic reactions. The review included some of the researchers' novel findings. The journal featured the perspective piece on its cover. LDRD funded the Los Alamos work, and Dub received a J. Robert Oppenheimer Distinguished Postdoctoral Fellowship.

PHYSICAL REVIEW LETTERS

The journal *Physical Review* Letters reported an interesting phenomenon of magnetic materials. The magnetization in magnetic materials can be regarded as a little arrow pointing in certain direction in space. In ferromagnets, the arrows align in the same direction. Scientists had noted in the 1970s and later that the arrows could self-organize into a peculiar localized texture due to the underlying microscopic interactions. In the language of field theory, the uniform ferromagnetic state can be regarded as a vacuum state and the localized magnetization texture is a particle-like excitation. Generally creating a "particle" in "vacuum" requires overcoming an energy barrier and costs energy. Therefore the particle is a metastable state. In the publication, Los Alamos researchers and collaborators found that in certain magnets, the "particle" has lower

energy than the "vacuum" once an impurity is introduced into the system, resulting in the spontaneous nucleation of "particles" out of a "vacuum." The findings suggest a novel mechanism to generate a thermodynamically stable skyrmion in a simple way, which could have a large impact on future applications of skyrmions in spintronic devices, such as memory and magnetic sensors. LDRD funded the Los Alamos research.

AGU PUBLICATIONS

The discovery of manganese oxides in Martian rocks suggests that the Mars was once more Earthlike than previously believed. A paper in *Geophysical Research Letters* led by Los Alamos researcher Nina Lanza reveals that NASA's Curiosity rover observed high levels of manganese oxides in Martian rocks, which could indicate that higher levels of atmospheric oxygen once existed on our neighboring planet. The journal featured the research on its cover. Now that researchers have discovered manganese oxides on Mars, the next step is to determine their origins. The team cannot conduct the study using ChemCam because they do not know if the manganese minerals they have observed there are biogenic (caused by life processes) or not. However, scientists can perform work at Los Alamos with the ChemCam engineering model. Lanza leads an LDRD Early Career Research project to investigate the chemical and mineralogical signatures of non-biogenic versus biogenic manganese, which is directly produced by microbes. The ChemCam instrument is a capability developed with funding from LDRD.

Los Alamos researcher Hsing-Lin Wang and collaborators published a review article on nanoelectrocatalysts that captured the March 2016 cover of the journal *Chemical Society Reviews*. Development of new, more efficient catalysts made from abundant materials is a key element in enabling industrial development of many energy-related technologies. Industrial fuel cells such as proton exchange membrane fuel cells, direct methanol fuel cells, and biofuel cells suffer from high cost, serious intermediate tolerance, anode crossover, sluggish kinetics, and poor stability of the catalyst. These fuel cells generally use precious metal such as platinum as the preferred electrocatalysts for the oxygen reduction reaction (ORR) at the cathode. The search for inexpensive electrocatalysts free from noble metals and practical for ORR has created one of the most active and competitive fields in chemistry and materials science. LDRD supported the Los Alamos research.

NATIONAL ACADEMY OF SCIENCES

Eliciting an immune response that can neutralize the large diversity of viral strains circulating in humans is a major challenge for developing an HIV type 1 (HIV-1) vaccine. Broad and potent monoclonal antibodies against HIV-1 have been discovered, which can neutralize a large fraction of a diverse panel of HIV-1 strains in vitro. However, their highly mutated nature and late emergence in infection make it difficult to determine how they arose. Thus, an effective HIV-1 vaccine is elusive according to Los Alamos researchers Alan Perelson and Shishi Luo. Harnessing the power of broadly neutralizing antibodies, which emerge years into a chronic HIV infection, could help overcome this challenge. The Los Alamos team used a mathematical model to examine how broadly neutralizing antibodies coevolve with HIV-1. The *Proceedings of the National Academy of Sciences* published their findings. The LDRD program funded postdoc research associate Luo.

ADVANCED FUNCTIONAL MATERIALS

Los Alamos researchers and a collaborator discovered why solution-processed, large-grain hybrid (organic/inorganic) perovskites produce solar cells with exceptional (approximately 18%) power conversion efficiencies. This class of materials offers low-cost solution processing preparation together with favorable intrinsic properties for optoelectronic applications. The journal *Advanced Functional Materials* published the findings. This discovery is an important step toward creation of solution-processed semiconductors that have properties comparable to materials grown by traditional high temperature methods. Hybrid perovskite materials have excellent optoelectronic properties that enable a wide variety of potential device applications. The research gives the team insight to develop this material for U.S. energy and global security applications, such as solar cells and sensors. LDRD funded some aspects of the work.

Awards and Recognitions

The LDRD program helps Los Alamos National Laboratory anticipate, innovate, and deliver solutions to some of the nation's toughest challenges. The driving force behind each impact has been the focused initiative of many talented scientists and engineers who choose to apply their knowledge and expertise in service to the nation. The LDRD program is proud to support the work of some of the Laboratory's most accomplished researchers, who in FY16 received many prestigious awards, honors, and recognitions.

IEEE Fellow

The Institute of Electrical and Electronics Engineers (IEEE) honored **Bruce Carlsten** with the title of Fellow. IEEE cited him "for contributions to high-brightness electron beams and vacuum electron devices." Carlsten is a pioneer in the production and use of high-brightness electron beams. His discovery of techniques enabling unprecedented beam brightness has led to a new generation of intense free-electron lasers, including the Lab's Navy Free Electron Laser (FEL), and MaRIE, a proposed premier x-ray FEL facility. These ideas are of such fundamental importance that virtually every free-electron laser in the world uses them. Carlsten currently leads a 2017 ER project.

ACA President

The American Crystallographic Association (ACA) elected **Tom Terwilliger** to be the 2016 President of the ACA. The ACA is a scientific organization of over 2,200 members in more than 60 countries who use x-rays, neutrons, and electrons to determine the structure of molecules at atomic (or near atomic) resolution. Terwilliger's research includes developing new methods for interpreting X-ray data so that researchers such as scientists in pharmaceutical companies can see their new drugs bound to protein molecules quickly and accurately. He currently leads a 2016 DR project.

ASM Fellow

ASM International named **Ellen Cerreta** to the 2016 class of Fellows. Recipients of one of the highest honors in the field of materials, ASM Fellows are technical and professional leaders who have been recognized by their colleagues and serve as advisors to the Society. Cerreta was cited for "outstanding contributions in the fields of dynamic and shock behavior of materials, as well as structure/property effects on mechanical behavior and damage evolution in materials." She is a past contributor to LDRD projects, served on the ER refresh panel, and has served on LDRD proposal review panels.

ECS Outstanding Achievement Award

Rangachary Mukundan received the 2016 Sensor Division Outstanding Achievement Award, presented biennially by the Sensor Division of the Electrochemical Society (ECS). The award is the highest recognition the division can bestow on a member. Mukundan is the co-inventor on six U.S. patents and has authored more than 125 papers including more than 50 in peer-reviewed journals that have been cited over 4,000 times. He is the technical editor in the area of sensors and measurement sciences for ECS journals. Mukundan currently leads a 2017 DR project and will serve on a DR proposal review panel for the FY18 LDRD proposal competition.

Alvin Van Valkenburg Award

Arianna Gleason received the Alvin Van Valkenburg Award at the 2016 Gordon Research Conference on High Pressure in Holderness, NH. Gleason was honored for her substantial contributions as an early career scientist to high-pressure physics in both static and dynamic compression. Gleason began conducting scientific research in 1998 on asteroid/comet detection and discovery with the group Spacewatch at the University of Arizona. She received a doctorate from the University of California, Berkeley in mineral physics and Earth sciences for her investigation of the elasticity and plasticity of Earth-relevant materials at extreme conditions. Gleason used static compression techniques combined with synchrotron sources. The work helps interpret Earth's seismic information and provides insight into the evolution of the Earth's interior. She joined the Laboratory in 2014 as a Postdoctoral Fellow supported by LDRD.

AAAS Fellow

The American Association for the Advancement of Science (AAAS) awarded the distinction of Fellow to **Dave Morris** for his pioneering contributions in chemistry research and leadership, including electronic structure and bonding in organoactinides and environmental speciation of actinides by optical spectroscopic probes. Throughout his career, Morris made unique and significant contributions in two very distinctly different areas of chemistry. The first is in the application of spectroscopic and electrochemical methods to explain electronic structure and bonding in organometallic f-element complexes. The second is in the development and application of electronic and vibrational spectral probes, in combination with X-ray absorption spectroscopies, to explain the partitioning of uranium in clay minerals and other important subsurface mineral phases. Morris has made several LDRD contributions as PI on ER projects.

Complex Natural & Engineered Systems

SHIELDS: Space Hazards Induced near Earth by Large Dynamic Storms - Understanding, Modeling, Predicting

Vania K. Jordanova
20150033DR

Introduction

Our society is increasingly dependent on technologies susceptible to harmful conditions in space, e.g., Galaxy 15, a $250M telecommunication satellite in geosynchronous orbit, failed to operate in 2010 due to a space storm, and its recovery operation cost was ~$3.5M. Predicting space weather hazards remains a big space physics challenge due to the complex multi-scale nature of the magnetosphere. This project will address this challenge using a cross-Laboratory team, LANL state-of-the-art models, computational facilities, and data from national security payloads. This project will develop a new capability, the SHIELDS framework, to understand, model, and predict one of the most important space weather hazards, the spacecraft Surface Charging Environment (SCE), i.e. the hot (less than few 100 keV) electron fluxes whose enhancement can lead to satellite failures during disturbed conditions. This project aims at addressing two mechanisms that may be crucial for the increase of the SCE, but are not included in any existing global model: a) particle injection during geomagnetic substorms (magnetospheric reconfiguration events), and b) scattering by plasma waves. Substorms may contribute significantly to the plasma pressure increase, causing sudden enhancements of the ring current (keV) fluxes. Plasma waves redistribute energy throughout the collisionless magnetospheric environment; wave-particle interactions can serve as a dominant mechanism for energy diffusion and particle loss. Including these processes requires models that are targeted at key regions/physics regimes, however, the coupling of these models across multiple spatial and temporal scales remains an extreme challenge. Guided by theory and observations, the goal of this project is to bridge macro- and microscopic computational models, allowing for the first time to study the SCE consequences on a global scale. New data assimilation techniques employing data from LANL instruments on Van Allen Probes and geosynchronous satellites will be applied for the first time to the global model.

Benefit to National Security Missions

Our national efforts in nuclear nonproliferation depend in many ways on our satellite sensing systems. Many of the nation's civilian and military space assets operate in the inner magnetosphere, an extremely hazardous region of space causing satellite failures and anomalies. The ability to reliably distinguish between various modes of failure is very important in anomaly resolution and forensics and may be used in decision-making exercises at the highest levels. The crucial national security need to maximize the safety of civilian and military satellites requires a capability to predict dynamic conditions in space, as called out in national studies supporting the National Space Weather Program by DOE, DOD, NOAA, NASA, and NSF. This is especially needed during solar maximum (in ~2015) with its expected high storm occurrence. Our SHIELDS framework will address the ubiquitous threats posed by surface charging and will specify the fast-changing Surface Charging Environment (SCE) which represents a seed population for the harmful radiation belts. SHIELDS utilizes unique data from DOE/LANL geosynchronous spacecraft, which are operational national security payloads that additionally provide scientific data at critical locations in the magnetosphere. SHIELDS is directly relevant to the Lab's Global Security Space Situational Awareness (SSA) and Energy Security missions and the "Complex Natural and Engineered Systems" priority area to understand key drivers of the radiation belts (e.g., seed populations, plasma waves) and advance toward prediction of the space environment. Being sought both nationally and internationally, such unique LANL capability will position us at the forefront of space science exploration.

Progress

Work on the Particle Tracing Model (PTM) focused on following off-equatorially mirroring particles and investigating the azimuthal extent of the injection boundary. We modeled several scenarios: an idealized substorm

with/without inner-magnetosphere coupling (RAM-SCB feedback to the MHD code), and a realistic substorm event that occurred in July 2013. We applied the PTM code for a range of equatorial pitch angles (and with adaptive switching between full-orbit and guiding-center equations) to each of these scenarios to obtain boundary conditions for the inner magnetosphere model (RAM-SCB). The dynamic fields from the global magnetohydrodynamics model (BATS-R-US) have also been used to trace the evolution of empirical injection boundaries to provide a cross-check/validation of the PTM results. Coupling of the inductive electric fields into RAM-SCB is ongoing.

We implemented the coupling between iPIC3D and BATS-R-US configured for multi-ion and/or separate electron pressure equation, allowing the BATS-R-US and iPIC3D to use different grids and different time steps. We improved the efficiency of the coupling substantially (the execution time was reduced from 80% to less than 2%) and the coupling is now fully parallel. We applied the MHD-EPIC code to Mercury where the separation of kinetic and global scales is moderate. The obtained magnetic field signatures showed very good agreement with MESSENGER observations. We now applied MHD-EPIC to the Earth, which is the main target for the SHIELDS project, putting the PIC box around the dayside reconnection site. We performed 3D MHD-EPIC simulations (with an ion mass set to 16) which worked very robustly and efficiently, showing several flux ropes forming at the dayside reconnection site covered by the PIC region.

The first data assimilation method we used for RAM-SCB was the localized ensemble transform Kalman filter (LETKF). The results from the LETKF effort were reasonable but not entirely satisfactory, due to inherent characteristics from the model and assimilation approach. In order to improve upon our previous assimilation effort, we developed a novel assimilation approach based on the singular value decomposition (SVD). The new approach decomposes the model solution into dominant modes, and projects onto these modes to perform the data assimilation. Subsequently, after the assimilation in the dominant modes, the model solution is then reconstructed with an improved error estimate. We implemented our new assimilation method to RAM and obtained encouraging results which are better compared to the LETKF results.

We have implemented both a time-dependent plasmaspheric density model and a new diffusion scheme in RAM-SCB. The plasmasphere density model, based on a formulation by Rasmussen (1993), was updated to utilize the latest version of IRI which includes detailed history files of a variety of geomagnetic indices including the global geomagnetic storm index (Kp) derived from magnetic field data. The Kp index is also utilized in a climatology of plasmaspheric wave amplitudes derived from the CRRES satellite by the British Antarctic Survey (BAS) that was also incorporated into RAM-SCB. Thus these two sub-models have self-consistent forcings. Work has begun on the new PIC-driven diffusion coefficients.

SHIELDS repositories were fully integrated into gitlab.lanl.gov. We worked on the development, implementation and incorporation of continuous integration into SHIELDS software development workflow. We performed large scope and scale execution/regression tests and initial unit tests, and incorporated automated build and test integration within RAM-SCB, SWMF, CPIC and particle tracing codes. We implemented RAM-SCB testing against the latest stable SWMF with capability to immediately identify issues. We helped to develop and deploy continuous integration infrastructure that has been made available to the entire institution.

We now have a working version of the spacecraft-charging Curvilinear PIC (CPIC) code ported on multi-block meshes. In particular, we (1) developed a multi-block Poisson solver using mimetic discretization techniques, (2) developed a particle mover on multiblock meshes (including an efficient parallelization method), (3) tested the new CPIC code on simple geometries, and (4) developed an interface to a commercially available mesh-generation software that will be used to generate the mesh conforming to the geometry of the spacecraft.

Finally, the SHIELDS workshop we organized in Santa Fe was a big success with 55 participants and a press release in PCmag and LANL Science Highlight. We submitted a copyright disclosure through CODES for open-sourcing RAM-SCB. We also created a SHIELDS website to publicly share major accomplishments: http://www.lanl.gov/projects/shields/index.php

Future Work

A major goal is organizing the SHIELDS challenge, simulation of the March 17-18, 2013 geomagnetic storm, to assess and demonstrate the effectiveness of our new modeling framework. Specific tasks are:

1) Fully integrate the injection-associated fluxes into RAM-SCB, together with the inclusion of the inductive electric fields. Simulate the SHIELDS challenge event and validate the results against GEO and Van Allen Probes observations. Explore the radial dependence of the injected particles.

2) Develop further the coupling of BATS-R-US and the iP-

IC3D code and extend the Earth simulations to the tail. Run the SHIELDS challenge event with this setup and provide output for the PTM code. Complete the direct coupling between multiple PIC regions. Develop methods to identify reconnection sites in an automated fashion.

3) Apply the newly developed SVD-based data assimilation scheme to the SHIELDS challenge event; incorporate flux data into RAM and find the appropriate self-consistent B field. Perform data assimilation with the coupled RAM-SCB and BATS-R-US system, where the assimilation estimates key MHD model parameters.

4) Develop a new capability utilizing off-line PIC simulations to inform the RAM diffusion coefficients. Since PIC simulations are computationally expensive, only space-time locations with unstable RAM populations will be used to seed PIC simulations. Demonstrate this new capability for the SHIELDS challenge.

5) Fully automate existing workflows to integrate data assimilation and particle tracing with RAM-SCB/SWMF. Extend continuous integration tests and ensure compatibility of distinct development efforts. Tie the components into a global SHIELDS framework, obtaining an automated workflow.

6) Perform spacecraft-charging simulations with CPIC for the Van Allen Probes (VAP) for the SHIELDS challenge event to (a) assess the fidelity of the numerical prediction of the VAP charging during orbit, and (b) to explain why, despite being a conductive spacecraft, VAP can charge quite negatively even when exposed to sunlight.

Conclusion

Using a new, system-level approach, we will provide the transformative understanding of mechanisms driving disturbed geomagnetic conditions, critically needed for their accurate prediction and to prevent damages to technological systems in space. We will obtain, for the first time, a realistic description of the magnetosphere, resolving short timescales of substorm dynamics and enabling a better prediction of the spacecraft Surface Charging Environment (SCE). We will examine, for the first time self-consistently on a global scale, the fundamental generation of plasma waves and their feedback on particle dynamics. We expect this to lead to new discoveries and high-impact innovative publications.

Publications

Birn, J., A. Runov, and M. Hesse. Energetic ions in dipolarization events. 2015. Journal of Geophysical Research - Space Physics. doi:10.1002/2015JA021372 (120): 1.

Denton, M. H., M. F. Thomsen, V. K. Jordanova, M. G. Henderson, J. E. Borovsky, J. S. Denton, Pitchford, and D. P. Hartley. An empirical model of electron and ion fluxes derived from observations at geosynchronous orbit. 2015. Space Weather. 13 (4): 233.

Denton, M. H., M. G. Henderson, V. K. Jordanova, M. F. Thomsen, J. E. Borovsky, J. Woodroffe, D. P. Hartley, and D. Pitchford. An improved empirical model of electron and ion fluxes at geosynchronous orbit based on upstream solar wind conditions. 2016. Space Weather. doi:10.1002/2016SW001409 (14): 1.

Godinez, H. C., Y. Yu, E. Lawrence, M. G. Henderson, B. Larsen, and V. K. Jordanova. Ring current pressure estimation with RAM-SCB using data assimilation and Van Allen Probe flux data. 2016. Geophysical Research Letters. doi:10.1002/2016GL071646 (43): 1.

Henderson, M. G.. The role of “plasma-bubbles” in the injection process. Invited presentation at Unsolved Problems in Magnetospheric Physics. (Scarborough, UK, 6-12 Sept. 2015).

Hou, E., A. Hero, and E. Lawrence. Penalized Ensemble Kalman Filters for high dimensional non-linear systems. 2016. Monthly Weather Review. : 1.

Jordanova, V. K.. Global modeling of wave generation processes in the inner magnetosphere. 2017. In Magnetosphere-ionosphere coupling in the solar system. Edited by Chappell, C., R. Schunk, P. Banks, J. Burch, and R. Thorne. Vol. Geophysical Monograph 222, First Edition, p. 155. American Geophysical Union: John Wiley & Sons, Inc.

Jordanova, V. K., G. L. Delzanno, M. G. Henderson, G. Toth, H. C. Godinez, C. A. Jeffery, E. C. Lawrence, J. D. Moulton, L. J. Vernon, D. T. Welling, J. R. Woodroffe, Y. Yu, and L. Zhao. The LANL SHIELDS Project. Presented at Twelfth European Space Weather Week. (Ostend, Belgium, 23-27 Nov. 2015).

Jordanova, V. K., W. Tu, Y. Chen, S. K. Morley, A. D. Panaitescu, G. D. Reeves, and C. A. Kletzing. RAM-SCB simulations of electron transport and plasma wave scattering during the October 2012 “double-dip” storm. 2016. Journal of Geophysical Research: Space Physics. doi:10.1002/2016JA022470 (121): 1.

Meierbachtol, C. S., G. L. Delzanno, D. Svyatskiy, L. J. Vernon, and J. D. Moulton. An Electrostatic Particle-In-Cell Code on Multi-block Structured Meshes. Journal of Computational Physics.

Meierbachtol, C. S., G. L. Delzanno, J. D. Moulton, L. J. Vernon, and V. K. Jordanova. CPIC: A Curvilinear

Particle-In-Cell Code for studying spacecraft-plasma interactions. Presented at Twelfth European Space Weather Week. (Ostend, Belgium, 23-27 Nov. 2015).

Peng, I. B., S. Markidis, E. Laure, A. Johlander, A. Vaivads, Y. Khotyaintsev, P. Henri, and G. Lapenta. Kinetic structures of quasi-perpendicular shocks in global particle-in-cell simulations. 2015. Physics of Plasmas. doi: 10.1063/1.4930212 (22): 1.

Toth, G., X. Jia, S. Markidis, B. Peng, Y. Chen, L. Daldorff, V. Tenishev, D. Borovikov, J. Haiducek, T. Gombosi, A. Glocer, and J. Dorelli. Extended Magnetohydrodynamics with Embedded Particle-in-Cell Simulation of Ganymede's Magnetosphere. 2016. Journal of Geophysical Research. 121 (2): 1273–1293.

Welling, D. T., V. K. Jordanova, A. Glocer, G. Toth, M. W. Liemohn, and D. R. Weimer. The two-way relationship between ionospheric outflow and the ring current. 2015. Journal of Geophysical Research. 120 (6): 4338.

Woodroffe, J. R., S. K. Morley, V. K. Jordanova, M. G. Henderson, M. M. Cowee, and J. G. Gjerloev. The latitudinal variation of geoelectromagnetic disturbances during large (Dst≤−100 nT) geomagnetic storms. 2016. Space Weather. doi:10.1002/2016SW001376 (14): 1.

Woodroffe, J. R., V. K. Jordanova, H. O. Funsten, A. V. Streltsov, M. T. Bengtson, C. A. Kletzing, J. R. Wygant, S. A. Thaller, and A. W. Breneman. Van Allen Probes observations of strong whistler-mode chorus inside a remnant plasmaspheric plume. Journal of Geophysical Research.

Yu, Y., G. L. Delzanno, V. K. Jordanova, I. B. Peng, S. Markidis, and T. Wang. PIC simulations of wave-particle interactions initialized by a physics-based electron distribution obtained from the RAM-SCB model. Journal of Atmospheric and Solar-Terrestrial Physics.

Yu, Y., V. K. Jordanova, A. J. Ridley, J. M. Albert, R. B. Horne, and C. A. Jeffery. A New Ionospheric Electron Precipitation Module Coupled with RAM-SCB within the Global Geospace Circulation Model. 2016. Journal of Geophysical Research. doi:10.1002/2016JA022585 (121): 1.

Yu, Y., V. K. Jordanova, S. Zou, R. Heelis, M. Ruohoniemi, and J. Wygant. Modeling subauroral polarization streams (SAPS) during the March 17, 2013 storm. 2015. Journal of Geophysical Research - Space Physics. doi:10.1002/2014JA020371 (3): 1738.

Zhao, L., Y. Yu, G. Delzanno, and V. Jordanova. Bounce- and MLT-averaged diffusion coefficients in a physics-based magnetic field geometry obtained from RAM-SCB for the March 17 2013 storm. 2015. Journal of Geophysical Research - Space Physics. doi:10.1002/2014JA020858 (4): 2616.

Critical Watersheds: Climate Change, Tipping Points, and Water Security Impacts

Richard S. Middleton
20150397DR

Introduction

Water is critical for domestic health, wealth, and security. Our changing climate will have a significant and detrimental impact on terrestrial ecosystems and subsequent water supply for the energy-water nexus (EWN). Currently, we do not understand the interactions and feedbacks between climate, forest mortality, wildfire, and hydrology. Without this understanding, we cannot predict and plan for climate-induced impacts on society and the EWN.

This project develops the necessary basic science and modeling capabilities to (1) predict, (2) quantify, and (3) mitigate climate-related impacts on our natural ecosystems and the EWN. The project focuses on the novel concept of "critical watersheds", watersheds that are both critical to society and vulnerable to climate change, and climate-induced extreme events. The project is advancing the predictive understanding of integrated watershed hydrology and the role of disruptive events in ecosystems. The project focuses on processes that operate and are manifested on multiple scales, requiring multiple study sites to capture the range of climate-ecosystem-hydrologic interactions. Our study sites range from small-scale ecosystem study plots and hillslopes (< 0.1 km2) and small watersheds (<2 km2) up to mesoscale watersheds and the entire Colorado River basin. The broad project focus will is on the US Southwest though the science, tools, and understanding developed will be broadly applicable to critical domestic and global watersheds. The project will use combination of existing data from LANL and multiple collaborators, new modeling approaches, new model-based data analyses and syntheses, and new experiments. The project will uniquely position LANL to predict, quantify, and mitigate the impacts of climate change on water supply to municipalities and energy producers, with multiple potential sponsors in DOE, state and federal agencies, and private industry.

The project will develop a first-of-a-kind fully-integrated framework to directly address interactions and feedbacks between climate, terrestrial ecosystems, wildfire, and hydrology.

Benefit to National Security Missions

The project directly addresses the energy security and environment missions, with anticipated substantial contributions to the DOE applied energy and science programs.

Environment mission: The project focuses on climate and energy impacts, specifically exploring climate change/extremes and water supply for the energy-water nexus (EWN). This includes all energy production/extraction that requires water including coal-fired and gas plants, nuclear power plants, renewable energy (e.g., hydropower), and conventional and unconventional oil and gas production. The stretch goal of the project is to develop quantitative mitigation plans—including remediation and restoration—that increase ecosystem resiliency (e.g., fire suppression, hydrologic stability) to changing climate and extremes. Science and modeling capabilities developed in this project directly address challenges set out by the DOE-SC including integrating fire behavior, drought mortality, and hydrology into standalone watershed frameworks as well as providing key input for DOE-SC's Accelerated Climate Model for Energy (ACME).

Energy security mission: The EWN is a key focus of the project, understanding how nuclear energy, fossil energy, and renewable energy/power will be impacted by climate change/extremes, particularly in critical watersheds such as the Colorado River.

Agency relevance: Project outcomes are designed to directly address challenges and needs set out by DOE-SC (see above) and DOD (e.g., SERDP). The project addresses applications critical to DOE-EERE (e.g., biomass

and hydropower programs). Long-term, the project could position LANL for non-traditional federal agencies including USDA (food security), EPA (environmental impacts), and Department of State (geopolitically critical watersheds such as the Nile River basin).

Progress

We identified three goals and three tasks in FY15 planning. During FY16 we have made significant progress and, three quarters through FY16, we are on track to meet and exceed all goals, tasks, and sub-tasks. In addition, we have made significant progress with identifying and meeting with future sponsors notably the DOE-SC Climate and Environmental Science (CESD) division. In particular, we have couched the Critical Watersheds LDRD-DR in terms of integrated disturbance science (IDS). With 15 months of the project remaining the CESD is already raising the prospect of a LANL scientific focus area (SFA) in the area of IDS and the Critical Watersheds LDRD-DR.

GOAL 1: We have advanced our understanding of coupled hydrology-drought impacts at the fine scale (Upper Jaramillo River (IJR) watershed; several square kilometers) and the regional scale (San Juan River (SJR) basin; 10,000s square kilometers). We have demonstrated coupled wildfire-hydrology impacts for the UJR and coupled drought-hydrology for the San Juan. One dedicated paper for each study will be submitted imminently, with several more manuscripts being developed by the end of FY16.

GOAL 2: We have developed a preliminary framework—the Advanced Terrestrial Simulator (ATS)—to couple processes representing climate, ecosystems, fire, and hydrology. In FY16 we demonstrated the framework for the UJR and presented preliminary results during the January 2016 appraisal. The demonstration is currently being updated including critical processes such as duff interactions. A manuscript is in preparation.

GOAL 3: The original white/concept manuscript is currently being parsed into two separate manuscripts: one focusing on modeling challenges and opportunities and one on IDS. A third related paper is expected in FY17.

Task 1.1 Drought ecology: We have identified key hydrologic impacts of plant stress/mortality and integrating them into ATS. This task is intensive and will continue into FY17. We have developed our firsl site in the UJR based on existing data and interactions with the Valles Caldera National Preserve (VCNP) and NSF's Critical Zone Observatory (CZO) project based in the Jemez Mountains.

Task 1.2 Vegetation succession/recovery: significant progress has been made integrating dynamic vegetation in to the ATS model. We anticipate with to be major scientific advance and uniquely position LANL in terms of science and sponsors. Progress will continue into FY17.

Task 1.3 Fire ecology: The QUICfire reduced fire model has developed rapidly and has already been tested and benchmarked for grassland fires. We anticipate QUICfire being tested in forested ecosystems by the end of summer 2016. TASK 2: Framework development: Key processes have been identified, including processes (such as duff) that we previously did not anticipate as being so important. We developed an approach to incorporate detailed vegetation understanding and fire impacts into the framework. Work in this task supported the UJR demonstration.

TASK 3 Build preliminary database: We fully developed a regional hydrologic model for the SJR basin and demonstrated the impact of temperature-drought mortality on regional water supplies. A manuscript will be submitted imminently. The study showed that climate-driven disturbances will have significant impact on water delivery particularly in terms of how the snow pack forms and melts for a snow-driven system. We have started to build a database/framework for the Upper Colorado River (UCR) basins. This work was completed with the existing Variable Infiltration Capacity (VIC) model.

Specific accomplishments:

- DTRA has begun funding (~1.5 FTE) the QUICfire model for urban applications. The QUICfire concept was entirely developed in this LDRD-DR.
- Primary convener for an AGU session on climate-driven disturbances and critical watersheds.
- Invited to the Environmental Science Systems (ESS) PI meeting held by DOE SC. Full presentation to all DOE-SC CESD program managers expected in August 2016.
- Multiple invite talks including Los Alamos' Pajarito Environmental Education Center (PPEC).
- Radio interviews with Los Alamos and Santa Fe radio stations.
- LANL currently filming 25-minute documentary/report on the LDRD-DR. Filming has already taken place for the SJR work and the wildfire work.
- Project covered in media including Christian Science Monitor, LA Daily Post, and New Mexico newspapers.
- Work appeared in the White House Water Summit fact sheet (only two national labs were represented).
- Developed relationship with NSF CZO project in the Jemez Mountains.

Future Work

GOAL 1: Develop new approach to upscaling climate-driven disturbance observations and experiments from the fine scale to the regional scale.

GOAL 2: Integrate dynamic vegetation (based on ALM-ED) and fire impacts (QUICfire) into a single framework to demonstrate coupled climate-ecosystem-hydrology feedbacks and impacts.

GOAL 3: High-level publication of results from years 1 and 2.

TASK 1 Basic science and fundamental model development for drought ecology, vegetation succession/recovery, and wildfire:

Task 1.1 Dynamic vegetation response: Identify critical vegetation processes to represent within the Advanced Terrestrial Simulator (ATS). Identify spatiotemporal upscaling from ALM-ED column model to ATS. Integrate projected temperature-drought forest response. Calibrate with local-to-regional observations of forest mortality and regional historic hydrologic observations.

Task 1.3 Fire ecology: Build second generation QUICfire approach for forested ecosystems. Test and benchmark fire behavior and resultant outputs against (i) FIRETEC run and (ii) historic observations. Develop post-processing approach to integrate soil heat transfer effects including hydrophobicity. Align/integrate QUICfire outputs with ATS input requirements.

TASK 2 Coupled modeling: Integrate climate-driven disturbances into ATS directly (as opposed to offline coupling). Demonstrate fully-coupled framework, including a manuscript, by project end.

TASK 3 Regional empirical hydrology: Analyze impact of climate-driven disturbance for the Upper Colorado River (UCR) basin using the empirical Variable Infiltration Capacity (VIC) model, based on preliminary work in the San Juan River (SJR) basin.Perform historic analysis/calibration of extreme events and land cover change.

Conclusion

They overarching goal of this project is to develop the science and modeling capabilities to predict and quantify climate impacts on critical watersheds and water supply. This will have a potentially transformative impact on our understanding of climate change and the energy-water nexus (EWN) and our ability to mitigate and adapt to climate change. Specifically, we are developing a new understanding of the interaction and feedbacks between climate change and extreme events, climate-driven disturbances such as wildfire, drought and forest mortality, hydrology, and water for the EWN.

Publications

Allen, C. D., D. D. Breshears, and N. G. McDowell. On underestimation of global vulnerability to tree mortality and forest die-off from hotter drought in the Anthropocene. 2015. ECOSPHERE. 6 (8).

Coon, E. T., J. D. Moulton, and S. L. Painter. Managing complexity in simulations of land surface and near-surface processes. 2016. ENVIRONMENTAL MODELLING & SOFTWARE. 78: 134.

Fisher, R., S. Muszala, M. Verteinstein, P. Lawrence, C. Xu, N. McDowell, R. Knox, C. Koven, J. Holm, B. Rogers, and others. Taking off the training wheels: the properties of a dynamic vegetation model without climate envelopes. 2015. Geoscientific Model Development Discussions. 8 (4).

Middleton, R. S., J. S. Levine, J. M. Bielicki, H. S. Viswanathan, J. W. Carey, and P. H. Stauffer. Jumpstarting commercial-scale CO2 capture and storage with ethylene production and enhanced oil recovery in the US Gulf. 2015. GREENHOUSE GASES-SCIENCE AND TECHNOLOGY. 5 (3): 241.

Middleton, R. S., J. W. Carey, R. P. Currier, J. D. Hyman, Kang, Karra, Jimenez-Martinez, M. L. Porter, and H. S. Viswanathan. Shale gas and non-aqueous fracturing fluids: Opportunities and challenges for supercritical CO2. 2015. APPLIED ENERGY. 147: 500.

Skurikhin, A. N., N. G. McDowell, and R. S. Middleton. Unsupervised individual tree crown detection in high-resolution satellite imagery. 2016. JOURNAL OF APPLIED REMOTE SENSING. 10.

Countering Pathogen Interference with Human Defenses

Thomas C. Terwilliger
20160054DR

Introduction

We will implement a key part of the Los Alamos National Laboratory Advanced Therapeutics and Vaccines initiative by bringing together an experienced experimental and theoretical team to obtain a detailed understanding of the way in which pathogens manipulate human defense systems. We will integrate Los Alamos National Laboratory expertise in modeling, structural biology, imaging, synthetic antibodies, and genomics to build on Los Alamos National Laboratory models of the human "autophagy" defense system and develop a detailed description of how influenza virus interferes with this system. The project will create a foundation for next-generation therapeutics that block the ability of viruses and bacteria to interfere with human defenses. Further it will lead to improved "signatures" of pathogens that will identify whether the pathogens can interfere with specific elements of cellular defenses.

Benefit to National Security Missions

This project will lead to an understanding of how pathogens such as influenza interfere with human defenses and provide a basis for developing therapeutics that counter this interference. This work will be directly relevant to National Institutes of Health goals of understanding basic biology and protecting human health. Our work will also provide a framework that can be extended to understand interference with host defenses by intracellular bacterial pathogens such as Burkholderia that are of interest to the Defense Threat Reduction Agency. Further our work will provide a basis for diagnostic tests that evaluate the pathogenicity of the strain of virus or bacterium that is involved in an infection.

Progress

We have brought together a multidisciplinary team from LANL and outside collaborators to address the way in which influenza virus manipulates the human autophagy system to its own advantage.

Our work during the past 12 months has focused on structure determination of complexes of human and viral proteins, modeling of the autophagy system, and identification of the roles of specific influenza proteins on the authophagy system.

We have identified from our collaborators the human protein CRK-1 interactions with viral NS1 protein as important for this viral interference with autophagy. We have expressed and purified the CRK-1 protein and NS1 protein and constructed a stable complex between the two proteins suitable for crystallization and structure determination.

We have developed both high-level and detailed models of the autophagy system. These models are now suitable for incorporating the roles of influenza proteins on the functioning of the autophagy system.

We have developed a assay systems for identifying the effects of influenza proteins on the autophagy process. One of these assays allows us to visualize the formation of autophagosomes during the autophagy process and to determine the effect of influenza proteins on the formation of these vesicles that ultimately can break down the virus. The other is a biochemical assay for identification of which parts of viral proteins bind to human autophagy proteins such as beclin-1.

Future Work

Task 1. Develop comprehensive models of autophagy and influenza subversion of this host process.

We will extend LANL models of autophagy to include additional elements of the known autophagy system and the effects of influenza proteins. We will then validate the models and identify the values of parameters in these models. We will monitor formation and degradation of autophagosomes after influenza infection and

identify effects of changes in expression of influenza genes. We will use these observations to estimate parameters in the model and to identify elements of the host system affected by specific influenza proteins

Task 2. Develop a molecular understanding of the interactions that allow influenza to manipulate autophagy. We will purify, crystallize, and make progress towards obtaining crystal structures of complexes between influenza proteins and the human proteins that they regulate and to create reagents that can be used to perturb autophagy. These complexes will include beclin-1 complexes with the influenza M2 protein and the CRK1 complex with influenza NS1 protein. We will create a panel of synthetic antibodies to the external domain of the viral M2 protein. We will use stabilizing antibodies to enhance the crystallization of M2 bound to Beclin-1. Antibodies generated against these components will be used to perturb apoptosis and influence the course of autophagy. We will use these observations to track and perturb the system for comparison with our model-based predictions.

Conclusion

Human cells can detect when they are infected by a virus or other pathogen and respond by activating machinery that destroys the infecting pathogen. To counter this, many pathogens such as influenza virus have evolved sophisticated methods to manipulate the control networks for these internal defense systems and evade destruction. In this project we will develop a detailed molecular understanding of how influenza virus interferes with “autophagy”, a cellular defense system that can engulf and digest pathogens. Our project will create a foundation for the development of a broad range of next-generation therapeutics that block pathogen interference with human defenses and restore the natural ability of infected cells to destroy infecting pathogens. Our work will also provide a framework that can be extended to understand interference with host defenses by intracellular bacterial pathogens, such as Burkholderia, that are pertinent to defense threat reduction.

Systems Out of Equilibrium

Angel E. Garcia
20160588DR

Introduction

Problems dealing with systems out of equilibrium are both ubiquitous and extremely challenging; many have been deemed "Grand Challenge" areas of science. 21st century science will need to address these scientific challenges using many of the hard-earned tools of statistical physics, nonlinear dynamics, applied mathematics, etc. The important feature of systems out of equilibrium is that to remain in a steady state energy is required to balance dissipation. For example, in the absence of sustenance, biological activity cannot be maintained. Similarly, fluid motion will decay in the absence of input energy owing to viscous dissipation, and the space weather generated by solar ejections would not exist in their absence. The balance of forcing and dissipation is at the core of a set of problems spanning biological function, fluid turbulence in geophysical flows and in hydrodynamic instabilities such as Rayleigh-Taylor, magnetohydrodynamics, plasma physics, astrophysical multi-physics phenomena, and nonlinear plastic deformation associated with glassy and granular materials and with geological matter associated with earthquake phenomena. We use broad scientific capability to address problems at the interface of fundamental science and important application areas and aid the development of new capability that underpins many national security programs. Using novel computational approaches coupled with experiment and theory, we will make progress in interpreting and predicting complex nonlinear phenomena far from thermodynamic equilibrium.

Benefit to National Security Missions

Hydrodynamic instability, turbulence and mixing have application in ocean and atmospheric modeling and in characterization of astrophysical explosions and nuclear weapons physics. We will engage a wide spectrum of Laboratory science in bridging laboratory scale experiments and direct numerical simulations (DNS) with astrophysical scale behavior where turbulence is often not included in a systematic manner. To achieve a self-consistent description will require so-called large eddy simulations that parameterize small-scale turbulent fluctuations. This process will help illuminate turbulent mixing processes of interest in NW programs going beyond the traditional Reynolds-averaging approach. With respect to plasma physics and magnetohydrodynamics, our work will impact infrastructure resilience (Applied Energy Programs) and satellite robustness with connections to Global Security and Threat Reduction programs. Finally, dynamics of materials have wide ranging importance and impact from MaRIE to NW materials applications. Additionally, earthquake dynamics involves potential societal impact in characterizing earthquake precursors.

Progress

One of the goals of this project is to utilize new computational algorithms to allow efficient computation of flow through fracture networks and use applied math approaches to develop quantitative models of flow in porous media. DFNWORKS is a parallelized computational suite to generate three-dimensional discrete fracture networks (DFN) and simulate flow and transport. Developed at Los Alamos National Laboratory, this code has been used to study flow and transport in fractured media at scales ranging from millimeters to kilometers. The networks are created and meshed using DFNGEN, which combines FRAM (the feature rejection algorithm for meshing) methodology to stochastically generate three-dimensional DENs with the LAGRIT meshing toolbox to create a high-quality computational mesh representation. The representation produces a conforming Delaunay triangulation suitable for high performance computing finite volume solvers in an intrinsically parallel fashion. Flow through the network is simulated in DFNFLOW, which utilizes the massively parallel subsurface flow and reactive transport finite volume code PFLOTRAN. A Lagrangian approach to simulating transport through the DFN is adopted within DFNTRANS to

determine pathlines and solute transport through the DFN. Example applications of this suite in the areas of nuclear waste repository science, hydraulic fracturing and CO2 sequestration are also included.

We have also studied the effect of advective flow in fractures and matrix diffusion on natural gas production. Although hydraulic fracturing has been used for natural gas production for the past couple of decades, there are significant uncertainties about the underlying mechanisms behind the production curves that are seen in the field. A discrete fracture network-based reservoir-scale work flow was used by us to identify the relative effect of flow of gas in fractures and matrix diffusion on the production curve. With realistic three-dimensional representations of fracture network geometry and aperture variability, simulated production decline curves qualitatively resemble observed production decline curves. The high initial peak of the production curve is controlled by advective fracture flow of free gas within the network and is sensitive to the fracture aperture variability. Matrix diffusion does not significantly affect the production decline curve in the first few years, but contributes to production after approximately 10 years. These results suggest that the initial flushing of gas-filled background fractures combined with highly heterogeneous flow paths to the production well are sufficient to explain observed initial production decline. These results also suggest that matrix diffusion may support reduced production over longer time frames.

We studied the implications of acoustic vibrations on triggering and slow slip in sheared fault gouge. Friction and deformation in granular fault gouge are among various dynamic interactions associated with seismic phenomena that have important implications for slip mechanisms on earthquake faults. To this end, in a recent article in the Journal of Geophysical Research, we proposed a mechanistic model of granular fault gouge subject to acoustic vibrations and shear deformation. The grain-scale dynamics is described by the Shear-Transformation-Zone theory of granular flow, which accounts for irreversible plastic deformation in terms of flow defects whose density is governed by an effective temperature. Our model accounts for stick-slip instabilities observed at seismic slip rates. In addition, as the vibration intensity increases, we observed an increase in the temporal advancement of large slip events, followed by a plateau and gradual decrease. Furthermore, slip becomes progressively slower upon increasing the vibration intensity. The results shed important light on the physical mechanisms of earthquake triggering and slow slip and provide essential elements for the multiscale modeling of earthquake ruptures. In particular, the results suggest that slow slip may be triggered by tremors.

Future Work

Our goals for FY17 include:

- Utilize new computational algorithms to allow efficient computation of flow through fracture networks and use applied math approaches to develop quantitative models of flow in porous media.
- Develop mathematical foundations for local hyperdynamics algorithms that significantly speed up molecular dynamics computations.
- Investigate the detailed mechanisms for granular rearrangements within the STZ theoretical framework in order to understand bulk plasticity, as well as pre-seismic slip during the occurrence of stick-slip instabilities and creep-like effects observed in laboratory experiments.
- Develop new theoretical characterization of glassy disordered systems, attempting to synthesize a dislocation dynamics approach with novel concepts including shear zone transformation theory.
- Continue studies of the implications of acoustic vibrations on triggering and slow slip in sheared fault gouge. Friction and deformation in granular fault gouge are among various dynamic interactions associated with seismic phenomena that have important implications for slip mechanisms on earthquake faults.
- Use machine learning approaches to analyze seismic time series to predict earthquakes.

Conclusion

At the most fundamental level, we will investigate experimentally and numerically a range of fluid instabilities including low-Reynolds number porous media flows, thermal convection, and stably-stratified shear flows. Hydrodynamic instability, turbulence, and mixing have application in ocean and atmospheric modeling and the characterization of astrophysical explosions and nuclear weapons physics.

Publications

Akçay, C., W. Daughton, V. S. Lukin, and Y. Liu. A two-fluid study of oblique tearing modes in a force-free current sheet. 2016. Physics of Plasmas (1994-present). 23 (1): 012112.

Ben-Naim, E., and A. Scheel. Pattern selection and superpatterns in the bounded confidence model. 2015. EPL (Europhysics Letters). 112 (1): 18002.

Bisset, R. N., W. Wang, C. Ticknor, R. Carretero-González, D. J. Frantzeskakis, L. A. Collins, and P. G. Kevrekidis. Robust vortex lines, vortex rings, and hopfions in three-dimensional Bose-Einstein condensates. 2015. Physical Review A. 92 (6): 063611.

Christov, I. C.. Comment on “The velocity field due to an

oscillating plate in an Oldroyd-B fluid" by C.C. Hopkins and J.R. de Bruyn [Can. J. Phys. 92, 533 (2014)]. 2015. Canadian Journal of Physics. 93 (12): 1651.

Cuevas-Maraver, J., P. G. Kevrekidis, A. Saxena, F. Cooper, A. Khare, A. Comech, and C. M. Bender. Solitary Waves of a -Symmetric Nonlinear Dirac Equation. 2016. IEEE Journal of Selected Topics in Quantum Electronics. 22 (5): 1.

Cuevas–Maraver, J., P. G. Kevrekidis, A. Saxena, A. Comech, and R. Lan. Stability of Solitary Waves and Vortices in a 2D Nonlinear Dirac Model. 2016. Physical Review Letters. 116 (21): 214101.

D'Ambroise, J., M. Salerno, P. G. Kevrekidis, and F. K. Abdullaev. Multidimensional discrete compactons in nonlinear Schr\"odinger lattices with strong nonlinearity management. 2015. Physical Review A. 92 (5): 053621.

Dewar, W. K., J. Schoonover, T. McDougall, and R. Klein. Semicompressible Ocean Thermodynamics and Boussinesq Energy Conservation. 2016. Fluids. 1 (2): 9.

Ecke, R. E.. Chaos, patterns, coherent structures, and turbulence: Reflections on nonlinear science. 2015. Chaos: An Interdisciplinary Journal of Nonlinear Science. 25 (9): 097605.

Ecke, R. E.. Scaling of heat transport near onset in rapidly rotating convection. 2015. Physics Letters A. 379 (37): 2221.

Ecke, R. E.. Chaos, patterns, coherent structures, and turbulence: Reflections on nonlinear science. 2015. Chaos: An Interdisciplinary Journal of Nonlinear Science. 25 (9): 097605.

Ecke, R. E.. Scaling of heat transport near onset in rapidly rotating convection. 2015. Physics Letters A. 379 (37): 2221.

Geller, D. A., R. E. Ecke, K. A. Dahmen, and S. Backhaus. Stick-slip behavior in a continuum-granular experiment. 2015. Physical Review E. 92 (6): 060201.

Geller, D. A., R. E. Ecke, K. A. Dahmen, and S. Backhaus. Stick-slip behavior in a continuum-granular experiment. 2015. Physical Review E. 92 (6): 060201.

Gertjerenken, B., and P. G. Kevrekidis. Effects of interactions on the generalized Hong–Ou–Mandel effect. 2015. Physics Letters A. 379 (30–31): 1737.

Gertjerenken, B., and P. G. Kevrekidis. Effects of interactions on the generalized Hong–Ou–Mandel effect. 2015. Physics Letters A. 379 (30–31): 1737.

Gilbert, I., G. Chern, B. Fore, Y. Lao, S. Zhang, C. Nisoli, and P. Schiffer. Direct visualization of memory effects in artificial spin ice. 2015. Physical Review B. 92 (10): 104417.

Gilbert, I., G. Chern, B. Fore, Y. Lao, S. Zhang, C. Nisoli, and P. Schiffer. Direct visualization of memory effects in artificial spin ice. 2015. Physical Review B. 92 (10): 104417.

Hyman, J. D., A. Guadagnini, and C. L. Winter. Statistical scaling of geometric characteristics in stochastically generated pore microstructures. 2015. Computational Geosciences. 19 (4): 845.

Hyman, J. D., A. Guadagnini, and C. L. Winter. Statistical scaling of geometric characteristics in stochastically generated pore microstructures. 2015. Computational Geosciences. 19 (4): 845.

Hyman, J. D., S. Karra, N. Makedonska, C. W. Gable, S. L. Painter, and H. S. Viswanathan. dfnWorks: A discrete fracture network framework for modeling subsurface flow and transport. 2015. Computers & Geosciences. 84: 10.

Hyman, J. D., S. L. Painter, H. Viswanathan, N. Makedonska, and S. Karra. Influence of injection mode on transport properties in kilometer-scale three-dimensional discrete fracture networks. 2015. Water Resources Research. 51 (9): 7289.

Hyman, J. D., S. L. Painter, H. Viswanathan, N. Makedonska, and S. Karra. Influence of injection mode on transport properties in kilometer-scale three-dimensional discrete fracture networks. 2015. Water Resources Research. 51 (9): 7289.

Kevrekidis, P. G., J. Cuevas–Maraver, A. Saxena, F. Cooper, and A. Khare. Interplay between parity-time symmetry, supersymmetry, and nonlinearity: An analytically tractable case example. 2015. Physical Review E. 92 (4): 042901.

Khare, A., and A. Saxena. Response to "Comment on 'Superposition of elliptic functions as solutions for a large number of nonlinear equations'" [J. Math. Phys. 56, 084101 (2015)]. 2015. Journal of Mathematical Physics. 56 (11): 113510.

Kim, E., R. Chaunsali, H. Xu, J. Jaworski, J. Yang, P. G. Kevrekidis, and A. F. Vakakis. Nonlinear low-to-high-frequency energy cascades in diatomic granular crystals. 2015. Physical Review E. 92 (6): 062201.

Lieou, C. K., A. E. Elbanna, and J. M. Carlson. Dynamic friction in sheared fault gouge: Implications of acoustic vibration on triggering and slow slip. 2016. Journal of Geophysical Research: Solid Earth. 121 (3): 2015jb012741.

Mertens, F. G., F. Cooper, N. R. Quintero, S. Shao, A. Khare, and A. Saxena. Solitary waves in the nonlinear Dirac equation in the presence of external driving forces. 2016. Journal of Physics A: Mathematical and Theoretical. 49 (6): 065402.

Palmero, F., J. Han, L. Q. English, T. J. Alexander, and P. G. Kevrekidis. Multifrequency and edge breathers in the discrete sine-Gordon system via subharmonic driving: Theory, computation and experiment. 2016. Physics Letters A. 380 (3): 402.

Pozharskiy, D., Y. Zhang, M. O. Williams, D. M. McFarland, P. G. Kevrekidis, A. F. Vakakis, and I. G. Kevrekidis. Nonlinear resonances and antiresonances of a forced sonic vacuum. 2015. Physical Review E. 92 (6): 063203.

Regev, I., J. Weber, C. Reichhardt, K. A. Dahmen, and T. Lookman. Reversibility and criticality in amorphous solids. 2015. Nature Communications. 6: 8805.

Reichhardt, C., D. Ray, and C. J. Reichhardt. Magnus-induced ratchet effects for skyrmions interacting with asymmetric substrates. 2015. New Journal of Physics. 17 (7): 073034.

Wang, W., P. G. Kevrekidis, R. Carretero-González, D. J. Frantzeskakis, T. J. Kaper, and M. Ma. Stabilization of ring dark solitons in Bose-Einstein condensates. 2015. Physical Review A. 92 (3): 033611.

Discovery Science of Hydraulic Fracturing: Innovative Working Fluids and Their Interactions with Rocks, Fractures, and High Value Hydro-carbons

Hari S. Viswanathan
20140002DR

Abstract

Shale gas is an unconventional fossil energy resource that is already having a profound impact on US energy independence and is projected to last for at least 100 years. Production of methane and other hydrocarbons from low permeability shale involves hydrofracturing of rock, establishing fracture connectivity, and multiphase fluid-flow and reaction processes all of which are poorly understood. The result is inefficient extraction with many environmental concerns. This project used innovative high-pressure microfluidic and triaxial core flood experiments on shale to replicate reservoir conditions to explore fracture-permeability relations and the extraction of hydrocarbon. These data are integrated with simulations including lattice Boltzmann modeling of pore-scale processes, finite-element/discrete element models of fracture development in the near-well environment, and discrete-fracture network modeling of the reservoir. The ultimate goal is to make the necessary measurements to develop models that can be used to determine the reservoir operating conditions necessary to gain a degree of control over fracture generation and fluid flow a key topic of interest in DOE's new SubTER program. Our results include the development of a model explaining key physical processes governing hydrocarbon production during hydraulic fracturing, the elucidation of fracture-permeability relations through a combination of novel experiments combining rock fracturing and x-ray tomography with finite/discrete element mechanical models, the demonstration of the effectiveness of supercritical CO2 as an alternative hydraulic fracturing fluid, and the characterization of pore-scale fluid migration by numerical simulations.

Background and Research Objectives

Shale gas is an unconventional fossil energy resource that is already having a profound impact on US energy sector, with reserves projected to last for nearly 100 years [1]. The increased availability of shale gas (i.e., methane), which produces 50% less CO2 than coal, is primarily responsible for US emissions in 2011 dropping to their lowest levels in 20 years [2]. Production of methane and other hydrocarbons from low permeability shale involves hydrofracturing of rock, establishing fracture connectivity, and multiphase fluid-flow and reaction processes, all of which are poorly understood. The result is inefficient extraction with many environmental concerns [3,4]. Industry is motivated to reduce the 70 to 140 billion gallon per year water demand because there are droughts in the west, a lack of deep injection disposal wells in the east, and possible forthcoming regulations [3]. Our goal is to use unique Los Alamos National Laboratory (LANL) microfluidic and triaxial core flood experiments integrated with state-of-the-art numerical simulation to reveal the fundamental dynamics of fracture-fluid interactions to transform fracking from an ad hoc tool to a safe and predictable approach based on solid scientific understanding. One approach is to develop CO2-based fracturing fluids and fracturing techniques to enhance production, reduce waste water, while simultaneously sequestering CO2 [4].

Determining the key controlling mechanisms in subsurface thermo-hydro-mechanical-chemical (THMC) systems has been impeded due to lack of sophisticated experiments that make direct observations at the (in situ) high temperatures (T), pressures (P), and stresses present in the subsurface. For example, fracture apertures, a key input to models, may be orders of magnitude smaller in situ than when examined ex situ, without stress. We have been developing experiments and models that can characterize coupled fracture generation, multiphase fluid flow, and chemical processes under in situ conditions.

Here, we describe the key aspects of our LDRD DR project 1) the integration of field data from shale gas reservoirs with a high performance computational suite for generating discrete fracture network models and simulating flow and transport therein; 2) a tomographic

triaxial coreflood system with measurements of fracture-induced permeability change under in situ conditions; 3) a microfluidic apparatus that operates at high-pressure conditions where we are conducting sweep efficiency studies with water and CO2 working fluids in shale; 4) experiment-benchmarked meso-, core-, and reservoir-scale models that incorporate fracture mechanics, fracture-permeability relations, and multiphase flow in order to fill in knowledge gaps of previous work lacking in situ measurements of key parameters and important processes. Our ultimate goal is to make critical measurements and develop models that can be used to determine the reservoir operating conditions necessary to gain control [5] over fracture generation, fluid flow, and interfacial processes over a range of geologic environments. Here we present an overview of the experiment and modeling capabilities at different scales and how these scales are linked. This summary is as an overview, and we reference our published manuscripts for additional detail.

Scientific Approach and Accomplishments

Reservoir Scale

Unconventional gas resources such as tight sandstone and shale have very low permeability (microdarcy-nanodarcy). Permeability in these formations is enhanced by hydraulically generating fractures from horizontal wells that are placed to stimulate the reservoir and capture the generated gas. Due to poor understanding of the basic gas recovery and transport mechanisms, gas recovery rates are still very low (for example, for shale gas the recovery rates are only 10–15% of what is known to be present) [3]. Additionally, the production rates rapidly decline after the first couple of years – approximately 50-60% of the gas is produced during this time [3]. Natural gas sustainability depends on improving the production curve decline. Developing new technologies for optimizing and enhancing the gas production requires a detailed analysis of the fundamental mechanics behind gas transport.

Although gas production analysis is frequently done in the industry, the methods used are either highly empirical or are based on simplified analytical models that depend on gross idealizations of the reservoir [6]. In this work, we develop a numerical modeling methodology for simulating gas transport and calibrating against field production curves that are built on more realistic conditions using well-characterized fracture datasets and incorporate all the major gas transport physics. Specifically, we enhanced the new computational workflow dfnWorks that is built on a suite of high-performance computing (HPC) modules and visualization tools developed at LANL and other national laboratories. The general workflow involves generating and meshing discrete fracture networks (DFN) using field data from geological surveys [7], solving for flow using the massively parallel subsurface simulator PFLOTRAN, and evaluating gas flow pathways and gas particle travel times using a unique particle tracking method that we developed for DFN [8].

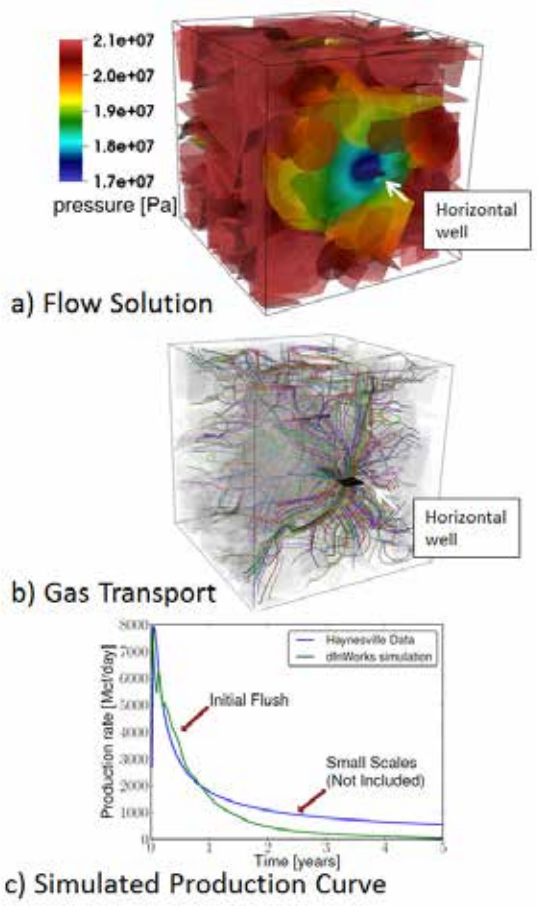

Figure 1. Reservoir scale simulation of hydraulic fracturing production.

Figure 1a and 1b shows a 100 m x 100 m x 100 m DFN based on the Pottsville Shale gas formation in Alabama. The DFN is generated using fracture properties from the site such as spacing, orientation, and aperture. A horizontal well along with hydraulically generated fractures is included at the center of the domain to simulate stimulation and production of the reservoir. We used operational values for pressure, aperture and porosity so the simulation is as realistic as possible. Figure 1a shows the flow solution with pressure being lowest at the horizontal well to create drawdown towards the well. Figure 1b shows a selection of particle trajectories to visualize transport pathways from the fracture network into the well. Details are published in Karra et al. (2015) [9].

Figure 1c compares production curves from site data (blue) to the one generated by the simulation (green). Interestingly, the first part of the production curve (initial flush)

is well matched by the simulation showing that the large hydraulic and natural fractures represented by the DFN control early production. At later production times, the simulation under-predicts the field data indicating that smaller-scale processes are contributing to production.

These results are consistent with discussions we have had with industry experts who believe early production is the result of draining large fractures whereas late time production is poorly understood because the small-scale physical mechanisms are not included in the above model [10]. Late-time production is critical to characterize, because wells often produce for decades and a slight increase in projection at late time can be a game changer for the industry. Our hypothesis is that late time production is a complex combination of mass transport from the damage zone between small fractures and the shale matrix, matrix diffusion, desorption and multiphase flow blocking. Our work at the core and pore scales addresses these mechanisms so that once characterized they can be incorporated into the reservoir-scale simulator.

Core Scale

One key limitation to improved efficiency of hydraulic fracturing is lack of knowledge of fundamental fracture network properties in shale. Core-scale (10 μm to 10 cm) fracture network processes are critical in characterizing the mass transfer of gas from the intact rock matrix to small fractures of the damage zone that connect to the large fractures represented by the DFN described in the previous section.

Our approach uses triaxial coreflood instruments to generate and characterize fracture formation and permeability at in situ temperature, pressure and stress conditions. We couple these in situ tomographic observations of rock fracturing with a finite element discrete element model (FDEM) [11,12] to characterize and predict fracture and hydrocarbon extraction in response to differing fluids, rock properties, and injection/pressurization schemes. The FDEM model we have developed can simulate fractures in the presence of fluid or when fluids propagate the fractures. Figure 2 compares a representative triaxial coreflood experiment with the FDEM model for a direct shear fracture experiment that uses a Utica shale sample provided by Chesapeake Energy. The FDEM model uses generic rock material properties for Utica shale rather than properties from this specific experimental sample, with the goal being to determine if qualitative agreement between model and experiment was possible without detailed shale characterization.

The experiment and model show good qualitative agreement. Both results show that the fracture network is dominated by a vertical fracture and two fracture arcs on either side of the central vertical fracture. We observed that the arcing fracture system is more strongly developed in the experiments than in the simulations. Interestingly, if fluid is not present in the fracture or if the layers of the shale are not considered, the model does not show good qualitative agreement to the experiment indicating that interface and fluid flow are key processes to consider in predicting fracture extent in shale. Details of this experiment and simulation can be found in Carey et al. (2015) [5].

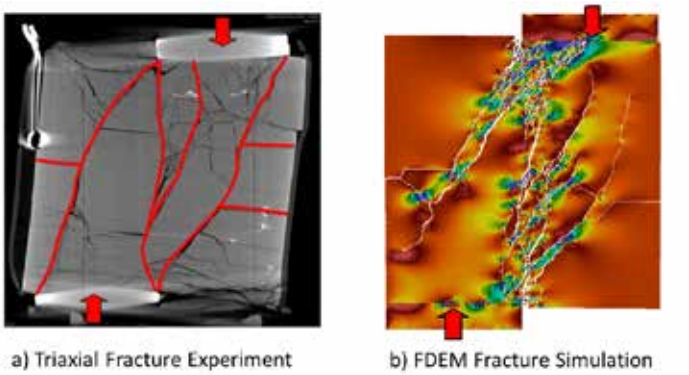

Figure 2. Comparison of fracture propagation experiment to simulation for shear fracture in shale.

Pore Scale

At the pore scale, we are characterizing the mechanisms governing the extraction of hydrocarbon from fracture networks using both aqueous and CO2-based working fluids in microfluidic experiments and lattice Boltzmann method (LBM) simulations. We are studying flow and multiphase fluid displacement in static mesoscale fracture networks either in simple geometries as shown in Figure 3 or complex fracture networks extracted from tomography collected following triaxial experiments as shown in Figure 2.

In order to be effective, fracking must create fracture networks at the mesoscale that drain the matrix of hydrocarbons [13]. Once in the fractures, the hydrocarbons must migrate through the network to the producing well. At the pore-scale, surface tension dominates fluid transport dynamics for the hydrocarbon-brine system and we hypothesize that undesired flow blocking prevents effective extraction to the small scale fracture network and thus to the well. We have identified several key phenomena to investigate in microfluidics experiments and LBM simulations: a) use of a working fluid that is miscible with hydrocarbon (e.g., supercritical CO2) will facilitate hydrocarbon migration in contrast to immiscible water that blocks flow of hydrocarbon at pinch-points within the fracture; b) wettability between shale and working fluid in combination with viscosity governs the penetration of the working fluid into complex branching fracture networks; c) dead-end

pores will trap hydrocarbon in aqueous systems but supercritical CO2 will dissolve into and liberate trapped hydrocarbon; and d) some components of natural gas, a complex multicomponent hydrocarbon, can condense as liquid due to pressure gradients at material interfaces causing flow blockage.

LBM is ideally suited to simulate these processes since it captures intra-pore geometries, complex flows, and all relevant physicochemical processes with high computational efficiency. Our models represent mesoscale simulations by considering multiphase flow, multi-component chemistry, and phase transitions. Figure 3 shows a microfluidic experiment in which a simple fishbone fracture pattern has been etched into Utica shale. A LBM of the experiment captures the fingering as the invading immiscible water displaces hydrocarbon, but bypasses the hydrocarbon in dead end fractures resulting in poor sweep (Figure 3b). At first glance, this example may appear simplistic. However, the finger width is controlled by flow rate and fluid viscosity ratios. Also, network geometry affects the finger width since fluid from the side channel narrows the finger. More details can be found in Middleton et al. (2015) [14].

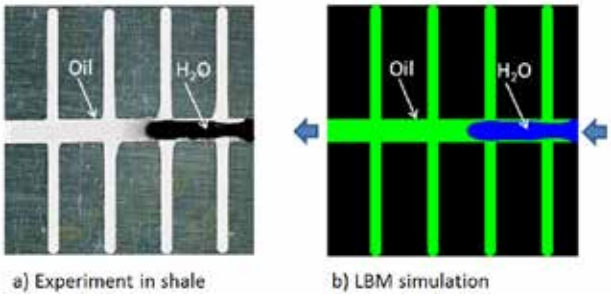

Figure 3. Comparison of microfluidic sweep efficiency experiment in shale and Lattice Boltzmann simulation.

Summary

The goal of this work is to integrate multiscale experimental measurements and computational modeling of coupled thermo-hydro-mechanical-chemical systems to understand and eventually control fracture formation and fluid flow during hydraulic fracturing. We anticipated that our results will provide key insights into processes that can lead to more efficient hydrocarbon extraction leading to the use of fewer wells and more complete use of the shale gas resource. Research on the growth and penetration of the fracture network also improves understanding of factors that allow the fracture network to be reliably contained within the shale layer and improve confidence in the protection of groundwater resources during shale gas production.

This project has so far produced 45 peer-reviewed publications and these serve as detailed results from the work discussed in this overview report. As part of this project the PI Viswanathan coedited an issue of Philosophical Transactions of the Royal Society on the Energy and the Subsurface [15]. The issue covers topics at the forefront of scientific research on energy and the subsurface ranging from carbon dioxide (CO2) sequestration to the recovery of unconventional shale oil and gas resources through hydraulic fracturing. Contributors to the issue were selected from attendees of the CNLS/CSES-sponsored Geological Fluid Mechanics Conference held in Santa Fe in September, 2015, which was co-organized by the LDRD team. Additional contributions to the issue include National Academy of Science members Zdeněk Bažant and Howard Stone, National Academy of Engineering member Mark Zoback, former CNLS director Robert Ecke, as well as several editors from leading technical journals and leading Oil and Gas industry R&D scientists.

The LANL contribution to this issue by Hyman et al. (2016) [16] serves as a technical overview of this project and weaves together the publications produced in the project into a coherent story. It provides more detail than is possible in this high-level overview.

Impact on National Missions

Predicting fluid flow through fractured systems is critical for LANL energy and global security missions. The project has been very successful in transitioning to applied (DOE-FE), basic science (OBES) and nuclear nonproliferation programs. In addition a new LDRD DR on advancing brittle fractures in areas of interest to PADGS and PADWP starts FY17 that uses the HOSS (current RD 100 finalist)and dfnWorks (DOE technology fund winner) software packages developed under this DR. Finally, an Energy Frontier Research Center on fluid and fracture flow is expected in FY17 and the capabilities developed under this DR will be part of EFRC proposals if a proposal call occurs.

References

Kargbo, D. M., R. G. Wilhelm, and D. J. Campbell. Natural gas plays in the Marcellus Shale: Challenges and potential opportunities. 2010. Environmental Science and Technology. 44: 5679.

Begos, K.. In a surprising turnaround, the amount of carbon dioxide being released into the atmosphere in the U.S. has fallen dramatically, to its lowest level in 20 years, and government officials say the biggest reason is that cheap and plentiful natural gas. 2012. Associated Press.

Moniz, E. J., H. D. Jacoby, and A. J. Meggs. MIT Study on the Future of Natural Gas. 2012. MIT.

Soeder, D. J., and W. M. Kappel. Water Resources and Nat-

ural Gas Production from the Marcellus Shale. 2009. U.S. Geological Survey Fact Sheet 2009-3032.

Carey, J. W., Z. Lei, E. Rougier, H. Mori, and H. S. Viswanathan. Fracture-permeability behavior of shale. 2015. Journal of Unconventional Oil and Gas Resources. : 27.

Patzek, T. M., F. Male, and M. Marder. Gas production in the Barnett Shale obeys a simple scaling theory. 2013. Proceedings of the National Academy of Sciences. 110 (49): 19731.

Hyman, J. D., S. Karra, N. Makedonska, C. W. Gable, S. L. Painter, and H. S. Viswanathan. dfnWorks: A discrete fracture network framework for modeling subsurface flow and transport. 2015. Computers and Geosciences. 84: 10.

Makedonska, N., S. L. Painter, Q. M. Bui, C. W. Gable, and S. Karra. Particle tracking approach for transport in three-dimensional discrete fracture networks. 2015. Computational Geoscience. : 1.

Karra, S., N. Makedonska, H. S. Viswanathan, S. Painter, and J. Hyman. Effect of advective flow in fractures and matrix diffusion on natural gas production. 2015. Water Resources Research. : 1.

Viswanathan, H., J. D. Hyman, S. Karra, J. W. Carey, M. L. Porter, E. Rougier, R. P. Currier, Q. Kang, L. Zhou, J. Jimenenz, N. Makedonska, L. Chen, and R. S. Middleton. Using discovery science to increase the efficiency of hydraulic fracturing while reducing water usage. 2015. In Hydraulic Fracturing: Environmental Issues, ACS Symposium Series 1216.. Edited by Drogos, D.. Vol. 1216p. 71. Laramie, Wyoming: Oxford University Press.

Lei, Z., E. Rougier, E. E. Knight, and A. Munjiza. A framework for grand scale parallelization of the combined finite discrete element method in 2D. 2014. Computational Particle Mechanics. : 307.

Zubelewicz, A., E. Rougier, M. Ostoja-Starewski, E. E. Knight, C. Bradley, and H. S. Viswanathan. A mechanisms-based model for dynamic behavior and fracture of geomaterials. 2014. International Journal of Rock Mechanics and Mining Sciences. : 277.

Bazant, Z., M. Salviato, V. T. Chau, H. S. Viswanathan, and A. Zubelewicz. Why fracking works. 2014. Journal of Applied Mechanics. 81 (10): 101010.

Middleton, R. S., J. W. Carey, R. Currier, J. D. Hyman, Q. Kang, J. Jimenez-Martinez, M. L. Porter, and H. S. Viswanathan. Shale gas and non-aqueous fracturing fluids: opportunities and challenges for supercritical CO2. 2015. Applied Energy. : 500.

Christov, I. C., and H. S. Viswanathan. Introduction: energy and subsurface. 2016. Philosophical Transactions of the Royal Society A Theme Issue on Energy and Subsurface edited by Christov and Viswanathan. : 1.

Hyman, J. D., J. Jimenez-Martinez, H. S. Viswanathan, J. W. Carey, M. L. Porter, E. Rougier, S. Karra, Q. Kang, L. Frash, L. Chen, Z. Lei, D. O'Malley, and N. Makedonska. Understanding hydraulic fracturing: a multi-scale problem. 2016. Philosophical Transactions of the Royal Society A. : 1.

Publications

Aldrich, G., J. D. Hyman, S. Karra, C. W. Gable, N. Makedonska, H. S. Viswanathan, J. Woodring, and B. Hamann. Analysis and visualization of discrete fracture networks using a flow topology graph. 2016. IEEE T Vis Comput Gr.. 22: 1.

Bazant, Z., M. Salviato, V. T. Chau, H. S. Viswanathan, and A. Zubelewicz. Why fracking works. 2014. Journal of Applied Mechanics. 81 (10): 101010.

Birdsell, D., H. Rajaram, D. Dempsey, and H. Viswanathan. Hydraulic fracturing fluid migration in the subsurface: A review and modeling results. 2015. Water Resources Research. : 1.

Carey, J. W., H. Mori, D. Brown, and R. Pawar. Geomechanical behavior of caprock and cement: Plasticity in hydrodynamic seals. 2014. Energy Procedia. : 5671.

Carey, J. W., Z. Lei, E. Rougier, H. Mori, and H. S. Viswanathan. Fracture-permeability behavior of shale. 2015. Journal of Unconventional Oil and Gas Resources. : 27.

Chen, L., J. D. Hyman, L. Zhou, T. Min, Q. Kang, E. Rougier, and H. Viswanathan. Effect of fracture density on effective permeability of matrix-fracture system in shale formations. To appear in AGU Books. By Carey, J. W..

Chen, L., L. Zhang, Q. Kang, H. Viswanathan, J. Yao, and W. Tao. Nanoscale simulation of shale transport properties using the lattice Boltzmann method: permeability and diffusivity. 2015. Scientific Reports. : 1.

Chen, L., Q. Kang, B. Carey, and W. Tao. Pore-scale study of diffusion–reaction processes involving dissolution and precipitation using the lattice Boltzmann method. 2014. International Journal of Heat and Mass Transfer. 75: 483.

Chen, L., Q. Kang, H. Deng, J. W. Carey, and W. Tao. Mesoscopic study of the formation of pseudomorphs with presence of chemical fluids. 2014. Geosciences Journal. : 1.

Chen, L., Q. Kang, H. S. Viswanathan, and W. Tao. Pore-scale study of dissolution-induced changes in hydrologic properties of rocks with binary minerals. 2014.

Water Resources Research. (50): 1.

Chen, L., Q. Kang, Y. Mu, Y. He, and W. Tao. A critical review of the pseudopotential multiphase lattice Boltzmann model: Methods and applications. 2014. International Journal of Heat and Mass Transfer. 76: 210.

Chen, L., Q. Kang, Z. Dai, H. S. Viswanathan, and W. Tao. Permeability prediction of shale matrix reconstructed using the elementary building block model. 2015. Fuel. : 346.

Chen, L., W. Fang, Q. Kang, J. Hyman, H. S. Viswanathan, and W. Tao. A generalized lattice Boltzmann model for flow through tight porous media with Klinkenberg's effect. 2015. Physical Review E. : 1.

Chen, Y., Q. Kang, Q. Cai, M. Wang, and D. Zhang. Lattice Boltzmann Simulation of Particle Motion in Binary Immiscible Fluids. 2015. Communications in Computational Physics. : 757.

Christov, I. C., and H. S. Viswanathan. Introduction: energy and subsurface. 2016. Philosophical Transactions of the Royal Society A Theme Issue on Energy and Subsurface edited by Christov and Viswanathan. : 1.

Frash, L. P., J. W. Carey, T. Ickes, and H. S. Viswanathan. High-stress triaxial direct-shear fracturing of Utica shale and in situ X-ray microtomography with permeability measurement. 2016. Journal of Geophysical Research: Solid Earth. : 1.

Hyman, J. D., A. Guadagnini, and C. L. Winter. Statistical Scaling of Geometric Characteristics in Stochastically Generated Pore Microstructures. 2015. Computational Geosciences. : 1.

Hyman, J. D., G. Aldrich, H. S. Viswanathan, N. Makedonska, and S. Karra. Fracture Size and Transmissivity Correlations: Implications for Transport Simulations in Discrete Fracture Networks. 2016. Water Resources Research. : 1.

Hyman, J. D., J. Jimenez-Martinez, H. S. Viswanathan, J. W. Carey, M. L. Porter, E. Rougier, S. Karra, Q. Kang, L. Frash, L. Chen, Z. Lei, D. O'Malley, and N. Makedonska. Understanding hydraulic fracturing: a multi-scale problem. 2016. Philosophical Transactions of the Royal Society A. : 1.

Hyman, J. D., S. Karra, N. Makedonska, C. W. Gable, S. L. Painter, and H. S. Viswanathan. dfnWorks: A discrete fracture network framework for modeling subsurface flow and transport. 2015. Computers and Geosciences. 84: 10.

Hyman, J. D., S. L. Painter, H. S. Viswanathan, N. Makedonska, and S. Karra. Influence of Injection Mode in Kilometer Scale Three Dimensional Discrete Fracture Networks. 2015. Water Resources Research. : 1.

Jackson, R. B., A. Vengosh, J. W. Carey, R. Davies, F. O'Sullivan, and G. Petron. The environmental costs and benefits of fracking. 2014. Annual Review of Environment and Resources. : 1.

Jimenez-Martinez, J., M. L. Porter, J. D. Hyman, J. W. Carey, and H. S. Viswanathan. Mixing in a three-phase system: Enhanced production of oil-wet reservoirs by CO2 injection. 2016. Geophysical Research Letters.. : 1.

Kang, Q., L. Chen, A. J. Valocchi, and H. S. Viswanathan. Pore-scale study of dissolution-induced changes in permeability and porosity of porous media. 2014. Journal of Hydrology. 517: 1049.

Karra, S., N. Makedonska, H. S. Viswanathan, S. Painter, and J. Hyman. Effect of advective flow in fractures and matrix diffusion on natural gas production. 2015. Water Resources Research. : 1.

Kelkar, S., K. Lewis, S. Karra, G. Zyvoloski, S. Rapaka, H. S. Viswanathan, P. K. Mishra, S. Chu, D. Coblentz, and R. Pawar. A simulator for modeling coupled thermo-hydro-mechanical processes in subsurface geological media. 2014. International Journal of Rock Mechanics and Mining Sciences. : 569.

Lei, Z., E. Rougier, E. E. Knight, and A. Munjiza. A framework for grand scale parallelization of the combined finite discrete element method in 2D. 2014. Computational Particle Mechanics. : 307.

Lei, Z., E. Rougier, E. Knight, A. Munjiza, and H. Viswanathan. A generalized anisotropic deformation formulation for geomaterials. 2016. Computational Particle Mechanics. : 215.

Lei, Z., E. Rougier, E. Knight, L. Frash, J. W. Carey, and H. Viswanathan. A non-locking composite tetrahedron element for the combined finite discrete element method. 2016. Engineering Computations.. 33: 1.

Liu, H., A. J. Valocchi, C. Werth, Q. Kang, and M. Oostrom. Pore-scale simulation of liquid CO< sub> 2</sub> displacement of water using a two-phase lattice Boltzmann model. 2014. Advances in Water Resources. 73: 144.

Liu, H., Q. Kang, C. R. Leonardi, B. D. Jones, S. Schmieschek, A. Narváez, J. R. Williams, A. J. Valocchi, and J. Harting. Multiphase lattice Boltzmann simulations for porous media applications--a review. 2015. Computational Geosciences. : 1.

Makedonska, N., J. D. Hyman, S. Karra, S. L. Painter, C. W. Gable, and H. S. Viswanathan. Evaluating the Effect of Internal Aperture Variability on Transport in Kilometer Scale Discrete Fracture Networks. 2016. Advances in

Water Resources. 94: 486.

Makedonska, N., S. L. Painter, Q. M. Bui, C. W. Gable, and S. Karra. Particle tracking approach for transport in three-dimensional discrete fracture networks. 2015. Computational Geoscience. : 1.

Middleton, R. S., J. S. Levine, J. L. Bielicki, H. S. Viswanathan, J. W. Carey, and P. Stauffer. Jumpstarting commercial-scale CO2 capture and storage with ethylene production and enhanced oil recovery in the US Gulf. 2015. Greenhouse Gases: Science and Technology. : 241.

Middleton, R. S., J. W. Carey, R. Currier, J. D. Hyman, Q. Kang, J. Jimenez-Martinez, M. L. Porter, and H. S. Viswanathan. Shale gas and non-aqueous fracturing fluids: opportunities and challenges for supercritical CO2. 2015. Applied Energy. : 500.

Middleton, R., H. Viswanathan, R. Currier, and R. Gupta. CO2 as a fracturing fluid. 2015. Energy Procedia. : 7780.

O'Malley, D., S. Karra, R. P. Currier, N. Makedonska, J. D. Hyman, and H. Viswanathan. Where does water go during hydraulic fracturing?. 2015. Groundwater. : 1.

Oostrom, M., Y. Mehmani, P. Romero-Gomez, Y. Tang, H. Liu, H. Yoon, Q. Kang, V. Joekar-Niasar, M. Balhoff, and T. Dewers. Pore-scale and continuum simulations of solute transport micromodel benchmark experiments. 2014. Computational Geosciences. 4-0: 1.

Padrino, J. C., B. VanderHeyden, X. Ma, and D. Z. Zhang. A separate phase drag model and a surrogate approximation for simulation of the steam assisted gravity grainage process. 2016. SPE. : 1.

Porter, M., J. Jimenez-Martinez, R. Martinez, Q. McCulloch, J. W. Carey, and H. Viswanathan. Geo-material microfluidics at reservoir conditions for subsurface energy resource applications. 2015. Lab on a Chip. : 1.

Summerscales, O. T., B. L. Scott, H. S. Viswanathan, and A. D. Sutton. Synthesis and reactivity of cis-FeH2(dcpe)2 (dcpe = 1,2-bis(dicyclohexylphosphino)ethane). 2016. Inorganic Chemistry Communications. 63: 57.

Viswanathan, H., J. D. Hyman, S. Karra, J. W. Carey, M. L. Porter, E. Rougier, R. P. Currier, Q. Kang, L. Zhou, J. Jimenenz, N. Makedonska, L. Chen, and R. S. Middleton. Using discovery science to increase the efficiency of hydraulic fracturing while reducing water usage. 2015. In Hydraulic Fracturing: Environmental Issues, ACS Symposium Series 1216.. Edited by Drogos, D.. Vol. 1216, p. 71. Laramie, Wyoming: Oxford University Press.

Zhang, L., Q. Kang, J. Yao, Y. Gao, Z. Sun, H. Liu, and A. Valocchi. Pore scale simulation of liquid and gas two-phase flow based on digital core technology. 2015. Science China Technological Sciences. : 1375.

Zhang, L., Q. Kang, L. Chen, and J. Yao. Simulation of flow in multi-scale porous media using the lattice Boltzmann method on quadtree grids. 2016. Communications in Computational Physics.. 19: 998.

Zubelewicz, A., E. Rougier, M. Ostoja-Starewski, E. E. Knight, C. Bradley, and H. S. Viswanathan. A mechanisms-based model for dynamic behavior and fracture of geomaterials. 2014. International Journal of Rock Mechanics and Mining Sciences. : 277.

Combating Antibiotic Resistance: Targeting Efflux Pump Systems at Multiple Scales

Sandrasegaram Gnanakaran
20140121DR

Abstract

Bacteria with multi-drug resistance (MDR) are a threat to public health and security. We increased quantitative understanding of this complex biological problem through experimental measurements and integrated modeling of structural properties, genetic regulation, and cellular effects. MDR efflux pumps of bacteria are complexes of three membrane proteins that pump antibiotics out of bacteria. MDR pumps provide resistance against antibiotics and pose a major barrier to treatment infections. Antibiotics induce bacteria to produce MDR pumps on the bacterial membrane to pump out the antibiotics. Efflux pumps can also bring in quorum signaling molecules that lead to the formation of bacterial biofilms that are impenetrable to antibiotics. Linked processes that determine antibiotic resistance include transport of antibiotics through the MDR pumps, genetic control of the MDR efflux pumps, and cellular effects from movement of bacterial metabolic products through the MDR pumps. In this project we discovered how structural, genetic, and cellular processes contribute to bacterial antibiotic resistance of Burkholderia pseudomallei, a high-priority bio-threat agent. We combined experiment and theory to understand each process, tested and validated our models, and identified key parts of each process that can be manipulated, paving the way for future work to combat drug resistance. Our work yielded a core capability for integrated modeling of complex adaptive molecular transport systems with broad applications in biosecurity, biofuel production, and microbial clearance of toxic materials and created a framework for developing integrated models for other complex biological systems.

Background and Research Objectives

Bacterial multi-drug resistance efflux pumps are complex molecular machines that expel multiple drugs and antibiotics. They also influence important genetic and cellular processes to confer additional drug resistance. Our project developed a multi-scale model that integrates structural, genetic, and cellular processes (depicted in Figure 1) to understand how efflux pumps work. This model will guide future designs of efflux pump inhibitors and therapeutic regimes to block specific steps in the efflux pump cascade and thus rescue the functions of drugs rendered ineffective by bacterial resistance. This project ws motivated the hypothesis that an experiment-based model that integrates structural, genetic, and cellular mechanisms to predict drug uptake and survival could provide a quantitative understanding and ability to predict how efflux pumps and the associated genetic and cellular systems defend bacteria against drugs and antibiotics.

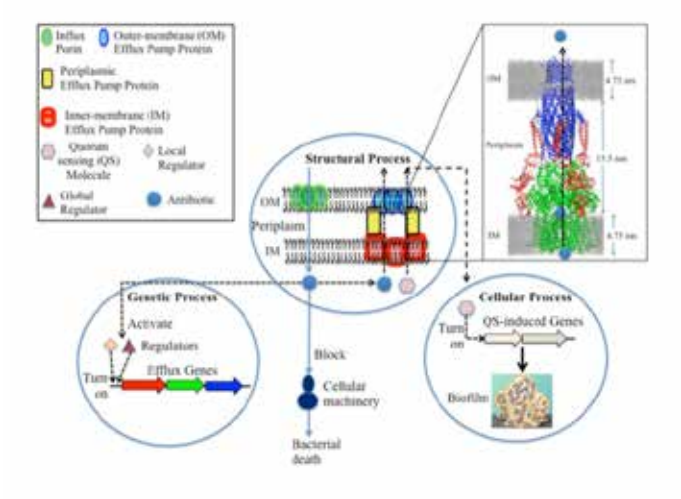

Figure 1. A schematic description of the complex structural, genetic regulatory, and cellular processes and their coupling underlying the overall function of an efflux pump.

Specific Research Goals

Efflux Pumps – A) Determine the three-dimensional structure of the tripartite efflux pump complex with and without drugs bound. B) Perform molecular dynamics (MD) simulations to describe the initial binding of a drug to the pump and its transport across the efflux channel spanning inner-membrane, periplasm, and outer membrane. C) Test predictions of the model by comparing

them with experimentally measured efflux rates of drugs through a pump.

Genetic Regulation – A) Analyze the roles of local and global transcriptional regulators by measuring the expression levels of efflux pump genes and those of their regulators after exposure to drugs. B) Develop a model that includes a gene regulatory component that describes the contributions of local and global regulators to drug- induced effects on expression of efflux/influx genes.

Cellular effects – A) Determine cell growth and mortality rates as a function of antibiotic concentration, which will be the key determinant of cell survival in the integrated model. B) Measure the dependence of these rates on biofilm formation and use this information to predict survival of mixed cultures of free and biofilm cells. C) Measure the release of quorum-sensing molecules through antibiotic induced efflux pumps and identify the quorum-sensing induced genes related to bacterial growth, virulence, and biofilms.

Integrated model- Develop an integrated model incorporating structural, genetic, and cellular processes underpinning the function of an efflux pump system.

Scientific Approach and Accomplishments

The three-dimensional structures the efflux pump components. We have crystallized BpeB, BpeF and OprA proteins of the tripartite efflux pumps BpeAB-OprB, BpeEF-OprC, AmrAB-OprA from the pathogen Burkholderia pseudomallei. The diffraction limits of these crystals are 6.0, 7.0, and 7.5 Å, respectively. We have obtained structural solutions for these crystals using the Molecular Replacement method and have built preliminary low-resolution models for those proteins. In collaboration with Prof. Huilin Li of Stony Brook University (SBU) and Brookhaven National Labs (BNL), we have obtained low temperature electron microscopy images of BpeB at 16 Å resolution. In collaboration with Prof. Satoshi Murakami of Tokyo Institute of Technology, we have determined the crystal structure of BpeB from B. cenocepacia at 3.6 Å resolution (see Figure 2). Structural and biochemical studies of the complete tripartite complexes have been progressing rapidly. We have generated expression vectors of the AmrAB-OprA and BpeEF-OprC complexes and have cloned them into E. coli expression systems. To link structure and function, future work will test the minimum inhibitory concentration (MIC) of antibiotics in E. coli expressing these pumps (from which the native pumps are deleted from the chromosome) including AmrAB-OprA-over-expressed E. Coli KAM3 (AcrB gene deleted) and W3104 (AcrA,B,D gene deleted). Strands with site-directed mutants of AmrAB-OprA were generated to test the effect on antibiotic resistance. We have established external collaborations with Prof. Huilin Li of Stony Brook University and BNL on cryo-EM imaging and analysis. We have collaborated with Prof. Satoshi Murakami of Tokyo Tech on structural studies of BpeB from Burkholderia. We have worked with Surajit Banerjee of Cornell University on APS data collection. We have worked on structural modeling and simulation. With the capabilities of membrane protein crystallography established in our labs in this LDRD project, we have obtained preliminary results needed for an NIH R01 proposal (PI: Kim) entitled "Structure determination of Burkholderia pseudomallei RND multi-drug efflux pumps" submitted in February 2016. We have obtained more preliminary data for resubmission of the proposal to external funding agencies.

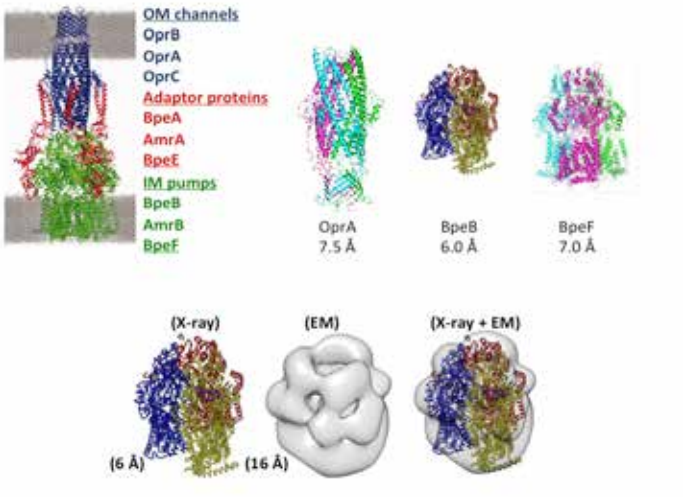

Figure 2. Model of assembled pump showing the 9 different proteins we used in the project. Outer membrane (OM), adapter proteins (which span between the inner and outer membrane proteins), and the inner membrane pump protein (IM). Each class of membrane protein component included 3 examples from different species or pumps (upper left); the proteins from each class of component we examined in detail OprA, BpeB, and BpeF (upper right); cryo electron microscopy (EM) and X-ray structures of BpeB showing the superposition of the X-ray structure on the EM surface (lower right).

Molecular dynamics (MD) simulations to describe the initial binding of a drug to the pump and its transport across the efflux channel spanning inner-membrane, periplasm, and outer membrane. We have used multi-scale and state of the art molecular dynamics simulations to study the assembly mechanism of the MDR pump of P. aeruginosa. We are the first group to computationally study the fully assembled pump (Figure 3, left) at the microsecond timescale and to dissect key elements responsible for its function. We observed that the outer membrane component (OprM) is activated by, and highly dependent on, the interaction with the periplasmic component (MexA) partner

through a “lock-and-key” mechanism. This insight revealed a new drug target to disrupt the engagement of the pump by specifically blocking these key interactions. By focusing on the pathogenic strain Pao-1 band-A antigen of P. aeruginosa we showed that low permeability to antibiotics derives from the external lipopolysaccharide (LPS) layer. This specialized structure (Figure 3, right) decreases the rates by which drugs can translocate into the bacteria, and we showed it is also responsible of the modulation of protein channels which otherwise may allow the active transport of drugs. This knowledge has brought a molecular understanding of how to increase drug intake by disrupting the structure of the LPS layer, improving the activity of already therapeutic treatments.

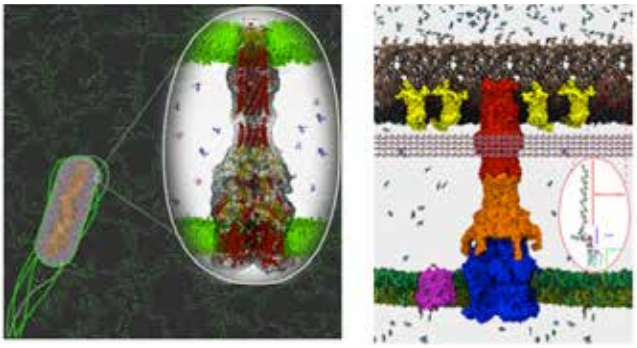

Figure 3. Assembly of the P. aeruginosa MDR pump in lipid model membrane. The pump is stable and functional in our computational simulation; bringing the possibility to study the molecular mechanism at atomistic scale (left panel); Cross-section view of a modeled P. aeruginosa cell envelope. The outside layer of the outer membrane (top of figure on right) has lipopolysaccharides (LPS) (pink color) “band A antigen”, and the inside layer of the outer membrane contains glycerophospholipids 1,2-dipalmitoyl-sn-glycero-3-phosphoe- thanolamine (DPPE). Green spheres are magnesium ions bound to O-chains and core polysaccharides of LPS. The inner membrane contains equal amounts cardiolipin, 1-palmitoyl-2-oleoyl-sn-glycero-3- phosphoethanolamine (POPE) and 1-palmitoyl-2-oleoyl-sn-glycero- 3-phosphoglycerol (POPG). Embedded in the outer membrane are the main porin OprF in a yellow surface density. The inner bilayer includes an MdfA transporter, represented in a magenta surface (bottom layer of figure on right). The modeled structure of the assembled MexAB-OprM multidrug efflux pump (MexB, (blue); MexA, (orange); OprM, (red)) spans both the inner and outer membranes. The structure of MexAB-OprM is from long duration (micro second scale) all-atom molecular dynamics simulations with the tripartite complex embedded in 1-palmitoyl-2- oleoyl-sn-glycero-3-phosphocholine (POPC) bilayers mimicking inner and outer membranes. The MexA component lacks the N-terminal lipid modification. The outer and inner membranes are based on separate protein-free all-atom MD simulations with the above composition. Other structures were taken from the Protein Data Bank. Ciprofloxacin molecules were added to illustrate a difference of concentrations created by slow diffusion across the outer membrane through porins and LPS-containing bilayer and the active efflux across the outer (MexAB-OprM) and inner (MdfA) membranes. Single representative LPS molecule from the simulations. The peptidoglycan is pictorially represented by fiber-like structures underneath the outer membrane (right panel).

We developed a mathematical model of the central component of the efflux mechanism - the active inner-membrane transporter of the RND efflux pump - that provides a connection between the observed structural properties and the efflux kinetics. The model shows that the specificity and throughput of the pump are not determined solely by the drug binding affinity - as thought conventionally - but can be modulated by the periplasmic pH, the membrane potential and the proton interaction with the transporter.

Web tool for assembly of efflux pumps. While the overall structures of Gram-negative tripartite efflux pumps are difficult to solve experimentally, the sequences of their component proteins (called inner membrane, outer membrane, and adaptor proteins) are readily accessible from various genome-sequencing projects. We have developed an optimized pipeline that lets a user input the component sequences for a pump of interest, and assemble a detailed atomistic model of the pump from these sequences, and returns the assembled model structure to the user. This pipeline can also accept component structures if available (for example the structures obtained in this project, see above). We have recently used the models predicted by this web tool, in combination with sequence analysis techniques, to look at sequence and structure variations among efflux pumps in three Gram-negative bacteria: E. coli, P. aeruginosa, and B. pseudomallei. In terms of the lengths of these pumps (i.e., the dimension that spans both membranes), we found that there is minimal length variation between pumps from E. coli and B. pseudomallei, suggesting that the periplasmic lengths of both bacteria are more uniform around their cells in order to fit these pumps. For P. aeruginosa, however, we found that the dominant efflux pump (MexAB-OprM) is uniquely shorter than the rest of the pumps, in particular for the adaptor protein (MexA) where sequence analysis shows gaps or missing residues. MexA has been observed to be more selective than other adaptor proteins in terms of which outer membrane proteins it can function with, and further research should provide insights if these observations are related to the length variation seen here for MexA.

Determination of antibiotic transport rates using computational milestoning. To develop kinetic models of antibiotic transport (influx and efflux) across Gram-negative bacterial membranes, the rate constants that govern the various transport processes need to be either measured experimentally or estimated computationally. In the case

of tripartite efflux pumps, there is little experimental data for their efflux rate constants. Measurements (ranging between 10-1000 molecules effluxed per second) are available for only a single class of antibiotics transported out by a single pump type in E. coli and in P. aeruginosa. To make computational estimates of these rate constants, we used an approach called milestoning that has been successfully used by others to estimate rate constants for various complex biomolecular processes (such as structural transitions in HIV reverse transcriptase upon binding of substrate). We tested this approach on a model system with smaller porin proteins (that act as channels for transport of molecules into the cell). Our preliminary results show transport through these porins faster than experimentally measured values. Combining the milestoning approach with techniques that can compute diffusion rates (e.g., Brownian dynamics simulations) should provide more reliable overall estimates of transport rate constants through both porins and efflux pumps.

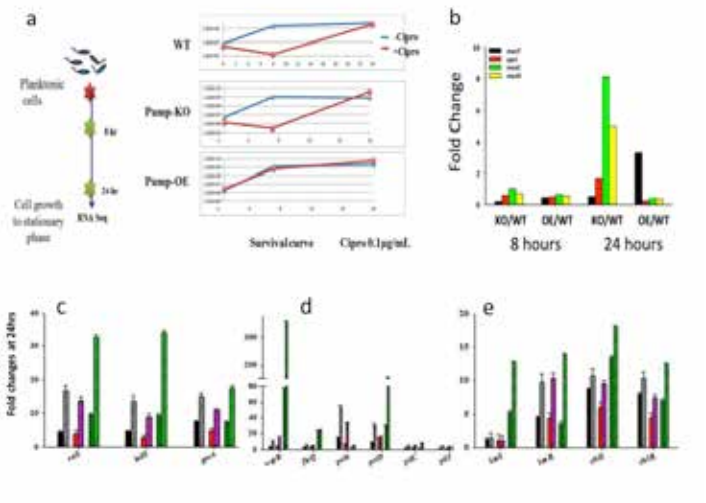

Figure 4. (a) Gene expression of mexT, mexC, mexD, and oprJ both in the presence and absence of ciprofloxacin; (b) survival curves of planktonic (free-swimming) P. aeruginosa wild-type (WT), mexAB-oprM knock-out (KO), and mexAB-oprM overexpressor (OE) strains exposed to 0.1 µg/ml Ciprofloxacin (red line) vs. untreated control (blue line); (c) critical genes for biofilm formation are upregulated in WT and Pump-OE in presence of 1 µg/ml Ciprofloxacin at 24 h (WT (grey/black), KO (red/purple), OE (dark green/green)); (d) expression of global regulators of biofilm formation are higher at 24 h cyclic-D-GMP (wspR) and polysaccharide gene (pelD) are higher in Pump-OE while the expression of motility genes (pilC, pilJ) are lower. This facilitates biofilm formation; (e) expression of quorum sensing genes also contribute to thick biofilm formation and thus confer antibiotic resistance.

Our gene expression, molecular, and cellular studies show that the RND efflux pumps play two different roles based upon the cellular states of P. aeruginosa. In addition to confirming their role extruding drugs, we showed that MDR efflux pumps also protect P. aeruginosa from drugs by forming biofilms and helping to lyse the first-line of host defense (host neutrophils) by releasing virulence factors that lyse neutrophils. First, in the planktonic "free-swimming" state, the RND pumps facilitate efflux of a drug before it can kill the bacteria (Figure 4a and 4b). Second, in the biofilm state, under antibiotic selection, the action of efflux pumps lead to expression of genes that contribute to the formation of a protective encapsulating layer of polysaccharide, DNA, and protein matrix to prevent drug entry (Figure 4c-d). In addition, the efflux pumps also facilitate the release of specific virulence factors that abrogate host innate immune defense. This is the first demonstration that the efflux pumps are more than pumps that not only facilitate extrusion of drugs but also regulate biofilm formation thereby providing additional resistance through the formation of biofilms. This study elucidates the role of efflux pumps in key resistance mechanisms in P. aeruginosa and also describes how different mechanisms are coupled. Our work shows how a detailed understanding of these mechanisms and their coupling will provide guidelines for developing novel therapeutic strategies against MDR P. aeruginosa.

Using a mathematical model, we showed that detailed information about drug import and export can be teased out of time courses of internal drug levels after a sudden exposure. The results suggest that membrane permeability can suddenly decrease during exposure to drug, accompanied by an increase, rather than a decrease, in the internal drug level. Our work centered on development of a dynamical model of drug accumulation in bacteria. The model captures key features in experimental time courses on ofloxacin accumulation: (1) initial uptake; (2) two-phase response; and (3) long-term acclimation (Figure 5). In combination with experimental data, the model provides estimates of import and export rates in each phase, the time of entry into the second phase, and the decrease of internal drug during acclimation. Global sensitivity analysis, local sensitivity analysis, and Bayesian sensitivity analysis of the model provide information about the robustness of these estimates, and about the relative importance of different parameters in determining the features of published time courses of ofloxacin accumulation in three different bacterial species: E. coli, S. aureus, and P. aeruginosa. The results lead to experimentally testable predictions of the effects of membrane permeability, drug efflux and trapping (e.g., by DNA binding) on drug accumulation. A key prediction is that a sudden increase in ofloxacin accumulation in both E. coli and S. aureus is accompanied by a decrease in membrane permeability. It is interesting to consider the importance of models of drug accumulation in light of a recent survey of physical properties of active compounds

in a drug screening collection and their relation to whole cell antibacterial activity. The survey reported on the difficulties encountered in simultaneously optimizing both biochemical potency and antibacterial activity, and concluded that "what is clearly needed is greater insight into medicinal chemistry strategies which optimize transport through porins and decrease efflux through the prolific efflux pumps." Our findings highlight how mathematical modeling of drug accumulation can provide these insights, and thus can be a key tool in enabling antibacterial medicinal chemistry.

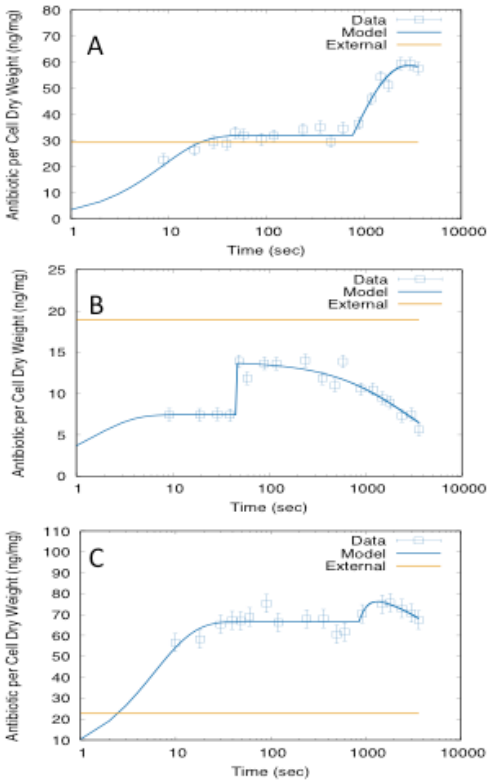

Figure 5. Ofloxacin accumulation data (open squares) with model fits (solid lines). (A) E. coli; (B) P. aeruginosa; (C) S. aureus. Each data point is assumed to have the same measurement error, estimated from the maximum values reported for norfloxacin (vertical bars). The external drug concentration of 10 mg/L is shown in each panel in ng/mg units (dashed straight lines), converted using the factors derived from the buoyant densities and dry fraction. The x-axis is plotted using a log scale, reflecting the time sampling of the data.

Impact on National Missions

We built a LANL capability that couples processes at multiple length and time scales: the nanometer molecular machine that pumps out drugs in seconds to minutes; the induction of gene clusters of multiple genes spanning hundreds of nanometers and their induction occurring over hours; and the formation of biofilm covering several microns over days. Each of these processes is crucial to the overall antibiotic resistance of B. pseudomallei; the fundamental approaches that we develop to integrate structural, genetic, and cellular processes can be used in the future to predict and engineer the functions of other biological systems. This will include engineering of microbes that are optimized for biofuel production through removal of toxic byproducts and development of inhibitors of human efflux systems for rescuing the activity of anti-cancer drugs. Multi-drug resistance poses a major hurdle in management of bacterial diseases encountered in both bio-threat and public health scenarios. Our capability in understanding and countering multi-drug resistance in bacteria directly benefits US and LANL missions in bio-security. Understanding multi-drug resistance in a bio-threat agent supports the Science of Signatures (SoS) bio-surveillance mission. The project has added LANL strength to the grand challenges in complex systems through the development of a capability in multi-scale modeling and manipulating biological machines.

Publications

Ganguly, K., M. Wren, J. Phillips, P. Pardington, H. Schweizer, M. Wall, S. Gnanakaran , and G. Gupta. Interdependence of multi drug efflux pumps and quorum sensing system in Pseudomonas. 2014. In International Congress on Infectious Diseases. (Cape Town, South Africa, 2-6 April). Vol. 21, Suppl 1, Edition, p. 92. International Journal on Infectious Diseases: --.

Hung, L. W., H. B. Kim, S. Murakami, G. Gupta, C. Y. Kim, and T. C. Terwilliger. Crystal structure of AcrB complexed with linezolid at 3.5 Å resolution. . 2014. Journal of Structural and Functional Genomics. . 14 (2): 71.

Phillips, J. L., Ganguly, Wren, Gupta, M. E. Wall, and Gnanakaran. Systems Level Study of Bacterial Multi-Drug Resistance from Efflux Machinery. 2014. BIOPHYSICAL JOURNAL. 106 (2): 791A.

Phillips, J., and S. Gnanakaran. A data-driven approach to modeling the tripartite structure of multidrug resistance efflux pumps. . 2015. Proteins: Structure, Function, and Bioinformatics.. 83: 43.

Vesselinova, N., B. S. Alexandrov, and M. E. Wall. Dynamical model of drug accumulation in bacteria: sensitivity analysis and experimentally testable predictions. To appear in PLoS One.

Zgurskaya, H., C. Lopez, and S. Gnanakaran. The permeability barrier of Gram-negative cell envelopes and approaches to bypass it. 2015. ACS Infectious Diseases. 1 (11): 512.

Quantitative Biology: From Molecules to Cellular Function

Angel E. Garcia
20140566DR

Abstract

Quantitative models of biological systems are becoming increasingly powerful in providing new insights into the structure and function of bio-molecules, intermediate-scale cellular structures, and full cellular function. Drawing from quantitative methods from physics, mathematics, statistical mechanics, chemistry, and computation, we advance the integration of cellular systems from molecular scales to full cell sizes. This involves the systematic coarse-graining of intermediate meso-scales that bridge macro-molecular components with compact models that describe cellular homeostasis and response to environmental stimuli. Often these compact models involve a very large number of interacting protein complexes that need to be described in a higher-level interacting network context that includes, for example, rule-based modeling methods. The application of our work is in the areas of biosurveillance, infectious disease modeling, bio energy systems of cellulosic and algal biofuels, and emerging challenges in drug resistant diseases and in developing vaccines for important human viral diseases such as HIV, HCV, and TB. Other collaborations in the areas of global security and energy security have been developed during this project.

Background and Research Objectives

The Center for Nonlinear Studies (CNLS) activities in biology are centered upon the quantitative analysis of biological systems covering the full range of scales from biomolecules, their assembly into intermediate scale structures such as membranes, the interaction of, for example, membrane proteins in facilitating cellular function, the intermediate network of cell regulatory mechanisms, and up to treating the cell as an entity with certain input/output characteristics on a quite phenomenological level. Because Los Alamos has a long history in leading the development of quantitative approaches to biology through computation and theory, it is natural for CNLS to take a role in amplifying that success and to add its strong physics, chemistry and mathematics capabilities to advancing the area of quantitative biology. In the past, we tended to look at complex biological systems as separate units owing the difficulties posed by trying to meld microscopic dynamics with overall cellular function. Increasingly, however, one can begin to piece together parts that do span from the microscopic to the mesoscopic and from the mesoscale to full cellular and intercellular activity. Our project focused on integrating efforts to span scales and to develop methods and models appropriate for multi-scale modeling of complex biological processes. This overall effort is, of course, not unique to Los Alamos as the impact of biological research touches everyone on a personal basis. In this area, however, we can make strong contributions based on our quantitative analysis foundations, on our history of exploiting new algorithms and architectures to produce world-class computer simulations, and on the combination of theory, computation, and experiment that we can bring together at a national laboratory.

Scientific Approach and Accomplishments

Stochastic control of intracellular gene regulatory networks

Genetic toggle switch --Stochastic genetic toggle switch is a ubiquitous gene regulatory motif that can produce bi- or multi-stability with only two genes of mutual repression. Toggle switch is important in the control of viral latency and activation, stem cell differentiation, and many other critical cellular processes. However, it is still unclear how the switching behaviors are regulated in these stochastic cellular circuits. In collaborating with Dr. Eduardo Sontag (Rutgers University), we built a stochastic model for generic genetic toggle switch to study how the switching rates from one distinct cellular macrostate (e.g. latent) to another (e.g. active) are controlled by the intrinsic rates of gene transcription, mRNA translation, protein-DNA affinity, as well as mRNA and protein decay. Using the “multi-finite buffer discrete Chemical Master Equation solution” (mb-dCME) method developed previously, we can directly solve the first passage

time distribution (FPTD) between two macrostates in the network, and therefore obtain the switching rates in different conditions. Preliminary results have shown strong nonlinear regulation of switching rates by transcriptions and translations. Also, protein translation and decay play much more significant roles than transcription and mRNA decay in regulating switching rates.

HIV latency and reactivation -- HIV latently infected cell reservoir is the major barrier to complete eradication of HIV infection. The latency and reactivation of HIV infected host cells appear to be stochastically controlled by the Tat regulatory circuit, a positive genetic feedback loop. By directly solving the steady state probability distribution of Tat mRNA and protein using the mb-dCME method, we are able to show the bistable behavior of the Tat circuit, which is largely unrecognized so far. This bistability of Tat can explain both the extreme stability of HIV latency, and the stochastic reactivation behavior. I further test various hypotheses as to how to induce the reactivation and/or suppress it in single cells by perturbing the Tat circuit with different drugs, and how these theoretical modeling results can be used to help developing better HIV therapies.

Stochasticity in single gene regulation -- Gene regulation is fundamental to cell behaviors. Experimental evidence shows that the expressions of the same gene can be highly stochastic in single cell level even in a homogeneous cell population, and the contribution of different reaction rates to the steady state protein abundance can be different. We explore how mean protein abundances and their noise levels are stochastically regulated in this fundamental process. We also study the effect of post-transcriptional regulations by microRNAs in controlling protein levels and noises using both the solution of chemical master equation and the stochastic simulation algorithm.

Prediction of optimal antibody combinations as anti-HIV prophylactic and therapeutic drugs

Recently, several potent broadly neutralizing antibodies (bnAbs) have been isolated from HIV infected individuals. It is now becoming clear that bnAbs develop due to the extensive co-evolutionary arms race within infected individuals between antibody responses evolving to try and neutralize the within-host viruses, which try to evolve resistance to such antibody responses. Even in individuals who develop exceptionally potent bnAbs the virus ultimately escapes and causes disease. However, the presence of bnAbs before the virus gets a chance to evolve resistance will be beneficial. Thus, administering of potent anti-HIV antibodies as prophylactic or therapeutic drugs, is an area of much current interest. One of the crucial advantages of antibodies over other antiretroviral drugs is that they can engage the host immune system in active killing of HIV infected cells, and hence if successful, antibody therapy can lead to HIV cure. Analogous to combination antiretroviral drug therapy, it is expected that a combination of antibodies will be needed for effective prevention and treatment of the highly diverse circulating HIV viruses. A key question is how many and which bnAbs would be most effective. Given the large number of bnAbs, an exhaustive experimental evaluation of bnAb combinations is not feasible. We have developed highly accurate modeling of neutralization by bnAb combinations. This modeling allowed us we can now predict and compare the performance of a comprehensive set of bnAb combinations.

In collaboration with NIH scientists, we analyzed the experimental data for a diverse set of viruses neutralized by single bnAbs and bnAb combinations. We found that a simple model, rooted in equilibrium mass action kinetics, gave very good predictions for the combination neutralization data. However, our modeling had some theoretical limitations, which we improved on to come up with a new model ("Bliss Hill Model").

Ongoing work uses the new Bliss Hill modeling approach to predict the best bnAb combinations from an extensive dataset, which was experimentally characterized by our collaborators at Harvard & Duke universities. In this study 16 of the most potent bnAbs known were tested against 200 HIV viruses, isolated from southern Africa ("Clade C panel"). A subset of data was tested as combinations, and the new experiments confirmed our predictions to be very accurate both for this dataset as well as the previous dataset we worked with. The real translational use of our modeling was that we were able to isolate the best few combinations from a total of ~1,600 potential bnAb combinations in this dataset.

Atomistic and Coarse-grained (CG) simulations of membrane proteins

Biological membranes are composed of a complex mixture of lipids, ions, proteins and other biomolecules. The interaction of proteins with the cell membrane will depend on the local ionic environment, the nature of the protein, and the lipids. Detailed atomistic simulations of membrane systems have been limited by slow relaxation of the lipid bilayer, and the complex interactions of proteins with the membrane. Coarse-grained molecular dynamics simulations enable the study of membrane proteins in large complexes and provide sufficient atomistic and energetic details needed to compare to experimental settings. We have worked on models of various membrane protein systems.

Membrane-mediated regulation of the immunoreceptor signaling -- The T cell receptor (TCR) recognition of

the peptide-major histocompatibility complex (MHC) is an essential step in initiating the host adaptive immune response. Upon TCR engagement with the peptide-MHC complex, intracellular signaling events are mediated in part by CD3e chain that contains an immunoreceptor tyrosine-based activation motif (ITAM). Even though the intrinsically disordered ITAM-bearing CD3e cytoplasmic tail is preferentially bound to negatively charged lipids in model membranes, the preferential binding and localization of CD3e are easily modified by the lipid composition and order in multicomponent systems mimicking biological membranes. Our modeling studies suggest a refinement of the roles proposed for "lipid rafts" in the activation of ITAM-containing immunoreceptors where changes in the local lipid environment may serve as a switch during the initial TCR activation. This work has been published (Lopez et al., Biophys J. 108, 2481-2491 (2015)).

Molecular Recognition of Diverse Epitopes in MHC-E -- Priming of rhesus macaques with Rh157.5/.4 gene-deleted rhesus Cytomegalovirus vectors leads to MHC-E mediated presentation of highly diverse peptide epitopes to CD8+ T cells. The nature of the functional plasticity of MHC-E that enables binding to such a diverse array of epitopes is not clear. Sequence analysis of 11 optimal MHC-E-restricted 9mer epitopes showed only one epitope with a canonical MHC-E-binding motif, whereas the other 10 optimal epitopes not only lacked this motif, but also manifested no statistically significant overlap with previously characterized sets of MHC-E bound peptides, including those presented in conditions of cellular stress. Structural analyses and molecular modeling suggest that unique conformational properties of MHC-E may drive the observed epitope diversity and breadth. Long time-scale all-atom molecular dynamics simulations of canonical peptide bound and unbound forms of the solved structure of HLAE* 01:03, human ortholog of Mamu-E, in comparison to simulations of the classical HLA-Ia protein HLA-A*02:01 revealed that HLA-E*01:03 preserves a relatively rigid peptide binding groove that remains open even in the absence of canonical peptide during the simulation timescales. In contrast, the binding groove of classical HLA-A02:01 molecules collapse in the absence of peptide. ROSETTA based docking analysis further suggests that the 11 optimal MHC-E restricted SIVgag epitopes described above can potentially bind to the relatively rigid MHC-E binging groove by adopting a similar backbone configuration while accommodating less stringent side chain requirements. This work was published in Science (Hansen, SG et al. Science, 351:714-720 (2016)).

Probing the activity of Mycolactone, a membrane-perturbing bacterial toxin -- Mycolactone is an exotoxin produced by Mycobacterium ulcerans and is a key virulence factor behind Buruli ulcer. It has been linked to a broad spectrum of pathological effects within the host organism. Although it has been shown that the toxin can passively permeate into host cells, its interactions with and distribution in lipids are unknown. We used multi-resolution molecular dynamics simulations to study the interaction of mycolactone with lipid membranes. Our preliminary results show that the exotoxin localizes in the water-membrane interface, with preference towards the glycerol moiety of lipids. This interaction modifies physical properties of the bilayer, including transition temperature, area per lipid, pore stability, and compression modulus. Furthermore, this exotoxin interacts with the saturated and unsaturated lipids of the liquid ordered-liquid disordered interphase, lowering the line tension. We show the tendency of mycolactone to behave as a linactant, (i.e., a molecule that localizes at the boundary between different fluid lipid domains in membranes and promotes inter-mixing of domains).

Engineering Effective Catalysts for Cellulose Conversion to Sugars. Challenges encountered during the conversion of biomass to biofuels are critically linked to the physical properties of the feedstock. Crystalline cellulose exists in various allomorphic states some of which are not found to occur naturally. A better understanding of unnatural cellulose allomorphs and their biodegradation will improve the efficiency of next-generation extractive ammonia based pretreatments. However, very little is known about how cellulases interact with such unnatural cellulosic allomorphs. We explore the interactions of various cellulolytic enzymes and their individual carbohydrate binding modules (CBMs) with cellulose allomorphs to gain insight into the mechanism of cellulose deconstruction. Interactions responsible for the stability and reactivity of cellulose were incorporated into the computational models. These computational models are used to understand and interpret experimental measurements that have revealed that both Type-A and Type-B CBMs (known to target crystalline and amorphous cellulose, respectively) have reduced affinity for non-native cellulose allomorphs (like cellulose III) compared to untreated cellulose (like cellulose I). This work was done in collaboration with the DOE Great Lakes Bioenergy Center. A manuscript has been published (Lopez et al., J Phys. Chem. B, 119, 465-473(2015)).

Conclusions

We studied biomolecular systems at scales ranging from molecular (e.g., proteins, RNA, etc.) to cells, with emphasis on the applications to biotechnology and human disease. We use physics-based theoretical and computational methods to study these systems at various degrees of complexity. There are challenges at each level of complexity that require the development of new models and

algorithms. We work closely with experimental groups studying our systems of choice such that we can help analyze data and validate our models. We have developed mesoscopic models that bridge scales in biofuel-relevant algae systems and provide a molecular level understanding and design principles for engineering more effective cellulosic biomass. We are developing multiscale models of pathogenesis in bacteria. We will use novel mathematical methods to improve rule-based methodology applied to bio-chemical reaction networks and employ them to understand and characterize specific cellular mechanisms. We will construct high-level models of infectious diseases including influenza, HIV and HCV based on systems-level understanding of immune response. We are developing high-performance computing and big data analysis to study the genetics of cancer. Using these methods we have identified markers for various cancers and aging.

Impact on National Missions

The fundamental discovery science associated with the CNLS biology effort has potential applications in energy security via algal and cellulosic biofuels modeling, in biosecurity through understanding and modeling of infectious disease epidemiology and cellular mechanisms, and in health related areas such as the ability to design effective vaccines using biological models of cellular function, and in identifying the origins of cancer from big genetic data analysis.

Publications

Abbink, , L. F. Maxfield, Ng'ang'a, E. N. Borducchi, M. J. Iampietro, C. A. Bricault, J. E. Teigler, Blackmore, Parenteau, Wagh, S. A. Handley, Zhao, H. W. Virgin, Korber, and D. H. Barouch. Construction and Evaluation of Novel Rhesus Monkey Adenovirus Vaccine Vectors. 2015. JOURNAL OF VIROLOGY. 89 (3): 1512.

Alexandrov, L. B., A. R. Bishop, K. Ø. Rasmussen, and B. S. Alexandrov. The role of structural parameters in DNA cyclization. 2016. BMC Bioinformatics. 17 (1): 68.

Bellissent-Funel, M., A. Hassanali, M. Havenith, R. Henchman, P. Pohl, F. Sterpone, D. van der Spoel, Y. Xu, and A. E. Garcia. Water Determines the Structure and Dynamics of Proteins. 2016. Chemical Reviews. 116 (13): 7673.

Chylek, L. A., Akimov, Dengjel, K. T. G. Rigbolt, B. i. n. Hu, W. S. Hlavacek, and Blagoev. Phosphorylation Site Dynamics of Early T-cell Receptor Signaling. 2014. PLOS ONE. 9 (8).

Chylek, L. A., B. S. Wilson, and W. S. Hlavacek. Modeling Biomolecular Site Dynamics in Immunoreceptor Signaling Systems. 2014. SYSTEMS BIOLOGY APPROACH TO BLOOD. 844: 245.

Chylek, L. A., D. A. Holowka, B. A. Baird, and W. S. Hlavacek. An Interaction Library for the FcεRI Signaling Network. 2014. Frontiers in Immunology. 5: 172.

Chylek, L. A., D. A. Holowka, B. A. Baird, and W. S. Hlavacek. An interaction library for Vie Fc epsilon RI signaling network. 2014. FRONTIERS IN IMMUNOLOGY. 5.

Chylek, L. A., L. A. Harris, C. Tung, J. R. Faeder, C. F. Lopez, and W. S. Hlavacek. Rule-based modeling: a computational approach for studying biomolecular site dynamics in cell signaling systems. 2014. Wiley Interdisciplinary Reviews: Systems Biology and Medicine. 6 (1): 13.

Chylek, L. A., L. A. Harris, J. R. Faeder, and W. S. Hlavacek. Modeling for (physical) biologists: an introduction to the rule-based approach. 2015. PHYSICAL BIOLOGY. 12 (4).

Chylek, L. A., L. A. Harris, Tung, J. R. Faeder, C. F. Lopez, and W. S. Hlavacek. Rule-based modeling: a computational approach for studying biomolecular site dynamics in cell signaling systems. 2014. WILEY INTERDISCIPLINARY REVIEWS-SYSTEMS BIOLOGY AND MEDICINE. 6 (1): 13.

Chylek, L. A., V. Akimov, J. Dengiel, K. T. G. Rigbolt, B. Hu, W. S. Hlavacek, and B. Blagoev. Phosphorylation site dynamics of early T-cell receptor signaling. 2014. PLoS One. 9: e104240.

Cooper, C. S., Eeles, D. C. Wedge, Van Loo, Gundem, L. B. Alexandrov, Kremeyer, Butler, A. G. Lynch, Camacho, C. E. Massie, Kay, H. J. Lmcton, Edwards, Kote-Jarai, Dennis, S. u. e. Merson, Leongamornlert, Zamora, Corbishley, Thomas, Nik-Zainal, Ramakrishna, O'Meara, Matthews, Clark, Hurst, Mithen, R. G. Bristow, P. C. Boutros, Fraser, Cooke, Raine, Jones, Menzies, Stebbings, J. o. n. Hinton, J. o. n. Teague, McLaren, Mudie, Hardy, Anderson, Joseph, Goody, B. e. n. Robinson, Maddison, Gamble, Greenman, D. a. n. Berney, Hazell, Livni, Fisher, Ogden, Kumar, Thompson, Woodhouse, Nicol, Mayer, T. i. m. Dudderidge, N. C. Shah, Gnanapragasam, Voet, Campbell, Futreal, Easton, A. Y. Warren, C. S. Foster, M. R. Stratton, H. C. Whitaker, McDermott, D. S. Brewer, and D. E. Neal. Analysis of the genetic phylogeny of multifocal prostate cancer identifies multiple independent clonal expansions in neoplastic and morphologically normal prostate tissue (vol 47, pg 367, 2015). 2015. NATURE GENETICS. 47 (6): 689.

Cooper, C. S., Eeles, D. C. Wedge, Van Loo, Gundem, L. B. Alexandrov, Kremeyer, Butler, A. G. Lynch, Camacho, C. E. Massie, Kay, H. J. Luxton, Edwards, Kote-Jarai, Dennis, S. u. e. Merson, Leongamornlert, Zamora, Corbishley, Thomas, Nik-Zainal, O'Meara, Matthews, Clark, Hurst, Mithen, R. G. Bristow, P. C. Boutros, Fraser, Cooke, Raine, Jones, Menzies, Stebbings, J. o. n. Hinton, J. o. n. Teague, McLaren, Mudie, Hardy, Anderson,

Joseph, Goody, B. e. n. Robinson, Maddison, Gamble, Greenman, D. a. n. Berney, Hazell, Livni, Fisher, Ogden, Kumar, Thompson, Woodhouse, Nicol, Mayer, T. i. m. Dudderidge, N. C. Shah, Gnanapragasam, Voet, Campbell, Futreal, Easton, A. Y. Warren, C. S. Foster, M. R. Stratton, H. C. Whitaker, McDermott, D. S. Brewer, and D. E. Neal. Analysis of the genetic phylogeny of multifocal prostate cancer identifies multiple independent clonal expansions in neoplastic and morphologically normal prostate tissue. 2015. NATURE GENETICS. 47 (4): 367.

Giorgi, E. E., D. O. Stram, D. Taverna, S. D. Turner, F. Schumacher, C. A. Haiman, A. Lum-Jones, M. Tirikainen, C. Caberto, D. Duggan, B. E. Henderson, L. Le Marchand, and I. Cheng. Fine-Mapping IGF1 and Prostate Cancer Risk in African Americans: The Multiethnic Cohort Study. 2014. Cancer Epidemiology, Biomarkers & Prevention: A Publication of the American Association for Cancer Research, Cosponsored by the American Society of Preventive Oncology. 23 (9): 1928.

Gottardo, R., R. T. Baller, B. T. Korber, S. Gnanakaran, J. Phillips, X. Shen, G. D. Tomaras, E. Turk, G. Imholte, L. Eckler, H. Wenschuh, J. Zerweck, K. Greene, H. Gao, P. W. Berman, D. Francis, F. Sinangil, C. Lee, S. Nitayaphan, S. Rerks-Ngarm, J. Kaewjungawal, P. Pitsuttithum, J. Tartaglia, M. L. Robb, N. L. Michael, J. H. Kim, S. Zolla-Pazner, B. F. Haynes, J. R. Mascola, S. Self, P. Gilbert, and D. C. Montefiori. Plasma IgG to linear epitopes in the V2 and V3 regions of HIV-1 gp120 correlate with a reduced risk of infection in the RV144 vaccine efficacy trial. 2013. PLoS One. : e75665.

Gundem, , Van Loo, Kremeyer, L. B. Alexandrov, J. M. C. Tubio, Papaemmanuil, D. S. Brewer, H. M. L. Kallio, Hoegnas, Annala, Kivinummi, Goody, Latimer, O'Meara, K. J. Dawson, Isaacs, M. R. Emmert-Buck, Nykter, Foster, Kote-Jarai, Easton, H. C. Whitaker, D. E. Neal, C. S. Cooper, R. A. Eeles, Visakorpi, P. J. Campbell, McDermott, D. C. Wedge, and G. S. Bova. The evolutionary history of lethal metastatic prostate cancer. 2015. NATURE. 520 (7547): 353.

Hansen, S. G., H. L. Wu, B. J. Burwitz, C. M. Hughes, K. B. Hammond, A. B. Ventura, J. S. Reed, R. M. Gilbride, E. Ainslie, D. W. Morrow, J. C. Ford, A. N. Selseth, R. Pathak, D. Malouli, A. W. Legasse, M. K. Axthelm, J. A. Nelson, G. M. Gillespie, L. C. Walters, S. Brackenridge, H. R. Sharpe, C. A. López, K. Früh, B. T. Korber, A. J. McMichael, S. Gnanakaran, J. B. Sacha, and L. J. Picker. Broadly targeted CD8+ T cell responses restricted by major histocompatibility complex E. 2016. Science. : aac9475.

Hong, M. K. H., Macintyre, D. C. Wedge, Van Loo, Patel, Lunke, L. B. Alexandrov, Sloggett, Cmero, Marass, Tsui, Mangiola, Lonie, Naeem, Sapre, P. M. Phal, Kurganovs, Chin, Kerger, A. Y. Warren, Neal, Gnanapragasam, Rosenfeld, J. S. Pedersen, Ryan, Haviv, A. J. Costello, N. M. Corcoran, and C. M. Hovens. Tracking the origins and drivers of subclonal metastatic expansion in prostate cancer. 2015. NATURE COMMUNICATIONS. 6.

Hovens, , Hong, Macintyre, Wedge, Van Loo, Lunke, Alexandrov, Slogget, Cmero, Mangiola, Lonie, Naeem, Sapre, Phal, Kerger, Pedersen, Ryan, Haviv, Costello, and Corcoran. Tracking clonal diversity in metastatic prostate cancer progression. 2015. JOURNAL OF CLINICAL ONCOLOGY. 33 (7).

Ismael, A., W. Tian, N. Waszczak, X. Wang, Y. Cao, D. Suchkov, E. Bar, M. V. Metodiev, J. Liang, R. A. Arkowitz, and D. E. Stone. Gβ promotes pheromone receptor polarization and yeast chemotropism by inhibiting receptor phosphorylation. 2016. Sci. 9 (423): ra38.

Kong, R. u. i., M. K. Louder, Wagh, R. T. Bailer, deCamp, Greene, Gao, J. D. Taft, Gazumyan, Liu, M. C. Nussenzweig, Korber, D. C. Montefiori, and J. R. Mascola. Improving Neutralization Potency and Breadth by Combining Broadly Reactive HIV-1 Antibodies Targeting Major Neutralization Epitopes. 2015. JOURNAL OF VIROLOGY. 89 (5): 2659.

Kozer, , Barua, Henderson, E. C. Nice, A. W. Burgess, W. S. Hlavacek, and A. H. A. Clayton. Recruitment of the Adaptor Protein Grb2 to EGFR Tetramers. 2014. BIOCHEMISTRY. 53 (16): 2594.

Krafnick, R. C., and A. E. García. Efficient Schmidt number scaling in dissipative particle dynamics. 2015. The Journal of Chemical Physics. 143 (24): 243106.

Langan, , Petridis, H. M. O'Neill, S. V. Pingali, Foston, Nishiyama, Schulz, Lindner, B. L. Hanson, Harton, W. T. Heller, Urban, B. R. Evans, Gnanakaran, A. J. Ragauskas, J. C. Smith, and B. H. Davison. Common processes drive the thermochemical pretreatment of lignocellulosic biomass. 2014. GREEN CHEMISTRY. 16 (1): 63.

Lopatina, L. M., and J. V. Selinger. Polymer-disordered liquid crystals: Susceptibility to an electric field. 2013. Physical Review E. 88: 062510.

Lopez, C. A., Bellesia, Redondo, Langan, S. P. S. Chundawat, B. E. Dale, S. J. Marrink, and Gnanakaran. MARTINI Coarse-Grained Model for Crystalline Cellulose Microfibers. 2015. JOURNAL OF PHYSICAL CHEMISTRY B. 119 (2): 465.

Lopez, C. A., Sethi, Goldstein, B. S. Wilson, and Gnanakaran. Membrane-Mediated Regulation of the Intrinsically Disordered CD3 epsilon Cytoplasmic Tail of the TCR. 2015. BIOPHYSICAL JOURNAL. 108 (10): 2481.

Martincorena, , Roshan, Gerstung, Ellis, Van Loo, McLaren, D. C. Wedge, Fullam, L. B. Alexandrov, J. M. Tubio,

Stebbings, Menzies, Widaa, M. R. Stratton, P. H. Jones, and P. J. Campbell. High burden and pervasive positive selection of somatic mutations in normal human skin. 2015. SCIENCE. 348 (6237): 880.

Mayes, H. B., Tian, M. W. Nolte, B. H. Shanks, G. T. Beckham, Gnanakaran, and L. J. Broadbelt. Sodium Ion Interactions with Aqueous Glucose: Insights from Quantum Mechanics, Molecular Dynamics, and Experiment. 2014. JOURNAL OF PHYSICAL CHEMISTRY B. 118 (8): 1990.

Merlevede, J., N. Droin, T. Qin, K. Meldi, K. Yoshida, M. Morabito, E. Chautard, D. Auboeuf, P. Fenaux, T. Braun, R. Itzykson, S. de Botton, B. Quesnel, T. Commes, E. Jourdan, W. Vainchenker, O. Bernard, N. Pata-Merci, S. Solier, V. Gayevskiy, M. E. Dinger, M. J. Cowley, D. Selimoglu-Buet, V. Meyer, F. Artiguenave, J. Deleuze, C. Preudhomme, M. R. Stratton, L. B. Alexandrov, E. Padron, S. Ogawa, S. Koscielny, M. Figueroa, and E. Solary. Mutation allele burden remains unchanged in chronic myelomonocytic leukaemia responding to hypomethylating agents. 2016. Nature Communications. 7: 10767.

Miner, J. C., A. A. Chen, and A. E. García. Free-energy landscape of a hyperstable RNA tetraloop. 2016. Proceedings of the National Academy of Sciences. 113 (24): 6665.

Morganella, S., L. B. Alexandrov, D. Glodzik, X. Zou, H. Davies, J. Staaf, A. M. Sieuwerts, A. B. Brinkman, S. Martin, M. Ramakrishna, A. Butler, H. Kim, Å. Borg, C. Sotiriou, P. A. Futreal, P. J. Campbell, P. N. Span, S. Van Laere, S. R. Lakhani, J. E. Eyfjord, A. M. Thompson, H. G. Stunnenberg, M. J. van de Vijver, J. W. Martens, A. Børresen-Dale, A. L. Richardson, G. Kong, G. Thomas, J. Sale, C. Rada, M. R. Stratton, E. Birney, and S. Nik-Zainal. The topography of mutational processes in breast cancer genomes. 2016. Nature Communications. 7: 11383.

Neale, C., H. Herce, R. Pomès, and A. García. Can Specific Protein-Lipid Interactions Stabilize an Active State of the Beta 2 Adrenergic Receptor?. 2015. Biophysical Journal. 109 (8): 1652.

Neale, C., R. Pomès, and A. E. García. Peptide Bond Isomerization in High-Temperature Simulations. 2016. Journal of Chemical Theory and Computation. 12 (4): 1989.

Nemenman, , J. R. Faeder, Gnanakaran, W. S. Hlavacek, Munsky, M. E. Wall, and Y. i. Jiang. The Seventh q-bio Conference: meeting report and preface. 2014. PHYSICAL BIOLOGY. 11 (4).

Nik-Zainal, S., H. Davies, J. Staaf, M. Ramakrishna, D. Glodzik, X. Zou, I. Martincorena, L. B. Alexandrov, S. Martin, D. C. Wedge, P. Van Loo, Y. S. Ju, M. Smid, A. B. Brinkman, S. Morganella, M. R. Aure, O. C. Lingjærde, A. Langerød, M. Ringnér, S. Ahn, S. Boyault, J. E. Brock, A. Broeks, A. Butler, C. Desmedt, L. Dirix, S. Dronov, A. Fatima, J. A. Foekens, M. Gerstung, G. K. Hooijer, S. J. Jang, D. R. Jones, H. Kim, T. A. King, S. Krishnamurthy, H. J. Lee, J. Lee, Y. Li, S. McLaren, A. Menzies, V. Mustonen, S. O'Meara, I. Pauporté, X. Pivot, C. A. Purdie, K. Raine, K. Ramakrishnan, F. G. Rodríguez-González, G. Romieu, A. M. Sieuwerts, P. T. Simpson, R. Shepherd, L. Stebbings, O. A. Stefansson, J. Teague, S. Tommasi, I. Treilleux, G. G. Van den Eynden, P. Vermeulen, A. Vincent-Salomon, L. Yates, C. Caldas, L. v. Veer, A. Tutt, S. Knappskog, B. K. Tan, J. Jonkers, Å. Borg, N. T. Ueno, C. Sotiriou, A. Viari, P. A. Futreal, P. J. Campbell, P. N. Span, S. Van Laere, S. R. Lakhani, J. E. Eyfjord, A. M. Thompson, E. Birney, H. G. Stunnenberg, M. J. van de Vijver, J. W. Martens, A. Børresen-Dale, A. L. Richardson, G. Kong, G. Thomas, and M. R. Stratton. Landscape of somatic mutations in 560 breast cancer whole-genome sequences. 2016. Nature. 534 (7605): 47.

Petljak, M., and L. B. Alexandrov. Understanding mutagenesis through delineation of mutational signatures in human cancer. 2016. Carcinogenesis. 37 (6): 531.

Phillips, J. L., and Gnanakaran. A data-driven approach to modeling the tripartite structure of multidrug resistance efflux pumps. 2015. PROTEINS-STRUCTURE FUNCTION AND BIOINFORMATICS. 83 (1): 46.

Rosenman, D. J., C. Wang, and A. E. García. Characterization of Aβ Monomers through the Convergence of Ensemble Properties among Simulations with Multiple Force Fields. 2016. The Journal of Physical Chemistry B. 120 (2): 259.

Russell, C. A., P. M. Kasson, R. O. Donis, Riley, Dunbar, Rambaut, Asher, Burke, C. T. Davis, R. J. Garten, Gnanakaran, S. I. Hay, Herfst, N. S. Lewis, J. O. Lloyd-Smith, C. A. Macken, Maurer-Stroh, Neuhaus, C. R. Parrish, K. M. Pepin, S. S. Shepard, D. L. Smith, D. L. Suarez, S. C. Trock, Widdowson, D. B. George, Lipsitch, and J. D. Bloom. Improving pandemic influenza risk assessment. 2014. ELIFE. 3.

Schulze, , Imbeaud, Letouze, L. B. Alexandrov, Calderaro, Rebouissou, Couchy, Meiller, Shinde, Soysouvanh, Calatayud, Pinyol, Pelletier, Balabaud, Laurent, Blanc, Mazzaferro, Calvo, Villanueva, Nault, Bioulac-Sage, M. R. Stratton, J. M. Llovet, and Zucman-Rossi. Exome sequencing of hepatocellular carcinomas identifies new mutational signatures and potential therapeutic targets. 2015. NATURE GENETICS. 47 (5): 505.

Shlien, , B. B. Campbell, de Borja, L. B. Alexandrov, D. M. Merino, Remke, Bakry, Dirks, Huang, R. G. Grundy, Durno, Aronson, M. D. Taylor, Z. F. Pursell, C. E. Pearson, Malkin, Bouffet, Hawkins, P. J. Campbell, and U. r. i. Tabori. COMBINED HEREDITARY AND SOMATIC MUTA-

TIONS OF REPLICATION ERROR REPAIR GENES RESULT IN RAPID ONSET OF ULTRA-HYPERMUTATED MALIGNANT BRAIN TUMORS IN CHILDREN. 2015. NEURO-ONCOLOGY. 17: 9.

Shlien, , B. B. Campbell, de Borja, L. B. Alexandrov, Merico, Wedge, Van Loo, P. S. Tarpey, Coupland, S. a. m. Behjati, Pollett, Lipman, Heidari, Deshmukh, Avitzur, Meier, Gerstung, Y. e. Hong, D. M. Merino, Ramakrishna, Remke, Arnold, G. B. Panigrahi, N. P. Thakkar, K. P. Hodel, E. E. Henninger, A. Y. Goeksenin, Bakry, G. S. Charames, Druker, Lerner-Ellis, Mistry, Dvir, Grant, Elhasid, Farah, G. P. Taylor, P. C. Nathan, Alexander, Ben-Shachar, S. C. Ling, Gallinger, Constantini, Dirks, Huang, S. W. Scherer, R. G. Grundy, Durno, Aronson, Gartner, M. S. Meyn, M. D. Taylor, Z. F. Pursell, C. E. Pearson, Malkin, P. A. Futreal, M. R. Stratton, Bouffet, Hawkins, P. J. Campbell, and U. r. i. Tabori. Combined hereditary and somatic mutations of replication error repair genes result in rapid onset of ultra-hypermutated cancers. 2015. NATURE GENETICS. 47 (3): 257.

Stieh, D. J., J. L. Phillips, P. M. Rogers, D. F. King, G. C. Cianci, S. A. Jeffs, S. Gnanakaran, and R. J. Shattock. Dynamic electrophoretic fingerprinting of the HIV-1 envelope glycoprotein. 2013. Retrovirology. 10 (1): 33.

Tripathi, S., A. E. Garcìa, and G. I. Makhatadze. Alterations of Nonconserved Residues Affect Protein Stability and Folding Dynamics through Charge–Charge Interactions. 2015. The Journal of Physical Chemistry B. 119 (41): 13103.

Veelen, V., Matthijs, S. Luo, and B. Simon. A Simple Model of Group Selection that Cannot Be Analyzed with Inclusive Fitness. 2014. Social Science Research Network.

Wagener, , L. B. Alexandrov, Montesinos-Rongen, Schlesner, Haake, H. G. Drexler, Richter, G. R. Bignell, McDermott, and Siebert. Analysis of mutational signatures in exomes from B-cell lymphoma cell lines suggest APOBEC3 family members to be involved in the pathogenesis of primary effusion lymphoma. 2015. LEUKEMIA. 29 (7): 1612.

Wagh, K., T. Bhattacharya, C. Williamson, A. Robles, M. Bayne, J. Garrity, M. Rist, C. Rademeyer, H. Yoon, A. Lapedes, H. Gao, K. Greene, M. K. Louder, R. Kong, S. A. Karim, D. R. Burton, D. H. Barouch, M. C. Nussenzweig, J. R. Mascola, L. Morris, D. C. Montefiori, B. Korber, and M. S. Seaman. Optimal Combinations of Broadly Neutralizing Antibodies for Prevention and Treatment of HIV-1 Clade C Infection. 2016. PLOS Pathog. 12 (3): e1005520.

Westrate, L. M., J. A. Drocco, K. R. Martin, W. S. Hlavacek, and J. P. MacKeigan. Mitochondrial Morphological Features are Associated with Fission and Fusion Events. 2014. PLoS ONE. 9 (4): e95265.

Westrate, L. M., J. A. Drocco, K. R. Martin, W. S. Hlavacek, and J. P. MacKeigan. Mitochondrial Morphological Features Are Associated with Fission and Fusion Events. 2014. PLOS ONE. 9 (4).

Yates, L. R., Gerstung, Knappskog, Desmedt, Gundem, Van Loo, Aas, L. B. Alexandrov, Larsimont, Davies, Li, Y. S. Ju, Ramakrishna, H. K. Haugland, P. K. Lilleng, Nik-Zainal, McLaren, Butler, Martin, Glodzik, Menzies, Raine, Hinton, Jones, L. J. Mudie, Jiang, Vincent, Greene-Colozzi, Adnet, Fatima, Maetens, Ignatiadis, M. R. Stratton, Sotiriou, A. L. Richardson, P. E. Lonning, D. C. Wedge, and P. J. Campbell. Subclonal diversification of primary breast cancer revealed by multiregion sequencing. 2015. NATURE MEDICINE. 21 (7): 751.

Zgurskaya, H. I., C. A. López, and S. Gnanakaran. Permeability Barrier of Gram-Negative Cell Envelopes and Approaches To Bypass It. 2015. ACS Infectious Diseases. 1 (11): 512.

Toward a Coupled Multi-physics Modeling Framework for Induced Seismicity

Satish Karra
20150693ECR

Introduction

The recent shale-gas revolution, has been accompanied by a five-fold increase in small to moderate magnitude (greater than 3) seismicity in the central and eastern US. It is likely that many of these earthquakes are induced by industry practice of disposing of fracking fluids into deep formations. The issue of induced seismicity presents a significant threat to US energy security, as regulatory barriers could curb the expansion of unconventional shale-gas operations as well as deployment of renewable energy technologies such as carbon sequestration and enhanced geothermal systems.

An induced earthquake occurs when pressurized fluid enters a fault and causes frictional failure. However, induced seismicity does not simply manifest as one single earthquake, but rather as a migrating, sporadic sequence of events. Modeling these sequences requires an understanding of the feedbacks between pressurization and fault rupture, and the ability to capture both small and large space and time-scales.

This project addresses the technology gaps in modeling induced seismicity. We propose a high-performance computing coupled multi-physics framework in which earthquakes alter fluid flow through fault networks, thereby influencing pressure migration and the location, timing and magnitude of subsequent earthquakes.

Benefit to National Security Missions

Shale gas, geothermal energy, carbon sequestration, and enhanced oil and gas recovery have a clear role in the U.S. energy policy, both in securing cost-effective energy and reducing atmospheric CO2. Injection-induced seismicity poses a significant mitigation challenge to the US energy sector, as it is intrinsically linked to the shale-gas fracking revolution, renewable energy technologies such as Carbon Capture and Storage and Enhanced Geothermal Systems, as well as underground waste water disposal. The coupled modeling framework developed in this work will form the basis for future forecasting tools. This will have a direct and immediate impact on policy-making as well as on the DOE's Offices of Fossil Energy (FE) and Energy Efficiency & Renewable Energy (EERE) programs in carbon storage, unconventional fossil fuels, and geothermal energy along with State agencies with regard to waste water disposal. Our research will also place LANL at the forefront when the DOE initiatives such as SubTER and Energy-Water Nexus commence.

Progress

The main goal of this project is to develop a coupled hydrology-seismicity framework that is aimed to be built on top of two HPC codes – PFLOTRAN (developed at LANL and other DOE labs) for flow and QK3 for earthquake slip dynamics. The overall goal of the previous FY was to develop the following capabilities to develop the coupled framework: a) coupled flow-geomechanics framework in PFLOTRAN, and b) coupling this capability in PFLOTRAN to QK3 earthquake slip dynamics simulator. Specific tasks achieved in previous FY include:

- Developed flow-geomechanics coupled framework for capturing poroelastic effects.
- Verified this implementation using well-established poroelasticity benchmark problems such as those proposed by Terzaghi and Mandel.
- The poroelastic model was then coupled to QK3 -- a simulator that models earthquake slip dynamics. Based on the stresses on a fault, a failture criterion (Mohr-Coulomb) was used to check if there is slip. If slip occurs, the stresses are passed to QK3 which then evaluates the slip and slip velocity, and thereby evaluates the propagation of an earthquake. Based on the slip, the permeability in PFLOTRAN can be modified as well to reflect opening and closing of faults due to slip.
- Preliminary simulations have been performed with

the coupled flow-seismicity PFLOTRAN-QK3 framework to demonstrate the capability.

Future Work

The main goal of this project is to develop a coupled hydrology-seismicity framework that is aimed to be built on top of two HPC codes – PFLOTRAN (developed at LANL and other DOE labs) for flow and QK3 for earthquake slip dynamics.

The overall goal of next fiscal year is to demonstrate the capabilities developed in this project, including: a) Coupled flow-geomechanics in PFLOTRAN; b) Induced seismicity framework that couples the flow-geomechanics process models in PFLOTRAN to QK3 earthquake slip dynamics model. The developed induced seismicity (geomechanics/slip and flow) framework will be used to perform the following tasks:

1. Perform inversion to evaluate the permeability and fracture characteristics using InSAR data of surface deformations due to injection/production activity around the Denver basin in CO. The InSAR data will be obtained from collaborators of the PI at UCBoulder.

2. Using site and injection data, we will evaluate estimates for stress state, slip and slip velocity for series of earthquakes at Rocky Mountain Arsenal, CO which have well-characterized site, injection and earthquake data.

Conclusion

Our primary goal is development of a new physics-based framework for induced seismicity that couples the traditionally separate fields of geomechanics (earthquakes) and hydrology (fluid injection). The coupling will be achieved through the use of innovative new fracture-permeability damage relationships that describe flow changes by as much four orders of magnitude in the fractured zone around a fault rupture. The framework uses recent advancements in two high-performance computing simulators – PFLOTRAN for subsurface flow and QK3 for fault dynamics. The methodology will have wide utility for industry, academic and government partners in carbon sequestration, waste water injection and enhanced geothermal systems.

Publications

Chang, J., S. Karra, and K. B. Nakshatrala. Large-scale Optimization-based Non-negative Computational Framework for Diffusion Equations: Parallel Implementation and Performance Studies. To appear in Journal of Scientific Computing (In press).

Grasinger, M., D. O'Malley, V. Vesselinov, and S. Karra. Decision analysis for robust CO2 injection: application of Bayesian-information-gap decision theory. To appear in International Journal of Greenhouse Gas Control. 49: 73.

Karra, S., and D. Dempsey. A coupled multi-physics modeling framework for induced seismicity. Presented at American Geophysical Union Fall Meeting 2015. (San Francisco, 14-16 Dec. 2015).

Mudunuru, M. K., S. Karra, N. Makedonska, and T. Chen. Joint geophysical and flow inversion to characterize fracture networks in subsurface systems. Statistical Analysis and Data Mining.

Mudunuru, M., S. Karra, D. R. Harp, G. D. Guthrie, and H. S. Viswanathan. Interpolation-based reduced-order models to predict transient thermal output for enhanced geothermal systems. To appear in Geothermics.

Riffault, J., D. Dempsey, R. Archer, S. Kelkar, and S. Karra. Understanding poroelastic stressing and in- duced seismicity with a stochastic/deterministic model: an application to an EGS stimulation at Paralana, South Australia, 2011. 2016. In 41st Workshop on Geothermal Reservoir Engineering 2016 . (Palo Alto, 22-24 Feb. 2016). Vol. 1, p. 855. Stanford: Curran Associates, Inc..

Next-Generation Sea Level Predictions with Novel Ice Sheet Physics

Matthew J. Hoffman
20160608ECR

Introduction

Ice sheet mass loss is the largest uncertainty in sea level change projections; current models are unable to predict rapid changes in ice dynamics to put an upper bound on future mass loss. Despite the fact that the sliding of ice sheets over their bed is the primary control on ice flux to the oceans, current ice sheet models reduce this process to a single parameter that cannot evolve. Because decades of research have demonstrated that the state of the subglacial hydrologic system is the primary control on sliding, ice sheet modelers have emphasized subglacial hydrology and its effects on basal sliding as a critical missing piece of current ice sheet models. This project will fill this void by applying a coupled model of ice sheet dynamics and subglacial hydrology to sea level projections. A subglacial hydrology model within the Community Ice Sheet Model will be improved by adding necessary missing physics of subglacial drainage and parallelization of the model. Applying parameter estimation tools to the completed model will allow for the first calibration of this coupled system. This model will be run into the future for different climate forcing scenarios to predict sea level contributions from the Greenland Ice Sheet, which experiences dramatic seasonal changes in sliding from surface melt draining and lubricating its bed.

Benefit to National Security Missions

A primary aspect of Climate and Energy Impact is sea level rise. Current predictions of sea level rise are missing important basal physics that allows the basal motion of ice sheets to evolve naturally. This project will remedy that deficiency. This improvement will have a major impact on other agencies researching climate and sea level changes, including the National Oceanic and Atmospheric Administration, the National Aeronautics and Space Administration, and research sponsored by the National Science Foundation.

Progress

In FY16, a prototype subglacial hydrology model was written in the high-level Matlab language. This prototype model is based on a new finite-volume implementation of the conservation equations for subglacial hydrology. The use of the high-level Matlab language facilitated rapid development and testing of different discretizations for parts of the equations that have proved unstable in the past. The results are ready for translation to a Fortran module in the ice dynamics code.
An additional accomplishment of FY16 was the investigation of a new component of the subglacial drainage system into the model. Recent borehole observations from Greenland (Andrews et al., Nature, 2014) have suggested that the current conceptual model for subglacial drainage is too limited, and a new component describing "swampy" areas of poor drainage is necessary. Using the observational data as a guide, I implemented a new model component for swampy areas and demonstrated that inclusion of this new component is necessary to reproduce seasonal changes in ice speed that have been observed. A publication on these results is currently in review at Nature Geoscience. While creation of this third component was not on the original proposed task list for this project, recent developments in the field indicated this was a necessary topic to explore to achieve reliable results from the model. The agile nature of this project allowed me to address this frontier in the field before other groups were able to.

Future Work

The primary task for FY17 is the completion of improvements to the subglacial hydrology model. These are primarily 1) the implementation of robust dynamic subglacial channels and 2) parallelization of the model. The milestone for this task is a completed robust subglacial hydrology model. This work was initiated in FY16 and will be completed in FY17.

The other main task is beginning the parameter estimation for the subglacial hydrology model. This consists of 1) increasing fluency in the DAKOTA parameter estimation framework using toy problems and 2) analyzing the topography of the Greenland Ice Sheet to define topographic regions that will be used to reduce the number of parameters to be estimated. The milestone for this task is setting up the framework for performing the parameter estimation.

Conclusion

Ice sheet basal sliding is the primary control on the flux of ice to the oceans; however, current predictions of sea level change from ice sheet models assume basal sliding will not change in the future, an assumption at odds with decades of research. Incorporating this crucial missing process will generate superior sea level predictions and a novel Earth System Modeling capability at Los Alamos. The impact of this work could be profound as sea-level change could potentially disrupt and displace costal infrastructure and communities – close to 150 million people live within 1 m of current sea level.

Deciphering Nature's Chemical Toolbox: Decoding the Logic of Biosynthetic Assembly Lines

Alexander Koglin
20140624ECR

Abstract

Natural evolution designed highly efficient enzymatic systems with an incredible and often enough not reproducible chemical diversity. Secondary metabolites, natural products with bioactive properties, represent the class of compounds with the highest diversity in their chemical structures, functional groups and properties. This class contains often heavily alternated non-ribosomal peptides; ketides or acyl-derived small molecules and combinations thereof. The diverse biological functions include the vast majority of all known antibacterial, antifungal, antiviral, anti-cancer, immuno-suppressant, analgesic, blood pressure reducing, signal transducing, energy-storage compounds and toxins. A variety of tailoring enzymes associated with the biosynthetic assembly lines define the chemical structure of all products and can tremendously modify these step-by-step synthesized molecules.

DNA sequences encode ribosomal peptides, resulting protein functions, and the order and assembly of enzymes into biosynthetic clusters. Neither the assembly order, nor all basic core function or tailoring enzymes that is responsible for the biosynthesis of vastly diverse secondary metabolites is currently known. This is key information for the identification of novel bioactive compounds as synthesis order defines the chemical structure of secondary metabolites. A basic annotation of biosynthetic core functions is available, but neither substrate specificity nor predictions of compound assembly is feasible based on current knowledge.

We investigated the genetic encoding and the biosynthetic organization of enzymatic functions in all known natural products with the goal to develop PYTHON and Perl-script based software tools to identify unknown natural products based only on their genetic encoding. These algorithms should not require any linear dependencies of peptide sequence motifs or enzymatic functions to identify novel secondary metabolites in all forms of life including bacteria, fungi and plants. Further, we created a SQL database to enable fully parallel searches of newly discovered assembly lines to predict the chemical composition of previously unknown natural products.

The main goal of this project was to develop methods that allow an accelerated genetic identification and structure prediction of novel secondary metabolites before compounds may be isolated and characterized to accelerate the basic development of bioactive compounds. This class of chemical entities represents the main source for all drugs.

Background and Research Objectives

This project focuses on methods to identify genes coding for new biosynthetic enzyme clusters that produce bioactive metabolites with new chemical properties (chemotypes) in genetic information of bacteria, fungi and plants and to predict the chemical composition or chemical structure of these biosynthesized natural products based on their encoding. It describes a "Genome-to-Drug" discovery route with the goal to create a searchable database of all known and newly identified enzyme clusters and produced compounds for drug development and to decipher the logic of enzyme cluster formation. Natural products represent the class of small bioactive molecules that are widely applied as antibacterial, antiviral, antitumor, antifungal, immunosuppressant and analgesic drugs. The search for new antibacterial and antiviral drugs supports the biosecurity mission of LANL and other federal government agencies as reflected in numerous recently issued press releases and several research funding announcements.

Meeting the great demand for novel bioactive agents requires improved discovery processes for bioactive compounds. It is clear that microbes continue as a major source of new drug leads. With short evolutionary cycles and natural pressure to protect their biological niches, soil and marine microbes are prime targets for identifica-

tion of novel compounds. This project couples advances in DNA sequencing and bioinformatics with biochemical and labeling techniques, structure elucidation methods and advanced knowledge in natural product biosynthesis. High- level expertise in these areas, combined with the Stable Isotope Resource, give LANL the potential to be an outstanding contributor to this field. This strategy gives us further insights into nature's way to produce bioactive compounds, significantly shorten the time span for natural product discovery, and consequently speed up and reduce costs for drug development. It will guide future developments of accurate prediction of natural product structures exclusively based on genomic DNA information. This supports the mission of Bioscience Division in biosecurity and LANL's mission in threat reduction and global security.

Scientific Approach and Accomplishments

During this project, we automatized the collection, analysis and deposition of protein sequences, the annotation of enzyme functions and of structural data in a library of biosynthetic clusters known to produce secondary metabolites. This class of bioactive small molecules contains non-ribosomal peptides (NRPS), polyketides (PKS), mixes of both (NRPS-PKS), also terpenes, fatty acids and further medicinal relevant natural products. For the bioinformatics part of the project, it was proposed to identify at least 10 new gene clusters encoding for biosynthetic machineries for natural product production. Instead, we used a more sophisticated approach of systematically analyzing all publicly deposited genomes of bacteria, fungi and plants. The analysis was carried out using primarily PYTHON and Perl-scripts and was compared to an adapted and heavily modified stand-alone version of the publicly available bioinformatic tool, AntiSMASH. Within the analyzed 2,831 genomes of bacterial strains, first successes are demonstrated with the identification of a total of 24,182 biosynthetic gene clusters in GENBANK-deposited bacterial and fungal genomes. Of these identified biosynthetic systems, approximately 16,500 represent the potential to produce entirely new natural products. In addition, 250 recently sequenced genomes have been made available by a federal agency. This collection represents the initial set to develop algorithms to predict the protein complex assembly and the chemical structure of the produced bioactive compounds. We programmed a searchable database with a graphical user interface that connects strain and genome information with cluster peptide sequences and structural information of the associated natural product of publicly available bacterial systems (GENBANK). We continue to expand the number of entries by including the NORINE and Merck Natural Product libraries to further improve the consistency of structural motifs used for our search algorithm and to enable a reliable prediction of the assembly orders in biosynthetic clusters. We developed a file format that is a one-cluster-per-file setup to allow cross-strain searches and alignments to identify similarity in biosynthetic processing of different natural products in different strains. This further helps to identify events of horizontal gene transfer between species and across strain families. In addition to the previously described recognition motifs (e.g. the phosphopantetheinylation site of thiolation (T) domains or the substrate recognition sites of adenylation (A) domains) in NRPS clusters, we identified short peptide sequence motifs that show high sequence similarity in all domains of a biosynthetic module in case the same substrate is processed. Homology modeling of T, A and condensations (C) domains revealed that those motifs are located on the surfaces of domains and proteins and seem to be highly conserved in their charge distribution if one particular building block is incorporated into the growing product chain. So far, these structural motifs seem to be consistently located at the interfaces of domains of an isolated module and at the proposed interfaces to neighboring modules. The identification of conserved peptide sequences, among all domains of one biosynthetic module that correspond to the processed substrate of this biosynthetic unit, suggests that a quality control mechanism to ensure the correct biosynthesis of natural products is embedded within the peptide sequence of natural product assembly lines. Although it seems necessary to ensure the correct biosynthesis of bioactive compounds, a proofreading mechanism has not been previously proposed. If we are able to prove this hypothesis for all incorporated substrate building blocks and in-trans active tailoring enzymes, then we can predict both complex formation of a biosynthetic module, even for a genetically distributed domain, and its clustering order into biosynthetic active assembly lines. In turn, this allows the prediction of the biosynthetic processing order of a natural product along its assembly line, since these clusters work in a step-by-step mechanism, and will enable us to make assumptions about the chemical structure of a natural product solely based on its genetic encoding.

We are confident that the generated information of bacterial, fungal and plant biosynthetic systems will enable the identification of new natural products and guide an informed isolation of those newly identified compounds based on predicted chemical composition and structure.

Impact on National Missions

This project supports the LANL public health mission (Homeland Security Act 2002, DOE Strategic Plan 2011, Public Health Security and Bioterrorism Preparedness and Response Act 2002) as well as its mission in global threat reduction. It also has direct appeal to our WFO spon-

sors and the base knowledge acquired can be applied to increasing efficiency of novel product synthesis to make it more cost effective. It both leverages and strengthens our capabilities in bioinformatics computing, genomic/meta-genomic analysis and isotopic enrichment in a multi-disciplinary project in support of the laboratory's missions in renewable energy, biosurveillance and biosecurity and development of countermeasures for bacterial infections under the Advanced Therapeutics Program.

Global Tree Mortality Prediction Based on Hydraulic Function Failure

Chonggang Xu
20150030ER

Introduction

Our prediction of future climate by Earth System Models (ESMs) greatly relies on how accurate we simulate the dynamics of terrestrial vegetation, which historically absorbed ~30% of anthropogenic fossil fuel carbon release. Unfortunately, recent studies have shown that current ESMs substantially underestimated the forest responses to drought. This underestimation is likely resulted from the fact that ESMs utilize carbon-based metrics of plant health to predict mortality, while our recent findings show that the universal signal of drought-caused tree mortality lies in the plant hydraulic function failure. To better predict vegetation dynamics under drought and vegetation feedbacks to climate, we propose to develop and evaluate the world's first global model of plant hydraulic failure within a DOE-Sponsored ESM. Our proposed work is built on a unique combination of LANL's world-class capabilities in dynamic vegetation modeling, drought-ecosystem research and remote-sensing-based monitoring of vegetation dynamics. The successful development and evaluation of our proposed global model will be able to provide the first global estimation of hydraulic-based tree mortality in past 112 years and for the future of this century. This tree mortality estimate will be the best in ESM history because it is based on the fundamentals of plant hydraulics and will be rigorously evaluated against the first high-resolution global disturbance database. The impact of success for our proposed research is enormous because our developed model will help improve climate projections released by Intergovernmental Panel on Climate Change (IPCC) and the tree mortality estimation can be utilized by the global communities who are concerned with vegetation changes at local to global scales.

Benefit to National Security Missions

The development of our global hydraulic model will represent an enormous step forward in our ability to predict terrestrial carbon feedback to the atmosphere, which is a key area of climatic change research in LANL's mission to mitigate the impacts of global energy demand. It will help LANL build a unique capability at the global scale, which is critical for LANL's involvement in the planned ACME (Airborne Carbon Measurements) project, DOE's initiative on a new Earth System Model. It will also enable LANL to play a stronger role in the pending DOE Office of Science's long-term program among several national laboratories ($10 million/year for 10 years), the Next Generation Ecosystem Experiment for the tropics, targeted to improve global climate predictions in ACME, the Accelerated Climate Model for Energy, which is the DOE's new Earth System model.

Progress

Hydraulic traits measurements

The tasks are finished as expected. In FY2016 we analyzed the measurement data obtained in FY2015 for xylem water retention curves (PV curves) and cuticular conductance for representatives of Boreal, Temperate and Arid zone (South West US) species. This analysis revealed that birch (Betula pendula) behaves anomalously under the standard protocol for measuring water retention curves and had to be excluded from the dataset. The anomalies are based on the observed conductivity of branches at very low water content. Under very low water content, the conductivity is normally low; however, for the birch species, we found that it can have a very high conductivity due to its fast refilling of water in stem conduits. Thus, our measurement is not representing the real conductivity at the specified water content due to the fast refilling. The values for birch could possibly be obtained via collaborators who use a different method for determining the water retention curves. Further studies on the reasons for this anomaly are conducted in collaboration with University of Helsinki. Local juniper and temperate oak also showed unexpectedly high cuticular conductance at low relative humidity and those measurements are repeated with stomatal conductance

measurements to understand the reason for the results. Excluding these anomalies, the data set for water retention curves and cuticular conductance is missing only final quality checks and almost ready to be released for modeling use.

Model evaluation metrics
The tasks are finished as needed. In FY2016, we analyzed the spatial patterns of different type of disturbances and attributed the US disturbances into harvesting and non-harvesting based on the Mat Hansen's map. We also differentiated fire from the non-harvesting disturbances based on the MTBS (Monitoring Trends in Burn Severity) fire map (http://www.mtbs.gov/). Finally, we also have drought indices to attribute the non-harvesting and non-fire disturbances into drought-induced and other type of disturbances. In summary, we have classified all the US disturbances into fire, harvesting, drought and others. The drought-induced disturbance is ready to be evaluated against model predictions.

Model development
The tasked are finished as expected. We have tested CLMED with hydraulic model in Sevelleta drought site in its capability to simulate water stress and carbon fluxes. Based on the site-level parameterization, we have applied the model for the whole SW US to identify the risk of drought-induced mortality for Pinyon pine.

Drought-risk assessment
We have identified the risk of drought impact on plant production. Based on the current 22 Earth system model predictions, we found the drought-associated reduction in plant net primary production (NPP) could increase by 2-5 times in the next one hundred years.

Future Work
For the Fiscal Year 2017, we are planning the following tasks.

- Compile all the hydraulic traits data from literature and our own measurements
- Parameterize our model globally using the complied global data on hydraulic traits
- Attribute the disturbances globally for harvesting, drought, fire and other types of disturbances
- Run the hydraulic model in DOE's Earth system model globally and test it using global transpiration data and the mortality data from our disturbance attributed map
- Assess the drought-induced carbon loss in the past and for the future.

Finally, we will finish the manuscript writing on disturbance attribution, model development and measurements.

Conclusion
The most important outcome of this project is a fully evaluated plant hydraulic function failure model at the global scale. Using this evaluated model, we will obtain drought-caused carbon loss in the past and for the future. Our laboratory measurements will provide a suite of complete datasets necessary for understanding plant hydraulics at the global scale, and our pattern-recognition approach will provide first drought-caused tree mortality dataset for model evaluations at the global scale. Finally, we will quantify the relative importance of insects versus hydraulic failure as causes of drought-induced disturbances for different regions of the world.

Publications

Christoffersen, B. O.. Linking hydraulic traits to tropical forest function in a size-structured and trait-driven model (TFS v.1-Hydro). To appear in Geoscientific Model Development .

McDowell, N., P. Williams, and C. Xu. Multi-scale predictions of massive conifer mortality due to chronic temperature rise. 2016. Nature Climate Change. 6: 295–300.

Sevanto, S., and C. Xu. Towards more accurate vegetation mortality prediction. 2016. Tree Physiology. : 10.1093/treephys/tpw082.

Wang, M., C. Xu, D. Johnson, G. Wang, and N. G. McDowell. Drought-induced tree mortality in the continental U.S. Nature Climate Change.

Wei, L., C. XU, and N. McDowell. Contrasting strategies for survival under water stress. New Phytologist.

XU, C.. Increasing drought impacts on terrestrial net primary production under future global climate change. To appear in Nature Climate Change.

Fighting Back Against Pathogens: Discovery and Validation of Novel Drug Targets

Ricardo Marti-Arbona
20150080ER

Introduction

Antimicrobial resistance (AMR) is an unavoidable effect of continuous use of antibiotics and our vulnerability to AMR is frightening. This project seeks to provide an answer to the question: "Are there any more antimicrobial targets left to be found?" and by doing so, will place LANL in the leading edge of antimicrobial research. We will develop a novel systematic approach to discover new ways to defeat AMR mechanisms in human pathogens. AMR pathogens can be defeated by finding novel antimicrobials or by deactivating the current AMR mechanism. This project addresses both paths, by developing RNA-based inducible modular regulatory elements (IMREs) that will mimic the antimicrobial effects of antibiotics. Antimicrobials act by inhibiting the activity of essential proteins and therefore creating a deleterious effect that is deadly to pathogens. IMREs will post-transcriptionally switch OFF the expression of 'putative' drug targets in response to an inducer molecule. IMREs are not antibiotics, but by mimicking the antibiotic's inhibitory action, they will identify essential proteins/genes that could be targeted for the production of novel drug chemotypes effective against AMR pathogens. As a proof of concept, we will focus on a list of 312 protein encoding genes that have been computationally predicted to be essential for the survival and pathogenicity of Burkholderia pseudomallei (model pathogen) and are not present in humans. Our overall goal is to engineer IMREs to identify and validate novel antimicrobial targets . This project creates a new capability to test and validate the suitability of a newly identified protein targets before committing major resources for characterization and drug development. Our platform will be crucial in the battle against pathogens and suitable to quickly identify drug targets in new threats, supporting national missions for biothreat reduction. Each identified target will have a high intellectual property value, and even higher medicinal significance.

Benefit to National Security Missions

This project builds capabilities required to address the Grand Challenge in complex biological systems: Bio-Security and Global Health Science, which seeks to develop therapeutic interventions to counter natural and man-made bio-threats. There is wide recognition that the discovery of new antimicrobial therapies is not keeping pace with the worldwide spread of antimicrobial resistance (AMR) and that AMR is now a serious threat to humans. The DoD (specially DTRA and DARPA) and DHHS (specially CDC and NIH) has been a leader in recognizing and protecting against the spread of AMR organisms. This project provides the proof of concept necessary to acquire funding from agencies including DTRA, DARPA and NIH to continue basic research on antimicrobial development.

Progress

We have been working on the validation of the use of Inducible Modular Regulatory Elements (IMREs) to post-transcriptionally switch OFF the expression of 'putative' drug targets genes. To summarize the FY 2015 accomplishments, we have validated the technique by switching off known antimicrobial resistance mechanisms in B. thailandensis. We have successfully targeted the gene (AmrA) encoding for one of the pump components that confers Gentamycin resistance and the gene (RecA) known to aid in the Ciprofloxacin (Cipro) antibiotic resistance for B. thailandensis and B. pseudomallei using IMREs. We confirmed the activity of the IMRE's in clinical isolate B. thailandensis CDC27211212 as well. In FY2016 we have finalized the development of two computational tools: The first allow the translation of a list of 'putative' antimicrobial protein targets from one organism to another; and the second identify unique nucleotide regions specific to the mRNA encoding for each of our 'putative' antimicrobial protein targets. We have applied both tools to B. thailandensis and S. typhimurium SB300 to obtain a detailed library of the IMREs that will control each

of their 'putative' antimicrobial protein targets. We have screened for the essential genes in B. thailandensis and S. typhimurium SB300 by transforming the libraries of all IMRE's and by assessing their impact on bacterial growth. We have started the patent application process and have recently received a positive email from The Laboratory Invention Disclosure Review Board (IDRB) stating that our IDEA 15-00097 / S133363 "RNA-based antimicrobial drug target discovery" will be filed as a provisional US patent application. We are currently in the last steps to finalize the results necessary to complete the final US patent application.

Future Work

Our overall goal is to engineer and apply Inducible Modular Regulatory Elements (IMREs) to identify and validate novel antimicrobial targets that are critical to pathogen's survival and antimicrobial resistance (AMR). The specific tasks for the fiscal year 2017 are the following:

Screening of essential genes in B. thailandensis and Salmonella

1. Validate the in vivo activity of our IMREs towards the post-transcriptional down regulation of the expression of essential genes by assessing the growth impact of the IMRE activity.
2. Correlate IMREs activity to the antibiotic's activity.

Development the technique automation

1. Robotic automation of the process of assessing the growth impact of the IMRE activity.

Assessment of the predicted 'putative' antimicrobial protein targets in the CDC stain of B. thailandensis and Salmonella

1. Correlate IMREs activity to the antibiotic's activity.

Conclusion

This project develops the technology to define novel protein targets for new drug chemotypes effective against antimicrobial resistance (AMR) pathogens. We will focus the initial discovery and validation of novel drug targets in Burkholderia because of its wide resistance to antibiotic therapies, high mortality and potential use as biological warfare agent. We will design, validate and apply RNA-based inducible modular regulatory elements (IMREs) to post-transcriptionally down regulate expression (thus inactivating them) of 312 protein encoding genes that are predicted to be critical to pathogen's survival and AMR. This will validate their usefulness as antimicrobial drug targets.

Enhanced Photosynthesis through Carbon Concentrating Mechanisms

Scott N. Twary
20150226ER

Introduction

This project will develop innovative methods for improving photosynthetic efficiency. It will be the first demonstration of chloroplast transformation in an algal production strain. The results will further define the critical role that specific enzyme structures perform in folding and pyrenoid structure formation. Key components required for pyrenoid functionality will be identified. The expression of the complex carboxysome structure requiring ten genes will be a significant advancement in designing and creating functional multi-component systems in chloroplasts. The improved carbon assimilation efficiency gains will have significant impact and applications to many photosynthetic production systems including plants and algae. Isotope models will be developed to define the system characteristics which will also establish a basis for further characterizing carbon utilization in many biological systems currently not studied.

Benefit to National Security Missions

Sustainable algal biofuel production requires increased rates of biomass production as defined by EERE BETO's productivity models. This work directly addresses this major limitation to the algal biofuel industry. Additional benefits would address the major cost of nutrient inputs by increasing nitrogen use efficiency potential. Successful creation of these biophysical structures in algae will also identify potential for increasing crop plant productivity in a similar manner. This will impact USDA goals for renewable cellulosic supplies and food production. Successful demonstration of functional biophysical structures coupled with isotope fractionation models will develop the basis for effective improvements in photosynthetic efficiency with related significant productivity impacts.

Progress

The green algae Nannochloropsis salina has been identified as a potential biofuel production strain due to its high oil production. Increasing the efficiency of algal production by a combination of genetic and cultural improvements is an important aspect towards economically viable biofuel production. The goal of our project is to engineer Nannochloropsis for enhanced photosynthetic carbon fixation. The photosynthetic carbon assimilation is a key determinant of biomass yield in algae. We have developed a biolistic gene gun chloroplast transformation system for Nannochloropsis to create designer hybrid ribulose bisphosphate carboxylase oxygenase (RuBisCO) proteins. RuBisCO is a two subunit protein catalyzing CO2 fixation. The small subunit is theorized to be responsible for formation of biophysical carbon concentrating structures called pyrenoids. The pyrenoids can enhance CO2 concentrations around RuBisCO 40X. Nannochloropsis does not form pyrenoids and we have discovered it is very leaky for CO2 retention in the cell. We have developed and utilized stable isotope discrimination tools to characterize and model CO2 dynamics in Nannochloropsis under both carbon saturating and carbon limiting conditions. During photosynthesis, RuBisCO preferentially fixes 12CO2 (CO2 with the carbon 12 isotope) instead of 13CO2 (CO2 with the carbon 13 isotope), resulting in different isotope signatures in algae under different conditions. We have successfully used this natural abundance 'fractionation' of carbon isotopes during photosynthesis to determine the conditions under which RuBisCO is saturated. We have measured the biomass, media, and headspace carbon isotope signatures under diverse carbon environments. These results are the first ever to measure theoretical saturation conditions in algae cultures. We anticipate that this powerful isotope tool will be incorporated into most of our future algal improvement programs for diagnosis and characterization. A manuscript describing this work has been submitted to a peer-reviewed scientific journal. The carbon starvation measurements have also implicated a metabolic shift during low CO2 conditions. The primary carbon source switched from CO2 to bicarbonate suggesting a limited carbon concentrating response

(CCM) in Nannochloropsis. We are currently genetically characterizing this CCM response to further understand its regulation and enhance its impact.

We have designed and developed an extensive molecular toolbox for genetically engineering Nannochloropsis chloroplast and nuclear genomes. We have created plasmid vectors directly targeting RuBisCO replacement by homologous recombination in the chloroplast resulting in differing selectable resistance schemes. We have also designed polycistronic nuclear vectors for expressing up to 4 genes concurrently. These plasmids contain fluorescent reporters and two antibiotic resistance genes for multiple genetic combinations. To improve the carbon use efficiency of this biofuel production strain we engineered a hybrid RuBisCO in an attempt to create pyrenoid structures. We identified a closely related algae species, Heterosigma akashiwo, known to produce pyrenoids. We genetically cloned the small subunit of RuBisCO from Heterosigma akashiwo and transformed it into Nannochloropsis to begin to engineer pyrenoid formation. We have successfully identified transformants containing the Heterosigma small subunit in Nannochloroposis resulting in hybrid RuBisCO protein. Chloroplasts contain multiple (tens) copies of their genome and require generations of selection pressure to achieve homoplasmy where all copies are identical. We have designed multiple selection schemes to vary the transformant selective pressure to achieve homoplasmy. We are currently screening engineered lines for carbon use efficiency, growth, biomass, and pyrenoid formation. Four potential accessory proteins have been identified in other pyrenoid forming algal species that may assist in pyrenoid folding or function. We have cloned these proteins into our transformation vectors including CIA6, LCIA, LCIB, and LCIC. We have transformed these proteins into the nuclear genome for expression and transport of the protein into the chloroplast. Since each of these accessory proteins do not have a well characterized biological function, we have expressed them individually to determine potential metabolic responses. We will then stack them together into one transformant line with the hybrid RuBisCO line to optimize pyrenoid function. We are currently awaiting transformant screening confirmation for each of these lines.

Future Work

Goal: Design an effective chloroplast transformation system for chloroplast targeted gene replacements to study protein sequence effects on pyrenoid folding and carboxysome formation.

Task 1. Create ribulose bisphosphate carboxylase replacement transformants. Create hybrid ribulose bisphosphate carboxylase transformants for pyrenoid initiation.

Task 2. Optimize pyrenoid folding by engineering accessory proteins into the hybrid lines for maximizing pyrenoid carbon assimilation efficiency.

Task 3. Create and verify homologous transformation in Nannochloropsis. Verify algae colonies growing under positive selection pressures by PCR, qPCR, and /or protein expression.

Task 4. Engineer the multi gene carboxysome operon into Nannochloropsis for expression of functional carboxysomes for maximum carbon localization around RuBisCO.

Goal: Identify responsive carbon isotope parameters for wild type Nannochloropsis.

Task 1. Develop Piccaro analysis techniques for native algae cultures under differing environments. This analysis will be used to characterize carbon use and efficiency. Measure real-time carbon dynamics under carbon starved and carbon saturating conditions to model algae responses and carbon use efficiency.

Task 2. Determine biomass and real-time gas isotope fractionation characteristics differing under varying environmental conditions. Isotope fractionation of biomass determines the final carbon fixed after complex interactions under different environments. This data will establish the basis for developing models describing the improvement mechanisms to carbon use efficiency engineered in. Measure the improved carbon use efficiency of engineered lines.

Task 3. Determine the genetic components of the Nannochloropsis carbon concentrating mechanism.
Conclusion

The project goals are to engineer biophysical carbon concentrating structures into the algal biofuel production strain, Nannochloropsis salina. These structures will increase photosynthetic efficiency by significantly concentrating carbon dioxide around the primary assimilating enzyme, ribulose bisphospate carboxylase/oxygenase reducing the wasteful oxygenase competing reaction. This process is the main route of carbon fixed into cells and will result in increasing potential biomass production rates and nutrient use efficiency. We will determine changes in carbon use through the modeling of enzyme isotope discrimination. This technology will impact sustainable algae and plant production system by increasing productivity with fewer inputs.

Ocean Acidification Over the Last 13,000 Years

Julianna E. Fessenden-Rahn
20150242ER

Introduction

This project will use LANL's 1280 Cameca Secondary Ion Mass Spectrometer (SIMS) to measure elemental and isotopic signatures on planktonic foraminifera shells to reconstruct oceanic pH, oxygen, temperature, and salinity over the last 13,000 years. We will use archived sediments taken from Santa Barbara Basin - upwelling zone in coastal California and pick planktonic foraminifera from the last 200 years (strong anthropogenic) and from the Younger Dryas (11-12.5 kybp; cold period with strong upwelling). We will measure pH proxies (B/Ca, B isotopes), temperature and salinity proxies (oxygen isotopes, Mg/Ca ratios), and redox proxies(U/Ca, Va/Ca ratios) in the shells of these foraminifera at a ~ 30 micron spot size allowing us to do these analyses on one single foraminifera shells (cutting edge, never performed before). This will eliminate diagenesis impacts on the chemical signatures/proxies, minimize chemical blank issues, and avoid dissolution and separation chemistry typically needed in traditional 20-50 shell aggregate measurements. This will also allow for determining the annual range of these parameters because each foram shell represents only a time frame of a few weeks.

High potential science: Accurate chemical data on current and historic oceanic pH, temperature, oxygen levels, and salinity will give predictive capabilities for future climate change/anthropogenic impacts on fisheries, commerce, transportation, and energy infrastructures. The program will unravel the mechanisms of oceanic pH changes and give parameters or boundaries on what we should expect in biological and chemical responses to continued acidification of the oceans.

Technology/Engineering advances: This project advances the 1280 Cameca SIMS analysis capabilities and methodologies to measure few-micron, multiple elemental and isotopic signatures on mixed/heterogeneous materials. It will advance the instrument in its use on nuclear, particle, explosive, biological, chemical materials.

Benefit to National Security Missions

This basic science project focuses on experimental analysis of chemical signatures in the oceans that will give information on climate change and impacts to local and global biological systems (fisheries, coral reefs, crustaceans) and anthropogenic infrastructure (bridges, oil platforms, peers). This research will develop LANL's 1280 Cameca Secondary Ion Mass Spectrometer (SIMS) to be able to analyze isotopic signatures and Laser Ablation Inductively Coupled Plasma Mass Spectrometry (LA-ICP-MS) to analyze elemental signatures of foraminifera shells. These chemical signatures will give direct information on past oceanic pH, oxygen levels, temperature, and salinity - all essential parameters for biological sustainment. The method development for the SIMS will help develop this tool and methods to be used in material interrogation of nuclear, particle, explosive, biological, wastes. The project will directly focus on climate impacts to energy, infrastructure, commerce by using fundamental chemistry signatures to understand material response to ocean acidification. The potential sponsors who will benefit from this project directly are: DOE - Office of Science, DOI, DOT, DOC. The potential sponsors who will directly benefit from the SIMS development are: NNSA, DoD, NASA, DHS, IC communities.

Progress

In FY16, we accomplished the following tasks:

- Conducted the d18O analysis on the Wisconsin SIMS instrument - analyzed 400 samples from 4 cores from SBB at 10 different time zones expanding the last 2000 years as well as over 250 years in the Younger Dryas period.
- Conducted the Ca, Mg, U, B analysis on the same foraminifera as the d18O measurements so we have elemental ratios of temperature, Oxygen, and pH proxies to compare to the d18O data. All of this data was made through LA ICP-MS analysis and nano-

SIMS analysis so we can compare bulk to point measurements.
- Worked on the LANL SIMS instruments on d18O analysis of calcite materials. Analyzed the same standards as used in the Wisconsin SIMS analysis to have standard to standard comparisons. We optimized the LANL SIMS instrument for d18O analysis using a new optical lens to help focus the Cs beam for smaller spot sizes.
- We are in the process of writing two manuscripts (one on the d18O and Ca, Mg analysis and one on the climate change impacts of this study). We are going to present this work at the next International AGU meeting in the Fall.
- We have started conversations wtih T-3 to advance this research with DOE Office of Science program managers as well as extend this research to a more global scale looking at more upwelling zones on the western margins of North and South America, and Africa.
- We have started conversations with the Civilian Nuclear Fuel Program office to advance this research to more waste mitigation and fate and transport tracing work (DOE NE or DOE EM).

Future Work

In FY17, the tasks to be accomplished are:

- Continue to perfect the SIMS measurements on the LANL instrument. We will finish the d18O measurements on standards and shells, and then move to new materials like glasses and oxides to tie the SIMS instrument to more LANL mission related work.
- We will move to d11B analysis on foraminifera and carbonate standards on LA-ICP-MS analysis to compare to the SIMS instrument analysis.
- We will compare our d11B SIMS analysis to other University analyses on d11B for comparision of our results.

Conclusion

This project will reconstruct oceanic pH, temperature, oxygen and salinity levels of current (last 1000 years) and historic (11-12.5 kyrbp) periods to determine anthropogenic and upwelling strength impacts on ocean chemistry. The program will also determine biological response to these chemical changes and predict the impact to fisheries, commerce, transportation, and energy infrastructures (cement in the oceans). This project will also advance the SIMS instrumentation to conduct multi-elemental and isotopic analyses on single foraminifera (few micron spot sizes) which could then be used to advance material interrogation for NNSA, DoD, IC, DHS, DOE sponsors and LANL missions.

Publications

Balestra, B., I. Orland, J. Fessenden, T. Rahn, A. Paytan, and J. Valley. Comparison of different proxies using in situ measurements in the benthic foraminifera genus Uvigerina: an example from the Santa Monica Basin. 2016. In Fall American Geophysical Union Meeting. (San Francisco, CA, 12-16 Dec. 2016). , p. 1213. San Francisco: University Press.

Balestra, B., J. Fessenden, and A. Paytan. Paleoceanographic reconstructions in the Santa Monica Basin during the last 22,000 years utilizing geochemical and benthic foraminiferal data sets. To appear in Paleoceanography Journal.

Griffiths, E., M. Fantle, E. Eisenhauer, and A. Paytan. Effects of ocean acidification on the marine calcium isotope record at the Paleocene–Eocene Thermal Maximum. 2015. Earth and Planetary Science Letters. 419: 81.

Paytan, A., A. Andersson, D. Kline, and P. Edmunds. Understanding ocean acidification impacts on organismal to ecological scales. 2015. Oceanography. 25 (2): 16.

Development of pH Responsive Protein Switches to Regulate Energy Capture and Conversion Processes in Photosynthesis

Richard T. Sayre
20150322ER

Introduction

Our overall objectives are to develop novel pH-regulated protein conformational switches that will accelerate the dissipation of excess energy harvested by the photosynthetic antenna systems to reduce photodamage and increase productivity. The challenge we are addressing is accelerating the slow (2-10 minutes) induction of non-photochemical quenching (NPQ) mechanisms that dissipate excess energy captured during high light conditions to less than one minute. To achieve these objectives will require the application of theoretical approaches to characterize energy transfer pathways, protein modeling studies to design switches, and biotechnology and biophysical approaches to develop and test the products. In this project, we will:

- Develop novel pH-controlled protein conformational switches that will accelerate the dissipation of excess energy captured by the photosynthetic light harvesting (LHC) antenna protein, CP29 to reduce photodamage, increase photosynthetic efficiency, and increase biomass or bioenergy productivity.
- Develop mechanistic models and design strategies based on molecular dynamics simulations of the CP29 protein-pigment complex in model thylakoid membrane lipid environments to predict potential CP29 conformational changes and reorganization of chlorophyll-carotenoid interactions that occur during the pH-induced transition from an energy non-quenching to an energy quenching state.
- Develop a quantum model of energy quenching in photosynthetic complexes to analyze the mechanisms of pH-regulated quenching of excited chlorophylls; describe and optimize the performance of relaxation channels including fluorescence and thermal energy transfer from excited chlorophylls to protein; incorporate interactions between chlorophylls and carotenoids in the CP29 complex, and between CP29 and the photosystem II reaction center involved in charge separation.
- Engineer CP29 deletion mutants of Chlamydomonas and express an engineered CP29 protein having a range of pH-responsive, protein conformational switches that accelerate conversion to the non-quenching in high light.

Benefit to National Security Missions

The major relevant program focus is sustainable production of clean energy. This effort will strengthen and build capabilities at the interface between computational and empirical sciences particularly in the area of photosynthesis and renewable energy systems. These efforts will position LANL to be more competitive for funding from the DOE-BES, -BER, and -BETO, as well as NIH, NSF and USDA. The development of protein switch technology has broader application for the control of metabolism in many engineered biosystems.

Progress

Computational approaches were used to investigate the conformational changes in the CP29 protein due to pH changes associated with the activation of the non-photochemical quenching (NPQ) mediated by energy transfer from chlorophylls to carotenoids and subsequent thermal dissipation. Our objectives are to understand how pH-induced conformation changes affect the pigment interactions and the NPQ process and how we can manipulate the pH-induced structural changes to make NPQ processes kinetically more responsive to rapidly changing light intensities and associated pH shifts. It is believed that pH-induced conformational changes in CP29 contribute to the activation NPQ process.

We conducted molecular dynamic (MD) simulations of the CP29 complex in a thylakoid membrane mimic at full atomistic resolution at high- and low- pH. We observed that the protonation of different susceptible protein residues at the lumenal interface triggers configurational changes that affect the internal motion of the protein as

well as the orientations of chlorophylls and carotenoids. Furthermore, using a coarse-grained approach, we found that localization of the carotenoids in the membrane is dependent on the epoxidation state and the structural phase of the bilayer.

Using a combination of homology modeling and geometrical modeling tools, we generated 30 model conformations each at high- and low- pH. Each of the 60 structures was prepared for electrostatic calculations at 61 different pH levels. These structures were used to solve for the electrostatic potential around the proteins. The charge asymmetry and charge density for the solvent accessible surface for each structure was then extracted, and the low-pH conformation results were subtracted from the high-pH conformation results to determine the change in charge asymmetry or density at each pH. Based on these evaluations, we find that the optimal pH for conformational transition in wild type CP29 is 4.8 consistent with the onset of NPQ.

Finally, we used our MD simulations to identify potential mutational sites that can be targeted as pH-responsive, protein conformational switches that will accelerate conversion to the quenching state in high light. We identified multiple sites that triggers the conformational changes in the transmembrane helices of CP29. We then proposed amino acids to be substituted at these sites according to pH responsiveness. Based on these evaluations, we recommended E128H (loop rearrangement), Y135S and T177H (promote favorable Xea-Nea exchange) and E114H (loop rearrangement) as the four substitutions for the first round of experimental studies. These mutations are being engineered into algae in which all of the LHC proteins have been simultaneously down-regulated to reduce potential background NPQ activity associated with other LHC family members.

M. Merkli, G. P. Berman, R. T. Sayre, S. Gnanakaran, M. Könenberg, A. I. Nesterov, H. Song, Dynamics of a chlorophyll dimer in collective and local thermal environments, Journal of Mathematical Chemistry, April 2016, Volume 54, Issue 4, pp 866-917. This research was oriented on a generalization of the exciton transfer rate, given by the well-known Marcus formula. We present a theoretical analysis of exciton transfer and decoherence effects in a photosynthetic dimer interacting with collective (correlated) and local (uncorrelated) protein-solvent environments.

Berman GP, Nesterov AI, Gurvitz S, Sayre RT, Possible role of interference, protein noise, and sink effects in nonphotochemical quenching in photosynthetic complexes, J Math Biol. 2016 Apr 30. We analyze theoretically a simple and consistent quantum mechanical model that reveals the possible role of quantum interference, protein noise, and sink effects in NPQ. The numerical simulations show that using proper combination of quantum interference effects, properties of noise, and sinks, one can significantly suppress energy transfer to the damaging channel.

Future Work

- Submit the paper on the classical molecular dynamics simulations study on the CP29 conformational changes
- Use DFT based calculations and ab-initio MD simulations to quantify the reorganization of chlorophyll-chlorophyll and chlorophyll-carotenoid interactions that occur during the pH induced transition as observed in the classical MD simulations of CP29 in thylokoid membrane mimic.
- Probe the mechanism and regulation of the violaxanthin cycle and its dependence on the different structural phases of the thylokoid membrane
- Calculate the contribution of the vibrational spectra to the electron transfer rates in strongly and weakly coupled chlorophyll dimers in CP29.
- Model and simulate the mechanism of charge separation on the LHC-RC boundary.
- Generate algal strains that do not accumulate any of the light harvesting complex (LHC) proteins.
- Re-transform the LHC minus mutants with WT and mutagenized CP29 encoding genes. The mutants have been identified as possibly amino acid residues that may regulate the pH-dependent control of non-photochemical (NPQ) processes.
- Characterize the LHC PSII complexes, NPQ properties and photosynthetic rates of WT and mutagenized CP29 transformants in the LHC minus backgrounds.

Conclusion

We will develop MD models that describe structural changes in CP29 when the pH is lowered including changes in Chl-Chl and Chl-carotenoid distances, Chl dipoles, and related time correlation functions as a function of pH and use them to connect to QM/mathematical models enabling comparison with measured spectral profiles. We will predict, design and characterize modified versions of CP29 protein that respond to rapidly changing light intensities by more rapid changes in NPQ. These modified CP29 transgenics will have increased resistance to photoinhibitory light treatments and increased productivity and biomass yield in fluctuating and high light environments.

Publications

Berman, G. P., A. I. Nesterov, G. V. Lopez, and R. T. Sayre. Superradiance Transition and Nonphotochemical

Quenching in Photosynthetic Complexes. 2015. J. Phys. Chem C. 119: 22289.

Ferrari, , G. L. Celardo, G. P. Berman, R. T. Sayre, and Borgonovi. Quantum Biological Switch Based on Superradiance Transitions. 2014. JOURNAL OF PHYSICAL CHEMISTRY C. 118 (1): 20.

Methane Coupling Chemistry Promoted by Catalysts Containing Inexpensive Metals

John C. Gordon
20150454ER

Introduction

Current methodologies for the conversion of methane (CH4) into commodity chemicals or fuels more amenable to transportation, storage and use either depend upon high energy input (Fischer-Tropsch) or on toxic/rare metals (e.g. Ir, Hg). The emerging importance of CH4 with respect to the Nation's energy portfolio makes this an unsatisfactory scenario. To have any hope of widespread implementation, any prospective CH4 functionalization catalyst must not require extensive energy input and must not be constructed of elements such that it is prohibitively expensive and/or impossible to obtain in sufficient quantities for Global utilization.

Our specific goal in this project is to prepare molecular systems comprised of inexpensive first row transition metals that can facilitate both C-H and C-C bond coupling chemistries utilizing CH4 to produce ethane (C2H6). C2H6 is itself a precursor to ethylene (C2H4), a valuable chemical feedstock used in the production of important commodity chemicals that include polyethylene, surfactants, detergents, alcohols and others. Annual worldwide production of C2H4 was 120 x 106 tons in 2008.

Benefit to National Security Missions

In direct line with the Chemistry & Chemical Sciences ER category, this project directly addresses how to advance our understanding of the chemistry and chemical methods that directly bear upon energy security, the impact of energy production, and mitigating that impact. In this case, the chemistry focuses on how to effectively upgrade an inert, abundant and cheap molecule in the form of CH4 into a useful C2 chemical feedstock. Moving away from precious metals to first row transition metals will potentially enable us to develop a catalytic system for C-H bond activation (a necessary step in functionalizing CH4) and C-C coupling chemistries that are economically scalable. This effort will capitalize on LANL's considerable expertise in catalysis using earth abundant metals. Success will competitively position LANL for funding from DOE OBES, DOE-FE, ARPA-E, and industry.

Progress

Manganese and ruthenium containing complexes have been screened by computations for their ability to promote the desired methane coupling chemistry. We have synthesized a variety of new examples of these. The manganese systems are inherently difficult to characterize because of their paramagnetic nature (no useful NMR resonances), although we have been able to structurally characterize an example of an amine-amide complex as a Lewis base adduct, due to its lack of solubility in non-coordinating solvents.

In order to complement this difficult manganese based chemistry, in parallel, we have moved to ruthenium based systems, partly because computations suggest that they can support the desired methane coupling chemistry and partly because many of these are diamagnetic and thus provide us with a spectroscopic handle (in the form of NMR spectroscopy) with which to understand structure and reactivity. We have characterized a number of these systems, although they tend to form bis-ligand rather than mono-ligand systems, which are our targets.

Future Work

We will begin the next FY by synthesizing and spectroscopically characterizing targeted phosphine and amine -amide complexes that have recently been identified as potential catalysts. The structural and magnetic properties of some of these complexes will also be used to benchmark DFT functionals and basis sets in order to determine the combination that most accurately describes the physical and electronic structure of complexes being used in this work without undue computational cost or compromising numerical accuracy.

Conclusion

The primary result from successful completion of this project will be experimental demonstration of each of the steps along the catalyzed pathway for conversion of CH_4 into C_2H_6.

While our ultimate goal is catalytic C_2H_6 production, even stoichiometric conversion of CH_4 to C_2H_6 would be a significant accomplishment.

Fundamental Actinium Science In Search of Radiotherapeutics

Eva R. Birnbaum
20150575ER

Introduction

We propose a multi-disciplinary effort to enable the rational design of actinium-225 complexes for targeted radiotherapy treatment of cancer. Actinium-225 is one of the most promising isotopes identified for use in targeted alpha therapy of cancer, a treatment strategy that utilizes high-energy alpha particles to selectively eradicate malignant tissue. The greater widespread clinical utility of 225Ac is hindered by radiotoxic side effects that result from detachment of the radiometal from its biological delivery vector. The design of ligands that effectively sequester actinium under biological conditions, however, has been impeded by a lack of fundamental knowledge of this rare, highly-radioactive element. The proposed work will launch, for the first time, a comprehensive investigation of the chemical and electronic properties of the element actinium in support of rational design of actinium ligands for medical use. The chemical hardness, coordination number, and covalency of actinium ions in solution will be determined. Preliminary data obtained with the stable analog lanthanum and a heavier actinide (plutonium) reveal that fluorescence spectroscopy and grazing incidence X-ray absorption spectroscopy can probe these important chemical properties while exhibiting high sensitivity for the detection of the extremely low concentrations of actinium available for investigation. In addition, density functional theory (DFT) calculations will be employed to interpret the spectroscopic data. With understanding of the electronic structure and basic chemical properties of actinium, rational ligand design will be pursued in the service of clinical use of 225Ac-containing compounds, which we hope can save lives.

Benefit to National Security Missions

An improved understanding of the fundamental chemistry of actinium is essential to the clinical use of 225Ac for the therapeutic treatment of disease, in particular malignant disease. The nature of the facilities required to produce large amounts of 225Ac ensures that only domestic facilities currently operated by the Department of Energy Office of Science have the capability to meet anticipated research demand for the isotope, if it can be shown functional in viable clinical trials. Among the National Institutes of Health's primary mission is the fight against cancer, and 225Ac's potential to incite a paradigm shift in treatment of this destructive disease in many forms is well recognized by the scientific community. We anticipate that our research into fundamental principles that govern the chemical bonding of actinium to biological vectors will catalyze further biological research, clinical trials supported by DOE isotope production infrastructure, and ultimately widespread, curative use of 225Ac in patients.

Progress

Over the past year, several EXAFS (Extended X-Ray Absorption Fine Spectrum) measurements have been made on Ac-227 solutions and this methodology is proving to be extremely successful for obtaining structural information about simple actinium complexes in solution. A number of key actinium compounds have been measured: actinium in water (which required significant preparation to remove any other potential ligands), actinium DOTA (tetraazacyclododecane-1,4,7,10-tetraacetic acid, a common compound used to bind a variety of metals) in acetate buffer, and actinium in concentrated hydrochloric acid (HCl). The methodology to analyze EXAFS data in combination with a theoretical approach (Molecular Dynamics DFT calculations) have been benchmarked with americium compounds. The analysis is complete for a comparison of americium in water, americium in concentrated HCl, and actinium in concentrated HCl. Results indicate that the actinium ion may prefer softer ligands than previously proposed, which would impact the design of future ligands. These results have been accepted for publication in Nature Communications. Further effort will be focused on studying

actinium with different chelates, both commercially available and synthesized for the project. This study will help us to identify actinium preference for soft or hard donors and the size of an optimized binding pocket.

In addition to X-ray based methods utilized in years 1 & 2, in year 3 the spectroscopic studies of Ac will be expanded to include a variety of other methodologies. Due to the spectroscopic innocence of Ac, we have decided upon a strategy of using strongly absorbing lariat crown ethers to facilitate these measurements. Synthesis of several prototype chromogenic containing lariat crown ethers has been completed, including phenol and catechol containing crown ethers. An efficient high-yielding synthetic route has been identified, which will enable the synthesis of several other modifications with minimal effort. With these new chromogenic chelates we have begun binding studies with Ac-225, Bi-207, and Lu-173 to compare differences among trivalent metal ions. In addition to tracer studies, spectroscopic measurements have been made with cold metals, including NMR and UV-Visible-NIR spectroscopy in order to identify the spectroscopic signatures of metal binding.

Future Work

In year three we plan to beginUV-Vis and other spectroscopic measurements utilizing our stock of Ac-227. In order to facilitate these measurements, techniques which are specific for very low volumes (<100 uL) will be used, allowing for the use of reasonable concentrations of Ac-227. These measurements will be contrasted with those obtained from studies of other trivalent metal ions, including both stable metals and actinides. From this basis of knowledge we will make modifications to the crown ether framework, determining how modifications on the crown ether cavity size, denticity, and ligand softness effect the metal-ligand binding. This will continue to build upon the relatively limited knowledge of Ac coordination chemistry, facilitating effective chelate development for the use of Ac as a radiopharmaceutical.

We will also continue to expand the XANES and EXAFS data sets for other simple actinium complexes. Building on the Cl data set just published, we will continue the analysis of collected data of the aquo complex. Further, data will be collected on DOTA (tetraazacyclododecane-1,4,7,10-tetraacetic acid) and HOPO (octadentate hydroxypyridinonate) complexes with actinium, to be compared with the acetate data collected in year one. A small amount of Ac-HOPO will also be sent to a new collaborator at LBNL who will use their own existing funding to attempt to collect a crystal structure of this complex inside a protein. These measurements will provide additional basis for analyzing more complicated actinium compounds ligated by the lariat crown ethers or other more complex ligands.

Conclusion

The proposed work will elucidate fundamental chemical properties of the element actinium to enable the rational design of actinium-225 complexes for targeted alpha therapy. A better understanding of the element, actinium, will allow application of the specific therapeutic isotope, actinium-225, in medicine for treatment of cancer.

Publications

Ferrier, M. G., E. R. Batista, J. M. Berg, E. R. Birnbaum, J. N. Cross, J. W. Engle, H. S. La Pierre, S. A. Kozimor, J. S. Lezame Pacheco, B. W. Stein, S. C. E. Stieber, and J. J. Wilson. Spectroscopic and computational investigation of actinium coordination chemistry. 2016. Nature Communications. 7: 1.

Wilson, J. J., E. R. Birnbaum, E. R. Batista, R. L. Martin, and K. D. John. Synthesis and Characterization of Nitrogen-Rich Macrocyclic Ligands and an Investigation of Their Coordination Chemistry with Lanthanum(III). 2015. INORGANIC CHEMISTRY. 54 (1): 97.

Wilson, J. J., Ferrier, Radchenko, J. R. Maassen, J. W. Engle, E. R. Batista, R. L. Martin, F. M. Nortier, M. E. Fassbender, K. D. John, and E. R. Birnbaum. Evaluation of nitrogen-rich macrocyclic ligands for the chelation of therapeutic bismuth radioisotopes. 2015. NUCLEAR MEDICINE AND BIOLOGY. 42 (5): 428.

Advancing Regenerative Medicine with Trinity: Defining a New State-of-the-Art for Biomolecular Simulation

Karissa Y. Sanbonmatsu
20150755ER

Introduction

Regenerative medicine offers the promise of generating replacement tissues and organs that are a perfect genetic match for the patient, alleviating the need for organ donors. Many regenerative therapies are based on stem cells, which are cells with the potential to be converted into any cell type in the body (e.g., eye, lung, brain, heart, etc.). Understanding exactly how to control the conversion of a stem cell into another type of cell is critical for therapeutic application. For example, one group has already succeeded in converting stem cells into dopamine-producing cells, resulting in a new treatment for Parkinson's disease in mice. A second group has converted stem cells into retinal pigment epithelial cells and used them recover vision in patients with macular degeneration, a common cause of blindness. Market Research Reports estimates that the market for regenerative medicine will grow from $16B (in 2013) to $67B in 2020. Pfeizer, GlaxoSmithKline and Johnson&Johnson have already made major investments in treatments for Alheimer's, Parkinson's and heart disease. A wide range of degenerative diseases remain potential targets for stem cell therapy and regenerative medicine; yet, converting stem cells into the appropriate specialized cell type remains a mystery. Current efforts in regenerative medicine have been largely spearheaded by trial-and-error strategies. Cell division is one of the key processes. Here, chromosome material (consisting of DNA threaded around thousands of molecular spools) undergoes a 70-fold collapse in volume from an extended form to a highly compact form. The atomistic details of this large-scale process have never been studied. LANL has the opportunity to become the leader in atomistic studies of this process, which is critical for stem cell programming and regenerative medicine.

Benefit to National Security Missions

In 2002, we were able to take the lead in biomolecular simulation, performing the first million atom simulation and the first simulation of the ribosome, approximately 8 times larger than any previous simulation. We now have the opportunity to reclaim the lead by performing a simulation 3 times larger than the largest to date. In addition, our collaboration with the GENESIS team gives us the opportunity to maintain this lead. While GENESIS scales to >200,000 cores, the next best scaling biomolecular simulation scales to ~10,000 cores. Expertise with GENESIS will allow us to continue to push the envelope. In addition, performing the large-scale simulations will build general capabilities for other applications in the area of enzyme optimization, nanoparticle clusters, and nanowires. The project is also directly related to understand how Anthrax infections alter host epigenetic programs. Biomolecular simulations are often more complex than atomic simulators used in materials science. Thus this work supports our national security mission in biosecurity, biosurveillance and human health, as well as enhancing our capability in information science and technology.

Progress

Significant progress was made toward preparing for the arrival of the full Trinity Phase 2 machine. The central goal of this project was porting and optimizing the GENESIS code to Trinity. We have compiled and run GENESIS on the B0 platform.

We have optimized GENESIS in terms of run time options, compilers and vectorization. We have identified hotspots. We have performed small scaling tests and find that 4 threads per MPI rank is about optimal. With 72 processors, the package would run at 18 PEs.

The next step is to optimize scaling once we have access to a large number of nodes. We have completed and published an initial condition for the simulations.

We are in the process of hiring a post-doc from the GEN-

SIS team. We have established synergy among the team, consisting of groups from LANL (Sanbonmatsu, Daniels, Tung, Wall and Adedoyin), RIKEN (Sugita, Jung and Nishima) and NYU (Schlick and Bascom). We have had several face-to-face meetings between the groups. Schlick and Sanbonmatsu presented at the Energy Landscapes CNLS conference in Santa Fe.

Additionally, in FY16 we published a paper on Hierarchical Looping of Chromatin Fibers Near Gene Regulatory Elements in the Journal of Physical Chemistry-B.

Future Work

For the next three months, we plan to optimize scaling to larger numbers of processors once these systems are available at LANL. We will also perform test simulations on our benchmark systems including the ribosome. We will also solvate our initial condition and perform early minimization and molecular dynamics. Once October begins, we will perform preliminary production runs and gradually ramp up to full production in anticipation of the arrival of the full phase 2 system.

Conclusion

A wide range of degenerative diseases remain potential targets for stem cell therapy and regenerative medicine; yet, converting stem cells into the appropriate specialized cell type remains a mystery. Current efforts in regenerative medicine have been largely spearheaded by trial-and-error strategies. Cell division is one of the key processes, but the atomistic details of this large-scale process have never been studied. We will perform the first atomistic simulations of condensation of chromosome material from an extended state to a condensed state. This will define a new state-of-the-art in biomolecular simulation, in terms of the number of cores used in a single simulation. In addition, performing the large-scale simulations will build general capabilities for other applications in the area of enzyme optimization, nanoparticle clusters, and nanowires. The project is also directly related to understand how Anthrax infections alter host epigenetic programs.

Publications

Bascom, G. D., K. Y. Sanbonmatsu, and T. Schlick. Mesoscale modeling reveals hierarchical looping of chromatin fibers near gene regulatory elements. 2016. The Journal of Physical Chemistry B. 120 (33): 1238.

Development of a Continuous Flow Reactor for the Conversion of Biomass Hydrolysates to Fuels and Feedstocks

Andrew Sutton
20160095ER

Introduction

The current approach to make fuel from biomass typically requires high temperatures (> 350 oC) and pressures (> 55 bar) using precious metal catalysts and then requires further refining to generate a fuel. We have developed routes to transform biomass into alkanes under substantially lower operating conditions (20.7 bar H2, 100 oC) using nickel and solid acid catalysts in high yield. These have been studied as batch reactions and in order to move towards economical, industrial-scale fuel synthesis we need to demonstrate the process in a continuous flow system and begin to develop a process flow-sheet and economic analysis. Commercial viability of this process hinges on reaction engineering and the fundamental understanding of the reaction kinetics as a function of processing variables (pressure, temperature, space-time, concentration etc.). We will develop kinetics rate models that will be used to identify process optimization pathways related to conversion, selectivity, yield, catalyst durability and ultimately cost and efficiency. The ultimate goal is to advance of our science discovery (currently TRL 3) to a viable, commercializable process to sustainably produce biomass derived liquid fuels (expected TRL 6/7).

Benefit to National Security Missions

This project will demonstrate the production of biofuels and commodity chemicals using a continuous flow reactor at very low temperatures in highly efficient reactors to address the Renewable Fuels Standard (RFS2) and to provide low green house gas fuels to the consumer. This work directly supports our mission in energy security and will benefit defense applications.

Progress

Initial work was carried out on improving the conditions and catalyst system for the separate parts of the hydrodeoxygenation (HDO) mechanism of biomass – this is the conversion of the ketone to an alcohol and the removal of the alcohol using solid acidic catalysts. Initial reactions used 5-nonanone as a model compound. Classic heterogeneous reduction catalysts – palladium supported on carbon (Pd/C), palladium supported on alumina (Pd/Al2O3), copper supported on silica (Cu/SiO2) and nickel supported on a mixture of silica and alumina (Ni/SiO2.Al2O3) – were investigated for their activity at similar conditions in batch reactions as reported previously (200 °C, 200 psi H2). It was found that Ni/SiO2.Al2O3 performed as well as the palladium-containing catalysts, achieving 90% conversion within an hour.

A number of solid acids were investigated for their catalytic activity for the removal of the alcohol species present in 5-nonanol (model compound for the intermediate in the oxygen-removal mechanism). These include acidic resins Amberlyst-15, Amberlyst-26 and Nafion, the acidic zeolite HZSM-5, as well as the crystalline compounds zirconia and alumina. Running the batch experiments at a range of temperatures, it was found that HZSM-5 can achieve complete conversion within 15 minutes at 150 °C, and within 10 minutes at 190 °C, though it is relatively inactive at lower temperatures. Combining the reduction and dehydration catalyst (Ni/SiO2.Al2O3 & HZSM-5) in a one-pot reaction with 5-nonanone at 200 °C and 200 psi H2, nonane was found to be the only product formed after an hour. This uses vastly cheaper catalysts in much faster reactions that our previous work (1 h vs >12 h).

After batch conditions and catalysts systems were optimized, initial tests were carried out on a continuous flow reactor (capable of processing ~1 L day-) for the separate stages of oxygen removal – dehydration and reduction. It was determined that HZSM-5 can completely remove the oxygen from 5-nonanol within a 6 minute space-time (time substrate spends in contact with catalyst), improving on the 10 minutes observed in batch. Conversion of 5-nonanone to 5-nonanol with Ni/SiO2.Al2O3 was found to reduce the ketone to an alcohol, and also remove the oxygen completely, converting 96% of the starting prod-

uct and producing nonane with 95% selectivity in a 3.3 min space time. Both conversion and selectivity reached 100% when the space time was increased to 10.1 min. This is a significant increase versus out initial 12 hour reaction time to perform this transformation and uses a catalyst system composed of abundant and cheap materials (Ni [$77/kg] vs Pd [$28000/kg]) and in a much shorter reaction period than has been reported previously (10 min vs. >12 h).

In addition we have been developing a state of the art predictive model for the determination of fuel properties from fundamental principals and this is significantly more accurate than the current model. This could prove to be a very valuable resource for the community. This is being coupled with a blending model for the prediction of how biofuel components act as blends with gasoline and diesel which could also be a significant tool for developing bio-blends.

Future Work

- Develop modular flow reactor and screen conversion of advanced bioderived molecules
- Optimize routes for the production of fuels and chemicals from aldol condensation reactions
- Perform initial process and economic analysis of conversion approach

Conclusion

The results of this research will be the characterization of the biomass catalytic upgrading process as a function of reaction engineering variables and reactor operating conditions. In addition, these results will be used to establish a process flow-sheet and preliminary economic analysis. The overall goal will be to produce mL quantities of fuel or fuel additive for future engine testing. This work directly supports our mission in energy security and will benefit defense applications.

Publications

Jenkins, R. W., C. M. Moore, T. A. Semelsberger, C. J. Chuck, J. C. Gordon, and A. D. Sutton. The effect of functional groups in bioderived fuel candidates. 2016. ChemSusChem. 9 (9): 922.

Sutton, A. D., C. M. Moore, R. W. Jenkins, M. T. Janicke, W. L. Kubic Jr., and E. Polikarpov. The use of acetone as a bio-derived building block for the simultaneous production of chemicals and fuels . ChemSusChem.

Investigations of the Magnetic Characteristics of Iron-Only Clusters

John C. Gordon
20160255ER

Introduction

The research herein outlines the development of new iron (Fe) clusters as these molecules have the potential to behave as single molecule magnets (SMMs). SMMs have been the target of chemists and physicists since the 1990s because of their potential applications in quantum computing, high-density information storage, spintronics and magnetic refrigeration. Iron has a number of attractive properties for such applications, including its low-cost and various physical properties.

Benefit to National Security Missions

The goals of this proposal are directly in line with maintaining and strengthening Laboratory scientific capabilities in theory, computation and modeling, and experimental chemistry that form the foundation for understanding new synthetic materials. Correlating the molecular structures of iron based clusters materials with their electronic structures and magnetic properties will be crucial in optimizing these systems for applications as Single Molecule Magnets. Developing new molecules and materials that do not depend on Rare Earth elements is also a priority for DOE. The expected properties of these molecules may lend themselves to applications important to the Laboratory (e.g. in quantum computing and high-density information storage using spintronics). The use of spintronics technologies could potentially revolutionize the electronics and computing industries by making it possible to store vastly more data in devices than is currently possible. Efficient spintronics technologies could also mean huge energy savings.

Progress

This past year, we have been working on optimizing the synthesis of an Fe9 cluster supported by phosphine ligands. This was a species that we serendipitously isolated in another unrelated set of chemistries. In order to characterize its magnetic properties, we needed to have a reproducible and scalable synthesis of this compound, which we believe that we now have.

This species has been characterized using a variety of magnetic field techniques and appears to exhibit some very interesting magnetic properties that may be as a result of the triangle of Fe irons that are connected to each other within the core of the cluster molecule. The detailed magnetic characterization of this molecule is ongoing, as it is important to know what effect that supporting ligands have on the magnetic properties of species such as this relative to the corresponding “naked” metal atom clusters that have been magnetically characterized in the gas phase, but cannot be physically isolated like we can using solution chemistry approaches.

Future Work

In FY17, we will synthesize more examples of Fe-core complexes and use a variety of physical techniques to characterize these molecules. We will computationally investigate target complexes via electronic structure calculations so that theoretical predictions can be made as to their physical and magnetic properties. Correlations will be made between experimental and computational work in order to validate and improve on our theoretical models. Optimized computational models will then be used to guide synthetic targets and strategies towards these. The magnetic characterization of a currently synthesized species will continue. A variety of magnetic techniques will also be applied to new clusters as they are made and isolated.

Conclusion

The expected high magnetic spins of these clusters may lend themselves to applications such as quantum computing and high-density information storage using spintronics. The use of spintronics technologies could potentially revolutionize the electronics and computing industries by making it possible to store vastly more data in devices than is currently possible. Efficient spintron-

ics technologies could mean huge energy savings due to the fact that reversing the electronic spins in such systems would require less power than the normal electronic charge. This work will build capabilities in theory, computation and modeling, and experimental chemistry that form the foundation for understating new synthetic materials.

Molecular Actinide Nitrides

Jaqueline L. Kiplinger
20160261ER

Introduction

The goals of the research outlined in this proposal are (1) the development of synthetic routes to the first molecular actinide diazide complexes and (2) the conversion of these azides to nitrides using reduction chemistry, thermolysis, and photolysis. Actinide nitrides [An≡N]x (where An = Th, U, Np, Pu) are candidates for accident tolerant nuclear fuels that have great potential for the expanding future of nuclear power. For example, binary uranium nitride [U≡N] is regarded as a superior material over uranium oxide fuels due to its higher melting point, higher thermal conductivity and increased density, whereas neptunium and plutonium nitrides have been proposed as attractive transmutation fuels. However, for both ceramic and molecular actinide nitride systems, few synthetic routes exist for their preparation, and next to nothing is known about their chemical behavior. The development of a fuel cycle involving any actinide nitride will require this basic information for the safe processing, preparation, use, storage, treatment, and eventual disposal of the used nuclear fuel. Recent advances in our laboratories have provided new insights for addressing important aspects within this knowledge gap using a molecular chemistry approach. In this work, we aim to develop routes for the synthesis of previously inaccessible thorium, uranium, neptunium and plutonium diazide complexes, then employ reduction chemistry, thermolysis, and photochemistry to generate their corresponding nitrides. In this pursuit, we will use previously unexplored reduction chemistry to prepare nitride-bridged bimetallic systems, An-N-M (An = Th, U, Np, Pu; M = Zr, Ir, U), where the nitride is bound to both an actinide and another metal. We anticipate that these new bimetallic complexes will provide valuable information about how actinide nitrides interact with other metals found in cladding material.

Benefit to National Security Missions

The goals of the research outlined in this proposal are (1) the development of synthetic routes to the first molecular actinide diazide complexes and (2) the conversion of these azides to nitrides using reduction chemistry, thermolysis, and photolysis. Actinide nitrides [An≡N]x (where An = Th, U, Np, Pu) are candidates for accident tolerant nuclear fuels that have great potential for the expanding future of nuclear power. For example, binary uranium nitride [U≡N] is regarded as a superior material over uranium oxide fuels due to its higher melting point, higher thermal conductivity and increased density, whereas neptunium and plutonium nitrides have been proposed as attractive transmutation fuels. However, for both ceramic and molecular actinide nitride systems, few synthetic routes exist for their preparation, and next to nothing is known about their chemical behavior. The development of a fuel cycle involving any actinide nitride will require this basic information for the safe processing, preparation, use, storage, treatment, and eventual disposal of the used nuclear fuel, all of which impacts our national security mission.

Progress

Our initial efforts have been focused on developing synthetic routes to thorium, uranium, neptunium, and plutonium azide complexes. Since metal azides can be converted into nitrides through the loss of dinitrogen using photolysis or thermolysis, both actinide azide and actinide nitride species are of interest due to their proposed use in accident tolerant fuel cycles.

In the first months of this project, we synthesized and characterized the first family of metallocene thorium diazide complexes, including the first organometallic actinide infinite coordination polymers. These compounds were characterized using X-ray crystallography, IR and multinuclear NMR spectroscopy, and for the first time for any structurally characterized actinide azide complex, Raman spectroscopy.

Importantly, we have found that thorium and uranium azide form different structures in solution and the solid-state. An examination of the published multinuclear uranium azide complexes suggests the beginning of a trend: the metallocene examples tend to form ring structures, with only two such examples in the literature: an organometallic octanuclear ring with alternating azides and nitrides and an organometallic uranium diazide trimer. Instead of rings, multinuclear thorium azide complexes form open polymeric infinite chains, which are dense in thorium and nitrogen.

Although comparable to bonding motifs observed for several transition metal systems, it is unclear why the thorium azides crystallize in open polymeric forms in contrast to the closed oligomeric ring structures observed for the uranium systems. While there is a measurable (0.05 Å) difference in metal ionic radius for Th(IV) versus U(IV), it is difficult to attribute such a significant structural difference to this property alone. Nevertheless, both the open polymeric (thorium) and closed oligomeric (uranium) diazide forms provide arrays dense in actinide and nitrogen, as well as opportunities for developing actinide nitride chemistry.

We have made less progress with neptunium and plutonium because of the highly radioactive nature of available isotopes of these elements (237Np and 239Pu). The practical consequences are small reaction scales (10-20mg), limited available analytical techniques, contamination control procedures that result in experiments taking much longer than for uranium or thorium (for example one simple proton NMR spectrum can take 3 hours to prepare, release, measure and dispose, compared with 30 minutes for Th/U), and an inability to screen scores of reaction conditions. Thus, when one considers that the proposed chemistry involves multiple nuanced reaction steps with isolation of intermediates required, achieving our aims pushes the practical limits of inert atmosphere transuranic synthetic chemistry and reinforces the need for guidance from optimized uranium and thorium chemistry. Indeed it is only possible to now attempt this chemistry due to our recent breakthroughs in access to Th(IV), U(IV), Np(IV) and Pu(IV) starting materials through the collaborative efforts of our team.

Before preparing Np and Pu azide complexes, it was first necessary to develop synthetic protocols for the generation of corresponding metallocene halide precursor complexes, which are poorly defined for Np and Pu, and never been structurally verified. Preliminary reactivity studies have focused on mimicking the synthetic protocols optimized by our team for the Th(IV) analogues discussed above.

The first attempt treated NpCl4(DME)2 (on ~ 14 mg scale) with 2 equivalents of KCp# (1,2,4-tBu-C5H2 or C5Me5) in a DME/Toluene solvent mixture resulting in formation of a red solution over 2 hours. An aliquot was taken for 1H NMR spectroscopy, which revealed the presence of a mixture of products, including the resonances at 6.49, 1.38 and 1.02 ppm, which we assigned to the target complex Cp#2NpCl2. A solution of the mixture of products in hexanes was stored at -35 °C resulting in deposition of a microcrystalline solid. NMR analysis revealed that one product had been selectivity crystallized from the other (with the presumed Cp#2NpCl2 species the major product remaining in solution). The small-scale of the reaction precluded isolation and structural verification of this very soluble species.

On the theoretical front, we have calculated the electronic structures of Cp*2AnCl2 for An = Th, U, Np, and Pu. These are the first calculations for the Np and Pu complexes in bent metallocene molecular framework. To understand the electronic structure change as substituted by azide, we also optimized a uranium azide complex (Cp*2U(N3)(C2N5H3), where the azide ligand is bound to the uranium center in a monodendate fashion.

Future Work

Synthesis of Th, U, Np, and Pu Diazide Complexes

- Th and U: start exploring the use of gold azide compounds as safe azide transfer agents to actinide metals; further explore tuning organoactinide azide structure, with an eye towards the number and nature of the azide ligands, as well as the conversion of new organometallic thorium and uranium azide complexes into nitrides.
- Np and Pu: continue our efforts to isolate the Cp#2NpCl2 species as well as exploring in situ efforts to generate the corresponding Cp#2Np(N3)2 complexes. We will initiate experiments with plutonium.
- Th-Pu: Structural, Spectroscopic, and Electrochemi

Characterization of New Molecules

- Predictive and Analytical Theoretical Studies: perform theoretical calculations on the monoazide, Cp*2An(N3)Cl and diazide, Cp*2An(N3)2 complexes across the series from Th to U to Np to Pu. Cp* = C5Me5.
- By comparing with the series of Cp*2AnCl2 accordingly, we will understand the electronic structure change induced by azide substitution.
- We will further study the reaction energetics of nitride forming reactions across the series if time allowed.

Conclusion

Few molecular examples of actinide nitrides are available

for study owing to the difficulties in synthesis. Recent advances have provided routes to actinide azide and nitride complexes that expands the options for developing actinide nitride chemistry. The development of new molecular azide and nitride systems remains a major challenge in the field of actinide chemistry. These systems will continue to provide insight into the bonding and chemistry of the An-N3 and An≡N bond, suggesting that a rich seam of novel reactivity is awaiting discovery. Several questions now present themselves. What stoichiometric and catalytic reactivity might be achieved with terminal nitride linkages? Could molecular systems such as the ones we propose to synthesize constitute useful low-temperature precursors to actinide nitride materials? To answer these questions and more, an understanding of the electronic structure and chemical behavior of actinide nitride functional groups is needed. This proposal will do just that. This effort is directly addresses the Los Alamos plutonium science research strategy, overlapping with several national security programs.

Using Therapeutic Bacteria to Treat Human Diseases

Jason D. Gans
20160340ER

Introduction

Gut flora affects our health by playing a role in the onset of diseases and providing protection against or support for gastrointestinal infections. Gut flora is a complex community, where many species depend on each other, but also antagonize one another. Understanding these inter-species interactions will enable the use of specific gut flora species for treatment of antibiotic resistant Clostridium difficile, a major cause of gastrointestinal infections that is responsible for ~30,000 deaths each year in the US alone. Fecal transplants are currently the only therapy for antibiotic resistant Clostridium difficile, but their use is limited, efficacy varies, and side effects are unpredictable. There is evidence that fecal transplants can cause serious changes in the patient's physiology, including weight gain and psychological changes.
We propose to develop a safe and reliable treatment for Clostridium difficile infections that uses specifically defined mixtures of natural gut bacteria. First, we will apply our existing high throughput screening process to human and mouse fecal samples to understand the interspecies interactions among the natural gut bacteria and between gut bacteria and Clostridium difficile. We will then identify the minimal subset of naturally occurring gut bacteria that can optimally fend off Clostridium difficile infection. Finally, we will carry out pre-clinical studies in lab animals to demonstrate the efficacy of our selected set of therapeutic bacteria for treating Clostridium difficile infections.

Benefit to National Security Missions

This project will enable studies of complex microbiological systems in all ecosystems on Earth, including commensal microbiomes. Applications will enable better medical treatments, improved biofuels production, enhanced NASA missions, and improved soldier preparedness.

Progress

Accomplishments since October 1, 2015 (8 months) include

- Hired a postdoc (Anand Kumar), who already has expertise in the area of gut microbiome, microbiology, and molecular biology needed for this project.
- Met with clinical collaborators at UNM (4 physicians) multiple times and discussed the details of the project. All four doctors are gastroenterologists and will work with us on the project.
- Obtained both IRB and IBC approvals to work with human blood and fecal samples obtained at UNM.
- Anand spent a week in another gut microbiome lab that works with Clostridium difficile and learned how to perform microbiology under anaerobic conditions, isolate C. difficile, and grow it.
- Purchased an anaerobic chamber and installed it in the lab.

Future Work

Aim 1: Identify best growth conditions and define baseline symbiotic and antagonistic interactions in the healthy gut flora

Defining the relative abundance/distribution of the natural gut flora species in our culturing system will be essential for the development of therapeutic bacterial cocktails and re-balancing the gut flora microbiome after C. diff. infection. This distribution profile will be used (in Aim 2) to determine when specific gut bacteria promote or enhance C. diff. growth and (in Aim 3) to create defined mixtures of therapeutic bacterial species that can be cultured in the lab.

Aim 2: Identify symbiotic and antagonistic relationships between the gut flora species and Clostridium difficile (C. diff.)

We will study the interactions of the natural gut flora species with C. diff., using the HiSCI process. C. diff. will be added to the gut flora before "packaging" the bacte-

ria into GMDs. Therefore, C. diff. will be given an opportunity to interact with all gut flora (a few species at a time), within MD microenvironments.

Conclusion

Clostridium difficile (C. diff.), is a major cause of gastrointestinal infections and is responsible for ~30,000 deaths every year in the U.S. alone. By the end of the project, we will demonstrate that a defined mixture of a few specific gut bacterial species can be used to effectively prevent and/or treat C. diff. infections in lab animals. The information gathered in this project will also help others better understand how equilibrium of species in a complex microbiome is established, and how it changes in response to various disturbances. This project will enable us to study the connection between the gut flora and several common inflammatory and auto-immune disorders, such as Crohn's disease, ulcerative colitis, cardiovascular disease, rheumatoid arthritis, etc.

Tracking Microbial Effects on Water-Uptake and Productivity of Plants

Sanna A. Sevanto
20160373ER

Introduction

The newest advances in plant science suggest that differences in the composition of microbial root associates such as fungi dramatically influence plant function from productivity to drought tolerance. This connection, shown with crops and non-herbaceous plants, is currently completely absent from the theories of plant stress responses, limiting our basic understanding of plant responses to their environment. This is mostly because the opacity, complexity, fragility and small size of soil-root interfaces make direct, in vivo studies of the influence of root associates on plants very challenging. To overcome this challenge we utilize and expand methods recently developed at Los Alamos National Laboratory for root associate identification and inoculation, Ultra-Low-Field Nuclear Magnetic Resonance (ULF NMR) and neutron radiography that images the effects of root associates on water uptake and productivity of intact plants at the sub-mm scale. Our objective is to develop these methods for studying soil-root interactions in detail and use them in targeted manipulation experiments to test the following hypotheses: (1) A healthy interaction with a mycorrhizal fungus promotes plant survival and recovery under drought conditions. (2) Good health of the plant:fungus interaction is manifested by a high water transport rate from the soil to the leaves, which leads to a positive cycle of higher desiccation tolerance and productivity during drought allowing more carbon investment of the plant to the fungus. (3) By employing a plant:fungus genomic approach on drought stressed and unstressed plants we can identify known classes and novel groups of expressed genes of both partners that influence plant performance. This information will provide keys to understanding and modeling variability in plant productivity and performance during stress, and is critical for improving predictions of vegetation responses in the era of global warming, increased desertification and pressure of food demand with increasing human population.

Benefit to National Security Missions

The work makes fundamental contributions to our basic understanding of plant function, interaction between plants and microbes, and how this relationship influences plant survival in the face of changing climate and environmental pressures. This knowledge, which is both a scientific gap and missing from our modeling of global climate change (with potentially profound implication), directly addresses important mission areas in energy security and environment. This project builds new capabilities at the interface of three programs (plant drought response, soil microbial biology and imaging techniques) with mission relevance to the DOE, NSF and USDA. The project specifically addresses a recurring request from DOE Biological and Environmental Research (BER) for LANL to build capability at the interface of mission needs in microbe-plant-climate science connections. Because all plants harbor root microbiomes, understanding and manipulating the integral role of the microbiome in shaping the form, function, and adaptive capacity of the plant has significant implications for missions in biofuel production, global climate change and food security. Our proposed work addresses a national priority and global need: reducing uncertainties about the future behavior of plant re-sources and forest ecosystems that have large feedbacks on global warming.

Progress

In the last FY we performed two sets of experiments with plants for imaging water uptake in the roots with neutron radiography at LANSCE. The first experiments were dedicated to finding correct soil and plant container material for neutron imaging and fine tuning the watering protocol for obtaining high enough contrast with D2O for visualizing the roots. Sandy, non-organic soil was determined the best soil material and aluminum was chosen for containers. The sandy soil turned out to be challenging for plant growth as it does not promote root biomass accumulation, but mixing that with small

amounts of local silt improved the soil quality for the plants without compromizing the image quality too much. With this system we succeeded in imaging root water uptake of small pinon pine seedlings and the water transport to the plant stems was verified with NMR. We also performed 3D neutron tomography on one pinon pine sample to determine the ability of the system to see water content differences within the root system. This imaging was very successful and the images could be processed to indicate water content gradients within the roots and soil system. For the second set we obtained a set of plant seedlings from drought tolerant and non-tolerant lines of the same species from Northern Arizona University. Half of these plants were inoculated with known, broad host range mychorrizal fungi and half not. We performed imaging experiments with six plants, but the data turned out challenging to interpret because the watering history of the plants affected both the image contrast and the plant water uptake rate. To improve our system and protocols for the next set of experiments we are building an automated actuator system to allow for measuring 2-3 plants simultaneously so that images can be compared directly between plants from different treatments and to a common standard. We have also refined and standardized our watering protocol and obtained a more sensitive neutron sensor to allow for higher contrast in the images. We have applied for more beamtime at LANSCE for the fall and, with these improvements, hope to obtain more easily interpreted data.

Future Work

To test our hypothesis we will perform a drought/re-watering experiment and carbon transport manipulations on trees with and without inoculation with their preferred mychorrizal fungi. During these experiments we will define three consecutive states of drought by the physiological response of plants: 1) stomatal closure, 2) fast declining water potential, 3) ceasing leaf respiration, and determine the timing of these stages relative to the onset of drought treatment. At each of these states we will perform a dynamic water uptake experiment on six randomly selected plants to measure the water uptake rate simultaneously at the roots, stems and shoots. We will then image these plants with neutron tomography to determine the extent of the intact root system at sub-mm scale, and sample half of them for plant:fungus metatranscriptome analysis. The other half will be re-watered and monitored for recovery from drought.

In the next FY we will continue refining the imaging methods using improved calibrations and detector resolution in neutron imaging and improving the stability of the ULF NMR system for long-term measurements. To test our hypotheses we will perform short drought experiments with pinon and ponderosa pine seedlings from a drought tolerant and drought intolerant seed line half inoculated with known, broad host range mychorrizal fungi and half not. These seedlings are currently growing in our greenhouse to obtain large enough root biomass for imaging.

Conclusion

A successful project will deliver first ever 1) world-class methods for studying plant-soil interactions, 2) in-vivo observations of the effects of mychorrizal fungi on plant water uptake and drought responses, and 3) plant activity on root associates. We will combine unique capabilities to lead an emerging scientific field integrating fungal associates with plant functional responses. We will also develop non-invasive, high-resolution methods needed for understanding soil-plant interactions. Our results could revolutionize theories on plant stress responses and tolerance representing significant gaps in our ability to predict plant productivity, vegetation changes and ecosystem-scale carbon cycling under changing climate.

Publications

Leigh, A., S. Sevanto, J. D. Close, and A. B. Nicotra. The influence of leaf size and shape on leaf thermal dynamics. Does theory hold up under field conditions?. To appear in Plant, Cell and Environment.

Vesala, T., S. Sevanto, Y. Salmon, T. Gronholm, L. Lindfors, E. Juurola, E. Nikinmaa, I. Riipinen, P. Hari, M. Mencuccini, and T. Holtta. Physical mechanism of reversed transpiration and enhanced water-use efficiency under plant water stress. To appear in Frontiers in Plant Science.

Expediting the Genetic Engineering of Microalgae for Industrial Production

Scott P. Hennelly
20160393ER

Introduction

There is a great deal of enthusiasm for the potential of algae as a systemic technology. Algae promise a carbon-neutral, environmentally friendly source of not only energy, but also a vast array of useful chemicals and materials, from the fuel in your tank to the tires you drive on. However, extensive genetic manipulations are required to realize algae's inherent potential. To date, progress has been slow, due to poorly characterized algal genetics and a lack of genetic tools such as plasmids, reliable transformation methods and viral vectors. We will develop these genetic tools, the same tools that have made biomedical research in other organisms possible. Our goal is to make algal genetic engineering routine. To accomplish this goal we will develop the means to deliver genes to algae, stably integrate them into the genome and express them. Historically, the main tools used for genetic engineering and molecular biology have been derived from viruses. Viral DNA elements have been co-opted to allow for the introduction of DNA to cells, its genomic integration and genetic expression in organisms from bacteria to humans. We will follow the same path to develop a set of tools and techniques for the engineering of algae. To this end we will; (1) isolate algal dsDNA viruses infecting production strains, (2) analyze the viral genomes to determine the components necessary to deliver, integrate and express genes of interest, and (3) combine the viral elements with cutting edge CRISPR/Cas genome engineering technology that allow for accurate targeted genome manipulations. Our success will make the now difficult task of algal genetic manipulation routine accelerating their development as a systemic technology.

Benefit to National Security Missions

This proposal aims to enable algal synthetic biology. The objective of these technologies is to co-opt algae's carbon neutral biosynthetic potential to produce biofuels and a wide array of useful chemicals and materials at an industrial scale. Additionally, since these organisms can thrive in reclaimed, produced and/or salt water, arable land and fresh water resources currently used to produce a number of important commodities can be freed up for other applications. For instance, the plant mevalonate biosynthetic pathway leading to the production of one of the most abundantly used biomaterials, rubber, is highly conserved in algae. Currently, the extensive genetic manipulations required to realize algae's inherent potential are difficult due to a lack of knowledge and tools. This project contributes to specific missions and agency goals by creating these tools and increasing our understanding of algal genetics.

The implications for biofuels production makes this effort of great interest for DOE, DOC and DOD. Beyond simple feedstock for energy production, harnessing the complex biosynthetic power algae would open new avenues for the production of a wide array of complex chemicals and materials that are of interest to DHHS (NIH, FDA) and DOD (DARPA). The fact that these technologies would be carbon neutral and replace traditional petrochemical precursors makes them very relevant to the missions of Energy security (Fossil Energy and Renewable Energy) and Environment (Climate and Energy Impact). Finally, this project will increase our understanding of algal genetics contributing to the mission ofScientificDiscovery and Innovation (Fundamental Bioscience).

Progress

We have made significant progress in developing the tools necessary to genetically engineer algae. We focused on developing a CRISPR-Cas delivery system that will avoid the published toxic effects of constitutive expression found in algal systems. To accomplish this, our aim was to deliver the Cas9 protein directly into the cell using Biolistic or chemical transfection techniques. We first constructed a Cas9 fusion with GFP. Following re-

combinant expression in E. coli and purification the fusion was shown to be active in DNA cleavage. We synthesized various sgRNAs (single-guide RNA) that associate with Cas9 and target the protein to specific DNA sequences for cleavage. The fusion was shown to be both active and specific in cleaving target DNAs. Cas9-GFP was expressed both with and without a nuclear localization signal (NLS) on the N-teminus of the fusion. To facilitate Biolistic transfection a tetra-Cys tag was also appended to the C-terminus. Biolistic transfection utilizes projectiles to normally deliver DNA vectors to host cells. These projectiles microscopic gold particles. As gold is highly thiophilic we reasoned the 4 thiols in the tetra-Cys tag would facilitate Cas-9 association with the gold projectiles. After various conditions for gold particle preparation and association were evaluated we were able to verify the association of Cas9-GFP using fluorescence microscopy. We also found the fusion can be release under mild reducing condition typically found in cells. As such the possibility of delivering Cas9 directly to a variety of cell types with relative ease now exists. Following delivery, we have recently demonstrated that the NLS tag allows for the localization of the CAS9-GFP to the nucleus of algal production strains Nanchloropsis salina and Chlorella sorokiniana. This study also showed that the fusion was stable for at least 24 hours post transfection. We are currently well positioned to derive a novel methodology for genomic engineering in algae.

Future Work

Goal 1. Building on our success in creating and delivering Cas9 into algal cells, we will continue to develop the CRISPR (Clustered regularly interspaced short palindromic repeats) delivery system for genomic manipulation of Algal production strains.

Task 1. Confirm nuclear localization of Cas9-GFP fusion in the presence of fluorescently labeled sgRNA (single guide ribonucleic acid).

Task 2. Use localized Cas9-sgRNA to edit genome at specific site, confirm through sequencing.

Task 3. Create chloroplast targeting Cas9-GFP fusion and validate chloroplast localization and editing.

Goal 2. Create targetable DNA delivery system using the ssDNA (single-stranded DNA) binding β-protein from Lambda-Red phage recombination system.

Task 1. Build protein expression vector for the expression and purification of nuclear targeted β-GFP fusion.

Task 2. Demonstrate DNA binding of β-GFP fusion using fluorescence anisotrophy.

Task 3. Demonstrate delivery into Algae and localization to the nucleus with labeled DNA.

Task 4. Demonstrate simultaneous delivery of β-GFP:DNA and CAS9:sgRNA to the host nucleus.

Task 5 Create chloroplast targeting β-GFP and demonstrate DNA delivery into chloroplast.

Goal 3. Use the tools outlined above to deliver cassette with selection to a neutral site within the Algal genome.

Task 1. Build modular cassette with promoter and terminator sequence and homology arms for site-specific recombination.

Task 2. Design sgRNA to target genomic site and excise sequence between homology sites demonstrate efficient cleavage and non-homologous end-joining repair.

Task 3. Use combination of targeted complexes (Cas9:sgRNA and β:DNA) to insert DNA constructs specifically into Algae.

Conclusion

Extensive genetic manipulations are required to realize algae's inherent potential as a systemic technology. To date, progress has been slow, due to poorly characterized algal genetics and a lack of genetic tools such as plasmids, reliable transformation methods and viral vectors. Our goal is to make algal genetic engineering routine. We will deliver a set of tools and methods to deliver genes to algae, stably integrate them into the genome, and express them. Beyond simple feedstock for energy production, harnessing the complex biosynthetic power algae would open new avenues for the production of a wide array of complex chemicals and materials of interest for national security applications.

Selective Extraction of Medically-Relevant Radionuclides from Proton-Irradiated Thorium Targets

Michael E. Fassbender
20160439ER

Introduction

The goal of this project is to develop a method to simultaneously produce and recover a unique suite of therapy radionuclides using a systems/process-engineering approach. We will develop a process flow sheet that optimizes the yield and purity of the promising therapeutic isotopes described below. The effort will leverage LANL's world-class 100 MeV proton irradiation capability at the Los Alamos Neutron Science Center (LANSCE) Isotope Production Facility (IPF) and chemical hot cells infrastructure.

Radionuclides under consideration in this proposal include 225/223/224Radium (potential alpha-therapeutic), 103Ruthenium/103mRhodium (potential auger therapeutic), 111Silver (potential β- therapeutic) which will establish a foundation for the development of cancer therapy research strategies and future treatment regimens with significant patient impact and revenue potential.

The aforementioned isotopes will be generated via proton irradiation of thorium targets at IPF and a battery of selective chemical extraction methods will be utilized for the development and optimization of integrated processes which isolate proposed isotopes from the target matrix in chemical form for subsequent medical use. Advantages of our proposed methods are 1) the isolation of several medically-relevant radionuclides that cannot be obtained by any other single production method, and 2) the simultaneous isolation and purification of these isotopes from a single target irradiation. Comprehensive systems engineering methodologies will be used to develop a process flow sheet that optimizes quality and yield of all of the critical isotopes outlined herein.
Benefit to National Security Missions

The National Isotope Program is managed under the DOE Office of Science, Office of Nuclear Physics and this work has A-level relevance to DOE/SC agency mission given the isotope focus of the proposal. The proposed effort grades B in other agency mission areas for NIH and DARPA where follow-on funding may be anticipated based on successful execution of the proposed scope related to therapeutic applications for cancer and/or infectious disease. For the same reasons, the effort is graded at B-level forNuclearSecurity and National Defense mission relevance given the potential of these agents as therapies for drug-resistant pathogens. Given the radiochemical separations focus of the effort and application for cancer therapy, the proposed effort is graded at A-level forScientific Discovery and Innovation mission relevance areas of fundamental chemistry and basic health science.

Progress

Key milestones for FY 16 proposed scope included testing of isolated isotope separation strategies for Ag, Ra and Ru isotopes as well as testing of the process protocol for simultaneous separation of Ac/Pa/Ra/Ru/Ag isotopes. Significant progress has been made for all FY16 milestones as detailed below:

Developing Separation of Ag: 111Ag purification has been explored using commercially available "Cl-Resin" manufactured by TrisKem International. This resin was designed for halide anion separation after loading with Ag cations. It permits high yield separation of 111Ag in relatively high purity. Purity maximization of isolated 111Ag will be the focus of remaining FY16 effort.

Testing Separation of Ru: 103Ru has been isolated using anionic sorption on a stationary phase of a strongly basic anion exchanger resin in a mobile phase of HCl as a method to separate 103Ru from a host of other fission products. Ruthenium-103 can be sorbed directly from a solution of irradiated thorium metal without prior treatment. Subsequent washing and desorption with HCl yields a pure 103Ru product. A combined manuscript

is in preparation detailing the specifics of the separation schemes of and protocols for 103Ru and 111Ag.

Testing of Ra Separation Strategies: an effective separation protocol for the separation of 225/224/223Ra has been demonstrated using cationic sorption on a strongly acidic cation exchanger resin as stationary phase in a citrate chelating matrix as mobile phase. This enables selective sorption of trivalent (Ac3+, radiolanthanides) and divalent (Ra2+, Ba2+) cations. Isolated Ac, radiolanthanides, Ra, Ba were further separated via DGA resin extraction chromatography (for Ac recovery) and a subsequent second cation exchange step (for Ra recovery). All steps can combined without in-between matrix evaporation or reconstitution. A manuscript is in preparation detailing the specifics of the separation scheme and protocol.

Simultaneous Separation of Ac/Pa/Ra/Ru/Ag: All separation steps above were designed as dependent modules and can be seamlessly integrated into a production batch process. This has been demonstrated multiple times in FY16 with good overall isolated yields and purities. Optimization effort will continue into FY17 as planned.

In FY17, particular focus will be dedicated to the advancement of a new 103Ru/103mRh generator concept using a novel, solid supported resin. We have approached a leading expert in the development of this resin and will receive samples to initiate work against this milestone by the start of FY17. We will work with the Feynman center to pursue potential patent of this generator technology as it is developed. In addition, we will continue to optimize the integrated process flow sheet with attention to enhanced product yields and purities for all isotopes outlined in the proposal. The final flow sheets will be detailed in the event that any/all of these isotopes would be pursued by the National Isotope Program (DOE OSc) for routine production.

Future Work

Starting with prior work on the isolation of 225Actinium from irradiated thorium targets, we will develop procedures to isolate 223/224/225Radium, 103Ruthenium and 111Silver. The main chemical engineering and overall technical challenge of this project will be the coordinated optimization of procedures for the isolation of the proposed radionuclides such that the new process is capable of providing all recovered radionuclides in sufficient chemical and radioisotopic purity for medical use.

FY16 scope focused on the development of individual, optimized separation chemical separation strategies for the Radium, Ruthenium and Silver isotopes outlined in this proposal. The significant milestone for FY16 to test a simultaneous separation of all isotopes under investigation and compare/contrast the performance of the simultaneous process to that of the previously investigated individual, optimized processes has been initiated and this effort will carry-on into FY17. In addition, FY17 scope will focus on the the development of a novel 103Ru/103mRh generator concept that will fully leverage the opportunity provided by high-quality 103mRh as a candidate for Auger therapy.

Conclusion

A set of promising isotopes will be generated via proton irradiation of thorium targets at the Los Alamos Isotope Production Facility and a battery of selective chemical extraction methods will be utilized for the development and optimization of integrated processes that isolate proposed isotopes from the target matrix in chemical form for subsequent medical use. Targeted radiotherapy will provide an alternative to surgical recision, chemo-therapy, and external beam therapy strategies.

Deciphering the Algal Phycosphere

Armand E. Dichosa
20140216ER

Abstract

A growing body of literature indicates that many microalgae, including biofuel production strains, require bacteria to provide essential nutrients and metabolites for optimal growth and survival. Nevertheless, most of the research conducted to improve the productivity of commercial algal systems relies on extrapolating growth studies conducted under axenic laboratory conditions, despite the fact that many algal production systems contain hundreds to thousands of species of bacteria. By traditional cultivation standards, it is not possible to recapitulate and assess even 1% of the possible intercellular interactions that positively (or negatively) influence algal productivity during cultivation. To address this need, we integrated gel microdroplet (GMD) technology with microfluidics to generate millions of culture microdroplets (MDs), whereby sequestering unique cell-to-cell interactions to facilitate both rapid identification and recovery of growth promoting bacteria via flow cytometry. Herein, we describe both the pipeline using off-the-shelf, commercially available technologies and the process by which seven microbial candidates that increase algal production are selected.

Background and Research Objectives

The main goal of this proposal is to isolate, identify, and characterize bacteria that grow in a symbiotic or epiphytic relationship within an algal habitat (the 'phycosphere'). Similar to a plant's rhizosphere, many unicellular algae require the presence of bacteria to provide essential nutrients and metabolites for improved fitness and survival in natural microbial ecosystems. Unfortunately, the scientific community is focused on 'mono-cultures' and little research has been completed to identify the extant bacterial mediated effects on algal nutrient utilization or growth.

Select unicellular photosynthetic microalgae have been targeted for commercial applications given their ability to efficiently accumulate biomass and lipids for conversion into renewable diesel and jet fuel. Specifically, Nannochloropsis salina and Chlorella sorokiniana, have been identified as strong candidates for outdoor production systems by LANL (unpublished results) and other industrial and academic partners. Two critical limitations to commercialization and improvement of these and other algal feedstocks are, 1) the high cost of external nutrient inputs and, 2) federal and state regulations that prohibit the use of genetically modified organisms (GMOs) in open algal production systems. Thus, overcoming these limitations will require significant improvement in biomass yield, reduction in external nutrient inputs, and necessitate the use/modification of non-GMO microbial populations. Furthermore, one of the most overlooked aspects of 'open pond' algal production systems is that most (if not all) are complex microbial communities containing hundreds to thousands of bacterial species intermixed with a dominant algae. Nothing is known about the function of the accompanying bacteria in most production facilities or natural ecosystems.

Scientific Approach and Accomplishments

Our overall scientific approach is to develop the HiSCI (Hi-throughput Sequencing of Cell-to-Cell Interactions) platform, that incorporates gel microdroplets (GMDs), flow cytometry, microfluidics, and genome sequencing technologies/bioinformatics to identify the top-performing algae and the associated bacteria. Our HiSCI platform initially captures algal cells with bacteria in individual GMDs. Thereafter, flow cytometry rapidly enriches the GMDs containing a single algal cell with ~5 bacterial cells, and are subsequently sequestered in MDs composed of algal growth medium (Figure 1). After a period of incubation, we harvest the GMDs and utilize flow cytometry to identify the GMDs containing algae with the greatest chlorophyll fluorescence to be individually sorted into a multi-well culture plate (Figure 2). The faster-growing algae are easily identified, resulting in the harvesting of the associated bacteria for downstream cultivation and genomic sequencing/identification.

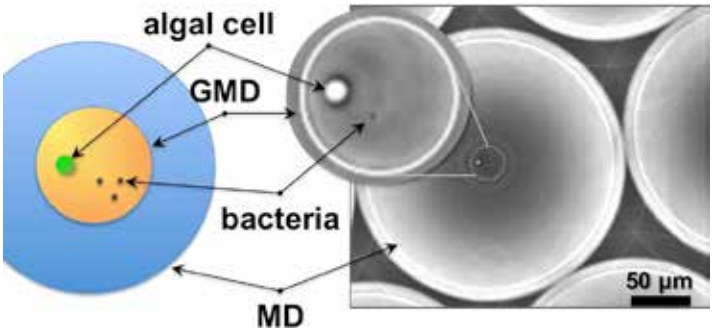

Figure 1. GMD with Algal Cell and Bacteria: GMDs containing a single algal cell and several bacterial cells are individually captured in MDs.

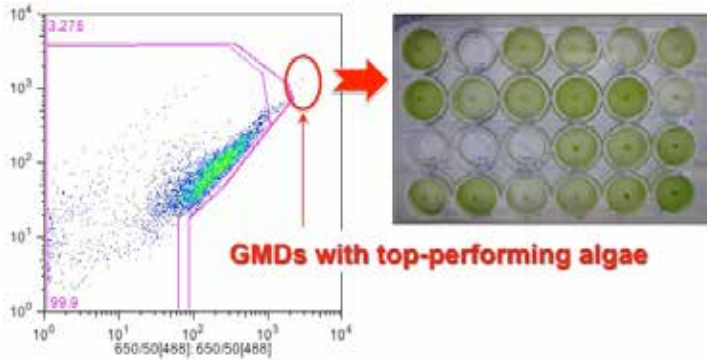

Figure 2. Selecting Top Performing Algae: Our HiSCI pipeline integrates flow cytometry post-incubation to rapidly identify and sort only the GMDs containing the faster-growing algae and the associated bacteria for subsequent cultivation in multi-well culture plates. Individual wells observed with the desired phenotype of rapid "green" growth are selected to isolate and genotype the associated bacteria.

Accomplishments

We have completed a novel HiSCI full-screen pipeline, which integrates GMDs, flow cytometry, microfluidics, and sequencing purposed to rapidly screen potentially millions of cell-to-cell interactions and recover/identify the cells.

We demonstrated the capability to detect improved algal biomass by flow cytometry through fluorescence (e.g., chlorophyll).

We developed a novel 16S rRNA phylotyping pipeline that utilizes the Illumina MiSeq platform and custom bioinformatics phylotyping methodologies. We are currently translating our wet-lab library protocol to an automated, robotics-based high throughput procedure.

From thousands of bacterial species, we down selected and isolated seven bacterial candidates via our HiSCI pipeline that potentially benefits algal biomass production. We are currently purifying one top candidate for necessary, subsequent validation studies and genomics.

We described our HiSCI pipeline in a manuscript that has been submitted to Biotechniques.

Impact on National Missions

As algae are widely accepted as a viable source for our country's energy needs, significant work is warranted to understand the basic biological processes that promote (and prevent) algal biomass production. Specifically, our work addresses this need to dissect and identify the associated bacteria that influence algal growth. Such fundamental understanding will greatly contribute to improving algal growth in a commercial production scale with greater efficiency (time, cost, and resources) and lesser environmental impact (nitrogen or chemical input).

Our work also contributes to the mission relevance of scientific discovery and innovation through fundamental bioscience. It is widely accepted that ~99% of environmental bacteria (including human microbiome, soil communities, etc.) cannot be grown as pure cultures under laboratory settings. A basic premise is that we cannot achieve the exact growth conditions as the native environment in the lab and that specific bacteria are required to signal growth. By using gel microdroplets (GMDs) for co-cultivation with high-throughput flow cytometry, we can greatly improve our current understanding of bacterial growth and cell-to-cell interactions, and their significance to our nation's health, ecology, and economy.

Furthermore, our work develops a novel pipeline in both the wet-lab and bioinformatics fronts to specifically investigate cell-to-cell interactions. Thus, the DHS, NIH, and DHHS will benefit from our work as our novel technology development can potentially address host-pathogen interactions and co-evolution (e.g., endosymbiosis) investigations.

Publications

Ohan, J., P. Nath, J. Huang, B. Pelle, B. Hovde, A. Dichosa, M. Vuyisich, and S. Starkenburg. High-throughput screening of cell-to-cell interactions by cultivation in gel microdroplets surrounded by oil microdroplets. Biotechniques.

Intrinsically Disordered Proteins: New Tools for Old Controversies

James H. Werner
20140307ER

Abstract

This project is building the tools to explore the molecular basis of how bacterial DNA is protected during spore formation. In particular, it aims to develop and exploit the tools necessary to study a class of proteins that play an important role protecting bacterial DNA during sporulation. Interestingly, these small acid soluble proteins appear to have no well-defined structure in solution, but appear to have a well-defined 3D structure when bound to and protecting bacterial DNA. This project aimed to develop instrumentation capable of monitoring single small acid soluble protein conformation before, during, and after binding to DNA, leading to a better understanding of this dynamic process that could inform strategies for more effective bacterial remediation or therapeutics.

Background and Research Objectives

Not all proteins have well defined 3D structure. An important class of proteins, termed intrinsically disordered proteins (IDPs), dynamically fluctuates between a large range of conformations and appears to have little well defined structure in solution. Interestingly, many IDPs fold into a more defined conformation when binding a target protein or DNA. While conventional experimental techniques to study the conformation of proteins with well-defined 3D structure (e.g. crystallography) can study the bound state of IDPs, these methods are generally ill-suited to the task of studying the conformations of IDPs before and during binding. By their nature, intrinsically disordered proteins almost demand methods that can identify, study, and delineate individual molecular conformations.

Single molecule spectroscopic techniques are a powerful method to explore individual biomolecular heterogeneity and these methods have recently been used to study the conformational dynamics of a handful of IDP systems. Most single molecule methods of studying protein conformation exploit single molecule fluorescence resonance energy transfer (smFRET) to measure specific site to site distances in the protein or biomolecule as a function of time.[1] These measurements can be performed on molecules diffusing through a fixed laser beam or by studying surface-immobilized molecules on a glass surface. Studies in solution have the advantage the conformation of the molecule of interest is not perturbed by surface attachment whereas studies on immobilized molecules have the advantage of long observation times. This work aimed to combine the best aspects of smFRET in solution (no perturbation on molecular dynamics due to immobilization) with the best aspects of smFRET on a surface (long observation times). In particular, this work aimed to directly follow and monitor molecular conformation in solution, exploiting our leading position in the development of 3D single molecule tracking methods. [2-4]

We developed these state of the art techniques to help explore a problem of substantial scientific and programmatic interest: the method by which bacterial DNA is protected during sporulation.[4] Our research goals included development of a 3D molecular tracking system capable of measuring smFRET during tracking, benchmarking this system on simple test materials (e.g. fluorescent beads), followed by demonstration of 3D tracking of single FRET labeled biomolecules (DNA and an intrinsically disordered protein important for protecting bacterial DNA during sporulation). A stretch-goal of this project was to observe biomolecular conformational dynamics of this intrinsically disordered protein directly in live bacteria.

Scientific Approach and Accomplishments

Our approach builds upon our prior efforts in the development of instrumentation and methods for following single fluorescent molecules or particles as they move in 3 dimensions in solution or biological milieu.[2-4] In brief, our 3D tracking microscope is a custom-designed confocal microscope that uses a unique spatial filter ge-

ometry and active feedback 200-500 times per second to follow fast, 3D motion inside live cells. Over the years our work advanced from Monte Carlo simulations to tracking quantum dots in glycerol water mixtures to tracking single quantum dot labeled proteins in live cells and tracking individual organic dyes or fluorescent proteins. For this project, we designed and constructed a new 3D tracking microscope capable of recording fluorescence in two distinct spectral regions (e.g. green and red for a donor and receptor organic fluorophores used as smFRET labeles) simultaneously. A schematic of the system developed in this project is shown in Figure 1. In particular, the original 3D tracking microscope used 4 confocal detection regions (arranged in a 3D tetrahedral geometry in the sample space) for 3D positional sensing and molecular tracking.[2-4] This new microscope uses a total of 8 detectors (4 for the donor and 4 for the fluorescence acceptor) to enable monitoring smFRET while tracking single molecules.

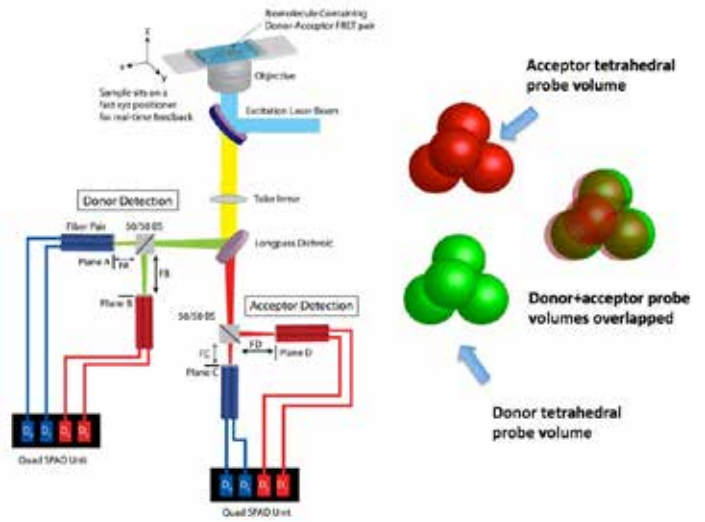

Figure 1. Left: Schematic of the 3D tracking microscope showing 8 detection channels (4 for the donor, shown in green and 4 for the acceptor channel, shown in red). Right: The projection of each set of the 4 optical fibers back into the sample space forms a 3D tetrahedron. The donor (green) and acceptor (red) probe volumes are overlapped as well as possible.

Expanding the system from 4 to 8 detectors required substantial modifications to our tracking code, in terms of feedback control and photon registration. These software and hardware modifications and others, including enabling time-resolved spectroscopy to be performed on the molecules being tracked were essentially finished by the end of the first year. Initial test samples included 3D tracking of fluorescent microspheres (200 nm in diameter) in water that emit fluorescence in both red and green spectral channels. A representative 3D bead trajectory is shown in Figure 2.

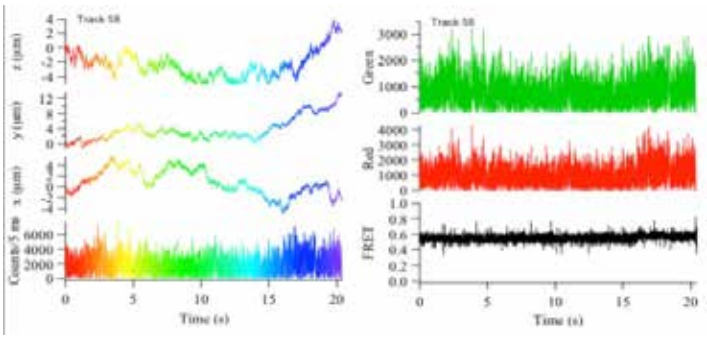

Figure 2. A 3D trajectory of a single 200 nm diameter fluorescent bead followed in the 3D tracking smFRET microscope. Left side shows the molecular position in X, Y, and Z as a function of time (0 to 20 seconds) as well as the sum of the counts on all 8 detectors used for real-time feedback and tracking. Right side shows the donor (green) and acceptor (red) counts separately as well as the apparent energy transfer efficiency as a function of time. The apparent FRET efficiency is defined as the counts in the red channel divided by the sum of the counts in the red+green channels.

Concurrent with instrument development efforts, we also began efforts to create an appropriately fluorescent donor and acceptor labeled intrinsically disordered protein construct. To this end, the gene encoding for wild type small acid soluble protein SspC was cloned into a pETa plasmid and custom synthesized by Blue Heron Technology, Inc. The plasmid was expressed into an Escherichia coli BL21 (DE3) strain. The expression and purification of SspC was adapted from a previously described protocol.[5]

To perform smFRET measurements of SspC, we introduced cysteine residues into the sequence of the protein so AlexaFluor 488 (donor) and AlexaFluor 594 (acceptor) dye labels could be attached via maleimide labeling. Cysteine residues were introduced at positions that would least likely to perturb the structural and functional characteristics of the protein, discovered through molecular dynamic simulations. We made the following mutant constructs: 1) A2C and H72C, 2) G40C and H72C, and 3) I31C and V51C (Figure 4). Circular dichroism (CD) measurements were done to characterize the secondary structures of these constructs relative to wt SSpC (Figure 3). The CD results show that the introduced cysteines did not significantly perturb the disordered nature of SspC.

During the course of the research, mass spectrometry analysis revealed that sometime during the labeling and purification of the constructs, it appeared that the first few N-terminal residues of SspC were cleaved off and as such, the AF-SspC 2/72 FRET pair was deemed a poor choice for further smFRET measurements. The AF-SspC 40/72 pair produced more promising results and showed significant FRET change upon addition of target dsDNA sequence.

Simultaneous with fluorescence labeling and purification of appropriately smFRET labeled SspC constructs, we began testing the tracking instrument to follow single fluorescent molecules, as opposed to the large and relatively bright fluorescent beads used in initial instrument alignment and testing. For these experiments, we used duplexes of DNA with Alexa 488 and Alexa 594 labeled at specific sites along the DNA, as illustrated in Figure 4. Double stranded DNA serves as a rigid rod to keep the fluorophores a known, fixed difference apart. Importantly, different DNA strands with Alexa 488 and Alexa 594 at different distances apart can be used to test our 3D tracking instrument performs at varying FRET efficiencies for IDP tracking.

Our initial DNA experiments began with 12 base pair separation between Alexa 488 and Alexa 594 as shown in Figure 4. Ensemble fluorescence lifetime measurements as measured by time-correlated single photon counting demonstrated a fluorescence resonance energy transfer efficiency of ~0.58 for this sample. A 3D trajectory for a single molecule of the A488/A594 DNA labeled sample is shown in Figure 5. A histogram of single molecule FRET efficiencies obtained from following several hundred 3D single molecule trajectories has an average value (0.57) in excellent agreement with the FRET efficiency determined from bulk fluorescence lifetime measurements (0.58). These results were presented at the 2016 Annual Biophysical Society Meeting, with a more detailed manuscript currently in preparation.

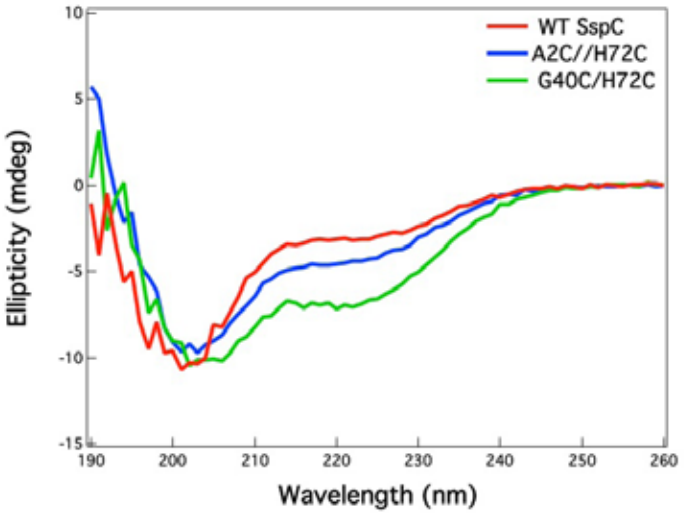

Figure 3. Circular Dichroism (CD) spectra shows fluorescence labeling does little to change the disordered structure of SspC

Figure 4. A cartoon depiction of the DNA test sample used to measure smFRET while tracking. The donor (Alexa 488 or AF488) and acceptor (Alexa 594 or AF594) are separated by 12 DNA bases, close enough for efficient Forster energy transfer.

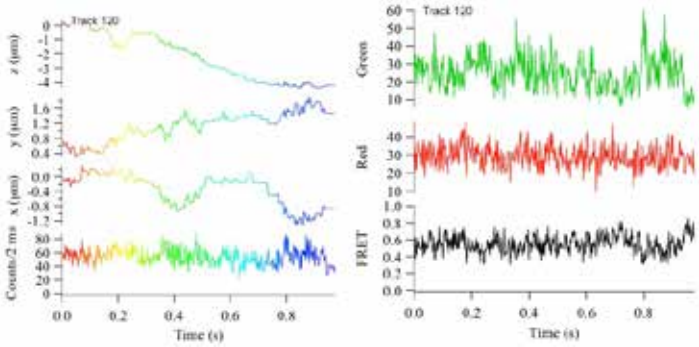

Figure 5. A 3D trajectory of a single molecule of DNA labeled with a donor (AF488) and acceptor (AF594) fluorophore pair. The left hand panel shows the molecular position as a function of time for the 3 Cartesian coordinates (X,Y, and Z) and the counts summed on all four detectors for tracking. The right hand panel shows the counts summed on the donor (green) and acceptor (red) channel, respectively, and the apparent energy transfer efficiency of this molecule as a function of time.

Impact on National Missions

Spores of Bacillus and Clostidium species have long been of interest due to their roles as agents of food-borne disease, food spoilage and bioterrorism (e.g. Bacillus anthracis). Small acid soluble proteins play a major role in long-term spore survival and bacterial persistence by protecting the spore DNA from numerous physical and chemical damages. An enhanced understanding of the molecular basis of spore DNA protection has the potential to lead to better eradication strategies. In particular, there is an emerging interest in understanding and combating bacterial sporulation. We further note that a successful demonstration of being able to simultaneously measure intra-molecular conformational dynamics and intra-cellular transport dynamics enables many applications of this system beyond better understanding IDP folding dynamics. Other systems include understanding and monitoring protein-protein interactions, including those important in how viruses and bacteria enter human cells, impacting Laboratory missions in the host-pathogen arena.

References

1. Roy, R., S. Hohng, and T. Ha. A practical guide to single-molecule FRET. 2008. Nature methods. 5 (6): 507.

2. Lessard, G. A., P. M. Goodwin, and J. H. Werner. Three-dimensional tracking of individual quantum dots. 2007. Applied Physics Letters. 91 (22): 224106.

3. Wells, N. P., G. A. Lessard, P. M. Goodwin, M. E. Phipps, P. J. Cutler, D. S. Lidke, B. S. Wilson, and J. H. Werner. Time-resolved three-dimensional molecular tracking in live cells. 2010. Nano letters. 10 (11): 4732.

4. Keller, A. M., Y. Ghosh, M. S. DeVore, M. E. Phipps, M. H. Stewart, B. S. Wilson, D. S. Lidke, J. A. Hollingsworth, and J. H. Werner. 3-dimensional tracking of non-blinking giant quantum dots in live cells. 2014. Advanced functional materials. 24 (30): 4796.

5. Hayes, C. S., Z. Peng, and P. Setlow. Equilibrium and Kinetic Binding Interactions between DNA and a Group of Novel, Nonspecific DNA-binding Proteins from Spores ofBacillus and Clostridium Species. 2000. Journal of Biological Chemistry. 275 (45): 35040.

Publications

DeVore, M. S., A. M. Keller, Cleyrat, M. E. Phipps, B. S. Wilson, and J. H. Werner. Simultaneous Confocal based 3D Tracking and Fluorescence Imaging. 2014. BIOPHYSICAL JOURNAL. 106 (2): 194A.

DeVore, M. S., D. G. Stich, A. M. Keller, Ghosh, P. M. Goodwin, M. E. Phipps, M. H. Stewart, Cleyrat, B. S. Wilson, D. S. Lidke, J. A. Hollingsworth, and J. H. Werner. Three dimensional time-gated tracking of non-blinking quantum dots in live cells. 2015. COLLOIDAL NANOPARTICLES FOR BIOMEDICAL APPLICATIONS X. 9338.

Werner, J., A. Keller, M. DeVore, T. Causgrove, and D. Vu. 3D Tracking single molecule fluorescence resonance energy transfer. Presented at 60th Annual Meeting of the Biophysical Society. (Los Angeles, Feb. 27-Mar 2 2016).

Electromagnetic Field Control of Cold Molecular Collisions

Brian K. Kendrick
20140309ER

Abstract

The study of cold and ultra-cold molecules and their collisions with other cold atoms and molecules represents a new virtually unexplored energy regime ripe for new discoveries and important technological applications. Experimental techniques to produce and collide cold molecules are continuing to evolve at a rapid pace. At these cold temperatures, the kinetic energy of colliding molecules becomes smaller than the electromagnetic field interactions routinely achievable in the laboratory. Thus, the control of the collision outcome is possible and this has been recently demonstrated experimentally. However, these initial control studies are only the beginning. Theoretical treatments of cold and ultra-cold molecular collisions including external electromagnetic field interactions are also under development. A notable deficiency in recent theoretical methods is their inability to treat reactive collisions within the cold energy domain where s-wave scattering is no longer valid and multiple reaction channels must be included. This project has successfully developed new capabilities for efficiently including electromagnetic field interactions for cold molecular collisions including higher partial waves and multiple reaction channels. The approach was based on LANL's APH3D quantum reactive scattering code which already has several unique computational capabilities. The new external field control capability developed in this project was demonstrated for the ultracold OH + O reaction. In addition, an entirely new quantum interference mechanism was discovered. This mechanism could provide a new experimentally realizable approach for controlling cold molecular collisions with unprecedented dynamic range and sensitivity. Extensive theoretical calculations for the fundamental H + H2 reaction system were pursued which clearly demonstrate the generality of the new interference mechanism and several experimentally measurable signatures of this new mechanism were predicted. The new external field control capabilities developed in this project and the unanticipated discovery of the new quantum interference mechanism will help enable the development of new technologies important to LANL's global and energy security missions.

Background and Research Objectives

Recent rapid experimental progress in cooling, trapping, and colliding cold molecules has opened up a new and exciting, unexplored energy regime which is ripe for new discoveries and technological applications.[1-5] The terms "cold" and "ultra-cold" refer to the relative translational motion of the molecules typically characterized by temperatures T < 1 Kelvin and T < 1 milli-Kelvin, respectively. Due to their unprecedented sensitivity, cold and ultra-cold molecular collisions are especially amenable to control by external electric and magnetic fields and recent experiments have begun to demonstrate this possibility.[3-5] The control of molecular collisions has been a long sought goal with many important fundamental and technological applications including: quantum computation, sensing, testing fundamental laws of physics, synthesis of specific molecular species of interest, elucidating quantum enhanced reaction mechanisms (i.e., interference, tunneling, resonances), and providing detailed information on molecular structure and intermolecular interaction potentials. Predictive theoretical and computational methods are critically needed to help design and interpret these new experiments and potential technological applications. Most previous theoretical and computational methods for including electromagnetic field interactions in treating cold and ultra-cold molecular collisions are limited to elastic and inelastic collision processes.[1-2] Notably lacking is the ability to efficiently and accurately treat reactive collisions. The primary goals of this research project were to develop, implement, and apply new theoretical and computational capabilities for including external electromagnetic field interactions in reactive scattering calculations of cold and ultra-cold molecular collisions. These new capabilities were applied to several important molecular systems of experimental interest to demonstrate the potential for controlling the dynamics

and most importantly the outcome of cold and ultra-cold molecular collisions.[6-14] In summary, the primary goals of this project were achieved. In particular, new theoretical/computational capabilities for treating external electric field interactions were developed and applied to ultra-cold reactive collisions of O + OH -> H + O2.[8,10] In addition, a new quantum interference mechanism was discovered which is unique to ultra-cold collisions but otherwise general.[8] This unanticipated new discovery could enable the control of ultra-cold molecular reactions with unprecedented dynamic range and sensitivity. It can effectively turn the reaction on or off depending upon whether the quantum interference is constructive or destructive, respectively. Furthermore, external electric fields can be used to control the nature of the interference[10] and therefore the reaction outcome! Additional objectives were pursued during the course of this project based on the newly discovered quantum interference mechanism. In particular, extensive calculations were pursued for the most fundamental molecular collision system H + H2 -> H + H2 (and its isotopic variants) which documented the general nature and broad impact of the new mechanism.[9,11-14] Several experimentally measurable signatures of the new mechanism were also identified for the hydrogen system.[9,11-14]

Scientific Approach and Accomplishments

The unique capabilities of the LANL quantum reactive scattering code (APH3D) were extended to include external electric field interactions and applied to ultra-cold reactive collisions of O + OH -> H + O2 , X + X2 -> X + X2 (where X = H, D and T), H + HD -> H + HD, H + HD <-> D + H2 , D + HD -> D + HD, D + HD <-> H + D2 , O(1D) + D2 -> D + OD, and Li + LiYb -> Yb + Li2.[6-14] In brief summary, the O(1D) + D2 calculations investigated isotope and vibrational excitation effects on the ultracold reaction rates,[6] the Li + LiYb calculations quantified the importance of performing exact quantum mechanical calculations of ultra-cold reaction rates through comparisons with other approximate methods,[7] the O + OH calculations led to the discovery of a new quantum interference mechanism,[8] external electric field control scenarios for the O + OH reaction were also investigated,[10] the calculations for H + H2 (and its isotopic variants) showed that the new quantum interference mechanism occurs for a large number of ultra-cold collisions.[9,11-14] Selected highlights from the O + OH and H + H2 calculations will be discussed in more detail below. In addition to the applications listed above, a reduced dimensional potential energy surface for the NaK + NaK collision system was also developed.

Figure 1 plots the ground electronic state potential energy surface for HO2 for a fixed O2 bond length. This surface represents the intermolecular potential that the hydrogen (red sphere) feels as it moves away from the O2 molecule during the O + OH -> H + O2 reaction. The scattering calculations are fully three-dimensional and the O2 bond (blue spheres) is allowed to vary (it is fixed in Figure 1 for visualization purposes only).

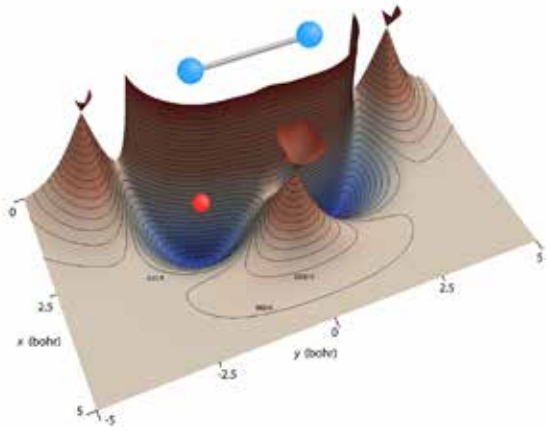

Figure 1. A two-dimensional slice of the Born–Oppenheimer potential energy surface for the ground electronic state of HO2 is plotted in the product region for a fixed O2 (blue spheres) separation of 2.28 bohr. The potential energy is plotted as a function of the xy location of the hydrogen (red sphere) relative to the center of the O2 bond. The prominent deep potential wells (dark blue regions) correspond to the bound HO2 molecule.

The dark blue regions correspond to attractive potential wells and three conical intersections (the sharp cone features) are clearly visible: One is located in the center (y=0) between the potential wells and the other two are located on each side (y=+/- 3.5 bohr) of the O2. Figure 2 plots a zoomed in side view of the central conical intersection.

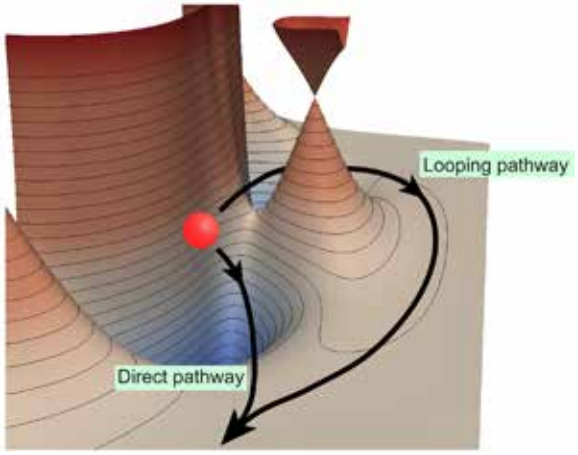

Figure 2. The direct and looping pathways of the hydrogen (red sphere) around the conical intersection for HO2 are sketched with the black arrows. The scattering amplitudes for each of these pathways are summed to obtain the total scattering amplitude for the reactive collision. The reactivity can be enhanced or

suppressed if the two scattering amplitudes interfere constructively or destructively, respectively.

The hydrogen (red sphere) can exit the reaction by traversing either of the two pathways indicated by the thick black arrows: the direct or looping pathway. The total reactivity is determined from the constructive or destructive quantum interference that can occur between these two pathways (in a quantum mechanical description the hydrogen is represented by a wave which effectively traverses both pathways simultaneously). If the interference is constructive (destructive) then the reactivity is enhanced (suppressed). Due to the unique properties associated with ultra-cold collisions, we discovered that the quantum interference in this case can approach its maximum theoretically allowed values! Thus, the reactivity can be essentially turned on or off (i.e. controlled) with unprecedented dynamic range and sensitivity. In addition to the quantum interference effect, there is an additional effect associated with a conical intersection called the geometric phase (or Berry phase). The geometric phase introduces an additional 180° phase shift on the looping pathway relative to the direct pathway in Figure 2 which causes the interference to change from constructive to destructive or vice versa. The correct theoretical treatment must also include the geometric phase.

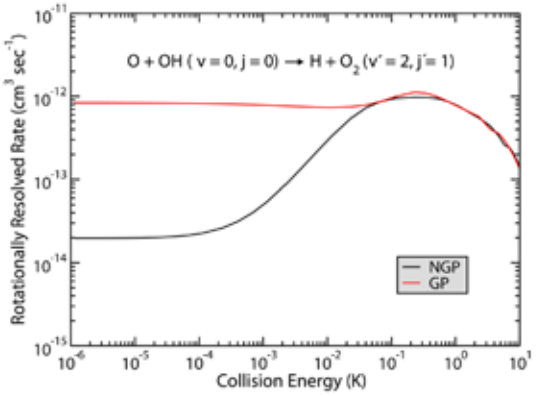

Figure 3. The scattering cross section is plotted as a function of collision energy and scattering angle for the D + HD(v = 4, j = 0) -> D + HD(v' = 3, j' = 0) reaction for odd exchange symmetry. Due to constructive quantum interference, the cross section which includes the geometric phase (plotted with the red mesh and labeled by the red GP) is enhanced at ultra-cold (10-6 K) collision energies relative to the cross section which does not include the geometric phase (plotted with the black mesh and labeled by the black NGP). A quantum resonance occurs in the GP results near 1K which corresponds to the sharply peaked oscillating ridge.

Figure 3 plots the theoretically computed rate coefficient for the O + OH -> H + O2 reaction for a particular initial vibrational (v=0) and rotational state (j=0) and final vibrational (v'=2) and rotational (j'=1) state. The red curve includes the geometric phase and the black curve does not. For this reaction, due to constructive quantum interference, the results which include the geometric phase (red) are dramatically enhanced relative to those with do not include the geometric phase (black) (which undergo destructive interference). The enhanced reactivity predicted in Figure 3 can be verified experimentally and will represent a confirmation of both the newly discovered quantum interference mechanism and the geometric phase effect. Several experimental groups world wide are actively pursuing these measurements. The newly developed capability for treating external electric fields was used to investigate possible control scenarios. Figure 4 plots the rate for the O + OH -> H + O2 ultracold (1 micro-K) reaction for several final states both with the geometric phase (red) and without (black) as a function of the applied electric field strength. The experimentally relevant results are those which include the geometric phase (red). Figure 4 shows that for electric fields between 400 and 500 kV/cm, the reactivity can be effectively turned off (due to destructive quantum interference). Thus, the ability to control ultra-cold reactions with unprecedented dynamic range and sensitivity is indeed possible!

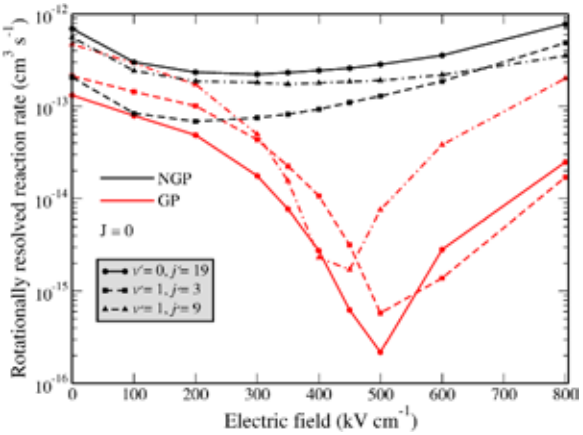

Figure 4. External electric field control of the O + OH -> H + O2 ultracold (10-6 K) reaction rate. Due to destructive quantum interference, the rates computed with the geometric phase (red) become significantly suppressed relative to those computed without the geometric phase (black) for electric field strengths between 400 and 500 kV/cm.

A comprehensive study was also completed for the most fundamental of all chemical reactions, the hydrogen exchange reaction: H + H2 -> H + H2 and its isotopic variants. These calculations demonstrated the generality of the newly discovered quantum interference mechanism and predicted several new experimentally realizable control scenarios based on nuclear spin state selection and isotopic substitution. Figure 5 plots the theoretically computed cross sections for the D + HD(v = 4, j = 0) -> D + HD(v' = 3,

j' = 0) reaction as a function of both collision energy and scattering angle (the direction of the outgoing HD molecule relative to the colliding D + HD). The results plotted with the red (black) mesh correspond to the calculations which include (do not include) the geometric phase. Due to constructive quantum interference, the results which include the geometric phase are enhanced at ultra-cold (1 micro-K) collision energies. A quantum resonance also occurs near 1K which gives rise to the sharp oscillating ridge structure. Both of these features provide experimentally detectable signatures of the new quantum interference mechanism and geometric phase.

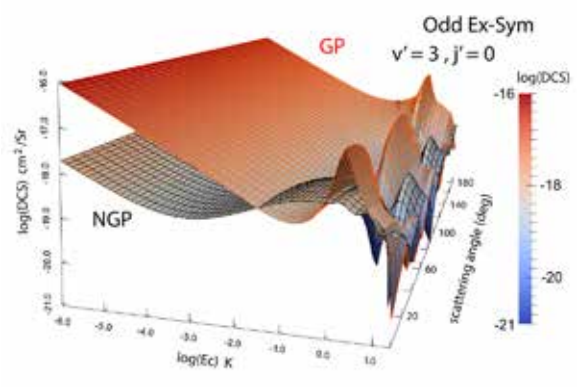

Figure 5. The scattering cross section is plotted as a function of collision energy and scattering angle for the D + HD(v = 4, j = 0) -> D + HD(v' = 3, j' = 0) reaction for odd exchange symmetry. Due to constructive quantum interference, the cross section which includes the geometric phase (plotted with the red mesh and labeled by the red GP) is enhanced at ultra-cold (10-6 K) collision energies relative to the cross section which does not include the geometric phase (plotted with the black mesh and labeled by the black NGP). A quantum resonance occurs in the GP results near 1K which corresponds to the sharply peaked oscillating ridge.

In addition to the highlighted results presented in Figures 1 – 5, this project has produced eight peer reviewed, high-impact publications.[6-12,14] The Nature Communications article[8] has been featured by three web news sites: http://phys.org/news/2015-08-mechanism-ultra-cold-chemical-reactions.html , http://www.technology.org/2015/08/05/ new-mechanism-discovered-for-controlling-ultracold-chemical-reactions/ , and http://www.ladailypost.com/content/lanl-mechanism-discovered-controlling-ultracold-chemical-reactions and in a LANL press release http://www.lanl.gov/discover/news-release-archive/2015/July/07.31-ultracold-chemical-reactions.php. The Physical Review Letter article[9] was selected as a PRL Editors' Suggestion. The Journal of Physics B: Atomic, Molecular and Optical Physics article[11] was published as an invited article in a special issue of the journal. The research from this project was also presented at several international conferences: two were contributed talks,[15,16] three were contributed posters,[17-19] and one was an invited talk.[20] In addition, two invited talks were given at Departmental Colloquia at the University of Nevada Las Vegas[21] and the University of Nevada Reno.[22] Two local (LANL) presentations of this work were also given to summer students and at the Quantum Materials seminar series (in addition to the annual oral LDRD review presentations).[23] This project also helped support a joint LANL/UNLV postdoc Dr. Jisha Hazra.

Impact on National Missions

This project has developed new fundamental capabilities in modeling and simulation which will enable the thorough investigation of molecular collisions and chemical reactions in the new unexplored cold/ultracold energy regime. In addition, this project has helped lay the foundation for potential technological applications based on cold/ultracold molecules including a new framework for realizing quantum computing, the development of sensors with unprecedented sensitivity, enabling new tests of fundamental symmetries, and the synthesis of specific molecular species and materials with novel properties. The control scenarios demonstrated in this project for cold/ultracold molecular collisions could also enable the formation of dense ensembles of cold molecules relevant for studying new exotic states of condensed matter and quantum phases. The fundamental understanding of cold molecular collisions and reaction cross sections computed in this project are also important in astrophysics models for the interstellar medium and molecular clouds. Relevant agencies include DOE's office of Basic Energy Sciences, NASA, DARPA, and the Offices of Army and Naval research.

References

1. Krems, Roman V.. Molecules near absolute zero and external field control of atomic and molecular dynamics. 2005. International Reviews in Physical Chemistry. 24 (1): 99.

2. Tscherbul, T. V., and R. V. Krems. Quantum theory of chemical reactions in the presence of electromagnetic fields. 2008. The Journal of Chemical Physics. 129 (3).

3. Knoop, S., F. Ferlaino, M. Berninger, M. Mark, H. C. Nagerl, R. Grimm, J. P. D'Incao, and B. D. Esry. Magnetically Controlled Exchange Process in an Ultracold Atom-Dimer Mixture. 2010. Phys. Rev. Lett.. 104: 053201.

4. Ospelkaus, S., K. K. Ni, D. Wang, M. H. de Miranda, B. Neyenhuis, G. Qu'em'ener, P. S. Julienne, J. L. Bohn, D. S. Jin, and J. Ye. Quantum-State Controlled Chemical Reactions of Ultracold Potassium-Rubidium Molecules. 2010. Science. 327 (5967): 853.

5. Parazzoli, L. P., N. J. Fitch, P. S. ifmmode dotZelse .Zfiuchowski, J. M. Hutson, and H. J. Lewandowski. Large Effects of Electric Fields on Atom-Molecule Collisions at Millikelvin Temperatures. 2011. Phys. Rev. Lett.. 106: 193201.

6. Pradhan, G. B., N. Balakrishnan, and B. K. Kendrick. Quantum dynamics of O(1 D)+D 2 reaction: isotope and vibrational excitation effects. 2014. Journal of Physics B: Atomic, Molecular and Optical Physics. 47 (135202): 1.

7. Makrides, C., J. Hazra, G. B. Pradhan, A. Petrov, B. K. Kendrick, T. Gonzalez-Lezana, N. Balakrishnan, and S. Kotochigova. Ultracold chemistry with alkali-metal-rare-earth molecules. 2015. Physical Review A. 91: 012708.

8. Kendrick, B. K., J. Hazra, and N. Balakrishnan. The geometric phase controls ultracold chemistry. 2015. Nature Communications. 6: 7918.

9. Kendrick, B. K., J. Hazra, and N. Balakrishnan. Geometric Phase appears in the Ultracold Hydrogen Exchange Reaction. 2015. Physical Review Letters. 115: 153201.

10. Hazra, J., B. K. Kendrick, and N. Balakrishnan. Importance of Geometric Phase Effects in Ultracold Chemistry. 2015. Journal of Physical Chemistry A. 119 (50): 12291–12303.

11. Hazra, J., B. K. Kendrick, and N. Balakrishnan. Geometric phase effects in ultracold hydrogen exchange reaction. 2016. Journal of Physics B: Atomic, Molecular and Optical Physics. 49 (19): 194004.

12. Kendrick, B. K., J. Hazra, and N. Balakrishnan. Geometric Phase Effects in the Ultracold D + HD → D + HD and D + HD ↔ H + D_2 Reactions. To appear in The New Journal of Physics.

13. Kendrick, B. K., J. Hazra, and N. Balakrishnan. Geometric Phase Effects in the Ultracold D + HD → D + HD and D + HD ↔ H + D_2 Reactions. 2016. arXiv:1607.05763 .

14. Kendrick, B. K., J. Hazra, and N. Balakrishnan. Geometric phase effects in the ultracold H + H_2 reaction. To appear in The Journal of Chemical Physics.

15. Kendrick, B. K., J. Hazra, G. Pradhan, and N. Balakrishnan. Quantum reaction dynamics of ultracold O + OH collisions: the geometric phase “controls” reactivity . (Columbus, OH, 8-12 June, 2015).

16. Kendrick, B. K., J. Hazra, and N. Balakrishnan. New Interference Mechanism Controls Ultracold Chemistry. (Providence, RI, 23-27 May, 2016).

17. Kendrick, B. K., J. Hazra, and N. Balakrishnan. New Interference Mechanism Controls Ultracold Chemistry. (Pacific Grove, CA, 28-31 Jan. 2016).

18. Hazra, J., N. Balakrishnan, and B. K. Kendrick. Geometric phase effects in ultracold chemistry. (Providence, RI, 23-27 May, 2016).

19. Ticknor, C., and B. K. Kendrick. Towards inclusion of excited vibrational states in ultracold molecule-molecule quantum scattering calculations. (Providence, RI, 23-27 May, 2016).

20. Kendrick, B. K., J. Hazra, G. Pradhan, and N. Balakrishnan. Cold Chemistry: Quantum reactive scattering calculations of O + OH → H + O2 and Li + LiYb → Li2 + Yb. (Denver, CO, 22-26 March, 2015).

21. Kendrick, B. K.. A Novel Quantum Interference Mechanism Controls Ultracold Chemical Reactions. (Las Vegas, NV, 14 Oct. 2016).

22. Kendrick, B. K.. A Novel Quantum Interference Mechanism Controls Ultracold Molecular Collisions. (Reno, NV, 4 Nov. 2016).

23. Kendrick, B. K.. A Novel Quantum Interference Mechanism Controls Ultracold Chemical Reactions. (Los Alamos, NM, 21 June, 2016).

Publications

Hazra, J., B. K. Kendrick, and N. Balakrishnan. Importance of Geometric Phase Effects in Ultracold Chemistry. 2015. Journal of Physical Chemistry A. 119 (50): 12291–12303.

Hazra, J., B. K. Kendrick, and N. Balakrishnan. Geometric phase effects in ultracold hydrogen exchange reaction. 2016. Journal of Physics B: Atomic, Molecular and Optical Physics. 49 (19): 194004.

Hazra, J., N. Balakrishnan, and B. K. Kendrick. Geometric phase effects in ultracold chemistry. Presented at DAMOP 2016, 47th Annual Meeting of the APS Division of Atomic, Molecular and Optical Physics. (Providence, RI, 23-27 May, 2016).

Kendrick, B. K.. A Novel Quantum Interference Mechanism Controls Ultracold Chemical Reactions. Invited presentation at LANL/CNLS Quantum Materials Seminar. (Los Alamos, NM, 21 June, 2016).

Kendrick, B. K.. A Novel Quantum Interference Mechanism Controls Ultracold Chemical Reactions. Invited presen-

tation at UNLV Department of Chemistry and Biochemistry Colloquium. (Las Vegas, NV, 14 Oct. 2016).

Kendrick, B. K.. A Novel Quantum Interference Mechanism Controls Ultracold Molecular Collisions. Invited presentation at UNR Department of Physics Colloquium. (Reno, NV, 4 Nov. 2016).

Kendrick, B. K., J. Hazra, G. Pradhan, and N. Balakrishnan. Cold Chemistry: Quantum reactive scattering calculations of O + OH → H + O2 and Li + LiYb → Li2 + Yb. Invited presentation at 249th National ACS Meeting – Division of Physical Chemistry Computational Chemical Dynamics: Advancing our Understanding of Chemical Processes in Gas Phase, Biomolecular & Condensed Phase Systems, Symposium in Honor of D. G. Truhlar. (Denver, CO, 22-26 March, 2015).

Kendrick, B. K., J. Hazra, G. Pradhan, and N. Balakrishnan. Quantum reaction dynamics of ultracold O + OH collisions: the geometric phase "controls" reactivity . Presented at DAMOP 2015, 46th Annual Meeting of the APS Division of Atomic, Molecular and Optical Physics . (Columbus, OH, 8-12 June, 2015).

Kendrick, B. K., J. Hazra, and N. Balakrishnan. The geometric phase controls ultracold chemistry. 2015. Nature Communications. 6: 7918.

Kendrick, B. K., J. Hazra, and N. Balakrishnan. Geometric Phase appears in the Ultracold Hydrogen Exchange Reaction. 2015. Physical Review Letters. 115: 153201.

Kendrick, B. K., J. Hazra, and N. Balakrishnan. Geometric phase effects in the ultracold D + HD → D + HD and D + HD ↔ H + D_2 reactions. 2016. xrXiv:1607.05763.

Kendrick, B. K., J. Hazra, and N. Balakrishnan. Geometric phase effects in the ultracold D + HD → D + HD and D + HD ↔ H + D_2 reactions. To appear in The New Journal of Physics.

Kendrick, B. K., J. Hazra, and N. Balakrishnan. Geometric phase effects in the ultracold H + H_2 reaction. To appear in The Journal of Chemical Physics.

Kendrick, B. K., J. Hazra, and N. Balakrishnan. New Interference Mechanism Controls Ultracold Chemistry. Presented at The 63rd Pacific Conference on Spectroscopy and Dynamics. (Pacific Grove, CA, 28-31 Jan. 2016).

Kendrick, B. K., J. Hazra, and N. Balakrishnan. New Interference Mechanism Controls Ultracold Chemistry. Presented at DAMOP 2016, 47th Annual Meeting of the APS Division of Atomic, Molecular and Optical Physics . (Providence, RI, 23-27 May, 2016).

Makrides, C., J. Hazra, G. B. Pradhan, A. Petrov, B. K. Kendrick, T. Gonzalez-Lezana, N. Balakrishnan, and S. Kotochigova. Ultracold chemistry with alkali-metal-rare-earth molecules. 2015. Physical Review A. 91: 012708.

Pradhan, G. B., N. Balakrishnan, and B. K. Kendrick. Quantum dynamics of O(1 D)+D 2 reaction: isotope and vibrational excitation effects. 2014. Journal of Physics B: Atomic, Molecular and Optical Physics. 47 (135202): 1.

Ticknor, C., and B. K. Kendrick. Towards inclusion of excited vibrational states in ultracold molecule-molecule quantum scattering calculations. Presented at DAMOP 2016, 47th Annual Meeting of the APS Division of Atomic, Molecular and Optical Physics. (Providence, RI, 23-27 May, 2016).

Multi-scale Probabilistic Resuspension Modeling of Spores and Radionuclides from Outdoor Surfaces

Michael J. Brown
20140444ER

Abstract

Small micron-sized radiological, biological, and/or heavy-metal-laden particles deposited on urban and rural surfaces during a nuclear or industrial accident, a terrorist attack, or inadvertently as a waste by-product can be resuspended into the air due to wind gusts and when breathed in can result in harmful exposures to the population over large areas and long time periods (particles that penetrate into the lungs are typically smaller than 10 microns, which is roughly 30 times smaller than the period at the end of this sentence!). Particle adhesion to surfaces – the main force that holds micron-sized particles to the ground – and the resultant resuspension process is poorly understood, however. In this project, our team devised accurate and repeatable methods for quantifying the particle-surface adhesion force using Atomic Force Microscopy (AFM) and modified a plume transport and dispersion model to include a more accurate particle resuspension algorithm that accounts for the probabilistic nature of the adhesion forces holding the particle to the ground and the wind-induced drag and lift forces trying to pull the particles off the surface. As a by-product of the experimental work, new (and sometimes surprising) findings were observed regarding the adhesion force on clean vs. "dirty" surfaces, for smooth versus roughened particles, for biological vs. non-biological particles, and in humid environments. Further, our experimental results confirmed that the current state-of-the-art resuspension models often incorrectly specify two important inputs: the average distance between surface asperities and the shape of the adhesion force distribution, and our modeling efforts confirm that the resuspended mass flux (i.e., the amount of particles blown off the surface) can be very sensitive to these inputs.

Background and Research Objectives

Based on assessment of controlled laboratory experiments, researchers were not able to predict the resuspension rate of inorganic spherical particles to within a factor of ±10; experiments using a surrogate for the Bacillus anthracis spore – the causative agent for the anthrax disease – resulted in resuspension rates of up to 1000x larger than predicted by current models [1, 2]. This means that current predictive capabilities are not able to quantify the amount of particles lofted into the air with enough accuracy to determine if a resuspension event is extremely hazardous to health or not of any concern whatsoever. This uncertainty is due in part to the prior inability to accurately measure particle adhesion to surfaces, previous focus on clean/pristine surfaces only, lack of knowledge regarding the microscopic structure of the surface itself, the confounding effects of humidity and moisture on adhesion, and the inherent stochasticity of the adhesion, lift, and drag forces.

For this project, our main research objective was to accurately measure adhesion force distributions using AFM for a wide range of particle and surface types under a wide range of environmental conditions. Secondary research objectives were to utilize the adhesion measurements to confirm or invalidate different theories used in particle resuspension algorithms and to accurately measure the microscopic surface morphology of a range of urban construction materials.

Scientific Approach and Accomplishments

During this project, we developed a new Atomic Force Spectroscopy (AFS) platform to overcome previous experimental limitations and conducted first-of-their-kind particle adhesion measurements on non-ideal urban/environmental systems. In this context, adhesion is the tendency of a particle and surface to cling to one another, and may result from chemical bonds, molecular attraction (e.g., van der Waals forces), electrostatics, or liquid-bridge-induced capillary forces. We conducted hundreds of thousands of individual adhesion force measurements using different-sized glass spheres, aspherical particles and biological particles on different surfaces like gold, mica, silicon, micro-fabricated surfaces, and

irregular urban construction surfaces like concrete, wood, clean glass and dirty glass. Figure 1 depicts how the AFM works and the resultant adhesion force map it measures across a surface of interest.

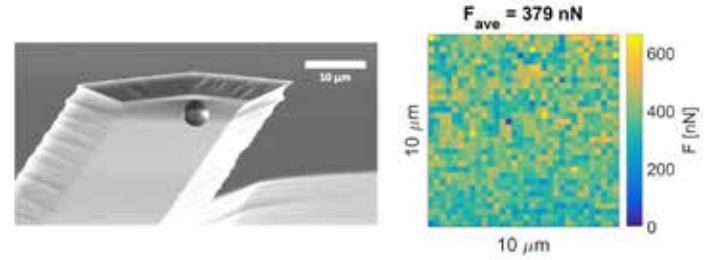

Figure 1. In Atomic Force Microscopy (AFM), a small particle is glued to the tip of a metal cantilever (left). The particle-cantilever probe is lowered vertically to the surface of interest and then slowly pulled away. As the probe is pulled away it bends downward due to the adhesion of the particle to the surface until it snaps up when the particle detaches. A laser precisely measures the subtle bend of the cantilever which is then converted to a force through knowledge of the cantilever stiffness. The probe is then moved horizontally to sample other locations across the (in this case 10 x 10 micron) surface of interest to produce a particle-surface adhesion force map (in nano-Newtons, i.e., 10-9 Newtons) between a glass sphere and a clean glass surface (right). Note that although the glass surface appears to be smooth and homogenous, the adhesion force is highly variable from location to location resulting from nanoscale (10-9 m) variations in the underlying surface topography.

A point of emphasis here is that we did not merely employ commercially available technology or traditional methods of measurement, but instead developed multiple capabilities and employed stringent performance thresholds that address typical AFS and other experimental approach limitations. Although not an initial goal of this proposal, we developed "in-house" probe manufacturing capabilities after we determined that variability in commercially-available colloidal probes limited the ability to generate reproducible adhesion data sets on even the most simplistic of designs (e.g. glass sphere on glass/silicon surface). Through efforts of this proposal, LANL can now reliably generate specialized probes for AFM and AFS investigations. Current probe capabilities include colloids of various size and composition and BSL-1 biological/synthetic microscopic materials of user request. A further development generated through modification of an existing Asylum Atomic Force Microscope, was the ability to control relative humidity from essentially ~0 to ~97+%. Variations in humidity can have a dramatic effect on adhesion due to the potential formation of a liquid bridge between the particle and the surface at higher humidities. In the sections that follow, we provide a few examples from our broad suite of adhesion and surface topology measurements that illustrate new findings, confirm theories hypothesized by other researchers, and call into question current assumptions in state-of-the-science particle resuspension algorithms.

Particle Size and Rough vs. Smooth Particles. Our adhesion force histogram measurements of 5 and 30 micron smooth glass spheres on flat glass surfaces confirm well-regarded theories that larger particles result in larger adhesion forces compared to smaller particles due to more particle-surface contact area in the former case (see Figure 2). In carefully controlled experiments, we also confirmed the hypothesis of Suresh and Walz [3] that roughened particles have lower adhesion than smooth particles of the same diameter (due to less particle-surface contact area). To put the differences of the adhesion force results in context, a wind gust that would resuspend the 5-micron roughened glass spheres would need to be 2-3 times stronger (owing to the wind load force being proportional to the square of the wind velocity) to resuspend the 5-micron smooth glass spheres. Notably, nearly all resuspension algorithms used in the plume dispersion modeling community do not account for the differences between smooth and rough particles.

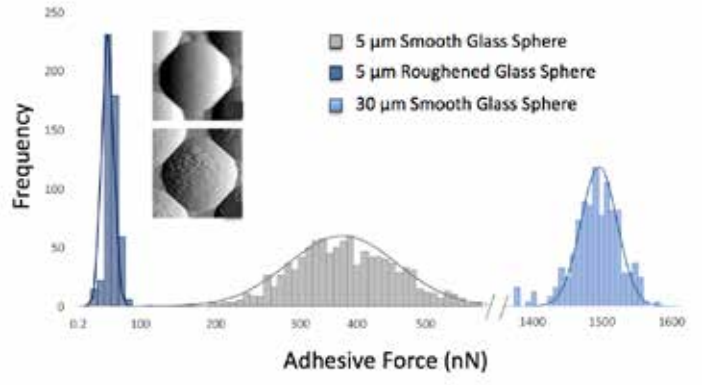

Figure 2. Adhesion force histograms showing the differences between 5-micron smooth, 5-micron rough, and 30 micron smooth glass spheres on clean flat glass. The two scanning electron microscope (SEM) images show the morphological differences between the five micron smooth and rough glass spheres.

Clean vs Dirty Surfaces. Experiments on particle-surface adhesion have consistently considered only laboratory-clean particles and surfaces for reproducibility. This fact raises two questions: (1) are the adhesion measurements representative of real outdoor urban surfaces, which are usually covered in dust, pollen, and other pollutants, and if not, (2) does the difference between clean and contaminated surfaces affect the resuspension rate? To answer these questions, we used AFM to measure the adhesion

force of a 5-µm glass sphere in contact with two glass surfaces, one cleaned and one that had been left outside for six weeks. As shown in in Figure 3, the measured adhesion force distribution of the clean glass was unimodal, while the dirty glass showed a bi-modal distribution. The low adhesion forces that show up for the dirty glass case are hypothesized to be due to soil, dust, and pollen particles that are attached to the glass, making it easier for the glass particle to detach from the surface. Scanning electron images confirmed the presence of contaminant particles on the glass, and concurrent measurements of surface topology and adhesion showed that regions of low adhesion were often associated with dust- and pollen-size surface deformities. These surprising results suggest that small wind gusts may be able to dislodge particles from dirty surfaces, while stronger winds are needed for clean surfaces. More experiments with different sizes and types of particles and different surface types are needed to see if these results hold more broadly.

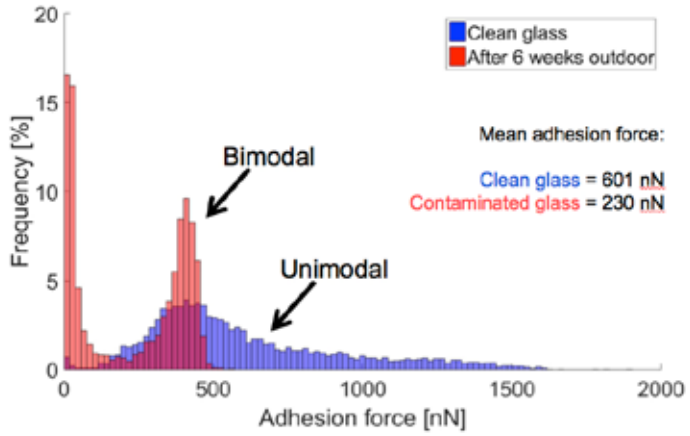

Figure 3. Adhesion force histograms showing the difference between a smooth 5-micron glass sphere on clean flat glass (blue) and "dirty" glass exposed to the elements for 6 weeks.

Humidity Effects. As part of this project, the AFS platform was equipped with a humidity control environment. It is commonly assumed in the literature, e.g., [4, 5], that above a certain relative humidity (RH) a liquid bridge will form between a spherical particle and the flat surface resulting in a huge jump in the adhesion force. Figure 4 shows the average adhesion force as a function of RH for 5 and 30 micron smooth glass spheres on glass, wood, and concrete surfaces. The 30 micron glass spheres show the expected low adhesion for RH < 30%, and then a sudden jump for larger RH as well as the expected gradual reduction in adhesion force as RH is increased further. Unexpectedly, the 5-micron glass spheres showed a nearly constant average adhesion force as the RH was varied. Other interesting results included a step-change in adhesion jumping up to much larger values at a RH = 75% for 30-micron glass particles on wood. The adhesion force for 5-micron glass spheres on wood and concrete remained small as a function of RH, while the 30-micron glass spheres on wood did likewise. The results for wood and concrete may be partly due to the large roughness and porosity of the surfaces. Further investigation is needed to better understand these results.

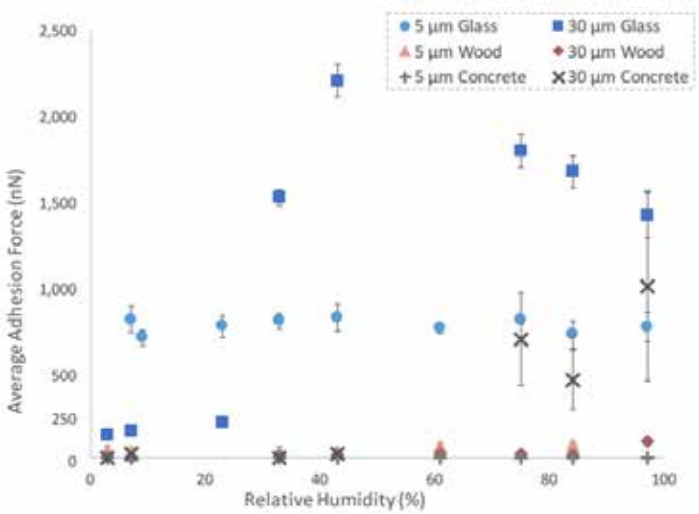

Figure 4. The impact of relative humidity on the average adhesion force for smooth 5- and 30-micron glass spheres on clean glass, unpainted wood, and concrete.

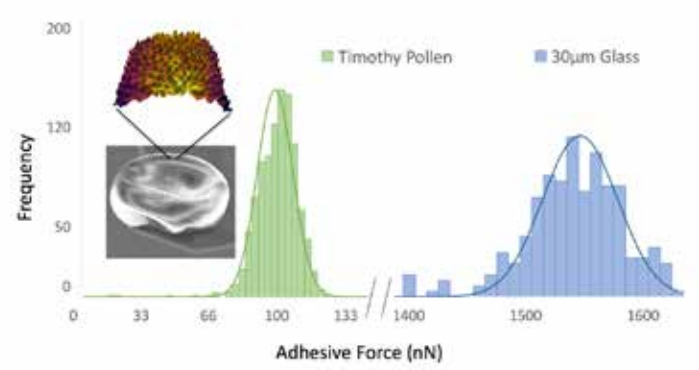

Figure 5. An example of an adhesion force histogram for a biological particle, in this case Timothy pollen (29 micron diameter) on a clean glass surface compared to a similarly-sized smooth glass sphere on a clean glass surface. These results suggest that a wind gust would need to be roughly 4 times larger to dislodge and resuspend the smooth glass spheres as compared to the Timothy pollen.

Biological Particles and Adhesion Forces. Initial attempts were made to measure adhesion between an actual biological particle and different surfaces. Figure 5 highlights the fabrication and adhesive force distribution of a timothy pollen particle (roughly 29 microns across) mounted onto an AFM cantilever using our in-house probe modification capability. The adhesion force distribution plot demon-

strates that the nanoscale roughness of the outer protein coat results in low adhesive force with only small variations over the glass surface. This indicates that particle surface roughness dominates discrete interactions between biological particles and the surface, a property shared with the roughened glass microspheres (recall Figure 2).

The Impact of Surface Asperity Spacing. The state-of-the-art Reeks and Hall resuspension algorithm [6] requires a number of inputs, among which is the ratio between the particle radius (r) and the horizontal distance between the peaks of the underlying surface (a) that act as pivot points; effectively, this is the ratio of the aerodynamic drag force lever-arm to the adhesion force lever-arm, the former required for estimating the pull-off force and the latter for the attachment force. There are no data in the literature on the mean value or the distribution of this ratio and further how important it is in calculating resuspension. Reeks and Hall defaulted to using r/a = 100. To help ascertain whether this value is appropriate we measured the "topography" of a glass surface using AFM and derived "a" via geometric arguments by letting a fictitious non-deformable spherical particle "fall" vertically until it touched the surface at one point, then rotate the particle until it touched a second point on the surface, and then calculated the distance between the two points to obtain the adhesion-force lever-arm a.

We investigated three particle radii and found that the average r/a = 66, 142, and 319 for 5, 20, and 100 micron spherical particles, respectively, on a clean glass surface. We found that the shape of the distribution of a depends on the particle radius, namely smaller particles are more likely to touch two nearby asperities, while larger particles touch nearby and more distant asperties with equal probability. To compute the resuspension rate, the Reeks and Hall algorithm was adapted to also include the distribution of r/a as an input, rather than just the fixed value. Using a range of adhesion forces and wind speeds, the resuspension rate calculated from the Reeks and Hall equation using the measured distribution was found to vary about a factor of two to five for the 100 micron particle size when compared to using the standard r/a = 100 value. Differences were nearly always less than a factor of two for the 20 and 5 micron cases. It is not clear at this time if these results can be extrapolated to other surface types with different morphologies.

Summary

Overall, the results of the experimental AFS measurements highlight the importance of nanoscale interactions and their dominance in controlling adhesive forces of micron-sized contaminates attempting to be modeled in the resuspension process. While far from exhaustive in their description of all particle-surface interactions, these findings highlight the importance of understanding discrete interactions when attempting to describe drag, lift, and adhesion forces experienced by particles.

Impact on National Missions

Resuspension of hazardous biological agents, heavy metal and radionuclide particles deposited on indoor and outdoor surfaces plays a role in numerous fields within LANL's national security mission, including counter-terrorism, nuclear power plant safety, plutonium storage, clean-up and remediation, and environmental risk assessment. The particle resuspension models developed and experimental data collected during this project will be of great interest to DoD, DHS, EPA and other agencies looking at chemical, biological, and radiological terrorist attacks, nuclear fallout after-effects, and Superfund contaminated sites, as well as internally at Los Alamos National Laboratory for environmental remediation and hazard risk assessment purposes. The new resuspension models developed in this project are now being applied in collaboration with the Naval Surface Warfare Center and the Edgewood Chemical and Biological Center to look at biological agent resuspension from contaminated military vehicles and other assets, a national security application. In addition, the experimental efforts of this proposal have resulted in new LANL/CINT capabilities that are being institutionalized for CINT user access, including reliable generation of specialized probes for AFM and AFS investigations. We envision extending our capabilities to include pseudo-cellular probes in a to-be-developed BioForce Platform, through collaboration with CINT staff scientists in the soft, biological, and composite nanomaterials thrust. Furthermore, approval for the extension of this research has been accepted as a CINT user proposal 2016AU0107: Effects of Surface Asperities on Colloid Adhesion.

References

1. Loosmore, G. A.. Evaluation and development of models for resuspension of aerosols at short times after deposition. 2003. ATMOSPHERIC ENVIRONMENT. 37 (5): 639.

2. Kim, , Gidwani, B. E. Wyslouzil, and C. W. Sohn. Source term models for fine particle resuspension from indoor surfaces. 2010. BUILDING AND ENVIRONMENT. 45 (8): 1854.

3. Suresh, L., and J. Y. Walz. Effect of surface roughness on the interaction energy between a colloidal sphere and a flat plate. 1996. JOURNAL OF COLLOID AND INTERFACE SCIENCE. 183 (1): 199.

4. Boer, M. P. de. Capillary adhesion between elastically

hard rough surfaces. 2007. EXPERIMENTAL MECHANICS. 47 (1): 171.

5. Butt, , and Kappl. Normal capillary forces. 2009. ADVANCES IN COLLOID AND INTERFACE SCIENCE. 146 (1-2): 48.

6. Reeks, M. W., and D. Hall. Kinetic models for particle resuspension in turbulent flows: theory and measurement. 2001. JOURNAL OF AEROSOL SCIENCE. 32 (1): 1.

Publications

Brambilla, S., M. Brown, G. Montano, M. Rush, and S. Speckart. Effect of environmental debris on surface roughness, adhesion force distribution, and resuspension. 2016. LA-UR-16-27262. To be submitted to Journal of Aerosol Science..

Brambilla, S., M. Brown, M. Rush, S. Speckart, and G. Montano. Impact of asperity distance distribution on the Rock 'n' Roll resuspension model. 2016. In preparation..

Brambilla, S., S. Speckart, and M. Brown. Forces involved in resuspension of spherical and rod-shaped particles: A review for plume dispersion modelers. 2016. LA-UR-16-27013. Submitted to Atmospheric Environment..

Brambilla, S., S. Speckart, and M. Brown. Resuspension rate models for plume dispersion applications and extension to rod-shaped particles. 2016. LA-UR-16-27096. To be submitted to Atmospheric Environment..

Rush, M., P. Adams, and G. Montano. A review of colloid force measurement procedures [for novices]. 2016. LA-UR-16-27316. To be submitted to Review of Scientific Instruments..

Rush, M., P. Adams, and G. Montano. Controlled adhesion measurements for colloid force spectroscopy in a dry air environment. 2016. LA-UR-16-27221. To be submitted to Review of Scientific Instruments..

Rush, M., S. Brambilla , S. Speckart , M. Brown , and G. Montano . Environmental effects on adhesion and redistribution of debris from building materials. 2016. LA-UR-16-27222. To be submitted to J. of Adhesion Science and Technology (In preparation).

Speckart, S., S. Brambilla, and M. Brown. Consequences of utilizing a rough surface model to estimate behavior of particle resuspension for smooth engineered surfaces. 2016. In preparation..

First Direct Observation of Weibel Instability in Collisionless Shocks

Sasikumar Palaniyappan
20140483ER

Abstract

Acceleration of charged particles as they interact with "collisionless shocks" is a widespread phenomenon occurring across the entire universe. Unlike the well-known collisional hydrodynamic shocks, in the collisionless shocks the particle collision time is much larger than the particle transit time through the shock. This astrophysical phenomenon occurs regularly in the cosmos, for example, at supernova shocks, during fast coronal mass ejection from the sun forming solar-wind shocks and at the planetary bow shocks [1-7]. A particular type of electromagnetic plasma instability known as Weibel instability is believed to be the dominant mechanism behind the formation of these collisionless shocks in the cosmos [8]. Weibel instability leads to an exponentially growing magnetic field arising from the electromagnetic micro turbulences in initially un-magnetized or weakly magnetized plasmas present in the vicinity of gamma ray burst sources, supernovae and galactic cosmic rays. How these magnetic fields are generated and what are their structures, which dissipation mechanism is dominant, which physical processes lead to shock formation, and how particles are accelerated in these shocks remain open questions. Apart from indirect spacecraft observations, there is no direct observation to date of collisionless shocks mediated by Weibel instability. Here we proposed first direct observation of Weibel instability mediated laser-driven collisionless shocks in laboratory plasmas diagnosed using laser-driven proton deflectometry [9]. At the end of the project period, we have successfully carried out the experiment at the Trident laser facility. Preliminary analysis of the experimental results indicates that we indeed see laser-driven collisionless shock in near-critical density plasmas. We are preparing a manuscript discussing the first laboratory observation of laser-driven collisionless shock in near-critical plasmas.

Background and Research Objectives

Collisionless shock acceleration of particles was originally proposed by Enrico Fermi in 1949 to explain the origin of cosmic rays in the interstellar space of the galaxy as particles interact with cosmic background magnetic field [10]. However their existence was speculative until spacecraft observations in 1964 of accelerated particles at solar-wind and planetary bow shocks gave insight into how acceleration may occur in astrophysical situations [11]. Very recently, the Cassini spacecraft crossing the bow shock region of Saturn has observed relativistic MeV energy electrons likely accelerated by strong astrophysical shocks [12]. It is generally believed from computer simulations and theoretical efforts that Weibel instability - a plasma instability originating from temperature anisotropy - leads to generation of large magnetic fields within the plasmas which moderates the collisionless shock formation. Weibel instability can develop in plasmas irrespective of whether they are initially magnetized.

In a collisionless shock, a charged particle gains energy by repeated scatterings across the shock from the converging magnetic field fluctuations acting like a magnetic mirror. This is similar to a tennis ball bouncing between two tennis rackets gaining energy as the rackets come closer to each other. Although, much more is known about these shocks now than a few decades ago, still many physics questions pertaining to the exact role of Weibel instability during the shock formation and particle acceleration remain unanswered. In this scenario, a first ever direct observation and demonstration of collisionless shocks mediated by Weibel instability in the laboratory would provide a tremendous opportunity to study and make quantitative measurements on this exotic phenomenon in a more controlled setting. The results would be extremely useful to model astrophysical shock phenomena accurately, and to test existing hypotheses in line with the spacecraft shock observations.

To form a collisionless shock in plasmas using lasers, the laser piston velocity should exceed the ion sound speed [13]. Figure 2 shows results from 2D Particle-In-Cell (PIC)

code 'OSIRIS' [14] simulation of linearly polarized ultra-intense laser (peak intensity of 5 x 1021 W/cm2 (a0 = 60); wavelength 1 µm) interacting with a thick fully ionized proton slab with density of 50 x 1021 electrons/cm3 (50 ncr) illustrating the collisionless shock formation in plasmas using intense lasers [13]. The results are snapshots of the interaction taken at 385 fs after the laser began to interact with the plasma (shock formation time ~250 fs). The initial plasma temperature is 1 keV. The simulation box size is 80 µm by 18 µm.

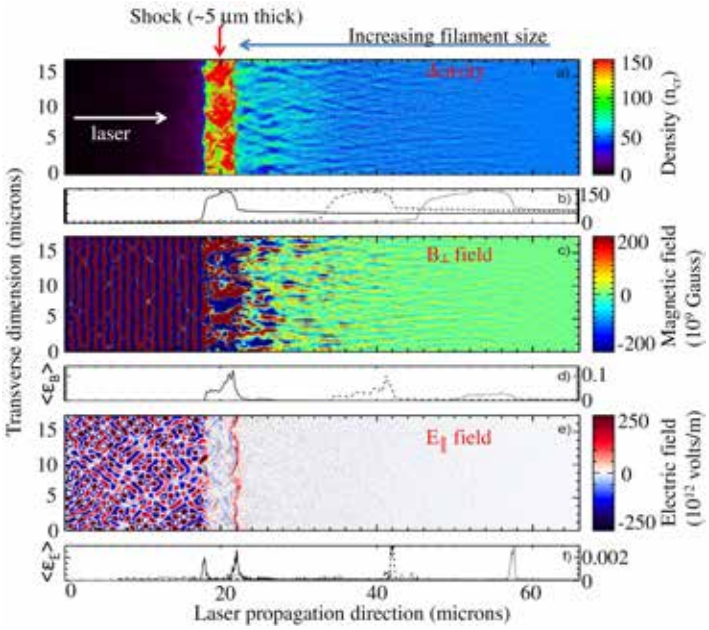

Figure 1. 2D 'OSIRIS' Particle-In-Cell (PIC) simulation of ultra-intense laser (peak intensity of 5 x 10 W/cm) forming collisionless shock in a thick fully ionized proton slab with initial plasma density of 50 .

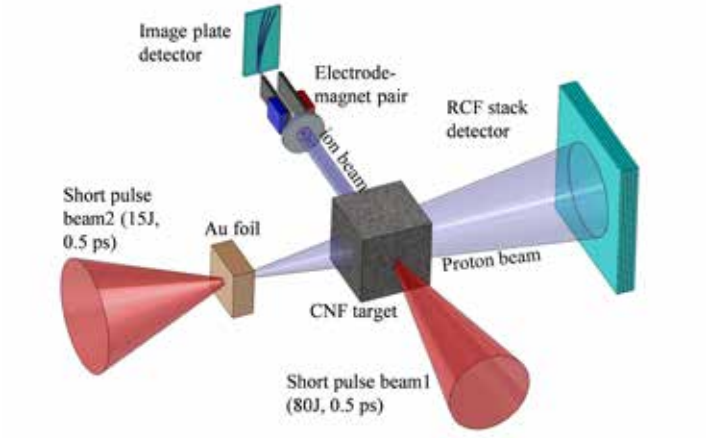

Figure 2. Experimental setup at the Trident west target chamber for studying laser-driven collisionless shock

Figure 1(a,b) show strong compression of the plasma due to laser piston action leading to shock formation along with strong filamentation. The transversely averaged plasma density in figure 1(b) shows results at 805 fs and 1134 fs too. At later time, the shock structure has evolved from initial ~5 µm to ~20 µm. Similar filamentary structures are observed in the upstream magnetic field perpendicular to the laser propagation direction (figure 1(c)) (Note that the laser is always behind the shock since the plasma remains opaque to the laser. Hence, the electromagnetic fields that are present within the shock and in the upstream region are not from the laser electromagnetic field). Since the hot and cold electron currents are largely limited to the laser propagation direction, the Weibel magnetic fields are perpendicular to those electron currents. The filament size evolves from electron skin depth (~25 nm) at the far upstream to ion skin depth (1 µm) close to the shock (Note the magnetic field in the downstream is from the laser). The magnetic energy peaks around the shock (figure 1(d)) and the magnetic energy density reaches 12% of equipartition with upstream kinetic energy density as measured in the downstream rest frame. The shock front is associated with a well-defined longitudinal electric field (Note: the laser has no electric field in the longitudinal direction). Even though the energy associated with the electric field is very small compared to the magnetic field, it could still reflect ~10% of the upstream colder ions as the shock moves forward, which could also be an experimental signature as these ions typically have narrow energy spread. As the reflected ions stream through the background cold ions, they could also enhance the upstream magnetic field due to ion Weibel instability. This is actually evidenced in figure 1(c) at the foot of the shock where ion reflections occur having the maximum Weibel magnetic field.

Scientific Approach and Accomplishments

Figure 2 shows the experimental setup implemented at the LANL Trident laser facility for observing laser-driven collisionless shocks in near-critical density plasmas. The 160 TW linearly polarized Trident short pulse 'C' beam (80J, 650fs) was focused using an f/8 off-axis parabola to focused intensity of 2 x 1019 W/cm2 (a0 = 4.5) on to a ~100 thick carbon foam with density of 12 mg/cm3 (4 ncr). The plasma density and the laser 'a0' value satisfy the condition for collisionless shock generations in laser-driven plasma [13]. The collisionless shock generated in the carbon foam was diagnosed using multiple diagnostics. Backscattered optical light was characterized using a time-integrated spectrometer and time-resolved single-shot FROG (frequency-Resolved-Optical-Gating) diagnostics. These diagnostics could reveal the dynamics of laser-plasma interaction which can be compared to the simulation results. The shock reflected ions were characterized using

Thomson parabola ion spectrometers. The shock speed can be deduced from the energy of the shock reflected carbon ions. The primary diagnostic for observing the laser-driven shock is the radio chromic film (RCF) stack. A second short-pulse laser (20J, 0.5 ps) was focused on to a 5m thick gold foil to an intensity of 1020 W/cm2 to produce laser-driven protons up to 25 MeV. When these protons traverse through the laser-driven carbon foam target, they get deflected due to the shock fields in the foam plasma. The deflected protons are then captured in the RCF stack. Protons of different energy range out in different RCF layers, thus providing information about the temporal evolution of the laser-driven collisionless shock in the carbon foam.

The low density foam targets (4ncr = 4.4 X 1021 electrons/cm3 i.e., density of 12 mg/cm3) are critical for the success of this project. Typical aerogel foam targets have micron size pores comparable or larger than the wavelength of the driving laser. Such large pores are more susceptible to filamentation of the incident laser, such that it is unable to drive the foam target like a piston and to form a collisionless shock. Here we proposed to use a novel carbon nanotube foam (CNF) low density target with pore sizes only of few tens of nanometers. The unpaid collaborator Dr. Wenjun Ma from Peking University, China has extensive experience in producing and characterizing the CNF targets for prior successful experiments involving CNF targets [15]. He provided the necessary CNF targets for this project.

Figure 3(a-i) shows the RCF images of deflected laser-generated protons as they traverse through the laser-driven collisionless shock in carbon nano foam. Each RCF layer corresponds to a specific time of the laser-plasma interaction. T = 0 ps corresponds to the peak of the shock-driving laser arriving at the carbon nano foam. The shock is formed in the near-critical foam plasma slightly after the peak of the driving laser. Figure 3 (a-i) show the temporal evolution of the Weibel filament and the shock front. Figure3 (j) and (k) are the zoomed images of the figures (f) and (g) respectively. The images indicate that the laser is indeed driving the foam target like a piston that launches longitudinal electron current filaments in the laser direction. The piston/shock front exists for >10 ps after the driving laser is gone, consistent with the simulations. We are in the process of generating synthetic proton radiographs to compare with the measured RCF images to interpret the data.

Figure 4 shows the carbon ion spectra measured by the Thomson parabola ion spectrometer. The ion spectrum shows ion spectral peak ~35 MeV. Cold ions reflected from the shock front get twice the velocity of the shock. The 35 MeV carbon ion energy corresponds to a speed of 7.8 % of the speed of light i.e., 23.4 µm/ps. This implies that the shock speed was 11.7 µm/ps, which is consistent with the expected piston speed of 0.035 'c' i.e., 10.5 µm/ps.

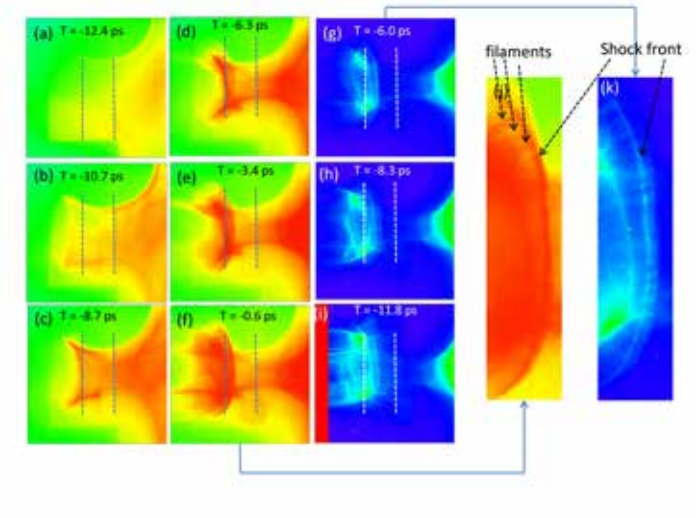

Figure 3. Radio chromic film images of the laser-driven collisionless shock probed by the laser-generated protons. The dashed lines indicate the boundaries of the initial target location.

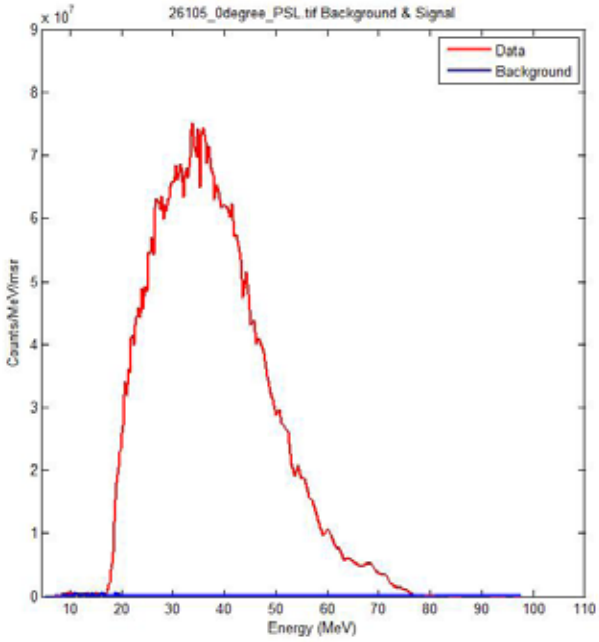

Figure 4. Carbon ion spectra showing ion spectral peak ~35 MeV measured by Thomson parabola ion spectrometer

Figure 5(a) shows the measured back scatter single-shot FROG as the plasma front reflects the incident laser light. The reflected intensity (solid red line) shows that the laser light did not filament in the carbon nano foam. The corresponding temporal phase indicates that the laser drove the plasma like a piston as expected. Instantaneous piston velocity can be deduced from the temporal phase of the reflected laser light. We have also measured the time-

integrated backscattered spectrum independently using an IR spectrometer. We see a wavelength red-shift of 30 nm from the central 1054 nm. This wavelength shift is consistent with the expected wavelength shift from the simulation. We are currently analyzing the experimental results and we plan to write up a manuscript soon. Finally, the ER project has resulted in several invited talks, conference presentations and publication.

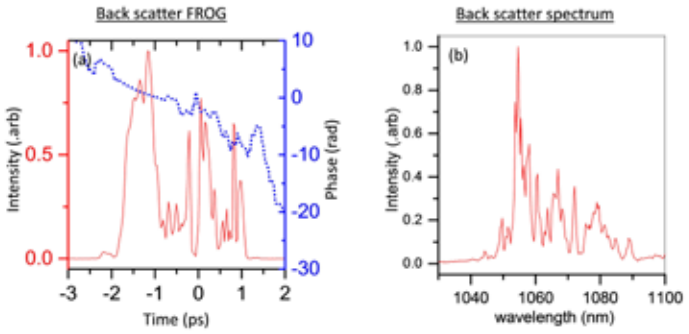

Figure 5. (a) Backscattered laser intensity (solid red line) and temporal phase measured using single-shot FROG; (b) backscattered laser spectrum measured by IR spectrometer.

Impact on National Missions

This project directly aligns with the LANL "Nuclear and Particle Futures" science pillar, specifically with its NPAC, HEDP, and (Advanced) Accelerators elements. Investment in this proposal would establish a unique LANL capability for studying astrophysical sciences using intense laser-plasma interactions. Studying laboratory astrophysics with intense lasers is at the heart of the LANL proposal High Intensity Laser Laboratory (HILL), submitted to the recent NNSA Experimental Science Facilities call, and squarely along the path of the LANL Laser Strategy. A first ever demonstration of Weibel instability mediated collisionless shock in the laboratory will have a tremendous impact on both the laser-plasma and the astrophysics community. It opens a new venue for closer evaluation of this exotic astrophysical phenomenon, which cannot be studied otherwise. The results could be used to test and evaluate several existing hypotheses explaining this phenomenon. Within LANL, astrophysics and cosmology is one of the focus areas under the "Nuclear and particle Features". Laboratory demonstration of an important astrophysical phenomenon would be a great capability for LANL, paving the way for future related explorations.

A first ever demonstration of Weibel instability mediated collisionless shock in the laboratory will have a tremendous impact on both the laser-plasma and the astrophysics community. It opens a new venue for closer evaluation of this exotic astrophysical phenomenon, which cannot be studied otherwise. The results could be used to test and evaluate several existing hypotheses explaining this phenomenon. Within LANL, astrophysics and cosmology is one of the focus areas under the "Nuclear and particle Features". Laboratory demonstration of an important astrophysical phenomenon would be a great capability for Trident laser facility and LANL, paving the way for future related explorations.

References

1. Kato, T. N.. Relativistic collisionless shocks in unmagnetized electron-positron plasmas. 2007. ASTROPHYSICAL JOURNAL. 668 (2): 974.

2. Piran, T.. Gamma-Ray Bursts. 2002. INTERNATIONAL JOURNAL OF MODERN PHYSICS A. 17 (20): 2727.

3. Spitkovsky, . On the structure of relativistic collisionless shocks in electron-ion plasmas. 2008. ASTROPHYSICAL JOURNAL LETTERS. 673 (1): L39.

4. Cassam-Chenai, , J. P. Hughes, E. M. Reynoso, Badenes, and Moffett. Morphological evidence for azimuthal variations of the cosmic-ray ion acceleration at the blast wave of SN 1006. 2008. ASTROPHYSICAL JOURNAL. 680 (2): 1180.

5. Bamba, A., R. Yamazaki, T. Yoshida, T. Terasawa, and K. Koyama. A spatial and spectral study of nonthermal filaments in historical supernova remnants: Observational results with Chandra. 2005. ASTROPHYSICAL JOURNAL. 621 (2): 793.

6. Remington, B. A., R. P. Drake, and D. D. Ryutov. Experimental astrophysics with high power lasers and Z pinches. 2006. REVIEWS OF MODERN PHYSICS. 78 (3): 755.

7. Aharonian, F. A., A. G. Akhperjanian, K. M. Aye, A. R. Bazer-Bachi, M. Beilicke, W. Benbow, D. Berge, P. Berghaus, K. Bernlohr, O. Bolz, C. Boisson, C. Borgmeier, F. Breitling, A. M. Brown, J. B. Gordo, P. M. Chadwick, V. R. Chitnis, L. M. Chounet, R. Cornils, L. Costamante, B. Degrange, A. Djannati-Atai, L. O. Drury, T. Ergin, P. Espigat, F. Feinstein, P. Fleury, G. Fontaine, S. Funk, Y. A. Gallant, B. Giebels, S. Gillessen, P. Goret, J. Guy, C. Hadjichristidis, M. Hauser, G. Heinzelmann, G. Henri, G. Hermann, J. A. Hinton, W. Hofmann, M. Holleran, D. Horns, O. C. de Jager, I. Jung, B. Kheilifi, N. Komin, A. Konopelko, I. J. Latham, R. Le Gallou, M. Lemoine, A. Lemiere, N. Leroy, T. Lohse, A. Marcowith, C. Masterson, T. J. L. McComb, M. de Naurois, S. J. Nolan, A. Noutsos, K. J. Orford, J. L. Osborne, M. Ouchriff,

M. Panter, G. Pelletier, S. Pita, M. Pohl, G. Puhlhofer, M. Punch, B. C. Raubenheimer, M. Raue, J. Raux, S. M. Rayner, I. Redondo, A. Reimer, O. Reimer, J. Ripken, M. Rivoal, L. Rob, L. Rolland, G. Rowell, V. Sahakian, L. Sauge, S. Schlenker, R. Schlickeiser, C. Schuster, U. Schwanke, M. Siewert, H. Sol, R. Steenkamp, C. Stegmann, J. P. Tavernet, C. G. Theoret, M. Tluczykont, D. J. van der Walt, G. Vasileiadis, P. Vincent, B. Visser, H. J. Volk, and S. J. Wagner. High-energy particle acceleration in the shell of a supernova remnant. 2004. NATURE. 432 (7013): 75.

8. WEIBEL, E. S.. SPONTANEOUSLY GROWING TRANSVERSE WAVES IN A PLASMA DUE TO AN ANISOTROPIC VELOCITY DISTRIBUTION. 1959. PHYSICAL REVIEW LETTERS. 2 (3): 83.

9. Li, C. K., F. H. Seguin, J. A. Frenje, Manuel, Casey, Sinenian, R. D. Petrasso, P. A. Amendt, O. L. Landen, J. R. Rygg, R. P. J. Town, Betti, Delettrez, J. P. Knauer, Marshall, D. D. Meyerhofer, T. C. Sangster, Shvarts, V. A. Smalyuk, J. M. Soures, C. A. Back, J. D. Kilkenny, and Nikroo. Proton radiography of dynamic electric and magnetic fields in laser-produced high-energy-density plasmas. 2009. PHYSICS OF PLASMAS. 16 (5).

10. Fermi, E.. On the Origin of the Cosmic Radiation. 1949. Physical Review. 75 (8): 1169.

11. NESS, N. F., J. B. SEEK, and C. S. SCEARCE. INITIAL RESULTS OF IMP 1 MAGNETIC FIELD EXPERIMENT. 1964. JOURNAL OF GEOPHYSICAL RESEARCH. 69 (17): 3531.

12. Masters, , Stawarz, Fujimoto, S. J. Schwartz, Sergis, M. F. Thomsen, Retino, Hasegawa, Zieger, G. R. Lewis, A. J. Coates, Canu, and M. K. Dougherty. Electron acceleration to relativistic energies at a strong quasi-parallel shock wave. 2013. NATURE PHYSICS. 9 (3): 164.

13. Fiuza, , R. A. Fonseca, Tonge, W. B. Mori, and L. O. Silva. Weibel-Instability-Mediated Collisionless Shocks in the Laboratory with Ultraintense Lasers. 2012. PHYSICAL REVIEW LETTERS. 108 (23).

14. Fonseca, R. A., L. O. Silva, F. S. Tsung, V. K. Decyk, W. Lu, C. Ren, W. B. Mori, S. Deng, S. Lee, T. Katsouleas, and J. C. Adam. A Three-Dimensional, Fully Relativistic Particle In Cell Code for Modeling Plasma Based Accelerators. 2002. Computational Science-Iccs 2002, Pt Iii, Proceedings. (2331): 342.

15. Bin, J. H., W. J. Ma, H. Y. Wang, M. J. V. Streeter, Kreuzer, Kiefer, Yeung, Cousens, P. S. Foster, Dromey, X. Q. Yan, Ramis, Meyer-ter-Vehn, Zepf, and Schreiber. Ion Acceleration Using Relativistic Pulse Shaping in Near-Critical-Density Plasmas. 2015. PHYSICAL REVIEW LETTERS. 115 (6).

16. Palaniyappan, , Huang, D. C. Gautier, C. E. Hamilton, M. A. Santiago, Kreuzer, A. B. Sefkow, R. C. Shah, and J. C. Fernandez. Efficient quasi-monoenergetic ion beams from laser-driven relativistic plasmas. 2015. NATURE COMMUNICATIONS. 6.

Publications

Palaniyappan, , Huang, D. C. Gautier, C. E. Hamilton, M. A. Santiago, Kreuzer, A. B. Sefkow, R. C. Shah, and J. C. Fernandez. Efficient quasi-monoenergetic ion beams from laser-driven relativistic plasmas. 2015. NATURE COMMUNICATIONS. 6.

New Chemistry Towards High Purity Uranium and Thorium Nitrides

Jacqueline M. Veauthier
20140504ER

Abstract
Actinide nitrides are becoming increasingly important materials within the intertwined landscape of global energy and security. Historically, these materials have been challenging to prepare pure in bulk quantities. This project unites LANL core capabilities in actinide and energetic materials chemistry to investigate innovative synthetic routes to high purity actinide nitrides. We have explored the experimental and theoretical chemistry of thorium and uranium with nitrogen-rich ligands and have significantly furthered of our understanding in this emerging field of actinide high nitrogen chemistry.

Background and Research Objectives
The quest to develop alternative sources of energy has implications far beyond the immediate objectives of technological advancement and scientific breakthroughs. According to the Annual Energy Outlook 2015 publication from the U.S. Energy Information Administration, nearly 20% of electricity production comes from nuclear power [1]. This power comes from 61 commercial plants located in 30 states in the U.S. In this context, it is no surprise that conducting research on various nuclear fuels is in the long-term interest of the U.S.

The research objective of this work is to ultimately produce pure actinide nitride materials in a high-yielding and synthetically straightforward procedure. Actinide nitrides are highly-desirable nuclear fuels for accelerator-driven reactors, due to their favorable physical properties such as high fissile metal density and high thermal conductivity. However, the current state-of-the-art method, carbothermic rediction and nitridation (CTR-N) of actinide oxides requires high temperatures, sophisticated equipment, and often yields products that contain carbon and oxygen impurities. Our approach was to simplify this process by implementing the use of actinide complexes containing nitrogen-rich ligands. We applied a tiered approach that first involved the aqueous synthesis of uranyl and thorium complexes containing a nitrogen-rich ligand, bitetrazolateamine (BTA). The second strategy involved synthesizing easily-understood model complexes so that the nature of the bonding between the metal and the ligand could be fully understood. This strategy has allowed us to make important conclusions about the donating ability of tetrazolate and ketimide tetrazolate ligands, and therefore has served as an important preliminary study for ultimately synthesizing actinide complexes that containing even greater percentages of nitrogen-rich ligands.

Scientific Approach and Accomplishments
Aqueous chemistry of thorium with bistetrazolateamine (BTA)
We have prepared new homoleptic complexes of thorium and uranium with a nitrogen-rich ligand by combining two equivalents of BTA with either Th(NO3)·6H2O or ThCl4·4H2O in water. Subsequently, we have shown that combustion of these new materials under an inert atmosphere yields high purity nanoparticulate UO2 and ThO2 respectively, as analyzed by X-ray powder diffraction and electron microscopy (SEM and TEM) as shown in Figure 1. These experiments involve mounting pressed pellets of the sample within an insert that is then placed inside of a combustion chamber. The chamber is then placed under an inert atmosphere (either N2 or Ar) and combustion is initiated by irradiating the sample with a high-power CO2 laser through infrared-transparent windows in the chamber and in the insert. These experiments have been scaled to yield up to 0.5 grams of high purity nanoparticulate UO2. Its efficacy as a new starting material to facilitate carbothermic rediction and nitridation for production of UN is being tested.

We devoted significant effort towards elucidating the coordination environment of Th in this material, as traditional molecular characterization methods (single crystal X-ray crystallography, solution-phase NMR spectroscopy, etc.) provided little insight into its structure. We therefore turned to the technique of high-energy X-ray spec-

troscopy (HEXS), which we performed in collaboration with Lynne Soderholm at the Advanced Photon Source Argonne National Laboratory. The intense synchrotron X-ray source at APS allowed us to collect a high-resolution diffraction pattern of the Th-BTA compound and to analyze it using a technique called pair distribution function (PDF) analysis.

We provided our theory collaborators (Neil Henson, Katie Maerzke, and Ping Yang at LANL) with possible chemical structures, and they calculated the stability of these structures and mapped all of the Th-X distances to determine how well these correlate with the experimental HEXS data. Thus far, we have several possible candidates for plausible structures for Th-BTA. We observe good correlation between experimental and predicted distances, especially at short (< ~ 4 Å) distances. We attribute the greatest significance to the good match in these shorter distances because it is within this regime that we expect the first coordination sphere of ligand atoms bound to Th. Difficulty in theoretically reproducing longer-range correlations in this manner stems from the nature of HEXS measurements on solid samples of even moderate crystallinity: intermolecular distances that repeat between unit cells are also captured in the HEXS data.

We are in the process of completing a manuscript for publication that summarizes the results of these efforts.

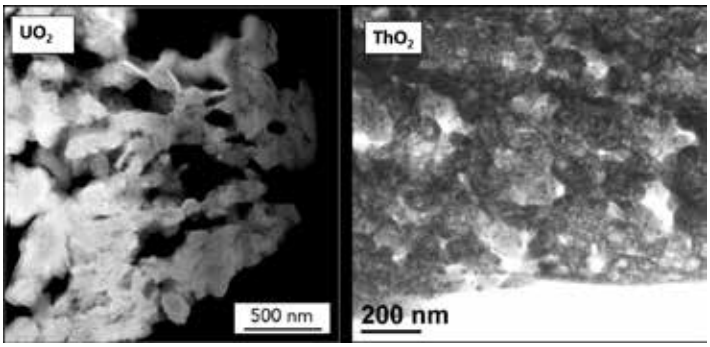

Figure 1. Micrographs of UO and ThO produced via combustion of U-BTA and Th-BTA, respectively.

Non-aqueous chemistry of thorium and uranium with tetrazole-based high-nitrogen ligands

We have worked extensively with 5-methyl-1H-tetrazole as a high-nitrogen ligand suitable for coordination to thorium and uranium. Upon protonolysis of the methyl groups of (C5Me5)2AnMe2 (An = Th, U) by the tetrazole ligand, we observe near-quantitative formation of (C5Me5)2An(eta2-tetrazolate)2 by 1H NMR spectroscopy, and we were able to grow single crystals of the Th and U analogs suitable for X-ray crystallography (Figure 2).

Analysis of the crystals structures shows that both compounds form a typical bent-metallocene structure of pseudo-tetrahedral geometry, with the tetrazolates coordinated within the wedge of the metallocene. The key difference between the two structures is in the orientation of the methyl groups of the tetrazolate ligands. Computational studies using Density Functional Theory (DFT) indicated that inversion of the tetrazolate ligands was possible for each compound, such that the Th structure in Figure 2 could have one of its tetrazolate rings invert so that the orientation of the methyl groups pointed towards one another. Likewise, the U structure could also undergo this tetrazolate inversion. This process was confirmed experimentally using variable-temperature 1H NMR spectroscopy, where the chemical shift of the methyl group protons for the Th structure in 5a was monitored as a function of temperature.

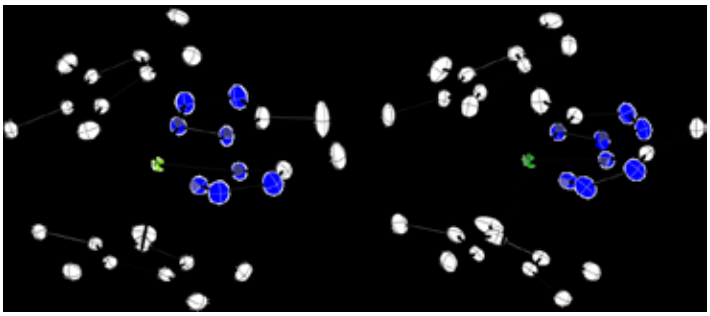

Figure 2. X-ray crystal structures of U, Th tetrazolate complexes.

For a chemical shift that varies as a function of temperature due to a change in the equilibrium population of configurational isomers, the ideal shape of the resulting plot is sigmoidal. By fitting the data points to the appropriate equations we can extract ΔG and determine that the 95% confidence interval at 298 K is -6.98 – 1.63 kJ/mol.

In addition to the structural properties of these two bis(tetrazolate) complexes of Th and U, we also characterized their electronic properties using electrochemistry and UV-visible-near-IR spectroscopy. Using these techniques we determined that the tetrazolate ligands behave primarily as sigma donor ligands. For example, the E1/2 potential for the U(IV)/U(III) reduction is -1.88 V versus the ferrocene/ferrocenium internal standard. When compared to other (C5Me5)UX2 U(IV) known complexes, this value places (C5Me5)U(tetrazolate)2 among complexes that have sigma donor ligands, such as CH2Ph, CH3, and Cl [2]. Electronic spectroscopy of the U complex in both the UV-visible and near-IR regions showed electronic transitions with extinction coefficients that fall within the range of those reported for other (C5Me5)UX2 complexes with sigma donor ligands. This work recently culminated in the publication of an article in Inorganic Chemistry, which, in addition to all of the experimental conclusions discussed above, contains a significant contribution from our theoret-

ical colleagues who employed DFT to validate our experimental results [3].

U(V) ketimide complexes

We've also explored a synthetic pathway towards imido-based analogs of tetrazole for coordinating to Th and U (Figure 3, a). The reaction of amino-tetrazole with one equivalent of (C5Me5)2AnMe2 (An = Th, U) is complete within minutes, but yields a species that is unstable in solution. We discovered that, in the case of uranium, a very efficient way to "trap" this complex is by immediately oxidizing the unstable U(IV) intermediate to the U(V) iodide using copper (I) iodide. There is ample precedent for this synthetic pathway yielding U(V) imido complexes [4] and so it came as a surprise when X-ray crystallography revealed that the product was a U(V) ketimide. Figure 3(b) shows how we envision this electronic rearrangement might occur to proceed from the imido to the ketimide.

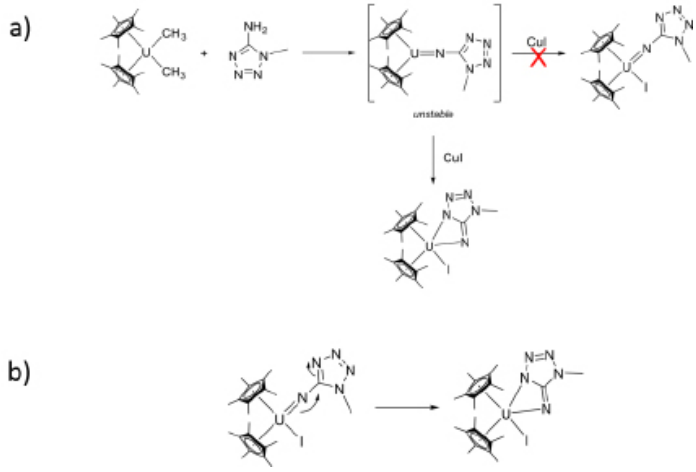

Figure 3. a) Synthesis of U(V) ketimide. The expected U(V) imido was not detected spectroscopically. b) Proposed electronic rearrangement from a transient U(V) imido to the observed U(V) ketimide.

This U(V) iodide served as a competent precursor for other derivatives in which the iodide was exchanged for other anionic ligands via salt metathesis. We have synthesized two additional complexes in this fashion, namely the azide and the tetrazolate derivatives. While we were unable to obtain single crystal X-ray structures of these azide and tetrazolate derivatives, spectroscopic evidence from 1H NMR points to the exchange of the iodide ligand for both azide and tetrazolate. Specifically, the upfield shift of the C5Me5 methyl group protons from the iodide, to tetrazolate, to azide derivatives, respectively, is consistent with displacement by increasingly pi-donating ligands. This same trend is confirmed for electrochemical measurements of all three compounds, with the U(V)/U(IV) reduction potential shifting to more negative values as the pi-donor nature of the ligand increases.

In an attempt to probe the mechanistic pathway that leads to the U(V) ketimide iodide – as opposed to the desired U(V) imido iodide. We attempted the U(IV)/U(V) oxidation using an alternate strategy. Instead of employing copper(I) iodide for the oxidation, we used a gold-based oxidant that relies on a similar redox process in which gold is reduced to its metallic form while uranium is oxidized. In addition to reactivity that is slightly different from that of copper iodide, gold(I) reagents have a triphenylphosphine ligand that makes them more soluble in organic solvents, typically speeding up reacitivity relative to the insoluble copper reagent. PPh3PAuN3 is a compound known to oxide U(III) to U(IV) and U(IV) to U(V); based on the decreased pi-donor nature of tetrazolate relative to azide, however, we decided that tetrazolate would be a better choice than azide. We successfully synthesized the gold(I) tetrazolate compound in one step from the gold(I) chloride precurser and potassium tetrazolate (Figure 4). Upon reacting this new reagent with the transient U(IV) imido species, however, the product was once again found to be the U(V) ketimide instead of the hypothesized U(V) imido.

Uranyl-BTA·DMSO complexes

In an effort to understand the nature of actinide-BTA coordination (the complexes discussed in Section I were not molecularly-identifiable through X-ray crystallography), we synthesized and characterized two DMSO adducts of uranyl containing BTA. Of note is the U(VI)/U(V) reduction of these complexes. The reduction of the monomer species (-0.98 V) is more facile than that of the dimer (-1.04 V), which we attribute to increased electron-donation by the bridging hydroxide ligands of the dimer that make its reduction more difficult.

The experimental electronic structure determined by UV-visible spectroscopy was reproduced faithfully by time-dependent density-functional theory, and aids in the assignment of the electronic transitions. The characteristic uranyl oxide-to-U(VI) charge transfer transitions in the 350-550 nm region are confirmed theoretically, and BTA-to-metal transitions were found to be relatively low in energy, as a consequence of the BTA ligand orbitals being closest to the HOMO in energy (and therefore possessing a relatively low HOMO-LUMO transition).

Towards increasingly nitrogen-rich actinide complexes

As part of our effort to move steadily away from actinide complexes with a high carbon content and towards complexes that feature more nitrogen-rich ligands, we synthesized (C5Me5)U(CH2Ph)3 as a starting material. Reaction of this known complex with three equivalents of 5-methyl-1H-tetrazole yields a stable product that is consistent with the desired nitrogen-rich low valent tris(tetrazolate) complex Figure 5), as determined by 1H NMR (which

shows formation of the expected toluene by product). This straightforward reaction proved the utility of protonolysis reactions to add the tetrazolate ligand to uranium, and more importantly illustrated the promise of moving a step further away from C5Me5-based ligands (here, one C5Me5 ligand as opposed to two) whose high carbon content may ultimately hinder combustion.

We are in the process of completing a manuscript for publication that summarizes the results of these efforts.

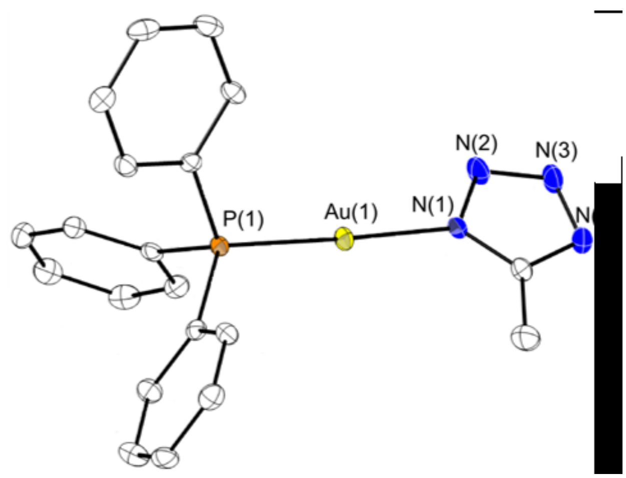

Figure 4. X-ray crystal structure of Au(I) tetrazolate complex.

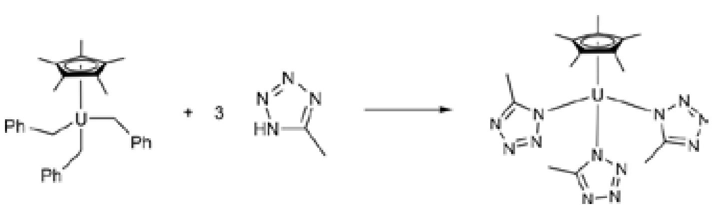

Figure 5. Synthesis of an organometallic U(IV) tetrazolate complex containing only one CMe ligand.

Impact on National Missions

This proposed work has brought together LANL expertise in actinide and energetic materials science, including chemists, theorists, and materials scientists. This work offers new ways to revolutionize production of advanced nuclear fuel materials. This collection of projects brings together two fields in which LANL has long been a pioneering and dominant player: actinide chemistry and energetic materials chemistry. The resulting bridge between these two fields establishes a new capability at LANL, and is already training future generations of actinide and energetic materials chemists. The discovery of a new method to produce pure, bulk actinide nitrides will place LANL at the forefront of a technological breakthrough, and can help secure our country's energy independence in the form of new nuclear fuels.

References

1. Annual Energy Outlook 2015 with Projections to 2040. 2015. U.S. Energy Information Administration.

2. Morris, D. E., R. E. Da Re, K. C. Jantunen, I. Castro-Rodriguez, and J. L. Kiplinger. Trends in electronic structure and redox energetics for early-actinide pentamethylcyclopentadienyl complexes. 2004. ORGANOMETALLICS. 23 (22): 5142.

3. Browne, K. P., K. A. Maerzke, N. E. Travia, D. E. Morris, B. L. Scott, N. J. Henson, Yang, J. L. Kiplinger, and J. M. Veauthier. Synthesis, Characterization, and Density Functional Theory Analysis of Uranium and Thorium Complexes Containing Nitrogen-Rich 5-Methyltetrazolate Ligands. 2016. INORGANIC CHEMISTRY. 55 (10): 4941.

4. Graves, C. R., B. L. Scott, D. E. Morris, and J. L. Kiplinger. Facile access to pentavalent uranium organometallics: One-electron oxidation of Uranium(IV) imido complexes with copper(I) salts. 2007. JOURNAL OF THE AMERICAN CHEMICAL SOCIETY. 129 (39): 11914.

Publications

Browne, K. P., D. E. Morris, B. L. Scott, D. E. Chavez, A. T. Nelson, B. C. Tappan, and J. L. Kiplinger. Actinide high-nitrogen chemistry. Invited presentation at Actinide high-nitrogen chemistry. (Denver, CO, 22-26, Mar. 2015).

Browne, K. P., K. A. Maerzke, N. E. Travia, D. E. Morris, B. L. Scott, N. J. Henson, Yang, J. L. Kiplinger, and J. M. Veauthier. Synthesis, Characterization, and Density Functional Theory Analysis of Uranium and Thorium Complexes Containing Nitrogen-Rich 5-Methyltetrazolate Ligands. 2016. INORGANIC CHEMISTRY. 55 (10): 4941.

Browne, K., K. Maerzke, N. Travia, N. Henson, D. Morris, B. Scott, P. Yang, J. Kiplinger, and J. Veauthier. Nitrogen-rich, organometallic complexes of thorium and uranium with 5-methyl-1H-tetrazole. 2016. In Abstracts of Papers, 251st ACS National Meeting & Exposition, San Diego, CA, United States, March 13-17, 2016. , p. INOR.

Henson, N., J. Veauthier, J. Kiplinger, and R. Martin. Computational studies of f-element complexes with high-nitrogen-containing ligands for separations processes. 2016. In Abstracts of Papers, 251st ACS National Meeting & Exposition, San Diego, CA, United States, March 13-17, 2016. , p. NUCL.

Maerzke, K. A., K. Browne, P. Yang, N. Henson, J. L. Kiplinger, and J. M. Veauthier. Organometallic actinide complexes with nitrogen-rich ligands. 2016. In Abstracts of Papers, 251st ACS National Meeting & Exposition, San Diego, CA, United States, March 13-17,

2016. , p. INOR.

Maerzke, K. A., N. Henson, J. M. Veauthier, and J. L. Kiplinger. Structure and stability of uranyl(VI) and uranium(VI) imido complexes with high-nitrogen ligands . Presented at 249th ACS National Meeting & Exposition. (Denver, CO, 22-26, Mar. 2015).

Travia, N. E., K. Browne, J. L. Kiplinger, D. E. Morris, A. Mueller, A. T. Nelson, A. Parkinson, B. Scott, B. Tappan, and J. M. Veauthier. 249th ACS National Meeting & Exposition. Presented at 249th ACS National Meeting & Exposition. (Denver, CO, 22-26, Mar. 2015).

Veauthier, J. M.. Synthesis and characterization of new nitrogen-rich metal complexes. 2014. ABSTRACTS OF PAPERS OF THE AMERICAN CHEMICAL SOCIETY. 248.

Veauthier, J. M.. f-Element complexes of nitrogen-rich ligands: Precursors to highly porous f-element nitride and oxide foams for nuclear fuel applications. Presented at The International Chemical Congress of Pacific Basin Societies 2015. (Honolulu, December 15-20, 2015).

Veauthier, J. M., J. L. Kiplinger, B. C. Tappan, N. E. Travia, K. P. Browne, B. L. Scott, N. Henson, A. H. Mueller, D. E. Chavez, and A. T. Nelson. Synthesis and combustion of nitrogen-rich f-element complexes. Invited presentation at Synthesis and combustion of nitrogen-rich f-element complexes. (Denver, CO, 22-26, Mar. 2015).

Veauthier, J., J. Kiplinger, K. Browne, K. Maerzke, N. Travia, B. Tappan, N. Henson, P. Yang, A. Mueller, B. Scott, and D. Chavez. Blending nitrogen-rich chemistry with f-elements for the development of new, high-purity routes to actinide nitrides. Invited presentation at Abstracts of Papers, 251st ACS National Meeting & Exposition. (San Diego, March 13-17, 2016).

Discovery and Implication of Negative Ions in the Earth's Magnetosphere

Herbert O. Funsten
20140546ER

Abstract

After more than 50 years of intensive study, our lack of understanding of mass and energy transport throughout the magnetosphere as well as the underlying physical processes that drive them is astounding: we still cannot predict geomagnetic storm onset, evolution, magnitude, and persistence. Using the HOPE mass spectrometer on NASA's RBSP mission that was designed to study the Earth's radiation belts within its harsh radiation environment, we have serendipitously discovered negative H and O ions at energies up to 50 keV. Because they (1) likely originate as cold ions in the upper ionosphere, (2) behave differently than positive ions in electromagnetic fields, and (3) respond differently than electrons to waves, these particles represent a fundamentally new and unique population. We attempt to answer fundamental questions of the presence and impact of negative ions in the terrestrial magnetosphere.

Background and Research Objectives

Upon commissioning of the Helium, Oxygen, Proton, and Electron (HOPE) mass spectrometers after launch of NASA's Van Allen Probes, the HOPE team observed tantalizing counts of negative ion species, which have not previously been observed in the Earth's magnetosphere. This project was structured to investigate these species and understand their origin and fate. This investigation required deep understanding and performance quantification of the time-of-flight subsystem of the HOPE mass spectrometers, which is comprised of a foil-based linear time-of-flight mass spectrometer.[1] The HOPE mass spectrometers are unique because they regularly report coincidence and non-coincidence count rates, as well as time-of-flight spectra, that contain a rich (and enormous) data set for understanding instrument backgrounds, performance (such as absolute detection efficiency [2]), and counting statistics.

Scientific Approach and Accomplishments

This project enabled a critical examination of the performance of time-of-flight plasma spectrometer that regularly reported coincident and non-coincident count rates, from which absolute detection efficiency can be derived [2]. Critical to this project was the quantitative understanding efficiencies of the detector subsystem for different ion species and types of backgrounds. Laboratory experiments were performed on components of the HOPE mass spectrometer (such as foils and channel electron multiplier detectors), as well as a spare mass spectrometer. These studies led to two paper publications [3,4] as well as an invited talk at a conference on space instrumentation. This work also contributed to incorporation of a mass analysis subsystem on a new instrument concept developed by Los Alamos [5]. The experiments indicated that negative H and O ions could be generated within the instrument as a background, although not at abundances observed in the HOPE data.

Much of the project was focused on analysis and interpretation of HOPE data, in particular understanding and quantifying the signatures of negative ions, understanding backgrounds, association with spacecraft location and local time, and correlation with other species present in the plasma environment. One of the major accomplishments of postdoc D. Olson was to quantify the time dependent correction to the HOPE detection efficiencies. He quantified detection efficiency degradation over time and developing a correction method that has been applied to data processing chain and has driven a reassessment of efficiency algorithms used for instruments on the Lab's nuclear detonation detection payloads.

Our analysis did not conclusively demonstrate that observed negative ions were of natural origin and not generated by scattering of positive ions within the HOPE instruments. We found strong correlation of negative ion flux with positive ion flux that was measured during the same acquisition interval, although we identified

six anomalous intervals in which negative hydrogen ions were observed are far higher fluxes that anticipated based on the concurrent proton measurements. These intervals remain under study.

Methods developed for quantitative understanding of the HOPE data, including absolute flux calibration and evolution of efficiency over time, have been incorporated into the HOPE data processing chain. The integrity of this data has been critical for series of studies of the structure and evolution of the radiation belts [6-9] using data from the HOPE mass spectrometers, and will be important for a series of future studies. Investigation into statistics and inference of sparse (low count) data led by B. Larsen (ISR-1) and B. Weaver (CCS-6) have opened, for the first time, a new avenue for application of Bayesian statistics to space plasma data, for which a publication [9] is in progress. This effort spawned an LDRD reserve that was added to this project in FY16.

The LDRD reserve project "Uncertainty quantification of space environment instrumentation enabling quantitate anomaly prediction and attribution" facilitated analysis by a team from three groups (ISR-1, CCS-6, ISR-3) and led by early career staff (B. Larsen, B. Weaver, K. Sentz) to understand the uncertainties with space physics particle measurements (sparse data) and the implication of these uncertainties on interpretation of the data. This effort developed and compared methods and insight on the problem of extreme value statistics applied to measurements in the Van Allen Radiation Belts. Many possible tools were utilized and analyzed, allowing for the development of candidate models to test the scientific hypothesis "is there a maximum number of particles in the radiation belts?" After substantiating this hypothesis, the team evaluated differences in statistical models and methodologies to accurately understand the radiation belt maxima question and to quantify the 10, 50, and 100-year particle event magnitude in a robust and defensible manner. These approaches are critical to both understanding the evolution of the radiation belts and the ability to design systems to operate within this harsh environment. Results demonstrate credibility of the approach as a basis for follow-on LDRD proposals (in two different institutional capability areas) as well as proposals to the USAF and NASA.

Impact on National Missions

This project has studied new signatures for understanding physical processes that drive the dynamics of the Earth's space environment. Furthermore, it has developed new methods for analysis and interpretation, as well as the accuracy and precision of sparse counting data within background. Understanding and predicting the space environment is directly applicable to our DOE space Nuclear Detonation Detection Program (SNDD) and is directly relevant to NASA's mission of understanding the space environment under its Living with a Star Program. Methods and algorithms developed and demonstrated under this project are being incorporated into the SNDD program.

The project has also supported three post-docs (W.-C. Tu, now at West Virginia Univ. in a tenure-track faculty position; D. Olson; and P. Fernandes) and one student (K. Pittman, two summers).

References

1. Funsten, H. O., R. W. Harper, and D. J. McComas. Absolute detection efficiency of space-based ion mass spectrometers and neutral atom imagers. 2005. Review of Scientific Instruments. 76 (5).

2. Funsten, . Helium, Oxygen, Proton, and Electron (HOPE) Mass Spectrometer for the Radiation Belt Storm Probes Mission. 2013. Space Science Reviews. 179 (1): 423.

3. Funsten, H. O., R. W. Harper, E. E. Dors, P. A. Janzen, B. A. Larsen, E. A. MacDonald, D. I. Poston, S. M. Ritzau, R. M. Skoug, and T. H. Zurbuchen. Comparative response of microchannel plate and channel electron multiplier detectors to penetrating radiation in space. 2015. IEEE Transactions on Nuclear Science. 62 (5): 2283.

4. Allegrini, F., R. W. Ebert, and H. O. Funsten. Carbon foils for space plasma instrumentation. 2016. Journal of Geophysical Research: Space Physics. 121 (5): 3931.

5. Skoug, R. M., H. O. Funsten, E. Möbius, R. W. Harper, K. H. Kihara, and J. S. Bower. A wide field of view plasma spectrometer. 2016. Journal of Geophysical Research: Space Physics. 121 (7): 6590.

6. Zhao, H., X. Li, D. N. Baker, J. F. Fennell, J. B. Blake, B. A. Larsen, R. M. Skoug, H. O. Funsten, R. H. Friedel, G. D. Reeves, H. E. Spence, D. G. Mitchell, L. J. Lanzerotti, and J. V. Rodriguez. The evolution of ring current ion energy density and energy content during geomagnetic storms based on Van Allen Probes measurements. 2015. Journal of Geophysical Research: Space Physics. 120 (9): 7493.

7. Kistler, L. M., C. G. Mouikis, H. E. Spence, A. M. Menz, R. M. Skoug, H. O. Funsten, B. A. Larsen, D. G. Mitchell, M. Gkioulidou, J. R. Wygant, and L. J. Lanzerotti. The source of O+ in the storm time ring current. 2016. Journal of Geophysical Research: Space Physics. 121 (6): 5333.

8. Zhao, H., X. Li, D. N. Baker, J. F. Fennell, J. B. Blake, B. A. Larsen, R. M. Skoug, H. O. Funsten, R. H. Friedel, G. D. Reeves, H. E. Spence, D. G. Mitchell, L. J. Lanzerotti, and J. V. Rodriguez. The evolution of ring current ion energy density and energy content during geomagnetic storms based on Van Allen Probes measurements. 2015. Journal of Geophysical Research: Space Physics. 120 (9): 7493.

9. Larsen, B. A., B. P. Weaver, D. K. Olson, H. O. Funsten, R. W. Harper, and R. M. Skoug. Uncertainty Analysis in Absolute Detection Efficiency of Space-Based Coincident Particle Instrumentation . 2016. In preparation for submission to J. Geophys. Res..

10. Denton, M. H., G. E. Reeves, M. F. Thomsen, M. G. Henderson, R. H. Friedel, B. Larsen, R. M. Skoug, H. O. Funsten, H. E. Spence, and C. A. Kletzing. The complex nature of storm-time ion dynamics: Transport and local acceleration. 2016. Geophysical Research Letters. : n/a.

Publications

Allegrini, F., R. W. Ebert, and H. O. Funsten. Carbon foils for space plasma instrumentation. 2016. Journal of Geophysical Research: Space Physics. 121 (5): 3931.

Denton, M. H., G. E. Reeves, M. F. Thomsen, M. G. Henderson, R. H. Friedel, B. Larsen, R. M. Skoug, H. O. Funsten, H. E. Spence, and C. A. Kletzing. The complex nature of storm-time ion dynamics: Transport and local acceleration. 2016. Geophysical Research Letters. : n/a.

Funsten, H. O., R. W. Harper, E. E. Dors, P. A. Janzen, B. A. Larsen, E. A. MacDonald, D. I. Poston, S. M. Ritzau, R. M. Skoug, and T. H. Zurbuchen. Comparative response of microchannel plate and channel electron multiplier detectors to penetrating radiation in space. 2015. IEEE Transactions on Nuclear Science. 62 (5): 2283.

Goldstein, J., D. N. Baker, J. B. Blake, S. De Pascuale, H. O. Funsten, A. N. Jaynes, J. M. Jahn, C. A. Kletzing, W. S. Kurth, W. Li, G. D. Reeves, and H. E. Spence. The relationship between the plasmapause and outer belt electrons. 2016. Journal of Geophysical Research: Space Physics. : n/a.

Kistler, L. M., C. G. Mouikis, H. E. Spence, A. M. Menz, R. M. Skoug, H. O. Funsten, B. A. Larsen, D. G. Mitchell, M. Gkioulidou, J. R. Wygant, and L. J. Lanzerotti. The source of O+ in the storm time ring current. 2016. Journal of Geophysical Research: Space Physics. 121 (6): 5333.

Larsen, B. A., B. P. Weaver, D. K. Olson, H. O. Funsten, R. W. Harper, and R. M. Skoug. Uncertainty Analysis in Absolute Detection Efficiency of Space-Based Coincident Particle Instrumentation . 2016. In preparation for submission to J. Geophys. Res..

Skoug, R. M., H. O. Funsten, E. Möbius, R. W. Harper, K. H. Kihara, and J. S. Bower. A wide field of view plasma spectrometer. 2016. Journal of Geophysical Research: Space Physics. 121 (7): 6590.

Zhao, H., X. Li, D. N. Baker, J. F. Fennell, J. B. Blake, B. A. Larsen, R. M. Skoug, H. O. Funsten, R. H. Friedel, G. D. Reeves, H. E. Spence, D. G. Mitchell, L. J. Lanzerotti, and J. V. Rodriguez. The evolution of ring current ion energy density and energy content during geomagnetic storms based on Van Allen Probes measurements. 2015. Journal of Geophysical Research: Space Physics. 120 (9): 7493.

Viral Disarmament: A Trojan Protein Approach

Murray A. Wolinsky
20140558ER

Abstract

Viruses evade our defenses by evolving rapidly. Typically, viruses evolve at rates approximately one million times faster than what the human genome can achieve. As a result of these rapid viral mutation rates, few effective antiviral therapeutics exist. Insight into viral mutation has helped inform a large percentage of the few existing therapeutic strategies we have today; but deeper insight is urgently needed. Despite its considerable scientific and medical importance, and despite numerous research studies, viral evolution remains poorly understood.

We are studying viral evolution by finding out how quickly a viral gene can lose its ability to perform its normal function. We do this by providing supplements ("Trojan proteins") to host cells that eliminate the need for viral genes to produce their protein products. These supplemental proteins alter (flatten) fitness landscapes and enable us to probe the rate of loss of function. Ideally, the supplements we introduce remove evolutionary pressure on the viral genome and allow it to accumulate what would otherwise be deleterious mutations.

It is not a goal of our effort to develop a therapeutic agent. However, we hope our work may provide a foundation for developing novel anti-viral therapeutics based on manipulating viral fitness landscapes. Many of the most effective current viral therapeutics are based on lethal mutagenesis – increasing the rate of viral mutation above a sustainable level. In practice, doubling the rate of viral mutation is usually sufficient to disrupt viral function. But, while effective, these mutagenic agents are often harmful to the host and typically require complementary drugs (adjuvants) to obtain maximum benefit. We believe that approaches based on Trojan proteins, as presented here, form a natural synergy with lethal mutagens and can serve as those adjuvants.

Background and Research Objectives

Viruses do battle with our immune system. To survive, they must evolve fast enough to outpace immune system resistance measures. But they cannot evolve too rapidly: if they "try" to do so, they are unable to maintain their identity. Manfred Eigen (1967 Chemistry Nobel prize) predicted a maximum mutation rate corresponding to an "error catastrophe." Observed viral evolution rates generally agree with Eigen's predictions. (Viruses evolve as fast as they can.) Some of our most effective antiviral agents exploit the error catastrophe by pushing the virus over the error threshold ("lethal mutagenesis.") The goal of this effort is to understand viral evolution better by manipulating viral fitness landscapes.

Mutations can be "silent" and have no effect on organism fitness. More interestingly, mutations can either augment or diminish organism fitness. We are primarily interested in mutations that affect fitness and, at the center of our effort, have developed a novel methodology that allows us to study the loss of fitness of viral genomes in a controlled manner.

We study viral infections of genetically engineered host cells. Our host cells have been modified to provide proteins which the infecting virus normally must produce by itself. We call these host-supplied proteins — which duplicate what the virus normally must produce for itself — "Trojan" proteins. By relieving the virus of the need to produce these proteins, the virus becomes more "free" to evolve. Our basic hypothesis is that the most likely result of eliminating the need for the virus to produce these proteins is for the virus to lose the ability to produce them. ("Lack of necessity is the mother of loss of capability.") If that is the case, the virus will become less infectious. However, it is possible that the opposite will take place: the virus may become more infectious — since it is less constrained and may be able to "explore" new opportunities that potentially increase its infectivity.

Our basic research objective therefore is to determine what happens when we remove selection pressure: [1] do viruses become less or more infectious? We then ask more detailed questions such as [2] how quickly do these changes occur, and (through the use of sequencing), we ask [3] how do these changes take place?

We collect transcriptomic data which allows us to examine further questions such as [4] how do the genetic modifications we have introduced affect host cells? and [5] how do normal ("wild-type") and modified host cells react to infection? (and are there interesting differences in how they respond?)

Scientific Approach and Accomplishments

Our approach is summarized in Figure 1. We performed viral passage experiments in unmodified ("wild-type") Madin Darby Canine Kidney (MDCK) host cells (top) and in two genetically-engineered MDCK host cell lines (labeled +HA and +M1) which stably express the influenza A viral (IAV) proteins HA and M1 (center and middle). We perform 10 passages for each condition and then infected wild-type MDCK cells with the final (passage 10) virus.

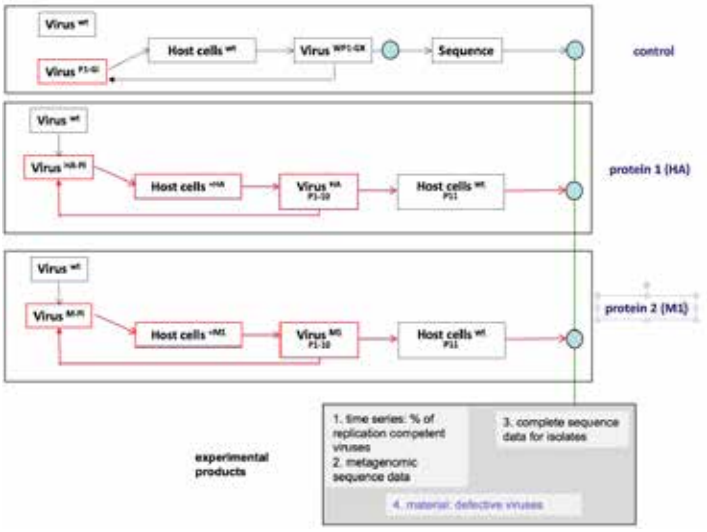

Figure 1. We performed viral passage experiments in unmodified ("wild-type") MDCK host cells (top) and in two genetically-engineered MDCK host cell lines (labeled +HA and +M1) which stably expressed the influenza A viral proteins HA and M1 (center and middle). We performed 10 passages for each condition and then infected wild-type MDCK cells with the final (passage 10) virus.

Performing this experiment was considerably more challenging than originally anticipated. Nevertheless, we have obtained promising results that are currently being analyzed.

Our first accomplishment was the establishment of two genetically engineered ("transfected") MDCK cell lines which express the IAV proteins HA and M1 stably. Most of the experimental effort performed for this project was directed at obtaining these cell lines. We started by trying all IAV proteins, and were able to produce viable clones for PB1, PB2, PA, M1 and HA IAV gene segments. The next step was to confirm the production of our protein by the modified host cells via western blotting. Only M1 and HA transfected cells showed positive western blot results (meaning the viral protein was produced (or "expressed"), while results for PB1, PB2, and PA were inconclusive. Based on these western blot results, we decided to proceed with M1 and HA transfected cells. At least three experimental modifications were required to obtain usable modified host cells: following others, we used the antibiotic Geneticin to favor our modified cells over wild-type ones; our initial ("parent") population of MDCK cells had to be replaced with a healthier population; and we needed to undo a modification we made early on to facilitate sequence analysis. (We initially added a "V5 tag" which, surprisingly, interfered with cell growth, and had to be removed.) These cell lines stably expressing viral proteins have been archived at LANL and may be useful in future projects.

Our second accomplishment was performing the passaging experiments. After generating our "tagless" transfectants, we were now ready to begin passaging our virus. Our parent strain (IAV Calif/2009/07) was cycled through both our M1 and HA transfected cells. The viral supernatant was collected after each infection, purified, and then reused to infect the next generation. Each IAV supplemented cell has its own dedicated viral population. The viral supernatant was collected for qPCR, for reinfection, for backup, and for sequencing purposes.

Our third accomplishment was obtaining sequencing data. Viral supernatant samples were collected for each passage from P1 to P10. We submitted samples for sequencing included the initial parent strain of Influenza A for control purposes, along with the final supernatant samples that were collected after P10. Illumina RNA libraries were made using proprietary library preparation methods, and run on Illumina NexSeq platform. Data is currently being processed through the EDGE bioinformatics platform and analysis is being performed as data becomes available. While the main focus of this project was to explore how viral mutagenesis occurs and under what circumstances, we decided it would also be interesting to explore the effects of how the transfected IAV gene segments impacted cell metabolism, and the infection process with the influenza A virus (i.e. increased or decreased the relative amount of Influenza A made that was measured in the supernatant via qPCR). M1 and HA transfected cells were grown, and had their RNA harvested. M1 and HA cell lysates were col-

lected in both infected and uninfected states. Illumina RNA libraries were made using proprietary library preparation methods, and run on Illumina NexSeq platform. This data is also currently being processed through the EDGE bioinformatics platform and analyses are being performed.

We have completed data collection (sequencing) and are finalizing data analysis. Our sequencing results are promising and we expect to publish the results.

While detailed analysis is ongoing, our preliminary results are interesting. It appears that the viruses passaged through HA and M1 supplemented cells exhibit opposite behaviors. The virus passaged through HA supplemented cells is less infectious than the original ("wild-type") virus. This is depicted in Figure 2 by the relative positions of the orange curve and the gray curve. The orange curve corresponds to viruses grown in HA supplemented cells and has a higher "CT" (Cycle Threshold) value than that for the wild-type cells (gray curve). Higher CT corresponds to slower growth and therefore diminished infectivity. For this supplement, the results are in agreement with our predictions. On the other hand, the viruses passaged through M1-supplemented cells are more infectious than wild-type cells. As shown in figure 3, the orange curve (now corresponding to M1 supplemented cells) lies below the gray curve and therefore has lower CT values, meaning faster growth. This is unexpected and contrary to our hypothesis.

We hope that the collected sequence data will allow us to understand the observed differences between these behaviors and enable us to predict which genes (such as HA) may correspond to Trojan proteins and which genes (such as M1) do not.

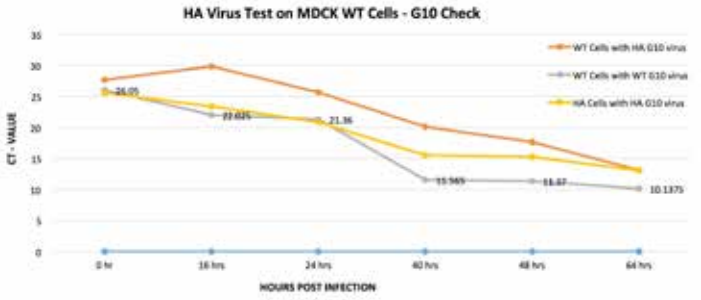

Figure 2. Viruses passaged through HA supplemented cells are less infectious than wild-type virus. Cycle Threshold (CT) is plotted against time. The orange curve corresponds to viruses grown in HA supplemented cells and has a higher CT value than that for the wild-type cells (gray curve). Higher CT corresponds to slower growth and therefore diminished infectivity. For this supplement, the results are in agreement with our predictions.

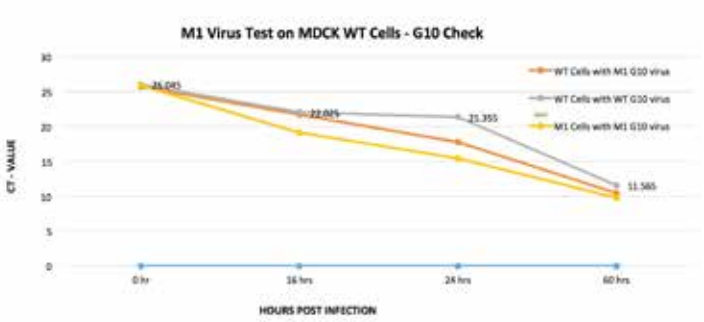

Figure 3. Viruses passaged through M1 supplemented cells are more infectious than wild-type virus. Cycle Threshold (CT) is plotted against time. The orange curve corresponds to viruses grown in M1 supplemented cells exhibiting a lower CT value than that of wild-type cells (gray curve). Lower CT corresponds to slower growth and therefore increased infectivity. For this supplement, the results are contrary to our predictions.

Impact on National Missions

Our work directly supports the Laboratory mission to address biodefense and public health concerns. The threat from existing and novel viruses has not abated (as demonstrated not least by the recent emergence of Zika virus). There are very few effective antiviral therapies and remarkably few novel ideas for producing new ones.

Three aspects of our work are relevant. First, our work addresses fundamental bioscientific issues in understanding viral evolution with potential relevance to combatting viral infections. Understanding the interplay of evolution, selection, and mutation may be crucial in developing effective new antiviral treatments or to otherwise mitigating the harm caused by viruses. Our work contributes new insights into what may be achievable and also what may need to be avoided.

Second, the project has suggested a direction for the development of actual countermeasures (therapeutics) that may be of value. The potential of interventions that exploit our methods is still uncertain and premature, but we intend to pursue additional funding and collaborators to explore this opportunity.

Third, the project developed a novel pipeline for further studies. Our work establishes a general "platform" for exploring viral evolution that can be used to perform related studies on additional viruses. After publication of our initial results, we will pursue further funding along this line.

Finally, and separately, this project directly led to the hiring of two new employees, who were both originally brought into the Laboratory to work on this project. Mr. Omar Ishak, who was a post-masters trainee directly involved in most of the activities of this ER project and in ensuring that

the work was successfully engaged. Is now a Technologist 5 in the Bioscience Division. Ms. Cheriece Margiotta was an undergraduate and postbaccalaurate student trainee in this project who is being hired in the Bioassay team in (C-NR) Chemistry Division. Both of these students were trained in cell culture, influenza work, and scientific procedures while on this project, and proved themselves essential in the troubleshooting processes that helped to solve the challenges that we faced in this project.

Genomics and Biomanufacturing

Patrick S. Chain
20160656ER

Abstract

Engineering organisms to generate high titers of bio-based products can be a slow process, and yet such molecules are paramount to replacing petroleum products and gaining U.S. oil independence. The overall goal of this 3-month project was to build a technical foundation in synthetic biology at Los Alamos related to the conversion of biomass feedstocks into high-value bioproducts in host organisms. In this project we aimed to develop and apply new molecular tools for regulating metabolic flux towards target molecules. We also adopted new host systems for expanding the range of target chemicals that can be produced synthetically; and applied a high throughput screening and selection process based on flow cytometry and cell sorting for identifying host cells with improved biosynthetic capabilities. Finally, we established a new collaboration with computational scientists at LANL to develop integrated genomics and transcriptomics analysis tools that will be used to gain insight into causal relationships and guide the design of gene regulators of synthetic pathways in the new host organisms. The new technologies and analysis tools will be broadly applicable to synthetic biology/advanced biomanufacturing research and development across several agencies and mission areas.

Background and Research Objectives

Current bioprocessing technologies, including those used to convert biomass resources to fuels and chemicals, require significant resources to reach market. Some of the most successful bio-based products have historically required 10-15 years to reach commercial production scales, and with an added capital expense on top of the R&D costs that often increases the total cost requirements somewhere between $500-1,000M. From an enterprise perspective, this implies that thousands of millions of dollars are expended annually by industry to develop new products achieved through biomanufacturing.

A vigorous biomanufacturing industry as a key component of the US Bioeconomy requires that product development be conducted in an accessible, integrated, and automated Design-Build-Test-Learn (DBTL) system that generates tunable organisms, genetic circuits, and conversion pathways to develop products of interest within industry “on-demand”. For a given biological process, the DBTL cycle includes selecting biological parts and pathways (Design); using genomic modification tools to generate a targeted library of strain variants (Build); assessing the performance of the constructed host strains that the parts and pathways will generate (Test); and ultimately evaluating the results to determine if the design was successfully realized or requires further improvement, and the ability to more efficiently operate the DBTL cycle and predictive designs of the next cycle or target (Learn).

Until now, we have independently developed several methods for optimizing metabolic flux for high titres of bioproducts and for delineating the relationship between genomic, transcriptomic, and phenotypic data. Starting with this project, we will re-direct and integrate our efforts to create a streamlined platform aligned with the DBTL system to produce bioproducts efficiently and with high yield.

Scientific Approach and Accomplishments

Our approach focused on building capabilities and expertise in 3 specific areas that bridge the interface between genomics and biomanufacturing and enable development of a robust platform to produce high bioproduct titers in industrially relevant host organisms with highest efficiency. In this project we specifically focused on muconate, a metabolic precursor to nylon production. To this end, we (1) Generated a fluorescence-based sensor to detect muconate-producing cells and demonstrated that this sensor works in an industrially relevant host; (2) Validated a new panel of gene switches that alter metabolic flux; and (3) Gained expertise with industrially

relevant host organism strains. Finally, an important goal of this project was to establish new collaborations that will position us for future projects and new funding opportunities.

We achieved the expected progress in each of these areas:

Develop a biosensor for muconate

In order to address the "Test" step of "Design-Build-Test" cycle for Biomanufacturing (1), we sought to create a whole-cell biosensor for a commodity chemical cis, cis muconate (ccM), where ccM formation is coupled to the fluorescence of the cell via activation of a custom transcription factor (2). The technology is adaptable to flow cytometry, which makes rapid screening of vast number of genetic variations (Build step) for enzyme evolution or pathway optimization feasible (3).

ccM is a high value commodity chemical, a precursor for adipic acid (with an annual demand of 2.6 million tonnes) (4) that finds a direct use in manufacturing of Nylon 6,6. Renewable routes to the production of ccM and adipic acid, will circumvent the current industrial route using nitric acid oxidation of benzene that results in release of GHGs (mainly Nitrous oxide) contributing to environmental deterioration and global warming (5). ccM production from lignin derived feedstocks has been shown to be very promising to meet the current global demands as an industrial precursor and also has potential to bring down the cost of biomass-derived fuels to a targeted selling price of ~$3/gge (gasoline gallon equivalent). The current titer of ccM from lignin based aromatic monomers using synthetic biology and metabolic pathway engineering in the Pseudomonas putida organism is 13.5 g/L and several bottleneck steps in the bioconversion have been identified that have stalled the current yield (6). In this project we focused on design of a whole cell sensing technique for intracellular ccM formation that could later be used as the biosensor to evolve a few bottleneck enzymes in the pathway that would potentially give a step-jump in the ccM titer towards the final goal of ~50 g/L.

Our approach was to use a natural transcription factor (TF) for ccM, and optimize it for the host strain. Currently there are at least three TFs from Acinetobacter sp ADP1 and Pseudomonas putida that have been identified to be regulated by ccM in the pathways involved in metabolism of aromatic molecules (7). Of these, BenM is a global regulator and has been found to respond to both benzoate and ccM via two distinct binding sites (8). This TF has been also used to create an intracellular sensor for ccM detection (9). Due to the broad specificity nature of the current TF and since we also sought to use benzoate as a feedstock for ccM production using Pseudomonas putida, we focused our effort towards the remaining two ccM regulated TFs, CatM and CatR from Acinetobacter sp ADP1 and P. putida, respectively.

P. putida as a host

Genetically modified strains of P. putida KT2440 can utilize a variety of feedstocks ranging from lignin derived aromatic monomers such as coumarate and ferulate or other aromatic molecules such as benzoate and phenol and metabolize them into ccM (6). A broad host specific vector, pBTL-2 (10) was used to incorporate sensor/reporter genes. Exploiting an endogenous TF, CatR in the host, we created a plasmid construct with the gfp gene and the CatR promoter sequence (11) (Figure 1). Simultaneously, we also created a construct to utilize Acinetobacter CatM. In this case a whole cassette that was designed previously for E. coli was transferred into the pBTL-2 vector, with some modifications (Figure 2). These plasmid-constructs were successfully transformed in the P. putida strain and were optimized for growth in minimal media supplemented with glucose as carbon source and different concentration of benzoate for ccM production.

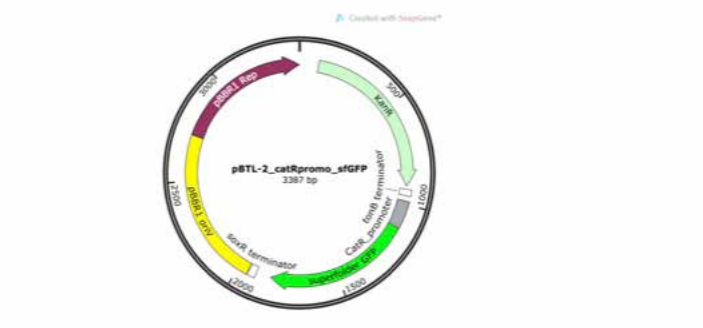

Figure 1. A broad host specific vector, pBTL-2 was used to incorporate sensor/reporter genes. Exploiting an endogenous TF, CatR in the host, we created a plasmid construct with the gfp gene and the CatR promoter sequence.

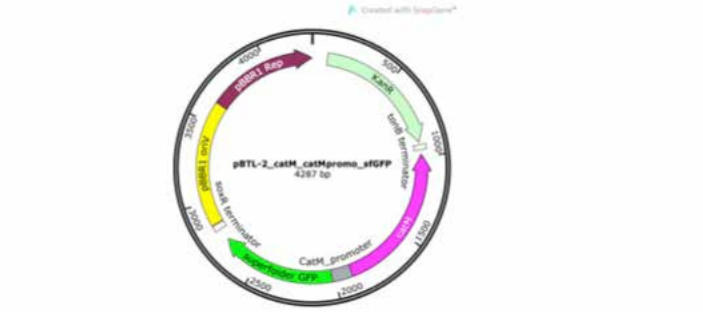

Figure 2. A construct was created to utilize Acinetobacter CatM. In this case the whole cassette that was designed for E. coli was transferred into the pBTL-2 vector, with an exception that E. coli RBS was switched back to the native Acinetobacter sequence.

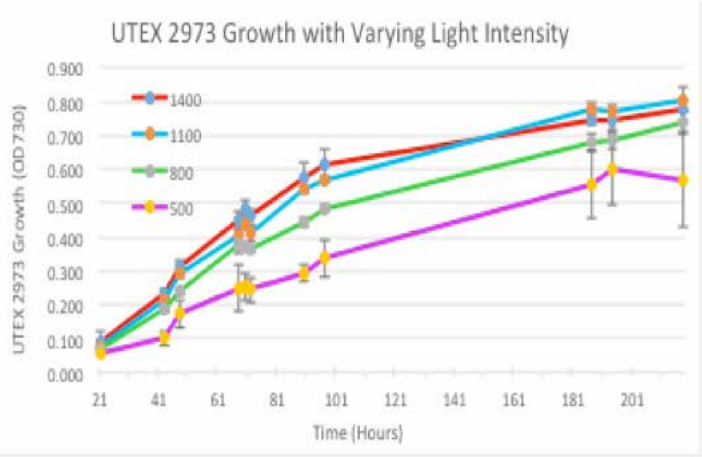

Figure 3. Growth of Synechococcus elongatus PCC 2973 cultures cultivated in Phenometrics environmental photobioreactors at 35°C, 3% CO, and constant light at intensities of either 500, 800, 1100 or 1400 µmol photons m s.

As a future direction, we will attempt to correlate the ccM production with the fluorescence of the cells. We will analyze the cells in a flow cytometer and then optimize the regulatory regions for the TFs for improved sensitivity and dynamic range (2, 12).

Develop a cis-repressor riboregulators for control of Green Fluorescent Protein (GFP) expression

The first goal of this task was to validate previous research and isolation of specific sequences responsible for specific protein (GFP) expression levels. We previously reported the design and demonstration of riboregulators that operate as pairs of Cis-repressors and Trans-activators (13). Using these pairs we were able to precisely tune the expression level of various reporter genes. We used fluorescence-activated cell sorting (FACS) to isolate 8 populations of E. coli cells containing RNA sequences that repressed GFP expression to varying degrees, resulting in 5 distinct levels of GFP expression, with a >50-fold dynamic range. This laid the ground work for tuning the expression levels of entire metabolic pathways; however, the eventual success of pathway engineering organisms using this system required the creation of multiple pairs that interact only with each other and reliably drive expression at predetermined levels. This requires generating multiple targeting sequences to guide their interaction that are both specific and performance-neutral.

In this project the aim was to show that only the cognate pair will activate expression and that each of the cognate pairs was able to activate to a similar degree. Over the course of this project we generated all combinations of 5 targeting pairs of Cis-Trans elements. This totaled 25 expression reporter constructs where each Cis element was tested against each of the 5 Trans targeting variants and each Trans elements is likewise tested with the 5 Cis targeting variants. In this approach, the genes of interest are turned off by the Cis elements and activated by Trans elements that were designed to turn on expression to specific levels. Briefly, the Cis elements repress expression of a plasmid encoded antibiotic resistance gene. The Trans element was also transcribed from the vector. The E. coli harboring each of these constructs was grown at increasing concentrations of the antibiotic and their growth rate at each concentration plotted. None of the non-cognate pairs showed appreciable activation, demonstrating our constructs are minimally cross-reactive and therefore specific. However, in some cases the cognate pairs did not activate to the same degree as our best performing pair. This is likely a result of targeting sequence variations. As a result we will continue testing alternative pairs, as well as performing analysis of the sequence variations that diminish performance in order to streamline and potentially automate the Design and Test cycle.

We reviewed the RNA sequences in each of these populations and chose two predominant sequences that were unique for each phenotype. These cis-repressing riboregulators were synthesized and independently cloned in front of the GFP reporter. This resulted in 16 different sequences with 10 different GFP expression phenotypes (some phenotypes were overlapping). The GFP expression levels varied across a broad 70-fold range from most dim to most bright. Also the resolution of these expression levels was quite high, with fold-intensities of as little as 1.5X from one culture to the next.

We were also able to complete one additional task and begin a third. In our original populations of 5 phenotypes, we noted that the distribution of GFP expression in each population was quite broad. To see if we could more tightly bin the GFP expression and therefore improve the resolution of these populations, we conducted an additional round of cell sorting. From the 8 populations (9, including a fully repressed construct), we sorted 14 new populations. These new populations had a >100x range in GFP expression, and tighter distributions per population, compared to the original populations. In the third activity, we are also tested the 16 cloned cis-repressors in a second expression system: the chloramphenicol acetyltransferase (CAT) gene, which confers resistance of the chloramphenicol antibiotic to the culture being studied.

These data show that libraries of different riboregulators can be sorted based on protein expression activity and that specific sequences can be recovered and used to induce specific levels of protein expression. These tunable regulators could be introduced in front of specific messenger RNAs of a pathway of interest, in order to optimize meta-

bolic flux in a natural or synthetic biological pathway. We aim to use these regulators in future projects to optimize the production of bioproducts of interest.

Gain experience in cultivation of new host organisms
Based on a literature search and our own experience, four strains of cyanobacteria, Synechococcus elongatus PCC 7942, Synechococcus elongatus PCC 2973, Synechocystis sp. PCC 6803 and Synechococcus sp. PCC 7002, were selected to evaluate their utility as phototrophic platforms to convert biomass into commodity chemicals. The selection criteria included: 1) reported ease of genetic manipulation, 2) maximal growth rates, 3) availability of genomic information, and 4) prior evidence that they could be used as a chassis to produce bioproducts. The four strains were purchased from culture collections, resuscitated in BG11 liquid medium, and transferred onto BG11 agar plates to obtain stock cultures for ongoing work.

First, we chose to evaluate the optimal phototrophic growth rate of S.elongatus PCC 2973 in our laboratory. This strain has been reported to exhibit exceedingly rapid phototrophic growth rates (doubling time of approximately 2.1 hr) (14). Cultures of S. elongatus PCC 2973 were cultivated in duplicate in Phenometrics environmental photobioreactors (ePBRs) at 4 different light intensities, 500, 800, 1100 and 1400 µmol photons m-2 s-1. In the Phenometrics ePBRs, with constant light at 35°C, doubling times of the S. elongatus PCC 2973 cultures were approximately 25-35 hrs (Figure 3). Growth rates appeared to saturate at approximately 1100 µmol photons m-2 s-1 in these photobioreactors. This growth rate is an order of magnitude slower than that reported by Yu at al. (14) but is similar to growth rates of closely related strains (i.e. S. elongatus PCC 7942) when grown in photobioreactors under less than optimal conditions. Currently, we are evaluating growth of S. elongatus PCC 2973 in photobioreactors that should allow greater light penetration than in the Phenometrics PBRs. Growth rates at different temperatures are being performed on all strains in batch cultures in Erlenmeyer flasks (~200 µmol photons m-2 s-1).

Finally, we established key collaborations with external and internal researchers. We established a new collaboration with NREL in the development of the muconate biosensor, and received their production strains and plasmids that are in use in their muconate research program. We held cross-disciplinary discussions with scientists in T and CCS divisions at LANL to determine which machine learning and statistical methods are most appropriate to implement software that can automate/improve discovery of biological networks from multi-omics datasets. These discussions are critical for defining strategies to pursue future funding opportunities.

Impact on National Missions

We have taken the first step to establish a new capability in synthetic biology at LANL that will ultimately be applied to replace petroleum-based platform chemicals and materials in a range of applications in energy, as well as medicine, defense, and national security in support of the emerging US Bioeconomy. Synthetic Biology is being used by the DOE Energy Efficiency and Renewable Energy (EERE) Office and the DOE Office of Science to expand options for bioenergy, and to provide bio-based, renewable replacements for petroleum-based chemicals and materials. The results of this project will enhance capabilities needed for "The Agile BioFoundry", to be funded by DOE-EERE's Bioenergy Technologies Office beginning in FY17.

References

1. Rogers, J. K., and G. M. Church. Multiplexed Engineering in Biology. 2016. TRENDS IN BIOTECHNOLOGY. 34 (3): 198.

2. Jha, R. K., T. L. Kern, D. T. Fox, and C. E. M. Strauss. Engineering an Acinetobacter regulon for biosensing and high-throughput enzyme screening in E-coli via flow cytometry. 2014. NUCLEIC ACIDS RESEARCH. 42 (12): 8150.

3. Harrington, L. B., R. K. Jha, T. L. Kern, E. N. Schmidt, G. M. Canales, K. B. Finney, A. T. Koppisch, C. E. M. Strauss, and D. T. Fox. Rapid thermostabilization of Bacillus thuringiensis Serovar Konkukian 97–27 dehydroshikimate dehydratase through a structure-sased enzyme design and whole cell activity assay . To appear in ACS Synthetic Biology.

4. Polen, , Spelberg, and Bott. Toward biotechnological production of adipic acid and precursors from biorenewables. 2013. JOURNAL OF BIOTECHNOLOGY. 167 (2): 75.

5. Vyver, Van de, and Roman-Leshkov. Emerging catalytic processes for the production of adipic acid. 2013. CATALYSIS SCIENCE & TECHNOLOGY. 3 (6): 1465.

6. Vardon, D. R., M. A. Franden, C. W. Johnson, E. M. Karp, M. T. Guarnieri, J. G. Linger, M. J. Salm, T. J. Strathmann, and G. T. Beckham. Adipic acid production from lignin. 2015. ENERGY & ENVIRONMENTAL SCIENCE. 8 (2): 617.

7. Maddocks, S. E., and P. C. F. Oyston. Structure and function of the LysR-type transcriptional regulator (LTTR) family proteins. 2008. MICROBIOLOGY-SGM. 154: 3609.

8. Ezezika, O. C., Haddad, T. J. Clark, E. L. Neidle, and Momany. Distinct effector-binding sites enable synergistic transcriptional activation by BenM, a LysR-type regulator. 2007. JOURNAL OF MOLECULAR BIOLOGY. 367 (3): 616.

9. Rogers, J. K., and G. M. Church. Genetically encoded sensors enable real-time observation of metabolite production. 2016. In PROCEEDINGS OF THE NATIONAL ACADEMY OF SCIENCES OF THE UNITED STATES OF AMERICA. Vol. 113, 9 Edition, p. 2388.

10. Lynch, M. D., and R. T. Gill. Broad host range vectors for stable genornic library construction. 2006. BIOTECHNOLOGY AND BIOENGINEERING. 94 (1): 151.

11. PARSEK, M. R., D. L. SHINABARGER, R. K. ROTHMEL, and A. M. CHAKRABARTY. ROLES OF CATR AND CIS,CIS-MUCONATE IN ACTIVATION OF THE CATBC OPERON, WHICH IS INVOLVED IN BENZOATE DEGRADATION IN PSEUDOMONAS-PUTIDA. 1992. JOURNAL OF BACTERIOLOGY. 174 (23): 7798.

12. Jha, R. K., Chakraborti, T. L. Kern, D. T. Fox, and C. E. M. Strauss. Rosetta comparative modeling for library design: Engineering alternative inducer specificity in a transcription factor. 2015. PROTEINS-STRUCTURE FUNCTION AND BIOINFORMATICS. 83 (7): 1327.

13. Krishnamurthy, , S. P. Hennelly, Dale, S. R. Starkenburg, Marti-Arbona, D. T. Fox, S. N. Twary, K. Y. Sanbonmatsu, and C. J. Unkefer. Tunable Riboregulator Switches for Post-transcriptional Control of Gene Expression. 2015. ACS SYNTHETIC BIOLOGY. 4 (12): 1326.

14. Yu, , Liberton, P. F. Cliften, R. D. Head, J. M. Jacobs, R. D. Smith, D. W. Koppenaal, J. J. Brand, and H. B. Pakrasi. Synechococcus elongatus UTEX 2973, a fast growing cyanobacterial chassis for biosynthesis using light and CO2. 2015. SCIENTIFIC REPORTS. 5.

Flow Cells for Scalable Energy Conversion and Storage Systems

Rangachary Mukundan
20160660ER

Abstract

There is a growing need for electrical energy storage as more renewable energy sources are brought into the power grid. A very promising scalable grid-level storage system is a flow cell, also called a redox flow battery. Current state of the art (SOA) flow battery technologies typically rely on aqueous acidic electrolytes and aqueous phase redox reactions that limit the volumetric energy density of the storage media and power density of the conversion process. To diverge from the current paradigm of acid aqueous-phase flow cells, we will develop anion exchange membranes (AEMs), non-aqueous electrolytes and new redox couples in synergy to build a non-aqueous flow battery. Iron based redox couples have tremendous potential to lower the cost of flow batteries, and ligands on the iron complex can be tailored to provide improved solubility and high redox potential. Design of highly soluble novel iron complexes for use with Ionic liquid (IL) electrolytes possessing high operating potential window has the potential to greatly enhance the energy density of flow batteries. New AEMs compatible with the ionic liquids and iron complexes are also required to improve the power density of flow cells and improve round trip efficiency and long term durability. In this four month feasibility project we synthesized Fe based complexes with redox active metal centers and ligands and demonstrated their capability for use in flow batteries. We also established a capability within LANL to construct, and evaluate both aqueous and non-aqueous flow battery systems. These capabilities will be utilized to build low cost high energy density Fe-based non-aqueous flow batteries in a follow-on LDRD project.

Background and Research Objectives

The U.S. has increasing needs for energy storage in its electrical power grid. Influencing this need is the rapidly growing use of renewables that produce power intermittently. Without grid scale energy storage, sufficient generating capacity must exist to handle peak demands resulting in large capital investments that sit idle for long periods of time (both daily and seasonally). Without technological breakthroughs in efficient, large-scale energy storage, it will be difficult to rely on intermittent renewables for much more than 20-30% of electricity produced in the US [1]. Due to their unique design, flow batteries provide several desirable features compared to other storage systems; (a) the ability to store large amounts of energy up to the grid level (MWh) in low cost tanks; (b) flexible modular design, which allows systems to be sized appropriately based on power and energy requirements; (c) the potential for much longer lifetimes since the electrodes are designed to primarily provide the electrochemically active surface for the redox reactions and do not undergo chemical changes as in standard battery systems, and; (d) inherent safety is built in due to the liquid state of the major constituents and separate storage of reactive materials, preventing catastrophic failures from an internal short circuit. All of these advantages, viz., large capacity, scalability, safety, and lifetime, translate into the potential for a much lower cost and more reliable energy storage system than any other battery technology [2]. However, the current Levelized Cost Of Electricity (LCOE) for various aqueous flow battery systems range from $400 MWh-1 to $1000 MWh-1 falling short of the DOE long and near-term targets of $100 and $200 MWh-1, respectively [3,4]. To make flow battery systems economically viable for effective energy arbitrage, the round-trip efficiency (charging + discharging) needs to be maximized and the capital system cost dramatically lowered by increasing the energy/power density and/or lowering the cost of the storage medium.

State of Art (SOA) flow battery technology relies on aqueous acidic electrolytes and aqueous-phase redox reactions. While progress has been made in decreasing the cost of these systems, the use of an expensive redox metal like Vanadium and fundamental limitations in energy density due to use of aqueous electrolytes, are still major barriers to overcome. The energy density in a flow

battery system is a function of the half-cell potentials of redox reactions, concentration of the charge carriers and number of electrons transferred. Currently, energy densities of SOA all vanadium aqueous systems are limited to ~43 Wh/L. This limitation results from the narrow voltage window of aqueous media (~1.5 V) and from the typical redox couples with limited solubility (~ 2 M) that only transfer one electron per molecule. To further decrease LCOE and make flow batteries economically competitive; new materials, chemistries, and designs resulting in larger operating voltages and multi-electron charge transfer must be developed along with an understanding of the complex interplay between reactant transport and electrode kinetics.

Scientific Approach and Accomplishments

Redox ligand synthesis: Our primary chemical focus during the four-month period of funding was a ligand archetype that we believed was both achievable within the work scope and would have promising properties. The basic concept is a bifunctional ligand that contains metal binding sites that prefer specific Fe valences so as to discourage ligand dissociation as the complex undergoes redox chemistry. For example, a pyridine moiety can serve as the binding site for Fe(II) whereas an imine can serve as the Fe(0) binding site. In complement, this ligand type is also redox active (similar to the related class of pyridine diimine (PDI) ligands) [5], which means that the ligand can become reduced instead of the metal to which it is attached. Moreover, these ligands are small enough that multiple ligands can be used to coordinatively saturate Fe (in order to dissuade decomposition reactions) and the synthesis can be conducted using inexpensive reagents. Ligand synthesis was accomplished through the condensation of pyridine-2-aldehyde with the desired primary amine (Figure 1). Our initial target was R = isopropyl because we believed that group would impart good non-aqueous solubility, but we also synthesized the R=methyl and R=phenyl derivatives. All of the ligands were successfully synthesized in multigram quantities and the 1H NMR spectra were consistent with literature reports.

Fe(OTf)2 (OTf = trifluoromethanesulfonate, triflate) was chosen as the Fe starting material because OTf is more likely to behave as an outer sphere anion than a halide and confers greater solubility in organic solvents than SO42-. Mixing Fe(OTf)2 with 3 equivalents of ligand in methanol yields dark purple solutions for all 3 ligands. These materials can be crystalized via diffusion of diethyl ether into acetonitrile solutions, but these crystals have not yielded solvable X-ray diffraction data. For this general ligand type and stoichiometry, mer and fac structural isomers are possible [6], and solid-state structures of both (with different R groups) have been reported [7,8]. 1H NMR data is consistent with multiple isomers and preliminary density functional theory energy calculations show that for R=isopropyl, the free energy difference between the mer and fac isomers is essentially zero. Thus, whatever form we eventually isolate in the solid state, we should generally consider it likely that multiple isomers/diastereomers are present in solution. Follow on work in the next project will initially focus on more fully characterizing these materials (including solubility) and attempting to isolate their reduction products.

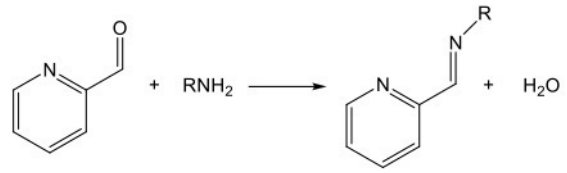

Figure 1. General Ligand synthetic scheme

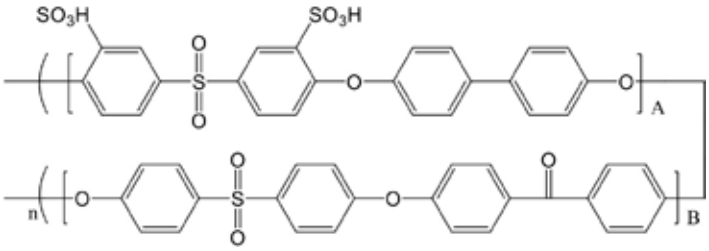

Figure 2. Chemical structure of the prepared cation exchange membrane (C185).

Membrane Synthesis: Membranes are a critical component in a flow battery system that separate the redox species in the catholyte and anolyte and also provide ionic conductivity. In this feasibility project new membranes were synthesized for replacing Nafion, which is the SOA membrane in current vanadium aqueous flow batteries. The synthesis of hydrophobic and hydrophilic oligomers and multiblock copolymers were carried out as follows. In a typical polymerization procedure, Biphenol, SDCDPS (Disulfonated co-monomers), and NMP (N-methyl-2-pyrrolidinone) were mixed and dissolved and K2CO3 and toluene were added. After dehydration at 150 C the polymerization proceeded at 190 C for 16 h. Then the reaction bath was cooled to 80 C, and the hydrophobic telechelic oligomer was dissolved in NMP and added to the reaction mixture. The bath temperature was raised to 95 C and kept at this temperature for 9 h. The reaction mixture was precipitated into isopropanol to obtain a brownish fibrous polymer. A series of block copolymers were synthesized, differing in ion exchange capacity and block length (Figure 2). This procedure will be further modified in the follow on project to synthesize membranes that are compatible with the

ionic liquids developed for the Fe-based redox complexes. The ability to tailor the functional groups in the membrane to improve conductivity in the electrolyte and decrease cross-over of the redox species will be critical to the design of low cost high performance flow batteries.

Flow Battery studies: Two new capabilities were added during this feasibility project. A system to evaluate aqueous flow batteries, and another to specifically evaluate non-aqueous flow batteries. The aqueous system was tested with a standard vanadium flow battery using 1 M VOSO4 – 2.5 M H2SO4 electrolyte, graphite flow fields and graphite felt electrodes. The newly synthesized C185 membrane possesses almost double the discharge capacity when compared to Nafion-117 in an identical environment. This could be attributed to its thickness, which is 3.5 times thinner than the Nafion-117 membrane. Due to its thinness, C185 membrane efficiently utilizes the transport of protons as well as vanadium ions. On the other hand, Nafion-117 membranes possess similar resistance (~ 30–35 mOhm) to the C185 membrane, yet its thickness prevents higher discharge capacity. The thinner C185 membrane shows coulombic efficiency little above 75%, compared to about 98% for Nafion-117 membrane owing to its thickness. The average energy efficiency for C185 and Nafion membranes are 47 and 48%, respectively. Though, the Nafion-117 membrane possesses higher coulombic efficiency and similar resistance, thinner C185 membrane outperforms in terms of voltage efficiency (49% for Nafion-117 vs 60% for C185). These preliminary results indicate the feasibility of designing custom membranes with functional groups tailored for high ion conductivity and low redox crossover.

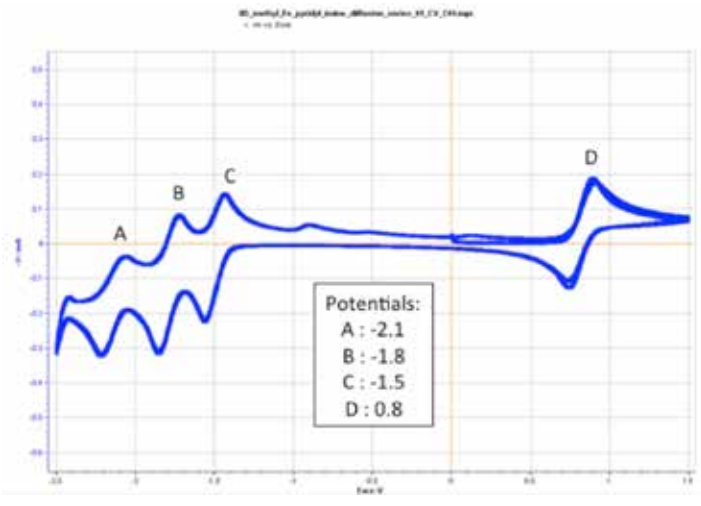

Figure 3. Cyclic voltammogram of the Methyl Fe-pyridyl complex in an acetonitrile solvent and Tetrabutyammonium hexafluorophosphate electrolyte.

The redox properties of the newly synthesized Fe based complexes were evaluated in a cyclic-voltammetry (CV) setup before incorporation into a non-aqueous flow battery system. The Fe complex (0.01M) was dissolved in acetonitrile solvent and a supporting Ionic liquid electrolyte (0.1M Tetrabutyammonium hexafluorophosphate: Bu4NPF6). A glassy carbon working electrode, a Pt wire counter electrode and a Ag/AgCl reference electrode were utilized for the CV studies. The CV of the methyl-pyridyl is shown in Figure 3 where the Fe(II)/Fe(III) transition is observed at +0.8V while three different transitions associated with the reduction of the ligand are observed between -1.5V and -2.1V. These preliminary results indicate that these Fe-complexes can support redox reactions that have the potential to be utilized in a non-aqueous flow battery system The potential difference between the Fe oxidation and the first ligand reduction peak is 2.3V and could be utilized in a non aqueous floe battery. Repeated cycling of this Fe compound indicated some degradation of the complex after cycling between +1.5V and -2.5V. The redox stability window of these complexes needs to be studied in detail and will be optimized in the follow-on project.

Impact on National Missions

Energy storage is a critical enabler for large-scale adoption of renewables into the grid. LANL, with its vast knowledge in the area of energy conversion devices and earth-abundant metal chemistry, is uniquely positioned to advance the development of flow batteries to fill the energy-storage need. With this feasibility demonstration project, we have taken the first steps to demonstrate the capabilities of Fe-complex based non-aqueous redox flow batteries. In any follow-on projects, we anticipate developing new chemistries, new IL based electrolytes and new anion exchange membranes that will result in low cost high energy/ power density flow batteries. We expect that these developments will improve energy storage that is critical to the energy security of our country.

References

1. Committee for The National Academies Summit on America's Energy Future, National Research Council, "The National Academies Summit on America's Energy Future: Summary of a Meeting," . 2008. National Academies Press, Washington, DC.

2. Soloveichik, G. L.. Flow Batteries: Current Status and Trends. 2015. CHEMICAL REVIEWS. 115 (20): 11533.

3. Technology Roadmap, Energy Storage . 2014. International Energy Agency.

4. Grid Energy Storage. 2013. U.S. Department of Energy .

5. Bart, S. C., Chlopek, Bill, M. W. Bouwkamp, Lobkovsky, Neese, Wieghardt, and P. J. Chirik. Electronic structure of bis(imino)pyridine iron dichloride, monochloride, and neutral ligand complexes: A combined structural, spectroscopic, and computational study. 2006. JOURNAL OF THE AMERICAN CHEMICAL SOCIETY. 128 (42): 13901.

6. BLANDAMER, M. J., J. BURGESS, D. L. ELVIDGE, P. GUARDADO, A. W. HAKIN, L. J. S. PROUSE, S. RADULOVIC, and D. R. RUSSELL. ISOMERIC FORMS OF TRIS-SCHIFF BASE COMPLEXES OF IRON(II) - STRUCTURE OF THE COMPLEX DERIVED FROM 2-ACETYL PYRIDINE AND METHYLAMINE. 1991. TRANSITION METAL CHEMISTRY. 16 (1): 82.

7. Serb, , Calmuschi-Cula, Dumitru, Englert, and Guran. Tris[4-(2-pyridylmethyleneamino)-phenol]iron(II) bis(perchlorate). 2008. ACTA CRYSTALLOGRAPHICA SECTION E-STRUCTURE REPORTS ONLINE. 64: M212.

8. Howson, S. E., L. E. N. Allan, N. P. Chmel, G. J. Clarkson, van Gorkum, and Scott. Self-assembling optically pure Fe(A-B)(3) chelates. 2009. CHEMICAL COMMUNICATIONS. (13): 1727.

Publications

Mukundan, R.. Flow Batteries for Scalable Energy Conversion and Storage. Invited presentation at 2016 New Mexico Regional Energy Storage and Grid Integration Workshop. (Albuquerque, 23 Aug. 2016).

New Ligands and Catalysts for the Hydrogenation of Renewable Compounds Containing Ketonic Substrates

Pavel Dub
20160666ER

Abstract

Carboxylic and carbonic acid derivatives form the majority of biologically derived, renewable feedstocks for replacing petrochemical resources [1]. The efficient conversion of these substrates to chemically reduced commodity chemicals and petrochemical substitutes remains a challenge [2]. Turnover efficiencies and stability have to be balanced with commodity scale production. We have recently developed ENENES, a cheap, air-stable and versatile ligand toolbox for the hydrogenation of C=O functionalities including fluorinated esters [3]. To increase the catalytic activity and stability of transition-metal complexes of Ruthenium and Iridium supported by these ligands, we have proposed the replacement of labile nitrogen centers by more stable phosphine motives. In this project we have now developed the efficient syntheses for these novel ligands and scaled the reactions to afford sufficient material for further evaluation.

Background and Research Objectives

The development of novel transition metal reduction catalysts for the practical synthesis of alcohols and amines from bio-renewable carbonyl-containing substrates has been a major effort in our group. In our previous work we have found that cheap ENENES (see Figure 1 for a representative example) can accomplish these conversions. The evaluation of these ligands suggested extending the initial proposed scope of the JRO Postdoc Fellowship to replace hemilabile nitrogen moieties with electron donating phosphine motives. We envisioned that these entirely new classes of ligands and derived catalysts may afford greater hydrogenation activities. The research objectives were development and scaling of the ligand syntheses, as well as evaluation of these novel ligands for catalysis.

Scientific Approach and Accomplishments

The thioamine phosphine ligand syntheses required generating thioethylamines depicted in Figure 2. The syntheses of the thiolamines proceeds in moderate to good yields from bromoethylamine hydrobromide and the thiol or thiolate, respectively, using freshly prepared sodiumethoxide (2.2 eq.) in ethanol and heating the reaction over 12 hours to reflux temperature. The addition of the thioethylamine derivatives to vinyldiphenyloxide yields mono and di – Michael addition products if conducted at reflux in water. Careful optimization of the reaction conditions showed that slow addition of a phosphine oxide solution to the amine in refluxing ethanol yields almost exclusively the mono-addition products in moderate to good yields as shown in Figure 3. These can be easily separated by flash column chromatography from vinylphosphine oxide starting material. Initial efforts to reduce the phosphine oxide focused on well known reported reductions with silanes, while excluding methods that require metal addition or metal catalysis to avoid metal binding to the products and the commensurate purification challenges. Screening of reduction reactions showed that trichlorosilane reductions with triethylamine in acetonitrile converts the starting materials efficiently at reflux temperature within 24 hours. The reaction was then adapted to microwave syntheses allowing the conversation to proceed within as little as 15 minutes as shown in Figure 4. Byproduct formation indicates that this process is highly dependent on the purity of the silane, a reduction agent with limited shelf life.

In summary, we have created a new class of ligands for Ru, Rh and Ir catalysts. Synthesizing these ligands allows the evaluation of these entities to increase the catalytic turnover for the reductive hydrogenation of carbonyl containing substrates. These novel entities will complement and extend our existing IP portfolio in catalysis; an IP disclosure is planned. We will further publish these new chemical routes in a high profile journal. We expect this work to provide to our strong foundation for future external funding in this area.

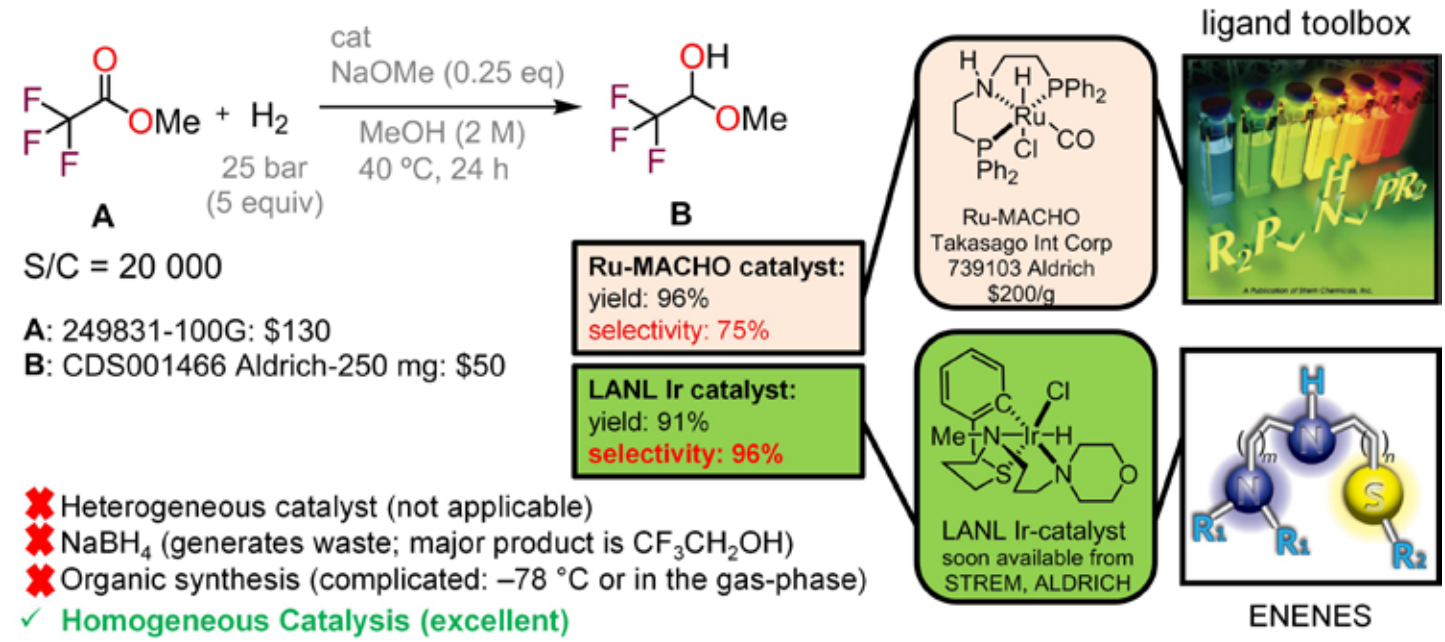

Figure 1. Practical synthesis of important synthon B by using a homogeneous catalysis approach

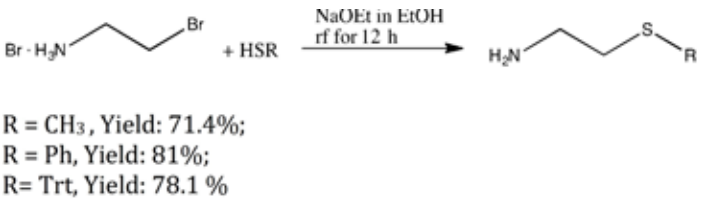

R = CH_3, Yield: 71.4%;
R = Ph, Yield: 81%;
R= Trt, Yield: 78.1 %

Figure 2. Thiopropylamine syntheses

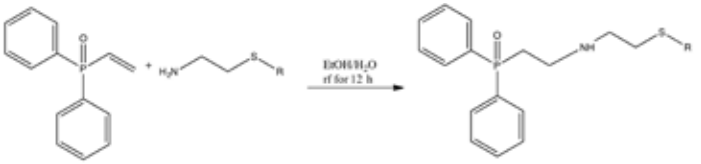

R = CH_3, yield: 68.9 %; yield based on consumed sm: 77.7%
R = Ph, yield: 77.4 %; yield based on consumed sm: 84 %
R= Trt, yield: 82.3 %; yield based on consumed sm: 85.3%

Figure 3. Phosphine-oxide ligand syntheses

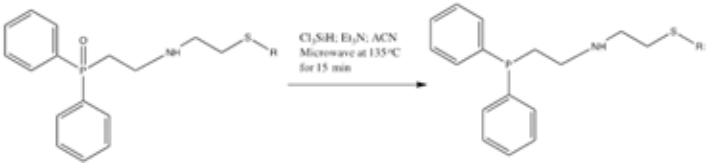

Figure 4. Rapid microwave assisted reduction of phosphine oxides

Impact on National Missions

The U.S. Department of Energy (DOE) has a goal of replacing 25% of industrial organic chemicals with bio-renewable chemicals by 2025. Major breakthrough technologies, such as increased hydrogenation turnover, are required to enable this goal and in particular catalysis and catalyst development to allow efficient conversion of oxygen rich biologically derived feedstock to chemically reduced commodity chemicals and petrochemical substitutes. We expect this work to have significant potential for addressing these challenges through DOE, industrial CRADA opportunities and within the context of Bioenergy Center efforts at LANL.

References

1. Bozell, J. J., and G. R. Petersen. Technology development for the production of biobased products from biorefinery carbohydrates-the US Department of Energy's "Top 10" revisited. 2010. Green Chemistry. 12 (4): 539.

2. Dub, P. A., and T. Ikariya. Catalytic Reductive Transformations of Carboxylic and Carbonic Acid Derivatives Using Molecular Hydrogen. 2012. ACS Catalysis. 2 (8): 1718.

3. Dub, P. A., B. L. Scott, and J. C. Gordon. Air-Stable NNS (ENENES) Ligands and Their Well-Defined Ruthenium and Iridium Complexes for Molecular Catalysis. 2015. Organometallics. 34 (18): 4464.

Bayesian Information Gap Decision Analysis

Velimir V. Vesselinov
20140000PRD4

Introduction

Bayes theorem is a mathematical technique that provides a way to determine the likelihood of different models given some observed data. Bayes theorem is mathematically rigorous, but its application is not always rigorous for two reasons: (1) We can enumerate the possible outcomes of dice-rolling, but not the possible outcomes of real-world problems like groundwater remediation. (2) We can determine conditional probabilities for coin-tossing, but substantial uncertainty surrounds the conditional probabilities in real-world problems. We circumvent these issues with a three-layered-onion approach. The middle layer employs Bayes theorem. The inner and outer layers employ a non-probabilistic uncertainty quantification (UQ) methodology called Information-Gap to overcome (1) and (2), respectively. This Bayesian-Information-Gap (BIG) UQ approach provides robust decision support for selecting a remediation approach after the site characterization been performed.

This project will extend this methodology to provide decision support throughout the site characterization process. A probabilistic model will be used to generate hypothetical data that might be obtained from measurement. The BIG UQ framework will be used to arrive at a decision before and after hypothetical site characterization. Characterization efforts that have a high chance of altering the decision are more worthwhile than those that have a low chance of altering the decision. This also informs the transition from uncertainty reduction to remedy selection. If all site characterization options are unlikely to alter the remedy selection, it is time to suspend site characterization and begin remediation. Techniques for estimating the progress and execution time of the analyses will also be developed.

The combination of flexible computational demands that arises from model independence and open source software means that this framework can also be used out at tens of thousands of contaminated groundwater sites across the USA. Applications to other fields are easily achieved due to the model independence.

Benefit to National Security Missions

This research aligns with the LANL mission and the strategic EES research goals as it aims to provide optimal decisions for national problems related to energy and environmental security; these national problems require development of strategic scientific capabilities to improve decisions in energy and water production, carbon capture and sequestration, waste disposition and storage, and restoration of contaminated sites. In all these areas, real-world applications require robust and accurate methods for capturing the existing uncertainties in the model analyses and decision process. The methods and tools developed in this work will satisfy these needs and strengthen existing research at LANL. This work will provide opportunity for future basic science and programmatic research growth working with new sponsors (e.g., DoD, SERDP, NSF, industry) and new research areas that require decision analyses for complex national security problems, such as counter-terrorism.

Progress

During the past year, the work under current project produced several important publications and developed an algorithm that has been made available as open-source code. O'Malley was listed as an author on 7 published papers. Dan was first author on 3 of the papers published in FY16.

Three of the papers (one published in Water Resources Research and two published in the International Journal of Greenhouse Gas Control) focused on the developed novel decision analysis theory based on Bayesian Information Gap (BIG) methodology. The paper published in Water Resources Research outlines the theory of Bayesian Information Gap (BIG) decision analysis. The papers published in International Journal of Greenhouse Gas

Control demonstrate the applicability to different practical problems. The work for the latter 2 papers was collaborative and included other LANL staff, students and postdocs.

Three of the papers (published in Groundwater, Journal of Hydrology, and Physical Review E.) focused on theoretical analysis on the underlying physics that is targeted in the current LDRD project and how these theoretical insights can provide understanding about conceptual uncertainties and related decisions. It is important to note that, the paper titled "Where does water go during hydraulic fracturing?" published in Groundwater, is collaborative work with another LDRD-DR project (PI: H. Viswanathan).

The paper published in Hydrologic Processes is work related to Arctic research with other LANL Earth and Environmental Sciences Division (EES) collaborators. The publication demonstrates the interest in Dan O'Malley's research outside of the current LDRD project.

In addition to the research papers, the developed algorithm have been incorporated in the open-source code MADS. MADS is a LANL-developed, high-performance, open-source framework for model-based decision support employing system and complex physics simulation models. The MADS code is available on the GitHub (http://github.com/madsjulia) and GitLab sites (https://gitlab.com/mads/mads.jl) and the documentation is available at the ReadTheDocs.org site (http://mads.readthedocs.org). Various demos, execution examples, and a tutorial are available at the MADS website (http://mads.lanl.gov). MADS test problems related to newly developed decision theory methods can be found at: http://mads.readthedocs.io/Examples/bigdt/source_termination.

In summary, the current LDRD project provided major contributions to the decision theory and its applicability to solve practical problems. The developed methods are already available in open-source codes (MADS; http://mads.lanl.gov).

Future Work

For the last six months of the project within FY17, Dan O'Malley plans to write to an overview paper that will summarize all the accomplishments. The paper will present the developed novel methodology and demonstrate its applicability using a series of synthetic example problems. The publication will target peer-review journals with high ranking such as the SIAM/ASA (Society for Industrial and Applied Mathematics/American Statistical Association) Journal on Uncertainty Quantification.

O'Malley also plans to work with other EES collaborators to demonstrate the methodology on a real-world problem. Most probably the real-world problem will be related to the LANL Chromium contamination site. The chromium plume at Los Alamos National Laboratory (LANL) is a complex contaminant-remediation site with spatial extent of several square kilometers. The LANL chromium problem is an extremely complex site for environmental management. The site is one of the most complex, data-rich, highly visible sites within the Department of Energy (DOE) complex. The analyses will also require the use of high-performance computational resources. This is because we are dealing with large data sets (>107 datum), complex models (>106 computational grid points), ambiguous uncertainties and challenging decisions.

O'Malley is going to work with researchers at UT-Austin and MIT to apply the developed novel methodologies under this project to problems studied at these institutions.

Conclusion

This project will provide a framework for making decisions related to complex problems with a focus on groundwater remediation, but benefits that go far beyond. Groundwater contamination is an important national problem with over $100 billion dollars in liabilities including around $20 billion within the DOE complex. A substantial challenge in groundwater remediation scenarios is to select between a variety of site characterization efforts and remediation options. This framework will provide insight into the value of different characterization efforts, inform the transition from studying the problem to solving the problem, and help select the best solution to the problem.

Publications

Cushman, J. H., and D. O'Malley. Fickian dispersion is anomalous. 2015. Journal of Hydrology. 531: 161.

Cushman, J. H., and D. O'Malley. Fickian dispersion is anomalous. 2015. Journal of Hydrology. 531: 161.

Grasinger, M., D. O'Malley, V. V. Vesselinov, and S. Karra. Decision Analysis for Robust CO2 Injection: Application of Bayesian-Information- Gap Decision Theory. 2016. International Journal of Greenhouse Gas Control. 49: 73.

Grasinger, M., D. O'Malley, V. Vesselinov, and S. Karra. Decision analysis for robust CO 2 injection: Application of Bayesian-Information-Gap Decision Theory. 2016. International Journal of Greenhouse Gas Control. 49: 73.

Hyman, J. D., J. Jimenez-Martinez, H. S. Viswanathan, J. W. Carey, M. L. Porter, E. Rougier, S. Karra, Q. Kang, L. Frash, L. Chen, Z. Lei, D. O'Malley, and N. Makedonska.

Understanding hydraulic fracturing: a multi-scale problem. 2016. Philosophical Transactions of the Royal Society A. 374: 2078.

Hyman, J., J. Jim'enez-Mart'inez, H. Viswanathan, J. Carey, M. Porter, E. Rougier, S. Karra, Q. Kang, L. Frash, L. Chen, and others. Understanding hydraulic fracturing: a multi-scale problem. 2016. Phil. Trans. R. Soc. A. 374 (2078): 20150426.

Lin, Y., D. O'Malley, and V. V. Vesselinov. A computationally efficient parallel Levenberg-Marquardt algorithm for highly parameterized inverse model analyses. 2016. Water Resources Research. 52 (9): 6948.

O'Malley, , V. V. Vesselinov, and J. H. Cushman. Diffusive mixing and Tsallis entropy. 2015. PHYSICAL REVIEW E. 91 (4).

O'Malley, , V. V. Vesselinov, and J. H. Cushman. A Method for Identifying Diffusive Trajectories with Stochastic Models. 2014. JOURNAL OF STATISTICAL PHYSICS. 156 (5): 896.

O'Malley, , and V. V. Vesselinov. Groundwater remediation using the information gap decision theory. 2014. WATER RESOURCES RESEARCH. 50 (1): 246.

O'Malley, , and V. V. Vesselinov. Analytical solutions for anomalous dispersion transport. 2014. ADVANCES IN WATER RESOURCES. 68: 13.

O'Malley, D., S. Karra, R. Currier, N. Makedonska, J. Hyman, and H. Viswanathan. Where Does Water Go During Hydraulic Fracturing?. 2015. Groundwater.

O'Malley, D., S. Karra, R. P. Currier, N. Makedonska, J. D. Hyman, and H. Viswanathan. Where does water go during hydraulic fracturing?. 2016. Groundwater. 54: 488.

O'Malley, D., V. V. Vesselinov, and J. H. Cushman. Diffusive mixing and Tsallis entropy. 2015. Physical Review E. 91 (4): 042143.

O'Malley, D., and J. H. Cushman. Anomalous dispersion. pres. In The Handbook of Groundwater Engineering. Edited by Cushman, John H, and Tartakovsky, Daniel M.

O'Malley, D., and J. H. Cushman. Fractional Fokker-Planck equations. pres. In Fractals in Geophysics. Edited by Ghanbarian B, and Hunt A.

O'Malley, D., and V. V. Vesselinov. Bayesian information-gap decision analysis applied to a CO2 leakage problem. 2015. Water Resources Research. 51: 7080.

O'Malley, D., and V. V. Vesselinov. ToQ.jl: A high-level programming language for D-Wave machines based on Julia. pres. In Proceedings of the 2016 Institute of Electrical and Electronics Engineers High Performance Extreme Computing Conference.

O'Malley, D., and V. Vesselinov. Bayesian-information-gap decision theory with an application to CO2 sequestration. 2015. Water Resources Research. 51 (9): 7080.

O'Malley, D., and V. Vesselinov. Groundwater remediation using the information gap decision theory. 2014. Water Resources Research. 50 (1): 246.

O'Malley, D., V. Vesselinov, and J. Cushman. A method for identifying diffusive trajectories with stochastic models. 2014. Journal of Statistical Physics. 156 (5): 896.

O'Malley, D., and V. Vesselinov. Analytical solutions for anomalous dispersion transport. 2014. Advances in Water Resources. 68: 13.

Throckmorton, H. M., B. D. Newman, J. M. Heikoop, G. B. Perkins, X. Feng, D. E. Graham, D. O'Malley, V. V. Vesselinov, J. Young, S. D. Wullschleger, and others. Active layer hydrology in an Arctic tundra ecosystem: quantifying water sources and cycling using water stable isotopes. 2016. Hydrological Processes.

Bottom-up Chemical Synthesis of Large, Well-Defined, and Organo-Processable Nanographene-based Triarylamine for Optoelectronic Applications

Hung-Ju Yen
20140666PRD2

Introduction

The main focus of this project is to develop synthetic strategies for making triarylamine-based nano-graphene (TAA-NG), a small piece of graphene with well-defined molecular structure. NG with flexible alkyl chains attached to the periphery of NG renders solubility in organic solvents and allows self-assembly of NGs with phase separation into nanoscaled morphology in composite materials. More importantly, the incorporation of heteroatoms such as triarylamine (TAA) into the graphene frameworks leads to a triangular shape and charge transfer characteristics, which, to the best of our knowledge, have never been attempted. The challenge of this project lies in the fact that the organic synthetic scheme for TAA-NG requires more than 20 steps. This is a costly and time-consuming process. Although synthesis of simple NGs have been demonstrated, synthesis of TAA-NG remains a challenge and the final yield of this compound may be low, which could impede us from developing applications using this materials. Therefore, our challenges are not only in the synthesis of TAA-NG, but also in finding ways to increase the yield of the final product.

We expect the as-prepared TAA-NG will reveal fine-tuned optoelectronic properties tailored for the applications in electrochromic, memory device, LED, photovoltaic cell, fuel cell, lithium battery, and super-capacitor. Success in demonstrating derivatized NGs in the above devices could have intellectual property value and warrants publications in high impact journals.

Benefit to National Security Missions

This project aims to develop nanographenes (NGs) with tunable electronic structures and optical properties. The integration of functional NGs into clean energy technologies could bridge the gap between basic research and commercialization of graphene-based energy devices. Further development of NG-based materials will strengthen our leadership role in NG research, which has strong ties to Laboratory mission in the areas of exotic materials and energy security.

Progress

For the past twelve months, we have prepared a series of novel three dimensional nanographenes through multi-step organic synthesis. The materials have shown very high specific capacitance and long term operational stability through hundreds of charging discharging cycles when fabricated as anode of Lithium ion battery. In addition, these materials have revealed electronic structure similar to that of the conjugated polymers and hybrid perovskite. All of the above exciting properties are mainly resulting from the unique, hierarchical self-assembled structures which can only be imaged by high resolution TEM in situ. The ultimate goal is to establish a structure-property relationship between nanographene structures and device performance; such systematic understanding has never been realized.

Future Work

In FY17, we will demonstrate the synthesis of heteroatom (P, N, or B) doped nanographenes through a newly designed synthetic route. Such synthesis includes Hydrogenation, Iodination, Curtis rearrangement, Sonogashira coupling, Suzuki coupling, Diels-Alder cycloaddition, and Ullmann reactions. The molecular structures and crystallinity of these nitrogen/boron doped nanographenes will be characterized by X-ray diffraction, scanning electron microscopy, scanning tunneling microscopy, atomic force microscopy, dynamic light scattering, MALDI-TOF Mass spectroscopy, infrared spectroscopy and nuclear magnetic resonance spectroscopy. Electronic and optical properties of these nitrogen doped nanographene will be determined by cyclic voltammetry, UV-Vis spectrometer and fluorescence spectrometer. The incorporation of heteroatoms in the nanographene is expected to increase the incorporation of metal atoms and rate of

diffusion. Therefore, we will incorporate these nitrogen-doped nanographenes as part of anode material in lithium ion battery (LIB) and evaluate the performance characteristics in terms of capacity, stability through hundreds of charging-recharging cycles. We will also evaluate the use of these novel nanographenes as new electrochromic material, and demonstrate the use of these materials as fuel cell electrodes.

Conclusion

We expect to achieve synthesis of processable nanographene (NG). Our proposed synthesis promises ways to control NGs with size-dependent band gap, optical absorptivity, and charge transfer functionality. If successful, this project will likely generate a new class of materials with emergent functionality previously not accessible through fabrication methods. The integration of functional NGs into clean energy technologies could bridge the gap between basic research and commercialization of graphene-based energy devices. Further developing NG-based materials will strengthen our leadership role in NG research, which has strong ties to Laboratory mission in the areas of exotic materials and energy security.

Publications

Cheruku, P., J. H. Huang, H. J. Yen, R. S. Iyer, K. D. Rector, J. S. Martinez, and H. L. Wang. Tyrosine-Derived Stimuli Responsive, Fluorescent Amino Acids. 2015. CHEMICAL SCIENCE. 6: 1150.

Kuo, C. Y., W. Nie, H. Tsai, H. J. Yen, A. D. Mohite, G. Gupta, A. M. Dattelbaum, D. J. William, K. C. Cha, Y. Yang, L. Wang, and H. L. Wang. Structural Design of Benzo[1,2-b:4,5-b ']dithiophene-Based 2D Conjugated Polymers with Bithienyl and Terthienyl Substituents toward Photovoltaic Applications. 2014. MACROMOLECULES. 47 (3): 1008.

Kuo, C. Y., Y. Liu, D. Yarotski, H. Li, P. Xu, H. J. Yen, S. Tretiak, and H. L. Wang. Synthesis, Electrochemistry, STM Investigation of Oligothiophene Self-Assemblies with Superior Structural Order and Electronic Properties. To appear in Chemical Physics.

Park, Y. I., O. Postupna, A. Zhugayevych, S. W. Kyu, , Y. S. Park, B. Kim, H. J. Yen, P. Cheruku, J. S. Martinez, J. Park, S. Tretiak, and H. L. Wang. A new pH sensitive fluorescent and white emissive material through controlled inter-molecular charge transfer. 2015. CHEMICAL SCIENCE. 6: 789.

Tsai, , K. S. K. Reddy, Yeh, Wang, Lin, Yen, Tsai, and Liou. Zinc and linkage effects of novel porphyrin-containing polyimides on resistor memory behaviors. 2016. RSC ADVANCES. 6 (91): 88531.

Tsai, , Wang, Lin, Tsai, Yen, You, and Liou. A novel porphyrin-containing polyimide for memory devices. 2016. POLYMER CHEMISTRY. 7 (16): 2780.

Yen, , Chang, Wu, and Liou. The steric effect of alpha- and beta-substituted anthraquinone units on high performance polymeric memory devices. 2015. POLYMER CHEMISTRY. 6 (44): 7758.

Yen, , Chen, Wu, and Liou. High performance polymers and their PCBM hybrids for memory device application. 2015. POLYMER CHEMISTRY. 6 (42): 7464.

Yen, , Liang, Chueh, Yang, A. K. Jen, and Wang. Large Grained Perovskite Solar Cells Derived from Single-Crystal Perovskite Powders with Enhanced Ambient Stability. 2016. ACS APPLIED MATERIALS & INTERFACES. 8 (23): 14513.

Yen, , and Liou. Solution-processable triarylamine-based high-performance polymers for resistive switching memory devices. 2016. POLYMER JOURNAL. 48 (2): 117.

Yen, H. J., H. Tsai, C. Y. Kuo, W. Nie, A. D. Mohite, G. Gupta, J. Wang, J. H. Wu, G. S. Liou, and H. L. Wang. Flexible memory devices with tunable electrical bistability via controlled energetics in donor-donor and donor-acceptor conjugated polymers. 2014. JOURNAL OF MATERIALS CHEMISTRY C. 2 (22): 4374.

Yen, H. J., P. W. Liang, C. C. Chueh, Z. Yang, H. L. Wang, and A. K.-Y. Jen. Single Crystal Perovskite Powders for Large Grained Perovskite Solar Cells. 2016. ACS Appl. Mater. Inter.. 8 (23): 14513.

Yen, H. J., and G. S. Liou. Solution-Processable Triarylamine-based High Performance Polymers for Resistive Switching Memory Devices. 2016. NPG POLYMER J.. 48: 117.

Yen, H., H. Tsai, M. Zhou, E. F. Holby, S. Choudhury, A. Chen, L. Adamska, S. Tretiak, T. Sanchez, S. Iyer, H. Zhang, L. Zhu, H. Lin, L. Dai, G. Wu, and H. Wang. Structurally Defined 3D Nanographene Assemblies via Bottom-Up Chemical Synthesis for Highly Efficient Lithium Storage. To appear in Advanced Materials.

Petabyte-Scale Computational Analyses of Genomic Data to Elucidate Aging Mechanisms

Ludmil B. Alexandrov
20140670PRD2

Introduction

The project has two objectives: 1) analyses of data from different species and 2) analyses of data from thousands of individuals and multiple human tissue types. To achieve the first objective, we will use the reference genome data available from NCBI to perform comparative genomics analyses across 25 species. Preference will be given to non-human primates and rodents because the species in these groups have similar genomes but diverse lifespans. For example, the naked mole rat lives up to 30 years, whereas its relative the house mouse lives only about four years. Additionally, in-depth analysis will be performed for different breeds of dogs due to the large amounts of available molecular data. Although all dogs share essentially the same genetic material, different breeds exhibit up to 2-fold differences in life expectancy.

The main outcome of this part of the project will be identification of homologous genes responsible for lifespan differences across species and the genes affected by nucleotide changes in different breeds of dogs. The second objective is focused on humans. We will use data generated by ICGC.

The primary goal of ICGC is identification of critical genes involved in oncogenesis, but a byproduct of this initiative is exhaustive characterization of the normal tissues (usually blood) and cancers of 25,000 individual patients. We have demonstrated that these abundant molecular data can be used to identity signatures of molecular processes causing somatic mutations. Moreover, these signatures can be mapped to molecular mechanisms. This study sheds new light on the origins of cancer but it just scratches the surface of what is possible. To achieve our second objective, we will use molecular data available for up to 25,000 individuals to identify molecular differences associated with age. We expect to characterize the rates of several distinct mutational processes occurring in 50 different tissue types.

Benefit to National Security Missions

The project will entail petabyte-scale data science. The methods used and lessons learned are likely to be relevant to many DOE mission areas such as biothreats and DOE Office of Science. The specific problem that will be addressed is highly relevant to the public health mission of NIH. By analyzing large amounts of genomic data, we hope to elucidate molecular signatures and causes of aging. Aging has been identified by the World Health Organization as one of the main healthcare and economic challenges of the 21st century. Remarkably, our current understanding of the mechanisms of aging is extremely limited and as a 2012 review in Cell concluded, “The underlying cause of aging remains one of the central mysteries of biology.” Two (not necessarily exclusive) hypotheses have been put forward to explain aging. The first postulates that aging is due to the accumulation of damage, which can come both from the external environment and from within our bodies and cells. The second theory suggests that aging follows a predetermined biological timetable in which certain genes get switched on and/or off to control lifespan.

Progress

During the past year, Ludmil Alexandrov’s accomplishments on the project include further optimizing the workflow allowing LANL to download and analyze large-scale genomics data. While the optimization is still ongoing in several respects, the current infrastructure has provided the capability to download up to 2PB of data per week. This powerful infrastructure has allowed cutting-edge biomedical research based on Big Data from external sources.

Throughout the past year, detailed bioinformatics and genomics analyses encompassing approximately 40,000 human cancers of various types have been achieved. It should be noted that the majority of results from these analyses are still unpublished (i.e., currently at various

stages of preparation and/or peer review). Nevertheless, we have managed to published some preliminary analysis on ~12,000 of these samples elucidating the activity of mutational processes in both neoplastic and normal aging cells. Overall, in the past year, this work has resulted in 8 articles published in high impact peer-reviewed scientific journals as well as in filing of 4 patent/copyrights disclosures and submission of another 13 manuscripts to well-respected scientific journals. From a scientific perspective, the project has provided the first description and quantification of ageing molecular clocks operative in all normal somatic human cells (published in Nature Genetics and highlighted by multiple news agencies), described a novel targeted cancer therapy based on mutational signatures (published in Nature Communication and highlighted as one of LANL's top 10 science stories of 2015), provided the first molecular portrait of CMML (published in Nature Communications), provided the largest and most comprehensive molecular analysis of breast cancer (published in two back-to-back papers in Nature and Nature Communications; highlighted by multiple news agencies), provided a comprehensive description of the role of structural parameters in DNA cyclization (published in BMC Bioinformatics), and written a mini-review article and a review article describing mutational signatures in human cancer (published respectively in Science and Carcinogenesis).

Lastly, during the past year, Ludmil's work on mutational signatures and human cancer has been recognized by multiple institutional and international awards: Prize for Young Scientists in Genomics and Proteomics, given by Science magazine & SciLifeLab; Postdoctoral Distinguished Performance Award, given by Los Alamos National Laboratory; Carcinogenesis Young Investigator Award, given by Oxford University Press & European Association for Cancer Research.

Future Work

From an operational perspective, we plan to finalize the automation process of our computational pipelines allowing easy analysis of external genomics data. The goal is to have a high capacity pipeline allowing the analysis of 1 PB of data within 2 to 3 weeks.

From a scientific perspective, we plan to processes ~12 PB of data in the next fiscal year accounting for about ~40,000 individual pairs of cancer-normal genomes. These data will allow us to develop the final universal set of signatures of mutational processes in human cancer as well as signatures of mutational processes that are part of normal aging processes. Currently, ~20,000 samples have already been analyzed with another ~20,000 to be processed by the end of the calendar year. We will associate the burden of these mutational signatures with environmental exposures, lifestyle choices, gene expression patterns, epigenetic profiles, and clinical data. We envision that this work will result in at least 10 high impact scientific publications.

Conclusion

The expected outcome is an in-depth characterization of the genetic changes that occur with age and the mutational processes responsible for these changes, which will have far-reaching implications for human health. In overcoming the technical challenges of the proposed work, we will establish a Big Data Science capability in Los Alamos that could be applied to diverse problems. The planned analyses will encompass roughly 25 petabytes of data and involve the use of advanced methods of multivariate statistics, novel method development, and new approaches to the use of computational resources to solve a Big Data problem.

Publications

Alexandrov, L. B.. Understanding the origins of human cancer. 2015. Science. 350 (6265): 1175.

Alexandrov, L. B., A. R. Bishop, K. Ø. Rasmussen, and B. S. Alexandrov. The role of structural parameters in DNA cyclization. 2016. BMC Bioinformatics. 17 (68): 1.

Alexandrov, L. B., P. H. Jones, D. C. Wedge, J. E. Sale, P. J. Campbell, S. Nik-Zainal, and M. R. Stratton. Clock-like mutational processes in human somatic cells. 2015. Nature Genetics. 47 (12): 1402.

Alexandrov, L. B., S. Nik-Zainal, H. C. Siu, S. Y. Leung, and M. R. Stratton. A mutational signature in gastric cancer suggests therapeutic strategies. 2015. Nature Communications. 6: 8683.

Alexandrov, L. B., Y. S. Ju, K. Haase, P. Van Loo, I. Martincorena, S. Nik-Zainal, Y. Totoki, A. Fujimoto, H. Nakagawa, T. Shibata, P. J. Campbell, P. Vineis, D. H. Phillips, and M. R. Stratton. Mutational signatures associated with tobacco smoking in human cancer. 2016. Science. 354 (6312): 618.

Connor, A. A., R. E. Denroche, G. Jang, L. Timms, S. N. Kalimuthu, I. Selander, T. McPherson, G. W. Wilson, M. A. Chan-Seng-Yue, I. Borozan, V. Ferretti, R. C. Grant, I. M. Lungu, E. Costello, W. Greenhalf, D. Palmer, P. Ghaneh, J. P. Neoptolemos, M. Buchler, G. Petersen, S. Thayer, M. A. Hollingsworth, A. Sherker, D. Durocher, N. Dhani, D. Hedley, S. Serra, A. Pollett, M. H. A. Roehrl, P. Bavi, J. M. S. Bartlett, S. Cleary, J. M. Wilson, L. B. Alexandrov, M. Moore, B. G. Wouters, J. D. McPherson, F. Notta, L. D. Stein, and S. Gallinger. ASsociation of distinct mutational signatures with correlates of increased immune activity in pancreatic ductal

adenocarcinoma. 2016. JAMA Oncology. : E1.

Hollstein, M., L. B. Alexandrov, C. P. Wild, M. Ardin, and J. Zavadil. Base changes in tumour DNA have the power to reveal the causes and evolution of cancer. 2016. Oncogene. : 1.

Hong, M. K., G. Macintyre, D. C. Wedge, P. Van Loo, K. Patel, S. Lunke, L. B. Alexandrov, and e. t. al. Tracking the origins and drivers of subclonal metastatic expansion in prostate cancer. 2015. Nature Communications. 6: 6605.

Merlevede, J., N. Droin, T. Qin, K. Meldi, K. Yoshida, M. Morabito, E. Chautard, D. Auboeuf, P. Fenaux, T. Braun, R. Itzykson, S. de Botton, B. Quesnel, T. Commes, E. Jourdan, W. Vainchenker, O. Bernard, N. Pata-Merci, S. Solier, V. Gayevskiy, M. E. Dinger, M. J. Cowley, D. Selimoglu-Buet, V. Meyer, F. Artiguenave, J. Deleuze, C. Preudhomme, M. R. Stratton, L. B. Alexandrov, E. Padron, S. Ogawa, S. Koscielny, M. Figueroa, and E. Solary. Mutation allele burden remains unchanged in chronic myelomonocytic leukaemia responding to hypomethylating agents. 2016. Nature Communications. 7: 10767.

Morganella, S., L. B. Alexandrov, D. Glodzik, X. Zou, H. Davies, J. Staaf, A. M. Sieuwerts, A. B. Brinkman, S. Martin, M. Ramakrishna, A. Butler, H. Kim, A. Borg, C. Sotiriou, P. A. Futreal, P. J. Campbell, P. N. Span, S. Van Laere, S. R. Lakhani, J. E. Eyfjord, A. M. Thompson, H. G. Stunnenberg, M. J. van de Vijver, J. W. Martens, A. Borresen-Dale, A. L. Richardson, G. Kong, G. Thomas, J. Sale, C. Rada, M. R. Stratton, E. Birney, and S. Nik-Zainal. The topography of mutational processes in breast cancer genomes. 2016. Nature Communications. 7: 11383.

Nik-Zainal, S., H. Davies, J. Staaf, M. Ramakrishna, D. Glodzik, X. Zou, I. Martincorena, L. B. Alexandrov, S. Martin, D. C. Wedge, P. Van Loo, Y. S. Ju, M. Smid, A. B. Brinkman, S. Morganella, M. R. Aure, O. C. Lingjærde, A. Langerød, M. Ringnér, S. Ahn, S. Boyault, J. E. Brock, A. Broeks, A. Butler, C. Desmedt, L. Dirix, S. Dronov, A. Fatima, J. A. Foekens, M. Gerstung, G. K. Hooijer, S. J. Jang, D. R. Jones, H. Kim, T. A. King, S. Krishnamurthy, H. J. Lee, J. Lee, Y. Li, S. McLaren, A. Menzies, V. Mustonen, S. O'Meara, I. Pauporté, X. Pivot, C. A. Purdie, K. Raine, K. Ramakrishnan, F. G. Rodríguez-González, G. Romieu, A. M. Sieuwerts, P. T. Simpson, R. Shepherd, L. Stebbings, O. A. Stefansson, J. Teague, S. Tommasi, I. Treilleux, G. G. Van den Eynden, P. Vermeulen, A. Vincent-Salomon, L. Yates, C. Caldas, L. v. Veer, A. Tutt, S. Knappskog, B. K. Tan, J. Jonkers, Å. Borg, N. T. Ueno, C. Sotiriou, A. Viari, P. A. Futreal, P. J. Campbell, P. N. Span, S. Van Laere, S. R. Lakhani, J. E. Eyfjord, A. M. Thompson, E. Birney, H. G. Stunnenberg, M. J. van de Vijver, J. W. Martens, A. Børresen-Dale, A. L. Richardson, G. Kong, G. Thomas, and M. R. Stratton. Landscape of somatic mutations in 560 breast cancer whole-genome sequences. 2016. Nature. 534 (7605): 47.

Notta, F., M. Chan-Seng-Yue, M. Lemire, Y. Li, G. W. Wilson, A. A. Connor, R. E. Denroche, S. Liang, A. M. Brown, J. C. Kim, T. Wang, J. T. Simpson, T. Beck, A. Borgida, N. Buchner, D. Chadwick, S. Hafezi-Bakhtiari, J. E. Dick, L. Heisler, M. A. Hollingsworth, E. Ibrahimov, G. H. Jang, J. Johns, L. G. Jorgensen, C. Law, O. Ludkovski, I. Lungu, K. Ng, D. Pasternack, G. M. Petersen, L. I. Shlush, L. Timms, M. Tsao, J. M. Wilson, C. K. Yung, G. Zogopoulos, J. M. Bartlett, L. B. Alexandrov, F. X. Real, S. P. Cleary, M. H. Roehrl, J. D. McPherson, L. D. Stein, T. J. Hudson, P. J. Campbell, and S. Gallinger. A renewed model of pancreatic cancer evolution based on genomic rearrangement patterns. 2016. Nature. 538 (7625): 378.

Petljak, M., and L. B. Alexandrov. Understanding mutagenesis through delineation of mutational signatures in human cancer. 2016. Carcinogenesis. : bgw055.

Schulze, K., S. Imbeaud, E. Letouze, L. B. Alexandrov, J. Calderaro, and e. t. al. Exome sequencing of hepatocellular carcinomas identifies new mutational signatures and potential therapeutic targets. 2015. Nature Genetics. 47 (5): 505.

Wegener, R., L. B. Alexandrov, M. Montesinos-Rongen, M. Schlesner, A. Haake, H. G. Drexler, J. Richter, G. R. Bignell, U. McDermott, and R. Siebert. Analysis of mutational signatures in exomes from B-cell lymphoma cell lines suggest APOBEC3 family members to be involved in the pathogenesis of primary effusion lymphoma. 2015. Leukemia. 29 (7): 1612.

Yates, L. R., M. Gerstung, S. Knappskog, C. Desmedt, G. Gundem, P. Van Loo, T. Aas, L. B. Alexandrov, and e. t. al. Subclonal diversification of primary breast cancer revealed by multiregion sequencing. 2015. Nature Medicine. 21: 751.

Access to Industrially Important Optically Active beta-X-alcohols via Direct Enantioselective Ester Hydrogenation

Pavel Dub
20140672PRD2

Introduction

Contrary to ketones, limited progress in the hydrogenation of less-electrophilic esters has been made during the last few decades. Industrial homogeneous reduction of esters still relies mostly on the use of metal hydride reagents such as LiAlH4 or NaBH4. Using these reagents, hydrogenation selectivities cannot be controlled and such spent (waste) reductants require energetically intensive regeneration input or disposal. Also the use of heterogeneous catalysis dictates the use of high temperatures and pressures and again selectivities cannot be controlled.

No reports describe detailed enantioselective ester hydrogenation despite the tremendous potential for synthetic organic chemistry. Current "state-of-the-art" catalysis in this area of chemistry has required complicated multi-step ligand synthesis as well and these ligands once synthesized often exhibit air-sensitivity. This work will thus focus on developing new well-defined chiral bifunctional molecular catalysts incorporating air-stable ligands for the enantioselective hydrogenations of esters via dynamic kinetic resolution.

Benefit to National Security Missions

Success in this chemistry could have significant positive impact for LANL, vis-à-vis the application of new approaches to chemicals, polymers, materials synthesis, energy applications, and in health related (e.g. pharmaceutical) R&D. Many of the molecules which we are interested in hydrogenating can be derived from bio-renewable sources (e.g. lignocellulosic biomass). This work if successful will potentially lead to high profile publications (Angew. Chemie., JACS, etc.) for the Laboratory and will place LANL at the forefront of this developing area of chemistry.

Progress

We made good progress in the last fiscal year in the synthesis and characterization of metal catalysts supported by NNS ligands. Some of these systems have proven to be effective catalysts for the hydrogenation of esters and other C=O containing species.

We also computationally investigated the mechanism of action of these complexes, as well as other related systems that have been reported in the literature. The body of evidence available from high level computations and experimental results for our own systems (as well as other widely studied and related systems) point to the fact that the mechanism of operation of these classes of catalysts is not concerted. It is instead stepwise, and a chelating ligand (typically containing an N-H functionality) remains chemically unchanged (i.e. is "innocent" rather than "non-innocent" during catalysis , in contrast to the currently accepted mode of action of such systems).

Future Work

In FY17, we will further develop our ligand chemistries to support new and effective catalysts for the hydrogenation of ketonic substrates. In particular we will target new classes of multidentate ligands that will lend themselves to higher catalyst stabilities. This feature may be required to effect the hydrogenation of more difficult (less electrophilic) substrates including esters, carboxylic acids and ureas.

Conclusion

In addition to the environmentally benign processes outlined above, our goals will go further: currently, the ruthenium (Ru) catalyzed asymmetric hydrogenation of ketones (R. Noyori, Nobel Prize 2001) is the main route to produce optically active secondary alcohols. The utilization of expensive Ru catalysts however is unattractive in terms of cost. It is envisioned that if the enantioselective hydrogenation of ketones could be catalyzed by less-expensive base metal complexes. We will incorporate

newly developed and synthesized air-stable chiral ligands onto cheap metals such as copper in order to perform catalytic asymmetric ketone hydrogenation.

Publications

Dub, P. A., B. L. Scott, and J. C. Gordon. Air-Stable NNS (ENENES) Ligands and Their Well-Defined Ruthenium and Iridium Complexes for Molecular Catalysis. 2015. Organometallics. 44: 4464.

Dub, P. A., B. L. Scott, and J. C. Gordon. First-row transition metal complexes of ENENES ligands: the ability of the thioether donor to impact the coordination chemistry . 2016. Dalton Transactions. 45 (4): 1560.

Dub, P. A., B. L. Scott, and J. C. Gordon. Why Does Alkylation of the N–H Functionality within M/NH Bifunctional Noyori-Type Catalysts Lead to Turnover?. 2017. J. Am. Chem. Soc.. 139 (3): 1245.

Dub, P. A., N. J. Henson, R. L. Martin, and J. C. Gordon. Unravelling the Mechanism of the Asymmetric Hydrogenation of Acetophenone by [RuX2(diphosphine)(1,2-diamine)] Catalysts. 2014. J. Am. Chem. Soc.. : 3505.

Dub, P. A., and J. C. Gordon. The mechanism of enantioselective ketone reduction with Noyori and Noyori-Ikariya bifunctional catalysts. 2016. Dalton Transactions. 45 (16): 6756.

Linking Scaling and Mortality Theory to Understand Climate Impacts on Vegetation

Nathan G. Mcdowell
20140685PRD4

Introduction

Postdoc Sean Michaletz will develop and evaluate new Metabolic Scaling Theory (MST) for predicting climate change effects on plant function from individual to global scales. He has extended MST to incorporate physical processes of vascular network hydraulics, leaf heat transfer and leaf photosynthesis, which together control the acquisition rates of essential resources for plant metabolism. He is now evaluating and refining this theory using plant growth, mortality, and resource flux data from two DOE water and temperature manipulation experimentsas well as the new DOE Next Generation Ecosystem Experiment-Tropics. Next, the theory will be parameterized with global climate and plant trait database data to predict (no free parameters) global plant performance data obtained from independent data sources (with Dr. Henry Adams). Data-based sensitivity analyses will be used to identify key plant traits that mediate plant responses to drought and heat climate stressors. In collaboration with Dr. Xu and Dr. McDowell (LANL Co-Mentors), the theory will then be used with the DOE's next generation Earth System Model ACME to forecast 1) plant performance and feedbacks under anticipated climate change scenarios and 2) plant traits that will and will not be successful for given areas subject to climate change.

Benefit to National Security Missions

Our work directly advances a critical current goal of DOE-BER, which is to understand and predict climate impacts on vegetation. Further, this project directly supports LANL's climate and energy impact mission.

Progress

Michaletz published three papers (one first author, two co-author) and one corrigendum, with an additional six manuscripts in revision or review (two first author, four co-author), and two co-authored manuscripts to be submitted within days, and gave two invited publications.

To assemble the several data streams that will be used in our analysis, 2e collected photosynthesis temperature response and leaf thermal traits at DOE SUMO (these data were used in Nature Plants submission, will also be used in planned analyses), as well as photosynthesis temperature response and leaf thermal traits at Rocky Mountain Biological Laboratory (these data were used in Nature Plants submission, will also be used in planned analyses). We also collected photosynthesis temperature response and leaf thermal traits along elevation gradient in Moxi China (these data will be used in planned analyses), and collected d18O data for leaf cellulose from elevation gradient at Rocky Mountain Biological Laboratory (these data will be used in planned analyses).

Michaletz has been collaborating with international PhD student of McDowell and Xu, and has been coaching student on scaling analyses of global wood decomposition rates. These results will be submitted to high-impact journal.

Future Work

In FY17, we will evaluate the new metabolic scaling theory (MST) for predicting climate change effects on plant function from individual to global scales. We will then refine this theory using plant growth, mortality, and resource flux data from two DOE water and temperature manipulation experiments as well as the new DOE Next Generation Ecosystem Experiment-Tropics. Next, the theory will be parameterized with global climate and plant trait database data to predict (no free parameters) global plant performance data obtained from independent data sources (with Dr. Henry Adams). Data-based sensitivity analyses will be used to identify key plant traits that mediate plant responses to drought and heat climate stressors. Finally, the theory will then be used with the DOE's next generation Earth System Model ACME to forecast 1) plant performance and feedbacks under anticipated climate change scenarios and 2) plant

traits that will and will not be successful for given areas subject to climate change.

Conclusion

This project is on the cutting edge of metabolic scaling and mortality theory, with the goal of understanding and predicting climate impacts on vegetation survival. We anticipate numerous high impact papers as well as a massive increase in model prediction accuracy of climate impacts on plants.

Remediation Process Simulation-optimization Under Complex Uncertainties

Velimir V. Vesselinov
20150711PRD2

Introduction

Environmental management and decision making is inherently associated with complex uncertainties that are involved in multiple parameters, multiple levels of information quality, and interactive parameter relationships. The is especially true for problems related to contaminated groundwater remediation and food-energy-water nexus. How to determine the optimal operating conditions under such complex uncertainties is seriously challenging decision makers. The proposed research aims to answer this question through development of innovative enhanced uncertainty quantification (UQ) and simulation-optimization methods for obtaining improved effectiveness.

This research is a logical extension of the interval-fuzzy subsurface modeling system (IIFMS) that we developed through incorporation of stochastic Bayesian UQ analysis, fuzzy UQ, and factorial design techniques. An integrated simulation-optimization framework will be established, including a numerical simulation model for predicting contaminant flow and transport, a nonlinear optimization model for optimizing remediation operating conditions, and a surrogate model for linking the simulation and optimization models. The proposed research represents a unique contribution to R&D of UQ and decision support methodologies. It will allow more systematic and comprehensive consideration of a number of factors that are related to groundwater remediation practices.

The research outputs will help identify optimal operating conditions for saving the costs and guiding practical and robust operations. The applicant will pursue excellence in both research innovation and practical applicability, through relying on the existing LANL field, laboratory and computational facilities, and utilizing existing models and data sets for the LANL contamination sites, which will benefit from the LANL expertise in theory, simulation and analysis of flow and transport in porous media.

This study will be able to bring significant environmental, economic and social benefits to the country by providing not only effective, but also cost-saving, methods for site remediation activities, and the same tools will have relevance for a number of complex national security problems.

Benefit to National Security Missions

The proposal targets development of a framework for optimal design of groundwater remediation activities under uncertainties. The research will focus on the theoretical and computational problems related to characterization of uncertainties related to groundwater flow and contaminant transport in geologic media. This research aligns with the LANL mission and the strategic EES research goals as it aims to address national problems related to energy and environmental security and information science and technology. These problems require development of strategic scientific capabilities to characterize and quantify uncertainties in model predictions related to energy and water production, carbon capture and sequestration, waste disposition and storage, and restoration of contaminated sites. In all these areas, real-world applications require robust and accurate models capturing the existing uncertainties. The novel methods and tools developed in this project will satisfy these needs and strengthen the existing research work at LANL. The work will provide opportunity for future basic science and programmatic research growth working with new sponsors (DoD, NSF, industry) and in new research areas that require uncertainty quantification for complex site settings. Our tools might be applied, e.g. to modeling proliferation sites.

Progress

Postdoc Xiaodong Zhang's research over the last fiscal year focused on the development of novel methods for decision analysis and risk assessment and their applicability related to (1) groundwater contamination manage-

ment and (2) Water-Energy-Food nexus.

On the first topic, a novel methodology for modeling of fuzzy and severe uncertainties has been developed. Decision analyses for management of contaminated groundwater sites are facing many challenges. Among them, quantifying uncertainties associated with numerous model parameters, factors and processes is very important since the uncertainties may significantly affect decisions related to groundwater remediation and risk management. Zhang developed integrated modeling approach to assess and quantify severe and subjective uncertainties associated with groundwater contamination using the information-gap and fuzzy sets theories. A representative synthetic case study is developed to demonstrate its applicability for generating scientifically-defensible decision alternatives for groundwater management. The representative synthetic case study was designed to be consistent with actual groundwater remediation sites at Los Alamos National Laboratory (Chromium and RDX plumes).

In addition, Zhang's research focused on socio-dynamic impacts on decisions related to groundwater remediation projects. Groundwater contamination may alter the behaviors of the public such as adaptation to such a contamination event. On the other hand, social behaviors may affect groundwater contamination and associated risk levels such as through changing ingestion amount of groundwater due to the contamination. Decisions should consider not only the contamination itself, but also social attitudes on such contamination events. A socio-dynamic model based on the theories of information-gap and fuzzy sets has been developed to address the social behaviors facing the groundwater contamination and applied to a synthetic problem. The obtained results demonstrated that scientifically-defensible decision supports for groundwater management in face of the contamination may need to account for socio dynamic impacts.

Related to the second topic, Zhang worked on application of developed novel methods for decision analysis and risk assessment related to Water-Energy-Food Nexus. Effective planning and management of limited water, energy and food resources to meet current and future social demands for sustainable development is challenging. Zhang developed an integrated decision analysis framework and tool called WEFO (Water-Energy-Food Optima), which is capable to address and decision trade-offs and uncertainties. The interrelationships and trade-offs among various system model components including energy supply, electricity generation, water supply and demand, food production are quantitatively analyzed. The obtained results demonstrate how these type of decision analyses can be helpful for decision-makers and stakeholders to make cost-effective strategies for optimally managing limited number of water resources, energy supplies, power generation, and food production for meeting the current and future demands of the society.

In the past year, Zhang published two papers regarding water management and decision making (shale gas wastewater under uncertainty, and surface/groundwater under climate change). These papers were published in the Journal of Environmental Management and Frontiers in Environmental Science, respectively.

Two additional papers have been finalized and submitted for publication.

Zhang also is actively working to present his research to the community. In FY16, Zhang gave 5 talks (4 as the primary presenter and 1 as secondary). The conferences are (1) 2016 SIAM (Society for Industrial and Applied Mathematics) Annual Meeting, (2) 2016 ASCE-EWRI (World Environmental & Water Resources) Conference, (3) CoDA 2016 (Conference on Data Analysis), and (4) 2015 AGU Fall Meeting.

In addition to his research accomplishments, Zhang was recently elected as Editorial Board Member of the Scientific Reports published by Nature. Zhang also organized a session and is a session chair at the upcoming American Geophysical Union meeting related to Food-Energy-Water Nexus.

Future Work

In FY17, we will:

- Further develop a methodology that incorporates the site probabilistic/non-probabilistic uncertainties into the fuzzy/Bayesian uncertainty quantification (UQ) framework.
- Initial code development of the proposed methodology is already completed. We develop computational tools in Julia. Julia is an open-source high-performance computing language developed at MIT. In the past year, Julia has been extensively tested to perform model analyses on the LANL high-performance computing clusters with a great success. The final version of the algorithms will be implemented in MADS (Model Analyses and Decision Support) computational framework (http://mads.lanl.gov).
- We have already performed initial testing of the developed methodology on a synthetic test problem. We would build additional test problems in FY17.
- Write a paper describing the methodology and the synthetic test analysis.

Conclusion

Groundwater contamination can lead to adverse impacts and risks to society and the environment. Remediation costs are typically high and there is a big need for cost-effective strategies. Uncertainties are inherently associated with conceptualization and modeling of the contaminant fate, transport, and remediation process. Site remediation management is composed of various interconnected components that exhibit more complexities than its individual parts do. Such interconnections may lead to various complexities such as uncertainties in parameters and parameter relations, associated with dynamic and multi-objective features. We anticipate this work will be directly useful for generating more cost-effective remediation management strategies with improved efficiencies and increased robustness. The developed methods/models can also be applicable to other research areas where complicated uncertainties exist such as energy systems planning and surface water resources management.

Publications

Zhang, X.. Conjunctive surface water and groundwater management under climate change. 2015. Frontiers in Environmental Science. 3: 59.

Zhang, X. D., and V. V. Vesselinov. Two-stage fracturing wastewater management in shale gas development. 2016. Industrial & Engineering Chemistry Research. : in reviw.

Zhang, X. D., and V. V. Vesselinov. Risk-based decision making for contaminant management. 2017.

Zhang, X. D., and V. V. Vesselinov. Bi-level decision making for supporting energy and water nexus. 2016.

Zhang, X. D., and V. V. Vesselinov. Decision analysis for water-energy nexus considering multiple objectives.

Zhang, X. D., and V. V. Vesselinov. A fuzzy optimization model for water-energy nexus management. 2016.

Zhang, X. D., and V. V. Vesselinov. Modeling of fuzzy and severe uncertainties in contaminated groundwater management. 2016.

Zhang, X. D., and V. V. Vesselinov. Integrated model-based decisions for water, energy and food nexus. 2015.

Zhang, X. D., and V. V. Vesselinov. Inexact socio-dynamic modeling of groundwater contamination management. 2015.

Zhang, X. D., and V. V. Vesselinov. Mathematical models for environmental decision-making under uncertainty. 2015.

Zhang, X. D., and V. V. Vesselinov. Quantification of hybrid uncertainties in groundwater remediation. 2015.

Zhang, X., and V. V. Vesselinov. Integrated modeling approach for optimal management of water, energy and food security nexus. 2016. Advances in Water Resources. : in revision.

Zhang, X., and V. Vesselinov. Mathematical Models for Environmental Decision-making under Uncertainty. Invited presentation at International Congress on Industrial and Applied Mathematics (ICIAM). (Beijing, 10-14 August, 2015).

Zhang, Xiaodong, Alexander Y. Sun, and Ian J. Duncan. Shale gas wastewater management under uncertainty. 2016. Journal of Environmental Management. 165: 188 .

Zhang, Xiaodong, and Velimir V. Vesselinov. Energy-water nexus: Balancing the tradeoffs between two-level decision makers. 2016. Applied Energy. 183: 77 .

Climate Correlates of Tree Mortality

Nathan G. Mcdowell
20150744PRD3

Introduction

There is much speculation that mortality rates are increasing in the tropics, with dire consequences on global carbon cycle because the tropics represent >50% of the terrestrial carbon sink that we depend on for mitigation of fossil fuel emissions, thus a decline in this sink due to mortality will accelerate climate warming. Postdoc Daniel Johnson is the first ever to compile and analyze a global dataset on pan-tropical forest mortality rates and traits and drivers associated with mortality and survival. This has not been previously attempted. The benefits of this project include both high impact, novel research findings regarding how trees die in the tropics, and the provision of this information in a model-friendly manner for improvement of our global vegetation models that are a focus of LANL, DOE, and international research currently. The impacts on our understanding of the tropical carbon sink could be revolutionary due to the first-time nature of his project coupled with the high profile and critical importance of the tropical carbon sink.

Benefit to National Security Missions

Integration of mortality vulnerability in to global carbon models will advance global change science. this work supports LANLs Climate and Energy Impact mission by quantifying the impacts of our global energy portfolio on a key terrestrial carbon sink, and be enabling better predictive modeling of the future impacts of our global energy portfolio.

This work directly supports DOE's Climate and Environmental Science Divisions goal to understand the role of terrestrial ecosystems in a changing climate and is intended to promote long-term programmatic growth. The products of this research will be of direct and immediate value to DOE models of vegetation change and climate, and will have significant impact on LANL's future model development, into which DOE has recently directed a large growth investment. Filling this key knowledge gap will greatly improve the projections of global change models that are needed to inform global climate policy.

Progress

In the summer of 2015 Dan Johnson attended a workshop organized by the Smithsonian Institution and met with tropical forest collaborators. He began amassing the datasets necessary to perform a pan-tropical analysis of tree mortality. He has made significant progress on that analysis at 8 widely distributed sites. He will be drafting a manuscript this summer. In collaboration with scientists at Lawrence Berkley National Lab, he also built software tools to process forest inventory data associated with the Smithsonian Institution's forest plot network to provide Earth System Models, such as the DOE's CLM(ED) and ACME models, with detailed benchmarking data.

Dan is also working on a continental scale analysis of tree mortality. With assistance from collaborators at the US Forest Service, Dan has analyzed tree survival for almost a million trees over the past fifteen years across the continental USA. Tree mortality is related to climate and key species traits in this analysis that will greatly advance our understanding of forest dynamics at very broad spatial scales. A manuscript reporting these exciting results is in preparation.

Dan has been collaborating with LANL scientists Richard Middleton and Katrina Bennett in EES-17 on a project examining the water-energy nexus in the Colorado River basin. Dan has been providing forest dynamics data to improve the modeling of water movement in the basin.

Dan gave an invited presentation at the Ecological Society of America meeting in August of 2015 on the spatial patterns of tree establishment in the eastern US. Dan has provided peer review for 12 manuscripts and reviewed two grant applications one for the NSF and one for Graduate women in Science Fellowships.

Dan has a manuscript published recently in Global Change Biology with collaborators from NASA and several sites around the USA. The paper examined the spectral signature of the leaves of tree species that have very different ecosystem functions in terms of carbon storage and nutrient use.

Dan has several publications in review or in preparation including an international collaboration on the traits of rare species in forests in Global Ecology and Biogeography. He also has two papers on the mortality of tropical seedlings, one in Panama and one in Taiwan. Dan has a paper in preparation on the spatial patterns of woody plants and the role that symbiotic fungi play in structuring forests.

Future Work

Dan is utilizing forest dynamics data from global observation networks to quantify changes in mortality rates related to climate and provide realistic parameters to improve model predictions of terrestrial carbon dynamics. A global scale analysis of mortality rates and their dependence on forest types, traits, or climate has never previously been attempted. Specifically, he is identifying the key climate variables and traits (e.g. height, leaf-type, wood density, and many others) that relate to mortality. Working with Dr. McDowell's lab, he is using the network of the Smithsonian Institution's Forest Global Earth Observatory plots that all follow a strict methodology and have tracked individual trees for decades along with supplemental data from other long-term forest datasets. He is exploring how droughts and rising temperatures modify community structure and identify responses related to functional traits. He is collapsing these diverse forests (10s to 100s of species per hectare) into functional guilds based on key traits linked to share responses to climatic changes for modelling on regional and global scales. We will then incorporate these trait-based predictions of mortality vulnerability into DOE's Community Land Model-Ecosystem Demography Model (CLM(ED)) to estimate vulnerability of global forests to climate change.

Conclusion

The overall technical goals of this project are to document if, when, and where forest mortality is accelerating (or decelerating) pan-tropically, to understand the drivers, e.g. climate, and traits of the trees that are associated with survival and mortality, and to provide these results to Los Alamos, DOE, and international modelers that desperately need this information to improve predictions of the future pan-tropical forest carbon sink. The impact will be on the ecology, climate change, and modeling fields.

Ab Initio Modeling of Organometal Halide Perovskites for Photovoltaic Applications

Sergei Tretiak
20150758PRD3

Introduction

The continued use of fossil fuels as our predominant source of energy poses a potentially large economic, political, and environmental security threat to this country. Sunlight is arguably the most plentiful source of clean energy capable of sustaining continued economic growth. While reasonable efficiency has been achieved for solar cell devices using single-crystalline materials such as silicon, the manufacturing processes, in terms of both materials and fabrication techniques, can be prohibitively expensive. The need for an affordable, clean, and abundant source of energy has generated large amounts of research in a variety of solution processed organic and hybrid organic-inorganic solar cells. A relative newcomer to the field of solution processed photovoltaics is the lead halide perovskite solar cell. In the last 5 years, the efficiencies of devices made from this material have increased from 3.5% to nearly 20%. Despite the rapid development of organic-inorganic perovskite solar cells, a thorough understanding of the fundamental photophysical processes driving the high performance of these devices is severely lacking. The majority of the research efforts to date have been focused on device development, with limited studies on charge carrier dynamics in CH3NH3PbI3 perovskite materials. An understanding of the charge generation and transport mechanisms in perovskite solar cells will provide valuable feedback to guide the materials design and device engineering.

Benefit to National Security Missions

The proposed research program promises to make LANL the world leader in photovoltaic and optoelectronic technologies based on perovskite materials. The work supports the broad goal of Energy Security work at LANL. Our proposal primarily addresses the Materials for the Future focus, while supporting the Complex Systems and Science of Signatures LDRD focus areas. It will strengthen our ability to perform co-design for functional materials, underpinning an important capability for MaRIE. If successful, key technological gaps for the deployment of low-cost PV technologies will be filled, generating a proprietary LANL Intellectual Property.

Progress

In the FY16, Amanda had several key accomplishments. Our experimental collaborators recently demonstrated the reduction in device efficiency in large grain crystalline MAPbI3 perovskite solar cells under constant solar illumination. The efficiency recovers to its original value in less than 1 minute in the dark. Preliminary calculations suggested that this behavior was because of localized charged states that strongly coupled to local structural lattice distortions and MA quasistatic configurations creating small polaron states [Nature Communications, 7, 11574, 2016]. Amanda then performed a more in depth computational study of small polaron formation, electronic structure, charge density, and reorganization energies. Through symmetry arguments and DFT calculations, it was shown that MA dipoles can align with a charge centered on a Pb atom. [Nano Letters, 16(6), 3809-3816, 2016]. Since this study showed that both volumetric strain and dipole rotation lead to charge trapping, replacing methylammonium (dipole moment 2.28D) with the larger formanmidinium (dipole moment 0.21D) should mitigate the degradation problem. Calculations are ongoing to show that this is indeed the case. In addition to our work on polaron stabilization, Amanda also been a part of a collaborative effort to study a form of layered 2-D perovskite known as Ruddlesden-Popper phases. These 2-D perovskites have shown promising stability against environmental influences but have historically exhibited poor photovoltaic efficiency. Our experimental collaborators recent results demonstrated devices with a photovoltaic efficiency of 13%, and industry-standard stability under constant light illumination and 65% humidity. The band gap of (BA)2(MA)n-1PbnI3n+1 can be tuned only from 1.52 eV to 2.24

eV for a single atomic layer [Nature, in press, 2016]. This study opens an entire field of degradation-free 2D confined perovskite architectures. Our theoretical simulations are able to significantly speed up the discovery process. Future Density Functional Theory simulations are expected to have very good predictive power in capturing quantum-confinement effects across a broad range of compounds. The existence and role of polarons remains an open question that is actively being investigated computationally.

Future Work

During the remainder of the project, postdoc Amanda Neukirch will use state-of-the-art computational techniques in order to characterize charge dynamics at the interface of perovskites in order to aide in materials design and device engineering. These include the high-level quantum mechanical calculations incorporating spin-orbit-coupling and the many body approaches, which help to identify the key electronic states involved in photoinduced dynamics. Future studies will focus understanding and overcoming the challenges with replacing the lead component with the less toxic, more environmentally friendly, Sn. In addition, with a greater understanding of the electronic and optical properties, the next step will be to monitor the charge dynamics and charge transfer at interfaces. In order to model the electronic and nuclear motions of a system after photoexcitation, it is necessary to go beyond the adiabatic Born-Oppenheimer approximation, and allow for electronic transitions using nonadiabatic molecular dynamics. The nonadiabatic molecular dynamics will be performed by combining time-domain density functional theory with the fewest switches surface hopping algorithm. By implementing the multistep procedure discussed above, the advantages and disadvantages of different design schemes will be revealed. More generally, the methods developed for the perovskite system will be applicable for other systems involving charge transfer at an interface.

Conclusion

The need for an affordable, clean, and abundant source of energy has generated large amounts of research in a variety of solution processed organic and hybrid organic-inorganic solar cells. A relative newcomer to the field of solution-processed photovoltaics is the lead halide perovskite solar cell. Using state-of-the-art computational techniques, we will characterize charge dynamics at the interface of perovskites in order to aide in materials design and device engineering.

Publications

Blancon, J. C., W. Nie, A. J. Neukirch, G. Gupta, S. Tretiak, L. Cognet, A. D. Mohite, and J. J. Crochet. The effects of electronic impurities and electron-hole recombination dynamics on large-grain organic-inorganic perovskite photovoltaic efficiencies. 2016. Advanced Functional Materials. 26: 4283.

Neukirch, A. J., Nie, Blancon, Appavoo, Tsai, M. Y. Sfeir, Katan, Pedesseau, Even, J. J. Crochet, Gupta, A. D. Mohite, and Tretiak. Polaron Stabilization by Cooperative Lattice Distortion and Cation Rotations in Hybrid Perovskite Materials. 2016. NANO LETTERS. 16 (6): 3809.

Nie, , Blancon, A. J. Neukirch, Appavoo, Tsai, Chhowalla, M. A. Alam, M. Y. Sfeir, Katan, Even, Tretiak, J. J. Crochet, Gupta, and A. D. Mohite. Light-activated photocurrent degradation and self-healing in perovskite solar cells. 2016. NATURE COMMUNICATIONS. 7.

Pedesseau, L., D. Sapori, B. Traore, R. Robles, H. H. Fang, M. A. Loi, H. Tsai, J. C. Blancon, A. Neukirch, S. Tretiak, A. D. Mohite, C. Katan, J. Even, and M. Kepenekian. Advances and Promises of Layered Halide Hybrid Perovskite Semiconductors. To appear in ACS Nano.

Tsai, , Nie, Blancon, C. C. S. Toumpos, Asadpour, Harutyunyan, A. J. Neukirch, Verduzco, J. J. Crochet, Tretiak, Pedesseau, Even, M. A. Alam, Gupta, J. u. n. Lou, P. M. Ajayan, M. J. Bedzyk, M. G. Kanatzidis, and A. D. Mohite. High-efficiency two-dimensional Ruddlesden-Popper perovskite solar cells. 2016. NATURE. 536 (7616): 312.

Characterizing Irregular Flows and Mass Transport in Microscopic Pore Spaces

Jeffrey D. Hyman
20150763PRD4

Introduction

Many of our emerging subsurface applications involve low permeability rock that require a detailed understanding of fluid flow in nanometer-sized pores. For example, extracting hydrocarbon from "tight" shales or geothermal energy extraction and storing CO2 or radioactive waste all involve low permeability rock, either as an energy resource or as a barrier to flow. Therefore, a fundamental understanding of pore scale fluid dynamics and how the irregular resistance offered by the pore structure induces a non-uniform fluid velocity field has never been more timely. Advanced pore scale studies characterizing fluid flow and mass transfer are needed to optimize energy extraction or containment strategies. However, sampling pore structures and then simulating flow and transport therein is expensive, both monetarily and computationally. Therefore, researchers commonly assume the ergodic hypothesis and replace ensemble averages with spatial ones obtained using a few samples. Simulating flow through realistic virtual pore spaces using the immersed boundary method (IB) is a powerful alternative because numerous simulations can be performed at low cost. Generating virtual realizations that are statistically identical to real samples is inexpensive compared to the sampling of pore spaces with X-ray tomography, and the IB formulation is ideal for these simulations because there is no mesh generation overhead, which is required for conformal mesh schemes. Additionally, the method is well suited for existing and future HPC architectures, such as GPUs and MIC, because the underlying mesh is uniform with regular connectivity, and the relatively small size of individual realizations permits embarrassingly parallel ensemble average computation.

Benefit to National Security Missions

Over 85% of our energy comes from the subsurface. Characterizing fluid flow in porous media and being able to control it is critical for our energy security mission. The work being performed can also be use for a wide variety of DOE interests spanning nuclear forensics, fossil energy, and nuclear waste storage.

Progress

Since the start of FY16 postdoc Jeff Hyman has published eight papers concerning various aspects of subsurface energy applications and has three more under review. The papers have been published in top journals such as Geophysical Review Letters, Water Resources Research, Philosophical Transactions of the Royal Society A, and IEEE Transactions on Visualization and Computational. He has primarily focused on transport and mixing processes during this year. In the earlier part of the year, he worked with a team from EES-14 to study three-phase mixing in laboratory experiments. His key contribution to the work was providing an analysis of upscaled continuum representation of the experimental data (Task 4 and Task 5 in the proposed work). Their work was published in Geophysical Review Letters, the top journal in geophysics. He has also prepared two manuscripts characterizing how regions of slow and fast velocity regions in a flow field lead to anomalous transport behavior (Task 3 in the proposed work). He noticed and capitalized on the opportunity that many of the tools he developed for Lagrangian transport analysis at the pore-scale (Task 3 in proposed work) were directly applicable to transport modeling in discrete fracture network models and has published and presented extensively on that subject as well. From March through May he visited the Fraunhofer Institute for Industrial Mathematics in Kaiserslautern, Germany as part of the Fraunhofer young researcher award he received from Intrepore last spring. While in Europe he gave eight invited presentations in Germany, Italy, Switzerland, France, Spain, and Sweden. This exposure provided opportunities for multiple international collaborations. In particular, he is working with a team of researchers at the Politecnico di Milano in Italy to advance computational methods for multiphase flow

simulations in computationally generated pore-spaces (Task 1 and 2 in the proposed work). In another new project with researchers from CSIC in Barcelona, Spain and CNRS at the University of Rennes, France he is generalizing pore-scale/continuum scale upcsaled transport models to discrete fracture network modeling (Task 4 in the proposed work). Overall it was a successful year for Hyman and he could not have done so without the support of the LDRD Director's fellowship.

Future Work

Perform direct numerical simulations of pore scale flow that will allow us to investigate the influence of pore structure on fluid flow, solute transport, and solute mixing all key for characterizing mass transfer and proper upscaling.

To complete this goal we will: (2) continue the development of the methodology to include patch-based adaptive mesh refinement, multi-fluid simulation, and solid-fluid interaction; (3) develop a suite of computational tools to analyze these flows; (4) test the applicability of continuum scale transport frameworks, a key issue for the use of upscaling to describe mass transport; (5) investigate how the pore structure induces the mixing of solutes and thus encourage chemical reactions; (6) investigate mixing in fracture networks at the in-plane scale, intersection scale, and network scale; (7) investigate particle tracking representatives of transport in fractured media using tool box developed at the pore-scale.

Conclusion

This project aims to determine the influence of pore structure on flow and transport, which will will increase our ability to extract the next generation of fuel as well as advance the study of groundwater flow and transport, the disposal of used nuclear fuel, filter and textile design, and medical applications including the delivery of drugs to tumors. It also aims to increase the efficiency of the Immersed Boundary methodology. Lastly, it will improve understanding of the effects of fluid-gas interactions in the pore spaces, and their effect on the macroscopic flow. The developed computational toolbox will be applied to discrete fracture networks and lattice Boltzmann simulations. Characterizing fluid flow in porous media and controlling it is critical for the energy security mission.

Publications

Aldrich, G., J. D. Hyman, S. Karra, C. W. Gable, N. Makedonska, H. S. Viswanathan, J. Woodring, and B. Hamann. Analysis and Visualization of Discrete Fracture Networks Using a Flow Topology Graph. 2016. IEEE T Vis Comput Gr..

Hyman, J. D., G. Aldrich, H. Viswanathan, N. Makedonska, and S. Karra. Fracture size and transmissivity correlations: Implications for transport simulations in sparse three-dimensional discrete fracture networks following a truncated power law distribution of fracture size. 2016. Water Resources Research.

Hyman, J. D., J. Jimenez-Martinez, H. S. Viswanathan, J. W. Carey, M. L. Porter, E. Rougier, S. Karra, Q. Kang, L. Frash, L. Chen, D. O'Malley, and N. Makedonska. Understanding hydraulic fracturing: A multi-scale problem. 2016. Philosophical Transactions of the Royal Society A. 374 (2078): N/A .

Jimenez-Martinez, , M. L. Porter, J. D. Hyman, J. W. Carey, and H. S. Viswanathan. Mixing in a three-phase system: Enhanced production of oil-wet reservoirs by CO2 injection. 2016. GEOPHYSICAL RESEARCH LETTERS. 43 (1): 196.

Makedonska, , J. D. Hyman, Karra, S. L. Painter, C. W. Gable, and H. S. Viswanathan. Evaluating the effect of internal aperture variability on transport in kilometer scale discrete fracture networks. 2016. ADVANCES IN WATER RESOURCES. 94: 486.

Laboratory Study of Fracturing and Hydraulic Conductivity through Heterogeneous Materials in Compressive Stress Environments

James W. Carey
20160642PRD1

Introduction

The focus of this project is to understand the relationship between mechanical damage and fluid permeability in heterogeneous materials. Small heterogeneities (e.g., grains, micro-cracks, and layers) have a strong effect on the mechanical behavior of materials and therefore control the ease with which fluids penetrate the damaged material. These relationships are critical to several Department of Energy missions including determining the effectiveness of CO2 sequestration (where leakage processes through damaged caprock or wellbore materials could allow CO2 to escape), hydraulic fracturing (where the goal is to generate a highly penetrating and highly transmissive fracture system), and the long-term isolation of nuclear waste (where fracture damage is a potential pathway for the escape of radionuclides to the environment). In this project, we use a unique Los Alamos apparatus that is capable of fracturing materials at high-pressure and temperature while simultaneously measuring in situ fracture permeability and collecting X-ray radiograph and tomographic images of fracture propagation and the 3D fracture apertures and patterns. This will allow for the first time direct measurement and imagery of fluid flow in fractures at high-stress conditions. The project will investigate both natural and synthetic specimens. Synthetic materials with controlled heterogeneity will be constructed using 3D printing and other methods to allow systematic investigation of fracture interaction with discontinuities and material interfaces. The results will also be applied to the aging/cracking behavior of high explosives, which are composite (heterogeneous) materials of great interest to weapons programs at DOE and DOD.

Benefit to National Security Missions

The experimental studies described in this project contribute directly to a "Basic Understanding of Material Properties". Our primary focus is to understand how mechanical damage (due to stress, temperature, fatigue, aging, chemical attack, etc.) to materials manifests as a changing permeability to fluids. We seek to understand how the interaction of stress and material properties (especially heterogeneity) allow or inhibit fluid movement. This understanding is critical to Department of Energy (DOE) environmental and energy missions in which fluid flow through earth materials governs success or failure including: development of hydraulic fractures in oil and gas as well as geothermal energy; consequences of fracture damage to caprock and wells that confine CO2 sequestered in the subsurface; and suitability of various rock types for the long-term containment of nuclear waste. The work considers the behavior of heterogeneous materials with a particular application to high explosives. Analysis of the impacts of aging and deterioration of these latter materials are critical to DOE missions in nuclear weapons and explosives. The project will pioneer new techniques for the direct observation of fracture growth and development under high-pressure and temperature conditions, which will advance DOE basic science efforts to understand and ultimately predict the performance of materials.

Progress

Luke Frash's accomplishments during the first six months (January-June 2016) of his Director's post-doctoral position included: 1) establishing collaborations to further his research aims both within and external to the Lab; 2) experiments and numerical modeling on fracture-permeability in shale and a submitted manuscript; 3) established procedures and began creating synthetic composites for fracture studies; 4) improved and updated the triaxial coreflood experimental system; 5) released software for controlling experimental equipment; and 6) contributed to a successful proposal to Basic Energy Sciences. Additional details on Dr. Frash's accomplishments are as follows:

1. Established collaborations with colleagues in EES-16

(fractured reservoir-scale modeling), EES-17 (dynamic fracture modeling), MST-6 (mechanical compression testing), MST-8 (high-explosives characterization), AET-1 (3D printing services), AET-6 (X-ray tomography and alternative 3D printing services), and ISR (machine shop services). He also arranged and coordinated a meeting with Apache Corporation in Houston, Texas, to discuss geomechanics research topics in shale gas and secured well-preserved shale rock core for use at LANL

.

2. Completed a combined experiment and modeling study on Utica shale in which fracture and fluid flow behavior at high-stress conditions were evaluated. The results showed lower than expected flow enhancement due to fractures, a favorable behavior for waste disposal (nuclear waste depositories or carbon sequestration) and an explanative behavior the low-efficiency of shear-stimulated reservoirs (oil and gas production or engineered geothermal energy). The study was conducted in close collaboration with EES-17 and AET-6 to leverage Frash's Abaqus models and the in-situ X-ray tomography data with finite element/discrete element modeling. A manuscript describing this study has been accepted with minor revision by the Journal of Geophysical Research.

3. Established a method for creating high-quality bi-material heterogeneous 3D-printed specimens that will be ideal for performing experiments on fracture propagation and fluid flow that can be coupled with predictive modeling. This method included development of a scalable porous 3D geometry. A batch of 12 specimens has been fabricated using this scalable geometry and a photocured resin printer with support from AET-6. A custom high-vacuum & pressure system was designed for controlled saturation of the 3D printed specimens with a catalyzed polyurethane resin and additional M&S funding has been applied for to enable construction of this system. This on-going work will soon be poised to produce experiment-ready specimens having controlled geometry, controlled boundary conditions, known internal material properties, and known interfacial properties, all of which are required for predictive numerical modeling.

4. Improved and updated the existing triaxial direct-shear equipment with the following features and capabilities: (a) added 8-channels of co-axial signal ports for improved passive acoustic monitoring sensitivity, (b) designed and fabricated a set of direct-shear adapters for improving equipment performance and reliability at high-confining pressures, (c) programmed a new proportional-integral-derivative algorithm that enables displacement-control of the triaxial piston for improved X-ray tomography quality and enhanced experiment control, and (d) upgraded and simplified the hydraulics system to improve gas-permeability measurement capabilities, increase the reliability of acquired pressure data, and enhance experiment control. He also designed and fabricated a new triaxial direct-shear apparatus to alleviate demand on the triaxial-tomography apparatus. The new apparatus, based on a Hoek-Cell confining stress concept, complements the existing apparatus by enabling high-throughput testing outside of the X-ray tomography cabinet. This new apparatus permits permeability testing with water or compressed air but forgoes in-situ X-ray imaging and passive acoustic monitoring.

5. Released DIsco, an advanced software utility for controlling Teledyne Isco D-series syringe pumps that was developed over the last year. This software simplifies remote pump controls for large arrays of pumps and also enables sophisticated fluid flow experiments to be executed with precision. DIsco was released using the LANL software distribution system through the Richard P Feynman Center for Innovation. This software was crucial for the new proportional-integral-derivative piston displacement-control.

6. Contributed to a BES proposal (now funded), co-written with my mentor, EES-16 staff, and EES-17 staff. His contributions included outlining a theoretical framework for integrating triaxial direct-shear experiments, HOSS modeling, microfluidics experiments, and dfnWorks modeling.

Future Work

Tasks and goals include organizing the collaboration among EES, AET and MST, developing methods in sample preparation and x-ray tomography, conducting experiments on fracture-permeability relations, and developing manuscripts describing results. The collaborations have as goals to establish a research approach to the study of mechanical damage of analogs to high explosives, developing improved methods of tomographic reconstruction to characterize 3D fracture patterns, and creating synthetic samples with controlled heterogeneity using 3D printing and other methods. We will conduct experiments on natural materials (shale and carbonate) using a direct shear method in order to investigate fracture-permeability relations and the dynamics of fracture growth. We will also conduct experiments on the new synthetic materials in order to develop fundamental relationships between permeability and fracture propagation through inclusions, layering and other sources of controlled heterogeneity. Experimental results

will be analyzed and used to prepare manuscripts describing fracture-permeability behavior of materials. As time permits, we will also collaborate to develop computational models that are based on the experimental results.

Conclusion

The experiments will provide the first-ever study and x-ray imaging of fracture-fluid interactions at high-pressure and temperature and significantly advance our understanding of the consequences of fracture damage. The work considers the behavior of heterogeneous materials with a particular application to high explosives. Analysis of the impacts of aging and deterioration of these latter materials are critical to DOE missions in nuclear weapons and explosives.

Publications

Carey, J. W., L. P. Frash, and H. S. Viswanathan. Dynamic Triaxial Study of Direct Shear Fracturing and Precipitation-Induced Transient Permeability Observed by In Situ X-Ray Radiography. 2016. In 50th US Rock Mechanics / Geomechanics Symposium held in Houston, Texas, USA, 26-29 June 2016.

Frash, L. P., J. W. Carey, H. S. Viswanathan, M. Gutierrez, J. Hampton, and J. Hood. Comparison of Pressure, Flow Rate, Stepped, and Oscillatory Control Methods for Fracture Permeability Measurements at Triaxial Stress Conditions. 2016. In 50th US Rock Mechanics / Geomechanics Symposium held in Houston, Texas, USA, 26-29 June 2016.

Frash, L. P., J. W. Carey, and H. S. Viswanathan. Notched Specimen Hydraulic Fracturing Method for Conducting Mechanical and Hydrological Experiments at Triaxial Reservoir Conditions. 2016. In 50th US Rock Mechanics / Geomechanics Symposium held in Houston, Texas, USA, 26-29 June 2016.

Frash, Luke P., J. William Carey, Timothy Ickes, and Hari S. Viswanathan. High-stress triaxial direct-shear fracturing of Utica shale and in situ X-ray microtomography with permeability measurement. 2016. Journal of Geophysical Research. 121: 5493.

Hyman, J. D., J. Jim'enez-Mart'inez, H. S. Viswanathan, J. W. Carey, M. L. Porter, E. Rougier, S. Karra, Q. Kang, L. Frash, L. Chen, Z. Lei, D. O'Malley, and N. Makedonska. Understanding hydraulic fracturing: A multi-scale problem. 2016. Philosophical Transactions of the Royal Society A. 374: 20150426.

Lei, Zhou, Esteban Rougier, Earl E. Knight, Luke Frash, J. William Carey, and Hari Viswanathan. A non-locking composite tetrahedron element for the combined finite discrete element method. 2016. Engineering Computations. 33: 1929.

Coupling Kinetic to Fluid Scales in Space and Laboratory Plasmas

William S. Daughton
20160647PRD2

Introduction

In this project, new simulation capabilities will be employed to study the influence of microscopic (kinetic) physics on the evolution of hot ionized gasses (plasmas). Two separate applications will be considered using a similar approach.

First, we will model some key space plasma processes around the Earth, where the magnetic field partially protects against the stream of energetic particles that are continually emitted from the sun. This interaction leads to the formation of the magnetosphere, a bubble of hot plasma surrounding our planet. During large solar storms, eruptions from the sun compress the magnetosphere and give rise to the injection of energetic particles that can damage satellites. It is a major challenge to model how these energetic particles are able to penetrate into the magnetosphere. This project will apply a new simulation approach in which the ions in the plasma are treated with a first-principles description to accurately describe the dynamics of this complex system, and offer predictions that will be compared with spacecraft observations.

The second application is inertial confinement fusion, where intense lasers are use to compress and heat small spherical capsules that are filled with a low-density hydrogen gas (deuterium and tritium). When compressed to sufficiently high-density, the gas becomes a hot plasma and undergoes thermonuclear reactions. Recent experiments have demonstrated a number of discrepancies that cannot be understood with existing fluid models. Researchers have speculated that ion kinetic physics may be playing an important role. To better understand these differences, we will perform advanced simulations of the fuel region using a kinetic description for the ions in the plasma. The goal is to understand the influence of this missing physics, and how to incorporate this kinetic physics back into standard fluid simulations that are widely used to model these experiments.

Benefit to National Security Missions

This research will exploit the newest generation of petascale supercomputers using a kinetic simulation code specially optimized for these machines. Some of these calculations will be performed locally at Los Alamos using NNSA computers, while other calculations will be performed on flagship DOE supercomputers such as Titan at Oak Ridge. These efforts are at the very forefront of high performance computing, both in terms of scaling the calculations to large numbers of cores (~100,000) and in remote visualization and analysis of the results. This research will increase our understanding of thermonuclear burn in inertial fusion regimes, which is directly relevant to experiments at DOE facilities such as OMEGA and NIF. In addition, the results from this research may benefit current and upcoming NASA missions focused on understanding the near-Earth space environment. For example, the Magnetospheric Multi-Scale (MMS) mission will focus on the kinetic physics of magnetic reconnection with the Earth's magnetosphere. The same space environment is where national security satellites that support nonproliferation missions fly. Finally, the simulations performed in this project will be among first to study the complex coupling between the kinetic and macroscopic scales for two forefront applications in plasma physics, important to our national security mission.

Progress

Excellent progress has been made towards the goals of this postdoctoral project. The research focus was evenly split between the numerical modeling of space plasmas and inertial confinement fusion. For both applications, we are employing hybrid simulations, which offer a rigorous kinetic description of the ions in the plasma, while the electrons are modeled with an approximate fluid description.

For the space physics simulations, we are using the hybrid code H3D, which has been ported to LANL clusters.

During the past year, a new electron closure relationship was implemented that captures electron temperature anisotropy, corresponding to different effective temperatures parallel and perpendicular to the magnetic field. This new closure was carefully tested for a series of problems, and the results were published earlier this year. Next, we modified the boundary conditions of the H3D code to study the dynamics of magnetospheres, which are bubbles of plasmas surrounding a planet or moon. Although our ultimate goal is the magnetosphere of Earth, our initial focus has been on the magnetosphere of Ganymede, the largest of Jupiter's moons. This test problem is computationally much easier than Earth. In addition, there is significant interest from our collaborators at NASA to compare our hybrid simulation results with spacecraft observations, and with other types of fluid simulations. We have presented our initial results for Ganymede at conferences and we are currently working towards a full paper.

As a final topic, we are also studying the microphysics of magnetic reconnection within the Earth's magnetosphere. For this problem, a new set of initial conditions were implemented within the fully kinetic code VPIC, which offers a rigorous description of both ion and electrons in the plasma. The problem setup was designed to allow simulations of reconnection at the magnetopause, where the shocked solar wind impinges on Earth's magnetic field. This new setup enables simulations of magnetic reconnection with large density and temperature asymmetries, a regime relevant to recent observations gathered by NASA's Magnetospheric Multi-scale Mission (MMS). Simulations were performed with parameters provided by our NASA collaborators to match two separate well-resolved MMS events. Using the new Trinity machine, one event was modeled in both 2D and 3D, and papers are currently under preparation describing new physical effects for strongly asymmetric reconnection layers at the magnetopause.

Good progress has also been made on applying hybrid modeling techniques to problems related to inertial confinement fusion. A verification problem involving the convergence and rebound of a spherical shock has been set up and run with the hybrid code LSP. The results will be verified using semi-analytical solutions and compared to a LANL-developed code, iFP. Finally, we are completing a simulation project with LSP to model laser fusion capsule implosion experiments performed at the OMEGA facility. These simulations, which include a kinetic treatment of both the fuel and the shell ions, are the first of their kind and may help explain some longstanding differences with fluid simulations. A paper assessing the influence of ion kinetics on fusion performance in these experiments is under preparation, and the results were presented at the Kinetic Plasma Effects workshop at Lawrence Livermore National Laboratory earlier this year.

Future Work

The research tasks in this project will be evenly split between two applications, both of which involve kinetic hybrid simulations of high-temperature plasmas:

During the next year of this PRD project, we will expand our 3D simulations of Ganymede (Jupiter's moon), and compare with both spacecraft observations and with recently published fluid simulations of this test problem. Our goal is to finish a paper on this topic during the next year. Next, we will begin performing larger-scale global simulations of other magnetospheres, starting with the limit of southward IMF where the dominant entry process is due to magnetic reconnection at the dayside magnetopause. Depending on how far we get, we will look for opportunities to compare our initial results with spacecraft observations. Finally, we will continue our study of the Earth's magnetopause using fully kinetic simulations, and we will compare against MMS observations. We anticipate several papers on this topic during the next year.

For the inertial fusion application, we will perform additional radiation hydrodynamic simulations using the HYDRA code to model the implosion of the dense shell material for a number of specific shots from the OMEGA facility. The evolution of the dense shell will provide the boundary conditions for LSP kinetic simulations of the low-density hydrogen fuel. We will investigate a variety of approaches for coupling these two simulations, in order to obtain the best agreement with experiments. Next, we will develop new diagnostics to explore the precise kinetic physics that is responsible for the observed deviations from simple fluid predictions. Finally, we will look for ways to characterize this missing physics for possible inclusion in future fluid simulations. We anticipate writing several publications describing these results.

Conclusion

The fluid equations currently used to model plasmas are not always well justified. This is particularly true in critical regions such as shocks and thin boundary layers. In this project, we will demonstrate the feasibility of simulations that more accurately describe the entire complex system. We anticipate this project may improve our ability to more accurately model a variety of applications, including the space weather environment surrounding the Earth, and also the plasma dynamics within the fuel region of inertial fusion capsules.

Publications

Egedal, J., A. Le, W. Daughton, B. Wetherton, P. Cassak, L. Chen, B. Lavraud, R. Torbert, J. Dorelli, D. Gershman, and L. Avanov. Spacecraft observations and analytic theory of crescent-shaped electron distributions in asymmetric magnetic reconnection. 2016. Physical Review Letters. 117: 185101.

Le, A., J. Egedal, and W. Daughton. Two-stage bulk electron heating during symmetric anti-parallel magnetic reconnection. 2016. Physics of Plasmas. 23: 102109.

Le, A., T. J. T. Kwan, M. Schmitt, H. Herrmann, and S. Batha. Simulation and assessment of ion kinetic effects in a direct-drive capsule implosion experiment. 2016. Physics of Plasmas. 23: 102705 .

Le, A., W. Daughton, H. Karimabadi, and J. Egedal. Hybrid simulations of magnetic reconnection with kinetic ions and fluid electron pressure anisotropy. 2016. Physics of Plasmas. 23 (3): 032114 .

Climate, Hydrology and Forest Disturbances in Southern and Western Watersheds

Richard S. Middleton
20160654PRD2

Introduction

We will develop a novel approach to quantifying changes in extreme events, with the goal of identifying critical watersheds where extreme streamflow (floods and droughts) threshold exceedance is of greatest risk and uncertainties are large. The proposed study focuses on headwater basins in the Colorado watershed, where key infrastructure and industry are located. A multi-faceted approach is needed to correctly capture local conditions and sub-daily responses for accurate representation of disturbance impacts. The project will: a) synthesize historical peak streamflow and precipitation observations using high resolution (4 km) 3-hourly fields from new runs of a Regional Climate Model (RCM) developed at the National Center for Atmospheric Research (NCAR); b) assimilate these data into the Variable Infiltration Capacity (VIC) hydrologic model at a 4 km resolution and calibrate for peaks flows; c) apply a climate sensitivity approach to the WRF data based on the future projections from Coupled Model Intercomparison Project (CMIP5) global climate models (GCMs); d) develop a novel, simplified model of dynamic landscape disturbances (fire, drought and pest infestations) for the region, and; e) produce coupled runoff/dynamic ecosystem scenarios for 1950-2100. Runoff, and water balances will be analyzed using robust statistical measures of extremes (e.g. Peaks-Over-Thresholds) and Monte Carlo simulation to assess changes in frequency/reoccurrence, intensity, duration, and magnitude of non-stationary events in disturbed and non-disturbed systems.

Benefit to National Security Missions

This work looks at the impact of climate and climate-driven disturbances on stream flow and water supply. This is critical for any infrastructure that could be impacted by water supply: too much (flooding), too little (drought), and intermittent/irregular. Infrastructure includes fossil (Fossil Energy) and nuclear (Office of Nuclear Energy) thermoelectric plants. Flood impacts is also aligned with critical infrastructure protection within DHS and, potentially, DOD.

This also directly ties into renewable energy (EERE). Office of Science (DOE-SC) is directly interested in understanding and predicting disturbances and disturbance impacts. The energy-water nexus is also a major cross-cutting DOE Big Idea that is significantly and directly impacted by climate change and climate-driven disturbances and the effect on water supply. NASA also has multiple calls for climate-impact proposals including in FY17 and this research would support future work for this mission. The Department of Commerce (specifically NOAA) has a direct interest in understanding climate change and climate impacts on water supplies. Other federal agencies will also have a direct interest in this work, though may not include potential sponsors, including Department of Interior (e.g., USGS) and the EPA.

This work directly and strongly supports LANL mission relevance in terms of Climate and Energy Impact.

Progress

- Variable Infiltration Capacity hydrologic model developed for the Colorado. Calibration 95% complete.
- Obtained alternative calibration approach using tools from the National Center for Atmospheric Research (NCAR).
- Gathered and analyzed regional climate model simulations of temperature and precipitation and sensitivities using the CMIP5 database of global climate models. Drafted results for journal paper.
- Developed a simple method to simulate landscape change in the San Juan basin 2006-2100 using two approaches; CMIP5 vegetation change and forest mortality estimates.
- Worked on collaboration with NCAR to access WRF climate data.
- Ran the climate and landscape changes through

the hydrologic model for San Juan, analyzed results. Drafted publication for journal submission.

Future Work

- Complete calibration of the Colorado basin and validate results.
- Develop a statistical method to simulate spatial distributions of landscape change into the future for the Colorado basin.
- Run the climate and landscape changes through the hydrologic model for the Colorado basin.
- Use Weather Research Forecast (WRF) model climate data for the Colorado basin to run the VIC model with this data, and analyze extreme streamflow in four watersheds.

Conclusion

The projected increase in frequency and intensity of billion-dollar weather and climate disasters, including severe storms, drought, and fire, is a significant domestic and global threat. We will develop a hydrologic model for the entire Colorado River basin (where key infrastructure and industry are located) that will be used to project future streamflow changes. One result will be a ranking of critical basins to determine the probability of future changes in extreme floods and droughts. This novel assessment of potentially destabilizing impacts will provide notable science results and new climate impact assessment technology to the national security community.

Publications

Bennett, K., N. McDowell, C. Xu, C. Wilson, and R. Middleton. Influence of forest disturbance on hydrologic extremes in the Colorado River Basin. Invited presentation at AGU Fall Meeting. (San Francisco, 14-18 Dec. 2015).

Bennett, K., R. Middleton, N. McDowell, C. Xu, T. Bohn, and E. Vivoni. Climate change and integrated forest disturbance impacts in the Colorado River basin. Invited presentation at Eric Wood Symposium. (Princeton, 2-3 Jun. 2016).

Wegner, , K. E. Bennett, de Vernal, Forwick, Fritz, Heikkila, Lacka, Lantuit, Laska, Moskalik, O'Regan, Pawlowska, Prominska, Rachold, J. E. Vonk, and Werner. Variability in transport of terrigenous material on the shelves and the deep Arctic Ocean during the Holocene. 2015. POLAR RESEARCH. 34.

Development and Application of Multi-scale Models for Disease Forecasting

Benjamin H. Mcmahon
20160662PRD2

Introduction

Providing robust, quantitative, and reproducible predictions of such complex phenomena as disease outbreaks requires several technological developments. We will develop these technologies by treating each use case from data to decision in five steps. First, we will identify the simplest model that is constrained by existing data, captures our understanding of relevant transmission mechanisms, and shows a path by which mitigations could control the epidemic. From this model, we can quantify the ability of this model to predict impacts of proposed mitigations, such as mosquito control, diagnostic deployment, or vaccine development. At this stage, we will select higher fidelity models capable of informing decisions, based on one of several possible strategies: First, we could incorporate the mechanistic assumptions necessary to predict, rather than simply extrapolate, the impacts of interventions. Second, we could provide geographic resolution to the model, so that fitting the model to successful control efforts in one region inform on the level of intervention required in other areas. Finally, it is possible to draw analogies among pathogens or diseases, accounting mechanistically for their differences.

Once the appropriate mathematical model is implemented, we will address the problem of propagation of statistical errors through the model and communicating results appropriately to decision makers. Statistical error propagation informs both the type and quantity of data collection needed to adequately characterize the epidemic for model prediction. Communication of predictions, model assumptions, and uncertainties is best achieved by producing an interactive version of the model, where the user has enough freedom to explore the broad scope of possibilities, while always being constrained to realistic scenarios. The ability to do this has been a long-standing grand challenge in epidemiology and public health, and advances in this area will transition to other problems in decision support and modeling of complex phenomena.

Benefit to National Security Missions

This work ties to LANL mission in several specific areas.

For biodefense planning purposes, it is important to extrapolate from deadly outbreaks of dangerous pathogens, which tend to occur in the developing world, to predict how such an outbreak might proceed in the homeland. In particular, the bi-annual biothreat risk assessment performed by DHS in accordance with HSPD-10 needs to make this assessment at a level of fidelity needed to inform investments in planning, logictics, and medical countermeasure development. DoD also has a mission-relevant need to accurately understand the risk to US personnel operating in areas of endemic disease, and how this risk can be mitigated with appropriate countermeasures.

In the area of climate and energy impact, emerging diseases of humans, wildlife, livestock, and crops are important sources of great consequence around the globe. The capabilities developed in this project are directly relevant to understanding how changes in rainfall (and thus disease vectors such as mosquitoes), land use, and social patterns lead to disease emergence impacting public health and food security.

Finally, this project is of importance to the basic science of disease emergence and medical countermeasure development, as quantitative epidemiological models are of direct value in quantifying the design of biosurveillance architectures and interpreting genomic data in terms of pathogen development and antibiotic resistance.

Progress

In her first few weeks, Dr. Manore has worked on mosquito models for Zika virus spread, presented results to Congressman Lujan, and is writing up results in a manuscript.

Future Work

Our tasks and goals for the first year will include work on each of the three distinct disease systems: Ebolavirus disease, Malaria-bacteremia co-infections, and Chikungunya / Zikavirus disease.

For Ebolavirus, we will develop the relationship between our existing coarse-grained model of the 2014 epidemic to more detailed simulations available with the EpiSims agent based model of disease spread. In particular, we will develop our understanding of how clustering of cases in families and family-like structures manifests itself in our models of geographically coupled regions that are assumed to be homogeneously mixed. This capability is essential to making any kind of model interactive for the purposes of decision support.

For the emerging virulence and antibiotic resistance work, we envision two tasks. First, Dr. Manore (postdoc) will work with undergraduates at the University of Portland to write a manuscript describing a cost-benefit model for the development and applications of molecular diagnostics in a high disease burden area. Second, Dr. Manore will perform a similar analysis for so-called intermittent prophylactic treatment (IPT) for malaria in high-risk groups such as infants and pregnant women. In both cases, the mechanism of emergence of antimicrobial resistance is central to the model.

For the Chikungunya and Zika viruses, a manuscript will be developed with university collaborators exploring the interplay of geography, vector (mosquito) control, and mitigations in forecasting the spread of Zika virus across the western hemisphere, drawing on analogies to the 2014 spread of Chikungunya and ongoing, endemic, fluctuations in Dengue virus infection levels.

To translate the results of this project to mission, Manore will work with mentors, Sara DelValle, Nicolas Hengartner, and Ben McMahon, to identify ties to existing programs across the Laboratory, speak at conferences, mentor students, publish peer-reviewed manuscripts, and engage with sponsors.

Conclusion

The expected results are of two types. First, we will have a greater understanding of the lessons to be learned from three specific epidemics of enormous importance to global public health: the West African Ebola outbreak of 2014, the emergence of virulence and antibiotic resistance in high disease-burden environments, and the spread of vector-borne disease. From these studies, we will gain insights into how demographics, climate change, and policy decisions can influence these and other cases of disease emergence. More generally, this work will provide an important catalyst for science-based decisions in other areas of the Laboratory.

Ultrafast Vacuum Ultraviolet Spectroscopy of Complex Materials

Dmitry A. Yarotski
20130814PRD4

Abstract

The last few decades have seen the discovery of novel classes of correlated electron materials (CEM) with exotic properties, such as high-temperature superconductivity and multiferroicity, that few would have imagined. Despite significant effort, the labyrinthine pattern of competing interactions among charge, lattice and spin has prevented development of predictive theoretical frameworks and basic principles required to harness CEM functionalities for technological applications. Experimentally, great strides in our understanding of CEM functionality have been made using well-established techniques such as thermodynamic measurements (heat capacitance, magnetization, etc.) and neutron scattering. Nevertheless, most of these techniques lack the specificity required for resolving (in both time and space) particular degrees of freedom, and the coupling between them, that are involved in the competition between different interactions. Therefore, conceptually new approaches are required to fully understand the emergent physics that evolves over multiple length and time scales, and to use this knowledge for designing materials with entirely new, or significantly improved, functionalities.

In this regard, ultrafast optical spectroscopy (UOS) offers unmatched ability to unravel the competing interactions and coupling between them in time domain, where UOS can track the evolution of electron, spin, and lattice with femtosecond temporal resolution. In particular, recent developments in nonlinear optical techniques have extended ultrafast measurements to soft X-ray frequencies and now allow direct access to the spin, lattice and charge excitations with high element specificity and nanometer spatial resolution. In this work, we will develop new time-resolved X-Ray magnetic spectroscopic capability at LANL and pioneer its application to selectively probe spin dynamics and its effects on CEM properties. This will be accomplished by leveraging unique LANL capabilities in ultrafast optical spectroscopy, synthesis and modeling of exotic magnetic materials. The results of this work are poised to make a broad impact on condensed matter physics and will open new directions in complex materials research.

Background and Research Objectives

The emergence of novel phases in complex materials, such as unconventional superconductivity, multiferroicity, and topologically protected states, derives from the strong interactions among spin, charge, and lattice degrees of freedom (DOF). Existing theories cannot predict the emergent behavior, partly because available experimental probes cannot decipher the interactions between particular DOF and can only extract an averaged response. Ultrafast optical spectroscopy offers an unmatched ability to separate various DOF and coupling among them in time domain because their dynamics occurs at different timescales. Therefore, the studies of time-dependent and element-specific processes hold the key to understanding the DOF interplay in CEM. Time-averaged measurements of the X-Ray linear or circular absorption dichroism (XMLD/XMCD), i.e. dependence on photon polarization, have provided many insights into spin ordering and its interaction with other DOF in various materials. Here, the X-Ray source acts as an element selective probe to monitor changes on a particular chemical site, since the absorption edges of different chemical species are unique. Rapid developments in nonlinear optics have recently enabled the tabletop ultrafast vacuum ultraviolet (VUV) sources that should enable time-resolved XMLD/XMCD spectroscopy at 3p→3d transitions (M absorption edges) in a majority of transition metals - the key elements of many complex materials. Although previous static measurements have demonstrated that these transitions are indeed very sensitive to magnetic ordering, the applications of ultrafast VUV sources to the time-resolved studies of element-specific spin dynamics in complex materials remain practically unexplored.

During this project, we have developed a new LANL capability in time-resolved XMLD spectroscopy that allows us to separate the dynamics of spin ordering from that of charge and lattice using all the benefits of X-Ray spectroscopic techniques: high element specificity, charge, and spin sensitivity, nanometer resolution and sensitivity to buried interfaces. We then applied this novel probe to reveal the spin dynamics and its coupling to other DOF in a set of complex materials, including antiferromagnetic (AFM) metals and multiferroics. Epitaxial heterostructures of CEM are currently of particular interest due to anticipated enhancement of emergent properties caused by proximity effects. Therefore, we have also utilized more penetrating probes with higher photon flux and better spatial/spectral resolution available at synchrotron facilities (Advanced Photon Source and Stanford Synchrotron Radiation Lightsource) to provide a new insight into exchange interaction and magnetoelectric coupling across the interfaces in CEM nanocomposites. The results of our work not only provide new capability at LANL for probing element-specific spin dynamics in CEM, but also unveil new details that will lead to better understanding of CEM functionality and development of the basic principles of complex material design.

Scientific Approach and Accomplishments

Our scientific accomplishments are significant considering the scale of the project. This can be testified by two refereed-journal articles currently in preparation and several presentations at the international conferences. In the following, we highlight most important technical accomplishments.

Time resolved XMLD capability development

The goal of this project is to probe ultrafast spin dynamics in CEM using time-resolved X-ray magnetic linear absorption dichroism (XMLD) spectroscopy. The XMLD technique probes p->d transitions of magnetic ions and is valuable tool for understanding how the spin order is coupled to other degrees of freedom (charge, orbital, lattice), because electrons on d-orbitals of transition metal ions are usually responsible for magnetism in complex materials. In particular, our recently developed ultrafast table top soft x-ray source is capable of spanning the 3p-3d transitions (M-edges) of many transition metal ions in CEM compounds. The dynamics of spin DOF is studied by photo-exciting (pumping) a sample with a femtosecond near-infrared laser pulse which takes the material out of equilibrium and perturbs the spin alignment through transient modulation of charge density or lattice distortions affecting exchange interactions. Subsequently, a soft X-Ray pulse probes the spin dynamics at the characteristic timescales (fs-to-ps-to-ns) by monitoring the evolution of absorption dichroism (polarization dependence) of the magnetic ion of interest. However, prior to applying an ultrafast X-Ray source and XMLD spectroscopic technique to elucidate non-equilibrium magnetic properties of CEM, we had to overcome several technical challenges related to unusually high surface sensitivity of M-edge measurements. First, we discovered that even under high vacuum and the cryogenic temperatures, a thin water layer can contaminate the sample surface and absorb a large portion of extreme ultraviolet (XUV) probe pulse. This problem has been mitigated by introducing a liquid nitrogen cooled shield around the sample that freezes out any water remaining in the vacuum chamber before the sample is cooled. A second obstacle was a high sensitivity of the XMLD signal to the sample roughness. By closely monitoring and controlling the position of the beam on the sample surface we could consistently measure the same region of the sample thus reducing signal variations cause by inhomogeneous surface profile. The new experimental capability (one of the few in the world) now allows continuous measurements of magnetic dynamics in a broad temperature range (5-450 K) in samples that move due to temperature dependent cryostat arm expansion/contraction.

Spin and charge ordering dynamics in antiferromagnetic Chromium

Chromium (Cr) is a peculiar material which undergoes several phase transitions involving AFM spin alignment in spin density waves and formation of charge density waves. We have applied our time-resolved XMLD capability to separate spin and charge dynamics in Cr and investigate the mechanisms of complex interplay between spin and charge density waves in this material. Measurements of temperature-dependent photo-induced XMLD dynamics in Cr crystals showed an increase in XMLD signal at ~310K consistent with the onset of AFM spin ordering. Interestingly, another transition at ~120K was also observed, which corresponds to the spin flip from transverse to longitudinal spin density wave order. Both of these observations clearly demonstrate high sensitivity of our table-top XMLD method to AFM spin order variations which were only observed before at large synchrotron facilities. Moreover, our ability to resolve sub-50 fs transients in photoinduced X-Ray absorption allowed us to distinguish between the dynamics of spin and charge degrees of freedom across the AFM phase transitions. Below the transition temperature, XMLD signals show a very fast (~1 ps) amplitude change that relaxes on time scales of >10 ps following photoexcitation. As the temperature is increased through the AFM transition, the amplitude of the ultrafast transient decreases and oscillations (~100 GHz) develop which correspond to coherent excitations in the material. The oscillation strength increases with increasing temperature. This behavior clearly indicates that magnetic order sup-

presses coherent excitation of charge density waves in Cr which implies strong coupling between these two orders. Theoretical modeling provided by our collaborators from LANL and Uppsala University will provide better understanding of the origins of such multiple-order coupling and its implications on the material functionality. The results of these experiments were presented at the 2015 APS March Meeting, and we are currently working on the manuscript that will summarize our findings and describe physical mechanisms responsible for the observed effects.

Strain and exchange-bias induced spin disorder in BiFeO3/La0.7Sr0.3MnO3 multiferroic nanocomposites

Multiferroics are technologically important materials with co-existing ferroelectric (FE) and (anti) ferromagnetic (FM/AFM) orders. The allure of these materials lies in the possibility of controlling the electric and magnetic responses with either electric or magnetic fields, which has the potential to revolutionize future sensing and information storage technologies. Despite substantial effort over the past decade, very few of the discovered single-phase multiferroics exhibit magnetoelectric (ME) coupling and then, only under conditions far beyond that of potential applications (i.e. extremely low temperature or high magnetic fields). Therefore, a new approach to creating multiferroic materials has recently gained extensive interest - epitaxial complex oxide nanocomposites where ME coupling is induced by strain or exchange-bias across the interface between ferroelectric and magnetic materials. In this project, we leveraged LANL unique facilities in material synthesis to create series of vertically aligned multiferroic nanocomposites of BiFeO3 (BFO, FE/AFM) and La0.7Sr0.3MnO3 (LSMO, FM) compounds where one phase is embedded into another in the form of nanopillar-in-matrix with controlled spatial distribution. The goal was to investigate the variation of ME response when the constituent phases evolved from pillar to matrix form (or vice versa). To probe the magnetic ordering at the interfaces as a function of nanocomposite structure, we have gained access to synchrotron facilities at Advanced Photon Source. Here, we have made temperature dependent measurements of element-specific spin structure by performing XMCD measurements at Mn and Fe absorption edges and revealed the microscopic signatures of strong coupling between FM order in LSMO and AFM order in BFO mediated by exchange bias across the interface in LCMO(x):BFO(1-x) nanocomposites with x in the 0.3-0.7 range. In particular, we have observed that FM order in LSMO induces FM spin alignment of Fe ions in otherwise AFM BFO. This effect has been observed before in XMCD experiments on BFO/LSMO superlattices, and thoroughly investigated by LANL team using neutron scattering and theoretical modeling. Interestingly, the observed effect is significantly more pronounced in 3D nanocomposite than in superlattices. Importantly, we have also discovered inverse effect where FM order in LSMO pillars is inhibited by proximity to AFM BFO. It is manifested by significant reduction in normalized XMCD response with decreasing LSMO fraction. This behavior has not been seen before due strong confinement to BFO/LSMO interfaces and small surface-to-volume ratio available in superlattices. Previously, large strain present in thin (< 5nm in thickness, which is on the order of pillar dimensions) LSMO films have been shown to suppress the FM spin alignment. However, such strain effect cannot explain our results because XMCD measurements conducted on a series of LSMO(x)/MgO(1-x) nanopillar composites with similar (x=0.3-0.7) LSMO fraction and strain levels, did not reveal as pronounced effects of LSMO pillar size on magnetization. Therefore, suppression of FM order in LSMO happens primary by exchange bias interaction across the interface with BFO. Dependence of this effect on the pillar density and structure provides essential insight for engineering ME coupling through manipulation of interfacial exchange bias in multiferroic composites. These results will be summarized in the second manuscript, and will be used as a groundwork and guidance for future ultrafast time-resolved XMCD studies.

Impact on National Missions

Our work directly addresses the Grand Scientific Challenges identified in the Basic Energy Sciences Advisory Committee (BESAC) report, which are central to DOE's missions in energy, science, and security in general, and to the LANL Materials Grand Challenge in particular. During this project, we collaborated or gained access to BES user facilities at APS and SSRL X-ray sources as well as CINT, NHMFL, and Lujan in accord with LANL institutional priority in supporting national user facilities. Moreover, the proposed work develops new MaRIE capabilities in ultrafast X-ray spectroscopies, which when combined with material synthesis, other ultrafast spectroscopic CINT capabilities and forefront condensed matter theory represents the LANL Materials Strategy and provides LANL, as well as BES-CINT, with the capability to investigate emergent properties of complex materials through observation of the dynamical behavior of relevant order parameters. Our thrust to interface materials science with ultrafast X-Ray coherent photon probes represents an essential element in the MaRIE strategy that connects the M4 facility to the Multi-Probe Diagnostic Hall. Proposed experiments will provide critical understanding of the mechanisms of magnetic ordering and its dynamics and thus enable the design and synthesis of new CEM with controlled functionalities.

Publications

Ahmed, T., B. McFarland, A. Chen, Q. X. Jia, D. A. Yarotski,

and J. X. Zhu. Site dislocation between Fe and Mn sites in double perovskite Bi2FeMnO6: A theoretical explanation for XMCD anomaly. Physical Review Letters.

McFarland, B. K., J. X. Zhu , R. P. Prasankumar, G. Rodriguez, R. L. Sandberg, A. J. Taylor, S. A. Trugman, and D. A. Yarotski. Ultrafast X-Ray Probe of Dynamics in Chromium. Presented at 2015 CINT User Meeting. (Santa Fe, September 21-22, 2015).

McFarland, B. K., J. X. Zhu, R. P. Prasankumar, G. Rodriguez, R. L. Sanberg, A. J. Taylor, S. A. Trugman, and D. A. Yarotski. Soft X-Ray Probe of Ultrafast Dynamics in Spin Ordered Chromium. Physical Review Letters.

McFarland, B., J. X. Zhu, R. Prasankumar, G. Rodriguez, R. Sandberg, A. J. Taylor, and D. A. Yarotski. Ultrafast Dynamics near the M-edge in Chromium. Presented at American Physical Society March Meeting. (San Antonio, Texas, March 2–6, 2015).

Tracking Microbial Activity to Predict the Impacts of Climate Change on Ecosystem Function

Cheryl R. Kuske
20140662PRD1

Abstract

Ecosystem processes such as nutrient cycling sustain life on earth, and are controlled in large part by communities of fungi and bacteria (collectively termed microbes) that reside in the soil. Global changes, such as nitrogen deposition, warming, elevated CO2, and altered precipitation, alter the abundance and biodiversity of microbial communities and significantly alter ecosystem functions. Soil microbial communities largely determine whether terrestrial ecosystems act as carbon sources or sinks under elevated CO2. However, biochemical processes mediated by complex microbial interactions in the soil remain a black box in terrestrial ecosystem models. A major hurdle in linking complex soil communities to major ecosystem processes is the ability to distinguish among the active and dormant members of the community. Understanding how dormancy structures microbial communities is of particular concern because it is a strategy for survival under unfavorable environmental conditions, and could determine whether microbial communities are sensitive or resilient in the face of current and predicted climate changes. We used a combination of high-throughput sequencing of ribosomal RNA and DNA with surveys of functional genes in two different field-collected soils in the laboratory to determine the relative contributions of the active populations, and to elucidate the biological and ecological constraints on the ability of microbial populations to enter and exit from dormancy. Collectively, these studies help us understand how the microbial community regulates climate change responses and feedbacks in the soil. We have completed two soil microcosm experiments: one that compares microbial community responses to increased moisture, increased nitrogen, and warming temperatures, and another that examines microbial response to environmental stress, including temperature, desiccation and starvation. We have also completed an 18 month field experiment that compares active and dormant microbes in seven microhabitats (biocrusts, plant root zones) in an arid grassland. We have published six manuscripts on this topic and have four more in preparation or review.

Background and Research Objectives

A long-standing scientific challenge is to understand how global change, primarily nitrogen deposition, will affect microbial communities, and in turn, important ecosystem functions, such as carbon cycling. Understanding how dormancy structures microbial communities is important for understanding both the long and short-term impacts of global change on microbial biodiversity because it is a strategy for survival under unfavorable environmental conditions, and is a potential pathway for resiliency of microbial communities to global change.

The goals of this project were to understand the relative contributions of active soil bacterial and fungal populations, and constraints on their ability to enter and exit from dormancy, to enable accurate predictions of C or N fluxes from the soil. In addition, by combining community surveys with measures of transcribed functional genes, we aimed to identify potentially novel pathways involved in dormancy. By quantifying microbial activity and dormancy under dynamic environmental conditions, our studies worked to determine how the microbial community regulates climate change responses and feedbacks in the soil, which are critical for development of soil process models and to define appropriate input variables in regional climate models. Our overall objective was to investigate how dormancy determines community response to global change and the implications of dormancy on soil processes.

Scientific Approach and Accomplishments

Approach

We conducted both controlled laboratory experiments and field surveys conducted over the course of 18 months, to study the response of natural microbial communities in two contrasting soils to a multiple environmental manipulations, including increased water availability, increased temperature and increased nitrogen

availability. The responses to these perturbations were tracked over time by quantifying soil respiration using gas chromatography. The active and total communities were measured using molecular analysis of rRNA and rDNA to link the composition of the active community to measures of soil respiration, and to quantify shifts in the active community over time. During postdoc Mueller's tenure, we applied for additional LDRD funds and were awarded funds to support metatranscriptome sequencing of many of the samples. These measures allowed us to determine the short-term community responses to predicted global changes, and to link those shifts with ecosystem function.

The longer-term field survey was conducted in a natural arid grassland, where soils were sampled monthly from seven microhabitats (a variety of biocrusts and plant root zones) to determine patterns of activity in those habitats and the influence of temperature, moisture, and photosynthetically active radiation over the course of a year. Total and active fungal and bacterial communities were assessed, along with environmental parameters.

Accomplishments

We compared the utility of a taxonomic marker (rDNA) and an enzyme-encoding gene (cbh1) to track soil fungal community responses over time (Mueller et al. 2014, Molecular Ecology; all publications are listed in the publications section). We designed and validated a new PCR primer set to survey for fungi, that is more compatible with the next-generation high-throughput sequencing platforms (Mueller et al. 2015, FEMS Microbiology Ecology). We then used this information to conduct a study of active and total fungal and bacterial communities along a natural environmental gradient (maple forest, Mueller et al. 2015, Microbial Ecology), and also applied them to this LDRD project. We assessed the quantity and composition of fungi and bacteria in an arid landscape after two years of simulated N-deposition (Mueller et al. 2015, Frontiers Microbiology). Postdoc Mueller participated in a workshop held in 2014, on prospects and challenges for fungal metatranscriptomics (Kuske et al. 2015, Fungal Ecology).

Over the next six months, we expect to generate two publications from the initial experiments, one linking soil respiration with community composition of fungal and bacterial communities, and another examining the dynamic rank abundance curves of active and dormant fungal and bacterial communities, which will also incorporate the findings from the metatranscriptome survey. We expect to generate an additional manuscript contrasting stress responses in fungi and bacteria within the two different soil types to further explore the relative effects of anthropogenic perturbations on community shifts and ecosystem functions. Finally, we plan to link the functional gene surveys from the microcosm studies to existing metatranscriptome datasets generated from field-based surveys, which also incorporate other functional measures, including ecoenzymes. In total, we expect that the above studies will lead to a minimum of four additional publications.

Overall, our studies have shown that (a) arid landscapes are very patchy in composition of soil fungi and bacteria, in association with the sparse plants and biocrusts, (b) that these surface soil communities are critical for recycling carbon and for responding to N, which is a limiting nutrient in these systems, (c) that arid ecosystems contain vastly different fungal and bacterial communities, and associated enzyme functions, compared to temperate forest communities and that this situation dramatically affects nutrient cycling in the surface soils, (d) that a combined DNA & RNA approach may differentiate active from total community members, but that each type of survey brings along its own biases that must be considered for quantification of the in situ community, (e) that soil chemistry, aeration and moisture are critical parameters to consider when assessing the activities and dormancy of resident fungi and bacteria.

Impact on National Missions

First, this project will help fill a significant information gap in our knowledge of and ability to predict the outcomes of processes that are mediated by complex microbial communities in soils. Soils are an enormous reservoir of carbon (C) on Earth, and the concerted activities of soil microbes regulate the storage or release of this C.

Second, the project directly contributes to DOE missions in biological systems science and climate change responses. It also advances metagenomics technologies and basic environmental surveys that enable more accurate, specific detection of target microorganisms in environmental samples, thus contributing to a technology base supporting biothreat detection. Third, this project advances our understanding of fungal and bacterial biomass and metabolic capabilities; these are organisms from which we have historically derived most of our antibiotics, as well as other pharmaceuticals and industrial enzymes. Fourth, many of the fungi we will be studying also have potential in processing C for biofuels applications. Through the course of these studies, we have cultured and archived over 2,000 new fungal isolates for further investigation.

Publications

Dunbar, , L. V. Gallegos-Graves, Steven, Mueller, Hesse, D. R. Zak, and C. R. Kuske. Surface soil fungal and bacterial communities in aspen stands are resilient to eleven years of elevated CO2 and O-3. 2014. SOIL BIOLOGY & BIOCHEMISTRY. 76: 227.

Kuske, C. R., C. N. Hesse, J. F. Challacombe, Cullen, J. R. Herr, R. C. Mueller, Tsang, and Vilgalys. Prospects and challenges for fungal metatranscriptomics of complex communities. 2015. FUNGAL ECOLOGY. 14: 133.

Mueller, R. C., Belnap, and C. R. Kuske. Soil bacterial and fungal community responses to nitrogen addition across soil depth and microhabitat in an arid shrubland. 2015. FRONTIERS IN MICROBIOLOGY. 6.

Mueller, R. C., L. Gallegos-Graves, D. R. Zak, and C. R. Kuske. Assembly of active bacterial and fungal communities along a natural environmental gradient. 2015. Microbial Ecology. : 1.

Mueller, R. C., M. M. Balasch, and C. R. Kuske. Contrasting soil fungal community responses to experimental nitrogen addition using the large subunit rRNA taxonomic marker and cellobiohydrolase I functional marker. 2014. MOLECULAR ECOLOGY. 23 (17): 4406.

Mueller, R. M., L. Gallegos-Graves, and C. R. Kuske. A new fungal large subunit ribosomal RNA primer for high throughput sequencing surveys. 2015. FEMS Microbiology Ecology 92 . 92: 6 pages.

Complexes Containing Redox-Active Ligands for the Synthesis of Fuels from Readily-Available Carbon Sources

John C. Gordon
20140664PRD2

Abstract

With its emphasis on catalysis, atom-economy, and utilization of readily-available starting materials, sustainable chemistry is a guiding principle in the construction and development of emerging chemical technologies and has the potential to positively affect national economic, environmental, and security interests. However, widespread and large-scale application of sustainable chemical processes has not yet been realized, and may not be achieved until approaches are developed to the point that they become more economically viable than current technologies.

A potentially important technology is the development of a system that converts readily available, highly oxidized precursors such as CO2, acetic acid, and glycerol into higher-order compounds containing more carbon atoms that can readily be converted into alkanes, which are the main components of transportation fuels. This work addressed both the synthesis of the higher order fuels precursors and their defunctionalization to produce hydrocarbons that would be suitable as fuels.

Background and Research Objectives

A potentially important technology is the development of a system that converts readily available, highly oxidized precursors such as CO2, acetic acid, and glycerol into higher-order compounds containing more carbon atoms that can readily be converted into alkanes, which are the main components of transportation fuels. This work attempts to address both the synthesis of the higher order fuels precursors and their defunctionalization to produce hydrocarbons that would be suitable as fuels

Scientific Approach and Accomplishments

The synthesis of a significant number of metal complexes supported by redox active ligands, including those containing iron and nickel have been achieved. During FY16 these were screened towards a number of reactions, including carbon-carbon bond coupling reactions, hydrogenations, hydroborations, etc. In particular, we prepared a nickel-based system that appears to exhibit interesting and unexpected redox behavior upon binding a ketonic (C=O bond containing) substrate that may have implication for how redox active metal complexes behave. This compound efficiently catalyzed a number of useful chemical transformations including the hydroboration of ketones, aldehydes, and imines.

Impact on National Missions

The goal of the project is the synthesis of molecules that can serve as fuels from readily available and sustainable molecules such as CO2, acetic acid, and glycerol. These goals are directly in line with DOE BES's interests in fundamental chemistry and catalysis science and DOE EERE's interests in sustainable and biorenewable chemistry. This work also directly impacts the area of climate and energy impact vis-a-vis the conversion of biorenewable and abundant small molecules into higher order carbon containing species with potential use as hydrocarbon fuels for transportation applications.

Publications

King, A. E., C. E. S. Stieber, N. J. Henson, S. A. Kozimor, B. L. Scott, N. C. Smythe, A. D. Sutton, and J. C. Gordon. "Ni(bpy)(cod): A Convenient Entryway into the Efficient Hydroboration of Ketones, Aldehydes, and Imines". 2016. European Journal of Inorganic Chemistry. 11: 1635.

Synthesis and X-ray Spectroscopy of Actinide Thiocyanates

Stosh A. Kozimor
20140677PRD3

Abstract

Covalency is a fundamental concept in chemistry used to describe chemical bonding in s-, p-, d-, and f-block elements. However, given the restrictions of existing experimental techniques, the degree of covalency of a given bond is difficult to measure and is often estimated or inferred. This situation was recently altered by the pioneering work of Solomon, Hedman, and Hodgson who used ligand K-edge X-ray Absorption Spectroscopy (XAS) to directly measure covalency in bonding. We are currently expanding this technique to complexes that contain heavy atoms in an effort to improve contemporary descriptions of covalency, electronic structure, and bonding in actinides. These studies are providing unique insight to evaluate the relative roles of d- and f-orbitals in bonding, and these results are being evaluated in the context of recent advances in f-element chemical reactivity that cannot be easily explained using a traditional description of f-element electronic structure.

Background and Research Objectives

As the need to develop a closed nuclear fuel cycle grows, there are a number of technological challenges that need to be overcome. One of the most difficult challenges is the separation of the minor actinides (Am3+ and Cm3+) from the trivalent lanthanide fission products, as they share many physical properties. A number of studies have shown that this separation is possible by employing soft ligands (such as those containing S or N donors), which preferentially bind the actinides (An) over the lanthanides (Ln). One particularly promising extractant is the SCN1- anion that provides enhanced separation of An over Ln. Although little is understood about why the SCN1- extractant is successful, it seems likely to be associated with the propensity of NCS1- to form more covalent An–NCS vs Ln–NCS bonds.

In this research we are characterizing the M–NCS interactions by synthesizing An(NCS)xy- (An = Pu, Am, Cm) complexes and subsequently analyzing the An(NCS)xy- compounds using ligand K-edge X-ray absorption spectroscopy (XAS) and DFT calculations.

Scientific Approach and Accomplishments

The goal of this research is to (a) develop a synthetic route to trivalent f-block SCN1- complexes, and (b) establish the bonding character of these complexes through multiple spectroscopic and theoretical techniques, primarily S, N, and C K-edge XAS and TDDFT. This will be accomplished by first establishing the interactions within the SCN1- ligand itself using S, N, and C K-edge XAS. These efforts are providing a framework for the subsequent efforts focused on characterizing electronic structure and covalency in the M–NCS bonds in the coordination complexes. Over the last year all of the analytes have been made and analyzed by S K-edge XAS. Follow-on efforts will center on conducing the N and C K-edge XAS experiments. Overall, the anticipated results will enable us to evaluate An–NCS bonding as a function of both actinide metal identity and actinide oxidation state, which represent the main factors affecting metal-ligand covalency in bonding.

Impact on National Missions

This research effort utilizes Justin Cross' experience in transuranic synthesis with LANL's proficiency in developing actinide bonding schemes through spectroscopy and theory. Follow-on work will mark the first synthesis of trivalent An3+(NCS)xy- compounds and the first transplutonium S, N, and C K-edge XAS experiments. Developing an understanding of the bonding in these complexes will shed light on both the differences in Ln/An–NCS interactions and highlight how An–NCS bonding varies as the 5f series is traversed from Pu to Cm. This investigation will develop a fundamental understanding of f-element bonding that can be applied to DOE's efforts to design practical and efficient separations of the lanthanides and minor actinides.

Publications

Macor, J. A., J. L. Brown, J. N. Cross, S. R. Daly, A. J. Gaunt, G. S. Girolami, M. T. Janicke, S. A. Kozimor, M. P. Neu, A. C. Olson, S. D. Reilly, and B. L. Scott. Coordination Chemistry of 2,2'-Biphenylenedithiophosphinate and Diphenyldithiophosphinate with U, Np, and Pu. 2015. DALTON TRANSACTIONS. ASAP (ASAP): NA.

Anaerobic, Solvothermal Synthesis of Lanthanide and Actinide Kagomé Antiferromagnets

Stosh A. Kozimor
20140681PRD4

Abstract

The goal of this project was to advance understanding of plutonium electronic structure, which is of fundamental interest and important to many areas of national security. The actinide series marks the emergence of 5f electrons in the valence shell. Whether the 5f electrons in actinide molecules, compounds, metals and some alloys are involved in bonding has been the central and integrating focus of actinide chemistry and physics. In the pure elements, those to the left of Pu have delocalized electrons while elements to the right of Pu are localized. Plutonium is trapped in the middle. For example, in the delta-phase metal the electrons seem to be in a unique state of being neither fully bonding nor localized, which leads to novel electronic interactions and unusual behavior. Given the complexity of plutonium, it is essential to identify new well-defined and pure-phase materials whose magnetism and electronic properties can be studied. As an example, the observation of superconductivity in PuCoGa5 provided an entirely new opportunity for evaluating electron delocalization in plutonium. This project focused on generating a new approach to generate magnetically frustrated systems for plutonium (as well as the other actinide elements) that we believed would (1) provide a platform for further advancing electronic structure descriptions for f elements and (2) might provide access to new actinide superconducting materials.

Background and Significance

Magnetism is important for many emerging technologies, i.e. information storage, high temperature superconductivity, and generators (to name a few). Magnetic properties and chemical bonding are fundamentally linked by a combination of the degree of covalency (orbital overlap), electron orbital and spin magnetic moments, and the Pauli exclusion principle. In the late 1950's Goodenough and Kanamori developed a set of rules to quantitatively understand the microscopic origin of magnetic interactions based on bonding in 3d-transition metal oxides (i.e. Fe3O4). Now, the Goodenough-Kanamori Rules are routinely used in designing novel transition metal devices, from multiferroics to high temperature superconductors. With the increased dependence on actinide elements in strategically important materials, it is imperative to develop analogous Goodenough-Kanamori Rules for predicting magnetic exchange in f-electron systems. Hence, the goal of this proposal is to demonstrate that magnetic properties in actinide compounds can be controlled and predicted based on local structure and covalent bonding.

Scientific Approach and Accomplishments

The isolation of a copper(II) 2D kagomé antiferromagnet led to (1) the first direct evidence for the resonating valence bond model in copper oxide superconductors and (2) the observation of a quantum spin liquid. Based on these studies, it seemed likely that trapping lanthanides and actinides (f-elements) in a 2D kagomé lattice would provide materials with unique magnetic properties and potentially impart similar unconventional f element superconductivity. However, frustrated f element 2D kagomé materials have not previously existed.

We set out to synthesize these 2D kagomé 4f and 5f materials for the first time. Significant effort in the first two years of this project focused on developing synthetic capability for these materials at TA-48. The efforts were successful and new solid-state and hydrothermal capabilities that were compatible with Plutonium and the other actinides were established. The choice of monovalent cations (A1+; Ag, Rb, Cs, etc) and the oxo dianions (MO42–; M = S, Se, Te, Mo, W, etc) was used as a template of the kagomé network and expand the lattice to incorporate the f elements. Initially work focused on Ce3+ (4f1) and Yb3+ (4f13) materials provided a new series of compounds, but did not meet the requirements of the kagomé framework. Additional efforts with uranium also provided a series of new uranium complexes that were characterized by powder XRD and XAFS. Again

these new compounds, while fundamentally interesting in their own right, did not meet the requirements of the kagomé framework.

Impact on National Missions

This two-year effort to synthesis 2D frameworks containing magnetically frustrated f elements established a new synthetic capability at Los Alamos for hydrothermal and solid state synthesis. The effort resulted in two publications, a third that is currently accepted for publication, and a fourth that is still in preparation. Future work using this capability will focus on establishing new design principles for unconventional actinide/lanthanide materials that might provide access to new types of actinide superconductors. Overall, these efforts will provide a strong scientific foundation for the DOE and its laboratories to directly support the national nuclear agenda and the integrated Plutonium Strategy.

Publications

Kiernicki, J., M. Ferrier, J. Lezama Pacheco, H. La Pierre, B. Stein, M. Zeller, S. Kozimor, and S. Bart. Examining the Effects of Ligand Variation on the Electronic Structure of Uranium Bis(imido) Species. To appear in Journal of the American Chemical Society.

Kozimor, S. A., and H. S. La Pierre. Spectroscopic and computational investigation of actinium coordination chemistry. 2016. Nature Communications. : 12312.

Kozimor, S. A., and H. S. La Pierre. Monomers, Dimers, and Helices: Complexities of Cerium and Plutonium Phenanthrolinecarboxylates . 2016. Inorganic Chemistry. : 4373.

Pierre, H. La, M. Loeble, J. Keith, E. R. Batista, K. Boland, S. Kozimor, R. Martin, S. Minasian, D. L. Clark, N. Kaltsoyannis, P. Yang, M. P. Wilkerson, L. E. Wolfsberg, J. A. Bradley, G. Seidler, S. Conradson, and D. K. Shuh. Covalency in Plutonium: A Cl K-edge XAS and DFT study. To appear in Journal of the American Chemical Society.

A Physics-Based Numerical Model for Next-Generation Laminar Flow Batteries

Qinjun Kang
20150700PRD1

Abstract

Flow batteries have emerged as an efficient and economical device for the storage of large quantities of energy. Significant research efforts have been devoted to making flow batteries economically competitive, most of which have focused on new materials and chemistries aiming to larger operating voltages and multi-electron charge transfers. A fundamental modeling effort to optimize flow battery design and architectures is lacking. The main objective of this project was to develop a physics-based numerical model to understand the coupled physicochemical processes in flow batteries, with the goal to optimize cell parameters to achieve higher efficiency and reduced costs. Scientific accomplishments of this project include the development of a numerical model for coupled flow, diffusion, conduction, and electrochemical reaction, accounting for the complex structures of the porous electrodes, as well as its application to catalyst layers of fuel cells and electrodes of vanadium redox flow batteries. Our work has resulted in multiple publications in important journals. This project targets transformative new energy technologies and to significantly enhance and extend the use of current technologies. It also supports DOE goals in promoting energy security.

Background and Research Objectives

The U.S. has increasing needs for energy storage in its electrical power grid because of the increasing use of renewables that produce power intermittently. Among multiple forms of energy storage, flow batteries hold the greatest promise for next generation grid-scale energy storage technology. Although various technologies are being developed to increase the power density and energy storage density of flow batteries, a fundamental modeling effort has thus far been lacking in flow battery research with the goal to optimize material design and architectures. Such optimizations can have an impact on the power density by nearly an order of magnitude.

The main objective of this research is to develop a novel, physics-based numerical model to understand the coupled physicochemical processes in flow batteries, with the ultimate goal to optimize cell parameters to achieve high power density and reduced cost.

Scientific Approach and Accomplishments

Building on our numerical models for simulating flow and transport processes in geological media, we have made quick progress towards our research goal. Particularly, we have developed a numerical model for coupled diffusion, conduction, and electrochemical reaction, accounting for the complex structures of the microporous electrodes. The governing equations for proton transfer in electrolyte and reactant transport in porous electrodes are solved using the lattice Boltzmann method (LBM), with the electrochemical reactions occurring at the electrolyte/electrode interface treated in the source term. We have used the model to predict transport properties of the catalyst layers of fuel cells and have made some important discoveries, including the overestimate of the effective diffusivities by the commonly used empirical relations, as well as the significant role of Knudsen diffusion plays in oxygen diffusion.

Following this line of research, we have carefully studied the non-Darcy behavior of gas flow in tight porous media and found that the actual permeability (measured by gas) of nanoporous media can be 10-100 times that of intrinsic permeability (measured by liquid), and that the traditional Darcy's Law greatly underestimates the gas transport rate in nanopores. Our work is the first one concerning slip flow in complex structures of nanoporous media.

Further, we have taken into account fluid flow in our model and applied it to simulate complicated multiphase flow and reactive transport in the electrodes of a vanadium redox flow battery. Both the permeability and diffusivity of the electrodes are predicted and compared with empirical relationships in the literature. Reactive

surface area of the electrodes is also evaluated and it is found that empirical relationship in the literature overestimates the reactive surface under lower porosities. Further, the effects of fiber diameter and porosity on electrolyte flow, ion transport and electrochemical reaction at the electrolyte-fiber surface are studied. Finally, evolutions of bubble cluster generated by the side reaction are studied. Our pore-scale studies successfully reveal the complicated multiphase reactive transport processes in the electrode, and the simulation results can be used to inform the design of flow batteries for improved performance and durability. This project has resulted in multiple publications in important journals, including Electrochimica Acta, Scientific Reports, and Fuel.

Impact on National Missions

This project successfully resulted in a comprehensive physics-based numerical model for coupled transport and electrochemical processes in flow batteries. The model may help the design of next-generation high power density flow batteries and facilitate their applications in energy storage and power supply. The capabilities developed in this project also have direct application to other earth and energy programs, including geological storage of nuclear waste and carbon dioxide, development of petroleum and geothermal reservoirs, fuel cells, and micro reactors. This project supports the LANL Grand Challenge to develop transformative new energy technologies and to significantly enhance and extend the use of current technologies in a manner that is sustainable and that mitigates negative environmental, social, and national security impacts. It also supports DOE goals in promoting energy security.

Publications

Chen, L., G. Wu, E. F. Holby, P. Zelenay, W. Tao, and Q. Kang. Lattice Boltzmann Pore-Scale Investigation of Coupled Physical-electrochemical Processes in C/Pt and Non-Precious Metal Cathode Catalyst Layers in Proton Exchange Membrane Fuel Cells. 2015. Electrochimica ActaElectrochimica Acta. 158: 175.

Chen, L., L. Zhang, Q. Kang, H. S. Viswanathan, J. Yao, and W. Tao. Nanoscale simulation of shale transport properties using the lattice Boltzmann method: permeability and diffusivity. 2015. Sci. Rep.Sci. Rep.. 5.

Chen, L., Q. Kang, R. Pawar, Y. He, and W. Tao. Pore-scale prediction of transport properties in reconstructed nanostructures of organic matter in shales. 2015. FuelFuel. 158: 650.

Resolving Kinetic Scales in 3D Global Magnetosphere Simulations

William S. Daughton
20150703PRD1

Abstract

The focus of this Director's Fellowship (PRD) project was to study the influence of ion kinetic physics on the global evolution of the Earth's magnetosphere. The project employed a hybrid simulation technique corresponding to a kinetic description of the ions in the plasma, together with a fluid description of the electrons. One key innovation in this project involves a new equation-of-state for the fluid electrons that approximately captures electron kinetic physics. This innovation may permit more accurate global magnetospheric simulations, which are critical for space weather modeling around our planet. This PRD project ended early, since the postdoc (Ari Le) was awarded the distinguished Feynman Fellowship, which started on February 22, 2016. The new project for the distinguished fellowship is a continuation and expansion of the Director's project described below.

Background and Research Objectives

The magnetic field of the Earth protects our planet against the stream of energetic particles that are continually emitted from the sun. This interaction leads to the formation of the magnetosphere, a bubble of hot ionized gas (plasma) surrounding our planet. During large solar storms, eruptions from the sun compress the magnetosphere and give rise to the injection of energetic particles that can damage satellites. It is a major challenge to understand and properly model how these energetic particles are able to penetrate into the magnetosphere. This project developed a new simulation approach to accurately describe the dynamics of this complex system, and to offer detailed predictions that can be compared with spacecraft observations.

This new simulation approach is far more accurate than current models of the magnetosphere, since it solves the most basic underlying equations (kinetic description) for the ions in the plasma. One major research objective of this project was to implement a new equation-of-state for the electron fluid within the hybrid simulation code. This approach has been shown to greatly improve the accuracy in small test problems, but has not yet been applied to large-scale modeling. Another major goal of this project was to perform high-fidelity modeling of magnetospheric boundary layers, in order to understand fundamental processes and to compare with spacecraft observations.

Scientific Approach and Accomplishments

During the one-year duration of this PRD project, excellent progress was made towards the research goals. The primary focus was kinetic modeling of magnetospheric dynamics, both on the global level using the approximate (hybrid) approach, and on the local level using a first-principles approach (fully kinetic). To accomplish these goals, we employed both hybrid kinetic simulations (kinetic ions and fluid electrons) with the code H3D, along with fully kinetic simulations (ions and electrons treated as kinetic species) with the Los Alamos code VPIC (vector particle-in-cell).

To carry out this project, we first ported the H3D code to LANL computer clusters. The H3D code has a rigorous description of the ions in the plasma, but only an approximate fluid description of the electrons. One of the primary goals of this project was to implement an improved fluid model for the electrons into the H3D code. This new equation-of-state accounts for the effects of electron pressure anisotropy, which in previous studies has been shown to play a critical role in the dynamics. During the first year, we implemented this new closure into the H3D code, and performed a series of two-dimensional test problems involving magnetic reconnection in a current sheet. Magnetic reconnection is a basic process that converts magnetic energy into plasma kinetic energy, while giving rise to changes in connectivity of the magnetic field. It is important to model this process accurately, since it gives rise to the entry of solar wind plasma into the Earth's magnetosphere. The results from our new hybrid approach agree quite well

with first-principles kinetic simulations performed with VPIC, the standard tool for these problems at LANL. These results show the development of intense current sheets within the reconnection outflow jets, and this feature is a key observational signature in the spacecraft data. The details of this work are described in a Physics of Plasma publication.

The next major focus was to employ the H3D code to model 3D magnetospheres. During the past year, we focused on modeling the magnetosphere of Ganymede, one of Jupiter's moons. This was selected as an initial test problem because Ganymede is of a computationally feasible size, and because comparisons could be made to both spacecraft observations, and to other fluid codes used by NASA collaborators. Improved boundary conditions were implemented, and 3D global simulations were compared to fluid simulations. Ion pressure tensor effects, which fall outside the scope of usual fluid models, were found to be important along the boundary layers and "Alfven wings" that form at Ganymede. We made comparisons of our kinetic results with scientists at NASA, and results were shown at the 2015 Fall AGU meeting in San Francisco, and also at a space weather meeting held at Princeton Plasma Physics Laboratory.

In addition to ion kinetics, electron physics can also play an important role in magnetospheric dynamics. During this project, we studied this issue using the fully kinetic code VPIC. The scaling of electron heating with plasma parameters was studied for anti-parallel reconnection, a configuration that serves as a starting point for understanding the dynamics of Earth's night-side magnetotail. To study reconnection at the day-side magnetopause, a new set of initial conditions was formulated for VPIC. The set-up allows simulations of reconnection at Earth's magnetopause, where the shocked solar wind impinges on Earth's magnetic field, by accounting for large density and temperature asymmetries, a regime relevant to recent observations gathered by NASA's Magnetospheric Multi-scale Mission (MMS). Simulations were performed with parameters provided by collaborators to match two separate well-resolved MMS events. This work has involved collaborations with NASA scientists, and has resulted in new papers currently in review.

Impact on National Missions

This research exploited the newest generation of petascale supercomputers using plasma kinetic simulation codes specially optimized for these machines. Most of these calculations were performed locally at Los Alamos using NNSA computers, including both Mustang and the new Trinity machine. These efforts are at the very forefront of high-performance computing, both in terms of scaling the calculations to large numbers of cores (~100,000) and in the visualization and analysis of the results. The scientific results from this research may benefit current and upcoming NASA missions focused on understanding the near-Earth space environment. In particular, the new Magnetospheric Multi-Scale (MMS) mission is currently in active operation and is producing very high-quality data on the kinetic physics of magnetic reconnection within the Earth's magnetosphere. The simulations performed in this project are among the first to study the complex coupling between these kinetic scales and the global dynamics, and the publications from this project are already impacting the MMS mission. Given the key role of space assets in nuclear nonproliferation programs, projects like this contribute better understanding of space weather constraints on space systems and therefore national security operations.

Publications

Egedal, , Daughton, Le, and A. L. Borg. Double layer electric fields aiding the production of energetic flat-top distributions and superthermal electrons within magnetic reconnection exhausts. 2015. PHYSICS OF PLASMAS. 22 (10).

Karimabadi, H., A. Le, V. Roytershteyn, and W. Daughton. Magnetic Reconnection. To appear in Space Weather Fundamentals. Edited by Khazanov, G..

Le, , Daughton, Karimabadi, and Egedal. Hybrid simulations of magnetic reconnection with kinetic ions and fluid electron pressure anisotropy. 2016. PHYSICS OF PLASMAS. 23 (3).

Ohia, , Egedal, V. S. Lukin, Daughton, and Le. Scaling laws for magnetic reconnection, set by regulation of the electron pressure anisotropy to the firehose threshold. 2015. GEOPHYSICAL RESEARCH LETTERS. 42 (24).

Hyperspectral 3D Tracking and Imaging Microscopy

James H. Werner
20150761PRD4

Abstract

This project aimed to construct a new particle tracking microscope that can follow the 3D motion of tens to hundreds of single fluorescent particles simultaneously. The microscope combines recent advances in light-field microscopy for 3D particle localization with established methods of recording emission spectra from point-like sources developed for looking at stars. In addition to computational modeling of the tracking system, we undertook experimental efforts aimed at finding the best cellular systems to be explored with this new capability once it is established.

Background and Research Objectives

Biological cells have a large number of proteins that can interact transiently and dynamically in time, with these interactions essential to life. Often, these interactions occur over the full 3 dimensional volume of the cell. The ability to track a large number of proteins simultaneously in three dimensions would be an incredibly powerful tool to understand the organization and signaling dynamics of living cells. While our lab and others have developed 3D single molecule tracking methods based upon a modified confocal microscope geometry, these methods can only follow one molecule at a time. [1] This project aimed to construct a new 3D tracking microscope that can follow many (tens to hundreds) of molecules or particles while simultaneously recording the emission color of each one. Such a 3D hyperspectral tracking microscope currently does not exist. This project builds upon new advances in light-field microscopy, where the 3 dimensional coordinate of an object in an image is inferred from the direction of the detected light rays. [2] The emission spectra (or color) of the particles being tracked are obtained by introducing a prism in the detection path. We envision the ability to follow ~100 molecules or particles within a volume comparable to a human cell (20 by 20 by 20 microns) simultaneously. This new microscope has the potential to contribute to our understanding of molecular disease. Additionally, this microscope represents a simple and robust method of obtaining 3D, spectrally resolved images and its operational principles could have applications in remote sensing in addition to cellular biology.

Scientific Approach and Accomplishments

In the past year, we have been exploring which cell lines and transport problems will be most impacted by the development of multi-particle 3D hyper-spectral tracking microscopy. In particular, the ability to follow the 3D motion of hundreds of individual particles/molecules simultaneously will have the most impact if demonstrated in a cell signaling system that best highlights the unique features of the technology. As such, we have focused initial efforts at studying the transport and diffusion dynamics of an important cellular receptor (epidermal growth factor receptor) in a polarized cell lines. Polarized cells have a defined orientation (e.g. one side may face the inside of a blood vessel to acquire nutrients whereas the other side interfaces with an organ). Polarized cells often form tight junctions between neighboring cells made from specific protein complexes. Polarized cells can be grown in laboratory environments, but the cell tight-junction interface is perpendicular to the porous substrate used for cell growth. This makes examining transport dynamics on this interface difficult by conventional microscopy methods (which generally image planes parallel with a supporting substrate). This makes polarized cells a good system to highlight the differentiating features of the proposed 3D multiple-particle tracking microscope.

In the past year, we have created a number of polarized cell lines that have key proteins important for tight junction formation (such as the protein Z0-1) labeled with a variant of a green fluorescent protein. We have also been creating cell lines that have the primary cilia protein ARL13B labeled fluorescently. Transport and diffusion along the cell's primary cilia is another polarized cell structure/feature difficult to observe or visualize with conventional optical microscopy measurements.

Our initial 3D tracking studies this past year exploited our existing (confocal-based) 3D tracking microscope, with important instrument upgrades (including two-photon excitation and simultaneous spinning disk imaging) needed for improved cellular visualization during tracking experiments. These experiments have been useful to determine how long polarized cells can remain stably labeled with the fluorescent proteins and provide quantitative data on diffusion rates for the EGFR receptor on the top (apical) side of the cell as well as in the proximity of the tight-junction (See Figure 1). While we have acquired hours of three dimensional tracking data (hours of trajectories, months of data collection), certain rare cellular events (such as EGFR diffusion on primary cilia) have proven difficult to capture with our existing 3D tracking microscope, which only follows one molecule at a time, underscoring the need for constructing a multiple-particle/molecule 3D tracking microscope to increase the probability of catching such rare events.

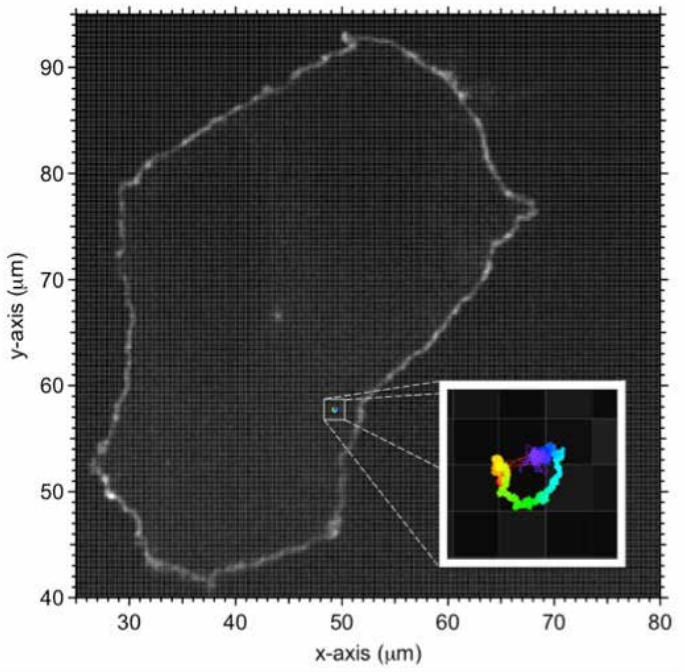

Figure 1. A polarized cell with its tight junction and primary cilia fluorescently labeled. The inset shows a 2D projection of a 3D trajectory recorded on this cell. The rainbow color code denotes the passage of time.

In addition to establishing and testing the viability/feasibility of important 3D molecular transport problems, in the past year we have made substantial strides in data analysis and visualization tools. In particular, the postdoctoral research associate supported on this project, Dr. Dominik Stich, has developed and implemented algorithms to account for stage drift during the measured 3D trajectories and has developed tools for rapid synchronization of camera images with our 3D tracking measurements (which are derived from the position of piezo-stages and not from a camera image). Stitch also has been working on methods for determining changes in molecular diffusion state by maximum likelihood estimators. Efficient analysis tools will also be of importance, especially with the increased data throughput of the proposed multiple particle tracking methods.

Impact on National Missions

Understanding how, when and why individual proteins interact in live cells is crucial to understanding and predicting cell response, including when or why a cell becomes diseased, develops cancer, or dies due to exposure to a biothreat agent. Such an understanding is a vital component of developing appropriate prophylactic or therapeutic strategies that are important for US citizens and warfighters. Along with biological applications, this microscope also supports Department of Energy (DOE) programs in Nanoscience. In particular, one component of the DOE sponsored Center for Integrated Nanotechnology (CINT) at Los Alamos and Sandia National Laboratories is the development of new state of the art instrumentation for nanomaterials characterization. The microscope we are building will be of use in CINT projects involving characterization of soft and composite nanomaterials and new fluorescent nanoprobes, such as quantum dots or noble metal nanoclusters. This project is developing/testing a new method of obtaining three dimensional, spectrally resolved data and benefits from a relatively simple optical design. Such a system can be readily transported/used in other environments/settings and may also be of use in Laboratory efforts in remote sensing.

References

1. Stich, D. G., M. S. DeVore, C. Cleyrat, M. L. Phipps, B. S. Wilson, P. M. Goodwin, and J. H. Werner. Advancing 3D Single Molecule Tracking by Time-Gating and Fast Simultaneous Spinning Disk Imaging for Contextual Information. 2016. Biophysical Journal. 3 (110): 632a.

2. Prevedel, R., Y. Yoon, M. Hoffmann, N. Pak, G. Wetzstein, S. Kato, T. Schrodel, R. Raskar, M. Zimmer, E. S. Boyden, and others. Simultaneous whole-animal 3D imaging of neuronal activity using light-field microscopy. 2014. Nature methods. 11 (7): 727.

Publications

Stitch, D. G., M. S. DeVore, C. Cleyrat, M. L. Phipps, B. S. Wilson, P. M. Goodwin, and J. H. Werner. Advancing 3D Single Molecule Tracking by Time-Gating and Fast Simultaneous Spinning Disk Imaging for Contextual Information. 2016. Biophysical Journal. 3 (110): 632a.

Information Science & Technology

Scalable Codesign Performance Prediction for Computational Physics

Stephan J. Eidenbenz
20150098DR

Introduction

We will develop a performance-prediction capability that relies on modeling architectural and algorithmic details of a computational-physics code running on a specified high-performance computing (HPC) architecture. This capability will fundamentally benefit a large number of HPC code projects by providing techniques for rapid evaluation of novel algorithmic ideas; rapid evaluation of middleware "mapping" concepts; optimizing method & architecture parameters for performance; and perhaps most intriguing semi-automated code generation for crucial subroutines. After the project ends, the performance prediction capability will be useable with minimal additional effort for other computational physics domains and architectures of the generations after next, and for decision support in HPC platform procurement to test vendor proposals against request specifications.

Building the performance prediction capability is our first goal, which will have a focus on models for state-of-the-art and conjectured architectures. Our second goal is to use the capability to assess novel solutions to the key exa-scale challenges of the data motion/movement, high-parallelism, and fault tolerance applied to radiation transport and hydrodynamics methods.

Our initial algorithmic ideas that we will develop, model and assess for the applications include: Determining optimal ways to hide communication and/or memory latencies on specific devices for discrete ordinates mesh sweeps and analyzing tradeoffs of non-sweep-based algorithms that increase independent work units and data movement for deterministic radiation transport. Models of the random access of memory and stochastic work generation of a Monte Carlo fixed source calculation and various approaches to task-based parallelism for stochastic radiation transport. Rapid analysis of tree-code algorithms on different architectures for hydrodynamics.

An initial set of middleware technologies that we will develop includes: Polyhedral optimization methods to minimize data motion, load-balancing schemes vs. data movement requirements, static graph-based automated parallelization approach for innermost loop computations of physics domain codes, Just-In-Time Parallelization schemes and alternatives to checkpoint-restart paradigm for failure tolerance.

Benefit to National Security Missions

Our future computational physics code base for hydrodynamics and radiation transport are of fundamental importance to DOE and LANL. Maintaining LANL's leadership role in national security will depend on our ability to consistently provide performance improvement in our codes for emerging architectures. Additionally, these techniques will be applicable to other application domains, in particular climate simulations and large-scale infrastructure simulations. Previous work related to AMD resulted in a successful transition of that project to the DOE Office of Science BES, which will now support the implementation and physics discovery work. Similarly in this project: If we are successful at identifying algorithmic variations with substantial predicted performance gains, programmatic sources, e.g., ASC, may be willing to support follow-on code development made possible by a successful LDRD project.

Progress

During FY16, we made substantial progress towards our goals:

- The SNAPSim application was validated against both serial and MPI based parallel runs on Cielo's hardware architecture. Several improvements to the hardware cache model have been implemented to achieve this goal.
- We are currently working towards the validation of Parallel Block Jacobi (PBJ) methods on Cielo's hardware. It is our expectation that the prior successful

validation of SNAPSim will pave the way to faster simulation app development for the PBJ method.

- A Simian discrete event simulation model for GPU hardware was developed using published facts about the NVidia GPU architecture. With this model which was first validated against available GPUs, we have been able to predict the expected performance boosts for the next generation NVidia GPU which has not been commercially released yet. This work was given the best paper award at the ValueTools conference held during Dec 2015.
- A middle-ware Simian model was implemented for MPI communication, and validated it against several supercomputer interconnect topologies. This work was presented at the PADS'16 conference. The MPI model has already been integrated with the SNAPSim application model.
- We developed a comprehensive suite of benchmarks to evaluate parallel discrete event simulation (PDES) engines. This was in response to a previous PDES community challenge.
- The LaPDES benchmarks were implemented for ROSS simulator and compared against our Simian PDES engine. The results showed that Simian is more than 5x better performing at higher computational loads when compared to ROSS in either the conservative or the optimistic mode. The higher performance of Simian can be attributed to our use of state of the art Just In Time compilers.
- Simian in JavaScript, another popular JIT enabled language, was implemented so that we have independent implementations with identical APIs in three popular languages: Python, Lua and JavaScript. The JavaScript version has similar top-of-class event-rate performance as the Lua version of Simian. In addition, JavaScript being a more popular language, it can potentially speed up adoption of Simian as the PDES platform of choice for a larger audience within the DoE complex. We now also have the capability to run Simin within all popular web-browsers with no change in the user model - this has applications in developing demos and educational tools using Simian as the PDES engine.
- We implemented a Python version of Simian which can run substantially faster (up to 100x) on GPU enabled clusters.
- Starting Feb 2016 we will perform preliminary work towards developing novel accelerated hardware architectures to speed up atomistic molecular dynamics (MD) methods. We have started work towards accomplishing the preliminary goals: several tools were developed to perform Spice characterization of the semiconductor device models at the field-effect transistor level, as well as for performing layout, placement and routing, as well as graphical visualization of nanometer sized semiconductor components on a given Silicon area budget. Verilog hardware description language models have been written for around half of the total expected component modules which will eventually be used as building blocks within the MD acceleration microchip which is being designed by us. We have also procured a small re-configurable hardware (known as FPGA) test platform to validate some of the individual modules being designed.

Future Work

For FY17 (year three of the DR), we will continue to expand the portfolio of hardware and software and middleware models within our Performance Prediction Toolkit (PPT). We consider our work going forward as categorized into three broader tasks:

1. Continue to add more features to the hardware models that describe the function of relevant architectures, including internode data movement (interconnect modeling), intranode data movement (memory hierarchy and cache structure modeling), failure resilience, and power consumption. Each new addition to the hardware modeling framework will be generalized and parameterized for simple extension to different architectures.
2. Expand our catalog of physics application domains to include stochastic radiative transport. Consider the inclusion of different computational kernels associated with radiative transport and hydrodynamics applications to ensure we are capturing all the relevant computational challenges associated with these types of numerical simulations. Begin exploring parallel solution algorithmic alternatives and their suitability for our existing suite of hardware models. We also will add models for hydrodynamics codes as well as Monte Carlo based methods.
3. Hardware and software model validation will be an important part of our third year activities. Ensuring that we have sound models will allow us to explore variations with confidence that alternatives are analyzed fairly and warrant further examination.

Conclusion

Based on results for different application domains and on preliminary analysis for transport and hydrodynamics, we anticipate to achieve at least one order of magnitude performance improvement for stochastic radiation transport codes as these codes have undergone few optimization efforts for current node designs of many cores and more complicated memory hierarchies. Deterministic radiation transport codes and smoothed particle

hydrodynamics codes have seen some optimization and we expect our models to predict another 2-3X improvement in performance.

Publications

Ahmed, K., M. Obaida, J. Liu, S. Eidenbenz, N. Santhi, and G. Chapuis. An Integrated Interconnection Network Model for Large-Scale Performance Prediction. 2016. Proceeding SIGSIM-PADS '16 Proceedings of the 2016 annual ACM Conference on SIGSIM Principles of Advanced Discrete Simulation. 2016 (1): 177.

Chapuis, G., S. Eidenbenz, N. Santhi, and E. J. Park. Simian integrated framework for parallel discrete event simulation on GPUs. 2015. In WinterSim 2015. (Huntington Beach, California, 6-9 Dec. 2015). Vol. Proc of the 2015 WSC, p. 1127. Huntington Beach, California: IEEE.

Chapuis, G., S. Eidenbenz, and N. Santhi. GPU Performance Prediction Through Parallel Discrete Event Simulation and Common Sense. 2015. In Valuetools 2015. (Berlin, Germany, 14-16 Dec. 2015). Vol. Proc 9th EAI PEMT Conf, p. 204. Berlin, Germany: ICST, Brussels.

Park, E. J., S. Eidenbenz, N. Santhi, G. Chapuis, and B. Settlemyer. Parameterized benchmarking of parallel discrete event simulation systems: communication, computation, and memory. 2015. In The Winter Simulation Conference. (Huntington Beach, CA, 6-9 Dec. 2015). Vol. Proc of the 2015 WSC, p. 2836. Huntington Beach, California: IEEE.

Santhi, N., S. Eidenbenz, and J. Liu. The Simian Concept: Parallel Discrete Event Simulation with Interpreted Languages. 2015. In 2015 Winter Simulation Conference. (Huntington Beach, CA, 6-9 Dec. 2015). Vol. Proc of the 2015 WSC, p. 3013. Huntington Beach, California: IEEE.

Zamora, R. J., A. F. Voter, D. Perez, N. Santhi, S. M. Mniszewski, S. Thulasidasan, and S. Eidenbenz. Discrete event performance prediction of speculatively parallel temperature-accelerated dynamics. 2016. Simulation: Transactions of the Society for Modeling and Simulation International. Online (Nov 2): -.

Cyberphysical Systems and Security

Scott N. Backhaus
20150215DR

Introduction

Many critical infrastructures, e.g., electric power grids and natural gas pipelines, are cyberphysical systems—physical networks whose flows are governed by the law of physics but are regulated by a control system coupled to cyber networks that transmit the information required to optimize and control the physical networks for reliability and efficiency. Crucial to the defense of cyberphysical systems is the concept of intrusion detection and localization, however, this is not sufficient. If a system is under attack, it cannot simply be brought down to purge the attacker. Doing so would grant the attacker his objectives, i.e. wide spread denial of the services from the cyberphysical network. A proportional response is required.

The overarching objective of this work is to develop advanced approaches to cyberphysical defense, which can be broken down into the following goals:

1. Detect and localize an attacker within the cyberphysical network without reference to a predefined attack vector. Attackers are creative and detection methodologies cannot be based on scripted attack scenarios.
2. Develop algorithms for proportional response and designing resilient cyberphysical networks—Proportional responses to attacks should weigh the estimated network degradation from the attack and the degradation caused by the response. Resilient cyberphysical designs will greatly improve this balance in favor of the cyberphysical operators.
3. Deploy, demonstrate and validate—The efficacy of cyberphysical intrusion detection and response methodologies will improve at much faster rates when their development and refinement is closely coupled with real-world experimentation that validates strengths and reveals weaknesses.

Benefit to National Security Missions

Cyberphysical systems are crucial to the reliable delivery of energy, water, and other resources, creating strong connections to LANL's National Security and Energy Security missions including those US Government agencies that monitor, analyze, or develop technology for critical infrastructure, e.g. DOE Office of Electricity, DOE Energy Efficiency and Renewable Energy, DOE Fossil Energy, and Department of Homeland Security.

Cyberphysical systems are composed of interdependent complex networks described by disparate mathematical models creating scientific challenges that go well beyond the modeling and analysis of the individual networks. Integration of approaches from complex systems, statistical physics, machine learning, and optimization will create a holistic and uniquely LANL approach that is able to localize attacks and develop appropriately scaled proportional responses. Both DOE and DHS are creating and running new programs in cyberphysical systems a creating significant programmatic pull. Many efforts in these programs are based on best practices or standard engineering analyses. Our approach based on the science of complex networks and probabilistic methods will advanced detection and defense capabilities to the US Government agencies identified above. Components of the NNSA Complex, including our own Laboratory, are cyberphysical systems with complex security issues, and this work will build capabilities for protecting the Complex.

Progress

Instrumentation and collection of NSSB HVAC communication system data

We completed our planned partial implementation of an instrumentation and data collection system for the HVAC communication system in the NSSB. We purchased and installed custom hardware and software to monitor and record data packets on the low-voltage communication

system that generates settings for and takes measurements of the building control devices. Working together with building maintenance engineers we decoded the data packets and used them to correlate with our other data streams of physical building measurements. The combination of these two signal time series data sets are enabling us to test our developed methodologies on real-world systems to ensure they are accurate and relevant.

Methodology for aligning time series

The data collection from the HVAC communication system generates time series of values from various building systems that measure diverse information such as temperature, air flows, valve angles, and fan speeds. In order to use these data streams for detection of anomalous behavior (faults or attacks) a method for establishing normal behavior was developed for the time series. The methodology is based on a continuous profile model approach to align and normalize the data using hidden Markov models. This approach is applicable to a wide variety of cyberphysical systems and allows computing residual (error) values from normal to enable anomaly detection methods.

Algorithms for detection of anomalies in cyberphysical systems

We developed a set of methods for detection and localization of failures in cyber-physical systems based on the analysis of correlations between physical time series. First, we developed a simple procedure for constructing a special correlation matrix out of detrended heterogeneous signals, making some assumptions on the anomaly signature we would like to be able to capture. Then, we used the correlation matrix to solve three crucial tasks: detection of the anomaly using spectral methods; localization of a subset of anomalous nodes within the system using low-rank approximations and biclustering methods, and identification of the functional role of the inferred anomaly based on the sensor labels. We validated our framework on experimental real-world data collected from the LANL NSSB building automation system.

Future Work

Milestones to be reached by end of FY17 include:

- Instrument remaining 3/4 HVAC communication hubs in the NSSB to complete testbed
- Design, develop, and execute full-building NSSB testbed intrusion detection experiments
- Extend mathematical algorithms to detect intrusions using full or partial data from combined physical and communications data from testbed experiments
- Develop machine learning algorithms for identifying features of anomalies in multi-modal testbed data time series

Conclusion

Information theory: We will develop algorithms for online learning of graphical models using operational time-series data collected from sparse measurements on cyberphysical systems.

Experimental validation: We will develop a unique cyber-physical test bed where we will deploy and test the tools and methods developed in the information theoretic and optimization thrusts.

Publications

Lokhov, A. Y., N. Lemons, T. C. McAndrew, A. Hagberg, and S. Backhaus. Detection of faults and intrusions in cyber-physical systems from physical correlations. 2016. arXiv preprint arXiv:1602.06604.

Hybrid Quantum-Classical Computing

Rolando D. Somma
20160069DR

Introduction

Recent breakthroughs in quantum technologies have proven extremely useful for solving certain problems with dramatic computational speeds, outperforming today's computers by a large margin. These devices, exemplified by D-Wave's "quantum annealer", begin to fulfill the promise of quantum computation. They implement a quantum-classical algorithm designed to simulate physical systems related to optimization problems, with applications from materials science to national security. In contrast to standard algorithms, quantum annealers exploit fundamental properties of quantum physics for fast problem solving.

The main goal of "Hybrid Quantum-Classical Computing" (HQCC) is to investigate, theoretically and experimentally, the performance potential of quantum annealers. Specifically, HQCC will 1- develop new algorithms for challenging optimization problems, 2- develop methods for benchmarking quantum annealers based on the dynamics of phase transitions, 3- develop a quantum programming compiler (QPC), and 4- conduct laboratory experiments of quantum annealing on physical systems that are ubiquitous in optimization. To this end, HQCC will develop advanced numerical tools for simulating physical systems that model quantum annealers. These numerical tools and the D-Wave device will then be used to solve optimization problems and for benchmarking. The QPC will transform classical computer code into a form suitable for a quantum annealer. The experiments will allow us to study dynamics of phase transitions that will play an important role in the efficiency of quantum annealers at very large scales, which are currently out of reach.

While previous work has investigated only ideal quantum systems, HQCC will be the first systematic study of physically realizable quantum computing technologies in optimization. Results from HQCC benchmarks and experiments will also be paramount in the design of future computing architectures. The QPC will move quantum programming from the realm of experts to a form accessible by lay programmers. HQCC will then enhance LANL's leadership in IS&T by exploiting an opportunity to collaborate with industry (Google).

Benefit to National Security Missions

Quantum-computing algorithms for optimization do have vast applications and potentially tie to several missions.

- Quantum computing technologies meet computational requirements in support of DOE's science mission (see: http://www.csm.ornl.gov/workshops/ascrqcs2015/)
- Quantum computing technologies provide novel capabilities to support Air Force research (see: https://www.fbo.gov/index?s=opportunity&mode=form&id=a93ff99b1850e9874fc0c0dfea99348a&tab=core&_cview=0)
- Quantum computing's ability to rapidly solve optimization programs makes it applicable to the ASC program. Team members are also exploring a way to use DWave to optimize the xRAGE code used for hydrodynamics considering the memory requirements of (phase II) Trinity.
- NASA, through the NASA Quantum Artificial Intelligence Laboratory, provides the space agency's hub for an experiment to assess the potential of quantum computers to perform calculations that are central in aerospace, earth sciences, and space exploration (see: http://www.nas.nasa.gov/quantum/)
- IARPA has several programs that fund quantum computing research (e.g., see: http://www.iarpa.gov/index.php/research-programs/csq)
- The development of new Monte Carlo algorithms is expected to find applications in many other areas.

DOE Office of Science supports various programs where quantum Monte Carlo techniques play an important role.

Progress

Computer Science (Tasks 1,2,5 in proposed work)
We have been investigating techniques for mapping problems onto the DWave architecture, to make programming this unusual hardware more approachable by classically trained programmers. To date, we developed a "quantum macro assembler" called QASM. QASM is a building block for future research that enables D-Wave programs to be described in terms of their logical rather than physical characteristics. QASM lets programmers name qubits symbolically, like "best" or "total", instead of by physical location, like "the qubit in the third row of the left partition of the unit cell that's five cells across and two cells down". QASM lets programmers define reusable blocks of code rather than having to manually replicate patterns of qubits. And QASM lets programmers express arbitrary inter-qubit interactions, which it then maps to the limited set of inter-qubit interactions supported by the underlying hardware.

We applied for and received approval (LA-CC-16-028, LA-CC-16-032, and LA-CC-16-033) for releasing the software being developed during this project under various open-source licenses. No software has yet been released, but we expect soon to do a public release of QASM. D-Wave Systems, Inc. is considering including a presentation of QASM in the hands-on advanced programming tutorial they give to their current and potential customers.

We developed new quantum computing algorithms for optimization that provide significant speedups with respect to known algorithms for these problems. The improvement in terms of precision is exponential and is polynomial in terms of the dimension of the configuration space. Such quantum algorithms require of a universal quantum computer and are not DWave implementable.

Numerical Methods (Task 3 in proposed work)
We are developing numerical methods to simulate the so-called quantum Linblad equation for open quantum systems. Of particular interest is to develop a method to simulate DWave under realistic decoherent processes. We already found a way to make our method efficient for simulating the Ising chain; this is a major step forward, since simulating the Lindblad equation usually takes exponential time. We are writing the code and looking for ways of parallelizing to simulate order of 100's of qubits, which is impossible to do with current techniques. Our methods will provide insight into the inner workings and the physics that dominates quantum annealing in DWave.

Phase Transitions in Quantum Annealing and Decoherence (Task 4 in proposed work)
We conducted studies of the scaling of the Kibble Zurek mechanism (KZM) in Ising systems similar to those of DWave. KZM dictates the number of "defects" that show up during a phase transition and can be related to how suboptimal solutions of optimization problems are.

New quantum master equations were derived to simulate the processes involved in DWave through its interactions with the environment. We sketched an algorithm to simulate these processes that is suitable for low rank density matrices. This method is more general than that of point B, but is less efficient. We are analyzing the effects of spectral gaps using adiabatic perturbation theory, to obtain better error bounds for how the quantum annealing time as a function of the system size.

DWave Simulations and Benchmarking (Task 5 in proposed work)
A very large number of simulations were executed in DWave and compared results with those of numerical simulations of an ideal quantum annealer. We found that DWave results are significantly different (see point B). Results from DWave simulations allowed us to characterize its error rates, i.e., how far are the DWave solutions from the optimal one. We realized that maximizing coupling strengths is key when encoding optimization problems into DWave- otherwise the results can be extremely noisy. We are now moving towards the simulation of frustrated systems, which resemble computationally hard optimization problems.

Experiments (Task 6 in proposed work)
To conduct quantum-annealing experiments in materials that resemble optimization problems in the large size limit, we designed and built a probe to perform magnetic experiments in pulsed high magnetic fields. This setup has the necessary rotation axis to achieve quantum annealing. Similar to DWave, these materials are magnets that correspond to Ising models but are not programmable. Our initial experiments on $Ca_3Co_2O_6$ revealed problems with both the probe and the quality of the crystals. Thus we requested new crystals from collaborators, which we are in the process of characterizing. In the near future, we will also attempt quantum annealing on another newly-discovered system: $Fe_2Mo_3O_8$ with different Zn dopings that can control magnetic remnant properties.

Future Work

Hybrid Quantum-Classical Computing (HQCC) will investigate and exploit the potential of available quantum-computing technologies in the context of hard optimiza-

tion problems. HQCC algorithms are based on the idea of quantum annealing, which requires several steps for their implementation. In FY17, HQCC will mainly establish a basis for methods and experiments. Specifically, in FY17 HQCC will:

- Develop and analyze different techniques to encode optimization problems in the architectures of currently available (D-Wave) quantum annealers,
- Use these techniques towards building a so-called quantum programming compiler, which is a method to transform classical code into an optimization problem suitable for a quantum annealer,
- Continue the development of classical numerical methods based on various diagonalization techniques to simulate quantum Ising systems, which are the systems that model quantum annealers,
- Use those numerical methods to analyze the interplay between physical phenomena, such as phase transitions, and the performance of quantum annealers,
- Continue work on quantum-annealing algorithms that avoid undesired complexities and are especially suited for frustrated models,
- Continue establishing the experimental setup at the NHMFL for quantum annealing experiments,

To accomplish these goals we will hold regular meetings to report progress and for collaborations. Provided that certain goals are met before the end of FY17, we will continue with D-Wave executions of some of our algorithms for benchmarking and for studying the power of DWave. As HQCC progresses, results and accomplishments are still expected to be published in peer-reviewed journals and presented at conferences, as we did during FY16.

Conclusion

"Hybrid Quantum-Classical Computing" (HQCC) provides the potential for orders-of-magnitude faster computation than is possible by today's computers. The main goal is to investigate the computing power of physically realizable quantum annealers, exemplified by a D-Wave's device. HQCC will deliver powerful algorithms for optimization, with potential applications that range from materials science to national security. These algorithms will be implemented in an available (D-Wave) quantum annealer and on conventional computers, using advanced numerical methods that simulate quantum annealers. HQCC will also conduct quantum annealing experiments, which will allow us to study the physical phenomena that can impact the efficiency of quantum annealers at very large scales.

Publications

Chikara, S., J. Singleton, D. Yarotski, N. Lee, H. Y. Choi, and V. Zapf. Electric polarization observed in single crystals of multiferroic Lu2MnCoO6. 2016. Physical Review B. 93: 180405 (R).

Daniels, M.. A programmable embedder. 2016. dwave.lanl.gov.

Francuz, A., J. Dziarmaga, B. Gardas, and W. H. Zurek. Space and time renormalization in phase transition dynamics. 2016. Physical Review B. 93: 075134.

Mun, E., F. Weickert, J. Kim, B. L. Scott, C. Miclea, R. Movshovich, J. Wilcox, J. Manson, and V. Zapf. Partially disordered antiferromagnetism and multiferroic behavior in a frustrated Ising system, CoCl2-2SC(NH2)2. 2016. Physical Review B. : 104407.

Pakin, S.. A quantum macro assembler. To appear in In Proceedings of the 20th Annual IEEE High Performance Extreme Computing Conference (HPEC 2016). (Waltham, Massachusetts, 13-15 Sep. 2016).

Somma, R., and A. Chowdhury. Quantum algorithms for Gibbs sampling and hitting-time estimation. To appear in Quantum Information and Computation.

Somma, R., and S. Boixo. Quantum algorithms for simulated annealing. 2015. arXiv.

Information-Driven Materials Discovery and Design

Turab Lookman
20140013DR

Abstract

The goal of this project was to demonstrate accelerated materials discovery by integrating the state- of-the-art statistical inference and optimization tools in order to find materials with desired or targeted properties. We proposed a data-centric approach as well as a knowledge-based approach to narrow the search space for improved prediction by teasing out hidden information that is present in the data for known materials. Until very recently, new materials have almost exclusively been discovered by intuition and costly trial and error. However, over the last 3-4 years, the use of statistical inference tools has begun to define the new field of materials informatics and this LDRD-DR has been at the cutting edge of this world-wide effort.. Our key innovation has been an integrated design loop - an excellent example of the paradigm of codesign. We have used tools from the fields of pattern recognition, operations research and bioinformatics, and applied them in a unique way to guide experiments and calculations to find materials. We have discovered new materials that otherwise would not have been possible because of the vast search space. These have included new NiTi-based shape memory alloys with the smallest thermal hysteresis, as well as lead-free piezoelectrics with the desired property of a temperature insensitive morphotropic phase boundary. We have also predicted the existence of new functional materials with novel properties and await for synthesis experts to validate our findings.

Background and Research Objectives

It has become increasingly clear over the last few years (e.g. DOE and NSF initiatives), in a range of domain sciences from drug discovery, biofuels and cancer genomics to materials science and advanced manufacturing, that there is a great need to learn from data and design approaches that seek optimal targeted solutions as efficiently as possible with minimal costs. Although some of the domain sciences may have only recently awakened to the concept of accelerating discovery and design, many of the tools and approaches that can potentially enable this task have been in the literature for several years. However, they have been spread across diverse fields spanning operations research, optimization, computer science and statistics and one of the challenges for the domain expert is how to bridge this divide. Industry and cancer genomics (bioinformatics) have been far more pioneering in the application and development of these tools than other fields (e.g. materials science). Yet, they are key to future innovation and productivity and afford LANL new opportunities to capitalize. Thus, the goal of this project was to demonstrate accelerated materials discovery by integrating the state- of-the-art statistical inference and optimization tools in order to find materials with desired or targeted properties. The challenge was very much to show how codesign could work in the materials context, very uncharted waters. Until very recently, new materials have almost exclusively been discovered by intuition and costly trial and error. Our work is a departure by applying informatics to materials science in a unique way.

Our approach was initially data-centric approach in order to narrow the search space for improved prediction by teasing out hidden information that is present in the data for known materials. Towards the end we also explored how materials knowledge, in the form of theory, could be incorporated within a probabilistic or Bayesian approach. Our key innovation was the integrated design loop for discovery of Figure 1 as a means to find materials with desired or target properties. Although we studied various materials in this LDRD, our focus in terms of design and the loop of Figure 1 was on the class of functional materials known as ferroics, of which shape memory alloys and piezoelectrics are examples. These are materials of extreme interest to industry and one of our key objectives related to finding new compounds with enhanced properties. Our second objective was to study how informatics or machine learning methods in general can be applied to a range of materials problems.

Such problems involve classification, that is, predicting materials that belong to a given class or have a given label, or regression, predicting materials with seemingly "best" properties. Note the distinction between this and the design question, which focuses on iteratively guiding experiments to find materials with desired properties.

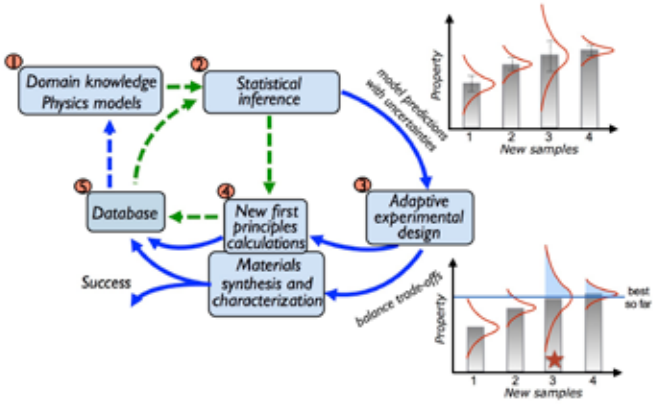

Figure 1. The design loop for accelerated discovery. Uncertainties in predictions drive the exploration in the vast search space.

Scientific Approach and Accomplishments

The work has resulted in 5 marquee papers (1 Nature Comm published and news releases, 1 Nature Comm in final review stage, 1 PNAS in final review). In addition, we will have published over 25 journal papers, four book chapters and 1 book. We had no prior expertise in this field at the start of the DR, but have moved into a position of leadership in the field. We briefly describe our major discoveries and then summarize other work. A substantial amount of work is still on-going and incomplete.

Figure 2 shows the design loop we executed in practice for our key discovery, namely, a new NiTi-based multicomponent alloy with a very small thermal hysteresis. We iterated the loop 9 times and in each iteration we predicted and synthesized 4 compounds. Of the 36 compounds so fabricated, the best alloy had a thermal hysteresis of 1.85K, a 42% improvement over the best in our training data. In all, 14 new compounds had a thermal hysteresis better than the best in the training data. This points to the efficacy of our loop and with a Fisher p index < .001, suggests that the probability of making this discovery by chance is very low. Although we didn't design for it, our new compound had a transition temperature in a very desirable range just above room temperature. It pointed to the need for performing multiobjective optimization and we have been implementing an appropriate strategy for this. At time of writing this work is still underway and is not completed. Beyond merely optimization, our density functional theory calculations provided insights as to why this composition has the desired low thermal hysteresis. It is because the Fe composition is tuned to an optimal value based on energetics and stability.

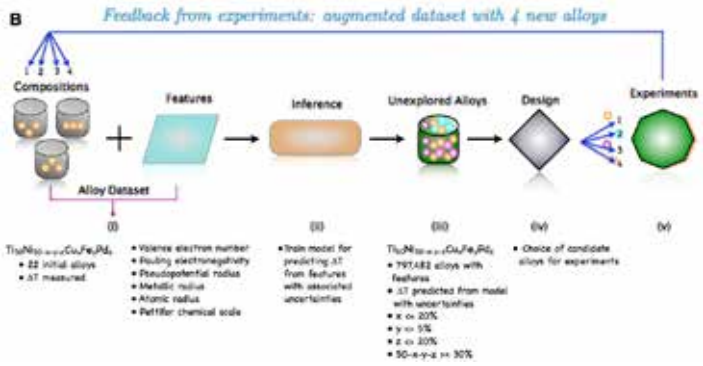

Figure 2. The design loop in practice for finding new NiTi-based alloys. Four experiments are suggested at a time and the data base is augmented with the findings for the newly synthesized materials.

Our second key discovery is a new Pb-free piezoelectric with a more vertical morphotropic phase boundary (MPB) (temperature insensitivity) than any BaTiO3 based piezoelectric known. Piezoelectrics are materials that produce a large strain if an electric field is applied, or a large polarization if stress is applied. The need is to find materials with a large response as they have numerous applications, from energy harvesting devices to sensors. Our design criterion for this work was to find a piezoelectric with a more vertical MPB as the piezoelectric response has been believed to be associated with how vertical the MPB is and controls how insensitive the response to temperature. In this regard the best-known piezoelectric, Lead Zirconate, is a prototypical example with an almost vertical MPB. In this work we utilized Landau theory to show how existing knowledge could be used in a Bayesian framework to predict posterior distributions, making use of the training data (Figure 3). This work thus went beyond a purely data-driven approach. The work predicted the new piezoelectric (Ba0.5Ca0.5)TiO3-Ba(Ti0.7Zr0.3)O3. As Figure 4 illustrates, although we achieved our design target (a 15% improvement), the piezoelectric response itself was relatively low. This therefore points to the need for optimizing both the verticality of the MPB and the piezoelectric response. This is ongoing work.

Our third marquee paper is an example of learning from data to design functional materials using computational and analysis. We predict in a data mining guided ab initio protocol to accelerate the design and discovery of non-centrosymmetric (NCS) materials. Our approach scaffolds applied group theory, informatics, and density functional theory (DFT) to uncover symmetry-chemistry-stability guidelines for computational design, which we applied to the A2BO4 Ruddlesden-Popper (RP) family. Informatics-

based inference tools (e.g. classification learning) were utilized to learn from available data on this crystal family, enabling formulation of design rules to identify candidate chemical compositions that fulfill the group theoretical postulates. Key to the success of this protocol was the use of machine learning methods to overcome the challenge of learning from small and imbalanced crystal-chemistry data sets ubiquitous in materials science. Informatics identifies 246 new compositions after screening 3,200 compounds with potential for NCS structures in bulk RP oxides, which is a 25-fold increase in the projected number of NCS materials from what was previously known. We validated our predictions for RP stannates, zirconates, hafnates and ruthenates using electronic structure calculations and confirmed the dynamical stability of the NCS ground state structures. The approach is very general and enables rational design and engineering of both crystal structures and functionalities, including (multi) ferroic properties, opto-electronic properties and non-linear optical responses.

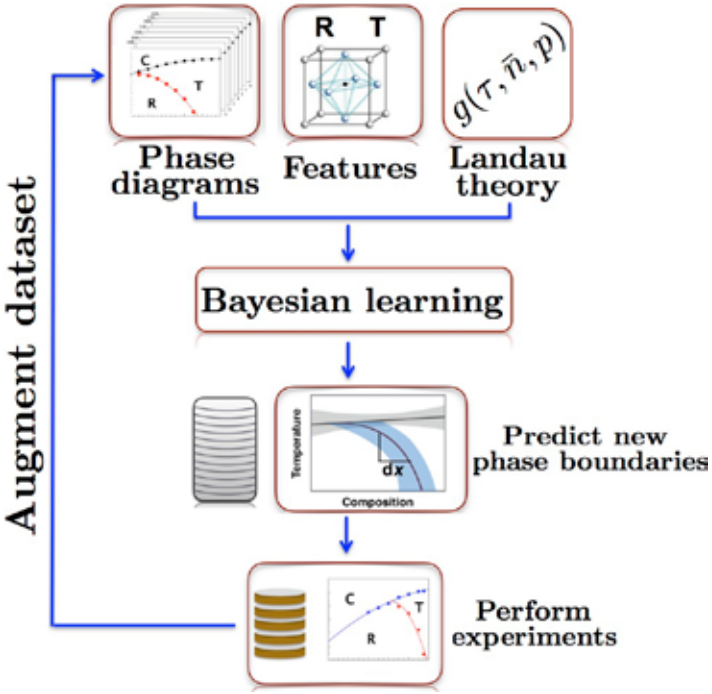

Figure 3. The design loop for piezoelectrics that incorporates Landau functional relationships in the learning.

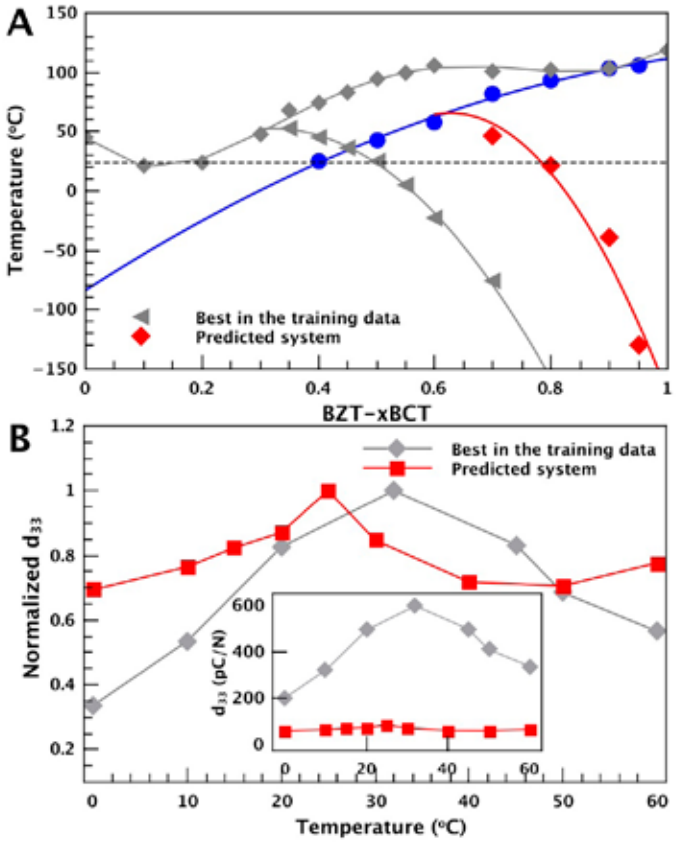

Figure 4. A comparison of the best piezoelectric in the training set versus the newly discovered compound with a more vertical phase boundary (15% improvement). The lower panel compares the normalized piezoelectric response, which is good. However, the inset shows that absolute piezoelectric coefficient or response is very low. This points to the need for multi objective optimization where the phase boundary shape and response are maximized.

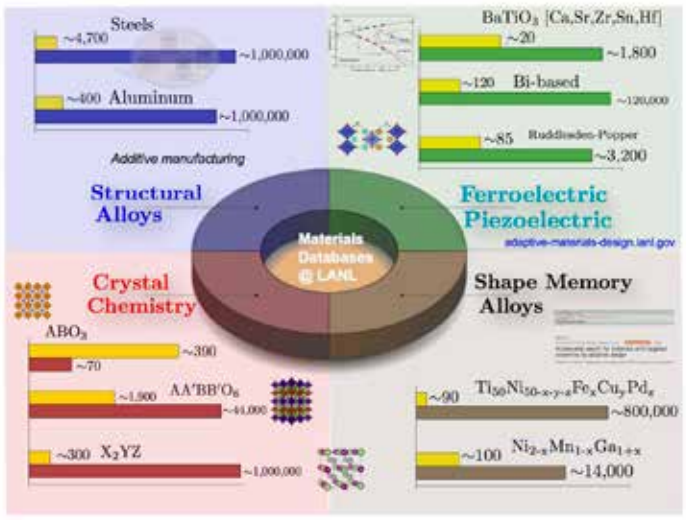

Figure 5. Databases in various materials classes assembled at LANL over the course of the LDRD.

We now summarize the breadth and importance of our other publications. Our key innovation has been to show how design with inference provides a recipe for discovery in materials science. In this regard, our benchmark work was published in [1] where we showed how uncertainties are fundamental to balancing the trade-off between exploration and exploitation to rank which materials should be explored next. We demonstrated our methodology on a data set from the literature on MAX compounds with the objective of finding the best material in as few iterations as possible. Essentially the same algorithm was also used in our work showing how to use an industry standard semiconducting materials code (APSYS) to design better Light Emitting diodes.

In order to learn for ourselves the scope of existing informatics methods and the innovations we needed to develop for materials, we also focused on solving classic materials problems studied in the last few years by the materials/ condensed matter community. These included classifying AB sp-bonded octet solids with six-fold coordinated rocksalt or four-fold coordinated zincblende/ wurtzite first studied in the 1970s. The idea is to construct two-dimensional maps to classify the AB compounds and we revisited this from a statistical learning perspective using classifiers such as decision trees and support vector machines to estimate the average classification accuracy and the associated model variance where a decision boundary is learned in a supervised manner. Our work has led to the importance of new material descriptors or features, such as the effective Born charge, for these problems. We have also studied a range of materials regression problems, from melting temperatures of solids to dielectric constants and band gaps of polymers, using machine learning tools such as kernel ridge and support vector regression as well as Bayesian-based Gaussian process models.

We have been responsible for generating unique and extensive databases on various materials classes (Figure 5) for the community. Some of these databases list over a million compounds of predicted properties. They were assembled from extensive literature searches of experimental data. For example, our inorganic perovskite database is unique in compiling all known experimentally validated perovskite compounds. No other databases (including Materials Project, AFLOWLIB or OQMD) are complete in this regard.

This work has not only focused on learning from data, but it has also demonstrated innovation in integrating physics based models with machine learning, for LED structures, shape memory alloys and for Landau-Ginzburg studies of pattern formation applicable to many systems. We have also contributed to innovation on the informatics side as well as introducing novel developments in optimal design from the cancer genomics community into materials science.

Finally, we have organized two international conferences, written a book (with a second book due out in 2017) and written reviews on materials informatics and design.

In summary, we set out to establish a paradigm for addressing complex optimization and discovery problems in materials science that include choices to incorporate domain knowledge. Further, we will have developed tools and algorithms to deal with error estimation with experimental design. Our success can be measured by our discovery of new materials with desired properties and greater insight into the dominant mechanisms (structure-property relationships) underlying materials phenomena.

Impact on National Missions

Accelerated materials discovery is of strategic importance and relevance to DOE/SC and national (e.g. MGI, ICAM) initiatives. Moreover, the development of information science predictive tools to enable accelerated materials discovery is key to this task. These tools are based on machine learning and optimization methods and are central to minimizing the number of complex experiments and calculations that need to be performed to obtain targeted solutions. LANL is a materials-centric laboratory and therefore the tools we have developed are of direct mission relevance. They can be also applied to many other areas, such as the National Cancer Initiative or biofuel research where the challenge is to seek parameters to optimize yield. The specific class of materials we have focused on (such as shape memory alloys, piezoelectrics and polymer dielectrics) are of direct interest to DOE/SC as they find applications as sensors and energy harvesting and storage devices. The design loop we propose is also an example of the paradigm of codesign (which is gaining greater traction within DOE, for example,) - where learning a “model” is performed iteratively guided by experiments and data.

References

1. Balachandran, P. V., D. Xue, J. Theiler, J. Hogden, and T. Lookman. Adaptive Strategies for Materials Design using Uncertainties. 2016. Scientific Reports. 6: 19660.

Publications

Information Science for Materials Discovery and Design. 2015.

Data Science and Optimal Learning for Materials Discovery and Design. Invited presentation at Data Science and Optimal Learning for Materials Discovery and Design. (Santa Fe, NM, USA, 16-18 May 2016).

Information Science for Materials Discovery and Design. Invited presentation at Information Science for Materials Discovery and Design. (Santa Fe, NM, USA, 4-7 Feb 2014).

Alexander, F. J., and T. Lookman. Novel Approaches to Statistical Learning in Materials Science. 2013. In Informatics for Materials Science and Engineering: Data-driven Discovery for Accelerated Experimentation and Application. Edited by Krishna, R.. Vol. 37, p. 37. London: Elsevier.

Balachandran, P. V., D. Xue, J. Theiler, J. Hogden, and T. Lookman. Adaptive Strategies for Materials Design using Uncertainties. 2016. Scientific Reports. 6: 19660.

Balachandran, P. V., J. Theiler, and J. M. Rondinelli. Materials Prediction via Classification Learning. 2015. SCIENTIFIC REPORTS. 5: 13285.

Balachandran, P. V., J. Young, T. Lookman, and J. M. Rondinelli. Learning from Data to Design Functional Materials without Inversion Symmetry . To appear in Nature Communications.

Balachandran, P. V., N. A. Benedek, and J. M. Rondinelli. Symmetry-adapted Distortion Modes as Descriptors for Materials Informatics. 2015. In Information Science for Materials Discovery and Design. Edited by Lookman, T., F. J. Alexander , and K. Rajan. , p. 213. Berlin: Springer-Verlag.

Balachandran, P., D. Xue, and T. Lookman. Structure--Curie temperature relationships in BaTiO 3-based ferroelectric perovskites: Anomalous behavior of (Ba, Cd) TiO 3 from DFT, statistical inference, and experiments. 2016. Physical Review B. 93 (14): 144111.

Dehghannasiri, R., D. Xue, P. V. Balachandran, M. R. Yousefi, L. A. Dalton, T. Lookman, and E. R. Dougherty. Optimal Experimental Design for Materials Discovery . To appear in Computational Materials Science, Elsevier.

Gubernatis, J.. Data Visualization and Structure Identification. 2014. LA-UR-14-22628.

Lookman, T.. Heterogeneities, The Mesoscale and Multifunctional Materials Codesign: Insights and Challenges. 2014. In Mescoscopic Phenomena in Multifunctional Materials, Springer Series in Materials Science . Vol. 198, p. 57. Berlin: Springer-Verlag.

Lookman, T., B. V. Balachandran, D. Xue, G. Pilania, T. Shearman, J. Theiler, J. E. Gubernatis, J. Hogden, K. Barros, E. BenNaim, and F. J. Alexander. A Perspective on Materials Informatics: State-of-the-Art and Challenges. 2015. In Information Science for Materials Discovery and Design. Edited by Lookman, T., F. J. Alexander, and K. Rajan. , p. 3. Berlin: Springer-Verlag.

Lookman, T., F. J. Alexander, and A. R. Bishop. Perspective: Codesign for materials science: An optimal learning approach. 2016. APL Materials. 4 (5): 053501.

Lookman, T., P. V. Balachandran, D. Xue, J. Hogden, and J. Theiler. Statistical Inference and Adaptive Experimental Design for Materials. To appear in Current Opinion in Solid State and Materials Science .

Lubbers, N., K. Barros, and T. Lookman. Learning low-dimensional representations of textures using convolutional networks. Invited presentation at Physics Informed Machine Learning . (Santa Fe, NM, USA, 19-22 Jan 2016).

Mannodi-Kanakkithodi, A., G. Pilania, J. E. Gubernatis, and T. Lookman . A Multi-objective Optimization Technique to Model the Pareto Front of Organic Dielectric Polymers. 2016. Comp. Mat. Sci.. 125: 92.

Mannodi-Kanakkithodi, A., G. Pilania, T. D. Huan, T. Lookman, and R. Ramprasad. Machine learning strategy for accelerated design of polymer dielectrics. 2016. Scientific reports. 6: 20952.

Pilania, G., A. Mannodi-Kanakkithodi, B. P. Uberuaga, R. Ramprasad, J. E. Gubernatis, and T. Lookman. Machine learning bandgaps of double perovskites. 2016. Scientific reports. 6: 19375.

Pilania, G., J. E. Gubernatis, and T. Lookman. Structure classification and melting temperature prediction in octet AB solids via machine learning. 2015. PHYSICAL REVIEW B . 91 (21): 214302.

Pilania, G., J. Gubernatis, and T. Lookman . Classification of octet AB-type binary compounds using dynamical charges: A materials informatics perspective. 2015. Scientific Reports. 5: 17504.

Pilania, G., P. V. Balachandran, J. E. Gubernatis, and T. Lookman. Classification of ABO3 perovskite solids: a machine learning study. 2015. Acta Crystallographica, Section B: Structural Science, Crystal Engineering and Materials. 71 (5): 507.

Pilania, G., P. V. Balachandran, K. Chiho, and T. Lookman. Finding New Perovskite Halides via Machine learning. 2016. Frontiers in Materials. 3 (19): 19.

Pilania, G., and T. Lookman. Electronic structure and biaxial strain in RbHgF3 perovskite and hybrid improper ferroelectricity in (Na,Rb)Hg2 & (K,Rb)Hg2F6 superlattices. 2014. Phys. Rev. B. 90: 115121.

Rouet-Leduc, B., K. Barros, E. Cieren, V. Elango, C. Junghans, and T. Lookman. Spatial Adaptive Sampling in Multiscale Simulation. 2014. Computer Physics Communications. 185 (7): 1857.

Rouet-Leduc, B., K. Barros, T. Lookman, and C. J. Humphreys. Optimisation of GaN LEDs and the reduction of efficiency droop using active machine learning. 2016. Scientific Reports. 6: 0.

Taverniers, S., T. S. Haut, K. Barros, F. J. Alexander, and T. Lookman. Physics-based statistical learning approach to mesoscopic model selection. 2015. Physical Review E. 92 (5): 053301.

Theiler, J.. Selecting the Selector: Comparison of Update Rules for Global Optimization. To appear in Journal Statistical Analysis and Data Mining .

Theiler, J.. Anomaly testing. To appear in Data Analytics for Materials Characterization. Edited by DeGraf, M., J. Simmons, L. Drummy, and C. Bouman .

Theiler, J., B. Zimmer, P. V. Balachandran, J. Hogden, K. Barros, and T. Lookman. POSTER: Selecting the selector: using statistics to discover new materials. Invited presentation at CoDA (Conference on Data Analysis). (Santa Fe, NM, USA, 2016).

Xue, D., P. V. Balachandran, J. Hogden, J. Theiler, D. Xue, and T. Lookman. Accelerated search for materials with targeted properties by adaptive design. 2016. Nature Communications. 7: 11241.

Xue, D., P. V. Balachandran, R. Yuan, T. Hu, X. Qian, E. R. Dougherty, and T. Lookman. Accelerated search for BaTiO3-based piezoelectrics with vertical morphotropic phase boundary: synthesis guided by learning . To appear in Proceedings of National Academy of Sciences (PNAS) .

Zong, H., Z. Ni, X. Ding, T. Lookman, and J. Sun. Origin of low thermal hysteresis in shape memory alloy ultrathin films. 2016. Acta Materialia. 103: 407.

Next Generation Quantum Molecular Dynamics

Anders M. Niklasson
20140074DR

Abstract

Molecular dynamics (MD) simulations are a mainstay of computational chemistry, biology, and materials science. Quantum-based Born-Oppenheimer MD (QMD), where the interatomic forces are computed on the fly from the relaxed electronic ground state structure of the system, is the most accurate method available today. In this project we have provided novel solutions to the computational bottlenecks that have limited the widespread adoption of QMD in real world applications. Our strategy is based on a co-design effort, where we reformulate the theoretical framework to allow the design of new algorithms and data structures that can harness the processing power of modern computational architectures.

We have developed fast solvers and graph-based electronic structure theory that reconcile, for the first time, the computational efficiency and accuracy of linear scaling sparse matrix methods with the trivial parallelism inherent to divide and conquer approaches. Our graph-based and sparse matrix algebra solvers have provided speed-ups of many orders of magnitude over traditional solvers. These methods have been implemented in the new, portable PROGRESS and BML libraries for use in a range of electronic structure codes. The time scales accessible in QMD have also been extended significantly through the use of accelerated MD methods. In addition, we have developed a machine-learning framework for the parameterization of interatomic potentials. In combination, these advances make QMD a practical alternative to empirical interatomic potentials for a new range of problems.

Our project has kindled a significant number of follow-on projects including an LDRD-ER, LDRD-DR, and a major DOE Exascale Computing Project. Further new funding sources directly related to this project include a DOE EFRC, ASC-HE, ExMatEx, Mars Inc., Proctor and Gamble, and NNSA Science Campaign 2. We have established new collaborations with the University of Bremen, the Fraunhofer Institute, Uppsala University, and US universities including Harvard, Stanford, and UC Berkeley. We played the key role in the 2015 IS&T summer school at LANL and supported numerous graduate students in the other years of the project. A postdoc hire made in the first year of the project is currently transitioning to a staff position at LANL.

Background and Research Objectives

MD simulation is a powerful and general method for understanding the properties of molecules and materials in atomic detail. It is a ubiquitous computational tool in chemistry, biology, and materials science. QMD, where the forces acting on the atoms are computed on-the-fly from the underlying electronic structure of the system, is the most accurate formulation of MD. However, tremendous computational obstacles exist that limit severely its application to many of the problems of interest to the laboratory and nation. Our objective was to systematically overcome these obstacles to the application of QMD in large scale, long duration simulation by reformulating the theoretical framework, redesigning its core algorithms, and harnessing modern heterogeneous computational architectures.

In QMD the positions of atoms are advanced incrementally using forces evaluated at the self-consistent electronic ground state. Computing the electronic ground state is traditionally an iterative process where a starting guess is improved incrementally. Each recalculation of the electronic structure is expensive and the total computational time scales with the cube of the number of atoms. Both of these factors have limited the type of problems that can be studied with QMD. We have significantly improved the performance of QMD by both removing the requirement for an iterative solution of the electronic structure at each time step and by reformulating the underlying algorithms so that they scale linearly with small and well-controlled errors. While the traditional algorithms of electronic structure theory are

complex and challenging to parallelize, we have succeeded in developing highly parallelized methods that are well suited to modern architectures.

Additional facets of QMD have been systematically improved during the project in order to increase the number of potential applications of the method. These include reconciling QMD with accelerated MD methods to greatly extend the accessible time scales, the use of machine learning techniques to rapidly parameterize new interatomic potentials, and the development of portable libraries for the high performance electronic structure solvers such that out methods can be used easily by other groups.

Scientific Approach and Accomplishments

The project has produced major advances in i) linear scaling electronic structure theory, ii) accelerated QMD, iii) the development of new parameterized models of interatomic bonding, and iv) applications of the extended Lagrangian Born-Oppenheimer MD formalism. Highlights from each of the project thrust areas are outlined below.

Linear scaling electronic structure theory: The LANL-developed QMD code LATTE was the testbed for most of the theory development in the project. LATTE had been used to demonstrate the first energy conserving, linear scaling AMD by combining the extended Lagrangian Born-Oppenheimer MD method with a recursive expansion of the density matrix in a series of sparse matrix-matrix multiplications. The original sparse matrix implementation of the SP2 algorithm could be executed on only one CPU core and was very difficult to parallelize. We demonstrated that by changing the structure of the sparse matrices in LATTE from the standard CSR format to ELLPACK, we could efficiently parallelize the algorithm over shared memory cores (OpenMP) as distributed memory MPI ranks [Cawkwell JCTC 2014, Mniszewski JCTC 2015]. These developments lead to significant speed-ups with respect to the original algorithm and we outperformed Intel's MKL standard by a factor of 2 to 3.

The computation of the inverse factorization of the overlap matrix is a major obstacle in electronic structure theory. Traditional algorithms for computing the matrix inverse scale with the cube of the number of atoms. Hence, the development of a new linear scaling solver for this step was imperative in order to achieve an overall linear scaling of the LATTE code in real applications. A new algorithm based on the iterative refinement of an approximate inverse in linear scaling sparse matrix algebra was developed. The extended Lagrangian formalism was used to propagate the approximate inverse factor in QMD simulations in order to achieve long-term energy conservation [Negre JCTC 2016].

The most significant outcome of the project is a new approach to QMD that reconciles linear scaling electronic structure theory with straightforward parallelism and rigorous error control via graph theory [Niklasson JCP 2016]. Our graph-based electronic structure theory allows a large, connected electronic structure problem to be broken up on the fly into non-interacting partitions that can the solved independently. While divide-and-conquer methods take an analogous approach, our method does not rely on pre-defined partitions but instead determines the communities naturally based on the connectivity of the underlying graphs. Hence, only our method enables straightforward parallelism with automatic error control. The fully distributed (MPI) graph-based electronic structure solver now enables QMD simulations on systems with up 105 atoms. This figure will improve significantly in the coming months.

A new type of graph partitioning problem, called CH-partitioning was formulated that minimizes the number of operations of a graph-based QMD. Several algorithms for solving that partitioning problem were developed, implemented, and analyzed [Djidjev SIAM 2016]. A dynamic version for the CH-partitioning problem in QMD was also developed [Ushijima-Mwesigwa In Prep 2016]. The work on graph partitioning inspired two successful ISTI proposals for implementing the partitioning algorithms on a quantum-annealing platform.

The LATTE code was overhauled during the project to enable the implementation of the new algorithms. The new solvers for the density matrix and overlap matrix inverse were separated from LATTE and put into the new PROGRESS library. The matrix algebra for PROGRESS was implemented in the new BML library. The latter takes care of math operations in different data formats (dense, sparse, etc.) so that users are not required to code up complex algorithms themselves. Moreover, BML allows the underlying matrix operations to be performed on a variety of computational architectures including multi-core CPUs, GPUs, and Xeon Phis. By separating the solvers from LATTE we ensure that other groups are able to use the developments made in this project by linking their codes to PROGRESS and BML. For instance, the DFTB+ code was quickly extended to call PROGRESS/BML, and BML itself has been used in unanticipated applications including the analysis of pore networks.

Accelerated QMD: The time scales accessible to regular MD are limited by the size of the time step used to integrate the equations of motion of the atoms. The accelerated MD methods developed originally by Voter can significantly boost the time scales accessible in simulations of rare events including the making and breaking of covalent bonds. The parallel replica accelerated MD method

enables systems to be studied over long time scales by effectively parallelizing time. We have combined reactive QMD driven by LATTE with the parallel replica method to study shock-induced reactions in benzene and diffusion in graphene at time scales inaccessible to regular QMD. Hence, in this project we have been able to significantly increase the time and length scales possible in QMD within a single code package.

Development of new DFTB parameterizations: Density functional based tight binding (DFTB) theory is the simplest model based explicitly on electronic structure that is capable of describing bonding in organic materials. It is a semi-empirical model, meaning that terms in the expressions for the total energy and forces are approximated and parameterized. The quality of the parameterizations largely determines the chemical fidelity of the simulations. Hence, we invested significant resources into the development of new computational tools for the generation and refinement of DFTB models. We established a new capability for the development of DFTB parameterizations directly from the minimal-basis density functional theory code PLATO. Machine learning approaches were used to refine these initial guesses so that errors in the DFTB models with respect to an accurate database of first principles calculations were minimized. These methods were collected in a new, general purpose optimization package, 'EPO'. EPO has been used to automatically reparameterize DFTB models for organic molecules and transition metals with good success.

Crystalline d- and f-electron materials: The LATTE code was extended during provide key capabilities for materials science applications. These now included the capability to simulate triclinic crystals, k-point integration, d- and f-orbitals, and a number of popular input formats. These new capabilities were exercised in the development of new models for titanium metal [Cawkwell JCTC 2015] and actinide species in solution. The EPO framework also enables us to develop parameterizations for new systems far more quickly than before.

Biomolecular applications: Our new theoretical and computational framework has been rigorously tested by a series of applications to biological systems. First, DFTB-theory was used to compute the ground state charge density of organic molecular crystals. The charge densities compared very accurately with those obtained from far more expensive density functional theory calculations. The charge densities were used to successfully refine x-ray crystallographic data [VanBenshoten PNAS 2016, Wall IUCrJ 2016].

Extended Lagrangian Born-Oppenheimer MD: The XLBO MD method, a LANL-invention that greatly improves the accuracy and speed of QMD, was applied in several new areas during the project [Niklasson JCP 2014]. First, the compatibility of the XLBO method with popular thermostats was evaluated in detail [Martinez JCP 2015]. We showed that thermal fluctuations generated by thermostats are only correct when the underlying microcanonical trajectory is accurate. The XLBO MD method provides extremely accurate microcanonical trajectories at minimal computational expense. The XLBO method was also applied successfully to QMD simulations of metals under charge constraints to overcome pathological 'charge sloshing' [Cawkwell JCTC 2015].

Quantum Response Theory: By calculating the response properties of a material on the fly along the molecular trajectories, we can extract information that is not available in a purely classical MD simulation. We developed a new canonical density matrix perturbation theory to achieve this [Niklasson PRE 2015].

Preliminary results shows that by using the new canonical quantum response theory in the calculation of the kernel in XLBO MD, even systems with severe electronic instabilities can be treated without requiring iterative self-consistent-field optimization or constrained charge conditions. This is an unexpected and potentially a very significant result.

Impact on National Missions

The significant advances made to the LATTE code in addition to the development of the new BML, PROGRESS, and EPO codes have led to several follow-on projects, new users, and new collaborations both inside and outside the laboratory. New capabilities for the simulation of d- and f-valent materials will be used in a new start LDRD-ER project (PI: Batista) for the simulation of actinides in complex solution environments and in a major DOE Exascale Computing Project (ECP) (PI: Voter, co-PI: Niklasson) for the simulation of nuclear fuels on next-generation exascale hardware. A subtask in Heavy Element Chemistry BES program at LANL will focus on developing DFTB parameters for actinide systems to study their ligand coordination and multiple species complexation and dynamic behaviors. Fast, accelerated MD simulations of high explosive chemistry are a cornerstone of a new start LDRD-DR project (PI: McGrane, co-PI: Cawkwell). The fast MD simulations of organic materials under high pressure, high temperature conditions that LATTE enables has also been adopted by ASC-HE (Leiding, T-1). A CoSP2 proxy application was developed in the ExMatEx project (PI: Germann). Intel, Nvidia, AMD, Reservoir Labs, and Rice University have explored CoSP2 on new architecture simulators, as part of sparse matrix library implementations, and for use with

task-based runtimes. The graph-based SP2 approach for QMD has been made part of the ECP Co-Design Center for Particle-Based Methods proposal (PI: Germann). Distributed versions will be developed based for distributed memory architectures per use of traditional OpenMP/MPI, graph-based, and task-based runtimes.

The BML and PROGRESS libraries have been integrated into the popular DFTB+ code by Balint Aradi (Bremen) and our team [Negre In Prep. 2016]. This development brings our new capabilities to a wider audience. New collaborations have been established with the Department of Chemistry at North Carolina State University, the Fraunhofer Institute for the Mechanics of Materials, and the Department of Materials Science and Engineering at Stanford University on the development of new DFTB parameterizations. Extensions to path-integral MD is pursued with Prof. Markland's group at Stanford and new integration techniques are under development with Prof. T. Head-Gordon's group at UC Berkley and Prof. Skylaris' group at the Universty of Southhampton. LATTE/BML/PROGRESS are being used in CRADAs with Mars Inc. and Proctor and Gamble to simulate chemical processes (Redondo, T-DO). Application to polarizable force-fields, orbital-free DFT for high-temperature simulations (Ticknor, T-1) as well as strongly correlated electron systems (PI: Barros, T-1) will also be pursued in the near future.

The project has been extremely beneficial for bringing new staff and students to the laboratory. Christian Negre joined the team as a post-doc from Yale. He is currently in the final stages of conversion to staff in T-1. An IS&T summer school was organized around this project which brought six graduate students to LANL from diverse academic backgrounds. Graduate students from the University of Missouri-Columbia, North Carolina State, and Clemson University were also supported during highly productive internships. A DOE Computational Science Graduate Fellow (CSGF) from Stanford University worked with our team for her practicum.

Publications

Bock, N., C. F. A. Negre, S. M. Mniszewski, B. Aradi, and A. M. N. Niklasson. The basic matrix Library (bml) for quantum chemistry. 2016. In preparation.

Cawkwell, M. J.. Fast quantum molecular dynamics simulations of shock-induced chemistry in organic liquids. Invited presentation at American Physical Society March Meeting 2014. (Denver, 3-7 March 2014).

Cawkwell, M. J., A. M. N. Niklasson, and D. M. Dattelbaum. Extended Lagrangian Born-Oppenheimer molecular dynamics simulations of the shock-induced chemistry of phenylacetylene. 2015. JOURNAL OF CHEMICAL PHYSICS. 142 (6).

Cawkwell, M. J., J. D. Coe, S. K. Yadav, X. -. Liu, and A. M. N. Niklasson. Extended Lagrangian Formulation of Charge-Constrained Tight-Binding Molecular Dynamics. 2015. JOURNAL OF CHEMICAL THEORY AND COMPUTATION. 11 (6): 2697.

Cawkwell, M. J., M. A. Wood, A. M. N. Niklasson, and S. M. Mniszewski. Computation of the Density Matrix in Electronic Structure Theory in Parallel on Multiple Graphics Processing Units. 2014. JOURNAL OF CHEMICAL THEORY AND COMPUTATION. 10 (12): 5391.

Djidjev, H. D., G. Hahn, S. M. Mniszewski, C. F. A. Negre, A. M. N. Niklasson, and V. B. Sardeshmukh. Graph Partitioning Methods for Fast Parallel Quantum Molecular Dynamics. 2016. SIAM Workshop of Scientific Computing .

Krishnapriyan, A., P. Yang, A. M. N. Niklasson , and M. J. Cawkwell. Parameterization of Density Functional Tight Binding Models Using Machine Learning. 2016. Journal of Chemical Theory and Computation. : In preparation.

Martinez, , M. J. Cawkwell, A. F. Voter, and A. M. N. Niklasson. Thermostating extended Lagrangian Born-Oppenheimer molecular dynamics. 2015. JOURNAL OF CHEMICAL PHYSICS. 142 (15).

Martinez, E., M. J. Cawkwell, A. F. Voter, and A. M. N. Niklasson. Thermostating extended Lagrangian Born-Oppenheimer molecular dynamics. 2015. JOURNAL OF CHEMICAL PHYSICS. 142 (15): 154120.

Mniszewski, S. M., M. J. Cawkwell, J. Mohd-Yussof, N. Bock, T. C. Germann, and A. M. N. Niklasson. Efficient parallel linear scaling calculation of the density matrix for Born-Oppenheimer Molecular Dynamics. 2015. Journal of Chemical Theory and Computation.

Negre, C. F. A., A. M. N. Niklasson, S. M. Mniszewski, T. Frauenheim, and B. Aradi. Linear scaling extended Lagrangian Born-Oppenheimer molecular dynamics for molecules and solids: a DFTB+ implementation. 2016. In preparation.

Negre, C. F. A., S. M. Mniszewski, M. J. Cawkwell, Bock, M. E. Wall, and A. M. N. Niklasson. Recursive Factorization of the Inverse Overlap Matrix in Linear Scaling Quantum Molecular Dynamics Simulations. 2016. JOURNAL OF CHEMICAL THEORY AND COMPUTATION. 12 (7): 3063.

Niklasson, A. M. N., M. J. Cawkwell, E. H. Rubensson, and Rudberg. Canonical density matrix perturbation theory. 2015. PHYSICAL REVIEW E. 92 (6).

Niklasson, A. M. N., S. M. Mniszewski, C. F. A. Negre, M. J. Cawkwell, P. J. Swart, Mohd-Yusof, T. C. Germann, M. E.

Wall, Bock, E. H. Rubensson, and Djidjev. Graph-based linear scaling electronic structure theory. 2016. JOURNAL OF CHEMICAL PHYSICS. 144 (23).

Niklasson, A. M. N., and M. J. Cawkwell. Generalized extended Lagrangian Born-Oppenheimer molecular dynamics. 2014. Journal of Chemical Physics. 141 (16): 164123.

Ushijima-Mwesigwa, H., C. F. A. Negre, S. M. Mniszewski, H. N. Djidjev, and A. M. N. Niklasson. Adaptive graph-partitioning methods for quantum molecular dynamics . 2016. In preparation.

VanBenschoten, A. H., L. Liu, A. Gonzales, A. S. Brewster, N. K. Sauter, J. S. Fraser, and M. E. Wall. Measuring and modeling diffuse scattering in protein X-ray crystallography. 2016. Proceeding of the National Academy of Sciences. 113 (15): 4069.

Wall, M. E.. Quantum crystallographic charge density of urea. 2016. International Union of Crystallography Journal. 3 (4): 237.

Optimization and Control of Dynamic Networks

Angel E. Garcia
20140565DR

Abstract

The interdisciplinary field of network science is an important part of the Los Alamos Information Science and Technology (IS&T pillar) and strategy. Network science research aims to develop new mathematical theory and models and to apply those models in application areas relevant to the Los Alamos mission such as optimization and control of power systems and detection of cybersecurity anomalies. The goals of this project were to develop interdisciplinary and collaborative progress on the theory and applications of dynamic networks. The Center for Non Linear Studies (CNLS) has played a leading role in the development of the field of network science both inside and outside of Los Alamos. Our interdisciplinary approach is key to identifying new and transformational science with impact on the frontier of discovery science and national security programs.

Background and Research Objectives

Network science research has been primarily focused on the simplification of dynamic graphs to static graphs and their topological characteristics. However, processes on networks such as the spread of a virus on a social network, traversal through a cyber network, and cascading failures in a power grid are critically dependent on the dynamic nature of the underlying network.

These dynamic graphs are at the heart of technological and scientific problems in electrical power grids. Deployment of new technologies, such as renewable generation and electric vehicles, is rapidly transforming electrical power networks by coupling previously distinct spatiotemporal scales and challenging traditional approaches for designing, analyzing, and operating power grids. The interactions of spatiotemporal scales in power systems are pushing the limits of power engineering best practices and require the development of general complex system models at the appropriate level of network detail necessary to isolate and analyze the relevant static, dynamic, and stochastic phenomena.

Computer networks are also inherently dynamic and non-stationary. Capturing the dynamics of user activity through coarse-level and high-fidelity modeling is critical to understanding normal activity and detection of anomalous activity. Only recently has a network-wide (graph theory) viewpoint been taken.

The CNLS brings a unique perspective in the integration of interdisciplinary approaches and ideas to the subject of network science. The CNLS has been a leader and innovator in Information Science and Technology. In particular, helping to provide new approaches in theory and modeling of networks for more than 10 years. It has helped nucleate efforts at Los Alamos for applications of networks in neurocomputation, smart grid, and cybersecurity.

Through this project, CNLS furthered theory and models for dynamic networks. This involved the development of mathematically principled models for temporal networks, which are tractable, can be fit to data, and can be efficiently generated for experiments. Components of the research involved mathematical description and investigation of the basic characteristics of the temporal graph models especially properties of connectivity such as reachability, optimization of the problem of fitting data to these models, and design of efficient, scalable algorithms to generate simulated networks. This project furthered and resulted in the development of temporal versions of several important static random graph models including the expected degree model, the random intersection graph, and the random motif graph.

This project investigated threshold behavior in the temporal random graph models for connectivity measures such as expected reachability, sizes of strongly and weakly connected components and lengths of shortest paths within nodes. This was accomplished through the creation of comprehensive ordinary differential equations/partial differential equations (ODE/PDE) models

for power systems, incorporating different devices and controls that are making inroads into electrical distribution networks, e.g., PV systems, electric vehicle charging, and frequency responsive loads. The ODE/PDEs approach addressed the interaction of emergent phenomena arising from the interaction of new smart-grid components. This project employed reduced-order stochastic models of the short-term dynamics, key to understanding power outage cascades. This project extended descriptions of heterogeneous collections of loads by proposing a new perspective on the Chapman-Kolmogorov equations. Additionally, through the course of this project the following were developed (1) new approximate statistical methods to capture underlying interactions and scale separations and seek effective parallel control algorithms to mitigate cascades; and (2) mathematical tools to capture system energy and thermal states with dynamic nonparametric probability distributions, where state transitions evolve according to Markov chains.

Scientific Approach and Accomplishments

This project furthered the development of fundamental mathematics, optimization theory, and algorithms for solving discrete nonlinear optimization problems. One of the focuses has been on developing methods that leverage structure arising from dynamic networks and applying these techniques to such networks. Results are in three fundamental areas.

State Estimation of Dynamic Complex Networks -- One of the key challenges in modeling and understanding complex networks is that the networks and their state are not completely observable. However, in order to make rigorous control and optimization decisions accurate and complete information about network system state is required. To address this problem, researchers have developed methods for estimating unobserved state in networks. These existing methods assume steady-state conditions and do not quantify uncertainty associated with the estimates. Addressing these limitations required the development of novel methods for estimating system state that accounts for fast timescale dynamics and quantifies the uncertainty. These novel approaches are able to quickly detect topology changes in networks (i.e. edge failures) with only sparse information and quantify the likelihood that such an event has occurred.

Optimization of nonlinear systems

Optimization of dynamic, complex networks are part of a larger, fundamental class of optimization problems: mixed-integer non convex optimization. These problems are NP-complete at best to solve. Under this CNLS project we have developed novel approaches to address the underlying fundamental problems (mixed-integer non convex optimization) as well as developed techniques that exploit structure in that appears in the subsets of these fundamental problems that arise in complex networks. On the fundamental side, our work has resulted in a novel method for solving mixed integer convex (but nonlinear) problems. This new solver, Pajarito, has already produced provably optimal solutions to problems that have never been solved before.(http://www.gamsworld.org/minlp/minlplib2/html/gams01.html) This solver is a building block for future work that will address mixed integer non-convex problems. In the area of complex network optimizations, results include developing methods for improving network stability based on local measurements (Garcia et al, 2014), developing optimization techniques for systems with ODE/PDE dynamics (Mak et al., under review), and making networks robust (Nagarajan et al, under review).

Optimization under uncertainty

Novel methods for combining uncertainty quantification with our new optimization techniques were developed in the course of this project. These approaches support optimization and control decisions that account for and are robust to this uncertainty. This includes operational decisions such as generator dispatch and unit commitment (Miles et al., in press; Sundar et al., in press) and design of resilient and robust networks (Yamangil et al,2015; Nagarajan et al., submitted).

Conclusions

This project furthered the understanding of fundamental, physics-based, approaches for working on complex networks and the application of these approaches to real life problems. The project results had three interlocking themes:

Dynamic Networks-- develop models and algorithms for temporal random graphs; seek theorems for connectivity and reachability in the models; and explore the range of possible temporal correlation patterns.

Power Systems -- create comprehensive ODE/PDE models for power systems; develop reduced-order stochastic models of network power-outage cascades; develop mathematical tools to capture system energy and thermal states.

Cybersecurity -- model as dynamic networks; develop techniques including hierarchical models to capture statistics of bursty network communication patterns; create inference methods and fit cyber authentication network data to the temporal random graph models.

Impact on National Missions

Information Science and Technology is a Laboratory strate-

gic pillar that touches a broad spectrum of science at LANL from discovery science to pivotal program needs. This proposal directly addresses Complex Networks capabilities through the modeling of dynamic networks and with applications to cybersecurity and power systems (``smart grids''). This project develops core information science and technology capabilities needed to address the open questions of the Office of Electricity that intersect with the scientific goals of DOE's Office of Advanced Scientific Computing Research (ASCR) Applied Mathematics Program such as uncertainty quantification in complex engineered networks. This project will innovate with basic research supporting LANL's internal cybersecurity programs and Global Security programs. Effective cyber defense of the weapons complex is essential to its security and effectiveness.

Publications

Bienstock, , Chertkov, and Harnett. Chance-Constrained Optimal Power Flow: Risk-Aware Network Control under Uncertainty. 2014. SIAM REVIEW. 56 (3): 461.

Chernyak, V. Y., Chertkov, Bierkens, and H. J. Kappen. Stochastic optimal control as non-equilibrium statistical mechanics: calculus of variations over density and current. 2014. JOURNAL OF PHYSICS A-MATHEMATICAL AND THEORETICAL. 47 (2).

Chertkov, M., M. Fisher, S. Backhaus, R. Bent, and S. Misra. Pressure Fluctuations in Natural Gas Networks Caused by Gas-Electric Coupling. 2015. In 2015 48th Hawaii International Conference on System Sciences (HICSS). , p. 2738.

Doerfler, , M. R. Jovanovic, Chertkov, and Bullo. Sparsity-Promoting Optimal Wide-Area Control of Power Networks. 2014. IEEE TRANSACTIONS ON POWER SYSTEMS. 29 (5): 2281.

Dvijotham, K., P. Van Hentenryck, M. Chertkov, S. Misra, and M. Vuffray. Graphical Models for Optimal Power Flow. 2016. arXiv:1606.

Dvorkin, Y., M. Lubin, S. Backhaus, and M. Chertkov. Uncertainty Sets for Wind Power Generation. 2016. IEEE Transactions on Power Systems. 31 (4): 3326.

Farrell, M., T. Goodrich, N. Lemons, F. Reidle, F. Villaamil, and B. Sullivan. Hyperbolicity, degeneracy, and expansion of random intersection graphs. 2014. arXiv.

Frolov, , Backhaus, and Chertkov. Efficient algorithm for locating and sizing series compensation devices in large power transmission grids: I. Model implementation. 2014. NEW JOURNAL OF PHYSICS. 16.

Garcia, M., S. Backhaus, and R. Bent. Power Flow-Based Adaptive Generator Controls. Invited presentation at 52nd Annual Allerton Conference on Communication, Control, and Computing. (Allerton, Illinois, 1-3 Oct. 2014).

Generous, N., G. Fairchild, A. Deshpande, S. Y. Del Valle, and R. Priedhorsky. Global disease monitoring and forecasting with Wikipedia. . 2014. arXiv.

Giani, A., R. Bent, and F. Pan. Phasor measurement unit selection for unobservable electric power data integrity attack detection. 2014. International Journal of Critical Infrastructure Protection. 7 (3): 155.

Goddard, , Klose, and Backhaus. Model Development and Identification for Fast Demand Response in Commercial HVAC Systems. 2014. IEEE TRANSACTIONS ON SMART GRID. 5 (4): 2084.

Hagberg, , and Lemons. Fast Generation of Sparse Random Kernel Graphs. 2015. PLOS ONE. 10 (9).

Jaworsky, , Turitsyn, and Backhaus. THE EFFECT OF FORECASTING ACCURACY ON THE SIZING OF ENERGY STORAGE. 2014. In 7TH ANNUAL DYNAMIC SYSTEMS AND CONTROL CONFERENCE, 2014, VOL 2.

Kundu, S., and I. A. Hiskens. Overvoltages due to Synchronous Tripping of Plug-in Electric-Vehicle Chargers Following Voltage Dips. 2014. IEEE Transactions on Power Delivery. 29 (3): 1147.

Kundu, S., and I. Hiskens. Nonlinear dynamics of hysteresis-based load controls. 2014. In The 19th World Congress of the International Federation of Automatic Control. (Cape Town, South Africa, 24-29 Aug. 2014). , p. 5419. Cape Town: IFAC.

Lokhov, A. Y., and T. Misiakiewicz. Efficient reconstruction of transmission probabilities in a spreading process from partial observations. 2015. arXiv:1509.

Lubin, M., E. Yamangil, R. Bent, and J. P. Vielma. Extended Formulations in Mixed-integer Convex Programming. 2016. arXiv:1511. 9682: 102.

Mak, T., P. Van Hentenryck, A. Zlotnik, H. Hijazi, and R. Bent. Efficient Dynamic Compressor Optimization in Natural Gas Transmission Systems. Invited presentation at American Control Conference 2016. (Boston, 6-8 Jul. 2016).

Mehta, , N. A. Sinitsyn, Backhaus, and B. C. Lesieutre. Safe control of thermostatically controlled loads with installed timers for demand side management. 2014. ENERGY CONVERSION AND MANAGEMENT. 86: 784.

Misra, S., M. Fisher, S. Backhaus, R. Bent, M. Chertkov, and F. Pan. Optimal Compression in Natural Gas Networks: A Geometric Programming Approach. 2015. IEEE Transactions on Control of Network Systems. 2 (1): 47.

Misra, S., M. W. Fisher, S. Backhaus, R. Bent, M. Chertkov, and F. Pan. Optimal compression in natural gas networks: A geometric programming approach. 2015. IEEE Transactions on Control of Network Systems. 2 (1): 47.

Nagarajan, H., E. Yamangil, R. Bent, P. V. Hentenryck, and S. Backhaus. Optimal Resilient transmission Grid Design. 2016. In 2016 Power Systems Computation Conference (PSCC). , p. 1.

Nagarajan, H., E. Yamangil, R. Bent, S. Backhaus, and P. Van Hentenryck. Optimal Resilient Transmission Grid Design. Invited presentation at Power Systems Computation Conference 2016. (Genoa, Italy, 20-24 Jun. 2016).

Nagarajan, H., M. Lu, E. Yamangil, and R. Bent. Tightening McCormick Relaxations for Nonlinear Programs via Dynamic Multivariate Partitioning. 2016. arXiv:1606.

Nagarajan, H., S. Rathinam, and S. Darbha. On maximizing algebraic connectivity of networks for various engineering applications. 2015. In Control Conference (ECC), 2015 European. , p. 1626.

Nagarajan, H., and S. Rathinam. On maximizing algebraic connectivity of networks for various engineering applications. Invited presentation at European Control Conference (ECC). (Linz, Austria, 15-17 Jul. 2015).

Roald, L., S. Misra, M. Chertkov, and G. Andersson. Optimal Power Flow with Weighted chance constraints and general policies for generation control. 2015. In 2015 54th IEEE Conference on Decision and Control (CDC). , p. 6927.

Stolbova, , Backhaus, and Chertkov. Fault-induced delayed voltage recovery in a long inhomogeneous power-distribution feeder. 2015. PHYSICAL REVIEW E. 91 (2).

Sulc, , Backhaus, and Chertkov. Optimal Distributed Control of Reactive Power Via the Alternating Direction Method of Multipliers. 2014. IEEE TRANSACTIONS ON ENERGY CONVERSION. 29 (4): 968.

Sundar, K., H. Nagarajan, M. Lubin, L. Roald, S. Misra, R. Bent, and D. Bienstock. Unit Commitment with N-1 Secuity and Wind Uncertainty. Invited presentation at Power Systems Computation Conference 2016. (Genoa, Italy, 20-24 Jun. 2016).

Tapia, A., N. LaLone, E. MacDonald, R. Priedhorsky, and M. Hall. Crowdsourcing rare events: Using curiosity to draw participants into science and early warning systems. . 2014. In International Conference on Information Systems for Crisis Response and Management (ISCRAM), 2014. (University Park, Pennsylvania, 18-21 May, 2014). , p. 135. Pennsylvania: ISCRAM.

Turcotte, M.. Detecting localised anomalous behaviour in a computer network . 2014. In Advances in Intelligent Data Analysis XIII, LNCS 8819 . (Leuven, Belgium, 30 Oct - 1 Nov, 2014). , p. 321. Belgium: Springer.

Vuffray, M., S. Misra, and M. Chertkov. Monotonicity of dissipative flow networks renders robust maximum profit problem tractable: General analysis and application to natural gas flows. 2015. In 2015 54th IEEE Conference on Decision and Control (CDC). , p. 4571.

Vuffray, M., and T. Misiakiewicz. Concentration to zero bit-error probability for regular LDPC codes on the binary symmetric channel: Proof by loop calculus. 2015. In 2015 53rd Annual Allerton Conference on Communication, Control, and Computing (Allerton). , p. 115.

Yamangil, E., R. Bent, and S. Backhaus. Designing Resilient Electrical Distribution Grids. 2014. arXiv:1409.

Yamangil, E., R. Bent, and S. Backhaus. Designing Resilient Electrical Distribution Grids. Invited presentation at Proceedings of the 29th Conference on Artificial Intelligence. (Allerton, Illinois, 1-3 Oct. 2014).

Zlotnik, A., L. Roald, S. Backhaus, M. Chertkov, and G. Andersson. Control policies for operational coordination of electric power and natural gas transmission systems. 2016. In 2016 American Control Conference (ACC). , p. 7478.

Zlotnik, A., M. Chertkov, and S. Backhaus. Optimal control of transient flow in natural gas networks. 2015. In 2015 54th IEEE Conference on Decision and Control (CDC). , p. 4563.

Real-Time, Real-World Time Series Forecasting Using Internet Data

Reid Priedhorsky
20160595ECR

Introduction

Estimates of disease incidence using internet data are accurate in many cases, based on traces such as social media sharing of symptoms or search logs. However, this is a "try it and see" field: if a particular combination of disease, location, and model is accurate, publish, if not, don't. The structure and parameters of the highly complex process between human event observations and apparently relevant internet traces have never been described; neither have controlled experiments been attempted, as opposed to observational studies. This limits progress on other emerging innovations, such as forecasting by coupling mechanistic (first principles based) models.

We will address these gaps by simulating outbreaks and related internet activity to obtain realistic ground truth that is completely observable, unlike the real world. These controlled experiments will be supported by a novel, rigorous description of the information pipeline and validated by real-world tests on diverse outbreaks.

Without this quantitative understanding, these tools cannot be trusted for life and death decisions. With it, they have the potential to revolutionize numerous situational awareness applications. Our approach brings together human field observations with other geographic time series to inform many nationally and globally important applications.

Benefit to National Security Missions

Disease dynamics and public health response are themselves global security issues, and reliable disease forecasting is a stated priority at the national policy level. The demise of Google Flu Trends underscores the difficulty of sustaining these efforts in the private sector.

Further, data science is an emerging priority for DOE. The techniques developed here are applicable in many areas of mission space, for example: (1) non-proliferation, where human observation of construction, truck traffic, and black market activity might be combined with sensor data and intelligence to forecast proliferation risk or interest in a given location; (2) smart grid, temperature comfort and travel plans with weather and energy sensor data to forecast energy de- mand; (3) climate, (dis)appearance of species, pollution effect, and fossil fuel transportation with space-based sensing to forecast treaty compliance; and (4) disaster response, situation reports with relief organization data to forecast resource needs and economic outlook.

The emerging scientific consensus is that models must be coupled with real-time, real-world observations — available en masse in internet data — in order to provide the most useful forecasts. This is key in the area of multi-int, which emphasizes the use of diverse data to solve situational awareness needs. Our work brings quantitative science to this challenge.

Progress

At the time of this writing, our project has been active for one month and is still in a startup phase. With respect to our FY16 tasks, we have:

Mathematical model of information flow

- Selected a theoretical framework on which to base our models (Shannon's information theory).
- Sarted developing an information flow graph and are working on the parameters and equations to model this flow.
- Evaluated disease simulation codes.
- Identified 8 specific codes and several simpler models and are evaluating them.

Evaluate data sources.

- Identified 10+ internet data sources (e.g., Twitter, Wikipedia, WebMD) and are evaluating them.

- Identified several analyses of internet use by demographics (e.g., Pew, U.S. Census) and are evaluating them.

Future Work

Between October 1, 2016 and September 30, 2017, we plan three tasks.

Task 1: Revise and improve mathematical model. We will complete and submit the manuscript drafted in FY16, and revise it based on peer review. The product will be an accepted manuscript on track for publication.

Task 2: Perform controlled experiments in one or more simulated outbreak settings. These have three goals: (a) validate our mathematical model of information flow, (b) quantify the sensitivity of estimate accuracy to the parameters identified in our model, and (c) quantify the value added by internet data to disease surveillance. The product will be one or more manuscripts submitted for publication.

Task 3: Prepare for real-world observational experiments. We will identify 5–10 real-world settings (disease outbreak, location, data sources, and information model parameters) for which our model predicts a range of estimation success outcomes. We will plan an observational experiment in these settings to test our predictions. The product will be this experiment plan.

Conclusion

The proposed work will make critical progress toward a deployed science of reliable disease forecasting with quantitative uncertainty, as well as in the broader data science of large-scale, real-world forecasting. While many of the individual tools are standard, their emergent behavior in a combined setting is novel.

Deliverables include a mathematical description of the information pipeline that transforms human observations into actionable knowledge via internet systems; validation of this pipeline using controlled experiments in a simulated setting; validation of this pipeline in diverse real-world settings; and quantification of the value of internet data for disease forecasting.

Assimilation Algorithms for Data Fusion in Large-scale Non-linear Dynamical Systems

Humberto C. Godinez Vazquez
20160599ECR

Introduction

Our primary goal is to develop a new class of data assimilation methods that can efficiently reduce the forecast error in large-scale nonlinear models. The method will use a novel spectral decomposition method, namely the Koopman modes, that capture the nonlinear dynamics of a model. The novel element is to project into the low-dimensional subspace defined by the Koopman eigenfunctions and perform the assimilation in this subspace, significantly reducing the computational cost of the assimilation while preserving the nonlinear behavior of the model.

The Koopman subspace has a number of desirable properties inherent in the Koopman operator, including the evolution of probability distributions functions, which we will exploit for data assimilation. This subspace is defined for any nonlinear model and does not rely on linearization of the dynamics: in fact, it captures the full information of the nonlinear system. A particular challenge will be to find the appropriate Koopman modes through the eigenfuctions of the Koopman operator, which can be utilized within the assimilation method. We plan to approximate the eigenfunctions by an iterative process, very similar in form to the eigenvalue power method.

We will explore a new approach to compute the Koopman modes using the Dynamic mode decomposition (DMD), which provides a practical numerical framework for the decomposition. The DMD is computed using an iterative method that does not require the Koopman operator explicitly, only its action on a vector. Additionally, we will develop Kernel generating methods to determine the appropriate eigenvalues and eigenfunctions. This approach will provide a computationally efficient way to obtain the Koopman eigenpairs and modes for large-scale dynamical systems.

The new assimilation algorithms will create a capability that will place LANL at the forefront of not only assimilation methods, but of several applied fields in its ability to predict physical phenomena of interest.

Benefit to National Security Missions

This project will advance LANL's Integrating Information, Science, and Technology for Prediction pillar by closely integrating new analytical and computational aspects to advance predictive capabilities for large-scale problems. Results of the proposed project will directly provide new computational tools that will support existing programs in space weather specification and forecasting, climate specification, and subsurface flow. Aspects of the modeling framework developed here are relevant for any high-dimensional nonlinear complex system, and will be of great interest to several DOE programs, positioning LANL to compete for new program space. The work is highly relevant to NASA, AFSOR, and DOE SC ASCR and BER program offices.

Progress

Our project just started about a month ago (June 2016). Nevertheless, we are in track with our plan on the project. In particular, we are currently working on developing a mathematical approach to estimate the Koopman eigenfunctions and have made great progress on this regard. We plan to submit a journal article once this work has been completed and will be presenting our results in the SIAM annual meeting this July 2016.

Future Work

Our main task is to develop and implement a Kernel method to determine the appropriate eigenvalues and eigenfunctions of the Koopman operator for our particular assimilation method. The subtasks are:

- Explore iterative Kernel generating methods for Koopman operator
- Implement our developed methods to approximate the eigenfunctions and eigenvalues to the 2D shal-

low water model, initial testing
- Present results in conferences
- Submit one or two journal articles describing our results

Conclusion

A new type of assimilation method will be developed that will greatly enhance the efficiency of assimilating data into large-scale models while still preserving the nonlinear dynamics. It will initially be tested on a 2D shallow water model, followed by a realistic space weather model. We will implement our methodology to the BATS-R-US, a Magnetohydrodynamic model, to correctly specify Earth's magnetosphere. We will study its applicability to LANL's space infrastructure, which will add critical forecasting to space awareness capabilities. A software library with the relevant assimilation method will be produced, tested, and released.

Publications

Linares, R., V. Vittaldev, and H. C. Godinez. Dynamic Data-Driven Uncertainty Quantification via Generalized Polynomial Chaos. To appear in Dynamic Data Driven Applications Systems Workshop. (Hartford, Connecticut, 9-12 August, 2016).

McLaughlin, C. A., H. C. Godinez, A. Sizemore, K. Barton, and P. Toledo. The Effects on Density and Orbit Propagation of Assimilating Various Data into General Circulation Models. To appear in Astrodynamics Specialist Conference hosted by the American Institute of Aeronautics and Astronautics and co-hosted by the American Astronautical Society. (Long Beach, CA, 13-16 Sept. 2016).

Mehta, P. M., A. C. Walker, E. Sutton, and H. C. Godinez. New density estimates derived using accelerometers on-board the CHAMP and GRACE satellites. To appear in Space Weather.

Schiller, Q., W. Tu, A. Ali, X. Li, H. C. Godinez, D. L. Turner, S. K. Morley, and M. G. Henderson. Simultaneous event specific estimates of transport, loss, and source rates for relativistic outer radiation belt electrons. To appear in Journal Geophysical Research.

Reducing Data Dimensionality in Seismic Inversion

Gowri Srinivasan
20150691ECR

Abstract

Seismic inversion (SI) refers to the science of using seismic observations to estimate the geophysical properties of the earth through a wave equation. SI is one of the primary techniques used to characterize reservoirs for applications like hydraulic fracturing, to maximize shale gas recovery. Inversion techniques are an integral part of DOE-critical mission areas such as energy production (induced seismicity during natural gas extraction) and national security (aspects of Comprehensive Test Ban Treaty verification) that rely on accurate estimations of geophysical properties. Errors in inversion are costly; the result is inefficient extraction of natural gas since fractures cannot be located, or inability to ascertain if an explosion was nuclear due to incorrect yield determination. Matching 1000s of terabytes of seismogram data to estimate a large number of nonlinearly related parameters in the wave equation is challenging and often computationally prohibitive. However, applying methods that reduce the dimensionality (number of independent parameters) of the problem without simplifying the physics will make the problem tractable and in addition, greatly increase the accuracy of predictions. New computational approaches that efficiently integrate the large amount of information gathered in these surveys to calibrate reservoir models are urgently needed. Our approach seeks to reduce the computational burden through reducing the dimensionality of the data, while respecting its inherently non-linear nature. We have adopted a kernel-based method that extends a promising linear technique Principal Component Analysis (PCA), to account for nonlinear correlations between parameters known as kernel PCA (kPCA). We demonstrate the efficacy of kPCA in seismic classification problems, where reducing the dimensionality produced not only a more computationally efficient classifier, but also increased its robustness. We further apply this reduced dimension classification capability to estimate complex geo-structures accurately using state-of-the-art machine learning techniques.

Background and Research Objectives

Seismic data is collected and used by geologists for a variety of applications including earthquake monitoring, detection and classification of manmade seismic disturbances, and characterization of structures in the earth's subsurface. These applications play a key role in many defense and energy applications. For example, a central theme in nuclear nonproliferation is to locate and characterize seismic events to distinguish natural events, e.g., earthquakes, from anthropogenic ones, e.g., underground nuclear weapons testing [1-3]. The recent claim by North Korea regarding the testing of a hydrogen bomb is one such instance where seismic signatures were analyzed to determine the nature of the event. In the energy sector, identifying the possibility of induced seismic activity, both minor and major earthquakes, resulting from the disposal of wastewater used in hydraulic fracturing operations is a pivotal concern [4,5]. In applications such as these, identifying and classifying the source and strength of the event accurately is of utmost importance.

Since wave propagation directly depends upon the medium traversed, geophysical properties such as density and permeability can be estimated from the observed wave characteristics (e.g. amplitude, arrival time, etc.). Current assumptions of isotropic and elastic media are problematic because most geologic formations are anisotropic in nature due to layering and heterogeneity. Furthermore, numerous laboratory studies have shown that it is important to understand the time-dependent (viscous) properties of rocks in order to predict the reservoir behavior over time since significant deformation of these types of rocks takes place by a time-dependent response not predicted by linear elasticity [6]. In recent years, seismic imaging techniques have advanced significantly, leading to higher fidelity data being recorded. Using thousands of terabytes of seismogram data to estimate a large number of nonlinearly related parameters in the wave equation [7,8] is challenging and often

computationally prohibitive [9]. In real world applications, physical parameters often exhibit nonlinear dependence on each other. For example, it has been shown in shale and other layered formations that the degree of anisotropy strongly correlates with the vertical velocity and vertical Young's modulus. Recent work has shown promise that computational burden in SI can be greatly alleviated by using Principal Component Analysis (PCA) [10] for dimensionality reduction [11]. However, assuming linear correlations between parameters is often not justifiable, particularly for seismic data, which typically exhibits high nonlinear correlations.

In newly published research, SVMs were used in classifying seismic data into earthquake and non-earthquake events [12]. Additionally, classifying seismic data into sets based on key features of interest remains an important first step to determining the structure characteristics and source locations. For example, knowing whether there is one or many strong underground reflectors can decrease the number of parameters in a subsurface model and thus reduce model complexity significantly prior to inversion, leading to large computational savings. State of the art seismological methods form subsurface estimates by assuming some class of model for the subsurface beneath the region that the seismic survey is over. These a priori models range from simplistic, one-dimensional layered models of the density and elastic properties of the subsurface, to complex heterogeneous models based on anisotropic elastic properties with a specified correlation structure. The seismic data is then used to estimate parameters in these models. However, selecting a class of a priori models is usually done ad hoc, either by attempting reconstruction using a few different model classes or by relying on expert knowledge of the substructure. For these reasons, there is a great need for methods that will perform classification of seismic data in a computationally efficient way while preserving accuracy.

Scientific Approach and Accomplishments

Combined Dimensionality Reduction and Classification

We have proposed and implemented a combined dimensionality reduction and classification algorithm specifically suitable for data that is highly non-linearly correlated. This combined method is especially powerful in the context of seismic data classification, where large data sets and the high nonlinear correlations necessitate nonlinear dimensionality reduction techniques. Traditionally, classification methods fall under the category of supervised learning algorithms, such as the Support Vector Machine (SVM)[13]. The SVM uses training datasets to learn the optimal separating hyperplane between the two sets being classified, which assumes that a linear separation exists. Our method maps the data into a higher dimensional plane where such a linear separation exists, using a suitable kernel mapping. It is now possible in this higher dimensional space to find the principle components, retain the first few components that contribute to most of the variations in the data and ignore the rest. This concept is identical to PCA described earlier, but is more accurate since it accounts for the nonlinearities in the data. We label this method kPCA-SVM since we perform dimensionality reduction prior to the classification.

In order to characterize the utility of kPCA-SVM in seismic classification problems we apply the methodology to a synthetic data set of seismograms generated using the scalar wave equation with heterogeneous acoustic profile and perfectly matched boundary layer. Within each sample there is either a single reflector or two reflectors and we seek to partition the data into disjoint sets based on the number of reflectors. Seismograms are sampled at known locations and we vary the depths and magnitudes of the reflectors to increase variably in the data. Our goal in applying kPCA-SVM is to identify whether a seismic signal is the result of one or multiple buried reflectors without resorting to seismic imaging methods. Performance of the method is quantified in terms of (i) the average classification score on a given set of sample points as the fraction of the set classified correctly, and (ii) the CPU time required for optimization convergence. The average score is a reliable metric for two-level classification algorithms when the training and test sets are made up of equal samples from each class. Details of the method can be found in [14] and the main results are summarized here.

Figure 1 plots the contribution of the singular values to the partial sums normalized by the sum of the entire spectrum against the singular value index for a set composed of one thousand samples, five hundred with one reflector and five hundred with two reflectors. The graph shows that over 90% variation in the spectrum of the kernel matrix can be accounted for by the first ten singular values and that the first one hundred singular values account for over 99% of the spectrum. This suggests that kPCA-SVM should obtain near optimal performance when one hundred features are used and that no additional benefits are gained thereafter. Our principal study uses a data set composed of four thousand samples, evenly split between one and two reflectors. Figure 2 plots the CPU times and cross-validated scores plotted as a function number of kPCA features used in the SVM classifier for a sample set with 4000 seismograms. The accuracy of the SVM plateaus after a small number of the kPCA features are used to build the SVM. The optimal CPU time for training the SVM occurs at this number of features as well. After this optimal number of features,

the CPU time increases linearly with the number of kPCA features included. In this case, the same accuracy of the classifier is obtained using approximately 250 features as with the entire data set, but at only a fraction of the CPU time (1/6). The results indicate that performing kPCA dimensionality reduction prior to SVM classification can significantly increase performance, reliability, and robustness of the classifier in seismic problems. This behavior suggests that for large problems, such as those encountered in real data, dimension reduction prior to classification can drastically improve computation times. The development of these types of classification techniques is needed in situations where limited seismic observation data is available and characterizing the source or acoustic profile model is a key first step in full seismic inversion. The presented method of kPCA-SVM is now applied to determine which seismic wave propagation model is best suited to invert a particular seismogram.

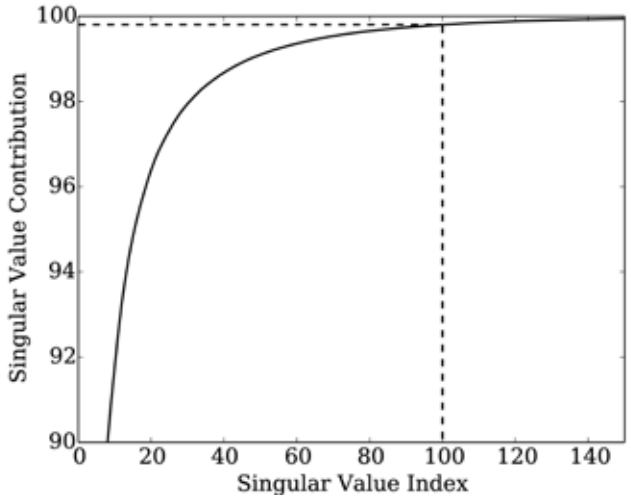

Figure 1. The contribution of the singular values to the partial sums normalized by the sum of the entire spectrum for the first 150 singular values of the kernel matrix constructed using a thousand samples. At 100 features, (10% of the total number of features) the singular values nearly capture the total variation of the sample set in feature space. The dashed line indicates the optimal number of features to maximize the accuracy in the independent test set. The large amount of the spectrum contained in the first 100 singular values indicates that using the subspace defined by these singular values should provide sufficient information for proper classification.

Model Selection

The adopted synthetic data described above is a caricature of many real world seismic situations including the monitoring of faults, detection of underground nuclear weapon testing, and surveillance of facility usage patterns. In the field, seismic inversion relies on assuming that the seismograms given were generated by a particular model of seismic wave propagation and a particular subset of

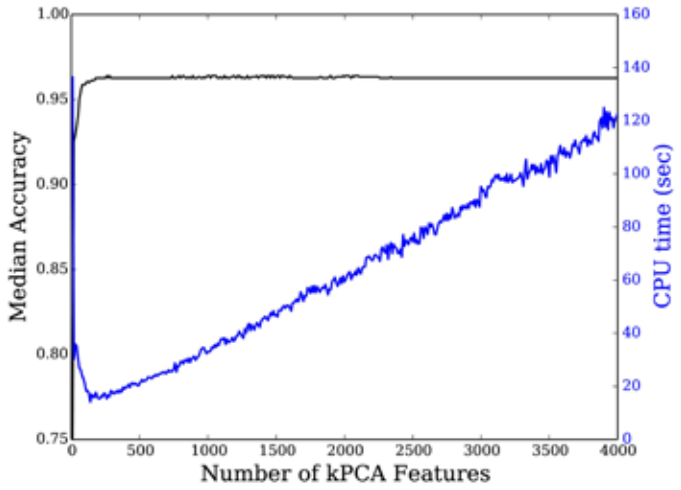

Figure 2. CPU times and cross-validated scores plotted as a function number of kPCA features used in the SVM classifier. The left ordinate is the median accuracy score and the right ordinate is the CPU time for the SVM fit. The optimal CPU time and SVM accuracy are achieved at the same number of retained features. As more kPCA features are included, the CPU time scales linearly but the SVM classier score does not improve. This behavior suggests that for large problems, such as those encountered in real data, dimension reduction prior to classification can drastically improve computation times.

acoustic profiles. Given a set of seismic measurements, the seismic inversion problem seeks to reconstruct an image of the elastic properties of the Earth's interior, or at least the elastic properties in some region of the Earth's subsurface. If acoustic measurements are given instead of directional seismic measurements, then the goal is to reconstruct just the acoustic properties. Though a great deal of success has been found using seismic inversion methods, the computational demand is very great. This computational demand can be reduced if macroscopic questions can be answered about the subsurface structure such as the existence of horizontal or strong compact reflectors or large changes in acoustic speed. The research described here involves the construction of a sparse convolutional-filter-based classifier able to classify seismograms by the presence or absence of these three particular macroscopic acoustic features in the subsurface. The three features picked here lead to eight combinatorial classes, each of which has a corresponding convolutional filter that can be learned. The training dataset is made up of seismograms such as the one shown in Figures 3 and 4. In this case, the seismogram corresponds to one generated by a heterogeneous medium with a strong compact reflector and a large change in acoustic speed.

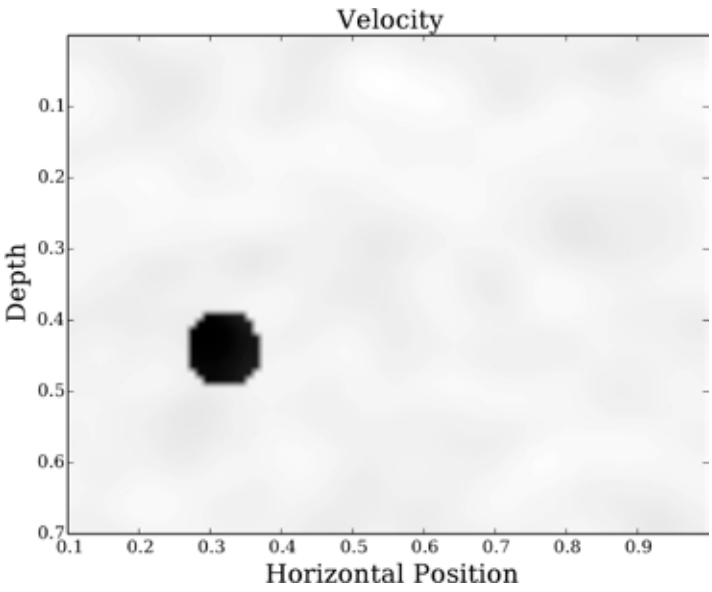

Figure 3. One of the features in our set of synthetic acoustic profiles is a compact strong reflecting inclusion. The inclusion is randomly placed with horizontal position between [0:2; 0:9] and vertical position between [0:5; 0:6]. Inclusions are circular with a random radius between [0:05; 0:1]. Within the inclusion the acoustic speed jumps to 2:0 which, when added to our Gaussian heterogeneous background makes the range of class 4 acoustic speeds between [1:75; 4:25].

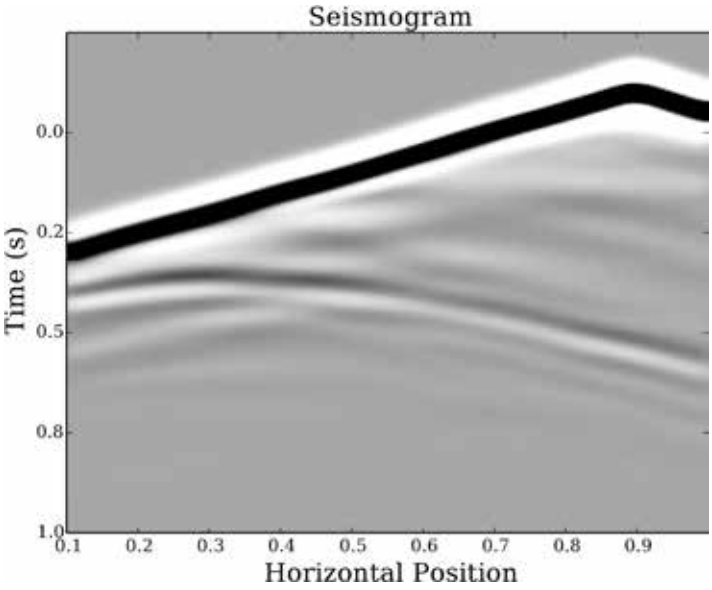

Figure 4. Seismogram corresponding to the feature shown in Figure 3. This seismogram is typical for a compact strong reflector with a large jump in acoustic speed.

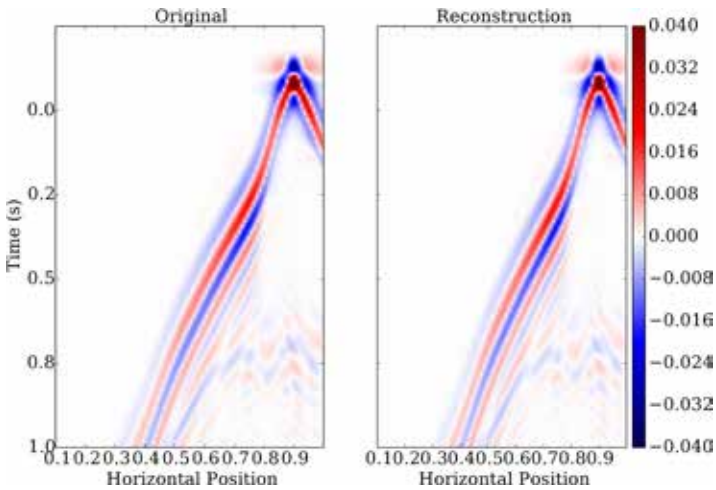

Figure 5. Here we show the reconstruction of a typical seismogram for a heterogeneous background with an acoustic jump at a random depth, ranging over [0:3; 0:6], and random background acoustic speed. Reconstruction was performed using the 9 filters learned through the sparse coding algorithm and shows excellent agreement with the original.

In learning the dictionaries, the computational burden grows with the number of training seismograms included in the problem. This makes solving the optimization problem, even with a very efficient algorithm, computationally intractable for more than tens of training samples. Our solution is to randomly sample training seismograms from a much larger bank of training seismograms. For our work here we used a set of 1000 seismograms generated from each class of acoustic profile, with a total of 8000 seismograms. The filter dictionary for a given class was then learned by randomly initializing the filter dictionary and approximately solving the optimization problem for a set of 20 training seismograms. The learned dictionary was then used as the initialization with a new set of 20 randomly selected training seismograms from the same class and the filter dictionary was further refined. This process was then repeated 20 times to arrive at a dictionary that has been informed by a large subset of the available training seismograms. Procedures like the one just described are known as mini-batch training methods and have been used successfully to train deep neural networks and convolutional neural networks in supervised learning problems with back-propagation algorithms. Figure 5 shows the original and reconstructed seismogram respectively using the filters learned through this sparse coding algorithm, revealing excellent agreement between the two. Once a set of dictionary filters is learned for each of the 8 acoustic profile classes, the dictionaries are combined into a superset dictionary that is used to construct our seismogram classifier.

Conclusions

Seismic data proved to be an excellent testbed to demonstrate our nonlinear dimensionality reduction technique in conjunction with classification algorithms. Our principle findings are as follows:

- kPCA-SVM provides a robust classification algorithm for partitioning seismic signals depending on the acoustic profile model generating them using a small fraction of the total feature space.
- kPCA-SVM obtains the same classification score as nonlinear SVM when a small fraction of the total number of kPCA features are used, sometimes as little as 10% of features at a fraction of the computational cost.
- Machine learning approaches such as convolutional filter-based dictionary learning provide an efficient and accurate way to identify important macroscopic features in the geostructure and can be used to identify the right wave propagation model to be used.

Impact on National Missions

This project helped advance LANL's IS&T pillar by closely integrating new analytical and computational aspects to improve predictive capabilities for large scale problems. Aspects of the modeling framework developed here are relevant for any high-dimensional nonlinear complex system, and are anticipated to be of great interest to several DOE programs. Our methods also address a topic of growing importance, data science at scale, and provide solutions through machine learning, or efficient classification methods to tackle computational burden. Our proposed work aligns well with the DOE ASCR (Advanced Scientific Computing Research) Machine Learning report that recognizes that "Resulting advances, both in the field of Machine Learning, as well as science domains, can potentially catalyze and revolutionize new breakthroughs." A recent DOE report from the BES (Basic Energy Science) Advisory Committee has listed mathematical algorithms, especially for challenging large data and computational problems, as a transformative opportunity in material science.

References

1. Bradley, C., and E. Jones. Modeling propagation effects from explosions in western China and India. 1998. Tech. Rep., Los Alamos National Lab., NM.
2. Denny, M., and J. Zucca. Introduction: DOE Non-Proliferation Experiment, Arms Control and Nonproliferation Technologies. 1994. DOE/AN/ACNT-94A.
3. Stump, B. W.. Practical observations of US mining practices and implications for CTBT monitoring. 1995. Tech. Rep., Los Alamos National Lab., NM (United States).
4. Ellsworth, W. L.. Injection-induced earthquakes. 2013. Science. 341 (6142): 1225942.
5. Vidic, R., S. Brantley, J. Vandenbossche, D. Yoxtheimer, and J. Abad. Impact of shale gas development on regional water quality. 2013. Science. 340 (6134): 1235009.
6. El-Naqa, I., Y. Yang, M. N. Wernick, N. P. Galatsanos, and R. M. Nishikawa. A support vector machine approach for detection of microcalcifications. 2002. Medical Imaging, IEEE Transactions . 21 (12): 1552.
7. Bui-Thanh, T., O. Ghattas, J. Martin, and G. Stadler. A computational framework for infinite-dimensional Bayesian inverse problems Part I: The linearized case, with application to global seismic inversion . 2013. SIAM Journal on Scientific Computing . 35 (6): A2494.
8. Martin, J., L. C. Wilcox, C. Burstedde, and O. Ghattas. A stochastic Newton MCMC method for large-scale statistical inverse problems with application to seismic inversion . 2012. SIAM Journal on Scientific Computing. 34 (3): A1460.
9. Fehler, M.. Status of simulations, The Leading Edge . 2012. SEAM Update: SEAM Phase I RPSEA update. 31 (12): 1424.
10. Jolliffe, I.. Principal component analysis. 2002.
11. Rezaie, J., J. Saetrom, and E. Smorgrav. Reducing the dimensionality of geophysical data in conjunction with seismic history matching. 2012. In SPE Europec/EAGE Annual Conference, Society of Petroleum Engineers. (, 2012). , p. . : .
12. Kortstrom, J., M. Uski, and T. Tiira. Automatic classification of seismic events within a regional seismograph network. 2016. Computers and Geosciences . 87 (2): 22.
13. Scholkopf, B., and A. J. Smola. Learning with kernels: support vector machines, regularization, optimization, and beyond. 2001.
14. Hickmann, K., J. Hyman, and G. Srinivasan. Efficient and robust classification of seismic data using nonlinear support vector machines. Computers & Geosciences..

Publications

Hickmann, K., J. Hyman, and G. Srinivasan. Efficient and robust classification of seismic data using nonlinear support vector machines. Computers & Geosciences.

Coupled ALE-AMR for 3D Unstructured Grids

Jacob I. Waltz
20150414ER

Introduction

This project researches and develops novel methods for the numerical modeling of high-speed material flows that are applicable to a wide range of scientific and national security problems. The basic concepts under exploration involve the combination of historically proven but heretofore independent techniques. The primary scientific challenge for the project lies in the development of a mathematical approach that couples the different techniques in a consistent manner. Such approaches have not been previously developed either at Los Alamos National Laboratory or within the broader computational science community. The new methods are designed to enhance fidelity and computational efficiency relative to existing methods.

Benefit to National Security Missions

We expect our research to lead to significant improvements in fidelity and computational efficiency for work related to NNSA Defense Programs, Nonproliferation, and Science Campaigns. The impacts of these improvements will include faster responses to programmatic questions; increased population sizes for Uncertainty Quantification and other sensitivity studies; greater detail in discovery-scale simulations; and an enhanced ability to model realistic 3D features.

Future Mission: The jump in simulation capability that results from our research will enable the solution of entirely new classes of problems and therefore has the potential to significantly expand the scope of the Laboratory's simulation tools. New application areas might include design of blast mitigation structures for urban environments, energetic disablement calculations of Improvised Explosive Devices, anti-personnel and anti-structural analysis, high-resolution studies of mix and ignition in Inertial Confinement Fusion targets, and astrophysics.

Progress

Two key accomplishments took place during the past 12 months.

The first involved a new local mesh force model that is more robust yet significantly less computationally expensive than existing models. The mesh force model blends characteristics of local mesh stiffeners (which are computationally inexpensive, but physically inaccurate) with mesh spring force models (which are computationally expensive since they require a global solve, but do not pollute the numerical solution with unphysical errors). The resultant algorithm is both inexpensive due to its local nature and physically accurate due to how it is integrated into the mesh motion procedure. The mesh force model was successfully coupled to the irrotational mesh motion procedure that was developed during the first year of the project. Combined, the two methods allow for robust physics-based mesh motion on a variety of complex problems, including those that involve both shock waves and vorticity.

The second accomplishment was the successful coupling of mesh adaption to mesh motion. This work involved the development of mathematically consistent constraints that allow the assumptions of both mesh adaption and mesh motion to be simultaneously satisfied. These constraints therefore constitute the mathematical foundation of the coupled method, and are key to enabling the overall goals of the project.

In addition to the research accomplishments, this work is being disseminated to the scientific community. A journal article describing the robust mesh motion procedure has been submitted for publication, and the results are scheduled to be presented at a major upcoming international conference.

Future Work

FY17 work will involve improved error metrics, along with final documentation and dissemination of research results. Specific tasks include:

- develop and implement mesh adaption metrics that account for a moving reference frame
- test the techniques on complex engineering-class problems
- document the research results in journal articles and/or conference presentations

Conclusion

The goal of this project is to develop a novel method for the numerical modeling of high-speed material flows. The impacts of this work will include significant enhancements in detail and accuracy; reduced uncertainty in simulation-based responses to programmatic issues; and advances in scientific understanding in the broader numerical modeling community. Given the unique nature of the work, it also will establish Los Alamos National Laboratory as an international leader in this area.

Publications

Bakosi, J., J. Waltz, and N. Morgan. Robust mesh velocities for 3D arbitrary Lagrangian-Eulerian methods. To appear in Journal of Computational Physics.

Waltz, J., J. Bakosi, and N. Morgan. A Helmholtz based approach for arbitrary Lagrangian-Eulerian mesh motion. Presented at World Congress on Computational Mechanics. (Seoul, South Korea, 25-29 Jul. 2016).

Waltz, J., J. Bakosi, and N. R. Morgan. A coupled ALE-AMR approach for shock hydrodynamics on tetrahedral grids. Presented at United States National Congress on Computational Mechanics. (San Diego, CA, 27-31 Jul 2015).

Globally Optimal Sparse Representations

Brendt E. Wohlberg
20150467ER

Introduction

One of the major computational challenges in the modern world is the processing and analysis of the growing deluge of data from such diverse sources as automated telescopes collecting astronomy data, physics data from particle accelerators, and intelligence data from remote sensing satellites, to name but a few. Many of these processing and analysis tasks require an effective model for the data at hand. Such a model is provided by sparse representations, which have found an extremely wide range of applications, often with state-of-the-art results. These representations are mathematically simple to define, but usually involve relatively expensive optimization algorithms to compute them. For practical reasons, this type of model is usually applied independently to small blocks of signal or image data. An alternative form of this representation that jointly models an entire signal or image exists, and has numerous advantages, but is not very widely applied, primarily due to the great computational cost.

Motivated by the recent development of significantly for efficient algorithms for these globally optimal sparse representations, this project will explore and develop the mathematical theory, algorithms, and applications of this approach. While there are numerous clear advantages of this form of sparse representation, there are a number of technical challenges in fully exploiting them. Potential applications include processing of and feature detection in hyperspectral remote sensing imagery, change detection in wide-field automated sky surveys, structural health monitoring for critical machinery and buildings, and detection and classification of features in radio frequency signals for non-proliferation monitoring. This work also has the potential for significant impact in the fields of signal and image processing, where sparse representations have become a major subject of research.

Benefit to National Security Missions

The project will develop a general data modeling technique, primarily with relevance to data in the form of sampled signals, images, or video. Given the generality of the method, it has potential relevance to any of the areas above that require processing or analysis of these types of data. As such, the primary mission relevance is to Information Science and Technology. Nevertheless, specific potential application areas that have already been identified include analysis of radio frequency data for non-proliferation monitoring (relevant to agency DOE/NNSA and mission Remote Sensing for Nuclear Nonproliferation), analysis of remote sensing data for non-proliferation and intelligence acquisition (relevant to DOE/NNSA and Intelligence Agencies, and mission Remote Sensing for Nuclear Nonproliferation), modeling of material properties and analysis of multiple modalities of materials science data (relevant to Basic Understanding of Materials mission), structural health monitoring for machinery, including vehicles (relevant to agency DOT and Commerce and Transportation mission), and analysis of astronomical and sky-survey data (relevant to agency NASA and mission Nuclear, Particle, Cosmology, and Astrophysics).

Progress

Technical: Progress has been made on all of the focus areas outlined the proposed work, but none of the issues have been definitely resolved. With respect to both signal representation and dictionary learning, a number of new approaches (some of which seem quite effective in practice) have been developed, and valuable insight has been obtained, but work on these complex questions is ongoing. Substantial progress has been made on algorithm development, including the design of efficient algorithms for various extensions (supporting additional capabilities that will have utility in practical applications) of the basic sparse coding and dictionary learning problems.

Papers: A journal paper ("Efficient Algorithms for Convolutional Sparse Representations") describing state-of-the-art algorithms for sparse coding and dictionary learning was published in IEEE Transactions on Image Processing in January 2016. (The paper has been featured in the list of 50 most frequently downloaded documents for that journal since publication.) Since June 2015, five conference papers have been presented on topics central to the goals of the project. These topics include extension of the method to multi-band images, the development of alternative regularization based on the graph Laplacian, and applications to audoo signal processing and anomaly detection. Two additional conference papers (addressing computationally efficient methods of imposing suitable boundary conditions, and applications to image noise reduction) have been accepted to be presented. Finally, two journal papers on signal processing applications of the method are currently under review.

Collaborations: A number of collaborations have been established, and are delivering results in terms of publications and progress on the technical goals of the project. These include work on low-rank/sparse models and video background modeling in collaboration with Paul Rodriguez at Pontifical Catholic University of Peru, work on sparse models for anomaly detection with Alessandro Foi at Tampere University of Technology as well as with a number of collaborators at Politecnico di Milano, and work on signal processing applications of convolutional sparse representations with groups at Academia Sinica and University of Rochester.

Students: Three students (two from UCLA and one from NCSU) were mentored over the summer of 2015. The work of one of these students lead to the development of a graph Laplacian regularization extension that has already been published as a conference paper. The two other students are returning this summer to continue their research.

LDRD Project Appraisal: The project received an "outstanding" rating in all categories during the November 2015 project review.

Future Work

The third fiscal year of the project will focus on the following main aspects of the project:

Dictionary learning: even in the case of standard sparse representations, the problem of learning a "dictionary" (the set of basic components from which the linear representation is assembled) is still rapidly developing, and is far from being a solved problem. Learning effective dictionaries in the convolutional setting presents an additional set of challenges related to the vastly increased redundancy of the representation, as well as to its unusual properties. Research will focus on understanding some specific properties that have been identified, and designing modified learning algorithms to avoid their associated problems. Examples include issues related to the representation of low-frequency signal components, sensitivity of the learning algorithms to the sparsity tuning parameter, and the construction of multi-scale dictionaries.

Algorithms: the development of even more efficient algorithms is critical to enabling application of these methods to large scale problems. Work will continue of online algorithms that avoid the need to simultaneously load the entire dictionary training dataset into memory, algorithms that support parallel processing and spreading of memory usage across multiple nodes, and GPU accelleration.

Applications: thus far, the project has concentrated on developing general techniques and algorithms for dictionary learning and sparse coding with convolutional sparse representations. In the final year of the project, attention will be given to using this method as a practical tool for solving inverse problems, both of general interest to the computational imaging community, and those of specific interest at LANL.

Conclusion

The major technical goals are the development of theory, algorithms, and applications of the globally optimal sparse representations. This work will primarily involve the development of signal processing theory and methods, together with associated algorithms. If successful, these developments have the potential to change the standard practice in the application of sparse representation methods to a wide variety of problems, together with improved performance and new capabilities of these methods. An open-source library will be released to make these techniques widely available to researchers in the field, as well as to practitioners in application areas.

Publications

Boracchi, Giacomo, Diego Carrera, and Brendt Wohlberg. Novelty Detection in Images by Sparse Representations. 2014. In Proceedings of the IEEE Symposium Series on Computational Intelligence (IEEE SSCI). , p. 47.

Carrera, Diego, Giacomo Boracchi, Alessandro Foi, and Brendt Wohlberg. Detecting Anomalous Structures by Convolutional Sparse Models. 2015. In The International Joint Conference on Neural Networks (IJCNN).

Carrera, Diego, Giacomo Boracchi, Alessandro Foi, and

Brendt Wohlberg. Scale-invariant anomaly detection with multiscale group-sparse models. 2016. In Proceedings of IEEE International Conference on Image Processing (ICIP). , p. 3892.

Cogliati, Andrea, Zhiyao Duan, and Brendt Wohlberg. Piano Music Transcription With Fast Convolutional Sparse Coding. 2015. In IEEE International Workshop on Machine Learning for Signal Processing.

Cogliati, Andrea, Zhiyao Duan, and Brendt Wohlberg. Context-dependent Piano Music Transcription with Convolutional Sparse Coding. 2016. IEEE/ACM Transactions on Audio, Speech, and Language Processing.

Jao, Ping-Keng, Li Su, Yi-Hsuan Yang, and Brendt Wohlberg. Monaural Music Source Separation using Convolutional Sparse Coding. 2016. IEEE/ACM Transactions on Audio, Speech, and Language Processing.

Jao, Ping-Keng, Yi-Hsuan Yang, and Brendt Wohlberg. Informed Monaural Source Separation of Music based on Convolutional Sparse Coding. 2015. In Proceedings of IEEE International Conference on Acoustics, Speech, and Signal Processing (ICASSP). , p. 236.

Luo, Xiyang, and Brendt Wohlberg. Convolutional Laplacian Sparse Coding. 2016. In Proceedings of the IEEE Southwest Symposium on Image Analysis and Interpretation (SSIAI). , p. 133.

Rodr'iguez, Paul, and Brendt Wohlberg. 11. 2016. In Incremental Methods for Robust Local Subspace Estimation. Edited by Thierry Bouwmans, Necdet Serhat Aybat, and El-hadi Zahzah. , p. 284. Chapman and Hall/CRC.

Rodr'iguez, Paul, and Brendt Wohlberg. Incremental Principal Component Pursuit for Video Background Modeling. 2016. Journal of Mathematical Imaging and Vision. 55 (1): 1.

Rodr'iguez, Paul, and Brendt Wohlberg. Translational and Rotational Jitter Invariant Incremental Principal Component Pursuit for Video Background Modeling. 2015. In Proceedings of IEEE International Conference on Image Processing (ICIP). , p. 537.

Rodriguez, Paul, and Brendt Wohlberg. Translational and Rotational Jitter Invariant Incremental Principal Component Pursuit for Video Background Modeling. 2015. In Proceedings of IEEE International Conference on Image Processing (ICIP).

Skau, Erik, Brendt Wohlberg, and Hamid Krim and Liyi Dai. Pansharpening via coupled triple factorization dictionary learning. 2016. In Proceedings of IEEE International Conference on Acoustics, Speech, and Signal Processing (ICASSP).

Sreehari, Suhas, Singanallur V. Venkatakrishnan, Brendt Wohlberg, Gregery T. Buzzard, Lawrence F. Drummy, Jeffrey P. Simmons, and Charles A. Bouman. Plug-and-Play Priors for Bright Field Electron Tomography and Sparse Interpolation. 2016. IEEE Transactions on Computational Imaging.

Wohlberg, Brendt. Endogenous Convolutional Sparse Representations for Translation Invariant Image Subspace Models. 2014. In Proceedings of IEEE International Conference on Image Processing (ICIP). , p. 2859.

Wohlberg, Brendt. Convolutional Sparse Representation of Color Images. 2016. In Proceedings of the IEEE Southwest Symposium on Image Analysis and Interpretation (SSIAI). , p. 57.

Wohlberg, Brendt. Boundary Handling for Convolutional Sparse Representations. 2016. In Proceedings of IEEE International Conference on Image Processing (ICIP). , p. 1833.

Wohlberg, Brendt. Convolutional Sparse Representations as an Image Model for Impulse Noise Restoration. 2016. In Proceedings of the IEEE Image, Video, and Multidimensional Signal Processing Workshop (IVMSP).

Wohlberg, Brendt. Efficient Algorithms for Convolutional Sparse Representations. 2016. IEEE Transactions on Image Processing. 25 (1): 301.

Enabling Automatic Parallelism and Transparent Fault Tolerance

Marion K. Davis
20150485ER

Introduction

One of the three major challenges in harnessing the potential of an extreme-scale computing system, as identified by the 2010 Summary Report of the DOE Office of Science Advanced Scientific Computing Advisory Committee (ASCAC), is exploiting massive parallelism. In particular, they state that software implementations will need new programming paradigms to make effective use of unprecedented levels of concurrency. Yet more recent is the 2011 DOE Advanced Scientific Computing Research (ASCR) Exascale Programming Challenges Report, specifically calling out the need to revisit functional-language concepts. DOE and DARPA have also recognized the potential of domain-specific languages (DSLs) for raising the level of abstraction of programming. In the broader scientific computing community it is becoming more widely understood that the only programming paradigm that can so scale will be data-dependence-based asynchronous scheduling of purely functional compute tasks. In turn, this paradigm enables a fault-tolerance mechanism much more light-weight than checkpoint/restart because compute tasks, being pure (side-effect free), can be safely restarted if their failure is detected. This project will develop and evaluate a robust and performant implementation of this paradigm in its purest form wherein compute tasks are both internally and externally (observationally) pure. While such systems have been proposed, and their theoretical properties are well-understood, no non-trivial implementation exists with an evaluation mechanism that is strict by default, i.e., exhibiting the behavior most commonly expected by programmers and required for high performance. By its nature such a system will be able to automatically extract maximal parallelism from a program, and in the presence of uncommitted compute resources allow speculative evaluation of results that may or may not be needed in the future. Further, it enables transparent (to the programmer) fault tolerance mechanism as previously described, and a type system that supports efficient deep embedding of DSLs.

Benefit to National Security Missions

High performance computing is fundamental to the advancement of many areas of science. While innovations in hardware technologies continue to allow us to build ever more powerful and complex computing systems, our modes of programming them have advanced conservatively. Both DOE and DARPA have recognized the need to re-examine the entire software stack that ranges from operating systems, runtime systems, programming systems, and applications. At the level of programming systems, the need to re-explore functional language concepts has been explicitly identified. This project directly addresses this need, as well as its corresponding runtime system. Breakthroughs in this area will benefit high performance scientific computing at large, and all scientific disciplines that use it.

Progress

The high-level goals for FY16 were stated to be

- largely complete serial implementation, and
- begin implementation of runtime support for parallel evaluation.

We previously reported that the bridging between the GHC Haskell compiler intermediate representation STG and our implementation of STG had been deferred as low-priority to the central goals of the project; this will also be addressed in the following.

Deliverables

The serial implementation was largely completed, which consisted mainly of enforcing invariants for dynamically consistent global state such that e.g. garbage collection can be performed in an asynchronous multi-threaded environment. Tail-calling is now fully implemented in user-level code, both for the STG abstract machine and the generated C code, both prerequisite for efficient parallel execution.

For the parallel runtime we have implemented a prototype Pthreads-based thread pool and a lock-free work queue, this latter critical for parallel performance. As an alternative thread pool we have implemented a thin wrapper around the ANL Argobots user-level thread library to provide equivalent semantics. This remains ongoing work for FY16.

Work on the previously deferred bridging to the GHC front end has been initiated and is scheduled for the remainder of FY16. As a stop-gap measure we implemented our own Haskell-subset front-end to facilitate the creation of test cases.

The semantic and syntactic concepts of function strictness and application strictness have been formally characterized and this distinction made in the choice of evaluation strategies and in the test suite.

On the software engineering front our test suite has grown considerably and our testing system currently performs ~1500 distinct tests automatically with every update to the code repository. We have implemented a logging mechanism for run-time diagnostics.

Our software has been released as open source under LANL LA-CC-15-073.

Future Work

The scope of work has changed as a direct consequence of budget cuts from the proposed $390K/yr to $342K for FY15 to $330K for FY16 and FY17. Specifically the investigation and implementation of a light-weight resilience mechanism for fault tolerance, originally proposed to begin in FY16 Q4, will be deferred indefinitely so that progress on the primary goal of automatic parallelization under variable evaluation strategies, and assessing the performance implications of variable evaluation strategies with automatic parallelization, will not be compromised. As such demonstrating fault tolerance as a specific goal has been elided from the project description, though its enablement by general design remains. Because the system has been designed with the resilience mechanism in mind, fault tolerance could be restored as a deliverable if funding were correspondingly restored.

Goals for FY17 include,

- Complete parallel implementation
- Implement performance counters and automate the collection and processing of performance data from the test suite
- Demonstrate linkage from user-level code to external C libraries.

Tasks for FY17 include,

Parallel implementation

- Design and implement thread-local stacks
- Design and implement thread-local heaps
- Design and implement various runtime changes for thread coordination for evaluation (computation), and for garbage collection
- Integrate work queue/thread pool with runtime

Performance profiling

- Implement performance counters and timers
- Design and implement logging
- Provide facilities for processing and presenting logged data

External C linkage

- Introduce mechanism for globally declaring external library function type signatures to type inferencer and code generator
- Augment build system to incorporate external library linkage

Conclusion

First is the strict pure functional language implementation itself, as open source--the first of its kind, even disregarding the automatic parallelization that this system will implement. Second, the practical validity of arguments for and against the strict but pure functional paradigm, in the context of scientific computing, while maintaining purity, will be testable. Third is the demonstration of utility of an environment in which the space/time implications of various evaluation strategies can be accurately instrumented and quantified.

Publications

Davis, K., D. Prichard, D. Ringo, L. Anderson, and J. Marks.

Inserting Nonlinear N-Material Coupling PDF Information into Turbulent Mixing Models

Jozsef Bakosi
20150498ER

Introduction

The project develops new mathematical models for turbulent mixing. We target applications in which the detailed simulation of turbulence is intractable and the purpose of "turbulence models" is to predict the statistics of turbulent mixing which is far more tractable. We address the mixing problem of multiple materials with very different densities. In such problems the velocity affects the material fields and more importantly, the material fields affect the velocity field. This results in strong two-way coupling between the fields that is not accounted for in current statistical computations.

The work introduces a new principle: Any model for the statistics must be derived from a relevant underlying probability density function (PDF), a higher order mathematical object that is consistent with the physics of coupled hydrodynamics and material mixing and contains information on all statistics. This ensures physical correctness at the mathematical and theoretical levels and has never been done.

We synthesize two evolution equations governing mass transport in two realms describing turbulent mixing: the mass fractions transport in physical space, and the Master Equation describing the transport of statistical information in probability state space. We also apply two averaging methods: Reynolds averaging in physical space and sample space averaging. This allows instantaneous constraints to be inserted into statistically averaged equations. This synthesis has never been done.

We bridge the multi-fluid and single-fluid descriptions of turbulent mixing. The Master Equation allows accounting for widely different underlying PDFs of the state space, representing very different non-equilibrium stages of the mixing process. This two-pronged strategy allows representing both sharp and diffusive material interfaces within the same method and allows a continuous bridging between multi and single fluid models, which has never been done.

The project entails mathematics, theory, computation, and validation, resulting in implementation of new models in a LANL production code.

Benefit to National Security Missions

Multi-component variable-density turbulent material mixing is a central element in many LANL programs. Material fields are required for a predictive science of turbulent mixing, reaction, and opacity. This work will directly and immediately impact modeling efforts and advance the predictive science in ASC (XCP) and various campaigns. The work will result in engineering models, directly relevant to LANL's large physics codes, in which the resolution of all scales are intractable and statistical methods are the only practical approach.

The results of the work will be translated in the 3rd year into programmatic engineering efforts by implementation of the developed equations into LANL's RAGE production code. To this end we are in contact with Robert Gore (XTD-IDA), and Marianne Francois (XCP-4), former and current project leads of various Campaigns.

Progress

In the second year of this project, we connected the first fiscal year's work on binary mixing to the existing moment method currently used in an unexpected way. We specified a new model expression for the fluid density variance required for modeling reaction rates. The new theoretical hypotheses underlying the new model have been verified using our new Monte Carlo code starting from multiple initial conditions representing different amounts of mixing fluids. The new model is currently being implemented in both FLAG and RAGE codes. This new density variance closure is an unexpected result that is directly useful at the Laboratory. A short report will be written on this result.

We continued work on the development and specification of the new turbulent mix model for two different-density fluids. In the first FY we only had functional forms for the model equations governing statistics. We now also have partial specifications for model coefficients.

We have also found a new way to derive a simple equation governing the primary variable responsible for variable-density mixing, used in the BHR model, the density-specific-volume correlation, b. Previously we had been using the material mass fraction variance, <y^2>, as a proxy but now use the a new equation for b. This is a very large breakthrough in that we are now able to have a model equation for b, derived from the Fokker-Planck equation, that once we finish modeling can be tested against data in the 1D and 3D BHR solvers. We have a general structure for the new b equation and are finishing up modeling it and comparing to high-fidelity direct numerical simulation (DNS) data using our Monte Carlo simulations.

We have also devised a new non-equilibrium time scale to address the transitional nature of mixing processes in general (i.e., not only variable-density mixing). Having this completed means that we have a basic template and recipe with which to address the multi species problem as well. Both the new b equation and the new time scale are unexpected results.

Instead of performing large eddy simulations (LES) to produce data for validation, we slightly changed course regarding our validation strategy and abandoned LES for this purpose. Instead, we obtained higher fidelity DNS data from Livescu. The new DNS data, resolving all physically relevant scales, provides the “true” solution for validation of our model for different amount of mixing fluids.

We have publicly released the Monte Carlo code (now open source, LA-CC-16-015, https://github.com/quinoacomputing/quinoa), used to validate the theoretical hypotheses within this project and useful for designing statistical moment approximations in general.

Future Work

Our goal is to finalize the specification of the binary material mix model by the end of the 2nd FY. After the model specification, validation will be performed in Schwarzkopf’s 1D code that solves ordinary differential equations governing spatially homogeneous mixing. This will be followed by final implementation in the RAGE code used.

In the third year of the project we plan to do analogous work (theory, Monte Carlo hypotheses testing, and validation) on the multi-material (ternary) mixing case.

Conclusion

The new turbulent material mix model will correctly account for the nonlinear coupling and constrained statistics in the mixing of multiple materials that do not exist in current approaches and will avoid the conventional passive-scalar approximations that are inadequate for LANL problems. The new model will be implemented in a production code for immediate impact on programmatic efforts. We expect sizable improvements over the currently used passive-scalar approximations for multi-material mixing problems and highly visible breakthrough-level results in the area of material mixing to be published in the open literature.

Publications

Ristorcelli, J. R., and J. Bakosi. Progress on the Density Variance in the Reaction rate. 2016. LANL Research Library.

Long-time Dynamics Using Trajectory Splicing

Arthur F. Voter
20150557ER

Introduction

Molecular dynamics (MD), the simulation of the evolution of individual atoms in a material, is an essential tool to further our understanding of materials at the nanoscale. Due to its inherently serial nature, however, MD is strongly limited in the timescales it can reach, a problem that becomes even more crippling on large-scale parallel computers. There is thus a pressing mission need for massively-parallel long-time MD simulation techniques. Building on our many years of experience addressing this issue, we are introducing a new paradigm in long-timescale simulation: parallel trajectory splicing (ParSplice). In this ParSplice approach, a long trajectory of arbitrary accuracy is assembled from many short, independent segments generated efficiently in parallel. Through the use of simulation simulators, i.e., simple models of the simulation framework, we will systematically explore the large design space of ParSplice methods to identify the best performing methods on existing and expected next-generation (or exascale) computer architectures, taking into account massive core counts, shorter mean times between failures, and energy costs dominated by data-motion. We will demonstrate the efficiency of the approach in production conditions by investigating problems important to the mission of the lab such as void and bubble evolution, annealing of defects at grain boundaries, and ionic transport in complex oxides. For systems where the trajectory is trapped in small regions of configuration space, we expect efficiency gains of several orders of magnitude at extreme computational scales compared to current approaches. ParSplice will revolutionize the way large-scale long-time MD simulations are performed.

Benefit to National Security Missions

The project directly addresses fundamental challenges of direct relevance to the lab and to DOE/SC/BES and DOE/SC/ASCR. Our project supports the Scientific Discovery and Innovation mission of the lab through two pillars: the basic understanding of materials, and IS&T. Indeed, our goal is to develop a novel capability that would enable the direct simulation of materials at the atomic scale over extremely long timescales. Such a capability is invaluable to investigate the microstructural evolution of materials and understand their performance in operation conditions. Applications to materials in extreme condition are directly relevant to the lab's mission, for example in support of the MaRIE effort. Application to nuclear materials are also directly relevant to BES and OFES. A second crucial aspect of the project is to develop a novel simulation paradigm that exploits state-of-the-art concepts in computer science. We are especially interested in the scalability of simulations up to the peta and exa-scales. Doing so requires the development of architecture-aware algorithms and codes that are scalable and fault-tolerant. Our project contains an important performance prediction component that will be used to predict and optimize the performance of the code on various architecture. These activities directly address challenges identified by ASCR.

Progress

During the past fiscal year, we have concentrated on improving the scalability of ParSplice in order to be able to exploit peta-scale computational resources, and beyond. We have developed a completely new implementation that relies on modern software design concepts. For example, communication is handled by a dedicated process at the node level to avoid network contention. This also allows the overlap of communication with computations in a very efficient manner. Task management is also carried at the node level. The new implementation relies on a high performance parallel database. Due to a tree-based communication pattern and a hierarchical caching framework, the database can maintain a high throughput even when the number of replicas is very high. The new implementation was deployed on Trinity as part of a Phase 1 open science project. The code was demon-

strated at scale, using up to 200,000 replicas.

The ParSplice code was used to study a range of problems. In collaboration with a DOE/SciDAC program, we carried out simulations of the evolution of vacancy/helium clusters in tungsten on Trinity. This has allowed us to highlight the crucial role of the complex interplay between Frenkel pair creation and annihilation. In collaboration with two DOE/BES programs, we have simulated the impact of point defects on the evolution of disordered oxides. We have also begun exploratory simulation of the evolution of vacancies in UO2, in collaboration with the DOE/NEAMS program.

Future Work

In the next fiscal year, we will concentrate on improving the performance of ParSplice for complex systems. Up to now, the internal model of the system that is used to predict the future evolution of the trajectory only contains states that have been visited before. Hence, ParSplice performs very well in situations where the trajectory is trapped within the same set of states for extended periods of time. We will extend our approach to cases where the system does not revisit states per se, but mostly evolves through pathways that have been seen before. This will entail being able to recognize and store transitions, as well as being able to map transitions to new states. This new approach should greatly increase the efficiency of ParSplice on more complex systems that do not revisit the same states often.

Concomitantly, we will apply our current code at intermediate scales (~1000 cores) in order to further demonstrate its practical uses in research settings. Possible application areas include complex defects in metals ceramics, nanoscale clusters, and dislocations.

Conclusion

We will develop the ParSplice method and deliver an implementation that is nominally exascale ready. This state of readiness will be validated through extensive simulations using our performance prediction approach. The design and parameter spaces will be thoroughly explored so as to be ready to adjust the implementation novel architectures emerge. We will also deliver a thorough formal understanding of the method. Based on this analysis, the class of systems that would optimally benefit from ParSplice will be identified. The power of the approach will be demonstrated on leadership-class computers on physical problems of interest to the lab.

Publications

Perez, D., E. D. Cubuk, A. Waterland, E. Kaxiras, and A. F. Voter. Long-Time Dynamics through Parallel Trajectory Splicing. 2016. JOURNAL OF CHEMICAL THEORY AND COMPUTATION. 12 (1): 18.

Spatial and Extreme Value Processes for Bridging Micro- and Macro-Scales in Materials

Scott A. Vander Wiel
20150594ER

Introduction

Advances in computing power have made it possible to simulate very small physical systems in remarkable detail, often making use of "first principles," or at least very reliable mathematical models for system evolution. However, bridging information from simulations at very small scales to the macro-scale required for modeling large-scale systems (e.g. the global ocean, a nuclear reactor, an implosion) remains a challenging and open problem. In materials science, advances in bridging scales are needed to develop more predictive models of material behavior given its micro-scale composition, enabling more reliable predictions of material properties in new, extreme environments, and enabling the design of new materials.

This project focuses on a basic problem in material science: How do heterogeneous, micro-scale descriptions of a polycrystal affect macro-scale mechanical response properties? Here the seemingly random spatial distribution of micro-scale material properties often results in spatially coherent stress fields (under loading), leading to damage or failure in the material. This project will focus on developing statistical theory, models, and tools to advance our ability to estimate macro-scale mechanical response properties from heterogeneous, random, microscale material descriptions.

Benefit to National Security Missions

There is a demonstrated need for advancement in computational prediction of damage and failure in polycrystalline metallic materials, particularly for our weapons calculations. This is largely a result of inadequate physics and material statistics representation. Although the computation mechanics and mechanics of materials communities continue to make advances in this arena, much of the work is lacking proper rigor in how extreme value physical processes are represented mathematically. This project is designed to address this shortcoming in how we represent such processes. The programs here at LANL with interest and need in these technological areas are ASC PEM Materials Modeling, Campaigns 1, 2, and 4. With increased interest in advanced and additive manufacturing processes, a rigorous statistical linkage to the material microstructure as we are proposing to do here will be important. In addition, the Office of Science is interested in funding work which offers the potential to promote energy efficiency. By improving our ability to predict damage and failure events in metallic materials, transportation sector industries can make more efficient use of materials and reduce the weight of vehicles and reduce manufacturing energy intensity.

Progress

We have developed a statistical model to represent the stress field in a multi-grain volume. The model incorporates several features observed in meso-scale computations: (i) each grain has its own nominal stress level, (ii) stresses tend to elevate at some, but not all, grain boundaries, (iii) boundary locations with elevated stress are correlated across grains. Fitting of the statistical model is challenging because meshes are on the order of half a million elements and this translates into vary large covariance matrices that represent spatial dependence in stress fields. Implementation of the statistical model is now complete.

Stress fields are represented as integrals of Gaussian Markov random fields. The structure of this model allows large-scale correlated fields to be computed blockwise in a Monte Carlo Markov chain (MCMC) calculation. The result is a posterior distribution of parameters that control correlation length scales and distances that elevated boundary stresses penetrate into grain bodies. This is a totally new approach to characterizing stress fields in polycrystalline materials with the potential to statistically bridge the gap between meso-scale and macro-scale models describing and predicting

how materials fail. Fitting the statistical model has been much more challenging that we anticipated, and we now recognize that the model form is inherently poorly conditioned for the original goal of producing new realizations of stress fields with spatial hot spots that mimic those of computational volumes. Nevertheless, we are writing up two papers for journal submissions to describe the work to statisticians and material scientists.

Flyer plate experiments on tantalum samples in combination with macro-scale damage model calculations of these experiments have provided quantitative information on stress conditions at the estimated point when material voids begin to grow. These boundary conditions are used as inputs to meso-scale polycrystalline models to interrogate the behavior of interacting tantalum grains. Finite element models of tantalum microstructure have been created with a 3D voxel structure that matches distributions of grain size, shape and crystal orientations. We can provide an endless supply of statistically equivalent microstructure realizations for further modeling efforts. We apply external stresses with time, representative of those in flyer plate experiments to the polycrystalline finite element meshes to produce stress fields throughout a representative volume of tantalum grains. These calculations show that stress tends to elevate at interfaces between two grains and more-so where three grains meet.

Curt Bronkhorst is presenting our work in LANL's Information Science and Technology Capability Review in June 2016. Peter Marcy gave two presentations and two posters on the work at various venues between March 2016 and May 2016.

Future Work

This effort will be conducted in two main phases. In the first phase, statistical theory and methodology will be developed in concert with a simulation campaign focused on simulated materials. Once methodology has been sufficiently refined, and kinks and problems have been worked out in the synthetic setting, we expect to move focus to actual materials.

Over the next fiscal year, we will:

- Develop a variety of statistical metrics for the spatial stress fields in polycrystalline structures, with special attention to conditions for elevated stress at grain boundaries and triple junctions
- Relate the spatial metrics from computed stress fields to those from random realizations of the statistical stress model as a means of demonstrating that the model carries accurate information about spatial distributions of stress hot spots.
- Relate the spatial metrics to crystal orientation and misorientation, to Taylor factors, and to boundary plane angles.
- Develop statistical models of the resulting stress field, characterizing the extremes of the field, as well as their spatial dependence.
- Analyze current computational experiments that vary stress conditions and numbers of slip systems to show how spatial hot spot distributions are impacted by these factors.

Conclusion

This effort will demonstrate a viable approach for statistically characterizing micro-scale properties of a polycrystal, and using these properties to predict the material's strength and damage properties at a macro-scale, under some rather simple loading scenarios. We also expect this effort will illuminate promising new directions for analysis approaches that can bridge the micro- and macro-scales. In particular, we will seek new statistically rigorous representations of damage nucleation in polycrystalline materials. As new experimental facilities come online, this work will serve to get some of the necessary analytical tools in place for gaining understanding from such experiments.

Publications

Bronkhorst, C. A., D. J. Luscher, H. M. Mourad, P. W. Marcy, S. A. Vander Wiel, N. Bourne, G. T. Grey III, V. Livescu, V. Livescu, and E. K. Cerreta. Meso to Macro Mechanics of Metallic Ductile Damage Under Dynamic Loading Conditions. Invited presentation at Society of Engineering Science 53rd Annual Technical Meeting 2016. (College Park, MD, 2-5 October, 2016).

Bronkhorst, C. A., G. T. Gray III, F. L. Addessio, Livescu, N. K. Bourne, S. A. MacDonald, and P. J. Withers. Response and representation of ductile damage under varying shock loading conditions in tantalum. 2016. JOURNAL OF APPLIED PHYSICS. 119 (8).

Bronkhorst, C. A., N. Bourne, G. T. Gray III, V. Livescu, C. B. Storlie, S. A. Vander Wiel, E. K. Cerreta, D. J. Luscher, M. Ardeljan, and M. Knezevic. Deformation Induced Porosity Nucleation Mechanisms in Polycrystalline Metallic Materials (keynote lecture). Invited presentation at International Symposium on Plasticity 2015. (Montego Bay, Jamaica, 4-8 January, 2015).

Bronkhorst, C. A., N. Bourne, G. T. Gray III, V. Livescu, C. B. Storlie, S. A. Vander Wiel, E. K. Cerreta, D. J. Luscher, M. Ardeljan, and M. Knezevic. Deformation Induced Porosity Nucleation Mechanisms in Polycrystalline Metallic Materials. Presented at Mach Conference 2015. (Montego Bay, Jamaica, 8-10 April, 2015).

Bronkhorst, C. A., N. Bourne, G. T. Gray III, V. Livescu, C. B.

Storlie, S. A. Vander Wiel, F. L. Addessio, D. J. Luscher, M. Ardeljan, E. K. Cerreta, and M. Knezevic. Porosity Based Damage and Failure in Polycrystalline Tantalum – Structural Linkages (invited). Invited presentation at TMS 2015. (Orlando, Florida, 15-19 March, 2015).

Bronkhorst, C. A., N. Bourne, G. T. Gray III, and V. Livescu. Porosity Based Damage and Failure in Polycrystalline Tantalum – Structural Linkages. Invited presentation at Information Sciences and Technology Capability Review for Computational Physics and Applied Mathematics. (Los Alamos, NM, June 2016).

Marcy, P. W., C. B. Storlie, S. A. Vander Wiel, and C. A. Bronkhorst. Modeling Material Stress Using Integrated Gaussian Markov Random Fields. Presented at Society for Industrial and Applied MAthematics Conference on Uncertainty Quantification. (Lausanne, Switzerland, 5-8 Apr 2016).

Marcy, P. W., C. B. Storlie, S. A. Vander Wiel, and C. A. Bronkhorst. Modeling Material Stress Using Integrated Gaussian Markov Random Fields. Presented at Conference on Data Analysis. (Santa Fe, NM, 2-4 Mar 2016).

Marcy, P. W., C. B. Storlie, S. A. Vander Wiel, and C. A. Bronkhorst. Modeling Material Stress Using Integrated Gaussian Markov Random Fields. Presented at Information Science for Materials Discovery and Design . (Santa Fe, NM, 16-18 May 2016).

Marcy, P. W., S. A. Vander Wiel, C. A. Bronkhorst, and V. Livescu. Modeling Material Stress Using Integrated Gaussian Markov Random Fields. 2016. Submitted to Annals of Applied Statistics..

Deep Sparse Columnar Neural Network (dSCANN)

Garrett Kenyon
20150752ER

Introduction

Understanding the computational capability of the human brain is a principal scientific grand challenge of this century, an enterprise that will require the application of large-scale, high-performance computing resources. In addition to providing insight into the intelligence that is the basis of all human technology, the effort will have transformational impact on computational science. Los Alamos researchers have become leaders in high performance neural simulation and neuromimetic applications, having developed codes that run efficiently on massively parallel computer architectures. In practice, however, it has not been possible to execute our neural simulations at anything close to the scale and complexity of cortical circuits, due to the limited memory and computational power of standard workstations and small clusters. The Trinity platform allows for a fundamentally different approach to large-scale cortical simulations, enabling an unprecedented leap in our ability to model cortical processing. We propose to implement a novel neural network architecture based on the columnar organization of the cerebral cortex, utilizing the Xeon Phi/KNL processors of Trinity Phase 2. As a specific problem, we will implement a hierarchical cortical network employing a local columnar architecture that will be trained to solve difficult spatial navigation and target detection tasks using motion, depth, and texture cues. We will also apply deep sparse columnar networks to global weather data, in order to determine whether the deep structure of the simulation results are similar to those obtained via direct measurement. We believe that similar techniques will ultimately be applied programmatically, to monitor, analyze and compare computational simulation to results of dynamic experiments.

Benefit to National Security Missions

DOE/SC: Our project is designed to demonstrate how deep neural network architectures can be mapped efficiently onto distributed supercomputer architectures.

DOD: Our project seeks to advance the state-of-the-art in automated spatial navigation and target detection tasks.

Intelligence Agencies: Our project seeks to develop new methods for automating the analysis of large data streams using supercomputer resources.

Fundamental Bioscience: Our project seeks to improve our understanding of cortical information processing.

Information Science and Technology: Our project seeks to develop fundamentally new approaches to neuromimetic computing.

Progress

We begin by summarizing the goals we expect to accomplish by the end of FY16 under the auspices of the Trinity Phase II open science project:

Optimization of PetaVision core convolutional routines for execution on single Intel KNL processors. The recently concluded discovery session with Intel engineers, attended by the PI and by Scot Halverson and Baram Yoon, demonstrated approximately 15-20% peak theoretical performance on KNL processors using test code based on core PetaVision convolutional operations. The optimization strategies employed by Scot and Boram included loop reordering to achieve better cache utilization, memory alignment and OpenMP thread optimization, yielding 5Xs - 10Xs speedups over the original unoptimized code. Further wins are anticipated by allocating memory in a dynamic manner so as to help localize the information required for individual threads and by exploiting lower resolution (float16) representations to reduce memory bandwidth and better utilize cache.

Optimization of PetaVision for execution on multiple Intel KNL processors. We will conduct runs this summer

in consultation with engineers from Intel and Cray on the Trinitie development platform to ensure that PetaVision performance scales approximately linearly with the number of KNL nodes. PetaVision employs a model-parallel execution model in which MPI is used to communicate activity between neighboring cortical columns, with each column implemented on a single node, and OpenMP is used to update the neurons within an individual column in a parallel manner. Our model-parallel approach is compute bound, using only local communication, and is expected to scale well across multiple nodes. Straightforward i/o optimization to allow read/write operations from more than one MPI rank, as well as fast checkpointing using burst buffers, will be implemented at this stage as well.

Implementation of deep, sparse, hierarchical model. We will use the Trinite development platform, as well as distributed platforms based on older processors, to test the deep, sparse, hierarchical model that we will ultimate execute on Trinity itself. Our deep model will learn to use stereo, motion and associated texture-flow and shading cues to estimate depth. This model is a natural extension of our existing models but involves a computational burden that requires large-scale compute resources to investigate.

Future Work

Proposed Work for FY17: Implementation and execution of open science runs on Trinity.
These runs to demonstrate how a scalable cortical architecture can learn to use visual cues to represent depth within a scene in an entirely unsupervised manner, analogous to how biological systems are hypothesized to self-organize during visual development.

Task 1: Model refinement runs conducted on Trinitite and other distributed architectures. Although the definition of the deep, sparse, generative model will be completed in FY16, additional model refinements will help to ensure the success of the final runs on Trinity.

Task 2: Execution and analysis of runs on Trinity.

Conclusion

Deep-learning algorithms based on convolutional neural networks loosely inspired by brain architecture have become the state of the art for classes of problems such as object/image classification and pattern recognition. These are problems that have not been adequately addressed with conventional algorithms. Using the Los Alamos supercomputer Trinity, we will implement a novel neural network architecture based on the columnar organization of the cerebral cortex. The results of this work could result in new methods for automating the analysis of large data streams using supercomputer resources, and advance the state-of-the-art in automated spatial navigation and target detection tasks.

Publications

A Deconvolutional Strategy for Implementing Large Patch Sizes Supports Improved Image Classification. To appear in Computational Models of the Visual Cortex (CMVC2015), 9th EAI International Conference on Bio-inspired Information and Communications Technologies (formerly BIONETICS). (Columbia University, New York, 2015).

Lundquist, S. Y., D. M. Paiton, P. Schultz, and G. T. Kenyon. Sparse Encoding of Binocular Images for Depth Inference. 2016. In 2016 IEEE Southwest Symposium on Image Analysis and Interpretation. (Santa Fe, 6-8 March, 2016). Vol. 0, 0 Edition, p. 121. Santa Fe: IEEE.

Paiton, D. M., X. Zhang, S. Y. Lundquist, W. Shainin, P. Schultz, and G. T. Kenyon. A Deconvolutional Competitive Algorithm for Building Sparse Hierarchical Representations. 2016. In Computational Models of the Visual Cortex, 9th EAI International Conference on Bio-inspired Information and Communications Technologies. (Columbia University, New York, 2015). , p. 0. New York: EUDL.

Efficient Exploration of High-Dimensional Model Structural Uncertainties

Nathan M. Urban
20160189ER

Introduction

Computer simulations of physical systems can have large uncertainties, which are due to the mathematical approximations necessary to efficiently solve the system's governing equations. Different choices of approximation, or "model structure", can result in different predictions. It is difficult to explore and quantify the range of possible predictions without manually and laboriously rewriting the simulation model code, and re-running time-consuming computer simulations, every time a new approximation is investigated.

We propose an automated method to efficiently generate and test a wide range of model structures for physical realism. It works by learning a mathematically compact representation of a computer model's structure. Once learned, it automatically suggests novel but related model structures. Many of these will be physically unrealistic, so it also automatically generates a simplified or "reduced" version of the complex simulation model, with which it can quickly evaluate the validity of the proposed structures without having to rewrite and re-run the original code. The result will be a set of different but physically plausible model structures, whose range of predictions then can be quantified.

Benefit to National Security Missions

The project primarily advances fundamental capabilities in computer model structural uncertainty quantification, and is most closely aligned with the Information Science and Technology mission. It impinges on any application area that uses complex simulations of physical systems described by partial differential equations, particularly related to fluid dynamics. Model structural uncertainties are often of significant importance across many agencies and missions, but are not often explicitly recognized as such by mission agencies. Therefore, for most applications, the work falls under "building underlying science / tools / capabilities" rather than "directly addressing identified mission challenges". Thus this work supports the mission challenges in the Office of Science and NNSA/Weapons program spaces.

Progress

We have constructed a test case of our method based on a numerical model of the two-dimensional rotating shallow water equations, an idealized geophysical fluid dynamics problem. We have successfully inferred the system dynamics by sampling the model output at the level of a single grid cell evolving over a single time step, and statistically reconstructing the local dynamical operator (LDO) that describes this evolution. This statistical reconstruction, using a regression approach, is essentially perfect in accuracy. However, it should be noted that in this test case, the LDO is a polynomial function that is easier to learn than a general nonlinear operator. Our LDO reconstruction procedure might be expected to lose accuracy in more complicated settings. This satisfies our Year 1 Goal 1 in the proposed work.

We have also constructed a reduced order model (ROM) for the rotating shallow water equations that exhibits reasonable accuracy in approximating the original numerical model while requiring almost 1000-fold fewer variables to describe the system's behavior. This ROM is constructed directly from the LDO we infer from simulation output, without any explicit knowledge of the underlying governing equations the simulation is solving. This represents a considerable advance over traditional projection-based ROM methods that require direct knowledge of the system equations. This satisfies Year 2 Goal 2.

These outcomes demonstrate that we can automatically construct an approximate description of a model's dynamics. However, they do not yet demonstrate an ability to explore alternate model structures (model structural uncertainty). In order to explore alternate

structures, a necessary (but not sufficient) condition is to determine which governing equations respect basic physical constraints such as the law of energy conservation. We are formulating our LDO inference problem as a constrained form of regression, such that the learned LDO is guaranteed to conserve energy (to the same accuracy as the original numerical simulation, at least). We have derived the form of the constraint equations and are in the process of implementing the constrained regression. This begins to address Goal 4, which was a Year 2/3 task.

We are also exploring the ability to learn model structures from lower-fidelity data. Our existing approach assumes that we have very fine-grained measurements of the system's behavior, at the level of individual grid cells evolving over single time steps. In reality, we may have only a few coarse statistics about the system's behavior, such as the direction, magnitude, speed, and wavelength of wave propagation. We are currently implementing an inference procedure that will attempt to determine which LDOs, describing the system's underlying dynamics, are consistent with these observable statistics (and also the above physical constraints such as conservation laws). This will lead to wider uncertainty about the system's governing equations since the inference procedure is not provided with as much data. This also addresses Goal 4.

In a new research avenue, not originally discussed in the proposed work, we are investigating an adaptive procedure to produce improved ROMs. One limitation of our current ROM algorithm is that it projects the system's dynamics onto a fixed set of modes of variability. These modes of variability are derived from simulation output. As we begin to alter the system's dynamics to explore the possibility of alternate model structures, there is no longer any guarantee that the original modes of variability will efficiently capture the new dynamics. Indeed, it is easy to see that at some point the original modes will fail to describe the system at all, if we perturb the dynamics so far that they no longer describe the original system at all (e.g. converting a wave equation into a diffusion equation). To ameliorate this problem, we are developing a method to alter the projection modes at the same time we alter the system's dynamics. Our new approach assumes that we can place an a-priori probability distribution on how likely we believe different model structures are. It then constructs a set of optimized projection modes that are designed to perform well, on average, over this entire distribution of model structures, rather than being tailored to one specific model structure.

Future Work

The overall project has four goals: (1) inferring a computer model's mathematical structure from its output (the local dynamical operator, or LDO); (2) constructing a reduced order model (ROM) of the computer model from its output; (3) perturbing the model's structure (LDO) and evaluating its predictions using the ROM; and (4) reducing the space of plausible structures with theoretical and experimental data constraints.

Year 2 will focus on applying our methods to more realistic problems, instead of the idealized problems of Year 1. We are contemplating two possible applications, but will only be able to carry out one of them this year. The first option is to construct a ROM for a commonly-used three-dimensional coastal flood model, defined on an unstructured mesh (a varying-resolution grid of data points), subject to uncertainties in boundary conditions such as wind stresses and ocean bathymetry. The second option is to construct ROMs and explore structural uncertainties in a series of groundwater transport models of differing structures and increasing sophistication. The advantage of the first option is that it is a fairly complex numerical model, and success would provide a compelling demonstration that our methods are widely applicable. However, it is higher-risk, and the effort required to produce a working ROM would slow its subsequent application to structural uncertainty quantification. The advantage of the second option is that the models are simpler and we can more easily explore structural uncertainties, but because the models are simpler, the application may be less compelling. Our current preference is to try the higher-risk first option, but this will require some preliminary feasibility studies, and we may end up working on the second option.

Conclusion

The goal is to automatically explore the computer-simulation uncertainties without having to rewrite and re-run the model for each new approximation. These uncertainties can be pervasive in many fields, such as climate science, fluid dynamics, material science, etc. We will test new automated uncertainty quantification techniques on a series of idealized problems from geophysical fluid dynamics to test the validity of the methods. If successful, this would revolutionize how computer model structural uncertainties are quantified. Currently, this work is done slowly, by hand, exploring only a narrow range of possible uncertainties.

Global Optimization Methods for Structural Bioinformatics

Hristo N. Djidjev
20160317ER

Introduction

The goal of this project is to develop a methodology for the design of scalable algorithms for exact solutions of hard combinatorial problems in bioinformatics that were previously solvable only approximately, with no accuracy guarantee, and/or on smaller instances. We are focusing on a key problem in structural bioinformatics – the determination of the 3D structure of a protein, given its amino acid sequence.

This problem is both very hard computationally and extremely important in practice. It is the shape of the protein that determines its properties and knowing its structure can be used to identify certain diseases or drugs to treat them; for instance, common diseases such as Parkinson's, Alzheimer's, and some cancers can be traced down to defects in the protein folding, many drugs are designed to bind to a target site of the protein structure. To find such drug candidates, high-throughput structure-based virtual screening techniques can be used to process databases of small molecules to determine ones that are most likely to bind to the given protein. In order for that to work, the 3D structure of the protein should be known.

In the same time, finding the protein structure is very hard computationally—currently the structures of about 90% of the human proteins have still not been determined, although their sequences are known. The most widely used current methods for finding the structure of proteins make use of local search and heuristics and usually find only locally optimal solutions as they get trapped in local minima, while only the optimal solution determines the correct protein folding.

We are offering a novel approach that involves the use of global optimization methods based on mathematical groundwork rather than heuristic ones, advanced relaxation methods, and use of high level of parallelism.

Benefit to National Security Missions

The relevance to the mission of the above agencies is mostly related to the importance of bioscience to national security and the fact that the properties of most proteins are closely related to their structure.

One of the missions of DHS is bio-defense and finding ways to counter bio-terrorism. For DHHS, our work can help in predicting or mitigating disease epidemics and pandemics. For the energy security mission, our work can lead to the development of energy-related biomaterials.

While this proposal focuses on bioinformatics, the global optimization framework that we develop can have great impact to the Information Science and Technology capability and has the potential to be extended and applied to other application areas such as cybersecurity and co-design.

Progress

During the report period of the first year of the project, we worked on the optimization problems related to the determination of protein structure of protein complexes. The specific problem we targeted was finding the structure of two-component proteins, where the structure of each component is given as input and the goal is to discover the best alignment of the two components with respect to the free energy. Our approach involves the following phases:

(i) The components are aligned based on geometry using an algorithm we designed for finding the longest alignment of two proteins. This problems is frequently reduced to the problem of finding (or enumerating) the largest cliques in the so called alignment graphs, a combinatorial problem known to be computationally very hard (NP-hard). In alignment graphs, each edge corresponds to matching of similar internal distances (up

to a user-defined threshold t). We find an efficient solution of the alignment problem by relaxing this condition and allowing cliques whose edges correspond to matching of similar internal distances up to 2t. For this relaxed problem, we design a polynomial algorithm and its efficient parallel implementation for aligning two protein structures that guarantees to return alignments with root-mean-square deviation (RMSD) less than 2t, if such alignments exist.

(ii) We extract the surface atoms of the input protein components (in order to reduce their sizes) using the tool MSMS (Sanner et al., 1996) and the biopython library (Cock et al., 2009), and apply the algorithm from phase (i) to the resulting structures. We get a list of candidate alignments for which large sections of the structures match (can be aligned closely). However, in such alignments, it is possible that other sections of the proteins will be overlapping, i.e., such alignments can not be realized in 3 dimensions. For that reasons, we need to filter out the results.

(iii) The first filtering step is based on geometry. We project each protein on a 3D mesh of points taking into account if the are internal, external, or boundary, allowing some flexibility for the boundary ones. Then we compute a matching between the corresponding arrays, assigning a very high penalty for a pair of internal points that match and smaller one for boundary pairs of nodes. Alignments with high penalty are discarded.

(iv) The second filtering step, on which we are currently working, is actually a scoring one, in which the remaining alignments are evaluated using a scoring function based on energy, where the fitness is estimated by summing the strength of intermolecular van der Waals and electrostatic interactions between all atoms in the complex. We are evaluating the available free tools NNScore, Zdock, and X-score.

We are also studying with our collaborators from University of Rennes the problem of genome scaffolding, the second phase of the genome sequencing and assembly problem, or the determination of the DNA sequences of a genome. During this phase, the contigs (gapless sequences of nucleotides that have been assembled based on short reads produced by the current high-throughput sequencing) need to be ordered into scaffolds on the basis of mate pairs information that provides relative distances and orientations between contigs. We are currently solving this problem as a mixed-integer linear programming (MILP) or mixed-integer linear programming (MIQP) problem.

Future Work

During the second year of the project we are planning to extend our results from two-component complexes to proteins with three and possibly more components. We are going to use the results of the pair-wise docking predictions (two-component complexes) as a starting point for the more difficult multi-component assembly problem. For a structure with N components, N(N-1)/2 pairs of components need to be aligned. If we take the top M alignments for each pair, the combinatorial assembly problem involves a total of MN(N-1)/2 pair-wise interaction energies and transformation matrices. Next, we represent those alignments as a fully connected weighted multi-graph. The vertices of this graph correspond to the component proteins, and the M edges between each pair of vertices represent the docking transformations with edge weights given by the docking scores. The combinatorial problem we need to solve is finding a minimum spanning tree, a problem of identifying a connected subgraph with no cycles and a minimum cost. This is an NP-hard problem (i.e., computationally very hard), which we are going to approach with global optimization methods using integer programming and branch-and-bound.

The second line of research we are planning for the second year is related to use global optimization methods for the scaffolding problem, the second phase of the genome sequencing and assembly problem. During this phase, the contigs, sequences of nucleotides produced by merging short reads during the first phase of the assembly, need to be ordered into complete genomes, a combinatorial problem of high computational complexity. Specifically, we plan to exploit the three-dimensional (3D) physical signature of chromosomes, information that only recently have become available, to bring a new level of resolution to scaffolding. We will work on this problem using data and in a close cooperation with our collaborators from the University of Rennes.

Conclusion

The proposed work will result in algorithms and tools for structural bioinformatics, focusing on predicting the structural alignment of proteins. We will restrict our focus to versions of those problems that can be modeled as quadratically constrained quadratic problems. Such problems include multi-component protein assembly, side-chain positioning, inverse folding, and multiple structural alignment. In order to validate our models and test the efficiency of our algorithms, we will use data banks such as the Protein Data Bank (PDB). While this proposal focuses on bioinformatics, the global optimization framework that we develop can have great impact to the Laboratory's

information science and technology capability and has the potential to be extended and applied to other application areas such as cybersecurity and co-design.

Publications

Aleksandrov, Lyudmil, Guillaume Chapuis, and Hristo Djidjev. Parallel shortest-path queries in planar graphs. 2016. In ACM Workshop on High Performance Graph Processing, HPGP 2016 ; Kyoto, , JPN ; 05/31/2016.

Chapuis, Guillaume Julien, and Hristo Nikolov Djidjev. Parallel Computation of Betweenness Centrality for Large Planar Graphs. 2016. SIAM Workshop on Network Science (NS16).

Eidenbenz, Stephan Johannes, Hristo Nikolov Djidjev, Balasubramanya T. Nadiga, and Eun Jung Park. Simulation-Based and Analytical Models for Energy Use Prediction. 2016. International Workshop on Performance Modeling: Methods and Applications (PMMA16).

Francois, Sebastien, Rumen Andonov, Hristo Djidjev, and Dominique Lavenier. Global Optimization Methods for Genome Scaffolding. 2016. 12th International Workshop on Constraint-Based Methods for Bioinformatics.

A Multiscale, Non-stochastic Approach to Model Collisions in Particle Systems

Luis Chacon
20160448ER

Introduction

This project aims at developing an efficient multiscale, non-stochastic (deterministic) alternative to Monte Carlo (MC) particle collision algorithms. Stochastic noise is currently one of the major efficiency and accuracy issues facing first-principles kinetic simulations with collisions. Our approach will be free of stochastic noise, will feature exact conservation properties and improved temporal convergence rates, and will be suitable for integration with modern LANL-developed multiscale particle algorithms. As a result, we will enable particle simulations in collisional regimes at an unprecedented level of fidelity while requiring far less computational resources than competing MC-based approaches. We will demonstrate the algorithm with two collisional kinetic systems of interest to LANL: thermal radiative transfer (TRT) and collisional plasmas. The successful demonstration of an efficient and accurate, particle-based deterministic collisional algorithm will provide LANL with a unique kinetic simulation capability advantage suitable for many mission drivers.

Benefit to National Security Missions

The project will develop novel algorithms to deal with arbitrary collisional regimes in radiation transport (photons, neutrons) and plasmas, and therefore the primary relevance of this project is for Information Science and Technology in the Scientific Discovery and Innovation mission. The algorithms stemming from this research, once successfully demonstrated, will impact a variety of mission spaces including the Nuclear Security Defense mission, and the Energy Security mission. This research is best aligned with DOE-SC, and in particular the Applied Scientific Computing Research Office and the Fusion Energy Sciences Office. It will also impact in a longer term the DOE-NNSA Defense Programs.

Progress

This project explores novel ways of treating collisions in particle-based descriptions of various physical systems in a deterministic manner (i.e., avoiding Monte Carlo randomness). The project focuses on two different physical systems of interest: thermal radiation transport (TRT), and collisional plasmas. We describe progress for these systems separately.

For TRT, we have implemented a multifrequency kinetic deterministic particle solver in Cartesian geometry, and we are currently working on generalizing it for spherical and cylindrical geometries. In the process of this implementation, we have found that the spatial discretization of the moment system, which is used to accelerate the kinetic solver in a multiscale fashion, is critical to obtain an accurate solution with reasonable spatial mesh sizes. Since accuracy of our method is mostly determined by the accuracy of (emission) source representation, a proper reconstruction of the material temperature is key. Desired properties of the source reconstruction approach include (1) preservation of asymptotic (equilibrium) diffusion limit, (2) minimization of numerical diffusion at material interface and (3) availability to an efficient linear/nonlinear solver algorithm. During this FY, we have tested several source reconstruction schemes, including standard linear discontinuous reconstruction, and continuous reconstruction for a finite volume-based moment system. In addition, we have developed and tested a new simple corner balance (SCB) discretization, which is a special lumped version of the discontinuous Galerkin discretization, for the moment equations. We have found that continuous reconstruction preserves an asymptotic equilibrium diffusion limit, but exhibits excessive numerical diffusion at large material discontinuities. We have also found that linear discontinuous reconstruction does not preserve diffusion limit. Currently, we are implementing a new continuous reconstruction with two linear slopes per cell, inspired by the plasma particle-in-cell (PIC) algorithm. We anticipate having a demonstration of the algorithm on the 1D Marshak wave problem in various geometries by the end of this FY.

For the collisional plasma application, we have made significant progress in the key element of the proposed algorithm, which is the coarse representation of the particle population for the collisional step. We have identified and adapted an optimal coarse graining approach based on finite mixtures of multivariate Gaussian or normal distributions. Although finite mixture models have been widely applied in many areas such as machine learning, social science, economics, biology, medicine, etc. the application of it on particle simulations with collisions is new. The basic idea is to replace a large number of particles by a set of small set of normal (Gaussian) distributions with accuracy and efficiency. The advantage of using Gaussians is that they are eigenmodes of the collision operator, and can be used to diagonalize it without needing to solve a partial differential equation. During this FY, we have derived the suitable governing equations for individual Gaussians according to the collision operator. We have also developed an algorithm that optimally maximizes the likelihood the mixture distribution with a given number of normal components. This is done by the conventional expectation-maximization (EM) algorithm, augmented by suitable splitting and merging steps. Splitting is done with an information-theoretic approach, the so-called minimum-message length (MML) criterion. We have designed a self-adaptive procedure that tries to fit the particle distribution by a mixture of isotropic normal distribution plus smaller, anisotropic ones. Merging of Gaussians is done analytically, and happens until the MML information criterion is satisfied. We are currently evaluating the effectiveness of the algorithm on some simple one-dimensional plasma physics simulations. We anticipate demonstrating the ability to deal with simple thermalization proof-of-principle test problems (in zero spatial dimensions, 0D, and one or more velocity dimensions, 1V or 2V) among multiple species by the end of this FY. We also anticipate that, by the end of the FY, we will have integrated our algorithm with a state-of-the-art 1D-1V PIC algorithm to test our proposed split time stepping approach.

Future Work

In both applications, we will continue to follow our proposed research plan. For TRT, we will continue investigating the optimal discretization for the LO system and source reconstruction scheme that provide accuracy in different physical regimes (streaming and diffusion). We will finish implementing and testing the deterministic particle method in both 2D XY Cartesian geometry and RZ Cylindrical geometry.

For plasmas, the plan is to finish integration within a particle-in-cell algorithm and demonstration in one-dimensional geometries, with one velocity and multiple velocity dimensions. We will verify the algorithm by comparison with Vlasov-Fokker-Planck simulations with the available 1D-3V iFP code. We will also test the algorithm on standard equilibration and transport benchmarks to verify the accuracy of the algorithm. We will begin to explore extending it to more realistic multi-dimensional applications.

Conclusion

We will demonstrate the feasibility, accuracy, and efficiency of deterministic (vs. stochastic) particle collisional treatments in two applications of relevance: thermal radiative transfer and semi-collisional plasmas. The successful conclusion of the research proposed in this project will enable unprecedented fidelity in the modeling of these two physical systems with far fewer computational resources, thus opening a new computational frontier. The methods proposed here will also conform naturally to modern architectures such as the Trinity supercomputer, thus opening the possibility of high utilization of modern computing architectures. The algorithms stemming from this research, once successfully demonstrated, will impact a variety of mission spaces including energy security and nuclear security defense.

From the Finite Element Method to the Virtual Element Method

Gianmarco Manzini
20140270ER

Abstract

The Finite Element Method (FEM) is a powerful numerical tool that is being used in a large number of engineering applications. Among the advantages of FEM is the relative flexibility to resolve complex geometries and the strong theoretical foundation describing its convergence properties. The classical FEM is constructed on triangular/tetrahedral meshes in two dimensions (2D) and quadrilateral/hexahedral meshes in three dimensions (3D). Yet, using these meshes is often not sufficient and extension to general polygonal/polyhedral meshes is highly desirable. Such an extension proved to be an extremely difficult problem that leads to very complex and computationally expensive schemes. The reason for this failure lies in the construction of the local basis functions on elements with a general geometric shape.

In this project we developed the Virtual Element Method (VEM), an extension of the FEM to general polygonal/polyhedral meshes. The VEM is a new family of numerical methods for the approximation of Partial Differential Equations (PDEs). We have successfully formulated, implemented and studied the VEM theoretically and numerically, and investigated their stability, robustness and accuracy for diffusion problems, convection-reaction-diffusion problems, the Stokes equations and the bi-harmonic equations.

Background and Research Objectives

In the last sixty years, a clear theoretical foundation of the FEM has been developed for many PDEs and the existence of such a theory with rigorous error bounds has become one of the attractions of this methodology. The FEM is usually considered on triangular/tetrahedral and quadrilateral/hexahedral meshes. On such meshes it is rather easy to build basis functions, e.g., polynomials, and a one-to-one correspondence between them and the discrete space of degrees of freedom, e.g., values at the vertices or other special nodes. Extending the FEM to general polygonal/polyhedral meshes is extremely difficult and leads to very complex and computationally expensive schemes. The reason for this failure is that the construction of basis functions matching with the degrees of freedom on elements with general shape is a non-trivial and complex task.

Nonetheless, there are many advantages to using polygonal/polyhedral meshes over purely triangular/tetrahedral or quadrilateral/hexahedral ones:

- polygonal/polyhedral meshes significantly simplify the partitioning of domains with a complex geometry;
- they can reduce the complexity of adaptive mesh refinement and coarsening algorithms as no special treatment of hanging nodes is required to maintain the conformity of the mesh;
- they may be dictated by the data coming from multi-physics applications.

Therefore, extending finite elements to polygonal/polyhedral meshes while keeping their solid theoretical foundation is of great interest to the community of physicists and engineers. However, doing that in a computationally efficient way without sacrificing the accuracy of the numerical approximation is a formidable task for the reasons that we will explain below. Instead, the virtual element approach is a very effective strategy to accomplish this task.

To explain why this topic is challenging we summarize the basic steps of the FEM construction:

- rewrite the PDE in a weak form: multiply by a test function, integrate over the domain, integrate by parts moving one derivative from the unknown onto the test function;
- partition the domain into elements and identify the degrees of freedom, e.g., the solution values at the

vertices of the elements;

- identify the shape functions and their gradients on each element;
- compute the elemental mass matrix and stiffness matrix by computing or approximating the integrals of the pairwise products of the shape functions and their gradients;
- assemble all the elemental matrices, solve the resulting linear system and post-process the numerical solution (if needed).

A straightforward extension of steps 1-5 to polygonal meshes has led to the development of the Polygonal Finite Element Methods (PFEMs). However, PFEMs are a generalization of the linear Galerkin FEM and thus provide a low-order approximation. Determining how to build higher-order accurate approximations, e.g., quadratic, and 3D approximations is still an open issue.

The critical point in the PFEM approach is represented by step 3: the construction of the elemental shape functions. On triangular/tetrahedral and quadrilateral/hexahedral elements the basis functions are determined as the unique solution of a polynomial interpolation problem for the degrees of freedom; hence, they are polynomials and are expressed by relatively simple formulas. For example, the shape functions of the linear Galerkin FEM on a triangle and a tetrahedron are the linear Lagrangian interpolants whose value is one at a given vertex and zero at the other vertices.

The situation is completely different on general polygonal and polyhedral elements because:

- the solutions of such interpolation problems are no longer polynomials;
- they are not uniquely determined, i.e., many different constructions for such interpolants are possible such as the Wachspress interpolants, the Sybson interpolants, the natural neighbor interpolants, the harmonic interpolants (just to mention a few), cf. Reference [12];
- no explicit formula is available for such interpolants and their gradients.

As no explicit formula is available, using such interpolants as shape functions is awkward. PFEMs are necessarily based on numerical quadratures and at each quadrature node a non-linear problem must be solved to determine the value of each shape function and its gradient. Depending on the accuracy of the quadrature rule and the number of quadrature nodes we may obtain either poor accuracy of the approximation (too few nodes) or a very expensive scheme (too many nodes). These issues become even more pronounced in 3D, making straightforward generalization of PFEMs prohibitively complex and computationally expensive.

Instead, in the virtual element formulation, only the part of the finite element space that refers to polynomials is constructed, while the behavior of the method on the rest of the space is approximated following a stability criterion. This fact has a dramatic impact on the computational complexity, which is greatly reduced as the implementation of VEM no longer requires the explicit construction of the shape functions. The VEM can thus be applied to meshes as in Figure 1 in 2D and 2 in 3D without any special modification in the method's formulation.

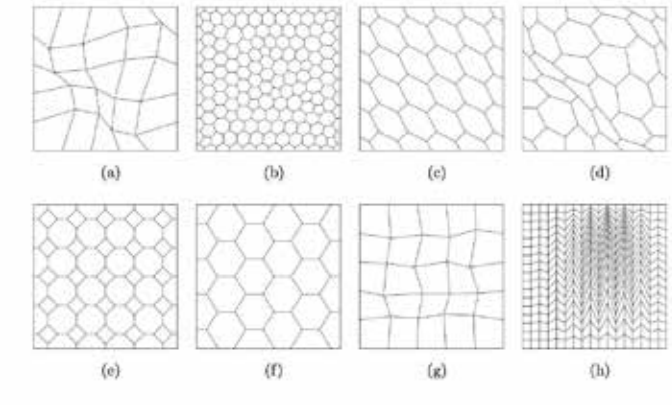

Figure 1. Typical meshes used to test the VEM: (a) smoothly remapped quadrilaterals; (b) Voronoi tessellations; (c) tilted hexagons; (d) smoothly remapped hexagons; (e) regular octagons and quadrilaterals; (f) regular hexagons; (g) randomized quadrilaterals; (h) highly skewed quadrilaterals.

The VEM may have an order of accuracy higher than two in the L2 norm and higher than one in the H1 (energy) norm. It may also have an order of regularity higher than zero (numerical solutions with continuous derivatives). The high order of accuracy is achieved by ensuring the exactness of the methods when the solution is a polynomial of degree higher than one. This property is normally achieved in the finite element method only on meshes of triangles and quadrilaterals in 2D and tetrahedra and hexahedra in 3D.

Scientific Approach and Accomplishments

Next we discuss the three major points where we were particularly successful.

Comparison with Polygonal/Polyhedral FEMs and hourglass stabilization

Generalized barycentric coordinates such as Wachspress

and mean value coordinates have been the unique available finite element formulation for polygonal and polyhedral meshes for about three decades. The VEM is an alternative, consistent and stable finite element method that works on polygonal and polyhedral elements. In the VEM, we use a projection operator to decompose the stiffness matrix into the consistency and stability matrices. The stability matrix must be positive semi-definite and is only required to scale like the consistency matrix. In Reference [12] we proved that the VEM decomposition provides a robust and efficient generalized barycentric coordinate Galerkin method where the consistent VEM matrix is adopted and computed using numerical quadratures. This approach facilitates the post-processing of field variables and provides a means to satisfy the patch test with efficient numerical integration in polygonal/polyhedral meshes. We also compared the accuracy and performance of the method with respect to the traditional PFEMs for Poisson problems in 2D (see Figure 3) and 3D and we established that linearly complete generalized barycentric interpolants deliver optimal convergence rates in the L2-norm and the H1-seminorm [12].

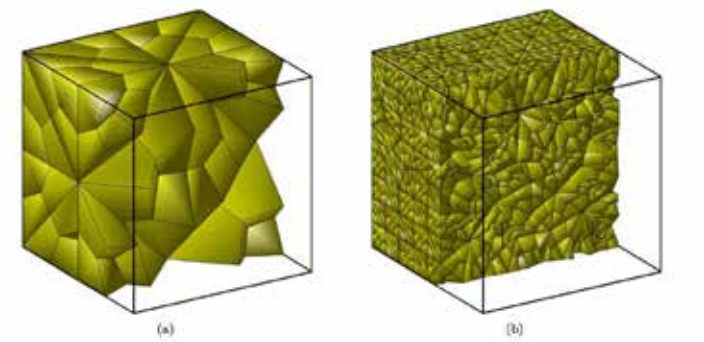

Figure 2. Example of unstructured hexahedral meshes: (a) base mesh; (b) first refinement.

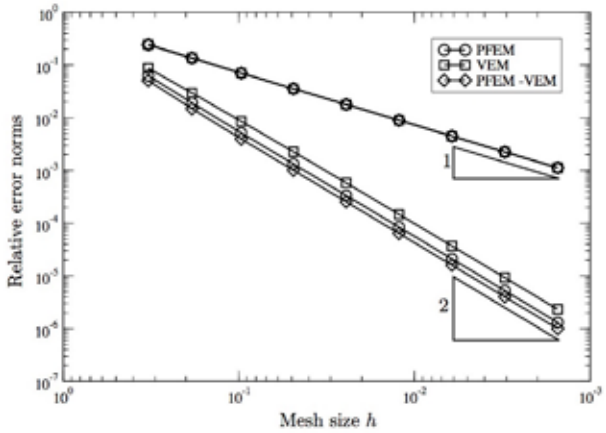

Figure 3. Comparison of the error curves of the solution of the Poisson equations using PFEM, VEM and PFEM-VEM (PFEM with the consistency term from VEM). H1 error (top curves), L2 error (bottom curves).

In [7] we established the connections between the VEM and the hourglass control technique that was developed by Belytschko and collaborators in the early '80s to stabilize underintegrated C0 Lagrange finite element methods. In particular, we proved theoretically that the variational approach adopted in the VEM affords a generalized and robust mean to stabilize underintegrated finite elements and the virtual element formulation is a natural theoretical setting to explain the hourglass stabilization technique. We focused on the heat conduction equation, and developed the virtual element formulation for the isoparametric 4-node quadrilateral and 8-node hexahedral element. In addition, we showed quantitative comparisons of the VEM consistency and stabilization matrices with those in the hourglass control method of Belytschko and coworkers. Numerical examples in 2D and 3D revealed that the virtual element method satisfies the patch test and delivers optimal convergence rates in the L2-norm and the H1-seminorm for Poisson problems on quadrilateral, hexahedral, and arbitrary polygonal meshes.

Conforming VEM: residual based a posteriori estimate and schemes with arbitrary regularity

A posteriori error estimation and adaptivity are very useful in the context of the virtual elements due to the flexibility of the meshes to which these numerical schemes can be applied. Nevertheless, developing error estimators for the VEM is not a straightforward task due to the lack of knowledge of the basis functions. In Reference [4] we developed a residual based a posteriori error estimator , we proved its reliability and investigated its performance when it is combined with an adaptive strategy for the mesh refinement (see Figure 4).

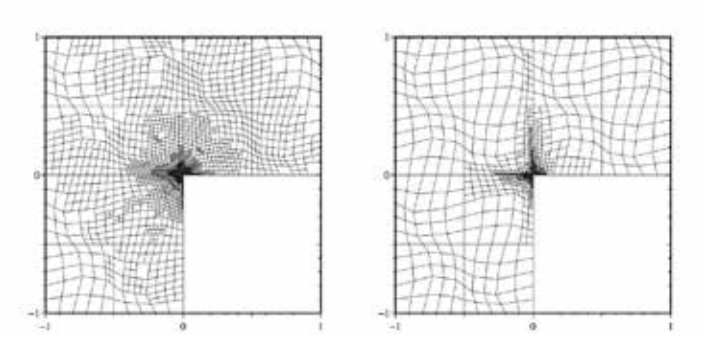

Figure 4. Adaptive mesh refinement driven by the residual based a posteriori error estimator from Reference [4].

In [3], we developed and analyzed a new family of virtual element methods on unstructured polygonal meshes for the diffusion problem in primal form that use arbitrarily regular discrete spaces. The degrees of freedom are (a) values of the function (solution) and its derivatives of various degree at suitable nodes and (b) solution moments inside

polygonal element. The convergence of the method was proven theoretically, an optimal error estimate was derived through the analysis and the proper behavior of the method was confirmed by the numerical experiments.

In Reference [10] we developed a conforming VEM with higher continuity (C1) for the solution of the biharmonic equation, which is used in plate bending theory. The challenge with discretizing the biharmonic equation is in the higher number of derivatives one should be able to take for the approximate solution. To address this challenge one can consider a mixed formulation or follow a Discontinuous Galerkin approach introducing penalty terms for the discontinuities (or both). In our VEM construction we were able to use the primal formulation by enforcing the C1-continuity of the approximation through a proper choice of the degrees of freedom. This was possible to do for any accuracy of discretization by introducing degrees of freedom at the vertices and edges that in addition to function values are also associated with the derivatives. Shared edge and vertex degrees of freedom therefore imply C1-continuity of approximations across adjacent elements.

Non-conforming virtual element methods

The first virtual element formulation can be considered as an extension of the classical conforming FEM, which is usually stated on simplicial and quadrilateral/hexahedral elements, to polygonal and polyhedral elements. During the first year of this project we realized that a non-conforming formulation is also possible. The non-conforming formulation offers a major advantage with respect to the conforming one: it does not require a hierarchical construction of the virtual element space when the number of dimensions is increased. Therefore, the total number of degrees of freedom is smaller in 3D than the number required by the conforming VEM. Moreover, as in the case of Stokes equations, the construction of the method is the same for any number of space dimensions and parity of the approximation. In contrast, conforming discretizations in 3D are notorious for their complexity.

In Reference [2] we first developed a non-conforming VEM for second order elliptic problems. The method was designed in 2D and 3D, and we highlighted the main differences with the conforming VEM and the classical nonconforming FEM. For this method, we also provided the error analysis and established the equivalence with the family of mimetic finite difference method previously developed by one of the authors, cf. Reference [11]. The performance of the new non-conforming VEM was validated by numerical experiments.

Then, in Reference [8] we developed a unified framework for the conforming and nonconforming VEM and extended the non-conforming formulation to 2D and 3D advection-reaction-diffusion problems. To this end, we split the differential operator of the continuum setting into its symmetric and non-symmetric parts and established conditions for stability and accuracy on their discrete counterparts. Under these conditions, we provided optimal L2- and H1-error estimates, which were confirmed by numerical experiments on a set of polygonal meshes. The accuracy of the two methods was shown to be comparable.

In the second and third year, we continued developing the non-conforming VEM and designed new VEM for the Stokes equations [6,9] and the biharmonic problem [1]. In the Stokes equations, the pressure is approximated using discontinuous piecewise polynomials, while each velocity component is approximated using the nonconforming VEM space. On each mesh element the local virtual space contains all the polynomials of up to a given degree plus suitable non-polynomial functions. The virtual element functions are implicitly defined as the solution of local Poisson problems with polynomial Neumann boundary conditions. As typical in the VEM approach, the explicit evaluation of the non-polynomial functions is not required. This fact makes it possible to construct nonconforming virtual spaces for any polynomial degree regardless of the parity, for two-and three-dimensional problems, and for meshes with very general polygonal and polyhedral elements. In [6] we showed that the non-conforming VEM is infirmum and supremum (inf-sup) stable and established optimal a priori error estimates for the velocity and pressure approximations. Numerical examples confirmed the convergence analysis and the effectiveness of the method in providing high-order accurate approximations.

In Reference [1] the non-conforming VEM was developed for the numerical solution of the biharmonic problem. This method uses both internal and boundary degrees of freedom locally defined on each mesh element to represent the functions of a special finite element space. The convergence of the method is theoretically proved by deriving optimal convergence rates, and a preliminary set of numerical experiments confirms the theoretical expectations.

Impact on National Missions

This research has provided unique capabilities in the DOE complex that combine world-class algorithms, their theoretical foundation and high-end HPC technologies and may have natural connections with Co-Design and Extreme-Scale Solvers with reference to the exascale initiative recently signed by President Obama. Our project was mainly focused on the design and analysis of new numerical methods. Implementation and testing were carried out mostly for academic problems. Nonetheless, these new

capabilities position us uniquely towards future opportunities in these areas. We expect indeed that virtual element algorithms may impact a wide range of modeling multiphysics applications, including climate and environmental modeling (e.g., climate, ocean and sea-ice modeling, ASCEM Project), plasma physics (e.g., Fokker-Planck equation in inertial confinement fusion simulations) and other CFD-based applications. This may lead to new funding in fundamental research on numerical methods by working with Office of Science ASCR managers.

References

1. Antonietti, P. F., G. Manzini, and M. Verani. Nonconforming VEM for biharmonic problems. 2016. Los Alamos Technical Report, LA-UR-16-26955.

2. Dios, B. Ayuso de, K. Lipnikov, and G. Manzini. The nonconforming virtual element method. 2016. ESAIM: Mathematical Modelling and Numerical Analysis. 50 (3): 879.

3. Beirao, L. da Veiga, and G. Manzini. A virtual element method with arbitrary regularity. 2014. IMA Journal of Numerical Analysis. 34 (2): 759.

4. Beirao, L. da Veiga, and G. Manzini. Residual a posteriori error estimation for the virtual element method for elliptic problems. 2015. ESAIM: Mathematical Modelling and Numerical Analysis. 49 (2): 577.

5. Bellomo, N., F. Brezzi, and G. Manzini. Recent techniques for PDE discretizations on polyhedral meshes . 2014. Mathematical Models and Methods in Applied Sciences . 24 (8): 1453.

6. Cangiani, A., V. Gyrya, and G. Manzini. The nonconforming virtual element method for the Stokes equations. To appear in SIAM Journal on Numerical Analysis.

7. Cangiani, A., G. Manzini, A. Russo, and N. Sukumar. Hourglass stabilization and the virtual element method. 2015. International Journal for Numerical Methods in Engineering. 102 (3-4): 404.

8. Cangiani, A., G. Manzini, and O. J. Sutton. Conforming and nonconforming virtual element methods for elliptic problems. To appear in IMA Journal of Numerical Analysis.

9. Gyrya, V., G. Manzini, and A. Cangiani. A non-conforming virtual element method for Stokes equations. Invited presentation at European Congress on Computational Methods in Applied Sciences and Engineering (invited, LA-UR-15-29189). (Crete, Greece, 5-10 June 2016).

10. Gyrya, V., and H. Mourad. C1-continuous Virtual Element Method for Poisson-Kirchhoff plate problem. 2016. Los Alamos Technical Report, LA-UR-16-27263.

11. Lipnikov, K., and G. Manzini. A high-order mimetic method on unstructured polyhedral meshes for the diffusion equation. 2014. Journal of Computational Physics. 272: 360.

12. Manzini, G., A. Russo, and N. Sukumar. New perspectives on polygonal and polyhedral finite element methods. 2014. Mathematical Models and Methods in Applied Sciences. 24 (8): 1665.

Publications

Antonietti, P. F., G. Manzini, and M. Verani. Nonconforming VEM for biharmonic problems.

Beirao, L. da Veiga, and G. Manzini. A virtual element method with arbitrary regularity. 2014. IMA Journal of Numerical Analysis. 34 (2): 759.

Beirao, L. da Veiga, and G. Manzini. Residual a posteriori error estimation for the virtual element method for elliptic problems. 2015. ESAIM: Mathematical Modelling and Numerical Analysis. 49 (2): 577.

Bellomo, N., F. Brezzi, and G. Manzini. Recent techniques for PDE discretizations on polyhedral meshes . 2014. Mathematical Models and Methods in Applied Sciences . 24 (8): 1453.

Cangiani, A., G. Manzini, A. Russo, and N. Sukumar. Hourglass stabilization and the virtual element method. 2015. International Journal for Numerical Methods in Engineering. 102 (3-4): 404.

Cangiani, A., G. Manzini, and O. J. Sutton. Conforming and nonconforming virtual element methods for elliptic problems. To appear in IMA Journal of Numerical Analysis.

Cangiani, A., G. Manzini, and O. J. Sutton. Numerical results using the conforming VEM for the convection-diffusion-reaction equation with variable coefficients. 2014. Los Alamos Technical Report LA-UR-14-27709 .

Cangiani, A., G. Manzini, and O. J. Sutton. The conforming virtual element method for the convection-diffusion-reaction equation with variable coefficients. 2014. Los Alamos Technical Report LA-UR-14-27710 .

Cangiani, A., V. Gyrya, G. Manzini, and O. J. Sutton. Virtual element methods for elliptic problems on polygonal meshes. To appear in Generalized Barycentric Coordinates in Computer Graphics and Computational Me-

chanics. Edited by Hormann, K., and N. Sukumar.

Cangiani, A., V. Gyrya, and G. Manzini. The non-conforming virtual element method for the Stokes equations. To appear in SIAM Journal on Numerical Analysis.

Dios, B. Ayuso de, K. Lipnikov, and G. Manzini. The nonconforming virtual element method. 2016. ESAIM: Mathematical Modelling and Numerical Analysis. 50 (3): 879.

Gyrya, V.. A non-conforming virtual element method for Stokes equations (invited, LA-UR-16-23638). Invited presentation at European Congress on Computational Methods in Applied Sciences and Engineering. (Crete, Greece, 5-10 June 2016).

Gyrya, V., G. Manzini, and D. McGregor. A non-conforming virtual element discretization for singularly perturbed advection diffusion reaction equations. 2014. Los Alamos Technical Report LA-UR-14-27995.

Gyrya, V., K. Lipnikov, G. Manzini, and D. McGregor. Extension of finite element methods to general polygonal (and polyhedral) meshes (invited, LA-UR-14-25735). Invited presentation at World Congress on Continuous Mechanics. (Barcelona, Spain, 21-25 July 2014).

Gyrya, V., and G. Manzini. On the local non-conforming virtual element spaces . 2014. Los Alamos Technical Report LA-UR-14-28831 .

Gyrya, V., and H. Mourad. C1-continuous virtual element method for Poisson-Kirchhoff plate problem. 2016. Los Alamos Technical Report.

Iaroshenko, O., V. Gyrya, and G. Manzini. Arbitrary order mixed mimetic finite differences method with nodal degrees of freedom . 2016. Los Alamos Technical Report LA-UR-16-26696 .

Manzini, G.. The virtual element method for flow and transport in porous media (invited, LA-UR-15-20412). Invited presentation at SIAM Conference on Mathematical and Computational Issues in the Geosciences . (Stanford, California, 29 June-2 july 2015).

Manzini, G.. The virtual element method (invited, poster, LA-UR-15-21780). Invited presentation at SIAM Conference on Computational Science and Engineering. (Salt Lake City, Utah, 14-18 March 2015).

Manzini, G.. The nonconforming virtual element method for the convection-reaction-diffusion equation (invited, LA-UR-15-25637). Invited presentation at X-DMS 2015. (Ferrara, Italy , 9-11 September 2015).

Manzini, G.. The non-conforming virtual element method for elliptic problems (invited, LA-UR-15-29585). Invited presentation at European Congress on Computational Methods in Applied Sciences and Engineering. (Crete, Greece , 5-10 June 2016).

Manzini, G., A. Russo, and N. Sukumar. New perspectives on polygonal and polyhedral finite element methods. 2014. Mathematical Models and Methods in Applied Sciences. 24 (8): 1665.

Large Fluctuations in Stochastic Dynamical Systems

Timothy C. Wallstrom
20140302ER

Abstract

The larger goal of our research is to understand dynamical systems in the presence of large random fluctuations. Such systems are ubiquitous in many areas of science and technology, but are not as well understood as systems with small fluctuations. New methods are needed.

In this project, we have focused on a particular class of dynamical systems: those governing evolution. In recent years, new models have been developed for evolutionary processes with large fluctuations. In order to understand whether these theories are relevant to nature, we have focused on the evolution of the Human Immunodeficiency Virus (HIV), the causative agent in AIDS, within the infected individual. There is strong evidence that large fluctuations play a role in this evolution. Our goal has been to develop methods for connecting the data to the theory, and thereby to better understand viral evolution in the infected host.

In order to improve on the mathematical results, which make some idealized assumptions that are unrealistic for real systems, we developed computational codes for simulating the behavior of the new models for real populations. We also developed statistical techniques for assessing the uncertainty in the behavior of these models. Using these advances, we were able to show that evolution of HIV within an infected individual is indeed better described by the new models with large fluctuations than with the older models with small fluctuations. We presented these results at conferences to interested researchers in biology, mathematics, and statistics. We have developed statistical methodology for testing the fit of the new models with the data. Finally, we have been studying whether our inferences can be related to the clinical progression of HIV in infected individuals.

Background and Research Objectives

The goal of this project has been to understand dynamical systems in the presence of large random fluctuations. Such systems are common in economics, physics, and several areas of biology. The usual analyses of random systems make certain technical assumptions on the size of the fluctuations, which are invalid when the fluctuations are too large. For these types of random systems, the usual analyses are invalid, and new methods are required.

We have focused on the dynamical systems that govern evolution, and specifically on the area of population genetics, which is the mathematical framework for the study of evolution. On the one hand, these systems are sufficiently rich to exhibit a broad range of phenomena. On the other hand, striking recent mathematical results have led to a complete characterization of the solution classes, under large fluctuations, of the equations of population genetics, in certain simple cases. Thus, these systems are tractable, but rich enough to provide general insights.

Our overall objective has been to connect the data to the theory. We are particularly interested in the understanding the Human Immunodeficiency Virus (HIV), which is the causative agent in AIDS. HIV mutates so rapidly that it undergoes significant evolution in a single infected individual. Existing models of HIV evolution have led to a number of stubborn mysteries, which we suspected were due to an inadequate modeling framework, which does not account for large fluctuations. There is empirical evidence of large fluctuations in HIV, and modern sequencing technology is available to permit detailed comparison of our models with experimental data.

Although there has been previous research in this area, several improvements were necessary in order to compare data and theory. Many of the existing results were mathematical results which only held in an idealized mathematical limit, which was of questionable relevance to actual data. Much of the statistical work

gave only mean values of statistical parameters, without giving ranges. Ranges are necessary for ruling out incorrect models. Finally, there was relatively little work on applying these large fluctuation models to HIV.

Our specific research objectives for this project have been designed to address these difficulties. We made significant progress on all of our objectives, including objectives that arose in the course of our research.

In order to deal with inadequacy of the idealized mathematical result, we wrote computer codes that were able to model actual populations much more accurately. The mathematical models were guaranteed to be accurate if the population was large enough, but it was unclear how large that had to be. To our surprise, we found that the idealized models were quite inaccurate even when inferring the evolutionary history of hundreds or thousands of individual viruses.

In order to deal with the inadequacy of statistical methods, we developed new methods that were able to estimate not only the mean values of statistical parameters, but their uncertainties as well. We then implemented these methods in computer code. Using these methods, we were able to show statistically that the classical models could be statistically ruled out for HIV evolution within the patient.

In order to deal with the lack of analysis of HIV data, we performed detailed analysis of numerous HIV datasets of different types, to help determine which types of data would lead to the best results. In this effort, we were assisted by access to high quality datasets from collaborators at the University of Pennsylvania. Our methods enabled us to assess the best data-collecting strategies for determining the correct model. For example, we could determine whether it was more useful to have a large number of short genetic sequences, or a small number of long sequences.

Initially, in fitting the model to the data, our objective was simply to determine whether Model A, say, was a better fit to the data than Model B. As the project developed, we came to appreciate how important it was to determine whether Model A, even when better than Model B, was really a good fit for the data in some absolute sense. That is, could the data have plausibly arisen from Model A? As a result, we developed methods to assess what statisticians call “goodness-of-fit,” a type of analysis that appears to be lacking in previous research in these models.

Scientific Approach and Accomplishments

We cite accomplishments in four key areas.

Applications to HIV

Our first main result was to show that HIV evolution within the patient was inconsistent with the classical models that have been used to analyze it. In statistical language, we showed that the classical models were “statistically ruled out.” Our analysis studied two different types of HIV sequence data, and for each type of data, we studied several individuals. This work was presented and well-received at a number of conferences, including the 23rd International Conference on HIV Dynamics and Evolution in Woods Hole, Massachusetts, where we gave a lecture on our work to an audience consisting mostly of HIV biologists. The work was also presented at conferences in Austin, Texas and Santa Fe, New Mexico, to audiences of mathematicians and statisticians, respectively.

We have also analyzed the HIV data in other ways. In the studies just cited, we analyzed data from the same HIV genomic region in many different patients. To complement this analysis, we studied a single patient in detail, and analyzed the evolutionary patterns across the genome, and at various stages of the infection, ranging from 16 days to 1187 days after infection. Again, we confirmed strong deviations from the behavior predicted by the classical model.

Finally, we have studied whether specific large fluctuation models are a good fit to the HIV data. There are many possible large fluctuation models, but specific choices have been proposed in the literature. We found that even though these models fit much better than the classical models, there were some systematic weaknesses in their fit. We have shown that the data is fit better by other models which, while more phenomenological, are also in the large fluctuation class.

Uncertainty analysis

In order to assess uncertainty in model fits, we developed a new statistical method for analyzing the sequence data, based on the general statistical method of “composite likelihood.” One of the problems with previous analyses is that for technical reasons, it was difficult to use all parts of the data, and researchers would use only one part, in the hope that that was good enough. Unfortunately, not only was much of the data not used, but the part that was used was often the most unreliable part. Our new method makes it possible to use all parts of the data in the inferences. We have developed this new method, implemented it in code, and applied it to answer important questions bearing on data collection. We applied this analysis to mitochondrial sequence data from the Atlantic Cod. We have completed a paper on our method, which is available as an unclassified Los Alamos report (LA-UR-16-27366), and which will soon be submitted to the journal Genetics.

3. Goodness-of-fit. We have developed new methods for assessing goodness-of-fit between sequence data and our generalized large fluctuation models. We have applied these tools to datasets from the Atlantic Cod and HIV.

Computer Code

One of the findings from our research is that idealized mathematical results were inadequate, and that in order to make reliable inferences it was necessary to simulate populations computationally. In order to carry out our research, we developed computer codes for (i) sampling from the evolutionary trees predicted by various models with large fluctuations; (ii) visualizing these trees; and (iii) implementing the uncertainty analysis described above, for various large fluctuation models. Our code is written in the open source computing language R, which has become the dominant language for statistical computing. Our code is documented and validated. Our code should be very useful to other research scientists in this area, and we plan to make it freely available.

Impact on National Missions

Our work has contributed to the understanding of dynamical systems in the presence of large fluctuations, which is an area of mathematics of importance to both the Office of Science (DOE/SC) and the NSF (Other Federal Agencies). The particular application on which we have focused is evolutionary dynamics, which is of broad interest, and is a central concern of Fundamental Bioscience. Models of evolutionary dynamics are relevant in many areas of biology, including cancer modeling. Our work has focused specifically on the evolution of HIV in the infected patient. Such research is of direct interest to the National Institutes of Health (NIH). The tools we have developed will be valuable for future advances in our understanding of HIV and other pathogens, such as influenza, which will have importance for Basic Health Research. Specifically, we have started to investigate, in conjunction with our colleagues at the University of Pennsylvania, whether the properties of the new models can be correlated with clinical progression of HIV in infected individuals.

Publications

Bhattacharya, T., E. Giorgi, T. Wallstrom, P. Hraber, G. Learn, T. Kreider, Y. Li, F. Gao, B. Korber, B. Hahn, and G. Shaw. Detecting Selective Sweeps in HIV. 2014. Presentation to Scientific Leadership Group of Center for HIV/AIDS Vaccine Immunology (CHAVI), July 30, 2014. Chosen for presentation to full CHAVI collaboration meeting, and presented there on September 29, 2014..

Wallstrom, T. C., T. Bhattacharya, and J. Wilkins. Quantifying uncertainty in the inference of generalized coalescents. 2016. LA-UR-16-27366.

Wallstrom, T., T. Bhattacharya, and J. Wilkins. Intrahost HIV evolution requires infinite-variance models. Presented at Conference on Data Analysis 2016. (Santa Fe, New Mexico, March 2-4, 2016).

Wallstrom, T., T. Bhattacharya, and J. Wilkins. Beta coalescents and Intrahost HIV evolution. Presented at Simons Conference on Random Graph Processes. (Austin, Texas, May 9-12, 2016).

Wallstrom, T., T. Bhattacharya, and J. Wilkins. Using Monte Carlo Sampling for Model Inference in Intrahost HIV Evolution. Invited presentation at 2016 Information Science and Technology Capability Review. (Los Alamos, New Mexico, June 26-29, 2016).

Wallstrom, T., T. Bhattacharya, and J. Wilkins. Generalized Coalescents may be Necessary for Modeling Intrahost HIV Evolution. Presented at 23rd International Conference on HIV Dynamics and Evolution. (Woods Hole, New York, April 24-27, 2016).

Accelerating Time Integration for Multi-scale Simulations

Shengtai Li
20140323ER

Abstract

We have developed new numerical methods and algorithms to accelerate the time integration for multi-scale problems. We have also implemented our algorithms to our software package LA-COMPASS (Los Alamos COMPutational Astrophysics Suite) and applied it to solve multi-scale problems in planet-disk interactions in dusty disks.

We developed several algorithms to handle different types of multi-scale problems. For problems with clear separation of the time-scale, we used the partial equilibrium state method to calculate the state of fast dynamics without using the small time step, and coupled it with slow motions of the slow dynamics. For multi-time-scale problems that do not have clear separation, we developed an implicit-and-explicit (IMEX) method to handle different physics with different time scales. For physics with fast dynamics, we used the implicit method to avoid using small time steps. For physics with slow dynamics, we used the explicit method. The resulting coupled system is easy to solve when compared with the fully-implicit method.

To solve the fast dynamics more accurately, we also developed a parallel-in-time method. We first used our reduced order method (ROM) or our IMEX method to predict the solution at coarse time levels. Then we applied the parallel-in-time method to solve the same problem using smaller time steps, where the early derived predicted values served as the initial guess at different time intervals. We observed remarkable speed-up for our target applications.

Using the algorithms and software, we simulated the formation of the proto-planetary disks. Our numerical model and simulations fit well with the observed data from ALMA telescope.

Our algorithms can be applied to other multi-time-scale problems with some modifications. They can also be combined with the space-domain decomposition parallel algorithm for parallel computing in both time and space. With more processors available, the combined space-and-time parallelization can speed up the simulations in another level and may have critical impact on exascale computing.

Background and Research Objectives

The need for a multiscale simulation capability is pervasive in many areas of science and engineering including, for example, environmental and geo-sciences, materials and combustion, high energy density physics and fusion, and biosciences. For our target application, planet-disk interaction in dusty disks, a broad range of timescales are involved in the simulation: from gas and dust coupling dynamics (~1 sec), gas hydrodynamics (~102 s), planet period (~107s), to planet formation (~1014s). It would take years to finish a simulation of planet formation (timescale of millions years) using the time step (~1sec) required for gas and dust coupling.

In this project, we developed an innovative numerical algorithm to speed-up the time integration for multi-time-scale problems. We also implemented our numerical algorithm as numerical software that worked efficiently on large-scale parallel computers. Furthermore, we also applied our algorithm and software to real physics problem and performed simulations that were previously out of reach.

Scientific Approach and Accomplishments

We first identified the bottle-neck in our time integration for our target application. We found that the time-step in our hydro method was controlled by the velocities in both radial and azimuthal direction. The larger the velocity, the smaller the time step. We also found that the azimuthal velocity is at least one magnitude larger than the radial velocity in every grid cell. Accordingly, we subtracted the large averaging azimuthal velocity in each azimuthal ring and used the residue velocity to calculate the time step. The averaging velocity was then added

back by a semi-Lagrangian approach to rotate each ring by an integer number of cells. This simple approach increased our time step by at least 30 times. We also combined this approach with our adaptive mesh refinement (AMR) to speed up our simulations. The results are published in [1].

For the coupled dust and gas simulations, we developed three algorithms to speed up the tine integrations. The first algorithm was a "brute force" method, employing small time steps allowed by the dust stopping time for whole simulations. This algorithm can be applied to relatively large dust particles, where the dust stopping time has a comparable value to the hydro time step. We applied this algorithm to study the formation the Oph IRS-48 proto-planetary disk (see Marel et al 2013 Science [2]). This particular disk depicts a strong asymmetric feature, useful for simulation testing. We selected a very massive planet to generate the Rossby vortex that attracts dust particles together to form the asymmetry. Our accelerating techniques enabled us to simulate the disk for a longer time than the published results; this was necessary to show the sustainability of the vortex and dust feedback to the gas. The results were published in Astrophysical Journal Letters (Fu et al. [3,4]). In the simulations, we also developed a new dust diffusion algorithm to avoid the possible numerical instability (see [5]). We also used our algorithm to study the sustainability of the asymmetric feature of the disks generated by the dead-zone theory. We have found that the vortex can be sustained for millions of years if a dead-zone is present in the disk. The results are published in [6].

The second algorithm assumed the time step from the stiff coupling of dust and gas was significantly smaller than the hydro time step. This is true for small dust particles or when the gas density is large. We separated the stiff part from other hydro evaluations and treated them in an operator split fashion. Due to the stiff coupling of gas and dust, the dust dynamics are slave to the gas dynamics and the mixture can reach partial equilibrium state quickly within one hydro step. Using a partial equilibrium state, we obtained a reduced order model (ROM) and via solving the ROM, we obtained the dust velocity and the gas velocity without solving the dust dynamic equations. This algorithm has been used in simulations of the HL-Tau proto-planetary disk and our model and simulations reproduce the observed data by ALMA telescope very well (see Jin et al. [7]. Figure 1 shows the comparison of the ALMA observation and our simulation result. In this simulation, we have found (see [8]) that the disk self-gravity plays an essential role in generating observable ring-type feature in the HL-Tau disk.

The third algorithm can be applied to a wide-range of the dust particles and gas surface density. Rather than split the stiff part from other hydro equations, we coupled them together in one step but treated them differently. The hydro part was solved using the explicit method, whereas the stiff coupled force between the gas and dust was solved using the implicit method. Using this implicit-explicit (IMEX) approach, we avoided solving the whole system using the fully implicit method, and as a result we realized significant economies by avoiding an expensive method. By treating the stiff part implicitly, we can use a very large time step without causing numerical instability. Since we solved the hydro and stiff drag terms together, our algorithm was reduced to the second algorithm for small dust species, and was reduced to the first algorithm for large dust species. We have developed a new Riemann solver for this algorithm. We also developed a fast implicit solver for multiple dust species using the Sherman-Morrison formula. We used this algorithm to model and simulate a new observed disk HD163296. Our results have been published in Phys. Rev. Lett. [9] recently and have gained scientific recognition around world (see news on APS front page at http://physics.aps.org/articles/v9/145).

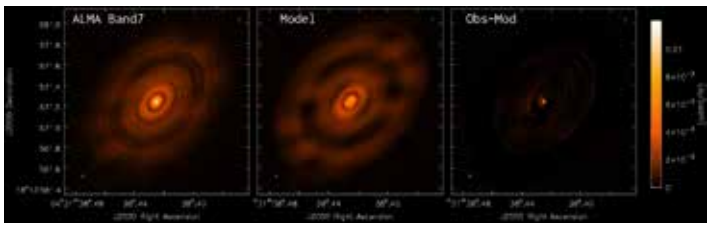

Figure 1. Comparison of the ALMA observation and our modeling and simulation results.

To increase the accuracy of our algorithm for small dust species, we have developed a parallel-in-time method. This method used the second or the third algorithm to predict the initial state at different time intervals. We then solved each time interval independently in parallel and iteratively corrected the predicted solutions until they are converged. We combined this time parallel scheme with our spatial domain decomposition whenever more computer processors are available. The parallel-in-time method sped up simulations by an order of magnitude.

We have implemented our algorithm in our software framework LA-COMPASS. We have developed a hybrid parallel mechanism using OpenMP, OpenACC, and OpenMPI. The OpenMP can speed up the performance by 30%. If the GPU processors are available, the combined OpenACC and OpenMPI can speed up the performance three times. Our new algorithms and software represent the best state-of-art numerical algorithm among the proto-planetary disk community. It enables us to perform simulations previously unattainable.

We have used our software in a number of simulations to study the planet formation and proto-planetary disk problems. More publications are expected.

Impact on National Missions

Advanced methods in computational physics are critical to the Lab mission of stockpile stewardship. Our project resulted in a better method to solve physical problems accurately and efficiently. It can be used immediately in modeling and simulation for the predictive science, such as climate modeling and subsurface flow prediction. It is directly related to Lab scientific challenges in information science and technology and understanding the universe beyond the standard model. The capability we have built throughout this project will be ideal for many astrophysical simulations and can be used as an alternative approach for many programmatic problems, such as materials simulations and fusion simulations.

"Parallel in time" seems to be a viable option to use more and more processors for future exascale computers. Our algorithm and code development in this project will help us to implement our new algorithm into ASC codes.

References

1. Li, S., and H. Li. Modified FARGO Algorithm and its Combination with Adaptive Mesh Refinement. 2016. Journal of Computational and Applied Mathematics. 307: 170.

2. Marel, N. van der, and E. van Dishoeck. A Major Asymmetric Dust Trap in a Transition Disk. 2013. Science. 340: 1199.

3. Fu, W., H. Li, S. Lubow, and S. Li. LONG-TERM EVOLUTION OF PLANET-INDUCED VORTICES IN PROTOPLANETARY DISKS . 2014. The Astrophysical Journal Letters. 788 (2): L41.

4. Fu, W., H. Li, S. Li, and S. Lubow. Effects of dust feedback on vortices in protoplanetary disks . 2014. Astrophysical Journal Letter. 795 (2): L39.

5. Li, S., and H. Li. Numerical treatment of dust diffusion in dusty proto-planetary disks. 2014. (Biarritz, France, 1-5 Jul 2013). Vol. 4881 Editionp. 96. San Francisco: Astronomical Society of Pacific Conference Series.

6. Li, S., and H. Li. Long-Time Sustainability of Rossby Wave Instability in Protoplanetary Disks with Dead Zone. 2015. (Long Beach, CA, 23-27 Jun. 2014). Vol. 4981 Editionp. 92. San Francisco: Astronomical Society of Pacific Conference Series.

7. Jin, S., S. Li, A. Isella, H. Li, and J. -H. Ji. Modeling Dust Emission of HL Tau Disk Based on Planet-Disk Interactions. 2016. Astrophysical Journal. 818: 76.

8. Li, S., and H. Li. The role of disk self-gravity on gap formation of the HL Tau proto-planetary disk. 2016. (Avigon, France, 8-12 Jun. 2015). Vol. 719p. 012007. New York: IOP Science.

9. Isella, A., S. Liu, H. Li, and S. Li. Ringed structure of the HD 163296 disk revealed by ALMA. 2016. Phys. Rev. Lett.. 117 (12): 251101.

Publications

Deng, W., H. Li, B. Zhang, and S. Li. Relativistic MHD Simulations of Collision-induced Magnetic Dissipation in Poynting-flux-dominated Jets/outflows. 2015. The Astrophysical Journal. 805 (2): 1.

Fu, W., H. Li, S. Li, and S. Lubow. Effects of dust feedback on vortices in protoplanetary disks . 2014. Astrophysical Journal Letter. 795 (2): L39.

Fu, W., H. Li, S. Lubow, and S. Li. LONG-TERM EVOLUTION OF PLANET-INDUCED VORTICES IN PROTOPLANETARY DISKS . 2014. The Astrophysical Journal Letters. 788 (2): L41.

Guan, X., H. Li, and S. Li. Relativistic MHD Simulations of Poynting Flux-Driven Jets . 2013. The Astrophysical Journal 12/2013; 781(1). . 781 (1): 1.

Isella, A., S. Liu, H. Li, and S. Li. Ringed structure of the HD 163296 disk revealed by ALMA. 2016. Phys. Rev. Lett.. 117 (12): 251101.

Jin, S., S. Li, A. Isella, H. Li, and J. -H. Ji. Modeling Dust Emission of HL Tau Disk Based on Planet-Disk Interactions. 2016. Astrophysical Journal. 818: 76.

Li, S.. A L-stable method for stiff hydrodynamic simulations in dusty disks. . To appear in AIP Conference Proceedings for ICNAAM 2016. (Rhode Island, Greece, 19-25 Sept. 2016).

Li, S., and H. Li. Numerical treatment of dust diffusion in dusty proto-planetary disks. 2014. In NUMERICAL MODELING OF SPACE PLASMA FLOWS: ASTRONUM-2013. (Biarritz, France, 1-5 Jul 2013). Vol. 488, 1 Edition, p. 96. San Francisco: Astronomical Society of Pacific Conference Series.

Li, S., and H. Li. Long-Time Sustainability of Rossby Wave Instability in Protoplanetary Disks with Dead Zone. 2015. In Numerical Modeling of Space Plasma Flows: ASTRONUM-2014. (Long Beach, CA, 23-27 Jun. 2014). Vol. 498, 1 Edition, p. 92. San Francisco: Astronomical Society of Pacific Conference Series.

Li, S., and H. Li. Modified FARGO Algorithm and its Combi-

nation with Adaptive Mesh Refinement. 2016. Journal of Computational and Applied Mathematics. 307: 170.

Li, S., and H. Li. The role of disk self-gravity on gap formation of the HL Tau proto-planetary disk. 2016. In Journal of Physics: Conference Series : ASTRONUM-2015. (Avigon, France, 8-12 Jun. 2015). Vol. 719, p. 012007. New York: IOP Science.

Liu, S., S. Li, and H. Li. Modelling the HD 163296 disk with the planet-disk interaction model . ApJ Letter.

Miranda, R., S. Li, and H. Li. Long-lived dust asymmetries at dead zone edges in proto-planetary disks. ApJ.

Su, H., and S. Li. Structure-Preserving Numerical Methods for Infinite-Dimensional Birkhoffian Systems. 2015. Journal of Scientific Computing. 46 (1): 196.

Su, H., and S. Li. Energy/Dissipation-Preserving Birkhoffian Symplectic Methods for Maxwell's Equations with Dissipation Terms. 2016. Journal of Computational Physics. 311 (1): 213.

Zhai, X., H. Li, P. Bellen, and S. Li. Three-Dimensional MHD Simulation of Caltech Plasma Jet Experiment: First Results . 2014. The Astrophysical Journal . 791 (1): 1.

Zhang, X., H. Li, S. Li, and D. Lin. RESONANCES OF MULTIPLE EXOPLANETS AND IMPLICATIONS FOR THEIR FORMATION . 2014. The Astrophysical Journal Letters . 789 (1): L23.

Automated Identification and Reverse Engineering of Malware

Christine M. Anderson-Cook
20140355ER

Abstract

Malware analysis is critical to our national security both to protect national secrets and to prevent corporate espionage. Almost all large government facilities and corporations employ highly trained cyber professionals, known as reverse engineers (RE), to analyze suspected malware. An organization cannot adequately respond to a malware infection or protect against future attacks from related code until they understand what it does. However, the RE can spend days to weeks uncovering the purpose of the malware, in an effort to discover who sent it and the extent of the attack.

The main goal of this project is to develop statistical tools for automated reverse engineering of malware. We have developed several approaches that will classify the program as belonging to an established family of malware given its static or dynamic trace, as well as determine the functionality of subroutines (e.g., disk I/O, network, GUI, registry, exploit, etc). For the family classification, matching to established families or flagging potential samples are helpful for establishing the phylogeny of the family. Defining a subroutine's purpose is an incredibly time consuming task when done manually. Our automated methods for determining subroutine functionality result in a list of most likely subroutine's functionality with corresponding probabilities. Thus, this work can substantially speed up RE times, providing a swifter response and thus reducing the expense and possibly severity of a malware infection. A second important consequence of this work is the ability to automatically assess the high-level functionality of a program as a whole with more accuracy than in previous work using the collection of subroutine's functionality. There has been little attempt until now to automatically arrange and classify the various tasks of a program, hence, the potential for a large impact due to this work.

Background and Research Objectives

Malware is a term used to describe a variety of forms of hostile, intrusive, or annoying software or program code. It was recently estimated that 30% of computers operating in the US are infected with malware [1]. More than 286 million unique variants of malware were detected in 2010 alone [2], and it is widely believed that the release rate of malicious software is now far exceeding that of legitimate software applications [3]. The cost incurred by US companies due to malware was estimated in 2011 to be $338 Billion/year [4]. A large majority of new malware is created through simple modifications to existing malicious programs or by adding some code obfuscation techniques such as a packer [5]. A packer compresses a program much the same way a compressor like Pkzip does, and then attaches its own decryption/loading stub which unpacks the program before resuming execution normally at the program's original entry point.

Malware is growing at such a rate that commercial antivirus vendors (AV) are not able to adequately keep up with new variants. Even though most new malware is very similar to known malware, it will often not be detected by signature-based antivirus programs [6, 7] until the malware signature is in the database, which can take weeks or even longer. There are two methods for antivirus scanners to implement their technology. The first is via a static signature scanning method, which searches for a sequence of known bytes in a suspected malicious program. The second method uses heuristic detection technologies that are intended to protect against zero-day (i.e., new) malware and malware not in the signature database. A goal of this work is to improve upon these heuristics technologies to complement existing AV software and thus provide the potential for CRADAs and/or external funding from industry.

Detecting malware on a machine in a computer network is a very important problem by itself, but it is not the end of malware analysis, rather the beginning. Once malware is discovered on a LANL host, for example, the time consuming process of reverse engineering [8] commences.

A highly trained cyber professional can spend a day to weeks uncovering the purpose of the malware, in an effort to discover who sent it and the extent of the attack. Not only does this tedious process require substantial time/labor expense, but it also results in a slower response. An organization cannot adequately respond to a malware infection until they understand its functionality (e.g., was a backdoor installed, was data stolen, personally identifiable information compromised? Should the whole network be shutdown, or just a few machines?). This delayed response to a known malware intrusion is the main motivation for the proposed work. Our approaches provide statistically-based tools that substantially speed up RE times, providing a swifter response and thus reducing the expense and possibly the severity of a malware infection.

The focus of the project has been on extracting and classifying information from static and dynamic traces. A static trace is a record of the sequence of instructions as they appear in the static binary, or the code, while a dynamic trace is the sequence of instruction as they are executed on a user's machine. There are benefits and drawbacks to both types of traces [9], static traces cannot be obtained if the program uses an unknown packer, while dynamic traces must be collected in a safe environment (e.g., a hypervisor) which is more time consuming than static analysis. If available, the static trace is often preferable as it allows all the code to be visible, where dynamic traces show only those calls that are executed. Thus, unused, legacy code will be available only from a static trace and can provide evidence to the author of the malware. In addition, the static trace allows the instructions of the program to be grouped into subroutines and calls between subroutines to be identified. A static trace also allows for an analysis of bigrams, or pairs of sequential instruction calls.

The major research objectives of the project were (1) to develop a novel, stochastic based approach using dynamic traces to perform initial classification of the sample as malicious or benign; (2) to determine the functionality of subroutines from static traces of known malware to identify the malicious components of the sample and probabilistically match them to known subroutines; (3) to group known malware samples into families that share common code and likely creators; and (4) to gain understanding about the phylogeny of the samples.

Scientific Approach and Accomplishments

To classify samples as benign or malicious, a method was implemented online in a sandbox environment (a security mechanism for separating running programs). The class of the program (malicious or benign) is modeled using a flexible spline logistic regression model with variable selection on the elements of the transition probability matrix, which are observed with error. Figure 1 shows a sample of instructions from a dynamic trace, with the conversion to a transition graph by identifying the function each instruction. The utility of the method was demonstrated on samples of traces from malicious and benign programs, and the performance of the method was superior to other leading detection schemes (both signature and classification based). The developed method is intended for eventual host-based use, providing concurrent sampling and analysis of the instructions executed by a given process, without disruption or substantial performance impact to the user [10].

Instr	Address
lea	ecx, [ecx]
sub	esp, 0x3C
sub	esp, 0x3C
mov	ebx, eax
mov	ebp, esp
add	ebx, 0x00410F1F
lea	eax, [ebp+]
mov	[esp+0x14], ecx
sub	eax, ecx
mov	[ebp+], edi
sub	edx, esi
or	edi, 0x0040A24E
xchg	[ebp+], esi

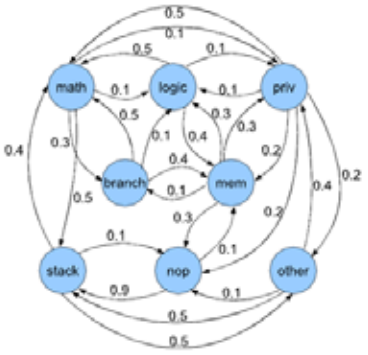

Figure 1. Markov chain transition probability representation of a dynamic instruction trace. The left hand side shows the first several lines from a dynamic trace, while the right side shows the conversion to transition probabilities based on categorization of the instructions.

To examine the functionality of subroutines, a new approach to malware classification was developed that probabilistically classifies programs based on their similarity with known malware subroutines [11]. Malware and benign programs can share a substantial amount of code, implying that classification should be based only on subroutines that occur infrequently, or not at all in benign programs. Figure 2 shows a sample of code, with expansion of subroutines and code blocks to illustrate the complexity of the code. This figure demonstrates how considering strategic elements can improve classification. Various approaches to accomplish this task were developed and compared. A simple approach that computes the fraction of subroutines of a program similar to malicious subroutines that are uncommon in benign programs was found to be the most effective. If this fraction exceeds around 1.5 %, the corresponding program can be classified as malicious at a 1 in 1000 false alarm rate. Combining a local and overall similarity based approach can lead to considerably better prediction.

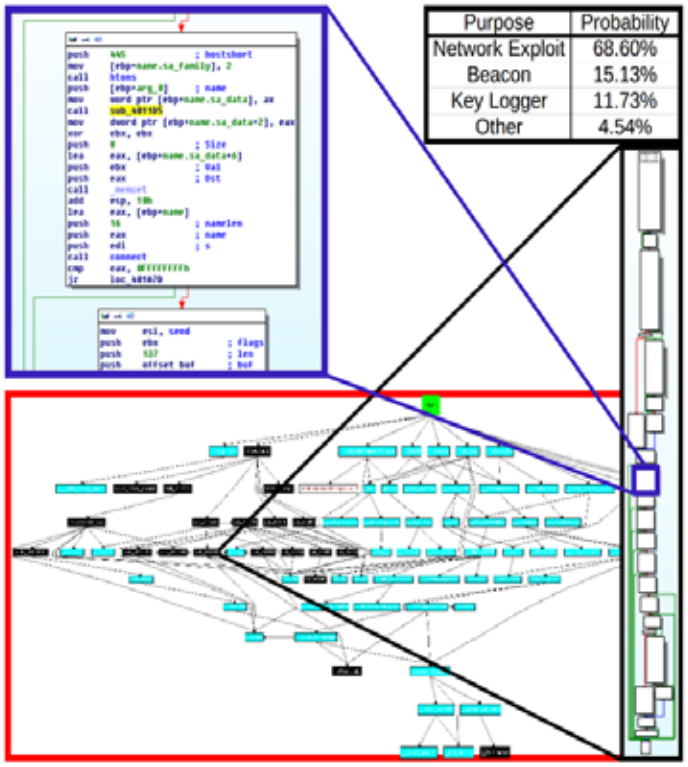

Figure 2. Code breakdown of the Sasser worm. The red box is a flowgraph of the subroutines, with one particular subroutine expanded and highlighted in black to show its code blocks. From that expanded code block, the individual instructions are shown in blue.

Static trace analysis through bigram and graph edit distance was shown to be effective at classifying identified malware into families or identifying new potential families. A three-stage method was developed to classify a new piece of malware into an existing family by comparing its similarity to static traces from a database of classified family members, and assigning it to the family with the most similar member [12]. First, a fast filtering method creates a shortlist of samples from the database with some similarity to the new malware, using a simple bigram comparison. The second stage uses the call graph, or the constructed graph of subroutines and the calls between them. Simulated annealing is used to estimate the graph edit distance, a measure of graph dissimilarity, between the call graph of the new malware and that of those on the shortlist. Figure 3 shows a summary of the correct classification of samples into families, with the small number of off-diagonal elements representing misclassified samples. Finally, a random forest or naïve Bayes classifier combines the previous two results to predict the family to which a new sample belongs.

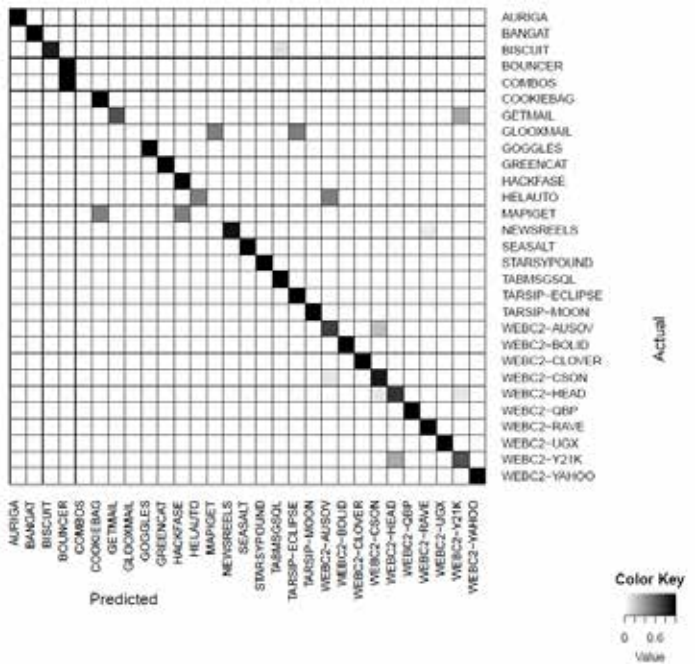

Figure 3. Heatmap demonstrating the classification matrix based on the simulated annealing method for calculating the graph edit distance.

Lastly, to gain understanding about the evolution and phylogeny of malware families, we built a Bayesian network structure, which combines human knowledge about the partial ordering of samples based on timestamps and statistical inference of conditional dependencies from observed data [13]. The flexible approach leverages complementary information from human knowledge and observed data to produce networks that reflect beliefs about the system while also fitting observed data. Figure 4 shows a collection of samples from a common family with a known phylogeny. The goal of this approach is to construct similar structure for a new family with unknown phylogeny. We provide an efficient implementation of the partial-order prior in a Bayesian structure discovery learning algorithm, as well as a related structure prior, showing that both priors meet the local modularity requirement necessary for an efficient Bayesian discovery algorithm. Our algorithm, when compared to existing malware phylogeny algorithms, is able to more accurately discover true dependencies that are commonly missed by other algorithms.

The developed collection of tools provides automated methods for reverse engineers to initially identify malware, and target subroutines that are likely malicious. This can streamline the process of gaining understanding about the functionality of the sample and begin the process of identifying a remedy. To leverage knowledge about existing samples and help with future identification, the classification of samples identified as malicious into families and

understanding their evolution can prove helpful.

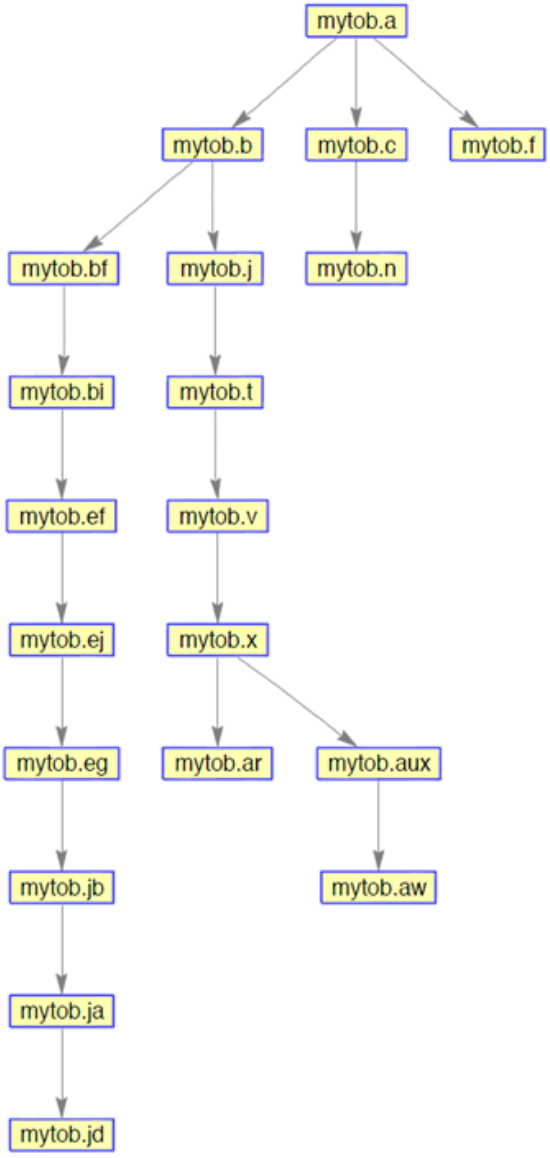

Figure 4. Desired output from a malware phylogeny learner.

Impact on National Missions

Malware analysis is a multi-billion dollar industry. Beyond that malware analysis is critical to our national security both to protect national secrets and to prevent corporate espionage. Almost all large government facilities and corporations employ trained cyber professionals to reverse engineer suspected malware. The statistical work developed as part of this project provides reverse engineers with tools to help automatically triage and classify different threats into new and established categories. This will allow them to not only investigate a larger percentage of the suspected malware discovered on their systems, but also allow a swifter response to those identified as threats. The preliminary classification work is already mature enough to be implemented on any enterprise network just as it already has been at LANL in Code Vision. The goal is to continue to develop tools to implement the new reverse engineering methodology developed in this project into a tool suite to be used by cyber professionals, allowing the methodology to be transitioned into practice at other government agencies and corporations. As the NNSA complex is a prime target for cyberattack, cybersecurity is an enabling technology for the nuclear weapons mission.

References

1. PandaLabs quarterly report. 2012. PandaLabs.
2. Internet security threat report. 2011. Symantec.
3. Internet security threat report, Trends for July–December 2007 (Executive Summary). 2008. Symantec.
4. Special report: Your security. 2011. Consumer Reports.
5. Royal, P., M. Halpin, D. Dagon, R. Edmonds, and W. Lee. PolyUnpack: Automating the hidden-code extraction of UnpackExecuting malware. 2006. In ACSAC. , p. 289. Miama, FL: IEEE Computer Society.
6. Christodorescu, M.. Static analysis of executables to detect malicious patterns. 2003. In Proceedings of 12th USENIX Security Symposium. (Washington, DC, 4-8 Aug. 2003). , p. 169. Washington, DC: USENIX.
7. Perdisci, R., D. Dagon, P. Fogla, and M. Sharif. Misleading worm signature generators using deliberate noise injection. 2006. In Proceedings of the 2006 IEEE Symposium on Security and Privacy. (Oakland, CA, 21-24 May, 2006). , p. 17. Oakland, CA: IEEE.
8. Chikofsky, E. J., and H. Cross. 1990. 1990. IEEE Software. 7: 13.
9. Anderson, B., C. Storlie, and T. Lane. Improving malware classification: Bridging the static/dynamic gap. 2012. In Proceedings of the 5th ACM Workshop on Security and Artificial Intelligence. (Raleigh, NC, 16-18 Oct. 2012). , p. 3. Raleigh, NC: ACM Digital Library.
10. Storlie, C. B., B. Anderson, S. Vander Wiel, D. Quist, C. Hash, and N. Brown. Stochastic identification of malware with dynamic traces. 2013. Annals of Applied Statistics . 8 (1): 1.
11. Sexton, J., C. B. Storlie, and B. Anderson. Subroutine based detection of APT malware. 2015. Journal of Computer Virology and Hacking Techniques. : 1.
12. Bolton, A. D., and C. M. Anderson-Cook. APT malware static trace analysis through bigrams and graph edit

distance. Statistical Analysis and Data Mining.

13. Anderson-Cook, C. M.. Optimizing in a complex world: Statisticians' roles in decision-making. To appear in Quality Engineering.

14. Anderson-Cook, C. M., and L. Lu. Much-needed structure: A new 5-step decision-making process helps you evaluate, balance competing objectives. 2015. Quality Progress. 48 (10): 42.

15. Oyen, D., K. Sentz, B. Anderson, and C. M. Anderson-Cook. Order priors for Bayesian network discovery with an application to malware phylogeny. Statistical Analysis and Data Mining.

Publications

Anderson, B., C. Storlie, M. Yates, and A. McPhall. Automating Reverse Engineering with Machine Learning Techniques. 2014. In The 7th ACM Workshop on Security and Artificial Intelligence. (Scottsdale, 7 Nov. 2014). , p. 103. Scottsdale: ACM Digital Library.

Anderson, B., T. Lane, and C. Hash. Malware Phylogenetics Based on the Multiview Graphical Lasso. 2014. In The Thirteenth International Symposium on Intelligent Data Analysis. (Leuven, Belgium, 29-31 Oct. 2014). , p. 1. Leuven, Belgium: Springer.

Anderson-Cook, C. M.. Optimizing in a complex world: statisticians' roles in decision-making. To appear in Quality Engineering.

Anderson-Cook, C. M.. Rejoinder for "Optimizing in a complex world: statisticians' roles in decision-making". To appear in Quality Engineering.

Anderson-Cook, C. M., and L. Lu. Much-needed structure: a new 5-step decision-making process helps you evaluate, balance competing objectives. 2015. Quality Progress. 48 (10): 42.

Bolton, A.. Malware static trace analysis through bigrams and graph edit distance. 2015. LANL Report.

Bolton, A. D., and C. M. Anderson-Cook. APT malware static trace analysis through bigrams and graph edit distance. Statistical Analysis and Data Mining.

Kao, Y., B. Reich, C. Storlie, and B. Anderson. Malware Detection Using Nonparametric Bayesian Clustering and Classification Techniques. 2015. Technometrics . 57 (4): 35.

Neil, J., C. Hash, A. Brugh, M. Fisk, and C. Storlie. Scan statistics for the online detection of locally anomalous subgraphs. 2013. Technometrics. 55 (4): 403.

Oyen, D., K. Sentz, B. Anderson, and C. Anderson-Cook. Application of Bayesian discovery with order priors to combining knowledge and statistical data. 2015. LANL Report.

Oyen, D., K. Sentz, B. Anderson, and C. M. Anderson-Cook. Order priors for Bayesian network discovery with an application to malware phylogeny. Statistical Analysis and Data Mining.

Sexton, J.. Anomaly detection of multistage network intrusions. 2015. LANL report.

Sexton, J., C. Storlie, and B. Anderson. Subroutine based detection of APT malware. 2015. Journal of Computer Virology and Hacking Techniques. : 1.

Sexton, J., C. Storlie, and J. Neil. Attack chain detection. 2015. Statistical Analysis and Data Mining. 8: 353.

Storlie, C., B. Anderson, S. Vander Wiel, D. Quist, C. Hash, and N. Brown. Stochastic Identification of Malware with Dynamic Traces. 2014. Annals of Applied Statistics. 8 (1): 1.

Temporal Graphs

Aric A. Hagberg
20140389ER

Abstract

Graphs, or networks, are increasingly being used to model complex techno-social networks such as the power grid, the Internet, as well as computer and social networks. Networks capture the interactions between elements of these systems and are fundamental structures used for studying them. Understanding how these networks function and behave under changing and dynamic circumstances is vital to several areas of national security including cybersecurity, which is the primary application for the theoretical and methodological work in this project.

We developed theoretical models for static and dynamic graphs that are relevant to cybersecurity infrastructure systems and examined the structure of those models. In addition we developed algorithms to efficiently generate instances of the models for statistical modeling and performance testing of algorithms. As part of this project, de-identified data sets of computer traffic were made available to the research community to engage our collaborators to develop algorithms for dynamic graph problems. This data was the basis for building temporal graph models and studying their properties as a way to estimate risk in computer authentication systems.

Background and Research Objectives

Network science research has been primarily focused on static graphs and their topological characteristics. However, all real-world networks are dynamic to some degree. Processes on networks such as the spread of a virus on a social network [1], traversal through a cyber network [2], and cascading failures in a power grid [3] are all critically dependent on the temporal nature of the underlying network. The need for modeling and analysis of temporal graphs was recognized at least 10 years ago, but only now is the topic gaining significant attention [4]. One reason for this oversight has been that the analysis of even static ``snapshots'' of the networks as time-series has proven complex. Indeed for the most part, such networks have resisted mathematical analysis.

This project focused on developing temporal graph models for classes of complex networks such as computer and social networks. Our objective was to elucidate the interplay between the structural evolution of the network, temporal properties of the network, and dynamic processes, such as the spread of a virus or information, occurring on the network. The research examined how sensitive networks are to perturbation, how to slow the speed of computer information spread and how to increase cybersecurity in the face of persistent attacks.

Scientific Approach and Accomplishments

Our approach to the theory and application of dynamic graph models centered around questions on the topic of security of networked computer systems. This approach consisted of three aspects: data collection, modeling and algorithms for the data, and mathematical theorems about the model properties. This approach grounded us in real-world data-driven problems and provided the power, through modeling, to reason about data properties to develop risk metrics and other related actionable information from the data.

Random Graph Structures

Our modeling approach was based on the well-established mathematical foundation of (static) random graph theory. We developed static and temporal random graph models that capture important structural characteristics of networks such as the degree distribution and clustering coefficient. One of the most relevant random graph models to social and computer systems is the random intersection graph (RIG). This graph model has parameters that represent the connectivity patterns between two sets of nodes (e.g. users and computers, or more generally people and groups). We developed mathematical proofs that show how the connectivity structure changes from completely unconnected, through mostly connected, and finally completely con-

nected as the group association parameters are changed. The surprising results are that the transitions between mostly unconnected and having a large fraction of the network mostly connected happens very dramatically for a small parameter change. This change in connectivity is very important for communication across the network and gives a type of threshold for easier transmission of information. This work is under review for the journal "Discrete Applied Mathematics" [5].

Algorithms

We invented a fast algorithm for generating large-scale random kernel graphs [8]. The random kernel model is a general model that can be designed to capture perceived important characteristics of real networks and that is mathematically tractable. For practical use in simulation large instances of graphs need to be generated and the naive algorithm, which takes quadratic time in the number of nodes, does not scale favorably. As real world networks are usually sparse and large, it is important for the running time of generation algorithms to scale linearly in the number of edges. We proved our algorithm scales linearly in the number of edges and demonstrated the performance with a software implementation. Further we have developed a way to modify a given kernel in the model that can change the assortativity, an important network property.

In addition to the manuscript, to show the practical performance and simplicity, we released a Python software implementation of the algorithm as part of the NetworkX software package [8]. We have new preliminary further results on this class of kernel models that appear to make it practical to generate networks with specified distributions of triangle, square, and higher order subgraphs.

Authentication System Modeling

Modern enterprise computer networks rely on centrally managed authentication schemes, which allow users to easily authenticate to many computer systems and applications. Authentication is typically required for users to access applications and information of importance to the enterprise. Examining this authentication activity gives insight into basic user behavior. In particular, authentication events imply relationships between computers and users, which can be represented as a bipartite graph. We find this to be an effective means to model the potential risk of credential hopping opportunities and to analyze potential mitigation strategies. A typical graph of the Los Alamos authentication network system at a given time is shown in Figure 1.

We developed a new modeling approach using random intersection graphs to capture the structure of computer authentication events. Authentication events imply relationships between computers and users, which can be represented as a bipartite graph. We used this graph to study the potential risk of credential hopping opportunities and to analyze potential mitigation strategies. Using graph-theoretical results for component sizes in random intersections graphs, we proposed two mitigation strategies, and performed experiments simulating their implementation. The results led to realistic, actionable risk reduction strategies. These models are helping understand the risk of using centralized authentication systems such as those found in most large organizations such as LANL. Our article "Connected components and credential hopping in authentication graphs," published as part of the International Conference on Signal-Image Technology \& Internet-Based Systems (SITIS) in November 2014 described our first results [9].

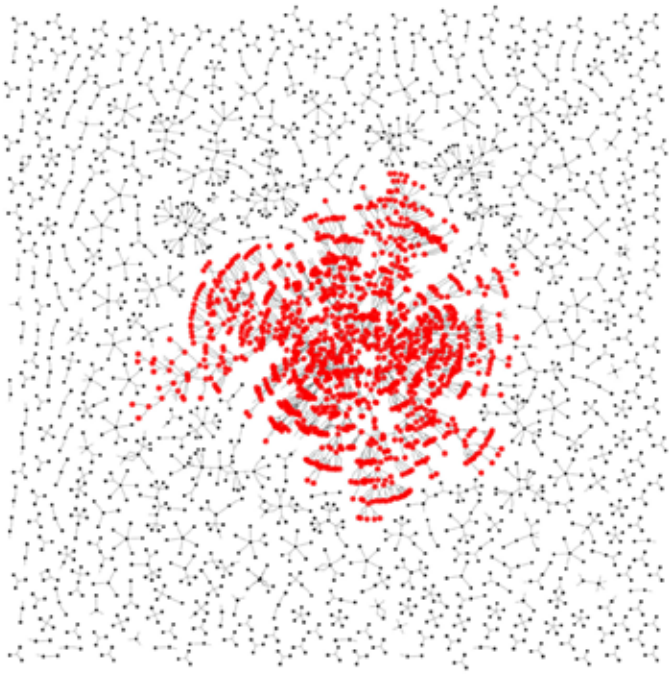

Figure 1. The authentication graph connecting computers and users at Los Alamos National Laboratory on a typical workday. Computers are shown as circles with those in the largest connected component colored red. The users credential nodes are suppressed and appear as junctions in edges between computers. The largest component has 1476 computers and 962 users. Understanding how to reduce the the typical size of the largest component is a goal of this research.

To further model computer authentication events we developed a method to characterize credential usage. One important research problem associated with credential systems is the analysis of theft or misuse, either by a malicious insider or an external adversary. Once compromised, a user credential can be used by adversaries to advance through the network and further their goals. Little attention is currently given to looking at computer event logs as

an aggregated multivariate data stream. We modeled user credential patterns by considering independently the time series of events generated by each user credential. Bayesian models were used to fit to the event data for each user credential, providing a flexible global framework for monitoring credentials on an enterprise network and identifying potentially compromised credentials [10].

Reachability

We investigated metrics for connectivity in temporal graphs that are relevant for real systems such as the authentication event data. For static graphs the connectivity of a node has a single simple definition of the set of other nodes that you can reach by crossing links. We developed a new definition of "reachability" that captures the dynamics of unauthorized credential usage in a computer network with centralized authentication. This definition provides a measure of how long it takes, starting at a given computer, to traverse the credential network and crossing as many edges as are available at the current time.

We constructed to new random temporal graph models based on the well-known static models the Erdos-Renyi and Chung-Lu random graphs. The models allow an adjustable rate of change for dynamic edges with preservation of the original static random graph structure. For these to models we proved theorems for the reachability time and the mixing time (the time it takes to thoroughly randomize any initial graph correlations). These theorems are published in the chapter "Temporal reachability in dynamic networks" of the book "Dynamics of Networks and Cybersecurity" [11].

Data Sets

Our modeling and analysis approach was inspired partly by challenges in understanding computer authentication system dynamics. In addition to modeling, improving data quality, reducing data parsing and normalization complexity, and increasing the size and number of useful data sets are all critical directions for the future of enterprise cyber defense data analysis. These directions will help improve and make future enterprise cybersecurity research more effective and efficient. In this project we collected, developed, and released two data sets and are in the process of finalizing a third data release.

The first data set contains de-identified authentication events from our enterprise computer network at LANL [12]. The time-series of events of logins by users to computers allows study of the dynamic properties of this data and facilitates common model-building and analysis tools in the research community. We learned from this data release that correlations between the authentication events and other cyber data such as flows across network routers, domain name system requests, and process start/stop data on computers is important for modeling and made a second data release that also includes those aspects [13]. This second data set also includes red-team activities for use in anomaly detection algorithms. For our third and final data release of this project we have adjusted, based on community feedback and results of this project, the processing to be enable easier correlations between the multiple source data. These data releases required the development of instrumentation to collect the data, tools for parsing, normalization, and de-identification of the data and design of a data format [14].

Impact on National Missions

We targeted a fundamental challenge in network science, namely modeling the time-dependent changes in complex networks. This project developed fundamental mathematical models and algorithms for complex evolving networks such as computer networks and social networks. This work will have direct applications in the fields of cybersecurity and infrastructure networks.

Our work develops new models, techniques and theorems for dynamically changing graphs that are the underpinnings for many applications of network science. For example, temporal graphs are a major research interest in cybersecurity and fill a missing gap in random graph models. Progress in modeling temporal graphs will provide capability relevant to DOD missions in cybersecurity anomaly detection. The data sets released as part of this project are providing a resource and focus for the community of academic, government, and corporate cybersecurity researchers to study algorithms for dynamic networks.

References

1. Barrett, C. L., S. G. Eubank, and J. P. Smith. If smallpox strikes Portland . 2005. Scientific American. 292: 54.

2. Neil, Josh. Scan statistics for the online detection of locally anomalous subgraphs. 2011. PhD Thesis, University of New Mexico.

3. Pfitzner, R., K. Turitsyn, and M. Chertkov. Statistical classification of cascading failures in power grids. 2011. Power and Energy Society General Meeting. DOI: 10.1109/PES.2011.6039412.

4. Holme, P., and J. Saramaki. Temporal networks. 2012. Physics Reports. 519 (3): 97.

5. Bradonji'c, Milan, Aric Hagberg, Nicolas W. Hengartner, Nathan Lemons, and Allon G. Percus. The phase transition in inhomogeneous random intersection graphs. 2016. In Review. : 1.

6. Farrell, . Hyperbolicity, Degeneracy, and Expansion of Random Intersection Graphs. 2015. In Algorithms and Models for the Web Graph: 12th International Workshop, WAW 2015, Eindhoven, The Netherlands, December 10-11, 2015, Proceedings. Edited by Gleich, F. David and Komj'athy, J'ulia and Litvak,. p. 29. Springer International Publishing.

7. Hagberg, Aric, and Nathan Lemons. Fast Generation of Sparse Random Kernel Graphs. 2015. PLoS ONE. 10 (9): e0135177.

8. Hagberg, Aric A., Daniel A. Schult, and Pieter J. Swart. Exploring network structure, dynamics, and function using NetworkX. 2008. In Proceedings of the 7th Python in Science Conference (SciPy2008). , p. 11.

9. Hagberg, A., N. Lemons, A. Kent, and J. Neil. Connected Components and Credential Hopping in Authentication Graphs. 2014. p. 416. IEEE Computer Society.

10. Turcotte, Melissa. 3. 2016. In Modelling user behaviour in a network using computer event logs. Edited by Niall Adams, and Nick Heard. Vol. 1p. 67. World Scientific.

11. Hagberg, Aric, Nathan Lemons, and Sidhant Misra. 9. 2016. In Temporal reachability in dynamic networks. Edited by Niall Adams, and Nick Heard. Vol. 1p. 181. World Scientific.

12. Kent, Alexander D.. User-Computer Authentication Associations in Time. 2014. 10.17021/1179829.

13. Kent, Alexander D.. Comprehensive, Multi-Source Cyber-Security Events. 2015. DOI:10.17021/1179829.

14. Kent, Alex. 2. 2016. In Cyber security data sources for dynamic network research. Edited by Niall Adams, and Nick Heard. Vol. 1p. 37. World Scientific.

Publications

Bradonji'c, Milan, Aric Hagberg, Nicolas W.Hengartner, Nathan Lemons, and Allon G. Percus. The phase transition in inhomogeneous random intersection graphs. 2016. In Review. : 1.

Farrell, . Hyperbolicity, Degeneracy, and Expansion of Random Intersection Graphs. 2015. In Algorithms and Models for the Web Graph: 12th International Workshop, WAW 2015, Eindhoven, The Netherlands, December 10-11, 2015, Proceedings. Edited by Gleich, F. David and Komj'athy, J'ulia and Litvak,. , p. 29. Springer International Publishing.

Farrell, M., T. Goodrich, N. Lemons, F. Reidl, F. S. Villaamil, and B. D. Sullivan. Hyperbolicity, degeneracy, and expansion of random intersection graphs. 2015. In to appear in the 12th Workshop on algorithms and models for the web graph.

Hagberg, A., N. Lemons, A. Kent, and J. Neil. Connected Components and Credential Hopping in Authentication Graphs. 2014. In Signal-Image Technology and Internet-Based Systems (SITIS), 2014 Tenth International Conference on. , p. 416. IEEE Computer Society.

Hagberg, Aric, Nathan Lemons, and Sidhant Misra. 9. 2016. In Temporal reachability in dynamic networks. Edited by Niall Adams, and Nick Heard. Vol. 1, p. 181. World Scientific.

Hagberg, Aric, and Nathan Lemons. Fast Generation of Sparse Random Kernel Graphs. 2015. PLoS ONE. 10 (9): e0135177.

Kent, Alex. 2. 2016. In Cyber security data sources for dynamic network research. Edited by Niall Adams, and Nick Heard. Vol. 1, p. 37. World Scientific.

Kent, Alexander D.. Comprehensive, Multi-Source Cyber-Security Events. 2015. DOI:10.17021/1179829.

Kent, Alexander D.. User-Computer Authentication Associations in Time. 2014. 10.17021/1179829.

Keszegh, B., N. Lemons, and D. P'alvolgyi. Online and Quasi-online Colorings of Wedges and Intervals. Order. : 1.

Keszegh, B., N. Lemons, and D. P'alvolgyi. Online and Quasi-online Colorings of Wedges and Intervals. 2015. Order. : 1.

Turcotte, Melissa. 3. 2016. In Modelling user behaviour in a network using computer event logs. Edited by Niall Adams, and Nick Heard. Vol. 1, p. 67. World Scientific.

Efficient Method for Large Scale Simulations of Fermionic Gases Interacting with Classical Fields

Kipton M. Barros
20140458ER

Abstract

We developed numerical tools to simulate a broad range of quantum mechanical phenomena that arise from strongly correlated electrons in actinide, lanthanide, and transition metal based compounds. These compounds are of special interest due to the formation of mesoscale super-structures that produce novel macroscopic functionality. Interacting quantum mechanical systems are notoriously difficult to simulate; existing numerical methods cannot span the gap between atomic and mesoscale. Our new algorithms are capable of performance calculations orders of magnitude faster than state of the art methods. Our new codes make mesoscale interacting quantum simulations accessible.

The algorithm and codes developed in this project have allowed us to simulate systems at unprecedented size, and helped to uncover exotic magnetic phases. We find a variety of complex mesoscale magnetic patterns emerging in magnetic ions interacting with low-density electron gases. For example, we have discovered new mechanisms for magnetic skyrmion formation. Another example is a super-lattice of merons and antimerons that arise due to a generic instability in Ruderman-Kittel-Kasuya-Yosida type interactions. Our numerical techniques also enable the study of correlated electron physics.

A rich mathematical theory underlies the algorithms of this project. We began with the Kernel Polynomial Method created at LANL by Silver and Roder [1], and performed an "automatic differentiation" transformation to calculate effective forces [2]. Throughout this project, we have discovered and applied beautiful techniques like probing methods for better stochastic convergence [3] and high-accuracy numerical dynamics [4].

The merits of this project can be evaluated through our many high quality publications (see Publications section) and a highly scalable hybrid MPI/GPU. Our methodologies have launched two new LDRD projects and continue to produce interesting science.

Background and Research Objectives

In this project, we consider a very generic task in condensed matter physics and quantum chemistry: We wish to solve quantum Hamiltonian matrices Hij [{S}] that represent the interactions between fermions and classical degrees of freedom S. In our condensed matter applications, the fermions are typically electrons and the classical field might represent local magnetic moments, charge density or a superconducting order parameter. In other quantum mechanical applications, the equations have a similar form, but a very different physical interpretation. In quantum molecular dynamics, for example, the classical degrees of freedom would represent positions of nuclei, treated within the Born Oppenheimer approximation. In lattice quantum chromodynamics (QCD), for example, the fermions would represent quarks instead of electrons, and the "classical field" would capture a bosonic functional integral over the gauge field. The point here is that this numerical problem is ubiquitous, and of general interest to many communities.

Here, we focused on applications to the Kondo lattice model (KLM), in which itinerant electrons interact with localized classical magnetic moments. Over the past decade, the KLM has been widely used to study giant and colossal magneto-resistance. In recent years, KLM studies have focused on a variety of new phases that have special transport properties. These new phases arise due to the complicated, effective many-body interactions of the classical field, obtained by "integrating out" the conduction electrons. Because electrons are quantum mechanical in nature, tracking the effective interactions for the evolving classical field S requires repeated diagonalization of the Hamiltonian matrix H. If we are working with a lattice of N sites, then typically the matrix H has size (cNxcN), with c a constant that typically ranges between 2 and 10. The classical field S typically contains order N degrees of freedom. The cost to diagonalize the

Hamiltonian matrix (i.e. find its eigenvalues and eigenvectors, which represent the possible quantum states of electrons) scales cubically with the system size – i.e. O(N^3). Moreover, we wish to obtain about 10^3 – 10^4 independent stochastic samples of the classical field S. Every time S changes, so does the Hamiltonian matrix H[S]. The repeated diagonalization of H quickly becomes a bottleneck. In a standard approach with direct diagonalization, the cost of a single sample of the classical field S scales quartically with system size, i.e. O(N^4). This naïve approach quickly fails for large lattices of order N=400 sites. The purpose of this project is to develop methods the reduce the computational scaling from O(N^4) to O(N), i.e. to a cost linear in the system size. To exploit our algorithms, we also developed a highly parallel, hybrid MPI/OpenMP/GPU code. The result is multiple orders of magnitude speedup compared to existing methods in real-world benchmarks.

Scientific Approach and Accomplishments

Our project begins with the Kernel Polynomial Method (KPM), a powerful technique originally developed at LANL [1]. In this method, one completely avoids explicit diagonalization of the Hamiltonian matrix H. That is, at no point in the calculation do we calculate the full set of eigenvectors and eigenvalues. Instead, KPM works by approximating the density of states (DOS), i.e. a rough count of eigenvalues at each relevant energy level. The total system energy E can be expressed as an integral over the DOS (i.e. a count of eigenvalues below a chemical potential threshold). Remarkably, KPM makes it possible to estimate the DOS and system energy E at a cost that scales linearly with system size N. The key ideas of KPM are: (1) Expansion of the DOS function in a Chebyshev polynomial series, and (2) approximation of the polynomial coefficients via stochastic estimation of the trace of the Chebyshev polynomials applied to the matrix H. Details of this method are provided in Ref 1.

For our applications, we desire statistical samples of the classical field S, and every change to S will generate a new Hamiltonian matrix H[S]. The system energy E is naturally also a function of S. Note that S typically has order-N elements. In the context of Monte Carlo sampling, a full sweep of the lattice, in which all N elements of S are updated, would require N calculations of energy E. Using KPM estimation of energies, the total cost would scale like N2.

In this project, we introduced a modification of KPM [2] that reduces the sampling cost from O(N^2) to O(N), i.e. linear in the system size. The idea is to transform KPM using the technique of reverse-mode automatic differentiation. KPM enables efficient estimates of energy E. Our transformation of KPM enables efficient estimates of the forces, fi = -dE/dSi for each component Si of the classical field. Note that all forces are obtained simultaneously; the complete set of N forces is calculated at the same cost as the single energy value E. Once the forces are available, we can use a Langevin dynamics to sample the full classical field S.

Recall that direct diagonalization costs O(N^4) to sample S. Our modified KPM method reduces this cost to O(N). In practice, the speedups are staggering. Whereas previous methods were restricted to systems of size N=400 sites, our new method can readily handles systems of size N=40,000 sites and larger. We obtain many orders of magnitude speedup compared to state-of-the-art methods on real world benchmarks. This is made practical by a combination of algorithmic developments and our highly optimized, highly parallel hybrid MPI/OpenMP/GPU code developed within the project. We have demonstrated good scaling on up to 100 GPUs on the Institutional Computing Moonlight cluster. Our code enables the first practical simulations of mesoscale quantum systems. Our simulations of the Kondo lattice model with tens of thousands of sites uncover various phenomena: chiral vortices and domains, skyrmions, bound hedgehog dipoles, and interacting vortices.

While working on this project, we discovered new mathematical techniques that further accelerate the modified KPM. There is a surprising and beautiful mathematical theory of “probing techniques” that enables KPM to achieve much better accuracy [3]. These techniques utilize the decay of the density matrix; by using “correlated” random vectors, fewer random vectors are required to obtain a good stochastic estimate of the trace.

In our project, we went beyond the prior work in Ref [3] by analyzing with what we call the energy matrix, which can be thought of as the anti-derivative of density matrix (i.e. the anti-derivative of the Fermi function, applied to the Hamiltonian). It turns out that the energy matrix has better decay properties than the density matrix. By using automatic differentiation, we can stochastically estimate the density matrix while still benefiting from the superior decay properties of the energy matrix. In the naive KPM method (our original ER proposal) the stochastic error scales like s^{-1/2}, where s is the number of random vectors. With our improvements, the error decreases exponentially with s for insulators. For metals, the error now scales like s^{-5/6} and s{-2/3} for 2 and 3-dimensional systems respectively. Our code is likely the only one capable of simulating the dynamics of metals in a linear scaling way.

This project supported many promising students. In partic-

ular, Julien Roussel visited us from France in the summer of 2015 and developed a Monte Carlo approach for the graph coloring problem. This work was necessary to effectively select KPM random vectors with appropriate correlations.

We have optimized various aspects of the code to improve builds times of the Hamiltonian matrix. In particular, we now calculate Hamiltonian matrix elements in a multi-threaded way using Intel's Thread Building Blocks (TBB) library. We also use TBB's parallel-sort capability to speed up construction of the Compressed Sparse Row (CSR) matrix format. Finally, using CUDA 6.5, our optimized code can now use Block- compressed Sparse Row (BSR) format, which takes advantage of the block matrix structure typically seen in multi-orbital Hamiltonians. The BSR format eliminates storage of most sparse matrix indices, thereby reducing GPU bandwidth loads, and enabling an effective speed-up of a factor of 2 for typical Hamiltonians. We also extended our KPM code to facilitate new application areas. For example, adding support for new types of Kondo Lattice Model now typically involves writing a couple new functions to specify the matrix hopping elements.

We have applied our new techniques to include correlations in quantum molecular dynamics via the so-called Gutzwiller approximation. We have produced the first prototype for modeling single-orbital systems (like Hydrogen). By using this approach, we have computed the self-diffusion coefficient as a function of the strength of the intra-orbital Coulomb interaction. Interestingly, we found that the self-diffusion coefficient exhibits a rather sharp maximum near the Mott transition. Our manuscript on this topic is in review.

Interaction with local quantum chemistry experts has suggested fruitful new methodological research directions. For example, after discussions with Anders Niklasson (T-1), we have learned that the Extended Lagrangian formalism could be very useful for solving dynamical self-consistency constraints that appear in condensed matter physics, such as strong magnets. These discussions have spun off a new-start ER proposal that begins in FY2017.

Our experience with Molecular Dynamics simulations has helped us to improve our methodology also for dynamical simulations of magnetic spin systems. In particular, we have implemented a predictor-corrector scheme for time integration of "stochastic Landau-Lifshitz" (SLL) dynamics [4]. This has had three benefits: (1) integration error now scales O(dt^2), making finite-temperature simulations much more accurate, (2) this richer dynamics now includes effective dynamical waves, which appear to decrease decorrelation times for equilibrium measurements, and (3) SLL dynamics is realistic, enabling us to perform non-equilibrium and dynamical magnet studies. This work is the subject of a manuscript now under review.

Finally, we mention that our methodological developments have enabled us to perform several groundbreaking studies in condensed matter physics and specifically frustrated magnetism. For example, we have found that crystals of merons and antimerons are solutions of Kondo Lattice Models on high-symmetry lattices. This important result shows that the Ruderman- Kittel-Kasuya-Yosida interaction is not enough to characterize the magnetic ordering of frustrated itinerant magnets. By combining our novel numerical approach with analytical treatments, only valid in the weak-coupling regime, we have discovered that exotic crystals of topological defects can also be stabilized in itinerant magnets. Our manuscript on the subject has been published in J. Phys. Soc. Jpn. As another example, we have found that frustration of multi-Q magnetic orders can enhance electron scattering at low temperatures, and thus provide a new mechanism for a resistivity minimum different than the Kondo effect. Our manuscript on the subject has been accepted for publication in Phys. Rev. Lett.

Impact on National Missions

We developed a tool that creates fundamentally new capabilities for bridging two LANL grand challenges: "Information, Science and Technology" (IS&T) and "Materials: Discovery Science to Strategic Applications"(MDSSA). This research was a direct response to FY13 IS&T Grand Challenge priorities: development of methods for inference and prediction of large-scale complex systems and design of algorithms to efficiently extract information from massive amounts of data. Our project also responds specifically to the LDRD "Materials for the Future" focus area and addresses the priorities of realizing design principles towards controlled functionality and developing multifunctional materials to transform structural and functional performance and integration, and tunable and emergent properties. In the BES report on Basic Research Needs, multifunctional materials are emphasized as solutions to a range of energy problems. The main bottleneck for understanding the complex behavior of interacting quantum systems is the lack of efficient algorithms for simulating the corresponding models. Developing this capability is crucial for addressing future Laboratory mission challenges such as inference and prediction of large-scale complex systems, and prediction and control of emergent phenomena in complex materials. The innovative codes that were developed under this project continue to be applied to the simulation of real compounds that are being investigated in our experimental groups. These codes helped support new program developments for modeling and simulating complex materials. This work will fundamentally advance

our understanding of unconventional states of matter. Such states have great application potential due to their unusual physical responses.

References

1. SILVER, R. N., and H. RODER. DENSITIES OF STATES OF MEGA-DIMENSIONAL HAMILTONIAN MATRICES. 1994. INTERNATIONAL JOURNAL OF MODERN PHYSICS C-PHYSICS AND COMPUTERS. 5 (4): 735.

2. Barros, , and Kato. Efficient Langevin simulation of coupled classical fields and fermions. 2013. PHYSICAL REVIEW B. 88 (23).

3. Tang, J. M., and Saad. A probing method for computing the diagonal of a matrix inverse. 2012. NUMERICAL LINEAR ALGEBRA WITH APPLICATIONS. 19 (3): 485.

4. Mentink, J. H., M. V. Tretyakov, Fasolino, M. I. Katsnelson, and T. h. Rasing. Stable and fast semi-implicit integration of the stochastic Landau-Lifshitz equation. 2010. JOURNAL OF PHYSICS-CONDENSED MATTER. 22 (17).

Publications

Barros, , Sinkovits, and Luijten. Efficient and accurate simulation of dynamic dielectric objects. 2014. JOURNAL OF CHEMICAL PHYSICS. 140 (6).

Barros, K., F. Venderbos, G. Chern, and C. D. Batista. Novel magnetic orderings in the kagome Kondo-lattice model. 2014. Physical Review B. 90: 245199.

Barros, K., and E. Luijten. Dielectric Effects in the Self-Assembly of Binary Colloidal Aggregates. 2014. Physical Review Letters. 113: 017801.

Gan, , Wu, Barros, Xu, and Luijten. Comparison of efficient techniques for the simulation of dielectric objects in electrolytes. 2015. JOURNAL OF COMPUTATIONAL PHYSICS. 291: 317.

Lin, , C. D. Batista, Reichhardt, and Saxena. ac Current Generation in Chiral Magnetic Insulators and Skyrmion Motion induced by the Spin Seebeck Effect. 2014. PHYSICAL REVIEW LETTERS. 112 (18).

Lin, , C. D. Batista, and Saxena. Internal modes of a skyrmion in the ferromagnetic state of chiral magnets. 2014. PHYSICAL REVIEW B. 89 (2).

Lin, S., C. Reichhardt, C. D. Batista, and A. Saxena. Dynamics of skyrmions in chiral magnets: dynamic phase transitions and equation of motion. 2014. Journal of Applied Physics. 115: 17D109.

Lin, S., X. Wang, Y. Kamiya, G. Chern, F. Fan, D. Fan, B. Casas, Y. Liu, V. Kiryukhin , W. Zurek, C. D. Batista, and S. Cheong. Topological defects as relics of emergent continuous symmetry and Higgs condensation of disorder in ferroelectrics. 2014. Nature Physics. 10: 970–977.

Ozawa, R., S. Hayami, K. Barros, G. W. Chern, Y. Motome, and C. D. Batista. Vortex Crystals with Chiral Stripes in Itinerant Magnets. 2016. Journal of the Physical Society of Japan. 85: 103703.

Ozawa, R., S. Hayami, K. Barros, and Y. Motome. Shape of magnetic domain walls formed by coupling to mobile charges. Physical Review B.

Wang, Z., K. Barros, G. W. Chern, D. Maslov, and C. D. Batista. Resistivity Minimum in Highly Frustrated Itinerant Magnets. To appear in Physical Review Letters.

Multi-Scale Model for Supercomputer Reliability Based on Field Data

Nathan A. Debardeleben
20160649ER

Abstract

As we move toward larger and more complex supercomputing facilities, the importance of modeling these machines in order to predict and understand behavior becomes crucial. We aim to develop a multiscale model of machine behavior, from low-level hardware to emergent behaviors, and we start by developing a model specifically for solid state drives (SSD) of Trinity used in the burst buffer / Data Warp component. We collect raw data using a tool provided by Intel, which measures a wide variety of important features, and conduct a preliminary analysis of this raw data. Our preliminary analyses find that the SSD drives were not significantly stressed during open science and early classified lifetime of Trinity, meaning that any model learned from this data will likely not apply to future SSD behavior. However, regardless of the quality of the data, we learn a model of statistical dependencies between the measured features, confirming some expectations and serving as a proof-of-concept that machine learning techniques can extract useful structural models from supercomputing data. We advocate for further data collection on Trinity when SSD drives are more heavily stressed to obtain better representative data and for further study to develop the later data into accurate predictive and explanatory models.

Background and Research Objectives

Research Goals

The objective of this work is to develop a multi-scale model for supercomputing systems, starting with the new SSD technology installed in the Trinity supercomputer. "Multi-scale" refers to the ability of a model to accurately describe a system on multiple levels, ranging from individual drives up through the overall emergent behavior of the machine. Such a model would be able to predict important features such as hardware lifetimes, and locations and causes of failures, as well as predicting changes in configuration that might improve performance. This model would be crucially useful for managing and monitoring current facilities as well as determining requirements for future machines.

Related Work

Our group has significant prior experience developing models of systems, particularly with developing models of DRAM faults. Previous work has involved investigating large-scale field studies of supercomputing data at LANL, and our most recent publications show that machine learning approaches can characterize DRAM faults faster and more accurately than the current state-of-the-art expert-designed algorithms. In addition, our group has been using machine learning to improve high performance computing in various other ways, including developing anomaly detection algorithms for the full data center.

Recent improvements in machine learning algorithms and theory have led to the discovery of methods for learning dependency structures from observational data. In this context, "observational data" refers to data collected passively from a system not under traditional controlled experimental designs. In particular, the data we investigate in this study is observational data collected during Trinity open science and early classified lifetime; we did not conduct (nor were we allowed to conduct) controlled experiments on the Trinity SSDs, simply collecting the data generated naturally by the codes run during the early lifetime of Trinity. Advances in the casual discovery sub-field of machine learning allow us to investigate the dependency relationships hidden with the available observational data, eventually leading to better models of supercomputing facilities.

Scientific Approach and Accomplishments

Available Data

Using a tool provided by Intel, we obtained snapshot datasets regarding SSD performance and projected lifetime. These datasets contain measurements of 44 features, including projected lifetime in years, wear lev-

eling count, erase fail count, write amplification, power on hours, and high and low temperatures.

Figure 1a contains blocks of text showing some of the output from this tool for just one of the SSDs in Trinity's burst buffer.

Figure 1. A: SSD Drive Info output; B: SSD SMART fields output

Telemetry data from Trinity's SSDs in the burst buffer were captured 5 times. This data had to be reviewed by a Derivative Classifier as it was moved from LANL's classified network to the open for evaluation and sharing with Intel. Over that time period, we saw the SSD Endurance field highlighted above as "EnduranceAnalyzer" reduce from roughly 1,300 years to 600 years. Certainly this trend is in the correct direction and indicates a beginning of usage of these devices, but nonethelessvit is an unreasonably high number and indicates extreme under-utilization of these devices.

One finding from the above snapshot was that many of the SSDs in Trinity were using an incorrect firmware version. While a simple finding, and perhaps pedestrian, this resulted in changes to the production techniques for monitoring for outdated firmware. So while not scientifically interesting, it had important mission impacts.

Another snapshot of data captured across every device is shown in Figure 1b. This includes all the SMART (Self-Monitoring, Analysis and Reporting Technology) data. As can be seen, there are counts in this SMART data related to thermal statistics, error correction, data read/written, and probably most importantly, wear leveling statistics. As can also be seen under the "Raw" fields for most of these elements, the devices have not been used much. This greatly impacts our conclusions but does not invalidate the process, workflow, nor modeling and will, in time, provide useful when the SSDs begin being used in production as expected.

According to these few snapshots, it appears that the workload was non-homogeneous across the SSD drives during open science, and almost all power cycles were due to unsafe shutdowns. We also find that the drives have outdated firmware. Unfortunately, the most significant finding from the raw data was that the SSD drives were not stressed during open science, meaning that any model built from this data will likely not apply in later phases when SSD usage changes drastically.

The main result of the SSD drives not being stressed during open science is unreasonably high predictions for drive lifetime, as shown in Figure 2. Across all SSD drives, the average expected lifetime was around 1,000 years, with outliers stretching up to above 4,000 years. This might be an encouraging observation if drive usage was expected to remain at the levels of open science; however, we expect SSD usage to increase dramatically as Trinity progresses to the closed phase. Figure 3 extends this analysis, showing expected drive lifetime as a function of write amplification. While a simple linear regression achieves an R2 value of 0.78 (where a value of 1.0 would be a perfect fit), the slope of the regression line is actually the opposite of that expected. That is, SSD lifetime should be negatively correlated with write amplification. This is further evidence that the available datasets will not be representative of future SSD behaviors. While a good predictive and descriptive model requires a representative dataset, we can still use the open science datasets as a starting point for building a multi-scale model. The extent to which the currently available data can be used to build a model is described in the following section.

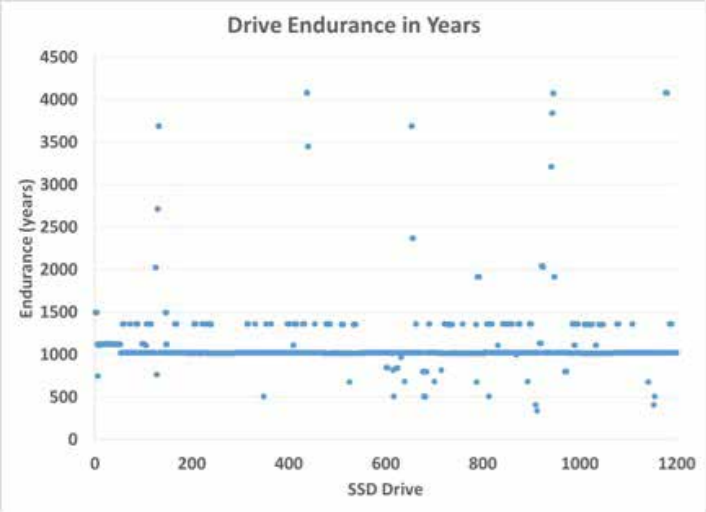

Figure 2. Expected SSD drive endurance. Note that the average value is around 1,000 years, with many outliers at up to around 4,000 years.

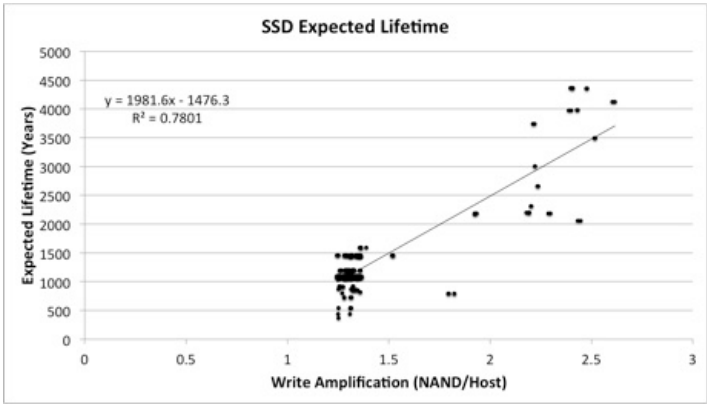

Figure 3. SSD expected lifetime as a function of write amplification, with a linear fit. Note that while the R value is fairly high, the slope is the opposite of expected.

Figure 4 shows the results of a temperature evaluation of the SSDs. The plot shows an interesting trend that, in discussion with Cray, revealed itself to be related to end of racks. As such, we suggest monitoring temperature to make certain the temperature maintains within acceptable tolerances.

Current Models

The Fast Causal Inference (FCI) algorithm from Spirtes et al. (2000) [1] discovers statistical dependencies between features in observational datasets, which ultimately gives a result that can guide the development of a structure for modeling systems. This algorithm works by testing conditional independence relationships between each pair of features, and orienting dependency edges logically based on statistically significant relationships in the data. Figure 5 shows the dependency structure discovered by FCI on the SSD data, at a statistical confidence level of 0.01.

The resulting graph is a directed acyclic graph, which can be used as the structure for a Bayesian network model, which would give predictions for each feature included in the model. As the available data is not representative of expected SSD usage, we do not yet have a reliable Bayesian model for SSD performance. However, these results regarding structure are an important starting point.

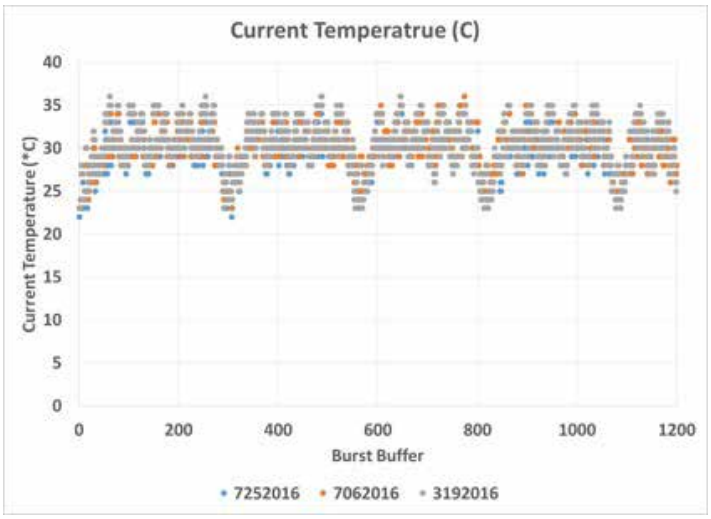

Figure 4. SSD temperature reveals trends related to physical placement within the data center and suggests a need to monitor closely.

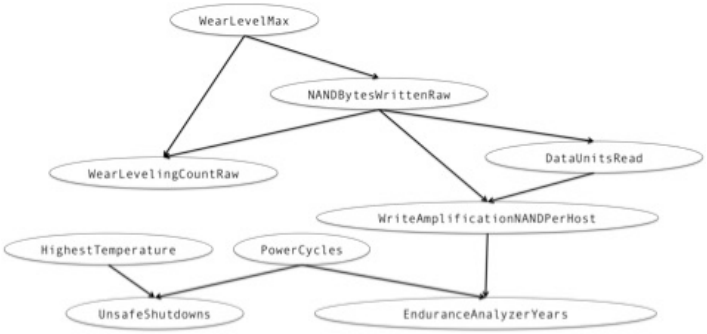

Figure 5. Results of the FCI causal discovery algorithm on the available SSD data. Nodes are individual measurable features, and edges indicate statistical dependencies.

As expected, we see a direct relationship between write amplification and expected drive lifetime, and between power cycles and expected lifetime (bottom right of Figure 5). We also see a relationship between the bytes written to the NAND device and the write amplification. This also makes sense. However, there exists a strange relationship discovered between the DataUnitsRead field and the write amplification. In consultation with Intel, we believe this to be anomalous. This is an example of a portion of the model that will settle down and be corrected when we have more accurate data. It is presented here to demonstrate the development of the tooling infrastructure rather than to show any conclusive results. We also see some

other relationships that do not necessarily make sense, such as wear level max affecting wear leveling count – this relationship probably would not be significant if the data-set was more representative of drive usage.

Conclusions and Future Work

Given the usage of SSDs during Trinity open science, our analyses predict that the lifetime of the drives will be, on average, 1,000+ years. This may be reasonable given that the SSD drives were not stressed during open science, however we do not expect the SSD usage to remain constant as Trinity moves into later phases. We have shown that the features measured by the Intel tool appear to be statistically significant for the metrics we would like to predict, but we strongly recommend collecting more datasets and further study in order to develop models and techniques that will be applicable to SSD drives under normal and high usage conditions.

While this report makes it appear as though these devices are capable of lasting for over 1,000 years, that is unrealistic. This is an artifact of the way the endurance analyzer calculates lifetime and is merely a metric used to predict aging and usage characteristics of the device. With better data and better usage in production, this number will become a useful metric.

In the event that quality data becomes available for Trinity, which we fully anticipate, the models developed in this effort are ready to be evaluated and used to impact the national missions discussed previously.

Impact on National Missions

Trinity was not fully operational during this project as expected when proposed. The work here provides a seed effort in modeling the burst buffer reliability and performance. A model of this portion of a supercomputer system will become part of a larger effort to study the entire system reliability. This larger model, a much larger effort, will have impact on LANL and DOE missions. It will allow system designers to evaluate prospective supercomputer designs and perform “what if” comparisons of different components. This will have an impact on procurement of these capital investments that will in turn impact the usage and usefulness of the HPC systems in production. Similarly, when in production, this model will inform application scientists and system operators so that they can plan accordingly. For instance, understanding expected failure intervals will influence the checkpoint intervals of application codes. From a production perspective, understanding the lifetime of the SSDs under evaluation can impact expected replacement rates and can be used to stage replacements to not impact users.

References

1. Spirtes, P., C. N. Glymour, and R. Scheines. Causation, prediction, and search.. 2000.

Reduced Data Corruption Through Erasure Codes

Laura M. Monroe
20160669ER

Abstract

Among system components, hard disks contribute significantly to storage failures. Field studies show that the annual disk failure rate typically exceeds 1%, with 2-4% common and up to 13% observed on some systems. When this occurs, the data on the disk is inaccessible, and is lost if it has not been saved or protected.

Erasure codes are a cutting-edge technology used to reconstitute the data from a crashed disk. In theory, these codes may also be used to correct corrupted data. Unfortunately, use in this manner decreases the number of disk failures that can be corrected at the same time, thereby reducing the usefulness of the erasure code.

In practice today, only disk failures are corrected, because the threat of data corruption is seen as negligible, in comparison to the risk of a disk failing. However, unprotected or error-ridden implementations of encoding and decoding may increase the risk of data corruption. For this reason, we are interested in investigating this problem.

Background and Research Objectives

We would like to protect against data corruption, while still retaining protection against disk failure. We proposed to do this by enhancing the erasure code with an arithmetic coding procedure independent of the erasure code.

We used ARM processors close to memory to perform the calculations for error detection. These processors are not extremely powerful, but they are good enough to carry out the calculations needed, and have the great advantage of being close to memory, thus minimizing data movement. This is a newer architecture and is very well suited to this use case.

This research made innovative use of underlying computational mathematics to demonstrate the use of experimental hardware to improve a cutting-edge error-correction technology.

Our approach is discussed in the next section. Using the funding allocated and available time, we were able to complete Steps 1 and 2, and addressed Step 3 but did not complete it. We also further developed the experimental hardware system identified in Step 5 for future use.

Current data fault handling by erasure codes

Erasure codes may correct both disk failures and bitflips, but correcting bitflips decreases the number of disks that may be corrected. It is thus advantageous to reduce the expected number of bitflip faults, so that the erasure codes may be used to full advantage for disk failures. We ask if it is possible to enhance these erasure codes to protect against the anticipated increase in data corruption, while at the same time leaving the disk failure protection untouched. Erasure codes alone cannot do this; asking for data protection decreases the amount of disk protection, However, by adding an independent error-detection/correction protocol for data faults, we believe we may protect data without interfering with disk protection.

Arithmetic codes and their application

Arithmetic coding is a technique to detect faults in data or sometimes in logic by purely arithmetic means [1,2]. We propose to use a form of arithmetic coding to detect data faults without interfering with disk failure protection. In the past year, the PI has developed an arithmetic method to correct Greatest Common Divisor (GCD) calculations, using methods related to classic arithmetic AN-codes [3]. The PI and her colleagues extended these classic techniques to include probabilism. These computational arithmetic methods extend to data protection and so seem suitable for implementation on a file system.

F-SEFI Fault Injector
To study this problem in simulation mode, we used the Fine-grained Soft Error Fault Injector (F-SEFI), a software fault injection tool developed by LANL [4].

F-SEFI capitalizes on the open source QEMU virtual machine hypervisor and works as a pluggable module. F-SEFI utilizes the QEMU virtual machine hypercalls to inter-communicate with the guest virtual machines (VMs). QEMU is widely used on emulating guest architectures which are different from the host physical architecture. F-SEFI inherits this feature and allows fault injections into architectures that are prototypes or are physically unavailable.

Fault injection with F-SEFI can be either coarse-grained or fine-grained. Coarse-grained fault injection is used when source code information is not available. This allows faults to be injected into portions of the application with little to no knowledge about the structure of the code. This approach allows for the inclusion of some information, such as the program counter and application state, allowing us to make inferences.

If source code is available and the application is compiled with debugging information, fine-grained fault injection is possible. With this approach, F-SEFI can place faults at any line number. In either case, faults are created based on a fault model that can be single or multi-bit, and can show any bit pattern desired in the faults simulated. For instance, faults can target only the mantissa of a floating-point operation

Scientific Approach and Accomplishments

Approach
We proposed to evaluate classical arithmetic codes for extension to erasure code calculations. One of the decoding methods for Reed-Solomon codes used in erasure coding is a form of Greatest Common Divisor. Based on our previous success with this method, we selected it as an appropriate method of coding.

The following was our intended technical approach:

Step 1: Study the vulnerability of common erasure code algorithms using the F-SEFI fault injector.

Step 2: Develop a model for faults occurring throughout the encoding and decoding process. We will quantify them in terms of the expected environment in the near-term.

Step 3: Work toward methods of addressing these faults. A first approach will be an investigation of the use of arithmetic codes to minimize data corruption.

Step 4: Validate using F-SEFI simulations. We will use F-SEFI to investigate the merits of this approach. F-SEFI has been widely used in the past to understand behavior in the presence of faults.

Step 5: Implementation, if possible, on the experimental storage system. This step will depend on the feasibility of actual implementation on the drives themselves. We will apply techniques developed to an experimental storage system owned by HPC-DES.

Step 1. Common Erasure Code Algorithms: Open-Source Jerasure Code Software
We used the Jerasure Erasure code library, an open-source software from the University of Tennessee [5]. Jerasure has implemented several coding methods in erasure coding library. The Reed-Solomon encoding method and the Cauchy-Reed-Solomon method are commonly used in cloud storage systems.

The Reed-Solomon encoding calculation and processing sequence is illustrated in Figure 1 and Figure 2. Reed-Solomon codes are block-based error-correcting codes with numerous applications in digital communication and storage. In Reed and Solomon code we normally use a pair (K, M) to illustrate the coding scheme. It can take a message, break it into K pieces, add M "parity" pieces, and then reconstruct the original from K of the (K+M) pieces.

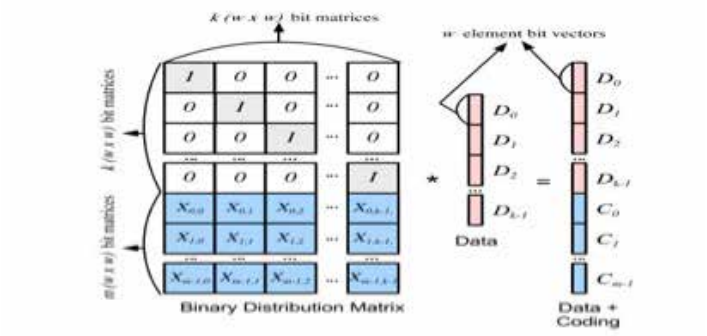

Figure 1. Matrix Calculation of Erasure encoding

Figure 2. Data coding processing sequence – encoding and decoding

Steps 1 and 2. F-SEFI pre-testing
Our preliminary experiments used LANL's Fine-grained Soft Error Fault Injector (F-SEFI) to study erasure codes intended for use on the hardware system described above. These experiments indicated that data corruption does cause error in the anticipated environment with its increased faults.

Our fault injection experiments were done using the Jerasure coding algorithm discussed above. For the original Jerasure coding algorithm, if two devices crash or data is erased/lost, the overall state of the stored information will be recoverable by decoding the coding blocks. In this example, the maximum of erasure is two - its tolerable number of lost storage devices.

However, if there are soft errors encountered during the encoding or decoding process, the erasure-coding algorithm is not able to detect the errors that affect the memory. The continuation of erasure coding encoding and decoding algorithms will corrupt the data and result in data loss. Our preliminary investigation using F-SEFI showed several examples addressing different behaviors that might occur in the wild, including the most severe: silent data corruption (SDC), in which the researcher never knows that anything is wrong, but merely continues.

Below we list several test cases and the resulting system state.

Case 1: Faults in decoding algorithm cause the corruption of recovered data. State of the system after decoding:

Data	Coding
D0 : 82 01 ea 48 ca 69 41 f4	C0 : c7 9c db 4b 88 53 f3 32
D1 : 06 d3 2d ec c9 f6 15 00	C1 : d7 81 ac dc 08 b6 af 5d
D2 : 7a cb 0c 45 e4 db 71 ec	
D3 : 9a c2 e7 b1 b5 7c 8f 9d	
D4 : bc 4c 40 ec 42 ce 30 73	
D5 : b8 f5 54 1d 8e 8b 4e 5d	
D6 : 3b 00 09 36 51 ea ff 91	
D7 : 9c fe ea dc 47 c4 d8 c9	

Case 2: Faults in decoding algorithm cause the loss of data during recovery. State of the system after decoding:

Data	Coding
D0 : 82 01 ea 48 ca 69 41 f4	C0 : c7 9c db 4b 88 53 f3 32
D1 : 06 d3 2d ec c9 f6 15 c1	C1 : d7 81 ac dc 08 b6 af 5d
D2 : 7a Na Na Na Na Na Na	
D3 : 9a c2 e7 b1 b5 7c 8f 9d	
D4 : bc 4c 40 ec 42 ce 30 73	
D5 : b8 f5 54 1d 8e 8b 4e 5d	
D6 : 3b 00 09 36 51 ea ff 91	
D7 : 9c fe ea dc 47 c4 d8 c9	

Case 3: Faults in encoding algorithm cause the corruption of data on a healthy storage device. Erased 2 random devices:

Data	Coding
D0 : 82 01 ea 48 01 69 41 f4	C0 : c7 9c db 4b 88 53 f3 32
D1 : 00 00 00 00 00 00 00 00	C1 : 00 00 00 00 00 00 00 00
D2 : 7a cb 0c 45 e4 db 71 ec	
D3 : 9a c2 e7 b1 b5 7c 8f 9d	
D4 : bc 4c 40 ec 42 ce 30 73	
D5 : b8 f5 54 1d 8e 8b 4e 5d	
D6 : 3b 00 09 36 51 ea ff 91	

Overall, we performed 3000 faults injection tests on the encoding and decoding algorithms randomly. The faults were injected randomly into an instruction of the algorithm. We observed the benign, crash, and SDC outputs. The results are shown in the following table.

Type	Crash	SDC	Benign
Percentage	46.2%	15.3%	38.5%

Benign faults have no effect on the calculation, and so are not considered a problem that must be addressed. Although crashes are a problem, they are obvious and detectable, and therefore not the most severe form of fault. The silent data corruption (SDC) rate of 15.3% is alarmingly high, especially considering their silent and non-obvious nature. Considering the high SDC rate, the importance of protection of encoding and decoding is clearly seen.

Step 3. Mathematical Development

We worked at first with a classical AN-coding approach, which is designed for standard arithmetic operations such as addition. This has worked well for such operations as GCD, on a previous project of the PI. Because decoding for Reed-Solomon codes is based on GCD, it was hoped that this method might easily apply to this problem.

We found that in this case, we needed distributivity over XOR, and the multiplication methods used in AN-coding do not provide this. We are now examining other methods of enhancing erasure codes arithmetically or otherwise.

Step 4. Software Enhancement

We developed a code suite testing the Jerasure codes for use in F-SEFI, and included methods of incorporating different error-correction schemes. We first tried running this system using the AN-coding method discussed above. As we develop further methods, we will use this code suite to test them as well.

Step 5. Hardware Testbed
Our small experimental test system has two EMC 1U servers, used for code development and testing. Each server had

- 32 Core CPU
- 256 GB DDR memory
- One Infiniband QDR interface to access Flash Array data
- Centos 7.1 OS is installed
- Jerasure 1.2 is installed

One EMC XtremIO All Flash Array is used as the destination storage system for ANCoding process.

Impact on National Missions

Exascale implications
As we move toward exascale, the incidence of faults is expected to increase. Future implementations of distributed storage systems may encode the disks using hardware without error-correction protection for cost and cooling reasons. Such a system will be more vulnerable to data corruption, and faults may propagate through the correction process.

ASC interest
As a follow-on to this preliminary study, the ASC program has indicated interest in continuing this research.

Future work
We intend to continue our mathematical investigations into alternative methods of coding, and as promising techniques are identified, implement them into the test suite and on the test hardware in the manner discussed above.

References

1. Brown, D. T.. Error detecting and correcting binary codes for arithmetic operations. 1960. IRE Transactions on Electronic Computers. EC-9: 333.
2. Chiang, A. C. L., and I. S. Reed. Arithmetic norms and bounds of the arithmetic AN codes . 1970. IEEE Transactions on Information Theory. 16 (4): 470.
3. Monroe, L., N. DeBardeleben, Q. Guan, D. Fu, and J. Daly. A resilient GCD algorithm. 2014. Technical Report.
4. Guan, Q., S. Fu, N. DeBardeleben, and S. Blanchard. F-SEFI: A Fine-Grained Soft Error Fault Injection Tool for Profiling Application Vulnerability. 2014. 28th IEEE International Parallel & Distributed Processing Symposium. : 1245.
5. Plank, J. S.. Jerasure: A library in C/C++ facilitating erasure coding for storage applications. 2007. Technical Report CS-07-603, University of Tennesee.

Trace Elements in Martian Rocks and Soils as Observed by ChemCam in Gale Crater, Mars, and Preparation for LANL's Next Mars Mission

Roger C. Wiens
20160650PRD2

Introduction

The Curiosity Mars rover brought unprecedented analytical capability to the surface of Mars when it landed three years ago. One of the instruments is the ChemCam remote-sensing composition instrument. It is the first use of laser-induced breakdown spectroscopy (LIBS) on another planet. A very substantial effort was devoted to accurate calibration for the major elements (silicon, titanium, aluminum, iron, magnesium, calcium, sodium, potassium). The ChemCam is also observing a number of minor and trace elements, many of which provide unique clues to Mars' geological and climate history. For example, nickel may help track the weathering of meteorites as their remains become mixed into the soil and sediments; copper may be concentrated by hot springs or hydrothermal activity, which is important for investigating Mars' habitability potential. The Curiosity rover is just about to arrive at several regions that defined the main goals of the mission, particularly a clay-rich region identified from orbit. Having better trace-element capabilities for this part of the mission will be very helpful in the overall goals of the rover mission.

Benefit to National Security Missions

The proposed work is aimed at improving the accuracy and detection limits for trace elements analyzed by laser-induced breakdown spectroscopy (LIBS), specifically for the ChemCam instrument on Mars. LIBS finds application in a wide variety of rugged environments, so it is potentially practical for detecting explosive residues, detecting transuranic elements and uranium isotope ratios, detecting contamination (e.g., Be, Pb), and even for making some medical detections. Results from the proposed work may be broadly applicable to these areas.

Progress

Since arriving at the Laboratory one month ago, Dr. Ollila has been working on Tasks 1 and 4. Task 1 (review of recent calibration data) takes some time, as there is a lot of data to ingest. This must be done before moving on to Tasks 2 & 3 (developing new calibration models and implementing them). For Task #4 (feed-forward to future missions; observation of Archean samples with reduction spots enriched in trace elements), she and I have had discussions with the provider of the samples and we are now making plans for laboratory analyses.

Future Work

Dr. Ollila's first task is to analyze the new calibration data that is now available from the LANL LIBS lab. A second task is to refine existing calibration models using the multivariate techniques of partial least squares (PLS) and independent component analysis (ICA), as well as using individual emission peaks for peak-area calibration. A third task is to apply these calibrations to targets observed recently along the Curiosity rover traverse, for example, looking for meteoritic input, hydrothermal alteration, and habitability potential. A fourth task is to investigate and look for feed-forward applications to SuperCam's laser-induced breakdown and Raman spectroscopies, as well as to other areas at LANL. In particular, we have just received some Archean biogenic targets from the PIXL team (another instrument on the Mars 2020 rover) that are enriched in relevant trace elements. These are perfect to understand the cross-instrument capabilities, including trace elements.

Conclusion

The rover will go to several regions that define the main goals of the mission, particularly a clay-rich region identified from orbit. Having better trace-element capabilities will be very helpful in the overall goals of the rover mission. LIBS can be applied in a wide variety of rugged environments, so it is potentially practical for detecting explosive residues, detecting transuranic elements and uranium isotope ratios, detecting contamination (e.g., Be, Pb), and even for making some medical detections.

Publications

Payre, V., C. Fabre, A. Cousin, V. Sautter, R. C. Wiens, O. Forni, O. Gasnault, J. Lasue, A. Ollila, W. Rapin, P. -Y. Meslin, S. Maurice, M. Nachon, L. Le Deit, N. Lanza, and S. M. Clegg. Alkali trace elements with ChemCam: Calibration update and geological implications of the occurrence of alkaline rocks in Gale crater, Mars. J. Geophys. Res..

Wiens, R. C., M. Bodine, S. M. Clegg, R. Newell, R. Newell, R. Newell, A. Ollila, R. McInroy, S. K. Sharma, F. Rull, and S. Maurice. Cross sections of common minerals using pulsed remote Raman spectroscopy. Spectrochim. Acta A.

Mixing and Diffusion in Granular Flows

Ivan Christov
20130792PRD2

Abstract

The theory of granular materials remains elusive. Under simple flow and forcing conditions, granular materials can exhibit a wealth of complex collective behaviors. Yet the relevance of granular materials cannot be understated as they are processed in almost all industries from pharmaceuticals to explosives. Even when static, granular materials are the building blocks of most subsurface porous formations from which we extract the majority of our energy resources. This project's aim was to analyze fundamental problems related to granular flow and flow through granular media. Theoretical models were constructed, then advanced mathematical and computational techniques were used to make key predictions, relevant for practical problems, from the models. For example, optimal methods for mixing granular materials in rotating containers were designed, quantitative predictions of the spreading of fluids through heterogeneous media were derived and experimentally verified, and novel types of nonlinear waves in continua with microstructure were found. While these problems are of clear fundamental scientific significance, their detailed analysis also has impacts on national missions in that the scientific results from this project can be used to address questions regarding waste storage and management, handling and transportation of high explosives or other powder materials, and the utilization of unconventional subsurface energy resources.

Background and Research Objectives

The project aimed to understand the complexity of force-carrying contacts in a granular medium, which can often lead to its destabilization (due to external forcing) along unexpected fault lines, as commonly observed in geophysical situations including earthquakes, mudslides, and avalanches. The goal was to interface advanced mathematical continuum models of granular materials with model experiments being conducted at Los Alamos of a granular medium between sheared. In addressing this complex problem, for which little prior work existed in the literature, the project had to solve several subproblems, all anchored on the common theme of continuum modeling of granular or otherwise microstructured media. In doing so, further connections were made to Los Alamos and DOE wide research efforts in the direction of subsurface flow and transport, hydraulic fracturing and unconventional energy resource utilization.

Specifically, a goal of this project was to understand universal emergent behaviors (clustering, ordering, topology) arising from the interplay between discontinuous granular mixing dynamics and microscopic physics. Few general unifying principles exist in this realm. As such, the goal was a high-risk undertaking, specifically as it relates to connecting the dynamics of granular materials in geophysical situations to laboratory scale experiments. Yet, the successful completion of this goal would imply the ability to extend the continuum concepts that have been so successful in fluid and solid mechanics to a new area.

A twofold approach was undertaken by first modelling how granular materials flow under the types of conditions encountered in geophysical processes, and then advanced mathematical techniques were used to extract key implications and obtain precise answers to practical questions. As the project's foundational problems were addressed, the topic of flow through static granular materials, such as porous media, had to be addressed. This led to the development of further mathematical models, which were then analyzed mathematically and computationally. As outlined in the Accomplishments section, through specific examples, the project accomplished the ultimate goal of using modeling and advanced mathematical techniques to obtain precise quantitative that inform our understanding of flow processes involving heterogeneous media and microstructured continua.

Scientific Approach and Accomplishments

The first major scientific accomplishments of the project

over its first twelve months included the first formulation and prediction of shear dispersion in dense granular flows. The dispersal of a passive solute in a pressure-driven laminar flow, a classical fluid phenomenon, can be described, at long times and far downstream from its injection point, by a cross-sectionally averaged advection-diffusion process in which the mean solute concentration is advected by the mean flow but diffuses with an effective dispersion inversely proportional to the solute's molecular diffusivity. We calculated the effective dispersivity for the rapid flow of a dry, cohesionless monodisperse granular material down an incline, assuming that volume fraction variations are negligible in the fully-developed Bagnold profile and that the diffusivity is proportional to the shear rate. This calculation has implications on fields ranging from pharmaceutical powder technology to ecology of geophysical events. For example, understanding granular dispersion is relevant for industrial separation processes such as the drying of powders for the purposes of dehydrating food. On the other hand, the distribution of debris upon the cessation of an avalanche or landslide can dictate the ecological impact of the geological event. By providing specific analytical results and scaling laws, this project advanced the knowledge base in these areas. This work was published in Granular Matter in 2014.

The second major accomplishment of the project over its first twelve months was the formulation and mathematical analysis of granular flow in a bi-axial tumbler (rotating container). The three-dimensional (3D) flow was expressed in terms of a mathematical object called a linked twist map, from which novel types of 3D chaotic dynamics were shown to be exhibited by the granular system. Through a mathematical analysis of the properties of the derived linked twist map, it was possible to make rigorous predictions regarding mixing quality and optimal operating conditions. For example, optimal rotation angles about each of the two axes were derived, such that unmixed regions in the container were minimized. These results have significant implications on the design of devices and processes for mixing of granular materials and pill preparation in the pharmaceutical industry. This work was published in the SIAM Journal on Applied Dynamical Systems in 2014.

An additional key accomplishment during the same time period, was the analysis of several problems of fluid flow through granular and heterogeneous porous media through the so-called Hele-Shaw analogy. Self-similar solutions were constructed that describe the spreading of very viscous fluids through granular and porous media. These solutions provide asymptotic scaling laws that can be used to determine the extent of spreading of a contaminant in the subsurface or for evaluating geological carbon capture and storage strategies. In the latter case, it is important to know the scaling relationship between the injection rate of supercritical carbon dioxide and its spatial spread in a heterogeneous reservoir or other subsurface structure. The results from this line of research provide such scaling laws, whereas most of the current theoretical literature has focused on the homogeneous case. This work was published in the Journal of Fluid Mechanics in 2014.

Over its initial twelve months, the project also yielded six invited presentations (at international conferences, departmental seminars and colloquia such as the Courant Institute at New York University) and three contributed presentations (international and regional conferences such as the American Physical Society's March Meeting and its Division of Fluid Mechanics Annual Meeting). A total of four journal publications appeared in top disciplinary and multidisciplinary journals (in the Proceedings of the Royal Society A, Journal of Fluid Mechanics, SIAM Journal on Applied Dynamical Systems, Granular Matter).

During the project's second twelve months, several of the successful research directions of the first twelve months were further pursued. Specifically, a novel flow regimes diagram for injection of a buoyant liquid into a confined porous medium was constructed based on computational and theoretical analysis. Although the dynamics of granular media under various forcing and excitations are of interest on their own, a common geophysical problem involves the penetration of a liquid into the pore space between static grains. Specifically, such fluid injection into a porous medium occurs in a large variety of geophysical and industrial processes such as seawater intrusion into coastal aquifers, geological sequestration of carbon dioxide, waste fluid disposal, and oil and gas recovery. When the injected and displaced fluids are immiscible, a free boundary problem can be formulated to describe the time evolution of the fluid-fluid interface. It is of interest to know how this interface evolves over time in order to understand the sweep efficiency of the injection process. This project focused on the case of two-dimensional vertically confined porous media. Assuming the injected fluid is denser than the displaced fluid, then the injected fluid only attaches to the bottom boundary at early times for point source injection. As time progresses, the injected fluid contacts the top boundary, and the fluid flow becomes confined. Results obtained in this project establish that during the propagation process, because of the change of the horizontal and vertical length scales, the interface exhibits a transition from an early time unconfined behavior to a late time confined behavior, and we derived a nonlinear advection-diffusion equation to describe the time evolution of the fluid- fluid interface. We analyzed this partial differential

equation in two distinguished asymptotic limits (early and late time) and found exact solutions in each case, resolving the structure of the moving front. Through detailed numerical simulations, we were then able to construct a phase diagram depending on two dimensionless quantities: the viscosity ratio of the displaced fluid to the injected fluid, and a dimensionless time. In doing so, the transition processes between the early and late time asymptotic limits were elucidated and the relevance of the early time and late time exact solutions were demonstrated for the first time in the literature. This work was published in the Journal of Fluid Mechanics in 2015.

Another scientific accomplishment of this project during its second twelve months was the Hamiltonian formulation of the equations for wave propagation in continua with microstructure, of which granular materials are a key example. Although a granular materials' microstructure is quite complex in practice, the collective (continuum) behavior has been observed and well documented. The simplest way to study wave propagation in such a context is to derive a generic (universal) model, based on extended thermodynamics, for a continuum with one inherent length scale (e.g., the grain size). Then, by standard techniques, one can obtain weakly nonlinear dispersive evolution equations for wave propagation through this continuum. What had not been appreciated in previous discussion of such equations in the literature is that they possess Hamiltonian structure, endowing them with a number of desirable physical properties. We constructed the Hamiltonian formulation of such nonlinearly dispersive wave equations for the first time, showing there is in fact a hierarchy of such nonlinearly dispersive evolution equations. Additionally, as another novel feature of our work, we derived exact solitary wave solutions of these equations with curious properties: namely, waves that are compact and peaked. This work was published as an invited contribution in the Proceedings of the Estonian Academy of Sciences in 2015. Additionally, a part of the objectives of this research direction of the project, the PI co-mentored a summer graduate intern at the Center for Nonlinear Students in 2014. The summer intern designed and implemented advanced numerical methods to simulate interaction of novel nonlinear waves just described. As of the time of writing of this final report, the numerical work is being prepared for submission as an invited contribution to the International Journal of Modern Physics B.

During its second twelve months, this project yielded over a dozen invited presentations and two contributed presentations (at international and regional conferences such as the American Physical Society's Division of Fluid Mechanics Annual Meeting). In addition, two journal publications appeared in top disciplinary and multidisciplinary journals (the Journal of Fluid Mechanics and Physical Review E).

Impact on National Missions

Granular materials are ubiquitous and are found in a host of applied programs. Hence, understanding mixing and flow of granular materials has impacts on the DOE and national missions. This project developed modeling and simulation capabilities for describing mixing and flow of granular materials from a continuum point of view. The ability to improve models of mixing of granular matter will impact energy applications including storage and transportation of energy-related materials (e.g., coal and biofuels). Granular materials tend to segregate according to size, a property that can be an obstacle in manufacturing and transportation processes. This project addressed precise mixing characteristics of granular materials and could lead to the design of optimized containers and protocols for improved mixing and more efficient transportation.

The accomplishments in the project's thrust on fluid flow through rigid granular (porous) media contributed to the DOE's SubTER initiative of "mastering the subsurface for energy production and storage." Specifically, the dynamical behavior of fluid interfaces in shaped cracks and heterogeneous porous media was analyzed mathematically for the first time. This analysis provides precise quantitative results on rates of spreading of various subsurface fluids in the presence of porosity and permeability gradients.

A further impact on programs at Los Alamos, the DOE and beyond was the ensuing 2015 workshop on Grand challenges in geological fluid mechanics sponsored by the Center for Nonlinear Studies and co-organized by the PI, Hari Viswanathan, Robert Ecke and Duan Zhang. The workshop surveyed the latest developments in the field and brought together theory and practice. In doing so, the workshop enabled cross-cutting collaborations and dissemination of research from academia, industry and the DOE complex at the interface of hydraulic fracturing, geothermal energy production, carbon capture and sequestration, nuclear waste disposal, and the environmental impact of these processes. A subset of the invited speakers at Grand challenges in geological fluid mechanics were subsequently asked to contribute manuscripts to a theme issue, co-guest edited by the PI and Hari Viswanathan, on "Energy and the subsurface" of the Philosophical Transactions of the Royal Society, in order to establish a self-contained volume detailing both the state-of-the-art and the research directions of this field. The Philosophical Transactions is the first modern peer-reviewed scientific journal, celebrating its 350th anniversary in 2015. The journal has high visibility and name recognition due to its storied history

and impact, which provides a key platform through which to disseminate research from the DOE enterprise to the broader scientific community.

In summary, the capabilities and knowledge developed as part of this project are also be relevant to other DOE programs and needs including, but not limited to, waste storage, waste handling and transportation, high explosives, and handling of materials produced in powder form.

Publications

Christov, I. C.. On a hierarchy of nonlinearly dispersive generalized KdV equations. 2015. PROCEEDINGS OF THE ESTONIAN ACADEMY OF SCIENCES. 64 (3): 2012.

Christov, I. C.. Comment on “The velocity field due to an oscillating plate in an Oldroyd-B fluid” by C.C. Hopkins and J.R. de Bruyn [Can. J. Phys. 92, 533 (2014)]. 2015. CANADIAN JOURNAL OF PHYSICS. 93 (12): 1651.

Christov, I. C., R. M. Lueptow, J. M. Ottino, and R. Sturman. A Study in Three-Dimensional Chaotic Dynamics: Granular Flow and Transport in a Bi-Axial Spherical Tumbler. 2014. SIAM JOURNAL ON APPLIED DYNAMICAL SYSTEMS. 13 (2): 901.

Christov, I. C., and H. A. Stone. Shear dispersion in dense granular flows. 2014. GRANULAR MATTER. 16 (4): 509.

Christov, I. C., and P. M. Jordan. On an instability exhibited by the ballistic-diffusive heat conduction model of Xu and Hu. 2014. ROCEEDINGS OF THE ROYAL SOCIETY A-MATHEMATICAL PHYSICAL AND ENGINEERING SCIENCES. 470 (2161): 20130557.

Christov, I. C., and P. M. Jordan. Corrections to Morse and Ingard’s variational-based treatment of weakly-nonlinear acoustics in lossless gases. 2015. JOURNAL OF THE ACOUSTICAL SOCIETY OF AMERICA. 138 (1): 361.

Christov, I. C., and P. M. Jordan. Maxwell’s “other” equations. 2015. The Royal Society Publishing Blog.

Khare, A., I. C. Christov, and A. Saxena. Successive phase transitions and kink solutions in phi(8), phi(10), and phi(12) field theories. 2014. PHYSICAL REVIEW E. 90 (2): 023208.

Zheng, Z., B. Guo, I. C. Christov, M. A. Celia, and H. A. Stone. Flow regimes for fluid injection into a confined porous medium. 2015. JOURNAL OF FLUID MECHANICS. 767: 881.

Zheng, Z., I. C. Christov, and H. A. Stone. Influence of heterogeneity on second-kind self-similar solutions for viscous gravity currents. 2014. JOURNAL OF FLUID MECHANICS. 747: 218.

Thermodynamics and Information Processing at the Nanoscale

Wojciech H. Zurek
20140667PRD2

Abstract

Quantum thermodynamics is a newly emerging field of modern research, which has recently attracted more and more activity. Although classical thermodynamics and quantum mechanics were developed side by side in the beginning of the twentieth century, the thermodynamic description of quantum systems has only recently become a major topic of modern research. This development has been spurred by the discovery of novel and fundamental generalizations of the second law of thermodynamics explicitly accounting for non-equilibrium fluctuations. These so-called fluctuation theorems changed the conventional focus of thermodynamics on work and heat to the study of entropy production -- a concept more accessible in quantum systems. To this end, three main avenues of research have been pursued: identifying fundamental notions of entropy and information production in quantum systems, studying the thermodynamics of information processing, and analyzing optimal quantum processes

Background and Research Objectives

Modern developments in nanotechnology lead to smaller and smaller devices, which are unavoidably subjected to the randomness of their thermal surroundings. It is a central goal of current research to synthesize molecular-scale motors that reliably perform specific tasks. To describe behavior that is more complex than one-dimensional directed motion, researchers developed the notion of stochastic networks, where one ignores microscopic details and restricts the model to a network of distinct states. In the description of quantum systems networks are not only a mathematical tool to describe a physical system with distinct configurations, but also constitute the underlying structure of prospective quantum computers. The hardware requirements for a quantum computer can be summarized as three main points: initially preparable in a well-defined state; controllable so that an arbitrary, entangled state can be launched; measurements performable with high quantum efficiency. Such a physical system can be realized with cold ions trapped in optical lattices (counter-propagating laser light), which is a network of distinct, controllable quantum states. The dynamics of optical lattices can, for instance, be described by methods developed in solid state physics. Thus quantum networks in optical lattices can also serve as a test bed for results from condensed matter theory. The theoretical description of optical lattices offers a rich potential for generalizations and applications to nanothermodynamics, and hence theoretical foundations of nanotechnology.

The main objective of this project has been the development of a coherent framework for the understanding, the design, and the theoretical foundations of nanothermodynamic devices, whose modes of operation allow to implement information processing, and which generically operate far from thermal equilibrium. In previous research, we also have been interested in the interplay of (quantum) information and thermodynamics. However, how to describe a quantum information reservoir, i.e. a fully quantum mechanical hard disk, and its thermodynamic properties has been an open question at the beginning of this project. Hence, we have been aiming at simple generalizations of the one-ion heat engines towards a minimal quantum Maxwell demon - a perfect device to study quantum thermo-dynamics and information theory. We also investigated fluctuation relations generalizing the statements of the second law of thermodynamics and their consequences on the dynamics of nanodevices.

Scientific Approach and Accomplishments

The methodology of the theoretical research and the scientific approach were based on the mathematical derivation and proof of rigorous statements, the analytical description of solvable systems, and numerical simulation of real experimental systems. This has led to a total of 11 publications in peer-reviewed, high ranking journals.

In a first sub-project, we studied the effect of interference of identical particles on the quantum work distribution. To this end, we evaluated the corresponding transition probabilities between many-particle eigenstates we obtained the quantum work distribution function for identical bosons and fermions, which we compared with the case of distinguishable particles. We found that the quantum work distributions for bosons and fermions significantly differ at low temperatures, while, as expected, at high temperatures the work distributions converge to the classical expression. These findings were illustrated with two analytically solvable examples, namely the time-dependent infinite square well and the parametric harmonic oscillator.

From there we moved on to diatomic molecules. In particular, we computed the quantum work distribution for a driven Morse oscillator. To this end, we solved the time-dependent dynamics for a scale-invariant process, from which the exact expressions for the transition probabilities were found. Special emphasis was put on the contributions to the work distribution from discrete (bound) and continuous (scattering) parts of the spectrum. The analysis was concluded by comparing the work distribution for the exact Morse potential and the one resulting from a harmonic approximation.

It quickly became clear that only focusing on Hermitian systems is too restrictive. Therefore, we turned to non-Hermitan systems, which are symmetric under parity (P) and time (T) reversal. In a first step, we showed that the quantum Jarzynski equality generalizes to PT-symmetric quantum mechanics with unbroken PT-symmetry. In the regime of broken PT-symmetry, the Jarzynski equality does not hold as also the CPT norm is not preserved during the dynamics. These findings were illustrated for an experimentally relevant system—two coupled optical waveguides. It turned out that for these systems the phase transition between the regimes of unbroken and broken PT-symmetry is thermodynamically inhibited as the irreversible work diverges at the critical point.

Non-Hermitian, but PT-symmetric systems can be understood as open system with balanced loss and gain. For any open system, however, optimal controlling and speeding up processes is an essential goal. To better understand this situation, we measured the quantum speed of the state evolution of the field in a weakly driven optical cavity QED system. To this end, the mode of the electromagnetic field was considered as a quantum system of interest with a preferential coupling to a tunable environment: the atoms. By controlling the environment, i.e., changing the number of atoms coupled to the optical cavity mode, an environment-assisted speed-up was realized: the quantum speed of the state repopulation in the optical cavity increases with the coupling strength between the optical cavity mode and this non-Markovian environment (the number of atoms).

In a similar system, in cavity QED it recently become possible to realize Dirac dynamics. Thus, we also showed that the Jarzynski equality readily generalizes to relativistic quantum mechanics described by the Dirac equation. After establishing the conceptual framework we solved a pedagogical, yet experimentally relevant, system analytically. As a main result we obtained the exact quantum work distributions for charged particles traveling through a time-dependent vector potential evolving under Schrödinger as well as under Dirac dynamics, and for which the Jarzynski equality was verified. Special emphasis was put on the conceptual and technical subtleties arising from relativistic quantum mechanics.

All these studies raised the question whether quantum devices could thermodynamically outperform classical engines. This is not the case! In particular, we showed that the definition of heat has to be modified to account for the thermodynamic cost of maintaining non-Gibbsian equilibrium states. Our theoretical findings were illustrated for two experimentally relevant examples.

Equipped with this insight, we returned to optimal quantum processes. In this context, a “shortcut to adiabaticity” is a finite-time process that produces the same final state as would result from infinitely slow driving. We showed that such shortcuts can be found for weak perturbations from linear response theory. With the help of phenomenological response functions, a simple expression for the excess work was found—quantifying the nonequilibrium excitations. For two specific examples, i.e., the quantum parametric oscillator and the spin 1/2 in a time-dependent magnetic field, we showed that finite-time zeros of the excess work indicate the existence of shortcuts. Finally, we proposed a degenerate family of protocols, which facilitates shortcuts to adiabaticity for specific and very short driving times.

This work was further extended to Dirac dynamics. As our main result we found that shortcuts to adiabaticity for the (1+1)-dimensional Dirac equation are facilitated by a combination of both scalar and pseudoscalar potentials. Our findings were illustrated for two analytically solvable examples, namely charged particles driven in spatially homogeneous and linear vector fields.

At the same time we also generalized our earlier work on PT-symmetric systems to more general non-Hermitian quantum mechanics, and we analyzed to what extent quantum thermodynamic relations are immune to the

underlying mathematical formulation of quantum mechanics. As a main result, we showed that the Jarzynski equality holds true for all non-hermitian quantum systems with real spectrum. This equality expresses the second law of thermodynamics for isothermal processes arbitrarily far from equilibrium. In the quasistatic limit however, the second law leads to the Carnot bound which is fulfilled even if some eigenenergies are complex provided they appear in conjugate pairs. Furthermore, we proposed two setups to test our predictions, namely with strongly interacting excitons and photons in a semiconductor microcavity and in the non-Hermitian tight-binding model.

These studies raised the question if it is legal to simply apply classical results, such as the Boltzmann-Gibbs distribution to quantum systems. In a much appreciated work we showed how to obtain statistical physics from symmetries of entanglement. Envariance—entanglement assisted invariance—is a recently discovered symmetry of composite quantum systems. We showed that thermodynamic equilibrium states are fully characterized by their envariance. In particular, the microcanonical equilibrium of a system S with Hamiltonian H_S is a fully energetically degenerate quantum state envariant under every unitary transformation. The representation of the canonical equilibrium then follows from simply counting degenerate energy states. Our conceptually novel approach is free of mathematically ambiguous notions such as ensemble, randomness, etc., and, while it does not even rely on probability, it helps to understand its role in the quantum world.

Finally, we turned to a study of how to measure work in quantum systems. Quantum work is usually determined from two projective measurements of the energy at the beginning and at the end of a thermodynamic process. However, this paradigm cannot be considered thermodynamically consistent as it does not account for the thermodynamic cost of these measurements. To remedy this conceptual inconsistency we introduced a paradigm that relies only on the expected change of the average energy given the initial energy eigenbasis. In particular, we completely omit quantum measurements in the definition of quantum work, and hence quantum work is identified as a thermodynamic quantity of only the system. As main results we derived a modified quantum Jarzynski equality and a sharpened maximum work theorem in terms of the information free energy. A comparison of our results with the standard approach allowed us to quantify the informational cost of projective measurements.

Impact on National Missions

This research has been directly relevant to advancing the frontiers of information science, which has value across our mission space. In particular, with the arrival of the DWave machine, which will take us beyond the limitations of silicon-based computers, underpinning the physical foundations of post-Moore's Law computing is becoming a main focus of researchers at LANL, and our work has been instrumental in doing the ground work.

References

1. Acconcia, T. V., M. V. S. Bonança, and S. Deffner. Shortcuts to adiabaticity from linear response theory. 2015. PHYSICAL REVIEW E. 92: 042148.

2. Gardas, B., and S. Deffner. Thermodynamic universality of quantum Carnot engines. 2015. PHYSICAL REVIEW E. 92: 042126.

3. Deffner, S., and A. Saxena. Quantum work statistics of charged Dirac particles in time-dependent fields. 2015. PHYSICAL REVIEW E. 92: 032137.

4. Cimmarusti, A. D., Z. Yan, B. D. Patterson, L. P. Corcos, L. A. Orozco, and S. Deffner. Environment assisted speed-up of the field evolution in cavity quantum electrodynamics. 2015. PHYSICAL REVIEW LETTERS. 114: 233602.

5. Gong, , Deffner, and H. T. Quan. Interference of identical particles and the quantum work distribution. 2014. PHYSICAL REVIEW E. 90 (6).

6. Leonard, , and Deffner. Quantum work distribution for a driven diatomic molecule. 2015. CHEMICAL PHYSICS. 446: 18.

7. Deffner, , and Saxena. Jarzynski Equality in PT -Symmetric Quantum Mechanics. 2015. PHYSICAL REVIEW LETTERS. 114 (15).

8. Deffner, S.. Shortcuts to adiabaticity: Suppression of pair production in driven Dirac dynamics. 2016. NEW JOURNAL OF PHYSICS. 18: 012001.

9. Gardas, B., S. Deffner , and A. Saxena . Non-hermitian quantum thermodynamics. 2016. SCIENTIFIC REPORTS. 6: 23408.

10. Deffner, S., and W. H. Zurek. Foundations of statistical mechanics from symmetries of entanglement. 2016. NEW JOURNAL OF PHYSICS. 18: 063013.

11. Deffner, S., J. P. Paz, and W. H. Zurek. Quantum work and the thermodynamic cost of quantum measurements. 2016. PHYSICAL REVIEW E. 94: 010103(R).

Publications

Acconcia, T. V., M. V. S. Bonança, and S. Deffner. Shortcuts to adiabaticity from linear response theory. 2015. PHYSICAL REVIEW E. 92: 042148.

Cimmarusti, A. D., Z. Yan, B. D. Patterson, L. P. Corcos, L. A. Orozco, and S. Deffner. Environment assisted speed-up of the field evolution in cavity quantum electrodynamics. 2015. PHYSICAL REVIEW LETTERS. 114: 233602.

Deffner, . TEN YEARS OF NATURE PHYSICS From spooky foundations. 2015. NATURE PHYSICS. 11 (5): 383.

Deffner, , and Saxena. Jarzynski Equality in PT -Symmetric Quantum Mechanics. 2015. PHYSICAL REVIEW LETTERS. 114 (15).

Deffner, S.. Shortcuts to adiabaticity: Suppression of pair production in driven Dirac dynamics. 2016. NEW JOURNAL OF PHYSICS. 18: 012001.

Deffner, S.. Viewpoint: Exorcising Maxwell's demon. 2015. APS PHYSICS. 8: 127.

Deffner, S.. Perspective: Quantum stochastic thermodynamics on harmonic networks. 2016. NEW JOURNAL OF PHYSICS. 18: 011001.

Deffner, S.. Im Brennpunkt: Den Maxwellschen Dämon bannen . 2016. PHYSIK JOURNAL. 15: 22.

Deffner, S., J. P. Paz, and W. H. Zurek . Quantum work and the thermodynamic cost of quantum measurements. 2016. PHYSICAL REVIEW E. 94: 010103(R).

Deffner, S., and A. Saxena. Quantum work statistics of charged Dirac particles in time-dependent fields. 2015. PHYSICAL REVIEW E. 92: 032137.

Deffner, S., and W. H. Zurek . Foundations of statistical mechanics from symmetries of entanglement. 2016. NEW JOURNAL OF PHYSICS. 18: 063013.

Gardas, B., S. Deffner , and A. Saxena . Non-hermitian quantum thermodynamics. 2016. SCIENTIFIC REPORTS. 6: 23408.

Gardas, B., and S. Deffner. Thermodynamic universality of quantum Carnot engines. 2015. PHYSICAL REVIEW E. 92: 042126.

Gong, , Deffner, and H. T. Quan. Interference of identical particles and the quantum work distribution. 2014. PHYSICAL REVIEW E. 90 (6).

Leonard, , and Deffner. Quantum work distribution for a driven diatomic molecule. 2015. CHEMICAL PHYSICS. 446: 18.

Materials for the Future

Aging in Delta Plutonium Alloys: A Fundamental Approach

Franz J. Freibert
20150057DR

Introduction

The mission of LANLs' Stockpile Stewardship program is to assess aging of our nation's stockpile materials. Both α-decay and thermodynamics are powerful physical processes in δ-Pu, with potential to couple strongly to phase changes in δ-Pu. Understanding the relative contributions of these processes is necessary to identify important aging mechanisms and accurately extrapolate induced effects on δ-Pu properties and performance over decades. This project, founded in Defects and Interfaces theme of the Materials for the Future Focus Area, is focused on the development of a mechanistic multi-scale understanding and control of defects and He bubbles, intrinsic and enhanced, across significant length, time and temperature scales of δ-Pu aging.

The goal is to quantify and understand the radiogenic changes in δ-Pu induced by the drivers of He ingrowth, defect accumulation and δ-Pu phase instability as determined by consensus of state-of-the-art experimental, computational and modeling tools. We will work to understand radiogenic defect accumulation as the mechanism of ambient temperature lattice swelling over a 1-2yr. transient ingrowth period; to control numbers and configurations of various defects separately from He bubbles and determine the influence radiogenic defects have on electronic and structural properties from nanometer to bulk spatial scale correlated with δ-Pu phase instability; and to understand defect accumulation interaction with He ingrowth as functions of experimental variables sufficient to induce and control void swelling.

This work will lay the fundamental groundwork for a Pu aging strategy by revealing the importance, rate, and scale of radiogenic changes in δ-Pu with exceptionally sensitive measurements, capable of showing aging effects in real time over a wide temperature range, with computational approaches describing defect structures and their relative stability. This approach supports unprecedented advances in understanding the physics of radiogenic damage process in δ-Pu exploring materials of controlled thermal histories, Ga compositions and alpha-decay dose.

Benefit to National Security Missions

The single most important mission of LANLs' Stockpile Stewardship program is to assess aging of our nation's stockpile; nonetheless, there are certain fundamental science questions that are not addressed in the program. Direct reuse of δ-Pu components expected to be in service for many decades requires that physics and engineering assessments have a firm scientific basis. Both a-decay and thermodynamics are powerful physical processes in δ-Pu, with potential to couple strongly to phase changes in δ-Pu. Understanding the relative contributions of these processes and their coupling are necessary to identify the important aging mechanisms and to accurately extrapolate induced effects on δ-Pu properties and performance margins over decadal time scales. Current physics-based lifetime estimates for US pits are approximately 100yr. These estimates were developed within a Quantifying Margins and Uncertainties (QMU) formalism for primary physics performance. However, the physics models for the QMU determinations do not contain fundamental physics and therefore are not predictive. The scientific work of understanding the effects of Pu aging must continue; otherwise today's solution to a Life Extension Program (LEP) problem might induce two or more unforeseen problems in the future.

Progress

Local Structure and Nascent State Defect Evolution - The project team has made progress towards the goal of using extended X-ray absorption fine structure (EXAFS) spectroscopy, as a probe of the local structure around defect sites. To further leverage the unique capabilities of the synchrotron experiments, we are redesigning our sample holders to make resistivity measurements simultaneously with structural measurements. We anticipate being able to make a full-scale test of the system

in advance of future synchrotron experiment. Finally, a manuscript entitled Isochronal annealing effects on local structure, crystalline fraction, and undamaged region size of radiation damage in Ga-stabilized δ-Pu (JR16-2818R1) has been accepted for publication in the Journal of Applied Physics. This work will be highlighted in the Pu Futures 2016 invited presentation EXAFS studies of self-irradiation damage in Pu.

Thermally Activated Defect Evolution and Kinetic Behavior–This currently involves allowing the samples to accumulate damage at 4 K for a short time and then heating the samples in-situ in the cryostat at various rates in order to investigate the annealing out of damage. Furthermore, characterization of the samples before and after various treatments, using X-ray diffraction technique (phase identification, any changes in peak position, shape and intensity, identification of any additional phases and/or impurities). This work will be highlighted in the Pu Futures 2016 oral presentation The Kinetic Evolution of Self-Irradiation Damage in Face-Centered Cubic Pu-Ga Alloys and a paper is in production.

Multi-State Configuration and Thermodynamics- Progress has been made in our understanding of delta phase Pu stability resulting in a new manuscript detailing the impact of multi-state configuration and its impact on thermodynamic properties of Pu. The manuscript entitled "Origin of the multiple configurations that drive the response of δ-plutonium's elastic moduli to temperature" (MS#: 2016-09215) has been submitted for publication in the Proceedings of the National Academy of Sciences.

Time Dependent/Defect Induced Thermodynamic Properties Changes - Using high-resolution, high temperature resonant ultrasound spectroscopy (RUS), we are measuring in real time at the 100 parts per billion level changes in the elastic moduli of unalloyed Pu and 2at%Ga-delta Pu to understand the relative contributions of radiogenic daughter product ingrowth, phase stability, and radiation damage. The drivers for such changes are the ingrowth of radioactive decay products, the thermodynamic stability of Pu-Ga phases, and the introduction of radiation damage.

We have observed two independent mechanisms of increasing elastic moduli changes at isotherms of increasing temperature. An article detailing this work entitled Changes In Aging With Temperature In Elastic Moduli Of δ-Pu239 Measured in Real Time is in production and this work will be highlighted as an invited presentation at the Pu Futures 2016 Conference entitled Real Time Studies of 239Pu Elastic Moduli using Resonant Ultrasound Spectroscopy.

Molecular Dynamic Modeling –Thus far, we have revised an existing meso-scale (100-10,000 nm) model to account for radiation-damage-suppression terms from a reaction-rate model. Furthermore, estimates have been made on interstitial defect transport rates as a function of gallium concentration in plutonium alloys. DFT simulations are being employed in development of a new fit to the modified embedded atomic method (MEAM) interatomic potentials for Pu-Ga alloys with collaboration of DR's Co-PIs with original MEAM developer Michael I. Baskes of UCSD with article detailing improvements in production.

Density Functional Theory Defect Modeling - Although indirect evidence of defect generation and ingrowth has been demonstrated through volume changes and the associated changes in elastic moduli, the one outstanding impediment to understanding Pu aging has been the lack of a systemic study of lattice damage and defect formation in a controlled manner experimentally and theoretically. Using DFT we can explore a variety of point defects in an unalloyed and Ga-alloyed δ-Pu 3x3x3 supercells (108 atoms), which consists of vacancies, octahedral interstitials, tetrahedral interstitials, <100> split-interstitials, and Frenkel pairs. Formation energy, Ef, of these defects may be calculated in order to gauge the stability of the defect within the lattice. In addition, these simulations will support experimental work. Furthermore, this work will be highlighted as an invited presentation at the Pu Futures 2016 Conference Insights into point-defects of δ-Pu and δ-Pu-Ga alloys using density functional theory and associated paper is in production.

Future Work

The goal of this project is to quantify and understand the radiogenic changes in δ-Pu induced by the drivers of He ingrowth, defect accumulation and δ-Pu phase instability as determined by consensus of state-of-the-art experimental, computational and modeling tools. This project is focused on the development of a mechanistic multi-scale understanding and control of inhomogeneities (i.e., defects and He bubbles), intrinsic and enhanced, across significant length, time and temperature scales that govern δ-Pu aging. In FY17, we will implement the given objectives and workscope: (1) Understand radiogenic defect accumulation as the mechanism of ambient temperature lattice swelling over a 1-2 yr. transient ingrowth period and into the steady-state decadal period. (2) Understand defect accumulation interaction with He ingrowth formations as functions of experimental variables currently recognized to induce and control void swelling in other face-centered cubic alloys. These objectives will be achieved with ongoing thermodynamic (e.g., resonant ultrasound spectroscopy, electrical resistivity, and heat capacity) and structural (e.g.,

EXAFS, neutron diffraction, and X-ray diffraction) measurements coupled with molecular dynamic (MD) simulations and kinetic rate fits for defect and/or impurity complex production/annihilation processes. Our interpretation (e.g. time dependencies and defect and/or impurity complex formation energies) and MD modified embedded atomic potential improvements are based on the results of a first principles density functional theory constructed on Ga alloying, radiogenically introduced defects and daughter product (U and He) ingrowth and their interactions. Our team now includes 2 postdocs, an undergraduate student and a high school intern. This will be the completion phase of this project and the team has been engaging with the Science Program, Plutonium Sustainment, and other mission related programs on transitioning our efforts for long-term sustainment.

Conclusion

This project will develop a physically sound basis for pit lifetime estimates advancing the understanding of fundamental radiogenic processes in δ-Pu. Because the focus of Defense Science Campaigns is the development of science impacting stockpile performance, an understanding of radiogenic effects in δ-Pu will impact experiment implementation. Because the focus of Directed Stockpile Work is the function of stockpile technology, aging indicators of performance impact could influence programmatic decisions on Pit Reuse and Lifetime Extension Programs and bound thermo-mechanical processing and supporting technological development for better definition of performance margins and uncertainties.

Publications

Conradson, S. D., Bock, J. M. Castro, D. R. Conradson, L. E. Cox, Dmowski, D. E. Dooley, Egami, F. J. Espinosa-Faller, F. J. Freibert, A. J. Garcia-Adeva, N. J. Hess, E. K. Holmstroem, R. C. Howell, Katz, J. C. Lashley, R. J. Martinez, D. P. Moore, L. A. Morales, J. D. Olivas, R. A. Pereyra, Ramos, S. P. Rudin, and P. M. Villella. Nanoscale heterogeneity, premartensitic nucleation, and a new plutonium structure in metastable delta fcc Pu-Ga alloys. 2014. PHYSICAL REVIEW B. 89 (22).

Conradson, S. D., Bock, J. M. Castro, D. R. Conradson, L. E. Cox, Dmowski, D. E. Dooley, Egami, F. J. Espinosa-Faller, F. J. Freibert, A. J. Garcia-Adeva, N. J. Hess, Holmstroem, R. C. Howell, B. A. Katz, J. C. Lashley, R. J. Martinez, D. P. Moore, L. A. Morales, J. D. Olivas, R. A. Pereyra, Ramos, J. H. Terry, and P. M. Villella. Intrinsic Nanoscience of delta Pu-Ga Alloys: Local Structure and Speciation, Collective Behavior, Nanoscale Heterogeneity, and Aging Mechanisms. 2014. JOURNAL OF PHYSICAL CHEMISTRY C. 118 (16): 8541.

Freibert, F. J.. Current research into the self-irradiation effects of δ-phase Pu-Ga alloys . 2015. In NUCAR 2015 . (Mumbai, India, 9-13 February 2015). , p. 42. Mumbai: Bhabha Atomic Research Centre.

Freibert, F. J., J. N. Mitchell, D. S. Schwartz, and A. Migliori. Radiogenic-thermally coupled lifetimes for defects of aged δ-phase Pu-Ga alloys. 2015. In Plutonium Futures 2014, The Science. (Las Vegas, NV, 7-12 September 2014). , p. 220. La Grange Park, IL: American Nuclear Society.

Hernandez, S. C., F. J. Freibert, and J. M. Wills. Density Functional Theory Study of Defects in Unalloyed δ-Pu. Physical Review Letters.

Maiarov, B. A., J. B. Betts, F. J. Freibert, and A. Migliori. Real-time aging studies and some high temperature measurements of Ga-stabilized δ-phase 239Pu . 2015. FY15 Annual Report.

Migliori, A., P. Söderlind, A. Landa, F. J. Freibert, B. Maiorov, B. J. Ramshaw, and J. B. Betts. Origin of the multiple configurations that drive the response of δ-plutonium's elastic moduli to temperature. 2016. Proceedings of the National Academy of Sciences. 113 (40): 11158.

Mitchell, J. N., F. J. Freibert, T. E. Mitchell, and D. S. Schwartz. Aging and the δ → α′ transformation in Pu-Ga alloys . 2015. In PTM: International Conference on Solid-Solid Phase Transformations in Inorganic Materials. (Whistler, Canada, 28 June-3 July 2015). , p. 523. : .

Olive, D. T., D. L. Wang, C. H. Booth, E. D. Bauer, A. L. Pugmire, F. J. Freibert, S. J. McCall, M. A. Wall, and P. G. Allen. Isochronal annealing effects on local structure, crystalline fraction, and undamaged region size of radiation damage in Ga-stabilized δ -Pu. 2016. Journal of Applied Physics, 21 July 2016, Vol.120(3) . 120 (3): 035103.

A New Approach to Mesoscale Functionality: Emergent Tunable Superlattices

Marc Janoschek
20150082DR

Introduction

The future availability of multifunctional materials is essential for the country to remain globally competitive and to ensure our energy and defense security. We must move beyond the current age of 'informed serendipity' towards a new era of 'materials by design' enabling controlled functionality that would allow rapid creation of novel applications required for an ever-changing world. Important technological functionalities are a consequence of mesoscale objects that respond to an external stimulus; e.g. magnetic memories and sensors are built upon the ability to switch mesoscale domains with magnetic fields. Here the mesoscale describes objects that have typical size in between the atomic-scale (i.e. sub-nanometer) and the macroscale (~1 mm). The critical step for mastering the designed functionality will be to achieve control of materials directly on this mesoscale. This is the potential promised by the recent discovery of a mesoscale object, a magnetic vortex called a "skyrmion" that emerges in magnetic materials . The stability of these topological objects makes them behave as particles when driven by external stimuli. Put differently, skyrmions are the new atoms of the mesoscale world. Similarly, just as different combination of atoms produce materials with different properties, different arrangements of skyrmions lead to distinct functionalities through coupling to electrical currents, magnetic and electrical fields, and temperature gradients. The resulting mesoscale architecture build from skyrmions is moreover clean, tunable, and movable, qualities that are vital for achieving enhanced macroscale functionality. This project will exploit the promising properties of those mesoscale magnetic whirls to find design principles for new functional materials, such as ultra-low-power high-density memory materials.

Benefit to National Security Missions

Our project responds specifically to the over-arching grand challenge of LANL's materials strategy. It addresses the priorities of realizing design principles towards controlled functionality and developing multi-functional materials to transform structural and functional performance, as well as tunable and emergent properties. In particular, the mesoscale magnetic whirls (so called "skyrmions") that will be investigated in this proposal hold great potential for multi-functional remote sensing, memory storage applications, and new computing technologies. In each case future devices using this technology will have ultra-low power consumption. Those new sensing, storage and computing devices are directly relevant for a new generation of defense and nonproliferation technologies, as well as improving information science and technology. The development of new mesoscale computational capabilities within this project that will be used to design these materials will additionally enable molecular dynamics calculations on the mesoscale, which is of broad relevance to the lab's material's strategy, and stockpile stewardship , weapon's research, and the study of matter at extremes in general. The mesoscale imaging and synthesis methods developed in this program will be crucial to study further functional materials directly on the mesoscale as required for stockpile stewardship, weapons research, and new materials for example required for the automotive, renewable energy, and defense industries.

Progress

Obtaining an improved understanding of the functionality that derives from magnetic mesoscale architecture based on skyrmion building blocks represents a multi-scale material science problem. Notably the competition of two or more atomic-scale magnetic interactions leads to the emergence of skyrmions, and controls their size and arrangement on the mesoscale. Those mesoscale parameters, in turn dictate the functionality of this assembly of skyrmions on the macroscale. In order to tackle this problem our team has tailored and improved our computing, synthesis and imaging capabilities to investigate these materials on each of those three length scales in the first year of this project. Building on the

capabilities established during the first year, our team has made progress in several areas:

During the last year, our theory effort performed unprecedented calculations on f-electron materials that suggest that the atomic-scale magnetic interactions present in this material class of interest to Los Alamos may also drive the creation of skyrmions. Building on these insights, we have investigated the conditions under which skyrmions may arise in f-electron materials. These calculations have shown that the most important parameter is the magnetic anisotropy: When the magnetic anisotropy is absent or small, no skyrmion lattice may exist in f-electron materials. Similarly, too large a magnetic anisotropy destroys the skyrmion state and a collinear or ferromagnetic state is observed. Thus, just the right amount of intermediate magnetic anisotropy (compared to the magnetic ordering temperature) is required to create skyrmion lattices in f-electron materials. Currently, our theory effort is screening the literature for promising candidates for f-electron skyrmion materials. Additional calculations have demonstrated that skyrmion-like magnetic states should, in principle, be more wide-spread than originally anticipated. If discovered, such materials could have additional functional properties compared to the materials already studied in this project. First-principle studies of the electronic structure have also been used how the mobility of skyrmions is changed by magnetic and non-magnetic impurities. The impact of impurities is notably important for possible devices based on skyrmion materials.

Experimentally, the largest progress was made by our neutron scattering effort. We have now carried out the first neutron spectroscopy measurements to quantitatively determine the change of the atomic-scale magnetic interactions in the skyrmion phase of manganese silicide. Our current theory can already qualitatively explain the observed magnetic interactions. An additional experiment to clarify further details is already approved and planned, and will be used to establish quantitative understanding of the atomic-scale interactions. We have further performed a series of small angle neutron scattering experiments to investigate the mesoscale structural properties of skyrmion lattices in the family of cobalt-zinc-manganese. We have found that the magnetic anisotropy appears to be larger compared to previously known materials such as manganese silicide, suggesting that this property indeed stabilizes skyrmion lattices as previously suggested by our theory effort. In addition, we have carried out a first experiment on uranium based f-electron material to search for skyrmion lattices in such materials. We have found that the anisotropy in this material is too large to form skyrmion lattices. However, more experiments for further f-electron materials are already planned. For the end of June, the first SANS experiment using the strain cell designed and developed during the first year is planned. The strain cell allows for in-situ tuning of the magnetic anisotropy, and we will investigate if this will indeed stabilize the skyrmion phase in manganese silicide.

In terms of synthesis, we have managed to synthesize a strontium-iron-oxygen compound that our theory effort has identified as suitable candidate for “artificial” skyrmion lattices. Here the aim is to grow this material on top of an artificial lattice of magnetic nano-pillars at MPA-CINT that will drive the emergence of skyrmions according to our theory. Unfortunately, this effort is currently delayed because of a broken hood that we require to carry out this work. The hood is hopefully being repaired soon, and we plan to finish this effort during the last year.

In summary, our project is making great progress building on the modeling-making-measuring capabilities created in the first year. Continuing the most promising studies will be our priority for the third and last year.

Future Work

Understanding the functionality of skyrmions represents a multi-scale material science problem that stretches from the atomic- over the meso- to the macroscale. In the first and second year our team has established that while the magnetic anisotropy is typically dominated by other atomic-scale interaction it is a central ingredient that influences both the stability and the properties of skyrmion lattices. In the second year, our theory effort has further demonstrated that if the magnitude of the magnetic anisotropy is just right, skyrmion lattices may also emerge in f-electron materials that are of interest to Los Alamos. Following the recommendations of the mid-project appraisal, our modeling effort has started to look at this possibility systematically, and we have started to carry experiments on candidate f-electron materials. During the last year of the project, we will experimentally screen more candidates. Notably, we will use the strain cell that we developed for small angle neutron scattering (SANS) experiments to actively tune the magnetic anisotropy in f-electron materials. Skyrmion-like states in f-electron materials are not only interesting in terms of the usual applications that are pursued for all kind of skyrmions, but will provide better understanding of actinide materials. Skyrmions are a so-called magnetic multi-Q state, i.e. a superposition of two or more mesoscale magnetic formations such as magnetic helices, where Q denotes their orientation. Such multi-Q states are relevant for the properties of actinides materials. For example, uranium dioxide exhibits a multi-Q state that is thought to be related to its low thermal conductiv-

ity, which limits its potential as nuclear fuel. Additionally, we will continue our effort to create 'artificial' skyrmion lattices via magnetic nano-pillars synthesized in MPA-CINT. Finally, we will complete our neutron spectroscopy efforts on the investigation of the atomic-scale magnetic interactions that drive the emergence of magnetic skyrmions, and our SANS studies of high-temperature skyrmion materials. We will emphasize connecting our modeling and experimental efforts.

Conclusion

In pursuing our objective, we will not only pioneer a new direction for material science at LANL, as well as for the international community, and respond directly to national, Laboratory and DOE priorities, but have the real potential of transforming the research on functional materials. Using our fully-integrated modelling-making-measuring loop we will find "design principles" for various mesoscale skyrmion architectures, which will immediately yield designed functionality via their unique properties. In particular, we expect to identify magnetic mesoscale architecture optimized for new memory or sensing applications.

Publications

Batista, C. D., Lin, Hayami, and Kamiya. Frustration and chiral orderings in correlated electron systems. 2016. REPORTS ON PROGRESS IN PHYSICS. 79 (8).

Chen, , Strigari, Sundermann, Agrestini, N. J. Ghimire, S. -. Lin, C. D. Batista, E. D. Bauer, J. D. Thompson, Otero, Tanaka, and Severing. Exchange field effect in the crystal-field ground state of CeMAl4Si2. 2016. PHYSICAL REVIEW B. 94 (11).

Choi, H., S. Z. Lin, and J. X. Zhu. Density functional theory study of skyrmion pinning by atomic defects in MnSi. 2016. Physical Review B. 93 (115): 1.

Enriquez, E., A. Chen, Z. Harrell, P. C. Dowden, N. A. Koskelo, J. Roback, M. Janoschek, C. Chen, and Q. Jia. Oxygen Vacancy-Tuned Physical Properties in Perovskite Thin Films with Multiple B-site Valance States. Small.

Enriquez, E., A. Chen, Z. Harrell, X. Lu, P. C. Dowden, N. A. Koskelo, M. Janoschek, C. Chen, and Q. Jia. Oxygen Vacancy-Driven Evolution of Structural and Electrical Properties in SrFeO3-δ Thin Films and a Method of Stabilization. 2016. Applied Physics Letters. 109: 141906.

Hayami, , Lin, and C. D. Batista. Bubble and skyrmion crystals in frustrated magnets with easy-axis anisotropy. 2016. PHYSICAL REVIEW B. 93 (18).

Hayami, S., S. Z. Lin, Y. Kamiya, and C. D. Batista. Vortices, skyrmions, and chirality waves in frustrated Mott insulators with a quenched periodic array of impurities. To appear in Physical Review B.

Kugler, M., G. Brandl, J. Waizner, M. Janoschek, R. Georgii, A. Bauer, K. Seemann, A. Rosch, C. Pfleiderer, P. Böni, and M. Garst. Band structure of helimagnons in MnSi resolved by inelastic neutron scattering. 2015. Physical Review Letters. 115 (9): 097203.

Lin, . Edge instability in a chiral stripe domain under an electric current and skyrmion generation. 2016. PHYSICAL REVIEW B. 94 (2).

Lin, , Hayami, and C. D. Batista. Magnetic Vortex Induced by Nonmagnetic Impurity in Frustrated Magnets. 2016. PHYSICAL REVIEW LETTERS. 116 (18).

Lin, S. Z., A. Saxena, and C. D. Batista. Skyrmion fractionalization and merons in chiral magnets with easy-plane anisotropy. 2015. Physical Review B. 91: 224407.

Lin, S. Z., and A. Saxena. Non-circular skyrmion and its anisotropic response in thin films of chiral magnets under tilted magnetic field. 2015. Physical Review B. 92: 180401.

Lin, S. Z., and A. Saxena. Dynamics of Dirac strings and monopole-like excitations in chiral magnets under a current drive. 2016. Physical Review B (Rapid Communications). 93: 060401.

Lin, S. Z., and S. Hayami. Ginzburg-Landau theory for skyrmions in inversion-symmetric magnets with competing interaction. 2016. Physical Review B. 93: 064430.

Ozawa, R., S. Hayami, K. Barros, G. W. Chern, Y. Motome, and C. D. Batista. Vortex crystals with chiral stripes in itinerant magnets. 2016. Journal of the Physical Society of Japan. 85 (103703): 1.

Ozawa, R., S. Hayami, K. M. Barros, and Y. Motome. Shape of magnetic domain walls formed by coupling to mobile charges. Physical Review B.

Saxena, A., and S. Z. Lin. Skyrmions in Functional Materials. To appear in Integrated Ferroelectrics. 116.

Wang, Z., K. M. Barros, G. W. Chern, D. L. Maslov, and C. D. Batista. Resistivity Minimum in Highly Frustrated Itinerant Magnets. To appear in Physical Review Letters.

Meso-Photonic Materials for Tailored Light-Matter Interactions

Houtong Chen
20150109DR

Introduction

Building on our internationally recognized expertise in metamaterials, we propose to tackle key science issues underpinning some "grand challenge" scale problems in photonics by developing transformational meso-photonic materials based on two core innovations: a meta-molecule concept and the integration of functional materials into meso-photonic structures. Meta-molecules are a collection of meta-atoms (sub-wavelength metal/dielectric resonators) with tailored internal interactions, enabling designer light coupling and propagation. Integration of functional materials (semiconductors, complex oxides, graphene, and transition metal dichalcogenides) results in tunable and reconfigurable photonic functionalities, enables novel optoelectronic architectures, and provides a means to exploit the greatly enhanced light-matter interactions to study a wealth of basic physics phenomena.

In our joint experiment-theory effort, we will demonstrate the unusual power of this meso-photonic platform in two connected focus areas: (a) Photonic phenomena and functionalities enabled by meta-molecule structures. We will demonstrate a host of photonic functionalities, including complete polarization control and arbitrary wavefront shaping based on the meta-molecule concept, and develop an efficient proof-of-concept solar thermophotovoltaics device for energy harvesting; (b) Enhanced meso-photonic functionalities through integration of functional materials into meta-molecule structures. We will realize real-time control of photonic functionalities, develop meso-photonic cavities for greatly improved optoelectronics, and explore the fundamental physics of strong light-matter interactions in low dimensional quantum materials.

Benefit to National Security Missions

Our proposed work supports the Emergent Phenomena central theme in the Materials for the Future science pillar. This project addresses some grand challenge questions regarding key technological gaps in photonics. The development of compact, lightweight, flexible, and integrated optical elements and optoelectronic devices will impact Threat Reduction and Global Security applications, such as flat lens antennas and focal plane array detectors for communications, imaging, and sensing, such as effluent detection, particularly for space and satellite sensing of nuclear nonproliferation. Indeed, in a recent presentation DoD has listed metamaterials and plasmonics as one of its six high priority S&T areas. The proof-of-concept meso-photonic solar thermophotovoltaics will create a pathway that greatly impacts renewable solar energy harvesting for our national energy security, a core mission of LANL and DOE. The exquisite control of photonic and electronic density of states in meso-photonic cavities will be of great interest to BES for fundamental studies of light-matter interactions enabling emergent meso-scale material properties and functionalities. The proposed research aligns with New Mexico's Technology21 Roadmap for Science and Technology, and contributes to the potential New Mexico Advanced Photonics Hub. It will also prepare us for the Mesoscale Science, Advanced Manufacturing, and National Photonics Initiatives.

Progress

- Metasurface antireflection coatings: We have designed, fabricated, and tested narrowband, dual-band, and broadband antireflection coatings employing metal-dielectric-metal metasurface structures, operating in the terahertz and mid-infrared frequency regions. The undesirable high Fresnel reflection from the surface of typical materials (e.g., silicon and gemanium) was dramatically reduced, and the transmission was greatly enhanced. Important advantages include the deep subwavelength thickness, simple fabrication, low loss, and no involvement of other materials except for metal.

- Terahertz metasurface flat lens: We designed and

successfully fabricated a a high-performance metasurface flat lens, which allows for tightly focusing the incident terahertz beam over a broad bandwidth (0.3 to 0.6 THz) and with low insertion loss. The device is currently under test with a raster scanner to evaluate the filed profile of the focused THz beam, in collaboration with the University of Adelaide.

- Broadband plasmonic absorbers for solar thermophotovoltaics: We have explored the use of refractory plasmonic materials (tungsten and titanium nitride) for the broadband metamaterial perfect absorbers that is required in solar thermophotovoltaics. Our preliminary testing results show that high absorptance was accomplished over the entire visible spectral range and the undesirable absorption in the near-infrared spectral range was suppressed.

- Instrumentation for solar thermophotovoltaic characterization: We have designed and constructed a new, start-of-the-art instrumentation for characterization and testing of metamaterial photonic structures for solar energy conversion, which occurs at temperatures up to 1800 degree C. We have acquired all of the components, finished the assembling, and performed some initial testing of the instrumentation.

- Meso-photonic photovoltaics: We have designed meso-photonic structures for enhancing the light-to-electricity conversion performance of thin film photovoltaics, through integrating organic polymer-based functional materials into metamaterial perfect absorbers.

- Graphene based active metasurface modulator: We have designed, fabricated and characterized active graphene metasurface devices with electrically tunable absorption for infrared spatial modulation and imaging, operating under low voltage bias that is compatible with commercial integrated circuit readouts. In the fabricated devices we observed that the absorption peak was actively tuned by applying low voltages (< 5 V) to the graphene layer, achieving an absorption difference around 10%.

- Light-matter interaction between colloidal quantum dots and epsilion-near-zero materials: We have developed a fabrication process using reactive sputtering to deposit indium-tin-oxide (ITO) nanolayers on both quartz and silicon substrates. We found that the epsilon-near-zero (ENZ) frequencies of the deposited ITO nanolayers (thickness ~ 30-40 nm) can be tailored at will through a post-deposition annealing step. This allows for the coupling of the ENZ mode supported by ITO nanolayers to the fluorescence of PbS colloidal quantum dots at ~1550 nm. The PbS colloidal quantum dots (CQDs) have been also synthesized and are ready to be spin-coated on the ITO layers.

- BCP QD/optoelectronic devices: An ultra-thin, metamaterial-based InAs quantum dot (QD) optoelectronic device has been proposed and simulated. The InAs quantum dots layer is embedded in a GaAs matrix and sandwiched between a gold ground plane and an array of gold nanoresonators. It allows near 100% absorption of the incident radiation in a dual-band fashion for optical excitation and photon emission, resulting in much faster decay rate of excited carriers via Purcell effect. We have prepared the InAs QDs through selective-area epitaxy (SAE) using metal-organic chemical vapor deposition (MOCVD), and a block-copolymer (BCP) template at the University of Wisconsin-Madison.

- Theory of optical response in TMD semiconductors, with the goal of understanding the characteristic frequencies of optical absorption and Kerr-rotation, which is important to understand feasibility of using new class of materials (TMDs) for optical applications.

- Theoretically investigated the physics of cavity quantum electrodynamics (cQED), which has emerged as a search of non-standard application of cQED to controlled generation of optical pulses with strong quantum interactions. We have derived a unique approach to solve cQED equations under conditions of explicit time-dependence of parameters. This theory opens the path to understand strongly interacting optoelectronic systems.

- Theoretically investigated and understood the effect of the reflection beam shift from the graphene surface, and the spatial dispersion effects in near-field heat transfer in grapheme systems. We further investigated non-reciprocal metamaterials for breaking Kirchhof's law of thermal radiation, and spatial nonlocal effects in non-equilibrium fluctuation-induced interactions.

Future Work

- Continue to design, fabricate and test new metasurface structures for broadband meso-photonic absorbers and narrowband emitters, by exploring refractory plasmonic materials including tungsten, tantalum and titanium nitride.

- Finalize the instrumentation for meso-photonic intermediate structures to be used in solar thermophotovoltaics.

- Continue to fabricate and characterize new metasurface structures that enable multiband or broadband antireflection performance, based on the success we have obtained.
- Explore broadband linear-to-circular polarization conversion in reflection, and its potential applications.
- Continue to fabricate and characterize the performance of a metasurface flat lens to focus broadband terahertz radiation, as well as other metasurfaces for arbitrary wave front generation and beam forming.
- Continue the design, fabrication, and characterization of thin film photovoltaic devices where metasurface structures are integrated.
- Continue to integrate semiconducting quantum structures to investigate light-matter interactions in the strong coupling region.
- Continue to optimize the design and fabrication of graphene-enabled independent tuning of a dual-band metasurface absorber.
- Continue the basic theoretical research to understand light-matter interactions with the presence of meso-photonic structures.

Conclusion

The anticipated deliverables are: a) Novel photonic functionalities from meso-photonic structures; b) Proof-of-concept highly efficient meso-photonic intermediate structure for solar thermophotovoltaic energy harvesting; c) Development of modeling and simulation capabilities for designing and understanding light-matter interactions in meso-photonic materials; d) Enhanced photonic functionalities enabled by functional materials integration; and e) Fundamental studies of strong light-matter interaction between meta-molecules and two dimensional electronic quantum materials. Our proposed work supports the Emergent Phenomena central theme in the Materials for the Future science pillar, and will have great impact on renewable energy, communications, imaging and sensing.

Publications

Azad, A. K., W. J. M. Kort-Kamp, M. Sykora, N. R. Weisse-Bernstein, T. S. Luk, A. J. Taylor, D. A. R. Dalvit, and H. T. Chen. Metasurface broadband solar absorber. 2016. Scientific Reports. 6: 20347.

Bartolo, N., F. Intravaia, D. A. R. Dalvit, and R. Messina. Non-equilibrium Casimir-Polder plasmonic interactions. 2016. Physical Review A. 93 (4): 042111.

Chen, H. T.. Semiconductor activated terahertz metamaterials. 2015. Frontiers of Optoelectronics. 8 (1): 27.

Chen, H. T., A. J. Taylor, and N. Yu. A review of metasurfaces: physics and applications. 2016. Reports on Progress in Physics. 79 (7): 076401.

Heyes, J. E., W. Withayachumnankul, N. K. Grady, D. R. Chowdhury, A. K. Azad, and H. T. Chen. Hybrid metasurface for ultra-broadband terahertz modulation. 2014. Applied Physics Letters. 105 (18): 181108.

Huang, L., B. Zeng, C. C. Chang, and H. T. Chen. Terahertz antireflection coating enabled by a subwavelength metallic mesh capped with a thin dielectric film. 2016. Terahertz Science and Technology. 9 (1): 1.

Intravaia, F., R. O. Behunin, C. Henkel, K. Busch, and D. A. R. Dalvit. Failure of local thermal equilibrium in quantum friction. 2016. Physical Review Letters. 117 (10): 100402.

Intravaia, F., R. O. Behunin, C. Henkel, K. Busch, and D. A. R. Dalvit. Non-Markovianity in atom-surface dispersion forces. 2016. Physical Review A. 94 (4): 042114.

Intravaia, F., V. E. Mkrtchian, S. Y. Buhmann, S. Scheel, D. A. R. Dalvit, and C. Henkel. Friction forces on atoms after acceleration. 2015. Journal of Physics-Condensed Matter. 27 (21): 214020.

Kort-Kamp, W. J. M., B. Amorim, G. Bastos, F. A. Pinheiro, F. S. S. Rosa, N. M. R. Peres, and C. Farina. Active magneto-optical control of spontaneous emission in graphene. 2015. Physical Review B. 92 (20): 205415 .

Kort-Kamp, W. J. M., N. A. Sinitsyn, and D. A. R. Dalvit. Quantized beam shifts in graphene. 2016. Physical Review B, Rapid Communications. 93 (8): 081410.

Li, J. X., S. Q. Chen, H. F. Yang, J. J. Li, P. Yu, H. Cheng, C. Z. Gu, H. T. Chen, and J. G. Tian. Simultaneous control of light polarization and phase distributions using plasmonic metasurfaces. 2015. Advanced Functional Materials. 25 (5): 704.

Liang, L., M. Qi, J. Yang, X. Shen, J. Zhai, W. Xu, B. Jin, W. Liu, Y. Feng, C. Zhang, H. Lu, H. T. Chen, L. Kang, W. Xu, J. Chen, T. J. Cui, P. Wu, and S. Liu. Anomalous terahertz reflection and scattering by flexible and conformal coding metamaterials. 2015. Advanced Optical Materials. 3 (10): 1374.

Liu, C., K. Agarwal, Y. Zhang, D. R. Chowdhury, A. K. Azad, and J. H. Cho. Displacement current mediated resonances in terahertz metamaterials. 2016. Advanced Optical Materials. 4 (8): 1302.

Lopez, P. Rodriguez, W. J. M. Kort-Kamp, D. A. R. Dalvit, and

L. M. Woods. Casimir force phase transitions in the graphene family. Nature Communications.

Lu, X., A. Chen, Y. Luo, P. Lu, Y. Dai, E. Enriquez, P. Dowden, H. Xu, P. G. Kotula, A. K. Azad, D. A. Yarotski, R. P. Prasankumar, A. J. Taylor, J. D. Thompson, and Q. Jia. Conducting interface in oxide homojunction: understanding of superior properties in black TiO2. 2016. Nano Letters. 16 (9): 5751.

Rodriguez, G., M. Jaime, F. Balakirev, C. H. Mielke, A. Azad, B. Marshall, B. M. La Lone, B. Henson, and L. Smilowitz. Coherent pulse interrogation system for fiber Bragg grating sensing of strain and pressure in dynamic extremes of materials. 2015. Optics Express. 23 (11): 14219.

Rodriguez-Lopez, P., W. K. Tse, and D. A. R. Dalvit. Radiative heat transfer in 2D Dirac materials. 2015. J. Phys.: Condens. Matter. 27: 214019.

Sinitsyn, N. A.. Exact results for models of multichannel quantum nonadiabatic transitions. 2014. Physical Review A. 90 (6): 062509 .

Sinitsyn, N. A., and F. Li. Solvable multistate model of Landau-Zener transitions in cavity QED. 2016. Physical Review A. 93 (6): 063859.

Sun, C., and N. A. Sinitsyn. Exact transition probabilities for a linear sweep through a Kramers-Kronig resonance. 2015. Journal of Physics A: Mathematical and Theoretical. 48 (50): 505202.

Sun, C., and N. A. Sinitsyn. Landau-Zener extension of the Tavis-Cummings model: structure of the solution. 2016. Physical Review A. 94 (3): 033808.

Szilard, D., W. J. M. Kort-Kamp, F. S. S. Rosa, F. A. Pinheiro, and C. Farina. Purcell effect at the percolation transition. 2016. Physical Review B. 94 (13): 134204.

Woods, L. M., D. A. R. Dalvit, A. Tkatchenko, P. Rodriguez-Lopez, A. W. Rodriguez, and P. Podgornik. A materials perspective on Casimir and van der Waals interactions. 2016. Review of Modern Physics. 88 (4): 045003.

Wu, L., W. K. Tse, M. Brahlek, C. M. Morris, R. V. Aguilar, N. Koirala, S. Oh, and N. P. Armitage. High-resolution Faraday rotation and electron-phonon coupling in surface states of the bulk-insulating topological insulator Cu0.02Bi2Se3. 2015. Physical Review Letters. 115 (21): 217602.

Xu, Q., X. Su, C. Ouyang, N. Xu, W. Cao, Y. Zhang, Q. Li, C. Hu, J. Gu, Z. Tian, A. K. Azad, J. Han, and W. Zhang. Frequency-agile electromagnetically induced transparency analogue in terahertz metamaterials. 2016. Optics Letters. 41 (19): 4562.

Yang, L., N. A. Sinitsyn, W. Chen, J. Yuan, J. Zhang, J. Lou, and S. A. Crooker. Long-lived nanosecond spin relaxation and spin coherence of electrons in monolayer MoS2 and WS2. 2015. Nature Physics. 11 (10): 830–834.

Zhang, B., J. Hendrickson, N. Nader, H. T. Chen, and J. Guo. Metasurface optical antireflection coating. 2014. Applied Physics Letters. 105 (24): 241113.

Zhang, Y., T. Li, B. Zeng, H. Zhang, H. Lv, X. Huang, W. Zhang, and A. K. Azad. A graphene based tunable terahertz sensor with double Fano resonances. 2015. Nanoscale. 7 (29): 12682.

Zhang, Y., T. Li, Q. Chen, H. Zhang, J. F. O'Hara, E. Abele, A. J. Taylor, H. T. Chen, and A. K. Azad. Independently tunable dual-band perfect absorber based on graphene at mid-infrared frequencies. 2015. Scientific Reports. 5: 18463.

Nuclear Science for Signatures, Energy, Security, Environment

Albert Migliori
20150646DR

Introduction

This project, "Nuclear Science Fellowships for Signatures, Energy, Security, Environment" will support research in nuclear science relevant to Laboratory mission areas by attracting and funding projects of a future generation of scientists and engineers with a high expectation, based on results from previous actinide research projects, of exceptional science and of retaining them as permanent employees. Nuclear science areas include materials, material properties, signatures, modeling, predictions, fabrication, detection, disposal, global security implications, forensics, and the specialized science surrounding actinides and especially plutonium, uranium, and their surrogates as fuels for energy and nuclear weapons. The aim is to advance nuclear science in a comprehensive project that ties targeted research with Los Alamos mission imperatives. The mechanisms for this are support of the research arising from a multi-year broad-based postdoctoral fellows project, and a summer student fellows research project. The project will be administered by the Los Alamos G. T. Seaborg Institute, which is a center for actinide and transactinide science.

An internal cross-institutional LANL advisory committee meets to select Nuclear Science Fellows. Fellow selection is based on the excellence of the science in the proposed projects, the quality of the candidate, and the strategic value of the proposed science. The quality of a candidate is measured by the candidate's transcripts, publication and presentation record, educational background and relevance, and letters of reference. Successful proposals have a clearly defined research proposal that supports nuclear science at the single investigator or small-team level, described in a one-page abstract, and is written by the student and mentor. These research plans address nuclear science topics connected to the objectives of this project and span the strategic breadth of nuclear science at LANL. Postdoctoral fellows work on a project that connects directly to nuclear science and that is not otherwise funded.

Benefit to National Security Missions

Actinide and nuclear science continues to be essential to the U.S. and central to the missions of the DOE and its NNSA laboratories, including nuclear weapons, global security, energy security, nuclear safeguards, nonproliferation, environmental restoration, and radioactive waste management. With nuclear weapons technology continuing to play an enduring role in defense policy for the foreseeable future, knowledge and expertise in the production, processing, purification, characterization, analysis, and disposal of actinide series elements specifically and nuclear materials in general is essential to U.S. national security. Nuclear science and detection technology development is extremely important to nonproliferation and global security. Moreover, the risks of global warming, and the environmentally destructive effects of burning coal are such that nuclear energy is expected to assume a greater role in the nation's electrical energy production in the future.

Of the actinide elements, plutonium, uranium and neptunium are especially important to Los Alamos missions. These elements are of technological and scientific interest largely due to radioactivity and it is this property which makes their study particularly challenging. Special facilities, instrumentation, and training, existing in only a small number of locations worldwide, are required for safe and secure handling of these elements, distinguishing actinide science from most other research. Fundamental actinide and nuclear science provides the technical basis for process and separations chemistry, metallurgy, characterization, and detection related to the national security mission of the Laboratory and the national Integrated Plutonium Science and Research Strategy.

Progress

Task: Using electron paramagnetic resonance (EPR) spectroscopy to study the difference in ligand bond strength between actinides and lanthanides elements.

Accomplishments: CW EPR on lanthanide and actinide samples and pulse EPR on some lanthanide materials with the Univ of Washington.

Task: Use of non-explosive and commercially available reagents that will enable synthetically and catalytically important [(C5Me5)2An(H)2]2 (An = thorium, uranium) complexes from (C5Me5)2AnCl2. Accomplishments: Synthesized [(C5Me5)2An(H)2]2 (An = thorium, uranium) complexes from (C5Me5)2AnCl2 and metal borohydride complexes. Understanding these processes in full allows for safer nuclear fuel and waste management strategies.

Task: Developing a portable, plasma-based, system for the separation & detection of actinides during in-field analysis.

Accomplishments: Began experiments on the system.

Task: Using Ga stabilized δ-Pu sample, may be able to probe the effect that Ga will have on the oxidation state of δ-Pu.

Accomplishments: Able to do various experiments on different Ga concentrations that involved exposures to atmospheric gases.

Task: Optical spectroscopy of nuclear materials for nuclear safeguards using laser induced breakdown spectroscopy (LIBS) and laser Raman spectroscopy.

Accomplishments: Optimized LIBS conditions for quantitative analysis of cerium and zirconium in a uranium oxide matrix.

Task: Analyzing plutonium compatibility with fluids to increase the precision of plutonium density measurements.

Accomplishments: Tested available fluids as potential perfluorocarbon fluid replacements. Developed basic multiphysics model of convective flow around a self-heating sphere. Fabricated Tungsten-alloy self-heating samples for experimental validation of convective flow models. Experimental set-up of Schlieren flow visualization and particle image velocimetry to validate model.

Task: Magnetic resonance techniques to perform non-destructive enrichment measurements and nuclear forensics.

Accomplishments: Began measurements on samples of enriched UO2.

Task: New synthetic approaches to the preparation of uranium & lanthanide starting materials.

Accomplishments: Synthesis & characterization of various uranium(III), uranium(IV), lanthanide(III) & lanthanide(II) complexes.

Task: Study the 5f-electron behavior of URu2Si2 by observing changes in the electronic configuration of the compound.

Accomplishments: 65 T pulsed magnet observation of quantum oscillations above 45 T in a single crystal of URu2Si2.

Task: Computational of bonding to provide support for selective separations in spent nuclear fuel, & for managing long-term nuclear waste storage.

Accomplishments: Accurate prediction have now been made.

Task: Effects of carbon on the defect accumulation kinetics & void swelling in ferritic Fe-Cr alloys under irradiation.

Accomplishments: High-dose Fe irradiation experiments performed & the irradiation-induced voids characterized by electron microscopes. Atom probe tomography characterization of irradiated samples was performed & the data is under processing.

Task: Exploring the ternary U-Si-X, (X=Al and Ti) systems to assess their oxidation resistance for use as accident tolerant fuels for nuclear reactor concepts.

Accomplishments: Published a paper on the oxidation resistance of the U-Si matrix compounds, Submitted another for publication on the synthesis of ternary systems. Preliminary oxidation testing is complete.

Task: Thermodynamic parameters for Pu-bearing oxides & alloys, U nitride/carbide, and other related materials and minerals.

Accomplishments: Set up a new actinide nano-material synthesis capability at RC1.

Task: Chelation behavior of isotopes such as actinium-225.

Accomplishments: Developed synthetic techniques, molecules synthesized, studied at the low levels expected when using radioisotopes.

Task: Modeling radiation-induced defect structures in plutonium materials for comparison to X-ray absorption spectroscopy.

Accomplishments: Defect structures simulated, using simple models based on damage in standard metal systems, & using state of the art DFT calculations on more complicated plutonium systems. Experimental x-ray absorption studies

conducted on plutonium alloys that have been acquiring damage for one to two months. Developing simulations to determine the best theoretical model for the experimental X-ray absorption data.

Task: Evaluate electronic structure & bonding in trivalent actinides to better understand their chemistry

Accomplishments: SSRL for X-ray Absorption Spectroscopy (XAS) experiments on actinides (actinium, americium, curium). Protocol to purify actinium form its daughter and from carrier (lutetium). Improved actinide solution XAFS measurements at SSRL. Publication of the first actinium XAFS experiment accepted in Nature Communications

Impact on the workforce pipeline

The project has already engaged 30 postdocs. Diversity has been good, with 12 of the 30 being female. 4 of the postdocs have been converted to staff at Los Alamos, and 2 more have been offered staff positions. 3 others have gone to positions at other national laboratories. 8 Laboratory divisions have been represented in the postdocs: C, P, T, MPA, NSEC, EES, MST, and M.

Future Work

R&D tasks under this project include:

- Develop a portable, plasma-based, system for separating and detecting of actinides.
- Chemical and isotopic measurement to understand nuclear fallout formation for nuclear forensics tools.
- Understand trivalent actinide chemistry from electronic structure and bonding.
- Utilize extremely low energy “ultracold” neutrons to induce fission in actinides near the material surface and characterize sputtered materials.
- Explore the ternary U-Si-X, (X=Al and Ti) systems to assess oxidation resistance for accident tolerant fuels in nuclear reactor concepts.
- Investigate the effects of carbon on defects involved in hardening and void swelling in ferritic Fe-Cr alloys under irradiation.
- Enhance detection and characterization of actinides in complex matrices using multiple, complementary, nondestructive analytical methods based on X-ray fluorescence spectrometry.
- Enhance understanding of correlated electron behavior of U-based compounds, to elucidate their exotic ordered states, and to discover new U-based superconductors.
- Validate sole observation of magnetic resonance signature of the 239Pu nucleus.
- Demonstrate potential of magnetic resonance for nondestructive measurements of enrichment levels for nuclear forensics tools.
- Develop methods to understand how actinides form bonds with other elements.
- Observe elastic mechanical properties of actinide and lanthanide compounds at extremes of pressure and temperature.
- Measure thermodynamic parameters for Pu-bearing oxides and alloys, U nitride/carbide, and other related materials to better understand structure-stability relations and complex behavior of 5f electrons in transuranic compounds.
- Develop characterization methods to measure O isotope concentration in UO2, which will then be used to test the feasibility of O isotope forensics.
- Fabricate U and Th nitride nuclear fuels via a novel chemical process, in which the precursors contain a high percentage of nitrogen and undergo combustion to make the nitride material.
- Solution chemistry approaches to explore solid state chemistry of nuclear fuels.
- Observe the effect that Ga has on the oxidation state of δ-Pu with surface electronic studies.

Conclusion

Improve our understanding of the electronic structure, phase stability, thermodynamics and thermal properties of nuclear materials and the dynamic behavior of plutonium, uranium, and some of their compounds across pressure, temperature, time, phase space, surfaces and interfaces for nuclear materials. Develop advanced chemical separations and synthesis processes and determine their signatures. Expand capabilities in detection, measurement, and analysis of signatures of nuclear and radiological materials. Improve understanding of the environmental behavior and signatures of nuclear materials. Expand the use of 242Pu to enhance understanding of plutonium aging, electronic structure and chemistry with minimal impact from nuclear decay processes.

Publications

(McDonald), J. L. Brown, B. L. Davis, B. L. Scott, and A. J. Gaunt. Early-lanthanide(III) acetonitrile-solvento ddducts with iodide and noncoordinating anions. 2015. Inorganic Chemistry. 54 (24): 11958.

(McDonald), J. L. Brown, M. B. Jones, A. J. Gaunt, B. L. Scott, C. E. Macbeth, and J. C. Gordon. Lanthanide(III) di- and tetra-nuclear complexes supported by a chelating tripodal tris(amidate) ligand. 2015. Inorganic Chemistry. 54 (8): 4064.

Ardeljan, M., R. J. McCabe, I. J. Beyerlein, and M. Knezevic. Explicit incorporation of deformation twins into crystal plasticity finite element models. 2015. Computer Methods in Applied Mechanics and Engineering. 295 (1 Oct): 396.

Barker, B. J., J. M. Berg, M. P. Wilkerson, S. A. Kozimor, and N. R. Wozniak. Visible and near-infrared excitation spectra from the neptunyl ion doped into a uranyl tetrachloride lattice. 2016. Journal of Molecular Structure. 1108: 594.

Brown, J. L., A. C. Montgomery, C. A. Samaan, M. T. Janicke, B. L. Scott, and A. J. Gaunt. Synthesis and characterization of potassium aryl- and alkyl-substituted silylchalcogenolate ligands. 2016. DALTON TRANSACTIONS. 45 (24): 9841.

Browne, K. P., K. A. Maerzke, N. E. Travia, D. E. Morris, B. L. Scott, N. J. Henson, Yang, J. L. Kiplinger, and J. M. Veauthier. Synthesis, Characterization, and Density Functional Theory Analysis of Uranium and Thorium Complexes Containing Nitrogen-Rich 5-Methyltetrazolate Ligands. 2016. INORGANIC CHEMISTRY. 55 (10): 4941.

Conradson, S. D., D. A. Andersson, P. S. Bagus, K. S. Boland, J. A. Bradley, D. D. Byler, D. L. Clark, D. R. Conradson, F. J. Espinosa-Faller, J. S. L. Pacheco, M. B. Martucci, Nordlund, G. T. Seidler, and J. A. Valdez. Anomalous dispersion and band gap reduction in UO2+x and its possible coupling to the coherent polaronic quantum state. 2016. NUCLEAR INSTRUMENTS & METHODS IN PHYSICS RESEARCH SECTION B-BEAM INTERACTIONS WITH MATERIALS AND ATOMS. 374: 45.

Guo, X., A. Navrotsky, R. K. Kukkadapu, M. Engelhard, A. Lanzirotti, M. Newville, and S. R. Sutton. Structure and thermodynamics of uranium-containing garnets. 2016. Geochimica et Cosmochimica Acta. 189: 269.

Guo, X., C. Lipp, E. Tiferet, A. Lanzirotti, M. Newville, M. H. Engelhard, D. Wu, E. S. Ilton, S. R. Sutton, M. Nyman, H. Xu, P. C. Burns, and A. Navrotsky. Structure and stability of UTa3O10, a U(V) -bearing compound. To appear in Dalton Transactions.

Guo, X., D. Wu, H. Xu, P. C. Burns, and A. Navrotsky. Thermodynamic studies of studtite thermal decomposition pathways via amorphous intermediates UO3, U2O7, and UO4. 2016. Journal of Nuclear Materials. 478: 158.

Guo, X., E. Tiferet, L. Qi, J. Solomon, A. Lanzirotti, M. Newville, M. Engelhard, R. K. Kukkadpu, D. Wu, E. S. Ilton, M. Asta, S. R. Sutton, H. Xu, and A. Navrotsky. U(V) in metal uranates: a combined experimental and theoretical study of MgUO4, CrUO4, and FeUO4. 2016. Dalton Transactions. 45: 4622.

Guo, X., R. K. Kukkadapu, A. Lanzirotti, M. Newville, S. R. Sutton, and A. Navrotsky. Charge-coupled substituted garnets (Y3-xCa0.5xM0.5x)Fe5O12 (M = Ce, Th): structure and stability as crystalline waste forms. 2015. Inorganic Chemistry. 54 (8): 4156.

Guo, X., S. Szenknect, A. Mesbah, N. Clavier, C. Poinssot, D. Wu, H. Xu, N. Dacheux, R. C. Ewing, and A. Navrotsky. Energetics of a uranothorite (Th1–xUxSiO4) solid solution. 2016. Chemistry of Materials. 28 (19): 7117.

Guo, X., S. Szenknect, A. Mesbah, S. Labs, N. Clavier, C. Poinssot, S. V. Ushakov, H. Curtius, D. Bosbach, R. C. Rodney, P. Burns, N. Dacheux, and A. Navrotsky. Thermodynamics of formation of coffinite, USiO4. 2015. Proceedings of the National Academy of Science, USA. 112 (21): 6551.

Hartig, K. C., J. Colgan, D. P. Kilcrease, J. E. Barefield II, and I. Jovanovic. Laser-induced breakdown spectroscopy using mid-infrared femtosecond pulse. 2015. Journal of Applied Physics. 118 (4): 043107.

Hawkins, C. A., C. G. Bustillos, May, R. o. y. Copping, and Nilsson. Hydrophilic Schiff base ligands for actinyl/lanthanide separations. 2014. ABSTRACTS OF PAPERS OF THE AMERICAN CHEMICAL SOCIETY. 248.

Hawkins, C. A., C. G. Bustillos, May, R. o. y. Copping, and Nilsson. Water-soluble Schiff base-actinyl complexes and their effect on the solvent extraction of f-elements. 2016. DALTON TRANSACTIONS. 45 (39): 15415.

Koutroulakis, G., T. Zhou, Y. Kamiya, J. D. Thompson, H. D. Zhou, C. D. Batista, and S. E. Brown. Quantum phase diagram of the S = 12 triangular-lattice antiferromagnet Ba3CoSb2O9. 2015. Physical Review B. 91: 024410.

Kundu, , S. C. E. Stieber, M. G. Ferrier, S. A. Kozimor, J. A. Bertke, and T. H. Warren. Redox Non-Innocence of Nitrosobenzene at Nickel. 2016. ANGEWANDTE CHEMIE-INTERNATIONAL EDITION. 55 (35): 10321.

Lichtscheidl, A. G., M. T. Janicke, B. L. Scott, A. T. Nelson,

and J. L. Kiplinger. Syntheses, structures, and 1H, 13C{1H} and 119Sn{1H} NMR chemical shifts of a family of trimethyltin alkoxide, amide, halide and cyclopentadienyl compounds . 2015. Dalton Transactions. 44: 16156.

Lichtscheidl, A., J. Pagano, B. Scott, A. Nelson, and J. Kiplinger. Expanding the Chemistry of Actinide Metallocene Bromides. Synthesis, Properties and Molecular structures of the tetravalent and trivalent uranium bromide complexes: (C5Me4R)2UBr2, (C5Me4R)2U(O-2,6-iPr2C6H3)(Br), and [K(THF)] [(C5Me4R)2UBr2] (R = Me, Et). 2016. Inorganics. 4 (1): 1.

Loble, M., J. M. Keith, A. B. Altman, S. C. E. Stieber, E. R. Batista, K. S. Boland, S. Conradson, D. L. Clark, J. L. Pacheco, S. A. Kozimor, R. L. Martin, S. G. Minasian, A. C. Olson, B. L. Scott, D. K. Shuh, T. Tyliszczak, M. P. Wilkerson, and R. A. Zehnder. Covalency in lanthanides. An x-ray absorption spectroscopy and density functional theory study of LnCl6x-(x = 3,2). 2015. Journal of the American Chemical Society. 137: 2506.

Macor, J. A., J. L. Brown, J. N. Cross, S. R. Daly, A. J. Gaunt, G. S. Girolami, M. T. Janicke, S. A. Kozimor, M. P. Neu, A. C. Olson, S. D. Reilly, and B. L. Scott. Coordination chemistry of 2,2'-biphenylenedithiophosphinate and diphenyldithiophosphinate with U, Np, and Pu. 2015. Dalton Transactions. 44 (43): 18923.

McIntosh, K. G., N. L. Cordes, B. M. Patterson, and G. J. Havrilla. Laboratory-based characterization of plutonium in soil particles using micro-XRF and 3D confocal XRF. 2015. Journal of Analytical Atomic Spectrometry. 30: 1511.

McIntosh, K. G., N. L. Cordes, B. M. Patterson, and G. J. Havrilla. Laboratory-based characterization of plutonium in soil particles using micro-XRF and 3D confocal XRF. 2015. Journal of Analytical Atomic Spectroscopy. 30: 1511.

McIntosh, K. G., S. D. Reilly, and G. J. Havrilla. Determination of plutonium in spent nuclear fuel using high resolution X-ray. 2015. Spectrochimica Acta Part B: Atomic Spectroscopy. 110: 91.

McIntosh, K. G., S. D. Reilly, and G. J. Havrilla. Determination of plutonium in spent nuclear fuel using high resolution X-ray. 2015. Spectrochimica Acta Part B: Atomic Spectroscopy. 110: 91.

Radchenko, V., J. W. Engle, J. J. Wilson, J. R. Maasen, F. M. Nortier, W. A. Taylor, E. R. Birnbaum, L. A. Hudston, K. D. John, and M. E. Fassbender. Application of ion exchange and extraction chromatography to the separation of actinium from protron-irradiated thorium metal for analytical purposes. 2015. Journal of Chromatography A. 2015 (1380): 55.

Radchenko, V., J. W. Engle, J. J. Wilson, J. R. Maassen, M. F. Nortier, E. R. BIrnbaum, K. D. John, and M. E. Fassbender. Formation cross-sections and chromatographic separation of protactinium isotopes formed in proton-irradiated thorium metal. 2016. Radiochemica Acta. 104 (5): 291.

Runnels, , I. J. Beyerlein, Conti, and Ortiz. An analytical model of interfacial energy based on a lattice-matching interatomic energy. 2016. JOURNAL OF THE MECHANICS AND PHYSICS OF SOLIDS. 89: 174.

Runnels, B., I. J. Beyerlein, S. Conti, and M. Ortiz. A relaxation method for the energy and morphology of grain boundaries and interfaces. 2016. Journal of the Mechanics and Physics of Solids. 94: 388.

Rusev, G., A. R. Roman, J. K. Daum, R. K. Springs, E. M. Bond, M. Jandel, B. Baramsai, T. A. Bredeweg, A. Couture, A. Favalli, K. D. Ianakiev, M. L. Illiev, S. Mosby, J. L. Ullmann, and C. L. Walker. Fission-fragment detector for DANCE based on thin scintillating films. 2015. Nuclear Instruments & Methods in Physics Research Section A: Accelerators, Spectrometers, Detectors and Associated Equipment. 804: 207.

Rusev, G., M. Jandel, B. Baramsai, E. M. Bond, T. A. Bredeweg, A. Couture, J. K. Daum, A. Favalli, K. D. Ianakiev, M. L. Iliev, S. Mosby, A. R. Roman, R. K. Springs, J. L. Ullmann, and C. L. Walker. Development of a thin scintillation films fission-fragment detector and a novel neutron source. 2015. SPIE ProceedingsSPIE Proceedings. 9593.

Sooby, E. S., A. T. Nelson, J. T. White, and P. M. McIntyre. Measurements of the liquidus surface and solidus transitions of the NaCl-UCl3 and NaCl-UCl3-CeCl3 phase diagrams. 2015. Journal of Nuclear Materials. 466 (November): 280.

Tamasi, A. L., K. S. Boland, K. Czerwinski, J. K. Ellis, S. A. Kozimor, R. L. Martin, A. L. Pugmire, D. Reilly, B. L. Scott, A. D. Sutton, G. L. Wagner, J. R. Walensky, and M. P. Wilkerson. Oxidation and hydration of U3O8 materials following controlled exposure to temperature and humidity. 2015. Analytical Chemistry. 87 (8): 4210.

Wei, , L. J. Broussard, M. A. Hoffbauer, Makela, C. L. Morris, Tang, E. R. Adamek, N. B. Callahan, S. M. Clayton, Cude-Woods, Currie, E. B. Dees, Ding, Geltenbort, K. P. Hickerson, A. T. Holley, T. M. Ito, K. K. Leung, C. -. Liu, D. J. Morley, J. D. Ortiz, R. W. Pattie Jr., J. C. Ramsey, Saunders, S. J. Seestrom, E. I. Sharapov, S. K. Sjue, Wexler, T. L. Womack, A. R. Young, B. A. Zeck, and Wang. Position-sensitive detection of ultracold

neutrons with an imaging camera and its implications to spectroscopy. 2016. NUCLEAR INSTRUMENTS & METHODS IN PHYSICS RESEARCH SECTION A-ACCELERATORS SPECTROMETERS DETECTORS AND ASSOCIATED EQUIPMENT. 830: 36.

Wilson, J. J., E. R. Birnbaum, E. R. Batista, R. L. Martin, and K. D. John. Synthesis and characterization of nitrogen-rich macrocyclic ligands and an investigation of their coordination chemistry with lanthanum(III). 2015. Inorganic ChemistryI. 54 (1): 97.

Wilson, J. J., M. Ferrier, V. Radchenko, J. R. Maassen, J. W. Engle, E. R. Batista, R. L. Martin, F. M. Nortier, M. E. Fassbender, K. D. John, and E. R. Birnbaum. Evaluation of nitrogen-rich macrocyclic ligands for the chelation of therapeutic bismuth radioisotopes. 2015. Nuclear Medicine and Biology. 42 (5): 428.

Wood, E. S., S. S. Parker, A. T. Nelson, and S. A. Maloy. MoSi2 oxidation in 670-1498 K water vapor. 2016. Journal of the American Ceramic SocietyJ. 99 (4): 1412.

Wood, E. Sooby, J. T. White, D. D. Byler, and A. T. Nelson. The synthesis and air oxidation behavior of U-Si-Al and U-Si-B compositions. ANS Transactions.

Wood, E. Sooby, K. A. Terrani, and A. T. Nelson. Sensitivity of measured steam oxidation kinetics to atmospheric control and impurities. 2016. Journal of Nuclear Materials. 477: 228.

Foldamers: Design of Monodisperse Macro-Molecular Structure by Selection of Synthetic Heteropolymer Sequence

Charlie E. Strauss
20160044DR

Introduction

While there are various materials under the rubric of "foldamer", we use the term exclusively to mean individual long chain heteropolymers that fold by themselves to atomically reproducible complex 3D monomer architectures. As such, none exist outside of biology. Our goal is to produce and characterize the first suite of non-biological (synthetic) foldamers that fold into defined, low entropy, 3D architectures using in-silico design and experimental evolution, and to ultimately apply those structures toward functions of catalysis, hierarchical self-assembly with other macromolecules, and high-specificity sensors. Non-biological Foldamers are anticipated to have the same extraordinary material properties achieved by proteins: copies of the same polymer may differ in their relative atomic positions by less than an angstrom, unlocking quantum processes (for energy production from sunlight and vision) or electron transfer (to catalyze reactions by factors of 10^18). Precision and reproducibility also enable hierarchical self-assembly into complex macroscopic materials such as photonic crystals.

We provide innovations that will overcome the gaps that have, so far, kept the non-biological foldamer grand challenge from being realized in the lab. As applications intended for transition to Global Security customers, we will create foldamers for select-agent pathogen detection (Ebola Marburg) and a catalytic hydrolysis of nerve agents (using lab-safe simulants). Technologies produced in this project will also revolutionize combinatorial manipulation of block polymers in general, by unlocking library screening technologies with millions of times higher throughput than conventional assays. The LANL team members are externally recognized as leading experts in the multiple component technologies, making the expected breakthroughs truly a hard-to-copy LANL proprietary capability. With this capability, we anticipate DoD, DOE and Industry will fund transitional research in non-biodegradable foldamers for destruction of Chemical Warfare agents, water filtration, catalysis in harsh reactors, high specificity sensors, low dose catalytic drugs, and chiral enantiomer separation.

Benefit to National Security Missions

We are creating a fundamentally new class of engineered material with inherently broad impact across many application domains. This is seen by analogy to the bio-materials, proteins, whose unique folding ability enable materials with extreme performance: Catalysts with kCat/Uncat improvements of 10^18 and individual molecules that bind other very specific molecules with picomolar sensitivity make ideal filters. Impact across diverse fields occurs because Catalysis, Filters, and Sensors (via Sensitive/specific molecular binding) are core enabling requirements. Catalysis and binding cross cut the front line problems of numerous fields such as Forensic isolation of rare materials, fuel production, nerve agent destruction, crystal growth, extraction of Uranium complexes, therapeutic assays, drugs, or self assembling electronics and optics. Our new class of folding material will have similar capabilities but will withstand harsh environmental conditions and can incorporate non-biological dynamic functional materials (e.g. optic or electronic moieties). For example, reactors for cellulosic biofuel production currently lack alternatives to expensive protein enzymes, but these degrade rapidly at the temperature and pH of the reactor; peptoids have thermal and pH stability orders of magnitude better. For example, proteins provide catalytic nerve agent destruction but they are easily degraded when used as materials in austere non-biological environments (like coating equipment, soldier-protective fabrics). Peptoids are not easily degraded or microbially digested. Folding also allows materials that switch configuration, providing a basis for stimuli responsive smart materials. Our targeted functions are also credible preliminary results for diverse sponsors especially DTRA, DARPA, NIH and certain Intel sponsors.

Progress

Our objectives for the first year and associated accomplishments/progress are as follows:

- Order major equipment and chemicals: Completed
- Synthesis of peptoid monomers: We are in process on this and have manufactured 3 initial momomer types and experimental synthesis is underway of 6 more types resembling amino acid analogs.
- Synthesis of monodispersed peptoid blocks: We have manufactured peptoid blocks ranging in size from 3 to 13 monomers. We have 4 different types of blocks, 3 of which have good water solubility and one that is soluble in organic solvent.
- Synthesize combinations of blocks: Experiments are underway for this but not complete. We have also placed an order for commercial (external) synthesis of one target block assembly using pre-existing monomer types. The purpose of this is to accelerate our NMR characterization capability in advance of our custom blocks and monomer.
- Develop mutual compatible protection chemistry for DNA, proteins and peptoids: We have experimented with several candidate technologies for this already and are in the process of developing others. We have not down selected on any one technology yet as so far it has not been necessary to have linked peptoid, DNA or peptides.
- Validate and optimize GFP based fold selection method.
- Modeling of peptoid peptoid interactions: Four different approaches are in use here to differing degrees. Our primary tools are combination of homology modeling and Molecular dynamic relaxation in a traditional forcefield for block-block interactions. We are also using traditional compchem models for small molecule configurations. And finally work has been done with modeling the importance of water and hydrogen bonding in proteins (where we can more easily validate the model with existing data). Rosetta based modeling will come into play later in the project to roll up the combinatorial data sets (not yet available) into a comprehensive model.
- Hire postdocs: Two PD have been hired, we are making an offer two others (who have agreed to come when they graduate next month), we are interviewing

We are thus well along on the synthetic chemistry and lagging on the GFP fold selection validation.

Future Work

Our scope, goals and tasks for the upcoming FY are detailed below.

Science Goal: Develop, model and characterize peptoid polymer blocks as fundamental building units for (later) Foldamers

Technical Tasks

- Assemble apparatus
- Synthesize peptoid monomers
- Synthesize peptoid blocks
- Synthesize block combinations
- Develop chemistry for simultaneous DNA and peptoid addition.
- NMR characterization of blocks and combinations.
- Evaluate and down select on alternative synthetic techniques for dual DNA and peptoid molecules.
- Establish controls for entropy and physiological selection of folded polymers.
- Establish controls for physical characterization by NMR and other structural analysis such as CD, and Dynamic Light scattering. Tasks: establishing NMR protocols for peptoid backbones.
- Establish a molecular dynamics simulation system and demonstrate that dynamics can be controlled by sequence.
- Establish platform for predicting multiple helix interactions.

Management Goal: Transition from baseline outcomes and controls in each discipline to sharing common work product. The driving force of integration is establishing the path that leads to the same peptoid sequences to be used in the modeling, characterization and synthesis during year 2.

Conclusion

Control over synthetic polymer 3D architecture (“foldamers”) remains a grand challenge in material science. We are creating a fundamentally new class of engineered material with inherently broad impact across many application domains. This is seen by analogy to the bio-materials, proteins, whose unique folding ability enable materials with extreme performance. Our new class of folding material will have similar capabilities but will withstand harsh environmental conditions and can incorporate non-biological dynamic functional materials. This work impacts

energy security objectives by establishing novel catalyst. materials suited for high-temperature and strong pH in biofuel reactors for the efficient use, generation, storage, and impacts mitigation of energy derived from fossil fuels or renewables entails an energy production/delivery/utilization system. Foldamers can also supply the sophisticated molecular recognition required for hierarchical molecular self-assembly spanning millimeter scales— impacting national advanced manufacturing objectives.

Topology and Strong Correlations: A New Paradigm

Filip Ronning
20160085DR

Introduction

Over, the past five years the notion of topology in condensed matter has revolutionized the field resulting in new classifications of matter. Importantly, this concept predicts the existence of new and technologically promising states of matter (e.g. metallic states on the surfaces of otherwise good insulating materials), which are insensitive to perturbations such as disorder or deformations. In other words, these conducting states can be considered to be "protected" by their topology. These topological states have been observed in uncorrelated materials, but the challenge is to explore topology in strongly correlated materials. Strong electronic correlations profoundly modify a system and generate many novel states of a matter. Combining the concepts of topology with the presence of strong electronic correlations is expected to lead to exotic topological matter that is quite distinct from its uncorrelated counterpart. This project will develop a design approach to discovering new materials that display exotic topological properties.

Benefit to National Security Missions

We will deliver the scientific foundations to design the functionality of strongly correlated materials with non-trivial topology. Our success in discovering new topological states of matter and their properties in strongly correlated materials with non-trivial topology will lay the scientific foundation for tailoring functionality in correlated topological matter. With high tenability, reduced dimensionality and large mobilities, these materials can address national security needs in many impact areas including: sensing, metrology, quantum information, nuclear fuels, and spintronics. Our integrated approach combining synthesis, measurement and theory will develop the capability to convert atomic scale structure to bulk functionality precisely as envisioned in the White House's "Materials genome initiative", the "Mesoscale science" report from DOE-BES, and LANL's materials' strategy. The capabilities we will develop extend well beyond this project to include: an improved understanding of the electronic structure of actinides, the ability to design collective magnetic phenomena f-electron materials through the development of the "f-electron Goodenough Kanamori rules", and the scanning Kerr microscope will be a powerful probe of spin currents in potential new devices exploiting spin (spintronics) rather than charge as in conventional electronics, regardless of whether they are topological. Investigations of uncorrelated topological matter have attracted some of the best minds and talent to the field. Not only will our success position us well to impact other programs, it will attract talented postdocs chosen for their skills and retention potential to become future leaders at LANL.

Progress

Below is a snapshot of things that have been accomplished in the first year.

A furnace was purchased and tested in which we will grow the plutonium hexaboride crystals (a proposed strongly correlated topological insulator)

We performed thermal conductivity measurements on Weyl semimetal MoTe2, and observed a superconducting transition at 100 mK. In addition there was no-linear thermal heat transport in these crystals. Trivial explanations such as heat losses through supports can be excluded. Additional measurements are in progress to test this novel phenomenon.

A thin slab of tantalum arsenide was prepared , and we investigated its magneto optical properties using our optical Kerr microscope in fields to 7 T and temperatures down to 1.5 K looking for signatures of the chiral anomaly in this candidate Weyl semi metal. Both polar Kerr and longitudinal Kerr geometries are being explored. No clear experimental signature has been observed thus far, but experiments with higher resolution are on-going.

We also investigated the rare-earth monopnictide system neodymium antimony (NdSb). If the electronic

structure is identical to the lanthanum analog this system should be topologically non-trivial. From angle resolved photoemission and quantum oscillation studies we showed that indeed it is. Furthermore, the magnetism from the Nd atoms interacts with the electrons, yet the system retains a topologically interesting electronic structure.

Measurements were performed on niobium arsenide (a topological Weyl semimetal) in the quantum limit where electronic correlations could strengthen. We found that the magnetization data shows influences of the topological electronic structure. Measurements to higher fields are in progress.

The electronic structure of Ce3Bi4Pt3 is being investigated theoretically. This electronic correlations required to create an insulating state are being implemented by dynamical mean field calculations. Comparisons with experiment are in progress.

Future Work

We will develop a protocol for determining the topological invariants of strongly correlated materials. New theoretical work will be developed and validated by the synthesis of new topologically non-trivial strongly correlated materials. A goal will be the discovery of novel fractional states of matter that occur as a consequence of this interplay. We will follow up on successes from the past year. Specific capabilities we will develop include: 1) the ability to compute the topological invariants of strongly correlated materials, 2) the ability to determine the magnetic exchange interaction which will enable prediction of topologically non-trivial states in the spin degrees of freedom and how they may influence the surface state of a topological insulator, 3) a scanning Kerr microscope for which topological states of matter can be identified by the spin accumulation during charge or thermal transport, and 4) the ability to measure transport, thermodynamic and spectroscopic measurements of air-sensitive samples. In the next year, these capabilities will be developed through the study of RX, RB6, and A2RX3 compounds (R=4f or 5f element, A = alkali or alkili-element). In addition we will test our protocol on new promising families of materials.

Conclusion

We will develop a “materials by design” approach using state-of-the-art theory combined with new and existing experimental capabilities to rapidly identify correlated topological materials with new functionalities. We will explore f-electron based insulators - a natural choice due to their inherent strong electronic correlations and large spin-orbit coupling, which will lead to new topological orders. Our success will lay the foundation for the discovery of new states of correlated topological matter and control over the protected conducting surface states, which are promising candidates for future technologies. With high tenability, reduced dimensionality and large mobilities, these materials can address national security needs in many impact areas including: sensing, metrology, quantum information, nuclear fuels, and spintronics.

Publications

Luo, , N. J. Ghimire, Wartenbe, Choi, Neupane, R. D. McDonald, E. D. Bauer, Zhu, J. D. Thompson, and Ronning. Electron-hole compensation effect between topologically trivial electrons and nontrivial holes in NbAs. 2015. PHYSICAL REVIEW B. 92 (20).

Luo, , R. D. McDonald, P. F. S. Rosa, Scott, Wakeham, N. J. Ghimire, E. D. Bauer, J. D. Thompson, and Ronning. Anomalous electronic structure and magnetoresistance in TaAs2. 2016. SCIENTIFIC REPORTS. 6.

Neupane, , M. M. Hosen, Belopolski, Wakeham, Dimitri, Dhakal, Zhu, M. Z. Hasan, E. D. Bauer, and Ronning. Observation of Dirac-like semi-metallic phase in NdSb. 2016. JOURNAL OF PHYSICS-CONDENSED MATTER. 28 (23).

Wakeham, , E. D. Bauer, Neupane, and Ronning. Large magnetoresistance in the antiferromagnetic semimetal NdSb. 2016. PHYSICAL REVIEW B. 93 (20).

Additive Manufacturing of Mesoscale Energetic Materials: Tailoring Explosive Response through Controlled 3D Microstructure

Alexander H. Mueller
20160103DR

Introduction

The design and control of the mesoscale structure(s) of energetic materials, the critical length scale at which initiation and reactive burn in detonation occurs, promises to provide a means for tailoring the initiation sensitivity and performance of energetic materials. Fabricating high explosive (HE) structures with well-defined features at dimensions of this scale, in the 1-100 µm range, has been impossible to date using current manufacturing techniques, and thus has made the systematic study of their roles difficult. With recent advancements in additive manufacturing techniques, the facile synthesis of hierarchically-structured energetic materials is now within experimental reach, and will lead to fundamentally new pathways for manipulating HE performance, sensitivity and safety by controlling chemical dynamics as shock waves couple to designed, ordered structures at the mesoscale. This work seeks to change this paradigm by directly assembling hierarchical structures to tailor and control the functionality of high explosives through manipulation of defects, wave interactions leading to the formation of "hot spots," and ultimately control the reactive flow and explosive performance properties. This overarching goal will be accomplished by the timely convergence of additive manufacturing (AM) capabilities, synthetic chemistry developments in energetic polymers / cast-cure explosives, mesostructure-informed reactive burn models developed at LANL, and the ability to measure the reactive flow using novel in situ diagnostics including the commissioning of the Dynamic Compression Sector at the Advanced Photon Source. Using AM methods, we will engineer structural features into novel HE hierarchies that have been simply not previously possible to produced in an on-demand, rapid manner. Using inert and energetic "scaffolds" in 3-dimensions, which will then be filled with secondary explosive formulations, or alternately building, "from the bottom up", controlled, multi-dimensional novel HE structures will be fabricated and investigated.

Benefit to National Security Missions

LDRD investment in AM-HE will strategically accelerate LANL into a leadership position demonstrating the capabilities and expertise for controlling HE performance via chemical dynamics at the mesoscale. NNSA is investing heavily in rapid-turnaround AM demonstration and AM capabilities throughout the complex. This work will serve as a fundamental scientific basis with which to build numerous highly applied programs. The topical themes of this project overlap wholly with DOE programs in the NNSA Science Campaigns, specifically DOE/NNSA Campaigns 1, 2, and ASCI, and future stockpile concepts (including all-IHE systems, Re-use and new 3D informed reactive burn models) by providing a scientific basis for the design of new energetic materials. It is expected that the IP developed during project execution will be of interest to stakeholders already engaged with the laboratory, ranging from GS agencies to industrial partners such as Chevron. We also anticipate answering mission needs from DoD/DTRA and DARPA for new AM-HE candidates and synthetic chemistry expertise.

Progress

In the first year of this project we have made progress on developing an additive manufacturing (AM) technology for high explosives (HE). This involved both the development and optimization of a number of formulations for 3 different deposition techniques, as well as developing the custom instrumentation for controlling the deposition of these materials. Current printing capabilities allow for the controlled introduction of voids within the structure at dimensions of just over 100 um, in parts that have been printed at sizes exceeding 5 cm^3.

Current feedstock and printing techniques have been developed for Direct Ink Write (DIW), a deposition technique requiring a post build thermal cure; UV-cured DIW, where the part is cured by exposure to UV photons; and Fused Deposition Modeling (FDM), a thermal extrusion build technique that does not require a post-build cure.

Initial development of laser sintering techniques has also begun, with a low-cost, easily configurable laser sintering 3D printer being on order to develop this technique into a capability available to the DR team.

These capabilities have been used to generate numerous HE parts, with the latest focus being directionally structurally anisotropic geometries for the demonstration of directional sensitivity within an HE part. These parts are of equivalent formulations and densities, yet have purposely introduced linear voids in a direction either co-linear or orthogonal to the input shock. This provides an initial sample series to investigate the material response to such structural modifications.

Modeling of these structures with the SURF and IG models have revealed a discrepancy in the two model's predictions. The desensitization included in the SURF model predicts that the included voids within the anisotropic structures will lead to dramatically differing directional responses, with the detonation extinguishing in the co-linear case and propagating in the orthogonal structure, while the IG model predicts both will fully burn. It is important to note that the model material inputs were PBX-9501, a well characterized explosive, and that the calculations will be repeated as soon as EOS data for the current formulation is determined from upcoming gas gun experiments. These predictions will be tested with physical experiments before the end of this fiscal year.

Current diagnostics for small scale detonation experiments include pin wire diagnostics and a high speed camera capable of imaging the detonation front as it travels through the part. We are procuring a ultra-high speed camera dedicated to this project that will be capable of both the time and spatial resolution necessary to observe the effect of sample structure on performance. This new camera has a 1 billion frame per second (fps) frame rate with sub nanosecond integration times, allowing for crisp resolution of the shock wave as it travels through the sample. This will eliminate the uncertainty in the current cameras images as its image integration time smears out the shock front, introducing error into the time information and destroying the ability to resolve the interaction of the shock with defects. This new capability will be available to the team before the end of the fiscal year.

Inert additive parts with controlled structure have been imaged under shock conditions at the advanced photon source at Argonne. Phase Contrast Imaging (PCI) and Pulsed Doppler Velocimetry (PDV) data taken at the IMPULSE gas gun revealed interesting structurally dependent dynamic behavior that can be used to control pressure localizations within structured parts. While these experiment initially performed to provide calibration and training opportunities for the eventual HE experiments at APS' IMPULSE facility, the data generated is the first time that control of the shock dynamics in structured materials has been directly imaged. The results have direct applicability to controlling, directing and localizing pressure fields within a structured HE part, leading to a method of controlling the parts explosive behavior. Finite Element Modeling (FEM) of this effect has been performed and matches well with the experimental results, which are being written up in a manuscript to be submitted to a high impact journal soon.

Presentations of the project's progress have been made at a Joint Army, Navy, NASA, Air Force (JANNAF) meeting, a JOWOG meeting focused on additive manufacturing at NNSA and AWE, as well as in an additive manufacturing session at the international THERMEC'16 conference.

Future Work

Novel AM-HE will be fabricated with input from theory simulations to guide idealized architectures. The full safety basis and will be explored and instruments will be modified and/or developed to precisely and rapidly produce desired HE structures. AM feedstocks will be developed and fully characterized for safety and ability to print in AM instrumentation. Initial experiments will be performed on structured materials with large (>100μm) features in order to quickly demonstrate the first controlled functionality in AM-HE. Development of a higher resolution deposition system will allow for the fabrication of finer structures containing gradients and / or inclusions to keep pace with theoretical guidance.

Plate impact driven shock initiation experiments on HE feedstock materials developed for printing will be performed using the Lab's unique large bore (2") two-stage light gas gun. We will employ embedded electromagnetic gauging to measure particle velocity wave profiles allowing us to obtain the initial shock state, reactive flow associated with the shock-to-detonation transition, and run-distance-to-detonation (shock sensitivity) of the materials. The electromagnetic gauges average the flow spatially (over mm) within the explosive, and will provide direct particle velocity waveforms for parameterization of the Surf+ reactive burn model. Detonation propagation behaviors will be quantified in high fidelity cylinder, sandwich, and failure cone configurations using traditional (shorting wires, framing cameras) and new (mPDV, optical Bragg grating) diagnostics. A particularly exciting aspect of the proposed effort is the ability to fabricate functionally-graded AM-HE, which will have the effect of grading the detonation velocity and pressure as a function of position. This will be accomplished by studying AM-HE structures that exhibit

structural anisotropies, leading to different detonation dynamics depending on direction of initiation.

Conclusion

This effort will lay the groundwork necessary to fabricate additive manufacturing-HE with novel controlled initiation and reaction zone characteristics by attaining prompt reactive burn through control of the internal structure of the HE part. We aim to tailor shock sensitivity and detonation performance, and envision AM-HE that exhibits better corner-turning capabilities for applications such as more effective HE boosters. Once detonating, the effects of the tailored chemical reaction zone dynamics on detonation critical diameter, confinement edge angles, and failure characteristics will be quantified. A combination of meso-scale-to-continuum scale data will be used to construct a new mesoscale informed reactive burn model.

Publications

Dattelbaum, D., B. Branch, D. Montgomery, B. Clements, A. Ionita, B. Jensen, B. Patterson, A. Schmalzer, and A. Mueller. Control of shockwave dynamics within periodic porous architectures. Physical review Letters.

Frontiers in Quantum Science

Angel E. Garcia
20160587DR

Introduction

Quantum science increasingly involves the application of the tools and concepts of quantum mechanics to realizable systems with novel functionality and technological application. From a discovery perspective, new topologically constrained states in materials offer foundations for potential robust quantum computation. We will explore how strong electronic correlations give rise to a new powerful family of topological materials. The consideration of such materials requires new algorithms and measurement techniques, both of which we will improve and develop in this project. On the algorithm front, we will investigate quantum annealing algorithms, electronic structure algorithms, and quantum electrons coupled to classical spins. One new measurement technique we will apply is quantum noise spectroscopy. In a related area, we explore the fascinating intersection of thermodynamics and quantum mechanics, two of the main pillars of modern physics. Despite its name, dynamics is absent from most thermodynamic descriptions, and the standard theory can only describe quasi-static processes that are a succession of equilibrium states. Moving to quite applied materials, we consider finite-time (non-equilibrium) processes at the nanoscale that necessitate a quantum mechanical approach, whereby not only dynamics but also thermal and quantum fluctuations are taken into account. Moving to the optical domain, the powerful approaches of quantum chemistry will be applied to excited-state photonic processes including the characterization and design of nano-structured materials with unique electronic and optical properties. Ranging over electronic materials, photovoltaics and quantum emitters to biological matter, a combined powerful approach including theory, modeling and simulation will complement experimental advances by providing rich and nuanced interpretation of data and by extracting critical information about photoexcitation, emission, transport and decay mechanisms, all of which are vital for designing new functional nano-materials and devices. In related work on quantum fluctuation-induced forces, we will explore fundamentals of Casimir-like interactions and their implications of meta-materials development.

Benefit to National Security Missions

Our project on Frontiers of Quantum Science underpins fundamental science in electronic structure of materials, in quantum information, and in atomic and molecular cold atom systems. Our work on developing new electronic structure algorithms and using existing and new approaches to understand and predict the properties of materials has relevance in developing new materials for energy applications such as photovoltaic materials, modeling and predicting properties of f-electron matter including Plutonium for NW/NNSA mission objectives, and developing materials for quantum computing applications. We will also apply quantum information algorithms to address new approaches to quantum computing relevant to intelligence agency mission. Our work on cold-atom experiments is relevant to the design and implementation of unique sensor technology relevant DOE Office of Science mission. Our overall work on quantum magnetism and topological order in strongly correlated systems is highly relevant to the Fundamentals of Materials area whereas

Progress

One of the goals of this project is to compute electronic properties of novel perovskite photovoltaic materials using density-functional theory with close collaboration with experimental materials scientists who are developing these materials. We have made advances in the production of solution-processed organometallic perovskite films with possible applications to solar cells. In a combined experimental and theoretical/computational effort, we have shown that the slow photocurrent degradation in thin-film photovoltaic devices is due to the formation of light-activated meta-stable deep-level trap states. We investigated several physical mechanisms to explain the microscopic origin for the formation of

these trap states, among which the creation of small polaronic states involving localized cooperative lattice strain and molecular orientations emerges as a credible microscopic mechanism requiring further detailed studies. This work was been published in Nature communications.

The electronic, magnetic and optical properties of nanomaterials were modeled. Spin noise spectroscopy (SNS) is a quickly evolving interdisciplinary field of research. It explores spin interactions by tracing dynamics of spontaneous spin fluctuations at or near the thermodynamic equilibrium without the need to intentionally polarize spins. Higher order time correlators of spin fluctuations reveal considerable information about spin interactions. In a recent paper, we argued that in a broad class of spin systems, one could justify a phenomenological approach to explore such correlators. We predicted that the third and fourth order spin cumulants are described by a universal function that can be parametrized by a small set of parameters. We showed that the fluctuation theorem constrains this function so that such correlators are fully determined by lowest nonlinear corrections to the free energy and the mean and variance of microscopic spin currents. We also provided an example of microscopic calculations for conduction electrons. This was published in PhysRevLett.

We studied the properties of materials relevant to quantum computing. In this case, we studied the three-stage decoherence dynamics of an electron spin qubit in an optically active quantum dot. The control of solid-state qubits requires a detailed understanding of the decoherence mechanisms. For spin qubits in semiconductor quantum dots, phenomenological models of decoherence include two basic types of spin relaxation: fast dephasing due to static but randomly distributed hyperfine fields (~ 2 ns) and a much slower process (>1 ms) of irreversible monotonic relaxation due either to nuclear spin co-flips or other complex many-body interaction effects. Here we show that this is an oversimplification; the spin qubit relaxation is determined by three rather than two distinct stages. The additional stage corresponds to the effect of coherent precession processes that occur in the nuclear spin bath itself, leading to a relatively fast but incomplete non-monotonic relaxation at intermediate timescales (~ 750 ns). This work was published in Nature Physics.

We also the studied quantized beam shifts in graphene. Reflection and refraction of light are among the most common phenomena in optics. For a plane wave impinging on an interface separating two media, the propagation of the reflected and transmitted waves are governed by the Fresnel and Snell laws. However, this standard geometric optics picture does not apply for a beam of finite width consisting of the superposition of several plane wave components. In this case, spatial and angular deviations from the expected ray trajectories occur, resulting in beam shifts within and transverse to the incidence plane, respectively called Goos- Hanchen and Imbert-Fedorov shifts. We predicted quantized Imbert-Fedorov, Goos-Hanchen, and photonic spin Hall shifts for light beams impinging on a graphene-on-substrate system in an external magnetic field. In the quantum Hall regime, the Imbert-Fedorov and photonic spin Hall shifts are quantized in integer multiples of the fine structure constant a, while the Goos-Hanchen ones in multiples of alpha. We investigated the influence on these shifts of magnetic field, temperature, and material dispersion and dissipation. An experimental demonstration of quantized beam shifts could be achieved at terahertz frequencies for moderate values of the magnetic field. Our studies revealed a plethora of magneto- optical effects that ultimately originate from the chiral properties of electrons in Landau levels. We envision that the effects predicted in this work could be enhanced by using graphene metasurfaces owing to their ability to tailor both the magneto- optical response of graphene and the spin-orbit coupling of photons.

Future Work

- Develop time-dependent orbital-based Kohn-Sham Density Functional Theory (KSDFT) with molecular dynamics, in order to capture the dynamics of the warm dense matter electronic structure on the quantum level exposed to extreme external conditions (e.g.: ultrafast and highly intense laser pulses).
- Develop computational methodology and application to the simulations of electronic structure studies of ground and excited states of transition metal complexes with application to catalytic processes, and actinide chemistry.
- Compute electronic properties of novel perovskite photovoltaic materials using density-functional theory with close collaboration with experimental materials scientists who are developing these materials. Band structure of perovskite to determine optimal PV function. Excited state dynamics photo-excited electrons and holes. Charge transport through interfaces.
- Continue developing algorithms for the computing dynamic transitions between quantum states with applications to excited state processes in macromolecular materials. Apply to organic chromophores in opto-electronic systems.
- Model electronic structure and optical properties of nano-graphene quantum dots and compare results with synthesis and characterization experimental studies.
- Develop theoretical and computational models of

topological states of quantum matter with applications to quantum computation and quantum memory.

- Explore new hybrid classical/quantum algorithms for computing novel states of matter involving quantum magnetism. Expand this hybrid approach to efficiently compute quantum chemistry (molecular) systems.
- Investigate quantum information algorithms applied to annealing of quantum states and compare with experimental results.

Conclusion

We apply concepts and algorithms of quantum computation to (1) understand the electronic structure of materials from complex correlated systems (2) explore novel functionality in topologically protected states such as skyrmions, and (3) bridge concepts of fluctuation-induced forces with new meta-material technology. This work has relevance in developing new materials for energy applications such as photovoltaic materials, modeling and predicting properties of f-electron matter, including plutonium, for NNSA mission objectives, and developing materials for quantum computing applications.

Publications

Acconcia, T. V., M. V. Bonança, and S. Deffner. Shortcuts to adiabaticity from linear response theory. 2015. Physical Review E. 92 (4): 042148.

Adamska, L., G. V. Nazin, S. K. Doorn, and S. Tretiak. Self-Trapping of Charge Carriers in Semiconducting Carbon Nanotubes: Structural Analysis. 2015. The Journal of Physical Chemistry Letters. 6 (19): 3873.

Bechtold, A., D. Rauch, F. Li, T. Simmet, P. Ardelt, A. Regler, K. Müller, N. A. Sinitsyn, and J. J. Finley. Three-stage decoherence dynamics of an electron spin qubit in an optically active quantum dot. 2015. Nature Physics. 11 (12): 1005.

Bisset, R. N., W. Wang, C. Ticknor, R. Carretero-González, D. J. Frantzeskakis, L. A. Collins, and P. G. Kevrekidis. Bifurcation and stability of single and multiple vortex rings in three-dimensional Bose-Einstein condensates. 2015. Physical Review A. 92 (4): 043601.

Bjorgaard, J. A., K. A. Velizhanin, and S. Tretiak. Nonequilibrium solvent effects in Born-Oppenheimer molecular dynamics for ground and excited electronic states. 2016. The Journal of Chemical Physics. 144 (15): 154104.

Bricker, W. P., P. M. Shenai, A. Ghosh, Z. Liu, M. G. Enriquez, P. H. Lambrev, H. Tan, C. S. Lo, S. Tretiak, S. Fernandez-Alberti, and Y. Zhao. Non-radiative relaxation of photoexcited chlorophylls: theoretical and experimental study. 2015. Scientific Reports. 5: 13625.

D'Ambroise, J., M. Salerno, P. G. Kevrekidis, and F. K. Abdullaev. Multidimensional discrete compactons in nonlinear Schr\"odinger lattices with strong nonlinearity management. 2015. Physical Review A. 92 (5): 053621.

Deffner, S.. Viewpoint: Exorcising Maxwell's Demon. 2015. Physics. 8.

Deffner, S.. Shortcuts to adiabaticity: suppression of pair production in driven Dirac dynamics. 2016. New Journal of Physics. 18 (1): 012001.

Deffner, S., and A. Saxena. Quantum work statistics of charged Dirac particles in time-dependent fields. 2015. Physical Review E. 92 (3): 032137.

Dewar, W. K., J. Schoonover, T. McDougall, and R. Klein. Semicompressible Ocean Thermodynamics and Boussinesq Energy Conservation. 2016. Fluids. 1 (2): 9.

Gardas, B., and S. Deffner. Thermodynamic universality of quantum Carnot engines. 2015. Physical Review E. 92 (4): 042126.

Ghosh, K., E. R. Balog, J. L. Kahn, D. P. Shepherd, J. S. Martinez, and R. C. Rocha. Multicolor Luminescence from Conjugates of Genetically Encoded Elastin-like Polymers and Terpyridine-Lanthanides. 2015. Macromolecular Chemistry and Physics. 216 (18): 1856.

Hayami, S., S. Lin, and C. D. Batista. Bubble and skyrmion crystals in frustrated magnets with easy-axis anisotropy. 2016. Physical Review B. 93 (18): 184413.

Kort-Kamp, W. J., B. Amorim, G. Bastos, F. A. Pinheiro, F. S. Rosa, N. M. Peres, and C. Farina. Active magneto-optical control of spontaneous emission in graphene. 2015. Physical Review B. 92 (20): 205415.

Kort-Kamp, W. J., N. A. Sinitsyn, and D. A. Dalvit. Quantized beam shifts in graphene. 2016. Physical Review B. 93 (8): 081410.

Kort-Kamp, W. ., N. . Cordes, A. Ionita, B. . Glover, A. . Duque, W. . Perry, B. . Patterson, D. . Dalvit, and D. . Moore. Microscale Electromagnetic Heating in Heterogeneous Energetic Materials Based on X-ray Computed Tomography. 2016. Physical Review Applied. 5 (4): 044008.

Li, F., S. A. Crooker, and N. A. Sinitsyn. Higher-order spin-noise spectroscopy of atomic spins in fluctuating external fields. 2016. Physical Review A. 93 (3): 033814.

Li, F., and N. . Sinitsyn. Universality in Higher Order Spin

Noise Spectroscopy. 2016. Physical Review Letters. 116 (2): 026601.

Lin, S., S. Hayami, and C. D. Batista. Magnetic Vortex Induced by Nonmagnetic Impurity in Frustrated Magnets. 2016. Physical Review Letters. 116 (18): 187202.

Lin, S., and S. Hayami. Ginzburg-Landau theory for skyrmions in inversion-symmetric magnets with competing interactions. 2016. Physical Review B. 93 (6): 064430.

Nie, W., J. Blancon, A. J. Neukirch, K. Appavoo, H. Tsai, M. Chhowalla, M. A. Alam, M. Y. Sfeir, C. Katan, J. Even, S. Tretiak, J. J. Crochet, G. Gupta, and A. D. Mohite. Light-activated photocurrent degradation and self-healing in perovskite solar cells. 2016. Nature Communications. 7: 11574.

Reichhardt, C., D. Ray, and C. J. Reichhardt. Magnus-induced ratchet effects for skyrmions interacting with asymmetric substrates. 2015. New Journal of Physics. 17 (7): 073034.

Wang, W., P. G. Kevrekidis, R. Carretero-González, D. J. Frantzeskakis, T. J. Kaper, and M. Ma. Stabilization of ring dark solitons in Bose-Einstein condensates. 2015. Physical Review A. 92 (3): 033611.

Photoactive Energetic Materials for Quantum Optical Initiation

Robert J. Scharff
20140005DR

Abstract

The demand for safer high explosives (HE) that do not sacrifice performance has led to increased interest in alternate means of initiation. Photochemical and to a lesser extent electrochemical pathways to initiation could eliminate the need for HE with sensitivities to mechanical and thermal stimuli. Although some progress has been made toward optical initiation of energetic materials, conventional explosives absorb weakly in the ultraviolet region of the electromagnetic spectra and do not absorb in the visible and near-infrared regions, limiting the efficiency of laser initiation. Systems with optical and energetic properties that can be tuned independently are necessary to improve the efficiency of optical initiation. Furthermore, the development of new photoactive explosive materials, which optically initiate through quantum controlled photochemical dynamics, would provide a transformational advancement in the laser-based ignition of explosive materials. Ideal photoactive explosive materials will have low initiation thresholds for specific optical pathways while simultaneously having high initiation thresholds for all other conventional stimuli. Optical control can only be effective in newly designed materials that are synthesized to take advantage of such control; consequently, quantum control of optical initiation requires a thorough understanding of the excited state molecular dynamics that leads to photochemical decomposition of the explosive. To date, our efforts have focused on making new explosive materials with energetic optical chromophores, validation of their non-linear optical response properties through experiment and simulation, and experimental safety and sensitivity testing to determine viability of the new explosive materials. As a result, the optical initiation of novel, low-sensitivity explosives via direct laser heating (thermal process) has been achieved. On the other hand, optical initiation via quantum control of chemical dynamics (photochemical process) remains elusive.

Background and Research Objectives

The state-of-the-art in optical initiation. Current efforts to initiate explosives with lasers are driven by the increase in electrical safety requirements of weapons. Ideally, an insensitive (e.g., to spark, friction, fire, lightning flash) explosive could only be initiated with a laser. While it is possible to initiate explosives with a laser, the process is indirect and requires high laser energies.1-8 There are also applications that use very sensitive explosives that can be initiated with only a flash of light.9, 10 For laser initiation of pentaerythritol tetranitrate (PETN),1-8 several established routes to couple a laser field to the explosive are utilized:11 (1) the beam directly impinges on an explosive target resulting in a thermal response.7, 8 (2) The beam directly impinges on an explosive target that contains absorbing particles used to create local “hot spot” regions where chemical reactions develop.1-3 (3) The beam is fiber-optically coupled to the explosive through a metal layer sputter coated to the end of the fiber.4-6 The laser pulse vaporizes the metal layer to create a plasma that inputs a quasi isentropic compression wave into the explosive. In the all instances, the mechanism of initiation is not a direct photochemical process, but rather an indirect, shock-less deflagration (burning)-to-detonation transition (DDT). The problems with current optical initiation schemes are: (1) high energies are required, (2) initiation is “indirect”, and (3) initiation of the chemical reaction is not “controllable.”

Photochemistry is the key to control. The term photochemistry applies to chemical reactions that are induced by light-matter interactions. Upon absorption of light, the ground state population in a molecular system can transfer to an electronically excited state where a subsequent chemical reaction ensues. Classic examples of 1-photon induced photochemistry are the Norrish reactions with ketones and aldehydes;12, 13 3D microfabrication with nonlinear photoinitiator polymers is an example of 2-photon induced photochemistry.14-21 Broadly defined, the term “nonlinear” includes simul-

taneous multi-photon absorption, cascaded (sequential) 1-photon absorptions, and "pump-dump" processes; all of which are physical mechanisms that can be optimized to control chemical dynamics.

Our project pursued an alternate initiation scheme that uses ultrashort (<100 fs) optical pulses to trigger and control a net exothermic photochemical-to-DDT reaction. This could provide a significant improvement to current laser ignition schemes because of the direct absorption of the laser field by the explosive and increased optical sensitivity that allows the energy of the excitation source to be reduced. Furthermore, the wide spectral bandwidth of ultrashort optical pulses could make it possible to control chemical reactions22-24 responsible for explosive decomposition.

In our research effort, we identified three critical research areas that had reached a level of maturity, which could be brought to bear on the realistic development of photoactive energetic materials: synthesizing photoactive molecules with specific optical activity; excited state molecular dynamics prediction of the excited state potential energy surface; and achieving optical initiation with quantum control.

Scientific Approach and Accomplishments

Our strategy to both create and optimize the controllability of explosive photochemistry centers around the theory-guided design of new explosive materials derivatized with an energetic and linear and nonlinear optical (NLO) chromophore.25-29 It was our hypothesis that the optimization of optical responses would enable efficient coupling of the laser field to the molecule and facilitate the quantum control of photochemistry in highly excited molecular states. Furthermore, a fundamental understanding of the underlying excited state molecular dynamics was developed to predict and tune photochemistry.

Chemistry. Design strategies and structure-functionality relationships to alter nonlinear excitation spectra and wavelength dependent optical cross-sections are well established. For the application of explosive initiation, the chromophore-derivatized explosive should possess a combination of high quantum yield for photodissociation and non-zero optical cross-sections in the visible-NIR range (350 nm – 1200 nm). The factors that influence optical cross-sections and resonant frequency include the electronic delocalization of the chromophore and polarity of terminal functional groups. Since our design strategy involves derivatization of known explosive materials, an additional requirement that the chromophore not be detrimental to the overall energetic performance (e.g., detonation velocity and pressure) must also be satisfied. For example, conventional laser dyes with large 1PA or 2PA cross-sections do not possess the latter requirement and have been found to degrade the energetic performance of the explosive in preliminary evaluations.30

Over the duration of the project, we have established a very interdisciplinary research program aimed at understating the photochemical reaction dynamics of several tetrazine derivatized energetic molecules. Tetrazine is a promising high nitrogen energetic chromophore that has a large heat of formation and versatile chemistry for attachment to a number of ligands. Petrin tetrazine chloride was the initial focus of detailed study, since petrin is the trinitrate analog of PETN, the current DOE detonator explosive. Replacing PETN with a PETN derivatized with an energetic chromophore was a logical first step. Tetrazine was also derivatized with 2 PETN molecules, with dinitroazetidine (DNAZ), 2 DNAZ molecules, and nitroglycerin. More complex molecules with 2 DNAZ and tetrazines linked through an azo group were tested as a means to achieve extended conjugation and increase the two photon absorption. An energetic copper complex with 2 tetrazines and 2 nitrate groups was synthesized to form a charge transfer complex upon photoexcitation, that could lead to enhanced photochemistry. Several triazine-based energetics were also formed, which are accessible to irradiation in the near ultraviolet.

The design and testing of a practical quantum optically initiated energetic material was an ambitious goal for this DR project. Although this wasn't fully realized during this project, the high-quality science generated was very impressive and significant progress was made. The project has resulted in the design and synthesis of a less-sensitive molecule to PETN for direct photoinitiation and the synthesis and testing of over 75 new optically active explosive molecules. The development of a non-adiabatic molecular dynamics capability is recognized as a unique state-of-the-art LANL capability and the extension to open-shell systems and the incorporation of solvent effects are significant advances in the field. Notably, theoretical predictions drove the synthetic strategy away from the PETN tetrazine chloride system to other formulations. This result has already had a significant impact on optical detonator research and development in DOE-NNSA. Experimental observations and predictive theory have led the team to a new design that integrates the chromophore and explosive functional groups into a single molecule unit (ATTO), whereas other molecules that have been synthesized and found not to have activity as optical initiators are now being considered for photothermal initiation applications. This project is good example of a high-risk high-reward investment that, although not delivering on the primary

goal, has delivered high quality science.

The project's major accomplishments are provided in details below:

- Over 75 new energetic materials have been synthesized, characterized, and isolated for evaluation as quantum control materials.
- The energetic properties have been fully characterized for most materials.
- Discovered a triazine-derivatized nitrate ester molecule with interesting sensitivity properties.
- An improved method for the synthesis of azo-bridged triazines that utilizes a solid oxidant instead of chlorine gas has been developed and has facilitated the synthesis of new energetic azo-bridged triazine compounds.
- Iron complexes of several energetic tetrazines have been synthesized and show intense MLCT (metal to ligand charge transfer) bands in the visible region of the spectrum.
- Complexes of energetic tetrazine derivatives with Zinc, Copper, Nickel, and Cobalt have been synthesized and show increased intensity for ligand-based absorption with tunable sensitivity and explosive properties.
- Simulation of one and two photon absorption spectra of 12 synthesized materials, IR spectra of DNAZ-Tz and Petrin-TZ, and detailed analysis of excited state structures of Petrin-Tz.
- Novel theoretically interesting and application oriented formulations of implicit solvation models for excited state properties of charge-transfer states relevant to photochemistry.
- Implementation of implicit solvation models for excited state Born-Oppenheimer molecular dynamics, including existing and newly developed models for dynamic calculations of charge-transfer states.
- Performed quantum chemistry based parameterization of the force field for benzene molecule chemisorbed to RDX periodic molecular layer. Energy minimization and equilibration are performed demonstrating system stability. Modeling of two-photon excitation of benzene-RDX complex and subsequent excited state molecular dynamics set the stage for non-equilibrium molecular dynamics.
- The photochemical ring opening in Tetrazine dichloride has been simulated using NA-ESMD and the timescale for the production of the first intermediate photoproduct has been measured to be ~1 ps with a quantum yield of 0.72.
- The photochemical quantum yield for tetrazine photochemistry in PETN functionalized tetrazine is determined to be 0.003 after 4 ps in NA-ESMD simulations, showing that PETN stabilizes the tetrazine ring.
- The mechanism leading to tetrazine photochemistry in PETN functionalized tetrazine has been determined using NA-ESMD to result from intramolecular vibrational energy transfer. Specifically, excess electronic energy in converted into kinetic energy localized in the tetrazine ring. On the other hand we observe that when vibrational energy is directed to the PETN portion of the molecule, NO2 dissociation would be possible.
- The capability to measure solid-state photochemistry product infrared absorption spectrum and determine quantum yield of photochemistry in novel photoactive energetic materials was established.
- The capability to measure the gas phase product mass spectra of photoactive energetic materials was established.
- The photochemical quantum yield of Petrin (pentaerythritol trinitrate) chlorotetrazine has been measured at 532 nm with continuous wave and pulsed ns laser light as a function of intensity. It was found that substantial enhancement of photochemistry could be achieved with high intensity irradiation accessing higher excited states. A joint paper between experiment and theory regarding this work is close to submission.
- The photochemical quantum yield was measured for 10 materials for pulsed irradiation at 355 and 532 nm excitation.
- Two photoactive energetic materials were found that exhibited evidence of chemistry on the conventional energetic moiety, Petrin-Tz-Petrin at 355 nm excitation and DNAZ-Tz-Cl at 532 nm excitation.
- Raman spectra were obtained for the 12 prototype materials. Some of this data will be used in a joint paper with chemistry and experiment. This paper is in preparation and close to submission.
- Ultra-violet- visible spectra were obtained for novel materials.
- The capability to measure fluorescence quantum yield was established and was used on the prototype mate-

rials.

- Ultrafast experiments with nitromethane revealed multiple decomposition pathways on very short timescales.

Impact on National Missions

Control over vibrational energy relaxation and transfer is essential to optimize optical initiation processes in energetic materials. Generally this research direction represents long-standing interest in relaxation phenomena and localization, shocks and intense localization heating in complicated molecular systems. The capabilities developed in this project have relevance to other programmatic activities and the project team is currently pursuing several of these. The team is well connected to DOE-NNSA defense programs and Department of Defense sponsors. Notably, there has been interest from AWE in the use of photoactive binder materials. The JMP and DSW programs are also avenues that have been explored. In DSW, there is a current interest for something more than ablative detonators. New materials development appears to be a current focus for the DSW program.

References

1. Aluker, E. D., A. G. Krechetov, A. Y. Mitrofanov, and D. R. Nurmukhametov. Photochemical and Photothermal Dissociation of PETN during Laser Initiation. 2011. Russian Journal of Physical Chemistry BRussian Journal of Physical Chemistry B. 5 (4): 658.

2. Aluker, E. D., G. M. Belokurov, A. G. Krechetov, A. Y. Mitrofanov, and D. R. Nurmukhametov. Laser Initiation of PETN Containing Light-Scattering Additives. 2010. Technical Physics LettersTechnical Physics Letters. 36 (3): 285.

3. Aduev, B. P., D. R. Nurmukhametov, and A. V. Puzynin. Laser Initiation of a Mixture of PETN with NiC Nanoparticles at Elevated Temperatures. 2010. Russian Journal of Physical Chemistry BRussian Journal of Physical Chemistry B. 4 (3): 452.

4. Stewart, D. S., K. A. Thomas, S. Clarke, H. Mallett, E. Martin, M. Martinez, A. Munger, and J. Saenz. On the Initiation Mechanism in Exploding Bridgewire and Laser Detonators. 2006. AIP Conference ProceedingsAIP Conference Proceedings. 845 (1): 471.

5. Akinci, A., K. Thomas, A. Munger, L. Nunn, S. Clarke, M. Johnson, J. Kennedy, and D. Montoya. On the Development of a Laser Detonator. 2005. SPIE Optical Technologies for Arming, Safing, Fuzing, and FiringSPIE Optical Technologies for Arming, Safing, Fuzing, and Firing. 5871: 1.

6. Nagayama, K., K. Inou, and M. Nakahara. 2001.

7. Tarzhanov, V. I., A. D. Zinchenko, V. I. Sdobnov, B. B. Tokarev, A. I. Pogrebov, and A. A. Volkova. Laser Initiation of PETN. 1996. Combustion Explosion and Shock WavesCombustion Explosion and Shock Waves. 32 (4): 454.

8. Bykhalo, A. I., E. V. Zhuzhukalo, N. G. Kovalskii, A. N. Kolomiiskii, V. V. Korobov, A. D. Rozhkov, and A. I. Yudin. INITIATION OF PETN BY HIGH-POWER LASER-RADIATION. 1985. Combustion Explosion and Shock WavesCombustion Explosion and Shock Waves. 21 (4): 481.

9. Benham, R.. Preliminary experiments using light-initiated high explosive for driving thin flyer plates. 1980.

10. Benham, R.. A new LIHE (Light Initiated High Explosive) test capability for spherical targets. 1987.

11. Bourne, N. K.. On the laser ignition and initiation of explosives. 2001. Proceedings of the Royal Society A - Mathematical, Physical, and Engineering SciencesProceedings of the Royal Society A - Mathematical, Physical, and Engineering Sciences. 457 (2010): 1401.

12. Norrish, R. G., and C. H. Bamford. Photodecomposition of aldehydes and ketones. 1936. NatureNature. 138: 1016.

13. Norrish, R. G., and C. H. Bamford. Photo-decomposition of aldehydes and ketones. 1937. NatureNature. 140: 195.

14. Baldacchini, T., H. Chen, R. A. Farrer, M. J. Previte, J. Moser, M. J. Naughton, and J. T. Fourkas. Multiphoton photopolymerization with a Ti : sapphire oscillator. 2002.

15. Baldacchini, T., R. A. Farrer, J. Moser, J. T. Fourkas, and M. J. Naughton. Efficient multiphoton polymerization for the fabrication of 3-dimensional microstructures. 2003. Synthetic MetalsSynthetic Metals. 135 (1-3): 11.

16. Belfield, K. D., and K. J. Schafer. Two-photon photoinitiated polymerization. 2003.

17. Engelhardt, S., Y. Hu, N. Seiler, D. Riester, W. Meyer, H. Krueger, M. Wehner, E. Bremus-Koebberling, and A. Gillner. 3D-Microfabrication of Polymer-Protein Hybrid Structures with a Q-Switched Microlaser. 2011. Journal

of Laser Micro NanoengineeringJournal of Laser Micro Nanoengineering. 6 (1): 54.

18. Gu, J., W. Yulan, W. Chen, X. Dong, X. Duan, and S. Kawata. Carbazole-based 1D and 2D hemicyanines: synthesis, two-photon absorption properties and application for two-photon photopolymerization 3D lithography. 2007. New Journal of ChemistryNew Journal of Chemistry. 31 (1): 63.

19. Ovsianikov, A., A. Deiwick, S. Van Vlierberghe, P. Dubruel, L. Moeller, G. Draeger, and B. Chichkov. Laser Fabrication of Three-Dimensional CAD Scaffolds from Photosensitive Gelatin for Applications in Tissue Engineering. 2011. BiomacromoleculesBiomacromolecules. 12 (4): 851.

20. Ovsianikov, A., M. Malinauskas, S. Schlie, B. Chichkov, S. Gittard, R. Narayan, M. Loebler, K. Sternberg, K. P. Schmitz, and A. Haverich. Three-dimensional laser micro- and nano-structuring of acrylated poly(ethylene glycol) materials and evaluation of their cytoxicity for tissue engineering applications. 2011. Acta BiomaterialiaActa Biomaterialia. 7 (3): 967.

21. Steenhusen, S., T. Stichel, R. Houbertz, and G. Sextl. Multi-photon polymerization of inorganic-organic hybrid polymers using visible or IR ultra-fast laser pulses for optical or (opto-)electronic devices. 2010.

22. Brumer, P., and M. Shapiro. Control of unimolecular reactions using coherent light. 1986. Chemical Physics LettersChemical Physics Letters. 126 (6): 541.

23. Tannor, D. J., R. Kosloff, and S. A. Rice. Coherent pulse sequence induced control of selectivity of reactions: Exact quantum mechanical calculations. 1986. The Journal of Chemical PhysicsThe Journal of Chemical Physics. 85 (10): 5805.

24. Tannor, D. J., and S. A. Rice. CONTROL OF SELECTIVITY OF CHEMICAL-REACTION VIA CONTROL OF WAVE PACKET EVOLUTION. 1985. Journal of Chemical PhysicsJournal of Chemical Physics. 83 (10): 5013.

25. Chavez, D. E., and R. D. Gilardi. Synthesis of 3,6-bis(3-azido-1,2,4-triazol-1-yl)-1,2,4,5-tetrazine. 2009. Journal of Energetic MaterialsJournal of Energetic Materials. 27 (2): 110.

26. Chavez, D. E., and M. A. Hiskey. Synthesis of the bi-heterocyclic parent ring system 1,2,4-triazolo[4,3-b][1,2,4,5]tetrazine and some 3,6-disubstituted derivatives. 1998. Journal of Heterocyclic ChemistryJournal of Heterocyclic Chemistry. 35 (6): 1329.

27. Chavez, D. E., M. A. Hiskey, and R. D. Gilardi. 3,3'-Azobis(6-amino-1,2,4,5'tetrazine): A novel high-nitrogen energetic material. 2000. Angewandte Chemie - International EditionAngewandte Chemie - International Edition. 39 (10): 1791.

28. Chavez, D. E., M. A. Hiskey, and R. D. Gilardi. Novel high-nitrogen materials based on nitroguanyl-substituted tetrazines. 2004. Organic LettersOrganic Letters. 6 (17): 2889.

29. Chavez, D. E., M. A. Hiskey, and D. L. Naud. Tetrazine explosives. 2004. Propellants, Explosives, PyrotechnicsPropellants, Explosives, Pyrotechnics. 29 (4): 209.

30. Chavez, D. E.. Private communication. 2010. LANL.

Publications

Bjorgaard, J. A., A. Sifain, T. R. Nelson, T. W. Myers, J. M. Veauthier, D. E. Chavez, R. J. Scharff, and S. Tretiak. Two-photon absorption in conjugated energetic molecule. 2016. T-1: PHYSICS AND CHEMISTRY OF MATERIALS.

Bjorgaard, J. A., K. A. Velizhanin, and Tretiak. Solvent effects in time-dependent self-consistent field methods. II. Variational formulations and analytical gradients. 2015. JOURNAL OF CHEMICAL PHYSICS. 143 (5).

Bjorgaard, J. A., Kuzmenko, K. A. Velizhanin, and Tretiak. Solvent effects in time-dependent self-consistent field methods. I. Optical response calculations. 2015. JOURNAL OF CHEMICAL PHYSICS. 142 (4).

Bjorgaard, J. A., Nelson, Kalinin, Kuzmenko, K. A. Velizhanin, and Tretiak. Simulations of fluorescence solvatochromism in substituted PPV oligomers from excited state molecular dynamics with implicit solvent. 2015. CHEMICAL PHYSICS LETTERS. 631: 66.

Bjorgaard, J. A., T. R. Nelson, D. E. Chavez, S. D. Mcgrane, M. T. Greenfield, C. A. Bolme, R. J. Scharff, and S. Tretiak. Linear and Nonlinear Optical Processes for Photochemistry. 2015. T-1: PHYSICS AND CHEMISTRY OF MATERIALS.

Brown, K. E., S. A. Clarke, T. W. Myers, and R. J. Scharff. Optical approaches for enhanced safety. 2015. M-9: SHOCK AND DETONATION PHYSICS.

Brown, K. E., S. A. Clarke, T. W. Myers, and R. J. Scharff. Photoactive HE Detonator Options. 2016. M-9: SHOCK AND DETONATION PHYSICS.

Brown, K. E., T. W. Myers, R. J. Scharff, and S. A. Clarke. Laser Initiation of a Novel Energetic Fe(II) Complex. 2016. M-9: SHOCK AND DETONATION PHYSICS.

Chavez, D. E., T. W. Myers, J. M. Veauthier, M. T. Greenfield,

R. J. Scharff, and D. A. Parrish. Pentaerythritol Trinitrate Substituted s-Tetrazine and s-Triazine. 2015. SYNLETT. 26 (14): 2029.

Chavez, D. E., T. W. Myers, J. M. Veauthier, M. T. Greenfield, R. J. Scharff, and D. A. Parrish. Pentaerythritol Trinitrate substituted s-Tetrazine and s-Triazine. 2015. WX-7: HE SCIENCE AND TECHNOLOGY.

Chavez, D. E., T. W. Myers, J. M. Veauthier, M. T. Greenfield, R. J. Scharff, and D. A. Parrish. Pentaerythritol Trinitrate Substituted s-Tetrazine and s-Triazine. 2015. SYNLETT. 26 (14): 2029.

Dennis-Koller, D., R. J. Scharff, and D. A. Fredenburg. Experimentally Obtained Hugoniot Measurements for Granular Solids. 2013. WX-9: SHOCK AND DETONATION PHYSICS.

Greenfield, M. T., S. D. McGrane, C. A. Bolme, J. A. Bjorgaard, T. R. Nelson, S. Tretiak, and R. J. Scharff. Photoactive High Explosives: Linear and Nonlinear Photochemistry of Petrin Tetrazine Chloride. 2015. JOURNAL OF PHYSICAL CHEMISTRY A. 119 (20): 4846.

Greenfield, M. T., S. D. McGrane, K. E. Brown, D. S. Moore, and R. J. Scharff. Towards optical control of energetic materials. 2014. WX-9: SHOCK AND DETONATION PHYSICS.

Greenfield, M. T., S. D. McGrane, K. E. Brown, D. S. Moore, and R. J. Scharff. Towards optical control of energetic materials. 2014. WX-9: SHOCK AND DETONATION PHYSICS.

Greenfield, M. T., S. D. McGrane, K. E. Brown, R. J. Scharff, and D. S. Moore. Toward quantum controlled initiation of explosives. 2013. WX-9: SHOCK AND DETONATION PHYSICS.

Greenfield, M. T., S. D. McGrane, R. J. Scharff, K. E. Brown, and D. S. Moore. Toward quantum controlled initiation of energetic materials. 2013. WX-9: SHOCK AND DETONATION PHYSICS.

Greenfield, M. T., S. D. McGrane, R. J. Scharff, and D. S. Moore. Optimal Dynamic Detection of Explosives (ODD-Ex). 2013. WX-9: SHOCK AND DETONATION PHYSICS.

Greenfield, M. T., S. D. McGrane, R. J. Scharff, and D. S. Moore. Towards controlled optical initiation of energetic materials. 2014. WX-9: SHOCK AND DETONATION PHYSICS.

Greenfield, M. T., S. D. Mcgrane, C. A. Bolme, D. E. Chavez, J. M. Veauthier, S. K. Hanson, T. W. Myers, and R. J. Scharff. Photoactive energetic materials: linear and nonlinear photochemistry of chromophore linked energetic materials. 2015. WX-9: SHOCK AND DETONATION PHYSICS.

Greenfield, M. T., S. D. Mcgrane, C. A. Bolme, D. E. Chavez, J. M. Veauthier, T. W. Myers, S. K. Hanson, and R. J. Scharff. Photoactive energetic materials: linear and nonlinear photochemistry of chromophore linked energetic materials. 2015. M-9: SHOCK AND DETONATION PHYSICS.

Greenfield, M. T., S. D. Mcgrane, C. A. Bolme, D. E. Chavez, J. M. Veauthier, T. W. Myers, S. K. Hanson, and R. J. Scharff. Photoactive energetic materials: linear and nonlinear photochemistry of chromophore linked energetic materials. 2015. M-9: SHOCK AND DETONATION PHYSICS.

Greenfield, M. T., S. D. Mcgrane, C. A. Bolme, J. A. Bjorgaard, T. R. Nelson, S. Tretiak, and R. J. Scharff. Photoactive high explosives: linear and nonlinear photochemistry of petrin tetrazine chloride. 2015. WX-9: SHOCK AND DETONATION PHYSICS.

Greenfield, M. T., S. D. Mcgrane, K. E. Brown, D. S. Moore, and R. J. Scharff. Towards optical control of energetic materials. 2014. WX-9: SHOCK AND DETONATION PHYSICS.

Greenfield, M. T., S. D. Mcgrane, K. E. Brown, and R. J. Scharff. Understanding excited state dynamics is key to controlling optical initiation. 2015. WX-9: SHOCK AND DETONATION PHYSICS.

Hebert, P., D. S. Moore, S. D. Mcgrane, R. J. Scharff, K. E. Brown, M. Doucet, and C. Saint-Amans. P116: Experimental study of shock-induced chemistry in explosives. 2015. CEA/DAM.

Hernandez, Alfonso, Nelson, Tretiak, and Fernandez-Alberti. Photoexcited Energy Transfer in a Weakly Coupled Dimer. 2015. JOURNAL OF PHYSICAL CHEMISTRY B. 119 (24): 7242.

Kilina, , Kilin, and Tretiak. Light-Driven and Phonon-Assisted Dynamics in Organic and Semiconductor Nanostructures. 2015. CHEMICAL REVIEWS. 115 (12): 5929.

Kippen, K. E., B. C. Tappan, R. J. Scharff, G. R. Parker, C. Liu, X. Ma, B. E. Clements, K. J. Ramos, J. A. Leiding, E. V. Baca, C. A. Bolme, J. A. Bjorgaard, C. M. Cady, M. J. Cawkwell, D. E. Chavez, S. A. Clarke, J. D. Coe, N. L. Cordes, N. Dallman, D. M. Dattelbaum, R. DeLuca, P. Dickson, M. T. Greenfield, R. L. Gustavsen, S. K. Hanson, E. M. Heatwole, B. F. Henson, M. D. Holmes, D. E. Hooks, A. Ionita, K. Lam, C. C. Long, M. L. Lovato, S. D. Mcgrane, R. Menikoff, E. A. Moro, T. W. Myers, T. R. Nelson, A. M. Novak, D. M. Oschwald, B. M. Patterson, A. Piryatinski, P. J. Rae, D. N. Seitz, C. B. Skidmore, L. B. Smilowitz, D. G. Thompson, S. Tretiak, L. D. Vaughan, J. M. Veauthier, D. K. Zerkle, and D. Z. Zhang. Energetic

Materials Posters. 2015. ADEPS: EXPERIMENTAL PHYSICAL SCIENCES.

McGrane, S. D., C. A. Bolme, M. T. Greenfield, D. E. Chavez, S. K. Hanson, and R. J. Scharff. Photoactive High Explosives: Substituents Effects on Tetrazine Photochemistry and Photophysics. 2016. JOURNAL OF PHYSICAL CHEMISTRY A. 120 (6): 895.

Mcgrane, S. D., C. A. Bolme, M. T. Greenfield, D. E. Chavez, S. K. Hanson, and R. J. Scharff. Photoactive High Explosives: Substituents Effects on Tetrazine Photochemistry and Photophysics. 2015. M-9: SHOCK AND DETONATION PHYSICS.

Mcgrane, S. D., M. T. Greenfield, C. A. Bolme, and R. J. Scharff. Spectroscopy and characterization team. 2015. WX-9: SHOCK AND DETONATION PHYSICS.

Myers, T. W., C. Snyder, D. E. Chavez, R. J. Scharff, and J. M. Veauthier. Electrochemistry in nitrate ester functionalized 1,2,4,5-tetrazines and 1,2,4-triazolo[4,3-b]-[1,2,4,5]-tetrazines. 2016. M-7: HE SCIENCE AND TECHNOLOGY.

Myers, T. W., D. E. Chavez, S. K. Hanson, R. J. Scharff, B. L. Scott, J. M. Veauthier, and R. Wu. Independent Control of Optical and Explosive Properties: Pyrazole-Tetrazine Complexes of First Row Transition Metals. 2015. M-7: HE SCIENCE AND TECHNOLOGY.

Myers, T. W., D. E. Chavez, S. K. Hanson, R. J. Scharff, B. L. Scott, J. M. Veauthier, and R. Wu. Independent Control of Optical and Explosive Properties: Pyrazole-Tetrazine Complexes of First Row Transition Metals. 2015. INORGANIC CHEMISTRY. 54 (16): 8077.

Myers, T. W., J. A. Bjorgaard, D. E. Chavez, S. K. Hanson, R. J. Scharff, S. Tretiak, and J. M. Veauthier. Energetic Chromophores: Tuning Charge Transfer in Explosive Fe(II) Tetrazine Complexes. 2015. M-7: HE SCIENCE AND TECHNOLOGY.

Myers, T. W., J. A. Bjorgaard, K. E. Brown, D. E. Chavez, S. K. Hanson, R. J. Scharff, S. Tretiak, and J. M. Veauthier. Energetic Chromophores: Low-Energy Laser Initiation in Explosive Fe(II) Tetrazine Complexes. 2016. Journal of the American Chemical Society. 138 (13): 4685.

Myers, T. W., J. A. Bjorgaard, K. E. Brown, D. E. Chavez, S. K. Hanson, R. J. Scharff, S. Tretiak, and J. M. Veauthier. Energetic Chromophores: Tuning Charge Transfer in Explosive Fe(II) Tetrazine Complexes. 2016. M-7: HE SCIENCE AND TECHNOLOGY.

Myers, T. W., J. A. Bjorgaard, K. E. Brown, D. E. Chavez, S. K. Hanson, R. J. Scharff, S. Tretiak, and J. M. Veauthier. Energetic Chromophores: Low-Energy Laser Initiation in Explosive Fe(II) Tetrazine Complexes. 2016. Journal of the American Chemical Society. 138 (13): 4685.

Myers, T. W., J. A. Bjorgaard, K. E. Brown, D. E. Chavez, S. K. Hanson, R. J. Scharff, S. Tretiak, and J. M. Veauthier. Energetic Chromophores: Tuning Charge Transfer in Explosive Fe(II) Tetrazine Complexes for Laser Initiation. 2016. M-7: HE SCIENCE AND TECHNOLOGY.

Myers, T. W., J. A. Bjorgaard, K. E. Brown, D. E. Chavez, S. K. Hanson, R. J. Scharff, S. Tretiak, and J. M. Veauthier. Energetic Chromophores: Low Energy Laser Initiation in Fe(II) Te-trazine Complexes. 2016. M-7: HE SCIENCE AND TECHNOLOGY.

Myers, T. W., K. E. Brown, D. E. Chavez, R. J. Scharff, and J. M. Veauthier. Factors influencing thermal stability, mechanical sensitivity and laser initiation in synthesized Cu(II) tetrazine explosives. 2016. M-7: HE SCIENCE AND TECHNOLOGY.

Nelson, T. R., M. T. Greenfield, S. D. Mcgrane, J. A. Bjorgaard, C. A. Bolme, S. Tretiak, and R. J. Scharff. Modeling photochemistry of chromophore-linked photoactive energetic materials. 2015. T-1: PHYSICS AND CHEMISTRY OF MATERIALS.

Nelson, T. R., R. J. Scharff, M. T. Greenfield, S. D. Mcgrane, C. A. Bolme, S. Tretiak, and J. A. Bjorgaard. Modeling Photochemistry with Nonadiabatic Excited State Molecular Dynamics. 2015. T-1: PHYSICS AND CHEMISTRY OF MATERIALS.

Nelson, T. R., S. Tretiak, R. J. Scharff, J. A. Bjorgaard, M. T. Greenfield, and S. D. Mcgrane. Ultrafast Photodissociation Dynamics of Nitromethane. 2015. T-1: PHYSICS AND CHEMISTRY OF MATERIALS.

Nelson, T., J. Bjorgaard, M. Greenfield, C. Bolme, K. Brown, S. McGrane, R. J. Scharff, and S. Tretiak. Ultrafast Photodissociation Dynamics of Nitromethane. 2016. JOURNAL OF PHYSICAL CHEMISTRY A. 120 (4): 519.

Rigg, P. A., R. A. Saavedra, and R. J. Scharff. Sound speed measurements in zirconium using the front surface impact technique. 2013. WX-9: SHOCK AND DETONATION PHYSICS.

Rigg, P. A., R. A. Saavedra, and R. J. Scharff. Sound Speed Measurements in Zirconium using the Front Surface Impact Technique. 2013. WX-9: SHOCK AND DETONATION PHYSICS.

Rigg, P., R. S. Hixson, R. J. Scharff, and M. Knudsen. Determining the window correction in LiF to the limit of transmissibility. 2015. Washington State University.

Scharff, R. J.. Excited State Processes in Novel Energetic Materials. 2016. M-9: SHOCK AND DETONATION PHYSICS.

Scharff, R. J.. Photo-Actice High Explosives. 2015. M-9: SHOCK AND DETONATION PHYSICS.

Scharff, R. J.. Photoactive energetic materials for quantum optical detonation. 2015. WX-9: SHOCK AND DETONATION PHYSICS.

Scharff, R. J.. Photo-Actice High Explosives. 2015. M-9: SHOCK AND DETONATION PHYSICS.

Scharff, R. J.. Photoactive High Explosives. 2015. M-9: SHOCK AND DETONATION PHYSICS.

Scharff, R. J.. Photoactive Energetic Materials for Quantum Optical Initiation. 2015. WX-9: SHOCK AND DETONATION PHYSICS.

Scharff, R. J.. Photoactive energetic materials for quantum optical initiation: Project Overview. 2015. WX-9: SHOCK AND DETONATION PHYSICS.

Scharff, R. J.. Excited State Processes in Novel Energetic Materials. 2016. M-9: SHOCK AND DETONATION PHYSICS.

Scharff, R. J., M. T. Greenfield, S. D. McGrane, D. S. Moore, D. E. Chavez, S. Tretiak, and T. R. Nelson. Novel energetic materials for quantum optical initiation. 2013. WX-9: SHOCK AND DETONATION PHYSICS.

Scharff, R. J., P. A. Rigg, and R. S. Hixson. Sound speed measurements in tantalum using the front surface impact technique. 2013. WX-9: SHOCK AND DETONATION PHYSICS.

Scharff, R. J., P. A. Rigg, and R. S. Hixson. Rarefaction wave propagation and longitudinal sound velocities in shock compressed tantalum to 105 GPa. 2013. WX-9: SHOCK AND DETONATION PHYSICS.

Scharff, R. J., P. A. Rigg, and R. S. Hixson. Careful determination of phase transitions from post-shock sound speed measurements: release wave propagation in shock compressed tantalum to 105 GPa. 2013. WX-9: SHOCK AND DETONATION PHYSICS.

Sifain, A. E., J. Bjorgaard, T. Nelson, T. W. Myers, J. M. Veauthier, D. E. Chavez, R. J. Scharff, and S. Tretiak. Two-Photon Absorption in Conjugated Energetic Molecules. 2016. T-CNLS: CENTER FOR NONLINEAR STUDIES.

Snyder, C., D. E. Chavez, J. M. Veauthier, T. W. Myers, and R. J. Scharff. A novel triazolotriazine-carbonitrile and related molecules. 2016. M-7: HE SCIENCE AND TECHNOLOGY.

Snyder, C., T. W. Myers, D. E. Chavez, J. M. Veauthier, and R. J. Scharff. A novel triazolotriazine-carbonitrile and related molecules. 2016. M-7: HE SCIENCE AND TECHNOLOGY.

Veauthier, J. M., D. E. Chavez, S. K. Hanson, T. W. Myers, R. Wu, B. L. Scott, and R. J. Scharff. New Materials for Controlled Initiation of Explosives. 2015. C-IIAC: INORGANIC ISOTOPE & ACTINIDE CHEM.

White, A. J., V. N. Gorshkov, Tretiak, and Mozyrsky. Nonadiabatic molecular dynamics by accelerated semiclassical Monte Carlo. 2015. JOURNAL OF CHEMICAL PHYSICS. 143 (1).

White, A. J., V. N. Gorshkov, Wang, Tretiak, and Mozyrsky. Semiclassical Monte Carlo: A first principles approach to non-adiabatic molecular dynamics. 2014. JOURNAL OF CHEMICAL PHYSICS. 141 (18).

Multiferroic Response Engineering in Mesoscale Oxide Structures

Dmitry A. Yarotski
20140025DR

Abstract

Multiferroic (MF) materials exhibit strongly coupled magnetic and ferroelectric (FE) orders and promise transformative technologies in energy, security, and information processing. However, the inability to synthesize epitaxial materials with desired 3D structure and to probe the emergent properties resulting from atomic-to-mesoscale evolution poses significant challenges to modern condensed matter theory in providing a predictive description of the strong coupling among spin, charge, orbital, and lattice degrees of freedom. As a result, new materials discovery has often relied on serendipitous findings rather than on scientific principles underpinning the magnetoelectric (ME) functionality. We applied a systematic co-design approach to the discovery of MFs based on a closed synthesis-characterization-modeling loop. We emphasize the rapid feedback from the experimental validation to theoretical prediction and vice versa. Our approach was enabled by a combination of recent LANL breakthroughs in first-principles modeling of complex electron correlation phenomena, controllable synthesis of 3D mesoscale films, and novel coherent photon probes of intrinsic dynamics of competing orders in MF composites. Together, they allowed us to unveil critical parameters of MF material performance and demonstrate the highest magnetoelectric coupling constant of ~2000 mV/cm-Oe observed to date in strain-coupled nanocomposites. This comprehensive suite of theoretical and experimental tools provides LANL with an unmatched capability for accelerated material discovery that will not only allow us to create MF materials with enhanced ME response but will also be vital to realization of LANL's vision on the design of other mission-relevant materials. Our approach and effort address LANL priorities in 'meso'-science development, align well with the MaRIE vision of 'material co-design,' and develops new integrated capabilities in synthesis, theory, and ultrafast x-ray characterization. Therefore, we expect this work to have a direct and significant impact on near- and long-term LANL programs in Advanced Materials, Global Security, Information Science and Technology, and Clean Energy.

Background and Research Objectives

The last few decades have seen the discovery of novel classes of materials where competing interactions lead to exotic properties that few would have imagined. Multiferroics stand out among them due to the ability to change magnetization and/or electronic polarization states with either electric or magnetic fields. Additionally, MF materials have the potential to revolutionize future energy, sensing, and information technologies. For example, MF material allows the realization of 4-state logic in a single device which has the advantages of low power consumption and high speed. This blending of attributes combines the best features of field-effect devices and magnetic memory elements.

However, the creation of solid-state materials with coupled magnetic and electric long-range orders has proven to be a challenging task. The difficulty arises from the seemingly incompatible origins of the two orders. Ferromagnetism (FM) and antiferromagnetism (AFM) (i.e. magnetic ordering) emerges from electron spin alignment in partially filled ionic shells, while FE polarization (i.e. electric ordering) is usually produced by coherent shifts of charged ions with completely filled or empty shells. Nevertheless, several bulk MF materials have been discovered, where the crystal symmetry induces weak interactions between magnetic and electric responses, albeit only at non-practical very low temperatures or high magnetic fields. To address this challenge, a new paradigm in understanding and controlling the functionality of correlated electron materials, including MFs, has recently been demonstrated by the growth of epitaxial transition metal-oxide multilayers. In these hybrid structures two or more materials with a particular set of orders are interfaced to produce new functionality unavailable in individual constituents. Limited success in producing ME coupling has been

demonstrated prior to our work by (i) combining magnetostrictive and electrostrictive components and coupling their responses through field-induced strain, and (ii) using exchange bias across an interface to couple FM order in one component to an anti-FM (AFM) order in the second material with weakly interacting AFM and FE orders. In spite of these advances, the conventional "making-then-measuring" approach has stalled producing strong ME coupling in layered or 2D MF composites due to inability of tackling the materials complexity and vast variety of possible nanocomposite geometries: the highest reported ME voltage figure-of-merit (FOM) αME = ΔE/ΔH did not exceed 50 mV/cm-Oe. Moreover, a growing body of evidence has revealed that ME response in a 2D (or layered) structure is often limited by the 'clamping' effects from the substrate. On the other hand, introduction of full 3D control in mesoscale films should have provided new pathway to design and manipulation of materials functionalities inaccessible in the 2D geometries, due to exceptional tunability of anisotropy, percolation, and range of interactions, and strain landscapes in 3D nanocomposites.

Therefore, our primary objective was to apply a systematic co-design approach based on a synthesis-characterization-modeling loop, envisioned by the Materials Genome Initiative, to develop scientific principles that underpin ME coupling in mesoscale 3D MF composite films and to enable a rational design of ME functionality. To reach this goal, we used our team's unique expertise in theoretical simulation of multifunctional metal oxide materials to identify the smost prominent composite structures and subsequently refine multi-scale (nano-to-meso) models by synthesizing and characterizing ME properties of such structures and comparing them to the theoretical predictions. In synthesis, we created new capabilities for fabrication of epitaxial MF materials with the desired nanopillars-in-matrix structure where size, distribution and ensuing strain fields around nanopillars can be reliably controlled by process speed, temperature and materials ratio choice. We have also developed new coherent photon techniques at LANL (high-intensity terahertz, ultrafast X-Ray magnetic spectroscopy and microscopy) and used existing advanced penetrating probes at neutron sources and synchrotrons in order to provide an adequate insight into emergent properties of MF nanocomposites resulting from strong coupling among spin, charge, orbital, and lattice degrees of freedom across multiple scales.

Together, these advances represent a long-sought co-design approach that will ultimately enable real-time refinement of theory, synthetic procedures, and composite geometry to achieve desired functionalities. In particular, it allowed us to reveal a number of physical parameters (interface/volume ratio, pillar size and spacing, interface termination etc.) that are critical to functionality of MF composites, and enabled demonstration of CoFe2O4:BaTiO3 heterostructures with the highest magnetoelectric coupling constant of ~2000 mV/cm-Oe observed to date. As such, this project provides LANL with an unmatched capability for accelerated material discovery that will not only allow us to create MF materials with enhanced ME response but will also be vital to realization of LANL's vision on the design of other mission-relevant materials such as superconductors and actinides.

Scientific Approach and Accomplishments

Our ultimate goal was to harness the 3D material structure to understand, manipulate, and control ME functionality of epitaxial oxide composites. Here, we highlight only several representative results, which reveal critical parameters for MF nanocomposite design but by no means encompass all of the accomplishments of this project.

Integration of synthesis and characterization with theory to demonstrate the full potential of the co-design loop is indeed the key to the success of this project. In an effort to build multi-scale modeling framework capable of predicting response of multiferroic oxide heterostructures, we have combined molecular dynamics (MD) simulation capability to extract the structural information at interfaces, and density functional theory (DFT) to study the electronic/magnetic responses of the obtained structures. Integration into a single simulation package TBM3 (Tight Binding Modeling for Materials at Mesoscale) allows: (i) simplified construction of various lattice structures, (ii) capturing interface/ microstructure electronic and magnetic properties, (iii) description of local and global dielectric properties, and (iv) significant acceleration of calculations with linear-scaling method. TBM3 not only enables simulations of surface terminations at specific interfaces, but also reveals the effects of lattice distortions such as dislocations and point defects. This package will be released for public use in the near future and will aid research groups around the world to model and understand emergent phenomena in materials with heterogeneities and strong coupling among multiple degrees of freedom.

We have used TBM3 and multiple experimental probes to reveal the mechanisms of magnetic coupling across the interface between multiferroic FE/AFM BiFeO3 (BFO) and ferromagnetic (FM) La1-xSrxMnO3 (LSMO). In order to understand the implications of BFO pillar structure in LSMO matrix on the ME coupling, we calculated the net magnetization induced in BFO and LSMO in the proximity of interfaces. Using initially AFM ordered BFO and FM ordered LSMO, we have shown that induced magnetiza-

tion in LSMO/BFO superlattice is expected to extend from the interface through several atomic layers of the BFO, in good agreement with polarized neutron reflectometry. [1] We have also electronically relaxed both system and found that collinear alignment of magnetization axis in both LSMO and BFO is more favorable than their perpendicular mutual orientation. These results explained the dependence of induced magnetization in BFO on the LSMO termination plane at the interface that was observed in our neutron scattering experiments.[2] Moreover, this effect should also lead to reduced magnetization in LSMO near the interface due to spin disorder induced by the exchange bias, which was again confirmed in our ultrafast optical and static X-Ray magnetic circular dichroism (XMCD) spectroscopy measurements on BFO/LSMO superlattices. Overall, these findings demonstrated an importance of materials chemistry and elemental termination at the interfaces for the final performance of the MF heterostructure, and can be used as control parameters in atomic layer-by-layer deposition that recently become available with molecular beam epitaxy methods.[3] Introduction of TBM3 have also allowed us to study magnetic interactions in double perovskite MF BiFe2Mn2O6 (BFMO) and at BFO/LSMO interfaces in the presence of oxygen vacancies.[4] Although this work is still in progress, our initial results show that a measureable density of oxygen vacancies in BFO and LSMO leads to a competition between degradation and enhancement of FE/DM responses due to different effects as a function of oxygen concentration and location in the lattice. This suggests that oxygen doping/depletion can be used as another control parameter for MF functionality in nanocomposites after these effects are understood and verified experimentally using thermodynamic measurements and X-Ray magnetic spectroscopies.

To determine effects of the nanocomposite structure on the strain landscapes and emerging properties, we have studied the problem of strain distribution and electronic localization/delocalization on magnetic properties in disordered FM systems. By targeting the structural disorder relevant to MgO pillars in LSMO matrix structure, we have found that with a given strength of an impurity barrier, there is a critical thickness, below which the low-energy electronic wave functions become localized. This work give a corresponding explanation to the experiment which measure the transport property for the LSMO system with a critical thickness. To test this prediction, we created a series of LSMO films of varying thickness and nanopillar samples where effective “thickness” of LSMO was continuously varied by changing LSMO fraction in LSMO/MgO composite from nanoscale pillar to mesoscale matrix. Magnetization and XMCD measurements have clearly shown continuous degradation of conductivity and FM response with increased strain in LSMO. On the other hand, large and uniform vertical strain that can be achieved in pillar-in-matrix nanocomposites within direct lattice matching framework, significantly modifies magnetic and magneto-transport properties and leads to an enhanced magnetoresistance in LSMO:MgO heterostructures. We have determined that the ultimate strain in these systems is controlled by the vertical interface area between the MgO nanoscaffold network and the film matrix. By changing the nanoscaffold density and dimensions, the strain state can be tuned, and so are the magnetic properties. We have established a strong correlation between the vertical interface area, —vertical strain and —magnetic properties in 3D nanoscaffolding thick films. These results proved that the vertical heterointerface area is a critical factor in both determining the ultimate strain and manipulating magnetic and magnetoelectric functionalities of 3D nanocomposite films.[5]

Finally, using all these control parameters we simulated an optimal composition and created high quality BaTiO3:CoFe2O4 (BTO:CFO) vertical nanocomposite thin films with FM CFO nanopillars in FE BTO matrix using our advanced pulsed laser deposition capabilities. Using piezoresponse force microscopy and second harmonic generation spectroscopy in magnetic field, we have demonstrated a longitudinal ME coefficient α31 of over 2000 mV/cm Oe - the largest achieved to date in strain-coupled heterostructures. It was found that the ME coupling at low magnetic fields in vertical nanocomposites is dominated by the volume change between the two phases rather than strain mediated vertical interface coupling mechanism in bilayers and heterostructures. As the field is increased, interfacial strain starts to dominate and changes the sign of the coupling constant while preserving the strength of ME coupling in this material. These results should aid in optimization of multiferroic functionality of other nanocomposites by controlling strain field distribution across the interfaces.[6]

In parallel to optimizing composite multiferroic architectures, we have continuously searched for new single-phase materials with enhanced magnetization, polarization and ME coupling that can be used in nanostructure fabrication. For example, double perovskite Bi2FeMnO6 (BFMO) is a potential candidate for the highly sought room-temperature multiferroic system. We have studied the magnetic, electronic and optical properties and their interplay in double perovskite Bi2FeMnO6 (BFMO) by using both the first-principles computation and experiment. Our ab initio calculations captured the complex exchange interactions between Fe and Mn sites which cause ferromagnetic (anti-parallel) spin alignment on these ions. The

predicted magnetic moment qualitatively agrees well with Goodenough-Kanamori theory but our calculations reveal the importance of onsite (on both Mn and Co) correlations that should be accounted for using Hubbard model. These correlations open up an insulating band gap providing the possibility for simultaneous existence of ferrimagnetic and FE ordering in BFMO. Initial modeling results disagreed with our XMCD spectra and measurements of magnetic moments of Fe and Mn ions which provided immediate feedback for improving our first-principle computation routines. Better match to experimental data could be achieved by accounting for complex interplay between the distortions and the disorder of the cation (Fe, Mn) sites as well as the magnetic structure. Improved accuracy of the calculations will enable better understanding and design of interfaced systems: recently, we used it to demonstrate strong dependence of net magnetization on strain in BFMO nanostructures which can be tested by varying substrate materials in XMCD and magnetization measurements.[7]

Impact on National Missions

This project aims to develop basic principles to control macroscale multiferroic (MF) functionality in mesoscale composites through tuning the interactions on the nanoscale. This research directly supports all three central themes of the Materials for the Future pillar in harnessing defects, interfaces and electromagnetic field extremes to control collective behavior in MF materials. Our approach also addresses LANL's priorities in 'meso'-science development and practical realization of design principles towards both tunable and controlled functionality of complex materials. The proposed effort aligns well with the MaRIE vision of 'material co-design' and develops new integrated capabilities in synthesis, theory, and ultrafast x-ray characterization for MaRIE. This project further leverages the user programs at LCLS, APS, CINT, NHMFL, and the Lujan Center in accord with the LANL institutional priority in supporting national user facilities. Materials with tunable functionality are enabling components in energy, sensing, and information technologies. Therefore, we expect this work to have a direct and significant impact on near- and long-term LANL programs in Advanced Materials, Global Security, Information Science and Technology, and Clean Energy.

References

1. Singh, S., J. T. Haraldsen, J. Xiong, E. M. Choi, P. Lu, D. Yi, X. D. Wen, J. Liu, H. Wang, Z. Bi, P. Yu, M. R. Fitzsimmons, J. L. MacManus-Driscoll, R. Ramesh, A. V. Balatsky, Z. Jian-Xin, and Q. X. Jia. Induced Magnetization in La 0.7Sr 0.3MnO 3/BiFeO 3 Superlattices. 2014. Physical Review Letters. 113 (4): 047204.

2. Jain, P., Q. Wang, M. Roldan, A. Glavic, V. Lauter, C. Urban, Z. Bi, T. Ahmed, J. Zhu, M. Varela, Q. X. Jia, and M. R. Fitzsimmons. Synthetic magnetoelectric coupling in a nanocomposite multiferroic. 2015. SCIENTIFIC REPORTS. 5: 9089.

3. Mundy, J. A., C. M. Brooks, M. E. Holtz, J. A. Moyer, H. Das, A. F. R□bola, J. T. Heron, J. D. Clarkson, S. M. Disseler, Z. Liu, A. Farhan, R. Held, R. Hovden, E. Padgett, Q. Mao, H. Paik, R. Misra, L. F. Kourkoutis, E. Arenholz, A. Scholl, J. A. Borchers, W. D. Ratcliff, R. Ramesh, C. J. Fennie, P. Schiffer, D. A. Muller, and D. G. Schlom. Atomically engineered ferroic layers yield a room-temperature magnetoelectric multiferroic. 2016. 537 (7621): 523.

4. Tai, Y. Y., and J. X. Zhu. Local charge variation enhanced spin canting of BiFeO3/La0.7Sr0.3MnO3 heterostructure. To appear in http://arxiv.org/pdf/1603.03107v2.pdf.

5. Chen, A., J. Hu, P. Lu, T. Yang, W. Zhang, L. Li, T. Ahmed, E. M. Enriquez, M. Weigand, Q. Su, H. Wang, J. Zhu, J. L. MacManus-Driscoll, L. Chen, D. A. Yarotski, and Q. Jia. Role of scaffold network in controlling strain and functionalities of nanocomposite films. 2016. MPA-CINT: CENTER FOR INTEGRATED NANOTECHNOLOGIES.

6. al, A. P. Chen et. Large Room Temperature Magnetoelectric Couplings in BaTiO3:CoFe2O4 Vertical Nanocomposites. to be submitted to Nature Materials.

7. Ahmed, T., C. Aiping, B. McFarland, W. Qiang, H. Ohldag, R. Sandberg, J. Quanxi, D. A. Yarotski, and Z. Jian-Xin. Site-mixing effect on the XMCD spectrum in double perovskite Bi 2FeMnO 6. 2016. Applied Physics Letters. 108 (24): 242907.

Publications

Ahmed, , Chen, McFarland, Wang, Ohldag, Sandberg, Jia, D. A. Yarotski, and Zhu. Site-mixing effect on the XMCD spectrum in double perovskite Bi2FeMnO6. 2016. APPLIED PHYSICS LETTERS. 108 (24).

Ahmed, , La-o-Vorakiat, Salim, Y. M. Lam, E. E. M. Chia, and Zhu. Optical properties of organometallic perovskite: An ab initio study using relativistic GW correction and Bethe-Salpeter equation. 2014. EPL. 108 (6).

Ahmed, T., A. Chen, D. A . Yarotski, S. A. Trugman, Q. Jia, and J. X, Zhu. Magnetic, Electronic and Optical Properties of Double Perovskite Bi2FeMnO6. 2016. Applied Physics Letters, Materials. : 1.

Atkins, R., M. Dolgos, A. Fiedler, C. Grosse, S. Fischer, S. P. Rudin, and D. C. Johnson. Synthesis and Systematic Trends in Structure and Electrical Properties of

[(SnSe)1.15]m(VSe2)1, m = 1, 2, 3, and 4. 2014. Chemistry of Materials. 26: 2862.

Chen, , Weigand, Bi, Zhang, Lu, Dowden, J. L. MacManus-Driscoll, Wang, and Jia. Evolution of microstructure, strain and physical properties in oxide nanocomposite films. 2014. SCIENTIFIC REPORTS. 4.

Chen, A.. Role of vertical strain and microstructure on magnetoresistance in vertically aligned nanocomposites. Invited presentation at Materials Science &Technology 2014. (Pittsburgh, PA, October 12-16, 2014).

Chen, A.. Tuning Functionalities in Ferroic Nanocomposite Thin Films. 2016. MPA-CINT: CENTER FOR INTEGRATED NANOTECHNOLOGIES.

Chen, A. P., W. Zhang, J. L. MacManus-Driscoll, H. Wang, M. R. Fitzsimmons, and Q. X. Jia. Role of interfaces on competing interactions of ferroic films. Invited presentation at 2015 MRS Fall meeting. (Boston, Massachusetts, 29 Nov - 4 Dec, 2015).

Chen, A., J. Hu, P. Lu, T. Yang, W. Zhang, L. Li, T. Ahmed, E. M. Enriquez, M. Weigand, Q. Su, H. Wang, J. Zhu, J. L. MacManus-Driscoll, L. Chen, D. A. Yarotski, and Q. Jia. Role of scaffold network in controlling strain and functionalities of nanocomposite films. 2016. MPA-CINT: CENTER FOR INTEGRATED NANOTECHNOLOGIES.

Chen, A., Q. Jia, M. Weigand, Z. Bi, W. Zhang, J. MacManus-Driscoll, and H. Wang. Role of Vertical Strain and Microstructure on Magnetoresistance in Vertically Aligned Nanocomposites. 2014. MPA-CINT: CENTER FOR INTEGRATED NANOTECHNOLOGIES.

Chen, A., and Q. Jia. Multiferroic Nanocomposite Thin Films. 2016. MPA-CINT: CENTER FOR INTEGRATED NANOTECHNOLOGIES.

Chikara, , Singleton, Bowlan, D. A. Yarotski, Lee, H. Y. Choi, Y. J. Choi, and V. S. Zapf. Electric polarization observed in single crystals of multiferroic Lu2MnCoO6. 2016. PHYSICAL REVIEW B. 93 (18): 180405.

Choi, E. M., T. Fix, A. Kursumovic, C. J. Kinane, D. Arene, S. L. Sahonta, Z. Bi, J. Xiong, L. Yan, J. S. Lee, H. Wang, S. Lamgridge, Y. M. Kim, A. Y. Borisevich, I. MacLaren, Q. M. Ramasse, M. G. Blamire, Q. X. Jia, and J. L. MacManus-Driscoll. Room temperature ferrimagnetism and ferroelectricity in strained, thin films of BiFe0.5Mn0.5O3. 2014. Advanced Functional Materials. 24 (47): 7478.

Dai, Y. M., Bowlan, Li, Miao, S. F. Wu, W. D. Kong, Richard, Y. G. Shi, S. A. Trugman, J. -. Zhu, Ding, A. J. Taylor, D. A. Yarotski, and R. P. Prasankumar. Ultrafast carrier dynamics in the large-magnetoresistance material WTe2 (vol 92, 161104, 2015). 2015. PHYSICAL REVIEW B. 92 (19).

Dowden, P. C., Z. Bi, and Q. X. Jia. Method for controlling energy density for reliable pulsed laser deposition of thin films. 2014. Rev. Sci. Instrum.. 85: 025111.

Fang, , Tai, Deng, Wu, Ding, J. u. n. Sun, and E. K. H. Salje. Fe-vacancy ordering in superconducting K1-xFe2-ySe2: first-principles calculations and Monte Carlo simulations. 2015. SUPERCONDUCTOR SCIENCE & TECHNOLOGY. 28 (9).

Haeusler, , Atkins, Falmbigl, S. P. Rudin, Neumann, and D. C. Johnson. Insights from STEM and NBED studies into the local structure and growth mechanism of misfit layered compounds prepared using modulated reactants. 2015. ZEITSCHRIFT FUR KRISTALLOGRAPHIE. 230 (1): 45.

Haeusler, , Atkins, Falmbigl, S. P. Rudin, Neumann, and D. C. Johnson. Insights from STEM and NBED studies into the local structure and growth mechanism of misfit layered compounds prepared using modulated reactants. 2015. ZEITSCHRIFT FUR KRISTALLOGRAPHIE. 230 (1): 45.

Jain, , Wang, Roldan, Glavic, Lauter, Urban, Bi, Ahmed, Zhu, Varela, Q. X. Jia, and M. R. Fitzsimmons. Synthetic magnetoelectric coupling in a nanocomposite multiferroic. 2015. SCIENTIFIC REPORTS. 5: 9089.

Jia, Q. X.. Effect of Interfaces on Ferroic Properties of Composite Films. Invited presentation at International Symp. on Emerging Multifunctional & Bio-Directed Mater.. (San Antonio, TX, 10 - 111, Oct.).

Kogoj, J., L. Vidmar, M. Mierzejewski, S. A. Trugman, and J. Bonca. Thermalization after photoexcitation from the perspective of optical spectroscopy. 2016. Physical Review BPHYSICAL REVIEW B 94, 014304 (2016). 94: 014304.

Lee, , S. A. Trugman, C. L. Zhang, Talbayev, X. S. Xu, S. -. Cheong, D. A. Yarotski, A. J. Taylor, and R. P. Prasankumar. The influence of charge and magnetic order on polaron and acoustic phonon dynamics in LuFe2O4. 2015. APPLIED PHYSICS LETTERS. 107 (4).

Lee, , Sangle, Lu, Chen, Zhang, J. S. Lee, Wang, Jia, and J. L. MacManus-Driscoll. Novel Electroforming-Free Nanoscaffold Memristor with Very High Uniformity, Tunability, and Density. 2014. ADVANCED MATERIALS. 26 (36): 6284.

Li, , R. u. n. Zhao, Tang, Chen, Zhang, X. i. n. Lu, Wang, and H. a. o. Yang. Vertical-Interface-Manipulated Conduction Behavior in Nanocomposite Oxide Thin Films. 2014. ACS APPLIED MATERIALS & INTERFACES. 6 (8): 5356.

Li, , W. e. i. Zhang, L. e. Wang, Gu, Chen, R. u. n. Zhao, Y. a. n. Liang, Guo, Tang, Wang, Jin, Wang, and H. a. o. Yang. Vertical Interface Induced Dielectric Relaxation in Nanocomposite (BaTiO3)(1-x):(Sm2O3)(x) Thin Films. 2015. SCIENTIFIC REPORTS. 5.

Li, B. o., Pan, Tai, M. J. Graf, Zhu, K. E. Bassler, and C. S. Ting. Unified description of superconducting pairing symmetry in electron-doped Fe-based-122 compounds. 2015. PHYSICAL REVIEW B. 91 (22).

Luo, , Li, Y. M. Dai, Miao, Y. G. Shi, Ding, A. J. Taylor, D. A. Yarotski, R. P. Prasankumar, and J. D. Thompson. Hall effect in the extremely large magnetoresistance semimetal WTe2. 2015. APPLIED PHYSICS LETTERS. 107 (18).

Mun, E. D., Chern, Pardo, Rivadulla, Sinclair, H. D. Zhou, V. S. Zapf, and C. D. Batista. Magnetic Field Induced Transition in Vanadium Spinels. 2014. PHYSICAL REVIEW LETTERS. 112 (1): 017207.

Mun, E., D. F. Weickert, J. Kim, B. L. Scott, C. Miclea, R. Movshovich, J. Wilcox, J. Manson, and V. S. Zapf. Partially disordered antiferromagnetism and multiferroic behavior in a frustrated Ising system, CoCl2-2SC(NH2)2. 2016. Physical Review B. 93: 104407.

Pan, , Li, Tai, M. J. Graf, Zhu, and C. S. Ting. Evolution of quasiparticle states with and without a Zn impurity in doped 122 iron pnictides. 2014. PHYSICAL REVIEW B. 90 (13).

Rudin, S.. Magnetic Structure, Cation Disorder, Octahedral Rotations, and Antiferroelectric Distortions in Bi2FeMnO6. Invited presentation at Electronic Structure Approaches and Applications to Quantum Matter. (Santa Fe, 20 May, 2015).

Rudin, S. P., and D. C. Johnson. Density functional theory calculations of the turbostratically disordered compound [(SnSe)(1+y)](m)(VSe2)(n). 2015. PHYSICAL REVIEW B. 91 (14): 144203.

Sandberg, R., B. Mafarland, R. Prasankumar, G. Rodriguez, A. Chen, Q. X. Jia, A. Taylor, D. Yarotski, A. Ried, and H. Ohldag. Probing multiferroic materials with soft X-ray spectroscopy and imaging. Invited presentation at SLAC User Workshop. (Menlo Park, CA, Oct. 10, 2014).

Sheu, Y. M., S. A. Trugman, L. Yan, J. Qi, Q. X. Jia, and A. J. Taylor. Polaronic transport induced by competing interfacial magnetic order in a La0.7Ca0.3MnO3/BiFeO3 heterostructure. 2014. Phys. Rev. X. 4: 021001.

Sheu, Y. M., S. A. Trugman, L. Yan, Q. X. Jia, A. J. Taylor, and R. P. Prasankumar. Ultrafast optical manipulation of magnetoelectric coupling at a multiferroic interface. 2014. Nature Communications. 5: 5832.

Sing, S., J. H. Haraldsen, J. Xiong, E. M. Choi, P. Lu, D. Yi, X. D. Wen, J. Liu, H. Wang, Z. Bi, P. Yu, M. R. Fitzsimmons, J. L. MacManus-Driscoll, R. Ramesh, A. V. Balatsky, J. X. Zhu, and Q. X. Jia. Induced magnetization in La0.7Sr0.3MnO3/BiFeO3 superlattices. 2014. Phys. Rev. Lett.. 113: 047204.

Tai, , C. -. J. Wang, M. J. Graf, Zhu, and C. S. Ting. Emergent topological mirror insulator in t(2g)-orbital systems. 2015. PHYSICAL REVIEW B. 91 (4): 041111.

Tai, Y. Y., H. Choi, T. Ahmed, C. S. Ting, and J. X. Zhu. Edge states and local electronic structure around an adsorbed impurity in a topological superconductor. 2015. Physical Review B. 92: 174514 .

Tai, Y. Y., and J. X. Zhu. Local charge variation enhanced spin canting of BiFeO3/La0.7Sr0.3MnO3 heterostructure. http://arxiv.org/pdf/1603.03107v2.pdf.

Talbayev, , Lee, S. A. Trugman, C. L. Zhang, S. -. Cheong, R. D. Averitt, A. J. Taylor, and R. P. Prasankumar. Spin-dependent polaron formation dynamics in Eu0.75Y0.25MnO3 probed by femtosecond pump-probe spectroscopy. 2015. PHYSICAL REVIEW B. 91 (6).

Talbayev, , Lee, S. A. Trugman, C. L. Zhang, S. -. Cheong, R. D. Averitt, A. J. Taylor, and R. P. Prasankumar. Spin-dependent polaron formation dynamics in Eu0.75Y0.25MnO3 probed by femtosecond pump-probe spectroscopy. 2015. PHYSICAL REVIEW B. 91 (6).

Trugman, S. A .. High temperature transport in the Holstein model. Invited presentation at Conference on Dynamics of Quantum Many Body Systems far from Equilibrium. (Krvavec, Slovenija, 15 December, 2014).

Wenrui, Z., F. Meng, L. Leigang, C. Aiping, S. Qing, J. Quanxi, J. L. MacManus-Driscoll, and W. Haiyan. Heterointerface design and strain tuning in epitaxial BiFeO 3:CoFe 2O 4 nanocomposite films. 2015. Applied Physics Letters. 107 (21): 212901.

Xiong, J., V. Matias, B. W. Tao, Y. R. Li, and Q. X. Jia. Ferroelectric and ferromagnetic properties if epitaxial BiFeO3-BiMnO3 films on ion-beam-assisted deposited TiN buffered flexible Hastelloy. 2014. J. Appl. Phys.. 115: 17D913.

Zapf, V.. Multiferroic behavior investigated at high magnetic fields: CdV2O4. Invited presentation at Telluride Workshop on oxide materials. (Telluride, CO, June, 2015).

Zapf, V. S., B. G. Ueland, M. Laver, M. Lonsky, M. Pohlit, J. Müller, T. Lancaster, J. S. Möller, S. J. Blundell, J. Singleton, J. Mira, S. Yañez-Vilar, and M. A. Señarís-Rodríguez. Magnetization dynamics and frustration in the multiferroic double perovskite Lu2MnCoO6. 2016.

Physical Review B - Condensed Matter and Materials Physics. 93 (13): 134431.

Zhang, , Chen, J. i. e. Jian, Zhu, L. i. Chen, Lu, Jia, J. L. MacManus-Driscoll, Zhang, and Wang. Strong perpendicular exchange bias in epitaxial La0.7Sr0.3MnO3:BiFeO3 nanocomposite films through vertical interfacial coupling. 2015. NANOSCALE. 7 (33): 13808.

Zhang, , Li, Lu, Fan, Su, Khatkhatay, Chen, Jia, Zhang, J. L. MacManus-Driscoll, and Wang. Perpendicular Exchange-Biased Magnetotransport at the Vertical Heterointerfaces in La0.7Sr0.3MnO3:NiO Nanocomposites. 2015. ACS APPLIED MATERIALS & INTERFACES. 7 (39): 21646.

Zhang, W., A. Chen, Z. Bi, Q. X. Jia, J. L. MacManus-Driscoll, and H. Wang. Interfacial coupling in heteroepitaxial vertically aligned nanocomposite thin films: from lateral to vertical control. 2014. Curr. Opin. Solid State Mater. Sci. . 18: 6.

Zhang, W., J. Jian, A. Chen, L. Jiao, F. Khatkhatay, L. Li, F. Chu, Q. X. Jia, J. L. MacManus-Driscoll, and H. Wang. Strain relaxation and enhanced perpendicular magnetic anisotropy in BiFeO3:CoFe2O4 vertically aligned nanocomposite thin films. 2014. Appl. Phys. Lett.. 104: 062402.

Zhao, , Tai, and C. S. Ting. Phase diagram of the isovalent phosphorous-substituted 122-type iron pnictides. 2015. PHYSICAL REVIEW B. 91 (20): 205110.

al., P. Bowlan et. Probing ultrafast spin dynamics through a magnon resonance in the antiferromagnetic multiferroic HoMnO3. 2016. Physical Review B. 94: 100404.

al., P. Bowlan et. Directly probing spin dynamics in insulating antiferromagnets using ultrashort terahertz pulses. arXiv:1608.05991.

Exploring Mechanisms of Catalysis on Plutonium Surfaces (U)

Marianne P. Wilkerson
20140051DR

Abstract

We have conducted a study to understand chemical reactivity on plutonium metal. Characterization of the molecular rearrangements that occur on metal surfaces is critical for predicting chemical behavior. In the case of plutonium, the presence of surface defect structures and the elemental impurities in the subsurface lattice likely influence these chemical transformations. The role of oxidation state and oxide form on reactivity is under debate as well. Through this LDRD-DR project, we developed a capability for probing chemical reactivity on plutonium surfaces. Instrumentation for high-resolution imaging (Atomic Force Microscopy and Scanning Tunneling Microscopy) has been established to characterize surface properties and evaluate defect structures, and Time-of-Flight Secondary Ion Mass Spectrometry and Fourier Transform Infrared Absorption Spectroscopy have been applied to identify surface speciation, providing new information about the role of small molecule adsorption on plutonium surfaces. We have used electronic structure and atomistic methods to model reaction mechanisms and thermodynamic stabilities of various plutonium materials. Furthermore, a comprehensive organometallic study was conducted to provide complementary information about metal-molecule binding. The experimental and theoretical results from this work have provided an initial understanding of the connections between composition, valence state, and structural properties of plutonium and potential susceptibility for catalysis.

Background and Research Objectives

It has been suggested that plutonium supports chemical processes that are catalytic in nature. However, it is widely-reported that plutonium rapidly forms a passivating oxide layer. The balance between this protective oxidized surface and chemical reactivity challenges our understanding of the response of plutonium surfaces to small molecules.

Our research objectives were to establish state-of-the-art capabilities for measuring surface properties and characterizing surface defect structures on plutonium metal alloys, and to develop instrumentation for measuring chemical speciation of adsorbates on these surfaces. We also proposed to theoretically model thermodynamic and structural properties associated with these defects in order to understand the propensity for formation of potential reaction intermediates.

Scientific Approach and Accomplishments

We developed experimental capabilities for characterizing the surface of plutonium on an atomistic scale. An Omicron variable temperature Scanning Tunneling Microscope (STM) housed in an ultra-high vacuum (UHV) system was modified to handle plutonium coupons. The UHV-STM system is comprised of an analytical chamber with a base pressure of 3x10-10 Torr, a sample preparation chamber with a base pressure of 1x10-9 Torr, and a load lock system for introduction and removal of tips and samples. The STM resides in the analytical chamber, which is also equipped with an Omicron Auger electron spectrometer used for determining sample cleanliness prior to STM imaging. The Atomic Force Microscope utilized is a Bruker MultiMode 8 equipped with an environmental control hood for controlled gas dosing experiments, and a sample heater-cooler stage with a temperature range of -35 to 250 °C. The AFM is housed in an inert argon atmosphere (<1 ppm O2, <1 ppm H2O) MBraun Labmaster 130 glovebox, which serves as containment for the Pu. Both instruments are housed in a ground floor room in order to minimize vibrations.

We have selected two capabilities for measuring the chemical speciation of adsorbed species on the plutonium metal surfaces. The polarization modulation-infrared reflection-adsorption spectroscopy capability consists of a Nicolet 6700 Fourier Transform infrared (FT-IR) spectrometer equipped with a module from ThermoScientific, a Refractor™ Reactor cell from Harrick Scientific,

a gas manifold for delivering gases to the reactor cell, and a Hiden quadrupole mass spectrometer for gas analysis. This technique provides the ability to conduct reactions at standard atmospheric pressures. In this surface sensitive technique, modulation of the infrared sources gives both S- and P-polarized light, and only molecular vibrations with some fraction of a dipole moment perpendicular to the surface are active, providing clues to the molecular orientation of adsorbed species.

Time-of-Flight Secondary Ion Mass Spectroscopy provides a unique analysis of the surface. SIMS is sensitive to all isotopes including hydrogen, and provides both a comprehensive survey of surface constituents as well as a useful tool for analyzing isotopically labelled experiments. It is surface specific, probing only the one to two monolayers. Operating in the static regime, where less than 1% of the surface atoms are sampled during the analysis time, the technique can be considered non-destructive.

Density functional theory calculations were performed using the Vienna Ab Initio Simulation Package (VASP), which implements the project augmented-wave method with pseudopotentials to describe the core electrons. The generalized gradient approximation as parameterized by Perdew, Burke, and Ernzerhof was used to describe exchange and correlation energy contributions to the system. A rotationally invariant Hubbard U parameter as described by Dudarev was added to the Pu 5f electrons in order to more accurately describe the strong correlations present in PuO2.

In this work, we have investigated the surface structure of a subset of plutonium alloys (2 at. % Ga stabilized plutonium and 7 at. % Ga stabilized plutonium) and a plutonium dioxide thin film prepared by polymer assisted deposition. Three-dimensional images of the plutonium surface of several materials reveal granular structures and sub-micron variations in the mechanical properties of the surfaces. Spectra collected using Time-of-Flight SecondaryIon Mass Spectroscopy suggest a range of adsorbates as a function of exposure to small molecules. Comparison of measurements by Fourier Transform Infrared Spectroscopy with absorption spectra reported in the literature has provided information about chemical speciation on plutonium surfaces. We have reported the first study to model atomic displacements in the periodic cell of delta-phase plutonium and to evaluate the role of elemental impurities on atomic positions in the lattice structure.

Impact on National Missions

The response of plutonium materials to molecular environments is a key component of laboratory missions related to Stockpile Stewardship. The development of the materials science and chemistry of the actinides, particularly plutonium, will advance and strengthen our position as the national Plutonium Center of Excellence.

Publications

Beaux, M. F., T. Durakiewicz, K. S. Graham, J. N. Mitchell, S. Richmond, E. D. Bauer, D. P. Moore, F. J. Freibert, P. H. Tobash, and J. A. Kennison. Electronic structure of polycrystalline d-Pu metal: a review of photoemission spectra interpretations. 2014. In Pu Futures - The 'Science' 2014. (Las Vegas, NV, 7-12 Sept. 2014). , p. CMP.9. Las Vegas NV: American Nuclear Society.

Hernandez, S. C., D. S. Schwartz, C. D. Taylor, and A. K. Ray. Ab initio study of Ga-Stabilitzed d-Pu bulk and surfaces. 2014. In Pu Futures - The 'Science' 2014. (Las Vegas, NV, 7-12 Sept. 2014). , p. M&MS.15. Las Vegas NV: American Nuclear Society.

Hernandez, S. C., D. S. Schwartz, C. D. Taylor, and A. K. Ray. Ab initio study of gallium stabilized d-plutonium alloys and hydrogen-vacancy complexes. 2014. Journal of Physics: Condensed Matter. 26 (3): 235501/1.

Hernandez, S. C., M. P. Wilkerson, and M. N. Huda. Understanding oxygen adsorption on 9.375 at.% Ga-stabilized delta-Pu(111) surface: A DFT study. 2015. Journal of Alloys and Compounds. 653: 411.

Hernandez, S. C., T. J. Venhaus, and M. N. Huda. Atomic oxygen adsorption on 3.125 at.% Ga stabilized delta-Pu(111) surface. 2015. Journal of Alloys and Compounds. 643: 253.

Hernandez, S. C., and C. D. Taylor. Density functional theory studies on atomic adsorptions on Ga stabilized d-Pu (111) surfaces. 2014. In Materials Research Society 2014 Spring Meeting and Exhibit. (San Franscisco, CA, 21-25 April 2014). , p. S6.05. San Franscisco CA: Materials Research Society.

Hernandez, S. C., and E. F. Holby. DFT+U study of chemical impurities in PuO2. 2016. Journal of Physical Chemistry C. 120 (24): 13095.

Holby, E. F.. Oxygen vacancies in PuO2 (110) surfaces via density functional theory. 2014. In Pu Futures - The 'Science' 2014. (Las Vegas, NV, 7-12 Sept. 2014). , p. III. Las Vegas NV: American Nuclear Society.

II, M. F. Beaux, M. S. Cordoba, A. T. Zocco, D. R. Vodnik, M. Ramos, S. Richmond, D. P. Moore, T. J. Venhaus, S. A. Joyce, and I. O. Usov. Development of First Ever Scanning Probe Microscopy Capabilities for Plutonium. Journal of Nuclear Materials.

Pugmire, A. L., C. H. Booth, T. J. Venhaus, and D. L. Pugmire. Structural insights into the oxide formed during the room temperature corrosion of Plutonium. 2014.

In Pu Futures - The 'Science' 2014. (Las Vegas, NV, 7-12 Sept. 2014). , p. SS&C.7. Las Vegas NV: American Nuclear Society.

Richmond, S., P. H. Tobash, and D. Schwartz. The synthesis of Pu6Fe from plutonium deuteride and iron powders. 2014. In Pu Futures - The 'Science' 2014. (Las Vegas, NV, 7-12 Sept. 2014). , p. M&MS.13. Las Vegas NV: American Nuclear Society.

Schwartz, D. S., S. Richmond, C. D. Taylor, A. I. Smith, and A. L. Pugmire. Hydrogen effects in Pu-Ga alloys: defects and thermodynamics. 2014. In Pu Futures - The 'Science' 2014. (Las Vegas, NV, 7-12 Sept. 2014). , p. II. Las Vegas NV: American Nuclear Society.

Smith, A. I., K. L. Page, S. Richmond, J. Siewenie, T. A. Saleh, M. Ramos, and D. S. Schwartz. Local structural investigation of the Pu-7at%Ga using neutron total scattering. 2014. In Pu Futures - The 'Science' 2014. (Las Vegas, NV, 7-12 Sept. 2014). , p. M&MS.7. Las Vegas NV: American Nuclear Society.

Summerscales, O. T., E. R. Batista, B. L. Scott, M. P. Wilkerson, and A. D. Sutton. Reversible formation of a cerium-bound terminal hydride: Ce(C5Me4SiMe3)2(H)(thf). 2016. European Journal of Inorganic Chemistry. : 1.

Sutton, A. D., and M. P. Wilkerson. Catalysis with cerium organometallic complexes. 2014. In Pu Futures - The 'Science' 2014. (Las Vegas, NV, 7-12 September 2014). , p. CCCC.11. Las Vegas NV: American Nuclear Society.

Venhaus, T. J., and D. P. Moore. Analysis of Pu surfaces with time-of-flight SIMS. 2014. In Pu Futures - The 'Science' 2014. (Las Vegas, NV, 7-12 Sept. 2014). , p. SS&C.8. Las Vegas NV: American Nuclear Society.

Wagner, G. L., M. T. Paffett, K. D. Rector, B. L. Scott, and M. P. Wilkerson. Characterization of products from hydrolysis of UF6. 2014. In Pu Futures - The 'Science' 2014. (Las Vegas, NV, 7-12 Sept. 2014). , p. CCCC.4. Las Vegas NV: American Nuclear Society.

Mesoscale Materials Science of Ductile Damage in 4 Dimensions: Towards the Computational Design of Damage-Tolerant Materials

Ricardo A. Lebensohn
20140114DR

Abstract

In this project we developed synergistic experimental and modelling approaches based on emerging techniques in the fields of Experimental Mechanics and Micromechanics towards the solution of one of the most difficult outstanding problems in Materials Science: the development of a predictive, microstructure-sensitive ductile failure model. With this goal, we integrated time-resolved three-dimensional (3-D) microstructural characterization of polycrystalline materials undergoing ductile damage with state-of-the-art micromechanical modeling able to operate directly on microstructural images. This combination allowed us to understand some of the controlling aspects of ductile damage at the mesoscale, paving the way towards a truly predictive ductile damage model. This also resulted in the advancement of novel experimental and analytical techniques that can be extended and applied to other problems of strategic interest for the Laboratory and the Nation.

Background and Research Objectives

The failure of structural materials has a significant impact on vast sectors of the economy, including energy, transportation and defense. The costs arise both from rare catastrophic events to the more mundane expenses of over-engineering or preventive part replacement. Consequently, there has been enormous effort in the past to gain fundamental understanding of failure mechanisms and thus enable the development of more reliable components. Most structural materials are polycrystalline aggregates, in which the constituent crystals are irregular in shape, have anisotropic mechanical properties, and contain a variety of defects. The deformation of these heterogeneous materials results in very dynamic and complicated responses. While centuries of metallurgical experience and post-failure analysis have given us insight into general aspects relating material processing and performance, our failure models remain empirically calibrated because we have yet to achieve a thorough understanding of the controlling processes at the scale of the materials' heterogeneity, i.e. the mesoscale.

This situation is especially acute in materials that undergo significant amounts of plastic deformation before ultimate failure. Here, the initiation processes are obscured by the accumulated damage, and cannot be discerned by standard post-mortem analysis. Additionally, 2-D in-situ observation has limited applicability because the initiation sites are controlled by the extreme values of the micromechanical fields, which are likely outside the plane of observation. The observation of damage evolution in 3-D bulk by non-destructive means is strongly preferred.

The recent development of novel synchrotron X-ray diffraction techniques, collectively known as High Energy Diffraction Microscopy (HEDM), is now enabling this 3-D characterization, providing tomography, crystal orientation fields and local stress mapping. This could dramatically advance our understanding of structural materials, in the same way 2-D electron backscatter diffraction (EBSD) revolutionized the field of materials characterization in the '90's. However, until very recently 3-D orientation and stress mapping have been performed separately, and have been limited to carefully prepared and slightly deformed materials. This prevents their application to more complex and realistic scenarios, such as ductile damage.

In this project we integrated and combined HEDM with state-of-the-art modeling formulations, to discover relationships between microstructure and ductile damage in selectively prepared polycrystalline aggregates. Following the volumetric deformation through time allowed us to understand some of the controlling aspects of ductile damage at the mesoscale, paving the way towards a truly predictive ductile damage model. This also resulted in the advancement of novel experimental and analytical techniques that can be extended and applied to other

problems of strategic interest for the Laboratory and the Nation.

Scientific Approach and Accomplishments

Our approach consisted in the integration of state-of-the-art experimental and spectral modelling techniques for the identification of microstructural effects on ductile damage. A summary of experimental/modelling accomplishments and an example of integration of both aspects for discovery of microstructural/damage correlations are given in the next subsections.

Experimental

Two different sets of experiments were conducted, to study microstructural effects on ductile damage of polycrystalline materials under quasi-static and dynamic loading conditions, respectively.

Quasi-static

Using powder metallurgy [1.2], we produced three types of materials: Cu, Cu-W and Cu-Nb plates with fully dense structure. Notched tensile specimens were machined from these plates using wire EDM method. We collected data from the in-situ deformation of these specimens using concurrent computed tomography (CT), HEDM near-field (nf) and far- field (ff), as part of two Advanced Photon Source (APS) 1-ID beamline General User Proposals entitled: "3-D in-situ characterization of ductile damage evolution in polycrystalline materials" and "Study of microstructural effects on ductile damage evolution in two-phase polycrystalline materials using 3-D in-situ HEDM characterization", and one Cornell High Energy Synchrotron Source (CHESS) F2 beamline proposal entitled: "In-situ grain strain measurements in notched tensile samples". In addition, we measured global internal stresses during the in-situ deformation of our Cu-W samples using neutron diffraction in LANSCE's Lujan Center. The results of these measurements are shown in Figure 1 (Cu) and Figure 2 (Cu-W).

Figure 1 shows the data collected at APS on a notched Cu sample. A full 3-D nf-HEDM characterization of the initial un-gripped state (S0) in the notched region was performed. Next, the sample was deformed and several nf-, ff-HEDM and CT measurements were carried out at different deformed states (S0-gripped + S1 through S7) during uniaxial tension loading. In the way it was possible to capture the evolution of: a) local orientation field in the narrowest section of the notch (2-D bulk measurement); b) grain stresses in the notch region; and c) voids formation in the notch, driven by local stress concentrations associated with both sample geometry and microstructural features. Analysis of the correlation between orientation fields, local stress triaxiality evolution (a first-of-its kind measurement) and damage initiation, as well FFT-based numerical simulations with direct input and validation from these microstructural images are underway and will continue as part of the transition of this LDRD-DR to programmatic activities.

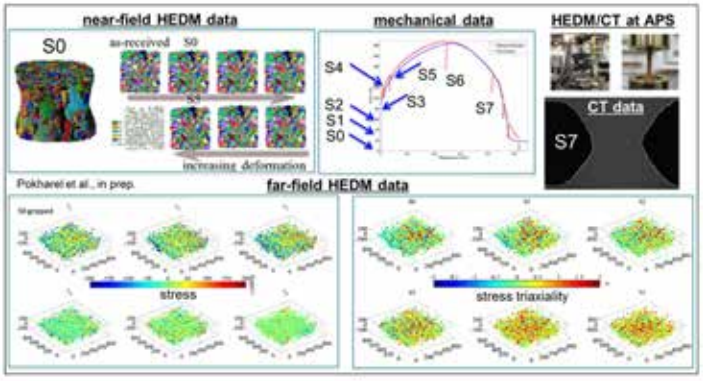

Figure 1. In-situ 3-D characterization of a notched Cu sample using HEDM techniques at APS, 1-ID beamline revealing the interplay between microstructure and damage.

Figure 2 shows the CT data collected at CHESS for the Cu-W sample. The three different phases are the Cu matrix (in gray) the W particles (in white) and the void phase (in black). Several CT images were taken at different deformed states during the loading. Voids nucleate by debonding of the weak Cu-W interfaces, producing the unload of the W phase at some critical stress (as confirmed by our ND measurements), and then grow and coalesce following a critical path in 3-D. HEDM data on orientation and grain stresses were also collected (not shown here). Registration of CT and HEDM images, analysis of the correlation between microstructural features, and direct FFT-based modeling is underway, as part of the transition of this LDRD-DR to programmatic activities.

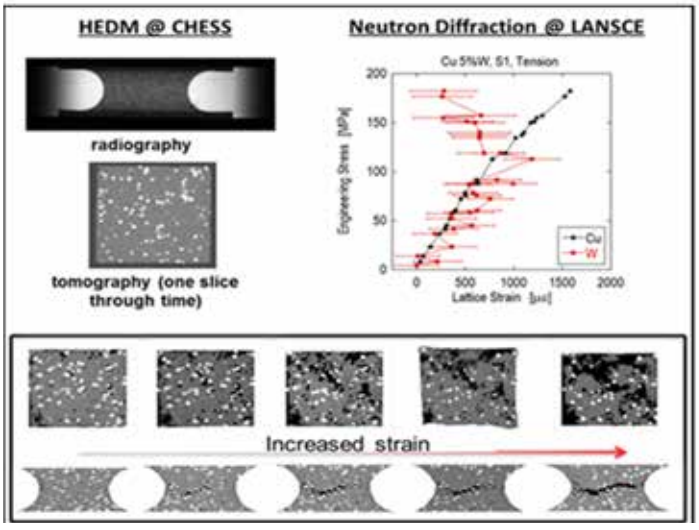

Figure 2. In-situ 3-D characterization of the interplay between microstructure and damage in a notched Cu-W sample using CT at CHESS and neutron diffraction (ND) at LANSCE.

Dynamic

3-D images of incipiently spalled Cu were obtained (Figure 3) [3]. The polycrystalline copper sample was pre-characterized in APS using nf-HEDM, then impacted in LANL with a velocity specifically selected to produce incipient spall voids. The recovered sample was then brought back to APS for nf-HEDM and X-ray tomography. The end result was a pair of 3-D orientation maps of the copper sample, both before and after the plate impact produced voids within the sample, with concurrent CT also providing 3-D images of the porosity distribution in the post-shocked sample. FFT-based simulations with direct input from the initial microstructure, coupled with Finite Element (FE) modelling of the shock experiment, were performed to obtain the micromechanical field distributions at the shock peak stress. This enabled establishing, for the first time, microstructure/porosity correlations [4] (see modelling section below).

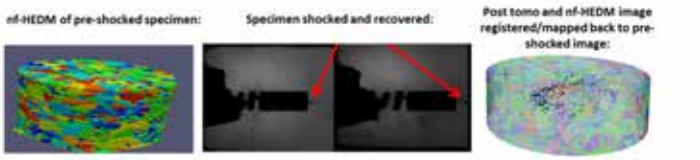

Figure 3. Nf-HEDM of pre-shocked Cu sample at APS, incipient spall experiment performed at LANL, and nf-HEDM combined with tomography of post-shocked sample at APS.

Modelling

Models for the prediction of ductile damage of polycrystalline materials—like in the experiments presented in the previous section—remain empirically calibrated due to a lack of knowledge of the controlling processes at the scale of the aggregate's heterogeneity. To overcome this limitation, our project further adapted a formulation developed in LANL over several years to enable microstructure-sensitive, three-dimensional prediction of ductile damage of polycrystals [5]. Specifically, two widely used micromechanical models, i.e. polycrystal plasticity and dilatational plasticity were combined within the framework of an efficient spectral formulation, to predict microstructural effects on porosity evolution with crystals and voids represented explicitly.

The classic crystal plasticity (CP) theory, a constitutive description based on considering the stress-controlled contribution to single crystal deformation of different slip systems, has been extensively used to solve the micromechanical behavior of crystalline materials. Previous to this project, CP constitutive laws were combined with a full-field Fast Fourier Transform (FFT)-based formulation. The CP formulations (rigid viscoplastic: VP-FFT and elasto-viscoplastic: EVP-FFT) that resulted from the latter were successfully applied to study microstructural effects on the plastic behavior of fully-dense polycrystalline aggregates. In particular, we demonstrated [6,7] good qualitative and moderate quantitative agreement (which can be improved by adopting more sophisticated constitutive descriptions) between FFT-based calculations with direct input from the initial nf-HEDM microstructures and the corresponding in-situ deformed images. Figure 4 shows the comparison between measured and predicted intragranular misorientation for a smooth Cu sample deformed 12% in tension, showing maximum misorientation along the <101>-<114> orientation line.

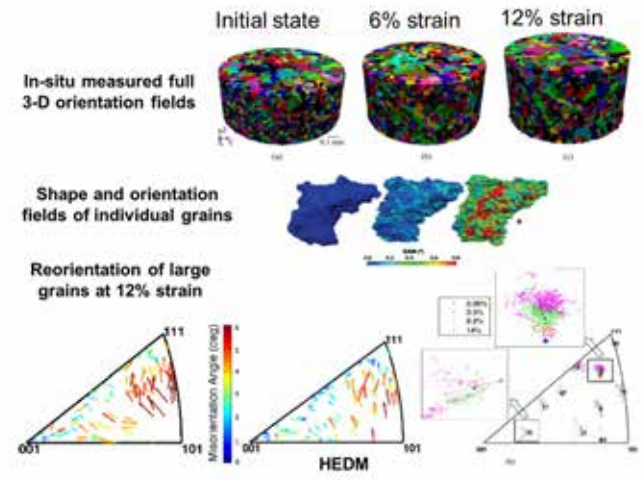

Figure 4. VPFFT simulations of intragranular misorientation development, with direct input and validation from nf-HEDM images of a smooth Cu sample deformed in tension.

As part of this project, the FFT-based formulation was extended to account for three critical aspects related to the formulation of a microstructure-sensitive ductile failure model, i.e. the interaction between crystals and pores, the influence of length-scale on the micromechanical behavior of polycrystalline aggregates, and the need of explicitly treatment of grain boundaries within the context of a voxel-based formulation.

Concerning the treatment of porosity and its evolution, dilatational plasticity formulations based on limit analysis, e.g. the Gurson model and its variants, have been successful in describing void growth in a homogeneous matrix. However, most polycrystalline materials have complex heterogeneous microstructures that affect damage evolution. With the goal of establishing correlations between the dilatational plastic behavior and the heterogeneous character of the matrix, the VP-FFT model was extended to the case of voided polycrystals with intergranular cavities. This dilatational formulation (D-VP-FFT) [5] makes it possible to follow the evolution of local porosity, i.e. growth of individual voids as determined by their local environment.

Regarding size effects, we have implemented a non-local EVP-FFT formulation [8], based on numerical procedures for the accurate estimation of higher-order derivatives of micromechanical fields, required for numerically stable feedback into single crystal constitutive relations. This new FFT-based implementation enables the analysis of the mechanical response of polycrystalline aggregates in three dimensions accounting for size dependence arising from plastic strain gradients with reasonable computing times.

Concerning the determination of grain boundary normals from voxelized microstructures, as those measured by CT and HEDM, these normal vectors are difficult to quantify due to the discretized nature of the measured microstructures. To overcome this, a new technique was proposed [9], based on first-order Cartesian moments of binary indicator functions to determine grain boundary normals directly from a voxelized microstructure image.

Application [4]

Using the pre-shocked image of the incipiently spalled Cu cylindrical sample shown in Figure 3, we embedded the nf-HEDM microstructure into a prismatic polycrystalline unit cell, representing the momentum traps in the spall experiment (Figure 5). FFT-based micromechanical simulations for this unit cell, coupled with FE modelling of the shock experiment to provide time-evolving strain-rate boundary conditions and hardening parameters to the EVP-FFT model, were used to compare distributions of predicted micromechanical fields at the peak stress, for the full set of grain boundary voxels ("full" distributions) versus the corresponding distributions restricted to those voxels that developed porosity after the shock ("restricted" distributions). This allowed the discovery of correlations between porosity and micro-mechanical response. The "usual suspect" micromechanical field for this comparison is stress triaxiality, which can be directly calculated from the stress tensor predicted by the EVPFFT model at every point in the material. The field of tractions normal to grain boundaries can also be calculated combining the stress tensor field with the grain boundary normal algorithm described in the previous subsection.

The comparison of the distributions of stress-triaxiality and normal tractions and are shown in Figure 5, second row. The violin plots, displaying a smoothed representation of the discrete probability distribution reflected with respect to the horizontal axis, show no significant correlation of these micromechanical fields with the subsequent void nucleation at grain boundaries. On the other hand, the full and restricted distributions of the difference in local Taylor factor across grain boundaries (ΔM, see definition in the figure, which describes the contrast in plastic response), are noticeably different, with the median for grain boundaries producing voids shifted to higher values compared to the full distributions. This implies that damage tends to occur preferentially on grain boundaries that are interfaces between crystals that have a greater contrast in plastic response. As the material deforms, these highly contrasted grain pairs begin to experience greater differences in local stress and strain that eventually leads to incompatibility that promotes damage.

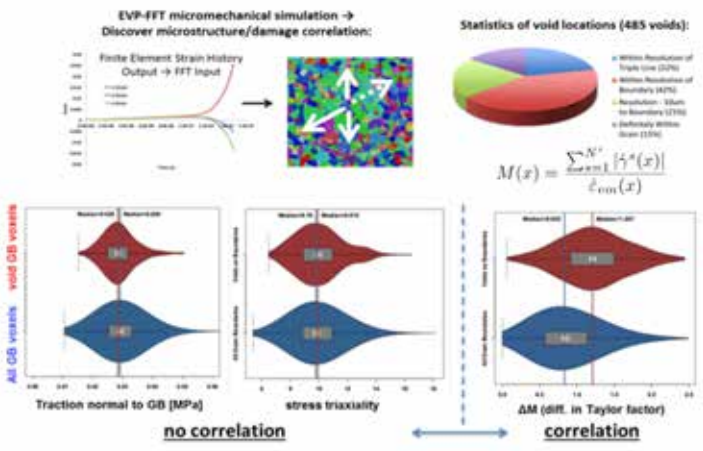

Figure 5. Statistical analysis based on results of FE/EVP-FFT calculations for a unit cell built from the nf-HEDM image of the pre-shocked Cu sample, showing propensity of void initiation at grain boundaries with large contrast in plastic properties.

Impact on National Missions

The work developed in this project directly addressed LANL's materials capability mission, integrating innovative characterization, analysis, and modeling capabilities. Progress has been made towards a predictive control of ductile damage response, and, more broadly, for future integrated materials design efforts.

The development of capability for advanced in-situ measurements at light sources, integrated with direct numerical modelling from these measurements, represent a test-bed for future research in extreme environments, e.g. dynamic experiments based on diffraction imaging that will be enabled by MaRIE. As LANL's experimental capabilities evolve towards dynamic measurements consisting of multiple snapshots with ~1 ps time resolution of ~1 mm3 samples and sub-micron spatial resolution, the tools that were developed in this project will be critical for the analysis of noise-prone, highly underdetermined problems. Proof of this has been the successful transition of the capabilities developed in this project to the MaRIE project, e.g. in terms of: a) very successful MaRIE presentations (R. Pokharel: "Enabling 3D reconstructions with single shot measurements at MaRIE", MaRIE's M4 Board of Directors Meeting, Los Alamos National Laboratory, December 2015) and External Advisory Board (EAB) (R.A. Lebensohn, R.

Pokharel and B. Clausen: "Towards an integrated experimental/modelling framework to account for microstructural effects on damage under extreme conditions", MaRIE External Advisory Board Meeting, Los Alamos National Laboratory, September 2016); b) appointments (E. Kober and R. Lebensohn) to MaRIE's Theory, Modeling and Computation (TMC) BOD; c) Participation (E. Kober, R. Pohkarel, R. Lebensohn) in MaRIE's Multi-Dimensional Imaging Technology Maturation Plan (TMP) working group.

References

1. Chen, C. F., D. Dombrowski, R. A. Lebensohn, B. Clausen, R. Forsyth, and R. Pokharel. Processing and consolidation of copper for mesoscale materials science of ductile damage in four dimensions. 2014. (Orlando, FL, 18-22 May 2014). p. 0946. Orlando, FL: APMI International.

2. Chen, C. F., R. Pokharel, M. J. Brand, E. L. Tegtmeier, B. Clausen, D. E. Dombrowski, T. L. Ickes, and R. A. Lebensohn. Processing and consolidation of copper/tungsten. To appear in Journal of Materials Science.

3. Menasche, D. B., J. Lind, S. F. Li, P. Kenesei, J. F. Bingert, and U. Lienert . Shock induced damage in copper: a before and after, 3D study. 2016. Journal of Applied Physics. 119: 154902.

4. Lieberman, E., R. A. Lebensohn, D. B. Menasche, C. A. Bronkhorst, and A. D. Rollett. Microstructural effects on damage evolution in shocked copper polycrystals. 2016. Acta Materialia. 116: 270.

5. Lebensohn, R. A., and R. Pokharel. Interpretation of microstructural effects on porosity evolution using a combined dilatational/crystal plasticity computational approach. 2014. Journal of the Minerals, Metals and Materials Society (JOM). 66 (3): 437.

6. Pokharel, R., J. Lind, A. K. Kanjarla, R. A. Lebensohn, S. F. Li, Kenesei, R. M. Suter, and A. D. Rollett. Polycrystal Plasticity: Comparison Between Grain-Scale Observations of Deformation and Simulations. 2014. Annual Review of Condensed Matter Physics. 5: 317.

7. Pokharel, R., J. Lind, S. F. Li, P. Kenesei, R. A. Lebensohn, R. M. Suter, and A. D. Rollett. In-situ observation of bulk 3-D microstructure evolution of polycrystalline copper using synchrotron radiation. 2015. International Journal of Plasticity. 67: 217.

8. Lebensohn, R. A., and A. Needleman. Numerical implementation of non-local polycrystal plasticity using Fast Fourier Transforms. To appear in Journal of the Mechanics and Physics of Solids.

9. Lieberman, E., A. D. Rollett, R. A. Lebensohn, and E. M. Kober. Calculation of grain boundary normals directly from 3-D microstructural images. 2015. Modelling and Simulation in Materials Science and Engineering. 23: 035005.

Publications

Anglin, B. S., R. A. Lebensohn, and A. D. Rollett. Validation of a numerical method based on Fast Fourier Transforms for heterogeneous thermoelastic materials by comparison with analytical solutions. 2014. Computational Materials Science. 87: 209.

Bingert, J. F., R. M. Suter, J. Lind, S. F. Li, R. Pokharel, and C. P. Trujillo. High-Energy diffraction microscopy characterization of spall damage. 2014. In Dynamic Behavior of Materials, Volume 1. , p. 397. : Springer International Publishing.

Chen, C. F., D. Dombrowski, R. A. Lebensohn, B. Clausen, R. Forsyth, and R. Pokharel. Processing and consolidation of copper for mesoscale materials science of ductile damage in four dimensions. 2014. In 2014 World Congress on Powder Metallurgy & Particulate Materials (PM 2014) . (Orlando, FL, 18-22 May 2014). , p. 0946. Orlando, FL: APMI International.

Chen, C. F., R. Pokharel, M. J. Brand, E. L. Tegtmeier, B. Clausen, D. E. Dombrowski, T. L. Ickes, and R. A. Lebensohn. Processing and consolidation of copper/tungsten. To appear in Journal of Materials Science.

Garcia-Cardona, C., R. A. Lebensohn, and M. Anghel. Parameter estimation in a thermoelastic composite problem via adjoint formulation and model reduction. To appear in International Journal of Numerical Methods in Engineering.

Lebensohn, R. A., J. P. Escobedo, E. K. Cerreta, Dennis-Koller, C. A. Bronkhorst, and J. F. Bingert. Modeling void growth in polycrystalline materials. 2013. Acta Materialia. 61 (18): 6918.

Lebensohn, R. A., and A. Needleman. Numerical implementation of non-local polycrystal plasticity using Fast Fourier Transforms. To appear in Journal of the Mechanics and Physics of Solids.

Lebensohn, R. A., and R. Pokharel. Interpretation of microstructural effects on porosity evolution using a combined dilatational/crystal plasticity computational approach. 2014. Journal of the Minerals, Metals and Materials Society (JOM). 66 (3): 437.

Lieberman, E., A. D. Rollett, R. A. Lebensohn, and E. M. Kober. Calculation of grain boundary normals directly from 3-D microstructural images. 2015. Modelling and Simulation in Materials Science and Engineering. 23: 035005.

Lieberman, E., R. A. Lebensohn, D. B. Menasche, C. A. Bronkhorst, and A. D. Rollett. Microstructural effects on damage evolution in shocked copper polycrystals. 2016. Acta Materialia. 116: 270.

Menasche, D. B., J. Lind, S. F. Li, P. Kenesei, J. F. Bingert, and U. Lienert . Shock induced damage in copper: a before and after, 3D study. 2016. Journal of Applied Physics. 119: 154902.

Ozturk, T., C. Stein, R. Pokharel, C. Hefferan, H. Tucker, S. Jha, R. John, R. A. Lebensohn, P. Kenesei, R. M. Suter, and A. D. Rollett. Simulation domain size requirements for elastic response of 3-D polycrystalline materials. 2016. Modelling and Simulation in Materials Science and Engineering. 24: 015006.

Pokharel, R., J. Lind, A. K. Kanjarla, R. A. Lebensohn, S. F. Li, Kenesei, R. M. Suter, and A. D. Rollett. Polycrystal Plasticity: Comparison Between Grain-Scale Observations of Deformation and Simulations. 2014. Annual Review of Condensed Matter Physics. 5: 317.

Pokharel, R., J. Lind, S. F. Li, P. Kenesei, R. A. Lebensohn, R. M. Suter, and A. D. Rollett. In-situ observation of bulk 3-D microstructure evolution of polycrystalline copper using synchrotron radiation. 2015. International Journal of Plasticity. 67: 217.

Rovinelli, A., R. A. Lebensohn, and M. D. Sangid. Influence of microstructure variability on short crack growth behavior. 2015. Engineering Fracture Mechanics. 138: 265.

Stein, C. A., A. Cerrone, T. Ozturk, S. Lee, P. Kenesei, H. Tucker, R. Pokharel, J. Lind, C. Hefferan, R. M. Suter, A. R. Ingraffea, and A. D. Rollett. Fatigue crack initiation, slip localization and twin boundaries in a nickel-based superalloy. 2014. Current Opinion in Solid State and Materials Science. 18 (4): 244.

Subedi, S., R. Pokharel, and A. D. Rollett. Orientation gradients in relation to grain boundaries at varying strain level and spatial resolution. 2015. Materials Science and Engineering A. 638: 348.

Controlling the Electronic Structure of Emerging Atomically Thin Materials Through Heterostructuring

Jinkyoung Yoo
20150659ECR

Introduction

The overarching goal of the research is controlling the physical properties of emerging two-dimensional atomically thin materials (2D-ATMs, e.g. graphene, monolayer transition metal dichalcogenides) through heterostructure formation with conventional semiconductor (silicon, germanium, gallium arsenide) growth on 2D-ATMs.

Though the emerging 2D-ATMs have attracted great attention in the last decade due to their exotic physical properties, there has not been methodology to control the physical characteristics of 2D-ATMs since chemical doping and alloying of 2D-ATMs are not permanently stable. Applying bias to 2D-ATMs through semiconductor on 2D-ATM enables us to control the electronic properties of 2D-ATMs in precise and on-demand manner. The preliminary results of the team show that high-quality semiconductor layers and nanowires can be grown on the 2D-ATMs through unconventional crystal growth mechanism. The project can make the breakthrough for 2D-ATM research field hindered by the absence of reliable method of controlling physcial properties of 2D-ATMs and for conventional semiconductor research field which has been suffered from the limit of inherent characteristics of conventional semiconductors.

The synergistic output through a combination of low dimensionality of 2D-ATMs and established science of semiconductors has broad impact in materials science and device manufacturing.

The research has four key goals:

1. Providing a reliable and robust way of tuning properties of 2D-ATMs in precise manner since the main approach of semiconductor growth on 2D-ATMs employs established semiconductor science and technology.
2. Controlling carrier transport characteristics of 2D-ATMs through semiconductors grown on 2D-ATMs.
3. Opening novel opportunities of observation of emergent phenomena in the novel heterostructures.
4. Utilizing the exotic physical phenomena (e.g. band gap opening in atomically thin materials, tunneling-mediated p-n junction properties) for semiconductor devices such as ultra-efficient photodetectors and artificial photosynthesis.

Benefit to National Security Missions

The goals of this LDRD project are closely related to semiconductor heterostructure formation and control of physical properties of emerging materials. Integrated studies, from materials preparation to device demonstration, offer benefits to basic science and applied research.

For basic science the project is directly relevant to the grand challenges set by DOE SC, ‘control at the level of electrons’ and ‘energy and information on the nanoscale’. The project provides materials systems composed of ultimately (atomically) thin material and semiconductors of which properties are precisely controlled to tackle the grand challenges.

The project provides a reliable way to utilize the exotic properties such as abnormally large optical absorptance of two-dimensional atomically thin materials (2D-ATMs) which are useful to develop ultrafast and highly efficient detectors (especially for MaRIE) due to extremely small capacitance and ultimately thin heterojunction expediting excited carrier separation as well as energy harvesting devices such as photovoltaic cells and water splitting for hydrogen production (Energy security, Renewable energy). Furthermore, the ultimate thinness of the semiconductor/ 2D-ATMs makes it possible to transfer high-quality heterostructures onto various substrates such as plastics and glasses without loss of physical characteristics. The transferrable heterostructures are the key building blocks of embedded and flexible devices. Thus, the concepts explored in the project can also find

diverse applications in electronic/photonic devices based on charged carrier management. Project success will pave the way for future research funded by Department of Homeland Security, Department of Defense, Department of Commerce, and pursuing initiatives in national nanotechnology and manufacturing.

Progress

The project is exploring novel heterostructures composed of conventional semiconductors and emerging atomically thin materials (ATMs) such as graphene, hexagonal boron nitride, and transition metal dichalcogenides (e.g. MoS2, WS2, NbSe2, etc.). In the past year we have made significant progress in the heterostructure formation and theoretical calculations of physical properties of the heterostructures. The achievements in the past year can be testified by a manuscript under review, two conference presentations, and an invention disclosure.

A progress in the heterostructure formation was growth of single crystalline semiconductor thin films on various ATMs. In addition to our previous achievement of Ge growth on MoS2 (semiconducting), crystalline Ge layer was successfully grown on graphene (metallic), hexagonal boron nitride (insulating), and NbSe2 (superconducting) via low-pressure chemical vapor deposition which is compatible to semiconductor industry. The complete set of materials combination encompassing metallic, semiconducting, insulating enables us to fabricate electronic devices such as diodes, transistors, inverters, etc. Additionally, Ge/NbSe2 heterostructure has been employed to fabricate Josephson junction in our team.

The studies on formation of semiconductor/ATM heterostructures revealed that 1) crystallographic orientation of Ge on ATMs can be controlled, 2) Strain-free crystalline Ge thin film can be prepared on ATMs, 3) first observation of atomic diffusion over van der Waals gap. In the following, we describe the technical accomplishments in detail.

The control of crystallographic orientations of Ge is achieved by change of growth temperature and reactor pressure. The most striking insight obtained from the growth study is that Ge can copy the in-plane hexagonal structure of ATMs. Hexagonal Ge has rarely been observed. Moreover there has not been successful hexagonal Ge thin film growth. Since decades-long theoretical efforts have predicted that hexagonal Ge has direct band gap, our achievement provides a revolutionary way of forming hexagonal Ge for light-emitting components.

ATMs do not have surface dangling bonds. Thus, conventional semiconductors (Ge, Si) with dangling bonds interact with ATMs through van der Waals forces. The absence of covalent bonding in the Ge(Si)/ATM heterostructures results in a strain-free interface. We confirmed that there is no strain in Ge/ATM (graphene, MoS2) heterostructures via Raman spectroscopy and X-ray diffraction mapping. Strain-free single crystalline semiconductor thin films prepared on ATMs can be building blocks for high-performance flexible devices because those can be easily transferred onto flexible substrates.

The main mechanism of Ge(Si)/ATM heterostructures is van der Waals interaction, not covalent bonding. There is sub-nm-gap at the interface between Ge(Si) and ATM according to transmission electron microscopy images. The gap acts as barrier for charged carriers such as electrons and holes. Thus, heterostructures composed of ATMs have been considered as an ideal system to achieve ultimately abrupt interfaces. However, our elemental analyses show that atoms can be diffused through the gap. The observation brings novel questions of heterostructure formation and interface control at nanoscale.

In parallel with the materials growth, we are developing the theoretical framework for materials preparation on ATMs. Previous theoretical calculations explaining semiconductor growth on ATMs are specific to materials combination. On the other hand, our theory provides the general mechanism of Ge(Si) formation on various ATMs with different in-plane lattice constants and surface energies. The key factors of our theory are van der Waals interaction and formation of image dipoles over the gap between ATMs and grown materials. The theory has been successfully employed to explain our experimental results.

Future Work

Since the milestones initially set in the proposal have been accomplished, two expanded goals for the last 4 months in FY17 are:

- Fabrication of semiconductor nanostructures on two-dimensional (2D) materials: Ge(Si) nanowire arrays will be fabricated on graphene, h-BN, transition metal dichalcogenides. The arrays will have ordering and addressable electrodes on tops of the wires. The electrical properties at the junctions between the nanowires and 2D material under biasing through nanowires will be explored. According to my preliminary studies, the junctions change carrier distribution in 2D material. Thus, inducing localization in 2D materials through biasing can open a novel research topic of reversible localization.

- Demonstration of flexible devices based on Ge(Si) vertical p-i-n junction photodetectors: 2D materials are usually prepared on dielectric (SiO2) substrates.

After preparation of Ge(Si) vertical p-i-n structures the Ge(Si)/2D materials can be easily detached from the dielectric substrates by wet etching. Then, the single crystalline and device-quality heterostructures can be transferred onto any flexible substrates. The device performance of photodetectors based on the Ge(Si)/2D heterostructures will be assessed.

Conclusion

The achievements are closely related to fundamental materials science from the perspectives of materials preparation and control of properties, which can be directly expanded to various device applications.

The ideal outcome of the research is the control of the physical properties of 2D-ATMs through semiconductor/2D-ATM heterointerfaces and the observation of emergent phenomena in the heterostructures such as tunneling-mediated transport, band gap opening, reversible strong localization of carriers, and other unexpected behaviors.

Additionally, the unconventional crystal growth mechanism, which is not based on chemical bonding between substrate and grown material, provides novel insights of preparing high-quality heterostructures composed incompatible materials.

Publications

Lin, Y. -C., I. Bilgin, T. Ahmed, R. Chen, D. Pete, S. Kar, J. -X. Zhu, G. Gupta, A. Mohite, and J. Yoo. Charge Transfer in Crystalline Germanium/Monolayer MoS2 Heterostructures Prepared by Chemical Vapor Deposition. 2016. Nanoscale. 8: 18675.

Lin, Y. -C., J. Yoo, I. Bilgin, A. Mohite, S. Kar, and D. Pete. Growth and characterizations of germanium/monolayer MoS2 heterostructures. 2015. 2015 Materials Research Society Spring Meeting.

A Novel Crystal Plasticity Model that Explicitly Accounts for Energy Storage and Dissipation at Material Interfaces

Jason R. Mayeur
20150696ECR

Introduction

This project is focused on developing a novel mesoscale theory and computational framework that can be used to enhance our understanding of the role that interfaces play in dictating microstructural evolution in nanoscale material systems. Recent work at LANL on fabricating bulk two-phase lamellar bimetallic nanocomposites has shown that these material systems possess superior strength and radiation damage resistance as compared the constituent metals and/or composites with more conventional layer thicknesses, e.g. larger than one micron. Experiments show that these nanocomposites have highly oriented microstructures and that there is a predominant interface relationship between grains along the bi-phase interfaces, which gives rise to their exceptional properties. The resulting microstructure in these nanoscale composites was unexpected based on conventional understanding of the fabrication process and active material deformation mechanisms. Earlier conventional mesoscale and atomistic simulations suggest that this unique microstructure arises due to a competition between the energy stored at the bi-phase interfaces and the stability of certain crystallographic orientations under the imposed deformation. In order to test this hypothesis, a mesoscale theory and computational framework that accounts for interface energy, the relevant plastic deformation mechanisms, and the associated lattice reorientation is needed. Such a modeling framework does not currently exist, and the goal of this project is to develop a tool to bridge this gap in understanding. The proposed path of model development would build upon an existing state-of-the-art nonlocal single crystal plasticity theory developed by the principal investigator to include the interface energy effects. The model would truly be one-of-kind and would uniquely position LANL to answer fundamental questions related to the role of interfaces in nanoscale polycrystalline material systems.

Benefit to National Security Missions

This project will deliver a simulation tool that addresses relevant physics of mesocale deformation mechanisms in polycrystalline metals with an emphasis on the role played by material interfaces. This enhanced understanding will enable the design of materials with properties tailored for specific applications, which is directly aligned with the Laboratory's Materials for the Future Science Pillar. The proposed modeling framework is also suited for bridging the mesoscale gap between atomistic and macroscale continuum methods, and would complement the modeling component of the Making, Measuring, and Modeling Materials (M4) facility as a part of the MarIE vision.

Progress

The past year's efforts were devoted to the theoretical development of a physics-based three-dimensional framework for modeling the size-dependent behavior of single crystal and polycrystalline metals and developing a robust and efficient numerical implementation of the theory into a finite element code so that the mechanical response of mesoscale polycrystalline ensembles can be simulated. The theoretical achievements reflect a review and implementation of ideas that reflect current state-of-the-art constitutive descriptions of ductile metals. A significant amount of effort in FY16 was devoted to upgrading the rudimentary numerical implementation that was used for the simpler constitutive models employed during the proof-of-concept stage of this work. At this stage, the numerical implementation has been thoroughly tested and benchmarked against conventional theories (and their implementation) for validation. Currently, simulations are being performed exploring mechanical size-effects in polycrystalline fcc, bcc, and fcc/bcc multilayered materials.

Future Work

- Develop a single crystal constitutive law applicable for body-centered cubic (bcc) materials.
- Implement the bcc single crystal constitutive law

within the nonlocal finite element framework.

- Develop the constitutive theory for the interface energy terms.
- Implement the interface energy constitutive theory within the nonlocal finite element framework.
- Perform nonlocal finite element simulations of face-centered cubic (fcc) nanocrystalline materials systems without interface energy effects.
- Perform nonlocal finite element simulations of bcc nanocrystalline materials systems without interface energy effects.
- Perform nonlocal finite element simulations of nanocrystalline fcc/bcc multilayer materials systems without interface energy effects.

Conclusion

The primary goal of this research is to develop a nonlocal crystal plasticity model to study the competition between bulk-dominated and interface-dominated polycrystalline plasticity at the mesoscale. The model will be used to study mechanical response of nanocrystalline face-centered cubic (fcc), body-centered cubic (bcc), and fcc/bcc lamellar composites. It is anticipated that the improved understanding of these nanoscale material systems obtained via simulation will facilitate next generation materials design by identifying relationships between process parameters and the resulting microstructure.

Publications

Mayeur, J. R., D. L. McDowell, and S. Forest. Micropolar and Micromorphic Crystal Plasticity. Handbook of nonlocal continuum mechanics for materials and structures. Edited by Voyiadjis, G. Z..

Mayeur, J. R., and D. L. McDowell. Micropolar crystal plasticity simulation of particle strengthening. 2015. MODELLING AND SIMULATION IN MATERIALS SCIENCE AND ENGINEERING. 23 (6).

Formation, Stability, and Chemistry of Tetravalent Actinide Nanocrystals

Ping Yang
20160604ECR

Introduction

Nanoscale materials bearing heavy elements, such as thorium and uranium oxide nanoparticles, play an increasingly important role in many stages of the nuclear fuel cycle, from recycling spent nuclear fuel during the precipitation step, to high temperature processing of actinide mixture, to mixed oxide fuels. The formation and stability of actinide nanoparticles are also vital to the multiple phases of long-term management of nuclear waste and assessment of contaminated sites due to environmental concerns Thorium and uranium are found to be in tetravalent state in nanomaterials due to their low solubility. For these reasons, there is a pressing need to understand both the inherent size-dependent chemical and physical properties of tetravalent actinide nanocrystals (NCs) and how surface passivating ligands contribute to their stability and formation. Actinide nanomaterials fill the gap between molecules, colloids, mesoscale and bulk materials, which is a grand challenge identified by DOE Basic Energy of Sciences. However, to date, little is known about the electronic structures, energy landscape, and proper- ties of actinide NCs. Therefore, a comprehensive understanding of the underlying electronic factors of actinide oxide NCs and of the influence of surfactants are crucial to achieve full control and predictability of nanoscale actinide systems with unique structures and selected chemical and physical characteristics.

We will employ a novel high-performance computational framework based on relativistic DFT to search for global minima of the nanocrystalline cores, identify the structural characteristics, as well as understand the interfacial chemistry between NCs and surface ligands. Computed results will be validated with published experimental results. The knowledge gained will provide guiding principles for predicting and controlling the formation and stability of actinide oxide NCs.

Benefit to National Security Missions

The proposed research directly addresses the LANL Plutonium Science and Research Strategy and LANL missions in Energy Security and Materials for the Future; we have initiated conversations and will continue to work closely with the LANL C-Division staff (Stosh Kozimor), to position us to compete for extramural energy funding. This proposal directly addresses a scientific grand challenge “Resolving the f-electron challenge to master the chemistry and physics of actinides and actinide-bearing materials”, identified in the 2006 Basic Energy Research Needs for Advanced Nuclear Energy Systems. Understanding the formation, stability and chemistry of AnO2 NCs will open the way to optimize their properties and advance the safe and secure usage of nuclear power, as discussed in the DOE Strategic Plan 2014-2018.

Progress

The research team started the process in identifying a potential postdoc for this project. Additionally, the procurement of four computing nodes that will be dedicated to this project was initiated.

Future Work

Going forward, the research team will focus on the following tasks.

- Implement basin-hopping algorithm interfacing with density functional theory package.
- Search for global energy minima of ThO2 NCs up to 1nm.
- Calculate structure and stability of surface ligand on ThO2 NCs

Conclusion

The long-term goal of this project is to build the knowledge foundation of structures, energetics, and chemical and physical characteristics of tetravalent actinide

nanocrystals as a function of particle size, composition, and surface ligands, using a novel high-performance computational frame- work. Understanding, predicting, and controlling their formation and chemical reactivity is crucial to improve the efficiency of the nuclear fuel cycle, long-term management of nuclear waste, and assessment of contaminated sites.

Microstructural Characterization of Shock-Recovered Explosives for Mesoscale Model Development

John D. Yeager
20160619ECR

Introduction

The goal of the research project is to characterize the microstructure of high explosives (HE) before, during and after dynamic loading which induces damage and partial reaction, focusing on data which provides insights into thermomechanical mechanisms of damage and can feed into grain-scale or mesoscale performance or damage models. The microstructure of HE is known to influence (if not control) initiation of chemical reaction and detonation performance under dynamic, high pressure loading. However, traditional in situ measurement techniques do not generally probe microstructure during loading, and the reactive and fragile nature of explosives has precluded post-shot sample characterization. Therefore, our specific research goals are to:

- For the first time at Los Alamos, develop and employ a recovery catch tank on one or more gas guns to catch damaged HE samples for post-shot characterization.
- Use new in situ techniques and post-shot characterization to quantify material response to planar shock and shear loading at sub-detonative pressures.
- Improve an existing mesoscale model to incorporate damage and calculate spatially resolved temperature to elucidate the microstructural features responsible for initiation.

This is a high-risk, high-potential project because it involves experimental work which has never been done before at LANL and involves some capability development, captures time and length-scale relevant data on HE to feed into new or improved mesoscale models, and studies two classes of HE (plastic-bonded and melt-cast) with very different thermomechanical responses to damage. While the research is essentially fundamental R&D on explosives, the output lays groundwork for MaRIE (particularly the multi-probe aspect in extreme conditions) and is of great interest to LANL weapons programs.

Benefit to National Security Missions

Successful execution of this program will provide fundamental understanding of high explosive materials in the form of data and models which inform thermomechanical codes, particularly for abnormal events such as fragment impact or low pressure shock. The primary focus is on explosives of interest to the Department of Energy (DOE) National Nuclear Security Administration (NNSA) stockpile with secondary focus on melt-castable materials of interest to the Department of Defense (DOD). Programs which have expressed interest in this type of data include the Joint Munitions Program (DOE/DOD), NNSA Science Campaigns 2 and 6, and Nuclear Counterterrorism (NCT). The multi-probe aspect of this research project supports and lays groundwork towards the MaRIE project, even if these experiments require multiple single or double-probe shots in order to build a complete dataset.

Building the capability to safely recover and characterize damaged explosives should result in long-term programmatic interest, particularly for those agencies already described. The combination of experiment and theory, using in-situ and post-shot measurements to collect data at the length and time scales of relevance to the models, is highly mission-relevant. Additionally, the usefulness of mesoscale models is still debated among some weapons safety experts. Advancing the sophistication of these models by providing difficult-to-measure experimental data and putting some effort into capturing the underlying physical mechanisms are both critical to validating their use at a large scale. Some of the key aspects of microstructurally-driven initiation of explosives are still under debate as well.

Progress

Due to a request from the LDRD office, our start date was pushed back until February 22, 2016. However, despite the short time period for the project so far, we have several accomplishments. On the modeling side,

we have identified a postdoc to assist on the modeling component of the proposal, and he will start working on the project in August. Through conversations with him and his LANL mentor (Co-I Luscher), we determined some preliminary experiments to gather mechanical properties of simplified material systems. These consist of various compression and tension tests on crystal-polymer-crystal stacked geometries while characterizing the material response using X-ray computed tomography (CT). We have started making these samples using the explosive HMX (the main component of PBX 9501, our ultimate target material) and a low-density polymer binder which is similar to the PBX 9501 binder. We expect initial tests on these materials to be completed this FY. The simplified geometry is identical to very localized microstructure in the heteregenous composite - essentially we are reducing a very complex material down to its simplest microstructural features. This helps validate the mechanical property and crystal-binder adhesion parameters in the mesoscale model, which otherwise would be inferred from other measurements in the literature which use several quasi-realistic assumptions.

Simultaneously, we have been researching existing "soft catch" systems for implementation on the gas gun at TA-09 in preparation for the mock explosive and ultimately PBX 9501 impact experiments. We found several existing designs at LANL for polymer and metal samples, but the metal samples have a much higher tolerance for the hardness of the catch system and often use catching materials that do not damage the metals but would damage the explosives. The polymers usually tested in this manner are also high hardness materials that similarly resist damage from catching materials. Thus we have been designing a modified catching system using softer materials such as foam. We have also been researching diagnostic improvements to the gun such as velocimetry measurements or high speed photography. We found that high speed photography can be employed at low / no cost. If the velocimetry diagnostics are ultimately too costly to implement, we may need to switch to a gas gun (e.g. at TA-40 or Ancho Canyon) which has the diagnostics already. This raises the cost per shot significantly over using the TA-09 gun due to the complexity of the other gun operations, so we will have to balance the overall cost with the usefulness of the data. This type of evaluation is currently ongoing. However, our preference is to borrow existing, unused equipment, and we have some leads on velocimetry diagnostics.

We have been designing shock experiments for in-situ X-ray characterization at the Advanced Photon Source and will be discussing scheduling and other matters with the appropriate personnel shortly.

Future Work

The primary goals of the next fiscal year work are 1) to continue developing and then implement a successful sample catching system on a gas gun and demonstrate applicability to soft materials, and 2) to improve the existing thermomechanical models by updating the coding and including cutting-edge experimental data. This latter point is currently being advanced by simplified measurements (e.g. mechanical properties of a two-crystal system with a polymer binder). A secondary goal is to begin in-situ measurements on high explosives (HE) at the Advanced Photon Source (APS).

Like all HE processes at LANL, it is desirable to first test the catching system using mock HE materials such as plastic-bonded sugar or certain polymers. We (Yeager [PI] and Thompson [Co-I]) will perform these tests using various impact conditions to demonstrate the limits of the system. We have been implementing some diagnostics on the gas gun, such as high speed photography or velocity measurements. The damaged samples will then be sent to Patterson (Co-I) for X-ray computed tomography (CT) to measure damage such as cracks and voids in three dimensions.

A postdoc has been identified and will start in August 2016. Luscher (Co-I) will serve as the primary mentor for the postdoc, who will be constructing and running mesoscale simulations.

A higher risk, higher reward goal (secondary) is to begin HE experiments at APS. We have experience doing this in the past but beamtime is perpetually in high demand and the experiments are expected to be challenging. At a minimum, if we do not accomplish the APS experiments in 2016, we will either have experiments lined up for next year or implement a suitable backup plan (such as increased focus on soft-catching HE and performing additional characterization techniques).

Conclusion

Relevant fields will be impacted in several ways: (1) Soft recovery (i.e. without further damaging the sample) would be a new capability for Los Alamos, (2) This type of mesoscale model has been difficult to validate using real data for high explosives, and (3) long-standing questions about the damage to initiation process will be addressed. Successful execution of this program will provide fundamental understanding of high explosive materials in the form of data and models that inform thermomechanical codes, particularly for abnormal events such as fragment impact or low-pressure shock.

Attosecond Dynamics of Correlated Electrons in f-Electron Materials

Steve M. Gilbertson
20140622ECR

Abstract

The knowledge and eventual manipulation of the dynamic properties of electrons in matter is the most critical goal in attosecond (1 attosecond (as) =10-18 s) science. While initial studies have been conducted on simple systems of atoms and molecules using intense (<1013 W/cm2) lasers to control the electronic structure in proof-of-principle experiments, the most exotic behaviors can be found in complex solid materials. In this work, we probed the quantum transient behaviors and interferences in the reflectivity of an isolated attosecond (as) extreme ultraviolet (XUV) pulse from a heavy-fermion material in the presence of a delayed, few-cycle near infrared (NIR) laser pulse. Through this work, we were able to observe and control atomic transitions in an actinide material for the first time and on the intrinsic timescale on the electrons themselves. This study has opened a novel avenue towards the understanding and control of coherence at the previously unavailable attosecond timescale.

To accomplish this work, an attosecond transient reflectivity setup was constructed consisting of a few-cycle NIR laser pulse, an XUV spectrometer, and an ultrastable interferometer for pump-probe experiments. The setup utilizes state-of-the-art technology for attosecond pulse generation and measurements and is an entirely unique capability at Los Alamos National Laboratory (LANL). Up to now, observations of dynamics at LANL were limited to timescales of several femtoseconds (fs) thereby leaving many fundamental questions concerning the actual electron motion unanswered. Using the as apparatus, we were able to conduct the first measurements of electronic dynamics in an actinide which is a class of materials that have particular interest to LANL through programmatic work in uranium and plutonium compounds. This work also allows for a new method of looking at the fastest dynamics that occur in other solid materials, which directly impacts the “materials for the future” scientific pillar at LANL.

Background and Research Objectives

The field of attosecond science has grown tremendously in the past few years. The initial experiments have provided new insight into the dynamics of electron motion in both atomic and condensed matter systems. However, studies of coherent behavior in quantum science remain practically untouched. This is especially true for solid-state systems, where very few experiments have been performed. By choosing f-electron systems, ones that LANL is particularly well suited to study, our research offered a unique opportunity to probe the effect of short, intense laser pulses on a solid material. Optically excited carriers would modify the reflectivity of the sample at certain energy levels. Through manipulation of the laser intensity and pump-probe delay, complete control over atomic transitions, and hence the overall energy structure of the system, could be accomplished for the first time on as timescales.

The rapid advance of laser technology over the past two decades has produced shorter pulse durations with increased control. Now, optical waveforms of as durations in the XUV have ushered in a new frontier where the motion of electrons can be explored, and perhaps, controlled at as time scales [1]. Through the technique of attosecond transient absorption [2, 3], sub-femtosecond dynamics have been reported in atomic and molecular targets similar to those seen in photoelectron measurements [4, 5]. Owing to the simplicity of atomic targets, these results have provided much insight into quantum interference within the atom.

Despite the complexity of producing and handling attosecond pulses (AP), some experiments have already been performed with APs in atoms [4, 6-8], molecules [5, 9] and solids [10]. Atoms have provided the best candidates for extracting the details of correlated temporal motion since the possible outcomes remain small and well-characterized, thus also yielding detailed, complementary theoretical and computational examination

[11]. Conversely, the experiments conducted on solids were mainly proof-of-principle and are of little practical interest to LANL. APs have never been used to study coherent effects in solids, and our results are poised to make a significant impact on this rapidly evolving field. No attosecond beam line existed at LANL prior to the start of this project so this was a major goal at the beginning of the experiment.

In this work we proposed to exploit unique phenomena in 5f Mott insulators and heavy-fermion materials, in particular uranium dioxide (UO2), to demonstrate quantum multi-path interference in the as response of these materials to a NIR laser pulse. Figure 1 shows an energy level diagram for UO2. Several transitions are available to typical attosecond pulses that can routinely be generated in the lab. We focused on reflectivity changes resulting from optically excited absorption structures in f-electron systems. Our technique allows for a material's reflectivity spectrum to be modified allowing measurement and possible control over the electron dynamics.

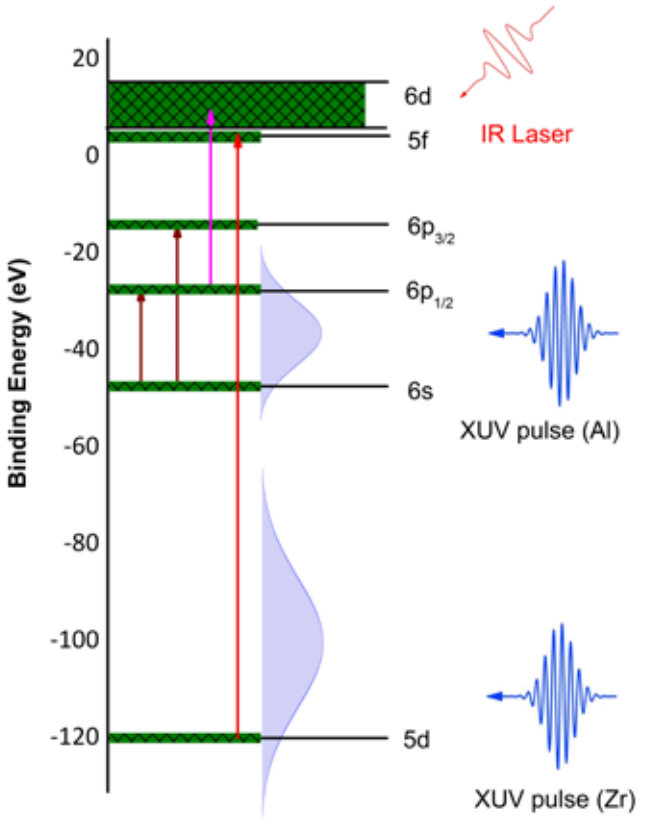

Figure 1. Various energy levels for UO2 are indicated as the green horizontal bars. Broad bandwidth XUV pulses filtered by an aluminum filter can cover the 6p and 6s levels while the 5d levels are accessible with XUV pulses filtered by a zirconium filter. Allowed transitions are indicated by the colored vertical arrows.

The specific research goals for this project are summarized below. First, construction of a hollow-core fiber assembly for generating few-cycle intense laser pulses was required. These laser pulses were used for generating the attosecond pulses as well as providing an intense laser to be used in a pump-probe experiment. This was accomplished in the first year of the project when sub-10 fs laser pulses with nearly 2 mJ of energy were created. Next, an XUV spectrometer had to be constructed that was capable of measuring broad spectra XUV pulses. Along with the spectrometer, attosecond pulses were generated for the first time at LANL. This portion was straightforward, although time consuming. The third portion was the most technically challenging portion of the entire proposal. This was to construct an ultra-stable interferometer capable of temporal jitter less than the attosecond pulse duration. In our case, we estimated sub 300 as pulses would be generated, meaning stability less than 100 as was desired. Through active and passive stabilization techniques this stability was acheived near the end of the second year. Finally, once the setup was complete, attosecond time-resolved reflectivity spectroscopy was conducted from a sample of UO2. This yielded the very first results of electron motion in an actinide. All research goals were met as planned and the resulting measurements have placed LANL in the position of being the sole laboratory capable of measuring attosecond electron dynamics in an actinide material and one of only a few labs worldwide capable of measuring attosecond electron dynamics in a solid material.

Scientific Approach and Accomplishments

Figure 2 shows a schematic of the experimental setup. The measurements for this work were made using a regenerative Ti:Sapphire amplifier which supplied 1 kHz, 3.5 mJ, 35 fs laser pulses. The output of the laser was sent to a 1 m long, neon gas filled hollow core fiber for spectral broadening [12] and temporal compression with multiple bounces from a set of chirped mirrors. The pulse duration were found to be sub-10 fs, as measured with a Grenouille [13]. The overall efficiency of the hollow-core fiber and chirped mirror set was typically 50-70%. Figure 2 shows the spectrum and temporal profile for a 10 fs laser pulse in red and a 30 fs input pulse in dashed black. These are the shortest high power laser pulses currently available at LANL. Their introduction alone represents a significant advancement in optical time resolved spectroscopy capabilities.

Next, the few-cycle infrared (IR) laser pulse was split with a 90/10 beamsplitter in a Mach-Zehnder style interferometer with the majority of the laser power used for generating the attosecond pulse. The laser pulse then passed through the first quartz plate, Brewster windows, and second quartz plate of the generalized double optical gating (GDOG) optics [14, 15]. The laser was then focused with a near normal incidence spherical mirror through a 0.5 mm

fused silica window into the vacuum chamber. After the window, the laser passed through the Barium Borate (BBO) crystal of the GDOG optics that generates the weak second harmonic contribution needed for breaking the symmetry of the driving laser [15]. Finally, the laser was focused onto a 1.5 mm thick laser drilled argon filled gas cell for generating the extreme ultraviolet (XUV) photons for attosecond pulse generation via the high harmonic generation (HHG) technique [16]. A spectrum of the attosecond pulse used for these measurements can be seen in Figure 2 as the solid black curve. The spectrum covered a bandwidth of ~11 eV centered around 40 eV. These attosecond pulses are the first ever created at LANL and the attosecond source is one of only a few worldwide. The source construction was a major milestone for this project and its completion allows LANL to begin studies of electron behaviors on attosecond timescales in gases and solid targets.

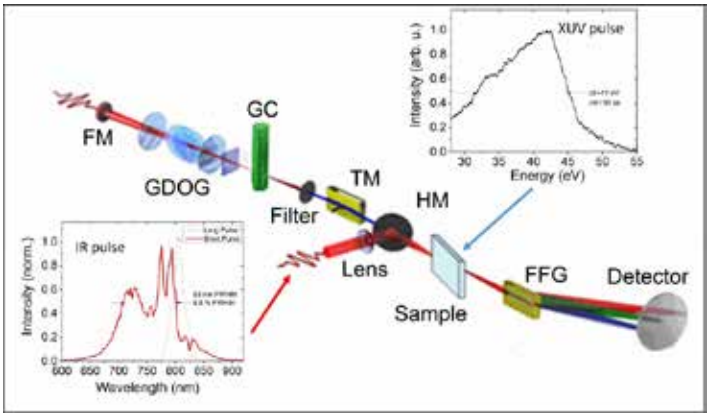

Figure 2. An input laser pulse is focused by a focusing mirror (FM) through the GDOG optics to generate an ellipticity varying pulse. The pulse is then focused onto a gas cell (GC) to generate an attosecond pulse of XUV photons. The residual IR is filter out and the XUV pulse is focused with a torroidal mirror (TM) through a hole drilled mirror (HM) onto the UO2 sample. The spectrum on a typical XUV photon pulse is shown in the upper inset. The reflected XUV photons are then dispersed with a flat field grating (FFG) onto the detector. The pump pulse for these experiments was another linearly polarized infrared laser pulse. This was focused with a lens, reflected off the hole drilled mirror, and was incident upon the UO2 sample. A typical spectrum of a sub-10 fs laser pulse is shown in the lower inset as a red solid line. For comparison, the spectrum of a 30 fs laser pulse is shown as a dashed black line.

After the attosecond pulse was generated, it passed through an aluminum or zirconium filter to remove the residual IR laser light. It then reflected from the material sample and was dispersed by a flat field grating onto a photon detector. The detector consisted of a microchannel plate and phosphor screen followed by a camera to capture images of the spectrum. At the sample, the remaining portion of the original beam acted as an optical pump of the sample for time resolved measurements.

In order for the attosecond measurements to be made, the temporal jitter between the two legs of the interferometer had to be suppressed as much as possible. This was accomplished through active and passive stabilization of the experimental setup. Details of the stabilization method can be seen in reference 17 [17]. Combining the active and passive stabilization, the interferometer could be stabilized to less than 40 attoseconds of temporal jitter, although only for a few minutes at a time. The stabilization of the interferometer to attosecond timescales was the most important milestone to be met., without which the experiments would have been limited to femtosecond timescales. Details of the experimental setup have been submitted for publication to the journal Review of Scientific Instruments.

The attosecond pulses generated had transform limited durations of ~160 attoseconds. Using argon gas allowed for high XUV photon flux requiring integration times of ~1 second. Figure 3 shows a spectrogram of accumulated attosecond spectra plotted versus pump-probe delay. The delay step size was ~200 attoseconds. Each spectrum was smoothed and normalized for presentation. Time zero was located where the modulation signal began. Without an electric field measurement, there was no way of being sure where time zero really occurred although we estimate that it began close to the beginning of the signal when the results are compared to other work [18]. Clearly, centered on 31 eV a modulation appears around time zero (peak overlap of the pump and probe) and continues for ~8 fs. The effect only occurs when the pump laser field is overlapped with the XUV probe and is suppressed very quickly after. Electrons in strongly bound states of UO2 were promoted into the conduction band by the XUV photons which was modified by the intense IR laser thereby changing the reflectivity of the sample. In order to maximize this effect, sufficiently high IR laser field strengths were required to increase the strength of AC stark shifts in the conduction band while staying below the damage threshold of the material sample. Through simple measurements of the laser intensity, the IR field strength was estimated at 2 V/Å on the sample.

Since the observed effects are induced by the oscillating electric field of the IR laser, in effect alternating current (AC) stark shifts, they occur at half the optical period of the pump laser. This can be seen as the modulations having a periodicity of 1.25 fs which is half the optical cycle of the 9.8 fs laser measured by the Grenouille. The dynamical properties of the induced polarization occur on timescales related to the inverse of the width of the conduction band which is several eV wide in UO2. This gives sub-fs tim-

escales for the transitions to occur. The inset in Figure 3 shows plots integrated over ~1 eV bands at 29 eV, 30 eV and 31 eV. The dashed lines on the spectrogram correspond to the locations of the curves shown in the inset. The increase in reflectivity was found to be ~3% total which is less than changes seen in SiO2 from a transient absorption experiment [18] where a nearly 10% change in the transient absorption was observed. We attribute the smaller changes seen in UO2 as stemming from the nature of a transient reflectivity geometry that measures small changes in surface states only.

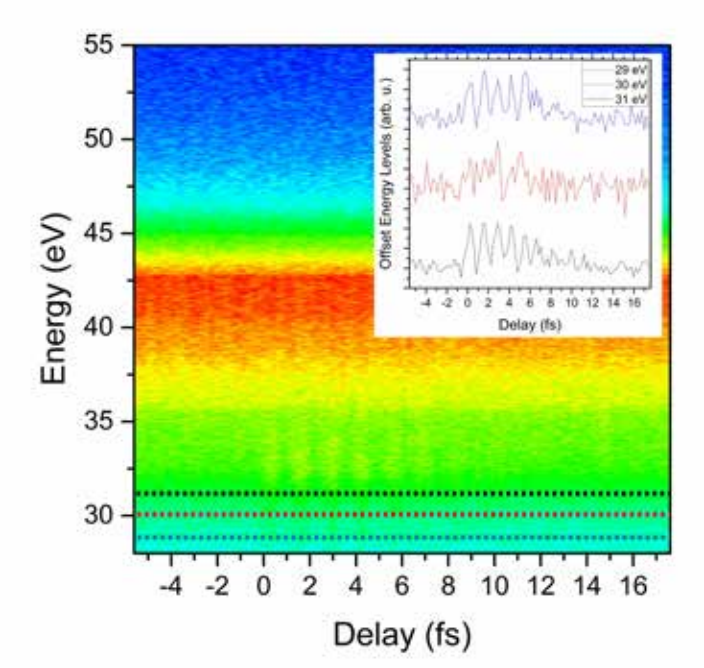

Figure 3. The 2-D image is a map of the energy spectrum of the attosecond pulse after reflection from the optically pumped UO2 sample, plotted as a function of pump-probe delay. Slightly after time zero, a modulation in the spectrum can be seenaround 35 eV. Lineout plots at 29, 30, and 31 eV and shown in the inset. The dashed lines on the 2-D image indicate the regions where the data was taken.

Comparing the experimental results to the energy level diagrams in Figure 1, we find the most probable transition we are measuring to be from a spin-orbit split pair of peaks around 17 eV and 27 eV below the Fermi level. Integrating across all times where the two pump and probe pulses are overlapped gives an "excited density of states" measurement. Each spectral slice was divided by a background spectrum taken when the pump laser was blocked to yield the reflectance. This can be seen in Figure 4. We observe that the reflectance increases over a wide range extending to nearly 34 eV. We attribute this to effects occurring within the entire conduction band. There are also two prominent peaks located at both 29 and 31 eV corresponding to possible UO2 transitions. These measurements represent the first ever attosecond time-resolved energy level measurements made in an actinide.

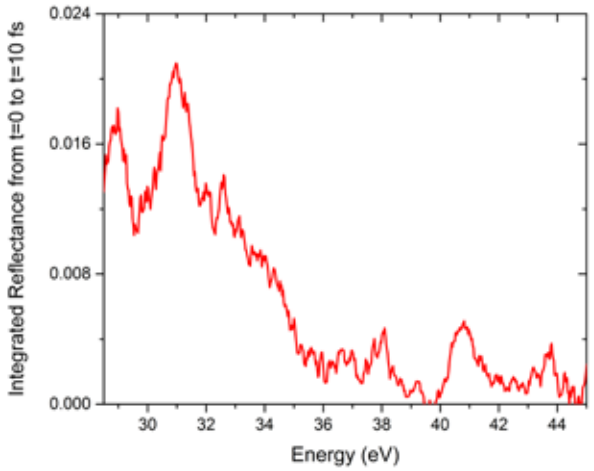

Figure 4. The plot shows the integrated reflectance between t=0 and t=10 fs. This is the temporal region where the temporal modulations were strongest. A double peaked structure is visible at 29 and 31 eV which is in agreement with possible dipole allowed transitions in UO2.

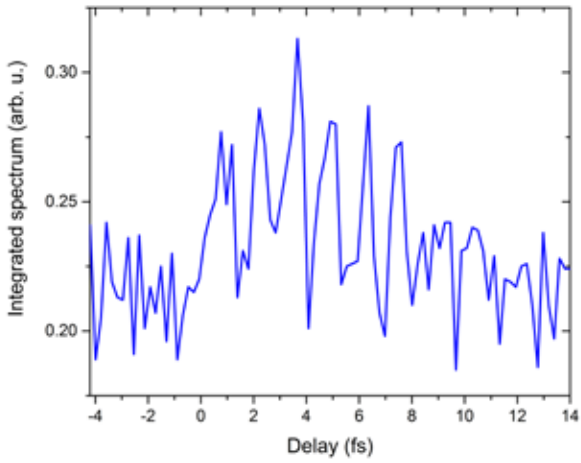

Figure 5. Fully vertically and horizontally binned spectrum of reflected XUV photons between 108 eV and 116 eV. These modulations represent the transient behavior of the optically perturbed 5d->5f transition in UO2. The temporal modulations have a periodicity of less than one optical cycle of the pump laser light and can only be measured with attosecond pulses. The low signal to noise of this figure is an artifact of the weak photon flux available in this energy range.

Finally, to capitalize on the f-electron nature of UO2, measurements of resonant U5d->U5f transitions were conducted. The transition energy is over 110 eV so higher energy XUV photons were required. Replacing the aluminum filter with a zirconium filter increased the transmitted bandwidth to over 100 eV with suppression of photons

below 50 eV. The reduced XUV flux at higher energies can be somewhat counteracted however since the 5d->5f transition is highly resonant as compared to the 6p->6d transitions seen in Figure 3. To overcome the difficulties associated with the reduced XUV flux, the data was fully vertically and horizontally binned over a near 8 eV bandwidth centered around 112 eV. The results can be seen in Figure 5. This plot represents the first transient 5f electron behavior ever measured in a material and was conducted with laser pulses having durations on the order of the intrinsic timescales of the electrons themselves. These results have been submitted for publication to the journal Physical Review Letters.

Impact on National Missions

The proposed application of attosecond sources to studies of coherent effects in solid state systems directly responds to the Grand Challenge in Materials: Discovery Science to Strategic Applications, which underpins all four Laboratory mission areas. The work is especially relevant to the "Materials of the Future" and "Science of Signatures" science pillars. It has provided LANL with a novel capability to investigate the quantum material behavior at the fundamental timescales of electronic motion. The attosecond transient reflectivity spectrometer built with this proposal is the first of its kind at LANL, one of three in the world, and the first to be used for measuring actinide material responses. This new capability will immediately place LANL at the forefront in material science and attract multiple new users to the CINT facilities, especially in actinide research. This project will also enable an important in situ characterization capability for MaRIE, LANL's future signature facility, since the ability to unravel the electron dynamics in complex materials is an important competence underpinning MaRIE's M4 facility.

References

1. Krausz, F., and M. Ivanov. Attosecond physics. 2009. Reviews of Modern Physics. 81: 163.

2. Chini, M., X. Wang, Y. Cheng, Y. Wu, D. Zhao, D. Telnov, S. Chu, and Z. Chang. Sub-cycle oscillations in virtual states brought to light. 2013. Scientific Reports. 3: 1105.

3. Gouleilmakis, E., Z. Loh, A. Wirth, R. Santra, N. Rohringer, V. Yakovlev, S. Zherebtsov, T. Pfeifer, A. Azzeer, M. Kling, S. Leone, and F. Krausz. Real-time observation of valence electron motion. 2010. Nature. 466: 739.

4. Gilbertson, S., M. Chini, S. Khan, Y. Wu, and Z. Chang. Monitoring and controlling electron dynamics in helium with attosecond pulses. 2010. Physical Review Letters. 105: 263003.

5. Sansone, G., F. Kelkensberg, J. Perez-Torres, F. Morales, M. Kling, W. Siu, O. Ghafur, P. Johnsson, M. Swoboda, E. Benedetti, F. Ferrari, J. Sanz-Vicario, S. Zherebtsov, I. Znakovskaya, A. L'Hullier, M. Ivanov, M. Nisoli, and M. J. J. Vrakking. Electron localization following attosecond molecular photoionization. 2010. Nature. (465): 763.

6. Mashiko, H., S. Gilbertson, M. Chini, X. Feng, C. Yun, H. Wang, S. Khan, and Z. Chang. XUV supercontinua supporting pulse durations of sub-one atomic unit of time. 2009. Optics Letters. (34): 3337.

7. Drescher, M., M. Hentschel, R. Kienberger, M. Uiberacker, V. Yakovlev, A. Scrinzi, T. Westerwalbesloh, U. Kleineberg, U. Heinzmann, and F. Krausz. Time-resolved atomic inner-shell spectroscopy. 2002. Nature. (419): 803.

8. Wang, H., M. Chini, S. Chen, C. Zhang, F. He, Y. Cheng, Y. Wu, U. Thumm, and Z. Chang. Attosecond time-resolved autoionization of argon. 2010. Physical Review Letters. (105): 143002.

9. Singh, K., F. He, P. Ranitovic, W. Cao, S. De, D. Ray, S. Chen, U. Thumm, A. Becker, M. M. Murnane, H. Kapteyn, I. Litvinyuk, and C. Cocke. Control of electron localization in deuterium molecular ions using an attosecond pulse train and a many-cycle infrared pulse. 2010. Physical Review Letters. (104): 23001.

10. Cavalieri, A., N. Muller, T. Uphues, V. Yakovlev, A. Baltuska, B. Horvath, B. Schmidt, L. Blumel, R. Holzwarth, S. Hendel, M. Drescher, U. Kleineberg, P. Echenique, R. Kienberger, F. Krausz, and U. Heinzmann. Attosecond spectroscopy in condensed matter. 2007. Nature. (449): 1029.

11. Lukin, M. D.. Trapping and manipulating photon states in atomic ensembles. 2003. Reviews of Modern Physics. (75): 457.

12. Mashiko, H., C. Nakamura, C. Li, E. Moon, H. Wang, J. Tackett, and Z. Chang. Carrier-envelope phase stabilized 5.6 fs, 1.2 mJ pulses. 2007. Applied Physics Letters. (90): 161114.

13. O'Shea, P., M. Kimmel, X. Gu, and R. Trebino. Highly simplified device for ultrashort-pulse measurement. 2001. Optics Letters. (26): 932.

14. Feng, X., S. Gilbertson, H. Mashiko, H. Wang, S. Khan, M. Chini, Y. Wu, K. Zhao, and Z. Chang. Generation of isolated attosecond pulses with 20 to 28 femtosecond lasers. 2009. Physical Review Letters. (103): 183901.

15. Gilbertson, S., Y. Wu, S. Khan, M. Chini, K. Zhao, X. Feng, and Z. Chang. Isolated attosecond pulse generation using multi-cycle pulses directly from a laser amplifier. 2010. Physical Review A. (81): 043810.

16. Corkum, P. B.. Plasma perspective on strong field multiphoton ionization. 1993. Physical Review Letters. (71): 1994.

17. Chini, M., H. Mashiko, H. Wang, S. Chen, C. Yun, S. Scott, S. Gilbertson, and Z. Chang. Delay control in attosecond pump-probe experiments. 2009. Optics Express. (17): 21459.

18. Schultze, M., E. Rothschafter, A. Sommer, S. Holzer, W. Schweinberger, M. Fiess, M. Hofstetter, R. Kienberger, V. Apalkov, V. Yakovlev, M. Stockman, and F. Krausz. Controlling dielectrics with the electric field of light. 2013. Nature. (493): 75.

In situ X-ray Imaging and Diffraction to Understand the Mechanics of Initiation Mechanisms in Explosive Single Crystals

Kyle J. Ramos
20140643ER

Introduction

The project is a joint experimental/theoretical investigation of the deformation mechanisms in the energetic molecular crystal (cyclotrimethylene trinitramine) RDX. The localization of mechanical deformation in explosives under shock compression has been linked to the on-set of chemical reactions and the initiation of detonation. New capabilities for real-time, in situ X-ray diffraction and imaging using the IMPULSE capability at the Advanced Photon Source will be employed to measure the evolution of the average lattice strain and spatially localized material failure in RDX single crystals during dynamic compression. These data will be interpreted and eventually predicted through the development of a single crystal plasticity model. The development of a validated, predictive thermomechanical model for RDX will enable us to model the response of more complex microstructures and defects at the completion of the project. The single crystal plasticity models will take as input existing data from the literature, in situ data from IMPULSE and the results of first principles electronic structure calculations of the orientation-dependent thermophysical properties of RDX. The use of first principles calculations are critical when we will model the high-pressure phase of RDX that cannot be recovered for characterization in the laboratory. The single crystal plasticity model will be validated via its implementation into a finite element simulation code from which we will compute diagnostics, including interface velocimetry and X-ray diffraction patterns that can be compared directly with in situ experiments.

The ability to measure the structure response of complex materials in the nanosecond time scales before they are destroyed during shock compression is a major innovation that this project will advance. Nevertheless, the integration of these measurements with theory and simulation that can rationalize and predict responses based on the activity of the underlying deformation mechanisms breaks new ground in shock physics.

Benefit to National Security Missions

Success in this project will motivate and guide technological development and further experimental work at the NNSA's Dynamic Compression Sector at the Advanced Photon Source and proposed facilities such as LANL's MaRIE.

The development of a mechanistic understanding of the response of energetic constituents to impact will provide the first framework for predicting the material conditions for initiation. This capability will significantly affect high explosive science at LANL and beyond and is critical to our national security mission. NNSA Advanced Simulation and Computing (ASC) and the Department of Defense (DoD) strongly support in situ measurements and emphasize the need for predictive materials models. In addition, new thermomechanical models and the ability to predict initiation are indispensable to the development of reduced sensitivity explosives for DoD and Department of Energy (DOE) insensitive munitions via particle and crystal engineering.

Progress

Continued application of shear stress to dislocations in alpha-RDX in atomistic simulations to evaluate barriers to dislocation motion

These data will inform the generation of single crystal plasticity models. The fundamental properties of dislocations in molecular crystals at the atomic scale have been investigated using a novel approach. The vast majority of atomistic simulations of dislocations in materials have been performed at zero temperature. It is questionable whether these traditional calculations are appropriate for molecular crystals since in most cases room temperature is in excess of 50% of their melting temperature. Hence, we have studied dislocations in the prototypical molecular crystal hexamine using Monte Carlo simulation methods to determine both the atomic scale structure and the temperature dependence of the

stress required to move dislocations. These results directly inform our single crystal plasticity models.

Continued development of an anisotropic equation of state, based on our new formalism, for gamma-RDX and/or other potential phases that are discovered in atomisitic simulations and XRD (X-ray diffraction) experiments.

We recently published in the Journal of Applied Physics free energy-based equations of state for the alpha and gamma polymorphs of RDX. These novel equations of state, based on statistical mechanics, electronic structure theory, and experiment, have enabled very accurate single crystal-level simulations of impacts on RDX, estimates of shock heating on the principal Hugoniot, and the development of a classical multiphase plasticity model for the RDX system. Our electronic structure calculations have identified a potentially new monoclinic phase of RDX that we shall investigate with in situ XRD.

Perform plate impact experiments for phase transformation investigation using XRD diagnostic

We performed the first ever in situ X-ray diffraction experiments on explosives under planar impact in March 2015. Following this success, we have systematically increased the peak loading pressure and varied the strain rate in experiments and simulations to investigate RDX response up to and through the phase transition. Impact experiments were performed at 1.5 and 3 GPa, which are just below the alpha-to-gamma phase transition. Simulations of the velocimetry using our newly developed multiphase plasticity model were in very good agreement with experiments. Predictions for higher pressures indicated a significant strain rate effect. Therefore, dynamic uniaxial loading experiments at lower rates have been planned and will be executed shortly. Combining the X-ray diffraction at multiple peak impact pressures and strain rates will provide information on the kinetics of phase transition.

Compare XRD experimental results with computed diagnostic from simulations

We have developed and validated new single crystal plasticity models and the necessary code to compute X-ray diffraction patterns from the results of the simulations. The single crystal plasticity simulations covered multiple impact pressures, crystal orientations, and crystal thicknesses for planar impact geometries. Overall, the level of accord between our predictions and experiment exceeded by far our most optimistic hopes. We will soon publish this comparison of computed versus experimentally measured velocimetry and are completing analogous comparisons for X-ray diffraction. The comparison with X-ray diffraction will ensure our models are reproducing the average crystal lattice response as well as the continuum response observed by velocimetry.

Apply the new models in the simulation of more complex microstructures

Now that our single crystal plasticity models have been validated, we have subsequently applied them in the simulation of shock propagation through an idealized RDX polycrystal and to predictive simulations of strain localization in a notched RDX crystal under dynamic compression. These simulations of RDX have provided new insights into the mechanics of localized deformation and heating in explosive composites and the role of crystal defects.

Future Work

Goals that we will pursue in the continuation of this project include:

- The theoretical prediction of in situ X-ray diffraction patterns from RDX single crystals under shock compression and experimental validation using either gas-gun or split Hopkinson bar apparatus at the Advanced Photon Source.
- Understanding the properties of dislocations in a prototypical molecular crystals (hexamine) with Monte Carlo-based atomistic simulations. These methods provide the basis for studying dislocations in more complex molecular crystals (ie., RDX).
- Application of our new single crystal plasticity model for RDX to defective and/or polycrystalline samples to understand strain localization and hot spot formation under impact.
- Validation of a phase transformation model for RDX by fitting the transformation kinetics to velocimetry data followed by experimental confirmation by in situ X-ray experiments at the Advanced Photon Source and/or Linac Coherent Light Source.

Conclusion

We will deliver a validated, anistropic thermomechanical model for the response of single crystals of the explosive RDX to shock compression. We shall construct anisotropic, temperature-dependent equation of state for RDX based on experiment and theory. The equation of state will be employed in a single crystal plasticity model that incorporates deformation mechanisms and phase transformations that have been observed experimentally. Rates for the deformation mechanisms will be parameterized to experimental data. The ability to model deformation processes

in explosives pertains directly to explosive initiation and safety, both of which are of considerable importance to ongoing NNSA and DoD missions.

Publications

Addessio, F. L., D. J. Luscher, M. J. Cawkwell, and K. J. Ramos . A high-rate, single-crystal model for cyclotrimethylene trinitramine including phase transformations and plastic slip. Journal of Applied Physics.

Cawkwell, M. J., D. J. Luscher, F. L. Addessio, and K. J. Ramos. Equations of state for the alpha and gamma polymorphs of cyclotrimethylene trinitramine. 2016. JOURNAL OF APPLIED PHYSICS. 119 (18).

Hooks, D. E., K. J. Ramos, C. A. Bolme, and M. J. Cawkwell. Elasticity of Crystalline Molecular Explosives. 2015. PROPELLANTS EXPLOSIVES PYROTECHNICS. 40 (3): 333.

Hooks, D. E., M. J. Cawkwell, and K. J. Ramos . Plasticity in crystalline molecular explosives–A key to unraveling "unpredictable" responses. 2016. Propellants, Explosives, Pyrotechnics. 41 (2): 203.

Luscher, D. J., F. L. Addessio, M. J. Cawkwell, and K. J. Ramos. A dislocation density-based continuum model of the anisotropic shock response of single crystal α-cyclotrimethylene trinitramine. 2017. Journal of the Mechanics and Physics of Solids. 98 (1): 63.

Enabling Mesoscale Science: Nonlocal Dislocation-Flux Crystal Plasticity Under Shock Loading Conditions

Darby J. Luscher
20140645ER

Introduction

Our team will develop and implement a novel physics-based model for dislocation-mediated single crystal plasticity, applicable under shock loading regimes characterized by large deformation, deformation rate, and high pressure and temperature. This endeavor is motivated by challenging mesoscale problems such as damage nucleation at material interfaces. The novelty of the proposed formulation stems mainly from its explicit representation of dislocation flow through the crystal lattice, coupled with a detailed accounting for elastic interactions between dislocations. These features establish a new paradigm for crystal plasticity, which is fundamentally different from existing models in that arena.

Specifically, our single crystal plasticity model will include (1) a proper treatment of the evolution of dislocation fields, built upon balance laws governing their transport through the lattice, (2) a physically consistent representation of long-range nonlocal interactions of dislocations, and their role in resisting (or enhancing) slip, (3) kinetics models for (a) dislocation nucleation, multiplication, and annihilation, consistent with large deformation rates and for (b) dislocation velocity, accounting for phonon-drag and inertial effects acting on dislocations, and (4) boundary conditions that have a direct physical interpretation. Our work will deliver (1) a coupled-physics, mixed-field implementation of the theory, amenable to numerical simulations of polycrystal response, and (2) novel simulations of dislocation pile-up leading to damage nucleation in copper polycrystals under shock loading.

High-risk aspects are numerical issues related to the computational implementation of mixed-field physics calculations, development of models for computing stress fields in the vicinity of dislocations, and the aggressive schedule of code implementations.

Benefit to National Security Missions

The length and time scales relevant in simulations of weapon performance motivate the development of macroscale models that capture the essence of dominant physical processes at finer scales. Examples include plastic slip, void nucleation, growth, and coalescence, phase transformation, and twinning. These physical processes depend critically upon microstructural details, such as grain morphology, orientation distributions, grain boundary characteristics, and defects. The development of macroscale models reflecting these processes demands an understanding of the underlying physics, which is often gained through experiment. Currently available diagnostic measurements for shock-regime experiments are often ambiguous in identifying specific mechanisms of these processes. For example, measurements of free surface velocity (VISAR) require speculative inference to draw conclusions about damage nucleation kinetics.

Development of new in-situ diagnostic technologies, for example, through MaRIE, promises to provide detailed data associated with these im-portant physical processes. In many cases, such newly available data would not be amenable to direct comparison with results obtained using existing models. The connection between microstructural processes and simulations of weapon performance demands insight from mesoscale modeling, to provide more detailed interpretation of currently available measurements and to be predictive on a commensurate level of resolution with anticipated diagnostics.

Our research will deliver a mesoscale simulation capability implemented into an ASC LAP code. These simulation tools are expected to deliver on the promise of nonlocal modeling strategies, namely the ability to predict scale-dependent material response as part of the solution of a multi-physics problem, without requiring any length-scale parameters to be specified as inputs.

Progress

In FY16 we continued to apply the prototype 1D code to simulations of various plate impact scenarios. These simulations were selected in order to challenge the numerical implementation and reveal where improvements to the reliability of the coupling and integration schemes can be made. We have successfully accomplished our goal of a multi-dimensional implementation of each sub-problem into an Advanced Simulation and Computing (ASC) Lagrangian Applications Project (LAP) code, FLAG. We have demonstrated full coupling of all of these sub-problems with application to 1D, 2D, and 3D simulations. We have successfully reached our Stage Gate 3: Tested implementation of each sub-problem into ASC code. A demonstration of the full coupling of these sub-problems to a 3D shock loading problem. Based on review committee feedback, we initiated a thorough code verification effort which has identified a small bug related to a prototype advection solver routine in our code and also identified a more significant bug in the FLAG subroutine used to compute gradients of fields. Both of these were rectified, the latter of which has an impact much broader than simulations for our project.

Future Work

We are on track to complete all of our project milestones and have successfully reached the proposed stage associated with FY16 (see next). In FY17 (funded only partial year) we will focus on publishing results of the ER project and demonstrating an overall TRL high enough to attract continued support from LANL programs. This effort will include running large scale simulations of polycrystal response on high-performance computing platforms and conducting phase-field and theoretical calculations of the interaction of dislocations with grain boundaries in order to enable the future development of interface constitutive models that can be added within our framework.

Conclusion

We will deliver simulation tools built around the mesoscale physics-based nonlocal models of plasticity developed by our research that will deliver on the promise of nonlocal modeling strategies, namely the ability to predict scale-dependent material response as part of the solution of a multiphysics problem, without requiring any length-scale parameters to be specified as inputs. Our research will have significant impact to LANL, the DOE's Office of Science, and the U.S., by virtue of its critical role in enabling mesoscale science needed for modeling nucleation and evolution of defects at material interfaces.

Publications

Luscher, D. J., J. R. Mayeur, H. M. Mourad, A. Hunter, and M. A. Kenamond. Continuum transport of dislocations during shock response of crystals. To appear in 24th International Congress of Theoretical and Applied Mechanics. (Montreal, Canada, 21-26 Aug. 2016).

Luscher, D. J., J. R. Mayeur, H. M. Mourad, A. Hunter, and M. A. Kenamond. A coupled dislocation-flux crystal plasticity theory for modeling shock response of single- and poly-crystals. Presented at 2016 Mach Conference. (Annapolis, MD, 5-7 April 2016).

Luscher, D. J., J. R. Mayeur, H. M. Mourad, A. Hunter, and M. A. Kenamond. A coupled dislocation flux crystal plasticity model applicable under shock loading conditions. Invited presentation at 2015 Mach Conference. (Annapolis, MD, 8-10 April, 2015).

Luscher, D., J. Mayeur, H. Mourad, A. Hunter, and M. Kenamond. Coupling continuum dislocation transport with crystal plasticity for application to shock loading conditions. 2016. International Journal of Plasticity. 76: 111.

Mayeur, J. R., H. M. Mourad, D. J. Luscher, A. Hunter, and M. A. Kenamond. Numerical implementation of a crystal plasticity model with dislocation transport for high strain rate applications. 2016. Modelling and Simulation in Materials Science and Engineering. 24 (4): 045013.

Mayeur, J. R., H. M. Mourad, D. J. Luscher, A. Hunter, and M. A. Kenamond. Numerical implementation of a continuum dislocation dynamics model of single crystal plasticity. Invited presentation at 2015 Mach Conference . (Annapolis, MD, 8-10 April 2015).

Mourad, H. M.. Numerical implementation of a crystal plasticity model with dislocation transport for high strain rate applications. Presented at The 53rd Annual Technical Meeting of the Society of Engineering Science. (College Park, MD, 2-5 Oct. 2016).

Schraad, M. W., and D. J. Luscher. Developing materials processing to performance modeling capabilities and the need for exascale computing architectures (and beyond). 2016. Los Alamos National Laboratory, LA-UR-16-26849.

Sub-Grid Meso-Scale Model for Twinning and Slip Processes

Curt A. Bronkhorst
20150431ER

Introduction

Plasticity is one of the most important means by which metallic materials accommodate imposed large deformations. Plastic slip, which involves dislocation motion on atomic glide planes, is one of the underlying mechanisms in plasticity. Under dynamic loading conditions, however, where dislocation-mediated processes alone cannot accommodate the high rate of imposed deformation, mechanical twinning can become prominent as an alternative mechanism, in competition with slip. In general, representation of slip-based processes in a computational setting is relatively straightforward because dislocations are very small (comparable to atomic length scales) relative to computational cells typically used in practice. This is true even when single crystals are resolved explicitly.

On the other hand, twins are plate-like structures that oftentimes span an entire single crystal, and where atomic planes are oriented differently with respect to the parent crystal. The formation of these features during deformation transforms the microstructure of the material and can contribute substantially to shock hardening in strategic materials. Representing this process numerically, in single crystal models implemented in a traditional finite element setting, has been a challenging task thus far, due to the large size of twinned regions relative to typical computational cells.

Work in this area has been limited to homogenized treatments, which don't resolve the microstructure, or highly resolved phase-field theories, which are computationally very expensive. The crystal plasticity finite element framework under development in the current project will have the unique capability of explicitly representing the morphological transformation due to mechanical twinning. If successful, this will be a transformative development that will allow us to model, in a single computational context, slip and twinning processes occurring simultaneously under general 3D loading conditions. This novel capability will also allow us to properly represent an important aspect of microstructural evolution under dynamic loading conditions, and account accurately for its effect on material response.

Benefit to National Security Missions

Much of our present weapon assessment and certification strategy relies upon numerical simulation of the shock and dynamic deformation behavior of metallic materials. At present, this deformation behavior is represented by highly phenomenological equations with only notional representation of complex physical processes leading to tenuous quantitative accuracy. In addition, this highly phenomenological material modeling strategy leads to numerical difficulties under certain loading conditions. At present, these models completely ignore the physical process of twinning on the shock hardening of metallic materials and also the impact that twinning has upon the structural evolution of materials and its impact upon their damage and failure response. This project will capitalize on LANL's expertise in plasticity modeling and begin to develop the meso-scale modeling tools to allow us to begin to quantitatively compute both dislocation slip and twinning processes in a way which is structurally accurate and allow us to quantify the influence of both of these processes on the way in which it changes under dynamic loading conditions. These developments can be used directly in weapons calculations in the future (selected regions of interest) or used to motivate the proper high length scale models to enable representation of slip and twinning together in a physically accurate way across the entire weapons system.

Progress

The first task in this project is concerned with the integration of a single crystal plasticity model with a sub-grid finite element model, initially developed for the treatment of adiabatic shear band formation. The main difficulty with the computational representation of shear bands stems from their small width (on the order of 10

microns) compared to the size of a typical structure being analyzed, which renders any attempt at explicitly resolving them prohibitively expensive (requiring excessive mesh refinement). The numerical representation of twins is challenging for similar reasons: they are thin lamellar structures, which oftentimes span an entire single crystal, yet their width is typically much smaller. Instead of attempting to resolve such slender structures via mesh refinement, a sub-grid finite element model was developed to allow them to be embedded within computational cells of larger dimensions, thus minimizing computational cost. The first step toward full integration of these two existing components was to reconcile the different kinematic variables used in each of them, such that the sub-grid finite element can pass a strain-like quantity to the crystal plasticity routine, which the latter can use to calculate a stress. This initial handshake capability was established in the past year, and simple computations were performed to verify the implementation of this basic aspect of integration.

With this capability in place, means of embedding a twinned region within a sub-grid element are currently under development. A sub-grid element formulation must ensure satisfaction of compatibility and equilibrium conditions between the twin and its parent crystal, and must obtain the stress response from the crystal model twice: once for the twin, and once for the parent grain. The added computational expense is minimal, because twins are embedded adaptively as they nucleate during the simulation in a small subset of the elements in the mesh. This adaptive strategy, however, requires the ability to answer questions regarding the probability of twin nucleation within a given finite element (and which twin variant is it likely to be), given the local state of stress. Task 2 is focused on producing a nucleation probability model that answers these questions. Existing models developed previously for use in homogenized treatments of twin nucleation in Zr and Mg are being developed further drawing upon experimental information from task 4 (detailed below). In particular, a missing length scale relevant to the twin nucleation process (the initial size of the twin) has been identified from experiments in the past year. The nucleation model is currently being modified to incorporate this important characteristic length scale.

Twins nucleate primarily at grain boundaries and then propagate across the grain, and subsequently grow in width. A twin growth model is therefore being developed (task 3). This model will allow each sub-grid element in a given simulation to calculate the rate of propagation and growth of their respective embedded twins. In the past year, the relevant literature has been surveyed to assess the state of the art in this area, and to study possible twin growth mechanisms in titanium. This study is underway and is currently guiding the growth model development effort. In addition, experimental results from task 4 are being processed quantitatively to identify linkages to single- and two-point relationships.

In support of nucleation and growth model development, low strain quasi-static compression experiments were conducted in the past year as part of task 4, to capture incipient twinning. Multiple high-purity Titanium samples were deformed to three successive levels of strain at strain rates of 0.1—1 /s. These samples were examined metallographically to extract crystallographic texture and twin morphology statistics information. Hopkinson bar dynamic experiments are underway, and the mechanical experiment plan is nearly complete.

Future Work

The anticipated tasks and accomplishment goals for this project in fiscal year 2017 are as follows:

The first task (lead by Mourad) is to develop the sub-grid computational technique for twinning and integrate it with existing single crystal model for slip based plastic processes and incorporate new treatments for nucleation and growth physics. Integration between the sub-grid element and crystal model will be carried out in fiscal year 2016 and 2017, followed by integration with the new twin nucleation and growth representations.

The second task (lead by Bronkhorst) will be to complete development and assist Mourad in implementing the analytical nucleation criteria for the initiation of twin lamellae within the ABAQUS code. We anticipate the development of the nucleation model and its implementation in fiscal year 2016.

The third task (lead by Bronkhorst) will be to develop the twin growth model for expansion of the laminate twin(s) with deformation. This model will be largely early in year two and and finalized in year three and will be coupled with the nucleation model and sub-grid code. Bi-crystal calculations will begin in year two to test numerical stability and begin to test the nucleation and growth criteria for growth of twins under simple shear conditions and will begin to integrate with experiments in year three.

The fourth task (lead by Livescu) will be to demonstrate the feasibility of the newly developed model by performing limited polycrystalline simulations of dynamic experiments conducted on high purity Ti and comparing results to the new experiments and quantitative metallographic information. A test plan has been developed and will be executed throughout the duration of this project. We will

draw upon these experimental results in the simulations we choose to focus upon.

Conclusion

This project will develop the numerical element to represent the morphological deformation of mechanical twinning in single crystal metallic materials. The kinetic and kinematic theory to represent the mechanism of twinning will be developed and taken from existing work. The theory will be implemented within the context of the new numerical element, coupled with existing theory for dislocation slip processes. This work will be supported by experimental data for HCP materials. This is exciting work and is anticipated to produce several publications. This will also allow us to institutionally broaden our computational material science capability.

Publications

Bronkhorst, C., H. Mourad, V. Livescu, I. Beyerlein, and O. F. Dippo. A study of twin formation and early stage growth in high-purity titanium. Invited presentation at MRS Fall Meeting. (Boston, Nov. 27 - Dec. 2, 2016).

Livescu, V., C. A. Bronkhorst, I. J. Beyerlein, H. M. Mourad, M. L. Lovato, and O. F. Dippo. Quantification of twinning for sub-grid mesoscale modeling. Presented at TMS Annual Meeting & Exhibition. (Nashville, Feb. 14-18, 2016).

Mourad, H. M., C. A. Bronkhorst, V. Livescu, E. K. Cerreta, J. N. Plohr, D. J. Luscher, J. R. Mayeur, and G. T. Gray III. Prediction and numerical representation of adiabatic shear banding in metals. Invited presentation at IUTAM Symposium on Integrated Computational Structure-Material Modeling of Deformation and Failure under Extreme Conditions. (Baltimore, June 20-22, 2016).

Mourad, H. M., C. A. Bronkhorst, V. Livescu, J. N. Plohr, and E. K. Cerreta. Modeling and simulation framework for dynamic strain localization in elasto-viscoplastic metallic materials subject to large deformations. 2017. International Journal of Plasticity. 88: 1.

Mourad, H. M., and C. A. Bronkhorst. Finite element simulations of dynamic shear localization in elasto-viscoplastic solids under adiabatic conditions. Presented at U. S. National Congress of Computational Mechanics. (San Diego, 26-30 July, 2015).

Higher Order Spin Noise Spectroscopy: from Foundation of Quantum Mechanics to Applications

Nikolai Sinitsyn
20150504ER

Introduction

Complete information about an interacting system is contained in the full set of correlators of its variables. However, one of the central results in statistical physics, called the fluctuation-dissipation theorem tells us that information provided by standard experimental measurement tools (e.g. conductivity, susceptibilities, or pump-probe experiments) is intrinsically limited: Accessible linear response characteristics are equivalent to measurements of only 2nd order correlators taken at thermodynamic equilibrium. Our main idea is that Spin Noise Spectroscopy, an optical technique pioneered at LANL, opens a unique opportunity to escape from the constraints of the fluctuation-dissipation theorem and measure higher-order correlators, which we will use to:

(i) characterize decoherence mechanisms in solid state qubits made of InGaAs quantum dots,

(ii) reveal interactions and disorder characteristics of conducting electrons in semiconductors,

(iii) explore spins entanglement in atomic gases and test quantum mechanics at new scales.

Studies of higher-order spin correlations will constitute a significant advance in the field of quantum measurement science. We will achieve the most precise understanding of the physics of a nuclear spin bath, determine whether macroscopic systems of ~109 interacting spins can still exhibit quantum properties that cannot be found in classical physics, and obtain qualitatively new information about many-body quantum electron interactions.

Benefit to National Security Missions

This project will build capabilities in the novel measurement methods that enable new scientific discovery at LANL. It is based on recent technological advancements that use the large data storage and manipulation capabilities. Until very recently this technology simply did not exist. The proposal will advance new Laboratory capabilities that underpin a wide variety of Laboratory missions including Nanotechnology and Quantum Information Science. Demonstration of new effects by measurements of higher order correlators in spin systems will generate worldwide attention and will form a robust platform for a mesoscopic spintronics program at LANL. The present project will lay the groundwork for future proposals for external funding to address national problems, including energy efficient applications (DOE). The team will work with A.Taylor to develop a BES Materials Science funded project.

Progress

The work on this project has advanced faster than it had been originally expected due to the additional interest from experimental teams at Chemistry Division at LANL (Klimov) and, on independent direction, by the group at U. Munich, Germany, which is lead by Prof. Jonathan Finely.

We achieved the following:

All members of the project (S. Crooker, F. Li and N. A. Sinitsyn) have published a research paper with first demonstration of the measurements of 4th order spin correlates in atomic vapor 41K.

Together with a group of J. Finely, N. Sinitsyn and F. Li have developed an alternative measurement technique that initially obtained spin correlates of InGaAs quantum dots and then measured the third order correlates. The first article in this series was published in Nature Physics and the second one, which was recently accepted to Phys. Rev. Lett. Results for higher order correlates, revealed very unusual behavior that can be explained only by purely quantum theory. The article in Nature Physics was extensively highlighted in mass media (over 30 online media publications). Currently, our team is working

on detecting similar effects using the LANL platform, which will open the path to use the discovered effects in a broad range of materials.

F. Li and Sinitsyn have finished the work on the theory of higher order correlations in conduction electrons. Results were published in Physical Review Letters.

Research lead by S. Crooker and V. Klimov has produced a new type of highly controllable spin register based on colloid quantum dots doped by magnetic ions. The team used Kerr rotation spectroscopy to detect collective dynamics of these spins. Results are published in Nature Nanotechnology.

Research lead by S. Crooker and Luyi Yang at LANL, partly in collaboration with N. Sinitsyn, led to characterization of optical effects in two-dimensional materials called TMDs. Our team discovered localized spin states that may be used for quantum information processing in those structures. Results are published in Nature Physics and Nano Letters.

N. Sinitsyn has written an invited review called “The Theory of Spin Noise Spectroscopy, the Review” for Reports of Progress in Physics. This review article is currently in press.

Future Work

Experimental studies during 2017 will focus on measuring 3rd-order correlator of the solid state spin qubit realized in InGaAs quantum dots. These spins are entangled with a dense bath of ~105 nuclear spins. Measurements of 3rd order correlators should provide considerable new insight in physics of this interaction. They will allow us to use our the central spin qubit as a nanoscale probe of local nuclear spin dynamics. Recently, we discovered that these correlators can be used to probe fundamental questions of quantum mechanics. Our team already obtained preliminary experimental results in this direction, on which we will develop our studies during 2017.

Theoretically, we will focus on higher order correlators of conduction electrons. We will explore the universality of their behavior due to thermodynamic constraints described by the higher order fluctuation dissipation relations. We will identify a small number of independent parameters that control the shape of higher order correlators and make predictions for their behavior in specific systems.

Conclusion

The goal of this project is to demonstrate the new material characterization method and use it to explore essentially new physical phenomena, previously unreachable by conventional means including some of the most fundamental problems in science such as the emergence of the macroscopic classical realism from microscopic quantum mechanics.

We will show that considerable stream of information provided by the spin noise signal is sufficient to precisely and non-invasively determine higher-than-2nd order correlators of variables even in mesoscopic quantum systems at thermodynamic equilibrium.

Publications

Bechtold, , Li, Mueller, Simmet, Ardelt, J. J. Finley, and N. A. Sinitsyn. Quantum Effects in Higher-Order Correlators of a Quantum-Dot Spin Qubit. 2016. PHYSICAL REVIEW LETTERS. 117 (2).

Bechtold, A., D. Rauch, F. Li, T. Simmet, P. Ardelt, A. Regler, K. Müller, N. A. Sinitsyn, and J. Finley. Three-stage decoherence dynamics of an electron spin qubit in an optically active quantum dot. 2015. Nature Physics. : x.

Li, , S. A. Crooker, and N. A. Sinitsyn. Higher-order spin-noise spectroscopy of atomic spins in fluctuating external fields. 2016. PHYSICAL REVIEW A. 93 (3).

Li, F., and N. A. Sinitsyn . Universality in higher order spin noise spectroscopy. 2016. Physical Review Letters. 116: 026601.

Rice, W. D., Liu, T. A. Baker, N. A. Sinitsyn, V. I. Klimov, and S. A. Crooker. Revealing giant internal magnetic fields due to spin fluctuations in magnetically doped colloidal nanocrystals. 2016. NATURE NANOTECHNOLOGY. 11 (2): 137.

Roy, D., L. Yang, S. A. Crooker , and N. A. Sinitsyn. Cross-correlation spin noise spectroscopy of heterogeneous interacting spin systems. 2015. Scientific Reports. 5: 9573.

Sinitsyn, N. A.. Exact transition probabilities in a 6-state Landau-Zener system with path interference. 2015. Journal of Physics A: Mathematical and Theoretical. 48: 195305.

Sinitsyn, N. A.. Solvable four-state Landau-Zener model of two interacting qubits with path interference. 2015. Physical Review B. 92: 205431.

Sinitsyn, N. A., and Y. Pershin . The Theory of Spin Noise Spectroscopy: a Review. 2016. Reports of Progress in Physics. 89: 106501.

Three-Dimensional Porous Nanographene for Highly Efficient Energy Storage

Edward F. Holby
20150532ER

Introduction

Graphene, due to its unique chemical and physical properties, has emerged as a new energy storage material for lithium ion battery anodes. However, over 50% of the graphene charge capacity is lost during charge-discharge cycles due mainly to restacking of graphene sheets into graphite-like structures. A lack of ideal model graphene systems that can be easily incorporated into Li battery anodes has hindered scientific investigation of Li reaction mechanisms and prevented development of robust graphene-based anode materials.

Using a novel synthetic method developing at C-PCS/MPA-11, we are able to synthesize a series of nitrogen-doped nanographene structures that allow for finely-tuned nitrogen doping and molecular structures and sizes. In this proposal, using these ideal nanographene model systems, we aim to elucidate Li ion adsorption/desorption/diffusion kinetics as functions of nitrogen dopant, molecular size, and structures of the synthesized nanographene. Based on the acquired knowledge, the 3D porous nanographene anodes with desired chemical and structural properties will be further prepared via a crosslinking synthetic strategy in order to maximize the specific Li storage capacity, diffusivity, and long-term charge/discharge stability.

In order to achieve these goals, we propose an innovative R&D approach by integrating theoretical predictions from density functional theory calculations and nanoscale dynamic simulations with experimental characterization using well-defined nanographene model systems. In turn, nanographene with optimally designed electronic and geometric structures will be realized though molecularly controlled synthetic methods.

By combining the multidisciplinary expertise, we expect to understand fundamental reaction mechanisms of lithium on the doped nanographene structures and ultimately, to propose a path forward to designing structurally stable and high-capacity graphene anodes for energy storage applications.

Benefit to National Security Missions

The proposed research enables a better understanding of fundamental mechanisms for Li behavior in porous graphene structures and provides a viable approach for fabricating functional nanomaterials for advanced battery technologies with high-power and high-rate performance. The project addresses fundamental challenges in materials, energy, and nanotechnology. Success will have wide-spread impact on the fabrication of high-performance rechargeable batteries for efficient energy storage. This research will strengthen our capability in addressing key LANL missions of materials functionality and energy security, positioning LANL in a new frontier of energy storage research. With this LDRD-ER effort, understanding the mechanisms that underpin battery reactions and developing high-performance electrode materials for energy storage will support new fundamental and applied follow-on projects in the Basic Energy Science (BES) and Energy Efficiency and Renewable Energy (EERE) offices, respectively.

Progress

We have demonstrated for the first time, a strong correlation between the nanographene structure and lithium ion battery property. Six nanographene derivatives have been synthesized and fully characterized. The structure-dependent charge capacity is clearly illustrated as the functional group dependent charge capacity varies from 380 mAh/g to 950 mAh/g. 950mAh/g is one of the highest charge capacities ever reported for a carbon based anode. State-of-the-art carbon based anode from high surface area carbon nanotube arrays has a charge capacity of 750 mAh/g. Therefore, nanographene is far more superior than the nanotube arrays. Theoretical charge capacity of such nanographenes can reach as high as 2038 mAh/g, three times the charge capacity of graphite.

We have carried out systematic investigation of how various experimental parameters impact the performance of lithium ion batteries. We have optimized the nature of the electrolyte, the composition of various components (binder/nanographene/acetylene black), and the coating method to reach optimized device performance.

In addition, nanographene based lithium ion batteries have shown stability for more than 200 charging-discharging cycles. The improvement in stability is another indication that carbon based materials should and will remain one of the major materials for future energy storage devices.

Future Work

In the coming fiscal year (2017), we will complete two main tasks: (1) Perform chemical synthesis and characterization of 2D and 3D nitrogen-doped nanographenes (NDNG) and their hierarchical structure via self-assembly. NDNG is expected to have a lower activation energy for Li diffusion in and out of the anode materials. Li diffusion is directly related to the charging and discharging rate of lithium ion battery. 2) Fabricate and characterize the performance of lithium ion batteries based on NDNG. We expect superior stability and rate from these novel materials. NDNG has never been synthesized and the demonstration of a NDNG lithium ion battery will represent a major advancement in rational design of anode materials for energy storage devices.

Conclusion

We expect to: (1) Develop new synthetic protocols to prepare a series of nanographenes with various functional groups (linker) and nitrogen doping to finely tune their physical and electronic properties. (2) Gain fundamental understanding of lithium adsorption/desorption and diffusion kinetics on doped graphene by using well-defined (e.g., molecular size, structure, and doping content and location) nanographene model systems. (3) Based on insight provided from experimental results and DFT predictions, design and synthesize novel 3D porous nanographene anodes with optimal chemical and structural properties to maximize Li capacity, diffusion rate, and cyclic stability for energy storage applications.

Publications

Yen, H. J., T. M. Zhou, E. F. Holby, S. Choudhury, A. Chen, L. Adamska, S. Tretiak, T. Sanchez, S. Iyer, H. Zhang, L. Zhu, H. Lin, L. Dai, G. Wu, and H. L. Wang. Structurally Defined 3D Nanographene Assemblies via Bottom-Up Chemical Synthesis for Highly Efficient Lithium Storage. To appear in Advanced Materials.

Controlled Helium Release from Composite Plasma Facing Materials through Interface Design

Yongqiang Wang
20150567ER

Introduction

The overall project goal is to demonstrate a tungsten (W) based plasma-facing material that continually outgasses helium (He) as it is being implanted, thereby preventing He assisted cavity growth and yielding a morphologically stable plasma-facing surface. This demonstration will be accomplished by designing and testing a tungsten-metal (W-M) nano-composite containing interfaces that provide stable pathways for controlled and continuous He outgassing. The interfaces will be designed such that the pathways self-organize under He implantation.

This project is built on recent research by our team into the interaction of He with solid-state interfaces in bcc-fcc multilayer composites, in which we discovered that that certain metal-metal interfaces are capable of stably storing up to several atomic % of He without forming He bubbles: far in excess of the bulk He solubility limit. The reason for this surprising lack bubbles as compared to the bulk counterparts is that implanted He aggregates into platelets that wet high-energy parts of the interfaces of interest and do not grow into voids even in the presence of radiation-induced vacancy supersaturations.

We plan to use this insight to design W-M interfaces with high-energy regions patterned into continuous pathways (nanochannels) that will first trap (or store) He and then allow it to outgas while maintaining morphological flatness, mechanical cohesion and thermal conductivity across the interface. Successful demonstration of this novel interface design concept will enable breakthrough improvements in the performance of W based plasma-facing materials under fusion-relevant conditions, and the insights gained will become a broader "toolkit" of materials science and engineering methods that may later be used in other fusion and non-fusion related applications where precipitation of impurities play an important role.

Benefit to National Security Missions

This research is important to LANL's core materials capabilities: discovering, understanding,and exploiting defects and interface in materials. To achieve the vision of prediction and control of materials functionality set by MaRIE vision, it is noted that "a key grand challenge is the ability to predictively manipulate microstructures to achieve desired macroscopic performance. Central to this challenge is the potency of defects, either to be exploited intentionally for enhanced performance or to suffer their deleterious effects." Our proposed research directly addresses this vision and will strengthen LANL's competency in the design of functional materials through exploiting defects and interfaces.

A recent report by the DOE Office of Fusion Energy Sciences' Advisory Committee emphasized that "the majority of [plasma facing component] materials research should be oriented towards tungsten" (p. xvi) with the specific goal of identifying and characterizing W-based materials suitable for fusion-relevant environments. The proposed project directly addresses the needs in this report.

We plan to design W-M interfaces with high-energy regions patterned into continuous pathways (nanochannels) that will first trap (or store) He and then allow it to outgas while maintaining morphological flatness, mechanical cohesion and thermal conductivity across the interface. Successful demonstration of this novel interface design concept will enable breakthrough improvements in the performance of W based plasma-facing materials under fusion-relevant conditions, and the insights gained will become a broader "toolkit" of materials science and engineering methods that may later be used in other fusion and non-fusion related applications where precipitation of impurities play an important role.

Progress

Experimental Efforts

Helium implantation induced bubbles are found to aggregate at defects, such as dislocations, grain boundaries and interfaces. We explored the planar distribution of helium bubbles at the Cu/V and V/Cu/V interfaces. Bilayer Cu/V and trilayer V/Cu/V thin films were synthesized on the MgO (111) substrate at elevated temperature, and the interface orientation follows the Kurdjumov-Sachs relationship. 20 KeV He+ implantation has been applied at 250oC, and transmission electron microscopy characterization and statistical analysis of helium bubbles distribution revealed the tendency of heterogeneous distribution of helium bubbles at the interface plane. We found that the bubbles that prefer to stay along certain crystallography directions or form some regular patterns are correlated with the trace of gliding dislocations and the interface misfit dislocation structure. There are also He denuded zones observed near the V/Cu interfaces. Our finding provides a potential method of manipulating the distribution of implanted bubbles through tailoring the boundary dislocation structure. A manuscript entitled "Exploring helium bubbles planar distribution at the Cu/V interface" is about to be submitted to Materials Research Letters in Summer 2016.

Considerable experimental effort went into high quality specimen preparation, in particular growing large grains in bi- and tri- metallic layers with desired crystalline orientations. First, the Cu-V bilayer and V-Cu-V trilayer films were fabricated by electron beam evaporation at elevated temperature using high-purity (99.999%) copper and vanadium targets. Second, W-Cu bilayer and W-Cu-W trilayer films were fabricated with magnetron sputtering. Third, we can use very high temperature to deposit pure W on single crystalline MgO or sapphire substrate with different orientations; this can produce very high quality interface of W/MgO and W/Al2O3 to better compare with model prediction of MDI distributions. These single layer W films are scheduled to be made during the summer.

Much of the characterization has been focused on reliably preparing TEM specimens for both cross-section and plane view observations. The focused ion beam (FIB) lift out technique was applied to prepare both plane view and cross-section transmission electron microscopy (TEM) foils. The plane view technique requires specific TEM capability to form a horizontal section rather than a vertical section. The most challenge part was keeping the metallic film intact when making a trench from MgO substrate side. Both microstructure and chemical analysis of He implanted TEM specimens have been conducted inside a FEI Tecnai F30 field emission gun TEM.

Modeling Efforts

We have completed development of a phase field model for He precipitate morphology evolution at interfaces in metal multilayers. We have implemented the model into INL's MOOSE software and used it to study precipitate coalescence and dewetting on an isolated interface. Moreover, D. Yuryev spent the fall 2015 semester at LANL on a DOE fellowship to work on integration of modeling and experimental work across the team. A manuscript entitled "Modeling growth, coalescence, and stability of helium precipitates on patterned interfaces" is about to be submitted to Modelling and Simulation in Materials Science and Engineering (MSMSE) in Summer 2016. We are also working on an additional batch of simulations—to be completed in the summer of 2016—that will also be written up and submitted for publication in a peer reviewed journal.

Our team has also made a number of conference presentations in the second year, including one oral presentation in 2015 MRS Fall Meeting, two oral presentations in 2016 TMS Annual Meeting, and one poster presentation in international conference on fusion reactor materials in the fall of 2015.

Future Work

The goal of the third year will be centered heavily on experimental efforts to better understand W-Cu nanocomposite structures for desired helium storage and controlled helium release while modeling/simulation efforts will be to complete the manuscripts writing and conference presentations (MIT-subcontract on modeling effort ends after the second year). First we will refine the physical vapor deposition synthesis parameters for making predictable W-Cu interfaces (bi-layer, tri-layer, and multi-layer); in addition to the conventional ex situ cross-sectional and planview TEM characterization of He-implanted bi-layer and tri-layer specimens, we will also perform in situ heating experiments in a transmission electron microscope. At elevated temperature, small helium bubbles will aggregate together to form either large bubbles or elongated gas channel along the misfit dislocation line at the interface. In situ TEM observation provides us the opportunity to capture this phenomenon. Finally, we plan to perform fusion relevant He plasma exposures on the pre-selected W-Cu multilayer specimens at UCSD's PIECES facility, a DOE Office of Fusion Energy Sciences' user facility for plasma-surface interactions research, to evaluate effectiveness of these novel nanolayered interfaces in managing/minimizing undesired morphologies (e.g. "fuzz" formation) at the plasma facing surfaces. Preparation of two publications is anticipated: one that explores the temperature effects on He precipitation, bubble formation and gas channel formation using in-situ TEM and another one concerning the

evaluation of these nano-engineered novel structures in a real plasma. We plan to present our work at the 2016 fall MRS meeting in Boston, 2016 International Conference on Application of Accelerators in Research and Industry, and/or 2017 annual TMS meeting in Phoenix.

Conclusion

The overall technical goals are to demonstrate a tungsten (W) based plasma-facing material that continually outgasses helium (He) as it is being implanted, thereby preventing He assisted cavity growth and yielding a stable plasma-facing surface. This demonstration will be accomplished by designing and testing a tungsten-metal (W-M) nano-composite containing interfaces that provide stable pathways for controlled and continuous He outgassing. Successful demonstration of this novel concept will enable breakthrough improvements in the performance of W based plasma-facing materials under fusion-relevant conditions as well as enhancing other applications where precipitation of impurities play an important role.

Publications

Chen, D., N. Li, D. V. Yuryev, J. Wen, K. Baldwin, M. J. Demkowicz, and Y. Q. Wang. Imaging the in-plane distribution of helium precipitates at a Cu/V interface. Materials Research Letters.

Li, N., M. Demkowicz, N. Mara, Y. Q. Wang, and A. Misra. Hardening due to interfacial He bubbles in nanolayered composites . 2016. MATERIALS RESEARCH LETTERS. 21663831: 1110730.

Qin, W. J., F. Ren, R. P. Doerner, Y. Y. Lian, Y. J. Feng, X. Liu, Y. W. Lv, S. Chang, L. Dong, H. Wang, L. L. Hu, J. Tang, M. Tang, and Y. Q. Wang. Enhanced radiation tolerance and thermal fatigue properties of nanochannel W films. Science Advance.

Yuryev, D. V., and M. J. Demkowicz. Modeling growth, coalescence, and stability of helium precipitates on patterned interfaces. To appear in Modelling and Simulation in Materials Science and Engineering.

Zhang, H. X., F. Ren, Y. Q. Wang, M. Q. Hong, X. H. Xiao, W. J. Qin, and C. Z. Jiang. In situ TEM observation of helium bubble evolution in V/Ag multilayer during annealing. 2016. Journal of Nuclear Materials. 467: 537.

Precision "Bottom-Up" Fabrication of Non-classical Photon Sources

Jennifer A. Hollingsworth
20150604ER

Introduction

"Quantum: light sources deliver photons in a strictly regulated fashion that defies the statistical distribution of photons that result from classical light sources, such as lasers, light-emitting diodes and thermal sources. A true single-photon source yields one photon when optically or electrically prompted, while non-quantum sources are always subject to a Poisson distribution in their photon statistics. Single-photon sources are needed as 'building blocks' toward next-generation quantum-information technologies – secure quantum communication (optical quantum bits/'qubits'), quantum networking (optical 'messengers'), quantum cryptography, quantum computation, and quantum sensing (including aiding development/qualification of sensors for quantum-information experiments and performance testing of low-light imaging systems).

Nanowire (NW) elements are nearly ideal structures for assembling photonic circuits due to their extreme shape asymmetry, which can afford optical confinement in two dimensions and opportunities for extensive transport in the long, third dimension, followed by photon out-coupling at the distal end. Integrating individual, otherwise isolated single quantum emitters within a NW cavity affords clear benefits for both systems – the wire is functionally "activated" by the emitter, while the emitter becomes accessible for a range of excitation routes, as well as to photon-information transport and collection. Although significant progress has been made in the past decade in emitter-in-wire single-photon sources by epitaxial-growth methods (top-down etching of planar structures containing self-assembled QDs, QDs self-assembled in a NW, and bottom-up nanodisc-in-wire structures), outstanding challenges remain.

The overarching goal is to address these challenges by combining novel fabrication principles with unique emitters to create quantum-emitter/NW-waveguide hybrid structures exhibiting: (1) on-demand single photons, (2) room-temperature photon purity, and (3) fast emission. Specifically, we will embed our so-called 'giant' QDs (g-QDs) within zinc oxide NWs, where the g-QDs will be structured to afford both room-temperature spectral purity and single-dot level optical stability (photons-on-demand), while the NWs will provide efficient subwavelength waveguiding.

Benefit to National Security Missions

With respect to our Science Mission, especially in regard to Materials Chemistry, Materials-by-Design, and Materials Properties, we will establish new methods for fabricating functional hybrid nanoscale structures that will exhibit designed emergent properties. We will establish new knowledge/new understanding regarding how to enhance/tune fundamental semiconductor radiative rates by field effects (proposed novel quantum-dot/dielectric metamaterial couple) and/or charge enhancement (quantum-dot/diode couple). More practically, we will demonstrate the first waveguided optically and electrically pumped single-photon sources based on solution-synthesized quantum emitters, characterized by an unprecedented combination of: ultra-pure photon statistics, high room-temperature efficiencies, and "on-demand" response that is not possible using conventional approaches. We also anticipate proving a path-forward to very low-threshold lasing resulting from our coupling of a novel emitter with a nanowire cavity (for strong cavity-emitter coupling). Thus, our Discovery Science aims will enable understanding/controlling collective properties of excitonic/dielectric hybrids using advanced spectroscopies, in-situ measurements & CINT (user facility). Toward applications relevant to nuclear nonproliferation, DoD, NIST, and IC, the work aims to establish new single-photon source capabilities for next-generation quantum information technologies – secure quantum communication, networking, cryptography, computation and sensing, with low-threshold lasers also useful for next-gen solid-state lighting and conventional communications. More specifically -- Photon-on-demand

are needed for DoD, DARPA secure communication, as well as non-proliferation programs (e.g., next-gen NCAM) - performance testing of low-light imaging systems, development and qualification of sensors for quantum information (QI) experiments, while entangled photon source will serve broad needs in QI science & secure communication (QKD & beyond).

Progress

In the second year of the project we continued to emphasize capability development most relevant to Objective 1 and underpinning for Objectives 2 and 3. Specifically, efforts in the nanoscale precision integration of 'giant' quantum dot (g-QD) quantum emitters with silica dielectric nanodisks by dip-pen nanolithography (DPN) were continued for optimization of both location precision and control over the number of quantum emitters placed per DPN "write" step. In particular, we observed that the previously favored scan-coating method for "inking" the DPN "pen" with g-QD solutions was challenging to reproduce. For this reason, we conducted a systematic study of the dip-coating process when applied specifically to suspensions of large, colloidal nanocrystals. We found that the DPN literature lacked any such study of technologically relevant "inks," as most reports have focused on molecular inks, while only one investigates the forces and processes involving writing of liquid inks. Significantly, our inks behave as liquid inks with respect to how they deposit from the DPN writing tip to the substrate, but the liquid deposition physics does not fully inform as to the manner in which large nanocrystals within the liquid transfer to the substrate. For this reason, we performed the first study of the effects of ink viscosity, ink-substrate contact angle, pen dwell time, pen rate of spot-to-spot motion and position of spot in a writing cycle (pattern of written spots) on (a) size of spot formed and (b) number of nanoparticles per spot. With this knowledge, we also used DPN to couple g-QDs with ZnO nanowires. The ZnO nanowires were synthesized for this project in two configurations. These were horizontal, lying-down wires for positioning g-QDs on the outside of the end of ZnO waveguide, as well as vertical stands of wires for deposition of g-QDs onto the top of the nanowire to be followed by continuation of ZnO growth to enclose g-QDs within the ZnS waveguide structure. To facilitate incorporation of the g-QDs into the oxide matrices, we have recently overcoated both visible-emitting CdSe/CdS and infrared-emitting PbSe/CdSe g-QDs with ZnO shells, imparting chemical compatibility between the two systems (semiconductor emitter and oxide waveguide). In addition, in support of Objective 3, we have synthesized a novel ZnO microdisk-on-wire structure whose optical properties are being calculated to assess the presence of whispering gallery modes in the disk portion of the structure into which photons in the wire-waveguide would be coupled. The progress made in integration and synthesis aspects of the project to date in year 2 will be key to demonstration of waveguiding and manipulation of photon characteristics in these hybrid structures by the end of this year of the project.

Future Work

In the remainder of the second year of the project we will focus on controlling the number of g-QDs (visible and near-infrared emitters) placed at the side-ends of horizontal ZnO wires and onto the tops of vertical nanowires. We will structurally and optically characterize these hybrid structures. Optical characterization will entail assessment of color and nanowire-diameter/length-dependent waveguiding toward single-photon emission performance. Tasks to be accomplished include experimental confocal microscopy studies to determine the efficiency of ZnO NW waveguiding process. In the thrid year, initial assessments of multi-photon/many-emitter systems will be extended to single-photon waveguiding, where the hybrid will necessarily comprise a single g-QD embedded in a ZnO nanowire. Single-nanostructure time-tagged, time-resolved photoluminescence spectroscopy will assess stability, linewidth, emission rate, polarization. In the third year, focus will shift entirely to single-photon behavior, which will necessitate optimization of single-nanoparticle writing by DPN (to increase chances of encountering one and only one g-QD on a ZnO platform) as well as conducting Hanbury Brown and Twiss and Hong-Ou-Mandel experiments to assess the purity and indistinguishability of the single-photon emission events (employing a new superconducting NW single-photon detector for experiments in the near-infrared). We anticipate that Objective 3 ('Speeding up' colloidally synthesized emitters) will at least be partially addressed with successful incorporation of g-QDs within the ZnO nanowire (via electromagnetic field enhancement). However, we now further suggest that co-deposition of g-QDs with plasmonic nanoparticles at the ZnO interface or on the ZnO pillars (for embedding with the ZnO waveguides) can be used as an alternative approach to field-based g-QD radiative rate enhancement in the event that field effects afforded by the ZnO component prove too weak. Furthermore, to meet Objective 2 (Electrically driven single-photon emission), we will focus our ZnO synthesis efforts on chemical doping during hydrothermal growth to create the required p-n junctions.

Conclusion

We will demonstrate the first waveguided optically (Objective 1) and electrically (Objective 2) pumped single-photon sources based on solution-synthesized quantum emitters, where our gQD emitters possess the unique advantages of ultra-pure photon statistics (complete antibunching) and

high room-temperature efficiencies compared to epitaxially grown emitters, combined with “on-demand” (non-blinking) response that is not possible using conventional colloidal QDs. We will also provide new understanding toward enhancing radiative rates by field effects (gQD/dielectric couple) and/or charge enhancement (gQD/diode couple) (Objective 3). Each new property will “emerge” as a direct result of the proposed design for a novel hybrid-material constructs.

Publications

Dawood, F., P. A. Schulze, C. J. Sheehan, M. R. Buck, A. M. Dennis, N. Karan, I. Staude, J. Dominguez, G. S. Subramania, A. R. James, I. Brener, N. A. Amro, and J. A. Hollingsworth. Precision placement of nanocrystals onto sub-micron three-dimensional dielectric antenna by dip-pen nanolithography. Small.

Peer, A., A. Singh, J. A. Hollingsworth, and H. Htoon. Coupling quantum dots to gold nanocups. Nanoscale.

Perovskite Solar Cells: The Next Frontier in Energy Harvesting

Aditya Mohite
20150612ER

Introduction

Recent discovery of incorporating organic–inorganic hybrid perovskites such as CH3NH3PbX3 (X = Cl, Br, I) as donor materials in a simple planar bilayer photovoltaic devices has revealed very high power conversion efficiency exceeding 15%1-4 without the need for nanostructuring or creating complex device architectures. In less than eight months, this work published in Nature1, 3 and Science4 has been cited more than 200 times. In spite of the celebrity status for this amazing new material, there is extremely limited scientific understanding on what intrinsic properties are responsible for endowing it with near ideal optical and electrical properties. Building on our extensive expertise in the organic photovoltaic (PV) devices 5, through a combined experimental and modeling effort, here we will formulate critical design strategies for high-performing devices based on hybrid perovskites by achieving synthetic control over light absorption properties, conversion of optical-to-electric energy, manipulation over charge separation and recombination.

Benefit to National Security Missions

This proposal focuses on developing perovskites and to gain unprecedented power conversion efficiency in photovoltaic (solar cell) devices. Perovskites with controlled crystallite domain size, defects, and morphology, coupled with an interfacial layer could redefine photovoltaic research as next generation solar cells with unprecedented high efficiency. The proposed work will strengthen our capability in addressing laboratory missions, particularly in the areas of materials development and energy security, and support new program development in Office of Science.

Progress

In the past year we mainly focused on achieving technologically relevant stability for perovskite solar cells: One of the key fundamental questions that will perhaps decide the fate of the perovskite based materials technology is stability. This year we have performed extensive work on understanding and resolving stability in hybrid perovskite based materials. These studies are outlined below.

We measured the degradation in the perovskite solar cell with continuous light soaking with a solar simulator. We discovered that this over time leads to the decrease in the current density of a perovskite solar cell. We attributed this to the formation of light-activated trap states. We also found that these light-activated trap states dissipate away when the solar cell is kept in the dark for a very brief time (<1 min). This leads to the complete restoration of the power conversion efficiency of the solar cell. We also used theoretical modeling to show that the microscopic origin for the formation of these light activated trap states is directly linked with the organic molecule methyl ammonium, which assists in the coupling of the light generated charge to the perovskite crystal lattice forming so called “polaronic states”. These results were reported in three papers published in Nature Communication 2016, Advanced Functional Materials 2016 and Nano Letter 2016.

Equipped with this finding, we then went on to investigate hybrid perovskite where we modified the organic cation from methyl ammonium to butyl amine, which forms a layered structure. We then applied our hot-casting technique discovered last year to achieve single crytalline films of this material and reported an efficiency of nearly 13%, which was a record for this material. We showed that these films exhibited technologically relevant stability when light soaked for >2000 hours in sunlight and humidity. These results were recently reported in Nature Letters 2016.

Future Work

In the coming fiscal year, we will focus on two aspects:

1. Increase the PV efficiency of our methyl ammonium hybrid perovskite to 20% for a large area device.

2. Explore the replacement of Pb with Sn and understand structure-property relationships as we increase the concentration of Sn. The goal is to achieve 10-15% PV efficiency with a 60-40 Pb-Sn concentration.

Conclusion

We expect to achieve an understanding of the intrinsic source of high photocurrent and voltage (open circuit voltage; Voc) in perovskite-based solar cell devices, as well as how the emergent ferroelectric properties of these unique materials can be tuned to surpass current device efficiencies and develop high efficiency low cost PV devices.

Publications

Nie, , Tsai, Asadpour, Blancon, A. J. Neukirch, Gupta, J. J. Crochet, Chhowalla, Tretiak, M. A. Alam, Wang, and A. D. Mohite. High-efficiency solution-processed perovskite solar cells with millimeter-scale grains. 2015. SCIENCE. 347 (6221): 522.

Tsai, , Nie, Cheruku, N. H. Mack, Xu, Gupta, A. D. Mohite, and Wang. Optimizing Composition and Morphology for Large-Grain Perovskite Solar Cells via Chemical Control. 2015. CHEMISTRY OF MATERIALS. 27 (16): 5570.

Defect-Induced Emergent Magnetism in (Nonmagnetic) Complex Oxides and their Interfaces

Scott A. Crooker
20150613ER

Introduction

Interest in oxide-based electronics has exploded in recent years, fueled by the ability to grow atomically-precise interfaces and heterostructures of various complex oxides. Strontium titanate (SrTiO3) -- a nonmagnetic wide-bandgap insulator -- is a foundational material in this field. Owing to its widespread use in materials science, its dielectric and lattice properties are well known. However, tantalizing evidence in recent years indicates that there may yet be much more to SrTiO3 than previously realized: Several groups around the world have recently reported unexpected emergent phenomena at these oxide interfaces, most strikingly magnetism and superconductivity. This is particularly remarkable because the constituent oxides (e.g., SrTiO3 and LaAlO3) are nominally nonmagnetic and insulating. Crucially, the formation and distribution of oxygen vacancies defects (VO) – which form readily in SrTiO3 and are mobile – are widely suspected to play an essential but as-yet-poorly understood role in these emergent interfacial phenomena.

Our team recently applied powerful magneto-optical techniques to bulk SrTiO3 crystals for the first time and discovered that, surprisingly, VO defects can generate an optically-induced and persistent magnetism in this nominally nonmagnetic material. However, the underlying physical mechanisms remain unknown. Nor is it known how deeply these findings inform on the interfacial magnetism discussed above. Therefore, motivated by these results and coupled with our state-of-the-art capabilities for pulsed-laser deposition (PLD) oxide growth at LANL, we propose to reveal the origin of (and ultimately engineer) the defect-related emergent magnetic properties in these bulk and interfacial complex oxides, focusing on the archetype SrTiO3. We will apply a powerful suite of magneto-optical techniques to SrTiO3 epilayers and SrTiO3/LaAlO3 interfaces grown by PLD and MBE techniques, including Optically-Coupled SQUID Magnetometry and also ultrafast magnetization dynamics via Time-Resolved Faraday Rotation. Controlled introduction and removal of VO defects via annealing protocols is a key component of this program.

Benefit to National Security Missions

This research is vital to LANL's core materials capabilities: Discovering, understanding, and exploiting defects and interfaces in materials. It not only strengthens LANL's existing competency, but also significantly expands capabilities for our future nanostructured materials via "external" control of interfaces and defects. Furthermore, the MaRIE Workshops report indicates that "interfaces and defects" must be addressed to solve the decadal challenges for accelerating materials discovery. To achieve the vision of prediction and control of materials functionality, it states "a key grand challenge is the ability to predictively manipulate microstructures to achieve desired macroscopic performance. Central to this challenge is the potency of defects, either to be exploited intentionally for enhanced performance or to suffer their deleterious effects. The role of defects is a microcosm of the broader impact of rare events and fluctuations that are a key stumbling block in achieving prediction and control." Our project directly addresses this vision. The ability to control defects will yield new and unique results since the materials we are going to explore will provide us the opportunity to obtain new and/or improved functionalities not obtainable through bulk materials or by simply changing material chemistry. Moreover, this research represents an opportunity for LANL to take the global lead in the fundamental understanding of oxide materials. LDRD's investment in such an effort will ensure continued leadership in nanotechnology and functional materials, which will enable LANL to respond effectively to future calls by BES and other funding agencies.

Progress

In the past year we have developed and used the experimental technique of Time Resolved Faraday Rota-

tion, the development of which was a primary goal of this proposal. We used this new capability to benchmark its performance on one of the new family of atomically-thin semiconductors, molybdenum disulphide (MoS2). These results turned out to be particularly interesting, and were published in the high-profile journals Nature Physics and Nano Letters. The full references are:

Spin coherence and dephasing of localized electrons in monolayer MoS2, by Luyi Yang, Weibing Chen, Kathleen M. McCreary, Berend T. Jonker, Jun Lou, Scott A. Crooker, Nano Letters 15, 8250 (2015)

Long-lived nanosecond spin relaxation and spin coherence of electrons in monolayer MoS_2 and WS_2, by Luyi Yang, Nikolai A. Sinitsyn, Weibing Chen, Jiangtan Yuan, Jing Zhang, Jun Lou, Scott A. Crooker, Nature Physics 11, 830 (2015)

As a result of this work, we received many invitations to present invited talks at international conferences, such as the 2016 March Meeting of the American Physical Society, and also talks at ICPS-2016 (Beijing) and also PASPS-9 (Kobe, Japan). These invitations ensure that LANL stays at the forefront of semiconductor physics.

Future Work

In the next fiscal year (FY17), we will focus on the following goals:

Optically-coupled SQUID magnetometry
We intend to measure the actual magnetic moment that is induced in oxygen-deficient SrTiO3 wafers by polarized light, by coupling polarized light down into the bore of a commercial SQUID magnetometer. Preliminary studies indicate that this approach will be successful. Of particular interest is the field dependence and temperature dependence of the optically-induced magnetization

Continue magneto-optical studies in our 8T magneto-optical cryostat
We will primarily rely on our "workhorse" setup for magnetic circular dichroism (MCD;), which has proven extremely effective at revealing magnetism in SrTiO3. Our Oxford Spectramag split-coil magnet at the NHMFL has direct optical access and is ideally suited for this purpose (T=1.5-300 Kelvin, B= 0-8 Tesla).

Growth and preparation of SrTiO3 epilayers and SrTiO3 / LaAlO3 interfaces, which will be performed at CINT-Los Alamos using our state-of-the-art PLD techniques. Direct comparison with similar samples grown by MBE forms a key piece of this proposal; these will come from established connections with Chris Leighton & Bharat Jalan (Minnesota) and Suzanne Stemmer (UCSB). Reduced concentrations of elemental impurities in MBE samples will allow us to ascertain whether, e.g., VO-Fe complexes play any role in the observed magnetic phenomena. In parallel, we will also continue to measure commercial "pure" SrTiO3 crystals as well as crystals that are intentionally and very lightly doped (0.01%) with Fe and Nb.

Controlled introduction and removal of VO via annealing in UHV and oxygen environments. This essential capability currently exists in U. Minnesota but we will emulate and improve it here at CINT to ensure quick turnaround of samples and rapid convergence on ideal annealing recipes.

Conclusion

The overall technical goal of this project is to study and ultimately reveal the origin of the recently-discovered magnetism and magnetic effects that emerge in many (nominally nonmagnetic) oxide semiconductors. We will focus on strontium titanate, which is the archetypical and foundational material in this new burgeoning field of 'complex oxide electronics'. Our plan is to directly compare magnetism and magneto-optical phenomena in SrTiO3 grown by bulk (commercial) methods, by pulsed laser deposition (PLD), and by molecular beam epitaxy (MBE). A key component is the rapid iteration of samples following controlled introduction and removal of oxygen vacancies.

Publications

Yang, L., N. A. Sinitsyn, W. Chen, J. Yuan, J. Lou, and S. A. Crooker. Long-lived nanosecond spin relaxation and spin coherence of electrons in monolayer MoS2 and WS2. 2015. Nature Physics. 11: 830.

Yang, L., S. A. Crooker, B. T. Jonker, J. Lou, and K. M. McCreary. Spin coherence and dephasing of localized electrons in monolayer MoS2. 2015. Nano Letters. 15: 8250.

Energetic Materials Cocrystal Engineering: Toward Superior Munitions

Philip Leonard
20150623ER

Introduction

This research is developing energetic materials with new and hopefully superior performance and safety properties via cocrystallization. Cocrystallization will allow us to exploit synergistic properties in existing energetic materials (EM) by alloying on a molecular level. Property modification via creation of stoichiometric cocrystals has been demonstrated with great success in pharmaceuticals and is beginning to bear fruit for explosives as well. For example, two EM that are powerful performers in terms of detonation velocity and shock pressure may separately be highly sensitive to impact, by cocrystallizing those molecules one might be able to achieve a layered structure where planar dislocations dissipate energy non-violently resulting in an acceptable handling safety. In the same vane, two insensitive materials which are non-performers due to inadequate density could cocrystalize into a form with a higher than average density as a result of superior packing. Given challenges in scaling and adopting new materials, creating better EM through cocrystallization has significant advantages. Cocrystallization of HE is critical as an alternative to formulation where the properties of molecules are always averaged - often with trade-offs in sensitivity and performance.

One challenge in this effort is coupling modeling and experiment. We are applying the latest in density functional theory (DFT) functionals to predict packing structures as well as modeling of single crystal X-ray data to determine structures. This active discourse will accelerate experimental achievement while also providing insight into the failings of our modeling assumptions.

Benefit to National Security Missions

Cocrystals have great potential for technological innovation. This project will perform fundamental research into the nature of intermolecular interactions in condensed matter that will enlighten cocrytallization in defense-related applications as well as life-science applications. An increased understanding of intermolecular bonding will be crucial to the development of explosives with superior properties in terms of energy density, handling safety, and specialized properties such as high melting and decomposition temperatures. Because explosives are widely used in the harvesting of fossil fuels, this research will improve our ability to extract energy resources from deeper or more difficult terrain. Improved explosive safety has direct application to DOD safety and DOE safety and surety missions. We envision that the capability to modify detonation velocity and pressure as a function of density will have important implications for the design of precision explosive applications such as linear and conical shaped charges and explosive lenses, applications which may be of interest to DARPA or NASA for controlled demolition such as rocket stage separation.

Progress

Initial screening

We have screened for cocrystal formation within a matrix of 12 different materials and found six likely cocrystals. Solvent grinding was performed for screening and produced mixed-phase material. This type of material is difficult to characterize for phase fraction and crystal structure of the constituents. The grinding technique was then iterated to determine processes for maximizing the phase purity of the formed cocrystal. Energy input and duration of grinding was systematically varied by performing vibratory or planetary ball milling and taking aliquots after different durations. Powder X-ray diffraction (PXRD) was performed and structure refinement analysis (i.e. both phase fraction and structure determination) is underway for this large dataset (i.e. 30 powder X-ray diffraction patterns down-selected out of 120). In the next two quarters, we will use other crystallization techniques to purify or scale up production of the most promising of these cocrystals.

X-ray analysis

One of the major challenges identified in the first year was analyzing powders that contain a mixture of crystalline constituents after solvent grinding. We took a two pronged approach: first, we improved the phase purity of our materials by optimizing our processing as discussed in task 1 and second, we used structure refinement analysis to quantitatively determine phase fraction and the crystal structures of each phase. We evaluated a number of different analysis software options and associated algorithms including GSAS, TOPAS, MAUD, and CrysAlisPro. We have also solicited specialized expertise through collaboration with crystallographers at LANSCE and will likely employ a student or postdoc for the analysis in the second year. In year 2, we will determine the best refinement structure analysis and determine phase fraction of the materials we are either screening or scaling up for sensitivity testing. The unit cell information for the pure cocrystal phase material will be used in modeling efforts.

Modelling
We have improved the refinement and prediction codes and worked on creating good sets of charges for the models. Further improvements to the code will be made as we compare real data to the calculated structures. Method integration will be performed as an investigation of trinitrotoluene (TNT) polymorphs for code validation.

Sensitivity and Performance Testing
We have expanded the nitrogenous structures based on trinitrophloroglucinol (TNPG) in an attempt to distinguish cocrystals from salts and network compounds. Salts of TNPG, including triaminoguanidine (TAG) at 1:1 molar equivalents and hydroxylammonia (HA) at 1:3 (TNPG-HA) molar equivalents have been successfully prepared on 2 g scales and baseline sensitivity data obtained. Both were shown to have high impact sensitivity, low friction sensitivity and moderate electrostatic discharge (ESD) sensitivity. Additionally, crystals of TNPG-TAG have been grown and are awaiting single crystal diffraction measurements.

The 1:1 salt of TNPG with melamine has been scaled up to 50 g and a single pellet of TNPG-Melamine at 1” diameter pressed for a rough estimation of ease of detonation.

Future Work
Initial screening
Cocrystal formation will be performed using solvent grinding and wet chemistry techniques. Solvent grinding is an efficient method in pharmaceuticals but is only now being utilized in explosives because we have overcome the inherent hazards. The LANL HE Crystal Lab has constant temperature and continuous circulation growth vessels, specifically designed for growth of cocrystals. Our goal is to create multiple highly crystalline materials for X-ray analysis.

X-ray analysis
In order to understand intermolecular interactions in the synthesized co-crystals we must determine their full atomic structure. We will apply atomistic simulation techniques to aid solution. Powder X-ray Diffraction (PXRD) on the cocrystals will enable us to identify their Bravais lattice and unit cell parameters. We will also measure vibrational spectroscopy in order to determine the number of unique molecules per unit cell. Our goal is to generate data sets for each new material for modeling.

Modelling
Using the Bravais lattice, unit cell parameters, synthon structures, and the number of unique molecules per unit cell, we will perform a series of Monte Carlo simulations with a generic force field to determine an optimal set of coordinates for the molecules of that lattice. The stability and heats of formation of those structures will be computed by condensed phase DFT calculations in order to identify which is energetically most favorable. Our goal is to be able to solve single crystal X-ray data and predict the correct packing structure (although possibly not exclusively).

Sensitivity and performance characterization
Sensitivity of new cocrystals will be assessed by the M-7 analytical team using standard drop-hammer, BAM friction, and electrostatic discharge (ESD) testing. Performance testing will confirm the calculated or expected detonation velocity and energy of promising new explosives. Our goal is to make safe energetic materials.

Conclusion
Our technical goals are to (1) develop and utilize rational crystal engineering strategies to discover cocrystals and (2) demonstrate superior explosive safety and performance and improved material properties. The first goal has broad relevance to chemistry in general as modification of physical properties are significant to everything from pharmeceuticals to non-linear optical (NLO) materials. Achieving a rational design process for cocrystallization based on more than intuition is critical to the future of the field. Developing new explosives is no less critical to national security as existing mainstays are being threatened due to environmental concerns.

Publications
Bowden, P. R., P. W. Leonard, J. P. Lichtardht, B. C. Tappan, B. L. Scott, and K. J. Ramos. Energetic salt of trinitrophloroglucinol and melamine. 2015. In APS Shock Compression of Condensed Matter. (Tampa, 14-19 Jun. 2015). , p. 6. Tampa, FL: American Physical Society.

Majorana Fermions for Quantum Information

Filip Ronning
20150628ER

Introduction

Quantum information processing offers great potential in terms of National Security, fundamental science, and commercial applications. However, quantum information is notoriously sensitive to small amounts of noise. A solution to this problem lies in using so-called fault tolerant topologically protected states to store quantum information. Majorana fermions, which were predicted over 70 years ago, but not yet definitely observed in nature, are examples of a topologically protected state that could be used for quantum information technology. Recent progress has suggested that appropriately engineered structures in solid state systems could realize Majorana fermions. Several promising first experiments have been performed, but disorder has limited further progress on existing materials. Instead, strongly correlated f-electron materials, such as SmB6 (samarium hexaboride), can also host Majorana fermions in appropriately engineered structures, and are much cleaner.

Benefit to National Security Missions

This work will address DOE Office of Science and national security mission needs. We propose to provide evidence for an exotic particle known as a Majorana fermion. A Majorana fermion has potentially a huge impact on national security as it can provide the platform for quantum information processing, which enables computations not possible on a classical computing architecture. The advantage of Majorana fermions is that they are much less sensitive to noise effects which can destroy other quantum information architectures. We will work on a material known as Samarium hexaboride. This material is interesting by itself as it may possess a unique surface state. Thus our studies will also shed light on a new type of matter found in Samarium hexaboride.

Progress

During the past year we attempted different ways to generate superconductivity in a topologically non-trivial electronic state. We tried to find superconductivity in the so-called Weyl semimetal NbAs, by applying pressure, and examining if this system goes superconducting under pressure. We learned that it does not. In addition, we deposited elemental Aluminum on crystals of samarium hexaboride(SmB6). We prepared of order of 15 such devices over the past year. Unfortunately, none of them demonstrated proximity induced superconductivity on the surface state of the SmB6 crystals. Our non-linear transport measurements suggest that the issue may be related to the low work function of the SmB6 crystals. Other approaches we attempted include different etch procedures to clean the surface prior to deposition. We also looked at an intrinsic junction created where residual Aluminum flux imbedded in the SmB6 crystal was used as the superconducting lead. This also did not help, suggesting surface termination is an important issue.

Future Work

Samarium hexaboride (SmB6) may possess an exotic electronic state on the material's surface. If it exists and superconductivity could be induced by proximity, one has the potential to create an exotic particle known as a Majorana fermion, which could be used in quantum information processing. We will explore the properties of devices made of SmB6. This will be accomplished by depositing an elemental superconductor on top of the SmB6 single crystals. If the interface between the SmB6 crystal and the elemental superconductor is transparent, then we will have the possibility of creating non-linear transport in such a device, which possesses a Majorana fermion. So far, we have been unable to generate the necessary clean interface, which may be due to the low work function of the SmB6 crystals. We are proceeding by trying different elemental superconductors with different work functions as well as different methods for preparing the surface before deposition including argon milling. We will continue to investigate thermal decoherence effects on the use of Majorana fermions for quantum memories.

Conclusion

We propose to provide evidence for the existence of the elusive Majorana fermions in hybrid structures using SmB6, and to further demonstrate that the position of the Majorana fermion can be moved. The physical exchange of Majorana states leads to exotic properties, which in the future can form the basis for quantum computation.

Publications

Ghimire, N. J., Y. Luo, M. Neupane, D. J. Williams, E. D. Bauer, and F. Ronning. Magnetotransport of single crystalline NbAs. 2015. JOURNAL OF PHYSICS-CONDENSED MATTER. 27 (15): 152201.

Luo, , N. J. Ghimire, E. D. Bauer, J. D. Thompson, and Ronning. 'Hard' crystalline lattice in the Weyl semimetal NbAs. 2016. JOURNAL OF PHYSICS-CONDENSED MATTER. 28 (5).

Materials Dynamics via Large-Scale Molecular Dynamics and Embedded Scale-Bridging Simulations

Timothy C. Germann
20150750ER

Introduction

Trinity simulations will provide insight into the dynamic behavior of tantalum, and demonstrate the use of multiple node types (Haswell, Knights Landing (KNL), and burst buffer) to execute embedded task-based scale-bridging simulations. First, using lessons learned from the CoMD proxy application, a KNL-optimized version of the Scalable Parallel Short-range Molecular dynamics (SPaSM) molecular dynamics code will be developed and optimized for the Trinity architecture. This will then be used to perform large-scale (multibillion-atom) simulations of the shock compression and spall failure of nanocrystalline tantalum samples, providing unprecedented insight into the fundamental microscopic processes controlling the strength of materials. Second, building upon efforts of the Exascale Co-design Center for Materials in Extreme Environments (ExMatEx), the newly developed Task-Based Scale-bridging Code (Tabasco) will be used to model the Taylor anvil impact of (polycrystalline) tantalum, to demonstrate the feasibility of at-scale heterogeneous computations composed of coarse-scale Lagrangian hydrodynamics tasks residing on Haswell nodes, dynamically launched constitutive model calculations executed on the KNL nodes, and whose results are stored for subsequent re-use in databases residing on the burst buffer nodes. Longer-term, the atomistic insight into the role that shock-induced dislocation slip, twinning, and phase transitions play in deformation and failure will be used to improve the mesoscopic constitutive model calculations, ultimately linking the microscopic SPaSM and macroscopic Tabasco simulation regimes.

Benefit to National Security Missions

This project addresses several advanced scientific computing challenges of key importance to the DOE Office of Science, Office of Advanced Scientific Computing (ASCR) and the NNSA Advanced Simulation and Computing (ASC) project. In particular, it will explore potential new uses for the additional memory layer ("burst buffers") in Trinity and subsequent high-performance computing (HPC) platforms, namely to store and manage a distributed database of fine-scale model evaluations for embedded scale-bridging computations. It will also advance the "computational co-design" efforts of ASCR and ASC by taking lessons learned from simple and flexible "proxy applications," which have been used to collaborate with computer science hardware (e.g. vendors) and software teams, and use these co-design efforts to optimize the existing Scalable Parallel Short-range Molecular dynamics (SPaSM) code for the new architecture of Trinity. SPaSM is used for scientific studies by several programs, including the ASC Physics and Engineering Models (PEM) project, and Office of Basic Energy Sciences (BES) projects. Computational co-design is also one of the main thrust areas of LANL's Information Science and Technology (IS&T) pillar.

Progress

During the Phase 1 Trinity Open Science period, we were able to demonstrate scale-bridging materials science simulations, and provide feedback and suggestions on the supporting software stack requirements for such simulations. Our three stated goals for this period were to:

1. use Trinity Phase 1 (Haswell nodes) to perform a petascale Task-Based Scale-bridging Code (Tabasco) demonstration calculation of the Taylor anvil impact of tantalum;
2. evaluate and benchmark the use of burst buffer key/value store intrinsics as an interface to, or an alternative for, standard database technologies such as Redis and RAMCloud, for our scale-bridging database storage, query, and interpolation; and
3. use lessons learned from the CoMD proxy application to develop and optimize a KNL-optimized version of the Scalable Parallel Short-range Molecular dynamics (SPaSM) molecular dynamics code.

Within the ASCR Exascale Co-design Center for Materials in Extreme Environments (ExMatEx), we have developed scale-bridging adaptive physics refinement approaches for materials simulation, and used these methods to evaluate various task-based programming models and runtime systems. The purpose of the Trinity Phase 1 portion of this project was to provide a petascale scale-bridging demonstration, and to evaluate the possibility of using burst buffer nodes for storing and managing the microstructure-response database which is populated and queried during the course of an adaptive sampling simulation.

We were able to develop a "proof of concept" demonstration of our Tabasco multi-scale physics code that was able to run at scale using an asynchronous task-based runtime, such as Charm++. Tabasco includes: (a) coarse-scale Lagrangian hydrodynamics; (b) dynamically launched constitutive model calculations, using a Taylor fine-scale plasticity model for Phase 1; (c) storage of the fine-scale evaluation results in a database for reuse; and (d) adaptive sampling which queries the database, interpolates results, and decides when to spawn fine-scale evaluations. Disabling the Adaptive Sampler is equivalent to a "brute force" simulation, where every Lagrangian element executes a fine scale model at each time step. The original (MPI-only) code was refactored as Charm++ chares, using the original data decomposition to allow for comparison. We also explored other task-based runtimes, libCircle and Vernon's MPI Task Pool.

Scaling runs were performed on partitions ranging from 1 to 4096 nodes. Strong scaling (in which the problem size is held fixed while the number of nodes is increased) was quite good to hundreds of nodes, as more cores are available to handle the numerically intensive fine-scale evaluations. Weak scaling (in which the problem size is scaled in proportion to the number of nodes) began to diminish around 100 nodes, due to the suboptimal decomposition of the Lagrangian hydrodynamics. Several production simulations were carried out that integrated tens of thousands of timesteps, until the compressive shock wave reached the end of the sample and the simulation was ended - thus achieving our goal of demonstrating at-scale scale-bridging simulations with dynamically spawned fine-scale calculations and database storage, query, and interpolation.

Use of the burst buffers for the database helped exercise the burst buffers and HIO library, but is currently unusable for our science runs. For example, Datawarp jobs experienced scheduling issues between the Datawarp allocation and the actual run, resulting in crashes. Our work with libHIO stimulated several library updates and made it a much stronger library as a result, but a version that resolved all of our issues was only obtained after the end of Phase 1. In lieu of this preferred solution, an "in memory" HashMap database proved to be a reasonably fast solution for short runs, and a Posix-based database was the best for larger longer scalable runs.

Optimization of CoMD for the KNL architecture was greatly enhanced by two events with Intel and Cray application engineers: the January 24-29 Trinity hackathon and June 7-9 Discovery Session. During these sessions, we were able to greatly enhance the single-node performance on Haswell (in January) and KNL (in June) nodes, with a speedup over 3x that of the original version. While most tests were run for a 1M-atom system. we also performed additional memory-intensive tests. Simulations with up to 20M atoms per KNL node fit in the high-bandwidth on-package memory (MCDRAM), which will suffice for our planned SPaSM runs, which will involve large-scale distributed Trinity simulations of up to 9.5B atoms.

Future Work

This project has several tasks and goals, for both Phase 1 and Phase 2 of Trinity and both scale-bridging and molecular dynamics materials science simulations. In particular, the following Phase 2 tasks are planned for the upcoming year:

1. Using lessons learned from the CoMD proxy application, a KNL-optimized version of the Scalable Parallel Short-range Molecular dynamics (SPaSM) molecular dynamics code will be developed and optimized.

2. SPaSM will be used on Trinity Phase 2 to perform large-scale (multibillion-atom) simulations of the shock compression and spall failure of nanocrystalline tantalum.

3. We will demonstrate the use of Trinity Phase 2 (Haswell, Knights Landing (KNL), and burst buffer nodes) for embedded scale-bridging using TaBaSCo, using an improved fine-scale model executing on the KNL nodes.

Task (1) will largely be completed in the remainder of FY16. As discussed above, during the past year, KNL-specific CoMD studies and optimizations have been performed, including at hackathons and discovery sessions. Incorporation of these lessons and optimized code into SPaSM is underway, and further tests and optimization on early KNL hardware will be completed prior to the availability of Trinity Phase 2 for Open Science runs (Task (2)), which will comprise the majority of this year's efforts.

Task (3) relies upon a software stack (job scheduler and MPI communication layer) that permits simultaneous allocation and use of both types of nodes (Haswell and KNL) within a single job. Based on our recent Phase 1 efforts,

such coordination (even between Haswell and burst buffer nodes) is quite challenging and requires outside assistance from vendors (Cray, Intel) and HPC support staff, so this task should be viewed as a stretch goal that will be attempted after successful completion of (1) and (2), and only if these non-project members are able to assist.

Conclusion

The scientific goal of these simulations is to better understand and model the dynamic response of materials (specifically tantalum), under impact and spall failure. Our computational goal is to evaluate the use of burst buffer nodes for the database query and interpolation which is central to our adaptive sampling scale-bridging. The results of this project will improve subsequent simulation codes and computer architecture designs.

Predicting High Temperature Dislocation Physics in HCP Crystal Structures

Abigail Hunter
20160156ER

Introduction

The primary goals of this project are to use a novel mesoscale model framework to (1) investigate high temperature deformation mechanisms, and (2) predict their effect on the overall mechanical response of hexagonal close packed (hcp) metals during manufacturing processes or accelerated aging experiments. These goals will be achieved through advancement of a 3D mesoscale code unique to Los Alamos National Laboratory (LANL) called phase field dislocation dynamics (PFDD). This model will become the first mesoscale model to account for both extreme temperature variations and plasticity in hcp crystal structures in a self-consistent, physical way. Beyond the award period, this novel temperature-dependent model will be sufficiently versatile for further advancements to phase transformations or void nucleation and growth.

Many hcp materials, such as Zr, Mg, and Be, are of interest in engineering applications because of their high strength and low density. To fully achieve our goals, this project requires tight coupling with experiments on Mg and Zr to both inform and validate the model. As part of this project, we will instrument a current rolling mill by refurbishing existing load cells, installing infrared cameras to track surface temperature entering and exiting the rolling mill, and installing high speed cameras to track plate exit velocity. These enhancements will allow variables such as temperature under rolling, load under rolling, and time under load to be extracted for specific localities within a plate. This will allow for finer control and repeatability of the roll bonding process and the output data will improve fidelity by providing data, such as applied load and initial temperature conditions, needed to initialize the hcp specific temperature dependent PFDD model. Separate from this LDRD, the instrumentation will convert an existing traditional manufacturing process into an advanced manufacturing process.

Benefit to National Security Missions

The temperature dependent phase field dislocation dynamics (PFDD) model aims to bridge the atomic to mesoscale gap, and produce predictive multiscale simulations crucial for understanding dislocation structure evolution under extreme conditions. Continuum-scale material models used in Los Alamos National Laboratory (LANL) codes lack physically based descriptions of mechanisms that many atomic, nano, and microscale models have shown to be important. The information gained during this project can be used to develop physically based constitutive models to describe strength and damage. Predicted stress-strain curves will reveal the impact temperature has on both the microstructural evolution and the global material strength response (e.g., flow stress and hardening) in relevant hexagonal close packed (hcp) metals, such as Zr, Hf, and Be. Furthermore, this project is centered around modeling kinetics at 'extremes' in temperature, which is paramount for understanding the effects of radiolytic aging on microstructure evolution. While self-annealing does not result in large temperature variations, small changes in the temperature have a significant impact on the microstructure and the overall material behavior. Understanding these effects becomes increasingly important for determining the performance, reliability, and safety of weapon systems, a primary mission of the Laboratory. The Physics and Engineering Models (PEM) Program has an interest in the problems addressed during this project and could represent a potential future funding source. Basic Energy Sciences (BES) is another potential future funding source. BES has identified 'Mastering Defect Mesostructure and its Evolution' as a primary research direction for mesoscale science.

Progress

Real materials exhibit varying degrees of elastic anisotropy which are manifest in measurable mechanical properties. In particular, accounting for anisotropy can be particularly important in hexagonal close-packed

(hcp) materials due to how they deform or how they are processed. Up until now, our Phase Field Dislocation Dynamics (PFDD) model has been constrained to elastic isotropy. To provide insight, and remedy the discrepancy between simulation and experiment, we have extended the PFDD model to incorporate full anisotropic elasticity. As a preliminary application, we have applied our model towards studying the effects of anisotropy on the equilibrium stacking fault width of Shockley partial dislocations. A manuscript on this work in currently under review, and we have been invited to present this work at a conference in October 2016.

Extending on this work, we are in the midst of applying our model towards computing the (finite) energy barrier necessary for constriction prior to cross-slip using both isotropy and anisotropy. Cross-slip is a thermally activated mechanism in face-centered cubic (fcc) and body-centered cubic (bcc) metals, and is an application for the temperature-dependent PFDD model. In addition, we are investigating the Ni3Al (superalloy) system which is both relevant across a range of industries, and is known to exhibit desirable mechanical properties which are highly dependent on the complex configuration of dissociated, spread dislocation cores. Superalloys show some unique behavior due to temperature changes (anomalous hardening), hence both superalloys and cross-slip will be good cases for testing the new temperature-dependent aspects of the PFDD model. Two manuscripts are in progress on this work.

This project proposed hiring and funding a post-doctoral research associate. Ben Szajewski started in Theoretical Division (T-3) in November 2015. During this first fiscal year, Ben has learned about the phase field approach and the Phase Field Dislocation Dynamics (PFDD) model central to this project. He has focused much effort on the PFDD advancements and studies detailed in the previous two paragraphs.

Some efforts have also been focused on modifying the PFDD model to work on a fcc lattice rather than a cubic grid. In other words, the grid points at which equations are solved will coincide with the atomic positions in an fcc lattice. Once this is achieved for these metals, we will have the capability to easily substitute in grids that also coincide with bcc and hcp metals as well. This will resolve some numerical issues with modeling hcp metals. We have also started implementing a kinetic Monte Carlo (kMC) algorithm with the PFDD algorithm to include temperature dependence.

In the first year on the experimental side, the primary goal was to instrument a current rolling mill by refurbishing existing load cells, installing infrared cameras to track surface temperature entering and exiting the rolling mill, and installing high speed cameras to track plate exit velocity. These enhancements will allow variables such as temperature under rolling, load under rolling, and time under load to be extracted for specific localities within a plate. This will allow for finer control and repeatability of the roll bonding process and the output data will improve fidelity by providing data, such as applied load and initial temperature conditions, needed to initialize the hcp specific temperature dependent PFDD model. This goal has been achieved and this capability now exists at LANL. Additional parts are currently being ordered and the final steps for refurbishing an existing rolling mill will be finalized in the last quarter of FY16.

Future Work

The primary goals of this project are to use a novel mesoscale model framework to (1) investigate high temperature deformation mechanisms, and (2) predict their effect on the overall mechanical response of hexagonal close packed (hcp) metals during manufacturing processes or accelerated aging experiments. These goals will be achieved through advancement of a 3D mesoscale code unique to Los Alamos National Laboratory (LANL) called phase field dislocation dynamics (PFDD). To fully achieve our goals, this project requires tight coupling with experiments on Mg and Zr to both inform and validate the model.

In the second and third years, this project proposed yearly milestones centered around experiment-simulation comparisons, which will probe increasingly complex temperature dependencies on deformation mechanisms in hcp metals, such as Zr and Mg. In the first fiscal year (FY 16), we focused on development of the temperature dependent PFDD model. During this time, instrumentation of an existing rolling mill at LANL was also completed. In the second fiscal year (FY 17), work will continue on development and testing of the temperature dependent PFDD model. We will use this code to start looking at temperature dependent material behavior in fcc metals and superalloys for validation purposes. We will also begin to incorporate slip systems and crystallography important necessary to model hcp metals (perfect dislocation motion). On the experimental side of the project, experiments on Zr and Mg will begin.

Conclusion

We will advance a 3D mesoscale code unique to Los Alamos called phase field dislocation dynamics (PFDD). The model aims to bridge the atomic to meso-scale gap, and produce predictive multiscale simulations crucial for understanding dislocation structure evolution under extreme conditions. Continuum-scale material models used

in weapons codes lack physically based descriptions of mechanisms that many atomic, nano, and microscale models have shown to be important. The information gained during this project will be used to develop physically based constitutive models to describe strength and damage.

Publications

Beyerlein, I. J., and Hunter. d Understanding dislocation mechanics at the mesoscale using phase field dislocation dynamics. 2016. PHILOSOPHICAL TRANSACTIONS OF THE ROYAL SOCIETY A-MATHEMATICAL PHYSICAL AND ENGINEERING SCIENCES. 374 (2066).

Mianroodi, J. R., Hunter, I. J. Beyerlein, and Svendsen. Theoretical and computational comparison of models for dislocation dissociation and stacking fault/core formation in fcc crystals. 2016. JOURNAL OF THE MECHANICS AND PHYSICS OF SOLIDS. 95: 719.

Quantum Optics of Solitary Covalent Dopants in Carbon Nanotubes

Han Htoon
20160172ER

Introduction

A solid state system capable of mimicking a two-level quantum mechanical system holds the key to realization of Quantum information technologies that promise novel applications including eavesdropping proof communication and solving enormous, complex problems impossible for conventional computers. Despite that many different systems ranging from individual ions trapped in vacuum to nitrogen vacancy (NV) centers in diamond have been explored for their potential in these technologies, none of the systems have emerged as an ideal candidate meeting all the critical engineering requirements that include an ability to operate in the telecommunication wavelength range (1.3 to 1.5 μm) at room temperature and allowing seamless integration with existing silicon based micro-electronic technologies. We recently discovered that oxygen dopants introduced in carbon nanotubes (CNTs) via simple deposition of a SiO2 layer can meet both of these critical requirements. Specifically, our study recently published in Nature Nanotechnology shows that oxygen dopant states can serve as room temperature, on-demand, two-level quantum emitters with their energy widely tunable to cover the 1.5 micron telecommunication band. Because our doped CNTs are encapsulated in a SiO2 matrix, they are fully compatible with well-developed Si fabrication technology and present an exciting opportunity for development of electrically driven single photon sources and integrated quantum photonic networks. While these preliminary results are extremely promising, establishing doped CNTs as transformative materials for quantum technologies demands a detailed understanding and control of their quantum coherence properties and fine electronic structure. The device integration potential mentioned above also needs to be demonstrated as well. This project aims to meet these challenges via three research tasks focusing on (1) understanding and control of quantum optical properties, (2) chemical manipulation of electronic structure and creation of coupled dopants, (3) proof of principle devices demonstrating electrically driven single photon generation and single photon switching.

Benefit to National Security Missions

By (1) attaining an understanding and control of the quantum optical properties of solitary covalent dopant states, (2) establishing the doped CNTs as transformative materials for a variety of quantum technologies and (3) developing devices that are fundamental building blocks of quantum information technologies that would allow protection of information critical for national security, our work directly addresses Information collection, Surveillance and Reconnaissance, National Defense mission as well as Basic Understanding of Materials, Fundamental Chemistry, and Information Science and Technology, Scientific Discovery and Innovation missions. It is therefore directly relevant to DOE/SC, DOD, DHS and Intelligence Agencies. Furthermore, as the devices we proposed to develop (single photon sources particularly) could also enable novel sub-diffraction imaging and ultra-sensitive absorption measurements, our project is also directly relevant to the DOC (NIST) and could indirectly address Fundamental Bioscience and Basic Health Research, Scientific Discovery and Innovation missions. Because doped CNTs could possess light harvesting properties attractive for photo-voltaic application, our project indirectly addresses Renewable Energy, Energy Security mission. Our project also responds to LANL's Materials for the Future Pillar: Advancing the Understanding of Materials Functionality and Developing Multi-functional Materials Architectures to Transform Structure/function Integration and Emergent Properties goals as well as IS&T Pillar: Emerging Challenge in National Security goal. Finally, through fulfilling the demands for new functional materials for quantum information processing and communication, we aim to support LANL leadership in the Materials Genome Initiative.

Progress

Understanding and control of quantum optical properties
We attained fundamental understandings necessary to optimize single photon emission and other key quantum optical properties of doped CNTs through control on (1) formation and recombination of multiple excitons states (2) trapping potential, (3) trapping of free charges, and (4) recombination dynamics.

Multi-excitonic processes of oxygen dopant states
While our preliminary study show that majority of doped CNT exhibit single photon emission, some emit photons in pairs. By applying a unique experiment developed in PI's lab, we separate the photon pairs in the time domain and determine their origin. The experiment revealed that the photon pair emission is originated from the consecutive recombination of two excitons (electron-hole pairs) in a dopant state. Control on formation and recombination of multiple exciton therefore holds the key for optimization of single photon emission. This work is currently under revision for Physical Review Letter.

Evaluation of trapping potential
The depth of the potential trap of dopant states determines thermal stability of the single photon emitting state. By performing temperature dependent photoluminescence spectroscopy and quantum chemistry calculations, we determined not only the depth of this trapping potential but also the strength of vibrational reorganization energy which plays a key role in stability of dopant states. The results provide strategies for developing deeper trap states needed for stable room temperature single photon emission. This work, performed in collaboration with S. Tretiak of T1 and Y. Wang of U of Maryland was published in J. Phys. Chem. C.

Role of free charge trapping in blinking of dopant state emission
While the emission of the dopant state is free of fluctuations between 150°K and 200°K, it becomes unstable at room temperature (RT). We performed a two-color photoluminescence imaging experiment to determine the mechanism responsible for this unstable emission. Our work identified the trapping of free charges in the potential well of dopant as the mechanism. This work showing the way to achieve fluctuation free RT, single photon emission was published in Nanoscale.

Recombination dynamics of diazonium dopant states
We measured for the first time the photoluminescence (PL) dynamics of the dopant states as a function of dopant and nanotube structure. This experiment revealed the existence of a dark state located below the emitting dopant state and identified multi-phonon coupling processes as the key non-radiative mechanism. This work has been submitted to ACS Nano.

Chemical manipulation of dopants
We have been collaborating with the Therien group (Duke University) to incorporate doped nanotubes into polymer matrices. These matrices are anticipated to enhance the stability and reduce inhomogeneous broadening of the single photon emission. To date, the Therien group has successfully wrapped our doped nanotubes in polymer. We are currently establishing the protocol to create polymer composite materials. We have also established a collaboration with the Ion-beam laboratory of Sandia National Lab to develop an ion beam based approach for deterministic placement of oxygen dopants.

Prototype devices
As the first step toward an electrically-driven single photon source, we are attempting to achieve electroluminescence from doped nanotubes. We are pursuing both single tube and thin film based device architectures. On the single-tube side, we are collaborating with the Krupke group (Karlsrue) and have our first generation devices in hand, on which we will next apply our solid state doping procedure to introduce oxygen defect sites and then characterize their ability to provide electrically stimulated defect-state emission. On the thin film device side, we have established protocols for depositing the necessary films and have in place shadow masks for depositing the required electrodes on the films. Our next steps will be to bring all materials together and characterize the devices optically.

Additionally, through collaboration with the Kato group (U of Tokyo), we have successfully coupled a thin film of doped CNTs with a cavity mode of 2 dimensional photonic crystal and demonstrated more than factor of 3 enhancement on emission rate. We have also developed a novel approach capable of placing a single doped CNT to the center of photonic crystal cavity. We anticipate performing cavity quantum electrodynamic experiments on this novel structure before the end of this FY.

Future Work

Understanding and control of quantum optical properties
Going forward, we will extend our advanced optical spectroscopy studies to individual as well as coupled diazonium dopants states and attained detail understandings on their electronic fine structure and quantum optical properties. In addition to low temperature PL spectroscopy and photon correlation spectroscopy studies applied in year 1, we will performed these advanced spectroscopies under 9T magnetic field. We expect these experiments to open a route to manipulate the spin and angular momentum behavior of the trapped excitons and initiate a new frontier

for CNT based spintronics and quantum computation.

Chemical manipulation

We will continue exploring diazonium chemistry to achieve ability to create dopant states capable of stable room temperature single photon emission at 1.5 micron and electronically coupled dopant pairs. We will also develop two novel approaches for deterministic placement of dopant. In the first approach we will use e-beam lithography to define sub 100 nm apertures on polymer mask placed on top of undoped CNT film and use ion beam to place oxygen dopants through the apertures. In the second approach we will use micropipette with 100nm aperture and a micromanipulator to introduce diazonium dopant on of prefabricated single nanotube or thin film devices with 1 micron precision.

Prototype devices

We expect to achieve single and thin film doped nanotube electroluminescence device by the end of year 1 and plan to optimize these devices to demonstrate electrically driven single photon emission by the end of year 2. We also anticipate to demonstrate coupling of single dopant state to a 2D photonic crystal cavity by end of year 1. We plan to optimize the coupling toward strong interaction regime and investigate cavity quantum electrodynamic phenomena such as Rabi-splitting and single dopant lasing.

Conclusion

A solid state system capable of mimicking a two-level quantum mechanical system holds the key to realization of Quantum information technologies that promise novel applications including eavesdropping proof communication and solving enormous, complex problems impossible for conventional computers. Despite that many different systems ranging from individual ions trapped in vacuum to nitrogen vacancy (NV) centers in diamond have been explored for their potential in these technologies, none of the systems have emerged as an ideal candidate meeting all the critical engineering requirements that include an ability to operate in the telecommunication wavelength range at room temperature and allowing seamless integration with existing silicon based micro-electronic technologies. We recently discovered that oxygen dopants introduced in carbon nanotubes (CNTs) via simple deposition of a silicon dioxide layer can meet both of these critical requirements.

Publications

Doorn, S. K.. Photon Statistics and Materials Development Towards Single Photon Emitters Based on Doped Single-Wall Carbon Nanotubes. Presented at PacifiChem 2015. (Honolulu, HI).

Doorn, S. K.. Covalently Doped Carbon Nanotubes: Photophysics and Emerging Potential for Nanotube Photonics. 2016. In Center for NanoScience, Workshop on Nanoscale Matter: Novel Concepts and Functions. (Sept. 2016).

Doorn, S. K.. Defect-Induced Exciton Localization for New Carbon Nanotube Functionality. Presented at Materials Research Socitey, Fall Meeting. (Boston, MA, Nov. 27-Dec. 2, 2016).

Doorn, S. K., N. F. Hartmann, K. Velizhanin, X. Ma, H. Htoon, J. Olivier, M. J. Therien, M. Kim, and Y. Wang. (Invited) Photoluminescence Relaxation Dynamics of Covalently Doped Carbon Nanotubes. 2016. In Meeting Abstracts. , 8 Edition, p. 653.

Hartmann, N. F., K. A. Velizhanin, E. H. Haroz, Kim, Ma, Wang, H. a. n. Htoon, and S. K. Doorn. Photoluminescence Dynamics of Aryl sp(3) Defect States in Single-Walled Carbon Nanotubes. 2016. ACS NANO. 10 (9): 8355.

Hartmann, N. F., S. E. Yalcin, Adamska, E. H. Haroz, Ma, Tretiak, H. a. n. Htoon, and S. K. Doorn. Photoluminescence imaging of solitary dopant sites in covalently doped single-wall carbon nanotubes. 2015. NANOSCALE. 7 (48): 20521.

Hartmann, N. F., X. Ma, H. Htoon, and S. K. Doorn. Angular Emission Properties of Single-Wall Carbon Nanotubes and Individual Covalent Dopant Sites. 2016. In Meeting Abstracts. , 8 Edition, p. 663.

Htoon, H.. New Building Blocks for Quantum Technologies: Doped Carbon Nanotubes and Plasmonically Coupled Quantum Dots Molecules . Invited presentation at META'16, the 7th International Conference on Metamaterials, Photonic Crystals and Plasmonics. (Melag, Spain, 25-28 July, 2016).

Htoon, H.. New Types of Artificial Atoms and Molecules for Quantum Information Technologies. 2016. In Frontier of Optics/Laser Science. (Rochester, NY, 17-21 Oct. 2016). , p. LTu3H. 3. Rochester, NY: Optical Society of America.

Htoon, H., X. Ma, N. Hartmann, L. Adamska, K. Velizhanin, S. Tretiak, J. Baldwin, and S. Doorn. Multi-Excitonic Emission from Solitary Dopant States of Carbon Nanotubes. Presented at APS Meeting Abstracts.

Kim, , Adamska, N. F. Hartmann, Kwon, J. i. n. Liu, K. A. Velizhanin, Piao, L. R. Powell, Meany, S. K. Doorn, Tretiak, and Wang. Fluorescent Carbon Nanotube Defects Manifest Substantial Vibrational Reorganization. 2016. JOURNAL OF PHYSICAL CHEMISTRY C. 120 (20): 11268.

Piryantinski, A.. Exciton Dynamics and Related Photon Emission Properties of Semiconductor Carbon Nanotubes. Presented at Excited State Processes in Electronic and Bio Nanomaterials (ESP-2016). (Snata Fe, NM, 13-16 June, 2016).

Piryantinski, A.. Diffusion, Recombination, and Photon Emission Properties of Interacting Excitons in Semiconductor Carbon Nanotubes. Presented at International Meeting on Photodynamics & Related Aspects. (Mendoza, Argentina, 9-12 May, 2016).

Piryantinski, A.. Exciton Diffusion, Recombination, and Photon Emission Properties of Carbon Nanotubes. Presented at Energy Materials and Nanotechnology Meeting (ENM 2015). (Hong Kong, 9-15 Dec., 2015).

Roslyak, O., and A. Piryatinski . Effect of Periodic Potential on Exciton States in Semiconductor Carbon Nanotubes. To appear in Chemical Physics.

Transient Thermal Conduction in Nonlinear Molecular Junctions

Dmitry A. Yarotski
20160180ER

Introduction

Non-equilibrium thermal dynamics in low-dimensional systems is an active research area aimed at understanding and harnessing nanoscale heat transfer phenomena to improve performance and reliability of molecular electronics devices. Reduced dimensionality leads to nonlinearity of heat conduction process that is mediated by a quantized spectrum of electronic and vibrational excitations and cannot be described by existing theoretical frameworks. DNA is an ideal system for studying nanoscale nonlinear heat transfer due to presence of large thermal fluctuations of the inter-strand separation (bubbles) that lead to high structural flexibility and nonlinear thermalization dynamics. However, few and controversial studies of DNA thermal properties exist despite recent surge of interest in heat dissipation in DNA scaffolds used for self-assembly of nanoscale devices and interconnects.

In this work, we will rely on the unmatched LANL integration of synthesis, advanced ultrafast optical spectroscopic techniques and forefront atomistic modeling of nonlinear fluctuations to reveal the mechanisms underpinning heat transport and dissipation in DNA. In pursuit of this goal, we will use a unique set of time-resolved fluorescence and Raman probes to determine the temperature-, sequence- and structural dependence of thermal energy flow through the DNA in the regime of nanometer distances, femtosecond time intervals and high temperatures. We believe these are the key parameters for capturing the essence of non-equilibrium molecular behavior. Experimental results will be used to benchmark the development of sophisticated coarse-grained DNA models that will reveal the fundamental physics of the non-linear molecular heat transport and unlock DNA for future applications in molecular electronic and heattronic devices.

Benefit to National Security Missions

Our program on understanding nonlinear thermal transport in molecular junctions directly addresses the Grand Scientific Challenges identified in the Basic Energy Sciences Advisory Committee (BESAC) report, which are central to DOE's missions in energy, science, and security in general, and to the LANL Materials Grand Challenge in particular. It leverages existing capabilities across the laboratory (both in the T and MPA divisions, and BES user facilities at CINT) and creates new ones, including analytical tools, numerical algorithms, nanofabricated surfaces, and ultrafast thermal interrogation techniques. Our thrust to interface materials science with ultrafast optical coherent photon probes represents an essential element in the MaRIE strategy that connects the M4 facility to the Multi-Probe Diagnostic Hall. The results of this work will strongly impact LANL missions in complex systems, nanotechnology and, especially, nanoelectronics, because better understanding of nonlinear heat transfer in molecular-scale systems is an enabling ingredient for technological applications of novel molecular electronic and heattronic/phononic devices. We believe that introduction of our integrated capabilities in modeling, synthesis and characterization of nanoscale thermal phenomena are poised to make a broad impact on the field, thus placing us in a favorable position to compete for external funding from BES, DOD, IC, and industrial sponsors.

Progress

The ultimate goal of our project is to reveal the mechanisms of nonlinear thermal conduction in DNA molecules and their dependence on various intrinsic DNA properties (sequence, presence of bubbles) and interactions with the environment. To reach this goal, we are capitalizing on a unique combination of team member's expertise in analytical and numerical modeling of complex nonlinear molecular systems, state-of-the-art biosynthetic and nanofabrication techniques, and ultrafast optical spectroscopies. One of our efforts in FY16 was directed towards development of a new experimental capability in dynamic characterization of thermal transport in mol-

ecules and nanostructured materials which could, in turn, be used to benchmark theoretical simulations. We have started with recently developed time-resolved Coherent Anti-Stokes Raman Scattering (CARS) spectroscopic capability which allows detection of stimulated Raman scattering signals in a wide spectral region with sub-picosecond temporal resolution. However, the low repetition rate (1 kHz) of the existing system proved to be inadequate for detecting low signals generated by sparse monolayers of oligonucleotides functionalized with Cy3 and Cy5 Raman markers. Therefore, we created a similar setup for detection of dynamic Raman/CARS signals, which is based on a high-repetition rate (250 kHz) ultrafast laser amplifier and provides significantly enhanced sensitivity due to lower noise and better data acquisition statistics. This capability can also use a streak-camera for resolving fluorescence emission from the heat markers at single-photon levels and picosecond timescales. The improved performance of the system is currently being verified on the monolayers of Cy3/Cy5 molecules after which the system will be applied to self-assembled monolayers (SAM) of DNA oligomers marked with the same molecules for local temperature detection and estimation of the DNA thermal conductivity at different average temperatures.

This milestone, which will be achieved by the end of FY16, will be enabled by our progress in making vertically aligned DNA SAMs on the gold film surfaces. In our approach, we used two commercially available strands of the DNA pre-labeled with a thiol (to attach to metal surface) and the standard Cy3 or Cy5 heat marker, respectively. The SAMs were formed by immersion of the substrate in the pre-labeled DNA solution. The average coverage density is ~ 1011 molecules within the laser spot which provide readily detectable signals in our new setup sensitive to 10-5 signal variations. This density can also be tuned by backfilling the space between DNA-marker complexes with short unmarked single stranded DNA fragments, which will be used in our future experiments to test the dependence of thermal conductivity on inter-molecular interactions.

Experimental advances in FY16 were matched by theory development aimed at better understanding of the role of interfacial resistance on the efficiency of transport processes on nanoscale. These questions are of critical importance for planning/guiding specific experiments within the project and for subsequent analysis of the experimental findings. Specifically, it has been demonstrated that the heat conductance of a molecular system (e.g., DNA) connected to a thermal bath (e.g., gold substrate) can depend non-monotonically on the strength of the molecule-bath coupling. This is critical knowledge that has to be taken into account when the dynamics of vibrational energy propagation through DNA from the transiently excited substrate to the heat marker is considered and compared to the experimentally extracted timescales. Detailed information about such interactions is thus essential for optimal tuning of DNA-metal substrate coupling within the present project. These important findings have been summarized in several manuscripts and have already resulted in two publications in high-profile peer-reviewed journals.

Future Work

The overarching goal of this work is to develop a comprehensive representation of heat transport dynamics in DNA. In pursuit of this goal, we will extend our synergistic efforts in theoretical simulations, biomolecular synthesis and ultrafast spectroscopies to study vibrational energy propagation in DNA with different structure. In early FY17, we will complete the optimization of our new ultrafast CARS/fluorescence experimental capabilities using fixed sequence DNA monolayers. Subsequently, we will create DNA SAMs with varying sequence, with exact nucleotide arrangements provided by the theory in order to narrow down the phase space of possible choices that lead to the desired heat conduction dynamics. Similar to FY16 work, the magnitude of DNA thermal conductivity will be extracted from matching theoretically predicted rates of vibrational energy propagation and equilibration within the molecules to the experimental values obtained for different DNA sequences. In addition to sequence, we will also vary molecular DNA lengths in order to investigate the time scales and mechanisms (ballistic vs diffusive) of vibrational excitations propagation at different average temperatures. We will also start developing the SAMs with DNA molecules where the DNA double-strand structure is disturbed by selective placement of the regions with weak hydrogen bonding or “bubbles”. We expect increase in nonlinear nature of heat transport of such structures. Theoretical/computational efforts will concentrate on applying the obtained general knowledge within the available models (coarse-grained and atomistic) to predict the time-resolved dynamics of the heat transport within the SAMs of DNA molecules with varying sequences, and possibly, bubbles. Experimental results will be used to verify theoretical predictions and further refine the models to provide best agreement with experiments. The theoretical efforts will also guide experimental effort by providing various spectroscopic parameters (resonance energies, optimal polarizations) required for finding most relevant spectral features and optimizing the experimental sensitivity.

Conclusion

We expect to reveal the fundamental physics of the nonlinear heat transport in DNA molecules. The close communication between the new dynamic thermal probes

and theoretical modeling should enable us to resolve the controversy between existing coarse-grained models (that reproduce equilibrium properties of DNA equally well but differ by orders of magnitude in the estimates of the non-equilibrium response) and develop predictive description of complex thermal conductivity of DNA oligomers. The results of this work will strongly impact national security missions that rely on complex systems, nanotechnology and, especially, nanoelectronics, because better understanding of nonlinear heat transfer in molecular-scale systems is an enabling ingredient for technological applications of novel molecular electronic and heattronic/phononic devices.

Publications

Gruss, D., K. A. Velizhanin, and M. Zwolak. Landauer's formula with finite-time relaxation: Kramers'crossover in electronic transport. 2016. Scientific Reports. 6: 24514.

Velizhanin, K. A., S. Sahu, C. Chien, Y. Dubi, and M. Zwolak. Crossover behavior of the thermal conductance and Kramers' transition rate theory. 2015. SCIENTIFIC REPORTS. 5: 17506.

Zwolak, M., K. Velizhanin, C. Chien, and Y. Dubi. Deconstructing Structural Transitions via Thermal Transport. 2015. BIOPHYSICAL JOURNAL. 108 (2): 176a.

Rigorous Development of Atomic Potential Functions in Terms of Strain Functionals

Edward M. Kober
20160220ER

Introduction

Extreme-scale molecular dynamics (MD) simulations of materials (containing more than a billion atoms) provide us with a powerful opportunity to gain a deep understanding of the response characteristics of realistically-sized material samples with micron dimensions. This critical regime is referred to as the mesoscale in materials science, and this is the focus of a current national initiative. At this scale, metals are composed of somewhat randomly ordered crystals, and the interactions between the crystals control the strength and failure of real materials. The distribution of the crystal orientations and defect structures depends on their initial manufacturing state and subsequent aging conditions, and we have limited predictive capability for which structures are dominant and controlling. Extreme scale MD simulations would be powerful tools for analyzing these factors. However, the accuracy of such simulations are restricted by how well the potential functions used to represent the atoms actually capture the fundamental interactions between them. Despite significant effort by many research groups over decades, the formulations used to achieve focus on high symmetry structures, and cannot be relied on to describe irregular geometries.

Our goal is to establish a robust method for developing potential functions for metals that can be calibrated against a large range of experimental data and first principles calculations. We have recently developed an approach that characterizes atomic geometries in terms of the different shapes of the neighborhood defined by the nearby atoms (e.g. how cubic, tetrahedral, sheared it is). This basis allows us to readily recognize the different geometries and defects of the atoms and describe them in a smooth and continuous basis. We will use these as the basis for the potential functions, so that arbitrary geometries can be captured accurately, enabling a much broader calibration regime.

Benefit to National Security Missions

Understanding the performance properties of metals and developing accurate models that can predict that behavior under a wide variety of circumstances (mechanical deformation, shock-loading, radiation damage, changes in manufacturing processes) is of critical importance to DOE and DoD missions, and also of significance to general manufacturing capability. Metals consist of agglomerations of crystalline grains, where the specifics of the manufacturing process determine how large these grains are and how they are oriented with respect to one another. While we have a good understanding of how the crystalline interiors of the grains respond to deformation processes, and a fair capability to model that, we have only a limited understanding of how the interfaces between the grains respond to deformations. This level of the material structure is referred to as the "mesoscale" and developing a better understanding of it is the focus of several national initiatives sponsored by DOE, NNSA, NIST and DOD.

To fully understand how both the bulk material and the grain boundaries respond to deformation processes requires large-scale atomistic simulations that can be performed using Molecular Dynamics (MD). However, these simulations are only as accurate as the classical potential functions that are used to describe the metals' properties. We will develop a much more robust and accurate method for analyzing and encoding this information into the potential functions. The resulting MD simulations will have significantly improved accuracy and would enable a predictive capability important to our national security mission.

Progress

The first primary task of the first year was to extend the geometric basis for our strain functionals out to sixth order. This has now been achieved where this includes both net shape deformation quantities, and the relative orientations between these types of distortion. The

shape deformations include, for example, the amount of shear (a second order distortion), trigonal symmetry (a third order distortion), cubic symmetry (a fourth order distortion) and hexagonal symmetry (a sixth order distortion). The orientation terms describe how the shear is oriented with respect to the trigonal or cubic symmetry axes, for example. Previous methods for developing potential functions have neglected these latter terms and so are based on incomplete geometric descriptions. The method we have developed for capturing these relative orientations should be similarly applicable to the general analysis of three-dimensional data sets and images, which also currently use incomplete basis sets.

Additionally, the vector derivatives of these shape functions have also now been defined. These describe the forces and displacements that would achieve the associated deformations. Consistent with the spherical coordinate frame used to define the deformations, these have been projected onto radial, azimuthal and tangential components as a means to establish orthogonality between the three vector components. The forces and displacements from our simulations will be projected onto this basis set for an orthogonal symmetry decomposition. As above, we have established relative orientation functions between the different order terms, which have not been previously identified. These could be applied for a more complete analysis of other vector fields such as complex fluid flow.

For the second primary task of the first year, we have developed a standardized database of copper atom configurations that will be used for the potential calibration. The database includes the geometries (the unit cell), the calculated forces, and all pertinent details of the calculations. All forces stem from highly accurate calculations performed with the density functional theory code VASP (Vienna Ab initio Simulation Package). The accuracy of the calculations is established in particular by comparison of calculated phonon frequencies with the experimentally measured values.

The configurations are systematically derived from copper's idealized crystal structure, which is face centered cubic, and are defined in three-dimensional periodic structures. The defect structures include vacancies (missing atom), interstitials (atom inserted between lattice position), Frenkel pairs (vacancy-interstitial combination), edge dislocation pairs (pairs of extra half planes of ions), and screw dislocations (circularly tapered displacement of ions). Structures with displaced atoms are based on the displacement patterns exhibited by high-symmetry phonons (lattice vibrations). The defect structures are generally snapshots taken from quantum molecular dynamics simulations at various temperatures. Consequently, each atom is in a unique geometry and provides calibration information for our force-matching procedure. Multiple snapshots are utilized for each type of defect.

Additional configurations to represent the liquid phase were introduced that are not based on a crystal structure. These rely on the Vibration-Transit theory of liquids and were taken (in a scaled volume) from recent simulations of liquid lithium. The unit cells contain 150 atoms and exhibit no symmetry. Performing such simulations directly for copper would be computationally prohibitive. The appropriately randomized structures should sufficiently sample the geometric phase space necessary for our calibration procedure.

The third primary task for the first year is to develop the numerical coefficients for our potential functions and to implement this into the SPaSM (Scalable Parallel Short-range Molecular dynamics) simulation code. This work is now beginning and should be complete by the end of the fiscal year. A post-doctoral research associate is being identified to assist with this. The work would include performing a least-squares fitting of the force-displacement data that we have assembled above. We expect that most of the data can be fit with low order polynomial expressions, though exponential repulsive terms may also need to be considered for shorter contacts between atoms. We expect that this process will identify geometric structures for which we do not have calibration points, and additional VASP calculations will be performed to characterize those geometries.

Future Work

The first primary task of the second year will be to complete the work on documenting our copper simulations. While previous potentials for copper accurately capture the structural and deformation aspects of the material, they are less accurate in capturing the lattice mode frequencies and the behavior of the liquid. We will perform molecular dynamics simulations with our potentials to document the level of improvement that we have achieved as well as the computational cost involved. Presentations of the work at national conferences are planned along with at least two journal publications.

The second primary task will be to extend this work to tantalum (Ta), which has a more complex structural response then copper. This is because it has a body centered cubic (bcc) structure compared to copper's face centered cubic (fcc) structure, and there are different defect structures and deformation processes available for it. From experiment, Ta does not appear to undergo any solid-solid phase transformations below 100 GPa, and only melts at very high temperatures (>3000K). However, one commonly

used potential for this material exhibited two shear-induced phase transformations. A subsequently derived potential did not exhibit these transformations. We will perform a similar calibration procedure that we used for copper, and specifically include the phases identified by the earlier simulations.

The third primary task will be to implement the Ta potential functions into the SPaSM (Scalable Parallel Short-range Molecular dynamics) code. These will be compared with the performance and accuracy of the two previous existing potential functions.

Conclusion

The overall goal is to develop atomic potential functions for the molecular dynamics (MD) simulations of metals that capture the very broad range of behavior including mechanical deformation, phase transitions and shock-loading. These will be calibrated to a combination of experimental data and electronic structure calculations. This will enable predictive MD simulations that will accurately capture the behavior of irregular atomic structures found around defects and grain boundaries in metals. This will allow us to more completely understand how the mesoscale structure of a metal affects its response characteristics, and enable the design of improved materials. Understanding the performance properties of metals and developing accurate models that can predict that behavior under a wide variety of circumstances is of critical importance to energy and defense missions, and also of significance to general manufacturing capability.

Publications

Kober, E. M., and S. P. Rudin. Strain Functionals for Characterizing Atomistic Geometries and Potential Functions. Presented at American Physical Society Meeting. (Baltimore, 15-17 Mar. 2016).

Kober, E. M., and S. P. Rudin. Strain functionals for characterizing atomistic geometries and deformation processes. Invited presentation at American Chemical Society Meeting. (Philadelphia, 22-25 Aug. 2016).

Stimuli-Responsive Coordination Polymersomes

Reginaldo C. Rocha
20160284ER

Introduction

We propose the development of novel stimuli-responsive polymer vesicles (polymersomes) where self-assembly, self-repair, and encapsulation/release of content are driven by the metal coordination of ligand-functionalized block copolymers. These proposed metallo-supramolecular assemblies are formed by dynamic metal-ligand binding with specific molecular recognition and are amenable to control over sensitivity to various stimuli. The tunability of coordination moieties and polymer-ligand components allows for introducing and manipulating chemical, optical, redox, and magnetic functionalities, making such platforms potentially ideal for applications in sensing, imaging, and targeted delivery. In these metal-ligand polymersomes as nanocarriers, mechanisms for controlled cargo release are based on the triggered disassembly that can be directed via responses of the metal-ligand moieties to physical and chemical stimuli. This research can also enable related forms of dynamic composite materials with controlled functionality across length scales, which are broadly relevant to the advancement of mesoscale materials at the interface of chemical and biological sciences.

Benefit to National Security Missions

This research supports the above missions by providing advancements toward the development and fundamental understanding of dynamic composite materials with controlled functionality across length scales (DOE-SC; LANL's 'Materials for the Future' science pillar) and applications in areas at the interface of chemistry and biosciences. The target applications in nanomedicine (e.g. drug delivery in cancer therapeutics and bio-sensing/imaging in diagnostics) are relevant to DHHS (NIH) and other sponsors; applications in optically and electronically responsive devices as well as materials healing and treatment - including nuclear/weapons components (e.g. triggered release of anti-corrosion agents) are relevant to the DOE, DOD (DTRA/DARPA), NNSA, DHS, and possibly other agencies.

Progress

In this early period of the project, our efforts have been primarily focused on establishing the synthetic methodologies and analytical techniques for the preparation and characterization of our metallo-polymer assemblies. We have explored several methods to control self-assembly of amphiphilic block copolymers into supramolecular structures in order to facilitate our target metal-coordination driven assembly of polymersomes. An important step toward our goal is to construct such supramolecular polymersomes in a reproducible, solution-processable fashion while minimizing heterogeneity and optimizing factors such as response to environmental stimuli and loading. In assessing feasibility of methodologies, proof-of-principle experiments were performed using multiple amphiphilic block copolymers [e.g. poly(butadiene)-b-poly(ethylene oxide) and poly(butadiene)-b-poly(acrylic acid)] with varying hydrophobic block/hydrophilic block ratio, block length, and thus total molecular weight. This variation also provides a key relationship in inducing and controlling the supramolecular formation of structurally different assemblies (e.g. micelle vs vesicle). A useful, applicable reference point in predicting the type of organization has been the critical packing parameter (Pc = v/a0lc; where v is the volume of the hydrophobic chain, a0 is the area occupied by the hydrophilic head group, and lc is the length of the molecule). Of the selected amphiphilic polymers, only those with Pc >0.5 tend to spontaneously assemble into vesicular structures with bilayer membranes (i.e. polymersomes).

The control over supramolecular structures via solution-processable strategies was tested using extrusion and probe sonication. Both methodologies are extensively used for liposome formation and have been demonstrated to form polymer vesicles as well. In extrusion, as our first attempted approach, polymers are passed through a nanoscale filter using gas-tight syringes. By forcing solutions of polymers through this filter, vesicle or micelles can be formed depending upon Pc. However, charac-

terization by dynamic light scattering (DLS) showed that product solutions typically exhibit a bimodal distribution of both types of structures with large polydispersities, dependent upon pore size. Another difficulty with this method is that, in the case of polymers with lower molecular weight (<3 kDa), polydispersion is increased. We attribute this to forcing amphiphiles to adopt non-equilibrium structures. The second approach attempted was probe sonication, which has proven to be effective in yielding unimodal distributions with much lower polydispersity compared to extrusion. However, in order to eliminate some aggregation observed at ~1 mM, we found that a third and most successful approach was sonication followed by extrusion. By using this method, it becomes possible to achieve a more uniform distribution of structures followed by removal of aggregates within the nanoscale pores of extrusion.

Although deemed as an acceptable method for the initial organization of our target metallo-polymers, a further optimization is desired to minimize loss of material through the multiple steps involved in the coupled sonication/extrusion approach described above. To this end, we have begun to implement a new approach termed solvent-exchange. In brief, polymers are first solubilized in a water-miscible solvent such as tetrahydrofuran and then water is slowly added to the mixture; upon evaporation of the organic solvent, the supramolecular polymer structure is self-assembled in the remaining water solution. In our exploratory studies of concentration and temperature dependence, we have found that control of dispersity levels is further improved when working at the critical concentration of each polymer. By adjusting the temperature, and effectively the exchange rate, this new method also appears to enable additional control over structure formation and homogeneity.

Parallel to developing the optimal self-assembly strategies, our efforts have involved polymer functionalizations with N,N,N-tridentate ligands in order to drive the organization of polymersome structures via metal-coordination crosslinking of ligand-ending block copolymers. By using reversible addition-fragmentation chain-transfer (RAFT) and atom-transfer radical polymerization (ATRP), our synthetic approach involves controlled radical polymerizations initiating from a meso R-group positioned opposite to the intermediate pyridyl N-site of terpyridine and bis(benzimidazolyl)pyridine derivatives. Upon characterizing the molecular weights and polydispersities of the ligand-terminated amphiphilic polymers (initially made of the same hydrophobic/hydrophilic blocks as above for comparison with the unfunctionalized analogues), our above approaches to assemble polymersomes will be further facilitated by the supramolecular crosslinking via metal-ligand coordination between the amphiphilic polymer bilayers. With these methodologies established, we will then turn to the characterization of optical and electronic properties underlying the targeted stimuli-responsive structures of metallo-polymersomes.

Future Work

With our synthetic and analytical methodologies successfully proven for the preparation and characterization of proposed supramolecular polymer assemblies, next we will develop structure-property relationships with a focus on the studies of 1) chemical stability and environmental sensitivity, 2) encapsulation and release of therapeutic molecular cargo, and 3) optical and electronic properties designed to govern the stimuli-responsive behavior of such assemblies. Through our approach involving a tight feedback between synthesis and measurement, these planned tasks will then lead to the mechanisms for triggered assembly/disassembly as a response of active metal-ligand centers to the chemical, electrical, or optical stimulation of metallo-polymersomes as nanocarriers for controlled transport and delivery.

Conclusion

The successful demonstration of functional metallo-polymersomes in this capacity will also have important implications as stimuli-responsive carriers of catalysts and reactants in the realm of electronic, photonic, and energy materials (e.g. damage self-repair and corrosion remediation). Because the broad field encompassing dynamic metallo-supramolecular polymers and functional metal-organic composite materials is still in its infancy, our research undertaking has a great potential for technical leadership and programmatic growth in areas of relevance to Los Alamos missions. There is potential for applications in optically and electronically responsive devices, as well as materials healing and treatment, including nuclear/weapon components.

Publications

Montano, G. A.. Pushing the lipid envelope: using bio-inspired nanocomposites to understand and exploit lipid membrane limitations. 2016. In American Physical Society, 2016 March Meeting. (Baltimore, Maryland, 14-18 March, 2016). Vol. Volume 61, Number 2 Edition, p. H53. College Park, MD: Bulletin of the American Physical Society.

High Efficiency, Low-cost Perovskite Solar Cell Modules

Aditya Mohite
20160320ER

Introduction

Photovoltaic power generation is a sustainable green technology that utilizes unlimited, clean solar energy to solve the global energy crisis. DOE Sunshot initiative is a national initiative that aggressively supports development of low-cost, high-efficiency photovoltaic (PV) technologies targeting $1/Watt by 2020 for grid-based deployment. A recent breakthrough by our team demonstrated a solution-processed approach (unique to LANL) to grow high crystalline quality thin-films and fabricated proof-of-principle PV devices with a power conversion efficiency (PCE) ~18%. Building on this work, the goal of this project is to achieve first of its kind prototypes of perovskite solar-cell modules with PCE >15% with long-lifecycle. Specific goals are as follows:

(a) Development of 3”x3” solar-cell modules using commercially scalable, large-area thin-film coating techniques such as Doctor Blading and spray coating.

(b) Long-term moisture stability of perovskite modules by developing encapsulation schemes using hydrophobic polymers, glass bonding and reduced graphene oxide and graphene films.

Benefit to National Security Missions

This proposed work aligns with the energy security mission of LANL. Proposed research promises to make LANL the world leader in low-cost photovoltaic technologies based on novel functional materials and meet the DOE EERE-SUNSHOT goal of producing power at levelized cost of electricity (0.6 c/kWh). Perovskite crystal devices can potentially be used as neutron and charge detectors. This project also opens up possibilities of the development of remote power sources for on-field personnel, which is of interest to DoD missions.

Progress

We have successfully demonstrated the working solar cell using the doctor blading technique with 7.3% efficiency. We systematically understood the engineering parameters for thin film optimization using the doctor blade technique, such as blade speed, blade to substrate distance, solution volume, substrate temperature. By extensive optimizations, we are able to achieve uniform pin-hole free hybrid perovskite thin film with large grains and desired crystal orientation. This study was published in “Applied Materials Today” early 2016.

In the last fiscal year, we put our major effort on understanding and improving the perovskite solar cell stability. There are two stabilities that continue to be the key challenges in the field of hybrid perovskite solar cell research, one is the photo stability (how long does the cell operate under constant light) and the other is environmental stability (how stable the material is under ambient environment).

In the photo-stability study, we found the perovskite solar cell undergoes degradation in constant light due to charge accumulation, and the performance can be recovered after sitting the cell in the dark. We have understood the physics behind the photo-degradation and proposed several approaches to stop the light-induced performance degradation: a) changing the device operation temperature, b) restoring the device in the dark and c) improving the device crystallinity to prevent the charge accumulation process. This work was published in “Nature Communications” in 2016.

In the environmental stability test, we tested our solar cell following the industry standard, a) in humid conditions (relative humidity =65%) and b) under heat conditions. We found the cell can degrade rapidly under humid conditions. The cells under humidity condition degraded within 2 hours without any encapsulation.

We further developed the encapsulation schemes to extend the lifetime against the humidity condition. We encapsulated the cell with glass slide bonded by epoxy and the cell lifetime can be significantly extended from a

few hours to a few hundred hours.

Future Work

We have set two key goals to accomplish going forward:

1. Continue work on fabricating large scale perovskite solar cell using the doctor blade technique, pushing the efficiency up to 15%. In the mean time, we will scale up the device area to 3” by 3”.

2. Focus on the stability test of our device. We will perform accelerated lifetime tests following the industry standard: constant 1sun illumination, in a humid environment and under heat. We will further develop an encapsulation scheme to protect the cell from degradation.

Conclusion

State-of-the-art-solar cells utilize high purity, single crystalline semiconductors to achieve power conversion efficiency (PCE) of ~20% and have dominated the PV industry. However, high-purity single-crystal growth requires high-temperatures, which manifests as an increase in the cost per efficiency (2.2 $/W) of the solar module production. Currently, there is no technology that offers high efficiency at low cost. Photovoltaic power generation is a sustainable green technology that utilizes unlimited, clean solar energy to address the global energy crisis. The success of this project is expected to transform the field of cheap low cost thin-film solar cell technology and take the perovskite technology closer to commercialization with a levelized cost of electricity of 6 c/KWh.

Publications

Mallajosyula, A. T., K. Fernando, S. Bhatt, A. Singh, B. W. Alphenaar, J. Blancon, W. Nie, G. Gupta, and A. D. Mohite. Large-area hysteresis-free perovskite solar cells via temperature controlled doctor blading under ambient environment. 2016. Applied Materials Today. 3: 96.

Tsai, H., W. Nie, J. Blancon, C. Stoumpos, R. Asadpour, B. Harutyunyan, A. J. Neukirch, R. Verduzco, J. J. Crochet, S. Tretiak, L. Pedesseau, J. Even, M. A. Alam, G. Gupta, J. Lou, P. M. Ajayan, M. Bedzyk, M. G. Kanatzidis, and A. D. Mohite. High-efficiency two-dimensional Ruddlesden–Popper perovskite solar cells. 2016. Nature. Online Only (Online): Online Only.

Near-unity, Stable, Scalable Down-conversion of High-power Light Sources

Jennifer A. Hollingsworth
20160357ER

Introduction

We aim to accelerate the development of a new class of semiconductor quantum dot (QD) – the "giant" QD (gQD) – as a replacement for rare-earth green and red-phosphor down-conversion materials. Doing so will enable high-efficiency/high-power warm-white light-emitting diodes (LEDs) for next-generation solid-state lighting (SSL). Working with industry and university partners, we will address: (1) Thermal quenching by nanoscale-materials engineering, (2) Lifetime performance by device engineering, and (3) Nanomaterial reproducibility/scaling toward 'advanced nanoparticle manufacturing' by chemical engineering. Impact will be in advancing energy security through high-efficiency lighting alternatives to conventional residential and commercial lighting that currently consumes ~20% of all electricity generated. Our program will address technical and socio-economic deficiencies of existing down-conversion phosphor materials (spectral properties, efficiency, stability, and/or cost/accessibility) resulting in dramatic improvement of consumer acceptance of white-light LEDs for general lighting. Without an optimization effort directed specifically toward thermal or photo-oxidative stability, gQDs already outperform state-of-the-art commercial QDs in preliminary accelerated lifetime testing (e.g., 0% decline under combined heat/flux to 500 h vs. 80% at 300 h, respectively), and gQDs solve "killer" issue of QD self-reabsorption. Here, we will transform the scientific discoveries achieved to date to enable gQD technology to address key remaining challenges limiting efficiency and utility of white-light LEDs. In Research Goal 1, we will probe ensemble and single-gQD-level thermal stability to identify which specific gQD structure affords targeted retention of emission efficiency at elevated temperatures. At the same time, in Research Goal 2 we will engineer the LED platform itself to limit sources of heating (conductive and light-to-heat conversion processes) via design/fabrication/testing of thermally-insulative/optically-transparent "spacer" layers and advanced ceramic phosphor matrices. In Research Goal 3 we will address the need for 'advanced nanoparticle manufacturing' by way of new automation of gQD synthesis to provide a novel path-forward to scale-able and reproducible synthesis.

Benefit to National Security Missions

A successful program will elevate a unique LANL capability in nano-emitters (LANL proprietary technology in "alternative down-conversion phosphors") from TRL 4 to TRL 6/7 in the context of efficient and high color-quality light-emitting diodes (LEDs) for solid-state lighting, supporting energy security through advancing energy efficiency (energy impact in residential, commercial and government sectors, where currently ~20% of all electricity generated is used for lighting). Clear new directions in applied-energy programs would be opened, e.g., in DOE-EERE, ARPA-E, and synergy with new EERE program established. Importantly, however, the potential impact extends beyond efficient lighting. The resulting advancement of light-emitting-materials understanding and device-engineering concepts will further support development of robust UV/infra-red bright and reliable bulk sources for nano-enabled tagging/tacking/locating & optical communication or sensing applications, e.g., enabling technologies for the intelligence agencies and DOE-DARPA, as well as ultra-bright and reliable (on-demand) single-photon sources for secure communication, non-proliferation, sensor/detector qualification, with direct impact to LANL programs as well as DoD and NIST mission space. Also significant, the program will establish new materials-engineering science, addressing Materials-for-the-Future Focus Areas in advancing understanding of materials functionality and developing materials architectures to transform structure/function integration. Lastly, the program will establish the utility of automated-synthesis approaches for nanomaterial scale-up and reproducibility, with clear impact on new initiatives in Additive Manufacturing. Notably, the PI will give an invited talk this fall at a national workshop on "Advancing Nanoparticle Manufacturing," thereby

demonstrating the unique role LANL can play in the rapidly emerging applications for ultra-bright and stable nano-emitter technologies.

Progress

Research Goal 1: Use structure:function correlations to identify green/red giant quantum dots (gQDs) with quantum yield (QY) at 85 ºC >90% peak QY

We have made substantial progress in the development of new green-emitting gQDs and in identifying structure:function correlations for thermal quenching behavior. Namely, in prior works, we discovered novel "non-blinking" (stable emission of light at the level of single QDs) red and near-infrared-emitting gQDs. Here, we have developed the first non-blinking/suppressed-photobleaching gQDs emitting in the green (manuscript in preparation). Furthermore, working with collaborators at Vanderbilt University, we have uncovered the key structural/compositional variables needed in order to achieve blinking-suppressed behavior. Importantly for application of any g-QD to solid-state lighting, we have also now confirmed a suspected correlation between single-QD photostability and device-level performance stability. The latter has entailed studying the photoluminescence behavior of single g-QDs as a function of several environmental stressors (light flux intensity, air and temperature to date), followed by comparison with device testing results for similar environmental stressors conducted by our industrial partner. The new analyses show a clear correlation between the two levels of performance -- single g-QD and g-QD ensembles in a device. In this way, the development of a non-blinking emitter in the green, to partner with our red-emitting non-blinking g-QDs, is an important breakthrough toward realizing stable, efficient white-light sources. In addition to single-dot/device correlations, we have further performed thermal quenching studies of g-QD ensembles in solution, as well as in silicone and acrylate polymer composites to correlate with thermal quenching properties at the single-gQD level.

These investigations have now been done for a range of g-QD samples representing different synthetic preparation methods and, thereby, structural characteristics (e.g., spherical vs. faceted or diamondoid vs. hexagonal pyramidal shapes). Result: For low photon fluxes, thermal quenching properties at the single-dot level match those of the ensemble composite; however, photon flux plays an extremely important role in both absolute levels of thermal quenching and reversibility of quenching. Together, these results are providing important understanding toward identifying key g-QD structural/chemical parameters for realizing full environmentally and performance stability.

Research Goal 2: Establish transformational long-term gQD-phosphor stability in light-emitting-devices

For environmental heating effects, we are focusing on direct heating using a heated sample holder at the level of g-QD/polymer composites or a heating in a cryostat in the case of single-dot measurements, as these methods afford greater control over the actual temperature applied compared to relying on conductive heating by a proximal light emitting diode (LED). For self-heating effects, we are comparing flux-dependencies in g-QD performance, where higher fluxes provide greater excess energy to the g-QDs that can be dissipated in the form of heat, i.e., energy not used to generate a photon of light is converted to heat. In the initial 9 months of the project, we are finding that the latter (high-flux-induced processes) has a larger impact on long-term stability than simple environmental heating alone. In fact, the ability of materials to recover from heat-induced quenching is strongly compromised in the case of high-flux experiments, suggesting photo and heat-initiated irreversible damage. The "identity" of this damage is under investigation in collaboration with Vanderbilt University and NIST, where recently NIST identified formation of a surprising oxygen-containing coating on permanently degraded g-QDs that was not present on recovered g-QDs, rather than the anticipated outside-in oxidative degradation that would entail particle shrinking and conversion of g-QD composition to an oxide.

Research Goal 3: Establish automated parallel synthesis for advanced nanoparticle manufacturing

Automated reactions are underway to assess batch-to-batch reproducibility and confirm equivalency to "traditional syntheses."

Future Work

Ensemble and single-gQD thermal quenching studies are underway, with important new understanding already established as described in Accomplishments. Single-dot correlation studies will be completed with our university collaborator for an unprecedented dot-by-dot assessment of single-dot environmentally dependent optical characteristics correlated with chemical/structural characteristics. The g-QDs (both red emitting and the new green emitting) with good thermal/flux stability (to 85 ºC) will be subjected to device-engineering RG2 goals and chemical-engineering RG3 goals. As required, materials-engineering the gQD itself (e.g., barrier shell, permanent surface passivation, interconnected-gQD xerogel strategies) will be employed, with initial results indicating that the core/shell interface may be playing a key role in thermal / flux quenching behavior.

Focusing on self-heating by Stokes-shift/QY-losses, we will

explore advanced ceramic-matrix alternatives to standard silicones for improving heat dissipation within the phosphor layer (M12-M18). As high flux now appears to be a key driver of both permanent thermal quenching losses and the previously uncovered charging and/or electric-field effects (causing unwanted spectral shifting), we will emphasize strategies for dissipating charges formed in flux that may accelerate photooxidation of g-QDs, their ligands or matrices, as well as change which excitations result in photoluminescence (neutral excitons, trions, multiexcitons, charged multiexcitons). We will conduct time-resolved PL/transient-absorption experiments with high-flux excitation to identify charging processes/dynamics and at low-flux in an applied electric field to distinguish charging/field effects and inform design of charging/field-"proof" gQD surface, internal interface and/or silicone/ceramic-matrix chemistry (M12-M24). We will work closely with our industrial partner on complementary device-level lifetime-testing as feedback to these investigations.

We will synthesize 20 g identical gQDs (± 2.5 nm; ±3% QY) 20-times faster than by standard methods (M6-M24). We will also develop synthetic protocol for adapting green-g-QD syntheses to the automated systems.

Conclusion

A successful program will lead to dramatic acceleration of the development of a novel class of quantum dot (QD) – the "giant" QD – as replacements for rare-earth down-conversion materials, underpinning advancements in white-light-emitting devices needed for next-generation solid-state lighting. In three Research Goals, we will solve remaining challenges limiting these otherwise ideal down-conversion materials: (1) Thermal quenching by correlating performance-under-temperature-stress with nanoscale structure for green and red gQDs, (2) Lifetime performance by engineering the LED to limit sources of thermal load, as well as addressing newly-identified detrimental photo-induced charging/field effects, and (3) Nanomaterial reproducibility/scale-up through new parallel-processing/automation strategies.

Publications

Mishra, N., N. J. Orfield, F. Wang, S. Click, H. Htoon, J. R. McBride, and J. A. Hollingsworth. Green-emitting 'giant' quantum dots nanoengineered for blinking suppression and single-emitter photostability. Nano Letters.

Nonequilbrium Dynamics and Controlled Transport in Skyrmion Lattices in Nanostructures

Charles Reichhardt
20160369ER

Introduction

Skyrmions are particle-like topological nanoscale magnetic objects that were discovered in chiral magnets in 2009. They have since been found in numerous materials, including recent observations of skyrmions that are stable at room temperature. Due to their size scale and the ease with which they can be moved, skyrmions could have a revolutionary impact on computational and information sciences which utilize magnetic storage, and could be used to create magnetic logic devices in which the skyrmions are the basic information unit. The key advantage to skyrmions is that they are smaller and can be packed far more densely than other comparable magnetic objects such as magnetic domain walls. Skyrmion-based devices can operate using orders of magnitude less power for read/write operations, significantly reducing heating.

The next advance in this field will be understanding and controlling skyrmion dynamics in nanostructured samples. Since skyrmions have many similarities to superconducting vortices, similar techniques for creating potential energy landscapes to control vortex motion could be applied to skyrmions, such as patterned structures that allow precise, thermally robust control of skyrmion motion under ac/dc driving. We will combine computational modeling of the nanostructured geometries to produce predictions of the skyrmion transport properties with experimental fabrication of these geometries and measures of transport.

The experimental results will validate the theoretical model and test the theoretical predictions. We will consider commensurate-incommensurate transitions on one-dimensional and two-dimensional periodic substrates and ratchet effects on asymmetric substrates. This will allow us to determine the optimal geometries for controlling the skyrmion dynamics and how to create the densest stable skyrmion packings. An important aspect that makes skyrmions very different from many other systems is the fact that their motion is dominated by the Magnus force rather than by dissipation. As a result, skyrmions represent a new class of dynamical systems.

Benefit to National Security Missions

The potential to create low power high density magnetic storage devices and other magnetic based logic devices would have a wide range of applications relevant for national security, including making smaller, more compact, lighter, and less energy costly devices for use by soldiers, aerial vehicles, and drones. Another possibility is the creation of an all-magnetic computer which would be able to start in the same state if it is shut off. This type of computer would much more durable in the field than conventional electronic devices. Skyrmions could be the next major player in this field due to their advantages over current magnetic domain wall technologies. Additionally, lower power, high density magnetic storage will be useful for big data storage and the ability to navigate through big data, and would help maintain the US and DOE at the very forefront of computer technology. Finally, the development of capabilities to model skyrmions on large scales could also be useful for modeling other systems where Magnus effects are relevant such as certain materials under extreme conditions.

Progress

For the fiscal year of Sept 15 to present we have published two papers and submitted four papers on skyrmion phases in pinning arrays. The first paper is on creating stable skyrmion crystals with periodic substrates. The second is is on how pinning creates a drive dependent skyrmion Hall angle which has been confirmed in experiments by the ANL group. The third paper is on Magnus-induced dynamics of driven skyrmions on a quasi-one-dimensional periodic substrate where we show how skymions can be guided and even accelerated by a 1D periodic substrate. The fourth paper is a comprehensive review on pinning/depinning phenomena including

what is the current state of the field of skymion dynamics. Additionally Charles Reichhardt has given invited four talks on Skyrmions and will be giving one more at an international workshop in Japan dedicated to skyrmion/vortex dynamics.

We have also published two papers in Physical Review B on this topic. The first one is on skyrmion/vortex ordering on a 1D periodic substrate which includes buckling transitions. The second is on a new kind of phase locking effect which occurs in skyrmion systems due to the Magnus term. In our experiments we have been able to measure the skyrmion Hall angle and will soon look at the effect of pinning on the Hall angle.

Future Work

During the next fiscal year, we will focus on dc driven motion of skyrmions to determine the effectiveness of the pinning landscapes and the ability of such landscapes to guide skyrmions along certain directions in the sample and measure the skyrmion Hall angle. Utilizing both continuum we will examine random, one-dimensional periodic, and two-dimensional periodic nanostructures for varied magnetic field and skyrmion densities. We will also examine skyrmion ratchet effects and noise fluctuations. The experiments will look at current driven dynamics with added pinning sites. These results will then be compared to the computational modeling to verify certain aspects of the input into the models to determine which modifications to the modeling are required.

Conclusion

In this project, we will model and understand how to precisely control skyrmion motion in nanostructured geometries along with the optimal geometries for the most effective way to move, write, read, and pack skyrmions in dense patterns which remain stable for long times. We will determine how to use transport measurements to detect skyrmion motion. We will use a combination of continuum and particle-based simulations to model these geometries and driving protocols. The potential to create low-power, high-density magnetic storage devices and other magnetic-based logic devices would have a wide range of applications relevant for national security, including making smaller, more compact, lighter, and less energy costly devices for use by soldiers, aerial vehicles, and drones.

Publications

Ma, F., C. Reichhardt, W. Gan, C. J. O. Reichhardt, and W. S. Lew. Emergent geometric frustration of artificial magnetic skyrmion crystals. 2016. Physical Review B. 94: 144405.

Ma, X., C. J. O. Reichhardt, and C. Reichhardt. Reversible vector ratchets for skyrmion systems. Physical Review B.

Reichhardt, C., and C. J. O. Reichhardt. Shapiro spikes and negative mobility for skyrmion motion on quasi-one-dimensional periodic substrates. Physical Review B.

Reichhardt, C., and C. J. O. Reichhardt. Depinning and nonequilibrium dynamic phases of particle assemblies driven over random and ordered substrates: a review. To appear in Reports on Progress in Physics.

Reichhardt, C., and C. J. O. Reichhardt. Noise fluctuations and drive dependence on the skyrmion Hall effect in disordered systems. 2016. New Journal of Physics. 18: 095005.

Reichhardt, C., and C. J. O. Reichhardt. Magnus-induced dynamics of driven skyrmions on a quasi-one-dimensional periodic substrate. 2016. Physical Review B. 94: 094413.

Reichhardt, C., and C. J. O. Reichhardt. Shapiro steps for skyrmion motion on a washboard potential with longitudinal and transverse ac drives. 2015. Physical Review B. 92: 224432.

Connecting Interface Structure and Functionality in Oxide Composites

Blas P. Uberuaga
20160501ER

Introduction

The goal of this effort is to connect functionality in complex oxides, particularly fast ion conduction, to the structure of the interface in oxide heterostructures. Our hypothesis is that the detailed atomic structure of the interface dictates the mobility of oxygen vacancies, which are responsible for ionic conductivity. By changing the chemistry of the oxide layers at the interface, we can modify that atomic structure and determine the subsequent effect on ionic conductivity.

This effort, an integrated modeling and experimental project, is aimed at determining, unambiguously for the first time, the role that the interfacial structure has on functionality. We will combine atomistic modeling with mesoscale modeling at the kinetic Monte Carlo level to develop models of ionic conductivity at oxide interfaces. These will be integrated with thin film growth and impedance spectroscopy to examine the connection between interfacial structure and ionic conductivity. We will use perovskite/rocksalt structures in which the interfacial atomic structure is very sensitive to the chemistry at the interface, providing a direct route to controlling interfacial structure without modifying the basic characteristics of the bulk materials.

The implications extend beyond ionic conductivity, as many materials functions, including magnetism and mutliferroic response, will depend on the atomic structure at the interface.

Benefit to National Security Missions

The DOE/SC mission involves controlled functionality, particularly in complex materials with a focus on materials design. Our effort directly addresses this challenge by examining how defect properties can be controlled with interfaces to enhance functionality. This also addresses the Mission Relevance of Renewable Energy and Basic Understanding of Materials as the types of complex oxides we are examining and their potential use as fast ion conductors provide new routes for developing fuel cell and battery materials, but based on a fundamental understanding of the relationship between interface structure and defect behavior. Finally, these same types of interactions are important for the development of radiation tolerant nanostructured materials and as such support the MaRIE mission.

Progress

On the modeling side, we have characterized the behavior of oxygen vacancies -- the carriers of ionic conductivity in these ionic conductors -- at two different structures of the SrTiO3/MgO interface. These interfaces differ in the chemistry of the SrTiO3 layer that is matched against MgO and, as a consequence, the misfit dislocation structure is significantly different. We have:

- used molecular dynamics to analyze the thermal stability of the interface and of the oxygen vacancy
- used molecular statics to calculate the energy of the oxygen vacancy as a function of location at the interface, accounting for the misfit dislocation structure
- constructed a kinetic Monte Carlo model that, under the assumption that the barriers between states is a simple function of the energies of the states, determines the mobility of oxygen vacancies at each interface
- calculated, using the nudged elastic band method, the actual energy landscape for the vacancy to traverse the fastest path identified in the kinetic Monte Carlo simulations

These simulation efforts have revealed that the mobility of oxygen vacancies is significantly slower at either interface than it is in the bulk. Further, it is much slower at the interface terminated by TiO2 chemistry than the one terminated by SrO chemistry. Together, these results indicate that the mobility of individual carriers is drasti-

cally reduced when they reside at the heterointerfaces. Thus, any increase in conductivity due to the presence of interfaces must be due to other factors, such as a high concentration of carriers or something more complex, such as an injection of carriers into the bulk of the material.

Experimentally, we have targeted, in the first year, the growth of SrTiO3 thin films that are suitable for ionic conductivity measurements via AC impedance spectroscopy. Films of STO were prepared by pulsed laser deposition (PLD) on MgO substrates. Initial conductivity measurements are being made in an in-plane configuration using Pt interdigitated electrodes. Measurements are being made over a range of oxygen partial pressure in order to assess the electronic and electrolytic regions of conductivity and identify the dominant charge carriers in each regime.

At the end of this fiscal year, we expect to have at least one manuscript ready for submission and significant results toward a second paper.

Future Work

In the second year of this project, we will continue developing thin film structures suitable for measuring ionic conductivity. As discussed in the proposal, isolating the role of the interface in the ionic conductivity while also eliminating any confusion as to contributions from electronic conductivity requires a rather sophisticated preparation of the sample. Our second year activities will focus on developing this process so that we can isolate the role of the interface on the ionic conductivity in this model system, SrTiO3/MgO.

On the theoretical side, we have demonstrated that the mobility of individual carriers are not enhanced by the interface. Thus, if the interface is a source of higher ionic conductivity, it can only be due to one of two factors: higher carrier concentrations, or a change in the nature of the carriers. We speculated that the later might be the origin of the high conductivity in these materials within our proposal and we will continue to pursue that line of interrogation in the second year of the proposal effort. In particular, we will develop kinetic models that account for both the mobility and the concentration of carriers at the interface as well as examine the likelihood that a different type of carrier is created by the interface.

Conclusion

Many technologically important applications, ranging from solid oxide fuel cells to supercapacitors and chemical sensors, rely on materials that exhibit high ionic conductivity, so-called superionic materials. However, despite the promise of these materials and the intensive research accompanying them, they still fall short of expectations. Not only will our work enable improved materials for applications such as fuel cells and supercapacitors, but the demonstration of controlling mass transport in complex materials via interfacial properties will be a first for Los Alamos and lead to a new ability to design materials for advanced applications involving superionics.

Controlling the Functionality of Materials through Interfacial Colloidal Gelation

Matthew N. Lee
20160519ER

Introduction

The overarching goal of this research is to develop a transformative "bottom-up" design paradigm for advanced materials, utilizing the spontaneous self-organization of nanoscopic particles at liquid interfaces to direct both structure and chemical functionality. Recent advances in photovoltaic cells, heterogeneous catalysis, and energy storage devices (e.g. high-performance batteries) have identified the key significance of interfacial engineering and its direct correlation with the performance metrics of these systems. However, few experimental methods exist to design, synthesize, and manipulate complex physical interactions across interfaces. Considering these present limitations, our research aims toward a rational design of porous and composite solids with controlled interfacial functionality using an emerging class of soft matter known as bicontinuous interfacially jammed emulsion gels, or Bijels.

Bijels are formed by arresting phase separation in multicomponent liquid mixtures, where the addition of solid particles to these systems can trap dynamic structures far from equilibrium. Because Bijels are a recent invention, our fundamental understandings of their physical assembly, aging, and mechanical properties are at an early stage. Moreover, Bijels have vast untapped potential in an array of current engineering applications, including interfacial catalysis and renewable energy systems. Hence, we will pioneer this area of research by 1) elucidating through a feedback loop of theory and experiment how the physicochemical properties of Bijels affect the physics of their assembly, and 2) applying this knowledge to the rational design of porous and composite structures with controlled functionality across multiple length scales.

As a pertinent example, we will demonstrate the strength of this approach through the design, synthesis, characterization, and application of novel electrode materials derived from Bijels. These results will provide critical advances for the optimization of porous structures in electrochemical systems (e.g. supercapacitors) while alluding to a broader potential of Bijel-based materials across an array of current technologies.

Benefit to National Security Missions

Successful realization of the proposed research objectives will provide critical advances in both theoretical modeling of multi-phase soft materials and novel materials synthesis techniques, paving the way for new generations of functional porous and composite solids for a diverse array of current technologies, including interfacial catalysis (e.g. CO2 sequestration and reduction), separations (e.g. pathogen detection, solute extraction), and energy systems (e.g. supercapacitors and high-performance batteries). More specifically, we will establish a fundamentally new design paradigm for composite structures based on a bottom-up assembly process, affording unprecedented control over the interfacial phenomena most crucial to the performance and economic viability of the applications listed above. This aspect of the work contributes directly to DOE Basic Science initiatives and is highly relevant to the Scientific Discovery and Innovation Mission and the Basic Understanding of Materials. The interdisciplinary and fundamental nature of this project also addresses clear challenges in the optimization of porous structures in energy storage devices, where success would have a clear impact on Mission Relevance in Energy Security (Renewable Energy). That these novel materials can also be utilized as filtration/purification membranes demonstrates even further relevance to the Environmental Missions (Climate and Energy Impact) as well as waste management and remediation technologies.

Progress

Our modeling efforts thus far in this FY have focused on: i) developing the field theoretical description of the phase separating blend plus nano particles; ii) implementing the model in a time-dependent Ginzburg-

Landau code (permitting a rough analysis of the process); and iii) marrying the field-theoretical method to a particle code that operates on the principles of Brownian dynamics for the colloidal motion and allows for probing directly the impact of colloidal shape, charge, concentration, dispersity, and size on the bijel formation process. This latter development will serve as a replacement for the envisioned lattice-Boltzmann method in the coming months, as we believe it will prove far more flexible and a better fit for our research objectives. This is a unique strategy for simulating bijel assembly, and is expected to provide significant benefits in the field when compared to existing techniques. Our team is in the process of servicing the fluorescent and photo-thermal confocal microscope (with C-PCS) to directly couple the simulations to our experimental data gathered from real bijel systems. It is expected that by the end of the current FY this microscopy system will be fully operational and we will carry out new experiments designed to more rigorously probe the interrelationships between bijel formation and their properties.

Our laboratory experiments have made several meaningful advances in FY16; bijels of water/lutidine have been reproducibly fabricated, and we now work with these on a daily basis. In addition, a new bijel system of the binary fluids diethyl maleate and undecane was discovered by a graduate student in MST-7 working on this project, which can offer several practical advantages to current systems including its stability at room temperature. This advance will be especially useful for the microscopy experiments described above. Beginning with bijels of water/lutidine, we have also prepared several novel materials from this system with immediate applications in HPLC and catalysis. Until now, bijels have only been transformed into porous materials using acrylic polymers. During this FY we have pioneered new routes to hierarchically porous polystyrene (PS) and PS-silica nanocomposites derived from bijels utilizing a double exchange process. We are currently exploring the use of these systems in flow-though separation columns. Separately, we have successfully discovered and fabricated a new class of aerogel materials based on bijels. Aerogels have many applications as insulators, capacitors, and sorbent materials, however, these are typically nanoscale solids that can be brittle and fragile. In addition, the size of pores in aerogels are on the order of tens of nanometers, which restricts their ability to accommodate high liquid throughput. Recently, our team has prepared two new aerogel materials derived from bijels. The first is made from carbonized polymer that is formed within the bijel once it is assembled; initial density measurements were on the order of just 20 milligrams per cubic centimeter, making this among the lightest ever carbonized aerogel materials prepared using this approach. Separately, we were astonished to discover that aerogel materials may be prepared from bijels simply by freezing and sublimating the solvents, leaving the self-assembled particles behind in a tortuous, 3-D arrangement. This can provide a crucial advance in aerogel-type materials, as ours prepared from bijels are macroporous in nature and may be wetted and dried without collapse. This also indicates that other types of aerogel materials may be derived from bijels prepared from different particles (e.g. metals or metal oxides). A paper describing these discoveries is in preparation, and an abstract to the MRS conference in Boston has been submitted.

To aid in the design and synthesis of novel bijel materials, this FY we sought to hire a postdoc with specific expertise in synthetic chemistry and catalysis. Over 60 applications were received for the position, and ultimately we were able to find a new postdoctoral researcher (Kyle Cluff) from UT San Antonio with an optimized skill-set for this project. Kyle joined LANL in the beginning of April 2016, and is now performing fundamental studies of new bijel systems prepared with exotic particles (e.g. gold nanoparticles and mesoporous silica particles). We are optimistic that bijels prepared from gold nanoparticles, coupled with our new-found ability to prepare aerogels from these systems will lead to an unprecedented new class of porous metal electrodes in the next FY.

Future Work

In the past FY our team has established both key theoretical and experimental capabilities that are necessary to study and explore bijel systems, and laid the groundwork for new experiments in FY17. In the second year of research, we aim to develop new functional bijel systems based on different particle chemistries/morphologies while continuing to optimize our newly-discovered synthesis routes to porous materials based on current bijel systems (developed during the current FY). For modeling, the new techniques based on the coupling of field-theoretical methods to a particle code that operates on the principles of Brownian dynamics for the colloidal motion developed this FY will be validated by probing the effect of the size/shape/number of colloids on the terminal domain size in the microstructure (for which we will gather experimental data to validate the codes). In our synthesis thrust, we plan to optimize our newfound ability to synthesis lightweight aerogel materials derived from bijels, and utilize these structures in separations and catalysis applications (e.g. high-performance liquid chromatography columns, where the bicontinuous nature of our materials coupled with their multimodal pore architecture is expected to allow for more rapid throughput and efficient separations when compared to existing methods). Similarly, for

hydrogenation catalysis applications we expected that Pd/Pt-decorated carbon aerogel materials derived from bijels will provide similar benefits: a combination of high active surface area for catalysis with high throughput necessary for economic feasibility. Lastly, our new postdoctoral researcher hired for this project will synthesize new bijel systems based on gold nanoparticles and higher-ordered mesostructured silica particles (to boost the available interfacial surface area even further for separation applications). The gold-based bijels will be utilized in catalytic reactions (e.g. CO oxidation), and as electrodes for energy applications such as super-capacitors.

Conclusion

The project goal is a rational design of porous and composite solids with controlled interfacial functionality using an emerging class of soft matter known as bicontinuous interfacially jammed emulsion gels, or Bijels. Because Bijels are a recent invention, our fundamental understandings of their physical assembly, aging, and mechanical properties are at an early stage. Moreover, Bijels have vast untapped potential in an array of current engineering applications, including interfacial catalysis and renewable energy systems. Successful realization of the proposed research objectives will provide critical advances in both theoretical modeling of multi-phase soft materials and novel materials synthesis techniques, paving the way for new generations of functional porous and composite solids for a diverse array of applications, including optimized energy storage devices and waste management and remediation technologies.

Publications

Santiago-Cordoba, M., K. J. Cluff, C. E. Hamilton, C. Grote, E. Weis, M. Herman, N. Parra-Vasquez, and M. N. Lee. Accelerating the Design of Low Density Materials with Bicontinuous and Hierarchical Porosity for Enhanced Energy-Driven Applications . To appear in Materials Research Society Fall 2016 Meeting & Exhibition. (Boston, Nov. 27th - Dec. 2nd 2016).

Emergent and Adaptive Polymers

Jennifer Martinez
20160528ER

Introduction

Optically (re)active materials are critical components in photovoltaics and sensing and emitting devices. These materials convert solar energy into hydrogen or electricity, create the signal in the transduction of biological detection, and form the dynamically changing colors of TV screens and implantable sensors, as just a few examples. The electrical or optical properties of these materials are dictated not only by the properties of polymers and their optical moieties but, more importantly, by the way in which the moieties are spatially ordered with respect to each other. Nature is a master of creating adaptive materials that respond dynamically to their environment converting one type of signal (e.g. chemical or photophysical) into another signal or emergent response and which are specifically ordered as is required for optically active materials. Stimuli-responsive polymers are an exciting class of materials that could be created to adapt, sense, and interact with their environment if only we can control polymer structure, the packing of their optical elements under a defined stimuli, and accelerate their discovery. We will create libraries of genetically encoded and optically active polymers, and through a technique akin to evolution sort for those polymers that exhibit a defined optical or adaptive response. Use of genetically encoded polymers (GEPs) allows us to create large libraries of stimuli-responsive polymers (far eclipsing current synthetic techniques) and to identify, en masse, those polymers with a defined function or physical property in a matter of days instead of decades. We target polymer light-emitting electrochemical cells (PLECs) and polymers for organic light emitting diodes (OLEDS)- producing electroluminescent polymers that respond to stimuli (e.g. specific potential) with output of a specific optical response(s) (luminescence).

Benefit to National Security Missions

Genetically encoded polymers are an exciting and impactful field on their own, but the creation of libraries and the facile selection of polymers with defined optoelectronic function is entirely novel. Not only is this a great intellectual challenge, but one with important practical consequences. We expect the results of this work to provide multifunctional materials for the next generation of PLECs and OLED used within implantable and wearable electronics and perhaps lighting. An investment in the field of optoelectronic libraries will open future funding opportunities from NIH, Intel, DOE, and the DoD. DOD (DTRA), for example, has listed Enabler #3: " We will pursue bioinspired and biomimetic integrated materials for application as coatings, elastomers, and structural and sensing materials". On the molecular electronics frontier, the DOE cites the need for "soft materials with tailored bandgaps, optical cross-sections, (and) luminescence efficiencies," to meet a BES Grand Challenge, to "…design and perfect atom- and energy-efficient synthesis of revolutionary new forms of matter with tailored properties". Our program addresses the LDRD Grand Challenge in Materials, which underpins all Laboratory mission areas.

Progress

Our goal is to dramatically alter the discovery landscape of functional materials using genetically encoded polymers and our combinatorial approach to select for polymers with a defined optoelectronic function, under the conditions of polymer use. Toward creating polymers with defined luminescent properties for downstream application in polymer light-emitting electrochemical cells (PLECs) and/or organic light emitting diodes (OLEDS) we will create the following:

Genetically encoded polymer libraries

We focus on developing coblock libraries of elastin-like polymer (ELP, e.g. springs) and structural blocks (coils, e.g. rods). Further encoded will be inorganic (metals) or organic (oligomers) moieties. Each of these blocks and redox/optical moieties will be randomly assembled into a target library of ~1 million in size.

Toward that goal we have designed a test matrix of ~9 different polymers, each differing in their composition of structural blocks (coils of 18 amino acids in length) and elastin-like polymers, where the position of conjugation to an optical moiety can be attached. Following further testing by PCR, we will use these below in testing microfluidic devices.

Microfluidic devices to create microemulsions and develop labeled polymers
We have narrowed down the microfluidic devices we need to reproduce for simple testing of our biological and optical processes.

We have a suite of lanthanide metal complexes, each with differing fluorescence that we are in the process of conjugating directing to E-ELP. This suite of fluorescent ELP will be used to benchmark the microfluidic sorting for either discreet fluorescence upon excitation and/or electroluminescence with application of current.

Further, we will use the 9mer matrix developed above to begin testing the correct biological and conjugation strategies within microfluidics –specifically testing how well we can make phage or conjugate polymer to optical moiety within the emulsions.

Evolved polymers from large libraries and rational design for those with defined functional properties (i.e. luminescence) following application of stimuli (i.e. current)
Downselected polymers will be identified and scaled from the embedded DNA of the polymer. We have finalized work where we have embedded a conjugated polyphenylene vinylene oligomer into a modified elastin. From this material we have made hydrogels and thoroughly characterized the rheological and optical parameters and have found new optical response with application of pH changes. This work has now been accepted into ACS Biomaterials Science and Engineering.

We are actively working up a first rationally designed construct, as low hanging fruit, that will be conjugated to three different transition metal complexes. These first constructs will be tested within a home built PLEC device and possible transferred to a colleague in Korea, for testing within OLED devices.

We have hired a staff member from Biosciences division to work on this project and have hired a postbac for the same.

Future Work
Our goal is to dramatically alter the discovery landscape of functional materials using genetically encoded polymers and our combinatorial approach to select for polymers with a defined optoelectronic function, under the conditions of polymer use. Toward creating polymers with defined luminescent properties for downstream application in polymer light-emitting electrochemical cells (PLECs) and/or organic light emitting diodes (OLEDS) we will create the following:

Genetically encoded polymer libraries
We focus on developing coblock libraries of elastin-like polymer (ELP, e.g. springs) and structural blocks (coils, e.g. rods). Further encoded will be inorganic (metals) or organic (oligomers) moieties. Each of these blocks and redox/optical moieties will be randomly assembled into a target library of ~1 million in size.

Microfluidic devices to create microemulsions and develop labeled polymers.

Evolved polymers from large libraries and rational design for those with defined functional properties (i.e. luminescence) following application of stimuli (i.e. current).
Downselected polymers will be identified and scaled from the embedded DNA of the polymer.

Conclusion
We will create libraries of genetically encoded and optically active polymers, and through a technique akin to evolution, sort for those polymers that exhibit a defined optical or adaptive response. Use of genetically encoded polymers (GEPs) allows us to create large libraries of stimuli-responsive polymers (far eclipsing current synthetic techniques) and to identify, en masse, those polymers with a defined function or physical property in a matter of days instead of decades.

Publications
Balog, E. R. M., Ghosh, Park, Hartung, Sista, R. C. Rocha, Wang, and J. S. Martinez. Stimuli-Responsive Genetically Engineered Polymer Hydrogel Demonstrates Emergent Optical Responses. 2016. ACS BIOMATERIALS SCIENCE & ENGINEERING. 2 (7): 1135.

Exotic States in U-based Superconductors

Roman Movshovich
20160572ER

Introduction

Ce-based superconductors (i.e. CeCoIn5 of the so-called 115 family) provide many examples of emergent behavior, where competition between Landau Fermi Liquid and magnetic ground states gives rise to states with exotic properties, such as unconventional and re-entrant superconductivity, non-Fermi Liquid behavior, and pseudogap state in the normal region just outside of the superconducting phase, with correspondingly very rich phase diagrams. Progress here was facilitated by the availability of high quality single crystals, allowing for specific heat and thermal conductivity measurements in a rotated magnetic field, which were instrumental in identifying not only the d-wave nature of the superconducting order parameter in CeCoIn5, but also a locations of its nodes (zeros) in the momentum space.

Similarly rich phase diagrams are also present in a number of U-based superconductors, e.g. URhGe and UCoGe ferromagnetic superconductors, where superconductivity is believed to be mediated by the ferromagnetic fluctuations. We have grown single crystals of these compounds, and employed recently developed electro-refining capability to purify the compounds and reduce the amount of crystalline disorder. Both compounds exhibit rich phase diagrams. In particular, resistivity and cantilever magnetometry studies of URhGe revealed re-entrant superconductivity at 8T, which is believed to be due to a magnetic reorientation transition around 12 T, which changes as the field is rotated away from the b-axis in an b-c plane. Our preliminary heat capacity studies of polycrystalline samples of superconducting U2PtC2 (T_c = 1.34 K) in magnetic field also indicate the presence of nodes in its superconducting energy gap. We will grow single crystal samples of U2PtC2. We have built a thermal conductivity cell coupled with a piezoelectric rotator, on a dilution refrigerator capable of achieving temperatures below 20 mK and magnetic field up to 14 Tesla. This system will be a powerful tool to study these U-based superconductors.

Benefit to National Security Missions

This work addresses the Grand Challenge: “Materials: Discovery Science to Strategic Applications”. It builds on the newly developed measurement capabilities and our expertise in high quality single crystal synthesis, and focuses on exotic emergent states such as unconventional superconductivity and its interplay with magnetism, and f-electron physics. Specific heat and thermal conductivity measurements at temperature down to few tens of millikelvins in a rotating magnetic field of up to 14 Tesla are a powerful suite of advanced measuring capabilities, and will support LANL’s position of leadership in the area of correlated electron research. We will apply these capabilities to investigations of superconducting and normal states in U-based intermetallic compounds, an area of traditional strong interest at LANL due to its focus on f-electron elements, especially actinide series. Overall, this project supports both themes of Emergent Phenomena and Defects and Interfaces, two of the three areas of the Materials Strategy at LANL.

Progress

We have successfully implemented rotation capability in low-temperature and high-field. A piezoelectric rotator was installed in a dilution refrigerator coupled with a 14 T superconducting magnet. In previous rotation experiments in our laboratory, heating at low temperatures as a result of friction in the mechanical rotator has been a major problem. In the current setup, the sample is rotated while maintaining the temperature below 200 mili-Kelvin. For monitoring the rotation angle, two Hall sensors perpendicular to each other are employed. The fine rotation and monitoring capability enables a rotation experiment with the angle resolution as low as 0.05 degrees.

A rotation frame mounted experimental apparatus for thermal conductivity measurements was successfully designed and assembled. For the standard steady state measurements, two thermometers and one heater were

calibrated and installed on a fiberglass-reinforced polymer frame that is suited for the rotator due to the light weight. The setup is capable of thermal conductivity measurements down to 50 mK with the sample's rotation range of more than 180 degrees.

The project's first experiment, the thermal transport measurement on unconventional superconductor CeCoIn5 in a rotating magnetic field, was successful. The systematic modulation of thermal conductivity by the 180 degree rotation in a magnetic field was observed. The modulation can be decomposed into two-fold oscillation by the contribution from the superconducting vortices and four-fold oscillation by the d-wave property of the unconventional superconductor. In addition, Duk Young has observed a sharp increase of thermal conductivity when the magnetic field is aligned parallel to the heat current or 33 degree away from the heat current direction, along the nodal direction of the d-wave superconductivity. These results indicates that exotic resonant states form, depending on the relative direction of magnetic field in the tetragonal crystal. We are preparing a publication on this observation.

In the low-temperature and high-field corner of the superconducting phase, CeCoIn5 has the so called Q-phase, in which an antiferromagnetic order coexists with the superconductivity. Duk Young has identified the switching behavior of the magnetic ordering with the angle-resolved thermal conductivity measurement. The measurement has revealed an anisotropy of the superconducting order parameter, which can be explained by the secondary p-wave pair-density-wave (PDW). This observation is important and interesting because it is a unique example of intertwined orders which is a concept of significant importance in understanding unconventional superconductivity. The reduction of the thermal conductivity in the Q-phase enables a quantitative prediction of the secondary order parameter, which has not been possible in any other experiment. The manuscript based on these observations has been submitted to Nature Communications.

Samples of UCoGe were grown; a piece of a rod was cut off, shaped into a thin disk appropriate for specific heat measurements, and oriented with the thin direction along the c-axis. The sample was annealed. We expect the residual resistivity ratio (RRR) in the range of 30-40.

We have successfully grown the first generation of the URhGe in a Bridgeman furnace with a thermal gradient. The samples are undergoing initial characterization with respect to purity, stoichiometry, and RRR.

Future Work

In FY17, we will continue to perform specific heat and thermal conductivity measurements on CeCoIn5. This will elucidate the nature of the third order parameter (we discovered in FY2016), which is intertwined with a d-wave superconductivity and an antiferromagnetic spin density wave (SDW) order in the Q-phase of CeCoIn5. We will also perform field-rotating investigations of superconducting in the entire superconducting phase of CeCoIn5 in a homogeneous (vortex, or mixed phase) state up to 10 T and from Tc to few tens of mK, to finish investigation of anomalous peaks in thermal conductivity at +/- 33 degrees. We will design and build a specific heat cell for rotator measurements. The work on synthesis of high quality single crystals of URhGe, UCoGe, and U2PtC2 will proceed further, and we will characterize the purity on crystallographic quality (defects) of these compounds (UCoGe is already available for investigation and first batches of URhGe have been produced). We will initiate their investigations via field-rotating specific heat and thermal conductivity measurements. We will continue our strong collaboration on this project with our theory colleague Shizeng Lin from T-4 of LANL, and with our external theory colleges, Ilya Vekhtor (LSU) and Anton Vorontsov (U Montana). In particular we will develop predictive capabilities for the thermodynamics and transport of p-wave order parameter superconductors (expected case for U-based superconductors) in a rotating magnetic field.

Conclusion

Uranium-based heavy fermion compounds offer a particularly fertile area to look for an emergent behavior, as they present a large variety of magnetically ordered ground states that seem to be connected to superconductivity. We will correlate the order parameter symmetry with the nature of magnetic fluctuations, accessing the microscopic origins of superconductivity in selected U-based superconductors. These results will help understand the origins of unconventional superconductivity in a wider range of materials, including high temperature cuprate and pnictide superconductors.

Publications

Kim, Duk Y., S. Lin, F. Weickert, M. Kenzelmann, E. D. Bauer, F. Ronning, J. D. Thompson, and R. Movshovich. Intertwined Orders in Heavy-Fermion Superconductor CeCoIn5. To appear in Physical Review X.

Target Projects in Theoretical and Experimental Materials Science: Novel Structural Models, Materials Imaging and Informatics, and Strength/Sensing Capabilities Integrated During Manufacturing

Alexander V. Balatsky
20160651ER

Introduction

The objective of this research project was to seed new ideas and develop new capabilities for Los Alamos within the area of materials science. This effort incorporated small-scale targeted projects encompassing both theoretical/modeling/simulation and experimental work. In particular, we focused on data mining and machine learning in materials science, dynamics of quantum materials, additive manufacturing, and methods for the facile morphological characterization of materials. Initial tasks included novel structural models, materials imaging, materials informatics, and focused manufacturing. This body of work brought together various lab strengths in modeling/informatics and imaging and manufacturing. A notable success was: development of a novel computational framework consisting of variational image segmentation and computational geometry techniques and development of an improved electrically conductive polymer for 3D printing applications that resulted in development and patent disclosure of a 3D-printed tamper-evident container.

Benefit to National Security Missions

Our R&D in Additive Manufacturing, modeling of correlated materials and understanding of materials defects provided technical products for the Laboratory to address missions in Additive Manufacturing, Complex Functional Materials and Materials Dynamics. In particular, we believe we are on the path to deliver new technical capabilities for Additive Manufacturing, modeling of correlated materials and data informatics, which have broad implications for materials in LANL mission applications.

Progress

Predictive design promises to revolutionize the creation of materials toward those with defined structure and function. However promising, to fully achieve in silico materials design the field requires improved understanding of structure-function relationships, methods to quickly image and analyze data to build databases for predictive algorithms, and methods to quickly create materials and to understand how those materials are grown with time (e.g. one must know failure mechanisms to best design next generation compounds). Toward reducing these knowledge gaps, the Institute for Materials Science targeted small-scale investment in high risk/high-reward tasks to allow the selected ideas to incubate. The Rapid Response (RR) process enabled the development of cutting edge and innovative science efforts at the nascent stage where there is potential for a scientific breakthrough. We identified tasks that targeted additive manufacturing, data informatics, and correlated and dynamic materials, all building toward predictive design. These areas have seen significant scientific excitement, are central to the Los Alamos mission and are aligned with the LANL materials strategy. During task selection, the potential for project failure (e.g. perceived risk), while to be avoided, was a secondary consideration to potential scientific impact. The risk-tolerant profile of RR complements other established modes of funding at LANL and adds to the full spectrum of the cutting-edge science pursued by LDRD.

By way of example of the project focuses we motivate here both structure-function and data analysis methodologies. Establishing a structure-function relationship in strongly correlated electron materials (SCEMs) has posed a significant challenge in the materials physics community. In particular, there are unresolved questions as to the temperature-driven multiple phases in Pu metal, as an example, and mechanism for migration of vacancies and defects in this metal. The need calls for powerful theoretical tools. In the past, molecular dynamics (MD) has played an important role in tracing dynamics of atomic-level phenomena of materials. Unfortunately, the classical MD approach is limited in the use of empirical potentials for the force fields while the quantum MD (QMD) approach, while more accurate, is computationally expensive. The drawback of quantum MD is that the

underlying DFT theory within its local density approximation is inadequate for the description of strongly correlated electronic materials. The object of this project was to go beyond DFT-based QMD and develop QMD with electronic correlation effects addressed explicitly. In our approach, the strong electronic correlation effects were treated within a real-space version of the Gutzwiller variational approximation (GA), which is suitable for the inhomogeneity inherent in the process of quantum MD simulations.

While image analysis techniques have advanced in recent years, automated extraction of microstructural features of interest from materials imagery remains a significant challenge resulting from the inhomogeneity in image background and noisy appearance of features of interest. Here our goal was to address these challenges by transitioning computer vision techniques that have been successfully used in the satellite imagery domain, and adapt them to the analysis of metal alloy solidification data collected by in-situ x-ray radiography.

Finally, toward facile methods to create libraries of new materials and to better define materials synthesis failure modes, we looked toward additive manufacturing processes. The quality of 3D printing processes is limited in part by the lack of build process monitoring and control. Toward these key gaps, we have developed methods to monitor the structural quality of printed parts and implemented a feedback system with the AM process to detect in situ defects.

Scientific Approach and Accomplishments

Capturing and Exploiting Microstructure-Aware Materials Data

This work developed Materials Genome Initiative (MGI) tools relevant for structural materials, whose mechanical properties depend nonlinearly on microstructure (e.g. image analysis for predictive design). The test problem was age-hardenable U-Nb alloys, whose literature (~40 papers) was small enough to be understandable by a subject matter expert without MGI tools, but large enough to sample the variability of data reporting in the literature. This effort focused on developing tools to streamline three key tasks of the scientific workflow:

1. Extraction: data digitizing (WebPlotDigitizer), staging (Excel), and conversion to XML + automated importing of data into the NIST Materials Data Curation System (Python).

2. Curation: semi-automated tools to map aging time-temperature space in terms of microstructure (lamellar vs. nonlamellar) and hardness trend (hardening vs. softening).

3. Analytics: interactive slice-and-data the datasets with automatic updates of model fits.

4. Finally, these tools were linked into an architecture called “Pinyon,” which capturing both code and documentation in one place (Jupyter notebook). It automated handoffs between the steps and tracked curation decisions.

Morphological Descriptors Developed Through Reduced Order Models

A new set of morphological descriptors for polycrystalline structures was developed based on the spatial gradients of the crystal orientation functions (quaternions) (e.g. data analysis for predictive design). These fully capture all of the degrees of freedom associated with grain boundaries and triple junctions, and provide a rotationally invariant basis with which to describe the relative orientations.

The completeness of the set was demonstrated with the mathematics of tensor decomposition and rotational invariance. Simple test problems of polycrystalline samples subjected to uniaxial strain were examined, and correlations between local regions of stress or strain build-up and extreme values in the descriptors were demonstrated.

A manuscript describing the work is currently in preparation. The postdoc on the project (CGC) has now been converted to LANL staff and continues to work in the area of developing reduced order models for describing complex material behavior.

Gutzwiller Variational Wavefunction Approach to Electronic Correlation and Lattice Dynamics in Multi—Orbital Models

Through this project, we developed a theoretical tool to perform Molecular Dynamics in strongly correlated electron systems. In this approach, the electronic correlation effects are addressed within a Gutzwiller variational wavefunction approximation. The developed capability has an impact in study of the structure-property relationship of actinide materials.

We considered a minimal one-correlated-orbital Anderson model with parameterized spatial dependence of tight-binding hopping integrals. The developed fast GA-MD method (Gutzwiller variational approximation- molecular dynamics) was benchmarked using exact diagonalization to solve the GA variational parameters. We found that the MD simulations based on SMA, and direct matrix diagonalization of the quadratic Hamiltonian (non-interacting or Gutzwiller-approximated) give a converged atomic structure fully consistent with each other. Noteworthy, for an ensemble of 1600 atoms, the SMA is two orders of magnitude faster than the matrix diagonalization method.

Physically, our GA-MD demonstrates the expansion of equilibrium lattice constant with the increase of Coulomb repulsion (Fig 1). This novel method will open up an unprecedented opportunity enabling large-scale quantum MD simulations of strongly correlated electronic materials. We are now generalizing this method further to simulate realistic materials.

Integration of Mechanical Reliability and Multifunctionality in High Quality Aluminum Nitride Films
Through this project, in situ dynamical mechanical tests have been performed at atomic scale in a transmission electron microscope (TEM) to explore the reversible phase transformation mechanism from Zinc Blende (ZB) to Wurtzite (WZ). The transition path can be characterized as the collective glide of Shockley partials on every two {111} planes of the ZB-AlN. This work provides an instructive method of mechanically controlling the crystalline phase in binary octet semiconductors.

The multilayers composed of alternating Al and AlN individual layers were deposited by reactive direct current magnetron sputtering on Si substrates. When the average thickness of the AlN layers is less than 1 nm, AlN exhibits ZB phase. On the other hand, when the AlN layer thickness is large, AlN presents in the WZ structure. Density functional theory calculations were carried out through collaboration with other LANL staff. We found that: as the biaxial strain due to coherency at the interface increases, the energy difference between the ZB-AlN/Al interface and the WZ-AlN/Al interface decreases.

This Rapid Response project provided the fundamental base and approach for the optimized design of both mechanical and functional properties of microelectronic materials. The performed work addresses the broader scientific challenges of discovering new mechanisms that enable simultaneous increases in material plasticity and toughness while preserving outstanding functionalities.

Optimizing Image Segmentation for Quantitative Studies of Materials
We transitioned computer vision techniques we have successfully used in satellite imagery domain, and adapted them to the analysis of metal alloy solidification data collected by in-situ x-ray radiography (Fig 2).

We developed and evaluated a novel computational framework consisting of variational image segmentation and computational geometry techniques. The image segmentation, i.e., extraction of features of interest (such as growing dendrites in metal alloys), was posed as an optimization problem, which takes into account both geometry and spectral image characteristics at local and global spatial scales. The segmentation step, that detected features of interest, was followed by structural characterization of the extracted features using 2D triangulation techniques.

The prototyped and validated computational framework provides core capabilities to accelerate the analysis of materials image datasets, which prior to this work, was primarily done manually. This new set of protocols have the potential to enable high-throughput materials processing experiments to be performed for the development and validation of multi-scale models in materials science.

Conclusion
Most of the funded tasks achieved their technical goals, demonstrating that small investments could make concrete technical progress. Project focus on nascent and rapidly developing areas enabled impactful science with relatively small-scale investments. To illustrate, J. Bernardin's project led to development of an improved electrically conductive polymer for 3D printing, and exploration of applications of the resulting technology. The ultimate deliverable arising from this research investment was the development and patent disclosure of a 3D printed tamper evident container. AM is a new and fast growing field where our research enabled new technology. Moreover, the image segmentation task developed and evaluated a novel computational framework consisting of variational image segmentation and computational geometry techniques for high-throughput analysis of large sets of microstructural imaging data.

Publications
Julien, J. P., J. D. Kress, and J. X. Zhu. Explicit inclusion of electronic correlation effects in molecular dynamics. Physical Reviews B.

Spin-state Transitions as a Route to Multifunctionality

Vivien Zapf
20140177ER

Abstract

Research in magnetoelectric materials is a new and accelerating trend motivated by the need for magnetic sensing and computing with orders of magnitude less power consumption and dissipation than existing technology. [1-4] In magnetoelectrics electric voltages rather than currents are used to control and sense magnetism, and the materials are electrically insulating. Thus, in contrast to spintronics, magnetoelectrics have orders of magnitude less power consumption and heat dissipation. Magnetoelectrics have also recently been shown to be useful for antennas, filters, resonators, gyrators and other devices where an applied electric or magnetic field can tune the frequency response in situ. [5]

To date, the majority of magnetoelectric research has focused on inorganic oxides where ferromagnetism can be coupled to ferroelectricity. [6] However, here we explore and demonstrate new approaches to magnetoelectric coupling in metal-organic compounds (single-molecule magnets, metal-organic frameworks, molecular magnets, etc). [7-15] These materials offer a large new territory in which to discover and design magnetoelectric properties, and to overcome limitations of existing materials. Their properties can be tailored and designed and they offer additional functionalities such as sensitivity to chemical absorbents, mechanical flexibility, transparency and interactions with light. However, historically the downside of metal-organics for magnetism has been low magnetic ordering temperatures well below room temperature.

In this work we show that we need not restrict ourselves to ferromagnetism and ferroelectricity – in metal-organics there are different native magnetic and electric functionalities that extend up to room temperature, which are less familiar to the condensed-matter physics community. We propose and demonstrate here that spin-state transitions can be used to create magnetoelectric coupling, and that organic guest molecules can be used to create ferroelectricity. Thus we have found entirely new routes to magnetoelectric coupling in the very large class of metal-organic materials with the potential to extend up to room temperature. This work is a collaboration between magnetic and electric measurements at MPA-CMMS, theory at T-4, metal-organic crystal growth at C-IIAC and crystal characterization at MST-11.

Background and Research Objectives

Spin state transitions

Magnets containing transition-metal ions can show spin-state transitions, when an electron transitions from one partially-filled magnetic orbital to another. In the process the overall magnetic properties of the ion change, e.g. the total spin of the ion may transition from S = 1 to S =2. This change in orbital occupation modifies the radius of the ion as much as 10%, and alters the shape, bonding, and dielectric properties (Figure 1) Thus spin-state transitions are a route to strong spin-lattice coupling. Spin-state transitions are generally found in d4-d7 transition-metal magnetic ions such as Co2+, Ni2+, Mn3+, Fe3+. They are rare in inorganic oxides at ambient temperatures and pressures because the stiff lattice and the crystal-electric field interactions are usually sufficient to suppress the spin-state transition. [16,17] However, in metal-organics such as molecular magnets, single-molecule magnets, metal-organic-frameworks where the transition-metal ion is bonded by organic linkers, the lattices are soft enough to accommodate the spin-state transition at room temperature or below and ambient pressure.

Thus, spin-state transitions are emerging as a major source of new magnetic functionality in metal-organics up to room temperature in the last ten years. [18-24] Spin-state transitions are cooperative phase transitions due to coupling between spin states of individual magnetic ions (as opposed to spin-state crossovers, which are the behavior of isolated magnetic ions). It has been previously shown that spin-state transitions can be used

to create hysteretic magnetic switching, can be triggered by light (albeit at temperatures well below room temperature), pressure, chemical adsorption, temperature, and magnetic field. [18-24] Here we show that the dramatic lattice reconfigurations that accompany spin-state transitions can also toggle ferroelectricity, thereby creating magnetoelectric coupling and multiferroic behavior.

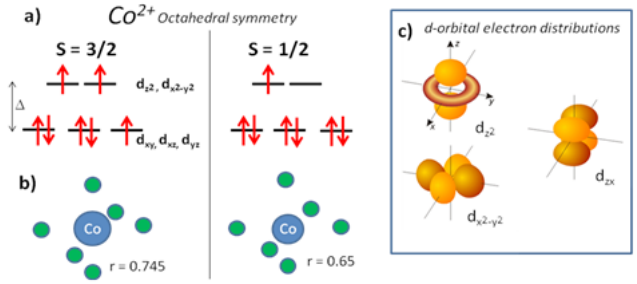

Figure 1. a) Spin-state transition from S = 3/2 to S = 1/2 in Cooccurs when an electron transitions to a different d orbital as a result of a change in temperature, pressure, magnetic field, chemical adsorption or light absorption. b) The effective ionic radius changes from 0.745 to 0.65 a.u. The green circles illustrate neighboring oxygens whose configuration changes to accommodate the spin-state transition of the Co ion. c) Shape of d-orbital electron distributions illustrating the change in shape and bonding of the magnetic ion as an electron transitions from one d-orbital to another.

Dielectric behavior in Metal-organic frameworks

Metal-organic frameworks (MOFs) are a subset of metal-organics where the crystalline lattice is porous at the level of individual unit cells. The structure consists of a framework and guest cations that are weakly bonded into the pores of the framework. This ability to adsorb and desorb guest molecules gives MOFs the potential for applications in gas storage and sensing, oil adsorption, and drug delivery. [7] Here we investigate their ferroelectric properties and show that electrically polar guest cations can form ferroelectricity that in turn can be modified by the magnetic framework. For example, dimethyl ammonium is an electrically polar molecule that can occupy the pores of a perovskite lattice consisting of transition metal ions bonded by formate molecules. [12] These electrically polar guest molecules can order ferroelectrically below 180 K. Thus electrically polar guest cations in MOFs offer another route to magnetoelectric coupling in metal-organics.

Scientific Approach and Accomplishments

Our two most important results are: 1) demonstrating for the first time that a spin-state transition can create ferroelectricity (being written up for publication), and 2) demonstrating magnetoelectric coupling and ferroelectricity in a metal-organic framework (in press with Nature Quantum Materials [25]). In addition to these two results we have, as part of this ER, generated or contributed to a dozen other papers on magnetoelectric coupling and metal-organics in high-impact journals including Physical Review Letters, Phys. Rev. X, Journal of the American Chemistry Society, Physical Review B, and a cover article in Reviews of Modern Physics. [26-37]

Spin state transition in Mn[taa] creates multiferroic behavior

Mn[taa] [H3taa = tris(1-(2-azolyl)-2-azabuten-4-yl)amine] is a molecular magnet, where the Mn[taa] molecules pack to form a cubic crystal structure (see Figure 2). [38] The Mn3+ ion is surrounded by six nearly equivalent nitrogen atoms. The Mn spin undergoes a sharp, cooperative spin-state transition at 50 K, dropping from the high-spin S = 2 to the intermediate-spin S = 1 state as the temperature is lowered. In the high-spin state, Mn3+ with S = 2 is Jahn-Teller active, meaning that it distorts its nitrogen cage along one of three nearly-equivalent axes. The distortion is dynamic; thus on average the crystal structure remains cubic. These distortions carry electric dipole moments; thus there is a large dielectric constant obeying a Curie-Weiss law above 50 K. As the temperature is lowered one might expect these dielectric structural fluctuations to freeze to form a ferroelectric state and trigger a structural phase transition. However, below 50 K the spin-state transition intercedes and the Jahn-Teller electric dipoles abruptly vanish before they have a chance to freeze, as the spin state lowers from S=2 to S=1. The interactions between spins and electric dipoles are primarily elastic in nature, since the magnetic or electric exchange path across intervening organic molecules is too long to be significant at 50 K.

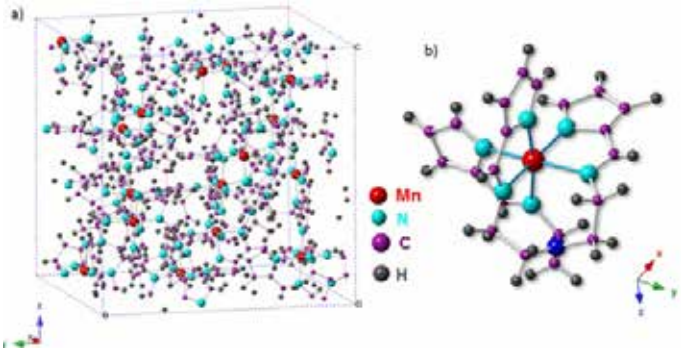

Figure 2. a) One unit cell of cubic Mn[taa] showing the packing of molecular units. b) One molecule of Mn[taa].

We postulate and then demonstrate that applying a large magnetic field allows the Mn spins to remain in the high spin state even at low temperatures, such that the electric dipoles have a chance to form a ferroelectric state. We demonstrate this using millisecond pulsed magnetic fields to 65 T and continuous fields to 45 T at the world-unique National High Magnetic Field Laboratory facilities. We find

that magnetic field-induced ferroelectricity forms at the spin-state transition in applied magnetic fields in Mn[taa]. Moreover, we observe a very large magnetoelectric coupling at the spin-state transition to within an order of magnitude of the largest magnetic field-induced changes in electric polarization that have ever been found. This is the first example, to our knowledge, of multiferroic behavior triggered by a spin-state transition, instead of conventional magnetic ordering. This result demonstrates that the vast field of metal-organic compounds with spin-state transitions can be exploited for multiferroic/magnetoelectric engineering.

Previous reports in the literature discussed neither synthetic detail nor the crystallization conditions. We were able to determine that the best commercially available Mn(III) precursor to use with the taa ligand was Mn(acac)3 (acac = acetylacetonate) as ligation releases pentane-2,4-dione which is easily removed under vacuum. [39] In contrast, materials such as Mn(acetate)3 and MnX3 (X = halide) generate acids such as acetic acid and HX and thus require the addition of a base and further purification steps. Single crystals grown from hexane diffusion into THF matched the reported structure. Our experimental and theoretical results are summarized in Figure 3.

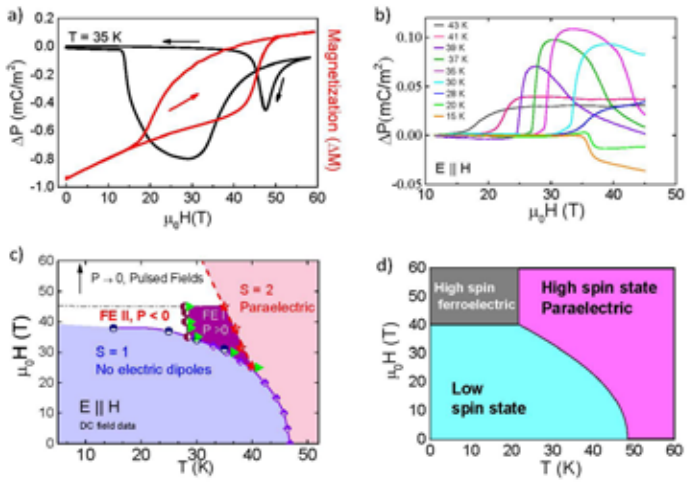

Figure 3. a) Electric polarization change DP and magnetization change DM relative to H = 0, in pulsed magnetic fields with sweep rates up to 4 kT/s. A spontaneous electric polarization indicative of ferroelectricity occurs for an intermediate region of magnetic fields during the spin-state transitions. b) Electric polarization vs magnetic field in continuous (slow) magnetic fields with sweep rates < 1 T/min. c) Phase diagram determined in continuous magnetic fields from electric polarization and capacitance measurements. d) Calculated phase diagram from a mean field 4-state Potts model.

Figure 3a shows the pulsed-field magnetization and electric polarization in applied fields undergoing a hysteretic spin-state transition. Figure 3b plots the electric polarization collected in slow continuous fields. Finally Figures 3c and d shows the phase diagram in continuous fields and our theoretically predicted phase diagram. In experiments there are two regions of ferroelectricity with opposite electric polarization. In the pulsed-field data we find that at the highest magnetic fields, when the spin-state transition is complete, the ferroelectricity vanishes. The samples are robustly insulating with a loss tangent of < 105, thus ruling out artifacts related to conductivity. The ferroelectric polarization only shows a small voltage dependence (<1% change by 100 V), which rules out artifacts due to magnetostrictive capacitance changes. There is a significant difference between our millisecond pulsed and the continuous field data – the phase diagram shifts to higher fields at higher speeds. This is consistent with the expected millisecond to microsecond dynamics of the magnetic field-induced structural phase transition. The theoretical phase diagram shown for comparison based on a four-state Potts model is not a perfect match to the experimental data, but captures the main result of magnetic field-induced ferroelectricity at the spin-state transition at the right temperature and fields. Details of the phase diagram observed in experiments will require a more detailed understanding of the elastic interactions that mediate the cooperativity of the phase transition via ab-initio calculations and synchrotron X-ray measurements, and is the subject of future work.

Metal-organic frameworks – ferroelectricity and magnetism

Moving on to our second main result, we demonstrate magnetically-controlled ferroelectricity in Mn(HCOO)3-(CH3)2NH2 (Mn-MOF). [12,25] This compound is a metal-organic framework shown in Figure 4a, where Mn ions are bonded into a perovskite structure by (HCOO)3 linkers, and the electrically polar (CH3)2NH2 reside in the pores of the structure. We demonstrate that the polar molecules order ferroelectrically below 180 K with ferroelectric domains. Moreover, a magnetic field up to 14 Tesla can modify the size of the electric polarization by up to 40%. We speculate that magnetostriction of the soft Mn(HCOO3) framework in a magnetic field in turn changes the size of the cavity in which the electrically polar (CH3)2NH2 molecule resides and therefore its electric properties. We calculate the ferroelectric properties using ab-initio approaches. The experimental results are shown in Figure 4 where panel b shows a picture of the ferroelectric domains collected by optical second harmonic generation and panels c and d show the electric polarization controlled by electric and magnetic fields. This result demonstrates that polar guest molecules can exhibit ferroelectricity and magnetoelectric coupling. Thus we find another non-traditional route to creating and coupling ferroelectricity and magnetism in

metal-organic materials. This result is in press with Nature Quantum Materials.

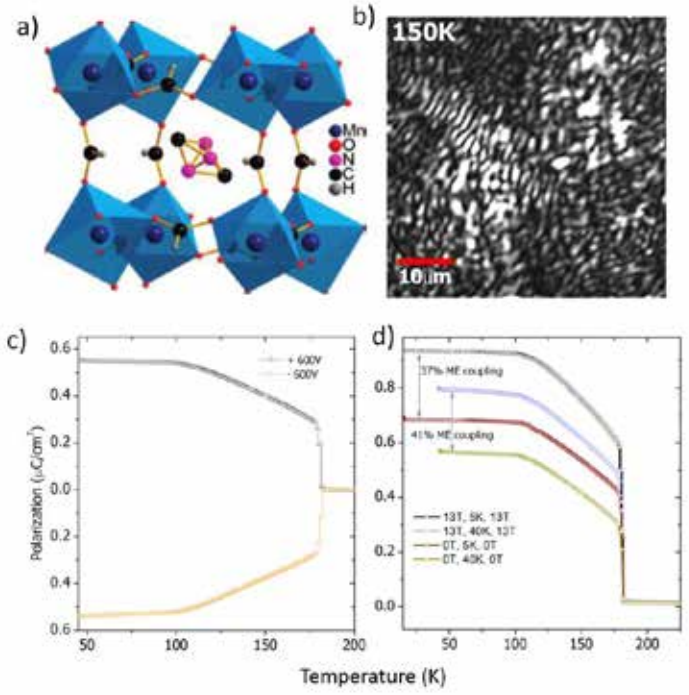

Figure 4. a) Crystal structure of Mn-MOF where Mn(HCOO-) forms the cubic framework, and electrically polar (CH)NHocupies the pore. All three possible rotational positions of the (CH)NH molecule are pictured simultaneously. b) Ferroelectric domains at 150 K collected using optical second harmonic generation. c) Spontaneous electric polarization across the 180 K phase transition measured by first applying an electric voltages while cooling through 180 K and then removing the voltage and measuring electric polarization on warming. d) Magnetic field effect on the electric polarization. [25]

In another similar compound, Co(HCOO)3-(CH3)NH3 [40], we demonstrate that at low temperatures, a complex magnetic ordering of the Co spins breaks the necessary spatial-inversion symmetry to allow for ferroelectricity. Thus magnetic ordering-induced ferroelectricity is demonstrated for the first time in this class of compounds. This result in published in the Journal of the American Chemical Society. [40]

Other work

We have also published or contributed significantly to work on frustrated magnetic configurations [26-32] for creating ferroelectricity and magnetoelectric couplings [33-37] in both inorganic and metal-organic compounds.

Finally we attempted several new metal-organic structures. A recent report of hysteretic spin crossover at high temperature [41] prompted our interest in the compound shown in Figure 5. As the bridging trizaole ligand (L) is anionic, it allows for the formation of a neutral molecule instead of a salt. The caveat of this is that the original complex is synthesized from Fe(ClO4)2, which results in the formation of dimethylammonium perchlorate as a byproduct. Organic perchlorates are potential explosive hazard, making the published route undesirable. This is especially true because all of the products are colorless and thus difficult to distinguish visually. Attempts to use other Fe2+ precursors such as Fe(SO4), FeX2 (X = halide), and Fe(OTf)2 (OTf = trifluoromethanesulfonate) under a variety of experimental conditions did not reproduce this complex. The original authors note that the trimer is insoluble once formed, so there must be some other species present in solution before trimer formation. In that case, it may be that a change in anion is affecting solubility or directing higher oligomer formation. This synthesis route towards metal-organic structures with potentially above room temperature magnetic and electric functionality is a future direction.

Impact on National Missions

Materials by design, nanostructured materials, multifunctional materials, and energy-saving materials are all themes reflected in the LANL Materials Strategy as well as BES National Needs. Magnetoelectric materials have the potential to revolutionize sensing and computing by vastly reducing the energy consumption utilizing electric voltages instead of electric currents to control and sense magnetic spins. This accelerating area of research is a new take on the traditional field of spintronics. The need for multifunctional materials that can be rationally designed is also the focus of the 2011 Materials Genome Initiative [42] and is called out in several BES Basic Research Needs reports including the "Basic Research Needs for Electrical Energy Storage," "From Quanta to the Continuum: Opportunities for Mesoscale Science," and most especially in "Directing Matter and Energy: Five Challenges for Science and the Imagination," [43]. Our results open a new class of materials – metal-organics – to the rational design of coupled magnetic and ferroelectric properties not just at very low temperatures but up to room temperature.

References

1. Coblenz, W. S., and S. A. Wartenberg. The DARPA HUMS program: revolutionizing magnetic field sensors using multiferroic materials and atomic gas vapor cells. 2012. Unattended Ground, Sea, and Air Sensor Technologies and Applications XIV.

2. Fiebig, M., and N. A. Spaldin. Current trends of the magnetoelectric effect. 2009. European Journal of Physics B. 71: 293.

3. Eerenstein, W., N. D. Mathur, and J. F. Scott. Multiferroic and magnetoelectric materials. 2006. Nature. 442:

05023.

4. Chen, , S. M. Gillette, Fitchorov, Jiang, Hao, Li, Gao, Geiler, Vittoria, and V. G. Harris. Quasi-one-dimensional miniature multiferroic magnetic field sensor with high sensitivity at zero bias field. 2011. APPLIED PHYSICS LETTERS. 99 (4).

5. Sun, N. X., and G. Srinivasan. Voltage control of magnetism in multiferroic heterostructures and devices. 2012. SPIN . 2: 1240004.

6. Cheong, , and Mostovoy. Multiferroics: a magnetic twist for ferroelectricity. 2007. NATURE MATERIALS. 6 (1): 13.

7. Yaghi, O. M., M. O'Keeffe, N. W. Ockwig, H. K. Chae, M. Eddaoudi, and J. Kim. Reticular synthesis and the design of new materials. 2003. NATURE. 423 (6941): 705.

8. Real, J. A., A. B. Gaspar, and M. C. Munoz. Thermal, pressure and light switchable spin-crossover materials. 2005. DALTON TRANSACTIONS. (12): 2062.

9. Southon, P. D., Liu, E. A. Fellows, D. J. Price, G. J. Halder, K. W. Chapman, Moubaraki, K. S. Murray, Letard, and C. J. Kepert. Dynamic Interplay between Spin-Crossover and Host-Guest Function in a Nanoporous Metal-Organic Framework Material. 2009. JOURNAL OF THE AMERICAN CHEMICAL SOCIETY. 131 (31): 10998.

10. Stroppa, , Di Sante, Horiuchi, Tokura, Vanderbilt, and Picozzi. Polar distortions in hydrogen-bonded organic ferroelectrics. 2011. PHYSICAL REVIEW B. 84 (1).

11. Stroppa, A., P. Jain, P. Barone, M. Marsman, J. M. Perez-Mato, A. K. Cheetham, H. W. Kroto, and S. Picozzi. Electric Control of Magnetization and Interplay between Orbital Ordering and Ferroelectricity in a Multiferroic Metal–Organic Framework. 2011. Angewandte Chemie . 123: 5969.

12. Jain, , Ramachandran, R. J. Clark, H. D. Zhou, B. H. Toby, N. S. Dalal, H. W. Kroto, and A. K. Cheetham. Multiferroic Behavior Associated with an Order-Disorder Hydrogen Bonding Transition in Metal-Organic Frameworks (MOFs) with the Perovskite ABX(3) Architecture. 2009. JOURNAL OF THE AMERICAN CHEMICAL SOCIETY. 131 (38): 13625.

13. Zapf, V. S., Kenzelmann, Wolff-Fabris, Balakirev, and Chen. Magnetically induced electric polarization in an organometallic magnet. 2010. PHYSICAL REVIEW B. 82 (6).

14. Zapf, V. S., Sengupta, C. D. Batista, Nasreen, Wolff-Fabris, and Paduan-Filho. Magnetoelectric effects in an organometallic quantum magnet. 2011. PHYSICAL REVIEW B. 83 (14).

15. Zapf, V. S., Wolff-Fabris, Kenzelmann, Nasreen, Balakirev, Chen, and Paduan-Filho. Multiferroic behavior in organo-metallics. 2011. In INTERNATIONAL CONFERENCE ON STRONGLY CORRELATED ELECTRON SYSTEMS (SCES 2010). Vol. 273.

16. Altarawneh, M. M., G. -. Chern, Harrison, C. D. Batista, Uchida, Jaime, D. G. Rickel, S. A. Crooker, C. H. Mielke, J. B. Betts, J. F. Mitchell, and M. J. R. Hoch. Cascade of Magnetic Field Induced Spin Transitions in LaCoO3. 2012. PHYSICAL REVIEW LETTERS. 109 (3).

17. Khalyavin, D. D., D. N. Argyriou, Amann, A. A. Yaremchenko, and V. V. Kharton. Spin-state ordering and magnetic structures in the cobaltites YBaCo2O5+delta (delta=0.50 and 0.44). 2007. PHYSICAL REVIEW B. 75 (13).

18. Bousseksou, A., N. Negre, M. Goiran, L. Salmon, J. P. Tuchagues, M. L. Boilot, K. Boukheddaden, and F. Varret. Dynamic triggering of a spin-transition by a pulsed magnetic field. 2000. European Physics Journal B. 13: 451.

19. Guetlich, , A. B. Gaspar, and Garcia. Spin state switching in iron coordination compounds. 2013. BEILSTEIN JOURNAL OF ORGANIC CHEMISTRY. 9: 342.

20. Halder, G. J., C. J. Kepert, B. Moubaraki, K. S. Murray, and J. D. Cashion. Guest-dependent spin crossover in a nanoporous molecular framework material. 2002. SCIENCE. 298 (5599): 1762.

21. Letard, J. F., P. Guionneau, and L. Goux-Capes. Towards spin crossover applications. 2004. SPIN CROSSOVER IN TRANSITION METAL COMPOUNDS III. 235: 221.

22. Ohtani, R. y. o., K. o. Yoneda, Furukawa, N. a. o. Horike, Kitagawa, A. B. Gaspar, Carmen Munoz, J. A. Real, and Ohba. Precise Control and Consecutive Modulation of Spin Transition Temperature Using Chemical Migration in Porous Coordination Polymers. 2011. JOURNAL OF THE AMERICAN CHEMICAL SOCIETY. 133 (22): 8600.

23. Real, J. A., A. B. Gaspara, and M. Carmen Munoz. Thermal, pressure and light switchable spin-crossover materials. 2005. Dalton Transactions. 2062: 2062.

24. Varret, , Boukheddaden, Codjovi, and Goujon. Molecular Switchable Solids: towards photo-controlled magnetism. 2005. HYPERFINE INTERACTIONS. 165

(1-4): 37.

25. Jain, P., A. Stroppa, D. Nabok, A. Marino, A. Rubano, D. Paparo, M. Matsubara, H. Nakotte, M. Fiebig, S. Picozzi, E. S. Choi, A. K. Cheetham, C. Draxl, H. W. Kroto, N. S. Dalal, and V. S. Zapf. Multiferroicity in a perosvkite metal-organic framework: a combined experimental and theoretical study. To appear in Nature Quantum Materials.

26. Lin, , Hayami, and C. D. Batista. Magnetic Vortex Induced by Nonmagnetic Impurity in Frustrated Magnets. 2016. PHYSICAL REVIEW LETTERS. 116 (18).

27. Aczel, A. A., Li, V. O. Garlea, J. -. Yan, Weickert, V. S. Zapf, Movshovich, Jaime, P. J. Baker, Keppens, and Mandrus. Spin-liquid ground state in the frustrated J(1)-J(2) zigzag chain system BaTb2O4. 2015. PHYSICAL REVIEW B. 92 (4).

28. Johnson, R. D., S. C. Williams, A. A. Haghighirad, Singleton, Zapf, Manuel, I. I. Mazin, Li, H. O. Jeschke, Valenti, and Coldea. Monoclinic crystal structure of alpha-RuCl3 and the zigzag antiferromagnetic ground state. 2015. PHYSICAL REVIEW B. 92 (23).

29. Koutroulakis, , Zhou, Kamiya, J. D. Thompson, H. D. Zhou, C. D. Batista, and S. E. Brown. Quantum phase diagram of the S=1/2 triangular-lattice antiferromagnet Ba3CoSb2O9. 2015. PHYSICAL REVIEW B. 91 (2).

30. Ma, J., Y. Kamiya, T. Hong, H. B. Cao, G. Ehlers, W. Tian, C. D. Batista, Z. L. Dun, H. D. Zhou, and M. Matsuda. Static and Dynamical Properties of the Spin-1/2 Equilateral Triangular-Lattice Antiferromagnet Ba3CoSb2O9. 2016. Physical Review Letters. 116: 087201.

31. Zapf, , Jaime, and C. D. Batista. Bose-Einstein condensation in quantum magnets. 2014. REVIEWS OF MODERN PHYSICS. 86 (2): 563.

32. Kamiya, , and C. D. Batista. Magnetic Vortex Crystals in Frustrated Mott Insulator. 2014. PHYSICAL REVIEW X. 4 (1).

33. Mun, , Weickert, Kim, B. L. Scott, C. F. Miclea, Movshovich, Wilcox, Manson, and V. S. Zapf. Partially disordered antiferromagnetism and multiferroic behavior in a frustrated Ising system CoCl2-2SC(NH2)(2). 2016. PHYSICAL REVIEW B. 93 (10).

34. Zhu, S., Y. Q. Li, and C. D. Batista. Spin-orbit coupling and electronic charge effects in Mott insulators . 2014. Physical Review B. 90: 195107.

35. Mun, E. D., J. Wilcox, J. L. Manson, B. Scott, P. Tobash, and V. S Zapf. The Origin and Coupling Mechanism of the Magnetoelectric Effect in TMCl2-4SC(NH2)2 (TM = Ni and Co). 2014. Advances in Condensed Matter Physics. 2014: 512621.

36. Mun, E. D., Chern, Pardo, Rivadulla, Sinclair, H. D. Zhou, V. S. Zapf, and C. D. Batista. Magnetic Field Induced Transition in Vanadium Spinels. 2014. PHYSICAL REVIEW LETTERS. 112 (1).

37. Lin, , Barros, Mun, Kim, Frontzek, Barilo, S. V. Shiryaev, V. S. Zapf, and C. D. Batista. Magnetic-field-induced phases in anisotropic triangular antiferromagnets: Application to CuCrO2. 2014. PHYSICAL REVIEW B. 89 (22).

38. Kimura, S., Y. Narumi, K. Kindo, M. Nakano, and G. Matsubayashi. Field-induced spin-crossover transition of [Mn-III(taa)] studied under pulsed magnetic fields. 2005. PHYSICAL REVIEW B. 72 (6).

39. SIM, P. G., and E. SINN. 1ST MANGANESE(III) SPIN CROSSOVER AND 1ST D4 CROSSOVER - COMMENT ON CYTOCHROME-OXIDASE. 1981. JOURNAL OF THE AMERICAN CHEMICAL SOCIETY. 103 (1): 241.

40. Gomez-Aguirre, L. C., B. Pato-Doldan, J. Mira, S. Castro-Garcia, M. A. Senaris-Rodriguez, M. Sanchez-Andujar, J. Singleton, and V. S. Zapf. Magnetic field-induced multiferroic behavior in [CH3NH3][Co(HCOO)3] Metal-Organic Framework. 2016. Journal of the American Chemical Society. 138: 1122.

41. Wang, , Liang, Yao, Zhai, and Fu. Tris[2-(pyrrol-2-ylmethyleneamino)-ethyl]amine. 2008. ACTA CRYSTALLOGRAPHICA SECTION E-STRUCTURE REPORTS ONLINE. 64: O629.

42. Materials Genome Initiative for Global Competitiveness. 2011. White House.

43. http://science.energy.gov/bes/news-and-resources/reports/basic-research-needs/. 2016. Basic Energy Sciences, Department of Energy.

Publications

Aczel, A. A., Li, V. O. Garlea, J. -. Yan, Weickert, V. S. Zapf, Movshovich, Jaime, P. J. Baker, Keppens, and Mandrus. Spin-liquid ground state in the frustrated J(1)-J(2) zigzag chain system BaTb2O4. 2015. PHYSICAL REVIEW B. 92 (4).

Gomez-Aguirre, L. C., B. Pato-Doldan, J. Mira, S. Castro-Garcia, M. A. Senaris-Rodriguez, M. Sanchez-Andujar, J. Singleton, and V. S. Zapf. Magnetic field-induced multiferroic behavior in [CH3NH3][Co(HCOO)3] Metal-

Organic Framework. 2016. Journal of the American Chemical Society. 138: 1122.

Jain, P., A. Stroppa, D. Nabok, A. Marino, A. Rubano, D. Paparo, M. Matsubara, H. Nakotte, M. Fiebig, S. Picozzi, E. S. Choi, A. K. Cheetham, C. Draxl, H. W. Kroto, N. S. Dalal, and V. S. Zapf. Multiferroicity in a perosvkite metal-organic framework: a combined experimental and theoretical study. To appear in Nature Quantum Materials.

Johnson, R. D., S. C. Williams, A. A. Haghighirad, Singleton, Zapf, Manuel, I. I. Mazin, Li, H. O. Jeschke, Valenti, and Coldea. Monoclinic crystal structure of alpha-RuCl3 and the zigzag antiferromagnetic ground state. 2015. PHYSICAL REVIEW B. 92 (23).

Kamiya, , and C. D. Batista. Magnetic Vortex Crystals in Frustrated Mott Insulator. 2014. PHYSICAL REVIEW X. 4 (1).

Koutroulakis, , Zhou, Kamiya, J. D. Thompson, H. D. Zhou, C. D. Batista, and S. E. Brown. Quantum phase diagram of the S=1/2 triangular-lattice antiferromagnet Ba3CoSb2O9. 2015. PHYSICAL REVIEW B. 91 (2).

Lin, , Barros, Mun, Kim, Frontzek, Barilo, S. V. Shiryaev, V. S. Zapf, and C. D. Batista. Magnetic-field-induced phases in anisotropic triangular antiferromagnets: Application to CuCrO2. 2014. PHYSICAL REVIEW B. 89 (22).

Lin, , Hayami, and C. D. Batista. Magnetic Vortex Induced by Nonmagnetic Impurity in Frustrated Magnets. 2016. PHYSICAL REVIEW LETTERS. 116 (18).

Ma, J., Y. Kamiya, T. Hong, H. B. Cao, G. Ehlers, W. Tian, C. D. Batista, Z. L. Dun, H. D. Zhou, and M. Matsuda. Static and Dynamical Properties of the Spin-1/2 Equilateral Triangular-Lattice Antiferromagnet Ba3CoSb2O9. 2016. Physical Review Letters. 116: 087201.

Mun, , Weickert, Kim, B. L. Scott, C. F. Miclea, Movshovich, Wilcox, Manson, and V. S. Zapf. Partially disordered antiferromagnetism and multiferroic behavior in a frustrated Ising system CoCl2-2SC(NH2)(2). 2016. PHYSICAL REVIEW B. 93 (10).

Mun, E. D., Chern, Pardo, Rivadulla, Sinclair, H. D. Zhou, V. S. Zapf, and C. D. Batista. Magnetic Field Induced Transition in Vanadium Spinels. 2014. PHYSICAL REVIEW LETTERS. 112 (1).

Mun, E. D., J. Wilcox, J. L. Manson, B. Scott, P. Tobash, and V. S Zapf. The Origin and Coupling Mechanism of the Magnetoelectric Effect in TMCl2-4SC(NH2)2 (TM = Ni and Co). 2014. Advances in Condensed Matter Physics. 2014: 512621.

Zapf, , Jaime, and C. D. Batista. Bose-Einstein condensation in quantum magnets. 2014. REVIEWS OF MODERN PHYSICS. 86 (2): 563.

Zhu, S., Y. Q. Li, and C. D. Batista. Spin-orbit coupling and electronic charge effects in Mott insulators . 2014. Physical Review B. 90: 195107.

Beyond the Chemical Reaction Zone: Detonation Product Gases in the Warm Dense Regime

Dana M. Dattelbaum
20140261ER

Abstract

Accurate thermodynamic descriptions of certain gases are important for understanding the detonation performance of high explosives. However, shock compression data often do not exist for molecular species in the dense gas phase, and are limited in the fluid phase. Ammonia (NH3) is a principal product gas resulting from explosives detonation, and the decomposition of other organic materials under shockwave loading (such as foams). Here, we present equation of state measurements of elevated initial density ammonia gas dynamically compressed in gas-gun driven plate impact experiments. Pressure and density of the shocked gases on the principal Hugoniot were determined from direct particle velocity and shock wave velocity measurements recorded using optical velocimetry (Photonic Doppler velocimetry (PDV) and VISAR (velocity interferometer system for any reflector)). Streak spectroscopy and 5-color pyrometry were further used to measure the emission from the shocked gases, from which the temperatures of the shocked gases were estimated. Up to 0.07 GPa, ammonia was not observed to ionize, with temperature remaining below 7000K. These results provide quantitative measurements of the Hugoniot locus for improving equations of state models of detonation products.

Background and Research Objectives

The most extreme states of matter accessible to experiment are those achievable by shock compression, a technique capable of dramatically raising pressure, temperature, and compression simultaneously. An understanding of material response under these conditions is essential to predictive simulation of weapons materials, the detonation of high explosives (HE), and to a variety of problems in planetary physics. Accurate thermodynamic description of atomic and molecular gases plays a central role in all of these contexts. Reactive flow modeling of HE detonation features prominently in a number of contexts central to the Lab's mission. The chemical reaction zone behind a detonation front comprises a dense fluid mixture of components such as N2, CO2, CO, CH4, and NH3, at densities ranging from 0.09 to 1.5 g/cm3. There is considerable overlap between the constituents of detonation product mixtures and those of planetary ices and atmospheres. Conditions relevant to planetary physics are often those of the warm dense matter (WDM) regime: too dense for weakly-coupled plasma models but too hot for standard condensed matter techniques. While these states are hotter and denser than those of the chemical reaction zone, multiple shocks may readily carry the product mixture through the WDM and into the dense plasma region: standard SESAME tables extend to T~10 keV and ρ0~106. Despite their vital importance in these contexts, however, molecular dissociation and ionization at elevated pressure and temperature are poorly characterized and constitute a significant source of potential error in our equations of state. To address these gaps, we will establish a synergistic experiment-theory-simulation effort focused on quantifying the P-V-T surfaces, and associated dissociation and ionization processes for the principal detonation product species: N2, CO2, CH4 and NH3.

Scientific Approach and Accomplishments

The objectives of the experimental effort are: 1) to quantitatively resolve the shocked states in detonation product species on the principal Hugoniot, and along a quasi-isentropic path to very high compression ratios and temperatures, and 2) to determine at what conditions dissociation and ionization (and possibly metallization) occur, and attempt to measure spectroscopic evidence of dissociation products.

Shock compression experiments

A series of dynamic compression experiments were performed on ammonia gas at 100 psi. These are the first experiments of their kind, as all prior experiments were on liquefied NH3. We measured the principle Hugoniot states of ammonia gas at 100 psi and 20 °C (0.0048 g/cm3) at several impactor velocities from 1 km/s to 4.3

km/s on the large bore two-stage gas gun. Figure 1 shows the experimental configuration for shocking elevated pressure gases, and the measured particle velocity profiles for shot 2S-811 with an impactor velocity of 3.5 km/s. The shock wave breakout at the Al drive plate/NH3 gas interface was measured using photonic Doppler velocimetry (PDV) (shown in red) and the shock wave breakout at the NH3 gas/sapphire window interface was tracked using velocity-interferometry-for-any-reflector (VISAR) (shown in green). The initial shock states on the principle Hugoniot were determined from the particle velocity profiles and are plotted in Figure 2, along with literature data for shocked liquid ammonia. Our experimental results are listed in Table 1 (*Asymmetric shot configuration; effective projectile velocity listed).

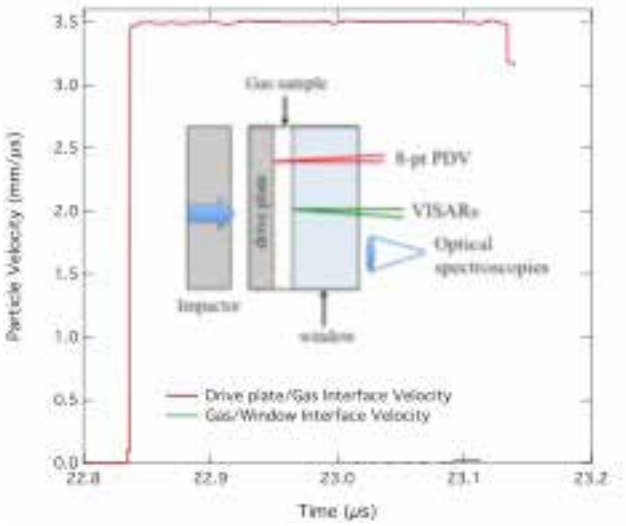

Figure 1. Experimental configuration and particle velocity profiles of shocked ammonia gas for shot 2S-811.

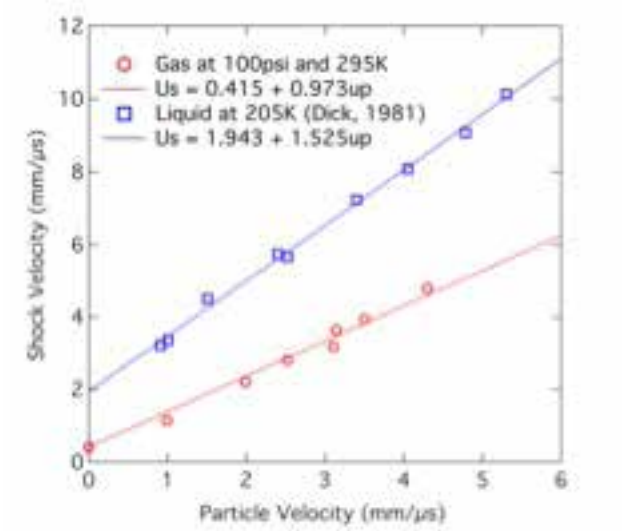

Figure 2. Shock velocity-particle velocity data for shocked gaseous ammonia (present work) and liquid ammonia (Ref. 1).

Shot No.	Projectile Velocity (mm/μs)	Particle Velocity (mm/μs)	Shock Velocity (mm/μs)	Pressure (GPa)	Density (g/cm³)	Temperature (K)
1S-1615	0.996	0.995	1.146	0.0054	0.0365	2200
2S-854	1.986	1.990	2.204	0.0213	0.0500	3700
2S-818	2.527	2.522	2.806	0.0341	0.0481	4600
2S-814	3.099	3.106	3.187	0.0486	0.1725	5650
2S-950	3.144	3.140	3.639	0.0544	0.0347	5200
2S-811	3.480	3.502	3.930	0.0665	0.0420	6800
2S-848 *	4.305 *	4.298	4.792	0.0988	0.0465	7590

*Table 1. Experimental results. *Asymmetric shot configuration; effective projectile velocity listed.*

Time- and wavelength-resolved emission and 4- or 5-color high-speed pyrometry measurements were performed for each of the shocked ammonia gas experiments. The streaked emission results from three of these experiments (1S-1615, 1 km/s; 2S-818, 2.5 km/s; 2S-950, 3.1 km/s) are shown in Figure 3. In all seven experiments, we observed unstructured (continuum) emission from the shocked ammonia gas.

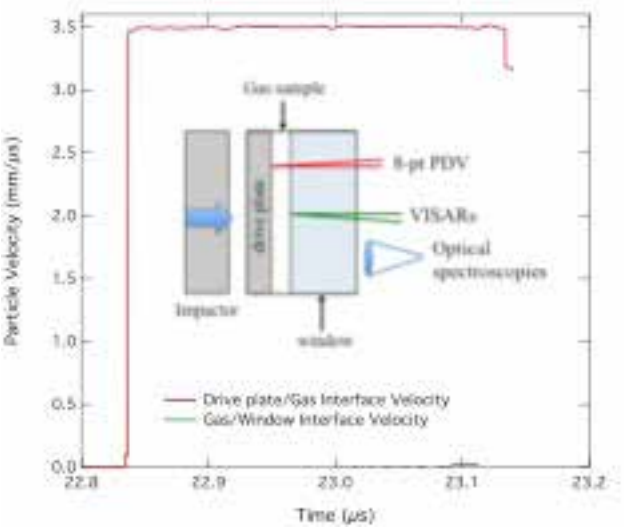

Figure 3. Time- and wavelength-resolved emission from shocked ammonia gas. (top) 1S-1615, 1 km/s, 250-590 nm; (middle) 2S-818, 2.5 km/s, 420-770 nm; (bottom) 2S-950, 3.1 km/s, 250-590 nm.

The temperature of the shocked ammonia gas was estimated using a pyrometry setup consisting of band pass-filtered high speed silicon photodiodes that monitored emission at four or five emission bands positioned between 290-750 nm. The pyrometry results from the first experiment (2S-811, 3.5 km/s) are shown in Figure 4. We did not see emission from the ammonia at the initial shock breakout into the gas (22.7 μs). The emission came at the first reflection of the shock from the sapphire window (23.1 μs). Assuming that the shocked gas emits as a blackbody (emissivity = 1), the peak gas temperature obtained from the peak radi-

ances measured at 488, 625 and 740 nm was in the range of 6750-6860 K. This is ~ 50% of the temperature in Argon at similar shock conditions.

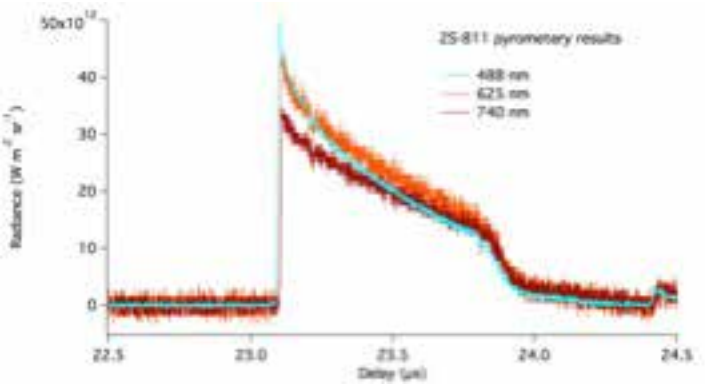

Figure 4. Pyrometery results from shocked ammonia gas from shot 2S-811.

The measured temperatures were compared to values calculated in hydrodynamic simulation using a legacy SESAME table and the PAGOSA hydrodynamic code. Calculated temperatures were systematically lower than the experimental measurements. From the data, we also determined that ammonia does not ionize on first shock.

Theoretical modeling of ammonia

The purpose of the theory work is twofold. First, we want to recover the phenomenological signatures (discontinuous variations in compressibility, for instance) seen in experiment. This gives us confidence that our methodology is sound. But then theory can provide something that experiment can't: a microscopic rationale for macroscopic features. In our case, we want to identify the conditions at which molecules dissociate and/or ionize, so that we can distill from these patterns simplified physics models. In order to do this, we wish to sample configuration and chemical space using atomistic simulation. The standard way to do this with high fidelity is ab initio molecular dynamics (AIMD). The difficulty with AIMD in this context is that it is both deterministic and computationally expensive. But depending on the thermodynamic state, making and breaking chemical bonds can be a rare event on atomistic timescales. At sufficiently high temperatures and densities, it will generate the correct equilibrium chemical composition because the system has enough thermal energy to surmount reaction barriers. However, it is difficult to know a priori at what temperatures and densities this will be the case. In order to redress this issue we have been developing tools for performing (for the first time) ab initio reactive Monte Carlo (AIRMC). We have been testing on ammonia, which undergoes the following reactions at various conditions:

$2NH_3 \rightarrow N_2 + 3H_2$

$N_2 \rightarrow 2N$

$H_2 \rightarrow 2H$

$NH_3 \rightarrow N + 3H$

The importance of each reaction can be estimated by calculating the chemical equilibrium constants from the quantum molecular partition functions. Ab initio reactive Monte Carlo (AIRxMC) solves tackles the rare event problem by adding to the standard set of Monte Carlo moves an additional move type in which chemical reactions are attempted. Thus, it efficiently samples both configurational and chemical space. A sample of the AIRxMC results for NH3 including reaction (a) are shown in Figure 5. The temperature is 4000 K and density is 0.75 g/cc (near that of the liquid density). Notice the relatively fast sampling of chemical space during the simulation. We also performed an AIMD run under the same conditions for comparison, and found that even 100 ps of simulation time (which takes approximately one month of supercomputer time to simulate) is insufficient to properly sample chemical space.

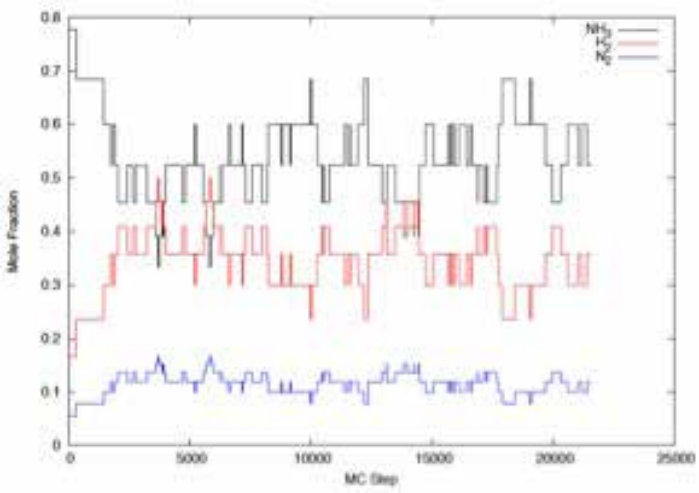

Figure 5. AIRxMC results for NH including reaction. The temperature is 4000K and density is 0.75 g/cc (near that of the liquid).

Impact on National Missions

This experimental-theoretical project provides critical and foundational data and models for improved confidence in weapons simulations. The outcome of the research has enabled development of experimental and theoretical tools for improvements in the treatment of detonation product gases. The results of this project are relevant to the NNSA Science Program and weapons assessments. In addition, the fundamental data obtained is relevant to planetary physics, and definitions of the conditions of the large gas

giant planets.

References

1. Dick, R.. Shock compression data for liquids. III. Substituted methane compounds, ethylene glycol, glycerol, and ammonia . 1981. Journal of Chemical Physics. 74: 4053.

Publications

Gibson, L. L., B. D. Bartram, D. M. Dattelbaum, J. M. Lang, and J. S. Morris. A gas-loading system for LANL two-stage gas guns. 2015. In Shock Compression of Condensed Mater - 2015. (Tampa, FL, 14-19 June 2015). , p. 0. Tampa, FL: AIP Proceedings.

Goodwin, P. M., B. R. Marshall, R. L. Gustavsen, J. M. Lang, A. H. Pacheco, E. N. Loomis, and D. M. Dattelbaum. Fiber-interferometric detection of gun-launched projectiles. 2015. In Shock Compression of Condensed Matter - 2015. (Tampa, FL, 14-19 June 2015). , p. 0. Tampa, FL: AIP Proceedings.

Topological Kondo Insulators

Joe D. Thompson
20140271ER

Abstract

The goal of this project has been to test a theoretical prediction that electronic correlations produce an electronic structure such that a material can be simultaneously a metal at its surface but an insulator in its bulk. This entirely new state of matter is a consequence of electrons' topology, and the material is termed a topological Kondo insulator. An essential prediction of theory is that topology protects the metallic surface state, that is, the surface remains metallic in the presence of defects. By irradiation damaging the surface of proposed topological Kondo insulators, we have shown for the first time that the concept of topological protection is robust and, moreover, that the response of a surface to irradiation damage can discriminate between proposed and real topological states.

Background and Research Objectives

Until recently, materials were classified generically as a metal, semimetal, semiconductor or insulator, the distinction being that the first two have no energy gap between conduction and valence bands and the latter two have a gap. As a result of their electronic structures, metals and semimetals have a finite electrical resistance, but the resistance of semiconductors and insulators is, in principle, infinite in the limit of very low temperatures. This historical classification of materials changed with the theoretical prediction in 2007 that, due to the topology of a material's electronic structure, a material could be simultaneously an insulator in its interior but a metal on its surface. [1] If such a topological insulator (TI) existed, it would represent an entirely new state of matter. The first experimental realizations of some of the theoretical predictions soon followed [2], and the theoretical and experimental study of topological insulators exploded, growing from about 30 publications per year in 2008 to over 1600 per year in 2015.[3] Though the theory itself is mathematically difficult, the conditions for a material to be a topological insulator are relatively straightforward to obtain from electronic structure calculations, which is why, in part, the field grew so rapidly. A drawback, however, was that materials predicted to be TI's tended be poor bulk insulators, which made comparison to theory questionable. Materials with strong electronic correlations, and, consequently whose electronic properties are more difficult to calculate, have much better insulating properties and are more directly comparable to theory. Basic ingredients of this theory are described below, but it is useful to begin with a simple discussion of topology.

A ball of play-doh can be deformed continuously into the shape of a cup, but it is not possible to form a donut without punching a hole in the ball. In terms of topology, the ball and cup have the same topology, but the donut is distinct—the topology of the donut is 'protected' from ever becoming a cup. Similarly, adding charge carriers to an insulator can continuously transform a bulk insulator into a bulk metal, and in this sense there is no change in electronic topology. It is not possible, however, to have a material with an insulating interior and a metallic (more precisely an electronically gapless) surface without changing the topology of electrons' wavefunctions, that is, topologically the metallic surface is protected by quantum mechanics from ever becoming an insulator. In the language of topology, the topological index of this material must be -1; whereas, the index for a conventional insulator is +1. This index of a material can be determined simply by counting the number of times electronic bands of even and odd parities cross the Fermi energy at high symmetry points of their momentum. [4]

Electronically correlated materials, such as SmB6 and Ce3Bi4Pt3, are ideal candidates to be topological insulators. In these materials, the Sm- or Ce-derived f-electrons, which have odd parity, hybridize with d-electrons (with even parity). This hybridization, generically called the Kondo effect due to strong correlations in these materials, creates a gap near the Fermi energy in the mo-

mentum-dependent energy band structure of the hybridized electrons. This is illustrated schematically in Figure 1. If the electron count in the material is such that the lower hybridized band is exactly filled, the material is a Kondo-derived insulator (for example, SmB6 and Ce3Bi4Pt3). The electronic structure in a real 3-dimensional material is far more complex than illustrated in Figure 1, particularly because quantum mechanics requires that bands with opposite parity cannot hybridize at high symmetry points, and this is what necessitates hybridized bands of opposite parity crossing the Fermi energy at those points. These band crossings are responsible for a metallic surface state. From their modelling of the electronic structure, Dzero and coworkers [5] argued that the topological index of SmB6 is -1, i.e., SmB6 should be a topological Kondo insulator (TKI). Later calculations on Ce3Bi4Pt3 suggested that it also should be a TKI.[6] Since those predictions, a large number of different kinds of experiments have found evidence for a metallic surface, typically but not always, supporting the calculated electron structure of SmB6 and suggesting that it is a TKI.[7] Because the interpretation of these experiments could be misguided due to the known peculiar surface chemistry of SmB6 and the possibility of impurity states in the Kondo-insulating gap, a more definitive test of theory would be to determine if the metallic surface state is protected. This has been the primary objective of our project.

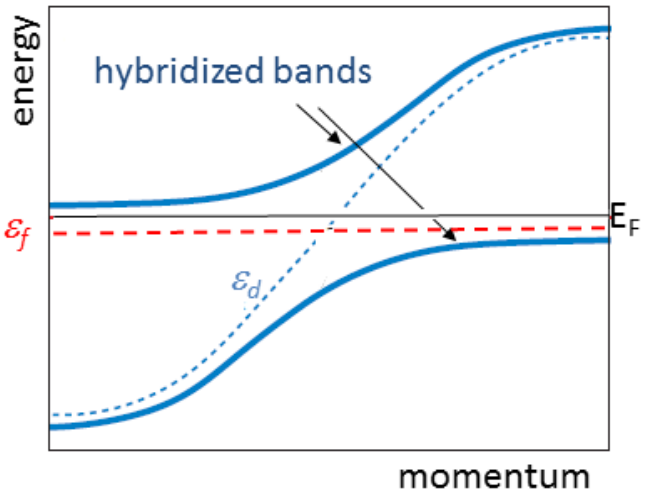

Figure 1. Schematic energy versus momentum electronic structure resulting from hybridization of a single bare (unhybridized) f-electron band with energy ε with a single bare band of d-electrons with energy ε. The hybridized bands have d-character at small (lower band) and large (upper band) momenta, but f-character at small (upper band) and large (lower band) momenta. If the lower hybridized band is filled with electrons and the upper band is empty, the material is a Kondo insulator. In this highly simplified illustration, the f- and d-bands cross below the Fermi energy E; however, in a real material, the combination of electronic correlations and quantum mechanics causes the hybridized bands with different parities to cross E at particular values of momentum. If the product of the number of crossing is odd, the KI is a topological KI.

Scientific Approach and Accomplishments

We have studied the transport and thermodynamics properties of single crystals of SmB6 and, to a lesser extent, Ce3Bi4Pt3 by electric resistivity, Hall effect, thermoelectric power, thermal conductivity, magnetic susceptibility and specific heat measurements, typically over a temperature range from about 1 to 300 K and in some cases as a function of applied pressure and magnetic field. This rather broad set of experiments was necessary to characterize the purity and electronic nature of the materials but most importantly to provide a foundation for interpreting the effect of heavy-ion irradiation of the surface of these crystals.

Chemical substitution is a common way to introduce defects into the bulk of a crystal and possibly affect a potentially protected metallic surface state. In contrast to chemical substitutions, which also modify hybridization as well as induce impurity states in the Kondo-derived energy gap, heavy-ion irradiation can be controlled to produce a desired number of defects within a specified depth from the surface of the crystal. For these experiments, we irradiated the surface with non-magnetic argon/xenon (Ar+/Xe+) and magnetic iron (Fe+) ions using capabilities of the Los Alamos Ion Beam Materials Laboratory. If a metallic state in SmB6 and Ce3Bi4Pt3 were due to topology, it should be protected against surface defects produced by irradiation with non-magnetic ions; however, introducing magnetic ions at the surface, like an applied magnetic field, should destroy a topologically protected metallic surface because they break time-reversal symmetry of the electronic wavefunctions.[4,7] A condition for topological protection is that the electrons' wavefunctions preserve time-reversal symmetry, i.e., an electron with spin 'up' moving with momentum +k must be equivalent to an electron with spin 'down' moving with momentum –k.

To test the theoretical prediction of topological protection, we could have chosen to study Bi2Se3, which is one of the first examples in which evidence for a topological metallic surface was discovered.[2] It, however, like similar materials being studied by others, is not electronically correlated and is highly susceptible to complications due to intrinsic disorder. The effect of this disorder is reflected in its temperature-dependent resistance [8] that is plotted in Figure 2 along with the resistance of SmB6 and Ce3Bi4Pt3. As seen in this figure, the much larger increase in resistance with decreasing temperature for SmB6 and Ce3Bi4Pt3reflects the robustness of their bulk semiconducting energy gap that is derived from electronic correlations

and the relative absence of substantial extrinsic disorder, both of which are important for a more straightforward interpretation of the consequences of ion-irradiation. The temperature-dependent resistance of SmB6 and Ce3Bi4Pt3 can be modelled simply as two resistors in parallel, one producing a thermally activated temperature dependence due to their bulk semiconducting energy gap and the other being a metallic resistor.

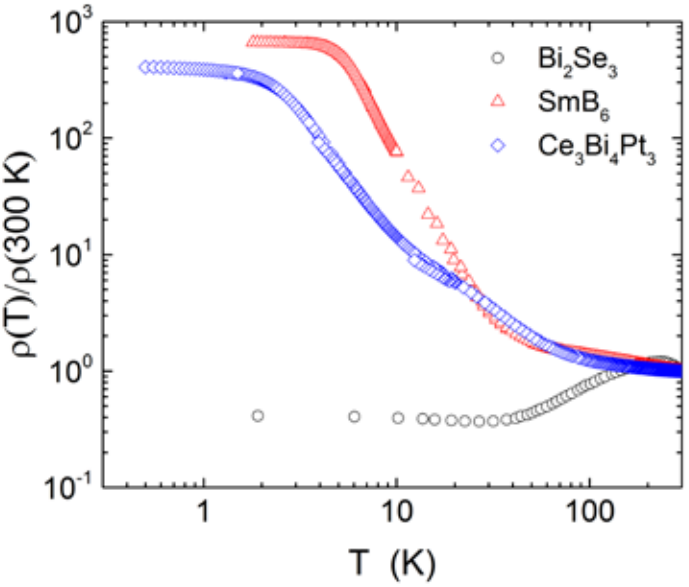

Figure 2. Comparison of the temperature dependence of the resistance of BiSe, SmB and CeBiPt. In this comparison, the sample's resistance is normalized by its value at room temperature. Data for BiSe are taken from [8]. The bulk energy gap of BiSe is about 0.3 eV (about 3000K), and, consequently, the resistance of BiSe should be orders of magnitude larger at low temperatures if there were no extrinsic disorder. The approach to a nearly constant resistance of SmB and CeBiPt at low temperatures could be due to the presence of a topologically protected metallic surface state or to impurity states in their Kondo-derived energy gap, which is about two orders of magnitude small than the gap in BiSe.

Theoretically, the thickness of a topological metallic surface is proportional to the velocity of those metallic electrons divided by the magnitude of the insulating energy gap of the sample's interior. This relationship allows an estimate of the surface state's thickness in SmB6 of roughly 10 to about 100 nm, where the variation comes primarily from different techniques used to determine the electrons' velocity. By controlling the acceleration energy of heavy-ions, their fluence, and exposure time of the sample to the heavy-ion beam, we systematically varied the depth of irradiation-induced damage from 13 to approximately 450 nm as well as changed the amount of damage in decadal steps from 10-3 to 1 DPA. At 1 displacement per atom (DPA), each atom in the irradiated area has been displaced on average once from its original structural site, and, consequently, the crystal structure in that area becomes effectively amorphous.

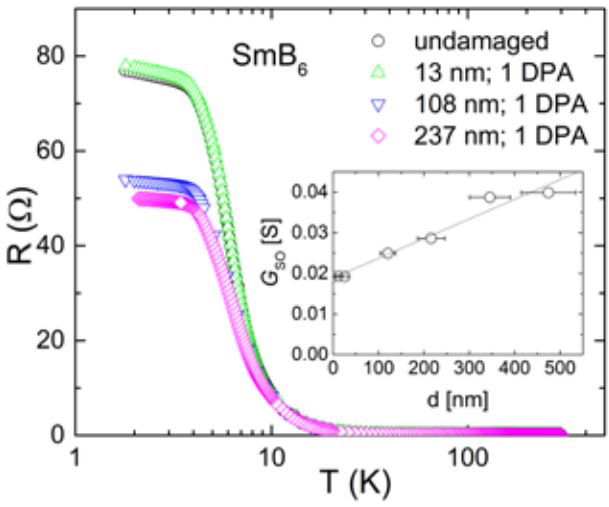

Figure 3. Temperature dependence of the resistance R of a representative SmB crystal damaged to the indicated depth on each of its plate-like faces. Additional curves were measured as each side of the crystal was damaged and at different depths of damage. The crystal's total thickness is 35 μm, approximately 70 times greater than the sum of damage-layer thickness d. The damage, produced by Ar/Xe irradiation, is fixed at 1 DPA in this example. The inset is a plot of the residual surface conductance as a function of damage depth d. Error bars on the values of d denote statistical error associated with uncertainty in the depth of damage.

Representative data from which we draw the primary conclusions for this project are plotted in Figure 3. These data show that the resistance at temperatures above about 10 K is not affected by the irradiation, consistent with damage being restricted to the surface and having no influence on the magnitude of the bulk insulating gap. In contrast, irradiation induces noticeable changes in the resistance at low temperatures, which is dominated by the metallic surface state. To interpret changes in the low-temperature resistance R0, it is useful to convert it to a residual sheet resistance Rso (equal to R0 multiplied by measured geometrical factors). As seen in the inset of Figure 3, the residual sheet conductance Gs0=1/Rso increases linearly with increasing depth of irradiation damage, i.e., Gs0 can be described as a parallel resistance Gs0=1/Rss +d/2ρDL where RSS is the residual sheet resistance of undamaged SmB6, d is the depth of damage and the fitting parameter ρDL is the resistivity of the damaged layer. If the metallic surface were not protected, Gs0(d) would have to be a non-linear function of d such that Gs0(d) at large values of d would be independent of 1/Rss, but our experiments show that this is not the case. Instead, the linearity of Gs0(d) with a finite d=0 value of 1/Rss strongly indicates that a metallic surface

with a residual sheet resistance of undamaged SmB6 is always present, even with substantial surface damage. That is, the metallic surface is protected. On this sample, the slope of Gs0(d) gives a value for ρDL = 1.0 ± 0.2 mΩcm, and from similar measurements on other crystals, we find an average value of (ρDL) = 1.7 ± 0.4 mΩcm. This average value agrees well with the resistivity (1.5 mΩcm) of SmB6 that was severely damaged throughout its bulk by sufficient neutron irradiation to make it amorphous.[9]

The obvious conclusion from these observations is that the metallic surface state of SmB6 reconstructs under the heavily damaged (effectively amorphous) surface. Figure 4 is a cartoon of this interpretation that follows straightforwardly from the experimental results of Figure 3 and the theory of topological insulators, namely that the metallic surface is protected from disorder as a consequence of the special topological electronic structure of the insulator that we have not changed by irradiating the surface with heavy ions.

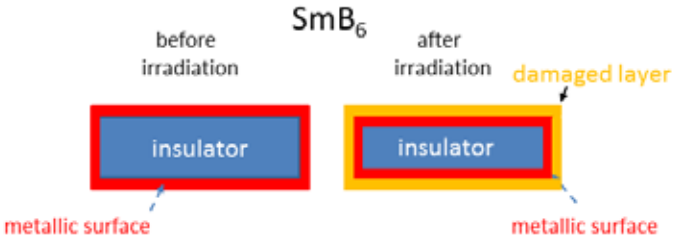

Figure 4. Schematic cross-sectional view of SmB, illustrating on the left that the bulk is an insulator and the surface is a metallic state. Rectangles in this illustration are not to scale. Crystals are typically 30 to 50 µm-thick by 300-500 µm-long; whereas, the metallic surface layer is of order 10-100 nm thick. After damaging to 1 DPA to a depth of order the thickness of the metallic surface layer, the metallic surface reconstructs under the damaged layer, as illustrated in the right-hand figure. In model calculations discussed in the text, we have taken the resistance of the insulating bulk to be infinite and have ignored the metallic contribution to the resistance coming from damaged and reconstructed areas at the sample's ends. We estimate that these approximations could introduce up to 30-40% error is determining the absolute value of resistivity of the damaged layer, which does not affect our primary conclusion.

This principal conclusion of our project was a surprise. We had expected that the metallic surface might survive small amounts of damage and above some damage threshold that it would collapse. To further test our main conclusion, we studied the effects of small (10-3 DPA) and intermediated (10-2 to 10-1 DPA) surface damage and found that the metallic surface state never collapsed with increased damage. Even more surprising was that irradiation with magnetic Fe+ ions produced the same response as that found with non-magnetic irradiation. As mentioned earlier, magnetic ions should break time-reversal symmetry of electrons' wavefunctions and destroy the metallic surface state. Instead, our experiments show that the metallic state again reconstructs under a strongly damaged surface layer. These results have broad implications for potential technological applications of topological insulators because they show that heterostructured devices can be built to take advantage of the special electronic properties of topologically protected states.

The Kondo insulator Ce3Bi4Pt3 also is predicted to be a topological KI,[6] but this possibility has been explored relatively little. Like SmB6, the low-temperature resistance of Ce3Bi4Pt3 is dominated by a metallic conduction path that shunts the continued increase of resistance due the underlying insulator state. By systematically irradiating the surface of Ce3Bi4Pt3 with increasing doses of Ar+ to produce damage ranging from 10-3 to 1 DPA, we found that the low-temperature resistance decreases monotonically with increasing dose and has no detectable effect of the insulating gap. Superficially, this response to heavy-ion damage is not so different from what we found in SmB6; however, the residual sheet conductance of Ce3Bi4Pt3 does not follow the simple relationship found for SmB6 (Figure 3 inset), suggesting that the 'metallic resistor' in Ce3Bi4Pt3 may not come from a topologically protected metallic surface state.

To test this suggestion, we measured the Hall resistivity at two thicknesses of an unirradiated but wedge-shaped single crystal of Ce3Bi4Pt3 at low temperatures where the metallic component of resistance dominates. If metallic conduction were due to a surface state, the Hall resistance should be proportional to thickness of the crystal at which the measurements are made. That is, the ratio of Hall resistances at two different sample thicknesses should be 1. In contrast, if metallic conduction originated from the bulk of the crystal, the Hall resistance should be independent of the thickness, and the ratio of Hall resistances should equal the ratio of the two thicknesses at which measurements are made. Results of our measurements are summarized in Figure 5 and compared to published results [10] on SmB6. As this figure shows, the ratio of Hall resistances in a single crystal of Ce3Bi4Pt3 at thicknesses of 590 and 175 µm scales well with the ratio of the crystal's thickness, consistent with a metallic conduction mechanism in the bulk of the crystal and not at its surface. These results stand in contrast with those on SmB6 where the Hall resistance ratio approaches 1 at the lowest temperatures, which is strong evidence for a surface metallic state. We conclude from these and the irradiation experiments that Ce3Bi4Pt3 is a Kondo insulator but is not a topological KI and that the metallic contribution that dominates its low-

temperature resistance likely is due to electronic impurity states in the bulk insulating gap that persist to the surface of Ce3Bi4Pt3.

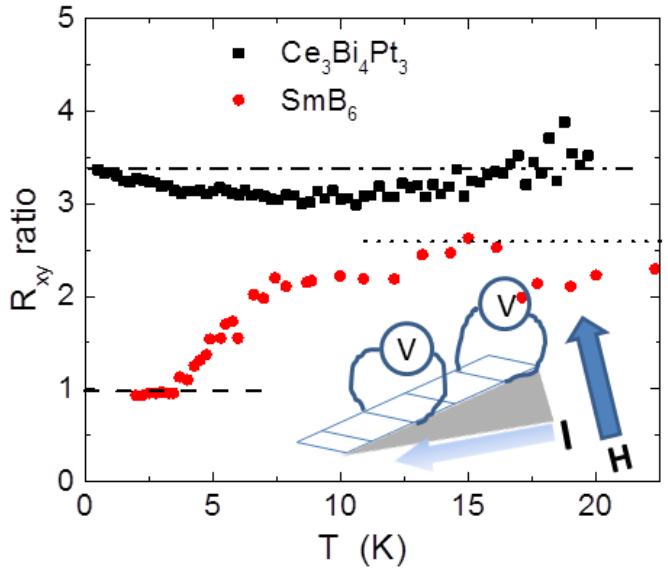

Figure 5. Temperature dependence of the ratio of Hall resistances R measured on a single crystal of wedge-shaped CeBiPt at points where its thickness is 590 and 175 µm. An illustration of the measuring geometry is shown at the lower right of this figure. The Hall resistance is determined by the transverse voltage V developed when a magnetic field H and current I are applied perpendicular to the voltage tabs. The upper dash-dotted line represents the ratio of sample thicknesses (590 µm/175 µm) at which the Hall resistance is determined. The data fall close to this line, indicating that electrical conduction is from the bulk of the crystal. Similar data, taken on a wedge-shaped crystal of SmB at thicknesses of 320 and 120 µm (whose ratio 2.7 is indicated by the dotted line), are shown for comparison. In the limit of low temperatures, the ratio of Hall resistances for SmB approaches 1, as expected for conduction by a metallic surface.[10]

Impact on National Missions

Since the idea of topological states in materials was introduced, a large number of technological applications of quantum topology has been envisioned, ranging from its use for quantum computing, dissipationless (or at least very low) energy transfer of information through interconnects in computing elements, creating plasmonic and spintonic circuits and low frequency photon detectors to discovering Majorana fermions, elementary particles that are their own antiparticles. Many of these energy- and defense-relevant uses of topological states, which rely on the presence of a protected metallic surface, are highlighted in a draft DOE/BES Basic Research Needs document on Quantum Materials for Energy Relevant Technology. This project has demonstrated that the topology-induced metallic surface state of SmB6 is protected from disorder, an important step in demonstrating that the potential of topological states can be exploited for technological applications.

References

1. Fu, L., C. I. Cane, and E. J. Mele. Topological insulators in three dimensions. 2007. Physical Review Letters. 98: 121306.

2. Hsieh, D., D. Qian, L. Wray, Y. Xia, Y. S. Hor, R. J. Cava, and M. Z. Hasan. A topological Dirac insulator in a quantum spin Hall phase. 2008. Nature. 452: 970.

3. Topological insulator. 2016. Web of Science.

4. Hasan, M. Z., and C. L. Kane. Colloquium: topological insulators. 2010. Reviews of Modern Physics. 82: 3045.

5. Dzero, M., K. Sun, P. Coleman, and V. Galitski. Theory of topological Kondo insulators. 2012. Physical Review B. 85: 045130.

6. Alexandrov, V., M. Dzero, and P. Coleman. Cubic topological Kondo insulators. 2013. Physical Review Letters. 111: 226403.

7. Dzero, M., J. Xia, V. Galitski, and P. Coleman. Topological Kondo insulators. 2016. Annual Reviews of Condensed Matter Physics. 7: 249.

8. Butch, N. P., K. Kirshenbaum, P. Sayers, A. B. Sushkov, G. S. Jenkins, H. D. Drew, and J. Paglione. Strong surface scattering in ultrahigh-mobility Bi2Se3 topological insulator crystals. 2010. Physical Review B. 81: 241301(R).

9. Larkin, A., Y. Akeshentsev, and B. Goshchitskii. Insulator-to-metal transition in SmB6 induced by neutron irradiation. 2007. Physics A. 460-462: 811.

10. Kim, D. J., S. Thomas, T. Grant, J. Botimer, Z. Fisk, and J. Xia. Surface Hall effect and nonlocal transport in SmB6: evidence for surface conduction. 2013. Scientific Reports. 3: 3150.

Publications

Wakeham, N., J. Wen, Y. Q. Wang, Z. Fisk, F. Ronning, and J. D. Thompson. The effect of magnetic and non-magnetic ion damage on the surface state of SmB6. 2016. Journal of Magnetism and Magnetic Materials. 400: 62.

Wakeham, N., P. F. S. Rosa, Y. Q. Wang, M. Kang, Z. Fisk, F. Ronning, and J. D. Thompson. Low-temperature conducting state in two candidate topological Kondo insulators: SmB6 and Ce3Bi4Pt3. 2016. Physical Review B . 94: 035127.

Wakeham, N., Y. Wang, Z. Fisk, F. Ronning, and J. D. Thompson. Surface state reconstruction in ion-damaged SmB6. 2015. Physical Review B. 91: 0851007.

Semiclassical Modeling of Non-adiabatic Processes in Molecular Materials

Dima V. Mozyrsky
20140293ER

Abstract

Prediction of the optical response and photo-induced processes of molecular systems is fundamental to a myriad of technological applications, ranging from sensing, imaging, solar energy harvesting, to optoelectronic devices. Theoretical modeling provides an understanding of the material's behavior, and could guide experimental efforts. The research objective of this project was to develop a novel quantum chemical methodology capable of modeling photo-induced dynamics and spectroscopic observables in the nano-sized molecular systems, and to apply these techniques to a number of materials particularly promising for energy technologies, to understand their emergent light-driven physicochemical behavior over multiple length and time scales. For this we have implemented the novel computational concept that was developed by our team and proved to be very accurate in several model problems. The method is based on a non-ad-hoc semi-classical description of the nuclei, which properly accounts for trajectory branching and phase correlations between nuclear paths, overcoming several critical deficiencies of existing methods. Our new algorithm is a controlled approximation (which can be systematically improved) with attractive computational scalability (invariant with respect to the number of vibrational degrees of freedom). This makes it particularly promising for applications to large molecular systems. The computational method developed here can be applied to several distinct classes of nanomaterials that are currently of intense interest for their promise in energy and (opto-)electronics technologies, such as conjugated dendrimers/macrocycles, polymer/fullerene blends used in solar cells, and biological light-harvesting systems. The acquired knowledge will allow for better analysis and interpretation of experimental data, understanding the photo-induced phenomena, and facilitating rational design of new materials with desired optical, light harvesting, energy and charge transfer properties.

Background and Research Objectives

Quantum chemistry has made enormous progress over the last several decades by enabling qualitative prediction of ground state properties of multi-atomic molecules thanks to the rapid development of efficient electronic structure methods. Now it faces a new challenge: It aims not only at evaluating the static properties (e.g. ground state) of molecular systems, but also at predicting the dynamics of such systems subjected to an external perturbation (i.e., chemical reactions). For example, when a molecule absorbs a photon, its electrons reach an unstable excited state, which leads to a non-equilibrium dynamics of coupled electrons and nuclei. As a result, the molecule can dissociate into several new species or it can undergo a certain conformational (i.e. geometrical) change or, end up in a long-living metastable state followed by a radiative (i.e. accompanied by an emission of a photon) decay into the ground state. All such outcomes can occur with a certain probabilities that can be deduced from the quantum mechanics, i.e., by solving (at least, in principle) the corresponding Schrodinger equation that governs such dynamics.

In reality, however, a direct solution via the Schrodinger equation is not feasible for multi-atomic molecules due to the exponential scaling of the computational complexity of the problem (and so the amount of needed computing resources) with the number of degrees of freedom, i.e. the number of atoms in the molecule. As a result one needs to resort to simplifying approximations that, typically, sacrifice accuracy and thus the predictive power for the sake of computational efficiency.

The main research goal of this project was to develop a computational approach that would provide sufficient accuracy without compromising computational efficiency; this balance was necessary to use the approach in large-scale simulations of photo-excited molecular dynamics. Such photo-excited dynamics involve electronic transitions between different electronic states and

therefore its mathematical description needs to account for various quantum mechanical effects related to the phase of the molecule's wave function (i.e., the so-called probability amplitude, whose absolute value squared describes probability for the molecule to be in a certain state). Proper accounting of the phase related effects, frequently termed as phase coherence effects, is critically important for a number of problems involving situations when the dynamics can propagate along several paths so that the "pieces" of the wave function associated with those paths interfere with each other. Such interference may significantly modify the probabilities of different outcomes (recall that since the probability is a square of the wave function, the cross terms corresponding to products of different pieces may significantly alter the result). Yet, in the most common approaches, such as mean field or the so-called surface hopping methods, the phase coherence effects are usually missed or treated incorrectly due to the ad-hoc nature of these methods.

In this project we have developed a systematic approach, derived from first principles and controlled by several physical parameters, that can properly account for the phase coherence effects and remain as computationally cost efficient as common approaches (e.g. mean field, surface hopping, etc.). Our method can be applied to a number of problems of molecular dynamics accompanied by electronic excitations/de-excitations. The method is expected to be particularly efficient when one is interested in such dynamics at relatively short times, i.e., at the femtosecond scale, which is the case for direct photo-dissociation of molecules.

Scientific Approach and Accomplishments

The method developed in this project is derived from the basic principles and is based on approximations consistent with semi-classical approximations, i.e., in the limit when the momentum of the nuclei is sufficiently high and the quantum uncertainty in their positions is sufficiently small. Under such an approximation and in the absence of electronic transitions the evolution of nuclei is classical (i.e. deterministic) and can be well described in terms of the Gaussian approximation, i.e., with a wave function of the nuclei being a Gaussian centered on its classical position. Electrons in a molecule cannot be described classically and therefore the semi-classical approximation needs to be significantly modified in order to account for the electronic transitions during the course of the dynamics. This program was carried out in Ref. [1], where the Gaussian approximation was extended to the situations involving inelastic transitions (i.e. accompanied by internal energy redistributions). It was shown that the wave function of systems that undergoes such transitions can be described as a superposition (i.e. sum) of Gaussian wave packets that arise as a result of coupling to the excited electronic states in the molecule. Furthermore in Ref. [1] we have proposed an algorithm that could simulate wave function by the Monte Carlo technique. In this approach, termed Semi-Classical Monte Carlo (SCMC) algorithm, the nuclei propagate under an assumption that electrons are in a certain state (ground or excited) and exert a certain force (on nuclei) that can be evaluated from electronic structure calculations. At the same time the electronic state can randomly change (with a probability prescribed by certain considerations based on quantum mechanics) and, afterwards, the dynamics continues with the assumption that electrons are in a new state. Similar stochastic dynamics is utilized in the surface hopping method, where probabilities are inferred from statistical averages of the simulation. In our approach such "hopping" trajectories were used to sample the wave function represented as a superposition of Gaussian wave packets, each associated with its trajectory. In other words, in Ref. [1] quantum trajectories are used to sample not probabilities, but rather the probability amplitude, which allows one to more accurately account for the phase coherence effects. This conclusion was confirmed by a set of numerical tests, which demonstrated the convergence of the corresponding Monte Carlo procedure to exact results, particularly in regimes where the surface hopping and the mean field methods would both fail quite dramatically.

While the SCMC algorithm demonstrated a reasonable computational efficiency, especially in comparison with other non-ad-hoc methods, its computational cost significantly exceeded that of the surface hoping method. The increase of the computational cost would become especially pronounced in systems containing extended regions of coupling between electronic states (usually termed non-adiabatic regions in the literature) or several distinct regions of non-adiabatic coupling. In such problems the simulations required tens to hundreds of thousands of trajectories, which would make it impossible to utilize such a computational approach in simulations of realistic molecular systems. The reason is that in such simulations the major computational cost comes from the electronic structure calculations, which are carried out "on the fly" with the propagation of nuclei, limiting the number of trajectories for most state-of-art simulations at most to several thousands. Therefore, while the theoretical framework of Ref. [1] provided a significant step forward in terms of accuracy and predictive power, there was a clear need for a new numerical method and the algorithm that could implement such theoretical approach much more efficiently.

Most of the following work on the project has dealt with

developing such numerical approach. In Ref. [2] we have studied the efficiency of the SCMC method as well as its accuracy dependence on parameters of the problem and size of the sample, while Ref. [3] studied certain theoretical aspects of generic non-adiabatic dynamics relevant for better understanding of physical picture behind it. In Ref. [4] we proposed a more efficient sampling technique that allowed us to significantly increase computational efficiency of the Monte Carlo approach (by approximately an order of magnitude).

A transformative improvement in the numerical method to carry out non-adiabatic simulations was made in Ref. [5]. In this paper we have developed an algorithm based on a theoretically modified framework, where dynamics is viewed as a graph which branches at every infinitesimal time step. That is, the wavefunction of the nuclei associated with a certain electronic state (i.e. a wavepacket) continuously creates offspring wavepackets linked with other electronic states. The corresponding graph is shown in Figure 1 (a), which schematically represents evolution of a wave function for a molecular system with two (relevant) electronic states. Obviously, such a continuous multiplication of wavepackets leads to the exponential growth of their number (e.g. the number of branches in the graph in Figure 1(a)), which creates an overflow after a sufficient number of computation steps. The problem can, however, be efficiently resolved if we note that wavepackets that are formed as a result of spawning at two consecutive (infinitesimal) time steps are infinitesimally close to each other in terms of their position, amplitude, phase and shape (i.e. width). Therefore the superposition (i.e. sum) of the two is a wavepacket with similar parameters, but (approximately) double amplitude. The critical step made in Ref. [5] is to replace the two wavepackets with a single one, such that the new wavepacket has optimal (i.e. maximum) overlap with the sum of two original wavepackets. We termed the procedure "renormalization", analogous to the renormalization procedure in the many-body quantum mechanics, where it is used in summing different orders of the so-called perturbative expansions. In our case, the renormalization procedure allows to dramatically reduce the number of wavepackets involved: While in the original scheme (i.e. without renormalization) after, say, 2 time steps one has 4 wavepackets as a result of the wavepacket spawning, the renormalization procedure reduces their number back to 2, which prevents the total number of the wavepackets from growing. Such reduction is shown schematically in Figure 1(b). However, the process of renormalization cannot be continued indefinitely: At some point wavepackets associated with different electronic states will separate in real and momentum spaces and, as a result, the renormalization procedure starts to fail. Physically this corresponds to the branching of the wavefunction: At that moment wavepackets are considered independent and propagate independently, creating new offspring and so on, e.g. Figure 1(c).

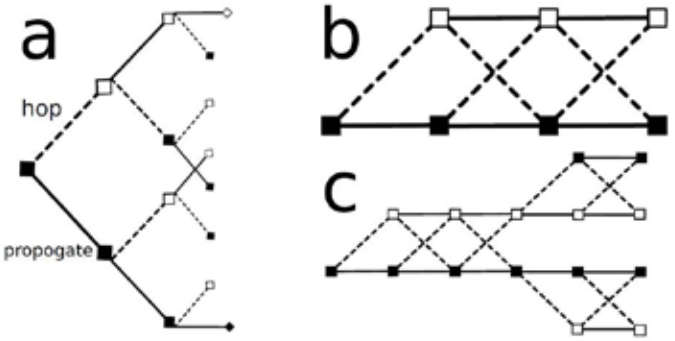

Figure 1. Schematics of the Coupled Wavepecket algorithm with two interacting potential energy surfaces (i.e. two electronic states): (a) Graph representing branching of the wavefunction, where wavepackets create offspring at each time step; (b) The graphical representation with the renormalization procedure; (c) Branching of the renormalized wavepackets.

The procedure described above has been implemented in a highly efficient numerical method that we termed the Coupled Wavepacket (CW) algorithm (since the renormalization procedure can be viewed as coupling between parent and offspring wavepackets). The new method can be viewed as a "smart spawning" procedure, where the wave function's branching (or spawning) occurs not at each elementary step, but only at points where it is prescribed by physical arguments which can be expressed in terms of well-defined physical parameters, such as wavepacket overlaps. As a result, the new CW algorithm dramatically reduces the computational cost of the simulation (by 2 to 4 orders of magnitude compared to the SCMC method!), thus making it possible to utilize it in modeling realistic molecular systems rather than a bunch of toy models of mostly academic interest (as it was in case of the original SCMC method). We believe that the CW method is likely to shape the non-adiabatic dynamics research as well as to be recognized as a powerful computational tool for predictive first-principle based simulations of photo-excited molecular dynamics.

Impact on National Missions

First and foremost our project has provided novel computational capabilities critical for understanding light-induced dynamics in many technologically relevant nanostructures. In fact, for the first time, experimental ultrafast spectroscopy will have its theoretical counterpart able to treat the material on the same footing. Consequently, we envision

extremely broad applications of developed tools, relevant to the current and future LANL/DOE missions. Our project addresses both the Los Alamos Information Science and Technology (IS&T) and Materials for the Future Pillars by providing innovative computational means for molecular materials suitable for clean energy: solar energy capture and energy storage. Consequently, proposed activities have potential for extending our program through LANL as well as through National Initiatives in energy and materials (e.g., BES calls of the EFRC renewals and the MESO initiative).

The application scope for the computational tool developed in the course of the project, e.g. the CW algorithm, is very broad: Our new unique theoretical capability can immediately provide a substantial boost to a number of already running programs and collaborations, focusing on different materials such as organic semiconductors, carbon nanotube/graphene materials, transition metal-based system, semiconductor nanocrystals and noble metal clusters. There are additional applications in LANL programs dealing with dynamics of materials under extreme conditions such as energetic materials. Next, there are many CINT users, who will tremendously benefit from these new theoretical tools. Finally, such development will attract attention of the world-wide community of spectroscopists.

References

1. Gorshkov, V. N., S. Tretiak, and D. Mozyrsky. Semiclassical Monte-Carlo approach for modelling non-adiabatic dynamics in extended molecules. 2013. Nature Communications . 4: 2144.

2. White, A. J., V. N. Gorshkov, Wang, Tretiak, and Mozyrsky. Semiclassical Monte Carlo: A first principles approach to non-adiabatic molecular dynamics. 2014. JOURNAL OF CHEMICAL PHYSICS. 141 (18).

3. Zhou, , Chen, Zhao, Mozyrsky, Chernyak, and Zhao. Ground-state properties of sub-Ohmic spin-boson model with simultaneous diagonal and off-diagonal coupling. 2014. PHYSICAL REVIEW B. 90 (15).

4. White, A. J., V. N. Gorshkov, Tretiak, and Mozyrsky. Non-adiabatic molecular dynamics by accelerated semiclassical Monte Carlo. 2015. JOURNAL OF CHEMICAL PHYSICS. 143 (1).

5. White, , Tretiak, and Mozyrsky. Coupled wave-packets for non-adiabatic molecular dynamics: a generalization of Gaussian wave-packet dynamics to multiple potential energy surfaces. 2016. CHEMICAL SCIENCE. 7 (8): 4905.

Publications

Gorshkov, V. N., Tretiak, and Mozyrsky. Semiclassical Monte-Carlo approach for modelling non-adiabatic dynamics in extended molecules. 2013. NATURE COMMUNICATIONS. 4.

White, , Tretiak, and Mozyrsky. Coupled wave-packets for non-adiabatic molecular dynamics: a generalization of Gaussian wave-packet dynamics to multiple potential energy surfaces. 2016. CHEMICAL SCIENCE. 7 (8): 4905.

White, A. J., V. N. Gorshkov, S. Tretiak, and D. Mozyrsky. Non-adiabatic molecular dynamics by accelerated semiclassical Monte Carlo. 2015. The Journal of Chemical Physics . 143: 014115.

White, A., V. N. Gorshkov, R. Wang, S. Tretiak, and D. Mozyrsky . Semiclassical Monte-Carlo: A First Principles Approach to Non-adiabatic Molecular Dynamics . 2014. The Journal of Chemical Physics . 141: 184101.

Zhou, N., L. Chen, Y. Zhao, D. Mozyrsky, V. Chernyak, and Y. Zhao. Ground state properties of sub-Ohmic spin-boson model with simultaneous diagonal and off-diagonal coupling . 2014. Physical Review B. 90: 155135.

Making nano-Mg a Reality

Rodney J. Mccabe
20140348ER

Abstract

There is immense interest in the aerospace, automotive, biomedical, consumer electronics and defense industries to grow the number of applications that use ultra-lightweight, formable Mg alloys. For example, with increasing public pressure to reduce fuel consumption for automotive applications, Mg alloys have risen to the top of the list as the next structural materials to replace or reduce the amount of aluminum and steel in cars. Mg has a high strength-to-weight ratio and low density, being 35% lighter than Al and 78% lighter than steel. If, for example, all the steel in your car were replaced with Mg, the weight reduction would boost fuel efficiency by approximately 55%. But elemental Mg is weak and its strength must be vastly improved in order to manufacture and shape ultra-lightweight devices and engineering components. Ten-fold strengthening is possible by nanostructuring, but to date nanostructuring of Mg is hindered by a mechanism called twinning. We worked towards developing novel Mg-X nano-composites with strength ten times that of pure Mg. The LDRD team was comprised of leading researchers from MST, T, and MPA divisions. The research team included undergraduate students, graduate students, and LANL scientists (both early career and advanced career) doing both modeling and experimental work. For this work, we combined severe plastic deformation processing, mesoscale process modeling, depostion and nanoemechanics testing at the Center for Integrated Nanotechnologies, and neutron diffraction techniques at the Lujan Center at LANSCE. We accomplished formation of Mg-Nb and Zr-Nb nanolaminates and demonstrated that these materials respectively were ten times and six times stronger than their coarse-grained counterparts.

Background and Research Objectives

With the need to reduce gas consumption, Mg alloys have risen to the top of the list as the next lightweight structural materials to replace steel. However, even if all the steel in your car (e.g., 30 mpg) were replaced with today's Mg, the weight reduction would boost fuel efficiency by only 54.6% (to 46 mpg), well below the Corporate Average Fuel Economy standards for 2020 (61 mpg). But if the strength of bulk Mg were to increase ten-fold, the gas mileage would boost from 30 mpg to 76 mpg, leading to a transformational impact on the automotive industry. For other structural metals (e.g., Al, Cu, Ni, steel), up to ten-fold increases have been realized by severe plastic deformation (SPD) techniques, which transform coarse-grained metals to nano-grained metals.

Unfortunately, all attempts to make "nano- Mg" in bulk sizes have failed. Bulk nano- Mg cannot be made because SPD causes deformation twinning in Mg. For this ER, we initially proposed a breakthrough in microstructural processing by design, where the key is to create a composite of Mg and a smaller amount of second metal phase, metal X, which in our ER X = Nb, and tune the Mg-Nb interfaces to suppress twinning, permitting Mg refinement to the nanoscale. This innovative approach gives rise to new scientific issues of Mg-Nb interface/defect processes. To tackle them, we posed two original hypotheses and used them to direct an integrated experimental and modeling strategy. Our bulk nano-Mg-Nb, as well as the science that enabled it and synthesis pathways that made it, will be in high demand by countless reputable research groups and industry (automotive, bio, and aerospace).

Scientific Approach and Accomplishments

To reach this goal, our approach was to synthesize a nano layered composite metal that combines two phases, one metal with a hexagonal close packed (hcp) crystal structure and another metal with a body centered cubic crystal (bcc) structure. Our main innovation behind this plan is the recognition that deformation twinning is the chief obstacle that has prevented so many scientists before us from achieving this goal. For the hcp phase, we used standard Mg and Nb metals as raw materials as our effort is meant to establish basic understanding. For the

bcc phase we used Nb. With these materials, we made Zr-Nb nanolayered composites via severe plastic deformation and Mg-Nb nano layered composites via physical vapor deposition. The reasons for making thin films is to 1) test different chemical compositions of Mg and Nb, 2) to determine the deformation behavior via micro pillar testing, and 3) to modify the interface structures in a controlled manner. We will at the same time carry out atomic scale simulations to determine which interface structures are energetically favorable and which deformation slip mechanisms are preferred. Using this knowledge, we performed crystal plasticity finite element (CPFE) simulations to understand microstructure evolution during bulk deformation processing. All of these efforts are new and innovative and have not been performed or reported in the literature.

We have successfully developed a method using accumulative roll bonding to produce nanolayered Zr-Nb composites with nanolayered thicknesses of ~90 nm. The quality of the Zr-Nb interfaces was characterized using energy-dispersive spectroscopy utilized within a transmission electron microscope and these scans showed no signs of intermixing and showed chemically distinct, pure phases in the layers to within 4.5 nm from the interfaces. In addition, Neutron Diffraction data obtained at LANSCE showed that deformation twinning was successfully suppressed. Prior to our work it was not known that dislocation-mediated plasticity free of deformation twinning could persist in hcp Zr down to the nanoscale. We are already revealing an innovative route to manufacturing hcp-based nanostructured metals as well as a novel material for pioneering hcp/bcc interface and nanoscale hcp research. To summarize, we are the first to synthesize and characterize hcp-bcc Zr-Nb composites using severe plastic deformation techniques and therefore this work represents the cutting-edge of the field.

Also progress was made towards the ultimate goal of making Mg/Nb composites. Mg/Nb nano layered composites was made using via physical vapor deposition. This fabrication method allows modification of the interface structures in a controlled manner as well as the determination the deformation behavior via micro pillar testing. An important discovery was that up to 5 nm layer thickness the Mg takes on a body center cubic (bcc) crystal structure. The 5 nm Mg/Nb composite achieved both outstanding ductility and strength. Interface and deformation studies of bccMg, were done using atomistic scale simulations as well as crystal plasticity finite element (CPFE) methods. This required significant development of the CPFE methodology. Similarly, the work on physical vapor deposition of Mg/Nb composites breaks new ground in the field, in particular the model development associated with this work have extended atomistic scale and well as crystal plastic finite elements methods significantly.

Impact on National Missions

Our bulk nano-Mg-X, as well as the science that enabled it and synthesis pathways that made it, will be in high demand by countless reputable research groups and industry (automotive, bio, and aerospace); the material and science have been chased for at least a decade. Nano- Mg-X will no doubt exhibit many other interesting properties apart from ultra high strength, such as corrosion resistance (aging), magnetism, conductivity, thermal stability, biodegradation resistance, and fracture toughness. Our project will fundamentally transform Mg research and manufacturing and make LANL the leader of this rapidly growing market. This ER notably fulfills all three pillars of LANL's Materials Strategy. 1) Defects and Interfaces: our innovation tunes interfaces to suppress emission of twinning dislocations. 2) Emergent Phenomena: all matter is controlled by their atomic structure and nearly 30% of nano-Mg-X will be Mg-X interface with a differing atomic structure than Mg or X. Hence new effects can be expected. 3) Extreme Environments: we exploit one extreme (severe strains) to produce nano-Mg-X, a material that will be tolerant in extremes of high stress, high strains (formable), and we expect, high temperatures.

Publications

Ardeljan, , I. J. Beyerlein, and Knezevic. A dislocation density based crystal plasticity finite element model: Application to a two-phase polycrystalline HCP/BCC composites. 2014. JOURNAL OF THE MECHANICS AND PHYSICS OF SOLIDS. 66: 16.

Ardeljan, M., D. J. Savage, A. Kumar, I. J. Beyerlein, and M. Knezevic. The plasticity of highly oriented nano-layered Zr/Nb composites. 2016. Acta Materialia. 115: 189.

Ardeljan, M., I. J. Beyerlein, B. A. McWilliams, and M. Knezevic. Strain rate and temperature sensitive multi-level crystal plasticity model for large plastic deformation behavior: Application to AZ31 magnesium alloy. 2016. International Journal of Plasticity. 83: 90.

Ardeljan, M., I. J. Beyerlein, and M. Knezevic. A dislocation density based crystal plasticity finite element model: application to a two-phase polycrystalline HCP/BCC composites. 2014. Journal of the Mechanics and Physics of Solids. 66: 16.

Ardeljan, M., M. Knezevic, T. Nizolek, I. J. Beyerlein, S. J. Zheng, J. S. Carpenter, R. J. McCabe, N. A. Mara, and T. M. Pollock. A multi-scale model for texture development in Zr/Nb nanolayered composites processed by accumulative roll bonding. 2014. Journal of Materials Science and Engineering. 63: 012170.

Beyerlein, I. J., J. S. Carpenter, Hunter, L. S. Toth, and Skrotzki. Nano-enabled orientation alignment via extreme shear strains. 2015. SCRIPTA MATERIALIA. 98: 52.

Cao, L. e. i., Hunter, I. J. Beyerlein, and Koslowski. The role of partial mediated slip during quasi-static deformation of 3D nanocrystalline metals. 2015. JOURNAL OF THE MECHANICS AND PHYSICS OF SOLIDS. 78: 415.

Carpenter, J. S., Nizolek, R. J. McCabe, Knezevic, S. J. Zheng, B. P. Eftink, J. E. Scott, S. C. Vogel, T. M. Pollock, N. A. Mara, and I. J. Beyerlein. Bulk texture evolution of nanolamellar Zr-Nb composites processed via accumulative roll bonding. 2015. ACTA MATERIALIA. 92: 97.

Carpenter, J. S., R. J. McCabe, J. R. Mayeur, N. A. Mara, and I. J. Beyerlein. Interface-Driven Plasticity: The Presence of an Interface Affected Zone in Metallic Lamellar Composites. 2015. ADVANCED ENGINEERING MATERIALS. 17 (1): 109.

Hunter, , R. F. Zhang, and I. J. Beyerlein. The core structure of dislocations and their relationship to the material gamma-surface. 2014. JOURNAL OF APPLIED PHYSICS. 115 (13).

Hunter, , and I. J. Beyerlein. Relationship between monolayer stacking faults and twins in nanocrystals. 2015. ACTA MATERIALIA. 88: 207.

Hunter, , and I. J. Beyerlein. Unprecedented grain size effect on stacking fault width. 2013. APL MATERIALS. 1 (3).

Hunter, , and I. J. Beyerlein. Predictions of an alternative pathway for grain-boundary driven twinning. 2014. APPLIED PHYSICS LETTERS. 104 (23).

Hunter, , and I. J. Beyerlein. Stacking fault emission from grain boundaries: Material dependencies and grain size effects. 2014. MATERIALS SCIENCE AND ENGINEERING A-STRUCTURAL MATERIALS PROPERTIES MICROSTRUCTURE AND PROCESSING. 600: 200.

Jahedi, , Ardeljan, I. J. Beyerlein, M. H. Paydar, and Knezevic. Enhancement of orientation gradients during simple shear deformation by application of simple compression. 2015. JOURNAL OF APPLIED PHYSICS. 117 (21).

Jahedi, , M. H. Paydar, Zheng, I. J. Beyerlein, and Knezevic. Texture evolution and enhanced grain refinement under high-pressure-double-torsion. 2014. MATERIALS SCIENCE AND ENGINEERING A-STRUCTURAL MATERIALS PROPERTIES MICROSTRUCTURE AND PROCESSING. 611: 29.

Knezevic, , Drach, Ardeljan, and I. J. Beyerlein. Three dimensional predictions of grain scale plasticity and grain boundaries using crystal plasticity finite element models. 2014. COMPUTER METHODS IN APPLIED MECHANICS AND ENGINEERING. 277: 239.

Knezevic, , I. J. Beyerlein, M. L. Lovato, C. N. Tome, A. W. Richards, and R. J. McCabe. A strain-rate and temperature dependent constitutive model for BCC metals incorporating non-Schmid effects: Application to tantalum-tungsten alloys. 2014. INTERNATIONAL JOURNAL OF PLASTICITY. 62: 93.

Knezevic, , Jahedi, Y. P. Korkolis, and I. J. Beyerlein. Material-based design of the extrusion of bimetallic tubes. 2014. COMPUTATIONAL MATERIALS SCIENCE. 95: 63.

Knezevic, , Nizolek, Ardeljan, I. J. Beyerlein, N. A. Mara, and T. M. Pollock. Texture evolution in two-phase Zr/Nb lamellar composites during accumulative roll bonding. 2014. INTERNATIONAL JOURNAL OF PLASTICITY. 57: 16.

Knezevic, , Zecevic, I. J. Beyerlein, J. F. Bingert, and R. J. McCabe. Strain rate and temperature effects on the selection of primary and secondary slip and twinning systems in HCP Zr. 2015. ACTA MATERIALIA. 88: 55.

Knezevic, M., T. Nizolek, M. Ardeljan, I. J. Beyerlein, N. A. Mara, and T. M. Pollock. Texture evolution in two-phase Zr/Nb lamellar composites during accumulative roll bonding. 2014. International Journal of Plasticity. 57: 16.

Kumar, A., I. J. Beyerlein, and J. Wang. First-principles study of the structure of Mg/Nb multilayers. 2014. Applied Physics Letters. 105: 071602.

Lentz, , Klaus, I. J. Beyerlein, Zecevic, Reimers, and Knezevic. In situ X-ray diffraction and crystal plasticity modeling of the deformation behavior of extruded Mg-Li-(Al) alloys: An uncommon tension-compression asymmetry. 2015. ACTA MATERIALIA. 86: 254.

Lentz, , Klaus, Wagner, Fahrenson, I. J. Beyerlein, Zecevic, Reimers, and Knezevic. Effect of age hardening on the deformation behavior of an Mg-Y-Nd alloy: In-situ X-ray diffraction and crystal plasticity modeling. 2015. MATERIALS SCIENCE AND ENGINEERING A-STRUCTURAL MATERIALS PROPERTIES MICROSTRUCTURE AND PROCESSING. 628: 396.

Xu, X. F., Y. Jie, and I. J. Beyerlein. A note on statistical strength of carbon nanotubes. 2013. Computers, Materials & Continua. 38: 17.

Xu, X. F., Y. Jie, and I. J. Beyerlein. A probability model for the strength of carbon nanotubes. 2014. American Institute of Physics Advances. 4: 077116.

Yuan, R. u. i., I. J. Beyerlein, and Zhou. Emergence of grain-size effects in nanocrystalline metals from statistical activation of discrete dislocation sources. 2015. ACTA

MATERIALIA. 90: 169.

Zhou, , C. J. O. Reichhardt, Reichhardt, and Beyerlein. Random organization in periodically driven gliding dislocations. 2014. PHYSICS LETTERS A. 378 (22-23): 1675.

Zhou, , Reichhardt, C. J. O. Reichhardt, and I. J. Beyerlein. Dynamic Phases, Pinning, and Pattern Formation for Driven Dislocation Assemblies. 2015. SCIENTIFIC REPORTS. 5.

Toward Tunable Functionalties Using Epitaxial Nanoscaffolding Films

Quanxi Jia
20140371ER

Abstract

Lattice-strained epitaxial nanoscaffolding films (epi-NSFs), in which a parallel array of nanoscaled material A interfaces with another material B and forms a regular lateral arrangement of A:B on a substrate, provide a new design paradigm to tune/manipulate functionalities that cannot be obtained in individual constituents (A or B). Tuning/controlling functionality of a broad range of materials has been emerging as an exciting direction in materials research community. Built on our expertise, integrated capabilities, this project has developed new capabilities toward tunable functionalities using epi-NSFs where the vertical interface can act as an active device. Specifically, we have investigated the tunable optical and resistive switching properties based on metal-oxide epi-NSFs. Our effort supports and strengthens the Laboratory's core scientific capabilities essential to discovering, understanding, and exploiting emergent phenomena in materials. Furthermore, this project has enabled the development of new experimental (advanced synthetic and diagnostic techniques) and theoretical capabilities (methods to model multiscale materials interactions) to probe the state of complex nanoscale materials.

Background and Research Objectives

Over the past several years, new discoveries and major advances have been made to enhance the understanding of improved functionalities and emergent behaviors in complex metal-oxides. Noteworthy examples include an extremely high mobility (>10,000 cm2/V·s) of the electron gas at the interface between otherwise strongly insulating LaAlO3 and SrTiO3 materials, arising from polarity discontinuities at the interfaces [1]. It should be noted that well-designed and accurately controlled superlattice or layered structures need to be synthesized to achieve these entirely new functionalities.

More recently, emergent behavior and/or improved functionalities have been also achieved through interfacing different oxides by forming epi-NSFs [2-5] instead of layered or superlattice structures. The most important features of epi-NSFs include: a) Emergent phenomena and/or improved functionalities can be induced through interfacing appropriate materials vertically; b) The thickness limitation for a full strain relaxation typically occurring by around 100 nm in a usual single layer or superlattice film can be circumvented, i.e. strained films with a thickness of an order of magnitude larger (compared to a single layer film) can be maintained in the epi-NSFs; and c) functionalities of an active phase in the epi-NSFs can be tuned by a second phase or a passive phase. Many technological applications require thicker films (>200 nm). This film thickness is well above the full strain relaxation thickness of superlattices and layered heterostructures.

While limited demonstrations of desired and/or new functionalities in epi-NSFs are technologically exciting, the tuning and control of functionalities in epi-NSFs are still in the very early stage. Furthermore, totally different surface morphologies of epi-NSFs have been reported from various research groups. Depending on the combination of materials (both the film and the substrate), the surface of epi-NSFs can appear as nanomaze [6], nanopillar [2,4], and/or nanocheckerboard [3]. As a result, this makes it difficult to determine the critical factors (such as surface morphology, vertical interface strain, and interface chemistry) that can lead to the emergent behavior and/or improved functionality. It is clear that a fundamental understanding of the relationship between the functionality and these factors is much needed.

Built on our expertise and preliminary experimental results, we focused new capability development on tunable functionalities using epi-NSFs. Specifically, we have investigated the tunable properties based on different metal-oxide epi-NSFs. Leveraging CINT's well controlled laser-MBE for the growth of complex metal-oxide films, we synthesized different epi-NSFs with controlled microstructures. In parallel with T-4's modeling effort, we

used computational results to guide the fine adjustment of processing parameters (which can affect the surface morphology of the film) and to tune the transport properties of interested materials.

Scientific Approach and Accomplishments

Leveraging CINT's well-controlled laser-MBE for the growth of complex metal-oxide films, we synthesize different epi-NSFs with controlled microstructures. In parallel with T-4's modeling effort, we use computational results to guide the fine adjustment of processing parameters (which can affect the surface morphology of the film) and to tune the transport properties of interested phases and resistive switching property (or so called "memristive" behavior) of the materials. Combining advanced TEM and high-resolution x-ray diffraction capability, we establish the processing-structure-functionality relationship of epi-NSFs. In a closed-loop between synthesis, probing, and simulation, we prove the tunable transport properties and memristive behaviors in epi-NSFs. We pursued the following three tasks across the project duration: i) Synthesize different epi-NSFs with controllable microstructures and desired functionalities; ii) Predict microstructures using phase-field modeling; and iii) Probe microstructural and functional properties of epi-NSFs to establish processing-microstructure-functionality relationship.

In the following, we highlight three important technical accomplishments. More accomplishments, detailed experimental work, and scientific results have been described in our many referred journal articles published from 2013 to 2016.

Strongly enhanced oxygen ion transport through samarium-doped CeO2 nanopillars in epi-NSFs [7]: Enhancement of oxygen ion conductivity in oxides is important for low-temperature operation of a range of devices such as solid oxide fuel cells, sensors, and other ionotronic devices. While huge ion conductivity has been demonstrated in planar heterostructure films, there has been considerable debate over the origin of the conductivity enhancement, in part because of the difficulties of probing buried ion transport channels. We have used highly crystalline micrometer-thick epi-NSFs that are composed of Sm-doped CeO2 embedded in supporting matrices of SrTiO3 to study this topical subject. We have found that the ionic conductivity is higher by one order of magnitude than plain Sm-doped CeO2 films by using such a structure. Via scanning probe microscopy, we have also shown that the fast ion-conducting channels are not exclusively restricted to the interface but also are localized at the Sm-doped CeO2 nanopillars. This work offers a pathway to realize spatially localized fast ion transport in oxides of micrometer thickness.

Self-assembled epitaxial oxide NSFs with tailored nanoscale ionic and electronic channels for controlled resistive switching [8]: Resistive switches are non-volatile memory cells based on nano-ionic redox processes that offer energy efficient device architectures and open pathways to neuromorphics and cognitive computing. However, channel formation typically requires an irreversible, not well-controlled electroforming process, resulting in difficult to independently control ionic and electronic properties. The device performance is also limited by the incomplete understanding of the underlying mechanisms. We have used epi-NSFs composed of self-assembled Sm-doped CeO2 and SrTiO3 as a memristive model material system to separate tailoring of nanoscale ionic and electronic channels at high density (~1012 inch−2). We systematically show that these devices allow precise engineering of the resistance states, thus enabling large on–off ratios and high reproducibility. The tunable structure presents an ideal platform to explore ionic and electronic mechanisms and we expect a wide potential impact also on other nascent technologies, ranging from ionic gating to micro-solid oxide fuel cells and neuromorphics.

Role of scaffold network in controlling strain and functionalities of nanocomposite films [9]: Strain is a novel approach to manipulating functionalities in correlated complex oxides. However, significant epitaxial strain can only be achieved in ultrathin layers. We show that, under a direct lattice matching framework, large and uniform vertical strain up to 2% can be achieved in epi-NSFs over a few hundred nanometers in thickness to significantly modify the magnetic anisotropy, magnetism, and magnetotransport properties. We have proposed the comprehensive designing principles to design large vertical strain in epi-NSFs. Furthermore, our phase-field simulations not only reveal the strain distribution but also suggest that the ultimate strain is related to the vertical interfacial area and interfacial dislocation density. By changing the nanoscaffold density and dimension, the strain and the magnetic properties can be tuned. Significantly, the established correlation among the vertical interface—strain—properties in nanoscaffold films from this research can consequently be used to tune other functionalities in a broad range of complex oxide films far beyond critical thickness.

Impact on National Missions

This work supports and strengthens the Laboratory's core scientific capabilities essential to discovering, understanding, and exploiting emergent phenomena in materials. In particular, this research develops/expands our key capabilities outlined in the Emergent Phenomena in Materials Functionality (EPM) LDRD ER category, e.g. i) functional design and optimization, ii) novel control and metrology

techniques exploiting emergent phenomena, iii) understanding mechanisms for control of material properties, and iv) synthesis and processing techniques that lead to control of emergent phenomena. Furthermore, this project enables the development of new experimental (advanced synthetic and diagnostic techniques) and theoretical capabilities to probe the state of complex nanoscale materials. This effort ensures LANL's continued and expanded leadership in nanostructured materials, innovative probing methods, and theoretical predication and design of new/improved functional materials.

This effort has also enabled LANL to respond effectively to future BES calls since our proposed work directly addresses the Grand Scientific Challenge identified in the BESAC report: how do remarkable properties of matter emerge from the complex correlations of atomic or electronic constituents and how can we control these properties? Beyond BES, this work has enormous ramifications in technological sectors such as memory and electro-optical devices. Finally, our effort enables an important capability for MaRIE, since the ability to design, synthesize, measure, and model functionality at different length scales in complex materials is the central competence underpinning MaRIE's envisioned M4 facility. Additionally, our effort exploits and expands the capabilities at two LANL National User Facilities: the Center for Nanotechnologies (CINT) and the National High Magnetic Field Laboratory (NHMFL).

References

1. Ohtomo, A., and H. Y. Hwang. A high-mobility electron gas at the LaAlO3/SrTiO3 heterointerface. 2004. Nature. 427: 423.

2. Zheng, H., and J. Wang et al. Multiferroic BaTiO3-CoFe2O4 nanostructures. 2004. Science. 303: 661.

3. MacManus-Driscoll, J. L., and P. Zerrer et al. Strain control and spontaneous phase ordering in vertical nanocomposite heteroepitaxial thin films. 2008. Nat. Mater.. 7: 314.

4. Harrington, S. A., and J. Zhai et al. Thick lead-free ferroelectric films with high Curie temperatures through nanocomposite-induced strain. 2011. Nat. Nanotechnology . 6: 491.

5. Lee, O., and S. A. Harrington et al. Extremely high tenability and low loss in nanoscaffold ferroelectric films. 2012. Nano Lett.. 12: 4311.

6. Chen, A., and W. Zhang et al. Magnetotransport properties of quasi-one dimensionally channeled vertically aligned heteroepitaxial nanomazes. 2013. Appl. Phys. Lett.. 102: 093114.

7. Yang, S. M., and S. Lee et al. Strongly enhanced oxygen ion transport through samarium-doped CeO2 nanopillars in nanocomposite films. 2015. Nat. Commun.. 6: 8588.

8. Cho, S., and C. Yun et al. Self-assembled oxide films with tailored nanoscale ionic and electronic channels for controlled resistive switching. 2016. Nat. Commun.. 7: 12373.

9. Chen, A., and J. M. Hu et al. Role of scaffold network in controlling strain and functionalities of nanocomposite films. 2016. Sci. Adv.. 2: 1600245.

Publications

Chen, A., M. Weigand, Z. Bi, W. Zhang, X. Lv, P. Dowden, H. Wang, J. L. MacManus-Driscoll, and Q. X. Jia. Role of microstructure and strain on the magnetoresistance of nanocomposite films. 2014. Scientific Reports. 4: 5426.

Cho, S., C. Yan, S. Tappertzhofen, A. Kursumovic, S. B. Lee, P. Lu, Q. X. Jia, M. Fan, J. Jian, H. Wang, S. Hofmann, and J. MacManus-Driscoll. Self-assembled oxide films with tailored nanoscale ionic and electronic channels for controlled resistive switching. 2016. Nat. Commun.. 7: 12373.

Jia, Q. X.. Self-assembled epitaxial nanocomposite films: their strain control and functionalities. Invited presentation at New Mexico Tech. (Socorro, NM, 7 March, 2014).

Jia, Q. X.. Effect of interfaces on competing interactions of functional complex metal-oxides. Invited presentation at Univ. of Connecticut. (Storrs, CT, 17 OCt. 2014).

Jia, Q. X.. Synthesis and characterization of epitaxial nanocomposite films: Effects of interface on the functionalities. Invited presentation at Electronic Materials and Applications. (Orlando, Jan. 20 - 22, 2016).

Jia, Q. X.. Control and manipulation of competing interactions of ferroic films. Invited presentation at International Mater. Res. Congress. (Cancun, Mexico, Aug. 16 - 20, 2015).

Jia, Q. X.. The role of interfaces on the functionalities of complex metal-oxide films. Invited presentation at Quantum Matter Workshop. (Santa Fe, NM, May 18 - 21, 2015).

Jia, Q. X.. Role of interfaces on competing interactions of ferroic films. Invited presentation at MRS Fall Meeting. (Boston, MA, Nov. 29 - Dec. 4, 2015).

Jia, Q. X., and C. W. Nan. Obtaining ultimate functionalities

in nanocomposites: Design, control, and fabrication,. 2015. MRS Bulletin. 40: 719.

Lee, S. B., A. Sangle, P. Lu, A. Chen, W. Zhang, J. S. Lee, H. Wang, Q. X. Jia, and J. L. MacManus-Driscoll. Novel electroforming-free nanoscaffold memristor with very high uniformity, tunability and density. 2014. Adv. Mater.. 26: 6284.

Lee, S. B., W. Zhang, F. Khatkhatay, H. Wang, Q. X. Jia, and J. L. MacManus-Driscoll. Ionic conductivity increased by two orders of magnitude in micrometer-thick vertical yttria-stabilized ZrO2 nanocomposite films. 2015. Nano Lett.. 15: 7362.

Lee, S. B., W. Zhang, Q. X. Jia, H. Wang, and J. L. MacManus-Dris. Strain tuning and strong enhancement of ionic conductivity in SrZrO3-RE2O3 (RE = Sm, Eu, Gd, Dy, and Er) nanocomposite films. 2015. Adv. Functional Mater.. 25: 4328.

Li, L., and L. Sun, et al.. Self-assembled epitaxial Au-oxide vertically aligned nanocomposites for nanoscale metamaterials. 2016. Nano Lett.. 16: 3926.

Lu, P., E. Roemro, S. B. Lee, J. L. MacManus-Driscoll, and Q. X. Jia. Chemical quantification of atomic-scale EDS maps under thin specimen conditions. 2014. Microscopy & Microanalysis . 20: 1782.

MacManus-Driscoll, J. L., A. Suwardi, A. Kursumovic, Z. Bi, C. F. Tsai, H. Wang, Q. X. Jia, and Q. J. Lee. New strain states and radical property tuning of metal oxides using a nanocomposite thin film approach. 2015. APL Mater.. 3: 062507.

Su, Q., and W. Zhang, et al.. Self-assembled magnetic metallic nanopillars in ceramic matrix with anisotropic magnetic and electrical transport properties. 2016. ACS Appl. Mater. Interface . 8: 2083.

Yang, S. M., S. B. Lee, J. Jian, W. Zhang, Q. X. Jia, H. Wang, T. W. Noh, S. V. Kalinin, and J. L. MacManus-Driscoll. Strongly enhanced oxygen ion transport through samarium-doped CeO2 nanopillars in nanocomposite films. 2015. Nat. Commun.. 6: 8588.

Zhang, W., L. Li, P. Lu, M. Fan, Q. Su, F. Khatkhatas, A. Chen, Q. X. Jia, X. Zhang, J. L. MacManus-Driscoll, and H. Wang. Perpendicular exchange-bias magnetotransport at the vertical heterointerfaces in La0.7Sr0.3MnO3:NiO nanocomposites. 2015. ACS Appl. Mater. & Interfaces . 7: 21646.

Zhao, R., W. Li, J. H. Lee, E. M. Choi, Y. Liang, W. Zhang, R. Tang, H. Wang, Q. X. Jia, and J. L. MacManus-Driscoll. Precise tuning of (YBa2Cu3O7)1-x:(BaZrO3)x thin film nanocomposite structures. 2014. Adv. Funct. Mater.. 24: 5240.

Direct-gap Group-IV Nanocrystals: Cheap, Versatile Materials for Solar Cells

Sergei A. Ivanov
20140446ER

Abstract

Such elements of the group IV as silicon and germanium are the most common building blocks of modern electronic devices due to their desirable band gap values, abundance and the relative ease of processing. Relatively small band gaps of these materials have ensured their applications in IR detectors and solar cells, despite the indirect nature of their band gaps, which gives rise to the reduced ability to absorb light. It has been shown from theoretical analysis that Si or Ge alloying with tin would produce better absorbing direct band gap materials. However, the miniscule solubility of Si and Ge in Sn due to large lattice mismatch and much higher cohesion energies of Si and Ge compared to that of Sn make alloying difficult to achieve in bulk. Nevertheless, the high surface-to-volume ratios and degree of curvature, available in small NCs, open up a unique possibility for a structural relaxation that reduces the strain from lattice inhomogeneity, making a wider range of alloys stable in the nanocrystalline form. Towards the goal of creating better absorbing Group IV materials, we have achieved the synthesis of SnxGe1-x nanocrystals with the full compositional range where tin content reaches x=0.951,2. Thorough investigation has confirmed the presence of homogenous alloys over the completely compositional range. Absorption spectroscopy of NCs of varying composition demonstrates a pronounced redshift and increase in molar absorptivity as a true indicator of solar relevance with increasing Sn-content. These results suggest that solution-processible NCs based on alloys of non-toxic and abundant Group IV elements are a promising material system for solar energy capture applications. We have investigated synthetic parameter space together with gaining experimental and theoretical insights into the mechanistic aspects of the reaction pathway leading to the formation of SnxGe1-x alloy. The resulting insights into the reaction mechanism allowed us to introduce the third element – silicon – into the binary alloy as well to move the material toward photovoltaic applications and beyond.

Background and Research Objectives

Cheap, non-toxic and abundantly produced, Group IV semiconductors (silicon (Si),germanium (Ge), tin (Sn)) are versatile materials for a broad range of devices. However, Si and Ge are indirect semiconductors, which make their interactions with light (absorption or emission) much less efficient than those of direct-gap semiconductors. This places severe limitations on how these materials can be used in solar cells, driving prices up and holding utilization down. If one could, instead, convert these materials into a more versatile form that could be handled and processed cheaply, and that offered better absorption properties, the effect on solar cell development and deployment would be transformative. Even simply rendering these materials amenable to, e.g., screen printing, spray deposition and other fabrication techniques suitable for roll-to-roll processing or the coating of surfaces of complex morphology, would enable a host of new civilian and military applications that are incompatible with rigid, brittle crystalline-Si. We propose to use the unique power and flexibility of colloidal synthesis to accomplish exactly that. The use of colloidal nanocrystal (NC) synthesis places the ability to create size-/composition-/shape-controlled NCs in device-relevant quantities into the hands of nearly any researcher. Importantly, colloidal NCs are amenable to low-cost solution based processing techniques, making them extremely versatile. We seek to exploit the power of colloidal synthesis to create a new class of Group IV alloy NCs with direct band-gap behavior at solar-relevant energies (1.0-1.5 eV) for use in a wide-range of emerging solar technologies.

Our project was targeting the following two research objectives: 1) synthesis of GexSn1-x and SixGeySn1-x-y alloy nanocrystals and 2) theoretical investigation of model alloy NCs to gain insights into their electronic structure and stability.

Scientific Approach and Accomplishments

Originally, we proposed to synthesize alloyed Ge-Sn nanocrystals using the halide route, where the mixture of GeCln (n = 2 or 4) and SnCl4 metal chlorides would be treated with alkyllithium (e.g., n-C4H9Li) reducing agent. First, we tested the reaction conditions for the reduction of individual halides, GeCln or SnCl4, separately. It was established that the reactivities for these precursors were so different, that there were no common conditions for both of them. Although, we have synthesized mono-elemental germanium and tin nanocrystals (NCs) using the proposed halide route, this path clearly was not viable for the synthesis of Ge-Sn alloyed NCs. We have modified the original approach and investigated the reactivities of alternative Ge and Sn precursors, GeIn (n = 2 or 4) and Sn(NTMS)2 (NTMS = N(Si(CH3)3)2).

The reactivity of the germanium iodide GeI2 was higher than that of GeCln, which implies the lower temperature of the synthesis, whereas the reactivity of Sn(NTMS)2 was lower than the corresponding chloride. As such, we have demonstrated that the reactivity of new precursors can be tuned to match each other (especially for Sn(NTMS)2). Using this new set of precursors and different temperatures, we were surprised to be able to prepare Ge-Sn alloyed nanocrystals within the complete compositional range, from purely monoelemental Ge NCs to SnxGe1-x NCs with x=0.98, which was confirmed by multiple characterization methods.

We have established a pathway for the formation for these alloyed nanocrystals. The reaction proceeds through the initial formation of a mix-metal cube-like complex with general formula SnmGe4-mL4 and its analogues. Pyrolysis of this complex leads to the original formation of small nanoparticles of molten tin with germanium being chemisorbed on their surface. Via diffusion, germanium gets incorporated into the particle interior where it is being kinetically stabilized against the phase separation during further heating and particle growth. From the established pathway it became apparent which particular tin precursors will lead to the formation of the alloy particles, namely organic tin amides. This was confirmed using a completely different tin precursor from Sn(NTMS)2, namely Sn(DIPAA)2, where DIPAA = di-isopropylacetamidinate). Theoretical investigation revealed that the germanium stabilitization inside of the molten tin particle happens due to the abrupt increase in the melting temperature of the material in the vicinity of each germanium atom, which drastically slows down the diffusion of germanium out of the particle. Synthesized nanocrystals were also studied with UV-Vis and photoluminescent spectroscopies to elucidate the nature of changes in the electronic structure of those products as a function of the amount of tin. Products with particular concentrations of tin even exhibited luminescence, the tell-tale sign of the direct transition. The results obtained to date indicate that previous theoretical models might have underestimated the amount of tin needed to convert germanium into the direct-gap material.

To maximize the application potential for the manufactured nanoparticles, that is to make them more air-stable and amenable for the post-synthetic chemistry to better incorporate into the materials matrices, we also developed the procedure to overcoat the particles with a thin layer of mix-metal sulfide GexSn1-xS2-δ. Treatment of the particles right in the original growth solution with the elemental sulfur solution renders them very air stable and subsequently the particles can easily undergo the surface ligand exchange to be soluble in a solvent of choice.

In parallel with the synthesis of GeSn alloyed nanoparticles, we modified our original approach to introduce the third element – silicon – into the composition of the alloy. Introduction of SiI4 into the reaction mixture appears to lead to the incorporation of up to 14% of silicon into GeSn nanoparticles. Direct incorporation of Sn into Si is yet an elusive goal, but the discovered modification of this approach with the initial synthesis of the ternary alloy followed by the minimization of germanium content is a viable alternative that might lead to the SnSi alloy formation.

Impact on National Missions

This work combines a number of marquee capabilities of the Laboratory, including world-recognized nanoscience efforts collectively at T, C-PCS and CINT, towards a goal of serious potential impact. These studies directly seek to understand and exploit the power of Defects and Interfaces in a material system of unique potential importance to applications in Energy Security, and as such lie at the core of the LANL “Materials for the Future” Pillar. The development of direct band gap Group IV NCs by low-cost methods is also extremely relevant to ongoing and future DOE Office of Science programs at LANL. Our approach lead to the broader compositional variability in the synthesis of thin films of Group IV alloys as well as nanorods and wires. Given the efforts that other groups apply to incorporate at least 10% of tin into germanium for the new lasing medium or solar cell material, the synthetic approach we developed and our results clearly enable and broaden the work in the synthesis of multicomponent Group IV alloys not only for photovoltaic applications, but also for the development of infra-red sensors, laser medium, and lithium battery anodes.

References

1. Ramasamy, K., P. Kotula, A. Fidler, M. Brumbach, J. Pietryga, and S. Ivanov. SnxGe1–x Alloy Nanocrystals: A First Step toward Solution-Processed Group IV Photovoltaics. 2015. Chemistry of Materials. 27 (13): 2640.

Publications

Ramasamy, , P. G. Kotula, A. F. Fidler, M. T. Brumbach, J. M. Pietryga, and S. A. Ivanov. SnxGe1-x Alloy Nanocrystals: A First Step toward Solution-Processed Group IV Photovoltaics. 2015. CHEMISTRY OF MATERIALS. 27 (13): 4640.

Ramasamy, K., P. G. Kotula, N. Modine, J. M. Pietryga, and S. A. Ivanov. Full compositional range in Sn-Ge system at nanoscale. To appear in Chem. Matters.

Metal and Semiconductor Nanocrystal Superlattices Under Pressure: Multiscale Tuning of Structure and Function

Jennifer A. Hollingsworth
20140456ER

Abstract

The overarching goal of this project was to explore and exploit high pressure as a novel means to precisely tune colloidal nanocrystal superlattices (NCSLs) from the atomic to the nano/mesoscale for new understanding of forces and interactions affecting supercrystal stability, novel NCSLs structures, and collective behavior resulting from interparticle interactions.

On their own, nanoparticle colloids of carefully controlled size/shape/surface properties will self-assemble into ordered two-dimensional/three-dimensional NCSLs that mimic atomic lattices. These can comprise single or multiple/different components, where the latter afford opportunities for developing new collective functional properties. Despite the rich opportunities in both novel structures and new functionality, key aspects of the field remain relatively or entirely unexplored. To date, examples of new functionality resulting from ordered arrays of dissimilar but interacting nanoparticles are very limited, while understanding of the comparative stabilities is almost entirely lacking.

We endeavored to fill these gaps by applying a novel approach – high-pressure methods as both an analytical and a synthesis tool. To achieve this, we pursued three research goals: (1) NCSL stability studies, (2) New NCSL structures through pressure, and (3) New binary NCSL functionality through pressure.

Background and Research Objectives

We aimed to fill gaps in understanding pertaining to the stability of nanocrystal syperlattices (NCSLs) and the nanocrystal components that they are made from, as well as gaps in our ability to obtain new functionality based on the assembled structures. Here, we applied a novel approach – high-pressure methods as both an analytical and a synthesis tool. To achieve this, we have pursued three Research Goals:

NCSL stability studies

We aimed to perform in-situ high-pressure small- and wide-angle synchrotron X-ray scattering on pre-assembled NCSLs to establish correlations between applied pressure and inter-NC distances as a function of composition, structure, and NCSL orientation. Coupling experimental results with computational chemistry approaches, we further aimed to infer NCSL thermodynamic stabilities.

New NCSL structures through pressure

We aimed to subject self-assembled NCSLs to high pressure in a temperature-controlled pressure cell to precisely tune inter-NC distances to the point of NC-NC fusing, creating new/permanent designed superstructures.

New binary NCSL functionality through pressure

We aimed to significantly advance the utility of NCSL structures beyond elegant curiosities to realize novel functionality inaccessible by other means, providing proof-of-concept in the form of unprecedented plasmon-enhanced excitonic emission: “superradiance” that extends over an entire supercrystal.

Scientific Approach and Accomplishments

Stability studies: We used pressure to study both NC stability and NCSL stability. Specifically, high-pressure diamond-anvil-cell (DAC) synchrotron Xray diffraction (XRD) studies of two series of core/shell QDs were conducted. Here, pressure was used to compare the relative stabilities of the core/shell systems against the tendency to form alloys. Namely, one system was anticipated to be highly susceptible to alloy formation via cation-cation migration and alloying, while the other was presumed less likely to alloy as the mechanism of alloy formation would have to be mediated by anion-anion exchange. Results from this analysis were published as part Publication Acharya et al. J. Am. Chem. Soc. 2015. Interestingly, we found that the system most susceptible to alloying in the solution phase, in particular during synthesis and

shell growth (CdSe/ZnSe core/shell NCs) was highly stable to both post-synthesis heating (to 310 °C) and to pressure (to 10.7 GPa) as investigated by obserserving effects on NC photoluminescence properties. Interestingly, we found that under high pressure, the core and shell behave independently. Consistent with literature, the wurtzite CdSe core transforms to the rock salt crystal structure above ~5.6 GPa and then to zinc blende upon return to 0 GPa. As expected for ZnSe (phase-transition pressure ≈ 13 GPa, the shell is unaffected by our experiment (~10 GPa) (Figure 1). The post-synthesis integrity of core/shell CdSe/ZnSe supports the hypothesis that surface-related processes during shelling are key to effecting shell versus alloy formation, rendering these NCs candidate building blocks for high-pressure formation and studies of NCSLs comprising core/shell semiconductor NCs. Second, we published new results pertaining to NCSL stability in Quan et al. PNAS 2014. Specifically, we observed that different structural polymorphs with very similar energetics can be made by slight changes in growth conditions. To our knowledge, this was the first direct experimental validation of a complex energy landscape for NCSL self-assembly. Our results suggested that fundamental thermodynamic driving forces can be harnessed to tailor specific assemblies of potential technological significance.

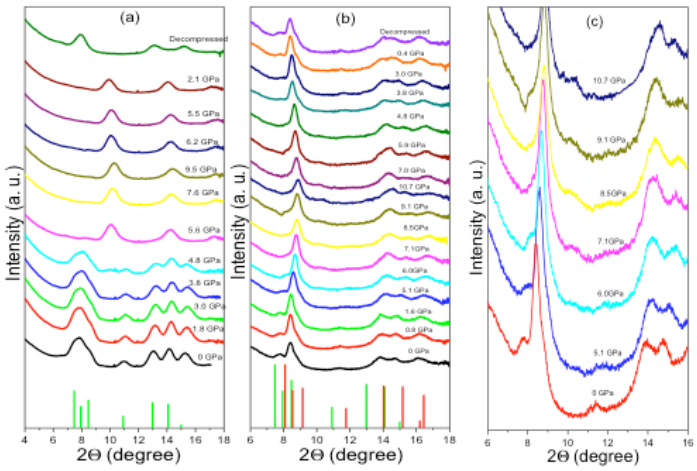

Figure 1. High-pressure X-ray diffraction patterns of (a) wurtzite CdSe core, (b) wurtzite CdSe/ZnSe (5 monolayer) core/shell QDs, (c) magnified pattern of (b) from 0 to 10.7 GPa. The weak and broad peaks shown in the green rectangle in (c) can be attributed to the rock salt (200) reflection of the high-pressure CdSe core. Green stick pattern is the bulk wurtzite CdSe reference pattern, and the red stick pattern is bulk wurtzite ZnSe.

New NCSL structures through pressure: We grew large single three-dimensional supercrystals from colloidal Pt nanocubes (NCus) and use a synchrotron-based two circle diffractometer to obtain an unprecedented level of structural detail from full sets of small/wide-angle X-ray scattering (SAXS/WAXS) patterns. Automatic indexing and simulations of X-ray patterns enabled detailed reconstruction of NCu translation and shape orientation within the supercrystals from atomic to mesometric levels. Individual NCu were found to orient themselves in a manner of atomic Pt[111] parallel to superlattice Rh[111]. We analyzed the superlattice structure in the context of three spatial relationships of proximate NCis including face-to-face, edge-to-edge, and corner-to-corner configurations. Detailed analysis of supercrystal structure revealed nearly direct corner-to-corner contacts and a tight interlocking NCu structure. We employed the correlations between strain and lattice distortion and established the first structural correlating mechanism between five superlattice polymorphs to elucidate the superlattice transformations and associated developing pathways. Although focused on a single component of our targeted binary superlattices – the metal NC framework – the developed experimental and modeling approaches together with the new understanding provide key information toward controlling design large-volume fabrication of NC functional materials with tailored structures and properties. This work was published in Li et al. Nano Lett. 2015.

New binary NCSLs: We made significant progress in our efforts to prepare phase-pure/discrete NCSLs in microfluidic droplet "microreactors." We identified this approach (only a single report in the literature on this novel application of microfluids to crystal growth) as the only clear route to obtaining large NCSLs phase separated from amorphous NC aggregates and even other NCSLs. We did so using both "well-behaved" NCs of uniform size/shape and ultimately also using the functionally more interesting larger and less uniform thick-shell quantum dots (giant QDs) and their hybrids with gold NCs, with the aim of realizing truly "collective" optical properties from the mixed excitonic-plasmonic systems. We obtained parameters for electrostatic NCSL formation, e.g., concentration of "screening" ions (as small charged NCs or salt additives), NC concentration, time, non-solvent concentration. Nevertheless, structural characterization and isolation of these types of NCSLs were challenged by difficulties faced in separating the NCSLs from the non-volatile medium in which they were prepared. For this and other reasons, we ultimately returned to the more conventional approach of growing NCSLs in non-aqueous media. With these new NCSLs we conducted simultaneous pressure and photoluminescence measurements. These data are currently being analyzed and we anticipate will be the subject of a fourth and final paper from this effort.

Impact on National Missions

The effort directly addresses Basic Science focus areas,

including Materials for the Future focus areas in advancing the understanding of materials functionality through co-design using extreme conditions, in situ measurements and User Facilities, as we made use of capabilities located at LANL CINT and Cornell's High-energy synchrotron source for x-ray scattering analysis (the CHESS facility). The work is also clearly responsive to envisioned MaRIE mission areas, especially "high-pressure nanoscience." We also support a focus area in developing multi-functional materials architectures to transform structure/function integration, performance and emergent properties. The capabilities and new understanding developed as part of the program will lay the groundwork for future programs in hybrid nanomaterials with potential applications in efficient lighting, light-based communication and information processes, and sensors. Beyond "light": the targeted ability to precisely organize interacting-nanocrystal superstructures comprising components of selected composition/functionality is key for energy harvesting (solar, thermoelectrics), catalysis, and energy storage, where coupled interfacial (e.g., charge-separation/transfer) and extended-transport issues dominate.

Publications

Acharya, K. P., H. M. Nguyen, Paulite, Piryatinski, J. u. n. Zhang, J. L. Casson, Xu, H. a. n. Htoon, and J. A. Hollingsworth. Elucidation of Two Giants: Challenges to Thick-Shell Synthesis in CdSe/ZnSe and ZnSe/CdS Core/Shell Quantum Dots. 2015. JOURNAL OF THE AMERICAN CHEMICAL SOCIETY. 137 (11): 3755.

Li, , Bian, Wang, Xu, J. A. Hollingsworth, Hanrath, Fang, and Wang. An Obtuse Rhombohedral Superlattice Assembled by Pt Nanocubes. 2015. NANO LETTERS. 15 (9): 6254.

Quan, Z., D. Wu, J. Zhu, W. H. Evers, J. M. Boncella, L. D. A. Siebbelese, Z. Wang, A. Navrotsky, and H. Xu. Energy landscape of self-assembled superlattices of PbSe nanocrystals. 2014. Proceedings of the National Academy of Sciences . : 9054–9057.

Interactions of Electrons with Quantum-Confined Systems Probed by Scanning Tunneling Spectroscopy

Victor I. Klimov
20140495ER

Abstract

The beneficial aspects of quantum confinement as a means for controlling light-matter interactions are well documented. On the other hand, the influence of confinement on interactions of solids with charged particles (electrons and holes) still remains largely unexplored. The case of charge injection is particularly important as most of the practical devices make use of this type of excitation. One expected effect of confinement is a diminished role of momentum conservation, which might lead to an intriguing situation where interactions of electrons with matter are constrained only by energy conservation. This would have major implications for several detection/sensing technologies, where the use of nanostructures could greatly increase sensitivity, potentially up to the fundamental limit defined only by energy considerations. Here, we address this problem via comprehensive studies of interactions of single electrons/holes with individual semiconductor nanocrystals (NCs). The specific focus is on impact ionization (ImI), that is, the collision of an injected charge with a valence-band electron, which is subsequently promoted to the conduction band. Electrons at well-defined energies are injected into the NCs from the tip of a scanning tunneling microscope and the ImI efficiency is inferred from measurements of the resulting luminescence and/or photocurrent. In addition to single-NC sensitivity, this methodology provides comprehensive information on how the structure of electronic states and carrier dynamics in NCs relate to their morphology. This project is well aligned with the topic of "Revolutionize Measurements" of the "Science of Signatures" Pillar and can potentially lead to the enhancement of capabilities across a range of disciplines from radiation detection and remote sensing to quantum communication.

Background and Research Objectives

Impact ionization (ImI) in semiconductors is a process in which a hot conduction band electron collides with a valence band electron and promotes it into the conduction band. Following the first observation of ImI in Ge-based photodiodes in 1957, this process has been extensively studied for many different semiconductors. A crucial step in these measurements is the generation of a hot electron with a sufficient excess energy (of at least the band gap, Eg) to undergo ImI. A variety of excitation mechanisms have been employed including photoexcitation, electrical charge injection, and irradiation with energetic particles. These studies as a function of excess excitation energy have revealed that instead of an ideal staircase shape with an onset at Eg, the ImI quantum yield (QY) shows a nearly linear growth with a threshold that is greater than Eg. The electron-hole pair creation energy (εeh), defined as the energy needed to create an additional electron-hole pair (when above the ImI threshold) has also been found to be greater than the ideal limit of one band gap. These observations have been explained by additional energy losses associated with translational momentum conservation and phonon emission. This represents a fundamental problem in bulk semiconductor-based devices, which limits, for example, the internal gain in avalanche photodiodes and energy resolution in radiation detectors.

There are several factors that can potentially lead to the enhancement in ImI in quantum confined NCs. They include (i) the discrete structure of electronic states which inhibits phonon emission due to a "phonon bottleneck", (ii) enhanced Coulomb interactions due to increased proximity between interacting charges and reduced dielectric screening, and (iii) relaxation of translational momentum conservation. The latter effect is, perhaps, most important as the "kinetic" energy loss associated with momentum conservation provides the dominant contribution to εeh.

This project's goal is to explore interactions of single charges (electrons or holes) with individual quantum confined semiconductor nanocrystals. In order to achieve this, we make use of a unique research tool,

optical scanning tunneling microscope (STM) (Figure 1a,b), which has been under development at C-PCS for the few past years. It represents a low-temperature, ultrahigh vacuum (UHV) STM equipped with optical ports for photo-excitation and light collection. It combines the capability for atomic-scale imaging with the power of optical spectroscopies, which allows for monitoring either the light-emission properties of NCs excited by a tunneling current (ST-luminescence, STL) or changes in the tunneling current when the NC is exposed to light (light modulated ST-spectroscopy, LM-STS). Additionally, using scanning tunneling spectroscopy (STS), we are able to map the structure of quantum-confined states, and thus infer the effect of the initial charge-injection state (its energy, symmetry, and a spatial distribution of charge density) on the effect of ImI.

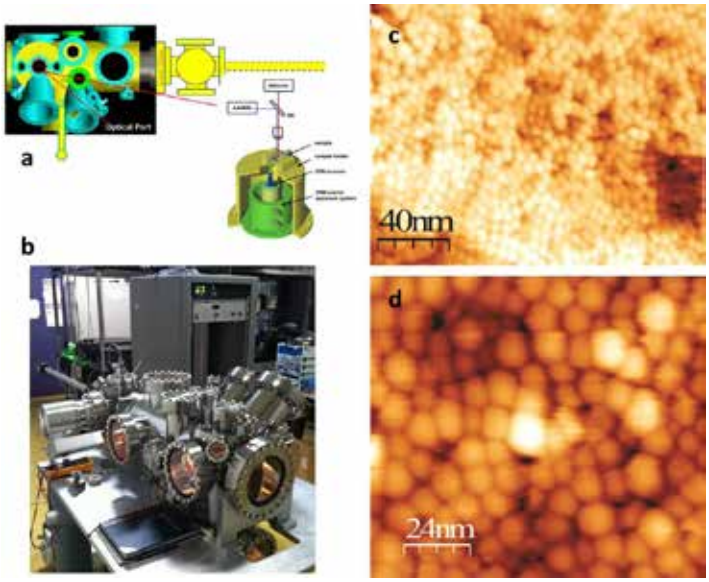

Figure 1. Drawing (a) and photograph (b) of the optical-access STM chamber with a special tip and head design (inset, panel a) that allows for optical excitation and efficient photon collection. (c,d) STM images of close-packed PbS nanocrystal layers obtained after special surface treatments and annealing that ensure removal of electrically insulating surface ligands and result in a film with high electrical conductivity.

Scientific Approach and Accomplishments

Optical Scanning Tunneling Microscope. A unique feature of the STM instrument developed as part of this project is a special design that allows for optical access to the sample and the tip through designated optical ports. In a classical STM head geometry, the STM tip together with the scanner unit is located above the sample substrate, which severely limits the solid angle from which optical signal can be collected. In our home-built STM, the scanners and the coarse approach motors are positioned below the sample substrate (see Figure 1a drawing and Figure 1b photograph). This geometry allows for unobstructed optical access either for photon collection or optical excitation. The STM system is housed in a UHV chamber for preventing sample contamination during the measurements. The second load-lock chamber is connected to the analysis chamber for quick sample loading from air (Figure 1a,b).

Scanning tunneling microscopy of nanocrystals. A key prerequisite for obtaining high quality STS information with or without optical excitation is the ability to image NCs with high spatial resolution. This ensures that the tunneling current feedback mechanism is stable enough to lock onto a selected NC when performing STS measurements. After testing numerous sample-preparation protocols, we have developed a reliable procedure for preparing “STM-grade” NC samples. It includes a special regime of spin-coating of a monolayer or multilayer NC film, ligand exchange to 1,2-ethanedithiol (EDT), and several well-defined annealing cycles in a vacuum oven or in the STM pre-chamber. This procedure allows for obtaining high quality STM images of colloidal nanoparticles as illustrated in Figure 1c,d, which displays a film of PbS NCs imaged with different scan windows and resolutions.

Scanning tunneling spectroscopy of nanocrystals. The STS technique allows us to study the electronic properties of the NCs. By electrically biasing the STM tip and bringing it in close proximity to a single NC, we can induce tunneling of electrons from the STM tip (tungsten in our case) into unoccupied quantum states of the NCs. Conversely, by reverting the bias voltage, we can collect electrons from the occupied states of the NC into the STM tip. These measurements can be used to gain knowledge of electronic structure in the individual NCs, including the band gap energy and the local density of states in NC’s conduction or valence band.

Figure 2 (top panel) displays the tunneling current between the STM tip and the PbS NC as a function of tip-to-sample bias voltage. As shown in the top panel, the tunneling current essentially vanishes in the region between −0.7 and 0.7 V. This region corresponds to the QD band gap where the density of states vanishes. For a more accurate analysis of the data, we plot the logarithm of the tunneling current as a function of bias voltage (Figure 2, bottom panel). Based on this plot we obtain that the apparent band gap of the specific NC probed in these measurements is 1.2 eV. In order to obtain a true band gap (Eg) based on the apparent value, we consider the interaction of the tip with the NC and the NC with the substrate within a so-called double barrier tunneling junction model (Figure 3a) and also account for the polarization correction to the band-gap energy.

According to refs 1 and 2, the bias (ΔVbias) measured by the STS technique, which corresponds to the energy sepa-

ration between the band-edge electron and hole states of the NC, can be related to Eg by the following expression: ΔVbias= (Eg + 2Σ)/η, where η is the division factor, which accounts for a finite capacitance between the NC and the substrate (CNC-Sub). The value of η can be calculated from the expression η = CNC-Sub (CNC-Sub + CTip-NC-Sub)-1 = (1 + C)-1 , where CTip-NC is the capacitance between the STS tip and the NC and C = CTip-NC/CNC-Sub [2]. Parameter C can be further related to the STS tip radius (rTip ~ 1nm), the NC radius (rNC), the effective dielectric constant of the medium (εEff), and the tip-NC (dTip-NC) and the NC-substrate (dNC-Sub) distances, as discussed in refs 1 and 2. In order to calculate εEff, we use the effective medium theory according to which (εEff - ε2)(εEff + 2ε2)-1 = ρ(εNC - ε2)(εNC + 2ε2)-1, where ρ is the volume fraction of the semiconductor in the NC film, εNC is the dielectric constant of the semiconductor (εNC = 161 for PbS), and ε2 = 1 for vacuum. Based on the above formalism, for the parameters of our STM experiment the division factor η is ca. 0.65.

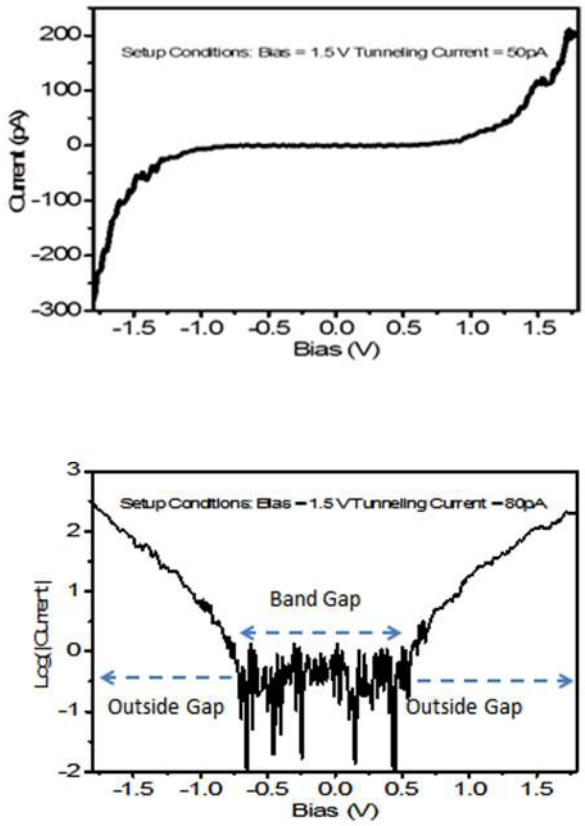

Figure 2. Current-voltage measurements of PbS quantum dots obtained by scanning tunneling spectroscopy with the band gap determined by the bias voltage region corresponding to a vanishing tunneling current. The top panel is a linear vertical scale, while the bottom panel is a logarithmic representation.

To calculate the electron polarization energy, Σ, we use theory of ref 2, which yields the dependence shown in Figure 3b. As evident from this plot, for samples studied in the present project (Eg < 1 eV), the correction due to Σ is quite small and does not exceed ~50 meV. Therefore, we neglect it in our analysis and assume that the "bias gap" can be directly related to the true band gap by factor η, i.e., Eg = η ΔVbias. Based on the data in Figure 2, ΔVbias = 1.2 eV, which leads to Eg = 0.78 eV. This value is remarkably close to the band gap of ~0.7 eV inferred from the optical measurements on the ensemble PbS NC sample.

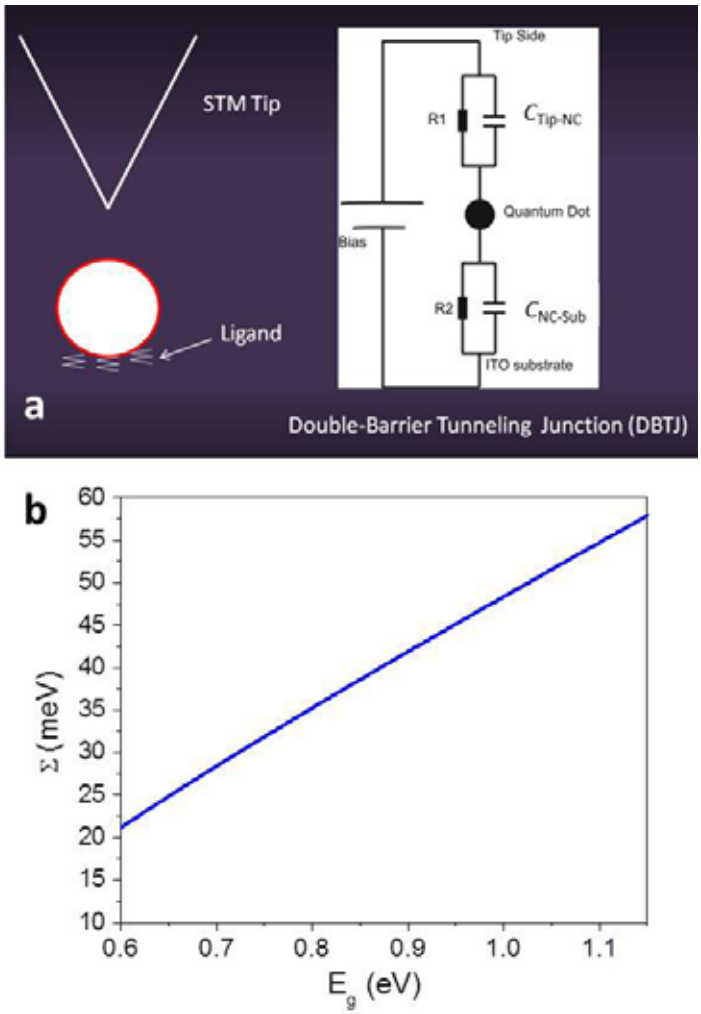

Figure 3. (a) Schematic of the double-barrier tunneling junction model that accounts for voltage drops at the QD-tip and QD-substrate gaps. (b) The dependence of the polarization energy on NC band gap.

Light-modulated scanning tunneling spectroscopy. As part of this project, we have also developed a capability for light-modulated scanning-tunneling spectroscopy (LM-STS), which is still a unique tool even in laboratories specializing in advanced STM measurements. To enable LM-STS studies, we have integrated a continuous wave (cw) 532-nm laser excitation source into the STM apparatus. The laser beam has been directed onto the studied sample through the top optical port of our instrument.

Its intensity has been modulated by electronics in order to avoid vibrations introduced by a mechanical chopper and the tunneling current was recorded as a function of time while the applied bias was slowly ramped from -2.5 V to 2.5 V. Figure 4a displays the I-V curve obtained from these measurements. As expected, the tunneling current increases upon photoexcitation (ON state) and drops back to the "dark" value (OFF state) when the laser beam is blocked. The difference between the ON and OFF currents yields the contribution purely due to photo-injected carriers, which can be treated as a photocurrent in, e.g., a traditional photodetector.

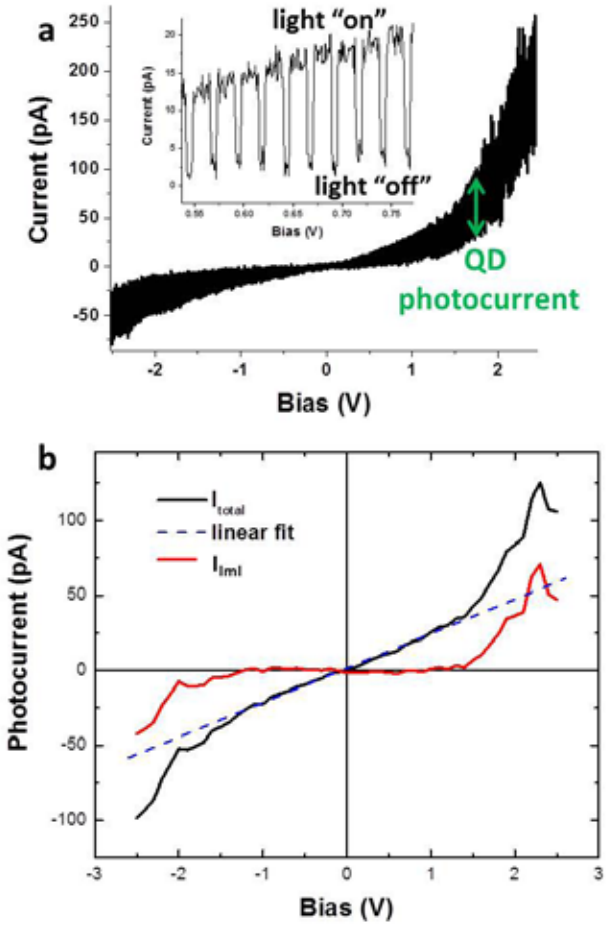

Figure 4. (a) Light-modulated scanning tunneling spectroscopy of PbS quantum dots with periodic on-off cycles in the laser excitation. The high-current envelope of the modulated spectrum corresponds to photoexcited quantum dots while dark tunneling is represented by the envelope with lower absolute values of the current. Inset of bottom panel shows a magnified view with visible on-off laser excitation cycles. (b) Photocurrent extracted from data in the top panel as a function of bias (black). The contribution due to ImI (red) is obtained by subtracting the linear fit (blue) to the "Ohmic" region from the total photocurrent.

The plot of the photocurrent (Iph) vs. tip bias is shown in Figure 4b. It displays a highly unusual behavior. For a standard photoconductor, the photocurrent would show an Ohmic behavior, i.e., a linear scaling between Iph and ΔVbias. We do observe such scaling up to biases of ~1.5 V, however, at higher voltages, the trend sharply changes to a fast super-linear growth. We believe this pronounced change is a sign of activation of ImI, that is, generation of additional electron-hole pairs via Coulombic collisions of photoinjected carriers with pre-existing valence-band electrons.

The model explaining our observations is depicted in Figure 5. PbS is characterized by mirror-symmetric conduction and valence bands. This symmetry implies that the energy of the incident photon (hv) in excess of the band gap is split equally between the conduction and the valence band, i.e., kinetic energies of a photogenerated electron and a hole (ΔEe and ΔEh, respectively) can be expressed as ΔEe = ΔEh = (hv - Eg)/2. In the present experiments ΔEe = ΔEh = (hv - Eg)/2 = (2.33 - 0.78)/2 = 0.78 eV. Based on the energy conservation requirement, in order for ImI to occur, the kinetic energy of the injected carrier must be at least equal to Eg. However, momentum conservation increases the threshold energy to ~1.5Eg, as discussed above. In our experiment, the kinetic energies of both the electron and the hole are around Eg, i.e., right at the energy-conservation-defined threshold but below the threshold expected if momentum conservation is taken into consideration. Therefore, ImI is unlikely in this situation and the photocurrent should exhibit a standard Ohmic behavior, as observed at low applied biases.

The transition to a non-Ohmic dependence observed at high biases likely relates to the electric-field-induced change in the mirror-symmetric picture of optical transitions. As was indicated by our previous STS measurements of PbS NCs [4], application of electric field can lead to mixing between states of different parity, which would make asymmetric transitions optically allowed. As a result, optical excitation can lead to the situation wherein one of the carriers "absorbs" most of the excess energy of the incident photon. For the parameters of our experiment, the carrier kinetic energy in the "asymmetric-excitation case" can reach the value of ~1.55 eV, which is equivalent to ~2Eg. This energy is sufficient to initiate ImI in the NCs, which likely leads to the sharp increase in the photocurrent detected at biases ΔVbias > 1.5 eV (Figure 4b).

In conclusion, we have developed a new unique experimental capability for simultaneous optical and STM/STS studies of nanomaterials and successfully applied it to colloidal NCs. An exciting result of these experiments is the first experimental observation of quantum-confined ImI at the single-NC level, which opens interesting opportunities for directly probing the effect of NC morphology on ImI

yields and ImI thresholds. We have also observed a considerable effect of applied electric field on the ImI efficiency, which we have attributed to field-induced modifications in optical selection rules due to mixing between states of different symmetries. This observation points towards practical strategies for enhancing ImI in existing NC materials as well as nanostructures under development. In addition to semiconductor NCs, the newly developed capability can be applied to other types of nanomaterials for investigating the implications of material's structural parameters on their interactions with photons and electrons.

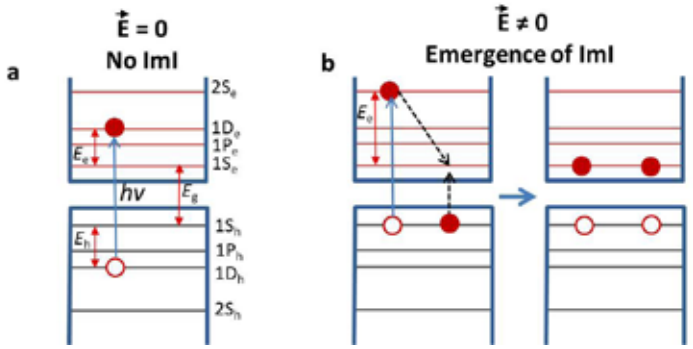

Figure 5. (a) Without electrical field, the excess energy of the incident photon (hv - Eg) is split equally between the photogenerated electron and hole; as a result the kinetic energy of either carrier is not sufficient to initiate ImI. (b) Applied electric field mixes states of different parity which makes asymmetric transitions (such as one shown by the green arrow) at least partially allowed. This increases the kinetic energy of one of the photogenerated carriers (an electron in the shown example) making it possible to trigger ImI (shown by dashed black arrows). As a result, absorption of a single photon produces two electron-hole pairs, which sharply increases the photocurrent.

Impact on National Missions

The proposed work directly addresses the Science of Signatures Pillar's "Revolutionize Measurements" Theme. This project pushes the boundaries in advanced instrumentation for studies of interactions of charged particles with individual nanostructures by combing scanning-probe and optical techniques. Further, this project exploits quantum confinement effects (e.g., relaxation of momentum conservation) for enhancing detection sensitivity. Since interactions of energetic radiation with matter are mediated by "hot" electrons, the investigated effects are directly relevant to radiation detection. Due to their potential use in infrared avalanche photodiodes, these studies also enhance capabilities in remote sensing and quantum communication, making these studies relevant to the Science of Signatures Pillar. Another application of impact ionization is for solar photovoltaics, relevant to the Lab's Energy Security mission. These studies also support the Materials Pillar and its underlying theme of materials-by-design with controlled functionality. Furthermore, the fundamental aspects of our work are also of interest to the DOE Office of Science.

References

1. Niquet, Y. M., C. Delerue, G. Allan, and M. Lannoo. Interpretation and theory of tunneling experiments on single nanostructures. 2002. Physical Review B. 65 (16): 165334.

2. Grinbom, G. A., M. Saraf, C. Saguy, A. C. Bartnik, F. Wise, and E. Lifshitz. Density of states in a single PbSe/PbS core-shell quantum dot measured by scanning tunneling spectroscopy. 2010. Physical Review B. 81 (24): 245301.

3. Moreels, I., K. Lambert, D. Smeets, D. De Muynck, T. Nollet, J. C. Martins, F. Vanhaecke, A. Vantomme, C. Delerue, G. Allan, and Z. Hens. Size-Dependent Optical Properties of Colloidal PbS Quantum Dots. 2009. ACS Nano. 3 (10): 3023.

4. Diaconescu, B., L. A. Padilha, P. Nagpal, B. S. Swartzentruber, and V. I. Klimov. Measurement of Electronic States of PbS Nanocrystal Quantum Dots Using Scanning Tunneling Spectroscopy: The Role of Parity Selection Rules in Optical Absorption. 2013. Physical Review Letters. 110 (12): 127406.

Unraveling Interfacial Charge and Energy Transfer Processes in Single Layer 2D Transition Metal Dichalcogenides

Aditya Mohite
20140540ER

Abstract

Transition metal dichalcogenides (TMDs) exhibit remarkable electronic and optical properties arising from the reduced dimensionality of a single unit cell perpendicular to the crystal plane that hold the promise for transformational research and development for next generation thin film optoelectronic applications. Unlike the semi-metal graphene (zero electronic band-gap), TMDs such as MoS2, MoSe2, WS2, WSe2, GaS, GaSe, InAs etc. are intrinsic semiconductors with band gaps spanning the entire solar spectrum. This provides a unique opportunity to create layered homo and heterostructures by combining two or more layers of these 2D materials and tailoring their interfacial properties to pave the path for current applications in phototransistors, photovoltaics, photodetectors, photo-catalysis (H2 evolution/water splitting) and light emitting devices (LEDs) and transformational technologies in spin and valley-optoelectronics. However in order to take advantage of the rich optoelectronic properties, it is critical to understand the charge generation, recombination and separation processes at the homo (create by two layers with semiconducting phase (2H) and/or metallic phase (1T) see Figure 3) or and hetero interfaces (created by dissimilar TMDs with semiconducting or metallic phase). Here we explore the properties of single atomic layers of TMDs and how to tailor the flow of carriers and energy at interfaces with other materials or electrodes in practical devices for photo-detectors, photovoltaics and light emitting.

Background and Research Objectives

The demand for clean energy is expected to force our civilization to research alternative, efficiency green energy sources. One of the leading prospects is light to energy conversion technologies such as photovoltaics and photo-electrochemical cells. Since the last 40 years, several photovoltaics technologies have been developed. In the pursuit of high efficiency per dollar, single crystalline wafer technology has been followed by nanostructure based thin film solar cells that rely on multi interface heterojunctions to separate light generated positive and negative charges to their respective electrodes. Several nanostructured materials have been tried and tested over the last two decades, but the ultimate goal of achieving high efficiency at low cost has not been achieved.

Understanding optical, electrical and structural properties of single layer TMDs

A key first step in developing a heterostructure-based device is to add to the limited knowledge about the intrinsic optical electronic and structural properties of each element as a single layer and multilayered forms [1,2]. We applied a host of powerful new and previously established correlated techniques (described in the scientific approach section) along with theoretical modeling to understand the nature of optical and transport properties such as the nature of excited states, absorption coefficients, binding energies of optically generated electrons and holes, recombination lifetimes, charge carrier mobilities, diffusion lengths, density of defects, etc. These figures of merit will be critical in basic design of the MoS2 and MoSe2 homo and heterostructure interface and will set the platform for characterizing the photo- physical properties arising at the interface.

Understanding the competition between charge separation and recombination across interface in heterostructures

A mandatory requirement for designing any optoelectronic device based on a homo or hetero interfaces is to understand the competition between charge separation and recombination. For instance, for a photovoltaic or photodetector device an efficient charge separation is preferred over recombination, while in an LED a high quantum yield of charge recombination at the interface is desired. We applied previously tested interface sensitive novel techniques to quantify the charge dissociation efficiency at the homo and hetero interfaces of MoS2 and MoSe2.

Develop proof of concept optoelectronic device

From the understanding gained from the above task, we will develop prototype heterostructure based thin film optoelectronic devices based on 2D materials that will offer tremendous advantages in its spectral response, sensitivity, stability and flexibility over existing nanoparticle thin film devices where the number of interfaces can be within the thermodynamic limits.

Scientific Approach and Accomplishments

Phase-engineered low resistance contacts for single-layer 2D TMD transistors and detectors

Part of this work was dedicated to finding solutions to reduce the contact resistance between semiconducting single layer TMDs and metal electrodes, in order to improve the performances of transistor and detector devices. To achieve this goal, we have developed at "phase-engineering" method to locally modify the phase of the TMD materials from semiconducting to metallic under the contact electrodes [1-3] (Figures 1 and 2).

This results in the reduction of contact resistance between the TMDs and metal electrodes by one order of magnitude, from 1.5 kΩ.µm down to 0.225 kΩ.µm. In other words, this results in a significant reduction of the Schottky potential barriers at the interface between the TMD and electrodes, by at least one order of magnitude from about 100 meV to below 25 meV [4] (Figure 4). To test the improvement of performances in (opto-)electronic devices, we fabricated field-effect transistors (FETs) and photo-detectors following conventional architectures as sketched in Figure 1, where the top metallic electrodes plays the role of source and drain and the doped Si(n++) acts as gate for the transistors. Using our phase-engineering method, we were able to improve the performances of these devices (Figures 3 and 4). In transistors all figures of merit are improved in the phase-engineered transistors as compared to the conventional devices (Figure 3), notably the mobility and on/off ratio are improved by several times [1,2]. Moreover, the responsivity (ability to convert light into electricity) of the photo-detectors is improved by more than 30 times in the phase-engineered devices [4].

Tailoring charge and energy flow at interfaces via materials control and heterostructures

The second approach to this project was to directly study the effect of the chemical composition and crystalline quality of the TMDs as well as metal contact choice on the charge and energy transfer at interfaces, either TMD/electrode contact interface or TMD heterostructure. The latter consists in the stacking of different types of 2D materials that can lead to new properties/functionalities of the heterostructures as compared to materials taken individually.

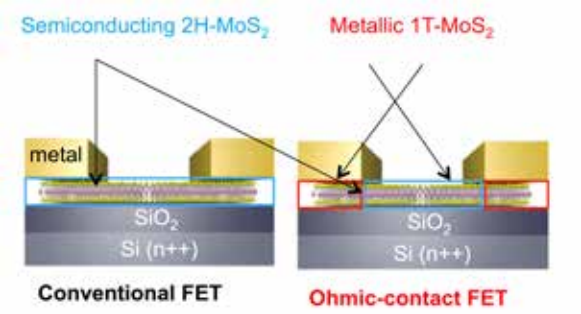

Figure 1. Phase-engineering of single layer TMDs to reduce contact resistance in (opto-) electronic devices. Typical devices for transistor and photo-detector applications; (left) conventional and (right) phase-engineered devices.

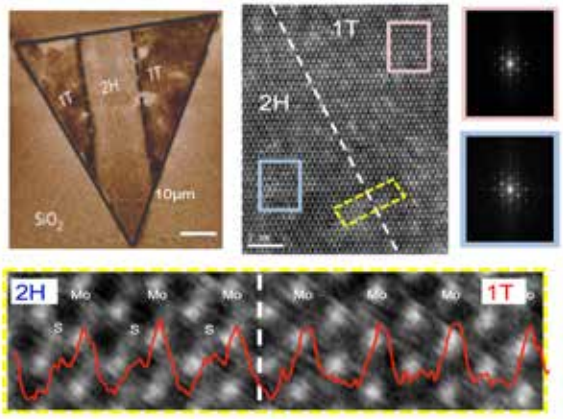

Figure 2. Examples of local phase modification of TMDs from semiconducting 2H-phase to metallic 1T-phase. (top-left) Electrostatic force microscopy. (right and bottom) Scanning transmission electron microscopy showing that the interface between 2H and 1T-phases is one atom thick.

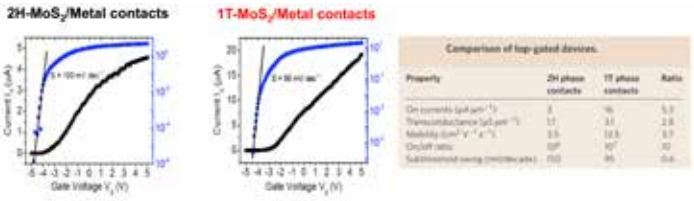

Figure 3. Figures of merit of field-effect transistors.

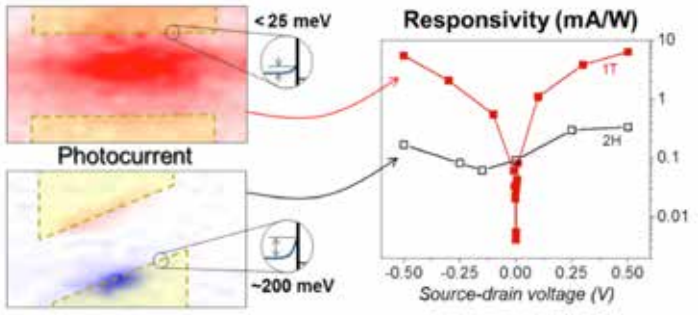

Figure 4. Photo-detector performances (right) and photocurrent distribution (left) resulting from change of Schottky barrier height (inset).

Here we developed some of the most successful single layer 2D materials obtained by exploring and developing new growth approaches to fabricate: (i) ultra-crystalline MoS2 using different precursor materials in chemical vapour deposition technique [5,6]. (ii) Ultra-thin optoelectronic devices were fabricated with active materials 2D ternary CuIn7Se11 and yields promising properties applications in ultra-thin photovoltaic devices7. (iii) InSe2 single layers [8] were used to fabricate photo-detectors with responsivity ~35 mA/W with fast response < 500 µs.

In addition, we have explored heterostructures where we combine one 2D TMD material with different types of interface materials in order to tailor the intrinsic electronic and optical properties [9. 10] of the whole system. (i) By inserting a hBN buffer layer between a single layer MoS2 and silicon substrates we were able to enhanced the physical properties of the 2D materials and therefore of the optoelectronic devices fabricated with this architecture [11]. (ii) By growing a Ge thin film on top of single layer MoS2 we observed impressive change of the transport properties of both materials, i.e. MoS2 transistor change polarity and undoped Ge becomes highly conducting, which are explained by charge transfer at the heterostructure interface [12]. (iii) Recently we also combined MoS2 2D layers with thin film organic-inorganic perovskite [13] and we have demonstrated that photodetector device properties can be tailored by changing the electronic properties of the 2D MoS2. (iv) Finally we demonstrate proof of concept for the synthesis of MoS2/WS2 composites which yield new functionalities which will be further explored in the future [14].

Application of TMDs for electrochemistry

In this project, we also discovered that the design principles that are important for achieving high efficiency devices are also critical for electrocatalysis using TMDs and was another major outcome of this project. Several papers were published in this area as well. [15-17]

Impact on National Missions

The novel physical phenomena we aimed to explore in this project will pave the way to make TMDCs viable asset in LANLs science pillar of materials for the future. The formation of interface states between TMDCs with an understanding of their fate and transport will allow us to go beyond intrinsic optical and electronic properties. This project, therefore, directly addresses the materials strategy of controlled functionality by tailoring materials to perform beyond their basic properties. The successful completion of this ER could lead to LANL opportunities and pave the way for future funding by BES and EERE.

References

1. Kappera, , Voiry, S. E. Yalcin, Branch, Gupta, A. D. Mohite, and Chhowalla. Phase-engineered low-resistance contacts for ultrathin MoS2 transistors (vol 13, pg 1128, 2014). 2014. NATURE MATERIALS. 13 (12).

2. Kappera, , Voiry, S. E. Yalcin, Jen, Acerce, S. o. l. Torrel, Branch, Lei, Chen, Najmaei, J. u. n. Lou, P. M. Ajayan, Gupta, A. D. Mohite, and Chhowalla. Metallic 1T phase source/drain electrodes for field effect transistors from chemical vapor deposited MoS2. 2014. APL MATERIALS. 2 (9).

3. Voiry, , Mohite, and Chhowalla. Phase engineering of transition metal dichalcogenides. 2015. CHEMICAL SOCIETY REVIEWS. 44 (9): 2702.

4. Yamaguchi, , Blancon, Kappera, Lei, Najmaei, B. D. Mangum, Gupta, P. M. Ajayan, J. u. n. Lou, Chhawalla, J. J. Crochet, and A. D. Mohite. Spatially Resolved Photoexcited Charge-Carrier Dynamics in Phase-Engineered Mono layer MoS2. 2015. ACS NANO. 9 (1): 840.

5. Bilgin, , Liu, Vargas, Winchester, M. K. L. Man, Upmanyu, K. M. Dani, Gupta, Talapatra, A. D. Mohite, and Kar. Chemical Vapor Deposition Synthesized Atomically Thin Molybdenum Disulfide with Optoelectronic-Grade Crystalline Quality. 2015. ACS NANO. 9 (9): 8822.

6. Saenz, G. A. L., C. Biswas, H. Yamaguchi, and C. N. Villarrubia. Effects of Synthesis Parameters on CVD Molybdenum Disulfide Growth. 2016. MSR Adv.. 1 (32): 2291.

7. Lei, , A. l. i. Sobhani, Wen, George, Wang, Huang, P. e. i. Dong, B. o. Li, Najmaei, Bellah, Gupta, A. D. Mohite, Ge, J. u. n. Lou, N. J. Halas, Vajtai, and Ajayan. Ternary CuIn7Se11 : Towards Ultra-Thin Layered Photodetectors and Photovoltaic Devices. 2014. ADVANCED MATERIALS. 26 (45): 7666.

8. Lei, S., L. Ge, S. Najamaei, A. George, R. Kappera, J. Lou, M. Chhowalla, H. Yamaguchi, G. Gupta, R. Vajtai, P. Ajayan, and A. Mohite. Evolution of the Electronic Band Structure and Efficient Photo-Detection in Atomic Layers of InSe. 2014. ACS NANO. 8 (2): 1263.

9. Seo, , Yamaguchi, A. D. Mohite, Boubanga-Tombet, Blancon, Najmaei, P. M. Ajayan, J. u. n. Lou, A. J. Taylor, and R. P. Prasankumar. Ultrafast Optical Microscopy of Single Monolayer Molybdenum Disulfide Flakes. 2016. SCIENTIFIC REPORTS. 6.

10. Opto-valleytronics imaging of atomically thin semiconductors. To appear in Nat. Nanotechnol..

11. Man, M. K. L., Deckoff-Jones, Winchester, Shi, Gupta, A. D. Mohite, Kar, Kioupakis, Talapatra, and K. M. Dani. Protecting the properties of monolayer MoS2 on silicon based substrates with an atomically thin buffer. 2016. SCIENTIFIC REPORTS. 6.

12. Lin, Y. C., I. Bilgin, T. Ahmed, R. Chen, D. Pete, S. Kar, J. X. Zhu, G. Gupta, A. Mohite, and J. Yoo. Charge transfer in crystalline germanium/monolayer MoS2 heterostructures prepared by chemical vapor deposition . 2016. Nanoscale. 8: 18675.

13. Wang, Y., R. Fullon, M. Acerce, C. Petoukhoff, J. Yang, C. Chen, S. Du, S. K. Lai, S. P. Lau, D. Voiry, D. O'Carroll, G. Gupta, A. Mohite, S. Zhang, H. Zhou, and M. Chhowalla. Solution-Processed MoS2/Organolead Trihalide Perovskite Photodetectors. 2016. Advanced Materials. : 0.

14. Delgado, A., J. A. Catalan, H. Yamaguchi, and C. N. Villarrubia. Characterization of 2D MoS2 and WS2 Dispersed in Organic Solvents for Composite Applications. 2016. MRS Advances. 1 (32): 2303.

15. Cummins, D. R., Martinez, Sherehiy, Kappera, Martinez-Garcia, R. K. Schulze, Jasinski, Zhang, R. K. Gupta, J. u. n. Lou, Chhowalla, Sumanasekera, A. D. Mohite, M. K. Sunkara, and Gupta. Efficient hydrogen evolution in transition metal dichalcogenides via a simple one-step hydrazine reaction. 2016. NATURE COMMUNICATIONS. 7.

16. Cummins, D. R., Martinez, Kappera, Voiry, Martinez-Garcia, Jasinski, D. a. n. Kelly, Chhowalla, A. D. Mohite, M. K. Sunkara, and Gupta. Catalytic Activity in Lithium-Treated Core-Shell MoOx/MoS2 Nanowires. 2015. JOURNAL OF PHYSICAL CHEMISTRY C. 119 (40): 22908.

17. Voiry, , Fullon, Yang, C. d. C. Castro e Silva, Kappera, Bozkurt, Kaplan, M. J. Lagos, P. E. Batson, Gupta, A. D. Mohite, Dong, Er, V. B. Shenoy, Asefa, and Chhowalla. The role of electronic coupling between substrate and 2D MoS2 nanosheets in electrocatalytic production of hydrogen. 2016. NATURE MATERIALS. 15 (9): 1003.

Publications

Opto-valleytronics imaging of atomically thin semiconductors. To appear in Nat. Nanotechnol..

Bilgin, , Liu, Vargas, Winchester, M. K. L. Man, Upmanyu, K. M. Dani, Gupta, Talapatra, A. D. Mohite, and Kar. Chemical Vapor Deposition Synthesized Atomically Thin Molybdenum Disulfide with Optoelectronic-Grade Crystalline Quality. 2015. ACS NANO. 9 (9): 8822.

Cummins, D. R., Martinez, Kappera, Voiry, Martinez-Garcia, Jasinski, D. a. n. Kelly, Chhowalla, A. D. Mohite, M. K. Sunkara, and Gupta. Catalytic Activity in Lithium-Treated Core-Shell MoOx/MoS2 Nanowires. 2015. JOURNAL OF PHYSICAL CHEMISTRY C. 119 (40): 22908.

Cummins, D. R., Martinez, Sherehiy, Kappera, Martinez-Garcia, R. K. Schulze, Jasinski, Zhang, R. K. Gupta, J. u. n. Lou, Chhowalla, Sumanasekera, A. D. Mohite, M. K. Sunkara, and Gupta. Efficient hydrogen evolution in transition metal dichalcogenides via a simple one-step hydrazine reaction. 2016. NATURE COMMUNICATIONS. 7.

Delgado, A., J. A. Catalan, H. Yamaguchi, and C. N. Villarrubia. Characterization of 2D MoS2 and WS2 Dispersed in Organic Solvents for Composite Applications. 2016. MRS Advances. 1 (32): 2303.

Kappera, , Voiry, S. E. Yalcin, Branch, Gupta, A. D. Mohite, and Chhowalla. Phase-engineered low-resistance contacts for ultrathin MoS2 transistors (vol 13, pg 1128, 2014). 2014. NATURE MATERIALS. 13 (12).

Kappera, , Voiry, S. E. Yalcin, Jen, Acerce, S. o. l. Torrel, Branch, Lei, Chen, Najmaei, J. u. n. Lou, P. M. Ajayan, Gupta, A. D. Mohite, and Chhowalla. Metallic 1T phase source/drain electrodes for field effect transistors from chemical vapor deposited MoS2. 2014. APL MATERIALS. 2 (9).

Lei, , A. l. i. Sobhani, Wen, George, Wang, Huang, P. e. i. Dong, B. o. Li, Najmaei, Bellah, Gupta, A. D. Mohite, Ge, J. u. n. Lou, N. J. Halas, Vajtai, and Ajayan. Ternary CuIn7Se11 : Towards Ultra-Thin Layered Photodetectors and Photovoltaic Devices. 2014. ADVANCED MATERIALS. 26 (45): 7666.

Lei, S., L. Ge, S. Najamaei, A. George, R. Kappera, J. Lou, M. Chhowalla, H. Yamaguchi, G. Gupta, R. Vajtai, P. Ajayan, and A. Mohite. Evolution of the Electronic Band Structure and Efficient Photo-Detection in Atomic Layers of InSe. 2014. ACS NANO. 8 (2): 1263.

Lin, Y. C., I. Bilgin, T. Ahmed, R. Chen, D. Pete, S. Kar, J. X. Zhu, G. Gupta, A. Mohite, and J. Yoo. Charge transfer in crystalline germanium/monolayer MoS2 heterostructures prepared by chemical vapor deposition . 2016. Nanoscale. 8: 18675.

Man, M. K. L., Deckoff-Jones, Winchester, Shi, Gupta, A. D. Mohite, Kar, Kioupakis, Talapatra, and K. M. Dani. Protecting the properties of monolayer MoS2 on silicon based substrates with an atomically thin buffer. 2016. SCIENTIFIC REPORTS. 6.

Saenz, G. A. L., C. Biswas, H. Yamaguchi, and C. N. Villarrubia. Effects of Synthesis Parameters on CVD Molybdenum Disulfide Growth. 2016. MSR Adv.. 1 (32): 2291.

Seo, , Yamaguchi, A. D. Mohite, Boubanga-Tombet, Blancon, Najmaei, P. M. Ajayan, J. u. n. Lou, A. J. Taylor, and R. P. Prasankumar. Ultrafast Optical Microscopy of Single Monolayer Molybdenum Disulfide Flakes. 2016. SCIENTIFIC REPORTS. 6.

Voiry, , Fullon, Yang, C. d. C. Castro e Silva, Kappera, Bozkurt, Kaplan, M. J. Lagos, P. E. Batson, Gupta, A. D. Mohite, Dong, Er, V. B. Shenoy, Asefa, and Chhowalla. The role of electronic coupling between substrate and 2D MoS2 nanosheets in electrocatalytic production of hydrogen. 2016. NATURE MATERIALS. 15 (9): 1003.

Voiry, , Mohite, and Chhowalla. Phase engineering of transition metal dichalcogenides. 2015. CHEMICAL SOCIETY REVIEWS. 44 (9): 2702.

Wang, Y., R. Fullon, M. Acerce, C. Petoukhoff, J. Yang, C. Chen, S. Du, S. K. Lai, S. P. Lau, D. Voiry, D. O'Carroll, G. Gupta, A. Mohite, S. Zhang, H. Zhou, and M. Chhowalla. Solution-Processed MoS2/Organolead Trihalide Perovskite Photodetectors. 2016. Advanced Materials. : 0.

Yamaguchi, , Blancon, Kappera, Lei, Najmaei, B. D. Mangum, Gupta, P. M. Ajayan, J. u. n. Lou, Chhawalla, J. J. Crochet, and A. D. Mohite. Spatially Resolved Photoexcited Charge-Carrier Dynamics in Phase-Engineered Mono layer MoS2. 2015. ACS NANO. 9 (1): 840.

Microstructure Based Continuum Process Modeling of Weapons Metals

Rodney J. Mccabe
20140630ER

Abstract

There is significant interest in the manufacturing sector in understanding the evolution in microstructure and properties that accompany thermo-mechanical processing to create engineering components. This is also true for the manufacture of uranium components that are of interest at Los Alamos. An improved understanding and models of these evolutions would allow for improvements in manufacturing design and greatly reduce scrap rates thus significantly reducing manufacturing costs and waste of nuclear materials. The purpose of this project was to develop a solid understanding of these evolutions in uranium and to develop modeling capabilities incorporating microstructure-evolution-based constitutive laws that integrate complex micro-scale physics of deformation and thermal behavior. Such a model would enable us to 1) gauge the properties of existing stockpile components, 2) analyze the sensitivity of manufacturing process variables, 3) examine alternative manufacturing processes resulting in similar microstructures and properties, and 4) directly assess the engineering performance of metal weapons parts in service. The LDRD team was comprised of leading researchers from MST, T, and Sigma divisions and collaborators from the University of New Hampshire and the University of Virginia.

The research team included graduate students, professors, and LANL scientists (both early career and advanced career) doing both modeling and experimental work. For this work, we combined rolling, forming, and annealing of uranium; microstructure characterization by electron backscatter diffraction (EBSD) and neutron diffraction techniques at the Lujan Center at LANSCE; and mean field and full field modeling of deformation and recrystallization. We made significant strides in understanding deformation processes and recrystallization of uranium and in developing modeling tools to predict the microstructures and properties that result from these processes.

Background and Research Objectives

Production of uranium and other metal weapons components requires complicated sequences of processes of mechanical deformation and thermal processes resulting in significant changes to microstructure and properties. The anisotropic microstructures and properties that result from wrought processing (thermo-mechanical processing) of uranium can cause significant problems for further processing and machining of engineering components, and result in non-uniform component properties. Previous uranium research resulted in a preliminary understanding and a mean-field based model of microstructure and property evolution during simple uranium deformation (simple tension and compression and bending). These models were not calibrated to large strain deformation typical of rolling and forming, are slow to scale up to the continuum level, and are not designed to model thermal annealing processes resulting in recrystallization. In fact, these models lack many microstructure details necessary to model recrystallization. There is a large body of work examining the recrystallization behavior of other metals, particularly metals with cubic crystal structures, but very limited efforts looking at the recrystallization behavior of low symmetry metals such as uranium.

The goal of this proposal was to establish rigorous microstructure-property relationships that accompany deformation and thermal processes and their effect on continuum level performance in uranium weapons components. This would be the first microstructure evolution based continuum modeling capability that incorporates the complex deformation behavior of these metals and the physics of thermal processing. To reach this goal, one objective was to integrate experiments and modeling to develop accurate constitutive laws describing the evolution of microstructure with thermal processing. A second objective was to develop a novel method for efficiently implementing the microstructure based constitutive laws into continuum level simulations.

Scientific Approach and Accomplishments

To reach these goals, our experimental approach was to define how the microstructural characteristics of recrystallizing uranium depend on the microstructural characteristics of differently deformation-processed uranium (i.e. different rolling schedules or rolling reductions) We characterized as-rolled and recrystallized microstructures for plates having undergone 3 different rolling schedules and, for one of the rolling schedules, seven different rolling reductions. In all cases we found that, relative to the deformed texture, the recrystallization texture is considerably weakened, and occurs without development of strong components that were not strong in the deformed material, which is in contrast to the behavior of many cubic metals. Our data strongly support the notion that recrystallization nucleation occurs along high angle grain boundaries in the deformed microstructure. There is no compelling evidence that either favored nucleation or favored growth has a significant effect on the recrystallization microstructure. The recrystallization texture is similar, but considerably weaker, than the deformation texture, and the texture of points along high angle grain boundaries in the deformed material is a good match for the recrystallization texture. In addition, while there is an orientation dependence on local misorientation, this dependence does not significantly affect the recrystallization texture. The distribution of high angle grain boundaries can be inhomogeneous within the microstructure, and nucleation of recrystallized grains correlates well with the spatial distribution of high angle boundaries. This inhomogeneous distribution of high angle boundaries causes clustered distributions of small and large grains, and twin boundaries, an important deformation mechanism in uranium, do not appear to act as recrystallization nucleation sites. These observations were validated by full-field recrystallization modeling results that have been submitted for publication.

Because of the previous work that had been done to develop mean-field models of the deformation behavior, it was desirable to try and use these models as the starting point for the recrystallization model. However, these experimental results compelled a fundamental change in the use of these models. A primary limitation of the standard mean-field formulation is that only the average values of the micromechanical fields such as the lattice rotation (and thus orientation) inside the grains are used to update the microstructure. With regard to recrystallization behavior, this approximation has two undesirable effects. Since intragranular misorientation is not accounted for, grain size reduction by grain fragmentation cannot be predicted based on strictly micromechanical considerations, and grain fragmentation is a primary means of increasing the high angle grain boundary contend during deformation processing. In addition, crystal orientations at high angle grain boundaries where recrystallization nucleation is expected to occur is no different than the average grain orientation. We have now developed an implementation of the mean-field model allowing us to calculate average intragranular fluctuations of lattice rotation rates in polycrystalline materials providing a measure of the trend of misorientation developing inside grains. The predicted lattice rotation rate distributions are now being used to estimate the evolution of average intragranular misorientations, which in turn are being used to extend the mean-field model to capture grain fragmentation and recrystallization based on micromechanical considerations.

Measured progress has been made in improving the speed of continuum level simulations of rolling and forming operations while incorporating microstructure based mean-field model at individual finite element integration points. We have developed a new implementation of a computationally efficient crystal plasticity model in a finite element framework where iterative solvers are replaced by a database of FFTs that allows for fast retrieval of the solution. The implementation has been validated for monotonic loading conditions and rolling for metals exhibiting simple deformation behavior and the predictions of the simulations compare favorably with experimental measurements. We also continue to incorporate the mean-field deformation model in FE as a user material sub-routine (UMAT). Significant improvements have been made to this approach by developing a new strain rate sensitive UMAT with improvements in computation speed of several times.

Impact on National Missions

The modeling tools developed in this program can be used to directly examine issues associated with manufacturing uranium components for programs of importance to LANL. With these tools, we will be simulating rolling and forming and annealing processes for actual components and predicting the residual stresses in the components after forming and recrystallization processes. These simulations will be used to survey the effects of various process parameter changes.

Publications

Ardeljan, M., R. J. McCabe, I. J. Beyerlein, and M. Knezevic. Explicit incorporation of deformation twins into crystal plasticity finite element models. 2015. COMPUTER METHODS IN APPLIED MECHANICS AND ENGINEERING. 295: 396.

Knezevic, M., J. Crapps, I. J. Beyerlein, D. R. Coughlin, K. D. Clarke, and R. J. McCabe. Anisotropic modeling of structural components using embedded crystal plasticity constructive laws within finite elements. 2016. International

Journal of Mechanical Sciences. 105: 227.

Lebensohn, R. A., M. Zecevic, M. Knezevic, and R. J. McCabe. Average intragranular misorientation trends in polycrystalline materials predicted by a viscoplastic self-consistent approach. 2016. Acta Materialia. 104: 228.

McCabe, R. J., A. W. Richards, D. J. Coughlin, K. D. Clarke, I. J. Beyerlein, and M. Knezevic. Microstructure effects on the recrystallization of low-symmetry alpha-uranium. 2015. Journal of Nuclear Materials. 465: 189.

Steiner, M. A., R. J. McCabe, E. Garlea, and S. R. Agnew. Monte Carlo modeling of recrystallization processes in alpha-uranium. Acta Materialia.

Zecevic, M., M. Knezevic, I. J. Beyerlein, and R. J. McCabe. Origin of texture development in orthorhombic uranium. 2016. Materials Science and Engineering A. 665: 108.

Zecevic, M., M. Knezevic, I. J. Beyerlein, and R. J. McCabe. Texture formation in orthorhombic alpha-uranium under simple compression and rolling to high strains. 2016. Journal of Nuclear Materials. 473: 143.

Zecevic, M., R. J. McCabe, and M. Knezevic. A new implementation of the spectral crystal plasticity framework in implicit finite elements. 2015. MECHANICS OF MATERIALS. 84: 114.

Solute and Microstructure Prediction during Processing (U)

Seth D. Imhoff
20140639ER

Abstract

Microstructure is fundamental to the properties and performance of a metal component. Because many of the important features of a microstructure are initially set during solidification, the ability to predict microstructural development during solidification is the first step in predictive materials property modeling. Another necessary step is being able to use this microstructure data to predict the properties of a material. We have made progress on both of these, first by developing a method of predicting spatially resolved microstructural features of cast metal parts from within Truchas, a part-scale, multi-physics casting code.

Our work on the microstructure-to-properties step has been to investigate how this microstructure data can be used in existing mechanical property simulation tools. One of the key features of this work has been to constantly compare simulation techniques to experiments in a way that is relevant to the MaRIE vision of data collection and analysis. Thus, model developments strongly rely on large amounts of experimental data gathered from a variety of beamline-type sources.

The largest volume of data for this project was collected using synchrotron x-ray radiation at the Argonne National Laboratory Advanced Photon Source (APS). Other beam-types and energies such as microfocus x-rays and proton radiography at LANL and electron radiography at Stanford Linear Accelerator Center were used as appropriate.

Background and Research Objectives

In many cases, solidification is the most influential time for microstructural development within a component. This is because many features of a microstructure (e.g. non-uniform distribution of alloying elements and the size, shape, and orientation of grains) are initially set during solidification and may not significantly change once the material is fully solid. Thus, linking processing to microstructure and microstructure to properties with experimentally-validated simulation techniques will make it possible to make spatially resolved predictions of the mechanical and chemical properties of a cast part. This type of information is particularly important to component designers who use simulations to assess how a particular part will perform in use.

It has been a long held goal of metallurgists to develop simulation techniques that can simulate a casting process to determine the microstructure of the part, and then use the microstructure data to compute spatially-resolved properties for the entire part. This goal seems reasonable since the link between processing conditions, microstructure, and material properties has been thoroughly studied and there are simulation techniques that can describe many of these phenomena; however, it is exceedingly difficult to combine these various methods because they operate at very different size/time scales. For example, many microstructural development models require a spatial discretization size on the order of a micrometer, whereas a continuum scale casting code has a total simulated domain of about a cubic meter. Performing micrometer-resolved simulations with scales like these would take on the order of several thousand years on a computer like LANL's new Trinity machine.

The goal of this work was to investigate and develop methods of bridging length/time scales or physical phenomena in computationally realistic ways. This was done in two ways:

- Add microstructural development and realistic solidification pathway modeling to an existing continuum-scale casting code
- Analyze state of the art methods of microstructure-to-properties modeling

An important feature throughout this work has been to validate the modeling efforts against experiments as of-

ten as possible. This is particularly true of the microstructure-to-properties work that uses experimental data as an initial condition and is compared to in-situ experimental measurements of material deformation behavior and overall mechanical properties.

Scientific Approach and Accomplishments

Microstructure modeling in Truchas

A flexible computational framework for microstructure modeling was implemented within Truchas, a LANL-developed multi-physics casting modeling code. The framework takes spatially-resolved data that is already computed in the heat and mass transfer portions of the simulation and passes it to a series of analytical models for predicting microstructure. These are time-dependent 0-D models, which makes them computationally inexpensive and also easy to extend to include additional physical phenomena in the future.

The first step of the microstructure model is to determine the growth morphology of the solid. There are three possible morphologies of the interface between the liquid and solid: planar, cellular, or dendritic; each of these are shown in Figure 1. For a given material, the growth morphology is largely determined by the thermal conditions at the solidification front, namely the temperature gradient (G) and solidification front velocity (V). Figure 1 shows a typical relationship between G, V, and growth morphology.

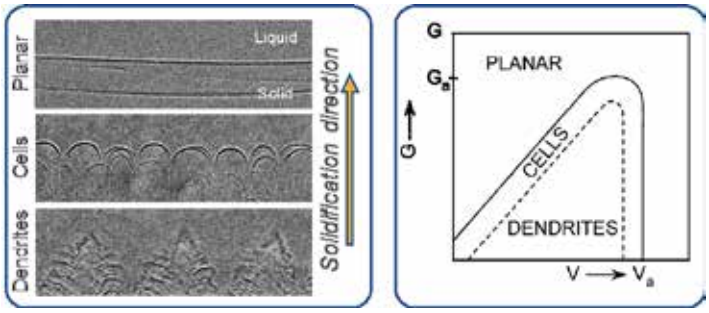

Figure 1. X-ray radiography images showing the three types of interfaces in an Al-Cu alloy. A typical growth morphology map is shown on the right. The dashed line between cells and dendrites reflects the difficulty in distinguishing these two morphologies very close to the transition.

For a fixed temperature gradient and low solidification speed, a planar interface is stable as it is the configuration that minimizes the total interfacial energy. With increasing interfacial velocity, the first growth morphology transition is from planar to cellular. This occurs because solute that is rejected from the growing solid phase piles up in front of the interface faster than diffusion can transport it away, which causes morphological instabilities on the interface to become stable and grow, eventually forming cells.

Continuing to increase the solidification speed at a constant gradient brings on the second transition from cells to dendrites. Dendrites are much like cells but in addition to the primary arms that are growing in the same direction as the overall solidification front, there are also secondary arms growing perpendicular to this. Because the most obvious difference between cells and dendrites is the presence of secondary branches on the dendrites, the distinction between these two growth modes is made by determining if there is enough space between the primary arms for secondary arms to grow and comparing this to the predicted primary dendrite arm spacing.

The nearly vertical lines on the right side of the plot, which show the transition to planar growth at very high interfacial speeds, are an interesting and important phenomena for certain processes like welding or additive manufacturing where it is possible to achieve solidification speeds that are on the order of meters per second; however, it is exceptionally rare to reach these speeds during casting processes, so the current model ignores this regime.

Once the growth morphology is known, it is possible to use the same input data to compute the feature sizes of the microstructure. For cellular growth morphology, this consists of the spacing between the cells and for a dendritic morphology, it is the spacing between the primary arms, as well as that between the secondary arms. These are important quantities because they are linked to mechanical properties like strength and ductility of a material. They also set the scale of chemical segregation, which determines the length of time required to homogenize the distribution of elements in a part.

To validate these new simulation capabilities, an experiment was performed in which a small (34 mm tall) wedge shaped casting was made and characterized. During the casting, temperatures of the mold were measured in 10 locations and the fluid-filling rate was measured with in situ proton radiography. This data was used to ensure that the existing heat and fluid flow were passing accurate information to the new microstructure portions of the code. The microstructure of the casting was analyzed and secondary dendrite arm spacings were measured and compared to those predicted by the simulation, as seen in Figure 2.

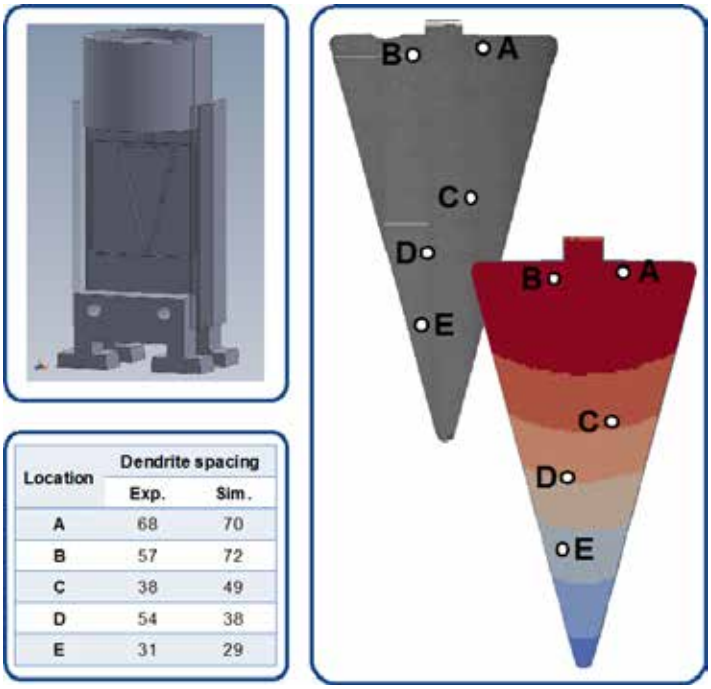

Location	Dendrite spacing	
	Exp.	Sim.
A	68	70
B	57	72
C	38	49
D	54	38
E	31	29

Figure 2. Schematic of the wedge shaped casting mold used in validating the microstructure modeling (top left). Microscopy image of the microstructure compared to predicted secondary dendrite arm spacings (right), and a table comparing these values at several points.

The second addition we have made to Truchas is the capability to input a tabulated solidification path, such as a table of phase fraction versus temperature. This modification now permits interfacing Truchas with thermodynamic equilibrium calculations, for instance using the CalPhaD method with the software ThermoCalc. One can now use any predefined solidification path, for instance using an equilibrium lever rule, or a Gulliver-Scheil model (liquid at equilibrium but no solid diffusion). This constitutes a first step towards including solute content influence in Truchas simulations.

In the example from Figure 3, we illustrate a test case for a simplified geometry of a square cross-section rod cooled down at both ends with a constant cooling rate and a constant temperature difference between them. We test six different solidification scenarios, namely using the lever rule or Gulliver-Scheil model for three different Al-Cu alloys at 5, 10, and 20 wt% Cu. While the temperature-time history is identical, the resulting solid fraction and local enthalpy measured at the center of the sample differ significantly. These differences could strongly affect the solidification at the continuum scale, for instance modifying the fluid flow in a casting of more complex geometry, in addition to affecting the formation of solidification microstructure.

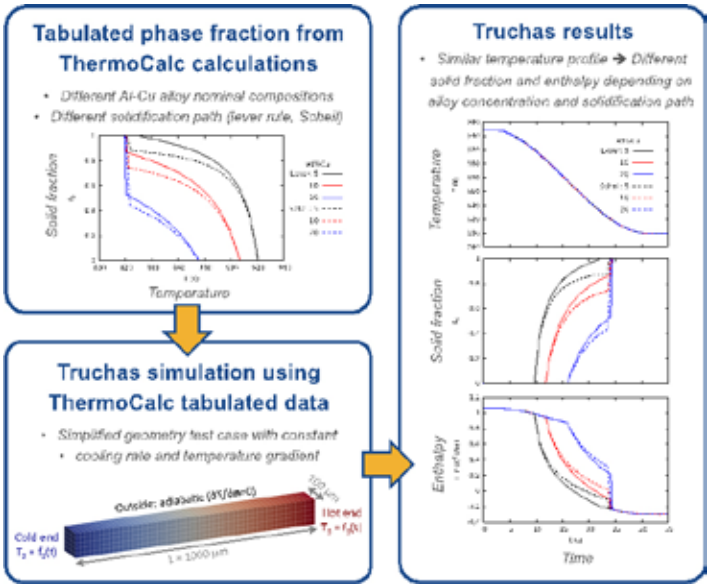

Figure 3. Sample Truchas simulations using tabulated data from ThermoCalc equilibrium calculations for different Al-Cu alloys (5, 10, and 20 wt% Cu) following the lever rule or a Gulliver-Scheil solidification path.

Microstructure to properties modeling

We have explored coupling strategies for monitoring, modeling, and bridging the different steps from controlled solidification processing with mechanical properties. For different Al-Cu alloys, we performed directional solidification experiments of thin samples (thickness ≈ 200 µm) at APS, using high energy X-rays to image the solidification in situ and in real time for various solidification conditions. In parallel, we performed multiscale simulations of the solidification experiments, using the newly developed Dendritic Needle network modeling approach, to directly compare predicted microstructural features, such as primary dendritic spacing critical to the strength of individual dendritic grains.

We saved the samples solidified under controlled and monitored conditions, and performed extensive characterization of the resulting microstructures. We used laser machining to extract microscale tensile specimens from the solidified foils. The gage length region of the microscale tensile specimens was imaged in 3D using lab-scale x-ray computed microtomography (micro-CT), and the tensile specimens were then tested using microscale tensile fixtures and in situ imaging. Both the micro-CT image volumes of the tensile coupons as well as the microstructures generated from multiscale solidification modeling were used to generate microstructural inputs for micromechanical simulations of the tensile tests via Elasto-Viscoplastic Fast Fourier Transform (EVPFFT) modeling.

This “processing-to-microstructure-to-properties“ part of

the study, illustrated in Figure 4, has demonstrated the feasibility of the complete integration of a broad suite of in situ x-ray imaging non-destructive tools, supported by predictive simulations for each step of the process.

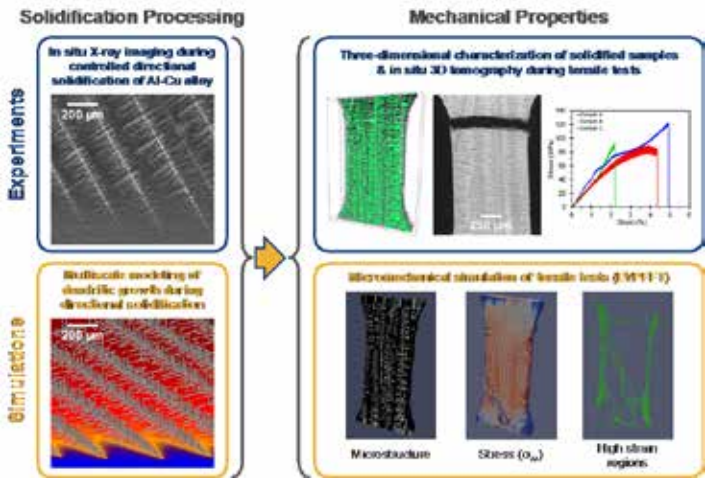

Figure 4. Bridging solidification processing with mechanical properties, using in situ imaging during controlled processing and mechanical testing together with multiscale modeling of the solidification process and micromechanical modeling of characterized microstructures.

While mostly exploratory, this very first comprehensive study of the entire pathway has allowed us to identify some critical aspects in linking approaches at different length scales, which should guide further efforts in progressing toward the long term goal of a fully integrated suite of tools to monitor and modeling processing-to-properties across length scales. One current major limitation is the lack of predictive modeling tools for processing up to a fully solid microstructure. Current capabilities, namely phase-field and dendritic needle network models, allow simulating the growth of a primary dendritic phase, but do not include growth of further secondary phases and structures, such as the eutectic structure. Addressing this issue would not only allow direct interfacing with a micromechanical model, but also with potential further processing steps such as heat treatment prior to mechanical testing. A second remaining open question pertains to the appropriate representation of the sub-micron two-phase eutectic microstructure (e.g. appearing in Figure 5) in the micromechanical simulations. Two typical representations have been suggested in the current study, namely using a fully lamellar structure oriented following the principal growth direction similar to the dendrites, or approximating a pseudo-isotropic structure using randomly oriented eutectic grains of size representative of the microstructure (e.g. the primary or secondary dendrite arm spacing).

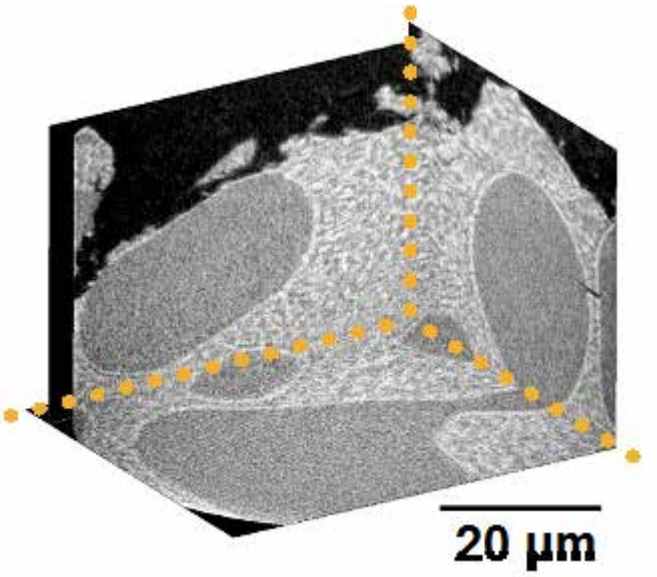

Figure 5. Orthogonal cross-sections reconstructed from 3D nano-tomography of the fracture surface region after tensile failure in an Al-12at.%Cu. The crack path appears at the interface between the dendritic Al-rich structure (darker gray) and the (Al + AlCu) eutectic (dark + light gray two-phase structure), as well as through the eutectic structure itself.

Impact on National Missions

Casting is a critical part of manufacturing both within the DOE/NNSA complex and in industry at large. The recent initiative for advanced manufacturing has pushed predictive modeling for microstructure and properties to the forefront of national strategies to increase overall manufacturing efficiencies.

Casting simulations have been performed at Los Alamos National Laboratory for over 20 years with continuum-scale codes, mainly the Truchas code. Truchas is a coupled multi-physics finite volume code that operates on an unstructured mesh, meaning that it can perform heat transfer and fluid flow calculations on complex geometries. It has been used to guide mold development and process parameter selection in both the uranium and plutonium foundries at LANL and has assisted in a wide range of projects from academic studies to determining casting parameters for stockpile components. Until now, however, Truchas has had no capability to predict spatially-resolved microstructure for alloy solidification. This work has added an initial model of this capability to Truchas, and established a foundation for building on in the future.

Additional exploratory work on modeling the complete metallurgical history of a sample from processing to microstructure to properties, supported by in situ imaging and monitoring of the entire pathway, has allowed us to identify some of the critical links warranting further effort in order to reach the long term goal of a fully integrated

predictive suite of metallurgical tools. Building such a quantitative suite of tools would greatly reduce the cost and time required for developing new alloys and processing routes by enabling a fully computational exploration, hence reducing significantly the number of experiments needed.

Publications

Gibbs, P. J., S. D. Imhoff, C. L. Morris, F. E. Merrill, C. H. Wilde, Nedrow, F. G. Mariam, Fezzaa, W. -. K. Lee, and A. J. Clarke. Multiscale X-ray and Proton Imaging of Bismuth-Tin Solidification. 2014. JOM. 66 (8): 1485.

Imhoff, S. D., P. J. Gibbs, M. R. Katz, T. J. Ott Jr., B. M. Patterson, W. -. Lee, Fezzaa, J. C. Cooley, and A. J. Clarke. Dynamic evolution of liquid-liquid phase separation during continuous cooling. 2015. MATERIALS CHEMISTRY AND PHYSICS. 153: 93.

Embedded Fiber Sensor Approach for Dynamic Pressure and Temperature Measurements in Explosives

George Rodriguez
20140650ER

Abstract

In this project we completed a set of in-situ high pressure and elevated temperature measurements in thermally ignited high explosives as experimental data input for the advancement of reactive burn models necessary for understanding thermodynamic behavior of burning high explosives important to the scientific and Laboratory programmatic communities. Measurements of the internal stresses and temperatures built-up over a very short instance of time in an operating high explosive are difficult to make because of the extreme operating conditions that sensors must survive initial heat conduction phase to approximately 200° C, self-reactive convective chemical burn, and subsequent detonation. Using a very small embedded optical fiber transducer called a fiber Bragg grating (FBG), we developed a high-speed optical sensor and recording system capable of operating to temperatures in excess of 250° C and dynamic pressures of 2x109 Pa (i.e., 1 atmosphere approximately equals 105 Pa).

The project successfully demonstrated use of this transducer to quantify the output detonation pressure of loosely confined HMX (octahydro-1,3,5,7-tetranitro-1,3,5,7-tetrazocine) based plastic bonded explosives (PBXs) upon ignition by an applied thermal stimulus in a series of cook-off type experiments. Two different explosives, PBX-9501 and PBXN-9, were studied, and are shown to have a significantly different peak pressure magnitude and temporal profile history attributed to differences in the chemical reaction violence and available exothermic output energy during detonation. The pressure output from PBXN-9 is approximately several times weaker and an order of magnitude slower than that of PBX-9501. The experimental methodology and results are presented below, and offers an approach that can yield data for quantifying predictive models important to both the Departments of Energy and Defense where such data is scant.

Background and Research Objectives

Characterization of a high explosive response to thermal stimuli is important to understanding the violence in thermal explosions [1,2]. To the extent that experimental observables such as density, temperature, pressure, and material flow, can be reliably monitored and recorded, new approaches that yield this information greatly aid predictive models of reactive violence in strong exothermic reacting explosives. HMX based PBX explosives can vary in their burn propagation rate from 10's to 100's of meters per second and can undergo a deflagration to detonation transition [3]. Radiography has been successfully used to determine differences in reaction rate violence in PBX based explosives [4]. Yet, additional material state information is still needed, and approaches to measure dynamic temperature and pressure is limited [5-7]. Direct pressure measurements in a burning high explosive are difficult to make because of the need for the sensor to survive elevated temperature, quasi-static volumetric flow due to the explosive material phase change, and high pressure. Additionally, the sensor must have high-speed (sub-microsecond) time response without introducing an obtrusive perturbation to the experimental assembly.

Recently, we reported on a successful embedded fiber approach that uses a single mode fiber Bragg grating to measure the response in thermal ignition experiments [8,9]. In this report we briefly summarize our objectives, approach, and accomplishments, but stress that these measurements represent the first significant modern advance of embedded in-situ dynamic pressure sensing in a burning high explosive over what has traditionally done using more intrusive techniques developed in the mid-1960s (i.e., manganin piezo and carbon resistor gauges). Our work takes advantage of combining a single-mode fiber Bragg grating transducer and ultrafast gigahertz photonics to measure thermodynamics during thermal conduction, convection, and subsequent detonation of a loosely confined high explosive. This work

represents a complementary measurement to flash x-ray radiography [10] and adds another important measurement quantity needed to understand the chemical violence of reacting explosives under extreme conditions. It should find wide impact among those researchers who use fiber photonic sensing systems that require high-speed interrogation methods, in particular applied to dynamic testing in extremes.

Scientific Approach and Accomplishments

Fiber Bragg grating (FBG) based sensors are used for research and commercial based strain, temperature, and pressure sensing [11]. They provide a very good basis for distributed sensing because their operational modality is rooted in multiplexing approaches from optical telecommunications technology [11,12]. Fiber Bragg grating sensors have predictable thermal and mechanical response properties [11-13]. However, much less is known about their performance in high-speed dynamic events that push the limits of FBG sensing to extreme environments under sub-microsecond transient loading conditions where both sensor and readout rates demand performance currently unavailable commercially [8,13,14]. Previously, the wavelength shift of the returning light spectrum has been studied as a function of temperature and applied pressure [10-12].

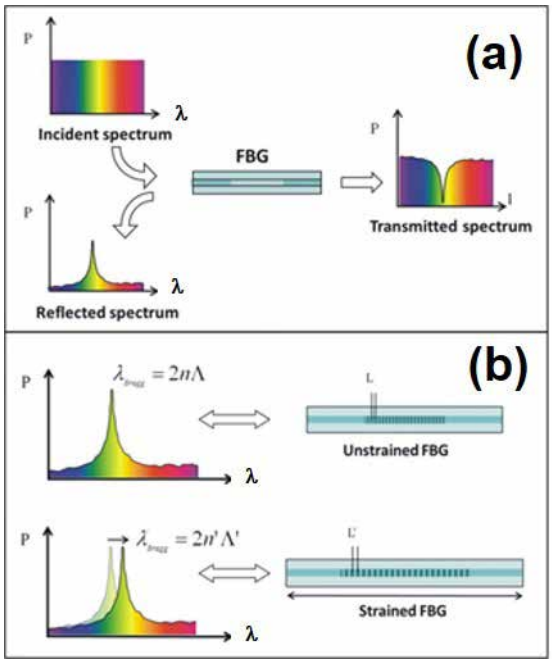

Figure 1. Operating principle of a fiber Bragg grating sensor. Incident broadband light is reflected (transmitted) at specific wavelength as shown in (a). Under stress or tension caused by pressure (P) or temperature (T), the grating is strained and the length, L, changes. The Bragg wavelength causes the reflected color wavelength, λ, to shift in proportion to the applied P or T as shown in (b).

Illustrated in Figure 1, under applied pressure, the fiber reflectance spectrum shifts to shorter wavelengths, and in elevated temperature, the reflectance spectrum shifts to longer wavelength. The pressure and temperature sensitivity shifts of fused silica FBG sensors are known to be approximately -3.8 nm/GPa and +0.011 nm/°C [8]. Thus, for a pressure wave to 1 GPa, a spectral shift of 3.8 nm at λ=1550 nm to shorter wavelength (λ=1546.2 nm) in the return FBG spectrum is expected and a shift of 2.5 nm to longer wavelength (λ=1552.5 nm) is expected at T=250°C. Therefore, it is possible to simultaneously measure temperature and pressure from a FBG if wavelength selective binning and recording of the return light spectrum from the FBG sensor is performed.

Experiments consist of placing an FBG sensor in a cylindrical aluminum case that houses the high explosive (HE). A schematic and photograph of the experimental package assembly is shown in Figure 2.

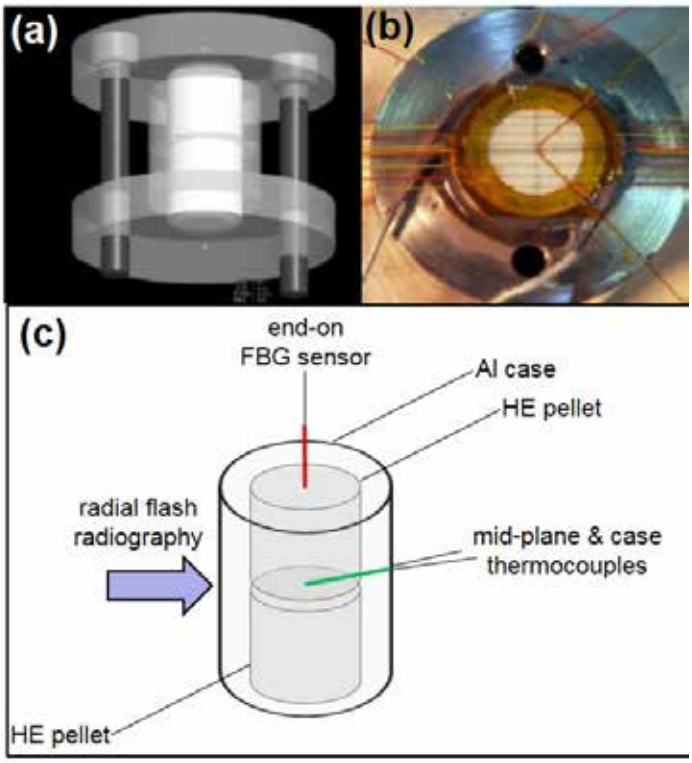

Figure 2. (a) Schematic, and (b) photograph, showing the relative sizes and location of the aluminum case and encased high explosive pellets. In (b), the mid-plane section between two pellet halves is shown to expose the placement locations of the array of thermocouples and a pair of IR pyrometer optical fibers originating from the center. The illustration in (c) shows the relative placement locations of all the diagnostics: FBG, thermocouples, and x-ray flash radiography.

Further details on the experimental package can be found in Refs. [8,10]. A pair of 12.5 mm diameter right cylinder pellets of plastic bonded explosives PBX-9501 (or PBXN-9)

is used for these measurements. The pellets are stacked on top of each other so that mid-plane diagnostics (temperature measuring thermocouples and a pair of infrared fiber pyrometer sensors) can be placed in the center volume portion of the assembly as in Figure 2(b). The HE pellets are housed in an end-capped aluminum sleeve. The HE is heated by a set of thin film resistive heaters attached to the case. A single 1-mm-long 1560 nm FBG is embedded into the HE. Experiments initially proceed by heating the sidewalls slowly over the period of 1.5 hours. Internal temperature measurements are continuously recorded using the signal from thermocouples, but since the FBG also responds to temperature, continuous recording of the FBG wavelength shift versus temperature is also done using the time integrating InGaAs arrayed spectrometer (Figure 3).

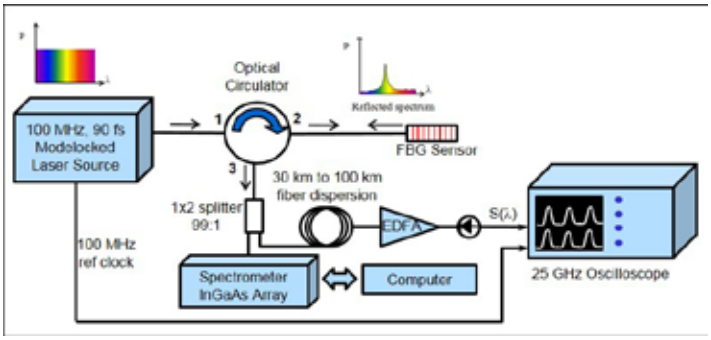

Figure 3. 100 MHz coherent pulse high-speed FBG interrogator system developed for temperature and pressure sensing in thermally driven explosions. The system is capable of measuring slow FBG sensor response with a light integrating InGaAs arrayed spectrometer, but can also measure the rapid FBG response every 10 ns using a coherent pulse time stretch spectroscopic method using gigahertz photonic time streaking. Details of operational characteristics can be found in Refs. [8,9].

Thermally driven explosion experiments proceed by monitoring observables (usually internal HE temperature) over the course of the heating phase from which real time indicators in temperature are able to track subtle changes such as material phase change and HE chemistry induced self-heating effects. These indicators yield a measure of thermal decomposition before internal chemical reactive kinetics give way to a full self-sustaining explosion with ignition and burn propagation. Thermal decomposition occurs over time scales of hours. As exothermic chemistry begins, the material self-heats and the decomposition accelerates. This causes a thermal runaway that leads to the thermal explosion. Final steps in the development of a thermal explosion are observed via temperature and density to evolve on the time scale of seconds. Ignition then occurs and a switch in energy release to post-ignition time scales of microseconds is observed. Post-ignition burn propagation occurs for tens to hundreds of microseconds and during this phase, extreme temperatures and pressures generated.

In Figure 3 we show the experimental setup schematic of the high- speed FBG interrogator developed under this project. The key feature of our FBG interrogator system is its capability of measuring the FBG sensor response under slow timing conditions (such as in the heat conduction phase which occurs over the course of thousands of seconds) using a light integrating spectrometer and under high-speed microsecond timing conditions (post-ignition and thru detonation) using the high-speed time-stretch spectroscopy FBG interrogator [8,9,14]. In the high-speed interrogator, the FBG is illuminated by broadband infrared (1510 nm-1610 nm) ultrafast laser pulses every 10 ns (100 MHz interrogation rate) from an Erbium fiber laser centered at 1560 nm. The FBG only reflects a very narrow portion of the spectrum (only 1 nm at approximately 1550 nm) that spectrally shifts with applied pressure or temperature as illustrated in Figure 1. After interrogating the FBG, the narrow band optical pulse from the FBG is then sent to a high chromatically dispersive fiber spool to stretch the pulse in time the colors that comprise spectrum of the return pulse from the FBG. Since the speed of light varies slightly with wavelength, a mapping of the color of the pulse to time is accomplished, and the temperature or pressure spectrally induced shift in the FBG spectrum appears as a time delay in the recorded signal at the detector. A very fast 35 GHz InGaAs photodetector converts the optical pulse to electrical pulses and is very sensitive to changes in the time delay (i.e., color spectrum) sensed by the FBG transducer. Post shot analysis is used to convert FBG pulse time delay to color spectrum shift, which is then converted to pressure and temperature upon applying the known temperature/pressure response coefficients for the FBG.

Figure 4 is a plot of the temperature time history of a thermal ignition event for PBX-9501 using the low-speed recording diagnostics. Plotted alongside the thermocouple data is the FBG data as recorded by the InGaAs spectrometer. Note the similarities in signature between the thermocouple data and the FBG data. The temperature was temporarily held at a couple of intermediate points (70°C, 175°C) before being held fixed at the final temperature of 205°C. At the 175°C point, the temperature is held to allow for material flow and rearrangement as the HE undergoes a volumetric expansion due to the β→δ crystalline phase transition. FBG data is subject to pressure as well as temperature, and during the β→δ phase change there was a slight temperature drop due to the endothermic phase change and commensurate with a volume expansion that slightly increased the pressure causing the FBG shift to lower wavelength. At the final hold temperature

of 205° C, reactive self-heating in the HE occurs in the final 1000 seconds prior to full ignition. The 100 MHz coherent pulse high-speed FBG interrogation system is used to record the final ignition event and explosively driven pressure build up in the package for the final 1 millisecond before the aluminum case containment fails and breaks up. Temperatures recorded during runaway to ignition are approximately in the 250°C range. In Figure 5(a) we show an example of the FBG measured results for a PBX-9501 shot.

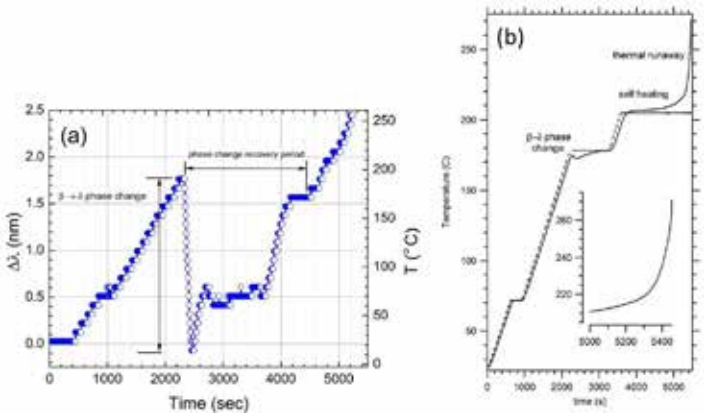

Figure 4. A plot of the FBG wavelength shift (Δλ) versus time for thermally heated PBX 9501 before ignition is shown in (a). The initial wavelength of the FBG was λ=1555.1 nm, and the corresponding temperature is given on the right ordinate labeled axis using a wavelength shift to temperature conversion constant of 11 pm/°C. The FBG data in (a) is, for a period during the heating and thermal conduction phase, disrupted by the β→δ material phase change that results in volume expansion and stress effects on the FBG response after t = 2200 sec. In (b), a plot of the thermocouple data for heated PBX 9501 (taken from Ref. [10]) is shown. The dashed plot in (b) represents the aluminum case temperature history, and the solid line is the temperature measured at the center of the PBX 9501 cylinder. Best agreement between the FBG and thermocouple data is before the phase change period and well after the phase change recovery time when self-heating of the explosive begins to produce thermal runaway in excess of 205° C.

The left ordinate axis in Figure 5(a) is the measured spectral shift as a function of time. The spectrum blue shifts to shorter wavelengths starting at 1556.9 nm and moving to as low as 1550.4 nm, a total blue shift of 6.5 nm. This shift is due to the pressure generated by the explosive during the post-ignition detonation burn phase. Applying the appropriate FBG pressure calibration constant of -3.8 nm/GPa, yields a peak pressure 1700 MPa. This right ordinate blue axis of Figure 5(a) shows the FBG shift in units of pressure. Figure 5(a) shows that the pressure build-up is rapid and occurs in less than 25 µsec. In Figure 5(b) a plot of a compendium of pressure measurements are shown for a series of thermal ignition measurements for the two types (PBX-9501 vs. PBXN-9) of explosives studied during this project. The plots in Figure 5(b), are the post-ignition buildup of pressure in the final millisecond as the explosive transitions to a detonating burn. The scatter in the amplitude pressure output varies somewhat since the initial ignition volume can vary by several millimeters from the mid-plane of the explosive, and as a consequence, the FBG sensor measures a slightly different pressure from shot to shot. However, the trend in the data between pressurization and its temporal burn history is clear. The PBXN-9 burn rate is nearly twenty times slower than PBX-9501, and the output pressure of PBXN-9 is several times weaker than PBX-9501. The slower and lower pressure output of PBXN-9 compared to PBX-9501 is a direct measure of the lower thermal reaction violence of PBXN-9. The data is now being input to models that describe thermal ignition burn histories in these explosives, and this project has successfully contributed by providing much needed model validation data. It is expected that future integration of the methods developed in this project will provide additional data on other explosive types for incorporation in programs that study performance of high explosives from both the application and safety perspectives.

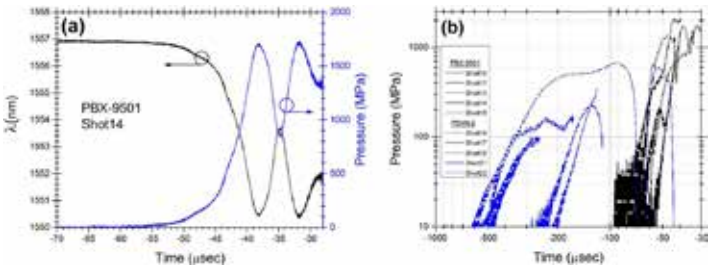

Figure 5. (a) Plot of the FBG dynamic response wavelength(λ) versus time for thermally heated PBX 9501 after ignition as recorded by the 100 MHz coherent pulse high-speed FBG interrogator system (Figure 3.). The left ordinate axis of (a) shows an initial FBG wavelength that dynamically shifts to shorter wavelength (i.e., increasing pressure) over a very short 25 µsec period. The right ordinate axis of (a) is the corresponding pressure achieved during detonation. A peak pressure of over 1700 MPa is measured. A compendium shots of pressure history is shown in (b). The black traces in (b) are from thermal ignition shots using the high explosive PBX-9501, and the blue traces are from shots with PBXN-9. Despite the somewhat stochastic nature of the ignition process, clear evidence in the differences of the pressure maximum produced and temporal explosive burn history between PBX-9501 and PBXN-9 are observed and quantified.

Impact on National Missions

This project has played a key role in establishing an approach for direct pressure measurement of thermal explosions in high explosives. Understanding thermal response violence with pressure measurements allows linkage between experimental data and modeling that establishes a validation data set for predictive models of reacting

chemical explosive materials under dynamic extremes. This work impacts the Laboratory's national security mission through scientific excellence to maintain world-class research and development capabilities in the science of high explosives supporting the weapons program, safety, and security. Specifically, impacted agencies include DOE NNSA and DOD high explosive science programs that include high explosive safety and surety, equation-of-state chemistry, and dynamics of materials under extremes.

References

1. Shock wave science and technology reference library vol. 5: non-shock initiation of explosives. 2009.

2. Tarver, C. M., and S. K. Chidester. On the violence of high explosive reactions. 2005. Journal of Pressure Vessel Technology. 127 (1): 39.

3. Esposito, A. P., D. L. Farber, J. E. Reaugh, and J. M. Zaug. Reaction propagation rates in HMX at high pressure. 2003. PROPELLANTS EXPLOSIVES PYROTECHNICS. 28 (2): 83.

4. Smilowitz, , B. F. Henson, J. J. Romero, and B. W. Asay. A COMPARISON OF THERMAL EXPLOSIONS IN PBX 9501 AND PBXN-9. 2009. SHOCK COMPRESSION OF CONDENSED MATTER - 2009, PTS 1 AND 2. 1195: 436.

5. Garcia, , K. S. Vandersall, J. W. Forbes, C. M. Tarver, and Greenwood. Thermal cook-off experiments of the HMX based high explosive LX-04 to characterize violence with varying confinement. 2006. SHOCK COMPRESSION OF CONDENSED MATTER - 2005, PTS 1 AND 2. 845: 1061.

6. Urtiew, P. A., J. W. Forbes, C. M. Tarver, Garcia, D. W. Greenwood, and K. S. Vandersall. Thermal cook-off of an HMX based explosive: Pressure gauge experiments and modeling. 2007. RUSSIAN JOURNAL OF PHYSICAL CHEMISTRY B. 1 (1): 46.

7. Glascoe, E. A., H. K. Springer, J. W. Tringe, and J. L. Maienschein. A COMPARISON OF DEFLAGRATION RATES AT ELEVATED PRESSURES AND TEMPERATURES WITH THERMAL EXPLOSION RESULTS. 2012. SHOCK COMPRESSION OF CONDENSED MATTER - 2011, PTS 1 AND 2. 1426.

8. Rodriguez, , Jaime, Balakirev, C. H. Mielke, Azad, Marshall, B. M. La Lone, Henson, and Smilowitz. Coherent pulse interrogation system for fiber Bragg grating sensing of strain and pressure in dynamic extremes of materials. 2015. OPTICS EXPRESS. 23 (11): 14219.

9. Rodriguez, G., L. Smilowitz, and B. F. Henson. Embedded fiber Bragg grating pressure measurement during thermal ignition of a high explosive. Applied Physics Letters.

10. Smilowitz, , B. F. Henson, J. J. Romero, and Oschwald. Thermal decomposition of energetic materials viewed via dynamic x-ray radiography. 2014. APPLIED PHYSICS LETTERS. 104 (2).

11. Fiber optic sensors: an introduction for engineers and scientists. 2011.

12. Handbook of optical fibre sensing technology. 2002.

13. Mihailov, S. J.. Fiber Bragg Grating Sensors for Harsh Environments. 2012. SENSORS. 12 (2): 1898.

14. Rodriguez, , R. L. Sandberg, B. M. Lalone, B. R. Marshall, Grover, Stevens, and Udd. High pressure sensing and dynamics using high speed fiber Bragg grating interrogation systems. 2014. FIBER OPTIC SENSORS AND APPLICATIONS XI. 9098.

Publications

Rodriguez, G., L. Smilowitz, and B. F. Henson. Embedded fiber Bragg grating pressure measurement during thermal ignition of a high explosive. Applied Physics Letters.

Rodriguez, G., M. Jaime, C. H. Mielke, et.al., Insight into fiber Bragg sensor response at 100 MHz interrogation rates under various dynamic loading conditions. 2015. In 2015 SPIE International Society for Optics and Photonics Defense, Security, and Sensing Conference: Fiber Optic Sensor and Application XII. (Baltimore, 20-24 Apr. 2015). Vol. 9480, p. 948004. Bellingham: SPIE.

Rodriguez, G., M. Jaime, F. F. Balakirev, C. H. Mielke, A. Azad, B. Marshall, B. M. Lalone, B. H. Henson, and L. Smilowitz. Coherent pulse interrogation system for fiber Bragg grating sensing of strain and pressure in dynamic extremes of materials. 2015. Optics Express. 23 (11): 14219.

Smilowitz, L., B. F. Henson, G. Rodriguez, D. Remelius, E. Baca, D. Oschwald, and N. Suvorova. Relationship between pressure and reaction violence in thermal explosions. 2016. AIP Conference Proceedings . : 100.

Smilowitz, L., B. Henson, G. Rodriguez, R. Sandberg, M. Holmes, A. Novak, E. Baca, and D. Oschwald. Following reaction progress from thermal decomposition to ignition and internal burning. 2015. In Proceedings of the 15th International Detonation Symposium. (San Francisco, 13-18 Jul. 2014). , p. 13. Arlington, VA, USA: Office of Naval Research.

Thin-Film Heat Switch for Active Thermal Management of CubeSat Payloads

Alexander H. Mueller
20150375ER

Abstract

The goal of this project was to develop a large-scale version of a novel heat switch demonstrated under a previous LDRD program and couple it to a thermal reservoir for regulating the temperature of a CubeSat payload . The heat switch area was scaled by 48x, and the thermal standoff distance was increased by 6x. We discovered that this scaling necessitated the optimization of the structured electrode intra-electrode line gaps. This was achieved by developing a comprehensive electrohydrodynamic device model using the COMSOL Finite Element Modeling software package. The model predicts that a thermal contrast of 30 is achievable by this system in the ON vs the OFF state. Experimental validations of these scaling effects were performed and allowed us to demonstrate improved performance for the heat switch device.

Background and Research Objectives

Satellites are exposed to a complex thermal environment: external heat loads change rapidly between solar exposure and eclipse, and internal heat loads are dictated by the operation of electronic payloads. While heat is most efficiently dissipated from the satellite during eclipsed (“cold”) periods, payload operation may follow different patterns as dictated by the mission. The resulting thermal management problems are magnified in small form factor CubeSats that have limited space to move, store, and release thermal energy.

Maintaining the temperature of satellite payloads within an optimum operating window is critical to the long-term operation of the instrumentation and communication devices deployed on these spacecraft. Current spacecraft thermal control is primarily a “passive” design and thus involves many compromises. The typical methods rely heavily on manipulating both the emissivity of exterior panels and thermal conduction paths (heat pipes). This requires a very “orbit average” view of thermal balance without the ability to adapt quickly and actively in relation to mission execution. These passive methods do not provide control of the thermal coupling between the heat source and the reservoir, allowing the heat to return to the payload once the thermal gradient reverses. Heat pipes can also suffer failure due to freezing during the “cold” state of the spacecraft. Research into applying electrochromic paints to provide switchable absorption as alternative to the satellite surface treatments, shape memory alloys as mechanical actuators for radiative cooling louvers, and active thermal gates for heat generating payloads have not yielded practical solutions. Given the magnitude of this problem, surprisingly, no practical “active” thermal management solutions have been developed!

A particularly relevant challenge is the temperature control of CubeSat batteries. The low solar flux in the CubeSat’s eclipsed part of the orbit results in the battery pack falling below a minimum temperature at which it can accept charge from the solar panels as the spacecraft moves into the illuminated part of the orbit. This results in the loss of time while the batteries first have to warm up by the solar exposure, or it requires the use of an active heater to pre-warm the batteries before entering the illuminated part of the orbit. The goal of this project was to fabricate the next generation heat switch and couple it to a phase-change material (PCM) in order to provide an active means of capturing waste heat in the PCM for later utilization. Specifically, excess heat generated during the charging and discharging cycle of the batteries in the illuminated half of the orbit would be moved into the PCM by activating the heat switch and then isolated and stored during most of the duration of the eclipsed part by deactivating the heat switch. Shortly before the satellite emerges from eclipse, the heat switch is reactivated to move the waste heat stored in the PCM to pre-warm the batteries so they can accept charge immediately upon entering the illuminated part of the orbit. This active thermal control scheme would greatly improve the power efficiency and thereby in-

crease the capabilities and agility of the CubeSat's mission assets.

Scientific Approach and Accomplishments

The project team has successfully demonstrated a novel concept of a "thermal transistor" as part of a previous LDRD project. The microfluidic device can be electrically switched between an ON state (active heat transport) and an OFF state (thermally insulating). The device concept is illustrated in Figure 1. When no electric filed is applied, the dielectric fluid acts as a thermal insulator and reduces the flow of heat across the gap. Applying an electric field across the dielectric fluid induces electrohydrodynamic (EHD) fluid motion which results in enhanced heat transport across the gap, cooling the hot and warming the cold side.

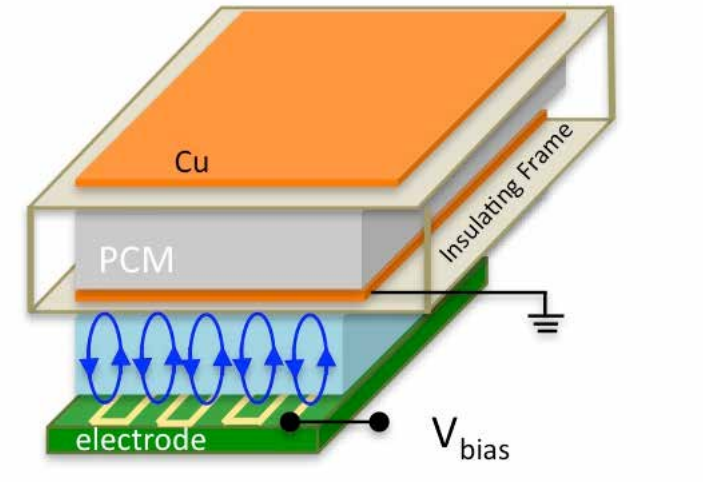

Figure 1. Schematic of the coupled heat switch and phase change material device. The structured electrode (bottom green) is biased relative to a planar Cu electrode across a layer of electrohydrodynamic fluid (light blue). This induces a vortex motion in the fluid that moves heat across the fluid and into the phase change material thermal storage media (gray).

The active element of the heat switch is the dielectric fluid layer that fills the thin (typically h>500 µm) gap between the structured gold electrode (shown in Figure 2) and the polished planar copper electrode. The structured electrode consists of thin metal lines deposited onto an insulating substrate. The project investigated electrodes consisting of line pairs (gap "a" between lines, gap "b" between line pairs, line width "w") as well as a uniform array of lines (gap "b" between lines). In the OFF state (no voltage applied), the thermal conductivity of the device is primarily determined by the thermal conductivity of the nominally stationary dielectric fluid. In the ON state (voltage applied across the dielectric fluid film), the fluid is in motion and the thermal conductivity is enhanced significantly by convection. This effect is demonstrated in Figure 3, which shows the thermal gradient ΔT across the fluid separating the hot (structured electrode) and cold (copper plate) sides of a 1-cm2 heat switch. Upon applying an electric field (-250 V DC) to the structured electrode, fluid flow is induced and transfers heat from the hot side to the cold side, thus reducing ΔT. The fluid velocity, and thus the thermal transfer rate, increases with increasing electric field up to a critical velocity beyond which the fluid does not remain in sufficiently long contact with the electrodes to complete the heat transfer. Thus, the rate of heat flow across the dielectric fluid film can be tuned via the applied electric field, creating a fully adaptable heat switch for a broad range of applications.

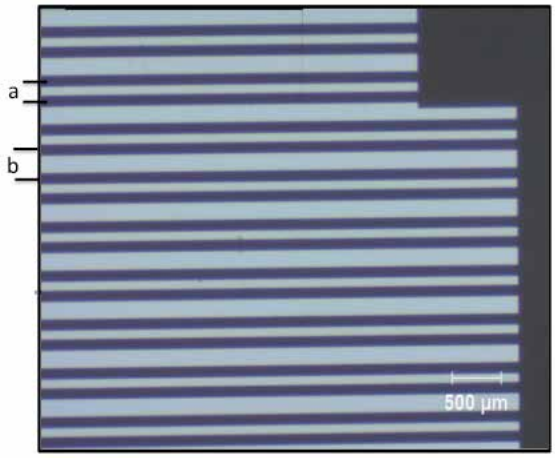

Figure 2. Micrograph of the structured electrode. This electrode is defined by metal line pair with an intra-pair distance of a and a pair to pair distance of b. These dimensions are important to optimize relative to the height of the fluid layer between the structured electrode and the planar ground electrode.

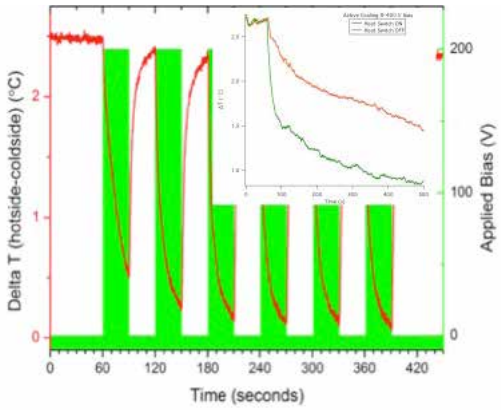

Figure 3. Reaction of the thermal gradient (represented in % gradient remaining) across the EHD fluid under bias cycling for varying electrode line spacings. It is observed that increasing the line spacings from 0.55 mm to 2.2 mm more than doubles the thermal response of the system. Shown in the inset is the magnitude of heat moved by the heat switch (blue line) at various electrode biases (black line). Thus a tunable system of heat transfer can be achieved using this technology.

The inset of Figure 3 shows ΔT during the cooling and thermalization of the device after the external heater is turned off. It can be seen that with the heat switch ON (400 V DC, green line) the fluid layer thermalizes (thermal gradient is destroyed) at a rate >10 times faster than under only conductive heat transfer conditions (heat switch OFF, orange line).

Electrohydrodynamically driven fluid flow is the result of a transport phenomenon produced by applying an electrostatic field and can be explained by electrokinetic or dielectrophoretic mechanisms. Electrokinesis is fluid transport produced by an electric field acting on a fluid having a net mobile charge where the velocity field everywhere is proportional to the electric field. In comparison, dielectrophoretic induced flow is produced by an electric field gradient on the induced dipole moment of the surrounding fluid. The dielectrophoretic potential field experienced is proportional to the difference between the particle and fluid polarizabilities. In order to distinguish between electrokinetic and dielectrophoretic fluid flow and to deduce the mechanism of the observed electrohydrodynamically driven flow, we looked at the change in temperature across the heat switch at varying field frequencies. Experiments determined that during application of an electric field below 20 Hz, the dielectric fluid continued to alter the thermal contact between the two electrodes. Above 20 Hz, there was very little temperature change across the heat switch. This confirms the frequency dependence of fluid flow, indicating an electrokinetic mechanism driving the fluid motion. Monitoring the electrode temperatures independently when applying voltages at 1 Hz, we observed that charged molecules travel from one side of the heat switch to the other, effectively transferring heat from the hot to the cold side. This behavior is indicative of ohmic current driving the fluid flow since the current and voltage are in-phase and changes in the field occur simultaneously, allowing the charged fluid molecules to travel from one electrode to the other. This behavior was not seen when the frequency was increased to 20 Hz where there is little heat transfer observed across the switch, although we continued to observe a slight change in temperature at the structured electrode. This slight change in temperature is the result of the initial motion of molecules at the electrode interface, but opposite polarity reverses the direction resulting in fluid motion across the gap not being established. This behavior suggests a transition from ohmic to a capacitive current mechanism, inhibiting fluid flow across the heat switch. Similar results were obtained at frequencies above 20 Hz. In the case of charge driven flow (electrokinesis), we would expect a pulsed DC field (+220 V) to result in accelerated fluid motion (higher thermal conductivity) compared to an AC field at 1 Hz. Although the molecules take longer to travel from one electrode to the other compared to a constant DC field, there is no opposite polarity to reverse the direction of flow as in the case of a true AC field.

Coupling this invention to a CubeSat battery pack required the scale up of the device and the characterization of the performance of the new iteration. Along with a nearly 50x increase in area from 1 cm2 to 48 cm2 to match the areal dimensions of a representative battery pack came an increase in the thickness of the EHD fluid layer in order to achieve better thermal insulation during the OFF state of the device. Scaling of the structured electrode shown in Figure 2 to match the increase in thickness of the EHD fluid gap was performed using a Finite Element Method computer model based on the electrokinetic mechanism determined by the above described experiment.

When an electrical field is applied on a dielectric fluid, the electrical charges released into the fluid induce an internal force acting on the fluid particles. As a result a velocity field is developed in the fluid. If a temperature gradient is considered, this results in heat transfer across the fluid layer. This problem can be described by the equations of electrohydrodynamics in conjunction with heat-transfer equations. Electrohydrodynamics then describes the electric charge density transport (not the individual charges) in the dielectric fluid when an electrical field is applied. It represents a coupling set of equations between electrostatic and fluid mechanics, the coupling term being the force induced by the electric charge density and electrical field. This force affects the fluid velocity field (electrokinetics), which in turn affects the electric charge density distribution in the fluid. The result is a fluid velocity field which affects the heat transfer problem in the fluid.

The abovementioned coupled set of equations were solved using COMSOL FEM (Finite Element Method) program for a two-dimensional case. The results of the numerical simulations are shown in Figure 4, which illustrates both the thermal distribution within the EHD Fluid (red to yellow color gradient) and the velocity field present in the fluid (represented by the scaled vector arrows). The inset of the figure shows the effect of the ratio of the structured electrode line gap dimension (dimension “b” in Figure 2) to the distance between the electrodes (fluid gap “h”) and the fluid velocity (red line) and thermal transfer (blue line). The structured electrode can be tuned to maximize the thermal transport between the scaled magnitude of the fluid gap. The model indicates that a 30x increase in thermal conduction relative to the OFF state should be achievable with an optimized device using an equally staggered line electrode structure. Other structure geometries have not yet been modeled. Figure 5 shows the switching of thermal gradients across a 1.1 mm fluid layer for three devices in which

the intra-electrode line gaps in the structured electrodes vary from 0.55 mm to 2.2 mm. We observe that the heat transfer scales with the introduction of field free regions through increasing the distance between the electrode lines, which allows for the establishment of stable mixing vortices in the fluid layer. The inset graph illustrates the thermal switching across the 2.2mm intra-electrode spacing device in Watts/m2 for increasing applied fields. It is observed that the heat transfer asymptotically approaches a maximum value with respect to the voltage applied to the device. While three different intra-electrode gaps were measured, additional measurements are necessary to experimentally determine the optimum and validate the model.

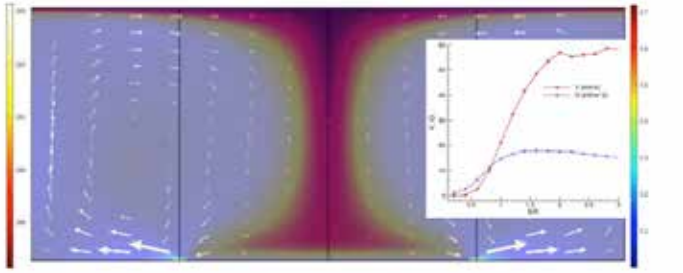

Figure 4. COMSOL Finite Element Model of the thermal gradient (red to yellow color gradient) established by the velocity field (white vector arrows) in the fluid. Inset: This velocity (red line) and thermal flux (blue line) can be increased by optimizing the structured electrode's intra-line spacing "b" with respect to the fluid layer dimension "h."

Integration of the heat switch with the phase change material (PCM) was accomplished by constructing a PCM reservoir, which has insulated sides exposed to the environment, and the boundary between the heat switch and the PCM consisting of a polished copper plate that acted as the counter electrode of the heat switch. Testing of the PCM material showed that 120 kJ of thermal energy was stored in the 7 mm thick layer of material. Measurements using the coupled heat switch indicated some heat transport to the thermal reservoir, however these measurements were made before the optimization of the intra-electrode line gap optimization and were difficult to reliably quantify. Additional measurement with an optimized heat switch will be necessary to determine the system's efficacy.

Impact on National Missions

Applications of this device range across technologies important to industry and US national security. A low power thermal switch and regulation device can be used to store and concentrate waste heat for energy applications in the home, such as variable insulation windows, and industry that would benefit from being able to concentrate waste heat into a more useable form. Aside from the satellite applications possible for the thermal regulation device developed in this project, the EHD technology employed can be used to "smear" out electronically generated heat onto a larger area in order to minimize temperature rises induced by the electronics. This capability has uses in cooling electronic equipment ranging from computer chips to flat screen technologies as well as being able to be used to mask thermal signatures of concealed devices. Being able to controllably couple the thermal conduction between heat sources and heat sinks using a device with sub-milliwatt power consumption is an important capability to enable modern mechanical and electronic technologies.

Publications

Branch, B. B., A. Ionita, N. Weisse Bernstein, D. Seitz, R. Eppstein, M. Hehlen, and A. Mueller. Heat Switch Based on Electrohydrodynamic Flow in a Thin Dielectric Fluid Film. Journal of Applied Physics.

Helium Bubble Growth in Tungsten Under Fusion First-Wall Conditions

Arthur F. Voter
20150725ER

Abstract

The nucleation of helium (He) bubbles in tungsten (W), and their subsequent growth and evolution until they burst at the W surface, is thought to be an important part of the process of "fuzz" formation on the surface of W when it is exposed to a He plasma. Gaining a better understanding of this detrimental fuzz growth process may be critical in advancing the fusion energy program, as W is the proposed first-wall material for the so called International Thermonuclear Experimental Reactor (ITER) tokamak fusion reactor now being built through international collaboration in the south of France. Although this type of bubble growth process can be directly simulated using molecular dynamics on picosecond-to-nanosecond time scales, we have recently found that simulation at much slower, more experimentally realistic, growth rates leads to different growth characteristics and different amounts of damage on the W surface. In this project, we use parallel replica dynamics and parallel trajectory splicing, which parallelizes time. By leveraging the massively parallel power of the Trinity supercomputer, we studied the growth and evolution over experimentally realistic microsecond-to-millisecond time scales of a He bubble that is nucleated at a realistic depth of 4 nanometers below the W surface. It has been unfeasible until now to grow a bubble at this depth at a realistic rate, so a detailed understanding of the bubble growth and bursting behavior under these realistic conditions has remained out of reach. We perform this study for the most important surfaces of W, giving us valuable insight into the bubble behavior and how it depends on the nucleation depth and the type of surface exposed to the plasma. This takes us a step closer to understanding how fuzz forms on the surface, and perhaps how to mitigate this effect, which will otherwise be a serious problem under fusion conditions. We also investigate the behavior of the nuclei of these bubbles, small vacancy/Helium clusters, in order to determine whether they are mobile. Note that this proposal was for computer time only; no funding was obtained.

Background and Research Objectives

Our goal was to carry out, and analyze, long-time molecular dynamics simulations of helium bubble growth near a tungsten surface. We performed these simulations using parallel replica dynamics on the Trinity supercomputer. Specifically, we simulated a bubble that is nucleated four nm below the surface (a realistic depth, although bubbles form at a range of depths) at T=1000 K (a realistic temperature), modeled with an embedded atom method (EAM) interatomic potential, for three different tungsten surface types. To capture the important physics, we added a new He atom to the bubble at regular time intervals, mimicking the irreversible arrival at the bubble, by diffusion, of He atoms surface-implanted by a He plasma. We used a growth rate of one He atom per ten ns. This is approximately two orders of magnitude faster than under real fusion plasma conditions, but is substantially slower than is possible with direct molecular dynamics. Based on our earlier study we believe this choice of depth and growth rate would allow us to probe the relevant physics most realistically and effectively within our provided computer resources. Other than this imposed growth, the bubble would be allowed to evolve freely. As the number of He atoms increases, the growing bubble pressure causes interstitial tungsten atoms to be emitted from the bubble and travel to the surface. The bubble itself grows in size, at some point sensing the surface through elastic interactions, affecting the growth characteristics. Ultimately the bubble bursts at the surface, releasing all its helium and leaving a crater of some shape. We were particularly interested in understanding the crossover to surface-directed growth, the shape (faceting, elongation, etc.) and size of the bubble at bursting, the characteristics of the crater and overall surface damage, and the dependence of these properties on nucleation depth and surface type. We further investigated the behavior of proto-bubbles, i.e., small complexes of Tungsten vacancies and He that act as nuclei for larger bubbles. Whether or not these defects can migrate in the material is currently unknown

and better understanding their behavior could significantly affect our ability to predict where and when He bubbles form in reactor operating conditions.

Scientific Approach and Accomplishments

The analysis of the results is still ongoing, but preliminary data indicates a rich set of unexpected phenomena. For the (100) surface orientation, we were able to simulate the growth of the bubble up to the bursting point. The growth of the bubble in this case was strongly biased towards the surface. During growth, we also observed new dislocation emission mechanisms that seem to stem from the interaction with the surface. We also observed novel mechanisms that activated as the bubble approached the surface, leading to the formation of a pinhole and to the subsequent escape of the He. In the case of the (111) surface, the bubble grew to about 1 nm away from the original surface. We also observed novel mechanisms that led to directed growth when the bubble was sufficiently close to the surface. However, because of the dislocation crystallography in this case, the surface is pushed away in front of the expanding bubble, so that bursting is not eminent. In the case of the (110) surface, the bubble is still far from bursting (figure 1). Interestingly, growth was much more isotropic in this case, an observation for which we have yet to find an explanation. These simulations each ran for about 30 us of simulation time with about 100,000 atoms.

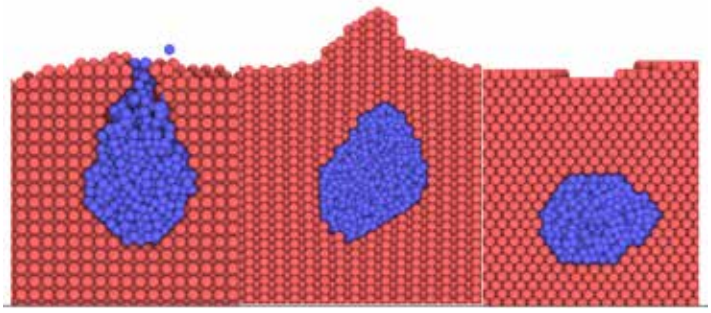

Figure 1. Snapshots of the He bubbles at the end of the simulations. Left: (100) surface; center: (111) surface; right: (110) surface.

In the case of the proto-bubbles, we investigated the behavior of V(M)+He(N) complexes (where V(M)+He(N) indicates a cluster of M vacancies with N helium atoms inside, for M=1,2 and N=0 to 20, at T=1000K Such complexes are the nuclei from which larger bubbles grow by absorption of interstitial He atoms that diffuse through the tungsten matrix. We were particularly interested in the mobility of these complexes. The results are very interesting, as the diffusivity proved to be very sensitive to the number of He, as shown in Figure 2. For example, V(1)He(0) (i.e., a free vacancy) diffuses on a nanosecond timescale with D=1x10-12 m2/s. The introduction of a single He (V(1)He(1)) appears to immobilize the cluster (we didn't see it move in ms of simulation time). This remains true under further addition of He until a sufficient number of heliums are present. At N~10, the complexes start to diffuse again, this time through the emission of a Tungsten interstitial, which eventually recombines and annihilates a vacancy; this leads to net motion of the complex when the annihilated vacancy is the original one. In order to diffuse according to this mechanism, N must be high enough for the emission of interstitials to occur at a significant rate, but low enough that recombination is also active. This leads to a strong dependence of the diffusivity on He content. For M=1, N=14 is such a magic number where diffusivity is a maximum, matching that of a free vacancy. As seen in Figure 2, in this regime, the addition of a single He can lead to changes in diffusivity of up to 2 orders of magnitude. The behavior is qualitatively similar for M=2, but more He are required to activate the motion of the complex.

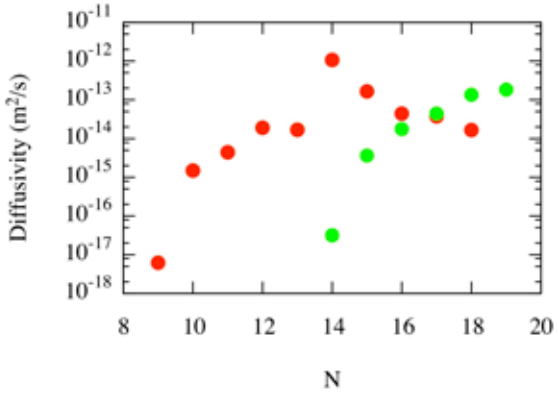

Figure 2. Diffusivity of V(m)+He(n) complexes for M=1 (red) and M=2 (green).

Impact on National Missions

Controlled nuclear fusion is poised to cross the threshold from basic experimental studies to demonstrable electricity production, as embodied by the ITER nuclear reactor under construction in France. However, serious hurdles remain before fusion energy becomes economically viable. Many of these challenges are related to materials. Indeed, the performance demands on plasma-facing components, first wall and blanket systems of future fusion power plants are beyond the capability of current materials. The United States National Academy of Engineering has ranked the quest for fusion as one of the top grand challenges for engineering in the 21st Century. Both the 2007 Fusion Energy Science Advisory Committee (FESAC) panel led by Martin Greenwald and the 2009 Research Needs for Magnetic Fusion Energy Report of the Research Needs Workshop (ReNeW) strongly highlighted the critical importance of improved understanding and modeling of the boundary plasma-materials interaction. The Greenwald FESAC report

found that four of the top five knowledge gaps in magnetic confinement fusion research were related to plasma surface interactions. Our focus, through the use of long-time molecular dynamics simulations at unprecedentedly realistic time and length scales, is understanding helium bubble growth and bursting near the surface of tungsten as it is bombarded by helium from the fusion plasma. This bubble growth and bursting is thought to be a key factor in the plasma-induced growth of "fuzz" on the tungsten surface, which threatens to disqualify tungsten as a first-wall material, despite the fact that it is currently slated as such in the ITER design.

Homogenization and Multi-Phase Strength Research Proposal

Darby J. Luscher
20160659ER

Abstract

This LDRD reserve funds research effort conducted over two quarters of FY16, has initialized a framework for comparing various continuum homogenization schemes used to compute the effective dynamic response of multi-phase materials. For example, a material that is stable in a specific phase or polymorph may change phases under shock loading to certain pressures and temperatures. During the transformation from one phase into another, there exists a time-evolving spatial distribution of both phases of the material that interact within the composite. A mixture of multiple material phases does not respond to dynamic events the same way either phase would respond independently, thus constitutive theories must address the manner in which they interact. This work has compared three separate continuum assumptions for the interaction of multi-phase materials and, more importantly, developed a set of tools to facilitate this research in future investigations.

Background and Research Objectives

There are numerous approaches for addressing the averaged response of a material comprising a mixture of distinct phases. Simple classical considerations for composite materials have assumed either a Voigt (uniform strain) or a Reuss (uniform stress) approach, which provide upper and lower bounds, respectively, on the strain energy within the homogenized material. Continuum models of phase transformation, which address either macro-mechanical or single-crystal scales of dynamic response, have been known to use the uniform strain assumption. However, the shock physics community has developed and parameterized expressions for the free energy and equilibrium phase diagrams of materials that are based on an assumption that each phase is at the same pressure. These models entirely neglect the effect of deviatoric stress (such as from shearing) on the transformation process. A logical extension of the uniform pressure assumption is to assume a uniform stress for the mixture of phases. However, assuming uniform stress within each of the phases is problematic when the yield strengths of different phases are disparate. On the other hand, assuming of uniform deformation within each of the constituent phases results in a model that is inconsistent with the equations-of-state developed and parameterized by the shock compression research community.

The objectives of this brief preliminary research effort are outlined as follows.

O1: Derive thermodynamically consistent system of equations for representing the individual and phase-averaged stress and deformation of a mixed-phase material under separate assumptions of (A) uniform pressure and (B) uniform deformation.

O2: Develop a numerical solution scheme for Hugoniot states based on each of the above cases that can be extended to include volumetric and isochoric deformation.

O3: Compare predicted Hugoniots and equilibrium phase diagrams with experimental data using previously developed and parameterized equations-of-state under both assumptions.

O4: Explore the efficacy including advantages and disadvantages of enhanced micromechanical approaches.

Scientific Approach and Accomplishments

The considered problem involves a material that can have n phases, each one of them described by a thermodynamic potential, Helmholtz free energy, which is the sum of energy associated with static lattice compression, and the vibrational and electronic excitation free energies. Under change of temperature, T, and/or pressure, P, phase transformation may happen. The equilibrium solution of the phase transformation process is obtained by maximization of the entropy or, likewise, by minimization of an appropriate thermodynamic potential. If the phase transformation is assumed to happen at uniform

temperature and pressure, then the appropriate thermodynamic potential is the Gibbs free energy, G, whereas a transformation at uniform temperature and strain finds its equilibrium at the minimum of the Helmholtz free energy. To realize objectives O1-O3, the kinetics of phase transformation were omitted and a thermodynamically consistent system of equations was developed to identify Hugoniot states and an equilibrium phase diagram for separate assumptions of (A) uniform pressure and (B) uniform deformation of the phases. The focus of this study was the shock induced α-ω, α-ε and α-ω-β phase transitions of titanium, iron, and zirconium, respectively.

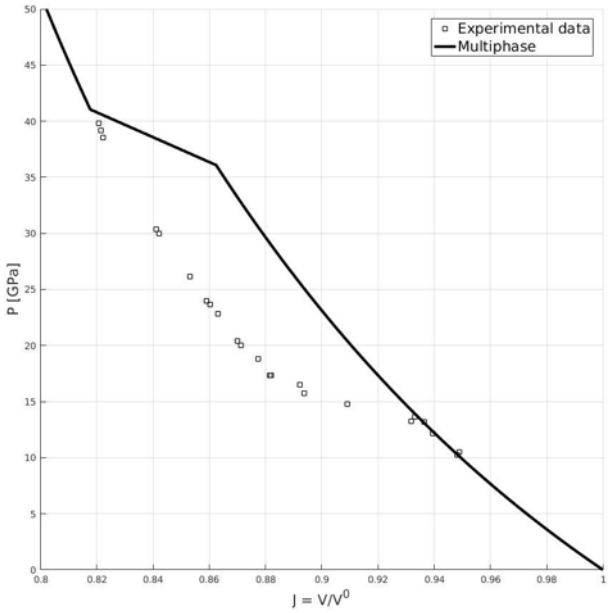

Figure 1. Iron Hugoniot, pressure vs. specific volume ratio computed using original free-energy potential.

Initial conditions were assigned to represent the material's ambient state and, using an iterative Newton-Raphson scheme, the reference volume is computed for each phase from the Helmholtz free energy. Once temperature and volume are known, it is possible to derive all the thermodynamic quantities from the material's thermodynamic potentials. Rankine-Hugoniot equations, which represent conservation of mass, momentum, and energy behind a passing shock wave were solved for varying values of impact or particle velocity in order to compute equilibrium Hugoniots. Maxwell construction was employed to plot the Hugoniot curve in the Us-Up and P-T planes. The Hugoniot curves for iron are shown in Figures 1 and 2. Both plots are obtained from minimization of the Helmholtz free energy assuming uniform temperature and strain; Figure 1 uses the original equation of state, whereas the free energy has been shifted for the calculations in Figure 2. Using the original equation of state, the α-ε phase transition is predicted for a shock pressure of 37 GPa, which is much higher than the 15GPa shock pressure required for transformation in experiment. The correct transformation pressure is captured by adjusting the static lattice potential of the ε phase by a constant energy term (consistent with Figure 2). Our results indicate that this strategy does not produce good results when applied to zirconium and titanium.

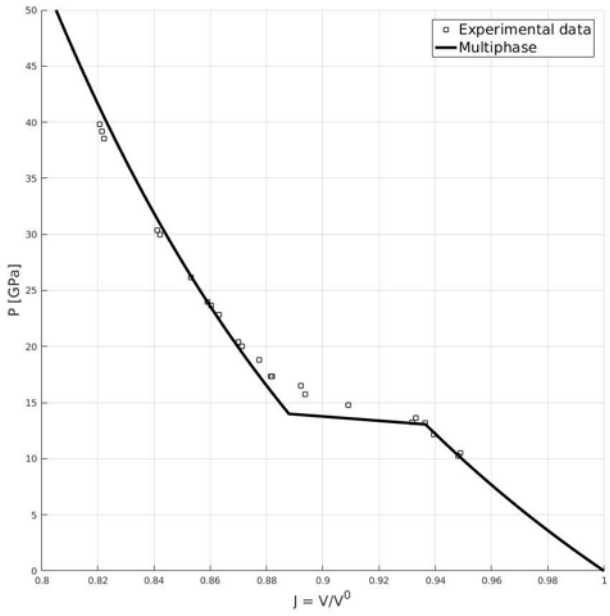

Figure 2. Iron Hugoniot, pressure vs. specific volume ratio computed using shifted free-energy potential.

Some Conclusions Regarding Objective O1-O3

Under uniform pressure and temperature, the published equations-of-state for relevant material phases can be used to reproduce experimentally measured Hugoniot states and equilibrium phase diagrams. This is largely because the assumption of uniform pressure and temperature between phases is consistent with assumptions made during the development and parameterization of the energy potentials for the material phases. On the other hand, these results demonstrate that potentials identified and calibrated based on the assumption of uniform pressure and temperature between phases cannot be used in a phase transformation framework that assumes the two phases are under uniform deformation and temperature without significant discrepancy from experimental data. In a sense, the assumptions used to develop the equations-of-state must be consistent with those used in the subsequent homogenization approach. This statement reinforces the original challenge motivating this exploratory research. Namely, constituents within a mixed-phase material cannot co-exist at the same uniform stress if these phases have disparate mechanical yield strengths. In order to address future generalization to cases of shear-driven phase transformation where this issue of non-uniform yield strengths is a significant concern, an additional microme-

chanics-based homogenization approach was evaluated in the context of this phase transformation problem to complete objective O4.

Objective O4 was achieved by introducing a simple kinetic rate for phase transformation within a Method-of-Cells (MOC) solution scheme. MOC is an established homogenization technique for the simulation of a composite material. A representative volume element of material (RVE) composed of a three-dimensional set of 2x2x2 subcells is considered. The first-order theory is used in this study such that the displacement field within each subcell varies linearly and the corresponding strain field is constant within each subcell. The theory assumes that displacements and tractions between cells are continuous and that stresses are equilibrated within each subcell. The constitutive behavior for subcells uses a Mie-Gruneisen equation of state with classical power-law hardening, isotropic plasticity.

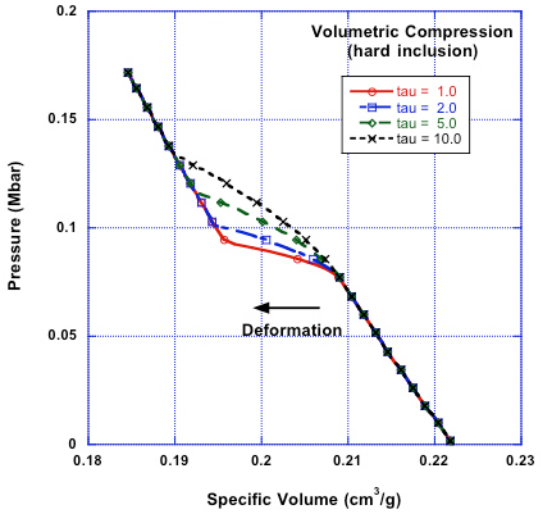

Figure 3. Average pressure versus specific volume during phase transformation for different relaxation times.

A range of deformation histories was investigated using the MOC technique. Here we address results from a simulation in which a hard phase is nucleated and grows within the composite material. A simple model for transformation kinetics that is linear in pressure was used for these simulations. The high-pressure phase is assumed to reside in a single subcell whose domain grows according to the evolving volume fraction. A plot of the average pressure-specific volume response for the conditions of uniaxial strain using several transformation time constants is provided in Figure 3. The transformation from the parent to the daughter phase is apparent by the step in the Hugoniot curve.

While these results demonstrate that the pressures of the two phases are identical are nearly identical, Figure 4 illustrates that the deviatoric (or shearing) stresses within the hard daughter phase (inclusion) are much higher than that for the relatively soft parent phase (matrix).

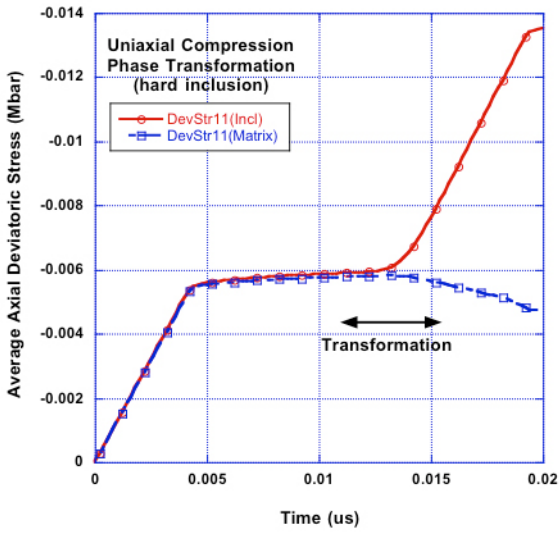

Figure 4. Average axial deviatoric stress evolution within the parent (matrix) and daughter (inclusion) phases.

Impact on National Missions

The findings from this investigation potentially impact the multi-phase equation-of-state and multi-phase strength and damage modeling efforts within the Advanced Scientific Computing's Physics and Engineering Models (ASC-PEM) program. The research conducted within that program thus far has focused separately on the rule of mixtures applied to the equations-of-state and that applied to the material's deviatoric constitutive response (e.g. strength and damage).

One conclusion from these results is that these communities could benefit from developing a consistent set of assumptions pertaining to mixed-phase material response. Conditions of uniform pressure are consistent with previously developed equations-of-state, but are physically incorrect and numerically ill-posed when extended to general states of stress experienced by plastically deforming constituent phases. In order to properly evaluate the applicability or effectiveness of other assumptions, researchers focused on the inelastic shear response of a material must collaborate directly with experts developing equations of state that are consistent with those varied assumptions. Physically-based equations-of-state developed and parameterized from discrete calculations such as density functional theory offer potential advantages in this regard over empirically determined counterparts. Homogenization approaches such as MOC offer a balance between the bounding assumptions of uniform pressure and uniform

strain, but do not obviate the concerns about appropriate equations-of-state.

We suggest future efforts focus on employing computational mechanics approaches to develop a statistical characterization of the stress and strain fields evolving within the volume of mixed-phase materials. The trends are certain to depend upon characteristics of the material phases e.g. the disparity in flow stress.

Efficient Carbon Nanotube Growth on Graphene-Metal Surfaces

Enkeleda Dervishi
20130785PRD2

Introduction

The project goal is to optimize the synthesis conditions that promote the catalytic conversion of graphene into high yield few-walled (1-2 layers) carbon nanotubes (CNTs). The approach will overcome typical drawbacks of nanotube synthesis that include use of harsh chemical treatments of growth substrates and include the need for multi-step purification processes. These challenges will be overcome by using graphene sheets as an innovative new substrate for growth that allows one-step synthesis of composite materials. Growth can also be attained at low-temperatures (~200 degrees C vs the typical 800 degrees or higher) which is essential for enabling development of composites based on multiple materials with very different ranges of temperature compatibility. Another innovative aspect is to use dip-pen lithography capability for fine-control over placement and morphologies of metallic nanoparticle growth catalysts. Optimization of our growth processes will require variation and study of the influence of multiple growth parameters. These will include modulation of catalyst particle size, composition, and placement. We will also study the effects of variable temperatures and reactant gas composition and flow rates. The resultant synthesis will directly provide nanotube/graphene composites that will be studied for their energy harvesting and storage potential. Low temperature growth processes are anticipated to also allow the use of gold nanoparticles for growth as well, which will be the key to enabling development of nanotube-nanowire hybrids (not yet attained) of interest for optical and electronics needs. The knowledge gained in these first synthesis directions will also allow us to tailor synthesis conditions to pursue growth of other novel composite materials including carbon nanotube hybrids with complex metal oxides. Such oxide thin films form the basis for superconducting and multi-ferroic materials of technological interest. Interactions with nanoelectronic materials such as nanotubes can introduce emergent electronic behaviors that may enhance the properties of interest.

Benefit to National Security Missions

The work is directly relevant to DOE Office of Science interests in the fundamental science of and development of multifunctional nanoscale materials. The work will also probe the fundamentals of carbon nanomaterial interactions with other materials, also of interest to DOE/SC. The nanotube/graphene materials are of significant interest for energy storage and energy harvesting, giving the work mission relevance for both energy security and the environment (climate and energy impacts). The effort is also directly related to development and basic understanding of nanomaterials with ultimate impact on electronics, sensing, and imaging needs as well, e.g. for nuclear nonproliferation applications.

Progress

In FY16, we continued with optimization of single domain large area growth and started exploring Fe-film catalyzed systems for “twisted” bilayer growth. Large area materials were fed into our heterostructure studies.

The team also continued graphene synthesis and provided materials to collaborators in the areas of biosensing and bioviability. Several manuscripts are on their way. We focused our efforts on the fabrication of graphene-membrane systems with tunable pore morphologies.

Evaluation of the Ge nanowire melting mechanism continued as well, and the team worked on the generation of test heterostructures for Raman spectroelectrochemical probing of the nanowire expansion process. In parallel we continued Si heterostructure growth strategies. Based on these results we wrote a strong LDRD/ER proposal that made it through the second review round.

Oxide heterostructures: We worked on optimizing the development of oxide heterostructures and performed thorough Raman studies to understand the interfacial properties between graphene and different type of substrates with varying morphologies. This work was

selected for an oral talk at a prestigious international conference.

Graphen Molecule Raman: In FY16 we completed all experiments and characterization of graphene molecules. We started working on a publication. This novel research was also selected for an oral and a poster presentation at two prestigious international conferences.

We also note that PI and former postdoc Dervishi has been converted to a staff position engaged in the weapons program.

Future Work

Large area, single domain graphene synthesis: In FY17 we will continue with optimization of single domain large area growth and push Fe-film catalyzed systems for "twisted" bilayer growth. Large area graphene will be used for our heterostructure studies.

In FY17, we will continue synthesizing large-area graphene and continue collaborations in the areas of biosensing and bioviability. We will also continue synthesizing Ge/Si nanowire-graphene heterostructures and develop new growth strategies. In parallel, we will work on developing a set up for Raman spectroelectrochemical probing of the nanowire expansion process during electrochemical cycling.

Oxide heterostructures: We will continue developing graphene-thin film heterostructures and perform thorough Raman spectroscopy studies to understand the relationship between the substrate morphology and properties of transferred graphene.

Graphen Molecule Raman: In FY17 we will continue the manuscript preparation on the Raman Spectroscopy studies of graphene molecules.

Graphene-based membranes: We will continue developing graphene-based membrane systems over various substrates and perform preliminary studies of new devices.

Conclusion

Our primary technical goal is now focused on generation of large-area graphene heterostructures. The methods we anticipate using will result in generation of functional hybrid carbon nanomaterials of interest for energy storage, electronic, membrane systems and multi-ferroic applications. These may include hybrid quantum dot/graphene materials, graphene/nanowire heterojunctions, and graphene composites with complex oxide thin films.

Publications

S. Trigwell, S. Snyder, W. Hatfield, E. Dervishi, and A. S. Biris. Carbon nanotube coatings as used in strain sensors for composite tanks. 2016. Particulate Science and Technology: An International Journal. : 1.

M. H Lahiani, E. Dervishi, I. Ivanov, J. Chen and M. V. Khodakovskaya. Comparative study of plant responses to carbon-based nanomaterials with different morphologies. 2016. Nanotechnology. : 265102.

Dervishi, E., Z. Li, M. Sykora, and S. K. Doorn. Raman spectroscopy of graphene molecules: Size dependent and reaction time studies. To appear in Under preparation.

Dervishi, E., Z. Li, N. Hartmann, M. Sykora, and S. K. Doorn. Spectroscopic studies of graphene molecules: Analysis of size and Crystallinity. Presented at The 17th International Conference on the Science and Application of Nanotubes (NT16) . (Vienna Austria, , August 7-13, 2016.).

Dervishi, E., Z. Li, N. Hartmann, M. Sykora, and S. K. Doorn. Raman Spectroscopy of Graphene Molecules: Size Dependent and Reaction Time Studies. Presented at The 229th ECS Meeting, . (San Diego CA,, May 29 -June 2nd, 2016.).

Gao, Y., O. Roslyak, E. Dervishi, N. S. Karan, Y. Ghosh, C. J. Sheehan, F. Wang, G. Gupta, A. Mohite, A, M. Dattelbaum, S. K. Doorn, J. A. Hollingsworth, A. Piryatinski, and H. Htoon. Hybrid Graphene-Giant Nanocrystal Quantum Dot Assemblies with Highly Efficient Biexciton Emission. . 2015. Advanced Optical Materials Highlighted on the Inside Front Cover. . 3 (1): 39.

Quantum Control of Tailor-designed Photoactive Energetic Materials

Tammie R. Nelson
20140668PRD2

Introduction

We will continue to develop a new excited state framework for implementation in the non-adiabatic excited state molecular dynamics (NA-ESMD) code to allow description of photochemical reactions in realistic environment. Photochemistry initiated by laser excitation in optically active high explosive (HE) materials can be the first step in a photodecomposition mechanism leading to direct optical initiation. Photochemical reactions often result in formation of radicals with unpaired electrons. In order to follow the dynamics of these fragments, we will develop an open-shell excited state description at the configuration interaction singles level. We will also derive the corresponding excited state gradients and non-adiabatic couplings for the open-shell with state specific solvation effects that are needed for propagating dynamics. We have already made a prototype code incorporating open-shell description for the ground electronic state. During the third year of the project our goal will be to extend this ground state framework to include electronic excitations. We will implement this new framework in the code including polarizable continuum model (PCM) solvent effects developed in the previous years of the project. The developed methodology will provide a better description of the entire evolution of bond breaking reactions. We will apply the new code to continue our studies of photoactive energetic materials with controllable optical functionality by identifying specific vibrational degrees of freedom responsible for bond breakage, rapid decomposition, and the onset of the exothermic chain reactions relevant to explosive initiation. Detailed numerical NA-ESMD simulations to investigate photoinduced pathways, timescales, branching effects, and multiple product formation, which can be experimentally validated by ultrafast spectroscopy capabilities, will be performed. Possible photoinduced reaction coordinates and electron-vibrational relaxation pathways to elucidate mechanisms for optical initiation will be assessed.

Benefit to National Security Missions

The proposed work will increase the controllability of chemical dynamics by predicting and controlling the functionality of materials. The proposed work will further LANL's reputation and prestige in quantum control and molecular design. Control of explosive initiation would be transformational for LANL's core missions of stockpile safety and energetic materials.

Progress

Over the past year, significant changes have been done to the non-adiabatic excited state molecular dynamics (NA-ESMD) codes toward implementation of solvent contributions and application to large molecular systems that are computationally demanding. To treat large molecules, a state limiting algorithm to reduce the number of excited states in surface hopping simulations "on-the-fly" has been implemented and tested on model systems of PPV oligomers and branched PPE dendrimers. This new algorithm provides a 2x reduction in computational cost in model systems and up to 5x speed up in larger systems. The results have been summarized in the article "Nonadiabatic Excited-State Molecular Dynamics: On-the-Fly Limiting of Essential Excited States" recently accepted for publication in Chemical Physics.We have informed the design of a new class of optically active "integrated" energetic chromophores and performed DFT and one- and two-photon absorption studies for a range of materials with different structural motifs. This work has been recently accepted for publication in Journal of Physical Chemistry A in the article "Two-Photon Absorption in Conjugated Energetic Molecules". Following this work, we have identified several molecular candidates with large absorption cross-sections to carry forward for molecular dynamics simulations. We have implemented excited state gradients and non-adiabatic couplings in the NA-ESMD code using the Polarizable Continuum Model (PCM) allows us to conduct simulations of non-adiabatic excited state dynamics in the presence of the simple solvent environment, we are now performing

NA-ESMD simulations to identify photochemical pathways in the new materials. In terms of applications, the photochemistry of the conventional high explosive nitromethane (NM) has also been investigated using the NA-ESMD code to verify excited state lifetimes, predict photoproducts and intermediates, and predict relative yields and timescales of different reactions. We were able to rationalize the experimental observation of isomerization products based on a two-step reaction supported by the predicted relative timescales for the two steps. The work is presented in detail in "Ultrafast Photodissociation Dynamics of Nitromethane" published in Journal of Physical Chemistry A.

Future Work

We will continue to develop a new excited state framework for implementation in the non-adiabatic excited state molecular dynamics (NA-ESMD) code to allow description of photochemical reactions in realistic environment. Photochemistry initiated by laser excitation in optically active high explosive (HE) materials can be the first step in a photodecomposition mechanism leading to direct optical initiation. Photochemical reactions often result in formation of radicals with unpaired electrons. In order to follow the dynamics of these fragments, we will develop an open-shell excited state description at the configuration interaction singles level. We will also derive the corresponding excited state gradients and non-adiabatic couplings for the open-shell with state specific solvation effects that are needed for propagating dynamics. We have already made a prototype code incorporating open-shell description for the ground electronic state. During the third year of the project our goal will be to extend this ground state framework to include electronic excitations. We will implement this new framework in the code including polarizable continuum model (PCM) solvent effects developed in the previous years of the project. The developed methodology will provide a better description of the entire evolution of bond breaking reactions. We will apply the new code to continue our studies of photoactive energetic materials with controllable optical functionality by identifying specific vibrational degrees of freedom responsible for bond breakage, rapid decomposition, and the onset of the exothermic chain reactions relevant to explosive initiation. Detailed numerical NA-ESMD simulations to investigate photoinduced pathways, timescales, branching effects, and multiple product formation, which can be experimentally validated by ultrafast spectroscopy capabilities, will be performed. Possible photoinduced reaction coordinates and electron-vibrational relaxation pathways to elucidate mechanisms for optical initiation will be assessed.

Conclusion

The proposed implementation of the quantum mechanical and molecular mechanical (QM/MM) approach will provide novel computational capabilities critical for understanding light-induced dynamics including realistic size and environment effects in many technologically relevant materials. Specifically, this will allow us to simulate large molecular systems where full ab-initio calculations are prohibitively expensive, and to describe systems that interact strongly with solvent environments. Such simulations have been done previously for the ground state but were never attempted for excited states due to computational complexity.

Publications

Bjorgaard, J. A., A. E. Sifain, Nelson, T. W. Myers, J. M. Veauthier, D. E. Chavez, R. J. Scharff, and Tretiak. Two-Photon Absorption in Conjugated Energetic Molecules. 2016. JOURNAL OF PHYSICAL CHEMISTRY A. 120 (26): 4455.

Bjorgaard, J. A., T. Nelson, K. Kalinin, V. Kuzmenko, K. A. Velizhanin, and S. Tretiak. Simulations of fluorescence solvatochromisms in substituted PPV oligomers from excited state molecular dynamics with implicit solvent. 2015. Chemical Physics Letters. 631: 66.

Greenfield, M. T., S. D. McGrane, C. A. Bolme, J. A. Bjorgaard, T. R. Nelson, S. Tretiak, and R. J. Scharff. Photoactive high explosives: linear and nonlinear photochemistry of petrin tetrazine chloride. 2015. Journal of Physical Chemistry A. 119: 4846.

Nelson, , Bjorgaard, Greenfield, Bolme, Brown, McGrane, R. J. Scharff, and Tretiak. Ultrafast Photodissociation Dynamics of Nitromethane. 2016. JOURNAL OF PHYSICAL CHEMISTRY A. 120 (4): 519.

Nelson, , Fernandez-Alberti, A. E. Roitberg, and Tretiak. Nonadiabatic Excited-State Molecular Dynamics: Modeling Photophysics in Organic Conjugated Materials. 2014. ACCOUNTS OF CHEMICAL RESEARCH. 47 (4): 1155.

Nelson, T., A. Naumov, S. Fernandez-Alberti, and S. Tretiak. Nonadiabatic excited-state molecular dynamics: on-the-fly limiting of essential excited states. To appear in Chemical Physics.

Probing and Controlling the Surface States of Topological Insulators

Scott A. Crooker
20140683PRD4

Introduction

Topological Insulators (TIs) are a recently discovered class of materials that have garnered significant attention in the last 5 years within the condensed matter physics community. They are bulk semiconductors such as Bi2Se3 and Bi2Te3 in which spin-orbit coupling gives rise to a topologically protected two-dimensional (2D) metallic surface, with a surface electronic structure similar to the Dirac cone spectrum of graphene. The surface states are protected from backscattering by time reversal symmetry, and therefore TIs have potential applications for spin logic devices and low-power electronics. Although there is tremendous excitement and interest in these novel materials within the physics and materials science community, the exploration of exotic spintronic properties in TIs such as spin photocurrent and current-induced spin-density properties are still at an early stage. The ability to control the topological surface states electrically or optically is the crucial key to the development of spin-based devices.

Luyi will probe, and ultimately manipulate, the spin degrees of freedom in TIs. A major part of this research will combine the unique optical and pulsed magnetic transport techniques at the National High Magnetic Field Laboratory at LANL to characterize spin structure and transport. In TIs it is possible to photoexcite currents whose charge, spin, and direction can be controlled by varying the helicity of the light. The subsequent spin currents and spin dynamics can be monitored and imaged via the magneto-optical Kerr effect. The unique nature of spin-momentum locking in the SSs suggests that the spin current in a TI can be generated with the same efficiency as charge photocurrent in a conventional insulator.

Benefit to National Security Missions

This project will build Laboratory capabilities in the areas of Materials Science, Emergent Phenomena, and Materials-by-Design, and also in novel measurement methods that enable new scientific discovery at LANL. It is based on the very recent discovery of a new class of so-called "topologically protected" materials, in which scattering and dissipative processes are prohibited from fundamental physics considerations. The experimental techniques that we will develop as part of this project will advance new Laboratory capabilities that underpin a wide variety of Laboratory missions related to Materials Science and Controlled Functionality in Materials. Beyond direct scientific impact, these studies have the potential to pave the pathways for new "topologically protected electronics"; that is, transport of charge and spin in new generations of lower-power, potentially more compact, and more efficient electronic devices, which has direct impacts on securing our energy future. In the longer term (10+ years) it is possible that next-generation electronic and 'spintronic' devices based on these materials could find their way to 1) advanced sensors and 2) quantum information processing applications, both of which would be relevant for Global Security interests. The present work helps establish the fundamental properties and underlying physics of this new generation of materials.

Progress

In the past year Luyi has obtained some breakthrough results that have been published in high-profile journals.

In the first paper (Nature Physics), Luyi studied a new family of two-dimensional semiconductors known as the "transition-metal dichalcogenides", which are composed of a single atomically-thin sheet of material. These materials have attracted significant amount of attention in the last two years owing to their promise for a new generation of low-power, high-efficiency semiconductor electronics. Luyi's paper describes the first-ever measurements of how magnetization develops and relaxes in these new materials.

In the second paper (Nano Letters), Luyi discovered that electrons in these 2D semiconductors actually exhibit the very interesting property of "coherence," which may

make them attractive for future device applications wherein information is encoded in an electron's 'spin' degrees of freedom.

These papers are the result of ultrafast optical measurements performed by Luyi, on a series of atomically-thin semiconductors (MoS2 and WS2) . As a result of this work, Luyi has received several invitations to give invited talks, for example at the 2016 March Meeting of the American Physical Society, as well as talks at the upcoming ICPS-2016 conference (Beijing) and PASPS-9 conference (Kobe, Japan). These presentations are important for maintaining LANL at the forefront of semiconductor physics in the international community.

Future Work

Luyi's Director's funded postdoctoral fellowship will end in October 2016. For the reminder of this fiscal year and for that portion of her Fellowship that runs into the next fiscal year, Luyi will focus on perfecting the infrared Magneto-Optical Kerr imaging microscope that allows us to directly image the spin currents in these topological insulator materials. Luyi will continue to benchmark a variety of mid-infrared quantum cascade lasers, and will continue to screen a variety of these topological insulator materials using magneto-reflectivity and absorption studies. She will also apply the microscope to a new class of related two-dimensional semiconductor materials that are believed to host interesting topological phases (eg, MoTe2).

Conclusion

The principal goal of this project is to image, via magneto-optical techniques pioneered at the NHMFL-Los Alamos, the spin currents that are predicted to form at the surface of TI materials. The results will allow direct visualization and spatial mapping of the topologically protected electronic states for the first time. Beyond direct scientific impact, these studies have the potential to pave the pathways for new "topologically protected electronics"; that is, transport of charge and spin in new generations of lower-power and more efficient electronic devices, which has direct impacts on securing our energy future.

Publications

Glasenapp, , N. A. Sinitsyn, Yang, D. G. Rickel, Roy, Greilich, Bayer, and S. A. Crooker. Spin Noise Spectroscopy Beyond Thermal Equilibrium and Linear Response. 2014. PHYSICAL REVIEW LETTERS. 113 (15): 156601.

Roy, D., L. Yang, N. A. Sinitsyn, and S. A. Crooker. Cross-correlation spin noise spectroscopy of heterogeneous interacting spin systems. 2015. Scientific Reports. 5: 9573.

Yang, , Chen, K. M. McCreary, B. T. Jonker, J. u. n. Lou, and S. A. Crooker. Spin Coherence and Dephasing of Localized Electrons in Monolayer MoS2. 2015. NANO LETTERS. 15 (12): 8250.

Yang, , Glasenapp, Greilich, Reuter, A. D. Wieck, D. R. Yakovlev, Bayer, and S. A. Crooker. Two-colour spin noise spectroscopy and fluctuation correlations reveal homogeneous linewidths within quantum-dot ensembles. 2014. NATURE COMMUNICATIONS. 5: 4949.

Yang, L., N. A. Sinitsyn, J. Yuan, J. Zhang, J. Lou, and S. A. Crooker. Long-lived nanosecond spin relaxation and spin coherence of electrons in monolayer MoS2 and WS2. 2015. Nature Physics. 11: 830.

Uniaxial Pressure to Elucidate Complex Electronic States in Actinides

Filip Ronning
20150702PRD1

Introduction

The development of a uniaxial pressure cell capable of nuclear magnetic resonance (NMR) measurements is key to this research. The cell should be tunable in situ and have the capability to reach cryogenic temperatures down to 20 mK and in magnetic fields up to 12 T. Following the design of Hicks et al. (RSI 2014) we will utilize piezoelectric stacks that are decoupled from a sample to maximize signal-to-noise ratio while simultaneously tuning uniaxial pressure in-situ in a magnet and cryostat. Once the cell is operational, the first NMR experiments will be carried out on uranium ruthenium silicide (URu2Si2). Recent elasto-resistivity measurements in collaboration with LANL reveal a hidden nematic order in URu2Si2, which can be exposed with the application of uniaxial pressure (Riggs 1405.7403). Measurements of the local spin susceptibility, electric field gradient, and spin lattice relaxation rate, which can be done with NMR will provide the necessary microscopic information to unravel the mysteries these systems present. In future work, this technique will enable new investigations of many other interesting anisotropic, heavy fermion, magnetic and superconducting materials.

Benefit to National Security Missions

Los Alamos has a long history in f-electron intermetallics from electronic tuning of plutonium to the discovery of the first 5f-electron heavy fermion superconductor, UPt3. Now, we are internationally recognized for developing an understanding of the rich and complex phenomena that occurs in strongly correlated (f-) electron systems. However, a detailed knowledge of the (competing) order parameters is still needed. Adam proposes to build a novel apparatus which will directly shed light on the electronic complexity exhibited by actinide materials. This will push us closer to the requisite understanding to achieve controlled functionality – one of the three objectives of the Los Alamos materials strategy.

This work directly addresses DOE-BES objectives as articulated in the Grand Challenge reports. Undoubtedly, success will enable studies of similar physics in d-electron systems. The study of spin fluctuations in actinide materials has relevance for nuclear materials. And the ability to study unconventional superconductivity may eventually lead to relevance for quantum information studies of so-called topological superconductors. This work also aligns with LANL's Energy Security strategy, and the understanding of electronic structure of actinides in general may eventually provide guidance to the LANL weapon's program.

Progress

The director's fellowship project entitled, "Uniaxial Pressure to Elucidate Complex Electronic States in Actinides" has progressed well since beginning in September 2015. Initial proof of concept nuclear magnetic resonance (NMR) experiments on a Uranium-Ruthenium-Silicon compound showed that the signal-to-noise ratio of the samples under study would be sufficient to proceed. A uniaxial pressure cell was designed, fabricated, assembled, and tested successfully. Software and hardware were developed to control, measure, and automate the application of uniaxial pressure with a computer. A significant radio frequency noise issue caused by the uniaxial pressure cell control electronics was overcome by constructing a filter device. Single crystalline samples were prepared with the appropriate orientation and dimensions for the experiment. One of the best samples has now been successfully mounted on the strain cell and the first experiments under applied uniaxial pressure are planned.

While preparations were underway for the upcoming experiments, other related zero-pressure measurements were conducted on samples known to be sensitive to uniaxial pressure or show related complex electronic states. Experiments were performed on a Cerium-Cobalt-Indium compound to determine the effect of introducing inhomogeneous strains (or internal pressures) via grind-

ing single crystals into a powder. NQR experiments were also performed on a similar Cerium-Rhodium-Iridium-Indium compound to quantitatively determine the amount of Rhodium and Iridium. Currently, NMR experiments are under way to ascertain the nature of a novel magnetic state in a related Cerium-Lanthanum-Bismuth-Platinum compound. Utilizing electronic density calculations the Lanthanum NQR spectrum was discovered and shows significant changes below the expected magnetic transition temperature at approximately 4 K. Further measurements are required to fully characterize the exact nature of this magnetic state.

Future Work

In the next year we will utilize our NMR strain device to measure the response of the spin degrees of freedom to uniaxial strain. We will begin with work on uranium-ruthenium-silicon compound known for its so-called “hidden order”. Subesequently, we will move to a well known set of cerium based compounds discovered at Los Alamos, known as the “115s”. In addition, we will continue standard NMR measurements on iron doped strontium-nickel-arsenide compound. This system shows a single ion Kondo effect from transport and resistivity measurements, and when doped with large amounts of iron shows a nematic transition which has been identified by strain measurements.

Conclusion

We will add an important new capability in the field of condensed matter research, which will enable new science to be discovered. Anticipated results include: addressing the microscopic origin of the so-called nematic order in URu2Si2, confirming or invalidating the presence of a chiral superconducting order parameter in UPt3, and possibly revealing the presence of a valence transition in PuCoGa5 and its role in mediating superconductivity. The response of these materials to uniaxial pressure could help answer major open questions about the nature of the complex electron interactions in a broad class of novel materials.

Publications

Kissikov, , A. P. Dioguardi, E. I. Timmons, M. A. Tanatar, Prozorov, S. L. Bud’ko, P. C. Canfield, R. M. Fernandes, and N. J. Curro. NMR study of nematic spin fluctuations in a detwinned single crystal of underdoped Ba(Fe1-xCox)(2)As2. 2016. PHYSICAL REVIEW B. 94 (16).

Dynamic Strength and Phase Transition Kinetics in Geophysical Materials

Arianna Gleason
20150707PRD2

Introduction

This project is performing cutting-edge science by using the most brilliant hard x-ray source available to examine the response of geophysical materials to strong shock waves. Only in the last few years has the ability to generate conditions of geophysical impacts been available at the same facility with a high brilliance x-ray source. This x-ray source is necessary to observe how materials like SiO2 and H2O (i.e., low atomic number and low symmetry) change their structures from crystalline solids to disordered materials, like liquids or glasses. Understanding the changes in lattice and electronic structures of these materials will provide new data about how these materials behave during geophysical impact events and about the basic material properties of constituent minerals that exist at simultaneous high-pressure and –temperature in planetary bodies including the Earth's interior.

An experiment was performed at the Linac Coherent Light Source (LCLS) to examine the strength of iron at high temperatures and pressures. These pressure and temperature conditions are similar to those found inside the Earth and will provide information at the atomic level about deformation mechanism and rheological behavior. The experiment was successful in collecting data up to the pressure at which iron melts under shock compression, and analysis is being performed to determine strength from the data.

Benefit to National Security Missions

This work contributes strongly to the basic understanding of materials by producing a new class of data that can be used to develop physically based models of dynamic materials response. This new class of data provides detailed information about the interatomic distances and the sizes and orientations of crystals in materials.

Due to the specific materials being investigated (i.e. materials that are very common in geophysical bodies, such as asteroids, comets, and rocky planets), this work will also directly contribute to astrophysical areas of research.

The Laboratory's proposed Matter-Radiation Interactions in Extremes (MaRIE) Signature Facility includes a hard x-ray free electron laser, similar to the facility in which this work performs experiments, and the work in this project will help to define the characteristics of the MaRIE free electron laser and the details of the experimental stations for MaRIE. Understanding the behavior of matter during extreme shocks is directly relevant to the nuclear weapons program.

Progress

In FY16, we completed a successful experiment probing the strength of shock-compressed iron using x-ray diffraction at LCLS. We collected data on iron compressed to the melt phase and observed interesting developments in the material texture. We have been working on developing analysis to account for both the iron texture and the material strength. The complicated analysis will be continued into the next fiscal year. Additionally, Gleason collaborated on 6 laser-driven shock experiments at the LCLS-Matter in Extreme Conditions hutch, including in-house beamtime.

Also this year, Dr. Arianna Gleason was selected to receive the Alvin Van Valkenberg award to recognize her substantial early career accomplishments in high pressure studies. She will be presented with the award at the 2016 Gordon Research Conference in High Pressure and will give an invited talk.

We have published three journal articles (in Journal of Physics B, Science, and American Mineralogist) and have one article currently in review (Review of Scientific Instruments).

Future Work

In FY17, we will complete analysis and submit a journal article on the formation mechanism of high density amorphous glass (SiO2) from shock compressed fused silica. Additionally, we will analyze the data on the strength of iron under shock compression that we recently acquired at the Linac Coherent Light Source (LCLS). These data will demonstrate a new measurement method for material strength under dynamic compression that is an extension of the radial diffraction technique used in static compression with diamond anvil cells.

Conclusion

The resulting information will advance the current level of understanding about how these materials behave in geophysical events, such as asteroid impacts and the dynamics of the earth's molten iron core. Understanding the behavior of matter during extreme shocks is directly relevant to the nuclear weapons program.

Publications

Gleason, A. E., C. A. Bolme, H. J. Lee, B. Nagler, E. Galtier, D. Milathianaki, J. Hawreliak, R. G. Kraus, J. H. Eggert, D. E. Fratanduono, G. W. Collins, R. Sandberg, W. Yang, and W. L. Mao. Ultrafast visualization of crystallization and grain growth in shock-compressed SiO2. 2015. Nature Communications. 6: 8191.

Nagler, B., A. Schropp, E. Galtier, B. Arnold, S. Brown, A. Fry, A. Gleason, E. Granados, D. Samberg, F. Seiboth, F. Tavella, Z. Xing, H. J. Lee, and C. Schroer. The phase contrast imaging instrument at the Matter in Extreme Condition endstation at LCLS. 2016. Review of Scientific Instruments. 87: 103701.

Reagan, M., A. Gleason, L. Daemen, Y. Xiao, and W. Mao. High pressure behavior of the polymorphs of FeOOH. 2016. American Mineralogist. 101: 1483.

Shahar, A., E. Schauble, R. Caracas, A. Gleason, M. Reagan, Y. Xiao, and J. Shu. A pressure effect on iron partitioning in iron alloys. 2016. Science. 352: 580.

In-situ, 3D Characterization of Solidification in Metals

John W. Gibbs
20150709PRD2

Introduction

Understanding the solidification behavior of metal alloys at the microscopic scale has seen great improvements through synchrotron x-ray experiments. The spatial and temporal resolution afforded by x-ray radiography is just right for visualizing both the shape of dendrites, which are the main features to form during solidification of metals, and how a handful of dendrites interact. This makes it possible to see how macroscopic conditions like temperature gradient or cooling rate affect microscopic features like the spacings between dendrites. Unfortunately, radiography relies on shining x-rays through the sample and collecting images of transmitted x-rays; thus, the resulting data is a projection through the thickness of the sample. Because of this, a relatively thin sample is required to avoid overlapping features, which artificially affects the interactions between dendrites.

By moving to x-ray tomography, it is possible to use a thicker sample and see dendrites interacting in 3D. This will provide a much better understanding of how a collection of dendrites arranges in more realistic scenarios and how morphological instabilities form and destabilize a planar interface. Another innovation of these experiments is to use a sample that is moving in a fixed temperature gradient. This makes it possible to have the liquid/solid interface in the field of view, which is approximately 2mm x 2mm x 2mm, during the full duration of the experiment while moving the sample over tens of millimeters. Such an experiment makes it possible to see how an interface responds to jumps in the interface velocity, which is difficult to observe because the changes often take many millimeters to reach a steady state.

Benefit to National Security Missions

NNSA/Science Campaigns: This project is tied to science campaigns by generating datasets of microstructure evolution during solidification experiments in which the thermal gradient, cooling rate, and alloy composition are independently and systematically varied. These datasets will give us a better understanding of solidification and will be made available to validate simulation methods, including a microstructure prediction model that is currently being implemented in the advanced simulation and computing (ASC) code Truchas.

MaRIE: In this project, we will be using multiple beams (e.g. proton and x-ray) to interrogate samples during solidification. This data can be used to access multiple size scales, since proton imaging has a resolution of ~20 µm and x-ray imaging typically has a resolution of ~1 µm. As both methods have a field of view about 1000 times their resolution, protons can be used to see large volumes of material, while x-rays can give higher resolution views of smaller volumes. The multiple characterization methods also provide opportunities to examine the chemistry of samples in higher detail, due to the differing contrast mechanisms between the two beam types. This work is in alignment with MaRIE, as multiple beams are envisioned to simultaneously characterize samples in the future. This research will also help to define what is currently possible with existing characterization methods and outline what capabilities should be included in future instruments.

Progress

In the past 12 months, which constituted the first half of the PRD, the major accomplishments have been to:

- design, purchase, and test a set of motion control stages that will enable tomography during metal alloy solidification
- design a furnace to work within the constraints of the tomography data collection process
- successfully request beamtime at the Advanced Photon Source (APS) for experiments, including testing time that occurred in May 2016

A tomography experiment consists of shining x-rays through a sample that is rotating and taking images

of the transmitted x-rays when the sample has rotated a specified amount. Typical amounts of sample rotation between images is about 0.25 degrees and the sample must be rotated through 180 degrees, so hundreds of images must be taken to collect a full dataset, which can take a significant amount of time. Thus, tomography requires stages that can move the sample into position and rotate it at the right speed. We are proposing to use a newly developed tomography scheme that, among other innovations, uses non-constant gaps between images in order to maximize the variation sampled under the constraint of a low sampling rate relative to the evolution of the sample. This allows for improved temporal resolution and the ability to capture early stage growth dynamics.

The experimental hardware and software that are required to enable the complex motion and integration with the imaging system has recently been completed. The software design makes the motion rotation pattern easily programmable, and the rotation stage is configured to slow down and trigger the camera to take a picture when it reaches the correct position. This capability has been tested at imaging rates as high as 100 Hz. This testing was done at the Advanced Photon Source (APS), which allowed us to test the integration between the stages and the x-ray imaging systems that we will be using.

The furnace design for these experiments is difficult because we need to achieve relatively large temperature gradients to accurately portray real castings, but to accommodate the tomography data collection process, the sample must be able to rotate freely so typical methods like direct heating and water cooling are not possible. To optimize the furnace design under this constraint, simulations have been used to guide the design process.

The main difference between the work that has been done and what was proposed last year is that we anticipated the first “in-beam” use of the system with pRad. Due to a shorter than anticipated run schedule, fewer days of beamtime were allocated at pRad, so instead we will be commissioning the set-up at APS. In addition to being more accessible, x-ray experiments afford higher resolution, smaller fields of view, and higher temporal resolution, which will be ideal for our first set of experiments.

Professional development accomplishments in the last year have included a week long LabVIEW class and participation in a 3 week Science of Signatures Advanced Studies Institute, hosted by the Engineering Institutes.

Future Work

The experimental setup required for this project consists of a set of linear and rotation motion control stages, a furnace, and the necessary software to coordinate motion and temperatures to perform four-dimensional microscopy of metal alloys during solidification. The motion control system is ready to use and was tested during a visit to the Advanced Photon Source (APS) in May 2016. The furnace has been designed and it will be assembled over the next few weeks. This will complete all of the preparation work for performing upcoming experiments.

The first experiments with this setup will be performed at APS in late July 2016. Our APS user proposal was granted 18 shifts (6 days) and we will be using half the allocation, so there is a possibility for follow-on experiments within the next year, if needed. Our experiments in July will focus on controlled directional solidification during tomography of a variety of aluminum alloys, which hasn’t been performed to date. Directional solidification will be achieved by moving the sample through a fixed temperature gradient, making it possible to watch interface evolution over tens of millimeters of growth, even though the field of view will only be 2 x 2 x 2 mm3. Aluminum alloys will be used because they have been previously studied with ex-situ experiments (i.e. fully solidified samples that are sectioned and undergo microstructural characterization) and in-situ experiments with thin sample radiography to study how single rows of dendrites evolve.

The next reporting period will be used to analyze the data from the upcoming visit to APS, write papers, and possibly perform another round of experiments, depending upon the outcome of our first experiments. Data analysis will be computationally intensive and may take several months to perform.

Conclusion

We will develop the capability to do tomography during controlled directional solidification in proton and x-ray beamlines across the U.S. DOE complex. We will probe solidifying metals with a variety of different diagnostic means to access a wide variety of spatial and chemical data. This will lead to an improved ability to compare experiments and simulations and better theories of solidification dynamics, particularly at non-constant solidification front velocity where there is relatively little data. These datasets will give us a better understanding of solidification and will be made available to validate simulation methods, including a microstructure prediction model that is currently being implemented in the advanced simulation and computing (ASC) code Truchas.

New Physics in New Materials

Priscila Ferrari Silveira Rosa
20150710PRD2

Introduction

The discovery of new physics in new materials is the engine that drives fundamentally new understanding and opens the possibility of previously unimagined new technologies. By its nature, research with this objective is exploratory and, though well-grounded in physical and crystal chemical principles, is intrinsically high risk, but the reward can be substantial. In a study of recently discovered materials, this research aims to discover entirely new electronic states in complex metals as well as to discover only the second example of a highly unusual type of coupled magnetism and unconventional superconductivity that is spatially modulated. The physics of such an unusual state is hotly debated by leading condensed matter theorists.

Benefit to National Security Missions

The discovery and understanding of complex electronic states that arise from multiple competing interactions and the ability to control those states from atomic to macroscopic scales have been and continue to be a priority of the DOE/Office of Science. The research goals of this project coincide precisely with those of the Office of Science. Specifically, this research aims to discover, understand and control new states that appear near a pressure-tuned, zero-temperature magnetic/non-magnetic boundary in new materials in which the magnetic order arises from strong electron-electron interactions and coupling.

Progress

The overall objective of this project is to discover new physics in new materials in which a magnetic transition is tuned to absolute zero temperature where new states of matter, such as exotic types of superconductivity, might emerge. This objective has been pursued through the study of three new materials, ThCo2Sn2 CaMn2Bi2 and CeRhIn5 in which a small amount of Cerium (Ce) has been replaced by Neodymium (Nd). At atmospheric pressure, each of these compounds orders antiferromagnetically at temperatures near 75, 150 and 3.5 K, respectively. We have shown that applying hydrostatic pressures to 2.5 GPa (about 25,000 atmosphere) reduces the magnetic transition temperature of the first two compounds by roughly 25 K and that 5-7 GPa should be sufficient to drive their transitions to zero temperature. To reach these much higher pressures, we have begun developing a new type of pressure device and made preliminary tests of it. Our design of the device is sound, and we fully expect to reach the desired high pressures in the coming few months. In parallel, a series of Nd-substituted CeRhIn5 crystals, Ce1-xNdxRhIn5 (with x greater than or equal of 0 and less than or equal to 1), have been grown and a manuscript has been submitted on their electrical, magnetic and thermodynamic properties at atmospheric pressure. These studies show that Nd-substitution acts in a very unusual way by introducing a type of magnetic frustration because the magnetic moment of Nd's f-electrons prefers to point along a particular direction in the crystals, and this direction is perpendicular to the direction of the ordered moment of Ce's f-electrons. Applying pressure to a crystal with 5% Nd (x=0.05) suppresses the Ce-derived antiferromagnetic transition toward zero temperature and induces superconductivity at a pressure of about 1.75 GPa. We have discovered that a new type of magnetism appears inside this pressure-induced superconducting state and have shown that it is a direct consequence of the presence of Nd. Specifically, a reasonable interpretation of these experiments is that the magnetic f-electrons of Nd become entangled in a very special way with superconducting electrons of Ce that also have magnetic character. The new state of entangled magnetic/superconducting electrons is very sensitive to an applied magnetic field, as demonstrated by the complete suppression of this state in a relatively small applied magnetic field. As this state is suppressed, however, another field-induced magnetic order emerges in the superconducting state, just as it does in pure CeRhIn5. To better understand

the nature of the magnetism due to entangled magnetic/superconducting electrons and its competition with the magnetism induced by high magnetic fields, we have begun developing a fiber-optical grating technique to measure extremely small field-induced changes in sample dimensions when the sample is under a high pressure. This development is in collaboration with scientists at the LANL National High Magnetic Field Laboratory (NHMFL) and will benefit research in this project as well as bring a new capability to the NHMFL.

Future Work

During the remainder of FY16 and into FY17, applied high pressures will be used to tune the magnetic transition temperature of single crystals of the new materials ThCo2Sn2 and CaMn2Bi2 toward absolute zero temperature and to use electrical resistivity and specific heat measurements to characterize the electronic state that emerges at this magnetic/non-magnetic boundary. To follow up on initial results, we will complete the development of a new type of pressure cell that will allow access to pressures approaching 7 GPa. In a parallel effort, pressure will be used to control the relationship between magnetic order and unconventional superconductivity in a crystal of CeRhIn5 in which a small fraction of the cerium atoms are substituted by neodymium atoms. This atomic substitution has proven to be a promising route to inducing an exotic electronic state of coupled magnetism and unconventional superconductivity, and to help understand this exotic state, we will use a new capability currently under development to measure minute changes in crystal dimensions when the sample is subjected to a magnetic field and simultaneously is under high pressures. Further, initial experiments suggest that substitutions of rare-earth elements in addition to neodymium may be a fruitful path. Crystals of these compounds will be grown, their atmospheric properties will be measured, and, depending on the outcome of this initial exploration, these crystals may be studied at high pressures and magnetic fields.

Conclusion

Exploring properties of promising new materials at extremes of low temperatures, high pressures and high magnetic fields is a very useful means to uncover new physics. This project proposes to use electrical resistivity and specific heat measurements to study new intermetallic compounds under extreme conditions. The goal is to show that quantum criticality and heavy electron superconductivity can be found in materials without f-electrons and without iron. We will also search for a second example of a heavy electron material that becomes superconducting and subsequently magnetic.

Publications

Rosa, P. F. S., Oostra, J. D. Thompson, P. G. Pagliuso, and Fisk. Unusual Kondo-hole effect and crystal-field frustration in Nd-doped CeRhIn5. 2016. PHYSICAL REVIEW B. 94 (4).

Rosa, P. F. S., Y. Luo, N. Wakeham, E. D. Bauer, F. Ronning, Z. Fisk, and J. D. Thompson. Competing magnetic orders in the superconducting state of heavy-fermion CeRhIn5. Proceedings of the National Academy of Sciences.

Dendritic Microstructure Selection in Cast Metallic Alloys

Damien Tourret
20150713PRD2

Introduction

Complex – so-called dendritic – microstructures are most commonly observed in metallic alloys. Their morphological and compositional characteristics determine the mechanical properties and performance of cast parts.

From a theoretical standpoint, dendritic growth is a long-standing example of complex pattern formation, involving structural and chemical changes over multiple length and time scales. Most theoretical studies have focused on diffusive dendritic growth, neglecting convective solute transport in the liquid. Yet, gravity yields significant convection, resulting in detrimental microstructure inhomogeneities.

The first implementation of a novel, multi-scale dendritic needle network (DNN) model is orders-of-magnitude faster than simulation methods like phase-field and hence permits simulations at the mesoscale. In this project, liquid convection will be added into this model, enabling dendritic solidification simulations under realistic gravity conditions at length/time scales relevant to experiments and casting processes for the first time. Computationally intensive implementations of phase-field models will also be used as a validation tool, in support of the DNN model development.

Convection effects at the microscopic scale will be studied with phase-field and at the scale of experiments with multi-scale DNN simulations. The model developments will be validated by quantitative comparisons to experiments performed by Clarke's team at LANL. The simulations will guide the design of new experiments that will be executed at U.S. DOE User Facilities. By combining controlled experiments with intensive simulations, we will reveal the fundamental mechanisms of microstructure selection in the presence of unavoidable convection, which is essential to the properties and performance of cast materials.

The development of cutting-edge simulation techniques that predict realistic solidification scenarios will provide LANL with unique capabilities for the prediction and control of solidification microstructures.

Benefit to National Security Missions

NNSA/Science Campaigns: The development of a simulation capability for microstructure solidification at realistic time/length scales and gravity conditions, which is currently missing at LANL, will be a critical step toward predicting and controlling solidification structure evolution, which is key for LANL to support advanced manufacturing initiatives and the design of innovative processing studies.

MaRIE: This project is strongly motivated by the capability to quantitatively simulate solidification microstructures in realistic gravity conditions to support the design of solidification experiments with in situ imaging at LANL with high energy X-ray and proton beams. The multiscale modeling approach will not only guide multi-scale characterization experiments with MaRIE, but should also bring fundamental insight into the relevant physics that need to be included in our models.

Basic Understanding of Materials: Because dendritic solidification involves a broad range of length and time scales, it has only been approached theoretically at the scale of a few dendrites in idealized conditions, such as a purely diffusive regime. The current project will provide the first tool to quantitatively explore the crucial effect of gravity-induced convection on spatially extended dendritic arrays.

Climate and Energy Impact: The reduction of energy consumption, for instance in transportation, requires the development of innovative materials with tailored microstructures and properties. The ability to explore microstructure design through simulations will also accelerate the development and deployment of energy efficient processes.

Progress

The main objective for FY16 was the implementation of the coupled Dendritic Needle Network (DNN) approach for crystal growth to computational fluid dynamics (CFD) calculations in the liquid phase. The implementation has been achieved for isothermal solidification conditions. It is currently being extended to non-isothermal conditions (for application to directional solidification experiments), which should be completed by the end of the FY.

After benchmarking possible integration pathways of the DNN approach within existing CFD frameworks (e.g. Truchas), we have decided to design a new CFD solver in 2D that could directly be integrated with the existing DNN code without fluid flow. The main reason for that decision was the possibility to shape the new solver in a similar manner as the DNN model, thus also assuring the implementation to be parallelizable in a similar manner, namely using massively parallel Graphic Processing Units (GPUs) in order to get the best computational efficiency. Therefore, we built a GPU-parallelized CFD solver in 2D for common solidification conditions (i.e. incompressible flow, with low Reynolds number, and gravity-driven buoyancy). We used standard CFD numerical methods such as finite differences with a staggered storage of the different fields (fluid velocity, pressure, and solute concentration), an explicit time scheme with adaptive time step, and a projection method for the resolution of the incompressible Navier-Stokes equations. We developed this CFD implementation so that it could be readily extended to 3D to meet the objectives of the next FY. We tested and validated the implementation of the CFD implementation in 2D against benchmark test cases from the literature for steady and unsteady flows, buoyant flows, and flows in the presence of obstacles in the liquid.

After thorough validation of the GPU-parallelized 2D CFD framework, we adapted the existing DNN code to allow it to be directly integrated within the CFD code. First, we built a coupled DNN-CFD model for isothermal solidification condition. During this process, we also extended the DNN implementation to expand its range of applications. For instance, the new implementation can now account for dendritic branches growing in any direction (while it was so far restricted to branches aligned with the square finite difference grid). This extension allows simulating crystalline structures of hexagonal symmetry (so far limited to cubic) and simulating polycrystalline solidification (so far limited to single crystal).

For isothermal solidification conditions, the coupled DNN-CFD implementation has been completed. The implementation of the coupled model for non-isothermal condition is currently underway. Its completion, expected by the end of the current FY, should allow direct comparisons to directional solidification experiments. A thorough validation of the coupled DNN-CFD model for both isothermal and non-isothermal conditions for cases of crystal growth in the presence of forced and natural fluid flow is the first objective of the next FY. It will be achieved through direct comparisons to phase-field simulations results from the literature and to measurements from experiments performed at Los Alamos.

In parallel to the DNN-CFD coupling in 2D, we have completed a thorough validation the DNN model for purely diffusive transport in 3D, using quantitative comparisons to analytical scaling laws, experimental measurements from the literature, and to data obtained from in situ observation of metallic alloys solidification experiments obtained by Amy J. Clarke's group at LANL. Resulting adaptations and improvements to the 3D DNN code without CFD will be crucial to orient the design of the coupled DNN-CFD model in 3D planned for the next FY.

Future Work

In FY16, we developed the first implementation of the two-dimensional (2D) model coupling the multi-scale Dendritic Needle Network (DNN) approach for crystal growth to computational fluid dynamics (CFD) calculations in the liquid phase. For isothermal solidification, the model was implemented for massively parallel calculations using Graphic Processing Units (GPUs). The implementation for non-isothermal directional solidification conditions is the main objective for the end of FY16.

For FY17, the objectives are two-fold. Firstly, we need to test and validate the 2D coupled DNN-CFD model. Secondly, we will develop a three-dimensional (3D) implementation of the model.

The validation of the 2D model will be achieved with direct quantitative comparisons to: (i) theoretical analytical solutions; (ii) results of more accurate but also more computationally expensive calculations, for instance using phase-field modeling; (iii) data from directional solidification experiments in the literature and from experiments performed at U.S. DOE User Facilities. Potential adjustments of the 2D model will be undertaken to ensure that it provides quantitative results within reasonable accuracy of reference models, such as phase-field. Once validated, the 2D model will be used to study fundamental aspects of fluid-crystal interactions at experimentally relevant length and time scales out of the reach of current state-of-the-art phase-field simulations.

The development of the 3D model may require substantial redesign of its numerical implementation, due to the

computational cost of full-3D CFD simulations. We will first build a direct 3D extension of the current 2D implementation, similarly parallelized on GPUs. Depending on the performance of the resulting extension, we may benchmark alternative optimized libraries for 3D CFD calculations. Like for the 2D model, the 3D implementation will need to be validated, primarily against experimental measurements of microstructural features in solidified metallic alloys.

Conclusion

Cutting-edge, multi-scale simulations validated by in situ experiments will shed light on the poorly understood, yet crucial effects of gravity on microstructure selection in metallic alloys during metallurgical processing. Understanding crystal growth under gravity-induced liquid flow across length scales will enable the control of microstructure and defects in cast parts. This project will mark a transformational leap toward reaching predictive capability for advanced manufacturing at Los Alamos, aimed at tailoring materials microstructures and properties relevant to national security and energy challenges. It will also provide new, predictive computational tools needed for future materials-for-the-future studies.

Publications

Tourret, D., Y. Song, A. Clarke, and A. Karma. Grain growth competition during thin-sample directional solidification of dendritic microstructures: A phase-field study. 2017. Acta Materialia. 122: 220.

Tourret, D., and A. Karma. Three-dimensional dendritic needle network model for alloy solidification. 2016. Acta Materialia. 120: 240.

Additively Manufactured High Explosive Materials with Controlled Mesostructure for Tuned Detonation Performance

Alexander H. Mueller
20150742PRD3

Introduction

Current High Explosive (HE) material's performance and safety characteristics are governed by the defects present in the finished part. However, the processing technology that has been used to produce these parts for well over 50 years has allowed no control over the introduction of such defects other than adding "grit" or gas bubbles into the material before beginning processing. Additive manufacturing promises to allow exquisite control over the location and magnitude of defects in the finished part by building them into the part's structure using computer control. This will allow for a new and more powerful avenue to tune the final HE part's ignition, detonation and burn as well as sensitivity properties, promising to increase both performance and safety.

Benefit to National Security Missions

Additive manufacturing (AM) of energetic materials has been designated as a priority to the NNSA and their stockpile stewardship mission. The development of this technology with relevant applications in lifetime extension programs (LEPs) and for the development of next generation materials (components of the future) has garnered much support throughout the agency. Furthermore, the development of AM processes for HE has received considerable interest in DoD programs and Intelligence sponsors to address their particular needs. The 2016 NNSA stockpile stewardship plan specifically writes of the importance of AM technologies and their tie-in to MARIE, with the understanding of the interactions of defects in HE during the buildup to detonation being an obvious material interaction in an extreme environment. The understanding that we will gain over the behavior of explosives gives this basic research relevance to the above marked program areas.

Progress

In the last year, Andrew has worked on developing the AM of HE capabilities at LANL. His work has focused on the formulation of extrudable explosives and inert feedstocks, and implementation of these on several different pieces of equipment for additively manufacturing explosives.

He has produced an inert PDMS material printable material from base polymer constituents to improve upon what is commercially available, and to understand what makes a printable DIW resin. This material has been successfully printed and dynamically shocked at the IMPULSE gas gun facility housed at APS.

He has successfully printed DIW HE parts on our high precision instrument after successfully printing both DIW and FDM parts on our modified commercial off-the-shelf 3D printer. Some of these parts have provided successful detonation tests where the detonation velocity of an additively manufactured part could be measured. The 3D printing success is also a result of his LabVIEW programming efforts to automate g-code generation for manufacturing parts with controlled structure and build schemes.

Andrew has worked on improving the printability of our feedstock in various ways. First, he has examined the effect of particle size distribution of HMX on the rheology of the DIW ink. As well, he has figured out how to formulate the binder such that it cures by exposure to UV radiation with the addition of a commercial UV initiating polymer.

He has presented his work at several conferences including at the THERMEC international conference on processing and advanced materials in Austria in June of 2016, the JOWOG 28 at LLNL in February of 2016, and the JOWOG AM at LLNL in June 2015. He has also authored a paper on radiative aging of addively manufactured siloxanes entitled "Gamma Radiation Effects on Siloxane-Based Additive Manufactured Structures," which is under revision in Rad. Phys. Chem. as of May 2015.

Future Work

Work relating to high explosives additive manufacturing will continue. In this regard, printing of new structures will be completed with the objective of building anisotropically sensitive explosives. The focus will be on producing explosives using both the Direct Ink Write (DIW) and Fused Deposition Modeling (FDM) methods of additive manufacturing with current and new feedstocks that are under development. These parts will undergo in house testing to determine mechanical and explosive properties. Once characterized, these materials will be fielded for dynamic testing at the IMPULSE gas gun facility housed at the Advanced Photon Source (APS) at Argonne National Laboratory (ANL).

Conclusion

We expect to develop a repeatable method of additively manufacturing HE parts for mechanical and performance testing. Using inert materials, the mechanical properties of structures developed using computer simulations will be assessed. After a down-selection of viable candidate structures, the selected structures will be rendered in high explosives by use of the developed additive manufacturing instrumentation. These parts will be performance tested using a unique suite of Los Alamos explosive characterization techniques.

Publications

Schmalzer, A.. Gamma Radiation Effects on Siloxane-Based Additive Manufactured Structures. 2017. Gamma radiation effects on siloxane-based additive manufactured structures. : 103–111.

Catalytic Generation of Gas Using Formic and Oxalic Acids for Pressure/Volume Work

James M. Boncella
20150743PRD3

Introduction

This project is directed towards discovery of a chemical system that can be used to generate gas pressure at low (>150oC) temperatures. We are focusing on formic acid, oxalic acid and other simple acids since these compounds can be decomposed into mixtures of hydrogen and carbon dioxide using transition metal catalysts. The pressure generated in this fashion can be used to do work, for example to move an actuator. While there are numerous examples of formic acid decomposition catalysts, there are no published examples of compounds that can accomplish similar chemistry with oxalic acid. Oxalic acid is an attractive substrate for such chemistry because it is a solid, and it will generate a greater pressure of gas than formic acid for the same mass of material. Such a pressure generation system could be used as a light weight alternative to storing pressure in a gas bottle or to avoid the use of a pyrotechnic gas generator such as the materials used in automobile airbags.

Benefit to National Security Missions

This project will investigate whether it is possible to use metal compounds to decompose oxalic acid and other simple organic acids. This process is important in biology because oxalic acid is toxic and various plants and fungi generate oxalic acid in the normal course of their metabolism. The naturally occurring metal containing enzymes, oxalate decarboxylates, serve this purpose in nature, but their function is poorly understood. By studying how metal compounds cause this reaction to occur, we will make a contribution to the fundamental understanding of an important biochemical process.

If successful in developing the conversion of oxalic acid to gases, we will be making a contribution to a potential application that we have identified as being important to certain defense programs. Thus, the program presents the opportunity to develop cutting edge science that has the potential to affect defense programs in a positive way.

Progress

Numerous (~40 -45) new transition metal (Mn, Fe, Co, Ru, Ir) complexes have been synthesized and evaluated as catalysts for the decomposition of formic acid to generate pressure through the formation of hydrogen and carbon dioxide. There have been a number of compounds and formulations that have been demonstrated to do this reaction effectively at less than 100 oC. One of the compounds that has been synthesized has demonstrated a remarkable ability to react cleanly with formic acid as well as with a large number of other substrates. This novel chemistry has led to three papers that have been published in the literature, with at least two more that are in preparation for future submission.

The results from this study will lay the groundwork for a much more thorough understanding of the chemistry is involved in these decomposition reactions. It also supports the programmatic application which is funded through other means. Furthermore, this project has also led to the discovery of other catalytic chemistry that will be disseminated over the rest of the project lifetime and likely far beyond.

Future Work

Using the novel compounds that we have synthesize in the previous year, we plan to evaluate the pressure generation characteristics of the decomposition of formic acid to carbon dioxide and hydrogen that is catalyzed by these manganese, iron, cobalt, ruthenium and iridium compounds and use this data to propose a mechanism for this process. The initial data that we have gathered is consistent with the mechanistic details of this reaction being highly dependent upon the identity of the metal complex and the reaction conditions.

Conclusion

Because oxalic acid and oxalate are toxic to various organisms (e.g. in humans, kidney stones are metal oxalates), Nature has evolved a class of enzymes to detoxify

this harmful material. By understanding how metal compounds can decompose oxalate, we will generate insight into how the class of enzymes known as oxalate decarboxylases function. The chemical insight gained from these studies will advance our knowledge in the general area of metal catalysis as well as offer the potential to develop a practical application. If successful in developing the conversion of oxalic acid to gases, we will be making a contribution to a potential application that we have identified as being important to certain defense programs.

Publications

Tondreau, A. M., B. L. Scott, and J. M. Boncella. A Tertiary Carbon-Iron Bond as an (FeCl)-Cl-I Synthon and the Reductive Alkylation of Diphosphine-Supported Iron(II) Chloride Complexes to Low-Valent Iron. 2016. ORGANOMETALLICS. 35 (11): 1643.

Tondreau, A. M., and J. M. Boncella. 1,2-Addition of Formic or Oxalic Acid to N-{CH2CH2(PiPr(2))}(2)-Supported Mn(I) Dicarbonyl Complexes and the Manganese-Mediated Decomposition of Formic Acid. 2016. ORGANOMETALLICS. 35 (12): 2049.

Tondreau, A. M., and J. M. Boncella. The synthesis of PNP-supported low-spin nitro manganese(I) carbonyl complexes. 2016. POLYHEDRON. 116: 96.

Novel Routes to Emergent Functionality in Multiferroics

Vivien Zapf
20150759PRD3

Introduction

Most modern electronic devices are based on systems with large generalized susceptibilities, such as systems that show a strong change in physical property in response to a small stimulus. In the quest for future devices with new functionality, it is important to study multifunctional materials, in which physical properties that are normally unconnected become strongly coupled. Systems of choice are multiferroic materials in which different ferroic orders are strongly coupled. This project seeks new approaches in the design of materials with strong magnetoelectric coupling, which could impact materials for the future design of sensing devices.

Metal-organic materials with spin-state transitions are an exciting new direction in which to search for magnetic and ferroelectric coupling that has not been significantly explored to date. A key innovation is to use spin-state transitions rather than long-range magnetic ordering patterns. Spin-state transitions are emerging as a dominant functionality of metal-organic materials, and they significantly couple to the lattice and to ferroelectricity since they involve re-arrangements of the orbital occupations of magnetic ions. In addition, the metal-organic class of materials is known to have sensitivity to chemical adsorption, pressure, and light, which adds additional properties to the multifunctional mix.

We expect to lay the critical groundwork for understanding new coupling mechanisms between magnetism and ferroelectricity. We will identify and characterize this coupling in existing and new chemical compounds that involve crystalline ordered lattices of magnetic ions and organic ligands.

Benefit to National Security Missions

This work advances our understanding of the physics and chemistry of metal-organic materials with spin-state transitions, specifically the spin-charge-lattice coupling mechanisms that allow spin-state transitions to interact with electric dipoles. The research impacts materials for the future - multifunctional coupling and materials by design. Metal-organic materials present a flexible tunable paradigm for materials design that allows us to combine magnetic ions with organic ligands. This hybrid approach creates many design parameters that can be modified to optimize the magnetic and electric properties.

The longer range goals of this area of research impact sensing and devices. Low power sensing is a needed technology for distributed in-the-field surveillance as well as numerous technological applications.

Progress

We have identified a compound that exhibits the sought-after multifunctionality, namely coupling between magnetism and ferroelectricity via a spin-state transition. This compound is a molecular material where the magnetism originates from Mn3+ ions coupled via organic ligands. When a magnetic field is applied, the spin of the Mn3+ ion doubles in size at the spin-state transition, and at the same time ferroelectricity is induced at a structural phase transition. The high spin state induced by fields has a Jahn-Teller distortion, which is a uniaxial distortion away from a cubic environment that creates an electric dipole in this material.

We have characterized the magnetic and ferroelectric properties in high magnetic fields here in Los Alamos in pulsed magnetic fields up to 65 Tesla, and at the National High Magnetic Field Laboratory in Florida in continuous magnetic fields up to 45 T. Since there is a structural phase transition involved, the properties are strongly dependent on the speed at which the transition is traversed, and we see significant tuning between millisecond pulsed fields and the continuous fields. Thus measurements in both the pulsed and the continuous-field facilities were necessary. We find a phase diagram consisting of a low-spin, non-electric state at magnetic

fields below 40 T, and a high-spin, ferroelectric state at high magnetic fields above 40 T and low temperatures, and finally a paraelectric high-spin state at temperatures above 50 K. Unexpectedly we found that the ferroelectric state is eventually suppressed as the magnetic field is further increased. We also observe two different ferroelectric states with opposite electric polarization.

The magnitude of the ferroelectricity varies between different measurements because the axis of ferroelectricity is chosen at random as the sample undergoes a phase transition from cubic to a lower symmetry. Thus the magnitude depends on this choice of axis made spontaneously by the sample in high magnetic fields and how this axis is angled compared to our measurement axis. The largest electric polarization that we observed ranges up to one quarter of the maximum magnetic field-induced electric polarization that has been seen in any material. This work is currently being written up for publication.

Our result is the first example of so-called "multiferroic behavior" (e.g. magnetic and ferroelectric behavior) that is induced by a spin-state transition instead of by the usual long-range magnetic ordering. Thus this is a significant new result. Moreover the effect is extremely large, as just discussed, involving a doubling of the magnetization and a significantly large ferroelectric polarization. However the temperature at which the multiferroic behavior occurs is well below room temperature and the magnetic fields are very high – well beyond those available in commercial magnets. The good news is that there are a practically infinite number of compounds showing spin-state transitions, and these range up to room temperature in metal-organic materials. Thus we plan to study additional compounds and find materials with higher temperatures and lower magnetic fields.

Future Work

Our goal is to identify and understand existing and new chemical compounds that exhibit magnetoelectric coupling based on spin-state transitions. We focus on metal-organic materials that are single or polycrystalline ordered lattices.

We are working with chemists and material scientists to grow these materials. We are continuing to perform a comprehensive suite of measurements of the magnetic, electric, lattice, and other thermodynamic properties over an extended range of temperature-magnetic field phase space. We are also collaborating with theorists to identify the magnetic Hamiltonian of these compounds, and calculate and model their properties. In addition, we are exploring other metal-organic and inorganic compounds with strong magnetic and electric response functions to identify promising new research directions for magnetoelectric functionality.

Our own focus is on measurements in extreme conditions though we collaborate closely with chemists and theorists. The ability to take a local spin-state transition on an ion and couple it through lattice distortions to create a cooperative phase transition is a key method by which the relative temperature and magnetic field scales can be tuned.

Measurements are being performed in superconducting magnets up to 14 Tesla, pulsed magnets up to 65 Tesla, and the flagship 100 Tesla magnet at the National High Magnetic Field Laboratory pulsed field facility in MPA-CMMS group at LANL. Measurement techniques include electric polarization induced by magnetic fields, magnetization, dielectric constant, and thermodynamic properties. Magnetostriction can also be performed on some materials.

Conclusion

Sensors rely on strong coupling between two properties - the property to be sensed and the circuit (generally electric) performing the sensing. Most commercial magnetic sensors such as those used in iPhones and hard drives couple magnetism to electrical transport properties. Unfortunately, most magnetic sensors today use high power and dissipate heat due to the need to drive electrical currents. By switching to ferroelectricity instead of electrical transport we vastly reduce the power consumption by manipulating voltages rather than currents. The longer range goals of this area of research impact sensing and devices. Low-power sensing is a needed technology for distributed in-the-field surveillance as well as numerous technological applications.

Publications

Chen, C. W., S. Chikara, V. S. Zapf, and E. Morosan. Correlations of crystallographic defects and anisotropy with magnetotransport properties in FexTaS2 single crystals (0.23≤x≤0.35). 2016. Physical Review B. 94: 054406.

Chikara, S., J. Singleton, J. Bowlan, D. A. Yarotski, N. Lee, H. Y. Choi, Y. J. Choi, and V. S. Zapf. Electric Polarization observed in single crystals of Lu2MnCoO6. 2016. Physical Review B. 93: 180405R.

Ho, P. C., J. Singleton, P. A. Goddard, F. F. Balakirev, S. Chikara, T. Yanagisawa, M. Brian Maple, D. B. Shrekenhamer, X. Lee, and A. T. Thomas. Fermi-surface topologies and low-temperature phases of the filled Skutterudite compounds CeOs4Sb12 and NdOs4Sb12. Phys. Rev. B.

Macroporous/Nanoporous Hierarchical Carbon Structure (MNHCS) for High-Performance Energy Storage Devices

Jeffrey M. Pietryga
20150760PRD4

Introduction

This project aims to develop next generation carbon-based porous materials for high performance energy storage devices such as lithium ion batteries and super capacitors.

One of the critical parameters that impact the performance of batteries and capacitors is the diffusion of electrolytes in and out of the electrodes. Graphene/graphite-based materials show great promise as they have high surface area, but the diffusion of electrolytes is limited by the d-spacing between layer. For example, a lithium atom has a diameter of 3.2 angstrom, and the d-spacing between graphene is only 3.3-3.4 angstrom, which barely accommodates one lithium atom. Diffusion of lithium (electrolyte) is therefore impeded by the d-spacing. To this aim, we strive to synthesize macro- and nanoporous 3D graphene materials that will expedite the diffusion of electrolyte by at least one order of magnitude.

Success of this project will answer the challenges faced by carbon-based energy storage materials by significantly improving the charge capacity and increasing the rate of charging and discharging. These are two long-sought-after solutions in energy storage devices.

Benefit to National Security Missions

We expect to design and synthesize novel high-performance 3D porous graphene materials with optimal structural and electrochemical properties, which will maximize specific capacitance, power density, energy density and cycle life for batteries and supercapacitors. Success in this project will have wide-spread impact on the development of high performance energy storage technologies. This research will strengthen our capability in addressing key LANL missions of materials functionality and energy security and position LANL for a new frontier of energy storage research.

Progress

We have prepared three dimensional porous graphene by incorporating nanoparticles into graphene oxide matrix in a liquid solvent and through hydrothermal reaction. The solvent was then removed by freeze drying to obtain highly porous graphene materials. The obtained three dimensional porous graphene were characterized by transmission electron microscopy, scanning electron microscope and energy-dispersive X-ray spectroscopy. All of the above results suggest highly porous structure nature.

The porous graphene was used to fabricate a supercapacitor and a lithium ion battery. They show improved charge capacity 20% higher than pure graphene materials.

Future Work

- Synthesis and characterization of 3D macroporous/nanoporous graphene materials. Crosslinking graphene oxide using nanographene and water-soluble fullerene through the formation of covalent bond between graphene oxide.
- Understanding the electrochemical properties of the porous graphene and demonstrate the use of these porous materials as electrodes (anode) for lithium ion batteries and supercapacitors.

Conclusion

We expect to achieve synthesis of 3D reduced nanoporous graphene oxides that offer several unique properties: i) an interconnected electrolyte-filled macroporous network that enables increased contact surfaces between the 3D network and electrolytic solution, and rapid ion transport, ii) short ion and electron transport lengths, iii) a high electrode specific surface area and (iv) high electron conductivity in the electrode assembly. This method will be extended to the synthesis of a variety of 3D conjugated systems that will render the

formation of conducting macroporous/nanoporous structures, ideally suited for the fabrication of highly efficient supercapacitors and lithium ion batteries. Success in this project will have widespread impact on the development of high performance energy storage technologies.

Investigating Complex Superconducting Phases via Field-Rotating Transport and Thermodynamic Measurements

Roman Movshovich
20150762PRD4

Introduction

The microscopic origin of the unconventional superconductivity remains elusive, and it is still one of the most challenging problems in condensed matter physics, after several decades of an intense research. A consensus about the important role of magnetic fluctuations in mediating unconventional superconductivity is beginning to emerge, based on a variety of studies of the interplay between superconductivity and magnetism. The so-called Q-phase, discovered in the high-field (above 10 Tesla), low-temperature (below 300 mK) corner of the superconducting phase of CeCoIn5, represents a unique and completely different relationship between magnetism and superconductivity. The antiferromagnetic order (with a wave-vector Q) of the Q-phase requires superconductivity for its very existence, as the magnetic order disappears in the normal state, once the superconductivity is suppressed by the superconducting critical field of 12 Tesla. There is a number of competing explanations for this behavior, including (1) a spatially inhomogeneous Fulde-Ferrell-Larkin-Ovchinnikov (FFLO) state and (2) a p-wave Pair-Density-Wave scenario, a combination of a d- and a p-wave superconducting order parameters. The investigations of the Q-phase is therefore directly related to the growing field of the intertwined order parameters, such as exist in cuprate high temperature superconductors and in pnictide-based superconductors.

The variation of specific heat and thermal conductivity in a rotating magnetic field was shown to be a powerful probe in resolving the nature of a superconducting order parameter. The thermal conductivity measurement in a rotating magnetic field within the Q-phase of CeCoIn5 will provide a direct information on the origin of this unprecedented state of matter. Our field-rotating thermodynamic and transport measurements of CeCoIn5 and other compounds with mixed and complex SC phases will directly probe the symmetry of these SC phases, making important contribution to the field of exotic and unconventional superconductivity.

Benefit to National Security Missions

This project will address the issue of unconventional superconductivity, by directly measuring the symmetry of the superconducting order parameter in a number of compounds. Some states that will be explored represent unique states of matter. This research is therefore of great interest to the mission of the basic understanding of materials. It is in the purview of the Basic Energy Sciences division of the DOE, and will contribute to the knowledge base in the area of unconventional superconductivity, magnetism, and correlated electron physics.

Progress

For thermodynamic measurements in rotating magnetic fields, Duk Young have successfully implemented rotation capability in low-temperature and high-field was successfully established. A piezoelectric rotator was installed in a dilution refrigerator coupled with a 14 T superconducting magnet. In rotation experiments at low temperatures, heating by friction has been a major problem. In current setup, a rotation of a sample maintaining the temperature below 200 milliKelvin has been demonstrated. For monitoring the rotation angle, two Hall sensors perpendicular to each other are employed. The fine rotation and monitoring capability enables a rotation experiment with the angle resolution as low as 0.1 degree.

The experimental apparatus for thermal conductivity measurements that can be mounted on the rotation frame was successfully assembled for thermal conductivity measurements. For the standard steady state measurements, two thermometers and one heater were calibrated and installed on a fiberglass-reinforced polymer frame that is suited for the rotator due to the light weight. The setup is capable of thermal conductivity measurements down to 50 mK with the rotation of sample more than 180 degrees.

As a first experiment of the project, the thermal trans-

port measurement on unconventional superconductor CeCoIn5 in a rotating magnetic field has been successfully performed. The systematic modulation of thermal conductivity by the 180 degree rotation in a magnetic field was observed. The modulation can be decomposed into two-fold oscillation by the contribution from the superconducting vortices and four-fold oscillation by the d-wave property of the unconventional superconductor. In addition, Duk Young has observed a sharp increase of thermal conductivity when the magnetic field is aligned parallel to the heat current or 33 degree away from the heat current direction, which was along the nodal direction of the d-wave superconductivity. These results indicates that exotic resonant states form, depending on the relative direction of magnetic field in the tetragonal crystal. We are preparing a publication on this observation.

In the low-temperature and high-field corner of the superconducting phase, CeCoIn5 has a so-called Q-phase, in which an antiferromagnetic order coexists with superconductivity. Duk Young has identified the switching behavior of the magnetic ordering with the angle-resolved thermal conductivity measurement. The measurement have revealed an anisotropy of the superconducting order parameter, which can be explained by the secondary p-wave pair-density-wave (PDW). This observation is important and interesting because it is a unique example of intertwined orders, a concept which has received significant attention in the unconventional superconductivity community. The reduction of thermal conductivity in the Q-phase enables a quantitative prediction of the secondary order parameter, which has not been possible in any other experiment. A manuscript based on these observations has been submitted to Nature Communications.

Future Work

In the next fiscal year we will perform thermal conductivity measurements in a rotated magnetic field to study the effect of Nd- doping on superconducting state of CeCoIn5. Recent neutron scattering measurements in 5% Nd-doped CeCoIn5 showed the existence of two spin densitiy wave (SDW) phases. The first one occurs in zero field, and is suppressed by magnetic field down to T=0 at 8T, at which point the second SDW phase develops and grows with further increasing magnetic field all the way up to the superconducting critical field Hc2 of just above 10 Tesla. The second SDW phase disappears at Hc2, a behavior identical to that of the Q-phase of CeCoIn5. We will explore the structure of the two SDW phases and similarity/difference of their behavior to that of the Q-phase.

Conclusion

Dr. Duk Young Kim will obtain thermal conductivity and specific heat data in CeCoIn5 at a dilution refrigerator temperatures and in high magnetic field up to 14 Tesla as a function of angle between the applied field and the heat current. The detailed analysis of the data will allow us to determine the symmetry of the superconducting state in CeCoIn5 and the character of the Q-phase in this compound. The investigation of the Q-phase will make an important contribution to the growing field of intertwined order parameters.

Publications

Kim, D. Y., S. Lin, F. Weickert, M. Kenzelmann, E. D. Bauer, F. Ronning, J. D. Thompson, and R. Movshovich. Intertwined orders in heavy-fermion superconductor CeCoIn5. To appear in Physical Review X.

Record-Low Lasing Thresholds Using Colloidal Type-II Quantum Wells

Victor I. Klimov
20150764PRD4

Introduction

Solution-processed optical gain materials hold promise for next generation low-cost and flexible laser devices. One class of such materials is colloidal semiconductor quantum dots (QDs). Gain thresholds in QDs are typically high due to the requirement of creating multiple excitons (MXs) for population inversion. Additional complications arise from a quick depletion of optical gain due to nonradiative Auger Recombination (AR) of MXs and QD photo-degradation. Previous studies have demonstrated approaches to boost the gain performances of QDs by either suppressing AR in interface-engineered "giant" core/shell QDs or employing single-exciton-gain strategies using type-II core/shell QDs with strong exciton-exciton repulsion. Recently, another class of colloidal materials, semiconductor nanoplatelets or quantum wells (QWs), has been studied in the context of their optical gain properties. This research has been partially motivated by the success of epitaxially grown QWs that have demonstrated record-low lasing thresholds due to their large absorption cross sections and slow AR. Here, we propose an integrated approach to achieving low-threshold lasing using colloidal type-II CdSe/CdTe QWs. These QWs combine the advantages of large absorption cross-sections, suppressed AR, and strong exciton-exciton repulsion which will facilitate the regimes of both single- and multi-exciton lasing and should result in extremely low lasing thresholds as well as an exceptionally large optical gain bandwidth.

Benefit to National Security Missions

The ultimate goal of this project is to reduce the optical gain threshold for colloidal nanomaterials in order to make them more feasible as wavelength-tunable lasers. The primary and secondary ties to LANL's mission is through the "Basic Understanding of Materials" and "Fundamental Chemistry" subcategories within "Scientific Discovery and Innovation", as the project seeks to explore general design, synthesis and fabrication principles in colloidal semiconductor nanomaterials for use as optical gain media. As both single- and multi-photon excitation will be explored to test gain thresholds, the materials will be engineered to withstand high radiation thresholds that result in the generation of up to 1021 carriers per cm3, and will provide valuable data for LANL's Matter-Radiation Interactions in Extremes (MaRIE) Signature Facility. Further development of colloidal quantum well materials into low-threshold, electrically pumped, highly tunable lasers can lead to useful remote sensing applications as portable, energy-tunable, coherent excitation sources, with application to national security problems such as nuclear nonproliferation.

Progress

During the past year we have synthesized CdSe nanoplatelets (NPLs) with a range of thicknesses and conducted their initial characterization using absorption and photoluminescence (PL) spectroscopies. We have also explored different approaches for NPLs processing into high-optical-quality films including spin-coating and doctor-blade deposition. The latter method has been found to allow for fabricating highly homogeneous, low-scattering films perfectly suited for evaluating optical gain properties of the NPLs. These studies are currently in progress.

In parallel, we have investigated photo-doping as a means for reducing gain and lasing thresholds by partially bleaching the band-edge transition. In these studies, we have used a mild reducing agent, lithium triethylborohydride, for removing a photo-injected hole from the quantum dot (QD). As a result of this process, photoexcited particles should become negatively charged. QDs used in this study are CdSe/CdS core/ shell structures with an intermediate alloyed CdSexS1−x layer inserted between the core and shell. This interfacial alloying allows for considerable suppression of Auger recombination, which is a necessary condition for extending optical gain lifetimes in photo-doped QDs.

Due to excess electrons produced by photo-doping, the QD samples exposed to lithium triethylborohydride in the presence of room light, show a pronounced bleach of the band-edge excitonic peak. Poisson statistics has been used to describe the charge distributions across the QD ensemble. Based on the quantitative analysis of absorption spectra, the average number of excess electrons, <Ne>, varies from ~0.2 to ~6.0 depending on the amount of lithium triethylborohydride. We detect the quenching of PL due to activation of the Auger decay pathway. However, even for the QDs with <Ne> ~ 2, the samples still preserve ~35% of the PL intensity of neutral QDs, indicating that Auger recombination of charged exciton states in these interface-engineered QDs is significantly suppressed compared to conventional QDs.

We have also monitored time-resolved PL dynamics for photo-doped QDs. With increasing <Ne>, the PL decay becomes faster and the initial signal amplitude increases versus that in neutral QDs. These are clear signatures of charged excitons that are expected to exhibit a higher emission rate and faster PL decay compared to neutral excitons. The analysis of the measured dynamics shows that the lifetime of a negative trion (a state with two electrons and one hole) is much longer (~5.6 ns) than in dots with sharp interfaces (<1 ns), indicating again the effectiveness of the strategy of interfacial alloying for suppressing Auger recombination.

The next step in our work will be direct evaluation of optical-gain thresholds as a function of <Ne>. If these measurements will indeed show the reduction of the gain threshold, we will apply similar photo-doping strategies to the NPL samples.

Future Work

- Measurements of optical gain thresholds as a function of the level of photo-doping in solution samples of core/shell CdSe/CdS quantum dots (QDs)
- Exploration of feasibility of photo-doping of solid state QD samples
- Development of techniques for film encapsulation and tests of stability of doping levels in solid-state samples
- Amplified spontaneous emission studies of photo-doped QD films
- Development of chemical approaches for photodoping of nanoplatelet (NPL) samples
- Spectroscopic studies of doping levels in NPL samples as a function of amount of reducing agent and applied light intensity.

Conclusion

The proposed studies will elucidate general design principles for colloidal optical gain media via an integrated approach involving parallel optinimation of all nanostructure paramaters relevant to lasing performance. The success of this work will provide an important milestone on the way to electrically pumped lasers based on colloidal nanomaterials. Further development of colloidal quantum well materials into low-threshold, electrically pumped, highly tunable lasers can lead to useful remote sensing applications as portable, energy-tunable, coherent excitation sources, with application to national security problems such as nuclear nonproliferation.

Discovering Highly Conducting Oxides by Combining High-Pressure and Thin-Film Techniques

Hongwu Xu
20160646PRD2

Introduction

As an important but underexplored thermodynamic variable, pressure offers a unique pathway for discovering materials with emergent or enhanced properties by tuning the interatomic distances to control their crystalline and electronic structures. However, since high-pressure phases are thermodynamically metastable at ambient conditions, many of them cannot be retained for real-world utilization. Taking advantage of the local stresses existing between thin films and their substrates, which are equivalent to external pressures, the aim of this research is to stabilize novel, high-pressure phases with desired properties, i.e. high conductivity, in the form of thin films at ambient conditions for technological applications.

In this project, we will first employ high-pressure synthesis with a diamond-anvil cell and multi-anvil press, coupled with in-situ characterization techniques (e.g. synchrotron X-ray diffraction, spectroscopies and physical property measurements), to develop a number of composite materials with superior transport properties. Then we will use thin-film growth techniques such as pulsed laser deposition and molecular beam epitaxy to introduce local strains in composite thin films with similar high-pressure phase properties. Major tasks include: 1) design and synthesize composite oxides with unique electronic properties, such as TiO2/ZnO, TiO2/SnO2 and TiO2/LaAlO3. Their interfaces could generate unique electronic structures with emergent properties, such as interfacial superconductivity and high-mobility 2D electron gas. 2) Examine pressure-driven property evolution using a suite of structural, spectroscopic, electronic and electrical probes to achieve a comprehensive understanding of the structure-property relationship. 3) Construct composite oxides into thin films with controlled interfaces and local strains via advanced film growth techniques by tuning the thickness and orientations. The local pressure can be created in both horizontal (using composite targets) and vertical (using a layer-by-layer approach) directions along the substrates. 4) Evaluate physical properties and performance of the films for energy-related applications (e.g., electrode or electron transport layer in photovoltaic devices).

Benefit to National Security Missions

This work will result in a number of new high-conducting oxide thin film materials and, more generally, will develop a novel synthetic route for functional materials design and innovation. Through combining high-pressure and thin-film techniques and taking advantage of the local stresses existing between thin films and their substrates, this work will open a new direction in stabilizing novel phases with enhanced or emergent properties, which are stable only at high pressure, in the form of thin films at ambient conditions for renewable-energy-related applications such as solar cells and batteries. This project will integrate material synthesis, extreme conditions, film deposition, and advanced synchrotron-based characterization to achieve an unprecedented understanding of structure-property relationships. This research directly supports DOE/LANL's missions in "Basic Understanding of Materials" by designing and developing novel functional materials with "emergent phenomena" at "extreme environments" - two research themes of LANL's grand challenge in "Materials for the Future." This work is also related to MaRIE - LANL's future signature facility.

Progress

Since the project started in late February 2016, we have made tremendous progresses. Specifically, we performed high-pressure synchrotron X-ray diffraction (XRD) experiments of black TiO2 nanoparticles and revealed a sequence of phase transformations as function of pressure. In addition, we conducted high-pressure experiments on a hybrid organic-inorganic halide perovskite, CH3NH3SnI3, using in situ synchrotron XRD, Raman spectroscopy, electrical resistance and photocurrent measurements. Our results show improved stability and properties of this compound after its high-pressure treatments. We

will describe these in details as follows:

Black titania: Black TiO2 nanoparticles with a crystalline-core and amorphous-shell structure exhibit superior optoelectronic properties in comparison with those of the pristine TiO2. We obtained black TiO2 nanoparticle samples with different anatase/rutile ratios, which show higher electrical conductivity than that of the pristine TiO2. In-situ structural characterization was carried out using synchrotron XRD coupled with a diamond-anvil cell (DAC) at the Advanced Photon Source (APS), Argonne National Laboratory (ANL). With increasing pressure, a phase transition from anatase/rutile to baddeleyite was observed at about 17 GPa, and this transition was complete at about 28 GPa. The baddeleyite phase was stable up to 48 GPa, the highest pressure we used. Upon decompression, the baddeleyite phase transformed progressively into a columbite-structured phase in the pressure range of 7 - 5 GPa, and this phase remained stable to ambient pressure. We will measure the corresponding transport properties of black TiO2 nanoparticles at high pressures in the near future.

Hybrid organic-inorganic halide perovskites: Hybrid organic-inorganic halide perovskites have demonstrated great potential for high performance photovoltaic applications (solar cells) with high power conversion efficiency (PCE) while economically feasible. However, these phases suffer from low stability at moisture and high temperature conditions, potentially resulting in degradation of hybrid perovskite-based photovoltaic devices in practical environments. Using state-of-the-art high-pressure techniques combined with in situ synchrotron and property measurements, we conducted a comparative investigation on the structural, electrical and optoelectronic properties of a lead-free (thus environmentally friendly) tin halide perovskite, CH3NH3SnI3, before and after its high-pressure treatments up to about 30 GPa. A sequence of pressure-driven phase transitions and resulting evolution in electrical and optoelectronic properties were revealed during two sequential compression and decompression cycles using in situ synchrotron XRD, Raman spectroscopy, electrical resistance and photocurrent measurements. Our results reveal improved structural stability, increased electrical conductivity (by 300%), and enhanced visible-light responsiveness of CH3NH3SnI3 via a pressure-induced amorphization and recrystallization mechanism. This study demonstrates that high pressure can be an effective approach for tuning the structure and properties of organic-inorganic hybrid perovskites and may open up new perspectives on understanding these materials vis-a-vis high performance solar cells with better stability. A manuscript based on these results was submitted to Advanced Materials and is currently under revision.

Future Work

In the next fiscal year, we intend to conduct the following tasks:

First, we will measure the transport properties of as-prepared black TiO2 nanoparticles with a crystalline-core and amorphous-shell structure at high pressures using a diamond-anvil cell (DAC) coupled with in-situ physical property measurements. From the obtained results, combined with our completed structural studies, the structure-property relationship will be established.

Second, based on our understanding of the pressure effects on black TiO2, we will use pulsed laser deposition technique to construct composite films of TiO2 homojunction to stimulate the crystalline-core and amorphous-shell structure in black TiO2. The interfaces with local strains and possible interfacial reconstructions could generate unique electronic structures, leading to emergent properties. The film quality and thickness will be tuned by adjusting deposition parameters. The electrical conductivities of the composite films will be evaluated using a physical property measurement system at temperatures down to 10 K, and their carrier concentration and mobility will be probed by Hall Effect measurements. Compositions and microstructures will be determined by X-ray diffraction, scanning transmission electron microscopy, electron energy-loss spectroscopy and other techniques. The comprehensive studies will provide valuable insights into the underlying mechanisms of the enhanced properties in black TiO2 and will in turn guide development of more advanced composite materials and their films.

Third, based on the insights obtained on TiO2 homojunction films, we will extend our studies to other oxide homojunction and heterojunction film systems: SnO2 bilayer films and Nb-TiO2/TiO2. Their structures and transport properties will be determined using similar methods.

Lastly, we will explore combining DAC with ultrafast laser spectroscopy to achieve in-situ characterization on pressure-driven evolution of electronic and optical properties in other materials such as composite oxides and topological insulators.

Conclusion

The overarching goal of this research is to design and develop novel materials with enhanced or emergent properties for energy-related applications by combining high-pressure and thin-film methods. Taking advantage of the local stresses existing between thin films and their substrates, which are equivalent to external pressures, we will stabilize novel, high-pressure phases with desired properties, i.e. high conductivity, in the form of thin films for

practical applications. This project addresses fundamental challenges at the interfaces between physics, chemistry and materials science, and its successful execution will have widespread impact on the development of energy devices using advanced composite films.

Publications

Lu, , Chen, Luo, Lu, Dai, Enriquez, Dowden, Xu, P. G. Kotula, A. K. Azad, D. A. Yarotski, R. P. Prasankumar, A. J. Taylor, J. D. Thompson, and Jia. Conducting Interface in Oxide Homojunction: Understanding of Superior Properties in Black TiO2. 2016. NANO LETTERS. 16 (9): 5751.

Lu, , J. W. Howard, Chen, Zhu, Li, Wu, Dowden, Xu, Zhao, and Jia. Antiperovskite Li3OCl Superionic Conductor Films for Solid-State Li-Ion Batteries. 2016. ADVANCED SCIENCE. 3 (3).

Lü, X., Y. Wang, C. C. Stoumpos, Q. Hu, X. Guo, H. Chen, L. Yang, J. S. Smith, W. Yang, Y. Zhao, H. Xu, M. G. Kanatzidis, and Q. Jia. Enhanced structural stability and photo responsiveness of CH3NH3SnI3 perovskite via pressure-induced amorphization and recrystallization. 2016. Advanced Materials. 28: 8663–8668.

Theory of Spin and Valley Dynamics in 2D Dirac Semiconductors

Nikolai Sinitsyn
20160648PRD2

Introduction

Conduction electrons in the new family of atomically thin materials, called Dirac semiconductors, behave as relativistic (Dirac) electrons despite much smaller electron velocities than the speed of light. This is an emergent phenomenon that follows from lattice structure and unusually strong spin-orbit effects. Relativistic Dirac equation predicts properties that have not been previously anticipated for conduction electrons, such as chiral anomalies that allow dissipationless charge transport, or Klein paradox that prevents electronic scatterings on impurities. One more consequence of Dirac physics is the presence of new binary quantum degree of freedom, known as valley magnetic moment. It is similar in properties to spin but arises from the nontrivial topology of the Dirac band structure. Valley moment couples both to magnetic fields and optical beams, which enables external control over its dynamics. However, valley magnetic moment does not experience numerous decoherence sources that are common to spins. These remarkable properties generate prospects for the emerging field of valleytronics that makes use of valley magnetic moments as carriers for information, including quantum information. Furthermore, effects of valley moment on collective effects, such exciton Bose condensation, in such materials are completely unstudied and may reveal essentially novel functionalities of new semiconductors.

Benefit to National Security Missions

This proposal is applicable to "Materials of the Future" research pillar of science at Los Alamos. Dirac semiconductors have the potential to replace commercial semiconductors for energy efficient electronics and solar cell applications. Such applications are of interest to the DOD and NASA. This work is also of potential impact to quantum information and quantum computing.

Progress

Work thus far has focused on producing preliminary results and searching for important problems. F Li has performed analytical calculation of Dirac exciton spectrum. Currently he is exploring the possibility to test predictions using Los Alamos expertise in DFT-type numerical calculations.

Future Work

Dr. Li will start with developing a theory for the Valley Hall Effect: emergence of valley currents in transverse to electric field direction, and make predictions for magnetic moment imaging by Kerr rotation spectroscopy. Using this theory, he will then explore possibilities to entangle spin and valley degrees of freedom by optical pulses, and estimate the relevant quantum lifetimes. This exploration will employ extensions of the nonequilibrium Green function technique to take into account Dirac electrons.

Conclusion

This emerging family of semiconductors is very similar in structure to grapheme but superior. The new 2D materials have an optical gap that makes them similar to commercial semiconductor, but being atomically thin and very stable, they will outperform all currently used semiconductors in energy efficiency, solar cells, and quantum information applications. Dirac semiconductors have the potential to replace commercial semiconductors for energy-efficient electronics and solar cell applications.

Publications

Sinitsyn, N. A.. Dynamic symmetries and quantum nonadiabatic transitions. 2016. Chemical Physics. : 1.

Plasmonics-Transformed Quantum Emitters Through Theory-Guided Synthesis

Jennifer A. Hollingsworth
20160653PRD2

Introduction

Theory has predicted that strong electromagnetic fields that develop inside plasmonic shells could be used to strongly enhance or change the emissive properties of quantum emitters placed inside metal shells. In practice, this effect has been little explored experimentally despite its strong potential for realizing emitter-field coupling in the full range from weak (e.g., Purcell effect quickens emission rates) to strong (e.g., Rabi oscillation) coupling. Control within this range will enable the removal of limitations for quantum dot (QD) emitters as single- and entangled-photon-pair sources: Purcell effects will speed emission toward GHz rates and enhanced coupling will enable entangled-photon-pair generation. To achieve this technological breakthrough, the postdoc will develop solution-processed hybrid photonic (QD)-plasmonic (metal-shell) systems as concentric core/spacer/shell architectures. His specific choice of plasmonic shell material and its "geometry" will be guided by theory. Working with LANL experts in quantum plasmonics, he will determine via theoretical calculations which plasmonic material can be tuned in thickness and distance from the QD emitter (defined by the dielectric spacer layer) to access either the weak or strong coupling regime. The latter (former) assumes minimal (significant) Ohmic losses. In addition to the novel architecture, unique attributes of the proposed research include combining his background and interest in complex ternary compound semiconductors, which provide full tunability of the semiconductor band gap from the ultraviolet to the infrared through composition tuning (not limited to QD size tuning) and non-toxic chemistry, with the novel LANL-developed approach for realizing single-photon emission uncomplicated by "blinking" (fluorescence intermittency), i.e., the "giant" QD (gQD). If the strong-coupling regime proves challenging to realize due to the "lossy" nature of metals, he will explore "dimer" formation (chemically coupling two structures) and ordered self-assembly of the nanostructures, where the interaction of many plasmonic shells closely associated may create a loss-reducing plasmonic cavity effect.

Benefit to National Security Missions

DOE SC and DOE other: Advanced quantum materials for a range of applications from single/entangled-photon sources or, in assemblies, as gain media for cavity-enhanced lasers. Such advanced light emitters are needed for next-gen communications, computing (light-enabled or even all-optical networks) and high power/high efficiency/low-energy-consumption general lighting sources.

DOD: Single-/entangled-photon sources for secure communication or sensor qualification, and optical circuitry to remove bottlenecks in communication networks, low-light detector/sensor qualifications, and tagging, tracking, and locating.

NIH / Pathogen Detection and Countermeasures: Multifunctional nanoparticles for ablation and imaging of cancer cells/tumors or infectious agents.

Remote Sensing for Nuclear Nonproliferation and Counterproliferation: Stand-off tagging, tracking, and locating.

Climate and Energy Impact: Components for efficient lighting.

Basic Understanding of Materials: Design principles for achieving new, emergent functionality in nanoscale hybrids through nanoscale integration enabled by materials synthesis and theory.

Progress

In his first three months as a LANL postdoc, Singh has made significant progress toward the three thrusts of his research -- synthesis of conventional and non-heavy-metal containing photonic (semiconductor) nanocrystals, synthesis of novel plasmonic doped metal-oxide nanocrystals, and assembly of hybrid photonic-plasmonic structures toward advanced plasmonics-enhanced optical properties. Namely, he has synthesized both spheri-

cal and cubic PbS quantum dots (QDs), as well as Cu-In-Zn-S nanorods and QDs, and obtained optical and structural characterizations. He has used colloidal synthetic methods to prepare both spherical and cubic-shaped tin-doped indium oxide (ITO) and obtained spectroscopic signatures of the size/shape and dopant dependent plasmonic resonances (tuned from the near to the mid-infrared). For assembly, spherical photonic particles will be matched with spherical plasmonic particles, and likewise for the cubic-shaped nanocrystals, to facilitate ordered organization into films and supercrystals. Finally, he has overcoated the ITO nanocrystals with a dielectric oxide spacer layer as a means for controlling spacing between the plasmonic nanoparticles and the photonic nanocrystals to ensure optimal plasmonics-based enhancement of semiconductor absorption and emission properties. He has also begun to prepare monolayers of the PbS QDs and the ITO nanoparticles with controlled ITO concentrations. These will be optically characterized in collaboration with LANL and Argonne National Laboratory collaborators.

Singh has shown significant initiative in his laboratory work and has also written a User Proposal ("Probing dopant heterogeneity in metal oxide nanocrystals") to obtain access to the advanced electron microscopy capabilities of the Molecular Foundry. The proposal was recently accepted and he will use Fellowship funds for the required travel. This capability will enable atomic-level characterization of dopants in his ITO nanoparticles, as well in-depth structural and compositional analyses of his semiconductor light emitters to aid in optimization of both components of his hybrid constructs.

Future Work

The postdoc Singh will work with LANL experts in quantum plasmonics to determine via theoretical calculations which combination of plasmonic material – Au/Ag, or non-conventional Al, Cu and even novel doped metal oxides (e.g., CsWO3, indium tin oxide) – can be tuned in thickness and distance from the QD emitter (defined by the dielectric spacer layer) to access either the weak or strong coupling regime. The latter (former) assumes minimal (significant) Ohmic losses. He will combine his background and interest in complex ternary compound semiconductors (e.g., CuIn(SSe)2, Cu2Zn(SSe)4), which provide full tunability of the semiconductor band gap from the ultraviolet to the infrared through composition tuning (not limited to QD size tuning) and non-toxic chemistry, with the novel LANL-developed approach for realizing single-photon emission uncomplicated by "blinking" (fluorescence intermittency), i.e., the "giant" QD (gQD). Specifically, he will attempt to synthesize gQD versions of the ternary / quaternary compounds, which have yet to be explored as the gQD structural motif. He will then encapsulate the new gQDs in dielectric and metallic shells to create the targeted core/shell/shell structures. He will perform basic optical/structural characterizations and work with the LANL advanced spectroscopy team to characterize the hybrid quantum optical properties.

Conclusion

The work will provide new fundamental understanding (experiment and theory) for the design of controlled plasmon-photon interactions across scale that will underpin the advancement of quantum dots as, e.g., useful single/entangled-photon sources or, in assemblies, as gain media for cavity-enhanced lasers. Such advanced light emitters are needed for next-gen communications and computing (light-enabled or even all-optical networks).

Publications

Hanson, C. J., N. F. Hartmann, W. J. De Benedetti, X. Ma, A. Singh, H. Htoon, and J. A. Hollingsworth. Giant PbSe/CdSe Quantum Dots: Ultrastable Single-Dot Near-infrared Photoluminescence. Journal of the American Chemical Society.

Peer, A., A. SIngh, J. A. Hollingsworth, and H. Htoon. Coupling quantum dots to gold nanocups. Nanoscale .

Topological Insulators

Joe D. Thompson
20130805PRD3

Abstract

The discovery and understanding of new states of matter fuel the engine that advances new scientific and technological opportunities important for the future energy and defense security of the Nation. Materials whose electronic structure acquires a certain topology can host new quantum states of matter and are an exciting scientific frontier with promise for entirely new approaches to quantum computing, thermoelectric cooling and sensing. This project has developed necessary new experimental capabilities and applied them to test theoretical predictions for proposed examples of non-trivial electronic topology in an electronically correlated insulator SmB6 and in topologically similar NbAs, which is semimetallic instead of insulating.

Background and Research Objectives

Metals, like copper, conduct an electrical current easily because electrons are free to move in them; whereas, in an electrical insulator, like paper, there are no free electrons and insulators do not conduct electricity. Virtually all solid materials that we know are basically either metals or insulators. The topology of their electronic states, that is, the relationship between electrons' energy and momentum, is trivial and in general can be calculated straightforwardly. Recently, however, theory has predicted an entirely new type of material in which its interior is an electrical insulator (like paper) but its surface is a metal (like copper). [1] Experiments have verified this prediction of a non-trivial topological insulator state where the metallic surface is 'protected' by certain symmetries that quantum mechanics imposes on the electrons. Because the topological insulator is so unusual, there has been an explosion of scientific research aimed at understanding conditions under which it can be found and at imagining the technological implications of such a metal/insulator. [2] So far, electrons in known topological insulators are uncorrelated, that is, behave independently of other electrons that are present. Recent theory has predicted that a new type of typological insulator might be possible in which the electrons are strongly correlated. [3,4] If this theory of topological Kondo insulators were proven to be correct, it could open new opportunities to understand and manipulate the remarkable properties of the inherently quantum mechanical topological state. A goal of this project has been to test the validity of the predicted topological Kondo insulator state in the most promising material SmB6 by using a set of measurements to separate the surface and interior contributions to the properties of this material. These experiments have involved the development of new techniques to measure the thermoelectric power as a function of pressure and to use very high magnetic fields to determine the microscopic configuration of surface electronic states.

Besides topological insulators, a closely related set of materials were discovered during the course of this project. [5] These materials are not insulating in their interior but instead are topological metals with nearly equal numbers of electrons and holes participating in metallic conduction. Nevertheless, conceptual ideas of topological protection developed to account for the very unusual properties of topological insulators also apply to topologically non-trivial semimetals, called Weyl semimetals because electrons associated with the non-trivial topology acquire chirality predicted by Weyl's quantum field theory of electromagnetic, weak and strong nuclear interaction in particle physics.[6] Like topological Kondo insulators, Weyl semimetals also hold potential for technical applications, in part because of the huge change in electrical resistance that an applied magnetic field can induce. Building on our study of SmB6, we have explored theoretical predictions for a candidate Weyl semimetal NbAs.

Scientific Approach and Accomplishments

Initial work focused on developing and optimizing experimental techniques to be used to test the theoretical prediction of a topologically protected metallic surface

state in Kondo insulators, such as SmB6. Tests of low-temperature, high-pressure, high-magnetic field techniques to measure electrical resistivity and Hall effect used the newly discovered topologically trivial Kondo semimetal CeNi2As2 as an example. These experiments led to the discovery of a new paradigm of a pressure-driven, zero-temperature (quantum) phase transition in the low carrier-density limit. In particular, the low carrier density in CeNi2As2, which should be even more pronounced in topological Kondo insulators, strongly influence the fundamental physics of materials such as SmB6 by exhausting the number of charge carriers necessary to form a Kondo-derived bulk insulating state in SmB6. This problem, called the Nozieres exhaustion problem, had not been considered in theoretical predictions of a topologically protected metallic surface state in SmB6. A manuscript based on these results is under consideration for publication in Proceedings of the National Academy of Sciences (USA).

Following these technique developments, studies began on the proposed topological Kondo insulator SmB6. Knowing that thermoelectric transport is sensitive to the topology of electronic states, we measured the thermoelectric power (the electrical voltage generated by a temperature gradient across a sample) and Nernst effect (the thermal Hall effect) on the (110) surface of SmB6 at atmospheric pressure. These experiments revealed an unexpected difference between thermoelectric transport on the (110) surface and previously studied (100) surface. Our analysis of thermopower, Nernst and Hall effect measurements found that thermal and electrical transport in the low-temperature metallic surface state of SmB6 appeared to be dominated by charge carriers with an unusually large effective mass, consistent with theoretical predictions that strong electronic correlations playing an essential role in SmB6. This conclusion, reported in a Physical Review article, is in stark contrast with conclusions from quantum-oscillation measurements by two independent groups [7,8] that claimed evidence for charge carriers with quite small effective masses. There are, however, significant qualitative differences in the way these groups came to these conclusions, and our use of thermopower measurement techniques show that apparent quantum oscillations in SmB6 can arise from spurious sources. Such spurious sources may be the origin of at least part of the disagreement between reports by these other groups. In contrast to small effective electron masses deduced from quantum oscillation measurements, a large effective mass of charge carriers suggested from our experiments supports a very recent theoretical prediction that such a large mass can arise from the breakdown of strong electronic correlations produced by a Kondo effect at the surface of SmB6.[9]

As noted above, a problem closely related to topological insulators is the theoretical possibility of a non-trivial topological semimetallic state, a so-called Weyl semimetal. As part of our study of quantum oscillations in the thermopower of SmB6, we have measured quantum oscillations in a theoretically proposed Weyl semimetal NbAs. These experiments not only found the anticipated huge (462,000%) increase in low temperature electrical resistance in an applied field of 18 T but also quantum oscillations in both electrical resistance and Hall effect measurements. Our analysis of these quantum oscillations showed that they arise from nearly equally small numbers of electrons and holes and that the electron states are topological protected but the hole states are topologically trivial. From this analysis, we concluded that the huge magnetoresistance in NbAs arises because of both the nearly equal numbers of electrons and holes and topological protection of the electronic states. These results, under consideration for publication in Physical Review X, provide a new mechanism for producing a technologically useful huge response of a material to an applied magnetic field.

In summary, our study of SmB6 has motivated the development of new experimental techniques, some unique in the U.S., that have proven useful in in covering new physics in this proposed topological Kondo insulator. Though not definitely proving that SmB6 is topologically non-trivial because of strong electronic correlations, our experiments are fully consistent with this interpretation and have placed new constrains on theoretical models. This project also has established for the first time the importance of topological protection in creating a huge magneto-electrical response in semimetallic NbAs.

Impact on National Missions

This project has explored and verified several theoretical concepts underlying the possibility of exotic topological quantum states that hold promise for new approaches to sensing, thermoelectric cooling, and quantum computing technologies. In pursuing a science-driven agenda aligned with DOE objectives of discovering and understanding new states of matter, this project has made important steps in realizing those objectives that will further the Nation's energy, defense and commercial competitiveness.

References

1. Fu, L., C. L. Kane , and E. J. Mele. Topological insulators in three dimensions. 2007. Physical Review Letters. 98: 106802.

2. Reich, E. S.. Hopes surface for exotic insulator. 2012. Nature. 492: 165.

3. Dzero, M., K. Sun, V. Galitski , and P. Coleman. Topo-

logical Kondo insulators. 2010. Physical Review Letters. 104: 106408.

4. Dzero, M., K. Sun, P. Coleman , and V. Galitski. Theory of topological Kondo insulators. 2012. Physical Review B. 85: 045130.

5. Xu, S. Y., I. Belopolski, N. Alidoust, M. Neupane, G. Bian, C. Zhang, R. Sankar, G. Chang, Z. Yuan, C. Lee, S. Huang, H. Zheng, J. Ma, D. S. Sanchez, B. Wang, A. Bansil, F. Chou, P. P. Shibayev, H. Lin, S. Jia, and M. Z. Hasan. Science. 2015. Discovery of a Weyl fermion semimetal and topological Fermi arcs. 349: 613.

6. Weyl, H.. Zeitschrift fur Physik. 1929. Elektron und gravitation. 56: 330.

7. Li, G., Z. Xiang, F. Yu, T. Asaba, B. Lawson, P. Cai, C. Tinsman, A. Berkley, S. Wolgast, Y. S. Eo, D. J. Kim, C. Kurdak, J. W. Allen, K. Sun, X. H. Chen, Y. Y. Wang, Z. Fisk, and L. Le. Two-dimensional Fermi surfaces of Kondo insulator SmB6. 2014. Science. 346: 1208.

8. Tan, B. S, Y. T. Hsu, B. Zheng, M. C. Hatnean, N. Harrison, Z. Zhu, M. Hartstein, M. Kiourlappou, A. Srivastava, M. D. Johannes, T. P. Murphy, J. H. Park, L. Balicas, G. G. Lonzarich, G. Balakrishnan, and S. E. Sebastian. Unconventional Fermi surface in an insulating state. 2015. Science. 349: 287.

9. Alexandrov, V., P. Coleman , and O. Erten. Kondo breakdown in topological Kondo insulators. 2015. Physical Review Letters. 114: 177202.

Publications

Luo, Y., F. Ronning, N. Wakeham, X. Lu, T. Park, Z. A. Xu, and J. D. Thompson. Pressure- and field-tuned quantum criticality in the antiferromagnetic Kondo semi-metal CeNi2As2 . To appear in Proceedings of the National Academy of Sciences (USA).

Luo, Y., H. Chen, J. Dai, X. A. Xu, and J. D. Thompson. Heavy surface state in a possible topological Kondo insulator:Magneto-thermoelectric transport on the [011]-plane of SmB6. 2015. Physical Review B. 91: 075130.

Luo, Y., H. Li, Y. M. Dai, Y. G. Shi, H. Ding, R. P. Prasankumar, and J. D. Thompson. Hall effect of the extremely large magnetoresistance semimetal WTe2. Applied Physics Letters.

Luo, Y., N. J. Ghimire, M. Wartenbe, M. Neupane, R. D. McDonald, E. D. Bauer, J. D. Thompson, and F. Ronning. A novel electron-hole compensation effect in NbAS. Physical Review X.

Probing and Modifying Intertube Interactions in Semiconducting Carbon Nanotubes

Stephen K. Doorn
20130808PRD3

Abstract

This effort was initially motivated by an interest in probing the electronic and optical properties of double walled carbon nanotubes, as surrogates for understanding intertube interactions in thin-film electronic applications. The effort ultimately focused on single wall tubes that provided routes to advancing the ability to isolate targeted nanotube structures. Such samples enabled Raman spectroscopy experiments aimed at probing the origins of non-Condon effects and establishing baseline behaviors of new phonon modes of interest for extending trends to those found in double walled tubes. New insights into nanotube surface chemistry, electronic structure, and electron-phonon interactions were the ultimate result.

Background and Research Objectives

The remarkable materials, electronic, and optical properties of single walled carbon nanotubes (SWNTs) make them promising elements for advances in optoelectronics and photonic applications. Many first applications will likely be in thin film networked architectures. The intertube interactions inherent to such devices ultimately will limit SWNT performance. It is therefore necessary to gain a better understanding and control of such interactions towards optimization of optical response. In this effort, double walled carbon nanotubes (DWNTs) were envisioned as well-defined model systems for understanding intertube interactions. This project sought to answer the following questions: Can the inner tube of a DWNT emit photo-luminescence? If not, can chemical functionalization of the outer wall switch on such emission? Baseline efforts toward isolation of appropriate tube samples, doping of tubes, and Raman and photoluminescence spectroscopy were carried out in preparation for working on actual DWCNT samples. Of particular interest with Raman would be probing of potential Raman interference effects arising from different types of electron-phonon coupling in pure tube samples of single chiralities. While extension to the DWCNTs of interest was not ultimately attained, significant advances in nanotube separations and Raman spectroscopy did result.

Scientific Approach and Accomplishments

Nanotube Separations

A major part of this effort were contributions made in advancing development of purification techniques to isolate pure single chiralities essential for obtaining spectra free of response from impurity species. Not all nanotubes are the same; how they are wound up ¬ – their chirality – is key to their physical performance. In order to make an unambiguous examination of the questions posed in the project description, we envisioned producing aqueous suspensions consisting of 100% DWCNTs. To that end, we are using a recent breakthrough in nanotube separation science known as two-phase aqueous extraction (ATPE). Because nanotube synthesis cannot be controlled to a level that allows for the production of material with specific physical properties (diameter, chiral angle, electronic type), as-produced material is heterogeneous, requiring post-synthesis separation to produce highly pure, single species samples required for these measurements. The ATPE method relies on the partitioning of carbon nanotubes, suspended in a mixture of surfactants, into two aqueous polymer phases of different hydrophobicity. The partitioning of the different nanotube species into the two polymer phases is controlled by the surfactant composition of the mixed micelles formed around the nanotube, effectively controlling the porosity of the nanotube surface with the aqueous environment and ultimately the hydrophobicity of the nanotube-surfactant complex. By tuning the surfactant composition with each cycle of extraction, separation of carbon nanotubes by diameter and electronic type has been achieved.

Here, we have produced two publications [1], [2] using the technique on SWCNTs over a diameter range 0.54-2.5 nm, which includes the diameters of both inner-

and outer-wall constituent nanotubes within a DWCNT. The results thus serve as a baseline for applying ATPE to DWCNTs. Ultimately, however, spectroscopy efforts took precedence over the final DWCNT preparation. A noteworthy aspect of the small-diameter nanotube separations is that we developed an efficient approach for isolating pure (5,4) nanotubes. These are typically the smallest diameter tubes available in any given sample. Access to these tubes provided us with unique limiting behaviors for new data in our Raman efforts. They were also important as enabling material for our interests in covalent doping efforts. Finally, we note that the large-diameter separations provided protocols of use for isolating pure samples of specific chiralities that are enriched in C13. These are necessary for the Raman experiments described below.

Raman Excitation Profiles

Significant effort went into Raman excitation profiling (REP) of pure chiralities as a probe of potential quantum interference effects that might arise in DWCNTs. As one area of interest, this work supported ongoing efforts at exploring non-Condon effects in the nanotube Raman response. In particular, it was of interest to demonstrate that similar effects to those already observed in semiconducting nanotubes might also be found in metallic tubes. Towards that end, this PRD effort provided REPs for the (5,5) metallic tubes that added to the overall conclusions that non-Condon effects are general behaviors found in all nanotube types. With the (5,5) being a particularly small-diameter tube, it also was a critical part of establishing the diameter trends found in the non-Condon behaviors [3].

We also exploited access to the (5,4) semiconducting structures to demonstrate unambiguously that for the lowest optical transitions, these non-Condon effects are significantly weakened or even absent. The results are contributing to the long-term goal of understanding the origins of these effects. To date, it is becoming clear that they result from the excitonic nature of the nanotube optical transitions. To probe this further, we are finishing measurements on C13 enriched nanotubes to probe the isotope dependences of the exciton-phonon coupling behaviors that are behind the non-Condon effects.

Novel Phonon and Phonon Coupling Behaviors

Finally, the pure chirality samples are providing a unique opportunity to probe phonon behaviors that were until now not possible to probe in detail. Our enriched single-chirality materials are exactly the types of samples required to overcome barriers to obtaining this data. Specifically, we have obtained so-called M-mode frequencies for 12 separate tube chiralities. A strong dependence on diameter is found, but in a unique manner. Within a given (2n+m) family of tubes, the frequencies deviate from an "ideal" armchair behavior in much the same way that nanotube transition energies do! This behavior has no other parallels for other nanotube phonon modes. Additionally, we find strong chirality dependences in the intensities. Most significantly, for tubes like the (11,0), for which we are also able to obtain M-Mode REPs (for the first time), we find the REP shape is completely unlike the excitonically-determined line shapes found for radial breathing modes and G-modes. The M-mode REP maxima do not match up with those found for the G and RBM modes. Tied to this behavior is that near resonance, the M-mode peaks themselves show two clear components. This contrasting behavior to the RBM and G modes suggests that the M-mode behavior is completely determined by the nanotube electron and phonon dispersions, as opposed to coupling to exciton levels. In addition to this new insight into carbon nanotube electronic structure, the M-mode data on these single wall carbon nanotubes will serve as a future baseline for comparisons to data being obtained through a CINT user project with a collaborator at the University of Alabama. Finally, the strong frequency dependence in this mode serves as a newly established signature of nanotube chirality, complementary to the RBM and G modes that have already been established through efforts at LANL.

As a final benefit of the pure chirality samples, the (5,4) tube has provided some unique advantages for probing electron-phonon coupling in nanotubes and for advancing nanotube doping chemistry. We have found that in the (5,4) tubes, strong phonon sidebands appear, indicating strong coupling to radial breathing modes and k-momentum phonons. The ease of resolution we observe is typically only found for larger diameter tubes at cryogenic temperatures. The (5,4) tubes are also providing the deepest exciton trap states and longest excited-state lifetimes that we find in any of our doped tube samples. These results will therefore form a strong basis for our ongoing studies linked to efforts at dopant chemistry of tubes and the unique optical behaviors that arise from them.

Impact on National Missions

Results of this project will have a direct bearing on developing optical and electronic properties of carbon nanotubes for photonic and optoelectronics applications, particularly based on the potential advantages that double-walled carbon nanotubes may present. As a result, this work will have direct relevance to the mission of the DOE-BES funded Center for Integrated Nanotechnologies and the potential applications will be of interest to agencies including DOE, DHS, and DOD. Our primary results will drive development and understanding of fundamental surface chemistry and spectroscopy of low-dimensional materi-

als. As such, their study supports DOE goals for expanding fundamental understanding of functional nanomaterials.

References

1. Fagan, J. A., C. Y. Khripin, C. A. S. Batista, J. R. Simpson, E. H. Haroz, A. R. H. Walker, and Zheng. Isolation of Specific Small-Diameter Single-Wall Carbon Nanotube Species via Aqueous Two-Phase Extraction. 2014. ADVANCED MATERIALS. 26 (18): 2800.

2. Fagan, J. A., E. H. Haroz, Ihly, H. u. i. Gui, J. L. Blackburn, J. R. Simpson, Lam, A. R. H. Walker, S. K. Doorn, and Zheng. Isolation of > 1 nm Diameter Single-Wall Carbon Nanotube Species Using Aqueous Two-Phase Extraction. 2015. ACS NANO. 9 (5): 5377.

3. Haroz, E. H., J. G. Duque, E. B. Barros, Telg, J. R. Simpson, A. R. H. Walker, C. Y. Khripin, J. A. Fagan, Tu, Zheng, Kono, and S. K. Doorn. Asymmetric excitation profiles in the resonance Raman response of armchair carbon nanotubes. 2015. PHYSICAL REVIEW B. 91 (20).

Publications

Fagan, J. A., C. Y. Khripin, C. A. S. Batista, J. R. Simpson, E. H. Haroz, A. R. H. Walker, and Zheng. Isolation of Specific Small-Diameter Single-Wall Carbon Nanotube Species via Aqueous Two-Phase Extraction. 2014. ADVANCED MATERIALS. 26 (18): 2800.

Fagan, J. A., E. H. Haroz, Ihly, H. u. i. Gui, J. L. Blackburn, J. R. Simpson, Lam, A. R. H. Walker, S. K. Doorn, and Zheng. Isolation of > 1 nm Diameter Single-Wall Carbon Nanotube Species Using Aqueous Two-Phase Extraction. 2015. ACS NANO. 9 (5): 5377.

Haroz, E. H., J. G. Duque, E. B. Barros, Telg, J. R. Simpson, A. R. H. Walker, C. Y. Khripin, J. A. Fagan, Tu, Zheng, Kono, and S. K. Doorn. Asymmetric excitation profiles in the resonance Raman response of armchair carbon nanotubes. 2015. PHYSICAL REVIEW B. 91 (20).

Lim, , A. R. T. Nugraha, Cho, Noh, Yoon, Liu, Kim, Telg, E. H. Haroz, G. D. Sanders, Baik, Kataura, S. K. Doorn, C. J. Stanton, Saito, Kono, and Joo. Ultrafast Generation of Fundamental and Multiple-Order Phonon Excitations in Highly Enriched (6,5) Single-Wall Carbon Nanotubes. 2014. NANO LETTERS. 14 (3): 1426.

Subbaiyan, N. K., Cambre, A. N. G. Parra-Vasquez, E. H. Haroz, S. K. Doorn, and J. G. Duque. Role of Surfactants and Salt in Aqueous Two-Phase Separation of Carbon Nanotubes toward Simple Chirality Isolation. 2014. ACS NANO. 8 (2): 1619.

Telg, , E. H. Haroz, J. G. Duque, Tu, C. Y. Khripin, J. A. Fagan, Zheng, Kono, and S. K. Doorn. Diameter dependence of TO phonon frequencies and the Kohn anomaly in armchair single-wall carbon nanotubes. 2014. PHYSICAL REVIEW B. 90 (24).

Understanding and Controlling Magnetism in Multiferroics with THz Pulses

Rohit P. Prasankumar
20130812PRD3

Abstract

Many modern technologies rely on magnetism, including magnetic data storage, magnetic resonance imaging, and magnetic levitation trains. These systems typically use ferromagnets (FM), where the magnetization can be controlled with an external magnetic field. However, magnetic fields have some drawbacks: there are limitations to how fast they can be switched, they are inconvenient to use, and they consume extra energy. Much effort has thus been devoted to the development of multiferroic materials, in which electric and magnetic polarizations exist simultaneously and can be coupled, enabling control of magnetism with an electric field (as well as control of ferroelectric (FE) order with a magnetic field) [1].

Recent advances in the ability to synthesize these materials has led to much effort towards increasing the magnetoelectric (ME) coupling between magnetic and ferroelectric order, especially near room temperature. This would make it possible to control magnetism with an electric field, greatly simplifying many existing technologies (e.g., by making them more energy efficient) while making new applications possible. However, the microscopic origin of this coupling is not well understood and can vary across different classes of materials. This is arguably the major limitation preventing multiferroics from finding a wider range of applications.

One approach to understanding ME coupling in multiferroics is through low energy magnetic, vibrational, and electronic excitations, which generally occur at terahertz (THz) frequencies [2]. These excitations are thought to play a key role in ME coupling, and therefore also offer a promising route to controlling it. Here, we used ultrashort optical and terahertz (THz) pulses to shed light on the microscopic origin of ME coupling, and in fact magnetic order itself, in different multiferroics [3-4]. We also developed a new technique for optically driving crystal vibrations and probing the resulting dynamics with surface sensitivity, which was used to shed light on vibrational dynamics in the topological insulator (TI) Bi2Se3 [5].

Background and Research Objectives

Low energy excitations serve as signatures of various types of order in complex materials. For example, specific vibrations of the crystal lattice, known as soft mode phonons, can emerge when a material displays ferroelectric order. Similarly, low energy excitations known as magnons appear when a material is magnetically ordered. In multiferroics, electromagnons represent the coupling between electric and magnetic order. These low energy excitations typically appear at frequencies ranging from ~0.1-10 THz, suggesting that THz pulses can be used to not only probe their dynamics, but potentially even control the order parameter associated with a given excitation. In fact, ultrashort THz pulses, typically generated from ultrashort optical pulses (with durations of 10-100 femtoseconds (fs)) through nonlinear optical processes, have been used to probe the low energy response of many materials for nearly two decades now. However, only recently has it been possible to generate intense THz pulses that can be used to drive specific low energy excitations, such as magnons in antiferromagnets, electromagnon excitations in multiferroics, and soft mode phonons in ferroelectrics [6]. Probing the resulting dynamic response has not always been straightforward, often necessitating the use of large, relatively inaccessible facilities such as synchrotrons and free electron lasers.

The primary goal of this project was thus to explore the use of intense THz pulses to both probe and control low energy excitations, initially focusing on multiferroic materials. Multiferroics possess soft mode phonons, magnons, and electromagnons at THz frequencies, making them an excellent model system for this effort, particularly since this could provide new insight into the origin of ME coupling. Furthermore, previous research has

shown that second harmonic generation (SHG) is an excellent technique for probing broken symmetry, whether due to FE order, magnetic order, or the presence of surfaces and interfaces [7]. An additional goal was thus to integrate SHG probing with intense THz excitation and apply this not only to multiferroics, but also other materials, such as the topological insulator Bi2Se3, a material of great contemporary interest in condensed matter physics.

Scientific Approach and Accomplishments

In the first year of this project, we began by building a high intensity source of femtosecond THz pulses. This was done by modifying an existing low-intensity THz setup to use a different generation crystal, with a tighter focus at the sample. This resulted in a very powerful tool for studying new materials at sample temperatures between 2.5 and 500 K, with electric (E) fields of 100-150 kV/cm in single-cycle pulses centered at 1.5 THz.

After testing and optimizing the setup, it was used to study the response of multiferroics. Rare earth manganite crystals were supplied by Sang-Wook Cheong at Rutgers University and Namjung Hur at Inha University in Korea. These have magnons that overlap well with the generated THz spectrum. As a first experiment, femtosecond optical pulses centered at 800 nm were used to excite the hexagonal antiferromagnetic (AFM) manganite HoMnO3, after which we monitored the transmission of a THz pulse through the crystal as a function of the time delay between the optical pump and THz probe pulses. Unlike typical optical-pump, THz-probe (OPTP) measurements, THz probing in HoMnO3 shows changes only at the magnon resonance, allowing us to directly track spin dynamics after optically exciting electrons (Figure 1(a)). We learned from additional measurements at different pump fluences and temperatures that the excited electrons couple to the spins via phonons, since the optically induced changes in the magnon resonance are consistent with steady state temperature increases. To test this physical picture, we also did optical-pump, optical-probe measurements. A slow rise time (of 5-10 picoseconds (ps)) was seen in these signals that was nearly identical to that seen in the THz data. This was attributed to spin-phonon relaxation through its temperature dependence, confirming that the magnon dynamics seen in our OPTP signals result from a phonon-mediated transfer of energy from electrons to spins, since they correspond to the spin-lattice relaxation time. Furthermore, by tracking the temperature dependence of this spin-lattice relaxation time (Figure 1(b)), we demonstrated that this process differs significantly between antiferromagnets like HoMnO3 (in which it decreases following a power law with increasing temperature) and the more extensively studied ferromagnetic manganites, in which it follows the magnetic specific heat. Our manuscript describing these results was published in Phys. Rev. B (Rapid Comm.) in 2016 [3].

Our next studies aimed at extending these experiments to the antiferromagnetic orthorhombic manganite TbMnO3, which has been extensively studied using a variety of techniques. In particular, optical spectroscopy has revealed electromagnon (magnons driven by the electric field of light) excitations in this material that only exist at low temperatures, where there is ME coupling between AFM and FE order. We performed OPTP experiments just as in HoMnO3 (Figure 2(a)), revealing that this material also has fast electron-phonon relaxation at early times that gives way to spin-lattice relaxation at longer times. As in HoMnO3, the amplitude of the signal and spin-lattice relaxation time decreases with increasing temperature (Figure 2(b,c)). This enabled us to draw a more general conclusion: spin-lattice relaxation in AFM manganites (and perhaps all AFM insulators) is governed primarily by direct modulation of the exchange interaction by lattice vibrations. Spin conservation prevents this process from occurring in FM manganites, where spin-lattice relaxation is governed instead by spin-orbit coupling. This work is currently under consideration at Phys. Rev. B [4].

Our next goal was to not only use THz pulses to probe magnetic order, but also to control magnetic order in these multiferroics. In principle, using THz pulses to modify magnetic order could in turn modify FE order, since these order parameters are coupled in these multiferroics. Therefore, we modified our experimental setup to excite the sample with intense THz pulses and probe any associated changes in the ferroelectric order through second harmonic generation. Unfortunately, we found that our THz electric fields were not strong enough to drive observable changes in FE order; recent work in this area has shown that fields at least twice as strong are likely required.

At this point, we realized that although THz-pump, SHG-probe experiments aimed at examining changes in magnetic or ferroelectric order would be difficult in multiferroics, the ability of SHG to probe changes in crystal symmetry at surfaces or interfaces could enable a completely new set of studies. We set out to demonstrate this on the topological insulator Bi2Se3, which has an optically active phonon at ~1.95 THz, well within the bandwidth of our intense THz pulses. Furthermore, TIs have unique transport properties, as they are insulating within the bulk material but have a topologically protected conducting surface state. SHG is only sensitive to this surface state, since Bi2Se3 is centrosymmetric in the bulk (and thus generates no SHG signal). Our goal was thus to photoexcite the 1.95 THz phonon and use time-resolved SHG to probe any resulting effects on the TI surface state, which would shed light on the cou-

pling between lattice and electronic properties.

Even at room temperature, using our intense THz pulses to drive this phonon mode produced an extremely large response, consisting of a ~50% initial change in the SHG signal, followed by oscillations at the phonon frequency as well as its second harmonic (Figure 3). The relative amplitudes of these components depended on the azimuthal angle of the Bi2Se3 films compared to the THz polarization, which indicates that the crystal symmetry transiently changes after photoexcitation. A simple model for the nonlinear polarization was used to show that oscillations at the phonon frequency were due to photoinduced changes in the surface symmetry, while oscillations at twice the phonon frequency originated from dynamic symmetry breaking in the bulk. We were also able to coherently control the oscillations using two time-delayed THz excitation pulses, which enabled us to either increase or decrease the oscillation amplitude. This work was recently submitted to Nature Photonics [5].

Finally, at the end of this project, we designed and implemented a collinear 2D THz spectroscopy system, capable of revealing new low energy excitations while also examining the coupling between both new and existing ones. We expect this system, and more generally, the techniques developed as part of this project (2D THz, THz-pump/SHG-probe, etc.)), to apply not only to TIs, but to a wide variety of other materials as well.

Impact on National Missions

In this project, we used intense THz pulses to both probe and drive low energy excitations in different quantum materials. This capability has already attracted much interest from colleagues working on using THz pulses for sensing applications, since molecular crystals also have resonances in the THz range. We believe that the generality of the technique should make it of interest to sponsors from the DOE Office of Science, as well as other programs within DOE, DoD, NIH, and NIST. It also connects well to LANL missions, including Materials for the Future and Science of Signatures. Finally, it will be of great interest to external collaborators through CINT by supporting our leadership in nanoscience/nanotechnology.

Figures

Figure 1. (a) Photoinduced transmission change in HoMnO versus time delay and frequency. (b) Spin-lattice relaxation time versus temperature.

Figure 2. (a) OPTP signals vs. time delay at different temperatures. (b) Amplitude of the OPTP signals vs. temperature. (c) Spin-lattice relaxation time vs. temperature.

Figure 3. (a) THz-induced changes in the SHG intensity vs. crystal angle and time delay. (b) THz-induced changes in the SHG intensity vs. time delay for different crystal angles.

References

1. Cheong, S. W., and M. Mostovoy. Multiferroics: a magnetic twist for ferroelectricity. 2007. Nature Materials. 6: 13.

2. Basov, D. N., R. D. Averitt, D. van der Marel, M. Dressel, and K. Haule. Electrodynamics of correlated electron materials. 2011. Rev. Mod. Physics. 83: 471.

3. Bowlan, P., S. A. Trugman, J. Bowlan, J. X. Zhu, N. J. Hur, A. J. Taylor, D. A. Yarotski, and R. P. Prasankumar. Probing ultrafast spin dynamics through a magnon resonance in the antiferromagnetic multiferroic HoMnO3. 2016. Phys. Rev. B (Rapid Comm.). 94: 100404(R).

4. Bowlan, P., S. A. Trugman, X. Weng, Y. M. Dai, S. W. Cheong, E. D. Bauer, A. J. Taylor, D. A. Yarotski, and R. P. Prasankumar. Directly probing spin dynamics in insulating antiferromagnets using ultrashort terahertz pulses. Phys. Rev. B.

5. Bowlan, P., J. Bowlan, S. A. Trugman, R. Valdes Aguilar, J. Qi, X. Liu, J. Furdyna, M. Dobrowolska, A. J. Taylor, D. A. Yarotski, and R. P. Prasankumar. Probing and controlling terahertz-driven structural dynamics with surface sensitivity. Nature Photonics.

6. Kampfrath, T., K. Tanaka, and K. A. Nelson. Resonant and nonresonant control over matter and light by intense terahertz transients. 2013. Nature Photonics. 7: 680.

7. Denev, S. A., T. T. A. Lummen, E. Barnes, A. Kumar, and V. Gopalan. Probing ferroelectrics using optical second harmonic generation. 2011. J. Am. Ceram. Soc.. 94: 2699.

Publications

Bowlan, P., D. A. Yarotski, N. J. Hur, A. J. Taylor, and R. P. Prasankumar. Direct observation of magnon dynamics in multiferroic HoMnO3. Presented at Quantum Electronics and Laser Science Conference. (San Jose, CA, 10-15 May 2015).

Bowlan, P., J. Bowlan, S. A. Trugman, R. Valdes Aguilar, J. Qi, X. Liu, J. Furdyna, M. Dobrowolska, A. J. Taylor, D. A. Yarotski, and R. P. Prasankumar. Probing and controlling terahertz-driven structural dynamics with surface sensitivity. Nature Photonics.

Bowlan, P., S. A. Trugman, J. Bowlan, J. X. Zhu, N. J. Hur, A. J. Taylor, D. A. Yarotski, and R. P. Prasankumar. Probing

ultrafast spin dynamics through a magnon resonance in the antiferromagnetic multiferroic HoMnO3. 2016. Physical Review B (Rapid. Comm.). 94: 100404(R).

Bowlan, P., S. A. Trugman, X. Wang, Y. M. Dai, S. W. Cheong, E. D. Bauer, A. J. Taylor, D. A. Yarotski, and R. P. Prasankumar. Directly probing spin dynamics in insulating antiferromagnets using ultrashort terahertz pulses. Physical Review B.

Bowlan, P., S. W. Cheong, D. A. Yarotski, A. J. Taylor, and R. P. Prasankumar. Directly probing antiferromagnetic order in HoMnO3 on an ultrafast time scale using optical-pump, THz-probe spectroscopy. Presented at Materials Research Society Spring Meeting. (San Francisco, CA, 6-10 April 2015).

Design Principles for High Performance Organic Photovoltaics

Aditya Mohite
20140658PRD1

Abstract

Present day electronic devices are enabled by design and implementation of precise interfaces that control the flow of charge carriers. However, unlike the well-controlled interfaces in conventional electronics based on silicon and other inorganic materials, organic semiconductor interfaces are relatively poorly characterized and understood, where majority losses are occurring. The ability to understanding, control and manipulate the interface recombination rates in organic photovoltaic cells (OPVs) is expected to bring about a scientific breakthrough that could lead to OPVs with high overall power conversion from sunlight to electricity. In this project, we have demonstrated how precise manipulation and control of organic-organic interfaces using innovative interface modification strategies can overcome a long-standing bottleneck of interface recombination in organic photovoltaic devices. We found by adding the monolayer of materials with different functionalities at the donor-acceptor interface, the rate of charge recombination/separation can be well controlled. By manipulating these rates, we are able to increase the photocurrent by ~350%, and increase the power conversion efficiency (PCE) by ~200%-500%. These lead to a dramatic increase in its power conversion efficiency of 2-5 times in a model bilayer system and from 4.0% to ~8.0% when these design strategies are applied to practical architectures like bulk heterojunction. These interface design strategies are universally applicable to any donor-acceptor interface, making them both fundamentally interesting and technologically relevant for achieving high efficiency organic electronic devices.

Background and Research Objectives

Organic photovoltaic cells (OPVs) are considered to be the next generation, cost-effective thin film solar cell in renewable energy utilization. However, its efficiency is far below the theoretical upper limit after 2 decades of research and development. To overcome such problem, one needs to understand the fundamental photo-physical process during the device operation. In OPVs, the photocurrent generation occurs via three basic photophysical processes: (a) Exciton generation in the donor (or acceptor) region and migration to a donor-acceptor interface; (b) Charge transfer (CT) state formation from an exciton at the interface and (c) CT state dissociation followed by charge collection at the device contacts. These processes are often expressed as charge dynamic rates: (i) exciton generation and migration to the interface, which competes with exciton recombination; (ii) exciton dissociation to CT state; (iii) CT state dissociation (or charge separation rate), which competes with CT state recombination. Therefore, controlling and manipulating these rates is critical for achieving maximum power conversion efficiency (PCE).

An efficient OPV device mandates that exciton dissociation to form the CT state (hole on donor and electron on acceptor) occurs faster than exciton recombination and that charge separation occurs at a rate faster than CT state recombination. OPVs based on bulk heterojunction (BHJ) architectures have been extensively studied over the past decade but the exact role of process parameters and structural features on recombination rates and mechanisms that suppress charge transfer remains ambiguous. Recent reports on the ultra-fast photo-physical dynamics have elucidate those fundamental processes and motivated studies on manipulating interface charge transport dynamics, however critical questions such as suppression of CT state recombination, mechanism of charge separation and role of interface microstructure at the donor-acceptor interface remains a major scientific challenge for the organic electronics community.

The objective for this project is to explore the approaches to manipulate the interface CT state recombination rate in the organic solar cell between the donor-acceptor interface to achieve high efficiency organic photovoltaic devices. Specifically, we add a spacer layer between the donor-acceptor interface with different functionalities

trying to slow down the electron-hole recombination through CT state.

Scientific Approach and Accomplishments

Approach: We study a model bilayer system where donor-acceptor materials are deposited on top of each other and being sandwiched between two selective electrodes for charge collection. At the interface of the donor and interface, we deposited monolayers of interface spacer layers with different functionalities: a) insulator, b) oligomers and c) heavy atom metal-organic complex molecules. We measure the photocurrent and current voltage curve under illumination to evaluate the charge separation efficiency and the overall power conversion efficiency.

Accomplishments

Model bilayer system We found by adding monolayer of those spacers, the device photocurrent increase by 3~5 times in the bilayer device. To understand the exact role of each of spacer layers, we varied the thickness of those layers while measuring the device characteristics such as current-voltage curves under light and under dark, photocurrent as a function of illumination light wavelength and the electroluminescence under magnetic field. We found by adding a) insulator (0~5nm), the photocurrent increase sharply with the spacer layer increase followed by exponential decrease for thicker insulator added. Such behaviour can be fitted well by a classical electron-tunnelling model: the electron can tunnel through the insulator at the interface, leaving the hole behind in the donor material, and thus suppress the recombination. When we add b) oligomers as spacer layer, the device photocurrent increases monotonically and reach a peak value around 5nm and then slow decreases when the spacer layer increases further. Such process can be described as an energy transfer process, where electrons can be transferred through energy transfer process from the donor to acceptor so that they are spatially separated from the hole in the donor, which is another way of suppressing the interface recombination. In the c) metal-organic complex molecules, we found the energy cascading is playing a role in the charge separation process. The molecules have proper energy levels that aligns well with the donor and acceptor that facilitate the electron to cascade from the donor to the acceptor.

Bulk-heterojunction system After understanding the fundamental process of the charge separation at the donor acceptor interface and explored possible spacer layers to slow down the recombination rate, we aimed to modify the device interface in a practical OPV device that employs a blend of donor-acceptor in the film with interface all through the bulk. We therefore add the oligomer into the blend trying to modify the interface. As a result, we observe similar photocurrent increase after adding those molecules with enhanced open circuit voltage and fill factor. This improvement is a classical indication of reduced recombination in the device majorly coming from the interface CT state. The overall power conversion efficiency is thus improved from 4% to 7%.

Impact on National Missions

This project developed a design principle for high performance photovoltaic devices using organic donor-acceptor materials. Solving the bottleneck of interface recombination in OPV system sheds light to the commercialization of the organic electronic technologies. The success of using solution processed organic material in photovoltaic devices will lead to broader PV applications for energy security.

References

1. Yin, S. u. n., Nie, A. D. Mohite, Saxena, D. L. Smith, and P. P. Ruden. Current-voltage characteristics of organic heterostructure devices with insulating spacer layers. 2015. ORGANIC ELECTRONICS. 24: 26.

2. Kuo, , Nie, Tsai, Yen, A. D. Mohite, Gupta, A. M. Dattelbaum, D. J. William, K. C. Cha, Yang, Wang, and Wang. Structural Design of Benzo[1,2-b:4,5-b ']dithiophene-Based 2D Conjugated Polymers with Bithienyl and Terthienyl Substituents toward Photovoltaic Applications. 2014. MACROMOLECULES. 47 (3): 1008.

3. Yen, , Tsai, Kuo, Nie, A. D. Mohite, Gupta, Wang, Wu, Liou, and Wang. Flexible memory devices with tunable electrical bistability via controlled energetics in donor-donor and donor-acceptor conjugated polymers. 2014. JOURNAL OF MATERIALS CHEMISTRY C. 2 (22): 4374.

4. Nie, , Tsai, Asadpour, Blancon, A. J. Neukirch, Gupta, J. J. Crochet, Chhowalla, Tretiak, M. A. Alam, Wang, and A. D. Mohite. High-efficiency solution-processed perovskite solar cells with millimeter-scale grains. 2015. SCIENCE. 347 (6221): 522.

5. Liu, , M. R. Kelley, S. A. Crooker, Nie, A. D. Mohite, P. P. Ruden, and D. L. Smith. Magnetoelectroluminescence of organic heterostructures: Analytical theory and spectrally resolved measurements. 2014. PHYSICAL REVIEW B. 90 (23).

6. Nie, , Chen, Smith, Xia, Hewitt, and Carroll. Nano graphite platelets enhanced blue emission in alternating current field induced polymer based electroluminescence devices using Poly (9,9-dioctylfluorenyl-2,7-diyl) as the emitter. 2014. ORGANIC ELECTRONICS. 15 (1): 99.

Publications

Crooker, S. A., F. Liu, M. R. Kelley, N. J. D. Martinez, W. Nie, A. Mohite, I. H. Nayyar, S. Tretiak, D. L. Smith, and P. P. Ruden. Spectrally resolved hyperfine interactions between polaron and nuclear spins in organic light emitting diodes: Magnetoelectroluminescence studies . 2014. Applied Physics Letters. 105: 153304.

Dun, , Huang, Huang, Xu, Zhou, Y. e. Zheng, Tsai, Nie, D. R. Onken, Li, and D. L. Carrollt. Hydrazine-Free Surface Modification of CZTSe Nanocrystals with All-Inorganic Ligand. 2014. JOURNAL OF PHYSICAL CHEMISTRY C. 118 (51): 30302.

Kuo, , Nie, Tsai, Yen, A. D. Mohite, Gupta, A. M. Dattelbaum, D. J. William, K. C. Cha, Yang, Wang, and Wang. Structural Design of Benzo[1,2-b:4,5-b ']dithiophene-Based 2D Conjugated Polymers with Bithienyl and Terthienyl Substituents toward Photovoltaic Applications. 2014. MACROMOLECULES. 47 (3): 1008.

Liu, , M. R. Kelley, S. A. Crooker, Nie, A. D. Mohite, P. P. Ruden, and D. L. Smith. Magnetoelectroluminescence of organic heterostructures: Analytical theory and spectrally resolved measurements. 2014. PHYSICAL REVIEW B. 90 (23).

Mok, J. W., Lin, K. G. Yager, A. D. Mohite, Nie, S. B. Darling, Lee, Gomez, Gosztola, R. D. Schaller, and Verduzco. Linking Group Influences Charge Separation and Recombination in All-Conjugated Block Copolymer Photovoltaics. 2015. ADVANCED FUNCTIONAL MATERIALS. 25 (35): 5578.

Nie, , Chen, Smith, Xia, Hewitt, and Carroll. Nano graphite platelets enhanced blue emission in alternating current field induced polymer based electroluminescence devices using Poly (9,9-dioctylfluorenyl-2,7-diyl) as the emitter. 2014. ORGANIC ELECTRONICS. 15 (1): 99.

Nie, , Tsai, Asadpour, Blancon, A. J. Neukirch, Gupta, J. J. Crochet, Chhowalla, Tretiak, M. A. Alam, Wang, and A. D. Mohite. High-efficiency solution-processed perovskite solar cells with millimeter-scale grains. 2015. SCIENCE. 347 (6221): 522.

Nie, W., G. Gupta, B. K. Crone, F. Liu, D. L. Smith, P. P. Ruden, C. Y. Kuo, H. Tsai, H. L. Wang, H. Ki, S. Tretiak, and A. D. Mohite. Interface Design Principles for High Performance Organic Semiconductor Devices . 2015. Advanced Science. : 2.

Sun, , Asadpour, Nie, A. D. Mohite, and M. A. Alam. A Physics-Based Analytical Model for Perovskite Solar Cells. 2015. IEEE JOURNAL OF PHOTOVOLTAICS. 5 (5): 1389.

Tsai, , Nie, Cheruku, N. H. Mack, Xu, Gupta, A. D. Mohite, and Wang. Optimizing Composition and Morphology for Large-Grain Perovskite Solar Cells via Chemical Control. 2015. CHEMISTRY OF MATERIALS. 27 (16): 5570.

Xia, , Chen, G. M. Smith, Sun, Yang, Nie, Li, Huang, Ma, and D. L. Carroll. High-performance alternating current field-induced chromatic-stable white polymer electroluminescent devices employing a down-conversion layer. 2015. JOURNAL OF LUMINESCENCE. 161: 82.

Yamaguchi, , Granstrom, Nie, Sojoudi, Fujita, Voiry, Chen, Gupta, A. D. Mohite, Graham, and Chhowalla. Reduced Graphene Oxide Thin Films as Ultrabarriers for Organic Electronics. 2014. ADVANCED ENERGY MATERIALS. 4 (4).

Yen, , Tsai, Kuo, Nie, A. D. Mohite, Gupta, Wang, Wu, Liou, and Wang. Flexible memory devices with tunable electrical bistability via controlled energetics in donor-donor and donor-acceptor conjugated polymers. 2014. JOURNAL OF MATERIALS CHEMISTRY C. 2 (22): 4374.

Yin, S. u. n., Nie, A. D. Mohite, Saxena, D. L. Smith, and P. P. Ruden. Current-voltage characteristics of organic heterostructure devices with insulating spacer layers. 2015. ORGANIC ELECTRONICS. 24: 26.

Synthesis of Novel Energetic Materials

David E. Chavez
20140659PRD1

Abstract

The project was focused on the development of new explosive materials with strong absorption of visible and near-infrared light for use in optical detonator systems. Previous work had shown that conventional materials lacked sufficient absorption of visible and near-infrared light, which in turn increased the laser energy required to initiate to impractical levels. During the project new explosive coordination complexes were designed and synthesized to address this need. Complexes of nitrogen rich tetrazine ligands with Cu(II) were synthesized and absorbed near-infrared light due to d-d transitions, but these transitions were too weak to lead to lower laser initiation thresholds. Complexes of nitrogen rich ligands with Fe(II) were synthesized and had intense charge transfer absorptions in the visible and near-infrared region of the spectrum. These Fe(II) complexes were shown to initiate at very low laser initiation thresholds while also being less sensitive to mechanical insult than conventional detonator materials. A majority of this work was published in a series of six peer reviewed journal articles and a non-provisional patent. The remainder of the work is being prepared for submission. The project has led to follow on funding to transition the discovered materials into a functioning optical detonator prototype. This follow on work has been supported by the pathfinder initiative and the joint munitions program. The project has also led to the conversion of Dr. Thomas Myers from a director's funded postdoctoral fellow to full time staff.

Background and Research Objectives

The project was motivated by several previous efforts at LANL and elsewhere to develop explosives for optical initiation. Previous work had demonstrated that conventional explosives such as PETN (pentaerythritol tetranitrate) could be detonated with high powered laser [1]. Furthermore, doping these systems with absorbent materials such as aluminum nano-particles reduced the energy required to achieve detonation [2]. However, in each case too much laser energy was required for practical implementation of optical initiation.

In order to develop a viable optical initiation system, this project sought to synthesize new explosive materials that had increased absorption of visible and near-infrared (NIR) light. It was hypothesized that integrating absorption and explosive properties on the molecular scale would increase the efficiency of laser light absorption while minimizing energy transfer requirements. In order to accomplish this goal, explosive coordination complexes were targeted. This approach allowed for the development of materials with the rich optical properties of inorganic materials without sacrificing the necessary oxygen balance required for an explosive material.

Throughout the course of this project over 25 new materials of this type were synthesized and characterized. As predicted these materials displayed typical optical properties of coordination complexes while still remaining explosive. The best performing materials developed were both less sensitive to mechanical insult than existing detonator materials and could be laser initiated at a lower energy threshold than existing materials. Overall, the goals of the project were well met, and the materials developed are currently being transitioned into an optical detonator prototype.

Scientific Approach and Accomplishments

The project sought to synthesize new coordination complexes that had both strong absorption of visible and near-infrared light in addition to favorable explosive properties. The combination of nitrogen rich ligands with first row transition metal salts was selected as class of target molecules. This selection was due to the favorable explosive properties that high nitrogen tetrazine ligands had exhibited in the past, in addition to the optical properties typical of transition metal complexes.

Initial work focused on the screening of a variety of first

row transition metals with simple tetrazine ligands. From this work it was determined that tetrazine ligands could successfully be bound to a variety of divalent transition metals to form explosive complexes. The complexes exhibited the d-d transitions in the visible region of the spectra characteristic of these type of complexes. Of particular note were the complexes of Cu(II) which had broad near-infrared absorptions. In addition, complexes of Fe(II) also had very intense charge transfer bands extending well into the near-infrared (Figure 1). This work was published in Inorganic Chemistry [3].

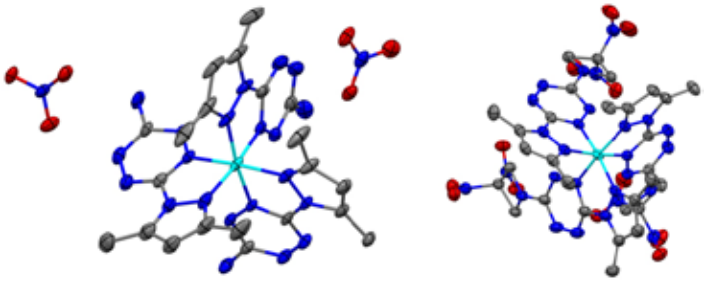

Figure 1. Solid state structures of Fe(II) complexes with tetrazine ligands.

Further work focused on the Cu(II) complexes discovered during the initial screening of potential complexes due to their near-infrared absorption. A new series of Cu(II) complexes were synthesized with a variety of explosive tetrazine ligands. It was found that the architecture of these complexes could be varied by subtly changing the reaction conditions (Figure 2). The series of complexes had a wide range of explosive properties, but very similar optical properties derived from the presence of the Cu(II) metal center. Unfortunately, none of the synthesized complexes could be laser initiated at low laser energies. This work was published in the European Journal of Inorganic Chemistry [4].

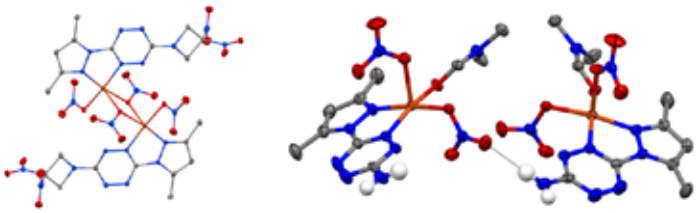

Figure 2. Solid state structures of Cu(II) complexes with tetrazine ligands.

Since complexes with d-d transitions did not appear to be viable candidates for laser initiation, efforts were shifted to the investigation of the Fe(II) complexes with charge transfer bands. In conjunction with theoretical modeling, synthetic efforts were focused on developing tetrazine based ligands to shift the absorption of the complexes deeper into the near-infrared region of the spectrum. By designing and synthesizing tetrazines with fused aromatic ring systems the charge transfer band was tuned over 200 nm into the near-infrared. This increased absorption in the near-infrared region allowed for successful laser initiation of these complexes with lower energy laser light (Figure 3). Furthermore, the discovered complexes were also less sensitive to mechanical insult than the conventional detonator material PETN. These exciting results were published in the Journal of the American Chemical Society [5].

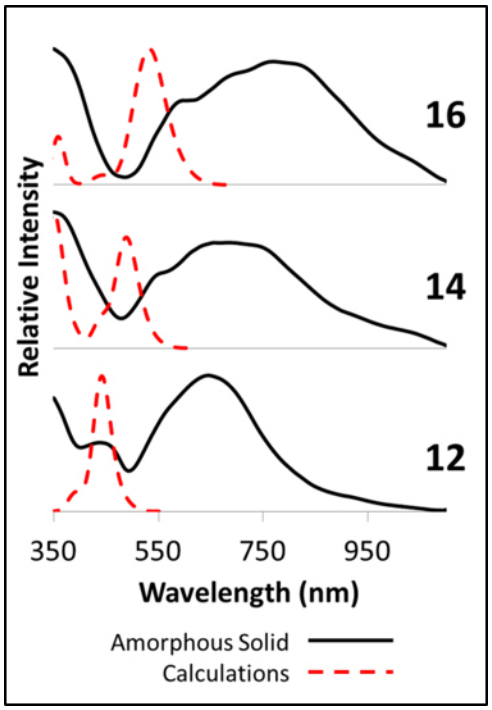

Figure 3. Tuning of the charge transfer bands in explosive Fe(II) tetrazine complexes into the near-infrared.

While the Fe(II) complexes could be initiated at low laser energies, they suffered from poor oxygen balances. New tetrazine ligands that contained higher percentages of oxygen and nitrogen were synthesized in order to generate complexes with more favorable explosive properties. However, these changes affected the ligand's ability to bind to the Fe(II) metal center. In some cases this prevented complex formation and in others it effected the coordination geometries of the resulting complexes (Figure 4). A manuscript draft summarizing this work is currently being prepared for submission.

All of the materials described above in addition to several proposed materials were patented [6].

During the project the electrochemical behavior of the tetrazine materials was also evaluated. This work led to several publications in a variety of journals [7-9]. Also, during the course of the project several new capabilities were developed. The capability to screen new explosive

materials for optical initiation behavior was developed. Collaboration between this project and M-9 scientists Kyle Ramos and Ken Windler helped establish X-ray diffraction for example samples at TA-9. Lastly, this project led to the conversion of Dr. Thomas Myers from a director's funded postdoc to full time staff (Scientist II).

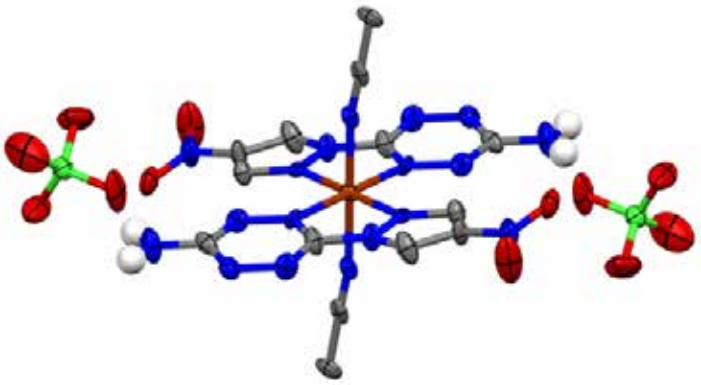

Figure 4. Solid state structure of an oxygen rich tetrazine ligand with Fe(II).

Impact on National Missions

This project has had a significant impact on laboratory missions. The project has led to follow on funding to transition the most promising materials discovered during the project into an optical detonator prototype. This follow on work is supported by the pathfinder initiative and the joint munitions program.

References

1. Renlund, A. M., P. L. Stanton, and W. M. Trott. Laser initiation of secondary explosives. To appear in Proceedings of the ninth international symposium on detonation. (Portland, Aug 23 - Sept 1).

2. Aduev, B. P., G. M. Belokurov, D. R. Nurmukhametov, and N. V. Nelyubina. Photosensitive material based on PETN mixtures with aluminum nanoparticles. 2012. COMBUSTION EXPLOSION AND SHOCK WAVES. 48 (3): 361.

3. Myers, T. W., D. E. Chavez, S. K. Hanson, R. J. Scharff, B. L. Scott, J. M. Veauthier, and Wu. Independent Control of Optical and Explosive Properties: Pyrazole-Tetrazine Complexes of First Row Transition Metals. 2015. INORGANIC CHEMISTRY. 54 (16): 8077.

4. Myers, T. W., K. E. Brown, D. E. Chavez, R. J. Scharff, and J. M. Veauthier. Correlating the Structural, Electronic, and Explosive Sensitivity Properties of CuII Tetrazine Complexes. 2016. EUROPEAN JOURNAL OF INORGANIC CHEMISTRY. (19): 3178.

5. Myers, T. W., J. A. Bjorgaard, K. E. Brown, D. E. Chavez, S. K. Hanson, R. J. Scharff, Tretiak, and J. M. Veauthier. Energetic Chromophores: Low-Energy Laser Initiation in Explosive Fe(II) Tetrazine Complexes. 2016. JOURNAL OF THE AMERICAN CHEMICAL SOCIETY. 138 (13): 4685.

6. Chavez, D. E., S. K. Hanson, R. J. Scharff, J. M. Veauthier, and T. W. Myers. Photoactive energetic materials. 2015. US patent application 14/713,807.

7. Myers, T. W., C. J. Snyder, D. E. Chavez, R. J. Scharff, and J. M. Veauthier. Synthesis and Electrochemical Behavior of Electron-Rich s-Tetrazine and Triazolo-tetrazine Nitrate Esters. 2016. CHEMISTRY-A EUROPEAN JOURNAL. 22 (30): 10590.

8. Chavez, D. E., T. W. Myers, J. M. Veauthier, M. T. Greenfield, R. J. Scharff, and D. A. Parrish. Pentaerythritol Trinitrate Substituted s-Tetrazine and s-Triazine. 2015. SYNLETT. 26 (14): 2029.

9. Breiner, M. M., D. E. Chavez, T. W. Myers, and R. D. Gilardi. 1,2,4,5-Tetrazinyl-Substituted Amino-1,2,4,5-Tetrazines. 2015. SYNLETT. 26 (4): 557.

Publications

Bjorgaard, J. A., A. E. Sifain, Nelson, T. W. Myers, J. M. Veauthier, D. E. Chavez, R. J. Scharff, and Tretiak. Two-Photon Absorption in Conjugated Energetic Molecules. 2016. JOURNAL OF PHYSICAL CHEMISTRY A. 120 (26): 4455.

Breiner, M. M., D. E. Chavez, T. W. Myers, and R. D. Gilardi. 1,2,4,5-Tetrazinyl-Substituted Amino-1,2,4,5-Tetrazines. 2015. SYNLETT. 26 (4): 557.

Chavez, D. E., T. W. Myers, J. M. Veauthier, M. T. Greenfield, R. J. Scharff, and D. A. Parrish. Pentaerythritol Trinitrate Substituted s-Tetrazine and s-Triazine. 2015. SYNLETT. 26 (14): 2029.

Chavez, D. E., T. W. Myers, J. M. Veauthier, M. T. Greenfield, R. J. Scharff, and D. A. Parrish. Pentaerythritol Trinitrate Substituted s-Tetrazine and s-Triazine. 2015. SYNLETT. 26 (14): 2029.

Myers, T. W., C. J. Snyder, D. E. Chavez, R. J. Scharff, and J. M. Veauthier. Synthesis and Electrochemical Behavior of Electron-Rich s-Tetrazine and Triazolo-tetrazine Nitrate Esters. 2016. CHEMISTRY-A EUROPEAN JOURNAL. 22 (30): 10590.

Myers, T. W., D. E. Chavez, S. K. Hanson, R. J. Scharff, B. L. Scott, J. M. Veauthier, and Wu. Independent Control of Optical and Explosive Properties: Pyrazole-Tetrazine Complexes of First Row Transition Metals. 2015. INORGANIC CHEMISTRY. 54 (16): 8077.

Myers, T. W., J. A. Bjorgaard, K. E. Brown, D. E. Chavez, S. K. Hanson, R. J. Scharff, Tretiak, and J. M. Veauthier. Energetic Chromophores: Low-Energy Laser Initiation in Explosive Fe(II) Tetrazine Complexes. 2016. JOURNAL OF THE AMERICAN CHEMICAL SOCIETY. 138 (13): 4685.

Myers, T. W., K. E. Brown, D. E. Chavez, R. J. Scharff, and J. M. Veauthier. Correlating the Structural, Electronic, and Explosive Sensitivity Properties of CuII Tetrazine Complexes. 2016. EUROPEAN JOURNAL OF INORGANIC CHEMISTRY. (19): 3178.

Myers, T. W., S. K. Hanson, Jacqueline M. Veauthier, and David E. Chavez. First row transition metal complexes of tetrazine based ligands as a new class of energetic materials . Presented at 249th ACS National Meeting & Exposition. (Denver, CO, 22-26, Mar. 2015).

Investigating Structure-Directing Agents in Nonconventional Nanowire Synthesis Using a Transmission-Electron-Microscope Flow-Cell Holder

Jennifer A. Hollingsworth
20140661PRD1

Abstract

Understanding the underlying mechanisms responsible for nucleation and growth of one-dimensional (1D) semiconductor nanostructures, especially complex 1D heterostructures such as superlattice, core/shell, and dumbbell-like structures, is essential for the controlled synthesis of these novel, functional nanomaterial architectures. Importantly, structural control is anticipated to enable control over properties, such as transport properties, charge separation efficiencies, and charge or energy transfer processes, relevant for a range of applications including energy conversion and storage, catalysis, and photodetection. However, controlled solution-phase growth of desired 1D heterostructures is still in an early stage compared to their 0D quantum dot counterparts. For this reason, improved methods for establishing underpinning mechanistic understanding and, thereby, increasing the pace of materials discovery and development are needed. The proposed work took advantage of the postdoc's expertise in solution-assisted low-temperature growth of tellurium-based semiconductor nanoheterostructures for thermoelectric applications. It also aimed to capitalize on new LANL capabilities in in situ liquid-phase transmission electron microscopy (TEM) [1] for real-time monitoring of nanowire and heterostructure growth and in flow-based nanowire synthesis using metal-catalyzed solution-liquid-solid (SLS) growth [2]. In particular, the postdoc attempted to elucidate the reaction parameters responsible for forming either alloyed or compositionally abrupt interfaces within axially heterostructured nanowires, i.e., nanowires for which composition is alternated along the nanowire length and for controlling the width of these segments. He investigated effects of precursor choice, concentration, and method of precursor introduction to the reaction. The work afforded new mechanistic insight into solution-phase heterostructured nanowire synthesis.

Background and Research Objectives

Understanding the growth mechanisms for one-dimensional (1D) semiconductor nanostructures, especially more complex 1D heterostructures including superlattice, core/shell, and dumbbell-like structures, is essential for the controlled synthesis of these novel architectures. Importantly, structural control is anticipated to enable properties control, where the ability to tune transport properties, charge separation efficiencies, and charge or energy transfer processes underpins a range of applications from energy conversion and storage to catalysis and photodetection. To date, however, controlled solution-phase growth of high quality and intentionally designed 1D heterostructures is still in the very early stage. Improved methods for establishing the structure-controlling mechanisms and, thereby, for increasing the pace of materials discovery and development are needed.

The work took advantage of the postdoc's prior experience as well as recently established capabilities at LANL. In particular, the postdoc's expertise in glycol-based solution-assisted low-temperature refluxing processes for synthesizing tellurium-based semiconductor nanoheterostructures for thermoelectric applications afforded a basis for tackling synthetic design for other metal chalcogenide materials systems.

Similarly, LANL's new capability in in situ liquid-phase transmission electron microscopy (TEM) [1] was to be used for direct monitoring of nucleation and growth processes, while our novel technique for flow-based metal catalyzed solution-liquid-solid synthesis laid the foundation for advanced hetero-nanowire growth studies [2]. The targeted ability to fabricate finely heterostuctured nanowires (complete composition changes over 10's of nanometers) is relevant for thermoelectric and topological insulator applications, as such "superlattice" structures are predicted to significantly enhance, for example, the thermoelectric figure-of-merit. Advanced

thermoelectrics technologies are needed for waste-heat energy harvesting (more than half of the energy generated worldwide is lost as heat), heat management in the electronics industry, remote power generation, etc.

Scientific Approach and Accomplishments

The postdoc focused on flow-enabled synthesis of heterostructured nanowires (toward addressing a need in the fields of thermoelectrics and topological insulators for ultrathin bismuth or lead chalcogenide nanowires (e.g., Bi2Te3 or PbTe, respectively) and their heterostructures (e.g., where PbSe/PbTe superlattices were predicted by Dresselhaus (PRB 2003) to afford a game-changing thermoelectric figure-of-merit: ZT >6, if nanowire diameter could be controlled to <5 nm and segment lengths to only 2-3 nm). He successfully re-established our laboratory's novel flow-solution-liquid-solid method for hetero-nanowire synthesis. He determined that lack of reproducibility in nanowire growth (even whether or not nanowire growth took place, e.g., in competition with quantum dot growth) could largely be attributed to the treatment of the growth substrate prior to deposition of the low-melting metal catalyst (bismuth). He determined that only HF treatment ensures that the metal film is sufficiently "active" and able to support/catalyze nanowire growth (without HF treatment, the metal appears not to break apart into the nanoscale catalytic "islands"). He successfully synthesized heterostructured nanowires comprising controllably abrupt or alloyed interfaces between segments of defined length. He controlled interface properties by exploring methods for depleting the catalyst droplets of precursor prior to initiation of growth of a second or third segment (eliminated the "reservoir" effect so common in gas-phase nanowire growth). His nanowires of alternating segments can be investigated by others going forward for thermoelectric properties, while those containing extremely short segments are being assessed for "quantum dot-in-wire" properties, e.g, enhanced photoemission from an embedded emitter in a wire. Lastly, we have established a capability for templating the growth of catalyst-metal arrays for ordered nanowire growth (polystyrene sphere template for directing metal deposition prepared using Langmuir-Blodgett sphere assembly). This comprises the first demonstration of ordered arrays of nanowires grown by a catalyzed solution-phase method.

Impact on National Missions

The work advanced fundamental understanding of nanomaterials growth mechanisms, which will enable new materials-by-design strategies. It also advanced our understanding of chemical processes that take place at nano/meso-interfaces and how these influence structure and ultimately function. Together, the new knowledge contributes directly to DOE/SC Basic Understanding of Materials and Fundamental Chemistry missions. Finally, the nanowire materials produced have direct relevance to energy harvesting (energy security, remote power generation) and cooling (e.g., spot cooling in electronics) applications, as well as to single-photon source applications in quantum optical information processing, with fundamental understanding translatable to other nanowire materials systems that have potential applications in chem/bio sensing.

References

1. Aguiar, J. A., S. Wozny, N. R. Alkurd, M. Yang, L. Kovarik, T. G. Holesinger, and J. J. Berry. Effect of Water Vapor, Temperature, and Rapid Annealing on Formamidinium Lead Triiodide Perovskite Crystallization. 2016. ACS Energy Letters. 1: 155.

2. Laocharoensuk, R., K. Palaniappan, N. A. Smith, R. M. Dickerson, D. Werder, J. K. Baldwin, and J. A. Hollingsworth. Flow-based solution–liquid–solid nanowire synthesis. 2013. Nature Nanotechnology. 8: 660.

3. Publications

4. Hollingsworth, J. A., G. Zhang, and R. Laocharoensuk. Controlling composition and interfaces in solution-grown semiconductor nanowires. Langmuir.

Ultrafast Carrier Dynamics in Novel Two-Dimensional Nanomaterials

Victor I. Klimov
20140675PRD3

Abstract

Semiconductor nanocrystals offer a versatile materials platform for exploring novel physical phenomena distinct from their bulk constituents. In particular, the physical size and shape of nanocrystals can induce unique optical and electronic properties, even allowing for facile control of the interactions between electrons. These materials have already shown promise for use in next-generation field-effect transistors, photovoltaics, down-converting phosphores, and light emitting diodes. However, the underlying electronic properties of these materials remain largely unexplored. Specifically, it still remains largely unknown how the effect of confinement in only one dimension is different from the effects of the two-dimensional and three-dimensional confinement realized, respectively, in nanorods and quantum dots. To address this gap in knowledge, we have conducted detailed studies of the optical and electronic properties of two-dimensional platelets of PbSe with femtosecond spectroscopies. Our findings have enabled a more detailed understanding of the effect of particle morphology on the optical and electronic properties of the low-dimensional lead chalcogenide systems.

Background and Research Objectives

Semiconductor materials provide the foundation for a large variety of technologies, most notably for transistors and light-emitting diodes, which comprise the principle component in electronic and optoelectronic devices. It is well known that shrinking the size of the semiconductor structures to nanometer dimensions has a profound impact on their properties. In particular, the band gap of the semiconductor, which directly relates to a variety of device performance parameters, can be tuned across a wide range of values through changing the size of the nanocrystal. Many other properties are additionally modified at the nanoscale, which results in novel physics, such as enhanced interactions between carriers enabling multiple charge carriers to be produced from the absorption of a single photon, termed carrier multiplication. In fact, the versatile nature of nanocrystals has already been developed to the commercial stage in recent display technologies, which rely on spectrally tunable and highly efficient emission of zero-dimensional quantum dots. Further developments could lead to additional practical technologies based on nanomaterials, such as efficient solar photovoltaics, light emitting diodes, and tunable laser sources.

However, the exact role that the particle shape plays in influencing the optical and electronic properties has remained largely unexplored. Recent studies of atomically thin layers of semiconductor MoS2 have shown great promise for a future generation of high- speed transistors. Previous results exploring the optical properties of elongated one-dimensional nanorods found the emergence of enhanced carrier-carrier interactions which enabled efficient carrier multiplication beyond that of both bulk and zero-dimensional quantum dots. While these reports show great promise of “engineered dimensionality” in controlling properties at the nanoscale, few studies have attempted to consistently evaluate the effects of confinement in one, two, and three dimensions.

Our initial target materials in this project were transition metal chalcogenide layered semiconductors that were recently isolated in the form of single-layered plates. We anticipated that following the methodology outlined in the published literature would enable us to prepare colloidal suspensions of single-layered MoS2 and characterize them with femtosecond optical spectroscopy. However, the sample preparation did not produce materials of sufficient optical quality for spectroscopic studies, with the suspensions containing a mixture of plates of differing thicknesses. Therefore, we instead focused on a different materials composition: PbSe. We synthesized high-quality two-dimensional platelets of controlled thicknesses for optical studies. Shown in Figure 1 is a transmission electron microscopy image of one of our nanoplatelets investigated in this work. The diffraction

pattern, shown in the inset, reveals the crystal structure and single-crystal quality of the nanoplatelets studied.

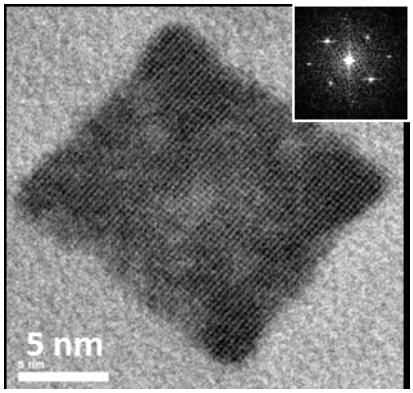

Figure 1. Transmission electron microscope image of one of the PbSe nanoplatelets studied in this work. The insert shows the two-dimensional Fourier transform of the image; it indicates the high level of crystallinity of the synthesized nanostructures.

We sought out to characterize the optical properties of these materials through the use of a variety of advanced femtosecond spectroscopies along with more traditional steady-state spectroscopic measurements. We were particularly interested in quantifying the carrier relaxation rates, carrier-carrier interactions, and the carrier multiplication yields. We were able to accomplish these goals for nanoplatelets of two different thicknesses. While we were able to synthesize a third, thicker nanoplatelet and characterize the steady-state optical properties, the photoluminescence quantum yield of this sample proved too low to perform detailed time-resolved measurements. The measurements performed allowed us to develop a comprehensive picture of how carrier interactions are modified when we change the particle morphology.

Scientific Approach and Accomplishments

To characterize the properties of our newly-synthesized PbSe nanoplatelets we have employed several advanced femtosecond spectroscopies along with steady-state spectroscopic measurements. Simple steady-state absorption and emission measurements allow us to quantify changes in the band gap with the thickness of the nanoplatelets, shown in Figure 2. Using a hyperbolic effective mass model we were able to explain the size dependence of the band gap as a function of the thickness of the material, which followed expectations based on studies of one-dimensional quantum rods and zero-dimensional quantum dots. The lack of sharp absorption features in Figure 2 suggested the lack of exciton formation, in contrast to measurements of one-dimensional quantum rods.

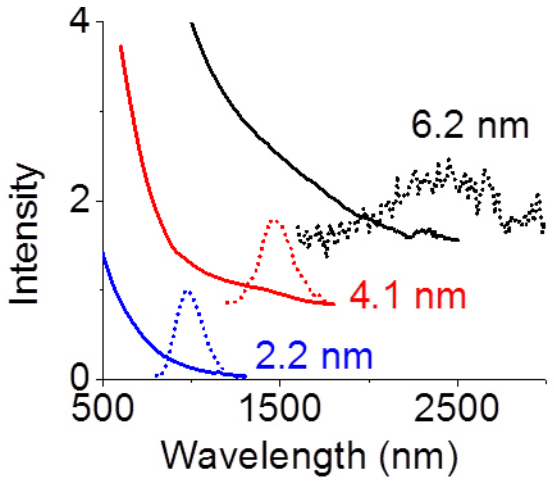

Figure 2. Absorption (solid lines) and emission (dashed lines) spectra of the nanoplatelets of different thicknesses (2.2 to 6.2 nm).

Femtosecond transient absorption experiments, whereby the change in the absorption spectrum following excitation with a short optical pulse is detected were utilized to characterize the interaction strength between carriers as well as the rate of carrier cooling. The build-up of the transient bleach at the band gap allows us to quantify the energy loss rate of hot carriers, shown in Figure 3 for the thinnest platelet. Interestingly, we find an increase in the carrier relaxation rate when compared to one-dimensional and zero-dimensional materials.

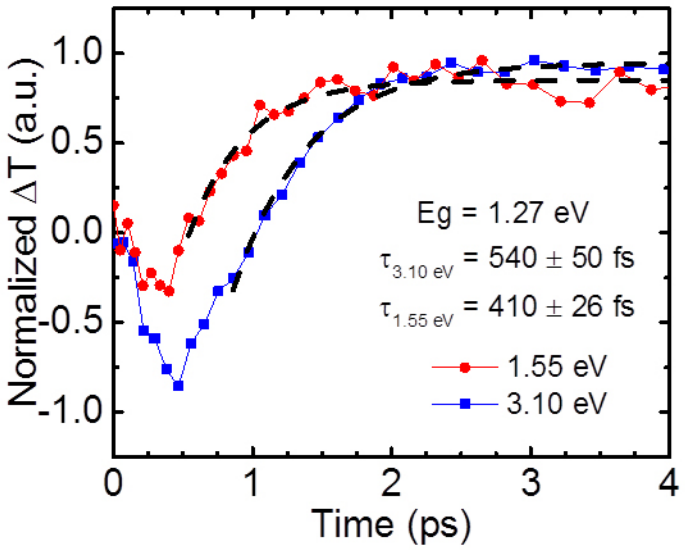

Figure 3. Femtosecond transient absorption data of the thinnest platelet (2.2-nm thick) reveal extremely fast timescales (400 – 500 fs) of carrier cooling for two different excitation energies.

The increase in the relaxation rate likely arises due to the increased density of states expected in two-dimensional materials. Furthermore, we were able to quantify the magnitude of the carrier-carrier interactions in bulk, two-

dimensional plates, one-dimensional nanorods, and zero-dimensional quantum dots. Interestingly, we found that one-dimensional materials exhibited the strongest interaction between carriers through a combination of dielectric and geometrical effects. While carrier-carrier interactions were found to be enhanced in our two-dimensional materials, interactions were insufficient to allow for the formation of room-temperature excitons along with other unique properties found in other two-dimensional materials.

Pump-intensity-dependent time resolved photoluminescence experiments provided detailed information about the absorption cross-sections along with multicarrier interactions (Figure 4). As the pump power is increased, multiple photons may be absorbed by a single nanocrystal, yielding a large local density of charges. The confinement of carriers induces enhanced interactions between the carriers resulting in fast non-radiative recombination of these multicarrier states. Analysis of the kinetics of the traces in Figure 4 yields the lifetimes of the two- and three-electron hole pair states (biexciton and triexciton, respectively). We find that the lifetimes follow the same trend found in zero-dimensional quantum dots and follow the volume of the nanocrystal. Similarly, the absorption cross section measured from the saturation of the photoluminescence with increasing pump fluence additionally followed established volume scaling laws. The scaling of the multicarrier lifetimes is consistent with a free carrier recombination model, confirming that excitons do not form in our structures at room temperature.

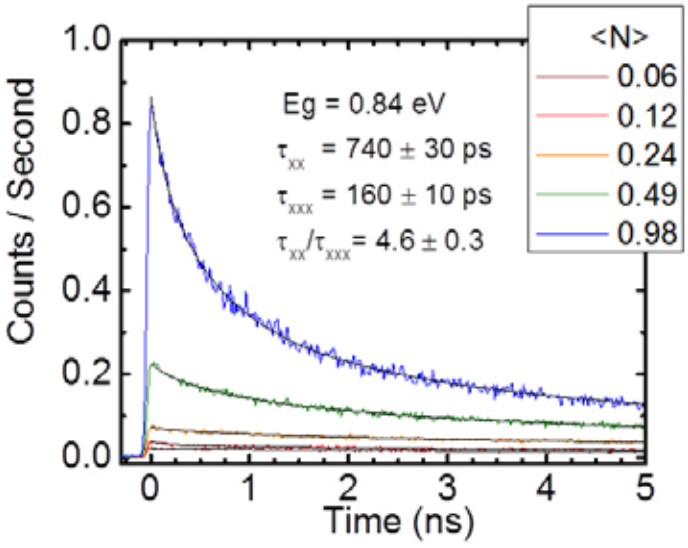

Figure 4. Time resolved photoluminescence transients for the middle thickness platelet (4.1-nm thick) as a function of pump fluence. These measurements reveal the time scale of intrinsic Auger recombination for biexcitons (τ) and triexcitons (τ).

Through tuning of the photon energy of the optical pump beam we can quantify the carrier multiplication yield through an analysis of the population of multiexciton states measured across the ensemble. We find that the carrier multiplication efficiencies in our materials are in good agreement for the values found in zero-dimensional quantum dots. Our results indicate that the photophysics of our PbSe nanoplatelets are quite similar to zero-dimensional quantum dots. However, for nanoplatelets of a similar band gap to that of a quantum dot, the rate of Auger recombination is found to be ten times slower. This result indicates that extracting the multiple charges generated through carrier multiplication could be more efficient in a solar cell comprised of nanaoplatelets, as the charge extraction time must be faster than the rate of Auger recombination. The results from this work were presented at the 2015 Fall Materials Research Society meeting in Boston MA and are currently being prepared for publication.

Impact on National Missions

The primary goal of this project is to explore the electronic properties of a new class of two-dimensional semiconductor materials. As such, the results will be valuable to the DOE Office of Science. Since we are studying charge carrier interactions at extremely high densities in these two-dimensional semiconductors, the insights from this project could potentially benefit MaRIE's mission of investigating time-dependent dynamic properties of matter under extreme conditions. Through ultrafast laser spectroscopy of these semiconductor nanoplatelets, we have established the role of two-dimensional quantum confinement on intraband carrier cooling, Auger recombination and other multi-carrier interactions, significantly contributing to the basic understanding of these novel nanomaterials. The materials developed in this project can be used as spectrally tunable light harvesters in photoconversion including both photovoltaics and generation of solar fuels. This makes this project directly relevant to LANL's Energy Security and Environment missions.

Publications

Fidler, A. F., S. Guo, O. Isaienko, W. Koh, K. A. Velizhanin, I. Robel, J. M. Pietryga, and V. I. Klimov. Carrier Multiplication in Quasi-One and Two-Dimensional Nanomaterials and Shape-Controlled Heterostructures. Presented at 2015 Fall Meeting of the Materials Research Society. (Boston, MA, Nov. 29 - Dec. 4, 2015).

Gao, J., A. F. Fidler, and V. I. Klimov. Carrier multiplication detected through transient photocurrent in device-grade films of lead selenide quantum dots. 2015. Nature Comm.. 6: 8185.

Guo, S., A. F. Fidler, K. He, D. Su, G. Chen, Q. Lin, J. M. Pi-

etryga, and V. I. Klimov. Shape-Controlled Narrow-Gap SnTe Nanostructures: From Nanocubes to Nanorods and Nanowires. 2015. Journal of the American Chemical Society. 137 (48): 15074.

Ramasamy, K., P. G. Kotula, A. F. Fidler, M. T. Brumbach, J. M. Pietryga, and S. A. Ivanov. SnxGe1–x Alloy Nanocrystals: A First Step toward Solution-Processed Group IV Photovoltaics. 2015. Chemistry of Materials. 27 (13): 4640.

New Room Temperature Multiferroic Thin Films Enabled by Strain Engineering

Quanxi Jia
20140676PRD3

Abstract

Superlattices and vertical nanocomposites with ferromagnetic (FM) and ferroelectric (FE) components have been synthesized to achieve room temperature multiferroic artificial materials. Different superlattices including BiFeO3/BiMnO3 (BFO/BMO), and BiFeO3/La0.7Sr0.3MnO3 (BFO/LSMO) have been synthesized by laser Molecular Beam Epitaxy (MBE). BiFeO3/BiMnO3 superlattices with magnetic transition temperature up to 470 K have been achieved. The interfacial interaction between FM and antiferromagnetic layers dominates the high Curie temperature in superlattices. In BiFeO3/La0.7Sr0.3MnO3 superlattices, enhanced magnetism in BFO has been achieved. Vertical nanocomposites with FM CoFe2O4 and FE BaTiO3 phases exhibit multiferroic properties above room temperature. Large room temperature magnetoelectric coupling coefficient (~2000 mV/cm Oe) has been confirmed by magnetic field dependent second harmonic generation (SHG) and piezoresponse force microscopy (PFM). Strain coupling along vertical interfaces plays a critical role in the property enhancement in these systems.

Background and Research Objectives

Multiferroic perovskite oxides with the coexistence of magnetism and ferroelectricity have drawn increasing interest due to their potential for multifunctional devices, for example, magnetoelectric random access memory, tunable multifunctional spintronic devices including four-state memory devices, and spin filters. Room temperature operating multiferroics are currently of intense scientific interest for these devices. However, single-phase multiferroic materials are very scarce due to their exclusive natural origins [1]. Here, we have targeted to develop new artificial multiferroic composites by using multilayer, superlattice and nanocomposite approaches. This allows choosing components with large ferroelectric properties and magnetostriction [2], so the resulting composites may have superior multiferroic properties and magnetoelectric couplings. Our research project aims to develop new artificial composite multiferroic materials with both FM and FE properties above room temperature. By adjusting the growth conditions, we have investigated the microstructure, strain and interfacial coupling effects on multiferroic properties.

Scientific Approach and Accomplishments

The objective of this project is to develop new room temperature multiferroic materials by using a composite approach. To accomplish the objectives, we deposited superlattices with FM and FE alternative layers, and vertical nanocomposites with two phases vertically aligned on substrates. Thus, we can integrate the multiferroicity into a composite format in both lateral and vertical manners. Taking advantage of our state of the art laser-MBE system in CINT, we have synthesized BiFeO3/BiMnO3 and BiFeO3/La0.7Sr0.3MnO3 superlattices with different periodicities. The Reflected High Energy Electron Diffraction (RHEED) system in the laser-MBE allows monitoring the unit cell by unit cell growth and thus we are able to manipulate the superlattice growth in the atomic scale. The sharp interface allows critical analysis of the interfacial interaction in superlattices. A TC of 410 K was observed for m = 1, and a TC of 320 K was observed for m = 2 in the BiFeO3/BiMnO3 system. This high Curie temperature is consistent with the theory prediction of TC (~406 K) with FM BMO–AFM BFO interactions. Artificial superlattices of ferroelectric BFO and BMO with interface-induced high temperature magnetism are an important prerequisite for creating practical magnetoelectric systems [3]. BiFeO3/La0.7Sr0.3MnO3 superlattices have been synthesized to study interface coupling, which is critical to understand magnetoelectric coupling in superlattices. Our polarized neutron reflectivity results indicate parallel alignment of magnetization across BFO/LSMO interfaces. We obtained an enhanced saturation magnetization of 110±15kA/m for an ultrathin BFO layer (2 unit cells) sandwiched between ultrathin LSMO layers (2 unit cells) [4].

By using pulsed laser deposition, we have also fabricated vertical nanocomposites with FM nanopillars in FE matrix by using two immiscible phases (CoFe2O4 & BaTiO3). In this work, we have investigated the multiferroic properties by temperature dependent SHG and magnetization. The ME coupling is evidenced by the magnetic dependent SHG characterizations. A large room temperature magnetoelectric coupling coefficient (~2000 mV/cm Oe) has been confirmed by magnetic field dependent piezoresponse force microscopy (PFM). The underlying physics governing the coupling between FE and FM phases in vertical nanocomposites is discussed [5]. This work opens up a new strategy to develop composite multiferroic materials with large room temperature magnetoelectric coupling.

We further explored the growth of new multiferroic materials by using two miscible composite phases such as BiFeO3-BiMnO3 and BiFeO3-BiCrO3 [6-8]. The growth window of new phases with potential room temperature multiferroicity has been explored. Our results have demonstrated that CeO2 serves as a general template for the growth of bismuth compounds with potential room-temperature multiferroicity. We have studied the magnetic properties in Fe and Mn site in double perovskite Bi2FeMnO6 thin films by using density functional theory simulations and x-ray magnetic circular dichroism measurements [9]. The strain effect on magnetic properties has been investigated in samples with different thicknesses. Our results demonstrated that exchange interaction between Fe and Mn sites is responsible for ferromagnetic ordering in BFMO films.

In summary, in this project, we have explored the synthesis of new artificial composite materials with room temperature multiferroic properties. We have explored different composite materials including superlattices (e.g., BiFeO3/BiMnO3 & BiFeO3/La0.7Sr0.3MnO3), vertical nanocomposites (CoFe2O4:BaTiO3) and single-phase new materials (BiFeO3-BiMnO3 & BiFeO3-BiCrO3). We have investigated the interfacial coupling and magnetoelectric coupling in these systems. The magnetoelectric coupling at room temperature in the vertical nanocomposites is as large as 2000 mV/cm Oe.

Impact on National Missions

This project directly contributes to LANL's advanced materials strategy of developing emergent phenomena via defects and interface engineering. It supports and strengthens the Laboratory's core scientific capabilities essential to discovering, understanding, and exploiting emergent phenomena in materials. This effort ensures LANL's continued and expanded leadership in nanostructured materials, innovative probing methods, and theoretical predication and design of new/improved functional materials.

References

1. Chen, A. P., and Q. X. Jia. Multiferroic nanocomposite thin films. 2016. In Multiferroic materials: Properties, techniques, and applications. Edited by Wang, J. L.. , p. xxx. CRC: Taylor & Francis Group.

2. Chen, A. P., and N. Poudyal et al. Modification of structure and magnetic anisotropy of epitaxial CoFe2O4 films by hydrogen reduction. 2015. Appl. Phys. Lett.. 106: 111907.

3. Choi, E. M., and J. E. Kleibeuker et al. Interface-Coupled BiFeO3/BiMnO3 Superlattices with Magnetic Transition Temperature up to 410 K. 2016. Adv. Mater. Interfaces. 3: 1500597.

4. Singh, S., and J. Xiong et al. Field-dependent magnetization of BiFeO3 in an ultrathin La0.7Sr0.3MnO3/BiFeO3 superlattice. 2015. Phys. Rev. B. 92: 224405.

5. Chen, A. P., and A. Eshghinejad et al. Large magnetoelectric couplings driven by strain induced new ground states. Adv. Mater..

6. Chen, A. P.. Stabilizing new thin film materials in bismuth compounds. To appear in J. Mater. Res..

7. Li, L. G., and w. Zhang et al. Strain and interface effects in a novel Bismuth-based self-assembled supercell structure. 2015. ACS Appl. Mater. Interfaces. 7: 11631.

8. Chen, A. P., and H. Zhou et al. A new class of room-temperature multiferroic thin films with bismuth-based supercell structure. 2013. Adv. Mater.. 25: 1028.

9. Ahmed, T., and A. P. Chen et al. Magnetic, Electronic and Optical Properties of Double Perovskite Bi2FeMnO6. To appear in APL Mater..

Publications

Ahmed, T., A. P. Chen, B. McFarland, Q. Wang, H. Ohldag, R. Sandberg, Q. X. Jia, D. A. Yarotski, and J. X. Zhu. Effect of Fe and Mn site mixing on the XMCD spectrum in double perovskite Bi2FeMnO6. 2016. Appl. Phys. Lett.. 108: 242907.

Ahmed, T., A. P. Chen, D. A. Yarotski, S. Rudin, S. A. Trugman, Q. X. Jia, and J. X. Zhu. First-principles study of magnetic, electronic and optical properties of double perovskite Bi2FeMnO6. 2016. APL Mater.. : xxx.

Chen, A. P., W. Zhang, J. L. MacManus-Driscoll, H. Wang, M. R. Fitzsimmons, and Q. X. Jia. Role of interfaces on competing interactions of ferroic films. Invited pre-

sentation at 2015 MRS Fall meeting. (Boston, Nov. 29 - Dec. 4).

Choi, E. M., J. E. Kleibeuker, T. Fix, J. Xiong, C. J. Kinane, D. Arena, S. Langridge, A. P. Chen, Z. Bi, J. H. Lee, H. Wang, Q, X. Jia, M. G. Blamire, and J. L. MacManus-Driscoll. Interface coupled BiFeO3/BiMnO3 superlattices with magnetic transition temperature up to 410 K. 2015. Adv. Mater. Interfaces. 3: 1500597.

Choi, E. M., J. E. Kleibeuker, T. Fix, J. Xiong, C. J. Kinane, D. Arena, S. Langridge, A. P. Chen, Z. Bi, J. H. Lee, H. Wang, Q. X. Jia, M. G. Blamire, and J. L. MacManus-Driscoll. Interface coupled BiFeO3/BiMnO3 superlattices with magnetic transition temperature up to 410 K. 2015. Adv. Mater. Interfaces. 3: 1500597.

Li, L., W. Zhang, F. Khatkhatay, J. Jian, M. Fan, Q. Su, Y. Zhu, A. P. Chen, P. Lu, and X. Zhang. Strain and interface effects in a novel bismuth-based self-assembled supercell structure. 2015. ACS Applied Materials & Interface. 7: 11631.

Lu, X., A. P. Chen, Y. Luo, P. Lu, Y. Dai, E. Enriquez, P. Dowden, H. Xu, P. G. Kotula, A. K. Azad, D. A. Yarotski, R. P. Prasankumar, A. J. Taylor, J. D. Thompson, and Q. X. Jia. Conducting interface in oxide homojunction: Understanding of superior properties in black TiO2. 2016. Nano Lett.. : 5751.

Zhang, W., A. P. Chen, M. Li, L. Li, Z. Xia, P. Boullay, L. Wu, Y. Zhu, J. L. MacManus-Driscoll, Q. X. Jia, and H. Wang. Two-dimensional layered oxide structures tailored by self-assembled layer stacking via interfacial strain. 2016. ACS Applied Materials & Interface . 8: 16845.

Search for the Topological States in F-electron Systems

Tomasz Durakiewicz
20140678PRD3

Abstract

Topological surface states are in the center of attention of the modern condensed matter physics. This proposal focuses on finding an experimental confirmation of such a state in SmB6, possibly the first f-electron system with such states. The direct evidence in terms of imaging and characterizing the surface states in energy – momentum space is still missing. Such direct evidence may be obtained from angle-resolved photoemission (ARPES).A set of focused low-photon-energy and low temperature ARPES measurements is proposed to detect and characterize the surface states and reveal the nature of the residual conductivity anomaly below 10K from a band structure and momentum-space perspective. With the use of ARPES and spin-resolved ARPES technique, the spin structure of the surface state in SmB6, was identified, and its possible momentum-spin locking properties will be analyzed. The search for topological surface states will be extended to other heavy Fermion compounds such as Kondo insulator CeNiSn, or skutterudites CeOs4As12 and CeOs4Sb12.

Background and Research Objectives

Materials with strong electronic correlations often exhibit exotic ground states such as the heavy fermion state, Mott and Kondo insulating states, and superconductivity [1, 2, 3]. The Kondo insulator SmB6 [4], recently attracted much attention due to the novel theoretical proposal that it may host topologically protected states within its Kondo bandgap [5]. This compound is metallic at room temperature, but the resistivity goes up at low temperatures and saturates to a finite value below 5 K. The anomalous residual conductivity present in SmB6 at low temperatures is believed to be associated with the surface states that lie within the Kondo band-gap. The nature of those surface states and their possible topological origin, remain unknown and form a center of a rapidly accelerating discussion [6, 7].

The main objective of this work was to discover the first examples of f-electron topological insulators and understand the role of f-electrons in forming the physical properties of these systems.

Scientific Approach and Accomplishments

The focus of this work was on topological properties of matter, with special emphasis on novel sub-groups of topological systems: topological Kondo insulators, Dirac semimetals, topological crystalline insulators and Weyl semimetals. In his experimental work the techniques of angle-resolved photoemission (ARPES) and time-resolved photoemission (TR-ARPES) were used to characterize the electronic structure aspects of materials.

Time-resolved ARPES: Discovery of the gigantic surface lifetime of an intrinsic topological insulator Bi2Te2Se, published in Phys. Rev. Lett. [8] was honored by a PRL Editor's Suggestion, associated with increased publicity on PRL webpages. Optical properties were found that are in sharp contrast to those of bulk-metallic topological insulators, including a gigantic optical lifetime exceeding 4 μs for the surface states in Bi2Te2Se, and a surface photovoltage, a shift of the chemical potential of the Dirac surface states, as large as 100 mV. The findings are of great significance for future devices utilizing photo-controlled topologically protected surface states.

Topological Kondo Insulators: In a series of three papers the topological properties of rare-earth hexaborides were presented, where the interest is fueled by possible coexistence of topological properties and strong correlations. In a paper published in Phys. Rev. Lett. [9], where Madhab Neupane is first author, it is shown that a theoretical prediction of YbB6 being a topological Kondo insulator is not supported by the details of its electronic structure. Specifically, it is shown that the Fermi level electronic structure of YbB6 has three 2D Dirac cone like surface states enclosing the Kramers's points, while the f orbital that would be relevant for the Kondo mechanism is ?1 eV below the Fermi level. This finding is a signifi-

cant novelty in rapidly growing field of correlated topological systems. These experimental and theoretical results provide a new approach for realizing novel correlated topological insulator states in rare-earth materials. Another hexaboride system, CeB6, was a topic of Phys. Rev. B [10] (first author), where it is shown that the Fermi surface electronic structure of CeB6 consists of large oval-shaped pockets around the X points of the Brillouin zone, whereas the states around the zone center Γ point are strongly renormalized, with quasiparticle states participating in the formation of hot spots at the Fermi surface, whereas the incoherent f states hybridize and lead to the emergence of dispersive features absent in the non-f counterpart BaB6. These results will be useful in understanding the nature of the exotic low-temperature phases in these materials. In a third paper from this hexaboride mini-series, Phys. Rev. B [11], the evolution of topological states and their orbital textures in the mixed-valence compounds SmB6 and YbB6 is discussed within the framework of the generalized gradient approximation plus onsite Coulomb interaction (GGA + U) scheme for a wide range of values of U.

Weyl semimetals: This particular area of research is growing rapidly. In a high profile paper published in Science [12], a discovery of a Weyl fermion semimetal and topological Fermi arcs in TaAs are shown. Surface Fermi arcs are directly observed for the first time, as well as the Weyl fermion cones and Weyl nodes in the bulk of TaAs single crystals. Fermi arcs terminate on the Weyl fermion nodes, consistent with their topological character. This work opens the field for the experimental study of Weyl fermions in physics and materials science. In a related paper which appeared in Nature Communications [13], Dr. Naupane identifies a topological Weyl semimetal state in the transition metal monopnictide materials class, and shows that in the TaAs-type materials the Weyl semimetal state does not depend on fine-tuning of chemical composition or magnetic order, which opens the door for the realization of Weyl semimetals and Fermi arc surface states in novel materials.

Impact on National Missions

Impact in the area of scientific excellence was provided by significant discoveries made in the course of this project and by publishing the results in widely respected and highly cited journals. Quantitatively, a total of 14 papers were published out of this project, including 2 papers in Science (Impact Factor = 33.6), 2 papers in Physical Review Letters (IF =7.5), 2 in Nature Communications (IF =11.5), one in Scientific Reports (IF = 5.6) and 6 papers in Physical Review B (IF = 3.7).

References

1. Mathur, N. D., F. M. Grosche, S. R. Julian, I. R. Walker, D. M. Freye, R. K. W. Haselwimmer, and G. G. Lonzarich. Magnetically mediated superconductivity in heavy fermion compounds. 1998. Nature. 394: 39.

2. Chandra, P., P. Coleman, J. A. Mydosh, and V. Tripathi. Hidden orbital order in the heavy fermion metal URu2Si2. 2002. Nature. 417: 831.

3. Curro, N. J., T. Caldwell, E. D. Bauer, L. A. Morales, M. J. Graf, Y. Bang, A. V. Balatsky, J. D. Thompson, and J. L. Sarrao. Unconventional superconductivity in PuCoGa5. 2005. Nature. 434: 622.

4. Menthe, A., E. Buehler, and T. H. Geballe. Magnetic and semiconducting properties of SmB6. 1969. Physical Review Letters. 22 (7): 295.

5. Dzero, M., K. Sun, P. Coleman, and V. Galitski. Theory of topological Kondo insulators. 2012. Physical Review B. 85: 045130.

6. Jiang, J., S. Li, T. Zhang, Z. Sun, F. Chen, Z. R. Ye, M. Xu, Q. Q. Ge, S. Y. Tan, X. H. Niu, M. Xia, B. P. Xie, Y. F. Li, X. H. Chen, H. H. Wen, and D. L. Feng. Observation of in-gap surface states in the Kondo insulator SmB6 by photoemission. 2013. arxiv 1306.5664, Cornell University Library.

7. Kim, D. J., S. Thomas, T. Grant, J. Botimer, Z. Fisk, and J. Xia. Robust Surface Hall Effect and Nonlocal Transport in SmB6: Indication for an Ideal Topological Insulator. 2012. arXiv:1211.6769, Cornell University Library.

8. Neupane, , Xu, Ishida, Jia, B. M. Fregoso, Liu, Belopolski, Bian, Alidoust, Durakiewicz, Galitski, Shin, R. J. Cava, and M. Z. Hasan. Gigantic Surface Lifetime of an Intrinsic Topological Insulator. 2015. PHYSICAL REVIEW LETTERS. 115 (11).

9. Neupane, , Xu, Alidoust, Bian, D. J. Kim, Liu, Belopolski, T. -. Chang, H. -. Jeng, Durakiewicz, Lin, Bansil, Fisk, and M. Z. Hasan. Non-Kondo-like Electronic Structure in the Correlated Rare-Earth Hexaboride YbB6. 2015. PHYSICAL REVIEW LETTERS. 114 (1).

10. Neupane, , Xu, Sankar, Gibson, Y. J. Wang, Belopolski, Alidoust, Bian, P. P. Shibayev, D. S. Sanchez, Ohtsubo, Taleb-Ibrahimi, Basak, W. -. Tsai, Lin, Durakiewicz, R. J. Cava, Bansil, F. C. Chou, and M. Z. Hasan. Topological phase diagram and saddle point singularity in a tunable topological crystalline insulator. 2015. PHYSICAL REVIEW B. 92 (7).

11. Neupane, , Xu, Alidoust, Sankar, Belopolski, D. S. Sanchez, Bian, Liu, Chang, Jeng, Wang, Chang, Lin, Bansil, Chou, and M. Z. Hasan. Surface versus bulk Dirac state tuning in a three-dimensional topological Dirac semimetal. 2015. PHYSICAL REVIEW B. 91 (24).

12. Xu, , Belopolski, Alidoust, Neupane, Bian, Zhang, Sankar, Chang, Yuan, Lee, Huang, H. a. o. Zheng, J. i. e. Ma, D. S. Sanchez, Wang, Bansil, Chou, P. P. Shibayev, Lin, Jia, and M. Z. Hasan. Discovery of a Weyl fermion semimetal and topological Fermi arcs. 2015. SCIENCE. 349 (6248): 613.

13. Huang, , Xu, Belopolski, Lee, Chang, Wang, Alidoust, Bian, Neupane, Zhang, Jia, Bansil, Lin, and M. Z. Hasan. A Weyl Fermion semimetal with surface Fermi arcs in the transition metal monopnictide TaAs class. 2015. NATURE COMMUNICATIONS. 6.

Publications

Belopolski, , Xu, D. S. Sanchez, Chang, Guo, Neupane, H. a. o. Zheng, Lee, Huang, Bian, Alidoust, Chang, Wang, Zhang, Bansil, Jeng, Lin, Jia, and M. Z. Hasan. Criteria for Directly Detecting Topological Fermi Arcs in Weyl Semimetals. 2016. PHYSICAL REVIEW LETTERS. 116 (6).

Chang, , Das, Chen, Neupane, Xu, M. Z. Hasan, Lin, Jeng, and Bansil. Two distinct topological phases in the mixed-valence compound YbB6 and its differences from SmB6. 2015. PHYSICAL REVIEW B. 91 (15).

Ghimire, N. J., Luo, Neupane, D. J. Williams, E. D. Bauer, and Ronning. Magnetotransport of single crystalline NbAs. 2015. JOURNAL OF PHYSICS-CONDENSED MATTER. 27 (15).

Huang, , Xu, Belopolski, Lee, Chang, Wang, Alidoust, Bian, Neupane, Zhang, Jia, Bansil, Lin, and M. Z. Hasan. A Weyl Fermion semimetal with surface Fermi arcs in the transition metal monopnictide TaAs class. 2015. NATURE COMMUNICATIONS. 6.

Lee, , Xu, Huang, D. S. Sanchez, Belopolski, Chang, Bian, Alidoust, H. a. o. Zheng, Neupane, Wang, Bansil, M. Z. Hasan, and Lin. Fermi surface interconnectivity and topology in Weyl fermion semimetals TaAs, TaP, NbAs, and NbP. 2015. PHYSICAL REVIEW B. 92 (23).

Neupane, , Belopolski, M. M. Hosen, D. S. Sanchez, Sankar, Szlawska, Xu, Dimitri, Dhakal, Maldonado, P. M. Oppeneer, Kaczorowski, Chou, M. Z. Hasan, and Durakiewicz. Observation of topological nodal fermion semimetal phase in ZrSiS. 2016. PHYSICAL REVIEW B. 93 (20).

Neupane, , Xu, Alidoust, Bian, D. J. Kim, Liu, Belopolski, T. -. Chang, H. -. Jeng, Durakiewicz, Lin, Bansil, Fisk, and M. Z. Hasan. Non-Kondo-like Electronic Structure in the Correlated Rare-Earth Hexaboride YbB6. 2015. PHYSICAL REVIEW LETTERS. 114 (1).

Neupane, , Xu, Alidoust, Sankar, Belopolski, D. S. Sanchez, Bian, Liu, Chang, Jeng, Wang, Chang, Lin, Bansil, Chou, and M. Z. Hasan. Surface versus bulk Dirac state tuning in a three-dimensional topological Dirac semimetal. 2015. PHYSICAL REVIEW B. 91 (24).

Neupane, , Xu, Alidoust, Sankar, Belopolski, D. S. Sanchez, Bian, Liu, Chang, Jeng, Wang, Chang, Lin, Bansil, Chou, and M. Z. Hasan. Surface versus bulk Dirac state tuning in a three-dimensional topological Dirac semimetal. 2015. PHYSICAL REVIEW B. 91 (24).

Neupane, , Xu, Ishida, Jia, B. M. Fregoso, Liu, Belopolski, Bian, Alidoust, Durakiewicz, Galitski, Shin, R. J. Cava, and M. Z. Hasan. Gigantic Surface Lifetime of an Intrinsic Topological Insulator. 2015. PHYSICAL REVIEW LETTERS. 115 (11).

Neupane, , Xu, Sankar, Gibson, Y. J. Wang, Belopolski, Alidoust, Bian, P. P. Shibayev, D. S. Sanchez, Ohtsubo, Taleb-Ibrahimi, Basak, W. -. Tsai, Lin, Durakiewicz, R. J. Cava, Bansil, F. C. Chou, and M. Z. Hasan. Topological phase diagram and saddle point singularity in a tunable topological crystalline insulator. 2015. PHYSICAL REVIEW B. 92 (7).

Wakeham, , E. D. Bauer, Neupane, and Ronning. Large magnetoresistance in the antiferromagnetic semimetal NdSb. 2016. PHYSICAL REVIEW B. 93 (20).

Xu, , Belopolski, Alidoust, Neupane, Bian, Zhang, Sankar, Chang, Yuan, Lee, Huang, H. a. o. Zheng, J. i. e. Ma, D. S. Sanchez, Wang, Bansil, Chou, P. P. Shibayev, Lin, Jia, and M. Z. Hasan. Discovery of a Weyl fermion semimetal and topological Fermi arcs. 2015. SCIENCE. 349 (6248): 613.

Xu, , Liu, S. K. Kushwaha, Sankar, J. W. Krizan, Belopolski, Neupane, Bian, Alidoust, Chang, Jeng, Huang, Tsai, Lin, P. P. Shibayev, Chou, R. J. Cava, and M. Z. Hasan. Observation of Fermi arc surface states in a topological metal. 2015. SCIENCE. 347 (6219): 294.

Xu, , Neupane, Belopolski, Liu, Alidoust, Bian, Jia, Landolt, Slomski, J. H. Dil, P. P. Shibayev, Basak, Chang, Jeng, R. J. Cava, Lin, Bansil, and M. Z. Hasan. Unconventional transformation of spin Dirac phase across a topological quantum phase transition. 2015. NATURE COMMUNICATIONS. 6.

Xu, S. Y., I. Belopolski, N. Alidoust, M. Neupane, G. Bian, C. Zhang, R. Sankar, G. Chang, Z. Yuan, C. C. Lee, S. M. Huang, H. Zheng, J. Ma, D. S. Sanchez, B. K. Wang, A. Bansil, F. Chou, P. P. Shibaye, H. Lin, S. Jia, and M. Z. Hasan. Discovery of a Weyl Fermion semimetal and topological Fermi arcs. 2015. Science. : 1.

Zhang, , Xu, Belopolski, Yuan, Lin, Tong, Bian, Alidoust, Lee, Huang, Chang, Chang, Hsu, Jeng, Neupane, D. S. Sanchez, H. a. o. Zheng, Wang, Lin, C. h. i. Zhang, Lu, Shen, Neupert, M. Z. Hasan, and Jia. Signatures of the Adler-Bell-Jackiw chiral anomaly in a Weyl fermion semimetal. 2016. NATURE COMMUNICATIONS. 7.

Rational Design of Multiferroics and Influence of Cationic Disorder on Multiferroicity in Perovskites

Blas P. Uberuaga
20140679PRD3

Abstract

New materials with pre-specified functionalities are desired for energy harvesting, storage and many other technologically relevant applications. Looking at the breakthroughs made in the recent past, it has become clear that computational and data-enabled strategies for rational materials design and discovery are much more effective in designing new materials as opposed to the traditional chemical intuition based trial-and-error Edisonian approaches. The work undertaken in this project has made important first steps in this direction. While the primary focus of the project was perovskite and related materials, we also explored well-studied materials classes, such as AB-type octet binary crystalline solids, as a means to develop and test our machine models. We not only addressed the effect of cation order (or disorder) on properties such as ferroelectricity, stability, and ionic conductivity of perovskites, but also developed and demonstrated new strategies using machine learning to explore vast chemical spaces and automated extraction of empirical rules from data (i.e., knowledge discovery from data). We also explored multi-objective-optimization techniques and multi-fidelity machine learning approaches as applied to materials problems — the areas that are currently in a state of infancy but bear an enormous potential for rational materials design.

Background and Research Objectives

The aim of the proposed theoretical research was (1) to develop an improved understanding of fundamental rules that govern the effect of cation order (or dis-order) on ferroelectric and ferromagnetic perovskite materials and (2) to develop and demonstrate state-of-the art machine learning and materials informatics based screening strategies to not only efficiently guide a targeted search of functional materials but also discover design-rules and insights from curated databases in an automated manner.

Scientific Approach and Accomplishments

During the course of the project, we have worked on the both fronts of the aforementioned objectives. For instance, in a recent paper [J. Appl. Phys. 117 (11), 114103 (2015)], we showed how one can combine two perovskite materials (with chemical formula ABX3, where A and B are cations and X is an anion, in this case Cl) to form a double perovskite that emphasized the strengths of each and minimized the weaknesses. In particular, we showed how combining CsCaCl3 and RbZnCl3 lead to a stable cubic double perovskite that had a strong ferroelectric response to strain. By themselves, CsCaCl3 is a very stable cubic perovskite that shows little sensitivity to strain while RbZnCl3 is unstable and easily distorts. By combining the two, we showed how a perovskite that is stable in the cubic structure but undergoes ferroelectric distortions under small strains leads to a new material with potentially improved functionality.

In another paper [Chem. Mater. 27, 5020 (2015)], we used accelerated molecular dynamics methods to examine the kinetic pathways for oxygen vacancies in double perovskites as a function of the cation ordering. Because of the structure of these materials, there are 9 high symmetry orderings of the A and B cations. We examined how oxygen vacancies, the important carrier of ionic conductivity in these materials, move through the material for the different cation orderings. We find that both the absolute mobility as well as the nature (one-dimensional or three-dimensional) depends significantly on the cation ordering. In particular, there are orderings in which the mobility is higher than in either of the component single perovskites (in this case, SrTiO3 and LaAlO3).

On the informatics side, we have built machine learning models to examine various aspects of material discovery, design and automated knowledge discovery (i.e., empirical rule mining). In particular, we have examined important properties of perovskite materials as these hold particular promise for a number of applications

involving ferroelectric, magnetic, catalytic properties and fast ion conduction. For examples, in two separate papers [Acta Cryst. B 71, 507 (2015), Sci. Rep. 6, 19375 (2016)], we have developed and demonstrated predicted power of machine learning approaches in predicting formabilities and bandgaps of perovskite materials, respectively. We have also developed new methods that allow us (1) to efficiently predict computationally expansive to compute properties of a given class of materials and (2) to search vast combinatorial chemical spaces for optimal materials with two or more desired properties (which often show inverse relationships) [cf., Comp. Mat. Sci. 125, 92 (2016), G. Pilania, et al., Multi-Fidelity Machine Learning Models for Accurate Bandgap Predictions of Solids, in preparation, to be submitted to Phys. Rev. B].

During the course of the project, in addition to the perovskites, we have also applied the developed machine learning approaches to other classes of materials such as polymers [Sci. Rep. 6, 20952 (2016)], AB-crystalline solids [Chem. Mater. 28, 1304 (2016)], and pyrochlores [G. Pilania, et al., Factors dictating the amorphization propensity of irradiated pyrochlores, under review, Nat. Comm.] to address challenges related to energy storage, high breakdown field strength and radiation damage.

Impact on National Missions

The research carried out and published during the course of this project is of direct relevance to the LANL's mission and specifically relates to the lab's science pillar of Materials for the Future. Ability to rationally design materials with targeted functionalities is highly desirable to enable novel and revolutionary future energy (both harvesting and storage), sensing, and information technologies, just to name but a few. The materials informatics based paradigm pursued here has the potential to mitigate the costs, risks and time involved in an Edisonian approach to the preparation and testing of potentially useful functional materials, and yields insights into the fundamental factors underlying materials behavior. Furthermore, an atomic-level understanding of the influence of crystalline (dis)order on stability and functionalities of perovskites would be important for designing new multi-functional complex oxide chemistries. As machine learning approaches mature, they will become a critical component of the materials science toolbox. This work has helped lay the foundation for that transition.

Publications

Kim, C., G. Pilania, and R. Ramprasad. Machine Learning Assisted Predictions of Intrinsic Dielectric Breakdown Strength of ABX3 Perovskites. 2016. Journal of Physical Chemistry C. 120: 14575.

Kim, C., G. Pilania, and R. Ramprasad. From Organized High-throughput Data to Phenomenological Theory using Machine Learning: The Example of Dielectric Breakdown. 2016. Chemistry of Materials. 28: 1304.

Lookman, T., P. V. Balachandran, D. Xue, G. Pilania, T. Shearman, J. Theiler, J. E. Gubernatis, J. Hogden, K. Barros, E. BenNaim, and F. J. Alexander. A perspective on materials informatics: state-of-the-art and challenges. 2016. In Information Science for Materials Discovery and Design. , p. 3. Switzerland: Springer International.

Mannodi-Kanakkithodi, A., G. Pilania, J. E. Gubernatis, T. Lookman, and R. Ramprasad. A Multi-objective Optimization Technique to Design the Pareto Front of Organic Dielectric Polymers. Computational Materials Science. 125.

Mannodi-Kanakkithodi, A., G. Pilania, T. D. Huan, T. Lookman, and R. Ramprasad. Informatics-Driven Strategy for the Accelerated Design of Polymer Dielectrics. 2016. Scientific Reports. 6: 20952.

Mannodi-Kanakkithodi, A., G. Pilania, and R. Ramprasad. Critical assessment of regression-based machine learning methods for polymer dialectrics. 2016. Computational Materials Science. 125: 123.

Pilania, , J. E. Gubernatis, and Lookman. Structure classification and melting temperature prediction in octet AB solids via machine learning. 2015. PHYSICAL REVIEW B. 91 (21).

Pilania, , and B. P. Uberuaga. Cation ordering and effect of biaxial strain in double perovskite CsRbCaZnCl6. 2015. JOURNAL OF APPLIED PHYSICS. 117 (11).

Pilania, , and Lookman. Electronic structure and biaxial strain in RbHgF3 perovskite and hybrid improper ferroelectricity in (Na,Rb)Hg2F6 and (K,Rb)Hg2F6 superlattices. 2014. PHYSICAL REVIEW B. 90 (11).

Pilania, G., A. Mannodi-Kanakkithodi, B. P. Uberuaga, R. Ramprasad, T. Lookman, and J. E. Gubernatis. Machine learning bandgaps of double perovskites. 2016. Scientific Reports. 6: 19375.

Pilania, G., J. E. Gubernatis, and T. Lookman. Multi-Fidelity Machine Learning Models for Accurate Bandgap Predictions of Solids. Physical Review B.

Pilania, G., J. E. Gubernatis, and T. Lookman. Classification of Octet AB-type binary compounds using Dynamical Charges: A Materials Informatics Perspective. 2015. Scientific Reports. 5: 17504.

Pilania, G., K. R. Whittle, C. Jiang, R. W. Grimes, C. R. Stanek, K. E. Sickafus, and B. P. Uberuaga. Using machine learning to identify factors that govern amorphization of irradiated pyrochlores. To appear in Nature Communications.

Pilania, G., P. V. Balachandran, C. Kim, and T. Lookman. Finding New Perovskite Halides via Machine Learning. 2016. Frontiers in Materials. 3: 19.

Pilania, G., P. V. Balachandran, J. E. Gubernatis, and T. Lookman. Predicting the formability of ABO3 perovskite solids: An initial machine learning study. 2015. Acta Crystallographica Section B. 71: 507.

Uberuaga, B. P., and Pilania. Effect of Cation Ordering on Oxygen Vacancy Diffusion Pathways in Double Perovskites. 2015. CHEMISTRY OF MATERIALS. 27 (14): 5020.

Studies on Functional Materials: Design and Optimization

Turab Lookman
20140682PRD4

Abstract

The goal of this project was to perform studies on ferroelectrics, such as piezoelectrics, and alloys to find new compounds with enhanced properties, thereby showing how accelerated materials discovery could be undertaken. The key results of this work are as follows: (1) discovery of new Lead free Ba-based compounds with the desired property of a temperature insensitive morphotropic phase boundary, and (2) new NiTi-based shape memory alloys with the smallest thermal hysteresis

Background and Research Objectives

Initiatives by DOE, NSF and the White House related to Materials Genome has catalyzed considerable activity in approaches to find new materials. Our objective was to exercise a closed loop with experiments and informatics to demonstrate a path towards realizing a goal of this initiative. We adopted a data-driven approach to narrow the vast space for improved prediction. Our key innovation was an integrated design to find materials with target properties. Our materials belonged to the ferroic class of functional materials that are of interest to industry.

Scientific Approach and Accomplishments

Our approach was to conduct experiments, in particular synthesis and characterization, guided by the accelerated design computational framework developed in an LDRD-DR effort. The work has resulted in several key papers, including 1 Nature Communication [1], 1 Nature Scientific Reports [2], 1 Physical review B [3], 1 Current Opinion in Solid State and Materials Science [in press], 1 PNAS in final review, and several other papers [4-7].

The work yielded a new NiTi-based multicomponent alloy with a very small thermal hysteresis. We iterated the loop 9 times and in each iteration we predicted and synthesized 4 compounds. Of the 36 compounds so fabricated, the best alloy had a thermal hysteresis of 1.85K, a 42% improvement over the best in our training data. In all, 14 new compounds had a thermal hysteresis better than the best in the training data [1]. This points to the efficiency of the loop and with a Fisher p index < .001, suggests that the probability of making this discovery by chance is very low. Although we didn't design for it, our new compound had a Martensitic transition temperature in a very desirable range just above room temperature. Our density functional theory calculations provided insights as to why this composition has the desired low thermal hysteresis. It is because the Fe composition is tuned to an optimal value based on energetics and stability [1].

Our second key discovery is a new Pb-free piezoelectric with a more vertical morphotropic phase boundary (MPB) (temperature insensitivity) than any BaTiO3 based piezoelectric known. A wide range of experiments were initiated and conducted for this project. Our design criterion for this work was a piezoelectric with a more vertical MPB as the piezoelectric response is associated with how vertical the MPB is and controls how insensitive the response is to temperature. For example, Lead Zirconate is a prototypical example with an almost vertical MPB. We used Landau theory and a Bayesian analysis. The work predicted the new piezoelectric (Ba0.5Ca0.5) TiO3-Ba(Ti0.7Zr0.3)O3. The compound provided a 15% improvement in the piezoelectric.

The project also generated a number of unique and extensive databases on materials classes. Some of these databases have a million compounds of predicted properties. They were assembled from extensive literature searches of experimental data.

Other work on this project related to algorithms for design with inference [2]. We showed how uncertainties are fundamental to balancing the trade-off between exploration and exploitation to rank which materials should be explored next. We demonstrated our methodology on a data set from the literature on MAX com-

pounds with the objective of finding the best material in as few iterations as possible.

Impact on National Missions

Accelerated materials discovery is of significant importance to DOE/SC/NSF and universities. The development of information science predictive tools to enable accelerated materials discovery is key to this task. As LANL is a materials-centric laboratory, the tools we have developed are of direct mission relevance. The specific classes of materials we have focused on (such as shape memory alloys, piezoelectrics and polymer dielectrics) are of direct interest to DOE/SC as they find applications as sensors and energy harvesting and storage devices.

References

1. Xue, , P. V. Balachandran, Hogden, Theiler, Xue, and Lookman. Accelerated search for materials with targeted properties by adaptive design. 2016. NATURE COMMUNICATIONS. 7.

2. Balachandran, P. V., Xue, Theiler, Hogden, and Lookman. Adaptive Strategies for Materials Design using Uncertainties. 2016. SCIENTIFIC REPORTS. 6.

3. Balachandran, P. V., Xue, and Lookman. Structure-Curie temperature relationships in BaTiO3-based ferroelectric perovskites: Anomalous behavior of (Ba,Cd)TiO3 from DFT, statistical inference, and experiments. 2016. PHYSICAL REVIEW B. 93 (14).

4. Xue, , Yuan, Zhou, Xue, Lookman, Zhang, Ding, and J. u. n. Sun. Design of High Temperature Ti-Pd-Cr Shape Memory Alloys with Small Thermal Hysteresis. 2016. SCIENTIFIC REPORTS. 6.

5. Zhang, , Xue, Wu, Ding, Lookman, and Ren. Adaptive ferroelectric state at morphotropic phase boundary: Coexisting tetragonal and rhombohedral phases. 2014. ACTA MATERIALIA. 71: 176.

6. Xue, , Zhou, Ding, Otsuka, Lookman, J. u. n. Sun, and Ren. Ambient-temperature high damping capacity in TiPd-based martensitic alloys. 2015. MATERIALS SCIENCE AND ENGINEERING A-STRUCTURAL MATERIALS PROPERTIES MICROSTRUCTURE AND PROCESSING. 632: 110.

7. Xue, , Gao, Zhou, Ding, J. u. n. Sun, Lookman, and Ren. Phase transitions and phase diagram of Ba(Zr0.2Ti0.8) O-3-x(Ba0.7Ca0.3)TiO3 Pb-free system by anelastic measurement. 2015. JOURNAL OF APPLIED PHYSICS. 117 (12).

Publications

Balachandran, P. V., Xue, Theiler, Hogden, and Lookman. Adaptive Strategies for Materials Design using Uncertainties. 2016. SCIENTIFIC REPORTS. 6.

Balachandran, P. V., Xue, and Lookman. Structure-Curie temperature relationships in BaTiO3-based ferroelectric perovskites: Anomalous behavior of (Ba,Cd)TiO3 from DFT, statistical inference, and experiments. 2016. PHYSICAL REVIEW B. 93 (14).

Xue, , Gao, Zhou, Ding, J. u. n. Sun, Lookman, and Ren. Phase transitions and phase diagram of Ba(Zr0.2Ti0.8) O-3-x(Ba0.7Ca0.3)TiO3 Pb-free system by anelastic measurement. 2015. JOURNAL OF APPLIED PHYSICS. 117 (12).

Xue, , P. V. Balachandran, Hogden, Theiler, Xue, and Lookman. Accelerated search for materials with targeted properties by adaptive design. 2016. NATURE COMMUNICATIONS. 7.

Xue, , Yuan, Zhou, Xue, Lookman, Zhang, Ding, and J. u. n. Sun. Design of High Temperature Ti-Pd-Cr Shape Memory Alloys with Small Thermal Hysteresis. 2016. SCIENTIFIC REPORTS. 6.

Xue, , Zhou, Ding, Otsuka, Lookman, J. u. n. Sun, and Ren. Ambient-temperature high damping capacity in TiPd-based martensitic alloys. 2015. MATERIALS SCIENCE AND ENGINEERING A-STRUCTURAL MATERIALS PROPERTIES MICROSTRUCTURE AND PROCESSING. 632: 110.

Zhang, , Xue, Wu, Ding, Lookman, and Ren. Adaptive ferroelectric state at morphotropic phase boundary: Coexisting tetragonal and rhombohedral phases. 2014. ACTA MATERIALIA. 71: 176.

Probing and Controlling the Surface States of Topological Insulators

Scott A. Crooker
20140683PRD4

Abstract

Topological Insulators (TIs) are a recently discovered class of materials that have garnered significant attention in the last 5 years within the condensed matter physics community. They are bulk semiconductors such as Bi2Se3 and Bi2Te3 in which spin-orbit coupling gives rise to a topologically protected two-dimensional (2D) metallic surface, with a surface electronic structure similar to the Dirac cone spectrum of graphene. The surface states are protected from backscattering by time reversal symmetry, and therefore TIs have potential applications for spin logic devices and low-power electronics. Although there is tremendous excitement and interest in these novel materials within the physics and materials science community, the exploration of exotic spintronic properties in TIs such as spin photocurrent and current-induced spin-density properties are still at an early stage. The ability to control the topological surface states electrically or optically is the crucial key to the development of spin-based devices.

Background and Research Objectives

The main goal of Luyi Yang's project was to probe, and ultimately manipulate, the spin degrees of freedom in novel topological and 2D materials. A major part of this research combined the unique optical and pulsed magnetic transport techniques at the National High Magnetic Field Laboratory at LANL to characterize spin structure and transport. In TIs it is possible to photoexcite currents whose charge, spin, and direction can be controlled by varying the helicity of the light. The subsequent spin currents and spin dynamics can be monitored and imaged via the magneto-optical Kerr effect. The unique nature of spin-momentum locking in these materials suggests that the spin current in a TI can be generated with the same efficiency as charge photocurrent in a conventional insulator.

Scientific Approach and Accomplishments

Yang's project and her tenure at LANL was extremely successful, with high-profile papers published in prominent journals including Nature Physics, Physical Review Letters, Nature Communications, and Nano Letters. She also gave invited talks at the APS March Meeting and also overseas in Japan, thereby raising LANL's profile in this burgeoning field. As described above in the Objectives, Yang used the ultrafast laser capabilities at the NHMFL-Los Alamos to perform time-resolved studies of spin dynamics in novel materials systems.

In her first paper (published in Nature Physics; see references listed at the end of this report), Yang studied a new family of two-dimensional semiconductors known as the "transition-metal dichalcogenides", which are composed of a single atomically-thin sheet of material. These materials have attracted significant amount of attention in the last two years owing to their promise for a new generation of low-power, high-efficiency semiconductor electronics. Yang's paper describes the first-ever measurements of how magnetization develops and relaxes in these new materials.

In a second breakthrough paper (published in Nano Letters), Yang discovered that electrons in these 2D semiconductors actually exhibit the very interesting property of "coherence", which may make them attractive for future device applications wherein information is encoded in an electron's 'spin' degrees of freedom.

Yang also played an important role in two other high profile papers published in Physical Review Letters and in Nature Communications.

Equally importantly, Yang has landed an excellent job at the end of her Director's-funded postdoc: a professorship position at the University of Toronto, which started in September 2016.

Impact on National Missions

This project established Laboratory capabilities in the areas of Materials Science, Emergent Phenomena, and Materials-by-Design, and also in novel measurement methods that enable new scientific discovery at LANL (namely, Yang developed capabilities for ultrafast measurements of magnetization dynamics using the Magneto-Optical Kerr Effect). It is based on the very recent discovery of a new class of so-called "topologically protected" materials, in which scattering and dissipative processes are prohibited from fundamental physics considerations. The experimental techniques that she developed as part of this project advanced new Laboratory capabilities that underpin a wide variety of Laboratory missions related to Materials Science and Controlled Functionality in Materials. Beyond direct scientific impact, her studies have the potential to pave the pathways for new "topologically protected electronics"; that is, transport of charge and spin in new generations of lower-power, potentially more compact, and more efficient electronic devices, which has direct impacts on securing our energy future. In the longer term (10+ years) it is possible that next-generation electronic and 'spintronic' devices based on these materials could find their way to 1) advanced sensors and 2) quantum information processing applications, both of which would be relevant for Global Security interests. Her work has helped to establish the fundamental properties and underlying physics of this new generation of materials.

Publications

Glasenapp, , N. A. Sinitsyn, Yang, D. G. Rickel, Roy, Greilich, Bayer, and S. A. Crooker. Spin Noise Spectroscopy Beyond Thermal Equilibrium and Linear Response. 2014. PHYSICAL REVIEW LETTERS. 113 (15): 156601.

Roy, D., L. Yang, N. A. Sinitsyn, and S. A. Crooker. Cross-correlation spin noise spectroscopy of heterogeneous interacting spin systems. 2015. Scientific Reports. 5: 9573.

Yang, , Chen, K. M. McCreary, B. T. Jonker, J. u. n. Lou, and S. A. Crooker. Spin Coherence and Dephasing of Localized Electrons in Monolayer MoS2. 2015. NANO LETTERS. 15 (12): 8250.

Yang, , Glasenapp, Greilich, Reuter, A. D. Wieck, D. R. Yakovlev, Bayer, and S. A. Crooker. Two-colour spin noise spectroscopy and fluctuation correlations reveal homogeneous linewidths within quantum-dot ensembles. 2014. NATURE COMMUNICATIONS. 5: 4949.

Yang, L., N. A. Sinitsyn, J. Yuan, J. Zhang, J. Lou, and S. A. Crooker. Long-lived nanosecond spin relaxation and spin coherence of electrons in monolayer MoS2 and WS2. 2015. Nature Physics. 11: 830.

Three-Dimensional Nitrogen-Doped Porous Nanographene for High-Performance Supercapacitor

Hsing-Lin Wang
20140684PRD4

Abstract

Graphene, a one-atom-thick a two-dimensional (2D) single layer of sp2-bonded carbon, has been considered as the basic building block of carbon materials of various dimensionalities. Because of its superior electrical conductivity, exceptional large specific surface area, and excellent structural stability, graphene has attracted tremendous attention in recent years as an ideal electrode material in energy storage devices such as (lithium ion battery and supercapacitor). However, graphene sheets often aggregate and restack during the graphene sheets synthesis, which not only decreases the graphene surface area but also deters the electrolyte from accessing to graphene sheets surface.

The most critical challenges are to find ways to prevent the graphene flakes from collapsing, retain maximum surface area available for the access of electrolyte ions and keep the natural electron mobility of graphene, achieving the exact control over design and synthesis of graphene materials with unique structures that is crucial in developing their use in supercapacitor energy storage devices

In this project, we used three dimensional nanographenes synthesized in our laboratory and crosslinked these small nanographene moieties to form mesoporous nanographene which will have a well-defined molecular structure, high surface area and most importantly structural homogeneity. The novel structural design is expected to achieve stability of very long operation time and exceeding hundreds of charging/recharging cycles. Most of all, mesoporous nanographene is expected to have very high surface area which could lead to high charge capacitance, exceeding 1200 mAh/g. In addition, we developed ways to dope these porous graphenes to render high conductivity to further improve their performances.

Background and Research Objectives

Our approach was to use three dimensional nanographenes (NG) synthesized in our laboratory and crosslinking these small nanographene moieties to form mesoporous nanographene which will have a well-defined molecular structure, high surface area and most importantly structural homogeneity. The design of this novel mesoproous nanographene was expected to exhibit very high capacitance and operational stability over a very long period of time. Our system is the first ever demonstrated to use mesoporous nanographene in energy storage devices. In addition, we worked to develop ways to dope these porous nanographenes to render high conductivity to further improve their performances. This project advanced understanding and future development of next generation energy storage devices.

Scientific Approach and Accomplishments

Nanographene Synthesis and Application in Energy Storage

We synthesized of a series of novel nitrogen-doped nanographenes with 3D porous structures by crosslinking the molecular building block (3Dnitrogen-doped-nanographene, Figure 1). During the synthesis, a wide range of linkers were chosen for the crosslinking reactions, which allowed us to fine-tune the surface area, pore size, and structural stability of 3D porous nanographenes. The potential applications for these 3D nitrogen-doped porous nanographenes as electrode materials in supercapacitors and lithium-ion batteries will be demonstrated. The synthesis-structure-property correlation will by systematically elucidated to obtain feedback, allowing us to further optimize their structure and device performance.

Physical characterization: Extensive physical characterization (high-resolution transmission electron microscope, scanning electron microscope, X-ray diffraction, X-ray photoelectron spectroscopy, Raman spectroscopy, Fourier transform infrared spectroscopy, Brunauer-

Emmett-Teller surface area analysis, etc,) were employed to determine the morphology, phase composition, hetero-atom doping, surface area and porosity of the as-prepared porous nanographene materials.

Electrochemistry and device tests: Electrodes prepared from the 3D porous nitrogen-doped nanographene were studied in supercapacitors and lithium-ion batteries. We studied the charge transfer limitations (electronic and ionic) in various porous nanographene structures using experimental techniques such as chemical delithiation, galvanostatic charge and discharge, galvanostatic and potentiostatic intermittent titration techniques (GITT and PITT), cyclic voltammetry, and impedance measurements, to gain insight into the structure-property-synthesis correlations.

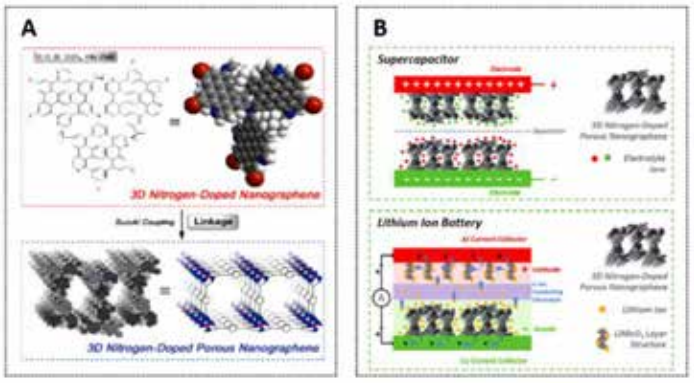

Figure 1. (A) Synthetic route and conceptual illustration of 3D nitrogen-doped porous nanographene. N atoms are shown in blue color. Additional functional groups (red)allowing crosslinking to form 3D porous structures.(B) Schematic illustration of a 3D nitrogen-doped porous nanographene based supercapacitor and lithium-ion battery.

Accomplishments

We developed a novel approach to synthesize a series of three-dimensional (3D) nanographenes (NGs) with well-defined molecular structures; in our synthesis, a variety of functional groups have been covalently attached to the NG flakes that enable fine-tuning of electron density on flakes and d-spacing between flakes. The multistep organic synthesis of 3D NG is designed to overcome the restacking observed in traditional rGO sheets and achieve graphene's intrinsically high Li storage capacity and diffusivity while simultaneously addressing the long-term stability issues.

We have carried out comprehensive structural characterization of the intermediate and NGs using MALDI-TOF, 1H NMR, and 13C NMR spectra. All the spectroscopic results are in perfect agreement with the proposed molecular structures, confirming the successful preparation of NGs. The thermal stability of NGs was examined by TGA . These NGs with various functional groups exhibit excellent thermal stability without significant mass loss up to 300oC under N2 atmosphere. The graphitized residue (char yield) of these NGs was more than 60% at 1000oC, which is attributed to their high aromatic (graphene-like) content.

Our 3D NGs reveal great promises for the fabrication of energy conversion and storage devices. We use NG as an anode for the Li ion battery, which was prepared for the first time to exhibit fantastic specific capacitance (> 900 mAh/g) - one of the highest ever reported for carbon based Lithium ion battery, and stability through hundreds of charging discharging cycles. Such performances are ranked the very top among all graphene based materials.

Results from this project were published in Chemical Society Review and ChemCatChem.

Impact on National Missions

This project's results furthered our fundamental understanding of the electrochemistry of 3D porous nanographene. Ultimately, the research will have wide-spread impact on the development of high performance energy storage technologies. This research strengthens our capability in addressing key Los Alamos missions of materials functionality and energy security.

Publications

Zhou, M., H. L. Wang, and S. Guo. High-efficiency nanoelectrocatalysts. 2016. Chemical Society Review. 45: 1273.

Zhou, M., and S. Guo. Electrocatalytic Interface Based on Novel Carbon Nanomaterials for Advanced Electrochemical Sensors. 2015. Chem Cat Chem. 7 (18): 2744.

Photophysical Properties of Self-Assembled Nanoclusters

Jennifer Martinez
20150704PRD1

Abstract

Metal nanoclusters are comprised of stable collections of small numbers of metal atoms (e.g. gold or silver, 2-144 atoms, ≤ 1.8 nm) that can have intriguing catalytic, magnetic or photophysical properties. Nanoclusters bridge the gap between atoms and nanoparticles, and in sharp contrast to larger nanoparticles, they exhibit these unique physical and optical properties not seen in bulk materials due to quantum effects. Fluorescent nanoclusters, in particular DNA templated silver (Ag) clusters, have drawn much attention, since they have tunable fluorescence emission, single-timescale photoblinking, high quantum yields, and thus have large potential for applications in bio- imaging and –sensing and for energy harvesting (within assemblies). Nanoclusters are called "superatoms" because they possess superatomic orbitals similar to atomic orbitals, where each atom of the nanocluster accounts for their properties, and where addition of an extra atom to a cluster completely changes its physical and optical properties. For this project we have studied their structure, size dependence, and ligand effects (particularly for DNA-templated clusters); assembly; distance-dependent energy transfer; and how the clusters behave as they are brought closer together (i.e. do their optical responses remain molecular or transition to plasmonic, due to inter-cluster coupling), as just a few examples. Thus, the use of noble-metal nanoclusters within assemblies allows us to investigate fundamental questions regarding their photophysical phenomena and to also provide important assembled optical responses.

Background and Research Objectives

Toward understanding the origin of the photophysical properties of nanoclusters, we have synthesized different cluster sizes, protected with either DNA or proteins. These clusters are synthesized by reducing the metal salt (gold and silver) in presence of DNA or protein (e.g. elastin). Taking the advantage of DNA hybridization, DNA clusters are designed to produce self-assembled structures, utilizing the length of DNA as a molecular ruler to control the distance between clusters in the assembly. In addition to DNA, protein polymer (elastin) protected nanoclusters are produced to make stimuli responsive assemblies that dynamically modulate cluster distances and photophysical reactivity. These created assemblies are then used to understand distance dependent cluster-cluster interactions (energy transfer) and to address the nature of cluster interactions (plasmonic or nonplasmonic).

Scientific Approach and Accomplishments

Nanoclusters are collections of a few atoms of silver or gold that exhibit size dependent optical properties, such as strong fluorescence. Little is understood about their optical properties (e.g. origins of their photophysical properties) and how to assemble clusters so that they can electronically "talk" to one another. In order to understand these questions we have developed strategies to self-assemble the clusters and study their photophysics (using a genetically engineered polymer and DNA), and to co-assemble the clusters with carbon nanotubes and enzymes to create a biocatalyst for alternative fuels.

To study how clusters talk to each other and how they may transition to have more advanced properties we have created a cluster templated within a genetically engineered polymer. Genetically engineered polymers consist of repeating units of amino acid sequence yielding a polymer with defined stimuli response, biocompatibility and programed assembly (as a function of changes in temperature). For the first time we report the direct synthesis of pure, single sized (144 atom), stimuli responsive, water-soluble and biocompatible elastin like polymer (ELP) templated Au nanoclusters (Figure 1). Optical absorption spectra and electron microscopy indicates that the particles synthesized were nanoclusters and their size was close to the boundary of plasmonic nanoparticles. From dynamic light scattering and electron microscopy we can observe that the clusters assemble with increase in temperature (Figure 2). With

their defined size and optical properties, we are now monitoring how they communicate with each other and have prepared a paper for submission to Nanoscale.

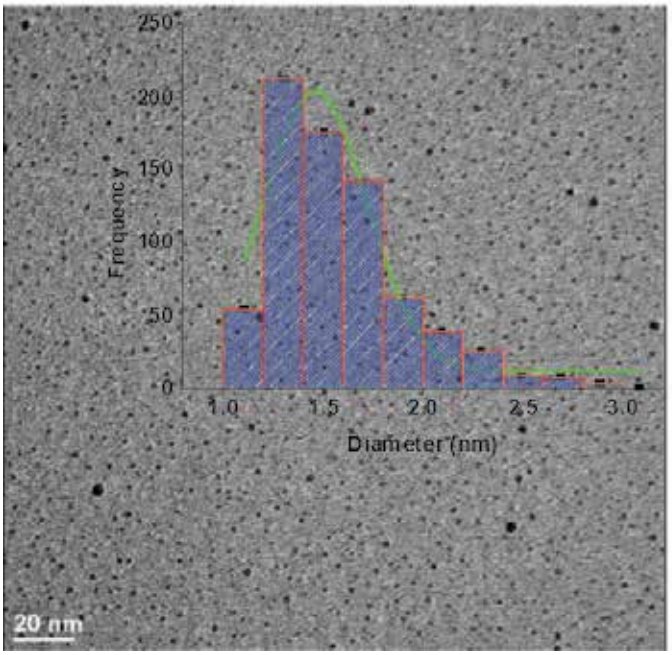

Figure 1. A modified genetically encoded polymer templates a gold nanocluster of 144 atoms, here imaged by TEM. Larger materials are from sintering and growth of smaller particles within the TEM beam.

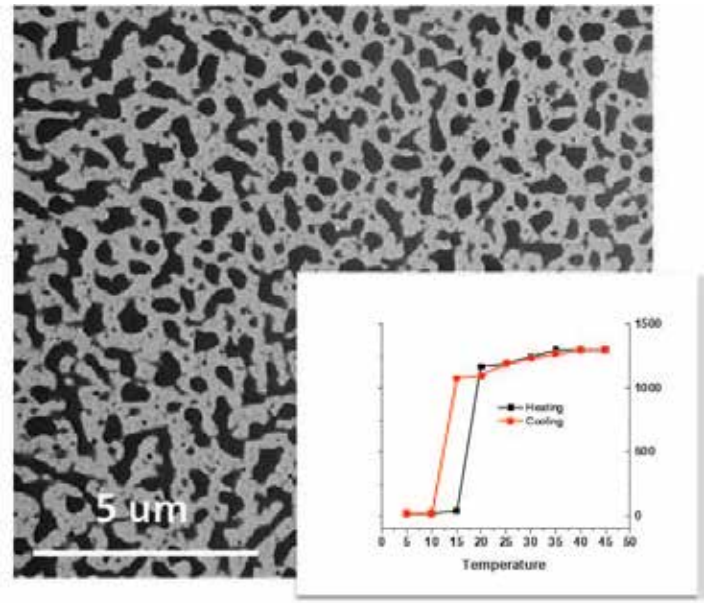

Figure 2. A gold cluster templated within a genetically encoded polymer is stimuli responsive as observed by the change in dynamic light scattering and TEM with temperature (Figure 1).

To more specifically assemble fluorescent clusters and study their photophysics we have used DNA. DNA is much like Velcro in that it can be designed to specifically bind its compliment and can serve as a molecular ruler by precisely spacing two materials away from each other, as to better understand at what distances the materials can communicate. We have created a highly fluorescent silver nanocluster templated within a piece of DNA (so called D3AgNC). To better characterize its properties we have determined that the cluster consists of 21 atoms of silver. From comparison of optical spectra to published silver clusters (without DNA on their surface), we believe that the D3AgNC is so very stable because it has a stable icosahedral core. We observed that as the clusters were concentrated (effectively causing the clusters to touch each other) that we substantially red shifted the resultant fluorescence and absorbance of the material (Figure 3).

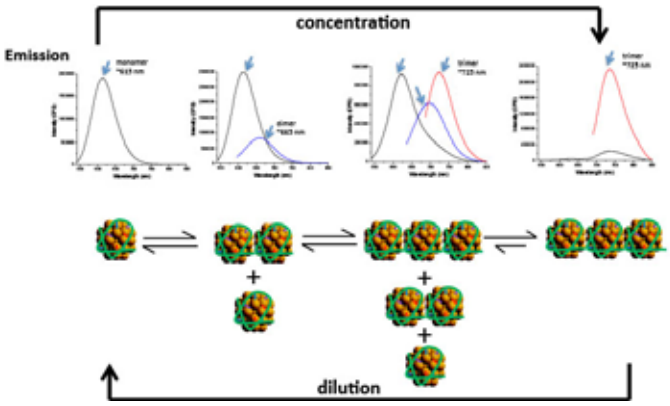

Figure 3. Silver nanocluster, D3, templated within DNA demonstrates emergent phenomena upon concentration. The effect is highly reversible.

This new "emergent" fluorescence was reversible with simple dilution of the clusters to reproduce the monomeric fluorescence. These initial results suggested that the clusters could electronically communicate. To better control this interaction we designed the cluster templating DNA to have a piece of overhanging DNA that could zipper together with its compliment (like Velcro). That complement contained the identical type of fluorescent cluster with a complementary overhanging DNA. We can control the separation of the two clusters with distances of 2, 4, and 6 nm. We find that the clusters communication (as seen by a substantial red shift in the fluorescence of 100 nm) decreases substantially with distance and drops off completely by 6 nm (Figure 4). As a control we have developed TEM methods to verify that the clusters, through their DNA velcro's, are attached at the lengths indicated. Because DNA is too fragile to withstand TEM conditions, we developed a process to embed the velcroed clusters within thin blocks of silica (Figure 5). Working with our theory colleagues we have indication that the clusters are coupling through dipole interactions that are as strong as strongly coupled (and touching) conjugated polymers, even though the clusters are far more separated than are polymers (suggesting that the clusters couple much more strongly

than current materials in the literature).

Beyond organizing cluster-cluster interactions, we have organized clusters to assemble with nanomaterials (carbon nanotubes) and enzymes in the hope of creating an efficient electrode that can be used as a catalyst for alternative fuels. With sources of fossil fuels dwindling, there is an urgent need to find cheap, renewable, and alternate forms of energy using naturally abundant resources such as sunlight, air, and water. Nanostructured materials and enzymatic fuel cells are showing great promise in this respect, if only we can increase their efficiency. We have created a new DNA-templated gold nanocluster (AuNC) of ~1 nm in diameter. When integrated with bilirubin oxidase (BOD) and carbon nanotubes (CNTs), the AuNC acts as an enhancer of electron transfer (ET) and lowers the overpotential of electrocatalytic oxygen reduction reaction (ORR) by ~15 mV as compared to the enzyme alone.

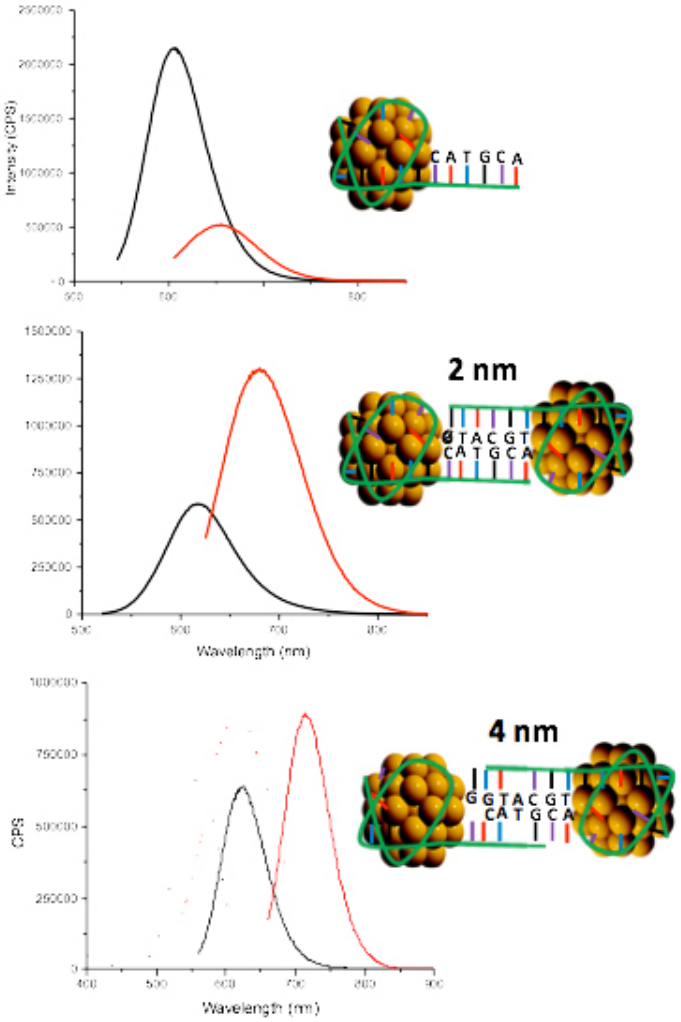

Figure 4. Silver nanocluster D3, velcroed together by DNA, show distance dependent emergent phenomena. The response drops off with addition of distance, as controlled by the DNA strand (e.g. 4 nm).

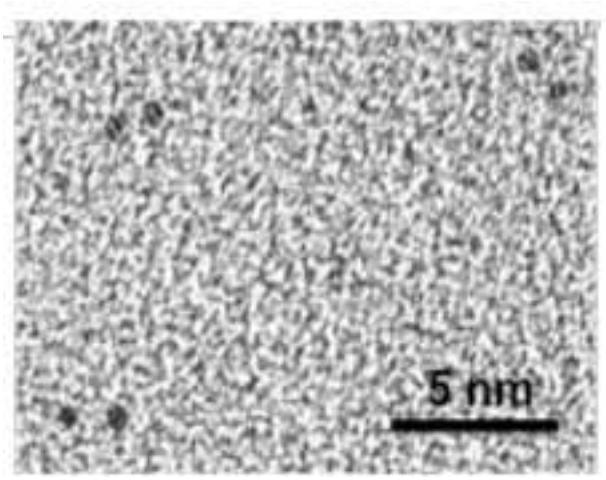

Figure 5. Silver nanoclusters, templated within DNA, are held at distances dictated by the DNA strand, as imaged embedded within silica by TEM.

Impact on National Missions

This project answers long-standing questions within the chemistry, materials and physics communities, by bringing a more thorough structure-function understanding of fluorescent silver and gold nanoclusters. Further, we bring fundamental understanding of how to modulate nanocluster physics so that they can behave as molecules in one instance and particles in another instance. This basic research project has applications to many important needs including biosensors, catalysis, batteries and solar harvesting and thus supports laboratory missions in emerging threats (science of signatures), materials for the future and energy security. The control of light energy and control of structure in self-assembled and biologically assembled material architectures, as discussed here, is important for numerous applications of relevance to the Department of Energy. “From Quanta to the Continuum: Opportunities for Mesoscale Science”, a BESAC report, identified a “grand challenge in materials science is to create multiscale functional structures that encode content; adaptively respond to their environment; and capture-transport, and utilize energy”. Basic Research Needs for Solar Energy Utilization was the focus of a BES workshop. Here, one of five identified cross-cutting issues relevant to priority research directions was “... novel methods for self-assembly of molecular components into functionally integrated systems.” Each of these areas was addressed within this project.

Publications

Chakraborty, S., R. C. Rocha, A. Desireddy, K. Artyushkova, T. C. Sanchez, P. Atanassov, and J. S. Martinez. Gold nanocluster formation using morpholino oligomer as template and assembly agnet within hybrid bio-nanomaterials. 2016. RCS Advances. 6 (93): 90624.

Chakraborty, S., S. Babanova, R. C. Rocha, A. Desireddy, K. Artyushkova, P. Atanassov, and J. S. Martinez. A DNA-Hosted Gold Nanocluster Enhances Enzymatic Reduction of Oxygen by Facilitating Efficient Electron Transfer. 2015. Journal of the American Chemical Society. 137 (36): 11678.

Fazelinia, H., E. R. M. Balog, A. Desireddy, C. E. M. Strauss, and J. S. Martinez. Elastomeric polymer arrays through zipper assembly. Soft Matter.

Karan, N. S., A. M. Keller, Sampat, Roslyak, Arefin, C. J. Hanson, J. L. Casson, Desireddy, Ghosh, Piryatinski, Iyer, H. a. n. Htoon, A. V. Malko, and J. A. Hollingsworth. Plasmonic giant quantum dots: hybrid nanostructures for truly simultaneous optical imaging, photothermal effect and thermometry. 2015. CHEMICAL SCIENCE. 6 (4): 2224.

Nuclear and Particle Futures

Probing New Sources of Time-Reversal Violation with Neutron EDM

Takeyasu Ito
20140015DR

Introduction

An electric dipole moment (EDM) measures the separation of positive and negative charges within a system and is an extremely sensitive probe of physics beyond the standard model, the accepted theory of elementary particles. The neutron EDM (nEDM) is said to have "killed more theories than any other single measurement."

This LDRD project is a joint experimental and theoretical project to probe new sources of time reversal violation (T violation) with the nEDM. Using the LANSCE (Los Alamos Neutron Science Center) Ultracold Neutron (UCN) source, we will develop a new nEDM experiment with a sensitivity goal of 3x10-27 e-cm, a 10-fold improvement over the current limit. More specifically, we will upgrade the existing UCN source which is expected to result in a 10-fold performance increase. In addition, we will build a prototype nEDM experimental apparatus. With the upgraded UCN source and prototype nEDM apparatus, we will demonstrate that it is possible to perform an nEDM experiment with a sensitivity of 3x10-27 e-cm. Note that the UCN density is the key parameter that is necessary for reaching the sensitivity goal.

At the same time, to match the anticipated experimental improvement, we will perform a comprehensive model-independent analysis of T violation beyond the standard model (BSM) and we will pioneer first-principles calculations of the matrix elements, essential in extracting and bounding the underlying BSM sources of T violation from EDM measurements.

The goal of this LDRD project is to reduce the technical risk of a full-fledged nEDM experiment at LANL with sensitivity of 3x10-27 e-cm.

Benefit to National Security Missions

The proposed research is central to both the LANL (Los Alamos National Laboratory) nuclear physics program and the future of the US (United States) program on fundamental symmetries in nuclear science. The proposed upgrade of the UCN (Ultracold Neutron) source is in line with the 2010 LANL NPAC (Nuclear, Particle, Cosmology, and Astrophysics) strategic plan that recommended development of a medium scale facility, and will benefit other experiments such as a neutron lifetime experiment, which received a strong community endorsement in a recent international workshop. Furthermore, completion of the proposed experimental tasks will provide a viable alternate approach to the high-risk SNS (Spallation Neutron Source) nEDM (neutron electric dipole moment) experiment, which has a large P division involvement. This will also lead to project funds coming to LANL if a decision is made to go forward with this new nEDM experiment.

In addition, this project will strengthen an already existing successful synergy of theory and experiment in fundamental neutron physics. This is a unique strength of LANL across US laboratories. This LDRD (Laboratory Directed Research and Development) will establish LANL T-division as one of the main US centers for nucleon matrix elements computations with lattice QCD (Quantum Chromodynamics). This will put a solid basis to seek additional external funding, through the channels of DOE (Department of Energy) Nuclear Theory topical collaboration centers as well as SciDAC grants in both High Energy and Nuclear Physics.

Additionally, the UCN source improvement will benefit fundamental neutron physics experiments, actinide sciences, and detection technology.

Progress

On the experimental side, during the October 2015 - February 2016 beam time, we performed the following three critical measurements successfully:

- UCN storage in a prototype nEDM chamber: we demonstrated that the storable UCN density with

the current UCN source (without the source upgrade) is already at the level that would allow us to perform an nEDM experiment at the several x 10^{-27} e-cm sensitivity level, comparable to the current best experiment.

- UCN storage in all the new UCN guide components: we demonstrated that all the new UCN guide components have the expected performance in terms of UCN storage.
- UCN storage in the new UCN source insert: we demonstrated that the new UCN source has a sufficiently long UCN storage time, although the measurement indicated a somewhat reduced (but still acceptable) Fermi potential.

After the beam time, we continued with the fabrication and assembly of the new UCN source insert. At the same time, we performed more measurements (using neutron and x ray reflectometry and XRF) on the UCN coating of the new UCN source insert, and decided to recoat the surface. We also prepared the area for the installation of the new UCN source, removing the shielding blocks. Furthermore, we prepared the area for the installation of the new cryocooler, which will be used to cool the cold moderator of the new UCN source.

In the remainder of this FY, we plan to complete the new UCN source insert and install it in place.

Within the theory effort, we have performed the Lattice QCD calculation of the nucleon tensor charges, that determine the neutron EDM induced by quark EDMs, with control over all the lattice systematics (lattice spacing, volume, quark mass), reducing the uncertainty to 10\%. With these improved matrix elements we have derived a stringent upper bound of $d_n < 4 \times 10^{-28} \, e$ cm for the neutron EDM in split-supersymmetry.

In parallel to the study of matrix elements, we have carried out a systematic study of the EDM constraints on non-standard CP-violating couplings of the Higgs to quarks, gluons, and electroweak gauge bosons, comparing the sensitivity of EDMs and collider processes.

Our major findings are:

(i) the electron EDM puts a bound on the electroweak dipole of the top quark that is three orders of magnitude stronger than previous existing bounds;

(ii) we have identified target goals for error reduction in the matrix elements, so that the constraining power of neutron and nuclear EDMs is maximized.

Future Work

In FY17, the main focus of the experimental part will be to 1) commission the new UCN source and characterize its performance, and 2) fabricate and assemble the necessary components of the nEDM experiment and perform the initial Ramsey resonance measurements. Note that we will not have the HV and elaborate magnetic shielding in this phase.

The commissioning and characterization of the new UCN source will be performed in the September 2016 - January 2017 beam time. After the beam time, the components necessary for the Ramsey measurements will be installed and characterized. In the beam time starting in August of 2017, we will continue to characterize the performance of the UCN source (and implement any possible improvement informed from the first UCN source test), and will perform the Ramsey measurement.

The theory effort will focus entirely on completing the first ever lattice-QCD calculation of the neutron electric dipole moment (EDM) induced at the quark-gluon level by the so-called quark chromo-EDM (a Time-reversal interaction induced in many leading extensions of the Standard Model). The relevant matrix element is currently uncertain at the order-of-magnitude level, clouding the interpretation of one of the high-profile DOE-NP experimental efforts, i.e. the search for the neutron EDM. Among other goals, our original proposal aimed at reaching order one uncertainty on this matrix element using Lattice QCD. With the formulation of the problem and preliminary studies at hand, we will proceed to production runs on lattices characterized by different quark masses, volumes, and lattice spacing. This will allow us to extract a central value for the matrix element and most importantly an estimate of the uncertainty.

Conclusion

By the end of the fourth year, we expect to achieve the following:

- Improved UCN source that increases flux by 20-fold
- Demonstration of the feasibility of an nEDM experiment with a sensitivity of 3x10-27 e-cm, through demonstration of the necessary UCN density stored in the prototype nEDM chamber
- First-principles calculation based determination of the relevant matrix elements, essential in extracting and bounding the underlying BSM sources of T violation from EDM measurements

Publications

Bhattacharya, T., V. Cirigliano, R. Gupta, E. Mereghetti, and B. Yoon. Dimension-5 CP-odd operators: QCD mixing and renormalization. 2015. arXiv:1502.07325 [hep-ph], submitted to Physical Review D. 92: 114026 .

Bhattacharya, T., V. Cirigliano, R. Gupta, H. W. Lin, and B. Yoon. Neutron Electric Dipole Moment and Tensor Charges from Lattice QCD. 2015. Physical Review Letters. 115: 212002.

Bhattacharya, T., V. Cirigliano, S. Cohen, R. Gupta, A. Joseph, H. W. Lin, and B. Yoon. Iso-vector and Iso-scalar Tensor Charges of the Nucleon from Lattice QCD. 2015. Physical Review D. 92: 094511 .

Bhattacharya, T., V. Cirigliano, and R. Gupta. Neutron Electric Dipole Moments from Beyond the Standard Model Physics . 2014. In 31st International Symposium on Lattice Field Theory (Lattice 2013). (Mainz, Germany, July 29- Aug 3 2013). , p. 299. Trieste, Italy: PoS LATTICE2013 .

Ito, T.. Science program at lanl ucn source. Invited presentation at The 2nd International Symposium on Science at J-PARC (J-PARC 2014). (Tsukuba, 12-15 Jul. 2014).

Ito, T.. New effort to develop an nEDM Experiment at LANL . Presented at International Workshop: Probing Fundamental Symmetries and Interactions with UCN. (Mainz, Germany, 11-15 April, 2016).

Ito, T.. Fundamental physics with Ultracold Neutrons in the U.S.A. Invited presentation at High Sensitivity Experiments Beyond the Standard Model. (Qui Nhon, Vietnam, 31 July - 6 Aug, 2016).

Jr., R. Pattie. Upgrades to the ultracold neutron source at Los Alamos Neutron Science Center. Presented at International Workshop: Probing Fundamental Symmetries and Interactions with UCN. (Mainz, germany, 11-15 april, 2016).

Tang, Z., E. R. Adamek, A. Brandt, N. B. Callahan, S. M. Clayton, S. A. Currie, T. M. Ito, M. Makela, Y. Masuda, C. L. Morris, R. Pattie, Jr. , J. C. Ramsey, D. J. Salvat, A. Saunders, and A. R. Young. Measurement of spin-flip probabilities for ultracold neutrons interacting with nickel phosphorus coated surfaces . 2016. Nuclear Instruments and Methods in Physics Research Section A. 827: 32.

Research Enabling a Next Generation Neutron Lifetime Measurement

Steven Clayton
20140568DR

Introduction

The lifetime of the free neutron is a fundamental input to the Standard Model of particle physics. At present the experimental situation with lifetime measurements shows a distribution of values for the lifetime that is outside the claimed accuracy of these measurements. Trapped ultra-cold neutrons (UCN) show great promise to both resolve existing discrepancies and to push the precision of lifetime measurements to the level of 0.1 sec . A major focus of this project will be the implementation of a new technique for in situ detection of UCN inside the trap. In the first year, we will test a proto-type system to do this. Subsequent years will make improvements to this system based on the experience in the first year. In the third year we expect to make extended running to make an initial lifetime measurement with well-characterized uncertainties controlled at the level of 1 second.

This project will develop and apply two major innovations to the study of neutron decay with UCN. We will make the first measurement of the UCN lifetime using an asymmetric trap that will serve to minimize systematic uncertainties caused by marginally trapped neutrons. Our measurement will also be the first to make an in situ measurement of the number of trapped UCN, which will eliminate uncertainties introduced in the alternate technique of measuring the surviving neutrons by draining them from the trap. Measurements at comparable accuracy to the present suite of experiments – but with fundamentally different and understood systematic uncertainties – will be key in understanding why earlier measurements underestimated their systematic uncertainties.

Benefit to National Security Missions

Better understanding the physical world - such as understanding the lifetime of the fundamental building blocks of matter, is central to the mission of the Office of science.

Nuclear physics experimental capability, specifically the ability to understand and make measurements with and about neutrons is a core capability of the nuclear weapons and nuclear nonproliferation programs which is sustained and advanced by this project.

Progress

In the past year, several upgrades to the UCNtau apparatus were completed, and data were taken during the 2015-16 LANSCE run cycle for several neutron lifetime measurements with 2-4 second statistical precision under varying conditions. Among the upgrades is a new active in situ ultracold neutron (UCN) detector (“active dagger”) to replace the originally-proposed in situ detector based on neutron absorption on vanadium-51. The active dagger is based on a new UCN detector technology developed by this project: a very thin (20 nm) layer of boron-10 coated onto a ZnS:Ag scintillator screen serves as a conversion layer for UCNs into charged particles (an alpha and lithium-7), which produce copious photons in the ZnS:Ag scintillator. Some scintillation photons are wavelength shifted and captured in optical fibers leading to photomultiplier tubes (PMTs). The new detector showed the anticipated statistical improvements over the vanadium absorber technique: 1) very good efficiency (~80%), and 2) elimination of the long counting period for vanadium-52 for a roughly 2-fold improvement in beam utilization.

By counting each UCN as it was absorbed on the detector surface, the active dagger provided unprecedented insight into the UCNtau trap dynamics. The active dagger enabled a series of data in which the detector was lowered in steps, counting the UCN population in the trap at successively lower heights. Removal of superbarrier UCNs (those not energetically confined to the trap) was extensively studied by varying e.g. the duration that a UCN-absorbing plate was lowered into the top of the trap, or whether or not the active dagger was positioned at the top of the trap to help remove these UCNs.

These studies showed that removing super barrier UCNs from the trap, without creating a systematic effect called phase-space evolution, may be more difficult than we had originally anticipated. Toward the end of the run cycle, a new large-area cleaner was added to the apparatus to improve removal of the super barrier UCNs. Monte Carlo studies of the UCN trajectories in the trap were performed and reproduce features in the experimental data such as absorption time spectra on the active dagger. Consistent with the experimental data, the Monte Carlo studies show that "deep cleaning" with the active dagger, in which the dagger is positioned lower than the horizontal absorber, can remove all super barrier UCNs but creates a phase space hole that is slowly repopulated over the storage time of the trap. Analysis of the experimental data, supported by Monte Carlo studies, indicate that adjusting the large-area horizontal cleaner somewhat lower in the trap (and better aligned with the smaller, active cleaner) will be sufficient to remove super barrier UCNs.

The data taken during the 2015-16 LANSCE run cycle were blinded by scaling the trap holding times (the duration that the UCNs are held in the trap before the survivors are counted) by a factor unknown to the individuals performing data analysis. This enabled relative comparisons between the extracted neutron lifetime under varying conditions (e.g. cleaning time, configuration) without bias due to knowledge of results from other experiments. Data analysis is ongoing.

Future Work

In the final year of this project, we will take additional production data for a 1-second precision neutron lifetime measurement (i.e. comparable to the current world-average precision) and take additional data to study systematic effects at this level, in particular to further characterize the systematic effects due to phase space evolution observed in the previous running period (2015-16 LANSCE run cycle). This data-taking period will follow a number of refinements and upgrades to the experimental apparatus including the following: 1) adjustment of the height of the large-area "cleaner" at the top of the ultracold neutron (UCN) trap for quasi-trapped UCN removal; 2) upgrades to the UCN guides leading up to the apparatus to remove gaps where UCNs are lost during the trap loading period; 3) upgrades to the data acquisition hardware and software; 4) upgrades to the valve control hardware and software for tighter timing of loading and unloading the trap. The apparatus upgrades and next run plan are motivated by data analysis of the previous run cycle, in which we observed phase-space evolution of the trapped UCN population after more aggressive removal of the quasi-trapped UCNs.

As a stretch goal, a new method to read out the in-trap active detector in parallel with the previous wavelength-shifting fiber method will be implemented. The new method uses optical lenses to image scintillation light escaping the active in-trap UCN detector onto a position-sensitive photomultiplier tube. This new method shows promise for a next-generation version of the present experiment, in which the position sensitivity could enable direct monitoring for phase-space evolution. Furthermore, segmenting the detector addresses event pileup issues that could become significant with more UCNs in the trap.

Conclusion

The overall goal of the project will be to characterize all systematic uncertainities involved in using this system to make a measurement of the neutron lifetime at the level of 1 second. A new measurement at the 1-second level will lower the uncertainty of the PDG evaluation of the lifetime. The neutron lifetime is one of its basic properties. It is an important input to the standard model of cosmology and understanding primordial nucleosynthesis. Combining neutron lifetime with the other parameters of neutron decay can be used to construct sensitive tests of the standard model of particle physics.

Publications

Morris, C. L., E. R. Adamek, L. J. Broussard, N. B. Callahan, S. M. Clayton, C. Cude-Woods, S. A. Currie, X. Ding, W. Fox, K. P. Hickerson, A. T. Holley, A. Komives, C. Y. Liu, M. Makela, R. W. Pattie Jr., J. Ramsey, D. J. Salvat, A. Saunders, S. J. Seestrom, E. I. Sharapov, S. K. Sjue, Z. Tang, J. Vanderwerp, B. Vogelaar, P. L. Walstrom, Z. Wang, W. Wei, J. W. Wexler, T. L. Womack, A. R. Young, and B. A. Zeck. A new method for measuring the neutron lifetime using an in situ neutron detector. Review of Scientific Instruments.

Salvat, D. J., E. R. Adamek, D. Barlow, J. D. Bowman, L. J. Broussard, N. B. Callahan, S. M. Clayton, C. Cude-Woods, S. Currie, E. B. Dees, W. Fox, P. Geltenbort, K. P. Hickerson, A. T. Holley, C. Y. Liu, M. Makela, J. Medina, D. J. Morley, C. L. Morris, S. I. Penttilä, J. Ramsey, A. Saunders, S. J. Seestrom, E. I. Sharapov, S. K. Sjue, B. A. Slaughter, J. Vanderwerp, B. VornDick, P. L. Walstrom, Z. Wang, T. L. Womack, and A. R. Young. Storage of ultracold neutrons in the magneto-gravitational trap of the <math xmlns="http://www.w3.org/1998/Math/MathML"><mi>UCN</mi><mi>τ</mi></math> experiment. 2014. Physical Review C. 89 (5): 052501.

Seestrom, S. J., E. R. Adamek, D. Barlow, M. Blatnik, L. J. Broussard, N. B. Callahan, S. M. Clayton, C. Cude-Woods, S. A. Currie, E. B. Dees, W. Fox, K. P. Hickerson, M. Hoffbauer, A. T. Holley, C. Y. Liu, M. Makela, J.

Medina, D. J. Morley, C. L. Morris, R. W. Pattie Jr., J. Ramsey, A. Roberts, D. J. Salvat, A. Saunders, E. I. Sharapov, S. K. L. Sjue, B. A. Slaughter, P. L. Walstrom, Z. Wang, J. Wexler, T. L. Womack, A. R. Young, J. Vanderwerp, and B. A. Zeck. Total cross sections for ultracold neutrons scattering from gases. To appear in Physical Review C.

Wang, , M. A. Hoffbauer, C. L. Morris, N. B. Callahan, E. R. Adamek, J. D. Bacon, Blatnik, A. E. Brandt, L. J. Broussard, S. M. Clayton, Cude-Woods, Currie, E. B. Dees, Ding, Gao, F. E. Gray, K. P. Hickerson, A. T. Holley, T. M. Ito, C. -. Liu, Makela, J. C. Ramsey, R. W. Pattie Jr., D. J. Salvat, Saunders, D. W. Schmidt, R. K. Schulze, S. J. Seestrom, E. I. Sharapov, Sprow, Tang, Wei, Wexler, T. L. Womack, A. R. Young, and B. A. Zeck. A multilayer surface detector for ultracold neutrons. 2015. NUCLEAR INSTRUMENTS & METHODS IN PHYSICS RESEARCH SECTION A-ACCELERATORS SPECTROMETERS DETECTORS AND ASSOCIATED EQUIPMENT. 798: 30.

k_effective: First Measurement of a Nanosecond-Pulsed Neutron Diagnosed Subcritical Assembly

Anemarie Deyoung
20150044DR

Introduction

Neutron generation is extremely sensitive to plutonium compressibility, and understanding the compressibility under the conditions encountered in a nuclear primary is key to Life-Extension Program (LEP) options (including pit reuse), guarding against untoward aging effects, and establishing the safety/surety characteristics for the future stockpile. These and other key drivers have been studied in a classified venue by our XTD Division advisors to the LDRD. In this project we will develop a precision measurement technique to determine the nuclear generation in a subcritical system, with an accuracy comparable to that obtained in nuclear testing. The Weapons Program requirement for an innovative alternative to nuclear testing is a dynamic pulsed measurement of neutron generation. The focus of this proposal is the feasibility of a subcritical static neutron generation experiment.

Previous subcritical experiments have not had the diagnostic capability to infer nuclear generation. Our project involving Neutron Diagnosed Subcritical Experiments (NDSE) provides neutron generation, which is an extremely sensitive integral constraint on both the distribution and nuclear properties of materials. Our proposed NDSE capability would enable inference of neutron generation or, more precisely, “alpha” (α), with the accuracy needed for weapons analysis. We will perform a high precision measurement of α using a static subcritical assembly. The challenge is to make the measurement under laboratory conditions with ~10 orders of magnitude fewer gammas than were available during nuclear testing.

We will develop a capability that includes (1) a pulsed neutron source and (2) a detector and data acquisition system with proper shielding and collimation to measure the gammas emitted from the package. The recent advances in pulsed neutron sources, detector technologies, fast electronics, and simulation-based analyses, have advanced the NDSE concept to a level that has a high chance of succeeding at a first ns-scale pulsed neutron generation measurement.

Benefit to National Security Missions

Success of this LDRD project would establish the technical feasibility of proceeding toward a large future weapons program in dynamic NDSE at the NNSS. Such a program would provide the first modern quantitative understanding of the neutronic properties of Pu at high pressures and thus provide experimental validation of weapons models which is key to Life-Extension Program (LEP) options (including pit reuse), guarding against untoward aging effects, and establishing the safety/surety characteristics for the future stockpile. This also has possible applications in the Global Security arena. The Nuclear Engineering and Non-proliferation (NEN) Division is expert in the use of passive and active diagnostic techniques for detection and characterization of configurations of special nuclear materials. The neutron generation measurement offers an opportunity to explore different techniques for simultaneously collecting, utilizing, and analyzing all the available time-dependent induced signatures.

Success of this project would advance the scientific state-of-the-art in gamma-ray detectors and DPF neutron sources. As well it would enable advanced criticality studies, e.g., study of fast pulse excitation of complex static critical assemblies. Measuring the alpha, using a fast neutron pulse, of a static but complex critical assembly, creates a new regime which permits advanced testing of simulation codes. Observation of alpha as it changes from an initial value (14 MeV excitation) to its equilibrium value, would allow separation of various contributions such as delayed neutrons, effects of cross section libraries for the unresolved resonance regions, and the time-dependence of complex moderation and reflection processes.

Progress

This year we successfully performed the first gamma fall-off measurement on a static 10B target (which has a gamma fall-off similar to SNM with keff~0.95) using the concrete line of sight at NNSS by March 2016, the first milestone for this project. We passed the external midterm review with Outstanding and Excellent ratings. As of now all components of the system are proving to be adequate for a dynamic measurement of alpha in the future. This next year we will quantify the precision with which we expect to be able to measure alpha on a dynamic system using the current design.

Working with our NSTec collaborators we designed and built a line of sight collimator and concrete shielding tunnel that was completed by October 2015. Extensive modeling using the MCNP6 Monte Carlo Transport code was required. Results are consistent between MCNP and the experiment. The DT DPF generated neutron pulses with yield and pulse shape of high caliber, meeting our requirements for the gamma measurement. New 'near-in' neutron detectors were shown to properly characterize the neutron pulse, as corroborated by data from a neutron shadow bar detector at 20m, and by data from the gamma detector at 15m measuring signal from a graphite target (4.4 MeV gamma resulting from the 14 MeV neutron pulse) after unfolding of detector system responses. Gamma falloff measurement of the 10B target were consistent with results measured in the laboratory using a counting-mode system. These results have generated excitement leading to plans for an SNM measurement within a year. Subsequent measurements of gamma falloff from the 10B target using DD DPF neutrons resulted in a better measurement.

DPF R&D modeling and characterization demonstrated excellent agreement between modeling and experimental results for the DD DPF neutron radial and axial mean energy and energy spread. 3D modeling of asymmetric rundown and run-in showed the capability to generate 'kink' mode instability; this (unfortunately) predicted a result that was subsequently seen on one of the DD DPF tubes. The LA-COMPASS magnetohydrodynamic code with nuclear physics post-processor has proved itself to be a powerful tool for characterizing the DPF, and for optimizing its performance.

MCNP modeling predicted that the large amount of copper in the DPF anode may be an issue for future experiments due to the creation of low energy neutrons; this is leading to a better design.

The four gamma detectors performed admirably. The 'liquid VI' scintillator has ultrafast nanosecond scale time response and little 'afterglow.' The large 15"x15"x8" cell however was found to cause a long ~15ns FWHM time response. By measuring the response and with unfolding from the data, excellent ultrafast results were obtained. Nevertheless, the design has been studied by NSTec and the team; a new smaller unit will be built for faster inherent time response.

Criticality studies in NEN contributed to the theory and analysis of data to infer the reactor physics parameters (Rossi-alpha, criticality, etc) that is embedded in the measured data for comparison with traditional methods of measuring such data.

Presentations were made at the NEDPC conference and given at other venues throughout the year. The team is collaborating with groups across the Complex on this project. A report on the graphite target test series comparing MCNP6 and experimental results is in progress.

Future Work

In FY17 we expect to be able to quantify the precision to which alpha can be measured in a dynamic shot using the system components we have at NNSS Area 11.

We are proposing the following plan for the FY17 NDSE project:

- Static experiments at Area 11
- Precision measurement on a second 10B target of slightly different slope from first target, to demonstrate capability to discriminate between two objects of slightly different keff, using DD neutrons
- Advance the capability to field precision measurements on both fissile and non-fissile targets
- Detector research
- Research to improve detector characterization of the DPF neutron flux
- Gamma detector research to improve time response (altered Liquid VI design and backup BaF2 scintillator design)
- DPF theoretical modeling and analysis
- 3D modeling of next gen DT DPF tube improving both yield and neutron pulseshape
- Studies to demonstrate whether DD DPF would be viable in a keff experiment
- Studies of analysis of the keff (t) to be derived from the data given the neutron source term
- TBD if funding exists – research on DPF radial and axial neutron energy spreads as a function of DD or DT burn
- LOS and target MCNP modeling
- MCNP modeling to enable the second 10B target measurement; Different slope surrogate object (reflected with Be plates or different diameter object)

- Comparison of B4C target to simulations (to date we have only done graphite)
- Journal article on B4C experiments and simulations
- Research studies on improvements to the existing Test Stand at Area 11 that would improve the keff measurement
- Nuclear Engineering: studies and methods for measurement of static SNM targets with different reflectors which would enable future precision keff measurements

Conclusion

We must develop novel gamma-ray detector technology to meet the requirements of the neutron generation measurement; this includes new materials to achieve a signal with large dynamic range and ultrafast few-ns scale time response. We must also develop a robust pulsed neutron source based on Dense Plasma Focus (DPF) technology; this lies at the forefront of plasma physics. With sufficient funding, in FY17 we expect to be able to quantify the precision to which alpha can be measured in a dynamic shot using the system design we have at NNSS Area 11.

Publications

DeYoung, A., A. C. Hayes, J. T. Goorley, G. L. Morgan, V. W. Yuan, A. W. Obst, R. S. Rundberg, H. Li, G. Jungman, M. A. Snowball, M. M. Fowler, E. Guardincerri, W. L. Myers, S. M. Sterbenz, R. S. King, and N. S. P. King. First NDSE LDRD Proof-of-Concept Experiments (LA-CP-16-20465). 2016. LDRD Annual Report for LDRD Office and DOE Headquarters.

DeYoung, A., V. Yuan, G. Morgan, C. Hagan, A. Obst, R. Rundberg, A. Hayes, T. Goorley, H. Li, G. Jungman, W. Myers, S. Hsu, T. Haines, J. Lestone, E. Guardincerri, M. Fowler, P. Koehler, J. Gatling, E. Hunt, M. Kelley, D. Lowe, B. Davis, and J. Tinsley. New diagnostic: neutron diagnosed subcritical experiments (LA-CP-14-20196). Presented at Nuclear Explosive Code Development Conference 2014. (Los Alamos, NM, 20-24 October 2014).

Hsu, S.. DPF benchmarking diagnostics: present and future. Presented at DPF Workshop. (LLNL, Livermore, CA, 29 June 2015).

Li, H., A. C. Hayes, G. Jungman, S. Li, K. A. Flippo, A. Rasmus, A. DeYoung, R. S. Rundberg, and C. Hagen. Using Magnetized HED Plasmas to Study Astrophysical Plasma Processes (LA-UR-16-23870). 2016. HEDLP Capability Review, 2016-06-15/2016-06-16 (Los Alamos, New Mexico, United States).

McKenzie, G. E., T. J. Grove, W. L. Myers, and R. G. Sanchez. Reactivity worth studies associated with a Rossi-Alpha measurement system (LA-UR-15-25941) . Presented at American Nuclear Society Winter Meeting. (Washington DC, November 2015).

Yuan, V., A. DeYoung, A. Obst, and G. Morgan. NDSE detectors development. Presented at 2015 Nevada working group meeting, LA-UR-15-22230 . (Las Vegas, Nevada, 31 March 2015).

Yuan, V., A. Obst, A. DeYoung, G. Morgan, R. Rundberg, and M. Fowler. Detector and boron target R&D for the NDSE LDRD project. 2016. LDRD review presentation.

Multi-Scale Kinetics of Self-Regulating Nuclear Reactors

Venkateswara R. Dasari
20150058DR

Introduction

Los Alamos is pioneering the development of self-regulating small compact nuclear reactors (SCRs). These reactors are of immense interest to the community of sponsors who have power needs in space, underwater and in remote areas. In this research, we propose to demonstrate the feasibility of self-regulation by developing and validating models for reactor behavior in tunable 'micro-engineered' materials specifically designed to achieve self- regulation. Reactors that self-regulate fission power to match varying operational needs and that protect the reactor core from exceeding thermal limits during accidents are ideal for unattended operations.

SCRs are significantly different in scale and design from conventional reactors. Making use of precisely engineered core and reflectors, SCRs can be designed to have relatively longer neutron life time, small excess reactivity in the core and low power density making them an ideal candidate for achieving self- regulation. The transformational goal of this DR is to precisely understand how novel SCRs can be designed to self-regulate with minimal control system or human intervention. In this research we are seeking a disruptive alternate based on the hypothesis that certain mesoscale properties of micro-engineered fuels can be 'tuned' so that emergent neutronic functionality maximizes SCR self-regulation. Building on this hypothesis, we have designed micro-engineered dispersed fuel composites that trigger and amplify negative reactivity feedback at different timescales and lengthen neutron lifetime by 'geometrically delaying' a significant portion of fissioning neutrons.

The focus of this research is to demonstrate the feasibility of our SCR concept by accomplishing three inter-related R&D objectives: to research and develop techniques to make limited quantities of tunable fuel composites that maximize self-regulation; to measure their neutronic and thermo-mechanical properties at different length-scales; and using this data to model the performance of the full-scale reactor to confirm self-regulation and quantify uncertainty.

Benefit to National Security Missions

Los Alamos is pioneering the design of self-regulating low-power small compact reactors. Such "fission batteries" are of immense interest to the community of sponsors who have power needs in space (NASA/DoD/IC), underwater (DoD/IC/DHS) and in remote areas coupled with renewable sources (DOE). Despite these transformative aspects, there is reluctance to adapt reactor technologies because they are perceived to be too financially risky and complex to operate.

In this Directed Research, we propose to demonstrate feasibility of self-regulation and develop and validate constitutive models of neutron kinetic behavior in tunable 'micro-engineered' materials specifically designed to achieve self-regulation. LANL is singularly qualified to undertake this research because of our unique ability to bring together computational nuclear engineering, computational and experimental nuclear materials science, and criticality testing facilities at NCERC.

Of particular importance are our capabilities (1) to precision design, engineer and fabricate nuclear components, (2) to build in proliferation resistance and (3) to test the system and its components relying upon methods developed as part of science-based stockpile stewardship. In addition to providing fundamental knowledge on nuclear materials, it also provides nuclear criticality data necessary for characterizing safety and non-proliferation implications of dispersed fuels and are likely to lead to fabrication of accident tolerant nuclear fuels. In summary we are leveraging specific capabilities being maintained at LANL for the purpose of carrying out our primary nuclear security mission, to meet needs of other national security sponsors, and refining those actinide science skills for future weapons and nonproliferation missions.

Progress

Accomplishments are listed by the three major focus areas of proposed research.

Fuel and Materials Fabrication

A key focus area is to demonstrate our ability to fabricate specially designed nuclear fuel composites. We have demonstrated our ability by:

- Establishing FBCVD, Fluidized Bed Chemical Vapor Deposition technique, for applying thin layers of thermal barrier coatings on fuel kernels. First demonstrated using surrogate non-nuclear materials (TiO2 and WC) and ultimately using uranium-carbide kernels
- Demonstrating that coated fuel kernels can be compacted into large fuel compacts without damaging the coatings. In our research we have achieved 60 vol-% of packing without adversely affecting stresses on the fuel. Fuel was characterized making use of equipment we have at LANL and that located at INL. Results were presented at the peer-reviewed conference
- Upgrading safety and authorization basis to fabricate low-enriched nuclear fuel composites. Progress here included revisions to glovebox safety/authorization basis.

Nuclear Testing

- Designed two sets of experiments to be conducted in the third year of this LDRD. Both experimental plans were reviewed by the host organization and raised no USQs (Unreviewed Safety Question). They are now progressing to be scheduled for conduct in the second quarter of FY17.
- First series of experiments will subject our specially fabricated fuel compacts to reactivity pulses from Godiva. In these tests, we expects the temperature of the fuel kernels to suddenly (0.05 seconds) increase by 200 C. This sudden increase will cause proportional expansion of the fuel kernels. We will study how the overall fuel compact might be able to survive such a pulse.
- Second series of experiments will examine feedback properties of the fuel using the Planet test reactor. These type of experiments are routinely performed by LANL.

Future Work

In the next fiscal year, we will focus on the following objectives:

- Fabricate large samples for nuclear experimentation. Several samples will be fabricated to fit into Godiva sample holders and ACRR Sample holders. These samples will be subjected to pulse experiments with results analyzed for coating performance.
- Fabricate additional materials at engineering scale to perform experiments that will measure reactivity worth and spectral shift.
- Characterize sample properties before and after each nuclear experiment. Because the nuclear experiments are of limited exposure we can perform post-irradiation examination within days after exposure.
- Build refined models that will be used to perform an integrated assessment of self-regulation. We plan to model the experiments and parts of the core in explicit detail to capture the effects of the micro engineered materials.
- Patent protection and publication. We believe that this research is likely to lead us to generating patentable information. We have engaged the Feynman Center to protect the information.

Conclusion

We are seeking a disruptive solution based on the premise that dispersed fuel composites can be 'tuned' at the micro-scale such that emergent neutron behavior can be designed to self-regulate a reactor with minimal control system or human intervention. Operationally, the Defense Science Board identified small compact reactors to be "game-changers" whose demand cannot be underestimated for space exploration, for underwater vehicles, for assured arctic awareness and satellites that can operate on the dark side of the globe. This research will demonstrate feasibility and readiness of such a technology for near-term use by a community of sponsors.

Publications

Cummins, D. R., E. Luther, A. Telles, and P. Pappin. Low Temperature Sintering of Silicon Carbide for New Self Regulating Reactor Design. Presented at Rio Grande Fuels Conference. (Los Alamos/ Albuquerque, September 2015).

Hurley, D.. Spatially Resolved Thermal Transport Measurements in PyC Coated Fuel Particles. To appear in Transaction of American Nuclear Society. (New Orleans, LA, August 2016).

Luther, E.. Fabrication and Characterization of Graphite Composite with Controlled Thermal and Mechanical Properties. To appear in TMS 2016. (Orlando, November 2016).

Rao, D. V.. Multipoint Kinetics of Compact Self-Regulating

Reactors. Nuclear Technology.

Usov, I., and D. V. Rao. Pyrolytic Carbon Coatings on Oxide and Carbide Microspheres. To appear in TMS 2016: the Materials and Fuels for Advanced and Current Nuclear Reactors. (Orlando, FL, November 2016).

Next-Generation Double Beta Decay Experiment

Steven R. Elliott
20150088DR

Introduction

If neutrinos are their own antiparticles, technically referred to as Majorana particles, theories that explain the matter-antimatter asymmetry of the Universe and hence our presence become plausible. Neutrinoless double beta decay experiments are the only practical technique to establish that neutrinos are Majorana particles. A next generation experiment using approximately a tonne of source will have an exciting opportunity to make this determination. This is especially true given the knowledge we have regarding neutrino mass from other experiments. It is clear that this is an ideal time to begin planning such an experiment.

There is some remaining R&D that is required to eliminate risks associated with a next generation experiment. This includes a number of technical and theoretical topics. This project intends to perform that R&D.

There is no DOE funding for this activity. DOE is planning for a future large double beta decay experiment, but they haven't chosen the technology yet. With this R&D, we hope to improve the case for the use of Ge detectors.

Benefit to National Security Missions

This is a critical time for this R&D. The DOE-NP office is planning to fund a large-scale double beta decay experiment and is making plans for that eventuality. NSAC has finished an assessment of the possible techniques that can accomplish the goal and a sub-committee has posted its report. The report to NSAC indicating the importance of the science and the critical nature of the next 2-3 years in determining the final choice of technology. Therefore, the R&D accomplished in the next few years will greatly influence the final decision. The Nuclear Physics Long Range Plan had a double beta decay experiment as its highest priority for a new start.

This research will also provide a significant improvement in HPGe detection limits, and the knowledge gained can be leveraged to lower backgrounds for operational (Global Security) relevant missions. The data acquisition and multiplexing will provide an excellent basis for better throughput in data collection and storage. The pulse shape discrimination (PSD) analysis work also may serve to improve detection sensitivities through recognition of background versus sample events. The PSD may also allow us to do better time coincidence measurements by looking for only coincidences with certain pulse shapes.

Low background gamma-ray detection has application to non-proliferation by lowering the limit of detection of radioactive effluent from reprocessing and other weapons production activity. This supports the Laboratories Science of Signatures Pillar.

Progress

This past year we made progress on all of the activities associated with our project. Our efforts are R&D aimed at improving the performance of a tonne-scale double beta decay experiment based on Ge detector technology. Some of our efforts are dedicated experiments at LANL, whereas other efforts exploit data from the Majorana Demonstrator presently operating at the Sanford Underground Research Facility and critical theory for understanding the expected decay rate.

The hybrid cryostat design requires operating detectors at high voltage. We made measurements of the breakthrough voltage of different candidate gases using the gas system and the cryostat. Currently, a draft for publication of this work is developed. A detector holder has been designed for the cryostat and we are getting ready to operate a detector in a cold gas.

Several ideas for multiplexing the detector signals and pulsers were pursued to determine if sufficient bandwidth could be provided while keeping the injected noise low enough to maintain a low energy physics capability. After consultations with electrical engineers and

several simulations it was determined that only an optical switch method holds any promise. This method will be pursued in the coming year.

We have begun laying out plans for studying Rn in our glove box system. We re-established the purge system for that glove box and did some initial baseline measurements of the Rn level. We have developed plans for a Rn removal filter to be added to the purge system and a sensitive Rn measurement system.

We have now installed an inverted robot that will be used to assess the performance of detectors. The robot is working properly and a gripper technology has been chosen. Software for the specific planned tests are now being prepared.

Muons are the primary cosmic radiation that reaches an underground lab and produce high-energy secondary neutrons. Simulations were performed, calculating the muon flux in the six leading underground labs worldwide taking into account the surface topology. The results show that the deepest underground lab in Jinping, China, has a disadvantage due to its surface topology and that SNOLAB, Canada or the deeper level in the Homestake Mine, SD provide the same level of shielding against cosmic rays. The results were presented at international meetings, like the next generation ton-scale meeting in Munich, Germany and a publication is in preparation.

The neutron-induced isotope, 73Ga can be generated through interactions between fast neutrons and germanium isotopes. Using its unique decay signature, we identified three candidate decay events of 73Ga in the commissioning data of Majorana Demonstrator. From these events, we estimate the corresponding neutron energy spectrum and the background induced by neutron-induced isotopes in the Region of Interest (ROI) for 76Ge neutrinoless double beta decays. Preliminary results have uncovered a problematic background generated by the fast neutrons for the next-generation germanium neutrinoless double beta decay. A deeper experimental site or different shield design will be necessary in order to reduce the neutron flux to an acceptable level.

We have been working to build an international collaboration that will execute a next generation double beta decay experiment that will use some of the results from this LDRD. We have met several times face to face and presently have routing conference calls.

We have completed calculations of single beta decay in light nuclei. These beta decays have a quenching similar to those seen in larger nuclei, but (10-20%) quenching. We have included both realistic nucleon-nucleon correlations and two-nucleon currents in these calculations. We find that the correlations reduce the matrix elements, the two-nucleon currents provide a very small increase in the relevant matrix elements to bring the total into agreement with experiment. These results are being written up for publication.

At higher momentum transfer calculations of neutrino response with the same interactions and current operators indicate a much smaller quenching, or in fact an enhancement at very large momentum, of the axial response, suggesting the absence or at least a much smaller quenching of the axial response. We are pursuing results in larger nuclei for both single and double beta decay.

We have continued our study of beyond the standard model effects for double beta decay with a paper submitted this year.

Future Work

For FY2017, we plan to make progress on several separate experimental R&D tasks. We plan to begin use of a new cryostat concept and test a detector. We have made down-select choices within the various possible multiplexing schemes with no great option and will consider one more plan. We plan to begin using a robot to perform certain repetitive tasks in detector assessment and assess its effectiveness. We plan to study improvements in low-radioactivity connectors and Rn removal inside a glove box. We plan to begin analysis of data from a present underground experiment to assess the depth requirement for such experiments.

On the theory front, we will continue our studies on the influence of the axial vector coupling constants on the matrix element for double beta decay. We will also continue the study of other potential influences from particle physics on the double beta decay rate.

Conclusion

Our expected results include assessments of new cryostat designs for Ge detectors, use of robotics in assessing detectors, new data acquisition techniques, understanding the depth requirement for such experiments and key theoretical issues in nuclear and particles physics required to fully understand a measurement of double beta decay.

Publications

Rielage, K., S. Elliott, P. Chu, J. Goett, R. Massarczyk, and W. Xu. Research and Development Supporting a Next Generation Germanium Double Beta Decay Experiment. Division of Nuclear Physics of the APS. (Santa Fe, NM, 28-31 Oct. 2015).

Cold Cathodes for Next Generation Electron Accelerators: Methodologies for Radically Improving Performance and Robustness

Nathan A. Moody
20150394DR

Introduction

Many grand challenges, including the quest for sustainable energy, continued scaling of computational power, detection and mitigation of pathogens, and study of the structure and dynamics of the building blocks of life require the ability to access, observe, and control matter on the frontier timescale of electronic motion and the spatial scale of atomic bonds. The only instruments with such capability are future coherent x-ray sources and advanced colliders, which demand increasingly high performance electron beams well beyond the present state-of-the-art. The purpose of this project is to address this technology gap and make parallel, transformational advances in the two critical performance areas of an electron source: lifetime and efficiency. Traditional approaches have failed because advances in one of these parameters have come at the expense of the other.

Transformational advance in electron source performance requires radical improvements in lifetime and efficiency. Previous work has succeeded in delivering increases in one, but at considerable expense of the other because of the competing underlying physical processes. The unique approach of this project is to decouple the competing mechanisms so that both lifetime and efficiency can be independently and substantially improved. The generalized hypothesis is that lifetime and efficiency of electron sources can be controlled by manipulating nano-scale structure of cathode materials, yielding emergent behavior which radically enhances performance. Our innovative approaches span three thrust areas and share a common theoretical framework: a.) Enhanced performance through nanostructure; b.) Enhanced lifetime through monolayer protective coatings, and c.) Integration of new physics in models, simulations, and technology demonstrations. Our progress to date has validated our research approach, which includes key risk mitigation and supporting engineering efforts, including the completion of an in-situ cathode synthesis and beam diagnostic instrument which provides correlation between material properties of the cathode and beam properties of the emitted electrons.

Benefit to National Security Missions

DOE/DOD/SC/MaRIE

This project represents an enabling technology for existing and future light sources and particle accelerators, including MaRIE, which is intended as a tool to study weapons-relevant materials among others. Light sources and particle accelerators are key to the DOE/SC mission requiring state of the art electron beams for generation of coherent x-ray light as well as all electron-beam-based DOD missions, such a high power free electron lasers and radio frequency source technologies. Improved cold cathodes with controllable parameters allows for higher performance, reduced complexity, reduced cost, and reduced system maintenance in almost every relevant application area. It is directly enabling for all accelerator-based approaches to remote detection of chemicals, pathogens, and nuclear materials . It would benefit accelerator-based solutions for management of nuclear waste as well as the production of critical medical radioisotopes.

The monolayer coatings we employ can potentially be functionalized to act as detectors, of interest to DHS/DHHS, or as a key element in energetic neutral atom imaging for remote space sensing (NASA).

Basic Understanding of Materials

X-ray free electron lasers (X-FELs) are the ideal tool to interrogate, understand, and even control matter in extremes. To date, nineteen Nobel Prizes have been awarded for x-ray science using beam-based x-ray light sources, and we can expect more in the future as these tools open vast science frontiers to probe matter-in-extremes at unprecedented temporal, spatial, and energetic scales. The work represented in this project closes critical technology gaps in the fielding of X-FELs as instruments of discovery science.

Progress

Theoretical Framework

Establishing a validated understanding of photoexcitation and photoemission from nanostructured materials using first principles and experimental comparisons.

Goal 1: Understand applicability of existing models

- Completed: Comparison between families of density functionals
- Completed: Modeled coatings on metals and semiconductors

Goal 2: Down-select from among existing models and adapt to include nanostructure

- Completed: Determine and incrementally implement methods to account for effect of monolayer protective coatings (publication milestone)
- Completed: Arbitrary stoichiometry, barrier geometry.
- Completed: implemented realistic scattering processes which match that of similar systems

Goal 3: Identify highest priority experimental parameters and measurements

- Completed: Direct validation of predictions for graphene on copper and semiconductor photocathodes.
- Completed: modeled multi-photon processes for first time

Thrust Area #1: Controlling and enhancing cold cathode performance through nanostructure

Goal 1: Validation of methods for controlling surface cathode properties

- Completed: Optimize conductivity of quantum dot films and compute effect of heterostructure layering to enhance optical absorption.
- Completed: demonstrated state of the art chemical vapor deposition growth of high performance photocathodes and alkali halide protective films.
- Completed: specify synthesis methods and demonstrate reproducability
- Completed: buildup of experimental chamber for femto-second laser excitation
- Completed: development of model explaining mechanism of electron emission from quantum dots.

Goal 2: Validation of methods for controlling bulk cathode properties

- Completed: Fabrication and measurement of straightforward, first-generation quantum dot (QD) photocathode samples (publication milestone).
- Completed: first electron beam emission measurements from quantum dots.

Thrust Area #2: Enhancing robustness and lifetime using monolayer barrier-shield coatings

Goal 1: Comparison between three primary methods for growing graphene

- Completed: Determine the advantages of each and degree of control over relevant parameters, down-selecting on primary methods.
- Completed: Identified key signatures of degradation mechanisms
- Completed: Adopted novel quantitative method of describing photocathode lifetime, resolving persistent ambiguities in literature data (publication milestone)

Goal 2: Demonstrate transfer of large-area films

Completed: Demonstrated large area transfer to metallic mesh scaffolds and successfully grew photocathode material on this suspended substrate (publication milestone)

- Completed: complete characterization of films using state-of-the-art tools
- Completed: demonstrated gas barrier function of graphene films

Thrust Area #3: Integration of new physics in technology demonstrations

Goal 1: Specify requirements, functionality, and design of multi-use cathode test environments

- Completed: engineering designs for all cathode test hardware, including the in-situ beam diagnostic and surface science stations; begin procurement/fabrication/assembly, and address any compatibility issues.
- Completed: procured commercial state-of-the-art surface science diagnostics, referred to as Auger spectroscopy and x-ray photoemission spectroscopy.

Goal 2: Prepare existing rudimentary test hardware to scale to project needs

- Completed: Update/upgrade vacuum system to pro-

vide immediate photoemission data from first samples to accelerate model validation and overall interface between theory and experiment

- Completed: tunable laser procurement and install
- Completed: Modeled performance of electron beam diagnostic and demonstrated required sensitivity

Overall Summary of Progress to Date

- 7 high impact journal submissions
- 5 conference proceedings
- 5 patent submissions completed and 1 awarded patent
- Significant post-doc development
- 1 post-doc to staff conversion
- Strategic partnerships with academia, industry, and other national labs

Future Work

Theoretical Framework

Establishing a validated understanding of photoexcitation and photoemission from nanostructured materials using first principles and experimental comparisons.

Goal 1: Extend computational materials methods

- Task: Demonstrate agreement over wider range of parameters (such as other ranges of thickness of graphene)

Goal 2: Test fidelity of predictions of beam parameters

- Task: Design experiments that allow for beam emittance to be modeled and then measured without removal from load-lock chamber

Goal 3: Inform optimization paths

- Task: Use surface science diagnostics to constrain parameters of models to conditions which actually exist at cathode surface during synthesis steps.

Thrust Area #1: Controlling and enhancing cold cathode performance through nanostructure

Goal 1: Demonstrate working prototypes in photocathode gun

- Task: Improve charge transport, photon capture, enhance Auger effects
- Task: Examine two-wavelength light bias enhancement

Goal 2: Cathode design procedures

- Task: Study photoemission from single quantum dot and measure emittance of quantum dot films
- Task: Compare emission data to extended photoemission model.

Thrust Area #2: Enhancing robustness and lifetime using monolayer barrier-shield coatings

Goal 1: Specify ideal properties of gas barriers

- Task: Tune thickness of barrier films to optimize electron emission
- Task: Controlled gas exposure tests

Goal 2: Correlate key performance metrics (efficiency and beam emittance) with layer depth and composition

- Task: In-situ and side-by-side beam measurements together with surface characterization

Thrust Area #3: Integration of new physics in technology demonstrations

Goal 1: Commission the in-situ multi-physics chamber

- Task: Individual chambers integrated together, calibrated.
- Task: photoemission model validation

Goal 2: Make comprehensive in-situ beam measurements of advanced cathode prototypes

- Task: Specify the correlation between changes in the electron beam properties with changes in the cathode material properties.

Conclusion

We will develop and demonstrate 'designer' cold cathode electron sources with tunable parameters (bandgap, efficiency, optical absorption) that outperform present technologies in terms of efficiency and lifetime, where success in either of these is considered transformational. We introduce fundamentally new approaches to address decadal weaknesses in performance and enable cathode properties to be tuned or engineered for specific Department of Energy missions and related applications. This project will specifically yield new understanding of nanoscale structure on cathode performance, new fabrication methodologies, validation of simulation and modeling tools, and prototype demonstrations of novel cold cathodes incorporating these new features.

Publications

Alexander, A., N. A. Moody, and P. Bandaru. Enhanced quantum efficiency of photoelectron emission, through surface textured metal electrodes. 2016. Journal of Vacuum Science and Technology A (JVSTA-A-15-292). 34 (021401): 0214010.

Carlsten, B. E, S. J. Russell, J. W. Lewellen, D. C. Nguyen, P. M. Anisimov, C. E. Buechler, K. A. Bishofberger, L. D. Duffy, F. L. Krawczyk, Q. R. Marksteiner, N. A. Moody, N. Yampolsky, and R. L. Sheffield. MaRIE XFEL physics design risks and risk mitigation plans. 2015. Los Alamos National Lab. (LANL), Los Alamos, NM (United States); DOE Contract Number: AC52-06NA25396; LA-UR--15-22069.

Jensen, K. L., N. A. Moody, A. Shabaev, S. G. Lambrakos, D. Finkenstadt, A. Mohite, G. Gupta, and F. Liu. Delayed Photoemission model for beam optics codes. 2017. Journal of Vacuum Science & Technology B . 35 (02C102): 02C1021.

Liu, F., and C. N. Villarubia, A. Mohite, G. Gupta. Single layer graphene protective gas barrier for copper photocathodes. To appear in Applied Physics Letters.

Makarov, N. S., J. W. Lewellen, N. A. Moody,, and I. Robel, J. M. Pietryga. Short pulse photoemission studies of quantum dot film. To appear in ACS Nano Letters.

Pavlenko, V., E. Batista, N. A. Moody, and F. Liu, M. Hoffbauer,. Kinetics of alkali-based photocathode degradation. 2016. AIP Advances. 6 (115008): 1150081.

Yamaguchi, H., F. Liu, and N. A. Moody. Active bialkali photocathodes on free-standing graphene substrates. Nature Photonics.

Cosmic Positrons from Pulsar Winds and Dark Matter: New TeV Theories and New TeV HAWC Observations

Brenda L. Dingus
20160007DR

Introduction

The discovery of an excess of high-energy positrons by several earth-orbitting satellites has generated enormous interest because of its potential origin from dark matter (DM). Another possible producer of these positrons are neutron stars called pulsar wind nebulae (PWNe). Detailed observations combined with advanced modeling of these systems, both of which produce positrons and gamma rays, are pivotal to understanding of the positron excess.

With the newly constructed High Altitude Water Cherenkov (HAWC) observatory, we will to increase the highest energy sensitivity by building an array of outrigger detectors. This sensitivity enables us to develop and constrain new theories of TeV particle production and search for nearby PWNe and/or DM sources. HAWC will make the highest energy observations of at least 18 PWNe to constrain their spectral, spatial, and temporal characteristics. We will perform relativistic magnetohydrodynamics and kinetic simulations to model PWNe and particle acceleration via reconnection. The gamma rays from PWNe models will be compared with HAWC observations. Second, HAWC's all sky surveys will provide the best sensitivity to search for DM annihilation of the most massive DM candidate particles. We will study high energy physics DM models, such as supersymmetry, to constrain such annihilation cross-sections. Third, we will model the positron propagation through the interstellar medium with both turbulent and coherent magnetic fields to determine the expected positron spectra and anisotropy that would be observed at Earth. In the end, our theoretical results will be compared with multiwavelength observations by HAWC and positron observations.

This proposal brings together a unique combination of recognized, long-held expertise at LANL in high-energy observational astrophysics, plasma astrophysics, transport physics and high-energy physics. Its success enables development in fundamental science capabilities and in tools that support LANL programs in detector, plasma and transport physics. It also enhances our ties with DOE Office of Science.

Benefit to National Security Missions

DOE/SC High Energy Physics program, the National Science Foundation's Particle Astrophysics program, and NASA are all interested in understanding the highest energy particles and gamma-rays from astrophysical sources and from dark matter. These objectives have been further endorsed by various reports, such as the National Academy's Astro2010: The Astronomy and Astrophysics Decadal Survey and the DOE/SC and NSF High Energy Physics Advisory Panel's report "Building for Discovery: Strategic Plan for U.S. Particle Physics in the Global Context". This project utilizes LANL's unique capabilities in theoretical modelling of both astrophysical sources and potential dark matter candidates as well as in observations of the highest energy gamma rays. Specifically, this project will address recent puzzling detections of high energy positrons by satellites orbiting Earth with gamma-ray observations by the High Altitude Water Cherenkov detector and detailed theoretical simulations of particle acceleration in pulsar wind nebula and theoretical calculations of gamma rays and positrons from potential dark matter candidate particles. These investigations will increase LANL's capabilities in information science and technology as well as remote sensing of radiation and other experimental techniques relevant to studies of our nuclear stockpile.

Progress

The outrigger construction has made excellent progress. Prototypes have been tested both at LANL and at the HAWC site. The new data acquisition (DAQ) system is being tested with the pre-deployment laser calibration system at LANL. The design of the outrigger array has been finalized and most parts have been ordered and will be delivered prior to the end of this fiscal year. An array of 10 outriggers is being constructed at the HAWC

site now and will be tested with the new DAQ before the end of the fiscal year. The parts for the rest of the outriggers are being tested and assembled at LANL and will ship to the HAWC site early in the next fiscal year for deployment.

The analysis of the HAWC data is also progressing well. First results were announced at the American Physical Society meeting in April and papers are being written. Several pulsar wind nebula have been detected including two that are very near to Earth. These two sources are the subject of several theoretical papers that claim these two are likely the origin of the excess positrons observed at Earth. HAWC data will be able to constrain the energy of the positrons that are produced by these sources as well as the energy losses the positrons suffer as they propagate away from their origins.

On the high energy theory effort, several kinds of TeV scale models of dark matter are being investigated. In the first class of models the dark matter arises from a phase transition that occurs in the early Universe, producing topological defects that could be dark matter candidates. The interest here is in how to couple such a sector to the Standard Model in order for dark matter annihilations to produce visible signals. In the second class of models, the dark matter candidate is a fermion charged under the Standard Model electroweak gauge group and has a multi-TeV mass. In this circumstance the model contains other charged particles that are nearly degenerate in mass with the dark matter candidate. This means that the effects of the interactions between these charged states and the dark matter candidate must be carefully included when evaluating the predicted relic abundance of the dark matter. The formation of bound states due to the exchange of the Higgs boson may also be an important effect to include.

The astrophysics theoretical and numerical studies have been carried out on two fronts: the physics of electron and positron acceleration in the pulsar wind nebulae (PWNe) and the possible impact of the electron/positron populations from PWNe to the detected positron excess.

We have studied relativistic magnetic reconnection in both electron-positron and electron-ion plasmas. We demonstrate that reconnection rapidly accelerates both ions and electrons into power-law distributions via first-principles kinetic simulation. The ongoing new 3D simulations investigate effects of turbulence on LANL's Trinity machine and open boundary conditions on Edison machine in the National Energy Research Scientific Computing Center. The preliminary results show particle acceleration in reconnection is a robust mechanism, even with the pre-existing turbulence and different boundary conditions. We will present detailed mechanisms in those 3D simulations in publications under preparation.

In addition, we have studied the electron/positron diffusion in the PWNe and the interstellar medium (ISM). We have built codes that can track the electron/positron diffusion that has time-, space-, and energy-dependence, as well as their radiative losses via synchrotron and Compton processes. We have studied the effects of different diffusion processes which give rise to different spatial diffusion times in our model. By comparing with the PWNe observations in X-rays and TeV gamma-rays, we need to employ slow spatial diffusion. In addition, we find that the magnetic fields inside the PWNe and the ISM are comparable, so that the diffusion coefficient that we find in the PWNe is applicable to the ISM as well. With such a slow spatial diffusion, we demonstrate that most of the electrons/positrons created by pulsars and PWNe are generally close to their sources. Therefore, the detected positron excess at Earth is unlikely due to the nearby pulsars/PWNe, but could be of other origins such as dark matter annihilations.

Future Work

The tasks for this project will be divided into 4 categories: 1) construction of an outrigger detector array, 2) study of high energy physics theories of dark matter (DM), 3) plasma astrophysics simulations of pulsar wind nebulae (PWN), and 4) models of cosmic ray propagation.

We will begin the outrigger construction by first installing a few prototype detectors at the HAWC site and operating them with spare electronics from the HAWC detector in order to test components. We have ordered the components for the full outrigger array and will continue to receive, test, and assemble them here at LANL. These components will then be shipped to the HAWC site for installation later this calendar year.

Theories of Beyond the Standard Model physics can be probed by HAWC. We will investigate two features of such theories that could increase HAWC's sensitivity to annihilations of DM to Standard Model particles. These are (i) the effect that additional exotic particles, nearly degenerate in mass with the DM, may have on the cosmological evolution of the relic abundance of DM; and (ii) the effect that new exotic particles have on the present-day annihilation rate of DM. We will determine HAWC's sensitivity to such theories.

Simulations will be performed that include multi-dimensional, relativistic, magnetohydrodynamics (MHD) to model the PWN spatial morphologies and investigate the dependence on the energy injection rate. We will also

carry out simulations to study particle acceleration by relativistic reconnection using the initial conditions from MHD simulations.

Existing radiation transport codes will be modified to treat the propagation of cosmic rays, which include positrons. Two different environments will be considered: (i) the escape of cosmic rays from their sources, and (ii) their deflection and diffusion by interstellar magnetic fields on the way to Earth.

Conclusion

While the existence of dark matter is well known, the nature of the particles that comprise dark matter is not. With this project, we will increase our understanding of the possible properties of dark matter. Also, the existence of high energy emission from pulsars is well known; however, the physical mechanisms by which the particles are accelerated is not. With this project, we will detect higher energies from pulsars and compare these observations with new theoretical models. Finally, we will use radiation transport simulations to predict the locally-measured, cosmic positrons from both dark matter and pulsars. These investigations will increase the Laboratory's capabilities in information science and technology as well as remote sensing of radiation and other experimental techniques relevant to studies of our nuclear stockpile.

Publications

Beresnyak, A., and H. Li. First Order Particle Acceleration in Magnetically-Driven Flows. 2016. ASTROPHYSICAL JOURNAL. 819: 90.

Deng, W., H. Zhang, B. Zhang, and H. Li. Collision-induced Magnetic Reconnection and a Unified Interpretation of Polarization Properties of GRBs and Blazars. 2016. ASTROPHYSICAL JOURNAL LETTERS. 821: L12.

Fowler, T. K., and H. Li. Spheromaks and how plasmas may explain the ultra high energy cosmic ray mystery. 2016. JOURNAL of PLASMA PHYSICS. 82: 595820503.

Guo, F., H. Li, W. Daughton, X. Li, and Y. H. Liu. Particle acceleration during magnetic reconnection in a low-beta pair plasma. 2016. Physics of Plasmas. 23: 055708.

Guo, F., X. Li, and H. Li. Efficient Production of High-energy Nonthermal Particles during Magnetic Reconnection in a Magnetically Dominated Ion-Electron Plasma. 2016. ASTROPHYSICAL JOURNAL LETTERS. 818: 9.

Harding, J. P., C. L. Fryer, and Mendel. EXPLAINING TEV COSMIC-RAY ANISOTROPIES WITH NON-DIFFUSIVE COSMIC-RAY PROPAGATION. 2016. ASTROPHYSICAL JOURNAL. 822 (2).

Li, X., F. Guo, H. Li, and G. Li. Nonthermally Dominated Electron Acceleration during Magnetic Reconnection in a Low-β Plasma. 2015. ASTROPHYSICAL JOURNAL LETTERS. 811: L24.

Zhang, H., W. Deng, H. Li, and M. Boettcher. Polarization Signatures of Relativistic Magnetohydrodynamic Shocks in the Blazar Emission Region - I. Force-free Helical Magnetic Fields. 2016. ASTROPHYSICAL JOURNAL. 817: 63.

Dark Matter Search with a Neutrino Experiment

Richard G. Van De Water
20160037DR

Introduction

The project goals are to search for sub-GeV dark matter by enhancing the capability of the short-baseline neutrino detector (SBND), which will be the near detector for the Short Baseline Neutrino (SBN) program at Fermilab. The DOE funded project SBND is to search for sterile neutrinos, while the LDRD funded project will add the capability to detect sub-GeV dark matter.

Direct observations of dark matter would be a revolutionary discovery that would have a big impact on particle physics, nuclear physics, astrophysics, and cosmology. Searching for sub-GeV dark matter is experimentally novel and theoretically motivated, which neutrino experiments are capable of performing if they have excellent low energy particle identification and background rejection.

The experimental part of the project will involve the design and construction of a photon detection system (PDS) for the SBND detector. A fast, well-designed PDS combined with the sensitive SBND liquid argon time projection chamber (TPC) will reduce backgrounds and will allow the nominal energy threshold for signal events to be reduced from 200 MeV to below 50 MeV. This will open up the ability to search for sub-GeV dark matter signatures, which are below 200 MeV. The combination of a TPC with a PDS may also have applications in other areas, such as threat reduction and nuclear nonproliferation.

The theoretical part of the project will improve the estimation of neutrino cross-sections, which are a background to dark matter searches, and will explore dark sector models involving sub-GeV dark matter, sterile neutrinos, and their impact on future neutrino and astrophysical experiments. These efforts are important for all future accelerator-based neutrino experiments.

Benefit to National Security Missions

This work contributes directly to nuclear, particle, cosmology, and astrophysics scientific discovery. The search for sub-GeV dark matter is of fundamental importance since we know that as much as one quarter of the energy density of the universe is in a form of matter we do not understand. The direct detection of dark matter would open up a new field of research and would have a big effect on cosmology and the evolution of the universe. The specific goals of this project are to enhance the SBN program by building a photon detection system for the SBND detector to enable it to search for sub-GeV dark matter, by improving the estimation of neutrino cross-sections on argon, and by developing models of the dark sector that involve sub-GeV dark matter.

The development of liquid Argon scintillation light detection capability at LANL could lead to applications in nuclear nonproliferation such as enhanced neutron and gamma-ray portal detection. Coupled with a time projection chamber, a liquid argon detector has extremely efficient signal identification and background rejection compared to many current technologies in use. The development of LAr technology for efficient neutrino detection can also be applied to remote sensing of nuclear reactors for nuclear nonproliferation. As well, the development of the LAr technology might find application in matter-radiation interaction in the extreme, where novel fast and efficient particle identification is a requirement.

Progress

During FY16, the following experimental results were achieved:

Working with the SBND collaboration, the PDS timing requirements were defined as 15 photo-electrons/MeV energy and 100 nsec timing, with a stretch goal of 1-2 nsec timing which would give the best background rejection. To this end, a system has been designed that will achieve 15 PE/MeV and 1-2 nsec goal. This will consist of 120 8” Hammamatsu R5912 PMT’s, which has 1.5

nsec timing resolution and excellent charge dynamic range. These PMT's have been purchased and delivery of 135 PMT's by the end of July. They will be mounted uniformly on a PMT mounting structure being designed by LANL hired engineer (Jan Bossevain). The design of the PMT support structure and cable feedthrus will be completed in FY16. The electronics system that will read out the PMTs are CAEN 1730 digitization boards that have a 500 MHz digitization rate with a 14 bit charge ADC. This will achieve the timing reconstruction and charge dynamic range that is required. Also, the support readout and trigger hardware, and HV system, has been specified with CAEN and a purchase order placed. The new postdoc is studying the design of a new PMT base, and prototype boards have been built. Design of a PMT test facility has been started. Work on scintillation light simulations has begun, with initial simulation results of the PDS system already helping to guide choice of PMT's and reflector foil designs.

Also, a great deal of work has been conducted on theory, with the following accomplishments.

In nuclear theory we have pursued complete calculations of the Carbon-12 response, calculations of the response for electron scattering can be directly compared with data. Those calculations are complete and is under review by Phys. Rev. Letters. Calculations of neutrino scattering for Carbon are well underway, the neutral current response is approximately 1/2 completed and should be finished this year, the charged current calculations will take a little longer because of the computer time required. We have also worked on developing more approximate methods that are faster and can be extended to heavier nuclei. These methods still include two-nucleon currents and correlations in an accurate manner. This code is still being developed but we have reproduced PWIA calculations with free-nucleon intermediate states and we have completed calculations of the interacting two-nucleon final states. We expect to have initial results of this approach this year.

In lattice QCD we have carried out two separate calculations of the axial form factors of the nucleon. The first uses the clover-on-HISQ lattice formulation with nine ensembles generated with 2+1+1 flavor of dynamical fermions. The second uses the clover-on-clover formulation with four ensembles of 2+1 flavor fermions. The analysis of these calculations to extract form factors covering the range of momentum up to 1~GeV is being done. Methods to improve the signal in correlation functions with momentum transfer larger than 1 GeV are being developed.

Future Work

Proposed work for the next fiscal year includes the detailed design of the Short Baseline Neutrino Detector (SBND) photon detection system (PDS) and using 8-inch phototubes covered with TPB wavelength-shifting coating. Included in the PDS design will be the electronics and data acquisition system and the interface of the PDS with the time projection chamber. A protoype of the PDS DAQ and trigger system will be tested with the MiniCAPTAIN TPC detector during a neutron run at WNR. In addition, orders will be placed for time critical PDS equipment such as cable feedthrough and PMT support structure. The PMT test stand will be designed and built and PMT testing completed in FY17. The new postdoc will begin work on the reconstruction of neutrino events and the rejection of background events using only scintillation light. Studies will also be performed on the collection and use of prompt Cherenkov light, which may further improve the event reconstruction. Proposed work for the theoretical part of the project will include continued calculations of large nuclear effects in neutrino-argon scattering and the estimation of electron-neutrino charged-current cross sections on argon. These calculations will improve estimates of neutrino background rates for dark matter searches with the SBND detector. This work will include lattice QCD studies of neutrino-nucleon form factors that are used as input to the nuclear calculations. In addition, work will begin on models that employ interacting sterile neutrino interaction and their connection to the dark sector. The cosmological history of sterile neutrinos and dark matter is complicated due to the effects of dark-matter and neutrino self-interactions, as well as dark matter - neutrino interactions. The effects of these on the cosmic microwave background (CMB) will be studied through solving the coupled Boltzmann equations.

Conclusion

Final state charged particles that interact in the SBND liquid argon time projection chamber produce recoil electrons, which in turn produce scintillation light that can be detected by the photon detection system (PDS). The PDS reconstructs the neutrino or dark matter event position and time from the scintillation light. The timing of the scintillation light is approximately one nanosecond, which enables the PDS to significantly reduce backgrounds and expand the physics scope of SBND by enabling a search for sub-GeV dark matter. The development of liquid argon scintillation light detection capability at Los Alamos could lead to applications in nuclear nonproliferation such as enhanced neutron and gamma-ray portal detection.

Publications

Water, R. G. Van de. SBND PMT System Review. 6. Fermi National Accelerator Laboratory Systems Review Nov 18, 2016 .

Rapid Response to Future Threats (U)

Charles W. Nakhleh
20160664DR

Introduction

The project aims to lay the groundwork for Los Alamos nuclear weapon designers to respond to 21st century national security missions quickly and efficiently. The project will tackle two main problems facing the design community. The first problem this project will address is the development of a set of modern design tools to enable a weapon designer to develop, iterate and optimize a design effectively. These tools will be integrated with our modern Accelerated Strategic Computing (ASC) weapons simulation codes and are meant to be one tool of many used by designers when working problems. The design community currently lacks these tools and so any design efforts are often burdened with individuals having to develop these tools on their own. Often, these tools are then lost once a project ends. The design community does not have a sustained effort to maintain a capability for new design work. Developing these tools is the first step on that path. These tools are meant as an aid to anyone looking the design a new or redesign an existing system.

The second problem this project addresses is the capability to design non-traditional weapons physics packages. The goal here would be to develop a capability that could be drawn upon in the future if the country needs it. Within the design community now the bulk of work revolves around a very specific set of subjects that are defined by the existing stockpile. If the stockpile needed to evolve beyond its current state, at this point in time, it would be difficult for the design community to tackle a problem that was a region of design space outside the existing stockpile. This project would help prepare Los Alamos for that possibility.

Benefit to National Security Missions

The products developed under this LDRD will lay the groundwork for Los Alamos to respond rapidly to 21st century national security mission. The project will combine the tools developed by the Advanced Strategic Computing (ASC) Program and the Science Campaigns over the last twenty years with the cutting edge Information Science and Technology capabilities at Los Alamos for the Laboratory to respond quickly to mission requirements from DOE's Defense and Nonproliferation Programs, as well as to requirements from the DoD and Intelligence Community.

Progress

As of the date of this entry (6/21/16), the project has been active for three weeks. The team has been assembled and has started on its work tasks, but it is too early to report on specific accomplishments.

Future Work

At the end of the first year of the project there will be two main products. The first will be an in depth study to understand how to use the modern codes in a design mode as opposed to an analysis mode. In an analysis mode, more often than not, the physics models and parameters need to be rather stringent which leads to longer times for calculations. In a design setting, one needs to push through many simulations to understand the sensitivity of a device to certain design parameters. This requires that we establish how we modify certain simulation parameters to decrease physics fidelity and run time without significantly polluting the solution such that it cannot be used for understanding. This assessment has not been done in significant detail with our newer codes.

The second product from the first year will be an assessment of how the design tools that are being built will interface with the codes. For example, it is likely that the codes will have to create new outputs that the design tools can utilize. So, in effect, the software for the design tools will not be complete in the first year but a framework for how those software tools will interface with the codes and how they might work with each other will be established so that the tools can be most effective.

Conclusion

At its end, this project will supply the first version of a set of design tools that will enable a designer to quickly and efficiently execute design iteration calculation with modern design codes. The project will also provide the calculational modeling for developing a weapon physics package non-traditional weapon design outside the design space of the existing stockpile.

Illuminating the Origin of the Nucleon Spin

Ivan M. Vitev
20130019DR

Abstract

The goal of this project was to make a fundamental advance in our understanding of the origin of the proton spin, through a unique synergy between theory and experiment. The proton is made up of quarks and gluons, the elementary particles of the strong interaction. However, the measured sum of the quark and gluon intrinsic angular momenta only accounts for ~1/3 of the total proton spin. This deficit has been referred to as the "proton spin crisis". The missing fraction of the spin is likely carried by the orbital angular momentum of the quarks and gluons.

In a strategic partnership with Fermilab, we have developed a new experiment (E1039) that can make the world's first measurements of the sea quark Sivers distribution, a quantity expected to be related to the orbital angular momentum. A proposal for the experiment was written and received stage-1 approval from Fermilab. Experiment E1039 requires the use of a new high-luminosity transversely polarized proton target, which we have successfully constructed and recently tested at the University of Virginia.

An equally important goal of this project was to understand the relative significance of these spin contributions in the theory of strong interactions, Quantum Chromodynamics (QCD), and how they manifest themselves in reactions with polarized proton beams and/or targets. We have developed the state-of-the-art theoretical and computational tools necessary to interpret the experimental results that will lead to a major breakthrough in our understanding of the structure of matter and the theory of strong interactions.

This project has successfully placed our team of experts at LANL in a leadership role to address this most urgent science question for the international spin physics community, which has become a top science priority for the US nuclear physics program.

Background and Research Objectives

Each atom that makes up everyday matter has a dense nucleus composed of nucleons (protons and neutrons). These nucleons are, in turn, composed of smaller particles called quarks and gluons. These facts are well established, but just how the quarks and gluons act together to give a nucleon its mass and spin is not understood. Spin plays a key role in the determination of the properties of fundamental particles and their interactions. Spin effects have often challenged our understanding of the underlying physics mechanisms of experimental phenomena. Only recently, however, has a strategy emerged of how to determine the individual contribution of quarks, gluons and their orbital angular momentum to the overall nucleon spin [1,2]. Implementing this strategy in a joint experimental and theoretical program will result in a new fundamental test of the theory of strong interactions, Quantum Chromodynamics, which will revolutionize our understanding of the structure of the proton [3]. The insight gained from these developments in theory and experiment is essential to construct, for the first time, an accurate 3-dimensional picture of the nucleon in momentum space [2].

Two of the best-known unpolarized reactions with nucleons are: (1) particle production from a proton target bombarded with energetic leptons (e, μ), known as Semi-Inclusive Deep Inelastic Scattering (SIDIS) and (2) lepton pair production from a proton target bombarded with a pion or a proton beam, known as the Drell-Yan (DY) process. In recent years, important progress has been made in SIDIS measurements with polarized targets at various laboratories across the world [4,5]. These measurements indicate that the sum of the quark spins, in the "valence" region where quarks carry a large fraction of the proton momentum, contributes only ~ 30% of the nucleon spin [6], a critical problem known as the "spin crisis". The spin program at the Relativistic Heavy Ion Collider (RHIC) has shown that the contribution of the gluon spins to the proton spin is small. A physics

picture is now emerging, which suggests that the orbital motion of quarks from the "sea" region, where they don't carry a large fraction of the nucleon momentum but are instead plentiful, contributes most of the proton spin. The correlation between the proton spin direction and the quark transverse momentum is described by the "quark Sivers distribution" f1T [7]. The Sivers distribution vanishes if the quarks have no orbital angular motion. One of the essential predictions of the theory of strong interactions is that the sign of the quark Sivers distribution must change when going from SIDIS to DY measurements with polarized targets: f1T(DY) = -f1T(SIDIS) [2]. No such DY experiment has ever been performed to test this prediction. An ongoing COMPASS experiment in Europe uses a pion beam to produce lepton pairs and probes the valence quarks. There exists a unique opportunity to advance the theory of transverse momentum dependent distributions (TMDs) and build a polarized target system for the first polarized Drell-Yan measurement in the US and the first polarized Drell-Yan measurement in the sea quark region. What sets the quest to understand the origin of the nucleon spin apart from other exciting questions in nuclear and particle physics is that experimental discoveries in this area are expected in the next five years, due to worldwide interest and intense competition.

To this end, we proposed a combined theoretical and experimental program to significantly advance the understanding on nucleon structure and pave the way toward a measurement of the Sivers asymmetry in the sea quark region using polarized Drell-Yan production. The objectives of the project were

Experiment
To construct a polarized ammonia target by modifying an existing LANL superconducting magnet, develop a new nuclear magnetic resonance (NMR) system to accurately determine the proton polarization, perform simulations to optimize the experimental setup and determine the accuracy of the Sivers asymmetry measurement, prepare proposals to Fermilab and DOE for the polarized target installation into the existing unpolarized SeaQuest experiment, consistent with the Fermilab beam schedule, and for two years of data taking and analysis.

Theory
To utilize the power of three complementary approaches, perturbatiive Quantum Chromodynamics (pQCD), a modern effective theory of the strong interactions – soft collinear effective theory (SCET), and lattice QCD to significantly advance the understanding of nucleon structure and the Sivers asymmetry in reactions with polarized nucleons.

Scientific Approach and Accomplishments

Experiment
We built and tested the world's highest luminosity capacity polarized proton target, which consists of several different major components that we describe in the following sections.

The central part of the experiment is the polarized target, consisting of a superconducting magnet, a refrigerator system and a microwave oscillator. Since a new superconducting magnet would have been beyond the financial limits of an LDRD project, we were able to identify an old existing magnet at LANL. However, this magnet has been in storage for 20 years and had a longitudinal coil configuration, instead of the transverse field we require. In order to reorient the coils into the required geometry, we had to send the magnet back to Oxford Instruments in Oxford, UK (the original manufacturer) and have the coils rearranged. Before the magnet was shipped, we performed a system test with the old configuration at the University of Virginia (UVa), in order to ensure that the magnet was still able to achieve the necessary field of 5T. After the successful completion of this test, Oxford performed the coil rotation and magnet refurbishment. In order to polarize ammonia in such a system, the requirements on the field homogeneity are extremely stringent and in Jan 2014, we went to Oxford to perform these measurements. By optimizing the shim coils, we were able to achieve the required homogeneity and had the magnet shipped back to the US. The superconducting magnet is shown being tested in Figure 1.

Due to aging, the helium refrigerator had developed leaks, which we detected in tests at UVa. Those leaks were fixed at the UVa machine shop and we refurbished the refrigerator with new Alan Bradley resistors and new electronics.

In order to achieve the low temperature of 1K, large mechanical vacuum pumps are needed. We designed a three stage ROOTS pump system based on the heat load from the microwave tube as well as the beam current. After purchasing this system, we installed the pumps at Fermilab and tested this system. In addition, we designed the pumping line and purchased all of the necessary components required for remote and safe operation.

To achieve dynamic nuclear polarization in a field of 5T, a 140 GHz microwave oscillator tube is needed. Our test of the microwave tube from the old system revealed that the tube had aged to such a degree that the power was too low for our new extended target. We therefore purchased a new tube with a new power supply and successfully put them into service.

Figure 1. Polarized Magnet

Furthermore, we designed a new target structure, holding four cells, where three contain the polarization material and the fourth is a calibration cell. Due to the extended target geometry needed for this experiment, our cells have three NMR coils distributed over the length of the target, in contrast to the usual one per cell geometry. This leads to a total of 9 NMR circuits per target stick, which would have made using the traditional Q-meter system from Liverpool dating from the 1990's prohibitively expensive. We therefore designed a completely new NMR readout system, which is based upon state of the art components and integrated in standard VME crates. Figure 2 shows one channel of the new NMR hardware in operation. Because of this new NMR design, we had to design, develop and build a new slow control system. In order to achieve better integration of all the components, we built a new software system, which now asynchronously controls all of the different processes.

Together with UVa, we produced the necessary frozen ammonia and went to the National Institutes of Standards and Technology, where we irradiated the material to produce the paramagnetic centers, necessary for the polarization.

The complete polarized target system was tested in April of 2016 and reached better than 90% polarization. Figure 3 shows the target polarization versus time as the microwave frequency is being optimized.

Extensive computer simulations of the spectrometer performance and experimental sensitivity to the Sivers function were performed in order to optimize the measurement. A letter of intent for the new experiment was then prepared and presented to the Fermilab Program Advisory Committee (PAC) in 2013 [8]. The letter was well received and the Director granted E1039 first stage approval. In 2015 we presented an update to the PAC, describing the progress and status of the experimental preparations.

Figure 2. The LANL NMR system

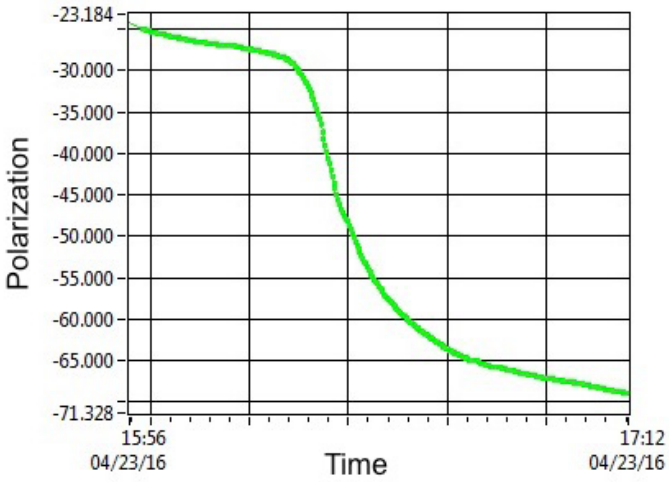

Figure 3. The results for the polarization tests at UVa. The y-axis shows the polarization in percent and the x-axis displays time.

We have since worked closely together with Fermilab to design and estimate the cost of the necessary changes to the existing spectrometer. New beam line optics, a new radiation shielding plan and a new cryogenic plant have all been designed. Additionally we have designed a new target actuator mechanism and mechanical configuration for integrating the target into the existing spectrometer.

With the costs for the new experiment now well understood, a construction proposal was written and is currently under review by the Department of Energy [9].

Theory

In theory we have pursued a three-pronged approach to elucidate the three-dimensional (3D) nucleon structure and to prepare the analysis tools for the upcoming polarized Drell-Yan (DY) measurements.

In the framework of perturbative QCD we have performed accurate theoretical calculations of asymmetric particle distributions (spin asymmetries) in reactions with polarized proton targets [10,11]. An important achievement was to understand the energy dependence of the particle production rates and the quark Sivers distribution in both SIDIS and DY processes. This allowed us to carry out a global analysis of existing SIDIS data and extract the Sivers function from the measurements [12]. A 3D plot of the up (u) quark Sivers distribution in momentum space is shown in Figure 4. The left-right asymmetry, which translates into asymmetric particle production, is clearly seen. We made predictions for the DY Sivers asymmetry relevant to our E1039 experimental kinematics. Our work and global analysis effort are recognized by the spin/TMD community as the most accurate study of the Sivers asymmetry in SIDIS/DY production. Toward the end of the DR project we developed a simulation package, which can be easily used to calculate the Sivers asymmetry for Drell-Yan production, and other vector bosons (for example, the W and Z elementary particles of the Standard Model). This package is flexible, and can be adapted to various experimental setups. It was used to calculate the Sivers asymmetry of W bosons at 500 GeV for the kinematics relevant to Relativistic Heavy Ion Collider (RHIC) at Brookhaven National Laboratory [13]. Recently, our calculations have been compared with the recent RHIC measurement for W production.

In the area of soft collinear effective theory we published a rigorous proof of the equivalence of traditional perturbative QCD and SCET methods of resummation of large logarithms and new ways to improve the accuracy of predictions using both methods for cross sections in momentum-space, for example Drell-Yan transverse momentum kT distributions [14]. The paper is viewed as “remarkable, likely to become a classic.” With support from the DR project the first proof that an important ingredient in the SCET formalism, the soft function, is the same in Drell-Yan production, deep Inelastic scattering, and electron-positron (e+e-) collisions up to two-loop order (high accuracy) [15]. That means that emission of up to two low-energy gluons affects observables in these three types of collisions in the same way. With existing known results on the two-loop e+e- soft function, this is the first two-loop result for the SIDIS and DY soft functions, and makes possible percent-level accuracy in predictions for all three types of cross sections. We began to develop technology for the definition, computation, and evolution of transverse momentum-dependent parton distribution functions (TMDPDFs) in SCET using a new rapidity renormalization group technique. We completed one-loop computations of quark and gluon TMDPDFs and also identified their transverse momentum (kT) evolution to high accuracy. Promising new strategies to resum kT distributions directly in momentum space rather than going through its Fourier transform into position (or impact parameter) space were identified. We are preparing a publication on these novel results to follow on soon after the close of the DR period.

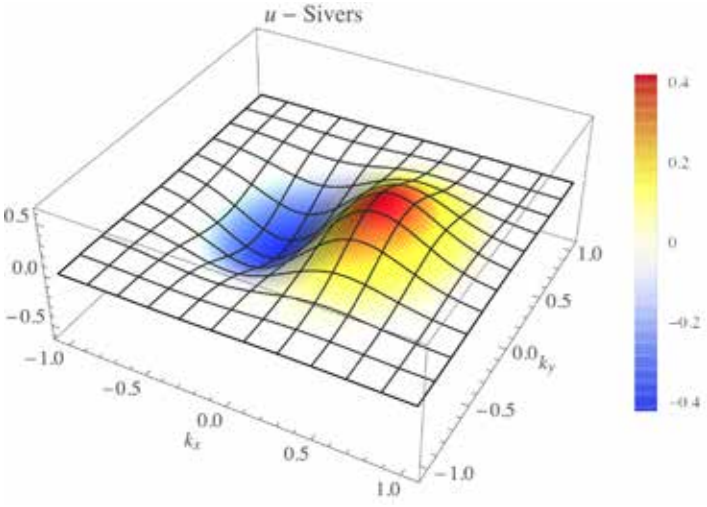

Figure 4. A three-dimensional view of an up (u) quark Sivers function at a momentum fraction x=0.1 as a function of the transverse momentum k obtained through our global analysis of experimental data. Note the asymmetric momentum distribution at an energy scale Q = 1.4 GeV.

Our lattice QCD effort included high statistics calculations of both Sivers and Boer-Mulders (another TMD) functions on two 2+1 quark flavor ensembles with different lattice actions, domain wall at lattice spacing 0.08 fm and Wilson-Clover at lattice spacing 0.114 fm, to study discretization errors. The pion mass in the two calculations was roughly the same, 300 MeV. Using bilinear quark operators with staple-shaped Wilson lines, we studied transverse momentum dependent parton distribution functions (TMDs) of the proton. For naively time-reversal odd observables, we calculate the generalized Sivers and Boer-Mulders transverse momentum shift in SIDIS and DY cases, and for T-even observables we calculated the transversity related to the tensor charge and the generalized worm-gear shift [16]. The higher statistics Wilson-Clover results allowed us to quantify the behavior as a function of the Collins-Soper parameter (zeta), which controls the approach to the physical limit. The lattice data was compared to and found to be compatible with a phenomenological extraction of the Sivers shift [12]. This can be seen in Figure 5. An important product of our work is a novel application of

machine learning techniques to lattice QCD calculations [17]. New quasi-parton distribution functions (QPDFs) that can be evaluated on the lattice have also recently been proposed. We presented a model calculation that allows us to determine the nucleon boost at which QPDFs approach standard PDFs [18].

The project team is grateful to the LDRD office for largely restoring budget cuts to this LDRD DR project, which allowed us to meet the project goals.

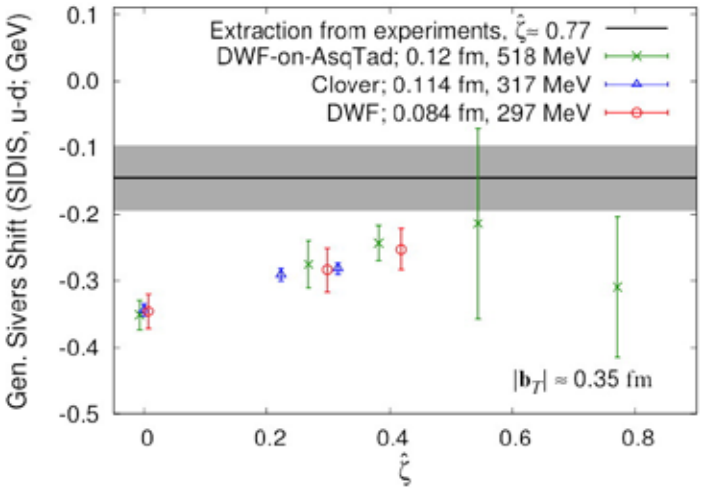

Figure 5. Comparison of the generalized Sivers shift for the difference of up and down quarks (u-d) for different lattice actions and pion masses. In the limit of large proton momentum lattice results approach the generalized Sivers shift obtained form fits to experimental data on reactions with a polarized proton target.

Impact on National Missions

This work has had significant impact on the Lab and National Missions. It strengthened LANL's role as a leader in polarized proton reactions. We constructed a state-of-the art high-luminosity polarized ammonium target, a new NMR system and developed the related theory for the most precise understanding of nucleon structure. LANL is now recognized as the spearhead in the effort to determine the Sivers function for sea quarks.

Our DR project brought outstanding young researchers to LANL. Zhongbo Kang, formerly an Oppenheimer Fellow, joined T Division. Kun Liu and Boram Yoon were converted to staff in P and CCS Divisions, respectively. David Kleinjan is getting his security clearance and looking forward to staying at LANL. The work on spin physics, new effective theories of the strong interaction, and transverse momentum dependent distributions helped leverage a prestigious DOE Early Career award for Christopher Lee. The important accomplishments of the DR project, experimental advances and new theoretical results, have strengthened our existing lines of funding for Medium Energy Nuclear Physics and Nuclear Theory, with additional support for work at Fermilab and the spin effort in T Division. The newly formed LANL-led E1039 polarized Drell-Yan collaboration was invited to write a proposal for two years of data taking at Fermilab by the DOE Office of Science, Office of Nuclear Physics. The proposal was recently submitted to DOE and there is interest in using our state-of-the art polarized proton target elsewhere. The synergy between perturbative QCD, SCET, and Lattice QCD used to attack this outstanding problem in nucleon structure, which our team envisioned and implemented in this DR project, became the model for the new global theory effort to map out the 3D landscape of the nucleon. This initiative grew into a US-wide Nuclear Theory Topical Collaboration to study transverse momentum distributions, one of only three Topical Collaborations funded by DOE Nuclear Theory for the next 5 years.

References

1. Florian, D. de, R. Sassot, and M. Stratmann. QCD spin physics: Partonic spin structure of the nucleon. 2012. Progress in Particle and Nuclear Physics. 67: 251.

2. al, D. Boer et. Gluons and the quark sea at high energies: Distributions, polarization, tomography. 2011. Institute for Nuclear Theory Program Report.

3. al, R. Tribble et. The frontiers of nuclear science: A long range plan. 2007. DOE Office of Science.

4. al, A. Airapetian et. Single-spin asymmetries in semi-inclusive deep-inelastic scattering on a transversely polarized hydrogen target. 2005. Physical Review Letters. 94: 012002.

5. al, V. Alexakhin et. First measurement of the transverse spin asymmetries of the deuteron in semi-inclusive deep inelastic scattering. 2005. Physical Review Letters. 94: 202002.

6. Bass, S.. The spin structure of the proton. 2005. Review of Modern Physics. 77: 1257.

7. Sivers, D.. Single-spin production asymmetries from the hard scattering of pointlike constituents. 1990. Physical Review D. 41: 83.

8. Klein, A., and X. Jiang. Letter of intent for a Drell-Yan experiment with a polarized proton target. 2013. Program Advisory Committee.

9. Klein, A.. SeaQuest with a transversely polarized target (E1039). 2016. Department of Energy.

10. Kang, Z. B., I. Vitev, and H. X. Xing. Transverse mo-

mentum-weighted Sivers asymmetry in semi-inclusive deep inelastic scattering at next-to-leading order. 2013. PHYSICAL REVIEW D. 87: 034024.

11. Dai, L., Z. Kang, A. Prokudin, and I. Vitev. Next-to-leading order transverse momentum-weighted Sivers asymmetry in semi-inclusive deep inelastic scattering: the role of the three-gluon correlator . 2015. Physical Review D. 92 (11): 114024.

12. Echevarria, M., A. Idilbi, Z. Kang, and I. Vitev. QCD Evolution of the Sivers Asymmetry . 2014. Physical Review D. 89: 074013.

13. Huang, J., Z. Kang, I. Vitev, and H. Xing. Spin asymmetries for vector boson production in polarized p+p collisions. 2016. Physical Review D. 93: 014036.

14. Almeida, L., C. Lee, S. Ellis, I. Sung, G. Sterman, and J. Walsh. Comparing and counting logs in direct and effective methods of QCD resummation. 2014. Journal of High Energy Physics. 1404: 174.

15. Kang, D., O. Labun, and C. Lee. Equality of hemisphere soft functions for e+e-, DIS and pp collisions at O(alphas**2). 2015. Physics Letters B. 748: 45.

16. Yoon, B., R. Gupta, and T. Bhattacharya. Nucleon transverse momentum-dependent parton distributions from Lattice QCD. Physical Review D.

17. Yoon, B.. Estimation of matrix trace using machine learning. Journal of Computational Physics.

18. Gamberg, L., Z. Kang, I. Vitev, and H. Xing. Quasi-parton distribution functions: a study in the diquark spectator model . 2015. Physics Letters B. 743: 112.

Publications

Almeida, L., C. Lee, S. Ellis, I. Sung, G. Sterman, and J. Walsh. Comparing and counting logs in direct and effective methods of QCD resummation. 2014. Journal of High Energy Physics. 1404: 174.

Dai, L., A. Prokudin, Z. Kang, and I. Vitev. Next-to-leading order weighted Sivers asymmetry in semi-inclusive deep inelastic scattering: three-gluon correlator. 2015. In DIS 2015. (Dallas, May 2015). , p. 246. Trieste: Proceedings of Science.

Dai, L., Z. Kang, A. Prokudin, and I. Vitev. Next-to-leading order transverse momentum-weighted Sivers asymmetry in semi-inclusive deep inelastic scattering: the role of the three-gluon correlator . 2015. Physical Review D. 92 (11): 114024.

Echevarria, M.. QCD Evolution of the Sivers Asymmetry. 2015. In QCD Evolution Workshop 2014. (Santa Fe, NM, 12-16 May, 2014). , p. 1560025. Singapore: World Scientific.

Echevarria, M., A. Idilbi, Z. Kang, and I. Vitev. QCD Evolution of the Sivers Asymmetry . 2014. Physical Review D. 89: 074013.

Engelhardt, M., B. Musch, T. Bhattacharya, R. Gupta, P. Hagler, A. Schaefer, S. Syritsin, and B. Yoon. Nucleon transverse momentum-dependent parton distributions from domain wall fermion calculations at 297 MeV pion mass . 2015. In 32nd International Symposium on Lattice Field Theory (Lattice 2014). (Brookhaven, NY, June 23-28, 2014). , p. 23. Trieste23: SISSA.

Gamberg, L., Z. Kang, I. Vitev, and H. Xing. Quasi-parton distribution functions: a study in the diquark spectator model . 2015. Physics Letters B. 743: 112.

Gamberg, L., Z. Kang, and A. Prokudin. Indication on the process-dependence of the Sivers effect. 2013. Phys. Rev. Lett.. 110: 232301.

Huang, J., Z. Kang, I. Vitev, and H. Xing. Spin asymmetries for vector boson production in polarized p+p collisions. 2016. Physical Review D. 93: 014036.

Jian, X.. Single Spin Asymmetries of Inclusive Hadrons Produced in Electron Scattering from a Transversely Polarized 3He Target. 2015. In QCD Evolution Workshop. (Santa Fe, NM, 12-16 May 2014). , p. 1560067. SIngapore: World Scientific.

Kang, D., O. Labun, and C. Lee. Equality of hemisphere soft functions for e+e-, DIS and pp collisions at O(alphas**2). 2015. Physics Letters B. 748: 45.

Kang, Z.. Single transverse spin asymmetries in polarized SIDIS and pp scattering. Invited presentation at The 5th Workshop of the APS Topical Group on Hadronic Physics. (Denver, 10-12 April 2013).

Kang, Z.. Nucleon spin: longitudinal, transverse, and evolution. Invited presentation at 2014 RHIC and AGS Annual Users Meeting. (Upton, NY, 17-20 Jun. 2014).

Kang, Z.. Advances in the determination of TMDs from global analysis. Invited presentation at E1039/E906 Collaboration Meeting. (Santa Fe, NM, February 11-13, 2015).

Kang, Z.. TMD evolution and global analysis. Invited presentation at The 6th Workshop of the APS Topical Group on Hadronic Physics. (Baltimore, MD, April 8-10, 2015).

Kang, Z.. Transverse single spin asymmetry of the W production at RHIC. Invited presentation at 2015 RHIC and AGS Annual Users Meeting. (Upton, NY, June 9-12,

2015).

Kang, Z.. Spin physics of Sivers, Collins, pA, and jets. Invited presentation at 2016 RHIC and AGS Annual Users Meeting, Brookhaven National Laboratory. (Upton, June 2016).

Kang, Z.. Recent progress on TMD study and future perspective at the EIC. Invited presentation at International Conference on the Structure of Baryons. (Tallahassee, May 2016).

Kang, Z.. TMDs: Theory overview. Invited presentation at APS April meeting 2016. (Salt Lake City, Apr 2016).

Kang, Z.. Transverse single spin asymmetry of the W production at RHIC. Invited presentation at 2015 RHIC and AGS Annual Users Meeting, Brookhaven National Laboratory. (Upton, June 2015).

Kang, Z.. TMD evolution and global analysis. Invited presentation at The 6th workshop of the APS topical group on hadronic physics. (Baltimore, Apr 2015).

Kang, Z.. Advances in the determination of TMDs from global analysis. Invited presentation at E1039/E906 Collaboration Meeting 2015. (Santa Fe, Feb 2015).

Kang, Z.. QCD frontiers in high energy nuclear physics: quantum correlation and many-body dynamics. Invited presentation at High energy and astro-particle (HEAP) seminar, department of physics and astronomy, UCLA. (Los Angeles, May 2016).

Kang, Z. B., I. Vitev, and H. X. Xing. Transverse momentum-weighted Sivers asymmetry in semi-inclusive deep inelastic scattering at next-to-leading order. 2013. PHYSICAL REVIEW D. 87: 034024.

Kang, Z., A. Prokidin, P. Sun, and F. Yuan. Extraction of quark transversity distribution and Collins fragmentation functions with QCD evolution. 2016. Physical Review D. 93: 014009 .

Kang, Z., A. Prokudin, P. Sun, and F. Yuan. Nucleon tensor charge from Collins azimuthal asymmetry measurements. 2015. Physical Review D. 91: 071501.

Kang, Z., A. Prokudin, P. Sun, and F. Yuan. TMD evolution for Collins asymmetries in e+e− annihilation and SIDIS. 2015. Int. J. Mod. Phys. Conf.. 37: 1560027.

Kang, Z., L. Gamberg, and A. Prokudin. Transverse momentum-weighted Sivers asymmetry in semi-inclusive deep inelastic scattering at next-to-leading order. 2014. Int. J. Mod. Phys. Conf. Ser.. 25: 1460018.

Kang, Z., and B. W. Xiao. Sivers asymmetry of Drell-Yan production in small-x regime. 2013. Phys. Rev. D. 87: 034038.

Klein, A.. An Experiment to Measure the Sivers Asymmetry of the Sea Quarks. 2015. In QCD Evolution Workshop. (Santa Fe, NM, 12-16 May, 2014). , p. 1560064 . Singapore: World Scientific.

Klein, A.. Drell Yan at FNAL with a Polarized Target. Invited presentation at DNP Fall Meeting. (Waikoloa, HI, 6-11 Oct. 2014).

Klein, A.. The status of the polarized target and E1039. Invited presentation at Fermilab PAC Meeting. (Batavia, IL, January 2015).

Klein, A.. Polarized Drell Yan with SeaQuest. Invited presentation at Physics Seminar, Mississippi State University. (Mississippi State, May 2016).

Klein, A.. Polarized Drell Yan with SeaQuest. Presented at 22nd International Spin Symposium. (Urbana-Champaign, Sep 2016).

Klein, A., P. McGaughey, and I. Vitev. Letter of Intent for a Drell-Yan experiment with a polarized proton target. 2013. Fermilab PAC .

Kleinjan, D.. A polarized Drell-Yan experiment at Fermilab. Invited presentation at CIPANP2015. (Vail, CO, 19-24 May 2015).

Kleinjan, D.. A future polarized Drell-Yan experiment at Fermilab. 2016. eConf Proceedings. : C150519.

Kleinjan, D.. Measuring nucleon TMD spin-momentum correlations via Drell-Yan at Fermilab E906/E1039 SeaQuest experiment. Presented at International Conference on the Structure of Baryons, Baryons 2016. (Tallahassee, May 2016).

Kleinjan, D.. Accessing the SeaQuark Orbital Angular Contribution to the Proton's Spin. Presented at Fall DNP Meeting 2015. (Santa Fe, Oct 2015).

Kleinjan, D.. E1039 target position and magnet studies. Invited presentation at E906/E1039 Collaboration meeting. (Santa Fe, Feb 2015).

Kleinjan, D.. E1039 Monte Carlo simulations and analysis. Invited presentation at E906/E1039 Collaboration meeting. (Batavia, June 2016).

Kleinjan, D.. E1039 slow control using Labview. Invited presentation at E906/E1039 Collaboration meeting. (Batavia, June 2016).

Kleinjan, D.. Understanding proton spin structure via the dynamics of its sea quarks. Presented at P-Division postdoc summer seminar series, Los Alamos National Laboratory. (Los Alamos, June 2015).

Kleinjan, D., and A. Klein. A Polarized Drell-Yan experiment

to probe the dynamics of the nucleon sea. Invited presentation at Diffraction 2014. (Primošten (Croatia), 10-15 Sept. 2014).

Lee, C.. QCD Resummation: Comparing Direct and Effective Methods. Invited presentation at Boston Jet Workshop. (Boston, MA, 21-23 Jan. 2014).

Lee, C.. Comparing and Counting Logs in Direct and Effective Methods of Resummation. Invited presentation at SCET 2014. (Munich, Germany, 24-26 March, 2014).

Lee, C.. The Evolution of Soft-Collinear Effective Theory. 2015. In QCD Evolution Workshop. (Santa Fe, NM, 12-16 May, 2014). , p. 1560045. Singapore: World Scientific.

Lee, C.. Towards High Precision Resummation and Evolution Using SCET. Invited presentation at E1039/E906 Collaboration Meeting. (Santa Fe, Feb. 2015).

Lee, C.. Direct and Effective Methods of QCD Resummation. Invited presentation at Loopfest XIII. (New York, 18-20 June, 2014).

Lee, C.. Introduction to SCET for LHC and collider physics. Invited presentation at KIAS Workshop on QCD and LHC Physics. (Seoul,, 26-28 April, 2016).

Lee, C.. Soft collinear effective theory in QCD. Invited presentation at at 2016 Huada School on QCD in the EIC Era. (Wuhan, 30 May – 3 June, 2016).

Lee, C.. Hadronization effects on event shapes and jets. Invited presentation at SM@LHC . (Pittsburgh, May 4, 2016).

Liu, K.. E906 improvements for E1039. Invited presentation at E906/E1039 collaboration meeting. (Santa Fe, Feb 2015).

Liu, K.. DAQ upgrade options. Invited presentation at E906/E1039 collaboration meeting. (Batavia, June 2016).

Liu, K.. Drell-Yan experiment with polarized proton target. Invited presentation at Opportunities for polarized physics at Fermilab. (Batavia, May 2013).

Liu, K.. The E906/SeaQUest Experiment: Present and future. Invited presentation at 46th Annual Fermilab Users Meeting, Fermilab. (Batavia, June 2013).

Liu, K.. The E906/SeaQUest experiment: present and future. Presented at 4th joint meeting of APS Division of Nuclear Physics and Physical Society of Japan. (Hawaii, Oct 2014).

Liu, K.. The E906/SeaQuest experiment. Invited presentation at 48th annual Fermilab users meeting. (Batavia, June 2015).

Liu, K.. Current and future DY spin and p-A activities at Fermilab. Invited presentation at RBRC Workshop Emerging Spin and Transverse Momentum Effects in pp and pA Collisions, Brookhaven National Laboratory. (Upton, Feb 2016).

Liu, M.. A new polarized solid proton target for Fermilab E1039 Drell-Yan experiment . Invited presentation at Spin2014. (Beijing, China, 20-24 Oct. 2014).

Mirabal-Martinez, J.. The E1039 NMR system. Invited presentation at E906/E1039 collaboration meeting. (Batavia, June 2016).

Mirabal-Martinez, J.. Update on E1039 NMR and microwave systems. Invited presentation at E906/E1039 collaboration meeting. (Santa Fe, Feb 2015).

Prokudin, A.. Transverse Spin Asymmetries and TMD Evolution. Invited presentation at POETIC V. (New Naven, CT, 22-26 Sep. 2014).

Vitev, I.. Transverse momentum-weighted Sivers asymmetry in semi-inclusive deep inelastic scattering at next-to-leading order . Invited presentation at QCD Evolution Workshop 2013. (Newport News, 14-17 May 2013).

Vitev, I.. Theoretical Spin Effort at LANL. Invited presentation at E1039 Collaboration Workshop. (Batavia, IL, 18 March, 2014).

Vitev, I.. A study of quasi-parton distribution functions in the diquark spectator model . Invited presentation at QCD Evolution 2015. (Newport News, VA, May 26-30, 2015).

Vitev, I., Z. Kang, and H. Xing. Transverse Momentum-weighted Sivers Asymmetry in Semi-inclusive Deep Inelastic Scattering at Next-to-leading Order . 2014. International Journal of Modern Physics Conference Series. 25: 1460019.

Yoon, B.. Disconnected Contributions to Nucleon Structure. Invited presentation at Lattice QCD 2014. (Upton, NY, 23-28 Jun. 2014).

Yoon, B.. Nucleon transverse momentum-dependent parton distributions: Comparing Clover and Domain wall fermion results at ~300 MeV pion mass. Invited presentation at The 33rd International Symposium on Lattice Field Theory. (Kobe, 14-18 July, 2015).

Yoon, B.. Nucleon TMDs from Lattice QCD . Invited presentation at 22nd International Spin Symposium. (Champaign, September 2016).

Yoon, B.. Nucleon structure using Lattice QCD . Invited presentation at 2016 OLCF User Meeting. (Oak Ridge, May 2016).

Yoon, B.. Nucleon TMDs: comparing Clover and domain wall fermion results at 300 MeV pion mass . Presented at The 33rd International Symposium on Lattice Field Theory. (Kobe, July 2015).

Yoon, B.. Estimation of matrix trace using machine learning. Journal of Computational Physics.

Yoon, B., R. Gupta, and T. Bhattacharya. Nucleon transverse momentum-dependent parton distributions from Lattice QCD. Physical Review D.

First Direct Measurement of High-Z/Low-Z Plasma Interface Evolution in Isochorically Heated Dense Plasma (U)

Brian J. Albright
20140029DR

Abstract

The evolution of high-Z matter embedded in high-density, low-Z plasma is of profound importance to understanding mix in settings of thermonuclear burn. This project sought to employ the unique capabilities of laser-generated ion beams at the LANL Trident laser to study this problem by rapidly heating a solid-density, multi-material target into a well characterized, dense plasma state and then by probing the evolution of high-Z/low-Z interfaces in this plasma over nanosecond time scales. Several experimental diagnostics enabled a comprehensive characterization of the dense plasma state achieved. What made this experiment unique was the highly uniform initial density and temperature, thus allowing for controlled experiments in this challenging experimental regime for the first time. Complementing and guiding the experiments were computer calculations using the RAGE and LASNEX codes as well as a large array of kinetic plasma codes: VPIC particle-in-cell, iFP implicit Fokker-Planck, and molecular dynamics simulations, to name a few, and advances were made in our understanding of interfacial diffusion and mix in plasmas. In the course of this project, the team discovered and published several new ways of diagnosing the properties of dense plasmas and presented equations-of-state results that were consistent with our SESAME tables. Research into laser-based ion source development led to significant, potentially groundbreaking advances in laser-based neutron and hard x-ray sources, both of impact to major Lab and complex priorities.

Background and Research Objectives

This research project sought to use the unique capabilities of the LANL Trident laser system to resolve long-standing questions in our understanding of mix in plasma: how do material interfaces evolve in plasma? What roles to electrostatic fields play in mix? What is the final state of the material? This problem is of critical importance to a wide range of settings, including astrophysics, fusion energy, and defense applications. Indeed, kinetic plasma simulations of plasma-phase mix confirm anomalously rapid mixing and a period of super-diffusive, i.e., faster than diffusive, growth of mix layers in plasma (see Figure 1).

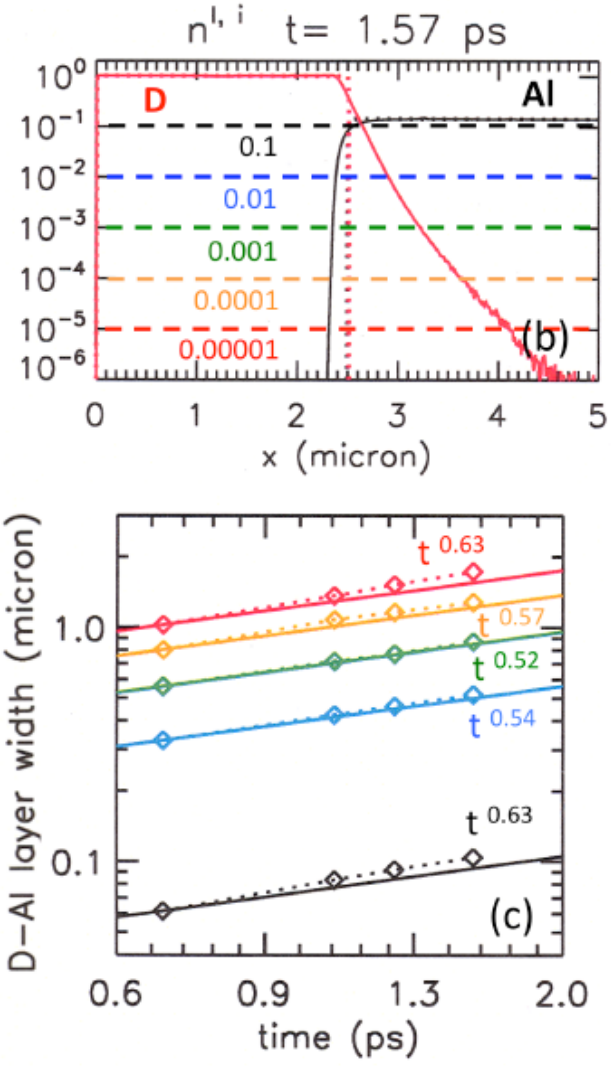

Figure 1. VPIC kinetic modeling of interfacial mix in a dense deuterium-aluminum plasma. The top panel shows the mix profiles at a time t=1.57 ps. The dashed curves in the bottom panel are level set separation distances as a function of time.

The solid curves are the diffusive scaling; that the dashed curves lie above the solid curves indicates that the mix layer grows faster than diffusively.

One of the reasons this problem is so hard to tackle experimentally is that making dense plasma requires enormous facilities, such as the National Ignition Facility at Lawrence Livermore National Laboratory or the Z Machine at Sandia National Laboratories; in such, the time scale over which plasma is assembled, tens of billionths of a second, is the same as that over which the plasma expands or "disassembles." Consequently, it is very hard to make plasma that is uniform in order to do a controlled experiment. Instead, experiments have large variations in temperature and density, making the results one obtains ambiguous and difficult to interpret.

This project instead employed ion beams made from the ultra-intense, short-pulse Trident laser to heat solid-density targets "isochorically," or much faster than the disassembly time. This meant that we could prepare highly uniform dense plasma in which to measure the plasma conditions to unprecedented precision, something that had never been done before. We used streaked optical shadowgraphy measurements to infer the material properties of the warm dense matter we prepared and we also measured the evolution of plasma interfaces using a series of x-ray "snapshots" with a gated x-ray camera. Streaked optical pyrometry measurements allowed us to further characterize and confirm the warm dense matter states obtained our experiments. Also, while we explored options to measure the interfacial electrostatic fields directly through proton deflectometry and spectroscopy, this proved untenable owing to limited shot time and budget for further diagnostics development.

Together with an integrated theory and modeling effort using ASC multi-physics codes and the world-leading VPIC kinetic plasma code, our objective was to advance the state of art in plasma mix research and we believe we have succeeded in this goal.

Scientific Approach and Accomplishments

The end goal of the project was to carry out high-power short-pulse laser experiments that were among the most complex and difficult ever fielded. To be successful, our approach required that we mitigate risk where possible by building up our experimental capability through a series of steps, each of which demonstrated a key component of our final experiments. In the end, we were able to field an integrated experiment incorporating all elements mentioned above.

The major steps taken in our experimental plan were as follows:

Improvement to the laser-based ion sources

An early success of this project was the discovery of a new method of controlling laser-based ion beams so that we can simultaneously achieve high ion beam current, high energy per nucleon, and a high degree of energy localization [1], accomplished through the interaction of the self-magnetic field structures behind the laser target with the laser-accelerated ions and electrons. The use of these novel ion beams enabled us to achieve more uniform heating of our targets and thus more controlled dense plasma formation in the desired state.

Design study of target materials and target plasma conditions. Through extensive use of the Stopping and Range of Ions in Matter (SRIM) code, we were able to guide our choice of target material compositions and thicknesses (see Figure 2).

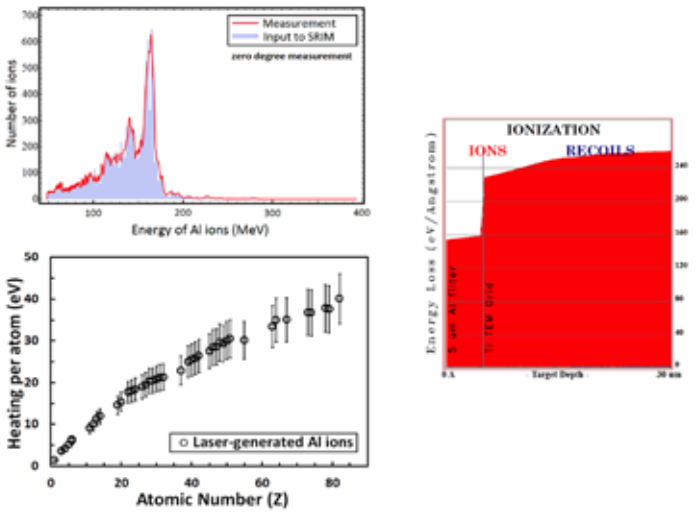

Figure 2. Representative results of stopping power modeling using the SRIM code used to design our targets. We use measured Trident quasi-monoenergetic aluminum ion beam enery spectra (top left) as input into our model. The right panel is heating energy as a function of penetration distance into the target material (the region at distance greater than 5 microns), indicating very uniform heating. (The leftmost five microns is an aluminum filter, which we account for in our design.) The bottom left panel indicates the heating per atom, showing that higher-Z atoms heat more from the incident ion beams.

Our objectives in this study were to find material combinations and thicknesses such that we achieve isochoric, uniform heating with our ion beams with total pressure across the material interface (nearly) constant, but large gradients in electron pressure, as required for large ambipolar fields, believed to be responsible for enhanced plasma diffusivity, to be achieved. In our composite targets, we sought configurations where one of the materials would be opaque to

the titanium K-alpha backlighter x-rays and the other material, transparent. We found multiple candidate combinations and down-selected to two that we would later field in our experiments: diamond-gold and aluminum-tin [2]

Characterization of the laser-ion heating

From the measured ion beam properties, we fielded composite targets with a vacuum gap between the two target materials. These targets, after heating, expanded into the gap and the rate of expansion was then measured using streaked optical shadowgraphy (Figure 3). Comparison of the measured plasma expansion rates with those predicted by SESAME equation of state tables and multi-physics RAGE simulations enabled us to infer the dense plasma conditions attained. This was an important consistency check of our physics understanding. [3]

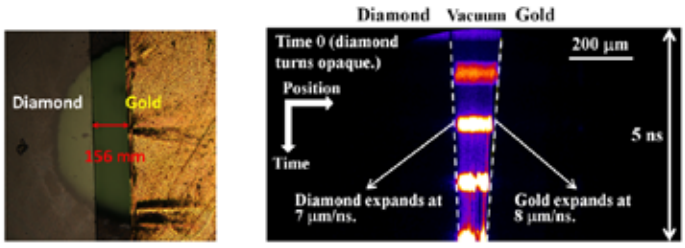

Figure 3. Optical shadowgraphy of gap closure in a multi-material target with a vacuum gap. The target is shown to the left. The right panel is a streaked optical shadowgraphy image, indicating that the diamond and gold expanded at 7 microns/ns and 8 microns/ns, respectively. This technique allowed us to diagnose and confirm our preparation of targets in the desired warm dense matter conditions for our experiments.

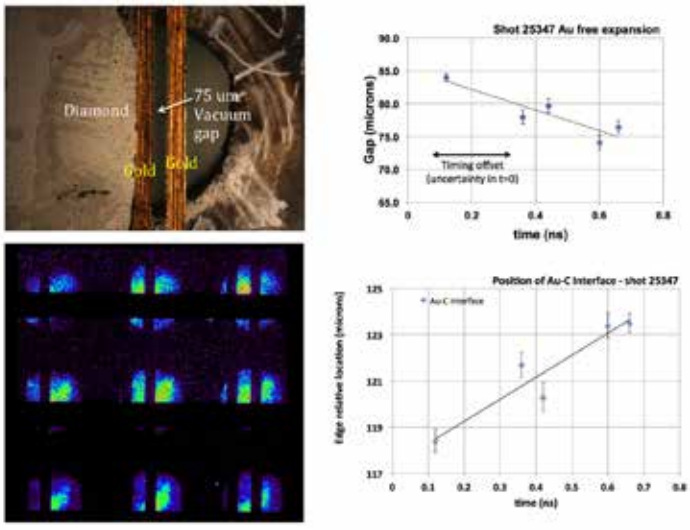

Figure 4. Preliminary analysis of gated x-ray imaging of gold-diamond interface with self-referencing target. An image of the target is shown in the upper left panel.The gold-diamond interface is as indicated with a second reference bar (expanding symmetrically into vacuum) located with a 75 micron vacuum gap. By measuring the expansion speed of the reference gold bar (top right) we can determine the rate of expansion of the gold. A representative gated x-ray image is shown in the bottom left; shown are successive snapshots in time, from which we make position measurements. The bottom right panel is the rate of motion of the gold propagating into the diamond; this expansion is comparable in speed to the free expansion of gold into vacuum, indicating super-diffusive mixing at the interface.

Initial gated x-ray measurements of evolution of interface

Based on an extensive design study, we were able to configure target and imaging systems such that we could obtain up to sixteen images at succeeding points of time of our interface, from which we could make measurements of the motion of the plasma interface. We included in our targets a fiducial element to eliminate the need for absolute referencing and instead make relative measurements of expansions of our targets. This modality was developed over three experimental campaigns to ensure high quality data could be obtained; preliminary data are shown in Figure 4.

Streaked optical pyrometry (SOP) diagnostics development and fielding

Independent measurement of target heating provides key confirmatory data for our experiments. To develop this, an optical pyrometer was designed, tested, and fielded on multiple campaigns. This work, conducted by our U. Texas at Austin collaborators and subcontractors Prof. B. Manuel Hegelich, Dr. Gillis Dyers, and Ms. Rebecca Roycroft, formed the basis of the Roycroft's Ph.D. dissertation.

Final campaign to measure Au-C and Sn-Al interfacial evolution

Our final campaign in Aug.-Sept., 2016 resulted in the acquisition of high quality data that we intend to analyze in the next month using techniques developed and refined in our prior campaigns. A notable improvement in this campaign was the recognition of a need for tighter requirements regarding precision of target fabrication and metrology. While this led to a delay in obtaining suitable targets (indeed, we were forced to postpone our April, 2016 campaign because of the unavailability of suitably constructed targets), we nevertheless were able to field a successful experimental campaign. We have five shots that yielded quality data that we intend to analyze.

Throughout our project, we made extensive use of radiation-hydrodynamics multiphysics codes for design and interpretation of our experiments. Our workhorse code was the RAGE code, developed in the Eulerian Applications Project of the LANL Advanced Simulation and Computing (ASC) Program. We also deployed the LASNEX code, developed at LLNL, as a cross-check to the physics. Our results and physics hypotheses were further corroborated by ab initio simulations using the LANL VPIC kinetic plasma

modeling code [4]. These calculations spurred theoretical work in this topical, which in turn led to an improved understanding of the evolution of plasma interfaces now the foundation for a spin-off effort funded by the ASC Program within the Thermonuclear Burn Initiative project.

With respect to visibility, work from this project has been documented and presented in many venues, including several scientific journal articles in top-tier journals, including Nature Communications, Physical Review Letters, Physical Review E, Physics of Plasmas, and (Nature) Scientific Reports [1-14], among others; also, several invited talks were given by various members of the project, including one at the Meeting of the American Physical Society Division of Plasma Physics, three at the Advanced Accelerator Conference, one at the International Conference on High Energy Density Physics, six University and Lab colloquia, two briefings at Dept. of Energy Headquarters, and five papers presented at US/UK Joint Working Group meetings and other DOE Technical Meetings.

Impact on National Missions

One of the early successes of this project was the demonstration of a new method of measuring and validating dense plasma properties, such as equation of state [5]. We also obtained for the first time high-quality validation data for dense plasma transport models, a high priority within several of the Lab's national security programs, making this a singular contribution to both Lab mission and the broader scientific community.

As mentioned, demonstration of our modeling capabilities led to a spin-off effort within the ASC Thermonuclear Burn Initiative to model the behavior of dense plasmas and to validate models in ASC multi-physics codes. This work required running simulations at the very largest scales and motivated a follow-on LDRD ER project to migrate the VPIC code to the many-core Trinity supercomputer in order to run "at-scale" simulations of plasma interfacial diffusion and turbulence. More broadly, national interest has been expressed by Exascale Computing Project leaders in VPIC as a relevant scientific platform. Indeed, VPIC development for modeling systems such as those in this project was proposed by the LANL Exascale leadership as a target computational application in the event of a rapid Exascale roll-out.

Refinement of laser-based ion sources led to pronounced advances in laser-based neutron sources, of utility for LANL applications such as Neutron Diagnosed Subcritical Experiments (NCSE) as part of the proposed Enhanced Capability for Radiographic Experiments (ECSE), neutron diagnostics at the proposed Matter-Radiation Interactions in Extremes (MaRIE) facility.

Recruitment and retention efforts were supported by this project; we fostered a pipeline of students with our U. Texas, Austin collaborators and hired from this institution both an experimentalist postdoc to help with the experiments and a theorist postdoc to work on simulation and modeling of laser-plasma acceleration.

References

1. Palaniyappan, S., D. C. Gautier, C. K. Huang, C. E. Hamilton, J. A. Cobble, C. Kreuzer, J. C. Fernández, and R. Shah. Efficient quasi-monoenergetic ion beam from laser-driven plasmas. 2015. Nature Communications. 6: 10170.

2. Bang, W., B. J. Albright, P. A. Bradley, E. L. Vold, J. C. Boettger, and J. C. Fernández. Uniform heating of materials into the warm dense matter regime with laser-driven quasi-monoenergetic ion beams. 2015. Physical Review E. 92: 063101.

3. Bang, W., B. J. Albright, P. A. Bradley, D. C. Gautier, S. Palaniyappan, E. L. Vold, M. A. Santiago Cordoba, C. E. Hamilton, and J. C. Fernández. Visualization of expanding warm dense gold and diamond heated rapidly by laser-generated ion beams. 2015. Scientific Reports. 5: 14318.

4. Yin, L., B. J. Albright, W. Taitano, E. L. Vold, L. Chacon, and A. Simakov. Plasma kinetic effects on interfacial mix. Physics of Plasmas .

5. Bang, W., B. J. Albright, P. A. Bradley, E. L. Vold, J. C. Boettger, and J. C. Fernández. Linear dependence of surface expansion speed on initial plasma temperature in warm dense matter. 2016. Scientific Reports. 6: 29441.

6. Jung, D., B. J. Albright, L. Yin, D. C. Gautier, B. Dromey, R. Shah, S. Palaniyappan, S. Letzring, H. C. Wu, T. Shimada, R. P. Johnson, D. Habs, M. Roth, J. C. Fernández, and B. M. Hegelich. Scaling of ion energies in the relativistic-induced transparency regime. 2015. Laser and Particle Beams. : 1.

7. Fernández, J. C., B. J. Albright, F. N. Beg, M. E. Foord, B. M. Hegelich, J. J. Honrubia, M. Roth, R. B. Stephens, and L. Yin. Fast ignition with laser-driven proton and ion beams. 2014. Nuclear Fusion. 54 (5): 054006.

8. Jung, D., L. Senje, O. McCormack, L. Yin, B. J. Albright, S. Letzring, D. C. Gautier, B. Dromey, T. Toncian, J. C. Fernández, M. Zepf, and B. M. Hegelich. On the analysis of inhomogeneous magnetic field spectrometer for laser-driven ion acceleration. 2015. Reviews of Scientific Instruments. 86: 059503.

9. Bang, W.. Disassembly time of deuterium-cluster-fusion plasma irradiated by an intense laser pulse. 2015. Physical Review E. 92: 013102.

10. Albright, B. J., L. Yin, and A. Favalli. Neutron generation from laser-accelerated ion beams: use of alternative deuteron-rich targets for improved neutron yield and control of neutron spectra. Physical Review Letters.

11. Huang, C. K., Y. Zeng, Y. Wang, M. D. Meyers, S. Yi, and B. J. Albright. Finite grid instability and spectral fidelity of the electrostatic particle-in-cell algorithm. 2016. Computer Physics Communications. 207: 123.

12. Meyers, M. D., C. K. Huang, Z. Yong, S. Yi, and B. J. Albright. On the numerical dispersion of electromagnetic particle-in-cell code: finite grid instability. 2015. Journal of Computational Physics. 279: 565.

13. Bang, W., H. J. Quevedo, A. C. Bernstein, G. Dyer, Y. S. Ihn, J. Cortez, F. Aymond, E. Gaul, M. E. Donovan, M. Barbui, A. Bonasera, J. B. Natowitz, B. J. Albright, and J. C. Fernández. Characterization of deuterium clusters mixed with helium gas for an application in beam-target-fusion experiments. 2014. Physical Review E. 90: 063109.

14. Jung, D., B. J. Albright, L. Yin, D. C. Gautier, R. Shah, S. Palaniyappan, S. Letzring, B. Dromey, H. C. Wu, T. Shimada, R. P. Johnson, M. Roth, J. C. Fernández, D. Habs, and B. M. Hegelich. Beam profiles of proton and carbon ions in the relativistic transparency regime. 2013. New Journal of Physics. 15 (12): 123035.

Publications

Albright, B. J.. Use of laser-generated ion beams for isochoric heating to dtudy plasma-phase mix at heterogeneous interfaces. Invited presentation at 16th Advanced Accelerator Concepts Workshop (AAC 2014). (San Jose, California, 13-18 July, 2014).

Albright, B. J., L. Yin, and A. Favalli. Neutron generation from laser-accelerated ion beams: use of alternative deuteron-rich targets for improved neutron yield and control of neutron spectra. Physical Review Letters.

Bang, W.. Disassembly time of deuterium-cluster-fusion plasma irradiated by an intense laser pulse. 2015. Physical Review E. 92: 013102.

Bang, W., B. J. Albright, P. A. Bradley, D. C. Gautier, S. Palaniyappan, E. L. Vold, M. A. Santiago Cordoba, C. E. Hamilton, and J. C. Fernández. Visualization of expanding warm dense gold and diamond heated rapidly by laser-generated ion beams. 2015. Scientific Reports. 5: 14318.

Bang, W., B. J. Albright, P. A. Bradley, E. L. Vold, J. C. Boettger, and J. C. Fernández. Uniform heating of materials into the warm dense matter regime with laser-driven quasi-monoenergetic ion beams. 2015. Physical Review E. 92: 063101.

Bang, W., B. J. Albright, P. A. Bradley, E. L. Vold, J. C. Boettger, and J. C. Fernández. Linear dependence of surface expansion speed on initial plasma temperature in warm dense matter. 2016. Scientific Reports. 6: 29441.

Bang, W., H. J. Quevedo, A. C. Bernstein, G. Dyer, Y. S. Ihn, J. Cortez, F. Aymond, E. Gaul, M. E. Donovan, M. Barbui, A. Bonasera, J. B. Natowitz, B. J. Albright, and J. C. Fernández. Characterization of deuterium clusters mixed with helium gas for an application in beam-target-fusion experiments. 2014. Physical Review E. 90: 063109.

Fernández, J. C.. High power density ion beams driven by lasers: progress and applications. Invited presentation at 2nd International Conference on High Energy Density Physics. (Beijing, China, 21-24 Sept. 2014).

Fernández, J. C.. Advancements in the Trident Laser Facility. 2016. Technical Report.

Fernández, J. C., B. J. Albright, C. W. Barnes, and K. F. Schoenberg. Harnessing relativistic laser plasmas to generate intense ion beams: a plasma science frontier white paper. 2015. LA-UR-15-24654, White Paper for Dept. of Energy Frontiers of Plasma Science Panel.

Fernández, J. C., B. J. Albright, F. N. Beg, M. E. Foord, B. M. Hegelich, J. J. Honrubia, M. Roth, R. B. Stephens, and L. Yin. Fast ignition with laser-driven proton and ion beams. 2014. Nuclear Fusion. 54 (5): 054006.

Hegelich, B. M., D. Jung, and L. Yin. Recent achievements on ion acceleration. Invited presentation at 41st European Physical Society Conference. (Berlin, Germany, 23-27 June, 2014).

Huang, C. K., Y. Zeng, Y. Wang, M. D. Meyers, S. Yi, and B. J. Albright. Finite grid instability and spectral fidelity of the electrostatic particle-in-cell algorithm. 2016. Computer Physics Communications. 207: 123.

Jung, D., B. J. Albright, L. Yin, D. C. Gautier, B. Dromey, R. Shah, S. Palaniyappan, S. Letzring, H. C. Wu, T. Shimada, R. P. Johnson, D. Habs, M. Roth, J. C. Fernández, and B. M. Hegelich. Scaling of ion energies in the relativistic-induced transparency regime. 2015. Laser and Particle Beams. : 1.

Jung, D., B. J. Albright, L. Yin, D. C. Gautier, R. Shah, S. Palaniyappan, S. Letzring, B. Dromey, H. C. Wu, T. Shimada, R. P. Johnson, M. Roth, J. C. Fernández, D. Habs, and B. M. Hegelich. Beam profiles of proton and car-

bon ions in the relativistic transparency regime. 2013. New Journal of Physics. 15 (12): 123035.

Jung, D., L. Senje, O. McCormack, L. Yin, B. J. Albright, S. Letzring, D. C. Gautier, B. Dromey, T. Toncian, J. C. Fernández, M. Zepf, and B. M. Hegelich. On the analysis of inhomogeneous magnetic field spectrometer for laser-driven ion acceleration. 2015. Reviews of Scientific Instruments. 86: 059503.

Meyers, M. D., C. K. Huang, Z. Yong, S. Yi, and B. J. Albright. On the numerical dispersion of electromagnetic particle-in-cell code: finite grid instability. 2015. Journal of Computational Physics. 279: 565.

Palaniyappan, S.. Magnetic electron trapping generates efficient quasi-monoenergetic ion beam from laser-driven plasma. Invited presentation at 16th Advanced Accelerator Concepts Workshop (AAC 2014) . (San Jose, California, 13-18 July, 2014).

Palaniyappan, S., D. C. Gautier, C. K. Huang, C. E. Hamilton, J. A. Cobble, C. Kreuzer, J. C. Fernández, and R. Shah. Efficient quasi-monoenergetic ion beam from laser-driven plasmas. 2015. Nature Communications. 6: 10170.

Yin, L., B. J. Albright, W. Taitano, E. L. Vold, L. Chacon, and A. Simakov. Plasma kinetic effects on interfacial mix. Physics of Plasmas .

The Role of Short-lived Actinide Isomers in High Fluence Environments (U)

Marian Jandel
20140046DR

Abstract

The population of short-lived isomeric states in U-236, a 688 keV (1-) state with the half-life T1/2=3.78 ns and a 1053 keV (4-) state with the half-life T1/2=100 ns, produced in neutron capture reaction of U-235 was determined to be between 15-35 %, for a wide range of neutron incident energies from a few eV to 100 keV. The new results were obtained using a newly developed compact array NEUANCE (NEUtron detector array at DANCE) that was installed in the central cavity of the Detector for Advanced Neutron Capture Experiments array (DANCE). NEUANCE enabled detection of prompt-fission neutrons and gamma rays and correlated time dependent gamma ray background originating from the products of the two reactions, fission and capture, and other relevant background components. We apply the statistical Hauser-Feshbach theory to support the DANCE experiments. It provides calculations of neutron capture cross section and probability of the decay into isomeric state. In addition, cross sections of neutron-induced reactions on excited unstable states can be obtained as well. The models involved are the photon-strength function, nuclear level density, optical potential for neutrons and nuclear fission, together with nuclear structure information provided in a database. To study isomers produced by a neutron capture event, it is necessary to include more experimental discrete levels that are feeding the isomeric states. We developed a new technique, where some discrete levels can be embedded in the continuum. The overlapping discrete and continuum regions allows us to see more discrete gamma rays originated from higher excitation energies. Finally, sensitivity studies were carried out and will be reported in a separated classified addendum.

Background and Research

Understanding nuclear reactions on excited nuclei is of physical interest for studying extreme environments such as nucleo-synthesis in nuclear astrophysics, nuclear weapon performance or the nuclear reaction process during ICF (Inertial Confinement Fusion). In a natural environment nuclear reactions normally take place on stable nuclei, with the target nucleus in its ground state or isomeric state if its half-life is long enough. In a high-density high-temperature neutron and gamma-ray environment, it is likely that neutron-induced nuclear reactions occur on the excited states, even though the life-time of the excited state is often on the order of nano-seconds. Example of the production/destruction network of the nuclear reactions around U-235 nucleus is shown in Figure 1.

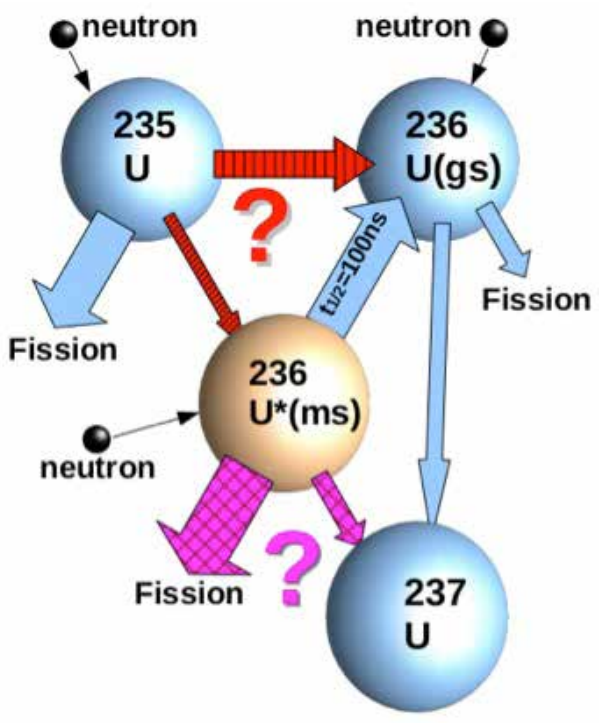

Figure 1. Production/destruction network of nuclear reactions around U-235.

The nuclear reaction rates on the excited states could be different from those on the ground state, primarily because of the difference in phase space of levels accessible: the spin and parity of the ground and excited states

usually differ, and the target excitation energy shifts the excitation energy of the compound system. This process can be calculated with the standard Hauser-Feshbach model with additional excitation energy on the target nucleus. Preliminary calculations of the 236U neutron-induced fission cross sections indicated that the enhancement of fission cross sections due to the additional excitation energy of the isomer was very large, two orders of magnitude.

Scientific Approach and Accomplishments

Our approach was to: 1) Develop new experimental capability that would address the complicated processes that occur in neutron-induced reactions measurements with U-235 and quantify the population of two isomeric states in U-236 compound nucleus. 2) Benchmark the measurements using improved theoretical models. 3) Improve LANL's capability to calculate the cross sections of neutron-induced reactions on short-lived states. 4) Carry out sensitivity studies to evaluate the impact of the population of these short-lived states of U-236 in high neutron fluence environments.

Measurements of capture gamma ray cascades leading to the population of short-lived isomers require very detailed knowledge of the prompt-fission gamma ray background. We have designed a compact neutron detector array NEUANCE that has been installed in the central cavity of the DANCE detector array. NEUANCE is shown in Figure 2.

Figure 2. NEUANCE - Neutron detector array consists of 21 stilbene crystals arranged in the cylindrical geometry around the beam pipe. The inner and outer rings of NEUANCE include 7 and 14 detectors, respectively.

NEUANCE enabled detection of prompt fission neutrons and time dependent gamma-ray emission after both fission and capture reactions. NEUANCE was designed and constructed using 21 stilbene organic scintillator crystals. [1, 2] Signals from the 160 BaF2 detectors of DANCE and the 21 detectors of NEUANCE were efficiently merged into a newly designed high-density high-throughput data acquisition system (DAQ) [3,4]. New digitizers VX1730B acquired from CAEN, are 14-bit, 500 MS/s digitizer with 5.12 MS/channel memory to store firmware events. On-board FPGA firmware is available for signal processing and data reduction of both fast organic/inorganic scintillators and slower semiconductor detector technologies. The triggering and readout scheme are asynchronous which massively improves the total acceptable trigger rate. Each DAQ channel independently triggers itself, with an external gate applied to select those events in the beam pulse window we are interested in. For the purposes of this project, the new DAQ permitted the measurement of a time window ~20x the size of the old DAQ, which made our use of beam time much more efficient. In short, the combination of onboard signal processing and move from an 8 to 14 bit ADC essentially permitted us to run with arbitrary experimental setups with or without the LANSCE neutron beam present, which represented a quantum leap in capability and allowed the project to take the data it needed to succeed.

The excellent pulse shape discrimination properties of stilbene enabled detection of neutrons with energy thresholds as low as 30-40 keVee [5]. A fission reaction tagging method was developed using a NEUANCE gamma-ray or neutron tagging. The probability of detecting a neutron from spontaneous fission of Cf-252 and U-235(n,f) using NEUANCE is ~47% and ~30%, respectively. The measurement with NEUANCE was performed in January, 2016 at DANCE flight path 14 in the Lujan Neutron Scattering Center at Los Alamos Neutron Science Center (LANSCE). New data acquisition codes and off-line data analysis codes were developed to enable a complex coincident events building from detectors of NEUANCE and DANCE. We have determined the yields of gamma-ray cascades leading to the ground state of the U-236 for several neutron resonances and continuous regions of incident neutron energies up to 10 keV. The procedure included subtraction of ambient, neutron beam induced and other components of background. The yield of gamma rays was determined for different duration of time intervals after neutron capture occurred, from 5 ns up to 200 ns. The population of the ground state increases with the increasing time interval of the measurement after the neutron capture, as is shown in Figure 3.

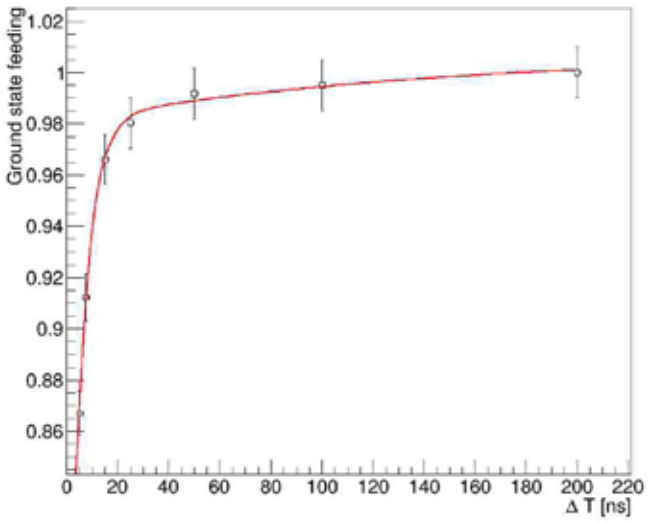

Figure 3. Population of the ground state of U-236 as a function of the time interval dT after neutron capture event, for incident neutron energy between 11.4 and 11.8 eV. The isomer population is estimated from the two component exponential decay fit using the known half-lives of 3.7 and 100 ns, for the states at 687 keV and 1053 keV, respectively.

The results are shown in Table 1 for different regions of neutron incident energy.

E_{n1} [eV]	E_{n2} [eV]	Y_0(gs)	Y_1(688 keV)	Y_2(1053 keV)
4.7	5.0	0.65	0.28	0.08
11.4	11.8	0.69	0.29	0.03
12	13	0.76	0.21	0.03
19	20	0.62	0.23	0.15
10	100	0.71	0.18	0.11
100	1000	0.74	0.11	0.15
1000	10000	0.84	0.11	0.07

Table 1. Results on the population of the isomeric states for incident neutron energy regions (En1,En2) shown in the first two columns. Total yield of the cascades leading to the ground state Y0 is compared to the population of Y1 and Y2 of the 688 keV and 1053 keV states, in the last two columns, respectively.

Prior this project, the statistical Hauser-Feshbach calculations for the neutron radiative capture process in the keV to MeV energy region were still unsatisfactory. This is mainly due to relatively large uncertainties in the model parameters used, in particular for unstable nuclei: the level density, the spin and parity distributions in the continuum, and the photon-strength function. Ullmann et al. [6] showed that the calculated neutron capture cross section for a deformed system is strongly influenced by the M1 scissors mode, although the amplitude of collective motion is expected to be small. When the energy of emitted gamma ray from a compound nucleus is low (< 1 MeV), such decay process has no impact on the calculated neutron capture cross section, because the gamma-ray transmission coefficient carries a phase space factor that will be very small at low energies. The M1 scissors mode, which is often seen in a few MeV region for deformed nuclei, may play an important role in de-excitation of a compound nucleus. We examine the enhancement in the calculated neutron capture cross sections for deformed nuclei due to the additional M1 strength. Since the enhancement could be remarkable for strongly deformed nuclei, we focus on the nuclei in the mass A = 100 - 200 region, then estimate its impact on actinides.

For the photon-strength function, we typically include the giant dipole resonance (GDR) in the generalized Lorentzian form, the spin-flip M1 resonance, and small contributions from higher multipolarities, E2 and M2. In addition to these commonly used strengths, we add the M1 scissors mode in a standard Lorentzian shape, then adjust it strength to reproduce evaluated neutron capture cross sections in the fast energy range in the mass region A=100 -200 [7]. This allows us to study a correlation between nuclear deformation and the M1 strength. The coupled-channels and Hauser-Feshbach theory is used for calculating the cross sections. The nuclear deformation parameters are taken from the finite range droplet model. The obtained M1 strengths for the target nuclei are fitted assuming a quadratic form in the nuclear deformation. This additional strength enhances the calculated capture cross sections on deformed nuclei by a factor of 2-3 in a wide mass range. The average deviations are -34~mb for the no-M1 case, and -7~mb for the with-M1 case.

In the area of fission process calculations, we advanced our current capabilities and improved the CGMF (Cascade Gamma and Multiplicity for Fission) code [8,9]. CGMF is a Monte Carlo Hauser-Feshbach code used to describe the statistical decay of excited primary fission fragments. By following the sequential emissions of prompt fission neutrons and gamma rays, on an event-by-event basis, CGMF can be used to study detailed and exclusive characteristics of prompt fission gamma rays. In particular, the known nuclear structure of fission fragments, including isomeric states, is used to compute the time evolution of gamma-ray data. The Monte Carlo technique is very powerful and straightforward to infer correlations among the many fission observables that are produced in a single fission event. The output of CGMF is a history file listing a sample of fission events, which include the fission fragments completely characterized by their momentum vectors in the laboratory frame and the prompt neutrons and gamma rays emitted during the de-excitation. By definition, the

prompt neutrons and gamma rays are emitted by the fission fragments, which then decay towards the valley of stability via beta emissions. This information was input into GEANT4 in order to model the response of the NEUANCE detector [10].

We performed an improved Hauser-Feshbach calculation, with the developments from 2), for the neutron-induced reactions on 235U by applying the discrete-continuum overlapping technique. The production cross-sections of the 688 keV, 1053 keV, and 2760 keV states are shown in Figure 4. The 688-keV state production is about a quarter of the total capture cross-section, and the 1053-keV state one-order of magnitude smaller than the ground state. It turned out that production of the 2760-keV state, which spontaneous fissions, is negligible. We also performed calculations of neutron-induced fission on excited states. When a sequential neutron interaction happens in a dense neutron environment, the excess energy of the isomeric states gives higher fission probabilities; hence we expect the fission cross section for the isomeric states are larger than the fission cross section for the ground state. This is shown in Figure 5. First we tuned the fission parameters to reproduce the evaluated fission cross sections of 236U in ENDF/B-VII.1, then applied the same parameters to the isomeric states. Although 236U has a fission threshold of about a half MeV, the excitation energies of 688 and 1053 keV allow the compound system to overcome its fission barriers.

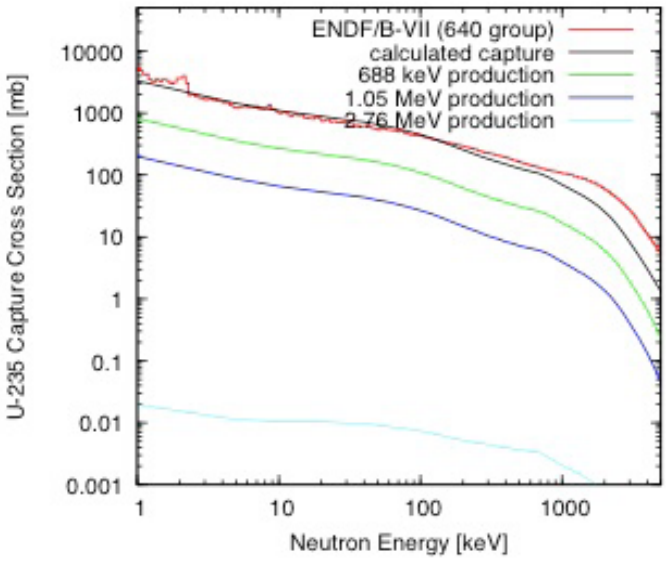

Figure 4. Isomeric state production cross sections for the neutron capture reaction on U-235.

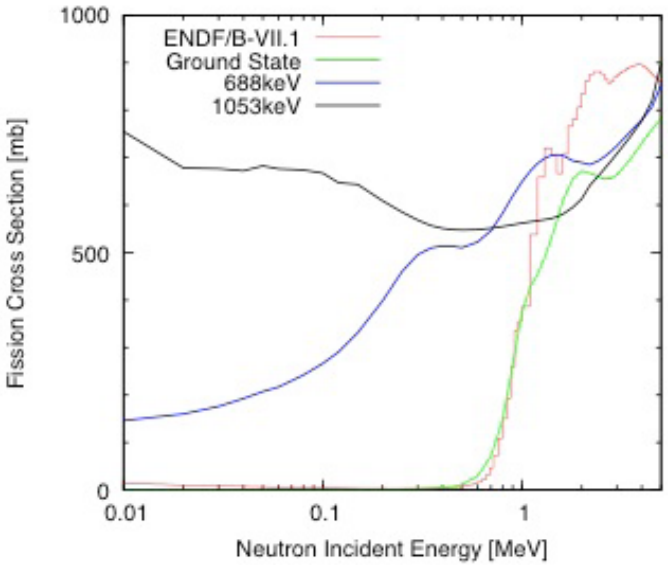

Figure 5. The calculated fission cross section of U-236 for the ground state (green curve), the first isomeric state (blue curve), and the second isomeric state (black curve).

We have expanded our uranium burn network codes to include the isomers of U-236, using the feeding of the isomers as measured in the experiments at LANSCE and the known half-lives. We ran a series of sensitivity studies in which the total neutron flux was varied within the range of interest to the program. We determined the circumstances under which the isomers have an effect on radiochemical diagnostics and quantified the magnitude of those effects. This work will be provided to the weapons community in a detailed report.

Impact on National Missions

Understanding the nuclear structure properties of the actinides is key to large areas of concern relevant to National Security as well as basic nuclear science. An enhanced interest of governmental agencies, such as NA-22, in more precise and correlated data on neutron-induced reactions will put the capabilities developed during this project into a great position to support future mission needs for systematic measurements of isomeric state production in neutron capture, correlated neutron-induced fission data, predictive modeling of capture and fission and refinement of transport codes such as MCNP to include important details on correlated radiation from neutron-induced reactions. New signatures for special material detection, nuclear proliferation and forensics will be the objectives of the follow up research, which is at the very core mission of this laboratory. The newly developed NEUANCE array enhances LANL capabilities of studying such correlated data in neutron-induced fission and capture reactions.

New correlated data for prompt fission neutrons and

prompt fission gamma rays were obtained for Cf-252 and U-235 using this high detection efficiency experimental set-up. Average properties of prompt fission neutron emission as a function of prompt fission gamma-ray quantities were also obtained, suggesting that neutron and gamma-ray emission in fission is correlated. This work will continue under NA22 funding and several new measurements with Pu-239 and other isotopes will be staged in FY17.

Our new results may have significant implications on our understanding of nuclear reaction networks in high neutron fluence environments such as those occurring in nuclear explosions. In these high fluence environments these isomers may interact with a second neutron before de-exciting. The results of the sensitivity studies performed under this project will be reported separately in a classified addendum to this project.

References

1. Jandel, M. et al. Capture and fission with DANCE and NEUANCE. 2015. The European Physical Journal A. 51: 179.

2. Jandel, M. et al.. Correlated fission data measurements with NEUANCE. 2016. in preparation for Nuclear Instruments and Methods A.

3. Couture, A. et al. Enhancing the Detector for Advanced Neutron Capture Experiments. 2015. The European Physical Journal Web of Conferences. 93: 07003.

4. Mosby, S. et al. Data acquisition upgrade for DANCE. 2016. in preparation for Nuclear Instruments and Methods A.

5. Baramsai, B. et al. Characterization and testing of EJ-309 and Stilbene scintillation detectors. 2015. In SPIE: Hard X-Ray, Gamma-Ray, and Neutron Detector Physics XVII . (San Diego, 9-13 Aug. 2015). Vol. 9593, p. 1. San Diego: SPIE.

6. Ullmann, J. L. et al. Cross section and g-ray spectra for U238(n,g) measured with the DANCE detector array at the Los Alamos Neutron Science Center. 2014. Physical Review C. 89: 034603.

7. Kawano, , Talou, M. B. Chadwick, and Watanabe. Monte Carlo Simulation for Particle and gamma-Ray Emissions in Statistical Hauser-Feshbach Model. 2010. JOURNAL OF NUCLEAR SCIENCE AND TECHNOLOGY. 47 (5): 462.

8. Watanabe, , Kawano, M. B. Chadwick, R. O. Nelson, Hilaire, Bauge, and Dossantos-Uzarralde. Calculation of Prompt Fission Product Average Cross Sections for Neutron-Induced Fission of U-235 and Pu-239. 2010. JOURNAL OF NUCLEAR SCIENCE AND TECHNOLOGY. 47 (5): 478.

9. Talou, , Becker, Kawano, M. B. Chadwick, and Danon. Advanced Monte Carlo modeling of prompt fission neutrons for thermal and fast neutron-induced fission reactions on Pu-239. 2011. PHYSICAL REVIEW C. 83 (6).

10. Walker, C.. Geant4 simulations of the NEUANCE array. 2016. in preparation for Nuclear Instruments and Methods A.

Publications

Baramsai, B., M. Jandel, T. A. Bredeweg, A. Couture, S. Mosby, G. Rusev, J. L. Ullmann, and C. L. Walker. Characterization and testing of EJ-309 and Stilbene scintillation detectors . 2015. In Proc. SPIE 9593, Hard X-Ray, Gamma-Ray, and Neutron Detector Physics. (San Diego, Aug 9). , p. 1. San Diego: SPIE.

Couture, A.. Enhancing the Detector for Advanced neutron Capture Experiments. 2015. EPJ Web of Conferences. 93: 07003.

Jandel, M.. Current and Future Research at DANCE. 2015. In CGS15 – Capture Gamma-Ray Spectroscopy and Related Topics . (Dresden, August 25-29). , p. 1. Online: EPJ Web of Conferences.

Jandel, M.. Capture and fission with DANCE and NEUANCE. 2015. European Journal of Physics A. 51 (12): 179.

Jandel, M., Baramsai, T. A. Bredeweg, Couture, Hayes, Kawano, Mosby, Rusev, Stetcu, T. N. Taddeucci, Talou, J. L. Ullmann, C. L. Walker, and J. B. Wilhelmy. Current and Future Research at DANCE. 2015. CGS15 - CAPTURE GAMMA-RAY SPECTROSCOPY AND RELATED TOPICS. 93: 02019.

Mosby, S.. A fission fragment detector for correlated fission output studies. 2014. Nuclear Instruments and Methods A. 757: 75.

Rusev, G., B. Baramsai, E. M. Bond, and M. Jandel. Fission-neutrons source with fast neutron-emission timing. 2016. Nuclear Instruments and Methods A. 817: 26.

Rusev, G., M. Jandel, B. Baramsai, A. R. Roman, J. K. Daum, R. K. Springs, E. M. Bond, T. A. Bredeweg, A. Couture, A. Favalli, K. D. Ianakiev, M. L. Iliev, S. Mosby, J. L. Ullmann, and C. L. Walker. Fission-fragment detector for DANCE based on thin scintillating films. 2015. Nuclear Instruments and Methods A. 804: 207.

Rusev, G., M. Jandel, B. Baramsai, E. M. Bond, T. A. Bredeweg, A. Couture, J. K. Daum, A. Favalli, K. D. Ianakiev, M. L. Iliev, S. Mosby, A. R. Roman, R. K.

Springs, J. L. Ullmann, and C. L. Walker. Development of a thin scintillation films fission-fragment detector and a novel neutron source. 2015. In Proc. SPIE 9593, Hard X-Ray, Gamma-Ray, and Neutron Detector Physics XVII, 959314 (August 26, 2015); doi:10.1117/12.2192440. (San Diego, Aug 9). , p. 1. San Diego: SPIE.

Stetcu, I.. Properties of prompt-fission gamma rays. 2014. Phys Rev C. 90: 024617.

New Technologies for a Tabletop Accelerator

Evgenya I. Simakov
20160002DR

Abstract

The fabrication of micron-scale dielectric photonic-band gap (PBG) structures is central to the development of new technologies for a tabletop accelerator. The purpose of this reserve project was to demonstrate viability of the additive manufacturing approach for fabrication of micron-scale PBG structures and significantly reduce the overall technical risk of subsequent R&D in this area.

Background and Research Objectives

Because of the electrical breakdown of metals induced by high electric fields, conventional particle accelerators, which consist of metal cavities driven by high-power microwaves, typically operate with accelerating fields of 10 to 30 MV/m. Devices based upon conventional technology are often large and expensive due to the accelerator length and the total stored energy needed to accelerate particles to high energy. Size and cost reductions are required for many applications.

Utilizing the extraordinary electric fields and high repetition rates of modern solid state laser systems for acceleration has long been a goal of advanced accelerator research, owing to the potential for higher accelerating gradient and reduced cost. Laser acceleration in structures closely mimics conventional microwave acceleration in cavities with linear accelerating fields, and thus is capable of producing accelerating bunches with controllable energy spread and emittance. Due to micron laser wavelength and similar dimensions of the accelerating structures, nano-meter emittances required by modern X-ray free-electron lasers (FELs) seem actually achievable in dielectric laser accelerators (DLAs). With accelerating fields in dielectric structures reaching gradients on the order of 10 GV/m, a laser accelerator structure driven at an IR wavelength could possibly have the footprint two orders of magnitude less as compared to a microwave accelerating structure, implying feasibility of miniaturized accelerators.

An operating DLA system (Figure 1) must include three critical components. First is the high power source of the electromagnetic energy (the laser), second is the electron beam source (cathode), and the third is the electromagnetic structure which ensures the transfer of the electromagnetic energy to the electron beam.

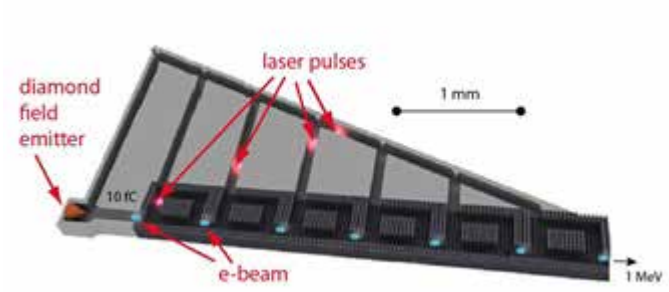

Figure 1. A schematic of dielectric laser acceleration in a structure.

IR (1-10 μm) laser systems capable of delivering the light in a pulse length of a few ps with the mJ pulse energies are now commercially available. However, the laser accelerator structure must be made to shape the laser pulse so that the electric field is longitudinal along the trajectory of the accelerated particle and the phase velocity of the wave is synchronous with the relativistic particles (close to the speed of light). The structures must be made of dielectric materials rather than metals due to large ohmic losses and low breakdown thresholds of metal surfaces at IR wavelengths. A woodpile PBG structure has been proposed by SLAC as a possible high efficient interaction structure. Initially it was suggested that fabrication of the woodpile structure would be compatible with photolithographic methods to produce micron-scale features. Multiple attempts of fabrication were performed with different degrees of success. However, the alignment of multiple fabricated sections could not be easily resolved precluding fabrication of a woodpile accelerating structures of a usable length. Currently, fabrication of appropriate dielectric accelerating

structures is an active area of research.

The major objective of this research project was to evaluate feasibility of fabrication of woodpile structures for accelerator applications with NanoScribe Photonic Professional GT. The work was supposed to start with the electromagnetic design of the woodpile structures for the wavelengths of 10 microns and 5 microns. Then it would proceed to fabrication of sample structures with NanoScribe proprietary resins. This work would demonstrate that we can produce and characterize objects at the required resolution, and allow us to have a better feel for the capabilities of the instrument. We planned to quantify fabrication tolerances and conduct simulations to evaluate the effect of the fabrication errors on performance of the accelerating structure. The second significant objective was to evaluate addition of fillers to the photolithography resin which may represent a significant change in the properties of the resin and the resin's performance with the Nanoscribe instrument. Addition of fillers is required to increase the dielectric constant of the resin material to fabricate the structure which would provide for the efficient interaction of the electromagnetic wave with the electron beam. That would allow us to learn if there are any real limitations for introducing particulate matter into printer's resins.

Scientific Approach and Accomplishments

The woodpile accelerating structures for laser acceleration confine the accelerating mode in a narrow channel (hollow waveguide at the center) with transverse dimensions of the order of a wavelength. Dielectric laser accelerator requires woodpile structures fabricated with high precision, made with vacuum compatible dielectric material with relatively high dielectric constant ($\varepsilon > 4$), low losses ($\tan \delta < 10\text{-}3$), and the ability to withstand high accelerating gradients.

We started utilizing a Nanoscribe Photonic Professional GT, a direct laser-writing device capable of maskless lithography and additive manufacturing, for the development of materials and structures to be used for target fabrication. The Nanoscribe can print at sub-micron resolution by focusing ultra-short, 760 nm laser pulses into a resin. The flux is only high enough for two-photon polymerization (2PP) at the focal point, allowing for lateral and vertical resolutions of 300 nm and 800 nm, respectively.

We have designed sample woodpile structures to operate at laser wavelengths of 5- and 10-µm. First we printed test matrices in Nanoscribe's acrylate-based 2PP resin (IP-Dip) of the unit cells of both 5- and 10-µm woodpiles to find the best printing parameters for a full-sized structure (shown in Figure 2). The laser power was varied between 15 and 60% of the full 50 mW, and scanning speed, the rate at which the focal point moves through the resin, was varied between 1000 and 20,000 µm/s. Selected features of the optimal prints for each of the 5- and 10-µm structures were measured in the scanning electron microscope (SEM) software and compared to the nominal value of the equivalent feature in the model. The inspection revealed that the acceleration defect size printed approximately 10% too wide and on the order of 5% too tall, but the departure from nominal is reproducible for different prints even with slightly different laser power. The departure from nominal was minimized for 40% laser power, and the scan speed of 5000 µm/s. These were chosen to be the optimal printing parameters for all future structures.

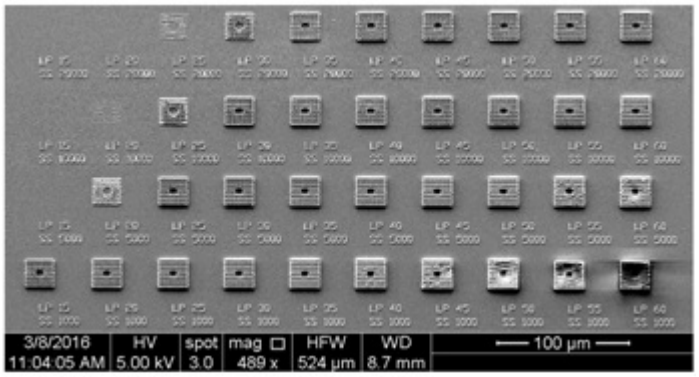

Figure 2. An SEM micrograph of the printing parameter test matrix for the 5 µm woodpile structure. In the upper left, no structures are printed because the amount of energy deposited in the resin was insufficient to cause polymerization, and in the lower right, the structures are partially decomposed and deformed, because too much energy was deposited.

Once the optimum printing parameters were found, several full-size woodpiles were printed and examined. SEM micrographs of full-size woodpiles are shown in Figure 3. We also analyzed the full-size parts with computed tomography (CT) for voids and imperfections through the whole length of the structure. To produce adequate contrast, 1% by weight of triphenyl bismuth was added to resin as an X-ray contrast agent.

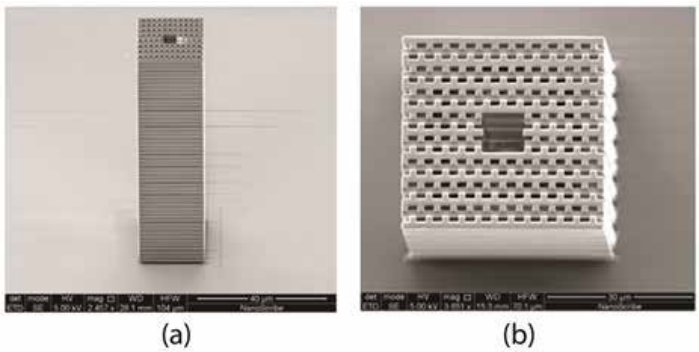

Figure 3. SEM micrographs of the printed full-scale 5-µm woodpile structure (a) and 10-µm woodpile structure (b).

Although we could produce the woodpile structures of correct dimensions with Nanoscribe's IP-Dip resin, those could not be employed for laser acceleration, because of the low dielectric constant of IP-Dip. Next, we tried to print a test matrix in a composite BTO-IP-Dip resin to demonstrate proof-of-principle of using composite resins with Nanoscribe. A composite resin was produced by sonicating BaTiO3 nanoparticles with triethyl phosphate in ethanol, combining the resulting suspension with IP-Dip, then driving off the solvent. An optical light microscope image of the printed test matrix is shown in Figure 4, demonstrating a print in a composite material.

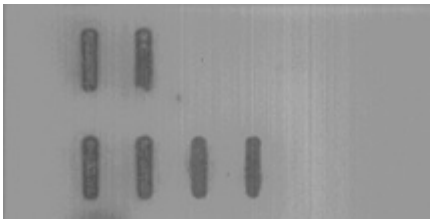

Figure 4. An image of the composite print. Bars are printed structures, 150 µm x 30 µm.

Thin films of resins and resin composites had to be prepared for measurement of their dielectric properties. The method of preparation was spin-coating onto a single-side polished silicon wafer, followed by curing under a metal-halide flood lamp, with an output of 225 mW/cm2 at 350 nm. The resins exhibited a wide range of viscosities, which made spin-coating a uniform layer difficult. We attempted to mitigate the effects of high viscosity with solvent, but found that solvent evaporation led to pronounced surface roughness upon photo-curing.

A series of trials with quarter-sectors of silicon wafers and different resins was carried out to determine the best spin-rate to coat a wafer to close to 10 µm thickness. For the IP-Dip resin, 30 seconds at 3000 rpm was sufficient to coat a section of the wafer with a 13 µm thick layer, but the high viscosity produced a splatter pattern around the edge of the wafer. The material was diluted with toluene, and appeared to flow better, but upon curing, showed a wavy surface. With limited time before the date for ellipsometric measurements, the first wafer, shown in 5(a) was selected. This particular mixture was found to cure to hardness in 1 minute under the flood lamp.

The PETA-Irgacure 819 resin, diluted with 10% toluene was spin-coated on a wafer for 120 seconds at 3000 rpm to give an 18 µm thick layer. During transit from the spin-coater to the flood lamp (approximately 2 minutes) the liquid layer was observed to pull back away from the edge of the wafer under its own surface tension. This blend does not adhere well to the wafer, resulting in a non-uniform coating regardless of dilution, and cured to hardness after 90 seconds under the flood lamp. The thickening of the edges is visible in Figure 5(b).

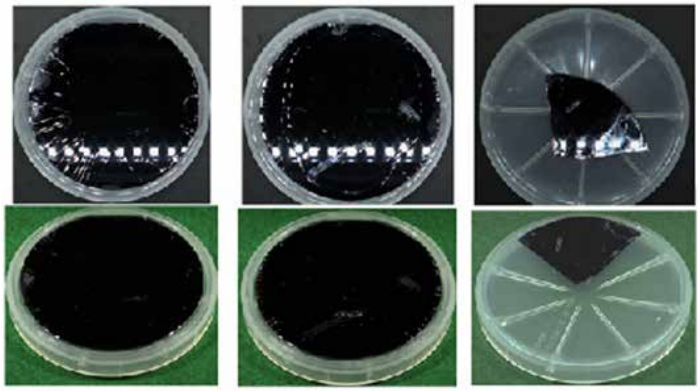

Figure 5. Spin-coated silicon wafers of resins. Top row, an above-down view in which the light source is visible as a series of bright spots. Bottom row, a view from 45°, illuminated from behind.

The undiluted VeroClear resin spun well, at 1000 rpm for 20 sec to give a 23 µm thick layer (Figure 5(c)). If time had permitted, a whole wafer would have been produced at 5800 rpm to give a 10 µm thick coating. The VeroClear resin cured in 30 seconds under the flood lamp.

Next, we worked with the composite resin of barium titanium oxide (BTO) and photopolymer that was produced by mixing an ethanol dispersion of nanometer-sized powdered BTO with resin. The ethanol dispersion of BTO was produced by suspending BTO particles in ethanol with triethyl phosphate, and intermittently sonicating (2 seconds on, 2 seconds off) the mixture with an ultrasonic disruptor for a total of three hours. Particle dispersion was assessed by particle size analysis. The ethanolic dispersion was mixed with VeroClear resin, and cast into photo-cured films for analysis by SEM and ellipsometry.

Particle size analysis of initial suspension (before resin addition) shows a maximum diameter of 200 nm, indicating fair dispersion. The film shown in Figure 5 was 12 µm thick, and had a surface roughness of about 0.1 µm. This roughness created a matte finish on the surface of the film, making it unsuitable for ellipsometry. SEM shows clusters of BTO particles with sizes ranging from 200 to 400 nm, composed on individual particles approximately 60 nm in diameter, which is consistent with the starting material. The ethanol suspension and the composite resin have a milky white appearance. The cure depth of the composite resin was found to be ~150 µm. A film of a similar composition, but with IP-Dip instead of VeroClear, was also cast. The surface finish of this sample was worse than the IP-Dip, possibly due to the absence of a more effective pho-

toinitiator. Improved dispersion may be achieved through the use of a high-speed mixer with the triethyl phosphate formulation. Coating the particles with polydopamine may also help with dispersion.

Ellipsometry is perhaps the best technique for determining the dielectric functions of a material. Light reflected from the surface of the material is compared in phase and intensity to the incident light. The differences in phase and intensity over the spectral region of interest can be used to compute the electrical permittivity and the dielectric loss as a function of wavelength.

A good sample for ellipsometry satisfies three requirements: the front and rear faces of the sample must be parallel and flat in the measurement area, it must be smooth, to minimize diffuse reflection from the surface, and it must have a thickness on the order of the wavelength of interest. The sample must also minimize specular reflectance from the rear, or be layered on the polished surface of a material with known dielectric properties, such as a polished silicon wafer.

Infrared ellipsometry experiments were conducted at CINT-Sandia. None of our samples that we had prepared had ideal surface quality, though samples of the TiO composite came close. The smoothest, flattest sample of TiO was 0.88 µm thick, but also showed many microscopic radial streaks, presumably an artifact of spin-coating, and the measurement was uninterpretable.

Each wafer we used was found to have a rear surface finish too smooth to allow for measurement. The preferred method for roughening the back of a wafer is to cover the front, sample side, with dicing tape, take the sample into a sandblasting unit, and sandblast the rear side to obtain a roughness (Ra) near 4 µm. Of the samples with good surface quality, none survived a spot test for the taping, in that some, or all, of the sample layer came away with a piece of dicing tape. The workers at the machine shop at LANL may be able to roughen the back with tooling, drawing grooves across the crystal to create a surface with the appropriate roughness, but we will need to consider the ramifications of the closely spaced grooves acting as a diffraction grating during the measurement.

Concurrently with efforts to produce useful ellipsometry samples, we are pursuing other ways of estimating the dielectric functions using measurement techniques that are less sensitive to sample quality, and more readily available. One technique, based on a determination of the index of refraction at one wavelength and the ATR-FTIR spectrum in the mid-IR range seems promising. The index of refraction can be determined from the effective optical path length through the sample, and the ATR-FTIR spectrum is used to estimate the value of the extinction coefficient k as a function of wavenumber. If the ATR spectrum is found to be underestimating k, we can use an integrating sphere to determine k(v) more precisely. The values of ε' and ε" are calculated from n and k.

Impact on National Missions

Compact accelerators are desired by a number of national security applications, including war-fighter support (weaponized FELs) and active interrogation (electron accelerators as compact front ends for muon active interrogation sources or to generate bremsstrahlung radiation). The compact dielectric laser accelerator that is being developed at LANL can provide relativistic electron beams to generate radiation for directed-energy-specific missions. Examples include directional gamma-ray beams through Compton scattering and terahertz radiation. With increased efficiency and decreased weight provided by DLA technology FELs might become fieldable on airborne platforms. In addition, the knowledge gained from employing the Nanoscribe system with customized non-standard dielectric composite resins is directly applicable to the development of novel resins to be used for the production of new and unique targets for the various High Energy Density Physics campaigns. Finally, the ability to create micron-scale parts in new materials supports LANL's position on the cutting edge of meso-scale science and engineering.

Publications

Simakov, E. I., H. L. Andrews, M. J. Herman, K. M. Hubbard, and E. Weis. Diamond field emitter array cathodes and possibilities of employing additive manufacturing for dielectric laser accelerating structures. To appear in Advanced Accelerator Concepts Workshop 2016. (National Harbor, MD, 31 July - 5 August, 2016).

Electron Transport in Warm and Hot Dense Matter

Charles E. Starrett
20150656ECR

Introduction

In this project we will develop a completely novel simulation capability for dense plasmas. Such plasmas exist in inertial confinement fusion plasmas (eg. at the national ignition facility (NIF)) as well as in astrophysics, for example, in the interiors of giant planets and in white dwarfs. Building on a existing computational tool developed by the PI, we will extend a method that has been very successful in condensed matter physics, into the dense plasma regime.

This method, known as KKR-Green's function, will provide an description of these plasmas with unparalleled realism across the temperature and density regime of interest. We will apply the method to the calculation of electrical conductivity, which is of importance to the modeling of inertial confinement fusion experiments. In the lower temperature regime the new capability will complement current high accuracy tools, while for hot dense plasmas the method will provide a gold standard where none currently exists.

Benefit to National Security Missions

The project aims to greatly improve our understanding of electron transport in dense plasmas. As such, it will ultimately provide a tool that could be used to provide crucial input information into hydrodynamical simulations of implosion experiments of inertial confinement fusion. Such experiments, like those conducted at the national ignition facility and elsewhere, are essential for the stockpile stewardship mission of the DOE NNSA.

The new method that we aim to develop will provide simulations of of unparalleled physical realism across the temperature and density regime of interest to the inertial confinement fusion community. It will put LANL at the forefront of the rapidly evolving field of electron transport in warm and hot dense matter.

Progress

In the last year, significant progress towards the final goal of the project has been made and the project remains on track.

The first significant milestone, the implementation of the single center Green's function code, was achieved and the result published (Starrett, High Energy Density Physics, Sept 2015). The second significant milestone was the development of the "structural constants" code. This was successful and was validated against available published results. This has been combined with the single center code and testing is ongoing.

On the theoretical side, this approach has provided routes to new approximations for calculating the conductivity using the single center approaches. We have published two papers based on this (Burrill et al, High Energy Density Physics, June 2016, and Starrett, High Energy Density Physics, June 2016). I presented some of this work at the American Physical Society's annual Division of Plasma Physics (DPP) conference in November 2015.

Future Work

In FY17 we will complete testing of the implementation of the conductivity and compare to published calculations. We will make new predictions of the behavior of the electrical conductivity in the warm dense matter regime and expect to write a paper for publication based on these results.

Conclusion

The ultimate result of this work will be a completely new computational framework for calculating electrical conductivity in warm and hot dense plasmas. The method will compare favorably to the existing gold standard methods at low temperature, and provide the gold standard at higher temperatures, where none currently exists. The method will lead to a new understanding of electron transport in dense plasmas and the resulting

calculations will of high relevance to the modeling of inertial confinement fusion experiments (eg. at the National Ignition Facility).

Publications

Burrill, D. J., D. V. Feinblum, M. R. J. Charest, and C. E. Starrett. Comparison of electron transport calculations in warm dense matter using the Ziman formula. 2016. HIGH ENERGY DENSITY PHYSICS. 19: 1.

Starrett, C. E.. A Green's function quantum average atom model. 2015. HIGH ENERGY DENSITY PHYSICS. 16: 18.

Starrett, C. E.. Kubo-Greenwood approach to conductivity in dense plasmas with average atom models. 2016. HIGH ENERGY DENSITY PHYSICS. 19: 58.

A Step toward Nuclear Reaction Studies for Applications at FRIB

Shea M. Mosby
20150683ECR

Introduction

The neutron capture reaction - in particular, the cross section - is of great importance for a variety of fields ranging from nuclear astrophysics to defense programs. This process must be understood across a whole host of elements and isotopes, with half-lives ranging from thousands of years to a fraction of a second. Current experimental access to this process is limited to stable and near-stable isotopes (half-lives ranging from months to years), and theoretical calculations are comparatively unreliable due to uncertainty in the nuclear structure inputs they require.

This project seeks to validate a potentially game-changing technique for measuring the necessary nuclear structure to accurately calculate the neutron capture cross section. Direct measurements using the Detector for Advanced Neutron Capture Experiments (DANCE) at Los Alamos National Laboratory will be made in parallel with indirect measurements using the Apollo instrument at Argonne National Laboratory. If successful, Apollo can be used to vastly improve our understanding of neutron capture on short-lived isotopes relevant for both nuclear astrophysics and defense programs.

Benefit to National Security Missions

Nuclear reaction rates (particularly neutron capture) on short-lived isotopes are known to have impact for basic science questions such as the origin of the elements heavier than iron, as well as radiochemical diagnostics used as part of our nuclear security mission. The current state of the art experimental methods for studying these reaction rates are limited to stable or long-lived isotopes. While several methods have been explored, no truly robust method of constraining neutron capture on short-lived isotopes has been demonstrated.

This project seeks to remedy that situation by performing the experimental work needed to validate a new method to constrain neutron capture rates on short-lived nuclei. The project will do this by performing two independent experiments on the same isotope - one using an established method for studying neutron capture, and one using the new method. By the end of the project, the two methods should provide consistent results for neutron capture, thus validating the new method and opening up hundreds of important isotopes for study.

Progress

Both of the experiments proposed for this project ran this FY, and online analysis of both measurements indicate that we have the data needed to extract our physics results. We have rough gamma-ray spectra (our physics observable) for both measurements.

The DANCE data calibrations are complete and at this point we are transitioning into the modeling phase of analysis. Sanity checks of the low-lying structure of 97Zr are happening, which serve to validate parts of the reaction model we wish to hold constant while constraining the interesting physics. We believe we have all the tools necessary in place, and the work is progressing quickly.

The Apollo rough analysis has taken place and much of the calibration work is complete. All the relevant data processing tools are in place. The theory/simulation tool chain is not yet complete but we expect to have that in place by the FY break. We have developed the means to characterize and subtract background.

Future Work

- Complete comparison of experimental gamma-ray yields with theoretical calculations.
- Estimate uncertainty of experimental constraint on neutron capture prediction for both direct and indirect methods.
- Submit results for publication.

Conclusion

The project will directly measure the 96Zr neutron capture cross section using DANCE, and constrain a theoretical calculation of the cross section using indirect techniques with Apollo. Furthermore, DANCE can make an independent measurement of the nuclear structure properties of 96Zr and independently constrain theoretical calculations of the capture cross section. It is expected that these three independent measurements will result in a consistent cross section prediction.

Optimization of Compton Source Performance through Electron Beam Shaping

Nikolai Yampolsky
20150690ECR

Introduction

The project aims to investigate a novel way for increasing brightness of light sources based on inverse Compton scattering (ICS). The key idea is to manipulate the electron beam phase space so that all the electrons emit photons of the same energy in some direction. During the course of the project we will study the feasibility of the scheme and determine how large an improvement can be achieved. Upon success of the project we will describe practical modifications to currently existing and future ICS light sources which should significantly improve their quality.

Benefit to National Security Missions

The proposed scheme may have a strong impact on MaRIE in its early stage. There is a possibility of reusing the planned MaRIE Injector Test Stand (MITS) as an ICS light source to enable early experiments. This project will also be beneficial for testing X-ray detectors planned for the MaRIE FEL.

Two ICS sources have been built and two future facilities are proposed to generate γ-rays through ICS for material science applications. Increasing the brightness of those sources will be beneficial for their host DOE facilities.

Recently, high-flux gamma rays have been proposed as approaches for detecting special nuclear materials and to address international nuclear proliferation concerns. A compact ICS source is an attractive option for generating these photons. The proposed method for conditioning the beam phase space will reduce the ICS bandwidth which will allow meeting the requirements. Moreover, increasing the brightness of such a source will allow reducing the power required to operate such a machine.

Progress

The initial project plan implied that the solution for the Wigner distribution function of the inverse Compton scattering (ICS) will be easy to achieve based on the well-known solutions for the emitted electric fields in the plane wave of the incoming laser. Turns out that the past experience is not applicable to the problem of interest since the homogeneous monochromatic radiation does not generate longitudinal Wigner function. The entire problem of the ICS has to be revisited to account for localization of the emitted radiation in time. Most of the time in FY15 was dedicated to finding the appropriate description of the light source properties in case of their localization in time (unlike conventional description with power spectra).

The single-particle motion in the field of the plane wave optical radiation has been revisited. The solution has been generalized to include the electron slow down due to the ponderomotive potential of the laser wave temporal envelope. The electric field of the radiation has been found including the temporal profile (unlike the conventional solution for the infinitely long monochromatic laser field). The general expression for the Wigner distribution function of a single-electron radiation in the ICS has been derived. To the best of our knowledge, this is the first time the 6D Wigner distribution function for any light source has been derived. Then the Wigner distribution function has been generalized to include the effects of the transverse and longitudinal localization of the incoming laser.

The Wigner distribution function of radiation emitted by the ensemble of electrons has been derived. The form for the monochromatic incoming laser wave was found. It has been concluded that the approximation of an infinitely long monochromatic incoming laser misses the important physics and it has to be generalized to include the temporal profile of the laser envelope. The work of finding the general 6D solution for the Wigner function of the scattered radiation produced by the entire bunch is underway.

Future Work

- Obtain the solution for the Wigner distribution function of the ICS source for arbitrary electron and laser distributions (defined through electron beam matrix Wigner function of incoming laser).
- Optimize the Wigner function of the ICS source through symplectic transforms of the electron beam distribution.
- Estimate the effects of the ICS source broadening for existing and planned facilities due to 3D envelope of the incoming laser wave packet.

Conclusion

We expect to demonstrate that ICS brightness can be increased through appropriate conditioning of the electron beam phase space. We expect to eliminate the largest contribution to the brightness degradation, i.e. either due to the angular divergence or the energy spread of the electron beam. At the moment, it is an open question whether both effects can be suppressed simultaneously. We conservatively anticipate that only one of them can be compensated and the final source brightness will be defined by the smallest rather than the largest effect.

Publications

Malyzhenkov, A. V., and N. Yampolsky. Optimization of Compton Source Performance through Electron Beam Shaping. To appear in 17th Advanced Accelerator Concepts Workshop. (National Harbor, 7/1/16-8/5/16).

Malyzhenkov, A. V., and N. Yampolsky. Optimization of Compton Source Performance through Electron Beam Shaping. To appear in North American Particle Accelerator Conference . (Chicago, 10/9/16-10/14/16).

Microscopic Fission Model for Data Needs

Ionel Stetcu
20140581ECR

Abstract

We have investigated nuclear fission within a microscopic framework, making use of the density functional theory (DFT) and its extension to time-dependent (TD) phenomena. Implementation of time dependent density functional theory (TDDFT) on computers using graphical accelerators (GPUs) has been a major part of the project, with significant improvement over our previous implementation on central processing unit (CPU) only architectures, the GPU version reaching speed up factors of up to 25 with respect to CPU-only version. This improvement has allowed us to make efficient use of leadership class machines and be well positioned in the current context of building new machines with the perspective of reaching exascale computing. With the new capability we were able to make several real-time calculations of the fission of an excited 240Pu nucleus. We found that the characteristics of the fission fragments (FFs) emerging from our calculations are comparable with the experimental information. Total kinetic energies of the FFs were predicted within 3% of the experiment, and that more excitation energy was available for neutron emission of fission from the light FF. Average light and heavy FFs mass numbers are also consistent with experimental information, especially taking into account that the errors on these quantities is around four mass units. We have found significant differences with respect to competing microscopic approaches that are most likely the result of more stringent approximations involved. We have shown that the evolution time from saddle to scission could be significantly larger than previously thought and obtained in other approaches, while some experimental data also points towards longer fission times. Although more development is necessary, the current capability is at a point that will allow us in the future to provide input in the phenomenological modeling of post-scission data: fragments yields, prompt gamma and neutron observables for a wide range of applications.

Background and Research Objectives

Fission plays an important role in applications to energy production, global security, weapons, astrophysics, etc. However, because of its complexity and despite the theoretical effort using different approaches [1], [2], [3], [4], [5], [6], [7], [8], more than seventy years after its discovery we still lack a quantitative and predictive quantum-mechanical description of this phenomenon. It is the main goal of this work to provide a first fully quantum-mechanical of the fission beyond the saddle point.

We have made use use of the latest-generation supercomputers to implement and study nuclear fission of actinides in the density functional theory (DFT) framework. At the end of the two-year period, we were be able to start with a nucleus in a deformed state beyond the fission barrier, and, in a consistent approach in which the structure is treated on the same footing with dynamics, release it and evolve the system further without any additional constraints. The system naturally evolves to a configuration of minimum energy, in which it will split into two fragments. In the process, we have the unique opportunity to study in a real-time dynamical approach the neutron emission at scission. Finally, once the system fissions, we extract average quantities for the light and heavy fragments, such as average charge and mass, average internal excitation energy, and average total kinetic energy (TKE). Other observables of interest, such as the fission fragment average angular momenta, require extensions of the DFT framework, which were not possible, nor proposed, for the two-year period.

Experiments provide a stringent test of the theoretical models. In particular for the fission of actinides (both induced and spontaneous), the properties of the prompt particles, emitted immediately after the fission fragment production and before any β decay, provide constraints for our simulation capabilities. In T-2, we have developed a code in which the starting point are the excited frag-

ments, fully accelerated by the Coulomb interaction. Making use of the statistical model of Hauser and Feshbach [9] to the de-excitation of compound nuclei, we can model the emission of prompt neutrons and gamma rays, taking into account the competition between them, until all the initial excitation energy is released [10], [11]. Several average quantities, like the neutron or gamma spectra, average number of particles emitted by a fission fragment, average energy released, etc., can be calculated and tested against experimental data. In addition, our Monte-Carlo implementation of the Hauser-Feshbach statistical model allows us to obtain more detailed information, such as correlations between the emitted particles. These have been or will be the subject of future experimental investigations at LANSCE and elsewhere, and will further test our prediction capability.

Data needs for applications go well beyond the existing and planned experiments. Therefore, it is important to have not only a simulation capability benchmarked against available experimental data, but one that can be reliably extended to other physical scenarios. At the moment, an input to our simulations is the experimental information on pre-neutron emission fission fragment yields as well as their kinetic energy, spin and parity distribution. We further assume a simple model for the sharing of the excitation energy between the fragments and that the particle emission starts after full acceleration of the fission fragments. For all these quantities, incomplete (e.g., yields) or indirect information (e.g., angular distribution) exists. In addition, the Hauser-Feshbach calculations rely on a number of other non-observables such as the optical potential used to model the neutron emission [12], the densities of states [13], or the Brink hypothesis for the gamma-ray strength function [14]. These are phenomenologically adjusted to reproduce data for nuclei close to stability, and might not reliably extrapolate to short-lived nuclei as those produced in fission. All these uncertainties reduce the predictive power of our model, even though it is based on the most sophisticated phenomenological approach. Hence, it is desirable to reduce the uncertainty of the input and the goal of this work is to provide microscopic predictions for production yields for fission fragments, their angular momentum distribution, and initial excitation energy sharing between fragments. Using such input can help constrain the other quantities involved in the calculations, for example the most appropriate optical model parameters for neutron emission. In this project, we have concentrated on obtaining average quantities, while future work will explore calculating the distribution widths.

An essential first step for the success of this approach was the efficient implementation of the code using GPUs, which allows for large-box calculations. In a sufficiently large box, an intermediary success will be to achieve fission by driving the system on the energy surface and releasing it before the scission point. This approach had to be altered as it was not possible to drive the system on the lowest energy surface. Instead, we started with a deformed solution by imposing deformation constraints on the system, and thus we were able to achieve fission at low excitation energy. The calculated average mass, charge and kinetic energy yields for the two fragments can be directly compared against existing experimental data. We have achieved qualitatively good agreement between theory and experiment, as discussed in the next section.

Scientific Approach and Accomplishment

State-of-the-art of the phenomenological approaches. Hahn and Strassmann (Nobel prize, 1944) put nuclear fission in evidence experimentally more than 75 years ago in 1939, and yet we still lack a microscopic quantum mechanical description of this phenomenon. To put it in perspective, superconductivity was discovered in 1911 by Kamerlingh Onnes (Nobel prize, 1913) and was given a theoretical description in less than 50 years, in 1957 by Bardeen, Cooper, and Schrieffer (Nobel prize, 1972). Nuclear fission is just the most prominent example of low-energy nuclear reactions that can be studied with the tools we have developed. Nuclear fission research has undergone a renaissance worldwide, and in particular at DOE/NNSA laboratories (in particular at LANL). Motivated by both basic science needs and applications to new signatures for material detection, proliferation and forensics, a vigorous experimental effort is dedicated toward understanding properties of actinides at the LANSCE facility at LANL (DANCE, GEANIE, ChiNu, SPIDER, etc.). This experimental program provides valuable input and benchmarks for the theoretical models developed. Particularly important for applications are the properties of prompt fission neutrons and gamma rays, which are emitted before the weak decays of the fission fragments toward stability. Such properties constitute an important research direction in the applied group at LANL and LLNL. In simulations of the fission spectrum, the fully accelerated fission fragments can be treated as compound nuclei and the input to such simulations typically is the experimental information (which is ether scarce or unavailable) on pre-neutron emission fission fragment mass/charge yields as well as their kinetic energy, spin and parity distributions.

Fission fragment properties are evaluated in the literature using a multitude of approaches. The scission-point model [15], [16] evaluates the energetics of various fragment configurations at a guess of the scission configuration of a given actinide nucleus. The method is based on counting

the number of available states in a phase space that includes basic nuclear shapes, proton and neutron numbers of fragments and it relies on the total equilibration of the intrinsic motion. One typical result is shown in Figure 1, where the amplitude of the uncertainties under variations of model parameters reaches 10%.

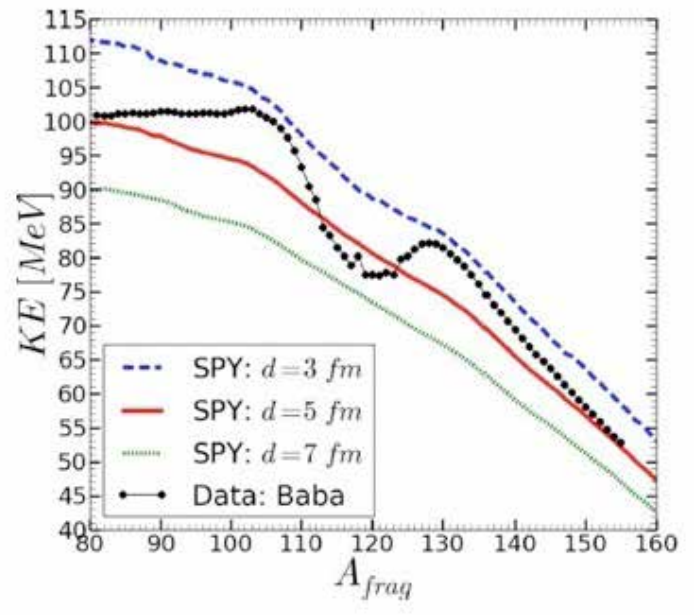

Figure 1. Fragment kinetic energies for different scission distances in the U(n,f) reaction, calculated with SPY, and compared with experimental data. Figure from Ref. [16].

The model by Brosa et. al. [17] is also based on the notion that the TKE is determined mainly by the nuclear shapes at the scission configurations, and thus fully ignoring the dynamics of the nuclear system until it reaches point. In Langevin approaches [5], [18], [19], one also assumes that the nuclear system is equilibrated and the evolution can be described by a classical diffusion model with phenomenological friction at a finite temperature and a potential energy surface calculated either at zero or finite temperature. This surface depends on a small number of chosen collective parameters typically 2-3 and no more than 5. Typical agreement with experiment is quite good when the number of collective degrees of freedom is large enough (5 in practice), which required the calculation of the nuclear potential energy surface for about five million configurations within the micro-macroscopic model. In the Langevin approach one determines typically only mass and charge yields. To illustrate the state-of-the-art ambiguities in predicting such distributions we show in Figure 2 predictions in superheavy nuclei from two competing phenomenological models (named GEF and SPY, respectively) for the same physical system. This demonstrates, likely in the extreme, the limitations of phenomenology.

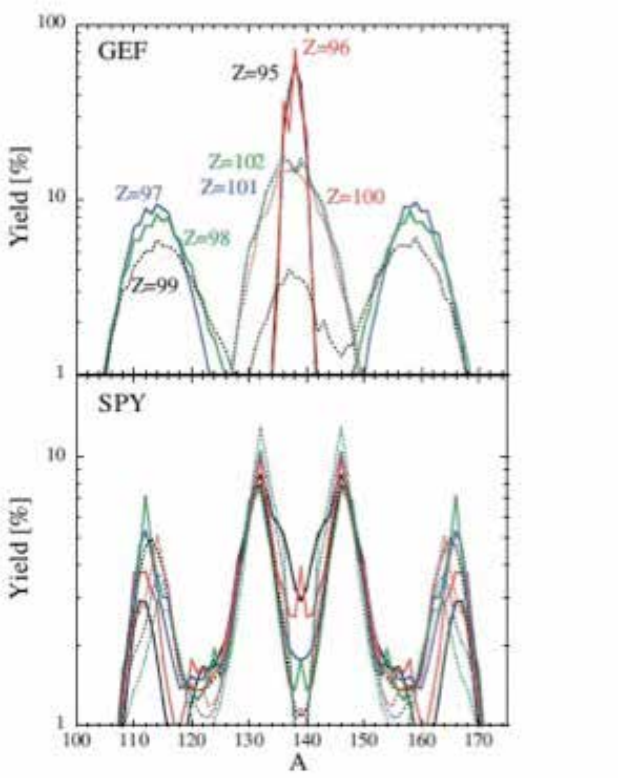

Figure 2. Fission fragment distribution predicted by GEF (upper panel) and SPY models (lower panel) for 7 A=278 isobars. Figure from Ref. [49].

State-of-the art of microscopic approaches. Attempts to use a microscopic approach based on the time-dependent Hartree-Fock (TDHF) theory to study fission go back to 1970s [20], when only some qualitative results were obtained. It was observed at that time that only by introducing unrealistically large pairing gaps (about 6 MeV) or starting at configurations where the neck is rather well formed could one have fission-like dynamics at low energies and starting from compact nuclear shapes. Interest in using TDHF and TDHF+BCS approaches was revived in the last couple of years, see [21], [22], [23], [24]. In all these studies it was determined that one can simulate fission dynamics only if one considers initial states relatively far away from the outer saddle point, see Figure 3. Note that the initial states considered in these studies are well below the ground state and can be reached only in some very unlikely photo de-excitation or neutron emission perhaps of a highly excited deformed nucleus. Otherwise the nucleus should be given an artificial boost, thus provided additional excitation energy. The physical reason for this behavior was explained almost two decades ago by Bertsch and Bulgac [25] using only general symmetry arguments and well-established nuclear properties. An axial symmetric nucleus (as the majority of fissioning nuclei at the outer saddle point appear to be in the majority of theoretical studies) has a large number of occupied single-particle states with

relatively large projections of the angular momentum on the fission axis. The population probabilities of states with high angular momenta are conserved in the dynamics, but at the same time such states do not exist in fission fragments. This situation creates an insurmountable dynamic barrier to fission, which can be overcome only by an additional boost, as observed in all these papers using TDHF or TDHF+BCS. In the case of TDHF+BCS the magnitude of the pairing field is constant throughout the entire space, though it can vary in time. Its time-dependent phase can be removed by a trivial gauge transformation, resulting in an insignificant renormalization of the chemical potential.

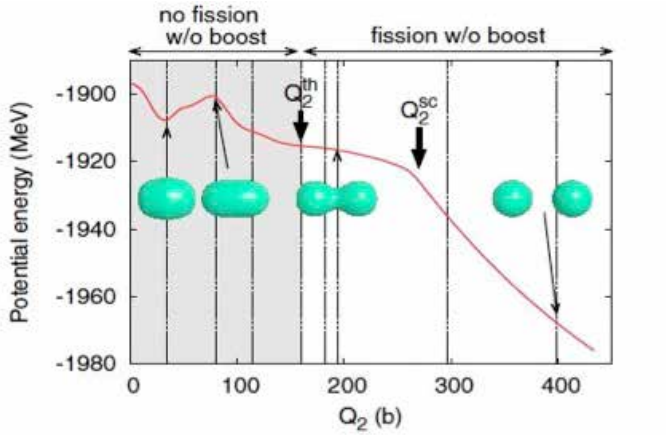

Figure 3. Potential energy curve of Fm nucleus, as a function of quadrupole deformation parameter. The vertical lines indicate the different starting points used in Ref. [22] as initial conditions for the time-dependent evolution. Figure from Ref. [22].

Our theoretical approach, the time-dependent superfluid local density approximation (TDSLDA), is based on the most advanced theoretical framework available today to describe both static and dynamic properties of strongly interacting many-fermion systems, using the only existing implementation of time-dependent superfluid dynamics in 3D. TDSLDA is an extension developed by the PI and collaborators of the local density approximation (LDA) implementation of DFT due to Kohn and Sham (1965) to real-time and superfluid systems. A previous extension of LDA to superfluid systems due to [26] is a non-local formalism, and thus nullified the great numerical simplicity of the original Kohn-Sham LDA, which would be extremely hard to implement numerically for nuclei even on exascale computers, and especially for time-dependent problems. DFT is the highly successful approach pioneered by Kohn (Nobel prize, 1998), Hohenberg, and Sham in 1964-1965 for many-electron systems in chemistry and condensed matter physics. These two ground breaking papers have garnered more than 70,000 citations according to Google Scholar. (TD)SLDA is relevant to a large range of quantum systems. It has been validated against a large number of experiments and ab initio results in cold atoms, neutron stars, and nuclei. (TD)SLDA provided actual predictions (as opposed to post-dictions) and often corrected interpretations of experiments with most of the results published in leading journals by a larger collaboration working DFT/TDDFT: [27], [28], [29], [30], [31], [32], [33], [34], [35], [36], [37], [38], [39], [40], [41], [42]. This approach is key to deliver accurate estimate of fission observables. Our numerical implementation of TDSLDA uses highly accurate numerical procedures and runs at scale with very efficient HPC implementations, originally on Jaguar using CPUs and subsequently on Titan with GPUs, for which support from the LDRD-ECR funding was essential. In Figure 4 we display the first-ever microscopic simulation of the real-time evolution of a heavy nucleus, 240Pu, from the outer saddle until scission.

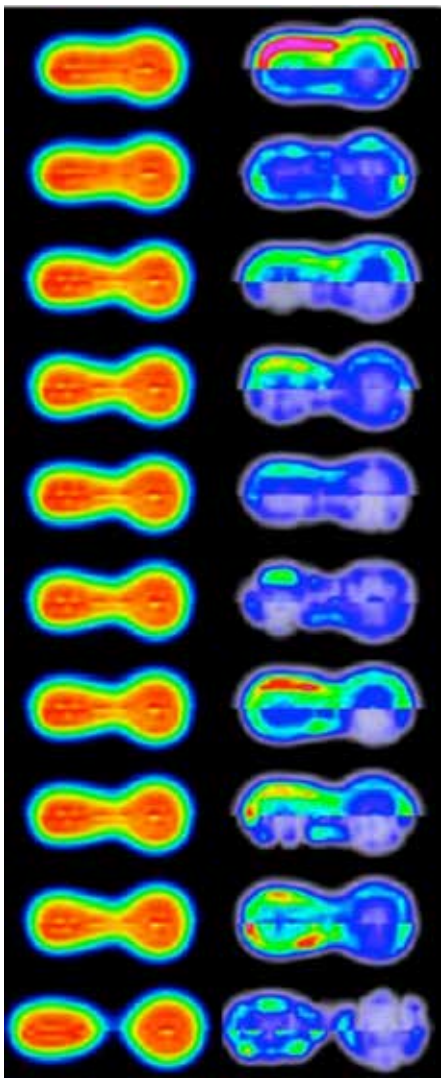

Figure 4. The left column shows the neutron/proton densities in the top/bottom half of each frame. In the right column the pairing eld for the neutron/proton systems are displayed in the top/bottom of each frame respectively. The time dierence between frames is dt=1600 fm/c. Figure from Ref. [42].

In particular, our approach is free of the ambiguities of defining the nuclear shape, the scission point, or a continuous potential energy surface needed in other approaches. Only a correct dynamical treatment of pairing correlations in TDSLDA, as in [42], can describe fission within a microscopic approach. The pairing correlations, due to their very-short range, are very effective at depopulating the "nuisance" high-angular momentum states in the mother nucleus. This situation is reminiscent of supernovae, which "refused" to explode in 2D simulations: A nucleus will not fission at low energies, started from a compact shape, unless all degrees of freedom are allowed to participate in the evolution. In Figure 5 we show the evolution of several degrees of freedom, excited during a complete simulation of the fission dynamics of 240Pu starting just above the outer saddle point, corresponding to an incident neutron energy of 1.5 MeV in a 239Pu(n,f) reaction.

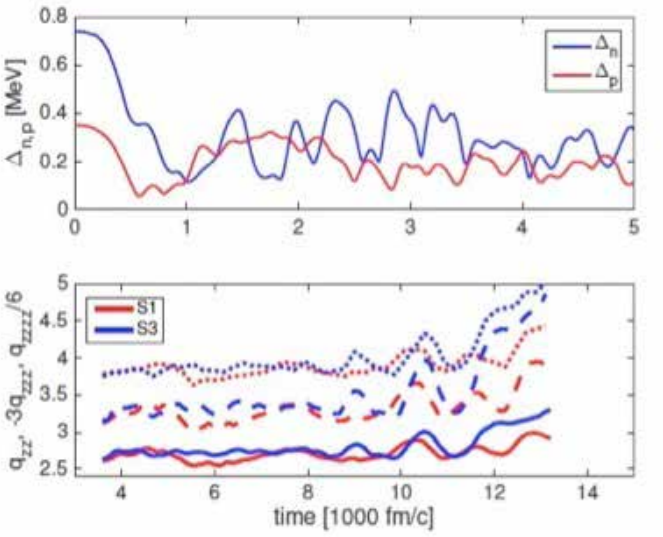

Figure 5. The time dependence of averaged absolute value of the the pairing field for protons and neutrons (upper panel) and scaled mass moments (lower panel). Figure from Ref. [42].

This illustrates the fact that many shape degrees of freedom are excited in fission dynamics, not only 2 or even 5. The crucial difference with previous simulations is in allowing for a complete unrestricted dynamics of neutron and proton pairing fields, both in space and time. Simulations of fission even at lower energies, below the neutron threshold, are also feasible. When such a full microscopic simulation is performed, even without trying to optimize the NEDF, many fission fragment properties emerge in surprisingly good agreement with experiment. The average TKE is reproduced with an accuracy of 3% or better, which is definitely superior to the scission-point models discussed above, see Figure 1, especially keeping in mind that in our approach there are no fitting parameters. In our simulations, see [42], we are able however to provide also some other crucial quantities such as the excitation energy of the fission fragments or information about angular momenta, which so far have been discussed in some phenomenological models only [43], [44] , [45], [46].

We have observed another remarkable qualitative feature, the fact that the saddle-to-scission time is greatly affected by the character of the pairing correlations namely by whether pairing is a volume or surface effect, or a mixture of them. Unfortunately ab initio useful information on this issue does not exist. Phenomenology also has no better answer. The analysis [28] of more than 200 semi-magic nuclei with known masses at the time and the more recent analysis [47] of 861 odd-even mass differences find almost no difference between various mixtures of volume and surface pairing mechanisms. Fission dynamics, however, appears to be the first nuclear phenomenon where one can observe a strong dependence of the saddle-to-scission time on the character of pairing, moreover this dependence appears to be non-monotonic too, which likely has a not too complicated explanation. There is another aspect of nuclear fission, which is less understood. Experimentally, the TKE decreases with the neutron incident energy En, which in case of 239Pu(n,f) reaction can be parameterized as follows: TKE = 177.80 MeV – 0.3489En according to Madland [48]. These two aspects, the long fission times and the TKE dependence on the incident neutron energy might be intimately related. Brosa et al [17] present sensible arguments that the TKE is determined by the geometry of the nuclear system at the scission point, the more elongated the nuclear system is at the time of the rupture, the smaller TKE is. Naturally, how long a system spends until it reaches the scission point, and what shape it acquires there are most likely very closely related aspects of the fission dynamics. The change in the TKE will in its turn affect the total excitation energy (TXE) as well, thus the neutron and gamma spectrum, and it might affect the mass and charge yields too. Due to the LDRD funding, we might be right now in the unique position, for the first time, to be able to crack these puzzles in a microscopic approach.

Scission neutrons were part of the proposed investigation. Our results suggest that the amount of neutrons produced at the time of separation of the two fragments is negligible, and thus further examination of the scission neutron properties were not necessary.

Impact on National Missions

The goal of the work funded by the LDRD program is to advance our ability to describe and predict complex non-stationary quantum phenomena, using state-of-the-art microscopic approaches, rather than phenomenological models, and increase the predictive power of our theoretical tools.

Nuclear fission is a remarkable problem in theoretical physics, which has been awaiting a description within a microscopic framework for almost 80 years. Furthermore, it is prominently featured as one the major research activities in The 2015 Long Range Plan for Nuclear Science (LRPNS) [science.energy.gov/np/nsac/], and the Workshop on Nuclear Data Needs and Capabilities for Applications, May 27-29, 2015, LBNL, Berkeley, CA, organized at the DOE NP request [bang.berkeley.edu/events/ndnca/whitepaper/], where nuclear fission was the only fundamental theoretical topic raised. On page 19 one reads: "A first principles understanding of nuclear fission would likely be of great importance to nuclear physics applications, since this understanding could lead to a predictive fission model that provides reliable information about fission nuclides and fission products at energies not normally accessed by experiment. Improved fission models will provide fission product information required by multiple applications. Without a high-fidelity fission models, one may still infer systematics from the limited existing experimental fission studies, which may introduce large uncertainties to calculated values in regimes that have not been addressed experimentally." Apart from being one of the basic unresolved problems in nuclear physics, nuclear fission is relevant to future reactors (new fuel compositions, new geometries), for the safety, management, and improvement of exiting fuel cycles, to national security, to non-proliferation and attribution, and to nuclear forensics (which is tasked with investigating nuclear materials by measuring a variety of physical and chemical properties in order to determine the source of the materials, whether they have been enriched, potential trafficking routes, etc.). Fission also has a broad impact across multiple branches of physics, from nuclear astrophysics and the determination of the origin of more than half of the elements heavier than iron, which are produced in core-collapsed supernovae and/or neutron star mergers during the r-process (rapid neutron capture) to nuclear reactions, condensed matter physics, dynamics of superfluids, studies of turbulence.

Particularly important for applications are the properties of prompt fission neutrons and gamma rays, which are emitted before the weak decays of the fission fragments toward stability. In such simulations, the fully accelerated fission fragments can be treated as compound nuclei and, making use of Monte-Carlo implementations of either the Weisskopf evaporation spectrum (LLNL) or the statistical model of Hauser and Feshbach to the de-excitation of compound nuclei (LANL), one can model the emission of prompt neutrons and gamma rays until all the initial excitation energy of fission fragments is released. A critical input to such simulations is the information on pre-neutron emission fission fragment yields as well as their kinetic energy, spin and parity distributions. For all these quantities only incomplete (e.g., mass/charge yields) or indirect information (e.g., initial angular distribution, or sharing of TXE) exists, which increases significantly the uncertainties and reduces the predictive power of the model. Theory guidance is thus essential to provide input to such reaction codes. In this project, we will have started the development of tools that can be aligned with these programs' needs.

References

1. NEGELE, J. W.. MICROSCOPIC THEORY OF FISSION DYNAMICS. 1989. NUCLEAR PHYSICS A. 502: C371.

2. REINHARDT, H.. SEMI-CLASSICAL THEORY OF NUCLEAR-FISSION. 1981. NUCLEAR PHYSICS A. 367 (2): 269.

3. Moller, P., D. G. Madland, A. J. Sierk, and A. Iwamoto. Five-dimensional potential-energy surfaces and coexisting fission modes in heavy nuclei. 2001. 4TH SYMPOSIUM ON NUCLEAR PHYSICS. 561: 455.

4. Moller, , A. J. Sierk, Ichikawa, Iwamoto, Bengtsson, Uhrenholt, and Aberg. Heavy-element fission barriers. 2009. PHYSICAL REVIEW C. 79 (6).

5. Randrup, , and Moeller. Energy dependence of fission-fragment mass distributions from strongly damped shape evolution. 2013. PHYSICAL REVIEW C. 88 (6).

6. Pei, J. C., Nazarewicz, J. A. Sheikh, and A. K. Kerman. Fission Barriers of Compound Superheavy Nuclei. 2009. PHYSICAL REVIEW LETTERS. 102 (19).

7. Staszczak, , Baran, Dobaczewski, and Nazarewicz. Microscopic description of complex nuclear decay: Multimodal fission. 2009. PHYSICAL REVIEW C. 80 (1).

8. Umar, A. S., V. E. Oberacker, J. A. Maruhn, and P. -. G. Reinhard. Microscopic description of nuclear fission dynamics. 2010. JOURNAL OF PHYSICS G-NUCLEAR AND PARTICLE PHYSICS. 37 (6).

9. HAUSER, W., and H. FESHBACH. THE INELASTIC SCATTERING OF NEUTRONS. 1952. PHYSICAL REVIEW. 87 (2): 366.

10. Becker, , Talou, Kawano, Danon, and Stetcu. Monte Carlo Hauser-Feshbach predictions of prompt fission gamma rays: Application to n(th)+U-235, n(th)+Pu-239, and Cf-252(sf). 2013. PHYSICAL REVIEW C. 87 (1).

11. Stetcu, , Talou, Kawano, and Jandel. Isomer production ratios and the angular momentum distribution of fission fragments. 2013. PHYSICAL REVIEW C. 88 (4).

12. Koning, A. J., and J. P. Delaroche. Local and global nucleon optical models from 1 keV to 200 MeV. 2003. NUCLEAR PHYSICS A. 713 (3-4): 231.

13. GILBERT, A., and A. G. W. CAMERON. A COMPOSITE NUCLEAR-LEVEL DENSITY FORMULA WITH SHELL CORRECTIONS. 1965. CANADIAN JOURNAL OF PHYSICS. 43 (8): 1446.

14. Brink, D.. No title. 1955. Ph.D Thesis.

15. Lemaitre, , Panebianco, Sida, Hilaire, and Heinrich. New statistical scission-point model to predict fission fragment observables. 2015. PHYSICAL REVIEW C. 92 (3).

16. WILKINS, B. D., E. P. STEINBERG, and R. R. CHASMAN. SCISSION-POINT MODEL OF NUCLEAR-FISSION BASED ON DEFORMED-SHELL EFFECTS. 1976. PHYSICAL REVIEW C. 14 (5): 1832.

17. BROSA, U., S. GROSSMANN, and A. MULLER. NUCLEAR SCISSION. 1990. PHYSICS REPORTS-REVIEW SECTION OF PHYSICS LETTERS. 197 (4): 167.

18. DAVIES, K. T. R., A. J. SIERK, and J. R. NIX. EFFECT OF VISCOSITY ON DYNAMICS OF FISSION. 1976. PHYSICAL REVIEW C. 13 (6): 2385.

19. Randrup, , and Moeller. Brownian Shape Motion on Five-Dimensional Potential-Energy Surfaces: Nuclear Fission-Fragment Mass Distributions. 2011. PHYSICAL REVIEW LETTERS. 106 (13).

20. NEGELE, J. W., S. E. KOONIN, P. MOLLER, J. R. NIX, and A. J. SIERK. DYNAMICS OF INDUCED FISSION. 1978. PHYSICAL REVIEW C. 17 (3): 1098.

21. Simenel, , and A. S. Umar. Formation and dynamics of fission fragments. 2014. PHYSICAL REVIEW C. 89 (3).

22. Scamps, , Simenel, and Lacroix. Superfluid dynamics of Fm-258 fission. 2015. PHYSICAL REVIEW C. 92 (1).

23. Goddard, , Stevenson, and Rios. Fission dynamics within time-dependent Hartree-Fock: Deformation-induced fission. 2015. PHYSICAL REVIEW C. 92 (5).

24. Tanimura, , Lacroix, and Scamps. Collective aspects deduced from time-dependent microscopic mean-field with pairing: Application to the fission process. 2015. PHYSICAL REVIEW C. 92 (3).

25. Bertsch, G. F., and A. Bulgac. Spontaneous fission: A kinetic approach - Comment. 1997. PHYSICAL REVIEW LETTERS. 79 (18): 3539.

26. OLIVEIRA, L. N., E. K. U. GROSS, and W. KOHN. DENSITY-FUNCTIONAL THEORY FOR SUPERCONDUCTORS. 1988. PHYSICAL REVIEW LETTERS. 60 (23): 2430.

27. Bulgac, A., and Y. L. Yu. Renormalization of the Hartree-Fock-Bogoliubov equations in the case of a zero range pairing interaction. 2002. PHYSICAL REVIEW LETTERS. 88 (4).

28. Yu, Y. L., and A. Bulgac. Energy density functional approach to superfluid nuclei. 2003. PHYSICAL REVIEW LETTERS. 90 (22).

29. Bulgac, A., and Y. L. Yu. Vortex state in a strongly coupled dilute atomic fermionic superfluid. 2003. PHYSICAL REVIEW LETTERS. 91 (19).

30. Bulgac, , and M. M. Forbes. Unitary Fermi Supersolid: The Larkin-Ovchinnikov Phase. 2008. PHYSICAL REVIEW LETTERS. 101 (21).

31. Bulgac, , and Yoon. Large Amplitude Dynamics of the Pairing Correlations in a Unitary Fermi Gas. 2009. PHYSICAL REVIEW LETTERS. 102 (8).

32. Bulgac, , Luo, and K. J. Roche. Quantum Shock Waves and Domain Walls in the Real-Time Dynamics of a Superfluid Unitary Fermi Gas. 2012. PHYSICAL REVIEW LETTERS. 108 (15).

33. Bulgac, , M. M. Forbes, M. M. Kelley, K. J. Roche, and Wlazlowski. Quantized Superfluid Vortex Rings in the Unitary Fermi Gas. 2014. PHYSICAL REVIEW LETTERS. 112 (2).

34. Stetcu, , C. A. Bertulani, Bulgac, Magierski, and K. J. Roche. Relativistic Coulomb Excitation within the Time Dependent Superfluid Local Density Approximation. 2015. PHYSICAL REVIEW LETTERS. 114 (1).

35. Bulgac, , Luo, Magierski, K. J. Roche, and Yu. Real-Time Dynamics of Quantized Vortices in a Unitary Fermi Superfluid. 2011. SCIENCE. 332 (6035): 1288.

36. Bulgac, . Local-density-functional theory for superfluid fermionic systems: The unitary gas. 2007. PHYSICAL REVIEW A. 76 (4).

37. Wlazlowski, , Bulgac, M. M. Forbes, and K. J. Roche. Life cycle of superfluid vortices and quantum turbulence in the unitary Fermi gas. 2015. PHYSICAL REVIEW A. 91 (3).

38. Bulgac, A.. Local density approximation for systems with pairing correlations. 2002. PHYSICAL REVIEW C. 65 (5).

39. Stetcu, , Bulgac, Magierski, and K. J. Roche. Isovector giant dipole resonance from the 3D time-dependent density functional theory for superfluid nuclei. 2011. PHYSICAL REVIEW C. 84 (5).

40. Bulgac, . Time-Dependent Density Functional Theory and the Real-Time Dynamics of Fermi Superfluids. 2013. ANNUAL REVIEW OF NUCLEAR AND PARTICLE SCIENCE, VOL 63. 63: 97.

41. Bulgac, A., M. M. Forbes, and P. Magierski. The unitary Fermi gas: from Monte Carlo to density functionals. 2012. In Lectures Notes in Physics. Edited by Zwerger, W.. , p. 305. Heidelberg Dordrecht London New York: Springer.

42. Bulgac, A., P. Magierski, K. J. Roche, and I. Stetcu. Induced Fission of 240Pu within a Real-Time Microscopic Framework. 2015. LA-UR-15-28092.

43. Schmidt, , and Jurado. Entropy Driven Excitation Energy Sorting in Superfluid Fission Dynamics. 2010. PHYSICAL REVIEW LETTERS. 104 (21).

44. Schmidt, , and Jurado. Final excitation energy of fission fragments. 2011. PHYSICAL REVIEW C. 83 (6).

45. Schmidt, , and Jurado. Thermodynamics of nuclei in thermal contact. 2011. PHYSICAL REVIEW C. 83 (1).

46. Schmidt, , and Jurado. Final excitation energy of fission fragments (vol 83, 061601, 2011). 2011. PHYSICAL REVIEW C. 84 (5).

47. Bertsch, G. F., C. A. Bertulani, Nazarewicz, Schunck, and M. V. Stoitsov. Odd-even mass differences from self-consistent mean field theory. 2009. PHYSICAL REVIEW C. 79 (3).

48. Madland, D. G.. Total prompt energy release in the neutron-induced fission of U-235, U-238, and Pu-239. 2006. NUCLEAR PHYSICS A. 772 (3-4): 113.

49. Goriely, . The fundamental role of fission during r-process nucleosynthesis in neutron star mergers. 2015. EUROPEAN PHYSICAL JOURNAL A. 51 (2).

Publications

Bulgac, A., P. Magierski, K. J. Roche, and I. Stetcu. Induced Fission of 240Pu within a Real-Time Microscopic Framework. 2015. Physical Review Letters (submitted); Report LA-UR-15-28092. .

Stetcu, . NUCLEAR STRUCTURE AND DYNAMICS WITH DENSITY FUNCTIONAL THEORY. 2015. ACTA PHYSICA POLONICA B. 46 (3): 391.

Stetcu, , C. A. Bertulani, Bulgac, Magierski, and K. J. Roche. Relativistic Coulomb Excitation within the Time Dependent Superfluid Local Density Approximation. 2015. PHYSICAL REVIEW LETTERS. 114 (1).

Relativistic Electrons in Magnetized Plasmas

Zehua Guo
20140605ECR

Abstract

Dynamics of runaway electrons in magnetic fields are governed by the competition of three dominant physics: parallel electric field acceleration, Coulomb collision, and synchrotron radiation. With the help of a recently developed tool that solves the relativistic Fokker-Planck equation in magnetic fields, it has been found that the presence of local vortex structure and global circulation is crucial to the saturation of primary runaway electrons. Identification of these velocity-space structures opens a new door to re-examine conventional understanding of runaway electron dynamics in magnetic fields.

Background and Research Objectives

Highly energetic electrons with MeV energy are expected to cause serious damage in the large tokamak fusion experiment, ITER, during a fast termination process of the hot confined plasma (disruption). With GeV energy, they are also well known in astrophysics for their role in Gamma-Ray-Burst during a supernova where large amount of explosion energy is converted into radiation. On our sun, relativistic electrons are thought to be the source of observed hard X-ray spectrum in solar flares. Since direct measurements of these highly energetic electrons are usually impossible, our understanding of the generation mechanism is still limited and sometimes can be controversial.

Originated from the study of electrical discharge during lightning events, these relativistic electrons are also called runaway electrons (RE). In tokamaks, REs are generated (> Mev) when the inductive electric field along the magnetic field overcomes the drag force due to Coulomb collisions with the background thermal plasma. REs can cause severe damage to the plasma facing components (PFC) in a tokamak, and affect the dynamics of the bulk plasma due to the current they carry. An urgent need for the success of the International Thermonuclear Experimental Reactor (ITER) is to develop robust capabilities to model the RE generation and their interaction with the bulk plasma so that more effective techniques can be designed to avoid REs or mitigate their damages to PFCs.

The major goal of this project was to develop a comprehensive physics model and the predictive capability for the generation and transport of relativistic electrons in magnetized plasmas.

Scientific Approach and Accomplishments

We have developed a parallel relativistic Fokker-Planck solver to simulate relativistic electrons in axisymetric geometries treating electric field acceleration, Coulomb collision, radiation damping, parallel free-streaming and radial drift on the same footings. By solving the relativistic Fokker-Planck equation, simulations using the tool developed in this project helped us reveal a novel saturation mechanism for the primary runaways via a global circulation in energy and pitch angle space. The global circulation is severely modified by magnetic trapping in a tokamak, resulting in a much reduced runaway population in saturation compared with the slab model. This offers the tantalizing possibility that even when an avalanche is triggered, runaway current may still be limited to be a fraction of the total plasma current, and runaway energy distribution can be similarly controlled, which would provide a much wider window of possibility to mitigate the wall damage by runaways. For studying the interactions between whistler waves and electrons, a parallel test-particle code has also been developed and applied to investigate the whistler spectra gap in radiation belt.

An invited talk on these physical findings was given in the 2016 Sherwood international Fusion theory meeting. A manuscript “Phase-space dynamics of runaway electrons in magnetic fields” was submitted to Plasma Physics and Controlled Fusion and is currently under review. Another manuscript “Magnetic trapping effect on runaway electrons” is also ready for submission. A case

study of the wave-particle interaction explains the formation of whistler spectra gap in the radiation belt, and the result has been published on Geophysical Research Letters, “Nonlinear subcyclotron resonance as a formation mechanism for gaps in banded chorus”. The capabilities developed in this ECR project also motivated and helped us to submit a new proposal, “Revisit the Ohm’s law for plasmas with relativistic electrons”, to DOE OFES in response to a call of “Basic Plasma Science”.

Impact on National Missions

It is now widely accepted that runaway electrons could severely damage the plasma facing components on any tokamak as large as ITER during a major disruption. This poses a significant risk for ITER, whose success is essential for eventually achieving magnetic fusion energy production. This is of high priority to the U.S. fusion program. The success of this LDRD Early Career Research (ECR) project has helped position LANL as a major player in a newly funded SciDAC project, ”Simulation Center for Runaway Electron Avoidance and Mitigation”, supported by DOE OFES and OASCR. With this programmatic support, we will contribute to the development of a reliable design tool for runaway mitigations.

Publications

Fu, , Guo, Dong, and S. P. Gary. Nonlinear subcyclotron resonance as a formationmechanism for gaps in banded chorus. 2015. GEOPHYSICAL RESEARCH LETTERS. 42 (9): 3150.

Guo, Z. H., C. J. Mcdevitt, and X. Z. Tang. Phase-space dynamics of runaway electrons in magnetic fields. Plasma Physics and Controlled Fusion.

Guo, Z. H., X. Z. Tang, and C. J. Mcdevitt. Magnetic trapping effect on runaway electrons. 2016. To be submitted to Physical Review Letters.

Spallation Neutrons for Radionuclide Production

Jonathan W. Engle
20160601ECR

Abstract
The demand for medical and research radionuclides is immense and growing. One promising option for large-scale production of novel radionuclides is spallation neutrons produced by charged particle beams but the necessary nuclear reactions are often so poorly characterized that feasibility cannot be realistically estimated. This project sought to develop the capability to investigate these reactions in a manner that will benefit the field of radionuclide production and generate nuclear data of interest in studies of dosimetry, accelerator driven systems, verification of nuclear transport codes, and to national security science.

Background and Research Objectives
Presently, no US domestic capability to measure the cumulative formation excitation functions for interesting radionuclides exists above approximately 30 MeV, though multiple accelerators can produce energetically "white" fluxes that could be used for radionuclide production. This means that assessment of the radionuclidic purity achievable by irradiating targets in neutron fluences is difficult to estimate. The goal of this research was to develop and verify a nuclear data measurement capability that is essential to estimate purities and yields of needed radionuclides made with spallation neutrons, in the process creating the capability to generate nuclear data useful to a variety of other fields.

Scientific Approach and Accomplishments
This proposal consisted of three parts: (1) development and testing of a direct quasi-monoenergetic neutron (QMN) measurement capability at the Lawrence Berkeley National Laboratory's (LBNL's) 88" cyclotron, (2) modification of established spectral unfolding codes to extract excitation functions from activation experiments in white neutron spectra, and (3) validation of results in experiments with well-understood white neutron spectra. The QMN capability for activation-style experiments cannot be built at LANL because of the limited number of discrete proton energies available in multi-user modes at LANSCE (100, 800 MeV).

The first objective has been partially completed. Extensive simulation experiments and close collaboration with the Sigma machining facility (Jason Cooley) and the Cyclotron Facility staff at LBNL have produced an Inconel-encapsulated Li target design that is compatible with a range of incident proton energies between 20 and 70 MeV. Preliminary test targets have been used in characterization experiments at LBNL, and full-scale targets capable of withstanding irradiation intensities of >20μA will be ready for shipment to LBNL by the end of FY16. Collaborating investigators at LBNL (Lee Bernstein) have dedicated student dissertation research projects to first experiments to activate materials of interest with secondary neutrons produced by irradiation of these Li targets over the next two years.

The second objective has been completed. SAND-II codes were modified by Dr. Michelle Mosby to complete both the forward operation (unfolding differential incident neutron energy spectra from activation yields and well-described excitation functions) and to solve the inverse problem (extraction of energy-dependent excitation functions from yield and differential energy spectra). It remains to implement this work in the context of new measurements.

The capability for white-spectrum activation measurements has been further developed at the Isotope Production Facility at LANSCE, with new target holders for materials of interest in neutron-initiated reactions fabricated in 2016.

Impact on National Missions
Expansion of the national nuclear data program beyond charged particle and low-energy (<20 MeV) reactions to medium energy neutrons will both contribute to the national nuclear data program (which has recently recog-

nized this precise need) and serve a long term need in US radionuclide production. This work is relevant to current DOE facilities and the planned large spallation sources of the future.

Hybrid Shock Ignition as an Alternate Concept for Fusion Energy

Eric N. Loomis
20140180ER

Introduction

Achieving energy gain from thermonuclear reacting plasmas in a laboratory setting is a fundamental aim of researchers around the world since, in time, it would lead to a new and controllable energy source, as well as a much needed platform for supporting aspects of Stockpile Stewardship. Inertial Confinement Fusion (ICF) has remained at the forefront of this research for many years and its flagship, the National Ignition Facility (NIF), is currently performing the experiments towards ignition anticipated for well over a decade. In the past year, however, thermonuclear ignition on NIF using conventional indirect-drive ICF has proven more elusive than previously expected. Even if ignition is achieved, new high yield concepts are needed for useful energy production as well as future "Applications of Ignition" experiments. In this project we present a novel platform with the potential for high energy gain implosions, which integrates the existing advances made in Indirect-Drive Inertial Fusion with the promising new scheme of Shock Ignition (SI). If successful, our Hybrid SI concept will provide a new platform by which to study hohlraum-based implosion physics, but which accesses different conditions than current NIF ignition attempts and stresses different aspects of our predictive capabilities, which we expect will lead to improved physics models in numerical radiation hydrodynamics codes.

Hybrid SI will use spherical hohlraums with a novel arrangement of symmetric laser entrance holes that allow both indirect-drive beam access to the hohlraum walls followed by shock ignitor drive beams that directly illuminate and provide requisite heating to the compressed fuel. Our exploratory research into this concept will involve multi-dimensional radiation hydrodynamics design calculations that demonstrate adequate implosion and ignitor symmetry. These calculations will then be used to study new physics associated with instabilities generated by collisions of converging rippled shocks.

Benefit to National Security Missions

Alternate Inertial Confinement Fusion (ICF) concepts, such as Shock Ignition (SI), will stress different aspects of the ignition problem compared to conventional indirect-drive and will help elucidate shortcomings in our predictive capabilities. This platform is also a potential low convergence design that at ignition-scale could out-perform current NIF implosions or at least be more predictable. This work addresses a major gap: LANL is currently the only major ICF laboratory without an investment in SI and, furthermore, LANL is the only ICF laboratory without an investment in any alternative ignition platform. The intent of this project is to begin to build an innovative Hybrid SI program with potential experiments on NIF within four years.

Progress

In FY15 we completed 2-D design studies of our OMEGA scale targets, target fabrication of complex geometry gold hohlraums for experiments originally planned in FY16, began investigations into optimized laser pulse shapes for hybrid-driven implosions, and discovered the potential detrimental effects of perturbations on converging shocks for shock ignition. Since efficient transfer of energy during the collision of the ignitor shock with the rebounding initial compression shock is essential for reaching optimal conditions for thermonuclear ignition, this last accomplishment will likely prove to be of utmost importance. For this reason we plan to have it as our central focus for the remainder of FY15 and into FY16.

This issue revealed itself as we were studying the results of 2-D target simulations. These simulations studied the implosion physics of x-ray driven capsules with direct-drive ignitor shocks. Capsule diameters were maintained at 550 microns and contained deuterium-tritium gas. Capsules had either 50 or 25 micron thickness and 50 or 25 atmospheres of DT, respectively. Thinner capsules were expected to give greater neutron yield at the expense of diminished hydrodynamic stability.

Low-mode drive asymmetry on the capsule was imposed using spherical harmonic expansion of the radiation flux from the hohlraum wall plasma. Radiation from the hohlraum wall emission to the capsule was then transported using multi-radiation group implicit Monte Carlo photonics. Finite statistics of this radiation field imposed high spatial frequency roughness at the ablation surface of the capsule; seeding ablative Rayleigh-Taylor perturbations similar to what is imposed on real targets with finite surface roughness. The combination of this high frequency roughness and the low mode drive asymmetry allowed us to study near experimental conditions in two dimensions. The hohlraum and laser geometry suggested that our targets are most likely to have mode 4 drive asymmetries so these were imposed on both the thick and thin capsule simulations. Modulations at the inner surface of the capsule grew rapidly into the gas at the time of capsule deceleration after feeding through the shell from the ablation surface. Thinner shells were observed to reach higher DT ion temperatures and neutron yield, but suffered greater instability growth and mixing during deceleration. Prior to the formation of the instability growth at capsule stagnation, modulations in pressure were observed in the gas due to asymmetries carried by the initial shock convergence. These gas modulations reached their maximum at the time of shock bounce at the center of the capsule, but then reduced somewhat during the bounce and divergence stage of the shock. There is some theoretical evidence for this unstable/stable asymmetry transition in spherical shock problems, but it has not yet been studied in regards to shock ignition, which relies heavily on the strength and stability of converging shocks.

From 1-D simulations in the first year, we discovered a need for tailored pulse shapes that had features well-suited for the separate stages of fuel compression and ignitor shock heating. These features need to be contained within a single, shaped laser pulse due to the OMEGA facility restrictions. To accomplish this a pulse was used that had a high-intensity short prepulse followed by a roughly 2 ns duration square pulse of moderate intensity. In a real experiment, the beams creating the ignitor shock would be time such that the high-intensity prepulse would irradiate the capsule just prior to capsule stagnation, thus maximizing the strength of the ignitor shock. This pulse shape was simulated in a laser-hohlraum calculation using the code Lasnex to generate the radiation flux source used in the capsule simulations discussed above. Under OMEGA laser intensities the hohlraums are predicted to reach about 200 eV radiation temperatures during the peak of the main 2 ns pulse stage.

Following this set of 2-D OMEGA capsule simulations we decided to start exploring the effect of gas modulations on shocks in spherical geometry. Our first method for studying this effect was to use very thin (i.e., 5 micron) capsules known as Exploding Pushers because these types of targets due not suffer from deceleration Rayleigh-Taylor growth and may be a good platform for studying them experimentally. In Hydra we used radiation flux asymmetries to change the gas shock conditions, but can now also place single mode modulations at the inner surface.

Future Work

We were not awarded facility time under the OMEGA laser Laboratory Basic Sciences (LBS) program so experiments are not likely to occur in this project as originally planned. For this reason we will continue to focus our efforts on detailed 2- and 3-D simulations of new physics issues associated with Shock Ignition that we have discovered in this LDRD. One issue, specifically, is determining the loss in energy transfer from the ignitor shock to the compressed fuel when the fuel has a modulated density field or when the ignitor collides with a modulated rebounding shock. The modulations in these cases grow much more rapidly due to convergence of the ignitor shock reducing the amount of shock heating to the fuel. In FY16 we will study this behavior using the LANL Rage code and the LLNL Hydra code by applying inner surface perturbations to our OMEGA scale capsules. These perturbations will imprint themselves into the fuel, which will produce growing modulations in the converging ignitor shock. By varying the initial wavelength of the inner surface perturbation we can change the spatial and temporal distribution of fuel density modulations and thus the amount of shock heating to the fuel as well. This effect should be present in both the direct-drive and hybrid concepts and may set lower limits on required ignitor shock pressure to overcome the loss in energy transfer efficiency. Part of our FY16 efforts will go into designing actual experimental platforms to test this effect, which we will then propose to the Inertial Confinement Fusion Science Campaign to support in out years.

In FY16 a new postdoc will be joining XCP to work on designs at NIF-scale. These designs will be used primarily to study instabilities, such as converging modulated shock collisions, at ignition conditions.

Conclusion

Success of this project is based on demonstrating the novel integration and nuclear performance benefit of a hohlraum-driven implosion with direct-drive Shock Ignition of the fuel. Specifically, the outstanding questions that must be addressed to declare success regards the achievable symmetry of the hohlraum-driven capsule implosion and the symmetry that must be attained by the ignitor beams

to result in enhanced nuclear performance (neutron yield, ion temperature, and areal density) beyond standard implosion techniques. We will also produce ignition-scale design calculations in order to predict feasibility for NIF.

Quantum Kinetics of Neutrinos in the Early Universe and Supernovae

Vincenzo Cirigliano
20140252ER

Introduction

Neutrinos are perhaps the most mysterious and elusive of the known particles, and yet play a crucial role in the early universe and the life of stars. Neutrinos interact only very weakly and have tiny masses, the heaviest neutrino being at least a million times lighter than the electron, the lightest charged particle. Moreover, observations of solar, atmospheric, reactor, and accelerator neutrinos indicate that the neutrinos come in three different flavors, that can morph into one another as they evolve, through a genuine quantum mechanical interference effect. Despite their elusive nature, neutrinos play a special role in the dynamics of the early universe (EU) and supernovae (SN), because they come in huge numbers and because through their flavor-dependent weak interactions they can set the ratio of neutrons to proton in both the EU and in the heated ejecta of a supernova. Such ratio is a key ingredient in understanding quantitatively what atomic nuclei are synthesized in these two environment.

The overarching goal of this project is to set up the analytic and computational tools needed to describe neutrino kinetics in the EU and SN environments, simultaneously keeping track of the effect of quantum mechanical morphing and the role of inelastic collisions with the medium. The appropriate tool to describe neutrino evolution in a hot and dense medium are the so-called Quantum Kinetic Equations (QKEs). To date, no self-consistent derivation of the QKEs exists, let alone numerical solution. Our proposed research will improve on the current state-of-the-art in two important aspects: first, it will provide a first-principle derivation of the QKEs, based on non-equilibrium field theory and a controlled expansion in ratios of widely separated length scales.

Benefit to National Security Missions

Understanding how neutrinos have shaped the evolution of the cosmos and of stars, including the implications for the synthesis of atomic nuclei, is a major goal of both the Nuclear Physics and High Energy Physics Office of Science.

Moreover, our project will develop cutting edge capability in transport theory. While this will be applied to neutrinos in supernovae and early universe, in the future the very same tools could be applied to programmatic work supporting our national security mission.

Progress

Theory

The research team demonstrated that n anisotropic environments a coherent spin-flip term arises in the Quantum Kinetic Equations (QKEs) which govern the evolution of neutrino flavor and spin in hot and dense media. This term can mediate neutrino-antineutrino transformation for Majorana neutrinos and active-sterile transformation for Dirac neutrinos. In an article published in Physics Letters B (V. Cirigliano, G. Fuller, A. Vlasenko, "A new spin on neutrino quantum kinetics", Phys. Lett. B747 (2015) 27-35) we discuss the physical origin of the coherent spin-flip term: the spin of a massive neutrino can precess due to the interaction with an axial-vector field generated by other neutrinos or other matter particles, such as electrons and protons, carrying weak charge. This spin precession does not require the presence of a magnetic field nor a neutrino magnetic moments. In the same article we have provided explicit expressions for the QKEs in a two-flavor model with spherical geometry, the first step towards a computational implementation of the new effect. In the context of this two-flavor model, we have also demonstrated that coherent neutrino spin transformation depends on the absolute neutrino mass and the so-called Majorana phases, parameters that are very difficult to measure in laboratory experiments.

We obtained the analytic expression for the collision term of the QKEs, accounting for neutrino scattering on other neutrinios, electrons, protons, and nucleons. We have also included neutrino pair production and an-

nihilation, in summary all the processes that are relevant in the early universe and supernova environments. We are currently putting these results in a form that will be suitable for computational implementation (e.g. we are reducing some of the integrals from five-dimensional to two-dimensional, more amenable for an efficient numerical calculation). Within FY15 we expect to summarize our results in a publication.

Computation

On the computational/astrophysical front, we examined whether the newly derived neutrino spin coherence could lead to large-scale coherent neutrino-antineutrino conversion. We have done so in a simplified model of a supernova envelope, using the so-called single-angle approximation for the neutrinos emitted by the surface of the compact object. In a linear analysis we found that neutrino-antineutrino transformation is largely suppressed, but we have demonstrate that nonlinear feedback can enhance it. We have pointed out that conditions which favor this feedback may exist in core collapse supernovae and in binary neutron star mergers. Our results have appeared as a preprint (V. Cirigliano, G. Fuller, A. Vlasenko, "Prospects for neutrino-antineutrino transformations in astrophysical environments", 1406.6724) under review in Physical Review Letter.

Future Work

In the upcoming fiscal year, we will finish the analytic calculation of the collision terms, valid both for the early universe isotropic conditions and for anisotropic conditions relevant to compact astrophysical environments. Submit the results for publication in high impact journals

Our goals are summarized as follows:

- Perform numerical simulations of the full quantum kinetic equations (QKEs) describing the evolution and decoupling of neutrinos in the early universe. We plan to do this both for the case of three active neutrinos and for the case of active-sterile mixing.
- Perform exploratory numerical simulations of the QKEs in a spherically symmetric supernova geometry.

Conclusion

The proposed research will enable us to address two sets of outstanding questions:

1. What is the energy and flavor composition of neutrinos about 1 sec after the Big Bang, when the light nuclei are first synthesized? How does this knowledge constrain the existence of possible new neutrino states, so called "sterile" neutrinos?
2. How do inelastic collisions affect collective flavor transformation in a supernova envelope? What are the consequences for the synthesis of heavy elements in the neutrino-heated supernova ejecta? What are the consequences for the neutrino signal that can be potentially detected from galactic supernovae?

Publications

Blaschke, D., and V. Cirigliano. Neutrino quantum kinetics: the collision term. 2015. LA-UR-15-25029.

Cirigliano, V., G. M. Fuller, and A. Vlasenko. A new spin on neutrino quantum kinetics. 2015. Physics Letters B. 747: 27.

Vlasenko, A., G. M. Fuller, and V. Cirigliano. Prospects for neutrino-antineutrino transformation in astrophysical environments . . To appear in arXiv:1406.6724.

Vlasenko, A., V. Cirigliano, and G. M. Fuller. Neutrino quantum kinetics. 2014. Physical Review D. 89 (105): 004.

Designing the Next Generation Compton Light Source

Nikolai Yampolsky
20140269ER

Introduction

The ultimate goal is to prove the feasibility of the new technology for light sources based on inverse Compton scattering using microbunched electron beams. In this setup the scattered light will be coherently amplified since the radiation generated by each microbunch adds up in phase. The idea has never been explored since there was no recognized mechanism for creating very short wavelength density modulations in relativistic electrons beams with relatively low energy (~100 MeV). We propose to create the beam distribution consisting of several well separated energy bands through a series of manipulations with the bunch phase space using laser modulation and conventional electron beam optics. Such a distribution will drive the two-stream instability resulting in the plasma wave, i.e. density modulation. The proposed scheme can be split into three well separated stages, namely (1) creating required beam distribution, (2) development of the two-stream instability causing beam microbunching, and (3) scattering laser pulse off the microbunched beam to produce radiation with increased coherency. We will study each of these stages and analyze start-to-end performance of this novel scheme. We anticipate finding the parameters region for which the novel scheme results in 5-6 orders of magnitude increase in brightness over existing Compton light sources in 1-10nm wavelength range.

The largest challenge of this project is in mitigating various deleterious effects which may suppress the instability leading to beam microbunching. Preliminary analysis shows that they are negligible at large wavelengths (on the order of 1 micron) and dominant at small wavelengths (on the order of 1 nm). During the course of the project we will identify the precise limit of the novel technology.

Benefit to National Security Missions

If successful, the project will lead to development of a new generation soft X-ray Compton light source having significantly better beam quality over existing ones. This source will be compact (~100m) and relatively cheap (less than $100M), which makes it suitable to be widely distributed to multiple national laboratories and major research universities. The high brightness, tunability, and short duration of these sources will allow for many experiments which currently have to be conducted at the 3rd and 4th generation light source facilities which are severely overbooked. Development of a cheap, competitive, high-brightness soft X-ray light source will cover several national light source needs and will boost many research areas such as Biology, Chemistry, Physics, and Material Science.

AOT division is currently designing the Injector Test Stand (ITS) needed for testing novel ideas in Beam Physics required for successful commissioning of the MaRIE hard X-ray free electron laser (FEL). The ITS can potentially be used as a Compton source for enabling early MaRIE related experiments prior to construction of the FEL both for refining MaRIE FEL parameters and for providing additional FEL justification and motivation. The capability developed through this proposed work will allow a larger number and breadth of preliminary experiments to be done. This source can be used even after the commissioning of MaRIE FEL, adding a complementary soft X-ray capability to the facility.

Progress

Start-to-end simulations have started. The simulations include simulation of the electron optics beamline required to generate the unstable electron distribution (ELEGANT simulations) and further development of the multi-stream instability in the following focusing channel (CPIC simulations). The analysis of the results is underway.

Future Work

- 3D simulations of the instability.

- Detailed start-to-end simulations using output of ELEGANT as an input for CPIC.
- Include intra-beam scattering into CPIC.
- Optimize performance of the scheme resulting in the largest growth of the modulation.
- Estimate the limit of the technology in terms of the shortest wavelength modulation which can be produced.

Conclusion

Perform detailed study of the two-stream instability in relativistic beams driven by the multi-stream distribution. Support conclusions with detailed analytical estimates and numerical simulations including all relevant effects.

Determine whether this mechanism for the microbunching instability may be used for improving quality of the Compton light source. Provide reliable quantitative estimates of the resulting source parameters.

Determine whether this mechanism for microbunching may be significant in other applications in Accelerator Physics, e.g. seeding schemes for free electron lasers (FELs).

Publications

Yampolsky, N. A., G. L. Delzanno, C. Huang, and D. Shchegolkov. Two-stream Instability at Soft X-ray Wavelengths for Increasing Brightness of Compton Sources. Presented at 35th International Free-Electron Laser Conference. (New York, NY, 25-30 August, 2013).

Yampolsky, N. A., G. L. Delzanno, C. Huang, and D. Shchegolkov. Two-stream Instability at Soft X-ray Wavelengths for Increasing Brightness of Compton Sources. Presented at North American Particle Accelerator Conference. (Pasadena, CA, 29/09/ - 4/10, 2013).

Yampolsky, N. A., G. L. Delzanno, C. Huang, and D. Shchegolkov. Two-stream Instability at Soft X-ray Wavelengths for Increasing Brightness of Compton Sources. Presented at 55th Annual Meeting of the APS Division of Plasma Physics.

Combined Klystron and Linac (Klynac)

Bruce E. Carlsten
20140351ER

Introduction

We propose an engineering prototype demonstration (Technology Readiness Level (TRL) of 5) of a novel accelerator system architecture, where the accelerator's RF power source is integrated with the accelerator structure itself. Using a klystron as the RF power source, we have named this architecture "Klynac" to represent the functionalities of both the klystron and linear accelerator (linac) parts. To quantify its potential impact, the Klynac technology may lead to a reduction of a factor of 5 to 10 in over-all weight of portable radiography systems when used with an existing LANL TRL 6 capability, the resonant air-core transformer (compared to the 1900-lb, 3-MeV Varian Linatron M3, intended for fixed or truck-mounted applications). The reduced weight and size of the Klynac will allow man-portable radiographic missions, including emergency response, and provide a new technology to reduce the cost of medical radiography systems.

Benefit to National Security Missions

This project aims to develop technology that can be used to reduce the size of portable MeV-class radiography systems (including those use for medical cancer treatments) from ~ ton weights to a few hundred pounds. The NA-22 roadmap "Special Nuclear Materials Movement Detection Program Radiation Sensors and Sources Roadmap" calls for high-repetition-rate linacs (1–10 kHz) to increase photon flux compared to traditional linacs, allowing detection of both prompt and delayed signatures. The roadmap specifically calls for development of next-generation accelerator concepts and development of compact, mobile photon sources, which can be addressed with the technologies developed by the proposed work.

Progress

In FY15 we finished the stability analysis of the Klynac design, showing good operational stability (i.e., it will turn on and reach a stable operating point that is not highly sensitive to beam parameters. We also received our 50-kV electron gun and the final drawings for our Klynac structure. The first half of the klynac structure is currently being fabricated in a local machine shop, soon to be followed by the second half. After fabrication, there will be a fine-tuning process where we ensure all Klynac cavities have the correct resonant frequency. We anticipate the entire Klynac structure will be delivered before the end of the fiscal year. By the end of the fiscal year, we will also have completed the necessary modification to our test beamline where we will experimentally demonstrate our Klynac structure in FY16. These modifications include support structures, vacuum pumping, new solenoids with power supplies, and modification of the 50-kV CLIA pulse power supply.

Future Work

All hardware components were received by the end of FY15. Additionally, all modifications to our test beamline were completed at the end of the fiscal year. In FY16, we will test operation of this device. The key test, the proof-of-principle demonstration, will be to measure higher final electron beam energy than injected by the electron gun (50 kV). We will measure the final electron beam energy with an X-ray spectrometer.

Conclusion

The main technical goal of this project is to demonstrate that a portion of the bunched klystron beam can be accelerated in a linac. For this demonstration, a low voltage resonant klystron and linac will be built, driven at 50 kV and accelerating the electron beam to 1 MeV. The S-band linac design is standard, and will be identical to that used in the previous linacs. Likewise, the electron gun design and the 4-cavity klystron design will follow standard design practices.

Multi-GeV Electron Radiography

Frank E. Merrill
20140591ER

Introduction

This project will investigate the potential for multi-GeV electron radiography to provide high spatial and temporal resolution measurements of dynamic materials at the multi-probe diagnostic hall (MPDH) proposed at the Matter and Radiation in Extremes (MaRIE) facility. This technique has been proposed as one of the major diagnostics on the MPDH, but has not yet been experimentally demonstrated. We plan to design an imaging system to utilize the multi-GeV beams at Stanford Linear Accelerator Center to test the concepts and performance of high energy electron radiography. Although this type of imaging has been demonstrated with MeV-GeV protons, it has never been attempted with high energy electrons. The demonstration of this measurement capability would provide a new window into the dynamic process of opaque materials at unprecedented time and length scales. This new window would allow a more fundamental understanding of material response to extreme environments such as is experienced within a functioning nuclear weapon system.

Benefit to National Security Missions

This work will test the concept of using multi-GeV electrons for radiography of thin dynamic systems. This concept is a major pillar of the proposed Multi-Probe Diagnostic Hall at the Matter and Radiation in Extremes (MaRIE) facility. It is envisioned that these high energy electrons will be used to study materials relevant to the future weapons program, measuring fundamental materials properties with very high temporal and spatial resolution. The successful development of this technology will support the fundamental material research efforts within the DOE Office of Science and the fundamental and applied research in the nuclear weapons program for both inert as well as reactive materials such as high explosives. This capability to measure dynamic material response will also be applicable to DOD programs for military applications.

Progress

We have identified a location at SLAC to test eRad concepts. We developed the suite of simulation tools to simulate eRad performance and we have identified existing SLAC equipment for these measurements and have designed a system to utilize this equipment. The system is being installed and first measurements will be collected in late July, fully meeting our second year goals.

Future Work

In the third year of this project:

- The first data will be collected at the end of the second fiscal year.
- Analyzing the second year's data, we will assess the performance of the fielded imaging system.
- From the analysis of this data we will determine if further refinement of the system is needed. If so, we will design and implement these modifications.
- We will perform a second iteration of measurements at SLAC to determine the performance capability of multi-GeV electron radiography.

Conclusion

This project plans to design, assemble and test the first ever Multi-GeV electron radiography system. These measurements will focus on characterizing the performance of this type of radiography system. This effort will provide important information for the MaRIE project in determining the electron radiography capabilities as well as specifying the requirements for a future facility.

Publications

Merrill, F.. Imaging with penetrating radiation for the study of small dynamic physical processes. 2014. Laser and Particle Beams.

Photocathodes in Extremes: Understanding and Mitigating High Gradient Effects on Semiconductor Cathodes in X-FELs

Nathan A. Moody
20140616ER

Introduction

At the frontier of many scientific disciplines is the goal to understand, and even control matter, especially when it is subjected to extreme and dynamic conditions, such as those encountered in combustion, explosions, or other excursions in temperature and pressure. The ideal tool to probe matter in such extreme conditions is what has become known as an x-ray laser, or x-ray free electron laser (X-FEL). An X-FEL produces pulses of light (coherent hard x-rays) with a wavelength comparable to the distance separating atoms in solid materials and a pulse duration nearly as short as the changes which occur in materials, such as the formation and breakage of chemical bonds. Consecutive pulses of these hard x-rays would allow movies to be made of atoms or molecules, providing first-ever crucial information about how matter interacts under extraordinary environmental conditions. Any FEL relies upon a very strictly defined electron beam and what stands in the way of building an X-FEL light source like the one described above is the lack of sufficiently bright electron beam. Designs for such a beam exist but call for electron beam sources (cathodes) with performance that has never been proven or verified. These large scale X-FEL instruments are very costly and time consuming to construct, thus their design should be built on known facts regarding electron beam source performance and capability. The dominant question regarding most X-FEL designs relates to the maximum electric field strength it can be exposed to (and for how long) before the material breaks down due to the stress of the extreme electric field (> 100 MV/m). This project answers the question of whether present-day cathodes can survive high electric field gradient and it also presents methodologies for addressing and mitigating this risk.

Benefit to National Security Missions

MaRIE: This project addresses the highest risk element in Matter-Radiation Interacting in Extremes (MaRIE) x-ray free electron laser (X-FEL) design: the unknown effect of high field gradient on semiconductor photocathodes. Because these effects irreversibly damage the emitted electron beam, they impact nearly every other aspect of an X-FEL design and must therefore be rigorously and experimentally understood, quantified, and mitigated before such designs mature beyond the conceptual stages. This project accomplishes all these goals.

DOE/DOD/SC: all next-generation light sources require a high brightness electron beam source. This research will answer fundamental questions concerning the behavior of cathodes under extreme conditions. The results will include fundamental research validating the basic approach to electron beam source design, and demonstrations of the enabling technology required to successfully utilize those cathodes in next generation light sources, user facilities, or weapons systems. We identify key technical challenges and solutions which simplify FEL designs and/or reduce the commissioning and operatation costs significantly.

Basic Understanding of Materials: x-ray free electron lasers (X-FELs) are the ideal tool to interrogate, understand, and even control matter in extremes. To date, nineteen Nobel Prizes have been awarded for x-ray science using beam-based x-ray light sources, and we can expect more in the future as these tools open vast science frontiers to probe matter-in-extremes at unprecedented temporal, spatial, and energetic scales. The work represented in this project closes critical technology gaps in the fielding of X-FELs as instruments of discovery science.

Progress

RF cavity fabrication

The cavity proper has undergone its last fabrication step, high temperature brazing, and it passed leak rate, flatness, surface finish, and dimensional tolerance inspections at the manufacturer on 6/18. The next step is similar inspections at LANL upon its arrival toward

the end of June. Design considerations, preparation and machining of these cavity components, to accommodate the high temperature braze process at a temperature of 1700 Fahrenheit in hydrogen furnace, are similar to those which will be used during eventual fabrication of the MaRIE photoinjector structure. Thus, this LDRD project has significantly advanced this critical LANL capability by documenting and demonstrating best practices relating to: braze joint design (horizontal versus vertical), component modularity, braze alloy composition and temperature dependence, braze form factor (shim versus paste), braze temperature dependencies (melting, diffusion, and erosion), component cooling rates, pre- and post-braze stress release anneals, braze dependencies on surface finish, and mitigation of virtual leaks.

The power coupler assembly was updated and modified to reduce fabrication cost and time, to make the coupler more modular (for ease of later upgrade or, if necessary, repair). This further reduces project risk, enhances portability, and improves compatibility with our high-power testing host institution, the Argonne Wakefield Accelerator.

We are preparing for fabrication and brazing of the RF power coupler assembly, and expect to have all parts of the test cell in-house by mid- to late-August.

RF cavity testing
We are on-track to have essentially all of the test cell parts in-house and assembled and initial low-power RF tests performed by early September 2015.

Cathode fabrication
We have demonstrated in FY15 a LANL routine which allows us to reproducibly manufacture cesium antimonide protocathodes with quantum efficiency (the ratio of vacuum emitted electrons to surface incident photons) of about 2% at 405 nm wavelength on thick optically flat substrates like silicon, glass, and single crystal metals. Having demonstrated the requisite repeatability, we have also completed the required modifications to optimize cathode stoichiometry which will bring quantum efficiency (QE) up to greater than 10%. This complements our earlier demonstrations of utilizing encapsulated alkali-antimonide cathodes in long-term storage. The biggest advantage of the alkali antimonide photocathode family is very high, up to approximately 30%, quantum efficiency at the optimum wavelength which lies in the visible part of the spectrum. The photocathodes of this class can only be manufactured and operated under UHV conditions, which is why we have developed this LANL capability for the later stages of this project. Wide tunable bandgap semiconductors, comprised of InGaN are also being investigated for their potential as efficient and robust photocathode candidates. Several InGaN semiconducting thin films with bandgaps in the 2.0 to 2.5 eV range are being screened with and without surface Cs treatment for their photocathode response following illumination with 405nm light. Other InGaN films will be grown with optimized photocathode properties and characterized immediately following growth under ultra-high vacuum conditions using 405 nm light and a Faraday charge collection device recently installed on the LANL ENABLE growth system. None of these semiconductor cathode classes have been investigated at the high electric field gradients targeted in this project.

Future Work

Complete low power RF Cavity Testing
Having completed the fabrication of the RF cavity structure in FY15, we will repeat several of last year's measurements but this time as a fully-assembled structure: RF coupling, cavity resonance, coupling co-efficient, RF joint compatibility, initial cathode integration using instrumented metallic surrogate, and low power characterization of RF cavity. Milestone: report data on each of the metrics listed above.

High power RF testing
Transport assembled RF structure (on strong-back chassis) to RF testing station and integrate with the local control system, diagnostics, and drive laser. Dark current measurements using surrogate cathode first. Milestone: report data on each of the metrics listed above.

Design and fabrication of movable cathode seal
The above tasks use a non-removable cathode for simplicity but first introduction of semiconductor cathode and/or other metal samples into cavity test cell at high power RF require a mobile RF joint to allow cathodes to be removed and inserted. We will design, fabricate and test this seal, allowing us to gain first indications of cathode performance as a function of electric field gradient for both removable and non-removable cathodes. Milestone: first publication of results.

Begin full cathode characterization
Begin parametric testing at a variety of field gradients (starting with the lowest first), mitigation efforts of field breakdown, quantify electric field damage thresholds as a function of RF pulse duration, test multiple cathode samples involving more than one type of semiconductor film, scan surface area of cathode to provide a "map" of quantum efficiency across the surface. Milestone: second publication.

Conclusion

This research will answer fundamental questions concerning the behavior of electron beam sources (namely, upper limit of electric field) when subjected to the conditions

associated with an electron beam based x-ray free electron laser (X-FEL). The results will include both fundamental research validating the basic approach to designing electron beam sources, and/or demonstrating the enabling technology required to successfully utilize those cathodes in a specific X-FEL design. Key technical challenges and solutions, such as cathode seal geometry and high electric field surface treatment, will emerge and the data will allow future X-FEL designs to be based on validated test results.

Publications

Carlsten, B. E., S. J. Russell, J. W. Lewellen, D. C. Nguyen, P. M. Anisimov, C. E. Buechler, K. A. Bishofberger, L. D. Duffy, F. L. Krawczyk, Q. R. Marksteiner, N. A. Moody, N. Yampolsky, and R. L. Sheffield. MaRIE XFEL physics design risks and risk mitigation plans. 2015. Los Alamos National Lab. (LANL), Los Alamos, NM (United States); DOE Contract Number: AC52-06NA25396; LA-UR--15-22069.

Lewellen, J. W., and N. A. Moody. High gradient cathode testing for MaRIE. 2014. In FEL2014. (Basel, Switzerland). , p. THP024. Basel, Switzerland: JaCOW.

Moody, N., H. Yamaguchi, G. Gupta, and A. Mohite. Graphene shield-enhancement of photosensitive surfaces and devices. 2014. Micro- and Nanotechnology Sensors, Systems, and Applications VI. 9083 (6): 9083331.

Superconducting Nuclear Recoil Sensor for Directional Dark Matter Detection

Markus P. Hehlen
20150437ER

Introduction

The universe consists of 72% dark energy, 23% dark matter and only 5% of ordinary matter. One of the greatest challenges facing the scientific community today is to understand the nature of dark matter. Dark matter detection is shaping experimental work in astrophysics and particle physics, and it is widely recognized as the most important problem in 21st century cosmology. Current astrophysics and particle physics models suggest that dark matter is made up of slowly moving, weakly interacting massive particles (WIMPs). They pass through the solar system and should leave signals in detectors. However, their interaction with ordinary matter is exceedingly weak, making their direct detection in the presence of ubiquitous backgrounds a monumental task. Detectors that can sense the predicted sidereal variation of the WIMP flux direction hold the greatest promise to unambiguously prove the Galactic origin of WIMPs. The goal of this project is to explore a novel concept of a solid-state WIMP detector with direction sensitivity. The high density of a solid detector may overcome the background noise limitations of current large-volume gaseous detectors. The proposed detector consists of a layered structure comprising superconducting traces applied to ultra-thin glass sheets. The anisotropic structure is key to enabling the detector's direction sensitivity. WIMP interactions within the glass create nuclear recoils that migrate forward through the glass and deposit their energy in the adjacent superconductor. The respective heat can cause the superconductor to transition to an electrically resistive state and produce a measurable voltage spike. The results of this study will allow us to formulate a roadmap for the development of the first solid-state WIMP sensor that offers direction sensitivity and high density. Such a detector could usher in the next generation of dark-matter experiments looking to sense the unambiguous direction signature of WIMPs for the first time.

Benefit to National Security Missions

This work builds new capabilities for the LANL Nuclear and Particle Futures Science Pillar, specifically the Nuclear, Particle, Astrophysics, and Cosmology (NPAC) thrust area. Developing advanced detectors that may enhance our understanding of the physics beyond the current standard model is of particular importance and directly ties into national funding agencies such as DOE and NSF. In particular, the fundamental nature and the direct detection of dark matter is one of the key focus areas of the "Cosmic Frontier" research in DOE's High Energy Physics (HEP) program in the Office of Science as well as NSF's Division of Physics (PHY). The DOE Cosmic Frontier in particular focuses on new experimental concepts and dark matter detectors. Success in this project will allow us to develop new DOE-sponsored programs and will position LANL to assume the leading role in a next-generation directional dark matter experiment. The present work is also relevant to the Science of Signatures Science Pillar. It builds underlying science and technology in areas of interest to nuclear nonproliferation, treaty verification, and global security where directional detectors can play a critical role.

Progress

During an initial phase, we carefully studied various options of producing a multi-layer device consisting of alternating WIMP interaction layers and superconducting traces. Several device architectures were assessed based on material availability, ease of processing, scalability, and expected detector sensitivity. Practical considerations and model calculations informed each other. We concluded that the initial approach of stacking a large number of sub-micron thick polymer layers faces significant layer adhesion and surface roughness challenges. A new device architecture was developed that consists of superconducting Nb traces patterned onto commercial ultra-thin glass sheets. This design (1) is significantly more scalable, (2) maintains the directionality of the detector, (3) can be tuned via geometry to a desired recoil

energy range (enabling means for active background rejection), and (4) offers an attractive low-mass target (silica glass) that is suited for interaction with low-mass WIMPs. While previous dark matter searches have focused on the ~100 GeV/c^2 WIMP mass scale, the lower WIMP mass region (few GeV/c^2) has gained interest due to recent observational and experimental hints as well as motivations from theory. The low mass regime is challenging as it requires very low (few keV) energy thresholds, a region dominated by large backgrounds that are very difficult to discriminate. Due to these challenges, the current limits on dark matter in the <=10 GeV/c^2 region are quite poor. Therefore, the technology pursued by our experiment, with its potential low-keV energy sensitivity, could make a strong impact in this regime even with quite small target masses, particularly if background discrimination/mitigation and directional sensitivity can be achieved.

Work was focused on modeling (Task 1) as well as fabricating and characterizing (Task 2) the first single-layer prototype of the new device architecture. The key accomplishments are:

We identified two types of ultra-thin (25-30 µm) glass sheets that are commercially available as AF32 and D263 products in high quality and square-meter-scale areas from Schott Glass. Test samples were obtained from Schott, and their composition was measured using Secondary Ion Mass Spectrometry (SIMS). The compositional information served as input for the nuclear recoil modeling task.

Our University of New Mexico collaborators calculated the nuclear recoil energy distribution in the thin glass for interactions with WIMPs of different masses. This data was then used to perform SRIM (Stopping and Range of Ions in Matter) calculations to determine the recoil range and thus predict the required superconductor thickness. From the calculated 50-300 nm thickness range we then predicted the width of the Nb trace to be on the order of 2-30 µm in order to offer sensitivity to 5-50 keV nuclear recoils. These dimensions are routinely achieved with standard deposition and photolithographic processes.

Nb films were deposited on sapphire test substrates using both RF sputtering and e-beam evaporation at both room temperature and 800 oC and using two different LANL sputtering chambers. Superconductive film quality can be strongly influenced by deposition parameters. Evaluating different deposition techniques allows us to determine the optimal process. The films were analyzed by X-ray diffractometry to assess crystallinity and crystal phases. Test structures with Nb traces of various lengths and widths were fabricated from these films using standard photolithographic processes.

A new cryogenic test station was designed and fabricated to allow for electrical testing of superconducting devices between room temperature and 3.8 K using an existing closed-cycle helium refrigerator. A sensitive 4-wire resistance measurement setup was implemented to allow for the automated acquisition of resistance vs. temperature curves.

Superconductivity was observed at a critical temperature of 5.9 K in a device containing a meandering trace of 5 µm width, 1600 µm length, and 200 nm thickness deposited by RF sputtering at 800 oC. Characterization of the other films is currently in progress, and the results will allow us to downselect both the deposition chamber and the deposition process.

Work has started to measure the critical current density of the Nb traces and to record the fast superconducting-to-normal transients expected upon an interaction. This will initially be tested with an Americium-241 alpha source placed inside the cryostat. Once successful, the setup will be relocated to the LANL Ion Beam Materials Science Laboratory (IBML) for a systematic exploration of the detector's energy and flux dependence.

Future Work

The work in the second project year (FY16) will focus on assessing the performance of the superconducting nuclear recoil sensor (SNRS) (Task 3) and fabricating a multi-layer device prototype (Task 4). The device modeling (Task 1) will be refined and continue to guide the design and data analysis. Specifically, Task 3 will involve the fabrication of a range of single-layer devices with varying geometry in order to experimentally determine the energy response of the detector. Initial work will be performed with sealed sources on the existing instrumentation, followed by experiments on the beamline at IBML. If successful, we will discover a lower energy threshold where the SNRS begins to detect, and upper energy threshold where the SNRS latches (no self-recovery from normal to superconducting state), and possibly energy information in the pulse shape within the active energy region. This information will be critical (1) to designing the Nb trace geometry to match the desired nuclear recoil energy range and (2) to developing active and passive background rejection strategies. These experiments will also demonstrate the directionality of the SNRS. Work will then begin to fabricate a multilayer (e.g. 10 layers) device prototype. This will involve developing methods for mechanically stacking the individual patterned ultra-thin glass sheets, establishing electrical connections to each layer, providing means to cooling the structure below the critical temperature, and reading out the signals form all layers in parallel.

Conclusion

The overall technical goal of the project is to demonstrate the novel concept of a layered glass/superconducting sensor for directional dark matter detection. We will (1) comprehensively model the nuclear recoil properties in the detector materials, (2) fabricate a single layered detector structure, (3) assess the sensitivity and directionality of the device using ion beams, (4) fabricate a multilayer prototype to assess scalability, and (5) measure the detector background performance. We expect this work to produce numerous high-impact publications and to deliver the quantitative information needed to formulate a roadmap for the future development of a large-scale solid-state detector.

Neutrinos and Fundamental Symmetries in Nuclei

Stefano Gandolfi
20150476ER

Introduction

Nuclei are the testing ground for many measurements of neutrino physics and for tests of Physics Beyond the Standard Model. Experimental probes of neutrino physics and tests of fundamental symmetries have reached astounding precision with recent measurements of neutrino oscillations and limits on non-standard interactions in beta decays, for example. Commensurate theoretical advances in weak interactions in nuclei are within reach. In this project we will implement for the first time realistic treatments of two-nucleon correlations and currents to enable higher-precision studies of neutrino physics at high energy and momenta, and use these same methods to improve the calculation of nuclear beta decays and related probes of physics beyond the Standard Model.

It is already clear that improved models of the weak currents are required. Neutrino cross-sections on nuclei are 20-30% higher than predicted based upon simple models, it is likely that the energy dependence produced by these models is also incorrect as they only include simple single-nucleon kinematics. Similar discrepancies between theory and experiment in electron scattering have been understood in terms of realistic nuclear interactions and currents. We will implement these same models for weak interactions and neutrino scattering to enable much higher precision nuclear experiments.

Benefit to National Security Missions

This research is important for the DOE Office of Science, nuclear and high energy physics offices.

Understanding quantitatively the neutrino interaction with matter is relevant to experiments measuring neutrino oscillations, double beta decay, and beta decay studies of physics beyond the standard model. These experiments need high precision weak matrix elements in the nuclei.

Progress

During the first year of the project we have finalized the calculation of electroweak imaginary-time response functions of 4He and 12C. In the electromagnetic case, we found that the contribution of two-body operators is very large as expected. The results are in excellent agreement with the available experimental data, for both the longitudinal and the transverse response. We have also calculated the weak imaginary-time response functions, and we are working to extract information on the neutrino-nucleus cross sections.

The research team developed the code to calculate the charge-changing weak currents. The matrix elements for those operators are related to the beta decay. The subroutines have been incorporated in the variational Monte Carlo code that we will use for light nuclei We are currently testing the code and then we will work to optimize the subroutines and then proceed to the calculation in light nuclei.

We have made very important progresses through the extension of Auxiliary Field Diffusion Monte Carlo code to calculate properties of medium nuclei. The ground state of closed shell nuclei, including oxygen and calcium, can now be solved for realistic nuclear Hamiltonians that include two-body forces. We are now working to also include three-body forces in order to reproduce the binding energies of nuclei. These are essential to get a reasonable description of the nuclear states involved in the weak transition.

Future Work

Our goals for the next fiscal year can be summarize as follows:

- Calculate the imaginary-time responses that are relevant for electron and neutrino scattering for a variety of nuclei up to A=12.

- Develop a theory to extract the high energy and momentum part of response functions from two-nucleon propagators.
- Develop the relevant two-body currents needed to calculate beta decay rates in light nuclei.
- Extend existing Auxiliary Field Diffusion Monte Carlo codes to simulate the ground state of medium nuclei.

Conclusion

At the completion of this project we will have a vastly improved capability to predict weak interaction rates for nuclei, both at the low energy and momentum scales relevant for beta decays, the moderate momentum transfer relevant for neutrinoless double beta decay matrix elements, and an accurate two-nucleon model for quasielastic neutrino scattering.

Publications

Carlson, J., S. Gandolfi, F. Pederiva, S. C. Pieper, R. Schiavilla, K. E. Schmidt, and R. B. Wiringa. Quantum Monte Carlo methods for nuclear physics. 2015. Rev. Mod. Phys.. 87: 1067.

Gandolfi, S., A. Gezerlis, and J. Carlson. Neutron Matter from Low to High Density. 2015. Ann. Rev. Nucl. Part. Sci., in press.

Lovato, A., S. Gandolfi, J. Carlson, S. C. Pieper, and R. Schiavilla. Electromagnetic and neutral-weak response functions of $4mathrmHe$ and $12mathrmC$. 2015. Phys. Rev. C. 91: 062501.

Lynn, J. E., I. Tews, J. Carlson, S. Gandolfi, A. Gezerlis, K. E. Schmidt, and A. Schwenk. Chiral Three-Nucleon Interactions in Light Nuclei, Neutron-alpha Scattering, and Neutron Matter. 2015. Phys. Rev. Lett., submitted.

Tews, I., S. Gandolfi, A. Gezerlis, and A. Schwenk. Quantum Monte Carlo calculations of neutron matter with chiral three-body forces. 2015. Phys. Rev. C, submitted.

Assessing the Quantum Physics Impacts on Future X-ray Free-electron Lasers

Mark J. Schmitt
20150508ER

Introduction

This project consists of theoretical and modeling efforts to develop a self-consistent model for the wave-electron interactions in x-ray free-electron lasers that includes quantum mechanical effects of the electrons. We conjecture that quantum mechanical spreading of the electron wave function down the wiggler, left out of current free-electron laser models, will degrade the extraction efficiency of these lasers. By including these effects in a new ab initio model, we hope to assess their impact for various laser configurations (e.g. fundamental and harmonic lasing) and determine the best way to optimize laser performance in their presence. The results of this new model will directly affect the design of future XFEL facilities and impact the capability for interrogating extreme states of matter.

Benefit to National Security Missions

This work directly impacts the design of the MaRIE 1.0 signature facility by providing an assessment of quantum effects potentially affecting the extraction of x-rays from energetic electron beams. This work will extend our current understanding of the generation of x-rays from high energy electrons relevant to astrophysics. The simulation models developed under this work will enhance the utility of MaRIE 1.0 and its ability to be used to interrogate materials in extreme states, directly impacting the validation of physics models used in weapons physics codes and for defense applications.

Progress

To accelerate the theoretical work of our research, Petr Anisimov spent the first three months of the ER in Wakoshi, Japan working with Dr. Franco Nori at RIKEN on the quantization of relativistic electrons in the magnetic field needed for a full quantum (QM) mechanical treatment of the FEL interaction. During this time Petr developed a QM mathematical formalism to describe the reduction in electron bunching and concomitant x-ray gain caused by the electron's QM phase uncertainty. Applying this theory to existing and planned x-ray FELs, the current model indicates that QM effects will cause electrons to spread by about 10% of the x-ray wavelength, resulting in a reduction in 3rd harmonic gain by a factor of about 2 for MaRIE-like parameters. A model for this reduced QM bunching has been added to the GENESIS code (the FEL code being used for the design of the MaRIE XFEL). Simulation results from the code show that degradation in gain increases with increasing x-ray harmonic wavelength, making operation at harmonic wavelengths more difficult that thought from a classical point of view. A presentation on the progress of this work is being prepared for presentation at the 2015 International Free Electron Laser Conference, organized by the Korea Atomic Energy Research Institute (KAERI), that will take place in August 2015 in Daejeon, Korea.

Future Work

Work for FY16 can be summarized as follows:

- Continue work on 3D quantum theory of XFEL operation incorporating feedback obtained from the scientific community. Milestone: Completion of 3D quantum theory.
- Implement the improved QM theory in a multi-electron Genesis code in conjunction with an existing classical radiation propagation model. Milestone: A numerical simulation code that describes quantum electrons and classical light in an XFEL.
- Conduct theoretical studies of the quantum startup regime where single photon light dynamics is important and compare results with the case where light is treated classically. Construct a fully QM startup module to be used in the main simulation code. Completed studies of the quantum startup regime and QM model.
- Submit publications/presentations of the work to refereed journals and scientific conferences and/or workshops.

Conclusion

As we construct our model, we will verify its predictions against conventional free-electron laser models in classical regimes, and validate its results against data generated at the LCLS facility. This new model will be used to predict the performance of future free-electron lasers including MaRIE 1.0.The successful execution of this high-leverage research would make a major advance in the XFEL field, placing LANL at the forefront of the design community for future XFELs

Publications

Anisimov, P. M.. Quantum Nature of Electrons in Classical X-ray FELs. To appear in International Free Electron Laser Conference - FEL 2015. (Daejeon, Korea, 23-28 Aug, 2015).

Transport Properties of Magnetized High-Energy Density Plasmas

Jerome O. Daligault
20150520ER

Introduction

There is a rapidly growing interest in exploring the application of magnetic fields to inertial confinement fusion systems in both laser and pulsed-power driven scenarios. The presence of magnetic fields change the fundamental properties of high energy density plasmas in ways that may bring significant rewards, but also present significant challenges for theory. Although decades of innovative research has led to a basic understanding of traditional inertial confinement fusion scenarios, the combination of high-energy density and strong magnetic fields requires extension of current physics models. In particular, understanding how strong magnetic fields, either induced or spontaneous, affect transport properties is a critical next step toward developing a theoretical understanding and modeling capability of these next-generation systems.

Combining numerical simulations and analytical modeling, we will enable a first-principles exploration of the transport properties of magnetized high energy density plasmas. We will develop a molecular dynamics simulation capability to account for both Coulomb interactions and magnetic fields over a wide range of Coulomb coupling and magnetic field strengths. This unique tool will be used to develop a fundamental physics understanding as to how the combined effects of many-body interactions and magnetic fields affect transport properties, and to validate new models of transport properties. We will augment our recent analytic transport theory for unmagnetized plasmas to include magnetic fields. Expressions for the transport coefficients will be cast in a form that is convenient for others to implement into the integrated simulation codes used to model ICF plasmas.

Benefit to National Security Missions

The results of this effort will introduce a new and unique simulation capability in modeling the influence of magnetic fields on high-energy density fusion plasmas at LANL. The capability will allow significant scope for exploration of non-equilibrium conditions in dense plasmas and materials under extreme conditions (e,g, radiation damage, ion slowing-down, non-equilibrium phase transitions). By enhancing our basic science capabilities, this project will help LANL meet its current and future applied missions and challenges, including the science campaigns, Advanced Scientific Computing (ASC) and national High Energy Density Laboratory Plasma (HEDLP) programs. This exploratory research has strong ties to the Nuclear and Particles Futures pillar.

Progress

The research team developed simulation capability to account for both Coulomb interactions and magnetic fields over a wide range of Coulomb coupling and magnetic field strengths. To this end, we added Lorentz forces in the Newton's equations for charged particles interacting through the Coulomb interaction in the presence of an external, homogeneous magnetic field. In the unmagnetized code developed by the PI in the past, the particle dynamics is integrated using the Verlet algorithm. The challenge was to develop an extension of the Verlet algorithm than can handle arbitrarily strong magnetic field. We first implemented existing velocity-dependent algorithms in the literature, including the Störmer-Verlet and the Boris algorithms, which are symplectic, stable, and arbitrarily accurate. However our numerical tests revealed that these algorithms were constrained to very small time steps (because the time step must be small compared to the Larmor cyclotron time, and therefore to short simulation time scales. This limitation prevents systematic studies over wide range of magnetic field strengths. We decided to design a new algorithm, where, unlike Störmer-Verlet and Boris, the choice of the time step is entirely independent of the strength of the magnetic field. The new scheme has been parallelized and incorporated successfully into our code.

We have begun a detailed study of the effect of magnet-

ic fields on the transport properties of high-energy density plasmas. After a long period of trial and error to determine the optimal simulation parameters, we have calculated for the first time the self-diffusion coefficients as well as the parallel-to-perpendicular temperature relaxation rates in one-component plasmas and in electron-ion plasmas, over a wide range of Coulomb couplings and magnetic field strengths. The analysis of the collected data and comparison with existing theoretical predictions are underway. Preliminary investigations reveal the limit of validity of the existing models and motivate the need for new theories. A paper on these results is in preparation.

We have derived and implemented the basic equations to include a magnetic field in our effective potential theory described in the proposal. Results from the effective potential theory will soon be compared to the molecular dynamics simulation results.

Our efforts this past year have been focused on the development of the new simulation capability, its testing, and the extension of the effective potential theory. We plan on publishing next year our numerical, analytical and physics results.

Future Work

The objective of this research is to develop a quantitative understanding of the dominant transport processes in magnetized high-energy density plasmas; including temperature relaxation, diffusion, electrical and thermal conductivity and viscosity. Models of transport properties will be developed and validated using molecular dynamics (MD) simulations. Our previous MD simulations and theoretical models have proven successful at capturing each of these transport properties in unmagnetized plasmas. The proposed work is a non-trivial extension to include an external magnetic field, which will contribute to individual particle equations of motion. Interaction forces will remain electrostatic. Extensive MD simulations will be carried out to unravel the microscopic particle dynamics in magnetized plasmas, and to develop a library of transport processes (diffusion, viscosity, resistivity, energy relaxation rate, dynamic structure factor, etc.) that will be used to validate the analytical models. Currently, our MD code allows for the simulation of classical systems of charges interacting through spherically symmetric potentials in a three-dimensional periodic domain containing up to several hundreds of thousands of particles and over long time scales. Currently, magnetic fields are not included. The inter-particle forces are obtained using the state-of-the-art particle-particle particle-mesh method, which combines high-resolution of close encounters and rapid, long-range force calculations. We will extend the present capability to account for magnetic fields, and apply it to explore a wide range of Coulomb coupling and magnetic field strengths. Two kinds of simulations will be done to explore the impact of magnetic fields: 1) We will develop our code to incorporate arbitrarily strong external magnetic fields. This requires adding velocity-dependent Lorentz forces in addition to the Coulomb forces in Newton's equations describing the particle evolution. 2) We will develop the effective potential to account for screened ion-ion interactions and then implement those effective potentials in our MD code and calculate ionic transport properties.

Conclusion

The primary result will be a microscopic-level understanding of the transport properties of magnetized plasmas across a broad range of coupling and magnetization strengths. Tangible products will be a numerical code and theory capable of describing these plasmas, and practical formulas that can be implemented into integrated simulation codes used to model ICF systems.

Publications

Baalrud, S., and J. Daligault. Modified Enskog kinetic theory for strongly coupled plasma. 2015. Phys. Rev. E. 91: 063107.

Daligault, J., and S. B. Baalrud. Plasma transport theory spanning weak to strong coupling. 2015. AIP Conf. Proc. . 1168: 040002.

Sjostrom, T., and J. Daligault. Ionic and electronic transport properties in dense plasmas by orbital-free density functional theory. Physical Review E Accessible at http://arxiv.org/abs/1510.00647.

Magnetic Rayleigh-Taylor Instability

Daniel Livescu
20150568ER

Introduction

While the goal of achieving economically viable controlled fusion remains remote in either the inertially (ICF) or magnetically confined configurations, it is generally believed that one of the main obstacles is the development of hydrodynamic instabilities. However, the complex physics associated with ICF makes such instabilities significantly more complicated than the classical Rayleigh-Taylor instability (RTI). The influence of magnetic fields, either self-generated or externally applied, has recently been an active research topic in the hope it may offer a way of controlling or inhibiting RTI and mixing in ICF. However, so far numerical investigations of this problem have been restricted to 2D, without realistic plasma transport properties, and the few existent studies investigating the coupling between magnetic fields and RTI seem to arrive at opposite conclusions.

In order to fill the gap in our knowledge of the coupling between RTI and magnetic fields, we will conduct a thorough study of the RTI in the variable-density (VD) magneto-hydrodynamics (MHD)-Hall limit using the first high-resolution 3D numerical experiments of plasma mixing with realistic plasma transport coefficients. In particular, we are aiming to address the following questions:

- Could a magnetic field suppress the late time growth of the RTI and, if yes, under what conditions and configurations?
- Could a robust lower limit on mixing exist in the Hall-magnetized plasma, similar to the bounds obtained earlier in the hydrodynamic limit? The existence of such a lower bound could impact the feasibility of obtaining ignition.

By examining a variety of configurations, we will not only answer the question regarding RTI growth in the presence of the MHD-Hall effect with realistic plasma transport properties, but also contribute to the understanding of the mix in ICF. In addition, the study will also address several astrophysical phenomena where the combined MHD-Hall effect and RTI occur.

Benefit to National Security Missions

Since one of the major sources of mix in Inertial Confinement Fusion (ICF) is Rayleigh-Taylor instability (RTI) development, controlling or suppressing this instability could have major implications in achieving ignition. In order to investigate this possibility, we will provide the first comprehensive studies using accurate numerical simulations of magneto-hydrodynamics (MHD)-Hall RTI with realistic plasma transport properties. The work will consider the role of external magnetic fields as well as various other effects (e.g. Biermann battery effect) on the development of RTI and electron thermal conductivity, at the conditions during the deceleration phase in ICF.

The results of the work could easily translate into future programmatic efforts. Thus, besides the importance of answering the central questions of the proposal, the mixing and turbulence characteristics we will identify may help address the physics of mix in ICF. For example, a recent DOE review regarding ICF concluded that the modeling of mix is likely inadequate and recommended "a program of scientific experiments and modeling focused on understanding the various physical effects, in isolation, that impact the integrated implosion experiments provides the best approach to eventually either achieve ignition, or to understand definitively why it may not be achievable." In addition, the extensive database we will generate of accurate simulations could be used to test and develop turbulence models and to test coarse mesh simulation codes of programmatic relevance. To this end, we are in contact with project leaders within several campaigns and the PEM program.

Progress

The project goals are to examine a variety of configurations, under late time ICF conditions, to understand the

role of the combined buoyancy, magnetic, and Hall effects on the Rayleigh-Taylor instability growth, turbulence, and mixing.

Work started by writing the full set of compressible equations describing the flow in a magnetized plasma: continuity, ion and electron momentum and energy, transport equations and Faraday's law. The heat and mass fluxes were derived, for the first time, using Onsager's relations for irreversible processes and Onsager's symmetry principle. The variable density density incompressible limit of these equations was derived assuming speed of sound much larger than any characteristic velocity, which is relevant to late time ICF conditions. The resulting equations have been implemented in the CFDNS code in both the Rayleigh-Taylor and homogeneous Rayleigh-Taylor configurations. Preliminary simulations have been started in both configurations. While the Rayleigh-Taylor set-up is directly relevant to ICF, the homogeneous set-up allows us to investigate the mixing problem under the ICF conditions, without the complications due to the presence of the edges.

In a related effort, we are finalizing a linear analysis of the compressible viscous Rayleigh-Taylor instability, with a background temperature gradient. The presence of a temperature gradient was never considered in such an analysis, yet in many problems (e.g. ICF or solar corona), there are strong temperature gradients. The results also address a recent controversy on the role of large plasma viscosity on the development of turbulence under ICF conditions. Thus, we show, for the first time, using realistic plasma viscosities, what are the likely perturbation wavelengths damped, in ICF, by the large increase in plasma viscosity and what is the range of wavelengths least affected.

Future Work

This is the first detailed study of the combined buoyancy, magnetic, and Hall effects on the Rayleigh-Taylor instability (RTI) growth, turbulence, and mixing. No previous study has been performed using realistic plasma transport properties and in 3D. The nominal case for the study addresses the conditions during the deceleration phase in Inertial Confinement Fusion (ICF). During this phase, the RTI development mixes hot and warm plasmas, which enhances thermal energy loss and produces a larger "warm-spot" instead of a hot spot. This undesirable effect could be mitigated by reducing the electron thermal conduction coefficient and/or the growth of RTI. As such, we aim to investigate the possibility of controlling the RTI development and electron thermal conductivity at the nominal conditions using external magnetic fields. We will also examine the turbulence and mix properties produced under these conditions. In order to be able to perform the study, during the second year we will focus on the following goals:

Theory

- Continue the analysis of the spectral range locality of the MHD-Hall equations, for the triply periodic case, following previous analysis of the pure MHD case.
- Examine the linear behavior of the MHD-Hall equations derived.
- Examine the structure of the MHD-Hall RT layer, in particular the verify the existence of an inner turbulent region and derive the scaling for the turbulent non-turbulent interface at the edges of the layer.

Computation

- Continue with the low resolution simulations to scope the parameter space, for the pure MHD and MHD-Hall cases in two configurations: triply periodic and classical RT.
- Start medium to high resolution simulations for the nominal cases.
- Start analyzing the data. In particular, examine the role of the increase of plasma viscosity with temperature on the turbulent evolution and/or suppression.

Conclusion

The central questions of the proposal, which we expect to answer, are related to the late time Rayleigh-Taylor (RTI) instability growth suppression using magnetic fields and the existence of a lower bound in the mix development. In seeking to address these questions, we will provide the first comprehensive studies using accurate numerical simulations of magneto-hydrodynamic (MHD)-Hall RTI with realistic plasma transport properties. We expect, along the way, to be able to address questions related to mix properties and the possibility of controlling mix in Inertial Confinement Fusion as well as many questions relevant to a multitude of astrophysical configurations.

Publications

Aslangil, D., D. Livescu, and A. Banerjee. Variable density mixing under variable mean pressure gradient. 2015. In 15th European Turbulence Conference. (Delft, The Netherlands, 25-28 Aug. 2015). , p. Paper number 122. Delft: TU Delft.

Aslangil, D., D. Livescu, and A. Banerjee. Reynolds and Atwood numbers effects on homogeneous Rayleigh-Taylor instability. To appear in 68th Annual Meeting of the American Physical Society Division of Fluid Dynamics . (Boston, 22-24 Nov. 2015).

Pulido, J., D. Livescu, J. Woodring, J. Ahrens, and B. Hamann. Survey and analysis of multi-resolution repre-

sentation methods using turbulence data. Computers and Fluids.

Reckinger, S. J., D. Livescu, and O. V. Vasilyev. Comprehensive numerical methodology for Direct Numerical Simulations of the compressible Rayleigh-Taylor instability. To appear in Journal of Computational Physics.

Wieland, S. A., D. Livescu, O. V. Vasilyev, and S. J. Reckinger. The compressible Rayleigh-Taylor instability and vortex dynamics in stratified media. To appear in 68th Annual Meeting of the American Physical Society Division of Fluid Dynamics . (Boston, 22-24 Nov. 2015).

Enhancing the Long-Baseline Neutrino Experiment Oscillation Sensitivities with Neutron Measurements

Keith R. Rielage
20150577ER

Introduction

The matter-anti-matter asymmetry of the universe is one of the key scientific questions of our time. In order to explain the asymmetry, a large violation of CP symmetry - particle vs. antiparticle behavior - is required. Of the two known types of matter particles - quarks and leptons - extensive studies of CP violation with quarks have been made and found to be too small to explain the asymmetry of matter and anti-matter in the universe. The discovery of neutrino oscillations gives us a mechanism to search for CP violation with leptons. The Long-Baseline Neutrino Experiment (LBNE), endeavors to make a comprehensive measurement of neutrino oscillation physics with a focus on measuring CP violation in the lepton sector for the first time. In addition, LBNE endeavors to over-constrain the leptonic mixing matrix giving unprecedented sensitivity to phenomena such as Non-Standard Interactions. LBNE will measure CP violation by making detailed studies of oscillation phenomena over a broad range of neutrino and anti-neutrino energies. They require an event-by-event reconstruction of the neutrino energy from the outgoing particles of the interaction - including neutrons. In this project, we will measure neutron interactions in a liquid argon time-projection chamber (TPC) in a well-understood neutron beam for the very first time.

Los Alamos has a unique neutron facility with a well-characterized, high-energy neutron beam. We will deploy a large liquid argon TPC in this beam in order to carry out the measurements. The theoretical part of the effort will be focused on determining the sensitivity of a variety of neutrino oscillation phenomena to the neutrino and anti-neutrino energy resolutions.

Benefit to National Security Missions

For neutrino oscillation experiments using liquid argon time-projection chambers, neutrons are a major challenge. Neutrino oscillation experiments employ neutrinos in the several hundred Mega-electron volts to several Giga-electron volt energies. At these energies, neutrons are often emitted in the neutrino interaction carrying away energy. Since the neutrino energy must be reconstructed using the outgoing particles, correlating neutron interactions in the detector with neutron kinetic energies is paramount. LANL has a unique high-energy neutron facility that enables these measurements.

The work will lead to a more robust approach to neutrino oscillation analysis that will be employed for searches of violation of CP symmetry (particle-anti-particle symmetry) as well as many other neutrino oscillation scenarios. CP violation in particular may be tied to the origin of the matter-anti-matter asymmetry of the universe.

This work contributes to the DOE Office of Science missions and directly supports the nuclear and particle futures pillar at LANL.

Progress

This three-year project aims to measure neutron interactions with argon and interpret the data in the context of neutrino oscillation analyses relevant to the international long-baseline neutrino effort currently being developed. The international long-baseline effort is being planned with the United States as the host country. The effort is currently called the Deep Underground Neutrino Experiment (DUNE). DUNE will employ an enormous liquid argon time-projection chamber (TPC) at a deep underground location in Western South Dakota. Our Laboratory Directed Research and Development (LDRD) project is designed to measure the response of a liquid argon TPC to neutron interactions at well-defined neutron kinetic energies up to 800 Mega-electron volts (MeV) using the Los Alamos Neutron Science Center's (LANSCE) Weapons Neutron Research (WNR) facility.

Since the beginning of the project in October, 2014, the team has carried out two liquid argon engineering runs

with the prototype detector for the Cryogenic Apparatus for Precision Tests of Argon Interactions with Neutrinos (CAPTAIN) program. The prototype, which we call Mini-CAPTAIN, consists of 1000 pounds of instrumented liquid argon. In our first test, we demonstrated our ability to achieve the very low electronics noise levels required for optimal operation. We then spent several months working on the purification system, conducting a variety of tests. We subsequently carried out the second engineering run and demonstrated good argon purity with respect to water. Our challenge now is to demonstrate good purity with respect to oxygen.

Since the second run, we have finished developing a gas-phase purification and condensing loop that will allow us to continuously purify the liquid argon and re-condense it. This system will allow us to obtain the optimal purity - especially with respect to oxygen. At the time of this writing, we have begun our third engineering run and begun operating the recirculation system. We will understand the performance of the recirculation system and determine if further modifications are necessary after this run. A neutron run is anticipated in fiscal year, 2016.

Several calculations and test effort has gone into the development of a neutron beam-flux monitoring system. Test data were taken in November and the system is now complete. The system will allow us to make flux and spectral measurements even at the low neutron rates we require to run the liquid argon TPC.

Future Work

During the first year, we have been working to commission the Mini-CAPTAIN detector. We are completing a second engineering run to demonstrate appropriate purity for the experiment. In tandem, we have put in a proposal to the LANSCE PAC to run at the WNR beamline 15R in the next run cycle. We expect to move the detector to the beam area in the beginning of FY16. The deployment and recommissioning of the detector requires significant set-up of cryogenic and electronics equipment. In addition, the detector will be filled with purified liquid argon that will be re-circulated to maintain optimum purity. The purity will be checked to assure high-quality data before taking beam. The detector will also be calibrated before taking beam.

Subsequently, the detector must be drained and removed from the beamline. The next experimental task will be to carry out a detailed data analysis as well as continued simulations.

The theoretical effort has stalled due to the departure of the T-division co-I. We are redirecting these resources into the commissioning of the detector. Detailed simulations will begin late this FY. The starting point is a detailed analysis of the energy resolutions of various charged particles and neutrons in liquid argon TPCs. The next step is to lay out what measurements will be made in the LBNE near neutrino detector. The final step is unifying the information from the near and far detectors in such a way that we can vary the resolutions of each piece of information in the oscillation analysis.

Conclusion

We will study neutron interactions on liquid argon in terms of their event signatures. We will use these results to test existing simulations of the interactions. We will then modify those simulations with our high statistics data-set. Ultimately, we will produce an oscillation analysis approach for LBNE that includes the impact of neutrons as well as a requirement to be sensitive to new physics. This analysis will create the near neutrino detector requirements essential for making the optimal design choices.

Direct Numerical Simulations of Magnetic Rayleigh-Taylor Instability

Daniel Livescu
20150732ER

Introduction

The development of hydrodynamic instabilities in the presence of complex plasma physics is one of the main obstacles in achieving ignition in both magnetic and inertial confinement fusion (ICF). Besides the important role of pure Rayleigh-Taylor instability (RTI) in many practical problems, magnetic RTI is very important for the compression (or lack thereof) efficiency in magnetic or inertial confinement fusion. Since the instability can limit the maximum compression achieved in the pinch or other inertial confinement fusion (ICF) implosions, controlling or, at least, understanding it is of critical importance.

At present, the role of a magnetic field on Rayleigh-Taylor Instability (RTI) growth is not well understood and the few existent studies seem to arrive at opposite conclusions. For example, recent numerical studies in 2D conclude that magnetic fields suppress instabilities and mixing while the only published study to explore the problem in 3D concludes that magnetic fields enhance the nonlinear growth of instabilities and mixing. Our recent simulations show that pure RTI growth is bounded from below by the growth of the inner turbulent region, which is independent of initial conditions or fluid properties at high enough Reynolds numbers. There is no systematic study examining the combined (magneto-hydrodynamics) MHD-Hall RTI turbulence and it is not known if such a lower growth bound exists for MHD-Hall RTI. It is also not known what effects the plasma transport properties could have on the growth of RTI. Moreover, there are many astrophysical systems which are not well understood, but where these effects likely play a role.

We propose to use Trinity Phase 1 to perform the first fully resolved 3D simulations, with realistic plasma transport properties, of the combined buoyancy, magnetic, and Hall effects on the RTI growth, turbulence, and mixing as well as electron thermal conduction, under realistic ICF conditions.

Benefit to National Security Missions

While the goal of achieving economically viable controlled fusion remains remote in either the inertially or magnetically confined configurations, it is generally believed that one of the main obstacles is the development of hydrodynamic instabilities. However, the complex physics associated with confined fusion makes such instabilities significantly more complicated than the classical Rayleigh-Taylor Instability (RTI). An example is the interaction between the confined plasma and magnetic fields. The influence of magnetic fields has recently been an active (experimental + numerical) research topic in the hope it may offer a way of controlling or inhibiting RTI and mixing or, more generally, understanding the role on the RTI development. For example, recent experiments on the Omega Laser facility resulted in the compression of an externally imposed magnetic field to around 20MG, which is dynamically important compared to characteristic RTI velocities.

Numerical investigations of this problem in the context of ICF have been limited to 2-dimensions (2D), and therefore are unable to capture the full 3-dimensional (3D) nature of magnetic RTI. It is well known that mixing and turbulence properties in 2D are completely different from 3D. We believe that conducting systematic investigations of magnetic field interaction with RTI in 3D would allow us to answer definitively whether or not magnetic fields can be used to control RTI.

This work will also benefit the stabilization of Trinity Phase 1 and further develop the CFDNS for efficient use on new and emerging architectures in support of our national security mission.

Progress

Our cycle on Trinity Phase 1 has not yet started. In preparation for the start date in mid July, the code has been ported to Haswell and small size simulations to test resolutions and parameter re=ranges are under way.

Future Work

This is a project for cycles on Trinity Phase 1 only. The simulations will be performed during the two month window for the stabilization process during the present fiscal year.

In order to study the instability growth and mixing characteristics due to the combined MHD-Hall RTI, we will conduct a series of numerical experiments, in the Hall-MHD limit that will cover typical conditions under the deceleration phase in ICF. Furthermore, we will compare the results with the MHD and hydrodynamic ($B \rightarrow 0$) limits to isolate the effects associated with magnetic fields and finite plasma skin depth. We are planning to use realistic plasma transport coefficients and fully resolve dissipation scales.

The project will use the OpenMP-MPI hybrid version of the CFDNS code. OpenMP is a library and API for shared memory multiprocessing, and is an industry standard for using threads within a code. It is expected that using MPI everywhere with upcoming many-core architectures, such as Trinity, will be too expensive. We plan on testing OpenMP by varying the number of threads used, and seeing if there are any performance increases. We have also made some changes to the code to increase the amount of vectorization to better utilize the more capable vector units found on Trinity. We will further test the implementation and use profilers such as Intel VTune and VampirTrace to identify potential bottlenecks.

Conclusion

In order to fill the gap in our knowledge of the coupling between instability development and magnetic fields in Inertial Confinement Fusion, we have proposed to conduct a thorough study of the Rayleigh-Taylor Instability (RTI) in the variable-density (magneto-hydrodynamics) MHD-Hall limit using high-resolution numerical experiments of plasma mixing with realistic plasma transport coefficients. In particular, we are aiming to address the following questions:

- Could a magnetic field suppress the late time growth of the RTI?
- Could a robust lower limit on mixing exist in the Hall-magnetized plasma, similar to the bounds obtained earlier in the hydrodynamic limit?

Publications

Srinath, A., R. Miller, and D. Livescu. OpenCL-based tridiagonal solvers for evaluation of compact finite differences on parallel architectures. 2015. Under preparation for a parallel computing conference.

Extreme-Scale Kinetic Plasma Modeling of Turbulence and Mix Using VPIC

Brian J. Albright
20150751ER

Introduction

VPIC is general-purpose, kinetic plasma modeling code that has been applied to and validated on a variety of problems, including laser-plasma instabilities in inertial fusion, dense plasma transport, thermonuclear burn, laser-driven particle acceleration, magnetic fusion, and applications in space and astrophysics. We propose to apply VPIC to three basic science problems central to our understanding of turbulence and mix in space and laboratory plasmas and particle acceleration arising in magnetized plasmas. To conduct this work, we will make several changes to the VPIC code base in order to enable its efficient use of the unique features of the Trinity supercomputer. Specifically, we will adapt the VPIC architecture to a four-tier structure that will enable exploitation of distributed-memory parallelism, task parallelism, data parallelism, and Trinity's specific single-instruction-multiple-data (SIMD) instructions. We will also examine the development of novel diagnostics taking advantage of the Burst Buffer capability Trinity has, a feature of the supercomputer enabling more extensive analysis of high data volumes than ever before possible, a potentially groundbreaking achievement. This modification to our flagship VPIC kinetic plasma modeling code will position the scientific community for effective use of Exaflop/s supercomputers in future years.

Benefit to National Security Missions

This work will vastly improve the state of the art in plasma kinetic modeling, a subject area with direct ties to many aspects of basic and applied science and national security.

The ability to resolve outstanding problems associated with plasma-phase mix ties directly to outstanding problems in high energy density science of direct importance to nuclear weapons programs.

Moreover, as noted in the research proposal, NASA missions rely heavily on large-scale simulations modeling magnetic reconnection and turbulence processes. Indeed, multiple active missions have been fielded specifically to advance our understanding of space science in these areas, which this project directly impacts.

Inertial fusion energy interests are also advanced by this project; not only is the VPIC computer code used to advance laser-plasma interaction science for direct- and indirect-drive inertial fusion energetics, but also plasma-phase mix of shell-fuel interfaces will be directly impacted by the atomic mixing studies we will conduct.

Finally, this work advances meaningfully the scientific community's ability to harness the power of modern and future supercomputers, making it of profound interest to the information science and technology communities. Also, the techniques developed to process large data volumes using the Trinity burst buffers may be of interest to information science applications involving similarly large data sets.

Progress

We have begun to assemble our team and issue work assignments for this project. No other progress yet to report.

Future Work

We will adapt VPIC to the Trinity architecture in a hierarchical way that reflects the physical characteristics of the system. As an overview, our approach will rely on asynchronous communication between compute nodes, task-parallel division across the intra-node single address space, data-parallel division within a task, and full vectorization within a thread of execution using AVX-512 intrinsics.

- Test performance of finer-grained MPI parallelism than employed previously. Assess performance tradeoffs when replacing MPI ranks with threads.
- Experiment with restricting task parallel threads to

optimize efficiency of the caches. Organize threads into user configurable groups such that each shares a replication of the field domain.
- Develop a hierarchical threading model combining atomic memory operations with stream reductions.
- Add support for AVX-512 intrinsics and find a suitable block size for processing particle data on Trinity. Explore new intrinsics available in AVX-512 and evaluate their effects on performance.
- Explore strategies for using Trinity high-bandwidth memory.
- Explore ways to use the new burst buffer capabilities of Trinity for checkpoint/restart and novel methods of high-data-volume postprocessing of simulation data
- Implement higher order particle weighting algorithm to VPIC to improve compute/data ratio
- Define key physics problems to be run “at scale” using Trinity during Phases 1 and 2 related to turbulence and mix of plasmas and particle acceleration
- Document and present results to the high performance computing and scientific communities.

Conclusion

At the culmination of this project, we will have made substantial progress toward resolving outstanding physics problems in plasma and high energy density science. Specifically, we will have revealed through large-scale calculations how dense plasmas mix with one another. We also will have advanced our understanding of the physics of magnetic reconnection and the acceleration of cosmic ray particles to very high energy. Another legacy of this project will be the development of our VPIC particle-in-cell kinetic plasma code for modern supercomputers such as Trinity and future multi-core platforms.

Publications

Huang, C. K., M. D. Meyers, Y. Zeng, S. Yi, and B. J. Albright. On the numerical dispersion and the spectral fidelity of the particle-in-cell method. To appear in 24th International Conference ont he Numerical Simulation of Plasmas . (Golden, Colorado, 12-14 Aug, 2015).

Huang, C. K., M. D. Meyers, Y. Zeng, S. Yi, and B. J. Albright. On the numerical dispersion and the spectral fidelity of the particle-in-cell method. To appear in Computer Physics Communications.

Nystrom, D.. Progress on optimizing VPIC for LLNL’s Sequoia Platform. To appear in 24th International Conference on the Numerical Simulation of Plasmas . (Golden, Colorado, 12-14 Aug, 2015).

Hybrid Shock Ignition as an Alternate Concept for Fusion Energy

Eric N. Loomis
20140180ER

Abstract

Inertial Confinement Fusion (ICF) is a concept for producing energy gain through the fusing of hydrogen isotopes (D, T) that was first conceived in the 1960's and has continued to evolve. If successful, it would open new doors into studying matter in unprecedented regimes and offer new directions for energy production. In recent years, the conventional designs for ICF have encountered difficulties suggesting the need for alternative fuel compression concepts. In this Laboratory Directed Research and Development project we have conceived of a modified concept that is based on the existing design known as Shock Ignition, but uses both x-rays and direct laser drive in order to function efficiently at the existing National Ignition Facility (NIF). In this report we discuss the avenues we have taken to evaluate this concept under realistic conditions and report our major findings and results.

Background and Research Objectives

Conventional ICF uses high-powered lasers or thermal x-rays to implode low-density spherical capsules containing D and T to densities and temperatures sufficient to produce a large number of thermonuclear reactions in a central "hot spot" in the resulting DT plasma [1]. If the fuel surrounding this hot spot is dense and thick enough to stop a large fraction of the alpha particles from the DT reaction then a thermonuclear burn wave will propagate outward, engulfing the remaining fuel. "Ignition" is achieved if a sufficient amount of this fuel is reacted in the burn wave so that more energy is released than the amount of energy used to initiate the implosion.

Shock Ignition is among the most attractive alternative concepts to succeed conventional ICF because of its predicted high gains [2-6], and has recently received significant attention both theoretically [4, 5, 7] and experimentally [8]. In SI the main compression pulse is not intense enough to initiate the burn by itself. Instead, it assembles the surrounding cold fuel to high areal density, but produces a central hot spot that is cooler and below the threshold required for self-heating by alpha-particle deposition [1-3]. Near the peak fuel compression time the capsule is uniformly irradiated with a high-intensity laser pulse that drives a strong spherically converging shock into the fuel, which reflects and amplifies the outgoing stagnation shock back into the hot spot, providing the requisite heating and compression to initiate the burn as illustrated in Figure 1.

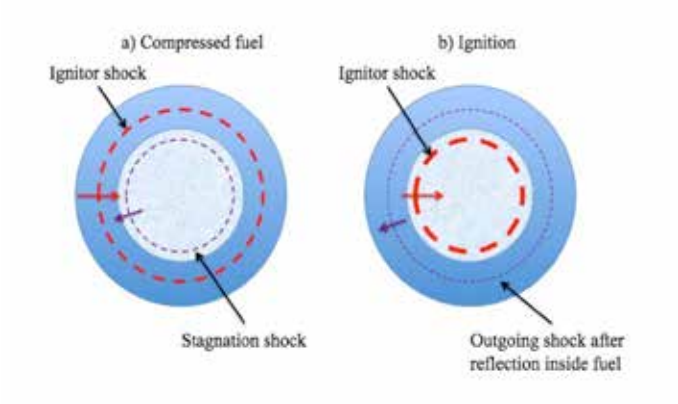

Figure 1. Illustration of Shock Ignition concept where fuel is first compressed by a main radiation pulse then the fuel is heated above the ignition threshold by a strong converging shock wave.

The objectives of the current project were to evaluate the possible benefits of a modified (Hybrid) SI concept that used both indirect (x-rays) and direct (lasers) drive in separate phases of the implosion. We intended for the project to have both theoretical design and experimental components; however, we were unable to secure facility time at the OMEGA Laser (Laboratory for Laser Energetics, Univ. Rochester, NY) through the standard Laboratory Basic Science (LBS) program. This allowed us to shift our focus on studying potential issues with Hybrid SI through numerical radiation hydrodynamics modeling. Our primary objectives ultimately were to:

(1) Evaluate the effects of low and mid mode (perturbation wavelength) drive and shell asymmetries on energy transfer in systems with converging strong shocks

(2) Design an OMEGA-scale experiment that could be used to measure energy transfer in converging asymmetric shock collisions

Scientific Approach and Accomplishments

Although not a major part of our original project plans, we discovered toward the end of the first project year the potential importance of evaluating the loss of energy transfer from the strong ignitor shock when it or the fluid ahead of it has departures from spherical symmetry. Converging shock waves exhibit diminished hydrodynamic stability relative to planar shock waves for all other conditions being equal [9-11]. We speculated that this diminished stability would result in less than ideal performance for SI if either the rebounding shock or ignitor shock possessed long or short wavelength modulations not captured in 1D simulations.

We began studying these effects using the Arbitrary Lagrangian-Eulerian (ALE) radiation hydrodynamics code HYDRA (Lawrence Livermore National Laboratory), which uses multi-phase tabular SESAME Equation of State (EOS) tables, multi-group radiation transport, and direct modeling of frequency dependent thermal x-ray or lasers as energy sources. Our first simulations modeled OMEGA-scale capsules [12] that had initial outer radii of 225 microns and were made from polystyrene (typical ICF ablator material). The polystyrene (CH) held between 25-50 atmospheres of deuterium gas and had shell thicknesses of 25-50 microns. For the OMEGA implosions a radiation temperature source was applied to the outer boundary of the numerical grid that lasted 2.5 nanoseconds and peaked at a temperature of 200 electron volts (eV). Radiation reaching the shell outer surface ablates material at high velocity, sending a strong 10's Mbar shock through the shell and eventually into the deuterium gas. Single mode (mode = 2 pi r/lambda, where r is radius of the interface) sinusoidal height perturbations were applied to the inner surface of the shell in contact with the outer boundary of the deuterium gas. Upon reaching this modulated interface the shock carried the modulations into the gas while the interface grew due to the Richtmyer-Meshkov (RM) instability [13] as shown in Figure 2. In these simulations we observed a transition regime near mode 20 where growth of the interface perturbation gave way to growth of the shock front perturbation moving toward the center. Both regimes can act to decrease the transfer of energy from the ignitor shock, albeit through different mechanisms. We focused on the lower mode effect where shock front perturbations were carried deeper into the deuterium gas, modulating the gas density and pressure as shown in the mode 8 simulations of Figure 2. The modulated gas then disrupts the propagation of the ignitor shock when it is launched just before the gas reaches peak compression.

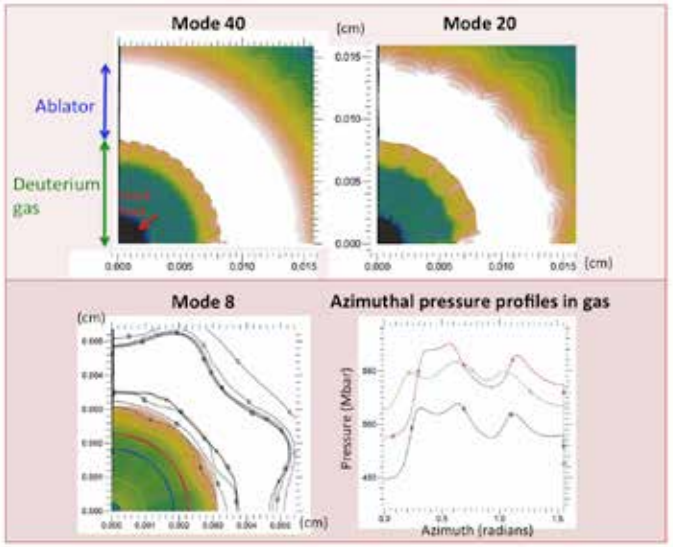

Figure 2. HYDRA simulations of inner shell surface perturbations. The top images show the difference in shock front modulation between mode 40 and 20. Bottom row show mode 8 modulations and target conditions just before ignitor shock. Black lines are contours of mass density starting at 0.5 g/cc and showing each 1.0 g/cc increment.

We performed a series of simulations using the initial mode 8 modulation on the ablator/gas interface that included the late time ignitor shock. The aim was to observe the growth of the gas pressure modulation as the initial interface perturbation amplitude was increased. Figure 2 (lower right image) shows an example of the initial pressure modulation as a function of azimuthal angle at three different radial positions in the gas just prior to the ignitor shock entering the gas.

From these results we see that increasing the surface perturbation amplitude slightly increases the mean pressure just prior to arrival of the ignitor shock while the peak-to-valley pressure modulation does not change significantly. Roughly 50 ps later the ignitor shock has traversed the gas itself and the mean pressure is raised into the 15 Gbar range. The peak-to-valley pressure modulation then reaches 3% of the mean pressure for the 1.125 micron perturbation and almost 10% for the 2.25 micron perturbation. In a NIF-scale target pressure (and temperature) modulations of 10% in the fuel could cool enough of the central gas to prevent initiation of the hot spot under marginal ignition conditions.

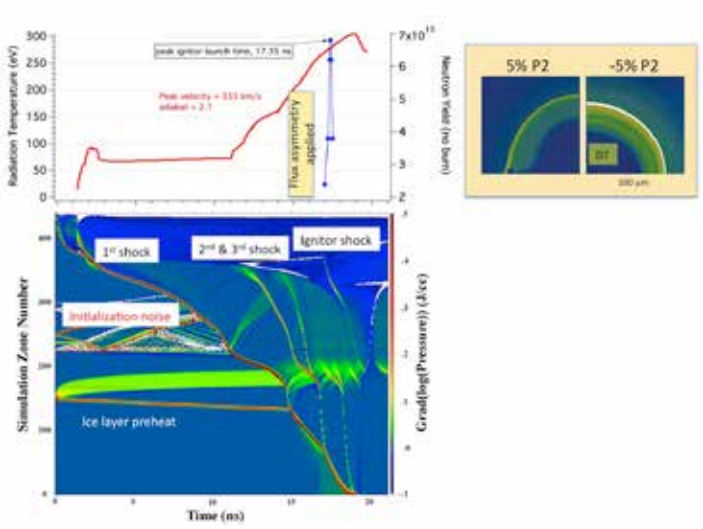

Figure 3. (Left) One-dimensional Helios simulations of the NIF high-foot plastic capsule where a shock ignition pulse has been added. The top left graph shows the hohlraum radiation drive from Clark et al. [15] along with the sharp ignitor timing peak with neutron yield maximizing at 17.35 ns launch time. Bottom left figure shows a shock front plot where shocks are observed propagating toward the center following each increase in radiation temperature. Here Zone 150 is the gas/ice boundary, Zone 225 is the ice/plastic boundary. (Above) In 2-D HYDRA simulations, a ±5% P2 flux asymmetry produces inverted fuel density shapes at bang time.

Questions about scaling from OMEGA to NIF in the case of Hybrid SI motivated us to begin studying potential degradation mechanisms at near-ignition scale (i.e., NIF). We started from existing NIF target designs rather than go through the lengthy process of designing a new and optimal target for Hybrid SI. We adapted as our baseline simulation the target and x-ray radiation pulse design of Dittrich et al. [14] and Clark et al. [15], which has been extensively benchmarked by actual experiments. These capsules have an outer radius of 1.13 mm and are fabricated with layers of Si-doped CH. A 70 micron thick layer of cryogenic deuterium-tritium ice is formed at the inner surface of the CH at a radius of 0.935 mm. Figure 3 shows our one-dimensional Helios (Prism Computational Sciences) simulations with radiation drive and the locations of shock fronts moving from the capsule toward the center of the fuel. With the x-ray radiation pulse is shown a direct-drive ignitor pulse that was 200 ps duration and 700 kJ total energy. The launch time of this ignitor pulse was adjusted in 100 ps increments until a maximum neutron yield (no alpha particle deposition) was found. This launch time peak (shown in the top left graph of Figure 3) is very narrow and is centered at 17.35 ns. When alpha particle deposition was turned on in the calculation the neutron yield increased up to 10E18 and ignition was predicted.

Two and three-dimensional effects will significantly diminish the yield from this idealized scenario. A primary degradation mechanism in current NIF experiments is the reality of time-dependent radiation flux asymmetries from complex hydrodynamic and radiation flow inside the hohlraum [16, 17]. To this end we have performed a series of HYDRA simulations where we applied a Legendre mode asymmetry to the radiation flux (Planckian spectrum) over the surface of the outer computational boundary. Previous work [16] has shown the most sensitive part of the radiation drive to flux asymmetries is during the rise to peak power. In the top right graph of Figure 3 we show a 2D HYDRA simulation near peak compression that was driven with +5% (left quadrant) and -5% (right quadrant) Legendre P2 mode from 15 to 16 ns. Here we observe that even with this minimal drive asymmetry an obvious non-spherical fuel shape is formed. We are currently finishing simulations that include the ignitor shock propagating through these asymmetric density fields, which we expect will significantly degrade the neutron yield since the ignitor will not efficiently transfer its energy to the fuel.

In Shock Ignition, the pressure of the transmitted shock is maximized in 1D, where there are no losses due to asymmetries [7]. In 2D and 3D however, the shocks may collide at an oblique angle due to radiation flux asymmetries, limiting the amplitude of the transmitted shock and giving rise to misaligned pressure and density gradients (and thus vorticity production). An understanding of the dynamics of asymmetric shock collisions and our code's ability to predict the resulting behavior is crucial to mitigating the losses in pressure amplification for shock ignition.

To this end, we have carried out a computational study designing experimental targets for the OMEGA laser facility to investigate asymmetric shock collisions using the Los Alamos RAGE code. Cylindrical targets are used to allow for better visualization of the shock collision with an axial X-ray backlighter [18]. The targets are nominally 430 µm outer radius and consist of a standard 1.04 mg/cc polystyrene shell with a low density (either 60 or 100 mg/cc) polystyrene foam interior. The shell thickness is varied between 20 and 40 µm. Our design simulations used a two-shock laser pulse – subject to facility energy and power limits - where the initial pulse drives a fast shock into the material resulting in modest compression of the target. The second pulse drives another shock into the target, with the collision being dependent on the timing of the second shock relative to the first. The timing of the second pulse is varied from 1.5 ns to 2.9 ns, relative to the onset of the first pulse, with the total energy in the pulse remaining constant at 18.95 kJ.

The spatial and temporal evolution of the high pressure

60 and 100 mg/cc foam simulations can be seen in the top row of Figure 4, which shows the logarithmic derivative of the pressure. Extrema in the logarithmic derivative correspond to shock fronts.

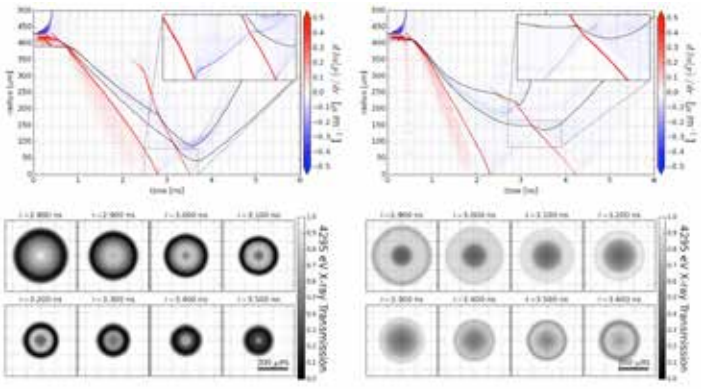

Figure 4. Simulations of OMEGA shock collisions in cylindrical targets from RAGE. (Top left) 60 mg/cc foam interior where shock fronts are shown in red and material interfaces in black, (top right) 100 mg/cc foam interior leading to reflected shock in blue colliding with second red shock front at 150 micron radius. (Bottom row) synthetic x-ray radiographs viewing down the cylinder axis for these two cases.

The first shock strikes the axis in both cases near 2.5 ns, and the subsequent collision of the second "ignitor" shock with the reflected shock occurs near 3.3 ns, as seen in the insets. Radial lineouts of the pressure, density, and material temperatures for the 60 mg/cc case are shown in Figure 5 at four different times highlighting the behavior for a typical shock collision. Synthetic diagnostics are used to construct X-ray radiographs of the implosion. Results with realistic instrumental blurring are shown in the bottom row of Figure 4. The first shock in the 60 mg/cc foam case is observed striking the axis at 2.8 ns, and the reflected shock is clearly visible up to 3.2 ns. The "ignitor" shock sweeps up what remains of the dense shell, and it breaks through just after 3.2 ns. The shocks collide just before 3.3 ns, and the transmitted shock and reflected shock are both visible at 3.3 ns. In the 60 mg/cc foam case, the shocks collide at about 60 µm, which limits the area of interaction. Increasing the density of the polystyrene foam in the interior reduces the convergence ratio, and delaying the second pulse longer relative to the first results in a collision farther out in radius. Lastly, reducing the shell thickness (and consequently the mass) allows the shocks to propagate through more quickly. All three effects can be used to alter where the shock collision occurs radially.

This can clearly be seen in the right-hand column of Figure 4, which shows the logarithmic derivative of pressure for a case with 100 mg/cc foam interior, a 20 µm shell, and a second pulse delayed 2.5 ns relative to the first. Here the shocks collide much farther out in radius, at about 150 µm, than in the 60 mg/cc case.

The goal in shock ignition is to create a peaked pressure profile following the shock collision. To that end, performance in these simulations can be quantified by the maximum value of the pressure on axis following the collision, as shown in Figure 5. As measured by this metric, performance increases as the shell thickness increases, corresponding to a decrease in the implosion velocity. The highest pressures are obtained with the 60 mg/cc foam interior, but the 100 mg/cc interior generally shows less variation in maximum pressure as the second pulse time is varied. From these designs we have begun 2D simulations with drive asymmetries, but they have not completed in time for this report. With these simulations and future experiments we can place tolerances on shock symmetry in full-scale shock ignition experiments.

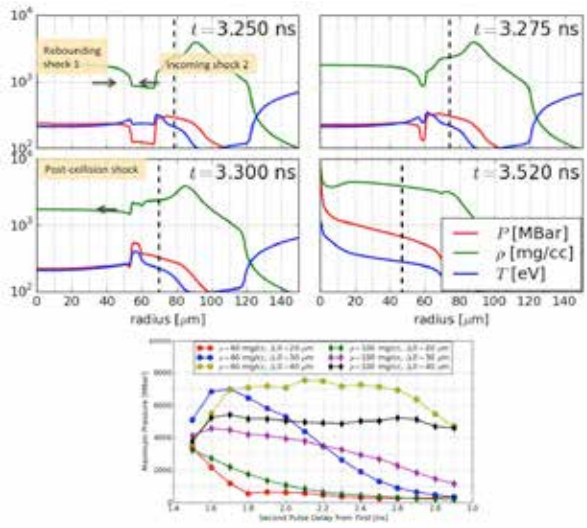

Figure 5. (Above) Radial profiles for a 60 mg/cc foam interior showing the evolution of shock collision in convergent geometry. (Lower) Summary of maximum pressure reached on axis after shock collision for all designs investigated.

Impact on National Missions

Achieving energy gain from thermonuclear reacting plasmas in a laboratory setting is a fundamental aim of researchers around the world since, in time, it would lead to a new and controllable energy source, as well as a much needed platform for supporting aspects of Stockpile Stewardship. In this LDRD research we have performed several novel simulation scenarios relevant to both conventional and Shock Ignition ICF including the impact of inner surface modes and time-dependent drive asymmetries. The post doc brought in for this research (Joshua Sauppe) has also designed a new experiment to study asymmetric shock collisions and vorticity production in convergent geometry as a means of benchmarking LANL codes under High Energy

Density conditions, which we plan to use in a proposal for Program funding and experimental support.

References

1. Lindl, J.. Development of the indirect-drive approach to inertial confinement fusion and the target physics basis for ignition and gain. 1995. Physics of Plasmas. 2 (11): 91.

2. Betti, R., C. D. Zhou, K. S. Anderson, L. J. Perkins, W. Theobald, and A. A. Solodov. Shock ignition of thermonuclear fuel with high areal density. 2007. Physical Review Letters. 98 (155001): 4.

3. Perkins, L. J., R. Betti, K. N. Lafortune, and W. H. Williams. Shock ignition: a new approach to high gain inertial confinement fusion on the national ignition facility. 2009. Physical Review Letters. 103 (045004): 4.

4. Ribeyre, X., G. Schurtz, M. Lafon, S. Galera, and S. Weber. Shock ignition: an alternative scheme for HiPER. 2009. Plasma Physics Controlled Fusion. 51 (015013): 19.

5. Lafon, M., X. Ribeyre, and G. Schurtz. Gain curves and hydrodynamic modeling for shock ignition. 2010. Physics of Plasmas. 17 (052704): 14.

6. Schmitt, A. J., J. W. Bates, S. P. Obenschain, S. T. Zalesak, and D. E. Fyfe. Shock ignition target design for inertial fusion energy. 2010. Physics of Plasmas. 17 (042701): 14.

7. Lafon, M., X. Ribeyre, and G. Schurtz. Optimal conditions for shock ignition of scaled cryogenic deuterium-tritium targets. 2013. Physics of Plasmas. 20 (022708): 10.

8. Theobald, W., R. Betti, C. Stoeckl, K. S. Anderson, J. A. Delettrez, V. Yu. Glebov, V. N. Goncharov, F. J. Marshall, D. N. Maywar, R. L. McCrory, D. D. Meyerhofer, P. B. Radha, T. C. Sangster, W. Seka, D. Shvarts, V. A. Smalyuk, A. A. Solodov, B. Yaakobi, C. D. Zhou, J. A. Frenje, C. K. Li, F. H. Seguin, R. D. Petrasso, and L. J. Perkins. Initial experiments on the shock ignition inertial confinement fusion concept. 2008. Physics of Plasmas. 15 (056306): 9.

9. Gardner, J. H., D. L. Book, and I. B. Bernstein. Stability of imploding shocks in the CCW approximation. 1982. Journal of fluid mechanics. 114: 17.

10. Davie, C. J., and R. G. Evans. Symmetry of spherically converging shock waves through reflection, relating to the shock ignition fusion energy scheme. 2013. Physical Review Letters. 110 (185002): 4.

11. Haines, B. M., F. F. Grinstein, and J. R. Fincke. Three dimensional simulation strategy to determine the effects of turbulent mixing on inertial confinement fusion capsule performance. 2014. Physical Review E. 89 (053302): 14.

12. Bennett, G. R., J. M. Wallace, T. J. Murphy, R. E. Chrien, N. D. Delamater, P. L. Gobby, A. A. Hauer, K. A. Klare, J. A. Oertel, R. G. Watt, D. C. Wilson, W. S. Varnum, R. S. Craxton, V. Yu. Glebov, J. D. Schnittman, C. Stoeckl, S. M. Pollaine, and R. E. Turner. Moderate convergence inertial confinement fusion implosions in tetrahedral hohlraums at Omega. 2000. Physics of Plasmas. 7 (6): 10.

13. Dimonte, G., C. E. Frerking, M. Schneider, and B. Remington. Richtmyer-Meshkov instability with strong radiatively driven shocks. 1996. Physics of Plasmas. 3 (2): 16.

14. Dittrich, T. R., O. A. Hurricane, D. A. Callahan, E. L. Dewald, T. Doeppner, D. E. Hinkel, L. F. Berzak Hopkins, S. Le Pape, T. Ma, J. L. Milovich, J. C. Moreno, P. K. Patel, H. S. Park, B. A. Remington, J. D. Salmonson, and J. L. Kline. Design of a high foot high-adiabat ICF capsule for the national ignition facility. 2014. Physical Review Letters. 112 (055002): 4.

15. Clark, D. S., J. L. Milovich, D. E. Hinkel, J. D. Salmonson, J. L. Peterson, L. F. Berzak Hopkins, D. C. Eder, S. W. Haan, O. S. Jones, M. M. Marinak, H. F. Robey, V. A. Smalyuk, and C. R. Weber. A survey of pulse shape options for a revised plastic ablator ignition design. 2014. Physics of Plasmas. 21 (112705): 14.

16. Scott, R. H. H., D. S. Clark, D. K. Bradley, D. A. Callahan, M. J. Edwards, S. W. Haan, O. S. Jones, B. K. Spears, M. M. Marinak, R. P. J. Town, P. A. Norreys, and L. J. Suter. Numerical modeling of the sensitivity of x-ray driven implosions to low-mode flux asymmetries. 2013. Physical Review Letters. 110 (075001): 4.

17. Kritcher, A. L., R. Town, D. Bradley, D. Clark, B. Spears, O. Jones, S. Haan, P. T. Springer, J. Lindl, R. H. H. Scott, D. Callahan, M. J. Edwards, and O. L. Landen. Metrics for long wavelength asymmetries in inertial confinement fusion implosions on the national ignition facility. 2014. Physics of Plasmas. 21 (042708): 10.

18. Tubbs, D. L., C. W. Barnes, J. B. Beck, N. M. Hoffman, J. A. Oertel, R. G. Watt, T. Boehly, D. Bradley, P. Jaanimagi, and J. Knauer. Cylindrical implosion experiments using laser direct drive. 1999. Physics of Plasmas. 6 (5): 9.

Quantum Kinetics of Neutrinos in the Early Universe and Supernovae

Vincenzo Cirigliano
20140252ER

Abstract

Neutrinos are perhaps the most mysterious and elusive of the known particles, and yet play a crucial role in the early universe and the life of stars. Neutrinos interact only very weakly and have tiny masses, the heaviest neutrino being at least a million times lighter than the electron, the lightest charged particle. Moreover, observations of solar, atmospheric, reactor, and accelerator neutrinos indicate that the neutrinos come in three different "flavors" that can morph into one another as they evolve; this occurs through a genuine quantum mechanical interference effect. Despite their elusive nature, neutrinos play a special role in the dynamics of the early universe (EU) and supernovae (SN), (1) because of their vast number, and (2) because they can set the ratio of neutrons to proton in both the EU and in the heated ejecta of a supernova through their flavor-dependent weak interactions. This ratio is key in understanding quantitatively what atomic nuclei are synthesized in these two environments. The overarching goal of this project has been to set up the analytic and computational tools needed to describe neutrino kinetics in the EU and SN environments, simultaneously keeping track of the effect of quantum mechanical morphing and the role of inelastic collisions with the medium. The appropriate tools to describe neutrino evolution in a hot and dense medium are the so-called Quantum Kinetic Equations (QKEs). Prior to this work, no self-consistent derivation of the QKEs existed. This project succeeded in a systematic first-principles derivation of the QKEs based on non-equilibrium field theory and a controlled expansion in ratios of widely separated length scales. The project uncovered the new phenomenon of coherent neutrino spin oscillations in anisotropic media and worked out in full detail the structure of the collision terms, including parts that cause de-coherence in the flavor and spin. Finally, by numerically solving the QKEs in simplified settings, the project explored impacts of spin-oscillations in an astrophysical environment and the effect of a non-zero lepton number in the early universe.

Background and Research Objectives

In hot and dense environments in astrophysics, like those associated with the early universe, core collapse supernovae, and compact object mergers, neutrinos may carry a significant fraction of the energy and entropy. The way these particles interact with and communicate with the medium is through the weak interaction. As a consequence, ascertaining the flavor states (weak interaction states) of the neutrino fields is these environments can be a key part of understanding, for example, how neutrinos set the neutron-to-proton ratio and deposit energy in supernovae, or whether neutrinos decouple in mass or in flavor states in the very early universe. A feature of both the early universe and core collapse supernovae is that neutrinos propagate from very hot, high energy density regions or epochs, where transport mean free paths could be short compared to neutrino flavor oscillation lengths, to environments where the opposite is true. Between these extremes, a poorly understood and complicated interplay of coherent neutrino flavor oscillations and scattering-induced de-coherence can govern how flavor develops. This intermediate regime is currently treated as "hard" surface, below which neutrinos interact and scatter, and above which neutrinos free-stream. Only a full QKE treatment can reveal the correct flavor, spin, and energy composition of the neutrinos emerging from a supernova explosion and coming out of equilibrium in the early phases of our universe's history. Through the course of this project we developed the foundations of such quantum kinetic equations, including relevant degrees of freedom for neutrinos (including spin, which is often neglected).

Scientific Approach and Accomplishments

The first main accomplishment of this project has been the complete formulation of Quantum Kinetic Equations for neutrinos starting from first principles, i.e. quantum field theory. The published results present a formulation of the quantum kinetic equations (QKEs) that govern the evolution of neutrino flavor at high density and tempera-

ture [1]. The QKEs are derived from the ground up, using fundamental neutrino interactions and quantum field theory. In the derivation we exploit a hierarchy of length scales (de Broglie wavelength, oscillation wavelength, mean free path, scale height of external potentials), working to second order in small ratios. We have shown that the resulting QKEs describe coherent flavor evolution with an effective mass when inelastic scattering is negligible. The QKEs also contain a collision term. This term can reduce to the collision term in the Boltzmann equation when scattering is dominant and the neutrino effective masses and density matrices become diagonal in the interaction basis. We also find that the QKE's include equations of motion for a new dynamical quantity related to neutrino spin. This quantity decouples from the equations of motion for the density matrices at low densities or in isotropic conditions. However, the spin equations of motion allow for the possibility of coherent transformation between neutrinos and antineutrinos at high densities and in the presence of anisotropy.

The physics of the new spin-coherence term in the QKEs has far reaching implications. If neutrinos are their own antiparticles (so-called Majorana fermions), this term can mediate neutrino-antineutrino transformation. If neutrinos are Dirac fermions, the new term drives active-sterile transformation, i.e. converts neutrinos into particles that do not feel the weak force. Even more surprisingly, none of these effects require the presence of an external magnetic field. Given the surprising implications of the new term, in our publication in Physics Letters, "A new spin on neutrino quantum kinetics",[2] we have discussed the physical origin of the coherent spin-flip term: the spin of a massive neutrino can precess -- much like a spinning top in gravitational field -- due to the interaction with an axial-vector field generated by other neutrinos or other matter particles, such as electrons and protons, carrying weak charge. This spin precession does not require the presence of a magnetic field nor neutrino magnetic moments. In the same article we have provided explicit expressions for the QKEs in a two-flavor model with spherical geometry, the first step towards a computational implementation of the new effect. In the context of this two-flavor model, we have also demonstrated that coherent neutrino spin transformation depends on the absolute neutrino mass and the so-called Majorana phases, parameters that are very difficult to measure in laboratory experiments.

Finally, to conclude our foundational work, we derived and published the collision term relevant for neutrino quantum kinetic equations in the early universe and compact astrophysical objects, displaying its full structure in both flavor and spin degrees of freedom [3]. In our analysis we included neutrino-neutrino processes, scattering and annihilation with electrons and positrons, and neutrino scattering off nucleons (the latter in the low-density limit), as illustrated in Figure 1. After presenting the general structure of the collision terms, we have taken two instructive limiting cases. First, we focused on the one-flavor limit that highlights the structure in helicity space. This has allowed for a straightforward interpretation of the off-diagonal entries of the collision term (the ones that drive de-coherence) in terms of the product of scattering amplitudes of the two helicity states. Second, we focused on the isotropic limit relevant for studies of the early universe. In this case the terms involving spin coherence vanish and the collision term can be expressed in terms of two-dimensional integrals, suitable for computational implementation. This article earned the status of "Editor's suggestion" in Physical Review D.

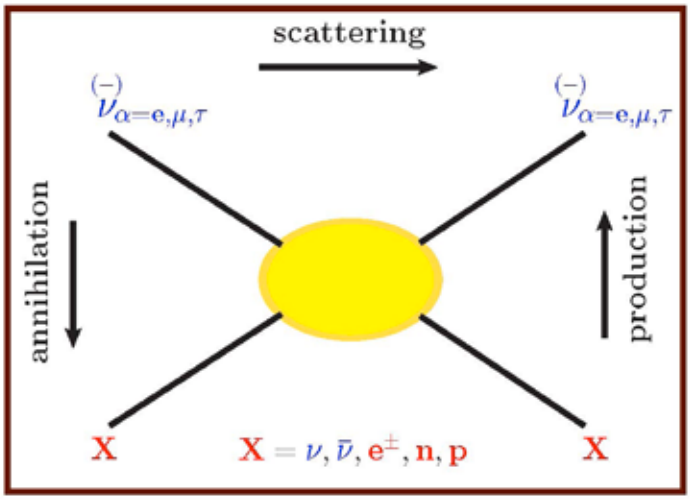

Figure 1. Illustration of the scattering, annihilation, and production processes that neutrinos of all flavors undergo in the early universe and supernovae environments. Target particles include neutrinos themselves, electrons, positrons, neutrons, protons, and nuclei (in supernovae).

During the course of the project, we also started the computational implementation of the QKEs, with two major highlights.

First, on the astrophysical front, we examined whether the newly derived neutrino spin coherence could lead to large-scale coherent neutrino-antineutrino conversion [4]. We did so in a simplified model of a supernova envelope, using the so-called single-angle approximation for the neutrinos emitted by the surface of the compact object. In a linear analysis we found that neutrino-antineutrino transformation is largely suppressed, but we have demonstrate that nonlinear feedback can enhance it. We pointed out that conditions favoring this feedback may exist in core collapse supernovae and in binary neutron star merg-

ers. Another interesting finding was that the novel effect depends linearly on the absolute mass of the neutrinos. Figure 2 shows an example of the result of a simple single-flavor neutrino-antineutrino conversion, using an absolute neutrino mass of 1eV and a density profile. These results have appeared as a preprint and are under review in Physical Review D [4]. Although the requisite conditions for neutrino-antineutrino conversion exist in the core collapse supernova and compact object merger environments, it is likely that only a self consistent incorporation of the QKEs in a sufficiently realistic model will establish whether or not significant neutrino-antineutrino conversion occurs.

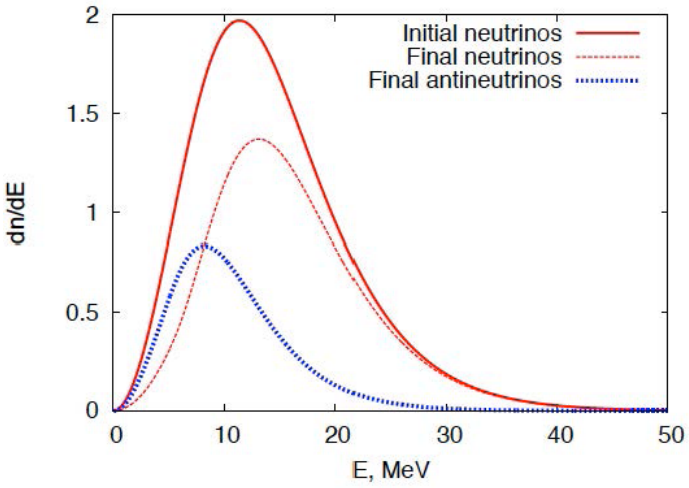

Figure 2. Illustration of neutrino-antineutrino conversion in a simple one-dimensional model for the supernova envelope. The model assumes an initial energy spectrum of electron neutrinos, that through evolution in the supernova envelope converts into a mixture of neutrinos and antineutrinos, populating a low-energy spectrum of antineutrinos. This simulations assume a neutrino mass of 1 eV and a density profile as specified in Ref. [4].

Second, we investigated neutrino flavor transformation in the early universe in the presence of a lepton asymmetry (i.e. a flavor-dependent difference in the number of neutrinos and antineutrinos), focusing on a two-flavor system with 1-3 mixing parameters [5]. We identified five distinct regimes that emerge in an approximate treatment neglecting collisions as the initial lepton asymmetry at high temperature is varied from values comparable to current constraints on the lepton number down to values at which the neutrino-neutrino forward-scattering potential is negligible. This work has uncovered an extremely rich set of oscillation regimes that further motivates the full implementation of the collision terms in the treatment of neutrinos in the early universe.

Impact on National Missions

Understanding how neutrinos have shaped the evolution of the cosmos and of stars, including the implications for the synthesis of atomic nuclei, is a major goal of both the Nuclear Physics and High Energy Physics Office of Science at the Department of Energy. Moreover, our project has developed cutting edge capability in transport theory. While this has been applied to neutrinos in supernovae and early universe, in the future the very same tools could be applied to programmatic work supporting our national security mission.

References

1. Vlasenko, A., V. Cirigliano, and G. M. Fuller. Neutrino quantum kinetics. 2014. Physical Review D. 89 (105): 004.

2. Cirigliano, V., G. M. Fuller, and A. Vlasenko. A new spin on neutrino quantum kinetics. 2015. Physics Letters B. 747: 27.

3. Blaschke, D., and V. Cirigliano. Neutrino quantum kinetic equations: the collision term. 2016. Physical Review D. 94 (3): 033009.

4. Vlasenko, A., G. Fuller, and V. Cirigliano. Prospects for neutrino-antineutrino transformation in astrophysical environments . To appear in Physical Review D.

5. Johns, L., M. Mina, V. Cirigliano, M. Paris, and G. Fuller. Neutrino flavor transformation in the lepton-asymmetric universe. To appear in Physical Review D .

Publications

Blaschke, D., and V. Cirigliano. Neutrino quantum kinetic equations: the collision term. 2016. Physical Review D. 94 (3): 033009.

Cirigliano, V., G. M. Fuller, and A. Vlasenko. A new spin on neutrino quantum kinetics. 2015. Physics Letters B. 747: 27.

Johns, L., M. Mina, V. Cirigliano, M. Paris, and G. Fuller. Neutrino flavor transformation in the lepton-asymmetric universe. To appear in Physical Review D .

Vlasenko, A., G. Fuller, and V. Cirigliano. Prospects for neutrino-antineutrino transformation in astrophysical environments . To appear in Physical Review D.

Vlasenko, A., V. Cirigliano, and G. M. Fuller. Neutrino quantum kinetics. 2014. Physical Review D. 89 (105): 004.

Designing the Next Generation Compton Light Source

Nikolai Yampolsky
20140269ER

Abstract

We have proposed and studied a novel scheme for creating the unstable beam distribution in relativistic electron bunches. We have studied all the aspects of this approach, namely (1) design and analysis of the beamline required to create the unstable beam distribution, (2) finding the growth rate of the instability analytically and benchmarking analytical results with numerical simulations, and (3) start-to-end simulations of the instability.

Background and Research Objectives

The two-stream instability develops in relativistic electron bunches if the electron distribution reveals two well separated energy bands. The instability is broadband and the central wavelength of the instability is proportional to the energy difference between the bands. Therefore, the two-stream instability can be potentially utilized in a broadband amplifier at small wavelengths [1]. However, the implementation of this scheme is a challenging task since it requires merging together two beams with close energies and ensuring their temporal and spatial overlap.

We have proposed an alternative scheme for generating the unstable beam distribution. The concept is similar to the echo-enhanced harmonic generation (EEHG) scheme [2] used for generating bunching in electron beams at high harmonic numbers [3]. The beamline for the scheme is outlined in Figure 1. First, the electron bunch interacts with a laser pulse inside the undulator and acquires sinusoidal in space energy modulation. Then the beam passes through the chicane, which shifts particles longitudinally proportionally to their energies. The energy distribution at any given spatial location resembles the multi-stream distribution.

Finally, the beam passes through the RF cavity, which imposes the energy chirp on the beam and eliminates the chirp in each individual stream of electrons. The resulting electron distribution is unstable and the multi-stream instability will develop in the following FOcus Drift DefOcus Drift (FODO) lattice long enough for observing growth of the microbunching.

The purpose of the project was to study the multi-stream instability in detail and find the parameter region where it can be observed. The particular application for the multi-stream instability is the possible enhancement of the inverse Compton scattering (ICS) light source. The scattering efficiency in ICS is proportional to the beam bunch at the scattered wavelengths. Development of the microbunching at EUV and soft x-ray wavelengths increases the bunching factor well above the random shot noise, which, in turn, increases the ICS efficiency.

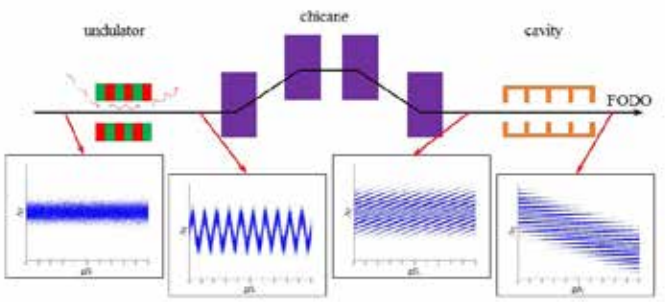

Figure 1. Schematics of the resulting in the multi-stream distribution and the longitudinal phase snapshots at different locations.

Scientific Approach and Accomplishments

We have studied all the aspects of the multi-stream instability. We have performed start-to-end analysis of the novel scheme. That analysis includes:

- Design of the electron beamline for generating the multi-stream distribution
- Simulating the designed beamline and optimizing the beam optics parameters
- Studying the instability analytically. Finding the

growth rate of the instability and the wavelengths where it is expected to develop

- Simulating the instability numerically and verifying analytical results

Beamline design and simulations

The design of the beamline resulting in the multi-band energy distribution was done using theory to describe the evolution of the modulated beams [4]. The dynamics of the beam distribution is traced in the Fourier space of the 6D phase space distribution. It can be shown that a monochromatic modulation remains monochromatic in the linear beamline and the transposed beam transform matrix describes that transform of the modulation wavevector. The analysis results in the conditions for the chicane strength and the imposed chirp depending on the desired number of energy bands in the output beam.

The exact beamline generating the multi-band distribution width was designed and simulated with the accelerator code ELEGANT [5]. The 120 MeV beam with 3 keV energy spread was modulated with 10 keV amplitude. The overall length of the beamline that creates the multi-band energy distribution is less than 5 m. The parameters of the beamline are optimized in ELEGANT to maximize the amplitude of the energy bunching (e.g. Fourier transform over the energy distribution). The output energy bunching is shown in Figure 2. Its amplitude is close to the analytical limit and is not significantly affected by the nonlinearities of the beam optics elements.

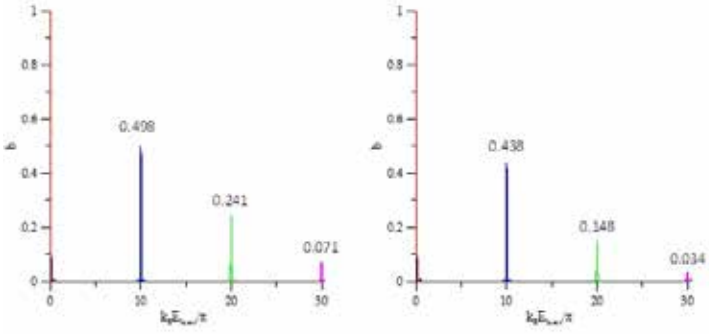

Figure 2. Energy bunch of the electron distribution simulated with ELEGANT code for linear (left plot) and including of each element (right plot).

The first-order design of the beamline performs exactly as expected. However, the ability to create the multi-band energy distribution significantly drops when the high order effects are taken into account. The largest deleterious effect on the beamline performance is the coherent synchrotron radiation (CSR). This effect results in the spatially dependent electric field along the bunch while it travels inside the chicane. As a result, the dispersion of the beam optics elements does not allow full recovery of the longitudinal phase space and the energy bands are smeared. The CSR can be mitigated by using long electron bunches. However, in this case, the transverse beam quality is poor since a high current needs to be generated at the photocathode and cannot be achieved through bunch compression. The second largest effect that degrades the scheme performance is the transverse beam quality, i.e. beam emittance. The angular divergence of the beam effectively increases the longitudinal plasma temperature in the beam frame. As a result, closely separated energy bands are washed out and the instability does not develop. The beam emittance has to be better than about 1 μm which is achievable with current photocathodes.

Analysis of the instability

The analysis has been performed in the Lorentz boosted beam frame where average electron velocity is zero. The electron beam in the beam frame can be treated as plasma. The energy bands in the original electron distribution translate to multiple streams of electrons in the beam frame. Such a plasma distribution is unstable and kinetic instability develops. The instability is similar to the conventional two-stream plasma instability except for the fact that the number of streams is larger than two.

We study the multi-stream instability under several assumptions. First, we focus on the longitudinal dynamics considering plasma to be uniform transversely. This assumption is valid if the characteristic wavelength of the instability in the beam frame is much smaller than the transverse beam size. Second, we consider the electron velocity distribution to be longitudinally uniform rather than periodic due to periodicity of the initially imposed modulation. This assumption is valid if the characteristic wavelength of the instability in the lab frame is much smaller than the wavelength of the laser used for imposing the modulation. The plasma dielectric function can be found analytically and the plasma modes supported by such a distribution can be found as zeros of the dielectric constant.

The dispersion relation for the plasma wave supported by the multi-stream distribution is presented in Figure 3. The analytical result is compared to the numerical result. The numerical dispersion was obtained using results described in Reference [6]. The real part of the frequency (left plot in Figure 3) is reproduced perfectly by the analytical expression. The imaginary part of the frequency (right plot in Figure 3) shows reasonable agreement between the analytical and numerical results.

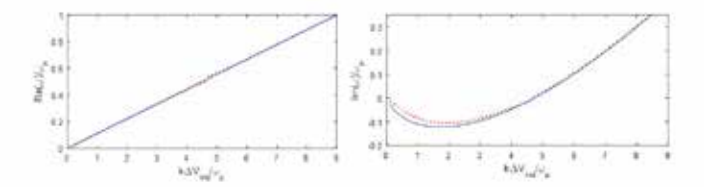

Figure 3. Dispersion relations the slowest plasma wave mode in the multi-stream instability for 9 bands and =0.5 bunching factor. Numerically found dispersion relation (red dotted lines) is compared with the analytical approximation (blue solid lines).

PIC simulations of the instability

1D electrostatic PIC code. The exact simulations of the instability are challenging since the output distribution shown in Figure 1 is not periodic due to the final chirp on the beam. Such a simulation requires resolving the entire bunch, which complicates simulations and limits the analysis of results. We approximate the exact beam distribution with the generic cosine distribution uniform in space. The instability was simulated inside a small plasma layer with periodic boundary conditions for particles and the electric field. The simulation was set up so that the second and the third spatial harmonics have similar growth rates close to the maximum and other harmonics are either stable or have substantially lower growth rates. The results of the simulations are shown in Figure 4.

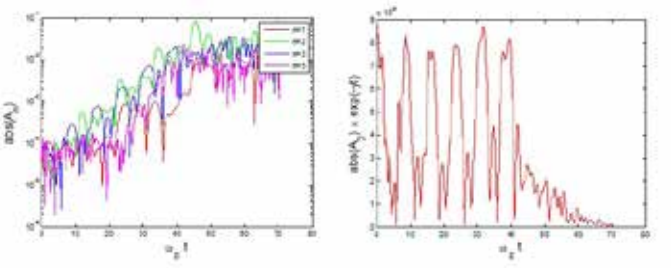

Figure 4. Left figure: growth of several low modes in the multi-stream instability. Right figure: change in time of the second spatial mode adjusted for the analytically expected exponential growth.

Figure 4 shows that multiple modes with different wavenumbers (the wavenumber of the mode is proportional to its number) grow in time until they reach saturation. The second and the third modes grow the fastest as expected. The time dependence of the density modulation can be well approximated as a product of the periodic and the exponentially growing functions (right plot in Figure 4). The growth rate and the frequency match theoretical expectations within the error of few percent. The periodic variation in the amplitude can be explained by the existence of multiple plasma modes at each wavenumber that are supported by the multi-stream velocity. The growth rates of those modes are almost identical and their frequencies are harmonics of the lowest frequency mode. The small deviation of the PIC results from the analytical expectations can be explained by small deviations of the modes frequencies and growth rates from the analytical expectations (the time evolution of the electric field adjusted for the exponential growth on the right plot of Figure 4 is slightly aperiodic).

The modes with a large longitudinal wavenumber do not grow at small time but their amplitude rapidly increases when the instability approaches the saturation (see the growth of the fifth mode on the left plot in Figure 4. This rapid growth is caused by the nonlinear two-plasmon coupling at large amplitudes of the plasma waves. The dispersion relation for the plasma mode in the multi-stream instability is actually the sound wave and the real part of the frequency linearly scales with the wavenumber as shown in Figure 3. As a result, two plasmons can recombine and yield the plasmon of a sum energy and momentum. This plasmon is supported by the plasma since its frequency and wavenumber matches the same dispersion as original plasmons because its phase velocity is equal to the phase velocities of each original plasmon.

Full bunch PIC simulations

We have also simulated the multi-stream instability using the output from ELEGANT as an input for the PIC code. These runs simulate the entire bunch since the phase space distribution is neither uniform nor periodic in space due to the presence of the energy chirp. The results are presented in Figure 5 and show the growth of the broadband instability at EUV frequencies.

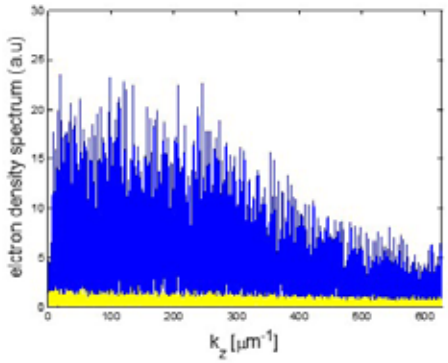

Figure 5. Spectra of the beam density at the beginning of the simulation (yellow line) and after the instability develops (blue line).

These simulations represent start-to-end analysis of the proposed scheme. We start with the beam distribution that is typical for conventional accelerators, model par-

ticles dynamics in the following beamline, which results in the multi-stream distribution, and then simulate the instability with the PIC code in which the coordinates of particles are passed from the accelerator code.

The proposed scheme for creating the unstable distribution in a single beam has been studied in details. We have confirmed that the original proposal is valid. The desired distribution can be generated and it results in the desired instability. However, our finding show that pushing the instability to EUV wavelengths for ~100 MeV electron bunches is challenging. There are three major limitations on the performance of the scheme:

- Beam emittance
- CSR effect
- Coulomb collisions

All these effects become a limiting factor at small separation between the energy bands in the electron distribution. As a result, one should increase the energy difference between the bands in order to avoid suppression of the instability. As a result, the wavelength of the instability increases. We conclude that the proposed scheme is not currently practical for increasing the brightness of the ICS source at soft x-rays to EUV region. At the same time, the proposed scheme can be practical for other accelerator-based applications such as optical stochastic cooling and broadband amplifier at optical to UV frequencies.

Impact on National Missions

The project has broadened Los Alamos expertise in Accelerator Physics, Beam Physics, and Plasma Physics. It has been demonstrated that conventional accelerator codes and plasma codes can be used simultaneously for studying different aspects of creating an unstable beam distribution in relativistic electron bunches. This capability can be expanded in future studies for the analysis of other problems of interest for Accelerator Physics such as microbunching instability driven by the longitudinal space charge. This work has implications for the development of accelerators for studies of matter in extremes.

References

1. Marinelli, A., E. Hemsing, and J. B. Rosenzweig. Using the Relativistic Two-Stream Instability for the Generation of Soft-X-Ray Attosecond Radiation Pulses. 2013. PHYSICAL REVIEW LETTERS. 110 (6): 4804.

2. Stupakov, G.. Using the Beam-Echo Effect for Generation of Short-Wavelength Radiation. 2009. PHYSICAL REVIEW LETTERS. 102 (7): 4801.

3. Hemsing, E., M. Dunning, B. Garcia, C. Hast, T. Raubenheimer, G. Stupakov, and D. Xiang. Echo-enabled harmonics up to the 75th order from precisely tailored electron beams. 2016. Nature Photonics. 10: 512.

4. Yampolsky, N. A.. Description of modulated beam dynamics. 2011. arXiv.

5. Borlund, M.. ELEGANT: A flexible sdds-compliant code for accelerator simulation. 2000. Argonne National Laboratory Advanced Photon Source Report No. LS-287 .

6. Xie, . Generalized plasma dispersion function: One-solve-all treatment, visualizations, and application to Landau damping. 2013. PHYSICS OF PLASMAS. 20 (9).

Publications

Yampolsky, N.. Two-stream instability in electron accelerators. Presented at Solved and Unsolved Problems in Plasma Physics. (Princeton, NJ, 28-30 March, 2016).

Yampolsky, N. A., G. L. Delzanno, C. Huang, and D. Shchegolkov. Two-stream Instability at Soft X-ray Wavelengths for Increasing Brightness of Compton Sources. Presented at 35th International Free-Electron Laser Conference. (New York, NY, 25-30 August, 2013).

Yampolsky, N. A., G. L. Delzanno, C. Huang, and D. Shchegolkov. Two-stream Instability at Soft X-ray Wavelengths for Increasing Brightness of Compton Sources. Presented at North American Particle Accelerator Conference. (Pasadena, CA, 29/09/ - 4/10, 2013).

Yampolsky, N. A., G. L. Delzanno, C. Huang, and D. Shchegolkov. Two-stream Instability at Soft X-ray Wavelengths for Increasing Brightness of Compton Sources. Presented at 55th Annual Meeting of the APS Division of Plasma Physics. (Denver, CO, November 11-15, 2013).

Yampolsky, N., G. L. Delzanno, C. Huang, and D. Shchegolkov. Development of the two-stream instability in a single bunch. To appear in 17th Advanced Accelerator Concepts Workshop. (National Habror, July 31 – August 5, 2016).

Combined Klystron and Linac (Klynac)

Bruce E. Carlsten
20140351ER

Abstract

A klynac is a klystron and linear accelerator (linac) combined into a single structure. The basic concept was originally described four decades ago but one has never been built and tested. Our approach is based on this earlier work but with an important modification: all cavities are coupled into one of two resonant circuits (a bi-resonant structure). This resonant coupling configuration leads to increased operational stability and can tolerate a significant temperature variation which greatly adds to the device's portability. In this project, we developed the underlying theory for the klynac, numerically designed one, and fabricated a prototype using that design. Preliminary testing of the fabricated klynac is validating the design approach.

Background and Research Objectives

Motivation: The intended purpose of a klynac device is to provide a compact and inexpensive alternative to a conventional 1 to 6 MeV accelerator requiring a separate RF source and linac and all the associated hardware needed for that configuration. Typical applications for compact 1 to 6 MeV electron beams are medical radiation therapy, nondestructive testing, and special nuclear material interrogation, all based on gamma-ray production from bremsstrahlung radiation from a conversion target at the end of the accelerator. For medical applications, the reduced size and weight of a klynac may significantly reduce the complexity and size of the cost-dominating gantries required for moving the radiation source about the patient, facilitating installation of radiation treatment instruments at smaller hospitals. For other applications, a compact, man-portable unit may be required for field operation.

Related work previous to this project: A klynac-like device was first described by Schriber in 1978 [1], where the output cavity of a klystron formed a single resonant structure with a linac section through coupling cells (operating in the $\pi/2$ mode, so there was negligible field in the coupling cells. More recently in 2003, Xie [2] demonstrated a klynac-like device where he directly attached a linac section to the output of a klystron. Some portion of the klystron beam was used as the linac beam. A hole in the collector was followed by a bending magnet, which provided an energy filter for the klystron electrons. The RF output of the klystron was externally connected to the linac section. In 2013, Potter [3] designed a resonant coupling cell with the same functionality as in Schriber's concept but where the klystron and linac are collinear and a small hole would allow some fraction of the klystron electron beam to be accelerated in the linac as in Xie's device.

Research objectives: The RF power generation section in Schriber's, Xie's, and Potter's designs all assumed (or in Xie's case actually had), a standard klystron architecture, where an input cavity is driven by an external, low-power RF source, and sequential gain cavities are driven by current modulation in the beam from previous cavities, as a convective instability. As in conventional standing-wave linacs, the accelerator cavities were resonantly coupled. We considered an alternative klynac architecture where the cavities in the klystron section are resonantly coupled in addition to the linac cavities, and the fields build up as an absolute instability.

This is a potentially important improvement. Because the klynac is a single structure with a single thermal mass, it has the potential to be much less sensitive to temperature variations than a system with a separate klystron and linac, as temperature variations will lead to more-or-less equivalent frequency shifts in both the klystron and linac cavities. This should allow operation without using active structure temperature control with a heated or cooled fluid flowing through the structure. An entirely resonant klynac structure would greatly enhance this ability because the frequencies of all cavities would be locked together.

Scientific Approach and Accomplishments

Basic design concept: To illustrate the basic concept, in Figure 1 we show the layout of the RF structure of a nominal 8-cavity bi-resonant klynac. The klystron input and gain cavities are K1, K2, and K3 and are resonantly coupled. An electron gun is to be bolted on the left of K1. Although in the location of a conventional input cavity, K1 shares the functionality as a gain cavity so, for this configuration, we will refer to cavities K1 through K3 as gain cavities. The klystron output cavity is K4, and the four linac cavities are L1 through L4 and these five cavities are also resonantly coupled. This structure resonates in the π/2 standing-wave mode, therefore the fields in the coupling cavities are negligible and they can be ignored in the following analyses. Note that this mode ensures that successive klystron cavities are 180o out of phase with the previous cavity, but the amplitudes can be designed to maximize the extraction power. (The amplitudes are fixed through varying the sizes of the coupling slots between the cavities [4].) Successive linac cavities are also 180o out of phase with the previous one.

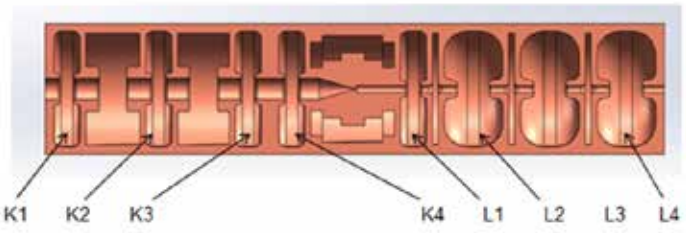

Figure 1. Layout of an 8-cavity, bi-resonant klynac structure. Klystron input/gain cavities K1, K2, and K3 form one resonant circuit and klystron output cavity K4 and linac cavities L1, L2, L3, and L4 form the second resonant circuit. There are on-axis coupling cells between cavities K1 and K2 and K2 and K3 in the first resonant circuit and between cavities K4 and L1, L1 and L2, L2 and L3, and L3 and L4 in the second resonant circuit.

The RF fields build up in the gain cavities as an absolute instability. The separation between K4 and L1 is adjusted to optimize the bunch capture in L1 and an intercepting aperture between cavities K4 and L1 reduces the beam current in the linac section to about 1% of that in the klystron section. The coupling cell between K4 and L1 is special because it is not open to the axis (it is a toroidal cavity instead of a pillbox cavity). Once the beam reaches L2, it is relativistic. Thus the separations between L2 and L3 and L3 and L4 are close to half the free-space wavelength of the klynac's operating frequency. Standard high-shunt impedance linac cavities designs are used. Note the coupling cells in the second resonant circuit have relatively short lengths. Both the gap in L1 and the center-to-center separation of L1 and L2 are shortened to provide for better capture of the initially low energy electron beam injected into the linac section.

Underlying physics: The klynac power balance is given by balancing the RF power generated to the power lost to Ohmic heating of the cavities plus the power absorbed by the electron beam. Power balance is established when the RF power generated in the klystron section is equal to the RF power dissipated in the linac cavities and the RF power that goes into the electron beam. Roughly speaking, we design the device to have about half the power going into the RF losses and half into the beam; if much less than half of the power goes into RF losses, the overall length can be shortened by increasing the gradient without too much performance degradation and if much less than half of the power goes into the beam, the beam power can be increased without a significant increase in overall length.

A key motivation behind the klynac is to minimize temperature tolerance requirement. It's worth considering the effect of temperature fluctuations for various coupling schemes. We note that the temperature expansion of copper is about 20 parts in a million per degree C; temperature variations in the structure will lead to frequency shifts due to geometrical changes. Typical separated klystron and linac systems need to be temperature regulated to less than 1 degree relative to each other to ensure the frequency of the klystron is close enough to the operating frequency of the linac to control the RF phase in the linac [5], based on a nominal linac Q of 104. In principle, the relative temperature requirement is simplified if the klystron and linac share the same thermal mass, as in a klynac, because temperature-induced frequency shifts in both the klystron and linac sections of the klynac should be equivalent.

There is an added complexity with the klynac design: in a conventional RF amplifier, the electron beam collector can be thermally separated from the RF interaction part of the tube. which minimizes temperature variations in that part. However, in the klynac, as shown in Figure 1, the beam interception is largely at the center of the structure and cannot be thermally isolated from either the klystron section or linac section cells. This leads to a temperature gradient along the klynac structure and the risk of cell frequency detunings relative to each other. Whereas relatively high-power klystrons or TWTs (~ kW average power) can operate with forced air cooling [6], a non-resonantly coupled klynac is limited to much lower power. Importantly, a π/2-mode resonantly coupled klynac can tolerate about an order of magnitude more power than a resonantly coupled klynac in another mode, and more than two orders of magnitude more power than an uncoupled klynac.

Design approach: Our original concept was to simplify

the device as much as possible by not requiring an input drive and designing the device to turn on by self-oscillation due to its internal feedback. Many RF sources have been designed and operated in this manner, starting with the Monotron in 1946 [7]. Specifically, we initially thought this device would operate like a discete monotron oscillator [8], which is topologically equivalent to the klystron section of the klynac. However, analysis and simulations showed that although the RF power section could oscillate by itself above some start current, the oscillations would be damped by beam loading in the linac section. The approach behind the design was to exploit this monotron instability for the gain section alone.

The klystron section of the nominal klynac shown in Figure 1 has five cells – three "klystron" cells and two coupling cells. As such, it has five modes, with 0, π/4, π/2, 3π/4, and π phase shift between cells. We want this device to turn on in the π/2 mode and not in the other modes. It is relatively easy to ensure this because the phase relationship of the cells and the harmonic currents are different for each mode. This problem is simplified if we can ignore the interaction of the electron beam with the coupling cells. We can do this by either making the coupling cavities coaxial like the coupling cell between K4 and L1 in Figure 1 or by minimizing the cell's transit time factor. Making the coupling cells coaxial leads to a risk of power-flow phase shift that needs to be stabilized by the cell's geometry, as in the coupling cell between K4 and L1 in Figure 1, which adds unnecessary complexity. It is easier to minimize the cell's transit time factor which is done through using a specific separation of the coupling cell's nose cones, which can be found numerically.

We can estimate the gap between the nose cones that will minimize the transit time factor. Using Warnecke and Guenard's expression [9] for the cavity fields that a beam sees, the transit time factor scales as J0(βed/2) where we are defining βe =ω/cβb, βb is the beam's velocity normalized to the speed of light, and d is the nose cone separation. This term can be made arbitrarily small by adjusting d so βed/2 approaches a zero of the J0 Bessel function. This occurs for a gap of about 2 cm at about 3 GHz. After minimizing the transit time factors of the coupling cells, there are only two competing modes because oscillations from higher frequency modes can be eliminated with a large enough beam-pipe radius so they are not cut off.

The basic design philosophy is based on two requirements, the first is to maintain a π phase variation between cavities K1, K2, and K3, and the second is that the gap voltages of K2 and K3 need to be very nearly π/2 out of phase with the harmonic current at those locations to keep the power transfer low. However, a design trick is needed to ensure the gain circuit turns on. The location of K3 is adjusted so the harmonic current there is at a slight decelerating phase of the RF at low RF amplitudes and approaches being π/2 out of phase as the amplitude increases, which ensures a stable operating point. After some iteration of cavity locations and gap amplitudes, we developed the following design with cavity amplitudes of 7.5 kV, 9.94 kV, and 54.7 kV for K1, K2, and K3, respectively, and axial center-to-center separations of 6.2 cm between K1 and K2 and 6.1 cm between K2 and K3. For the nominal operating parameters, the electron beam power exchange is -860 W, -331 W, and 967 W with cavities K1, K2, and K3, respectively, where a negative sign indicates the beam absorbs RF power. This design is stable and the gain section circuit will ring up, as shown in Figure 2. If the gain cavity amplitudes are below the design point, the beam will generate excess power, increasing the cavity amplitudes. If the gain cavity amplitudes are above, the beam will extract power from the cavities, decreasing their amplitudes.

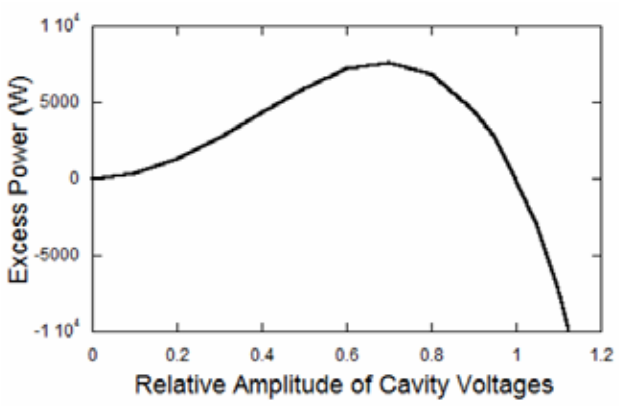

Figure 2. Excess RF power generated by the cavity locations and gap voltage ratios for the type (2) klynac design, as a function of cavity voltage amplitudes relative to those in the text.

Fabrication and testing: We fabricated the klynac shown in Figure 1. This device was cold tested, identifying the resonant modes and the relative field amplitudes as shown in Figure 3. Proof-of-concept tests have started on the klynac. The experimental set up is shown in Figure 4, with the electron gun and vacuum system installed. Due to the geometry and the location of the vacuum pump, the cathode heater is used to help bake out the device (to achieve a better vacuum). As the vacuum improves, we have been able to test the klynac at successively higher voltages. So far, the maximum voltage has been 45 kV, which is about the threshold for building up fields in the klystron gain section. A typical oscilloscope trace of the fields in the klystron gain section is shown in Figure 5, indicating the device has achieved stable oscillations.

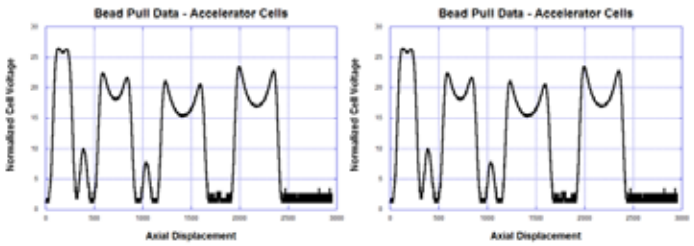

Figure 3. Cold test data. Field amplitudes in the klystron section (left) and in the linac section (right).

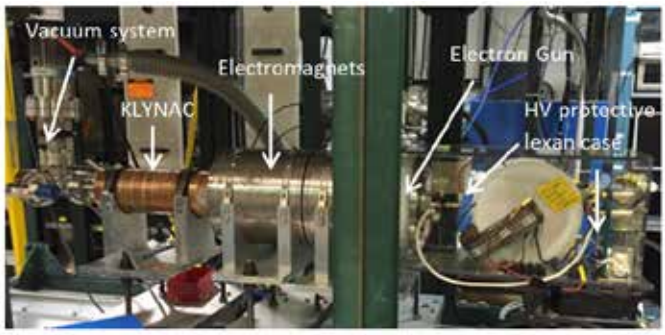

Figure 4. Current 8-cell KLYNAC under test at LANL. The 50-kV, 10-A electron gun is about 20-cm long and the KLYNAC structure is about 60-cm long. Two electromagnets confine the electron beam in the klystron section. A solid-state, diode-directed MARX pulser is used to drive the electron gun.

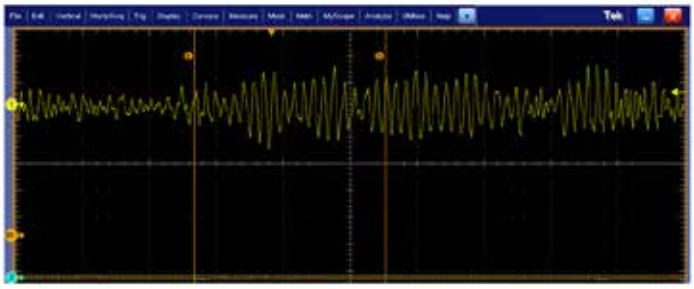

Figure 5. Typical test results – field in the klystron gain sections. The gain section is oscillating.

Impact on National Missions

A compact, man-portable X-ray source is a priority for both NNSA's Office of Defense Nuclear Nonproliferation Research and Development (DNN R&D) Nuclear Weapons and Material Security (WMS) Team and for The Domestic Nuclear Detection Office (DNDO) of the Department of Homeland Security. DNDO recently submitted a call for proposals (HSHQDN-16-R-0003) that includes a requirement for development of accelerators with applications to homeland security. We believe this technology is ideal for that application.

References

1. Schriber, S. O.. Klystron-accelerator system. 1978. Canadian patent 1040309.

2. Xie, J. L.. A combined source of electron bunches and microwave power. 2003. Review of Scientific Instruments. 74: 5053.

3. Potter, J. M.. The klynac, an integrated klystron and linear accelerator. 2013. AIP Conference Proceedings (CAARI Aug. 5-10, 2012). 1525: 178.

4. Gao, J.. Analytic formula for the coupling coefficient beta of a cavity-waveguide coupled system. 1992. Nuclear Instruments and Methods Physics Research. A309: 5.

5. Wangler, T.. Design of coupled-cavity linacs. 1998. In RF linear accelerators. By Wangler, T.. , p. 119. New York: John Wiley and Sons.

6. Gilmour, A. S.. Klystrons, traveling-wave tubes, magnetrons, crossed-field amplifiers, and gyrotrons. 2011.

7. Marcum, J.. Interchange of energy between an electron beam and an oscillating electric field. 1946. Journal of Applied Physics. 17: 4.

8. Carlsten, B. E., and W. B. Haynes. Discrete monotron oscillator. 1996. IEEE Transactions on Plasma Science. 24: 249.

9. Warnecke, R., and P. Guenard. Les tube electroniques a commande par modulation de vitese. 1951.

Publications

Carlsten, B. E., and K. E. Nichols. Bi-resonant klynac. To appear in Physical Review Accelerators and Beams.

Multi-GeV Electron Radiography

Fesseha G. Mariam
20140591ER

Abstract

Transmission electron microscopy was pioneered in the early 1900s, providing the first electron images through very thin samples [1,2]. This early work was followed by decades of technical advancement culminating in the award of the Nobel Prize in physics in 1986 for the development of the scanning electron microscope. The benefits of using electrons over photons for microscopy are two-fold. First, the de Broglie wavelength of energetic electrons is significantly shorter, which enables higher resolution microscopy and, second, the penetrating capability of the electron provides the ability to image structure within opaque materials. Traditional Electron Microscopy, however, is limited to ultra-thin samples (~100nm to 500 nm thick, depending on the accelerating voltage) and typically applied to nearly static samples. Recently, >10GeV electrons provided by the Stanford Linear Accelerator Center (SLAC) were used to demonstrate the extension of the capabilities of transmission electron microscopy to this very high energy regime. Our new technique, called Transmission High Energy Electron Microscopy or THEEM, provides two new capabilities to electron microscopy. First multi-GeV electrons are much more penetrating than lower energy (keV) electrons, thus enabling imaging through significantly thicker samples. Second, the accelerating mode of the radio-frequency linear accelerator provides very fast exposures. These short exposures, down to 1 picosecond, are ideally suited for flash radiography to study the evolution of material processes under extreme dynamic loading. Initial investigations looking at static and quasi-dynamic objects have been performed to demonstrate this type of measurement for future applications to study dynamic measurements.

Background and Research Objectives

The technique of transmission high-energy electron microscopy (THEEM), which uses electrons of greater than 10 GeV, is more similar to proton radiography [3] than standard Transmission Electron Microscopy (TEM). TEM uses a combination of electrostatic and magnetic lenses to form images. Because of the large electron momentum employed in THEEM imaging, electrostatic lenses cannot be used to form the electron images and magnetic lenses are required to focus the high-energy electron beam. Electron interactions with materials are similar to proton interactions, but because of the small mass of the electron at >10GeV, ultra-relativistic bremsstrahlung is the dominant energy loss mechanism. This energy loss within the material, which is relatively large, can result in image degradation through chromatic aberrations as the electrons are focused by the magnetic fields of the lens system. One of the major goals of these measurements was to study the effect of this large energy loss mechanism on image formation.

Scientific Approach and Accomplishments

For these demonstration experiments a simple magnifying lens system was formed from four magnetic quadrupoles in a Russian quadruplet configuration and deployed in the End Station A Test Beam (ESTB) [4] at the Stanford Linear Accelerator Center. Picosecond length electron beam pulses, at variable energies ranging from 4 GeV to 16 GeV, are delivered to the ESTB at a fixed rate of 5 Hz. Each pulse consists of about 1.6 x 109 electrons.

The four quadrupole magnets were located close to the object to be imaged and the image was formed at a distance of 26.55 m, providing an image magnification of about 11. The layout of the imaging system is shown in Figure 1.

The magnetic imaging system was designed utilizing the beam optics code COSY [5] to determine the optimal values of the quadrupole strengths, the quadrupole separations and the location of the collimators. The diffuser, located at 36 m upstream of the object location, consists of an Al foil a few microns thick. The incident electron beam, with a 0.1 mm spot size, scatters in the Al and diverges to a spot roughly 1.5 mm (rms) width at the

object location. This enlarged beam provides illumination over the 6 x 6 mm field of view of the imaging lens. The distance from the diffuser to the object plane determines the location of the so called Fourier plane of the imaging system, where electrons scattered in the object are sorted into radial positions proportional to the angle of scattering in the object. A collimator (aperture restriction) of a given size placed at this Fourier plane therefore acts as a filter for electrons scattered outside the collimator aperture, while those scattered through smaller angles continue on to the detector at the image plane where they are focused to form a magnified image. This is illustrated in Figure 2, which is beam-optic code (COSY) rendition of the trajectories of electrons through the imaging lens after multiple Coulomb scattering in an object at the object location. Because multi-GeV electrons are highly penetrating, a collimator at the Fourier plane is essential to generate image contrast. The size of the collimator opening thus controls image contrast; it also affects the resolution.

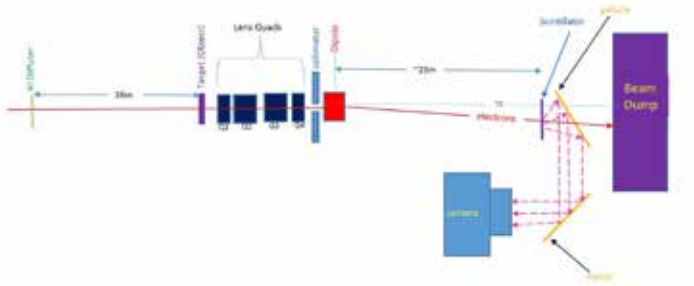

Figure 1. Schematic diagram of the experimental setup. The diffuser is used to expand the beam spot size at the object. The collimator is a set of horizontal and vertical jaws placed symmetrically about the Fourier plane. The dipole is used to separate the gammas from the electrons. The scintillator a 10 x 10 cm^2 piece of columnar ScI convertor. The quadrupoles, Q1-Q4, are tuned to provide a sharp image at the scintillator. The light from the scintillator is directed to two cameras. Only a simplified version of the actual optical train is shown in this diagram.

A 10 cm by 10 cm rectangular piece of columnar CsI scintillator at the image plane was placed at the image location. Electrons interacting with the CsI scintillator deposit a small amount of energy, which is promptly converted to photons by the scintillator. A pellicle and two turning mirrors placed downstream of the scintillator were used to reflect the light to a pair of high-speed cameras, with exposures synchronized to each accelerator pulse.

Simulations performed during experimental planning indicated that bremsstrahlung gammas produced by the electrons interacting with the diffuser and the object would constitute a serious source of background to the image – showing up as a bright spot at the center of the radiographic image formed by the electrons. This was later confirmed by measurements early in the experiment. To mitigate this effect, we installed a small dipole downstream of the collimator (see figure 1), which deflected the transmitted electrons, separating the image formed by the electrons from the bremsstrahlung gammas. This is illustrated in the images of a setscrew in Figure 3. Left uncorrected, the bremsstrahlung photons superimposed on the images, would have led to intractable complications in the measurement of system resolution and transmission.

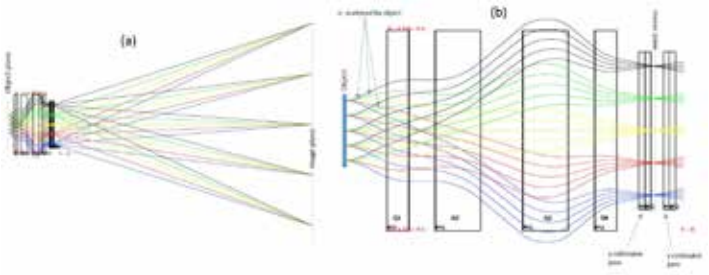

Figure 2. COSY rendition of the magnetic imaging lens. (a) The overall lens system from object plane to Image plane. (b) A zoomed section of (a) from the object to the Fourier plane. The positions of the collimator jaws are shown. Electron trajectories of the same color represent scattering by the same angle. Regardless of their spatial origin at the object, at the Fourier plane, all rays are imaged onto radial positions proportional to the scattering angle.

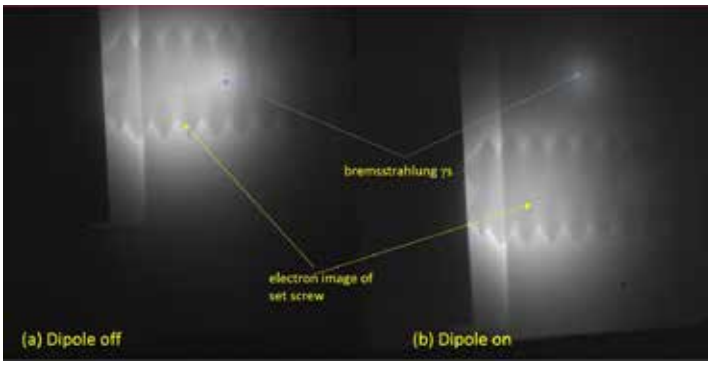

Figure 3. Radiography of a set screw without (a) and with (b) dipole on. The dipole of strength ~0.07 Tm, deflects the 13.89 GeV electron beam by 28.4 mm at the image plane.

As discussed earlier, two fast-gated cameras were used to capture the radiographic images formed by the transmitted electrons. The optical layout from the scintillator to one of the two cameras is schematically shown in Figure 1. The lenses on both cameras are focused at the scintillator plane. While one of the cameras (DIMAX) was set to view all the available scintillator area of about 10 cm by 10 cm, the other (EDGE) was fitted with a zoom lens with much reduced field of view covering only the central ~3 cm by 3 cm portion of the scintillator. Most of the data in the transmission studies were collected using the DIMAX while most the resolution data was collected using the higher

resolution EDGE camera. Standard optical patterns such as the Air Force test pattern (1951 USAF resolution test chart) were used to establish the spatial calibration and also to measure the inherent resolution of the two camera systems.

The inherent resolution of the cameras, including that due to the optical train, the camera lenses and sensors was measured from fitting the edge transition in the images of a USAF resolution test chart.

In charged particle radiography using magnetic lenses, it is well established that the resolution is limited by chromatic blur [3]. When charged particles pass through material located at the object location (OL), the particles undergo multiple Coulomb scattering and energy loss. Charged particles passing through objects with complicated geometry will experience differing amounts of mean energy loss and straggling, depending on the amount of material (areal density) they encounter. The imaging magnetic lens, on the other hand, can only be set to focus particles of a given energy at the image location (IL). An important property of such imaging magnetic lenses is the chromatic length, which is a measure of the attainable system resolution.

It is generally accepted practice to use the lineout of the step in transmission across the boundary of a straight edge to measure system resolution. The resulting transmission profile (also known as the edge spread function – ESF), is the integral of the point spread function (PSF) along the lineout. If one assumes that the system resolution PSF is Gaussian, the resulting ESF can be modeled in a straightforward manner, allowing us to extract the system resolution from an image of this step.

The system resolution from the fits is determined to be 12 microns. Note that this is the overall resolution with contributions from the magnetic lens and from the optical train. As discussed earlier, the latter includes the optical elements (turning mirrors and camera lens) and the camera itself.

Similar analysis using features of the AFTP yield 9 microns for the intrinsic resolution of the optical train (OT) including the camera. Assuming that the overall resolution is a quadratic sum of the contributions, the resolution of the magnetic lens is found to be 8 microns.

In the final two days of the allotted experimental time, we installed induction heaters and chillers to melt and freeze samples of metal alloys and monitor the formation of metallic crystalline aggregates. Radiographic images were taken at a rate of 5Hz during the melting and freezing phases of these materials. These type of dynamic experiments, which are relevant to the understanding of additive manufacturing, and metallurgical casting processes, have been performed using proton radiography, x-rays and synchrotron radiation at various spatial and temporal scales [6,7].

For these demonstration experiments using THEEM, solid samples were placed in thin-walled boron nitride crucibles and melted by means of induction coils. Once melted, a sample was held in its molten state for a specified length of time before initiating the freezing process using water chillers. It is during this process, that one observes the temporal evolution of metal segregation and formation of crystalline structures. A sampling of the resulting THEEM radiographs is shown in Figures 4 and 5. All the data was collected with the high resolution Edge camera.

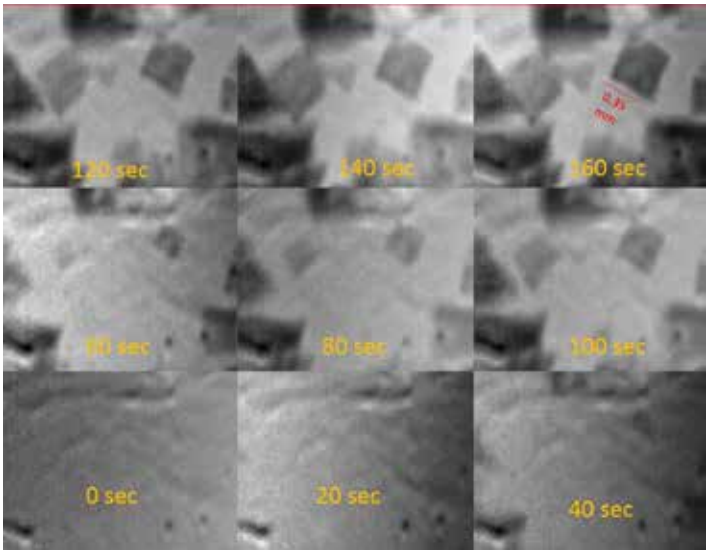

Figure 4. Temporal evolution of BiSn alloy during freezing. At "0 sec" the sample is mostly in molten phase. As the sample cools down Bi rich crystals form. The pictures shown here cover a span of 160 seconds. The spatial scale is shown by the diamond shaped Bi-rich feature which is about 0.35 mm wide.

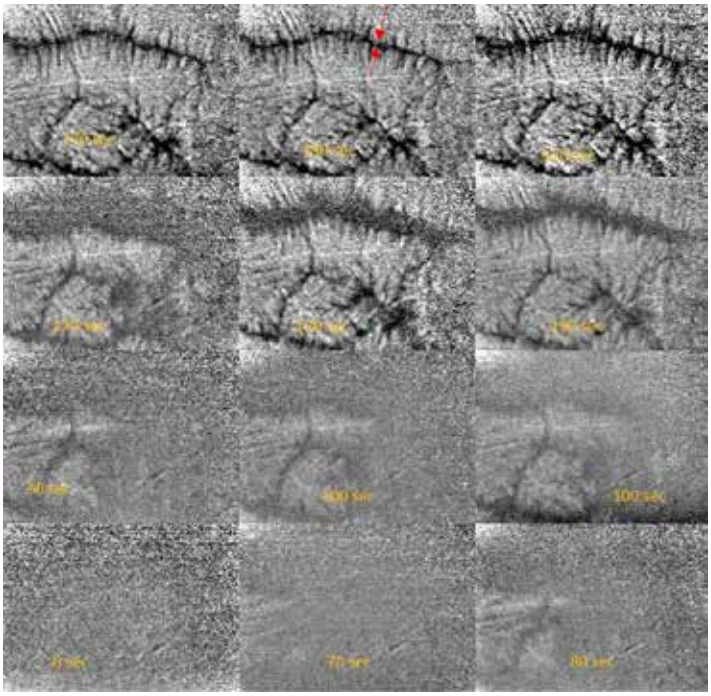

Figure 5. Observation of dendrite growth in AlAg alloy using THEEM. The images shown are over a span of 320 seconds starting from the onset of freezing. The spiny feature at 320 sec is about 20 microns wide.

We have demonstrated that Transmission High Energy Electron Microscopy (THEEM) utilizing GeV energy electron beams is a viable radiographic tool for the study of thin samples. We have also demonstrated that relatively slow dynamic processes, such as melting and freezing of alloys, can be studied using THEEM. As has been shown, bremsstrahlung, produced by the interaction of the ultra-relativistic electrons with the diffuser and/or the target materials, constitutes the main source of background in THEEM. We have so far analyzed only a small portion of the available data. In particular, an extensive set of data to study the dependence of transmission on the size of the collimator at the Fourier plane is yet to be analyzed fully. Coupled with realistic simulations, this will lead to the development of analytic tools for the evaluation of areal densities from measured transmission in THEEM.

There are several publications that can come out of this LDRD project. We have already started drafting a paper that will soon be submitted to APL for publication. We also intend presentations at SCCM (Shock Compression of Condensed Matter) and PAC in 2017 and at the next heavy ion fusion conference in 2018. Each of these will be accompanied by conference proceedings. These are the conference series that have been following this effort. There is also the possibility of presenting the results at the next Femtosecond Electron Imaging and Spectroscopy (FEIS) workshop. There may also be a paper devoted to the comparison of GEANT4 simulations to data. All these, including ongoing data analysis efforts, will depend on available support.

Impact on National Mission

Preliminary results from this project indicate the promise for high resolution imaging with high-energy electrons, proving the possibility of fielding new diagnostics at existing and future x-ray free-electron laser facilities which use high energy electrons to produce the secondary x-ray beams. Supplementing with this new technique, experimenters can greatly extend the scientific reach of these state-of-the-art facilities by making real-time, precision measurements of density variation in the types of thin samples traditionally studied at XFEL, a clear gap in capability of x-ray radiography alone.

References

1. Pietzsch, Joachim. Perspectives: Life through a lens. 1986. In Bell System Technical Journal.

2. Williams, D. B.. Transmission Electron Microscopy. 1996. In Transmission Electron Microscopy. By Carter, B. C..

3. Mottershead, T. C.. Magnetic Optics for Proton Radiography. 1998. Vol. 1397-9.

4. Hast, C.. A New Test Beam Facility at SLAC. 2012. SLAC-PUB-14602.

5. Berz, M.. COSY INFINITY Version 8.1. 2001. Michigan State University, MSUHEP-20703.

6. Clarke, A.J.. Proton Radiography Peers into Metal Solidification. 2013. 3.

7. McKeown, J.T.. Time Resolved in-situ Measurements During Rapid Solidification: Experimental Insight for Additive Manufacturing. 2016. 68.

Publications

Multi-GeV Electron Radiography. APL.

Merrill, F.. Imaging with penetrating radiation for the study of small dynamic physical processes. 2014. Laser and Particle Beams. : 1.

Nuclear Physics Techniques to Significantly Advance Cancer Imaging and Treatment

Dale Tupa
20160549ER

Abstract

This project worked towards a capability to image tumors less than 2 mm in diameter with proton radiography (PR). This successful research resulted in important tools and calculations for the application of PR and magnetic resonance imaging (MRI), unique capabilities developed at Los Alamos National Lab (LANL). Ultimately, a future goal is to demonstrate the feasibility of real-time imaging of cancer patients during proton beam therapy (PBT) treatments. Our work at the Los Alamos Proton Radiography Facility (pRad) [1] showed that image-guided PBT using high-energy protons can increase tumor-targeting accuracy by an order of magnitude over current PBT treatments. This will be made possible through targeted [2] contrast agents to which both PR and MRI are sensitive, allowing for secondary verification. The ability to make high resolution images to guide high-energy PBT in real time will enable the treatment of tumors much smaller than those currently treatable by PBT and enable PBT treatment of inaccessible tumors in the vicinity of crucial biological structures by minimizing the dose deposited in nearby sensitive tissues. With Director's Reserve funding, we showed that adequate contrast for PR may be achievable in a relevant tumor phantom, with standard labeling methods.

Background and Research Objectives

Proton therapy [3] is now a well-established method in treatment of various diseases, with 24 facilities in the US and 11 more in development [4]. It currently uses protons of energies 60-250 MeV to exploit the Bragg peak [3, 5] to deposit the radiation dose at a targeted depth. However, the maximum dose is delivered over a range of about a cm (Figure 1)[5]. We have modeled a proton beam passing through material to show how the beam is also dispersed in the transverse direction by multiple scattering, greatly increasing the transverse profile of the beam (Figure 2) [6]. If a patient is instead treated with higher energy protons, in the plateau of the absorption curve seen in Figure 1 rather than at the Bragg peak, the diameter of the relativistic proton beam remains small because of drastically-reduced lateral scattering. This dramatically improves the precision compared to all other radiotherapy modalities. Because of these advantages, relativistic protons are proposed for radiosurgery in Berkeley and in use at PNPI. In contrast with Bragg peak therapy, cancers will be treated with radiation introduced from various directions intersecting in the tumor to reduce the relative dose in healthy tissue, which necessitates moving the patient, introducing uncertainty in the target location as soft tissue moves. To truly take advantage of the increased precision afforded by a higher-energy beam, a method of targeting the proton beam in real time during therapy is needed. Fortunately, PR can exploit the same proton beam for imaging.

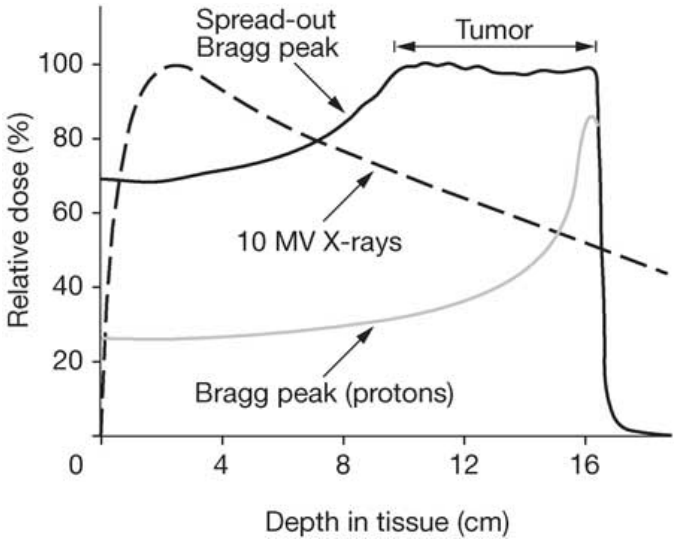

Figure 1. The relative dose deposited in tissue from radiation therapy. For dose deposited near the Bragg peak from a single treatment is distributed over a depth of ~ 1cm.

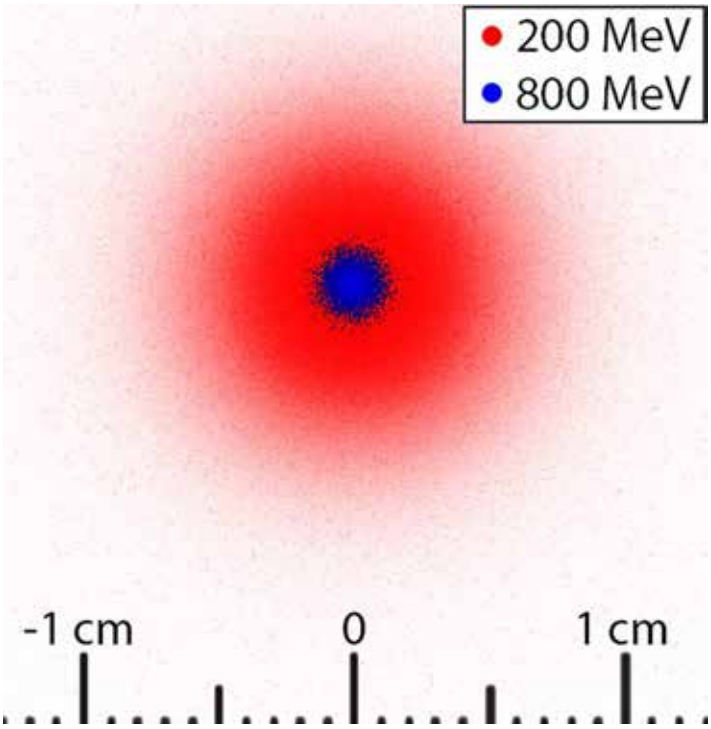

Figure 2. Monte-Carlo [6] of the spatial profile of 200 MeV and 800 MeV proton beams after traversing 20 cm tissue-equivalent plastic.

Modern PR, invented at LANL, employs a magnetic lens after the object, giving unprecedented spatial resolution with high-energy protons. Our recent experiments [7] generated images of sufficient resolution to guide a PBT beam (Figure 3). But normal and cancerous tissues are very similar in density; they do not produce enough contrast to guide high-energy protons to sub-millimeter precision. To increase the density of cancerous tissue relative to healthy tissue, we propose to label the tumor with a contrast agent of dense material, such as gold nanoparticles, using the same technology as for targeted drug delivery. Our team has experience with these targeted contrast agents [8], which are commonly used in medical applications [9, 10]. A targeted contrast agent consists of a nanoparticle core within a molecule containing antibodies specific to a cancer cell receptor. With this LDRD Director's Reserve funding, we have made phantoms of tumors treated with targeted contrast agents, showing that we have the capability to design and safely craft tissue phantoms with agarose gel and gold nanoparticles. We have also made proton radiographs of these preliminary phantoms. This demonstrates the techniques we will need to make a systematic study of the proton radiography of tissue phantoms with features of typical tumor sizes and labeling concentrations. Our studies will determine if we have sufficient radiographic contrast to distinguish small tumors from healthy tissue with resolution good enough to guide PBT at an acceptable proton dose.

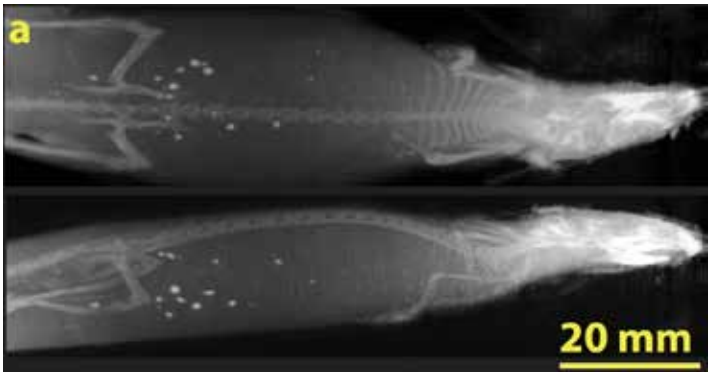

Figure 3. A proton radiograph of a preserved mouse made at the Los Alamos Proton Radiography Facility.

PR is typically used to image components of interest to national security at sub-microsecond time resolution in explosively-driven experiments. Imaging very thin targets (where "thickness" is a product of the density of the object and its physical length) and systems with very low contrast, such as tumors enhanced with targeted contrast agents, requires a different radiographic techniques and a modified configuration of the pRad accelerator beam line. We have modeled the proton beam optics at pRad and then optimized the beamline configurations to best image these thin, low-contrast systems. We have submitted our results for publication and expect that these studies will allow us to improve pRad studies of phenomena central to the LANL core mission, such a shock-induced ejecta, shocks in single-component and mixed gases, and thin-target experiments such as alloy solidification and Pu casting experiments.

Our ultimate goal is to demonstrate with a live mouse model that a tumor can be tagged with a targeted contrast agent and produce a PR image of the tagged tumor. The image will be of sufficient resolution to guide PBT and at a dose acceptable for the safety of a patient. Work with live animals requires careful planning in advance. During this 5-month funding period, we have met with our representative on the LANL Live Animal Handling Committee and formed a collaboration with researchers at the University of New Mexico (UNM) Keck-UNM Small-Animal Imaging Resource (KUSAIR), who will provide animals and animal handling services.

Scientific Approach and Accomplishments

We have used additive machining techniques to construct a framework for biological phantoms based on agarose gel. The gel mimics the density of tissue and differing concentrations of gold nanoparticles were incorporated into tumor phantoms embedded in the gel. We then made proton radiographs of this first-generation phantom, completing a demonstration of all the laboratory techniques and safety procedures required for a full, systematic study of

the resolution of pRad in the thickness and contrast regime expected for imaging tumors tagged with contrast agents. A photo and diagram of the phantom and a radiographic image are shown in Figure 4. When radiographing these phantoms, we took dosimetric data to evaluate the radiation dose that would be incurred during PR. Analysis of the images is under way in order to design a detailed, quantitative experimental run, for which we will incorporate our experience with the first-generation phantom to design an improved series of phantoms.

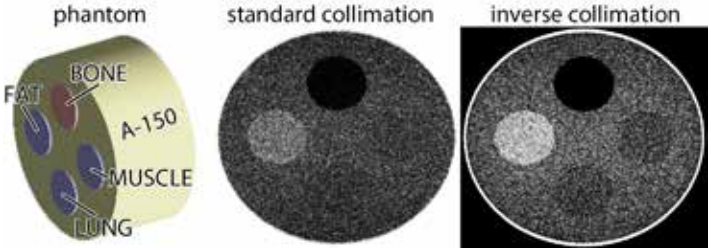

Figure 4. A cylindrical phantom of A-150 tissue modeled in Geant4, with inserts of bone, muscle, fat and lung tissue. A comparison of the projected radiographs with collimation and with inverse collimation shows increased contrast for soft tissue.

We have modeled the pRad proton transport beam line with the particle transport code Geant4 [11] in order to evaluate the current beam line and for biological imaging applications, and to start designing modifications that will improve the quality of radiographs in this regime. Results of the modeling are shown in Figure 5, where an inverse-collimation technique increases the contrast in PR for relevant tissues. Our results have been submitted for publication and are in the revision stage.

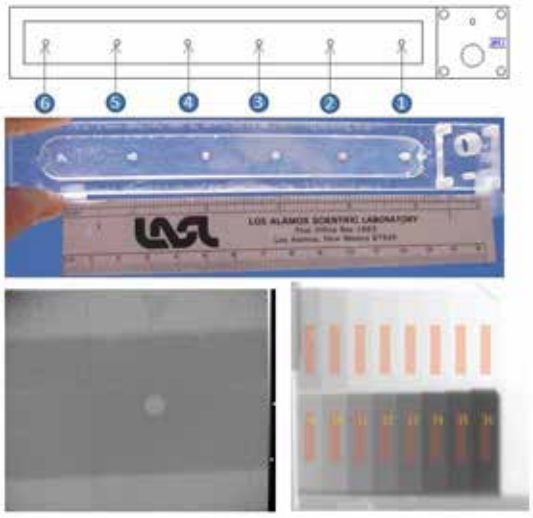

Figure 5. Proton Radiographs of phantoms to evaluate resolution for bioimaging. (Upper) Schematic of an additively-manufactured holder for biological phantoms made of agarose gel with and without inclusions of gold nanoparticles. (Center) A photo of the phantoms. (Lower left) A proton radiograph of one of the phantoms. (Lower right) A proton radigraph of a step wedge phantom of tissue-equivalent plastic to quantitatively evaluate the density resolution obtained by PR in this density regime.

This LDRD Director's Reserve funding allowed us to conduct the necessary calculations on a preserved specimen to support future live animal measurements at pRad; a future goal is to obtain compelling data with an image of a tumor in a live animal model. Our work with our KUSAiR collaborators has provided us with a defined set of requirements in order for them to provide animal handling services within the scope of their approvals. Our calculations also allowed us to evaluate the type and level of activation we might expect in the course of radiography, and we have obtained a preserved specimen to measure this experimentally.

Impact on National Missions

This reserve project brings numerous benefits to LANL. It further improves the utility of pRad for important LANL mission applications by developing methods to detect low-contrast features in low-Z materials such as high explosives, jets, shocked gases, ejecta, and materials undergoing phase transitions. It also continues our leadership in unconventional MRI and multi-modality imaging methods and analysis via new diagnostics for medicine [12] and materials.

References

1. The National Association for Proton Therapy: Proton therapy centers.

2. King, N. S. P., E. Ables, K. Adams, K. R. Alrick, J. F. Amann, S. Balzar, P. D. Barnes, M. L. Crow, S. B. Cushing, J. C. Eddleman, T. T. Fife, P. Flores, D. Fujino, R. A. Gallegos, N. T. Gray, E. P. Hartouni, G. E. Hogan, V. H. Holmes, S. A. Jaramillo, J. N. Knudsson, R. K. London, R. R. Lopez, T. E. McDonald, J. B. McClelland, F. E. Merrill, K. B. Morley, C. L. Morris, F. J. Naivar, E. L. Parker, H. S. Park, P. D. Pazuchanics, C. Pillai, C. M. Riedel, J. S. Sarracino, F. E. Shelley, H. L. Stacy, B. E. Takala, R. Thompson, H. E. Tucker, G. J. Yates, H. J. Ziock, and J. D. Zumbro. An 800-MeV proton radiography facility for dynamic experiments. 1999. NUCLEAR INSTRUMENTS & METHODS IN PHYSICS RESEARCH SECTION A-ACCELERATORS SPECTROMETERS DETECTORS AND ASSOCIATED EQUIPMENT. 424 (1): 84.

3. NIH: national Cancer Institute Targeted Therapy Factsheet. 2016. http://www.cancer.gov/cancertopics/factsheet/Therapy/targeted.

4. Tommasino, F., and M. Durante. Proton radiobiology. 2015. Cancers. 1 (7): 353.

5. Yock, T. I., and N. J. Tarbell. Technology insight: proton beam radiotherapy for treatment in pediatric brain tumors (vol 1, pg 97, 2004). 2005. NATURE CLINICAL PRACTICE ONCOLOGY. 2 (4): 222.

6. Freeman, M. S., Allison, Espinoza, J. J. Goett III, Hogan, Hollander, Kwiatkowski, Lopez, Mariam, Martinez, Medina, Medina, F. E. Merrill, Morley, Morris, Murray, Nedrow, Saunders, Schurman, Sisneros, A. m. y. Tainter, Trouw, Tupa, Tybo, and Wilde. 800-MeV magnetic-focused flash proton radiography for high-contrast imaging of low-density biologically-relevant targets using an inverse-scatter collimator. 2016. MEDICAL IMAGING 2016: PHYSICS OF MEDICAL IMAGING. 9783.

7. Prall, , Durante, Berger, Przybyla, Graeff, P. M. Lang, LaTessa, Shestov, Simoniello, Danly, Mariam, Merrill, Nedrow, Wilde, and Varentsov. High-energy proton imaging for biomedical applications. 2016. SCIENTIFIC REPORTS. 6.

8. Karan, N. S., A. M. Keller, Sampat, Roslyak, Arefin, C. J. Hanson, J. L. Casson, Desireddy, Ghosh, Piryatinski, Iyer, H. a. n. Htoon, A. V. Malko, and J. A. Hollingsworth. Plasmonic giant quantum dots: hybrid nanostructures for truly simultaneous optical imaging, photothermal effect and thermometry. 2015. CHEMICAL SCIENCE. 6 (4): 2224.

9. Tiwari, P. M., Vig, V. A. Dennis, and S. R. Singh. Functionalized Gold Nanoparticles and Their Biomedical Applications. 2011. NANOMATERIALS. 1 (1): 31.

10. Hathaway, H. J., K. S. Butler, N. L. Adolphi, D. M. Lovato, Belfon, Fegan, T. C. Monson, J. E. Trujillo, T. E. Tessier, H. C. Bryant, D. L. Huber, R. S. Larson, and E. R. Flynn. Detection of breast cancer cells using targeted magnetic nanoparticles and ultra-sensitive magnetic field sensors. 2011. BREAST CANCER RESEARCH. 13 (5).

11. Agostinelli, S., J. Allison, K. Amako, J. Apostolakis, H. Araujo, P. Arce, M. Asai, D. Axen, S. Banerjee, G. Barrand, F. Behner, L. Bellagamba, J. Boudreau, L. Broglia, A. Brunengo, H. Burkhardt, S. Chauvie, J. Chuma, R. Chytracek, G. Cooperman, G. Cosmo, P. Degtyarenko, A. Dell'Acqua, G. Depaola, D. Dietrich, R. Enami, A. Feliciello, C. Ferguson, H. Fesefeldt, G. Folger, F. Foppiano, A. Forti, S. Garelli, S. Giani, R. Giannitrapani, D. Gibin, J. J. G. Cadenas, I. Gonzalez, G. G. Abril, G. Greeniaus, W. Greiner, V. Grichine, A. Grossheim, S. Guatelli, P. Gumplinger, R. Hamatsu, K. Hashimoto, H. Hasui, A. Heikkinen, A. Howard, V. Ivanchenko, A. Johnson, F. W. Jones, J. Kallenbach, N. Kanaya, M. Kawabata, Y. Kawabata, M. Kawaguti, S. Kelner, P. Kent, A. Kimura, T. Kodama, R. Kokoulin, M. Kossov, H. Kurashige, E. Lamanna, T. Lampen, V. Lara, V. Lefebure, F. Lei, M. Liendl, W. Lockman, F. Longo, S. Magni, M. Maire, E. Medernach, K. Minamimoto, P. M. de Freitas, Y. Morita, K. Murakami, M. Nagamatu, R. Nartallo, P. Nieminen, T. Nishimura, K. Ohtsubo, M. Okamura, S. O'Neale, Y. Oohata, K. Paech, J. Perl, A. Pfeiffer, M. G. Pia, F. Ranjard, A. Rybin, S. Sadilov, E. Di Salvo, G. Santin, T. Sasaki, N. Savvas, Y. Sawada, S. Scherer, S. Seil, V. Sirotenko, D. Smith, N. Starkov, H. Stoecker, J. Sulkimo, M. Takahata, S. Tanaka, E. Tcherniaev, E. S. Tehrani, M. Tropeano, P. Truscott, H. Uno, L. Urban, P. Urban, M. Verderi, A. Walkden, W. Wander, H. Weber, J. P. Wellisch, T. Wenaus, D. C. Williams, D. Wright, T. Yamada, H. Yoshida, and D. Zschiesche. GEANT4-a simulation toolkit. 2003. NUCLEAR INSTRUMENTS & METHODS IN PHYSICS RESEARCH SECTION A-ACCELERATORS SPECTROMETERS DETECTORS AND ASSOCIATED EQUIPMENT. 506 (3): 250.

12. Matlashov, , P. e. r. Magnelind, Sandin, Espy, Anderson, and Mukundan. SQUID Instrumentation for Early Cancer Diagnostics Combining SQUID-Based Ultra-Low Field MRI and Superparamagnetic Relaxation. 2013. In 2013 IEEE 14TH INTERNATIONAL SUPERCONDUCTIVE ELECTRONICS CONFERENCE (ISEC).

Publications

Freeman, M. S., J. Allison, C. Espinoza, J. J. Goett, G. Hogan, B. Hollander, K. Kwiatkowski, J. D. Lopez, F. G. Mariam, M. Martinez, J. Medina, P. Medina, F. Merrill, D. Morley, C. Morris, M. M. Murray, P. Nedrow, A. Saunders, T. Schurman, T. Sisneros, A. Tainter, F. Trouw, D. Tupa, J. Tybo, and C. Wilde. 800-MeV magnetic-focused flash proton radiography for high-contrast imaging of low-density biologically-relevant targets using an inverse-scatter collimator . 2016. In Medical Imaging 2016: Physics of Medical Imaging. (San Diego, February 27, 2016). Vol. 9783, p. 97831X. San Diego, CA: SPIE.

Prall, , Durante, Berger, Przybyla, Graeff, P. M. Lang, LaTessa, Shestov, Simoniello, Danly, Mariam, Merrill, Nedrow, Wilde, and Varentsov. High-energy proton imaging for biomedical applications. 2016. SCIENTIFIC REPORTS. 6.

X-Ray Time Domain Astronomy

Richard M. Kippen
20160661ER

Abstract

This LDRD Reserve project successfully allowed us to define hardware and software instrumentation designs applicable to future space-based imaging X-ray astronomy telescopes. Specifically, we investigated: (1) design of data processing electronics hardware for a wide-field X-ray imager; (2) flight firmware and software to enable rapid, on-board source identification and localization, and overall instrument operation.

Background and Research Objectives

In early 2016 we began to investigate instrument concepts for a space-based X-ray Wide Field Imager (WFI) based on "Lobster-eye" optics, ideally hosted on the International Space Station (ISS) or a free-flying satellite in low earth orbit. The prime scientific driver is to capture and precisely localize X-ray emission from Gravitational Wave (GW) events as the ground-based LIGO/VIRGO GW observatories reach their full sensitivity. This process identified the need for a feasibility study in two important gap areas: (1) WFI X-ray event processing electronics and firmware ("event extractor") and (2) instrument-level data processing electronics and flight software to autonomously identify and locate astronomical X-ray sources. This LDRD Reserve project served to perform these studies, including important investigation of the driving factors related to available X-ray focal plane detectors and expected data throughput needs. The primary goal was to determine which designs could accomplish such a mission. The designs have applicability beyond the one possible mission, with relevance to a range of space-borne sensing problems.

Scientific Approach and Accomplishments

As proposed, the project performed design study work by (1) evaluating key driving requirements and concepts for the event extractor, instrument processor/computer, and related software & firmware and (2) refining and maturing those ideas into a limited, viable set of options. The following is a summary of the resulting designs.

Instrument Processing Electronics Hardware

Early concepts for WFI processing electronics performed X-ray event extraction in a logic box near the X-ray focal plane detectors (charge-coupled devices; CCDs), and then piped resulting event-by-event digital data to a Main Electronics Box (MEB) for further, higher-level processing and analysis (including functions for on-board source identification and localization, which are critical to meeting science requirements). The advantages of this concept were that many of the electronics solutions of the MEB might be procured as semi-custom items. However, it became clear throughout the study that there was no existing solution that sufficed. Furthermore, there remained a need for a fully custom electronics box (the Event Extractor; EE) to process X-ray data coming from the CCD array.

Incorporating Los Alamos expertise and capabilities into the design consideration we identified that a simpler concept could better meet the needs, and that many of the elements of that design were already existing or in development as part of LANL's Joint Architecture Standard — a flexible, nodal electronics architecture being used for future LANL space instrumentation projects. As illustrated in Figure 1, the key design feature is to utilize a high-speed serial link to communicate raw data directly from the CCD array Front End Electronics (FEE) to a re-envisioned MEB. This approach obviates the need for a dedicated EE box. Instead, the event extractor functions are performed within the MEB using an existing LANL Reconfigurable Processor (RP) node and its embedded, high-performance (by space standards) Field Programmable Gate Array (FPGA). This approach reduces complexity, mechanical and electrical design costs, and power. Furthermore, if LANL RP node hardware designs were used, they enable additional flexibility by providing (on-orbit) re-configurable event extraction processing capability. Such capability could allow for modifications

to adapt to conditions that were not anticipated prior to fielding, such as higher-than-expected backgrounds or partially failed components.

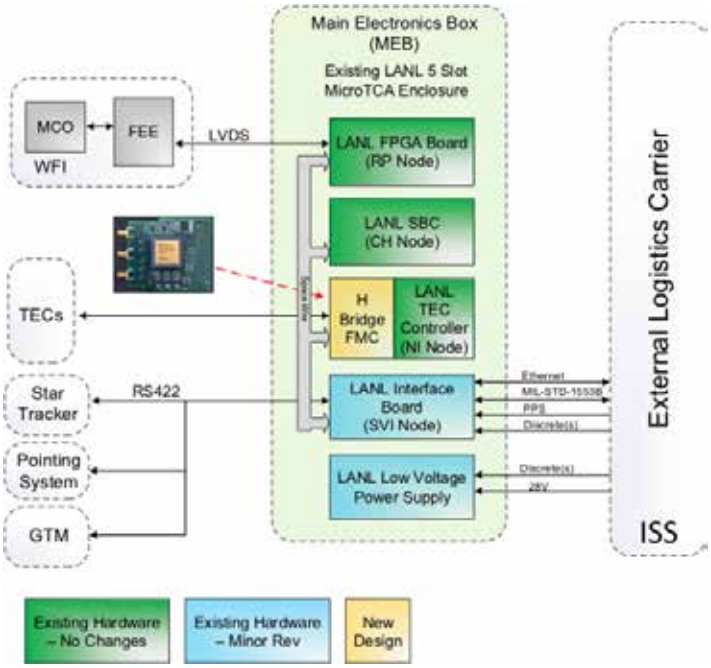

Figure 1. A design that maximizes re-use of LANL JAS modules.

In the final design concept, the MEB employs an existing LANL 5-module electronics box, including an existing configuration and host node module (CH; single board computer) and an existing RP node module (FPGA Board). Software and firmware on the CH and RP modules would be adapted to support specific WFI instrument needs, but the hardware designs could be used as is. The existing LANL Space Vehicle Interface node module (SVI Interface Board) would be modified to support the specific WFI instrument-to-host platform interfaces, but this node was designed for straightforward modification in support of different applications. An existing LANL low-voltage power supply design (LVPS) may or may not be able to be used without revision— further investigation based on a specific host platform characteristics would be needed. In this concept, one new electronics module will be needed, a small FPGA mezzanine card (FMC) that has the high-current bridge and transistors to support pulse width modulated control of the WFI thermal electric coolers (TECs). This would be a relatively small hardware development effort based on similar existing LANL FMC designs.

We considered several variants of this design that could be investigated further based on cost/schedule/performance needs. These include:

- A design that incorporates architecture/functionality shown in Figure 1, but is procured as a semi-custom box from an industrial supplier. We investigated one such supplier (Moog Inc.) and came to the conclusion that cost/schedule were actually worse compared to a LANL-built solution.
- A hybrid design using LANL CH & RP nodes, but with modified mechanics and backplane (or just cables) to support procured TEC and LVPS modules. We concluded this would only make sense if an industrial solution existed for a particular module.

We believe this basic approach in any of its variants could meet the needs of the of a WFI instrument, and is also adaptable to mission variants that might include more than one WFI telescope. The main difference is that larger missions would likely require multiple RP nodes (and possibly an additional CH node). This expandable capability is inherent in the JAS technology approach, and has already been demonstrated in other LANL development activities.

WFI Data Processing Firmware and Software

A fundamental requirement of any WFI-based mission is to autonomously process WFI data to identify and localize new or persistent X-ray sources on the sky. A further requirement is to use this capability to autonomously search the sky for new X-ray sources given a specified search area (such as the location of a gravitational wave source). Such capability has never been demonstrated with a wide field X-ray telescope. The key enabling technologies are the WFI, itself (mounted on slewing gimbal), the electronics processing architecture, and the software & firmware running on the electronics.

In the course of our study, we investigated the following aspects of the software challenge:

- Efficient event extraction from the CCD array into a form useable for on-board source localization. The basic conclusion was that the tremendous processing power of FPGAs was underutilized in early design concepts, and that many aspects of the source identification/localization algorithm could be realized in firmware rather than (slower) software. This trade remained open at the end of our study lacking specific algorithm choices and low-level details of the CCD interface throughput.
- WFI source identification algorithms (i.e., “triggering”
- WFI source localization algorithms
- Mission observations and telemetry management, where the basic conclusion is that existing software from the NASA Swift gamma-ray burst mission would provide a 90% solution as a solid design basis.

Fundamental algorithms for most of these functional aspects are reasonably mature, with the exceptions of (a) and (b). We further investigated these items in the context of the early design concepts. These were used to generate key trades and refined design concepts. For the event extractor functions, we generated a preliminary firmware design schematic and evaluated resource needs that are well within the capabilities of the target FPGA hardware. For the source identification and localization software, we evaluated the early design concept, which is graphically illustrated in Figure 2.

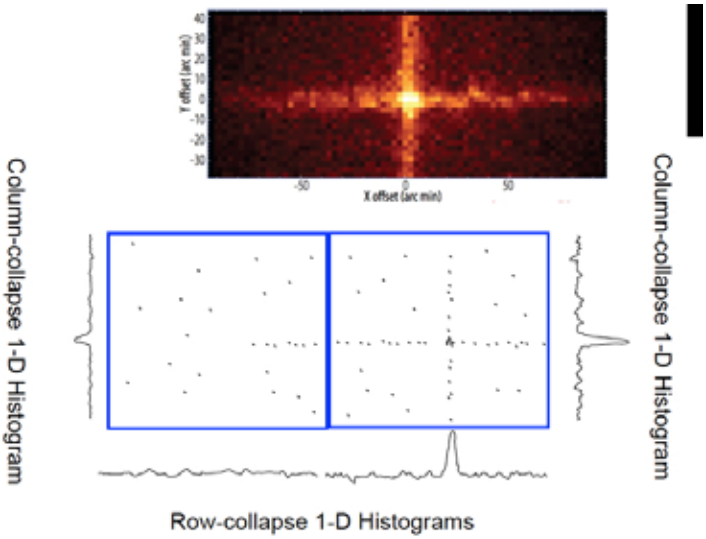

Figure 2. Evaluation of early design concept.

The basic concept for WFI source imaging is to leverage the two-dimensional nature of the Lobster-eye optics point spread function, and reduce the imaging algorithm to a set of two one-dimensional centroiding operations (in several different energy and time windows, simultaneously). We concluded that this approach would work in the target hardware architecture, and further that the architecture affords the possibility of speeding up the imaging process by implementing several of the fundamental operations in firmware rather than software. While this general algorithmic approach is simple and fast, we concluded that information is being lost in the reduced dimensionality, which ultimately limits sensitivity to detect and localize weak sources. Our refined concept would perform source identification and centroiding functions directly in two-dimensional image plane space, thereby retaining full sensitivity and enabling maximum science return. This approach introduces additional computing complexity to the algorithm, but we evaluate that this complexity is within the capacity of the target processing hardware, particularly if commonly-repeated processes are implemented in firmware.

Impact on National Missions

The design work performed under this project gave our electrical and software engineers and scientists a valuable opportunity to evaluate and apply current LANL space capabilities in the context of a novel imaging instrument application. This experience provides good lessons for future national security space missions, which also seek to exploit imaging sensor technologies with which LANL has little experience. In going through the WFI design process we confronted challenges in data throughput and algorithmic trades that drove us to consider a highly integrated (yet scalable and flexible) hardware, software, firmware architecture. We believe this process and approach will be applicable to future astrophysics and national security missions.

Investigating Properties of Quark-Gluon Plasma Using Jets and Heavy Quark Production at RHIC

Michael P. Mccumber
20140665PRD2

Introduction

Jets measurements feature prominently in the current set of Large Hadron Collider (LHC) results. Measurements at Relativistic Heavy Ion Collider (RHIC) will provide insight into properties of the Quark Gluon Plasma (QGP) under different physical conditions than can be explored with the LHC alone. The 400 person PHENIX collaboration is planning to propose the construction of a new $30M detector, sPHENIX, to DOE to provide a comprehensive set of jet measurements at RHIC and to prepare for the construction of an electron-ion collider (EIC). These physics goals are much beyond the original design capabilities of the PHENIX experiment, which was designed two decades earlier. To achieve these measurements, this LDRD-PRD project proposes to spearhead the development and construction of a new RHIC detector needed to bring a world-class experimental jet physics program to LANL. The new detector is crucial to the full exploration and understanding of the Quark-Gluon Plasma.

This LDRD-PRD project is focused on a new research area of Heavy Ion Physics (using particle jet production as a probe to study the properties of Quark-Gluon Plasma). We propose to lead the development of the future upgrade of the PHENIX detector, opening up a new research direction for LANL's Nuclear Physics Program, which will go beyond the current capabilities of the DOE-funded program. The current DOE-funded Heavy Ion Physics program in P-25 has focused on higher energy muon detection through a magnetic spectrometer at the forward angle, and using a silicon vertex detector to separate primary muon from secondary decays. Our work in this project will go beyond this limitation by initiating a new set of detector systems (sPHENIX) which is designed specifically for high energy jet measurement. Therefore, technical schemes and scientific goals of this LDRD-PRD project are beyond existing DOE funded non-LDRD projects.

Benefit to National Security Missions

This project is highly relevant LANL's Scientific Discovery and Innovation mission, in the area of Nuclear, Particle, Cosmology, and Astrophysics. Quantum Chromodynamics (QCD), the Standard Model theory governing the behavior of quarks and gluons, predicts that a new phase of matter is present in the relativistic collisions of large nuclei. Matter generated by these collisions is at such high temperature and density that quarks and gluons are no longer imprisoned in hadronic states, but are instead free to interact with one another directly, a state of matter known as Quark-Gluon Plasma (QGP). The new phase of matter is being actively studied at hadron collider facilities such as the Relativistic Heavy Ion Collider (RHIC) at Brookhaven National Laboratory and the Large Hadron Collider (LHC) at CERN. Research work on the understanding of properties of Quark-Gluon Plasma will also contribute and lead to new resources of nuclear energy in the next generations.

Progress

FY2016 has been a crucial period for advancing the proposal for a new detector at the Relativistic Heavy Ion Collider (RHIC), named sPHENIX, into a reality. McCumber has been a leading physicist advancing the new experiment and a gatekeeper for the experiment's tracking physics. After a successful science review in FY2014, a new scientific collaboration was formed to carry out the experiment which is currently focusing its efforts on the sPHENIX detector design. During this time the project also successfully underwent a cost & schedule review. McCumber's contributions have been instrumental in these positive developments.

McCumber has a deep involvement in simulations of the sPHENIX detector which are being utilized to characterize detector concepts against the physics needs of the science program, an important part of the detector design process. He is responsible for many of the sPHENIX software libraries representing half of the experiment's

code base, including the tracking software, jet reconstruction and simulation evaluation tools. He is most deeply involved in the tracking design development with a particular focus on the inner tracking layers which will be used to identify heavy flavor jets, one of the three pillars of the sPHENIX science program. He has provided many insights into the strengths and weaknesses of multiple designs being proposed within the collaboration. For instance, he examined the efficiency problems of reusing existing silicon pixel detectors and demonstrated their insuitability for heavy flavor physics. He also discovered issues with backgrounds produced by joining readout channels in one of the outer silicon detector designs. Early recognition of these weaknesses have subsequently resulted in design revisions or the advancement of new technology options—these are large positive impacts on how the sPHENIX experiment will be built that will benefit its science capability and would not have happened without McCumber's insights. The effort currently underway is the examination of the new sPHENIX baseline configuration which includes a MAPS-based inner tracker proposed by Los Alamos combined with an outer TPC tracking system. The new configuration is the result of strong scientific leadership from McCumber on the detector needs for heavy flavor jets and large momentum jet fragment reconstruction. McCumber developed simulation evaluation tools for the tracking system that are also used throughout the experiment to examine different detector designs, greatly aiding the decision points beyond the tracking. Examples include the evaluation of 1D and 2D projective calorimeter tower designs, and hadronic calorimeter plate design that were performed within McCumber's framework. As additional service work for the collaboration, he greatly improved the processing speed of the simulations (x3) and disk storage compression (x70) allowing more throughput for every study being performed.

This year McCumber obtained a sample of an advanced silicon tracking technology, Monolithic Active Pixel Sensor (MAPS), which has a very fine segmentation that makes it ideally suited to sPHENIX. The technical evaluation of that sample advanced quickly after McCumber set up a test stand at LANL. He has started an effort to integrate the new binary data stream from the prototype sensor into sPHENIX. McCumber also visited Nevis Laboratories where he diagnosed readout issues with the sPHENIX HCAL electronics prototype.

McCumber has continued to defend the sPHENIX proposal in scientific conferences, presenting at multiple meetings and seminars. He presented the sPHENIX bottom jet observables at the RHIC & AGS Users meeting. He was also invited to present the sPHENIX science case at the International Conference for New Frontiers in Physics in August 2015. These presentations have been invaluable in creating broad community support for the program. In addition to these presentations, McCumber has organized many workshops to foster sPHENIX's tracking capabilities. These include a tracking workshop in October 2015, the Santa Fe Jet Workshop in January 2016, an inner tracker workshop in March 2016, and a heavy flavor jet workshop at BNL in May 2016.

In recognition of his leadership, McCumber was recently designated as the heavy flavor jet convener where he is organizing the effort to bring the latest mechanical detector designs under simulation to guide the detector design optimization. In addition to his sPHENIX duties, McCumber continues to be active in PHENIX where he participated in supporting the detector and readout during its final year of operation and sits on the PHENIX Speakers Bureau.

Future Work

This LDRD-PRD project focuses on a new research area of Heavy Ion Physics (using particle jet production as a probe to study the properties of Quark-Gluon Plasma) and leading the development of the future upgrade of the PHENIX detector. Our research will open up new and exciting research directions for LANL's Nuclear Physics Program, which is striving to move beyond the existing capabilities of the currently funded DOE program. The current DOE-funded Heavy Ion Physics program in P-25 has been focusing on higher energy muon detection through a magnetic spectrometer at the forward angle and using a silicon vertex detector to separate primary muons from secondary decayed muons. During FY15, our work on this project surpassed this limitation by initiating a new set of detector systems (sPHENIX) which is designed specifically for high energy jet measurement. During FY17, our work will focus on optimizing the details of the calorimeter and charge particle tracking detectors and preparing for full scale detector R&D. Therefore, the technical schemes and scientific goals of this LDRD-PRD project enable us to push the research boundaries beyond the existing DOE-funded non-LDRD projects.

As a topical working group convener in sPHENIX on heavy flavor physics, Postdoc Mike McCumber will direct the development of heavy flavor jet analysis techniques and the construction of advanced tracking algorithms needed by the project for topics including modified jet fragmentation, heavy quark energy loss, and quarkonia production. McCumber's convenership will advance the physics capabilities of the new experiment.

sPHENIX detector at RHIC: in FY17, we will provide leadership of the detector research and development needed for

the construction of a jet-focused experiment at Relativistic Heavy Ion Collider (RHIC) covering both mid- and forward-rapidity in preparation for an Electron-Ion Collider (EIC) detector. This will include readout tests of the advanced silicon sensor prototype obtained in FY16 and integration of the technology into the sPHENIX readout in preparation for test beam studies.

Conclusion

A key piece of physics necessary to obtain in the desired data is the energy loss of massive quarks in the Quark-Gluon Plasma (QGP). Mike will take a leadership role in the first direct analysis of heavy quarks at forward rapidity using the Forward Vertex (FVTX) detector (a LANL-led DOE project) from the heavy ion data collected in 2014. This work presents a pivotal test of the models describing the interaction of fast moving quarks with the QGP and thus will prepare the field for the suite of measurements to come using the sPHENIX detector.

Publications

Adare, A. M., M. P. McCumber, J. L. Nagle, and Romatschke. Examination whether heavy quarks carry information on the early-time coupling of the quark-gluon plasma. 2014. PHYSICAL REVIEW C. 90 (2).

McCumber, M.. Future b-jet Measurements with sPHENIX. Invited presentation at RHIC and AGS Users Meeting 2015. (Upton, New York, 9-12 Aug. 2015).

McCumber, M.. Updated Jet Performance and Algorithm Approaches. Invited presentation at sPHENIX Department of Energy Science Review. (Upton, New York, 30 April 2015).

McCumber, M.. An Opportunity for Forward Jet Single Spin Asymmetry Measurements at RHIC. Presented at 6th Workshop on APS Topical Group on Hadron Physics. (Baltimore, Maryland, 8-10 April 2015).

McCumber, M.. fsPHENIX: Forward Jet and Drell-Yan Single Spin Asymmetries at RHIC. Presented at Joint Nuclear Physics Division Meeting of the APS and JPS. (Waikoloa, Hawaii, 7-10 Oct. 2014).

McCumber, M.. sPHENIX: An Upgrade Proposal from the PHENIX Collaboration. 2015. arXiv:1501.06197.

McCumber, M. P.. Back-to-back pair suppression at large transverse momentum in root s(NN)=200 GeV Au + Au collisions at PHENIX. 2011. NUCLEAR PHYSICS A. 855 (1): 408.

McCumber, M. P.. High p(T): Energy Loss Physics at PHENIX. 2013. NUCLEAR PHYSICS A. 904: 154C.

McCumber, M. P.. High p(T): Energy Loss Physics at PHENIX. 2013. NUCLEAR PHYSICS A. 904: 154C.

Nagle, J. L., Adare, Beckman, Koblesky, J. O. Koop, McGlinchey, Romatschke, Carlson, J. E. Lynn, and McCumber. Exploiting Intrinsic Triangular Geometry in Relativistic He-3 + Au Collisions to Disentangle Medium Properties. 2014. PHYSICAL REVIEW LETTERS. 113 (11).

Neutron Star Mergers Revisited

Wesley P. Even
20150712PRD2

Introduction

Neutron star mergers are the primary candidates for the advanced gravitational wave (GW) detectors (LIGO, VIRGO), coming into operation in the next few years, with estimated rates of several events per year. However, due to the poor directional sensitivity of GW detectors, we will remain blind to the location of the mergers, unless they are accompanied by a short gamma-ray burst. The latter only happens in a few percent of cases, when the merger axis is oriented towards the Earth. Recently, a new type of electromagnetic transients known as macronova or kilonova has been proposed, which can assist in locating the mergers. Macronovae emit isotropically and thus can be detected for any orientation of the merging system. It is powered by radioactive decay of heavy r-process elements, which are synthesized in merger ejecta. Depending on the parameters of merging system and its orientation, macronova can peak in the infrared or visual bands on a timescale of a few days.

A new optical and infrared survey system BlackGem is currently being deployed and will be targeted for systematic searches of macronovae. Therefore, theoretical understanding of the properties of merger ejecta is crucial for locating and interpreting macronovae. Many of these properties are still currently uncertain, including (i) the amount of mass ejected through different channels (dynamical, neutrino-driven winds, viscous winds), (ii) morphology of the ejecta, and (iii) its nuclear composition.

The main difficulty in simulating the ejected matter lies in the fact that it has much lower density compared to the merging stars. Previous studies with different prescriptions for gravity, nuclear and neutrino physics yielded contradictory conclusions about morphology and composition of the ejecta.

Benefit to National Security Missions

The simulations produced by this effort will play a vital role in the discovery and analysis of the electromagnetic counterparts to the first direct observations of gravitational waves. Previous simulations by Dr. Korobkin are currently used as the gold-standard for researchers designing instruments to observe these phenomena. The models being developed in this project will allow LANL to be a world leader at predicting electromagnetic counterparts for gravitational wave signals.

Because this project involves the development and usage of large-scale multi-physics codes that include nuclear reactions it has relevance to the stockpile stewardship work at the laboratory. Insights gained from this project have the potential to impact the development of future methods for fundamental physics that could be used for stockpile stewardship. However, the work being done in this project is in a very different regime and does not have direct application to stockpile stewardship.

Progress

In the past year, we have been developing a new particle hydrodynamics code, borrowing from the best practices of the previous codes (2HOT and the Einstein Toolkit) while also being readable and modular to allow for clear and straightforward coupling between hydrodynamics and gravity. We estimated that adding fully dynamical general-relativistic gravity treatment is just as efficient as adding post-Newtonian approximations. We therefore opted for the former option, namely coupling SPH code to a full Einsteinian gravity on a grid.

At the initial stage, we concentrated on developing the modular and scalable code base infrastructure, allowing for uniform treatment of both the particles and the grid, using hashed trees for subdomain treatment and parallelization. An allocation proposal for supercomputing time (IC2016) with the new code will be submitted; this request will be for time only (no associated funds) to test the results of the initial stage of this project.

As expected, initial toy implementations revealed that the energy-momentum tensor produced by the standard 2nd-order SPH prescription is rather noisy, and stable simulations require highly dissipative numerical settings. To address this problem, we developed and implemented high-order particle derivatives, similar to the ones employed in the moving least-squares particle hydrodynamics (MLSPH). This has been done in collaboration with Dr. Gary Dilts (CCS-2).

In a parallel effort of this project with more immediate outcome, we were working on the observational signatures of neutron star merger ejecta. This work is based on our previous results with Newtonian gravity, where each merger ejects about 1% Solar mass of highly neutron-rich material. We used previously computed ejecta morphologies to simulate macronova light curves. These light curves use the state-of-the art detailed atomic opacities of heavy elements, calculated by Dr. Chris Fontes (XCP-5), which to our knowledge are the best currently available in the field. Accurate radiative transfer simulations, providing expected light curves and spectra of macronovae, were accomplished with the SuperNu code, developed by Dr. Ryan Wollaeger (CCS-2). A paper (Wollaeger et al. 2016) summarizing our results and their astrophysical implications, is currently in preparation.

Macronova light curves require detailed knowledge about how much energy escapes in neutrinos as compared to the power in gamma-, beta- and fission fragments. We have developed a fast decay module to compute these heating rates and accurate ejecta abundances. This module will be used for the next step of our project where we investigate sensitivity of the light curves and spectra to the specific composition of decaying matter and the morphology of the outflows. Preliminary results show that polar outflows produce brighter transients, which are also bluer and peak earlier (around 1 day after the merger).

Future Work

For the 2017 fiscal year this project will complete the development and testing stage of the new parallel MPI-OpenMP code with the acclaimed robust coupling of (ML-) SPH and general relativistic gravity.

The project will open with the typical battery of general relativistic hydrodynamics tests, which include oscillations of a rotating relativistic star, migration of an overdense compact star to a stable branch, relativistic collapse and formation of a black hole, and Abramowicz-Sikora-Jaroszynski stationary tori around Schwarzshild black holes. This project will be done in collaboration with Dr. Stephan Rosswog at Oskar Klein Centre, Stockholm, and Dr. Erik Schnetter at Perimeter Institute.

At the next stage the project will move to the main production phase, which is the neutron star merger problem. It will begin with a test of symmetric merger of two 1.4 solar-mass neutron stars with a simple polytropic equation of state, that will be straightforward to compare to previous grid-based simulations.

In the final stage we will run the merger problem with a variety of more realistic microphysical equation of state, given by tabulated data both from external sources and using the new theoretical developments supplied by T and XCP division. The final product of each of these simulations we will be: a) a snapshot of a (quasi-)stationary hypermassive neutron star, surrounded by an accretion disk; b) an unbound debris with detailed morphology and composition; and c) gravitational wave signal (here we plan to adopt established code from the Einstein Toolkit).

This data will be compared to previous Newtonian studies and gridbased relativistic simulations. The dynamical ejecta information will be further utilized for predicting a macronova transient. As a final product we will have a coherent picture of high-fidelity simulations of merging neutron stars with conclusive statements about macronovae - gravitational wave burst connection, with the related uncertainties.

Conclusion

The resulting simulations will take advantage of numerical algorithms being developed at Los Alamos to scale ten to one hundred times the resolution that current models are typically conducted. The models will also include microphysics (i.e. opacities) in which Los Alamos experts are currently leading their fields. These simulations will be critical for locating sources and interpreting the results of the first gravitational wave signals from advanced gravitational wave detectors, such as LIGO. This research could have profound impact on the detection of neutron star mergers. It will also impact nuclear physics because neutron star mergers have been recently shown to be the main site for the r-process nucleosynthesis.

Publications

Eichler, M., A. Arcones, R. Käppeli, O. Korobkin, M. Liebendörfer, G. Martinez-Pinedo, I. V. Panov, T. Rauscher, S. Rosswog, F. K. Thielemann, and C. Winteler. The impact of fission on r-process calculations. 2016. Journal of Physics: Conference Series. 665 (1): 12.

Korobkin, O.. Evolution of the gamma- and X-ray radioactive source in macronovae from compact mergers. Presented at 2016 JINA-CEE Frontiers in Nuclear Astrophysics. (South Bend, IN, 29-31 Mar. 2016).

Korobkin, O.. Introduction to the Einstein Toolkit. Invited presentation at Einstein Toolkit EU School and Workshop. (Trento, Italy, 13-17 Jun. 2016).

Martin, D., A. Perego, A. Arcones, F. K. Thielemann, O. Korobkin, and S. Rosswog. Neutrino-driven winds in the aftermath of a neutron star merger: nucleosynthesis and electromagnetic transients. 2015. The Astrophysical Journal. 813 (1): 14.

Studying Nuclear Sstrophysics and Inertial Fusion with Gamma-rays

Alex Zylstra
20150717PRD2

Introduction

The proposed work will study nuclear astrophysics and basic nuclear physics using the unique capabilities of inertial confinement fusion (ICF) implosions. The plasmas created in ICF implosions closely mimic conditions in astrophysical systems, such as stellar cores. By studying nuclear reactions in this environment, we will greatly improve our understanding of how the elements were produced in the universe. This work will be conducted with the plasma physics (P-24) and broader ICF and nuclear physics communities at LANL, in particular Dr. Hans Herrmann.

Benefit to National Security Missions

The field of nuclear astrophysics will benefit from high-quality measurements at low energies; the direct applicability of ICF plasmas to conditions in the universe is a unique opportunity to make substantial contributions to our understanding of stellar and big-bang nucleosynthesis. Basic nuclear physics of these few-nucleon systems will be simultaneously studied. Improved nuclear diagnostics for experiments at National Ignition Facility are important for achieving our goal of fusion ignition, in support of stockpile stewardship and fusion energy applications. This research proposal is an ambitious program to make high-level contributions to these programs. Gamma-Ray studies in inertial confinement fusion platforms directly support High Energy Density and Weapons Physics. This work is relevant to our national security mission.

Progress

The T3He fusion reaction was studied on the OMEGA laser facility. This fusion reaction produces 6Li, emitting a gamma ray. By measuring the gamma ray, we were able to measure the fusion cross section using inertial fusion implosions. This reaction is important for big-bang nucleosynthesis, as it could explain an anomaly in 6Li abundances measured in primordial material. Our data are the first in the energy range relevant to the big bang, and conclusively show that this reaction cannot explain the 6Li abundance, pointing towards a non-nuclear explanation. This work is also the first use of an inertially-confined plasma to answer an open question in nuclear astrophysics, and has been submitted to Physical Review Letters.

Secondly, a new technique for hydrodynamic mix experiments was developed. Mix of high-Z material into the fuel is a critical degradation mechanism for inertial fusion, and achieving fusion ignition will require a good understanding of mix. In deuterated plastic shells filled with HT gas, we simultaneously measure the HT and DT fusion gamma rays. This is a time-dependent measurement of the mix of deuterium into the fuel over the nuclear production period. This technique will enable many new experiments to benchmark LANL mix models relevant to the weapons program.

Future Work

First, I will extend current studies of the p+D and T+3He gamma producing reactions using existing diagnostics and data. The p+D reaction is relevant to brown dwarfs and protostars; additional measurements at lower energy than previously done are important for modeling these systems. For T+3He, the new `super' Cherenkov detector enables much higher- precision measurements than has been done previously; this reaction is relevant to Big- Bang production of 6Li and nuclear physics of six-nucleon systems. Analysis of recently-acquired data on these reactions will continue in the next FY. A concept for a low-energy gamma detector will be explored; this detector could used to study two reactions for the first time in ICF facilities: the 3He+4He reaction (gamma at 1.6 MeV), important for the proton-proton II and III chains in low-mass stars, with implications for the stellar neutrino problem, and secondly, the T+4He reaction (gamma at 2.5 MeV), which is important for production of 7Li during the Big Bang. An experiment will also be

performed at the OMEGA laser facility to study the energy loss (stopping power) of charged particles, produced by nuclear reactions, as they transit HED plasmas. This work will be done in collaboration with the LANL gamma team, and nuclear physics collaborators at LANL and other institutions.

Conclusion

The field of nuclear astrophysics will benefit from high-quality measurements at low energies; the direct applicability of ICF plasmas to conditions in the universe is a unique opportunity to make substantial contributions to our understanding of stellar and big-bang nucleosynthesis. Basic nuclear physics of these few-nucleon systems will be simultaneously studied. This project will result in improved nuclear diagnostics for experiments at National Ignition Facility, which are important for achieving our goal of fusion ignition, in support of stockpile stewardship and fusion energy applications.

Publications

Kagan, , Svyatskiy, H. G. Rinderknecht, M. J. Rosenberg, A. B. Zylstra, C. -. Huang, and C. J. McDevitt. Self-Similar Structure and Experimental Signatures of Suprathermal Ion Distribution in Inertial Confinement Fusion Implosions. 2015. PHYSICAL REVIEW LETTERS. 115 (10).

Rinderknecht, H. G., M. J. Rosenberg, A. B. Zylstra, Lahmann, F. H. Seguin, J. A. Frenje, C. K. Li, M. G. Johnson, R. D. Petrasso, L. F. B. Hopkins, J. A. Caggiano, Divol, E. P. Hartouni, Hatarik, S. P. Hatchett, Le Pape, A. J. Mackinnon, J. M. McNaney, N. B. Meezan, M. J. Moran, P. A. Bradley, J. L. Kline, N. S. Krasheninnikova, G. A. Kyrala, T. J. Murphy, M. J. Schmitt, I. L. Tregillis, S. H. Batha, J. P. Knauer, and J. D. Kilkenny. Using multiple secondary fusion products to evaluate fuel rho R, electron temperature, and mix in deuterium-filled implosions at the NIF. 2015. PHYSICS OF PLASMAS. 22 (8).

Rosenberg, M. J., F. H. Seguin, P. A. Amendt, Atzeni, H. G. Rinderknecht, N. M. Hoffman, A. B. Zylstra, C. K. Li, Sio, M. G. Johnson, J. A. Frenje, R. D. Petrasso, V. Y. Glebov, Stoeckl, Seka, F. J. Marshall, J. A. Delettrez, T. C. Sangster, Betti, S. C. Wilks, Pino, Kagan, Molvig, and Nikroo. Assessment of ion kinetic effects in shock-driven inertial confinement fusion implosions using fusion burn imaging. 2015. PHYSICS OF PLASMAS. 22 (6).

Zylstra, A B, J A Frenje, P E Grabowski, C K Li, G W Collins, P Fitzsimmons, S Glenzer, F Graziani, S B Hansen, S X Hu, M Gatu Johnson, P Keiter, H Reynolds, J R Rygg, F H Séguin, and R D Petrasso. Development of a WDM platform for charged-particle stopping experiments. 2016. Journal of Physics: Conference Series. 717 (1): 012118.

Zylstra, A. B., H. S. Park, J. S. Ross, F. Fiuza, J. A. Frenje, D. P. Higginson, C. Huntington, C. K. Li, R. D. Petrasso, B. Pollock, B. Remington, H. G. Rinderknecht, D. Ryutov, F. H. Séguin, D. Turnbull, and S. C. Wilks. Proton pinhole imaging on the National Ignition Facility. 2016. Review of Scientific Instruments. 87 (11).

Zylstra, A. B., H. W. Herrmann, M. G. Johnson, Y. H. Kim, J. A. Frenje, G. Hale, C. K. Li, M. Rubery, M. Paris, A. Bacher, C. R. Brune, C. Forrest, V. Y. Glebov, R. Janezic, D. McNabb, A. Nikroo, J. Pino, T. C. Sangster, F. H. S'eguin, W. Seka, H. Sio, C. Stoeckl, and R. D. Petrasso. Using Inertial Fusion Implosions to Measure the $mathrmT+3mathrmHe$ Fusion Cross Section at Nucleosynthesis-Relevant Energies. 2016. Phys. Rev. Lett.. 117: 035002.

Zylstra, A. B., J. A. Frenje, P. E. Grabowski, C. K. Li, G. W. Collins, Fitzsimmons, Glenzer, Graziani, S. B. Hansen, S. X. Hu, M. G. Johnson, Keiter, Reynolds, J. R. Rygg, F. H. Seguin, and R. D. Petrasso. Measurement of Charged-Particle Stopping in Warm Dense Plasma. 2015. PHYSICAL REVIEW LETTERS. 114 (21).

A Kinetic Theory Based Study of Type II Core-Collapse Supernovae

Terrance T. Strother
20150741PRD3

Introduction

The overall technical goal of this project is to provide a first-ever fully self-consistent description of the impact that finite mean free path neutrinos have on the dynamics of core-collapse supernovae and document our findings. This is high impact science because this mode will provide a first-ever fully self-consistent description of the impact that finite mean free path neutrinos have on the dynamics of core-collapse supernovae.

Benefit to National Security Missions

Los Alamos National Laboratory is known for its cutting-edge research on implosion-driven systems such as inertial confinement fusion capsules as well as nuclear physics. The continuation of the development of Dr. Sagert's first-of-a-kind kinetic theory based core-collapse supernova model capable of resolving the system's macroscopic hydrodynamics that treats neutrino transport for all mean free paths identically and on equal footing with the nuclear matter will enhance Los Alamos National Laboratory's ability to model these systems. Thus this work is relevant to our national security mission.

Progress

Code development: We have been working on the modification of our Monte Carlo kinetic particle code architecture into a modular form. This includes the implementation of initial and boundary conditions, particle properties, output, checkpointing and gravity into the main code via modules. The different modules (e.g. periodic, reflective or free boundary conditions) are interchangeable which allows an easy and quick setup of different simulations according to the need of the user and highly facilitates future code development (e.g. usage of non-relativistic or relativistic particles). In combination with the modular architecture, we created a suite of unit tests that are performed after each code update to ensure a correct functionality.

In the previous version of our code, the dimensionality of the physical problem dictated the number of particle degrees of freedom and thereby the equation of state of the simulated matter, i.e. in a two-dimensional (2D) problem, matter was fixed to be an ideal gas with two degrees of freedom. Due to the high computational cost of 3D simulations, code verification tests in the literature (kinetic and hydrodynamic) are often performed in 2D, however, using an ideal gas with three degrees of freedom. To enable one-to-one comparisons with such studies we extended the abilities of our kinetic code to perform 2D simulations using an ideal gas with three degrees of freedom.

Our current work involves the collaboration with LANL scientists (Ben Bergen, Wesley Even, Josh Dolence) to use the Flexible Computational Science Infrastructure FLeCSi for parallelization of our code via Message Passage Interface (MPI) and the implementation of a tree method to efficiently calculate gravitational and Coulomb forces.

Physics development: We have continued and finalized the benchmarking of our code via standard shock and fluid instability tests. Previous studies included the standard Sod, Noh and Sedov shock tests and simulations of Rayleigh-Taylor fluid instabilities. In order to apply our code in core-collapse supernova (CCSN) and inertial confinement fusion (ICF) capsule implosion studies, the remaining necessary standard hydrodynamic test was the simulation of Kelvin-Helmholtz (KH) fluid instabilities. We performed these tests in the continuum limit and saw good agreement with hydrodynamic codes. In addition, we studied KH simulations in various kinetic regimes to test the impact of large particle mean-free-paths. Our results were presented at the High Energy Density Laboratory Astrophysics (HEDLA2016) conference in May 2016 and will be shown at the 30th International Symposium on Rarefied Gas Dynamics (30RGD) in July 2016. We have been discussing our results with LANL fluid dynamics experts (Daniel Livescu, Jon Baltzer)

with the corresponding publication being in preparation (I.S., Wesley Even, Terrance Strother).

To prepare our code for CCSN and ICF studies, we performed simple gravitational collapse and implosion tests. The first were simulations of a self-gravitating cold gas cloud. This problem possesses an analytic solution and comparisons with our simulations showed excellent agreement. This test was also used to check for energy and momentum conservation during the gravitational collapse. In addition, we performed simple ICF-like implosion simulations and compared our results with the LANL Radiation Adaptive Grid Eulerian hydrodynamic code RAGE (Wesley Even) as well as previous RAGE studies in the literature (Chris Fryer et al.). The implosion tests showed very good agreement and were used to check for effects arising from the finite number of particles in the kinetic simulations. The results were presented at HEDLA2016 and will be shown at 30RGD. A manuscript is currently in preparation (I.S. Wesley Even, Terrance Strother).

Future Work

The goals for this project for the next fiscal year are to publish the results generated simulating instabilities and implosions with our code and to finish fully parallelizing the code using a LANL message passing interface algorithm and integrate an existing neutrino production/propagation code to model astrophysical systems.

Conclusion

The algorithm is capable of resolving the system's macroscopic hydrodynamics and treats neutrino transport for all mean free paths identically and on equal footing with the nuclear matter. This first-of-a-kind kinetic theory based core-collapse supernova model capable of resolving the system's macroscopic hydrodynamics that treats neutrino transport for all mean free paths identically and on equal footing with the nuclear matter will enhance the Laboratory's ability to model these systems, making the work relevant to our national security mission.

Publications

Sagert, I.. 2D Implosion Simulations with a Kinetic Particle Code. Physical Review E.

Revealing the Particle Nature of Dark Matter with Cosmic Gamma Rays

Brenda L. Dingus
20160641PRD2

Introduction

The High Altitude Water Cherenkov Observatory (HAWC) is observing the gamma-ray sky from 100 GeV to 100 TeV, which makes it sensitive to Dark Matter (DM) masses from about 0.5 to 1000 TeV. Postdoc Andrea Albert plans to continue the hunt for a gamma-ray DM signal with the HAWC team at LANL. As a member of the Fermi Large Area Telescope Collaboration (LAT), Albert will be able to merge results from both NASA's Fermi LAT and HAWC to produce a combined likelihood analysis over a broad energy range in addition to performing new DM searches with HAWC. Albert will search for DM signals from key targets like the Virgo Cluster, dwarf galaxies, and the Galactic Center (GC). Since the DM emission from these targets is expected to be extended, the large field of view and continuous monitoring provided by both HAWC and the Fermi LAT makes them ideal and complementary instruments for these searches.

Specifically, Albert plans to continue her investigation of the effect of modeling uncertainties on the so-called 'GeV excess' in the GC in the Fermi LAT data. Additionally, Albert will search with HAWC for gamma-ray spectral lines from the GC: a smoking gun for DM. Though typically a rare process, Sommerfeld enhancement may also increase the branching fraction of DM annihilations into line channels. The planned upgrade to HAWC will increase both the range and sensitivity of DM searches. Albert will work on the calibration and study of this upgrade since a deep understanding of instrumental and event reconstruction details are necessary when searching for faint signals like those expected from DM.

Benefit to National Security Missions

DOE, NSF, and NASA are all funding fundamental research to investigate the nature of dark matter. Dark matter is believed to have about ten times as much mass as regular matter; however, it's characteristics are largely unknown. This makes the search for dark matter important to astrophysics and cosmology as well as particle physics. One of the leading theories for dark matter predicts that dark matter will emit high energy gamma rays. With this project, we will look for evidence of these gamma rays in order to discover the existence of this type of dark matter or to constrain the theoretical predictions with measured limits on the flux of gamma rays from dark matter. In addition, this project builds capabilities at LANL relevant to nuclear weapons research and nuclear nonproliferation through the development and analysis of data from complex detectors and relevant to information science and technology with the collection and reconstruction of peta-Byte data sets.

Progress

Postdoc Andrea Albert arrived on March 28, 2016. Since then Albert has continued her research into quantifying the systematic uncertainties that effect the so-called "Galactic Center GeV excess" in the Fermi LAT data. This tentative signal has been attributed to dark matter, but many other gamma ray sources excess in that region, some of which are highly correlated with potential dark matter signals. Albert and her LAT collaborators plan to submit the paper to internal review within the Fermi LAT Collaboration by the end of July. Albert showed preliminary results at the Galactic Center IAU Symposium this July. Albert also continues to be the coordinator of the Dark Matter and New Physics working group within the Fermi LAT Collaboration.

Albert has also begun learning High-Altitude Water Cherenkov (HAWC) data analysis techniques and have started developing tools to calculate the sensitivity of HAWC to signals from axion-like particles, which are a dark matter candidate. Albert is serving as internal referee for the upcoming HAWC paper on searches for dark matter signals from dwarf galaxies. Albert helped update the public HAWC website to prepare for the HAWC press release last April and started a HAWC Twitter account to facilitate public outreach. Albert is also currently helping to test and calibrate the new photodetectors for the

HAWC upgrade. This also involves training the summer students in the calibration techniques.

Future Work

- Search for gamma-ray emission from dwarf spheroidal galaxies with the High-Altitude Water Cherenkov (HAWC) data set.
- Develop search strategies for identifying energy spectral signatures consistent with the predictions of dark matter candidates.
- Create new energy parameter for reconstructing the energy of individual HAWC events using new expanded array.
- Monitor HAWC performance and data as is required for all scientists working on HAWC.
- Serve as Dark Matter & New Physics working group coordinator within the Fermi LAT Collaboration
- Test and calibrate new photodetectors and data acquisition system for HAWC upgrade.

Conclusion

This project will result in the most sensitive searches for gamma-ray signals from massive DM candidates. These searches will rule out some models of the DM if no signal is detected; however, if a signal is detected then other observations from the High Altitude Water Cherenkov Observatory and Fermi Large Area Telescope will have to be consistent with this signal. This would be a major discovery solving one of the longest standing problems in astrophysics, cosmology, and particle physics. The project also builds capabilities relevant to nuclear weapons research and nuclear nonproliferation through development and analysis of data from complex detectors.

Publications

Albert, A., S. Funk, T. Kawashima, M. Murphy, A. Okumura, R. Quagliani, L. Sapozhnikov, H. Tajima, L. Tibaldo, J. Vandenbroucke, G. Varner, and T. Wu. TARGET 5: a new multi-channel digitizer with triggering capabilities for gamma-ray atmospheric Cherenkov telescopes. Astroparticle Physics.

LAT, F., T. DES, and A. Albert. SEARCHING FOR DARK MATTER ANNIHILATION IN RECENTLY DISCOVERED MILKY WAY SATELLITES WITH FERMI-LAT. Astrophysical Journal (ApJ).

Precision Theoretical Analysis of Reactions with Protons Polarized in a Strong Magnetic Field

Ivan M. Vitev
20160645PRD1

Introduction

Precise theory to extract the transverse distribution of quarks and gluons, collectively called partons, in the proton, understand their behavior as a function of the collision energy, relate them to the orbital motion and the proton spin, and recreate the 3D image of the nucleon is absolutely essential to enable breakthroughs in the field of spin physics. Development of this theory and its application to analyze the results obtained by LANL scientists, in close collaboration with experiment, is the central topic of this project. Building upon earlier work, at the beginning of the project we will first perform an accurate calculation of the Drell-Yan production rate to incorporate previously neglected quantum correlations between the partons in the nucleon, which are further enhanced in a strong magnetic field. These play an essential role for the data set that will be collected by a LANL-led Fermilab experiment and control the energy dependence of the parton's transverse distribution. The next logical step is to relate this distribution to the orbital motion of quarks and gluons.The advances in analytic theory will be incorporated in fast simulation packages on local computer clusters. In the second part of this project, we will use the newly-developed analysis tools to precisely extract the parton transverse distribution from the Drell-Yan experimental measurements. We will present accurate predictions for the contribution of the parton orbital motion to the nucleon spin, an important step toward the resolution of the "spin crisis''. Last but not least, we will recreate the 3D picture of the nucleon in a variety of collision energies.

Benefit to National Security Missions

This work is central to the vision of the US Department of Energy (DOE) and the National Science Foundation (NSF) for the future of Nuclear Physics. In the recently released 2015 Long Range Plan for Nuclear Science, which sets priorities for both DOE and NSF, the study of the internal structure of the nucleons is prominently featured. Specifically, the plan recommends promptly carry out an experimental polarized proton target program at Fermilab, which will be led by LANL. This program will produce the world's most accurate polarized Drell-Yan data in proton-proton reactions. Our project will develop the theoretical analysis tools; it is a timely and in direct response to the DOE mile-stone to "test unique QCD predictions for relations between single-spin phenomena in p-p scattering and those observed in deep-inelastic scattering". The project also directly supports the priorities of the Nuclear, Particle, Cosmology and Astrophysics pillar of our Scientific Discovery and Innovation Mission. "Open questions related to the quark-gluon plasma, the nature of the color phase diagram, and nucleon structure and quark gluon dynamics are among the highest priorities of the Office of Science Nuclear Physics program and are an important part of understanding the Universe from first principles."

Progress

Although this project started near the end of FY16, we have made progress toward meeting its goals. To understand the role of novel quantum correlations between the constituents of the proton, quarks and gluons collectively called partons, we calculated the production rate of light elementary particles in reactions with protons polarized in a strong magnetic field. Specifically, we focused on the case when one proton is polarized transversely to the beam direction and the second is polarized longitudinally to it. We investigated how such polarized reactions produce asymmetries in the particle production rates and how they can be related to three-parton correlation functions in the proton. The three-parton correlation functions are intimately related to 3-dimensional (3D) spin structure of the proton and are unique ways to probe the distribution of its constituents in transverse momentum – the so-called transverse momentum distributions (TMDs).

Future Work

In the first year of the project we will focus on the

derivation of the Drell-Yan cross section, both unpolarized and polarized, in strong magnetic field proton targets. The distribution of quarks, fundamental building blocks of matter of Precise theory to extract the Sivers distribution, understand its behavior as a function of the collision energy, relate it to the orbital angular momentum of the nucleon, and recreate its 3D image is absolutely essential to enable the breakthroughs in the field of spin physics anticipated by the world-wide community. Development of this theory and its application to analyze the data collected by LANL scientists is the central topic of this proposal.

Building upon earlier work, at the beginning of this project we will first perform an accurate (next-to-leading order) calculation of the Drell-Yan Sivers asymmetry and incorporate gluon correlation functions. Gluons are expected to play an important role in the kinematic region probed by the LANL-led Fermilab experiment and control the energy dependence (evolution) of the quark Sivers function

Conclusion

This project will allow unprecedented understanding of the internal structure of protons and neutrons. It will extend the applicability of the theory of strong interactions to reactions with particles polarized by strong magnetic fields, and extend the theory's applicability to reactions with particles polarized by strong magnetic fields. Precision analysis of measurements from the polarized proton experiment at Fermilab will help construct a 3D picture and solve the longstanding problem about the origin of the nucleon spin. This work addresses DOE's vision for the future of nuclear physics and priorities set for DOE to study the internal structure of nucleons.

Publications

Hatta, Y., B. Xiao, S. Yoshida, and F. Yuan. Single spin asymmetry in forward pA collisions. 2016. Physical Review D. 94 (5): 054013.

Koike, Y., D. Pitonyak, and S. Yoshida. Twist-3 effect from the longitudinally polarized proton for ALT in hadron production from pp collisions. 2016. Physics letters B. 759: 75.

Using X-Rays with Protons for a Material-Identification Capability at pRad

Levi P. Neukirch
20160652PRD2

Introduction

Dr. Neukirch will combine x-radiography with proton radiography (pRad) to produce a pixel-by-pixel material identification diagnostic of dynamic systems. This will establish important new capabilities called for in the pRad Long Range Plan. Dr. Neukirch will develop experimentally a method to alternate multiple x-ray imagers with layers of materials that absorb different components of the spectrum of a broadband x-ray source. The combined data from the different images can recreate a 3-D image sensitive to different elements composing the system for a particular moment in time. An x-ray system is being installed at pRad for 3-D and thin-target imaging; using proton radiographs in conjunction with the x-ray images will make this technique yet more sensitive to constituent materials.

Benefit to National Security Missions

The proposed work will offer a new diagnostic for material identification, provide additional details about chemical mixing or fractionation induced by shocks, melting, or solidification, all relevant to the stockpile stewardship mission. It will enable spatially resolved measurements of the composition of ejecta and plumes.

Pushing pRad's spatial resolution below 10 μm will reach the regime of proton microscopy, even allowing individual metallic grains to be resolved within targets. Together with a supplementary x-radiography capability for spatially-resolved material identification will add to pRad's performance in current measurements and enable new types of experiments. They will guide the design and implementation of pRad capabilities into next-generation diagnostic systems for MaRIE.

Progress

Dr. Neukirch wrote a preliminary version of a computer program in Geant4, a open-source program for particle and radiation interactions, that models the x-ray attenuation in targets and detector sensitivity. This model has predicted the radiographs that would result from x-ray imaging of various test objects.

He has constructed test objects of aluminum and lead and imaged them at the 150 KeV x-ray source operated by AET Division in collaboration with Dr. Michelle Espy. Multiple simultaneous images, each with differing amounts of shielding, were made of the test object. The shielding materials were molybdenum, tin, tantalum, lead, and copper. This allowed for each plate to record a different x-ray energy spectrum. This data is currently being analyzed and compared to the predictions of the model.

To mate an x-ray source with the proton radiography facility, the source and the x-ray detectors must be shielded from damage during dynamic experiments. Thus, it is necessary to identify an appropriate window material that will allow x-ray penetration and is also strong enough to withstand the explosive pressure bursts and shrapnel. So-called "frag tests," proofing a candidate window material in real tests with high explosives, have been conducted to assess Spectra, a trade-name ultra-high molecular weight polyethylene fiber. The damage to the windows was consistent with expectations, so further development of Spectra windows will continue.

Dr. Neukirch wrote and presented a formal proposal for proton radiography (pRad) beam time to the pRad Program Advisory Committee.

Future Work

- Produce a computer model to test a proposed method to image objects with different energies of x-rays.
- Vary parameters in the model to determine a viable way to use different configurations of absorbers and imagers for an imaging diagnostic for materials identification for two or three demonstration experiments.

- Learn imaging techniques at the pRad facility.
- Build several static test objects that can be imaged at an x-ray facility and at pRad.
- Image the test objects at the pRad facility.
- Image the test objects at an x-ray facility in the configuration determined in task #2.
- Combine the data and evaluate this first-generation technique.
- With the experimental results, data analysis, and computer model, propose a refined technique suitable for quantitative measurements.

Conclusion

The project aims to combine x-radiography with proton radiography to produce a pixel-by-pixel material identification diagnostic of dynamic systems. This technique will help answer very important questions about materials transport in shock physics experiments, such as what are the constituents of gas plumes and ejecta and where these constituents originated. Even a proof-of-principle demonstration of the technique with a static manufactured model will produce a high-impact publication of an important novel diagnostic.

Theoretical Investigation of Nucleon and Nuclear Structure at Very High Energies

Zhongbo Kang
20130783PRD2

Abstract

Nucleons (protons and neutrons) are known to be the building blocks of matter, and also known to be bound states of quarks and gluons – the partons, whose dynamics is best described by Quantum Chromodynamics (QCD). To understand the nucleon structure and map out how its basic building blocks (quarks and gluons) are distributed inside the nucleon is of fundamental importance to science. Through 30+ years of research performed by the community, we now have a good understanding of the longitudinal motion of quarks and gluons inside the fast moving nucleon, in other words one-dimensional "image" of the nucleon. Recent theoretical advances and experimental progress have made it possible to extract the information on the transverse momenta of quarks and gluons inside the nucleon as well as large nuclei, which are highly boosted along the longitudinal direction in high energy scattering experiments. Such a breakthrough for the first time provides a way for three-dimensional tomography of the nucleon structure. In this project, we have developed theoretical techniques and computational tools to accurately extract the information on the transverse momentum dependence of the quarks and gluons from the existing experimental data. Our work has two main thrusts. First, we focus on transverse spin dependent experimental observables, which are very sensitive to the parton's transverse motion through a correlation between the transverse spin and the transverse momentum. Second, we study the novel nuclear dependence in lepton/proton-nucleus collisions, in which the effects of parton's transverse momentum can be amplified by the nuclear size. Our theoretical framework has been used to map out important novel elements of the nucleon structure, and to explain new exciting experimental data from the HERMES experiment at DESY, COMPASS experiment at CERN, Relativistic Heavy Ion Collider (RHIC) at Brookhaven National Laboratory (BNL), and Large Hadron Collider (LHC) at CERN.

Background and Research Objectives

The theoretical study and experimental exploration of the internal structure of nucleons (protons and neutrons) and nuclei are of fundamental importance to science and have recently entered a new exciting phase. In the past decades an understanding of nucleons in terms of quarks and gluons, the degrees of freedom of QCD, has successfully emerged. Progress has been made in constructing a "one-dimensional" picture of the nucleon, in the sense that we "only" know about the longitudinal motion of partons in fast moving protons and neutrons. In the last few years theoretical breakthroughs have paved the way to extending this simple picture in the transverse as well as longitudinal momentum space (2+1 dimensions). This new information is encoded in the novel concept of "Transverse Momentum Dependent parton distributions" (TMDs), which help address the long-standing questions concerning the motion of quarks and gluons inside the nucleon. How do they move in the transverse plane? Do they orbit, and carry orbital angular momentum? How is the motion modified in the nuclear environment?

Since the transverse momentum component of a parton is usually much smaller than its longitudinal component, it is critical but very difficult to design sensitive experimental observables and develop accurate theoretical tools to extract this information. The main goal of this project is to accomplish precisely that, thereby bridging the biggest gap in our understanding of the nucleon and nuclear structure at very high energies. A cornerstone result of this research will be to construct for the first time accurate 3D images of nucleons and nuclei in terms of the elementary constituents of matter. We attacked this problem through two unique but complimentary approaches. One is through the transverse spin dependence of experimental observables, since transverse spin can correlate with the parton's transverse momentum in the correlation observables. The other way is through a discovery of a novel nuclear dependence, as the small

transverse motion can be amplified by the large nuclear size. Focusing on the spin dependence, we set up a general formalism to evaluate the measured transversely polarized cross sections. Such type of cross sections can be directly linked to the TMDs within the theory, and thus the analysis of the experimental data of such kind leads to important extraction of the associated TMDs. On the other hand, anomalous large nuclear dependence has been measured for a series of experimental observables in processes involving large nuclei. Such nuclear dependences provide further information on the parton's transverse motion and its modification in large nuclei. Understanding such novel nuclear dependence not only solves experimental puzzles, but also provides unique ways to extract parton's transverse motion.

Scientific Approach and Accomplishments

During the three-year course of this project, we achieved the major goals outlined in our original proposal. 22 Journal papers were published and 20 invited talks were given at the international conferences/workshops. We have developed a solid theoretical framework that can utilize both methods to pinpoint the partons' transverse motion. For the spin-dependent observables, since data is often taken at different energies, we derived the energy evolution of the TMDs to interpret all experimental data in a unified framework. By resumming subsets of partonic scattering processes to all orders through these evolution equations, we improved the precision of the theoretical predictions by almost an order of magnitude. In particular, we have used this newly developed theoretical tool to perform the global analysis of the so-called Sivers function. The Sivers function describes the unpolarized quark distribution inside a polarized nucleon through a correlation between transverse momentum of the parton and transverse spin of the nucleon. The relevant transverse spin asymmetries (associated with Sivers function) have been measured by HERMES, COMPASS, and JLab experiments through semi-inclusive deep inelastic scattering (SIDIS) process. With derived factorization framework (next-to-leading logarithmic accuracy), we extracted the Sivers function (both longitudinal dependence and transverse momentum behavior) through global fitting of existing experimental data. We further made predictions for the spin asymmetries for Drell-Yan process in proton-proton collisions. We then extended such a study to the transverse momentum dependent fragmentation functions, where the generated hadron has transverse momentum dependence with respect to the fragmenting parton in the hadronization process. One of the most important TMD fragmentation functions is called the Collins function. We extract the functional form of these functions from the spin asymmetries at SIDIS and e+e- experimental data.

On the nuclear dependence part, we computed multiple scattering effects in the backward rapidity region for both light hadron and heavy meson production in p+A collisions. Such multiple scattering is generated through the small transverse momentum kicks from the partons inside the large nuclei, and thus provides precisely the magnitude of the parton transverse momentum. Our calculation provided a first explanation for the enhanced cross sections in this region as measured by both RHIC and LHC, and described the experimental data rather well. We further performed the first calculation of the multi-parton interaction contributions to the e+A and p+A collision cross sections with full next-to-leading order accuracy, which finally allow us to reliably constrain the partons' transverse motion inside a big nucleus.

Impact on National Missions

This project positioned LANL as one of the leaders of the theoretical effort to understand the quark and gluon transverse motion in nucleons and nuclei, relevant to experiments at all collider facilities that push the limits of our understanding of the theory of strong interactions at very high energies. Besides providing new and unique 3D-imaging information for the nucleon structure at unprecedented level, this project also give essential insights into how the QCD quark and gluon dynamics are modified in a large nucleus. It produced theoretical tools for the community to accurately and reliably extract such information from data collected at JLab, HERMES, COMPASS, RHIC and LHC, which provided much-needed theoretical guidance for and interpretation of the experimental results from the flagship hadronic and nuclear physics program at LANL, in the U.S. and abroad. This project also helped firm the scientific case for a future Electron Ion Collider.

Publications

Aschenauer, E. C., A. Bazilevsky, K. Boyle , R. Fatemi , C. Gagliardi, M. Grosse-Perdekamp, Z. B. Kang, Y. Kovchegov, and J. Lajoie. The RHIC Spin Program: Achievements and Future Opportunities . 2013. White Paper on RHIC spin physics to the Tribble Panel and Nuclear Science Advisory Committee.

Dai, L. Y., Z. B. Kang, A. Prokudin, and I. Vitev. Next-to-leading order transverse momentum-weighted Sivers asymmetry in semi-inclusive deep inelastic scattering: the role of the three-gluon correlator. PHYSICAL REVIEW D. 92: 114024.

Echevarria, M. G., A. Idilbi, Z. B. Kang, and I. Vitev. QCD Evolution of the Sivers Asymmetry. 2014. PHYSICAL REVIEW D. 89: 074013.

Gamberg, L., Z. B. Kang, A. Metz, D. Pitonyak, and A. Prokudin. Left-right spin asymmetry in ℓN↑→hX. 2014.

PHYSICAL REVIEW D. 90 (7): 074012.

Gamberg, L., Z. B. Kang, I. Vitev, and H. Xing. Quasi-parton distribution functions: a study in the diquark spectator model. 2015. PHYSICS LETTERS B. 743: 112.

Gamberg, L., Z. B. Kang, and A. Prokudin. Indication on the process-dependence of the Sivers effect. 2013. Physical Review Letters. 110 (23): 232301.

Huang, J., Z. B. Kang, I. Vitev, and H. Xing. Spin asymmetries for vector boson production in polarized p+p collisions . 2016. PHYSICAL REVIEW D. 93: 014036.

Huang, J., Z. B. Kang, and I. Vitev. Inclusive b-jet production in heavy ion collisions at the LHC . 2013. PHYSICS LETTERS B. 726: 251.

Kang, Z. B.. Polarized p+A, single spin asymmetries. Invited presentation at BNL-LANL-RBRC Joint Workshop on The Physics of p+A Collisions at RHIC. (Upton, NY, 7-9 Jan. 2013).

Kang, Z. B.. Single transverse spin asymmetries in polarized SIDIS and pp scattering. Invited presentation at The 5th Workshop of the APS Topical Group on Hadronic Physics. (Denver, CO, 10-12 Apr. 2013).

Kang, Z. B.. Forward physics from a theoretical perspective. Invited presentation at STAR Meeting on eSTAR Letter of Intent, Forward-Upgrades and Results from U+U Collisions. (Los Angeles, CA, 28-30 Aug. 2013).

Kang, Z. B.. Double parton fragmentation function and its evolution in quarkonium production . 2014. In QCD Evolution 2013. (Newport News, VA, 6-10 May 2014). Vol. 25, p. 1460040 . Singapore: International Journal of Modern Physics.

Kang, Z. B.. Unique opportunities in p+A collisions at RHIC and LHC. Invited presentation at APS Division of Nuclear Physics 2014 Long-range plan: Joint Town Meetings on QCD. (Philadelphia, PA, 13-15 Sept. 2014).

Kang, Z. B.. Nucleon spin: longitudinal, transverse, and evolution. Invited presentation at 2014 RHIC and AGS Annual Users Meeting. (Upton, NY, 17-20 June 2014).

Kang, Z. B.. TMD evolution of Sivers asymmetry. Invited presentation at Studies of 3D Structure of Nucleon. (Seattle, WA, 24-28 Feb. 2014).

Kang, Z. B.. QCD evolution of TMDs: what works?. Invited presentation at Indiana-Illinois Workshop on Fragmentation Functions. (Bloomington, IN, 12-14 Dec. 2013).

Kang, Z. B.. TMDs: Mechanisms/universality with ep and pp collisions. Invited presentation at QCD Frontier 2013. (Newport News, VA, 21-22 Oct. 2014).

Kang, Z. B.. TMD evolution and global analysis. Invited presentation at The 6th Workshop of the APS Topical Group on Hadronic Physics. (Baltimore, MD, 8-10 April 2015).

Kang, Z. B., A. Prokudin, P. Sun, and F. Yuan. Nucleon tensor charge from Collins azimuthal asymmetry measurements . 2015. PHYSICAL REVIEW D. 91: 071501.

Kang, Z. B., A. Prokudin, P. Sun, and F. Yuan. Extraction of Quark Transversity Distribution and Collins Fragmentation Functions with QCD Evolution. 2016. PHYSICAL REVIEW D. 93: 014009.

Kang, Z. B., E. Wang, X. N. Wang, and H. Xing. Next-to-Leading QCD Factorization for Semi-Inclusive Deep Inelastic Scattering at Twist-4 . 2014. Physical Review Letters. 112: 102001 .

Kang, Z. B., I. Vitev, E. Wang, H. Xing, and C. Zhang. Multiple scattering effects on heavy meson production in p+A collisions at backward rapidity . 2015. PHYSICS LETTERS B. 740: 23.

Kang, Z. B., I. Vitev, and H. Xing. Transverse momentum-weighted Sivers asymmetry in semi-inclusive deep inelastic scattering at next-to-leading order. 2013. Physical Review D. 87 (3): 034024.

Kang, Z. B., I. Vitev, and H. Xing. Next-to-leading order forward hadron production in the small-x regime: the role of rapidity factorization . 2014. PHYSICAL REVIEW LETTERS. 113: 062002.

Kang, Z. B., I. Vitev, and H. Xing. Multiple scattering effects on inclusive particle production in the large-x regime . 2013. PHYSICAL REVIEW D. 88: 054010.

Kang, Z. B., I. Vitev, and H. Xing. Initial-state cold nuclear matter energy loss effects on inclusive jet production in p+A collisions at RHIC and LHC. 2015. PHYSICAL REVIEW C. 92: 054911.

Kang, Z. B., R. Lashof-Regas, G. Ovanesyan, P. Saad, and I. Vitev. Jet quenching phenomenology from soft-collinear effective theory with Glauber gluons. 2015. PHYSICAL REVIEW LETTERS. 114 (9): 092002.

Kang, Z. B., S. Mantry, and J. W. Qiu. Probing nuclear dynamics in jet production with a global event shape . 2013. Probing nuclear dynamics in jet production with a global event shape . 88: 074020.

Kang, Z. B., X. Liu, and S. Mantry. The 1-Jettiness DIS event shape: NNLL + NLO results. 2014. PHYSICAL REVIEW D. 90: 014041.

Kang, Z. B., Y. Q. Ma, J. W. Qiu, and G. Sterman. Heavy Quarkonium Production at Collider Energies (I): Factorization and Evolution. 2014. PHYSICAL REVIEW D. 90:

034006.

Kang, Z. B., Y. Q. Ma, J. W. Qiu, and G. Sterman. Heavy Quarkonium Production at Collider Energies: Partonic Cross Section and Polarization . 2015. PHYSICAL REVIEW D. 91 (1): 014030.

Kang, Z. B., Y. Q. Ma, and R. Venugopalan. Quarkonium production in high energy proton-nucleus collisions: CGC meets NRQCD. 2014. Journal of High Energy Physics. 01: 056.

Kang, Z. B., and B. Xiao. Sivers asymmetry of Drell-Yan production in the small-x regime. 2013. Physical Review D. 87 (3): 034038.

Vitev, I.. Transv. Invited presentation at Transverse momentum-weighted Sivers asymmetry in semi-inclusive deep inelastic scattering at next-to-leading order. (Newport News, VA, 6-10 May 2013).

New Tools to Probe Matter with an Electron-Ion Collider

Christopher Lee
20140671PRD2

Abstract

Protons and neutrons (hadrons) were once thought to be indivisible elementary constituents of ordinary matter. One of the greatest discoveries of the 20th Century, through electron-proton collisions, was that hadrons themselves are made of smaller "quarks." We also discovered that quarks are bound together by gluons, which transmit the force called the strong interaction. Now in the 21st Century, the focus of US nuclear physics is to map out the structure of this dynamic system in unprecedented detail at a new Electron Ion Collider (EIC), which will collide high-energy electrons and protons to probe their internal structure and test predictions of Quantum Chromodynamics (QCD), the theory of the strong interaction. Crucial measurements will include the strength of the interaction between quarks and gluons, called the strong coupling, and the 3-D momentum distribution of all the different kinds of quarks and gluons within the proton. One treasure trove of information in EIC collisions will be hadronic jets, collimated bunches of strongly interacting particles produced by the collisions. In the last decade, a powerful theoretical tool called soft-collinear effective theory (SCET) has led to unprecedentedly precise predictions for jet production, including determination of the strong coupling to incredible precision < 1% in electron-positron collisions. However, the value extracted this way disagrees with numerical simulations of strong interactions by more than 3 standard deviations, a puzzle urgently demanding resolution.

Our work has contributed to pushing the frontier of precision jet physics at the EIC using SCET. Together with the EIC, a concomitant effort to improve accuracy of theoretical predictions is essential. Our work on 2-jet production in electron-proton collisions has led to new methods to compute jet cross sections to any desired accuracy. We have used this power to compute EIC jet cross sections to the highest precision to date, allowing us to use future EIC data to resolve the existing discrepancies in determining the strong coupling.

Background and Research Objectives

The goals of this project included predicting cross sections to produce two hadronic jets at EIC (Figure 1) to the highest precision to date, and so reduce theoretical uncertainty by up to an order of magnitude, and then to predict multi-jet production in EIC collisions, which exhibit even greater sensitivity to the strong coupling, alpha_s. These results will make possible the most precise extractions of alpha_s from DIS data and shed light on the current tension among different methods of extraction. alpha_s is a fundamental constant of nature and affects all predictions at colliders involving the strong interaction.

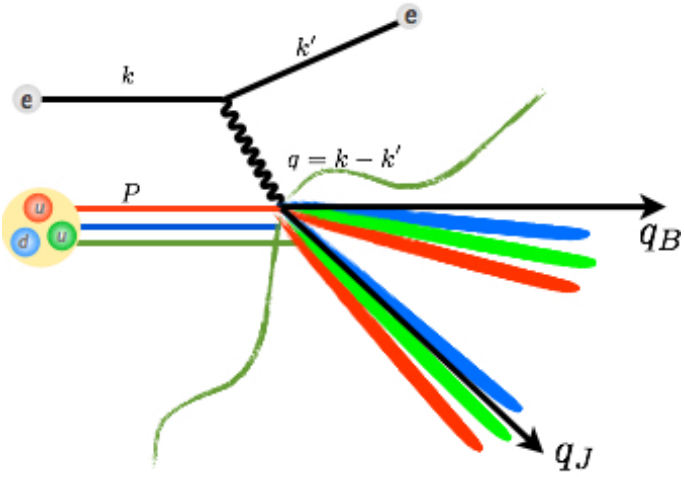

Figure 1. Deep inelastic scattering (DIS) of an electron and a proton. The proton is broken apart by the electromagnetic interaction in the collision with the electron. A jet of quarks and gluons (which bind into hadrons) is created along the direction qJ, and radiation from the proton itself creates a jet in direction qB. 1-jettiness event shape observables measure the degree to which the final-state hadrons are collimated along these two directions.

2-jet production in electron-positron (e+e-) collisions have long been one of the most precise sources of information about the strong coupling. In the past

several years, theoretical advances in SCET have led to unprecedentedly precise (one percent uncertainty) predictions in QCD perturbation theory for 2-jet cross sections in e+e- collisions, as well as rigorous treatment of the dominant nonperturbative effects, which cannot be computed perturbatively (as a power expansion in alpha_s) and are due to the strong binding of quarks and gluons into hadrons. The improved theoretical predictions as a function of alpha_s can be compared to world's data on these collisions. Doing this while including nonperturbative effects yields a value for the strong coupling measured at the energy scale of the Z-boson mass of alpha_s(M_Z) = 0.1123 +/- 0.0011. This is in tension with the world average using all methods of determination of the strong coupling, alpha_s(M_Z) = 0.1186 +/- 0.0007. (Figure 2) These are in significant disagreement. The reason for the discrepancy is still unknown. This is an unsatisfactory state of affairs about one of the most fundamental quantities in Nature.

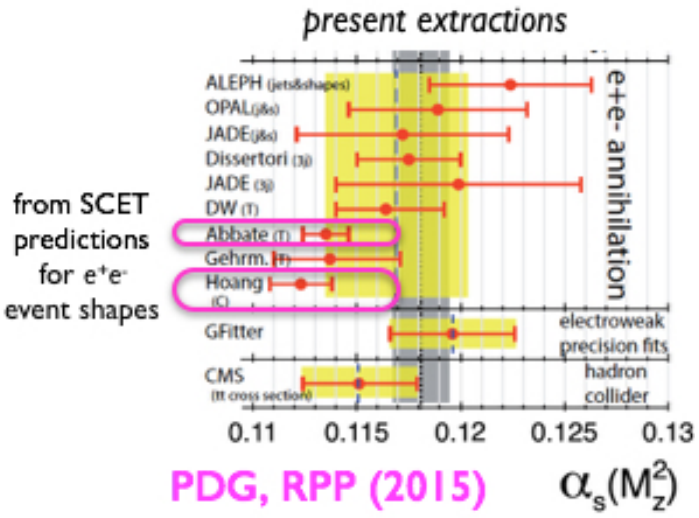

Figure 2. Soft collinear effective theory (SCET) methods have produced predictions for similar event shapes in electron-positron (e+e-) collisions that yield some of the most precise determinations in the world of the strong coupling alpha_s. However the extracted value is significantly lower than the world average, and the source of this discrepancy remains a mystery.

The goal of this project was to make similar theoretical advances in predictions for 2-jet cross sections in electron-proton collisions or deep inelastic scattering (DIS). We measured the 2-jet structure of the final state with an observable called 1-jettiness (1 for the jet that is additional to the one created by radiation directly from the proton beam). By applying the same theoretical techniques to a completely different collider environment, and performing a similar determination of alpha_s from these data, we can hope to identify the cause of the above discrepancy as a theoretical or experimental issue. A reliable value for alpha_s is crucial for accurate predictions in all hadronic colliders and for our understanding of the fundamental force binding the constituents of all ordinary matter.

Scientific Approach and Accomplishments

We have focused on computing cross sections in Deep Inelastic Scattering (DIS) of electrons and protons, differential in one of several event shape variables known as "N-jettiness". These measure the degree of collimation of final state hadrons into N energetic "jets" in addition to radiation along the beam direction. We measure final states with two total jets in DIS with 1-jettiness.

In November 2014, together with Iain Stewart at MIT, we published a paper in the Journal of High-Energy Physics on "Analytic Calculation of 1-Jettiness in DIS at O(alpha_s)" (JHEP 1411, 132) on the fixed-order computation in Quantum Chromodynamics (QCD) of the 1-jettiness distribution in Deep Inelastic Scattering (DIS) to first order in the strong coupling constant alpha_s. This enables a more precise prediction of the 1-jettiness (tau_1) distribution at large values of tau_1. This is an important step towards predicting DIS jet cross sections to a precision sufficient to perform percent-level extractions of alpha_s from experimental measurements.

In September 2015, together with PhD student O. Labun at Arizona, we published a paper in Physics Letters B (PLB 748, 45-54) on "Equality of hemisphere soft functions for e+e-, DIS, and pp collisions at O(alpha_s^2)" on two-loop, or second order in the strong coupling alpha_s, soft functions that contribute to event shape distributions in the three types of collisions. These functions describe the effect of soft gluon radiation on jet cross sections in these collisions and are an essential ingredient to achieve percent-level accuracy in perturbation theory for jet distributions. Since the e+e- (electron-positron) 2-loop soft function was already known, our proof of equality of the e+e-, DIS, and pp (proton-proton) soft functions immediately fills our previous gap in knowledge of the corresponding soft functions for DIS and pp.

In the last year of the project, we put together the above ingredients along with other necessary results from our own past work and as well as other recent results from other groups around the world. We have completed our prediction of DIS 1-jettiness cross sections to so-called next-to-next-to-next-to-leading logarithmic (NNNLL) accuracy in resummed perturbation theory in QCD, never before achieved for DIS observables, and necessary for reaching percent-level theoretical uncertainties (Figure 3). We are in the final stages of preparing a publication on this groundbreaking calculation. We have already presented preliminary results from this work at various interna-

tional workshops. The work has attracted the attention of physicists both working on the future EIC as well as a group at the DESY Laboratory in Germany, which ran DIS experiments in the past and is still analyzing its archived data. DESY has already performed analyses of its data to obtain cross sections for our 1-jettiness variables. We have begun a collaboration to combine our predictions with their analyses to obtain a determination of alpha_s. This would be a landmark step before the EIC can be built and run. We anticipate publications both on the theoretical work and the experimental analysis to follow on soon after the formal close of this project. Postdoc Daekyoung Kang is continuing at LANL for a third year, supported by a DOE Early Career grant won by PI Christopher Lee, to complete this work.

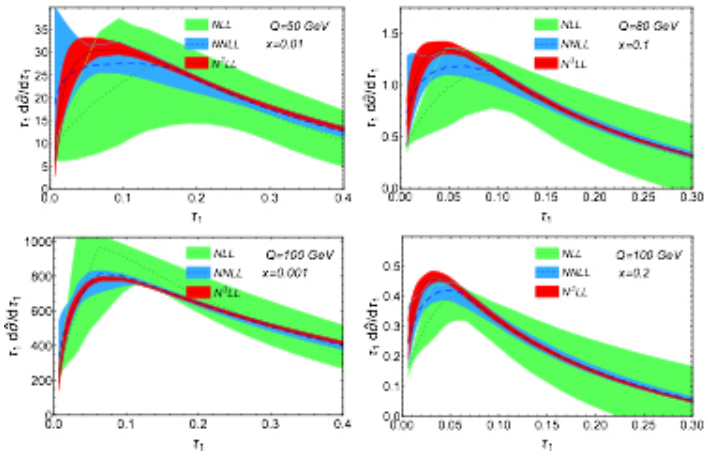

Figure 3. Preliminary results for 1-jettiness distributions in DIS achieved by this project. The red bands are at the so-called next-to-next-to-next-to-leading logarithmic accuracy, that is, three orders of subleading accuracy in resummed QCD perturbation theory. The remaining theoretical uncertainty.

Impact on National Missions

This research is directly aligned with LANL and national priorities in physics at a future electron-ion collider (EIC), a machine that plans to probe the structure of the proton and the nature of the strong interaction in unprecedented detail. The proton is a ubiquitous component of all ordinary matter in the universe, and the strong interaction is what binds the constituents of the proton (quarks and gluons) together and protons and neutrons to each other in nuclei. Understanding protons and the strong interaction is key to our fundamental understanding of Nature. Central to this research was the development and application of Soft Collinear Effective Theory (SCET) to provide the high precision predictions necessary to interpret the unprecedentedly detailed data on nucleon structure that will come from EIC. The calculations we performed will allow us to use EIC data to resolve current disagreements in measurements of the strong coupling, a fundamental constant affecting all studies of nuclear matter (e.g. LHC, RHIC). EIC physics and SCET are high priorities under the LANL Nuclear & Particle Futures Pillar, under the research thrust "Advancing our understanding of QCD and the fundamental properties of nuclear matter." The 2015 NSAC Long-Range Plan for DOE identified construction of the EIC as its top recommendation for future facility construction; this research strengthens LANL and US leadership in this exciting international endeavor.

Publications

Kang, D.. DIS Event Shapes at N3LL. Invited presentation at DIS 2015: XXIII International Workshop on Deep-Inelastic Scattering and Related Subjects. (Dallas, TX, 27 Apr - 1 May 2015).

Kang, D., C. Lee, and I. W. Stewart. Analytic Calculation of 1-Jettiness in DIS at O(alpha_s). 2014. Journal of High-Energy Physics. 11: 132.

Kang, D., O. Z. Labun, and C. Lee. Equality of hemisphere soft functions for e+e−, DIS and pp collisions at O(alpha_s^2). 2015. Physics Letters B. 748: 45.

Electric Dipole Moments of Hadrons from Lattice Quantum ChromoDynamics

Vincenzo Cirigliano
20140673PRD2

Abstract

Permanent electric dipole moments (EDMs) of elementary particles and certain atomic nuclei, atoms, and molecules, violate the discrete symmetries of time reversal (T) and parity (P), or equivalently CP, where C is the charge conjugation operation. Since CP is the symmetry that interchanges particles with antiparticles, the laboratory study of EDMs in closely tied to the mystery of the matter-antimatter asymmetry in the universe. In this project we studied strong-interaction uncertainties that affect the determination of the electric dipole moment of nucleons (neutron, proton) and nuclei. We have developed a strategy for a substantial reduction of the uncertainties affecting the determination of important couplings, such as time reversal violating pion-nucleon couplings. We applied this strategy to the leading source of CP violation in strong interactions (the so-called theta term), determining the leading pion-nucleon coupling with 10% uncertainty. For a class of operators induced by physics beyond the Standard Model (BSM) we have also derived relations between the pion-nucleon couplings and modifications to the particle masses. We have studied their robustness and set the stage for a computational implementation within lattice quantum chromodynamics (QCD), which describes the strong nuclear force in the non-perturbative regime.

The theoretical uncertainties that affect first principle calculations of the nucleon and nuclear EDMs have a strong impact on the constraints imposed by EDM experiments on models of BSM physics. In light of the discovery of the Higgs boson at the LHC, we studied the complementarity between collider and EDM experiments in determining CP-violating interactions of the Higgs boson to quark and gluons. We found that existing uncertainties in hadronic and nuclear matrix elements have a significant impact on the interpretation of EDM experiments, and we quantified the improvements needed to fully exploit the power of EDM searches. While with the current theoretical uncertainties the best bounds on the anomalous time-reversal violating Higgs interactions come from a combination of EDM measurements and the data from LHC Run 1, future theoretical and experimental EDM developments will greatly improve the reach of EDM experiments, putting them out of the LHC reach.

Background and Research Objectives

The observation of a permanent electric dipole moment would be a clear signal of physics beyond the Standard Model. In fact, while the Standard Model has a source of CP violation (the phase of the Cabibbo-Kobayashi-Maskawa (CKM) quark mixing matrix), this phase generates EDMs that are orders of magnitude away from the experimental capabilities. Thus EDM experiments are free of any SM background, and a non-null result in any of the next generation experiments will be an exciting evidence of new physics. For this reason, several new EDM experiments have been planned and will be realized in the next few years, with the goal of improving EDM bounds by one to two orders of magnitudes. These experiments will use different systems, going, in order of complexity, from the muon, to the neutron, proton, and light nuclei, to diamagnetic and paramagnetic atoms, and molecules.

While an EDM signal will indicate new physics, taking full advantage of the experimental information to discriminate between possible new physics models is a much more complicated problem, involving physics on a wide range of scales, from the low-energy atomic and nuclear scales at which the experiments are performed, to the high-energy scale where the T-violating dynamics originates. In particular, the expression of the nucleon, nuclear and atomic EDMs in terms of the parameters of the BSM theory at high energy requires the calculation of hadronic and nuclear matrix elements of CP-violating operators, a problem complicated by the non-perturbative nature of QCD at scales around the mass of proton, mp.

This difficulty is reflected in the unsettled status of the determination of such matrix elements. At energy scales around mp, after integrating out heavy degrees of freedom such as the Higgs, W and Z bosons, or the top quark, time reversal violation is parameterized in terms of a handful of operators, including the QCD theta term, the electric and chromo-electric dipole moments of the light quarks (qEDMs and qCEDMs) and the gluon chromo-electric dipole moment (gCEDM). These operators induce at low energy T-violating couplings between nucleons, pions and photons. The most important nucleon-photon couplings are the neutron and proton EDMs, which, in addition to their intrinsic interest, determine the single-body component of the EDMs of light nuclei, such as deuteron or 3He. In addition, a very important role is played by pion-nucleon couplings, which mediate long-range T-violating nucleon-nucleon forces, crucial for the computation of nuclear EDMs, from deuteron to mercury. These pion-nucleon couplings can respect the isotopic symmetry of nuclear forces (isoscalar term g0) or violate it (isovector term g1).

The T-violating isoscalar pion-nucleon coupling g0 induced by the leading T-violating quark-gluon coupling, the so-called QCD theta term, has been estimated a long time ago (see [1] and references therein), using the so-called flavor symmetry of strong-interactions to relate the coupling to the mass difference of the Σ and Ξ baryons. However, a theoretical error was never assigned to the estimate, which we found to over-estimate g0 by 50%. For other operators, the estimates are affected by even larger errors. For example, sum rule calculations of g0 and g1 induced by the qCEDM have 100% theoretical uncertainties [1].

Similarly, at the beginning of this project there were a few lattice QCD calculations of the nucleon EDM induced by theta, at values of the pion mass far from the physical value [5], and no lattice calculations for the remaining sources. The nucleon EDM from the qCEDM or the gCEDM was estimated with QCD sum rules, again with errors in the 50% to 200% range [1]. These large uncertainties, if taken seriously, considerably weaken the constraints on new physics scenarios [2,3,4].

Scientific Approach and Accomplishments

The main goal of the project was to devise strategies that, combining tools from low-energy Effective Field Theories and Lattice QCD, could improve the theoretical knowledge of CP-violating couplings, leading to more solid constraints on new physics scenarios.

In Ref. [5], we reanalyzed the T-violating pion nucleon coupling g0 induced by the QCD theta term, in the framework of Chiral Perturbation Theory (ChiPT). In the two-flavor theory, where only the u and d quarks are considered light, chiral symmetry relates g0 to the component of the neutron-proton mass difference arising from the different light quark masses. The framework of ChiPT allows one to systematically study higher order corrections to this relation, which we found to be very robust, and violated only by finite next-to-next-to leading order terms, to which we conservatively assigned a size of at most 10%. We then repeated the analysis adding the strange quark. In addition to the relation to the nucleon mass splitting, the larger symmetry group allows, at leading order, to express g0 in terms of other baryon masses, such as the Σ and Ξ baryons mass difference. However, our analysis shows that these additional relations are badly broken by higher order corrections, and are unreliable for a precise determination of g0. Using recent accurate lattice calculations of the neutron-proton mass splitting, we were able to obtain a new determination of g0. The central value is about 40% lower than previous estimates, and, more importantly, the theoretical uncertainties are estimated (for the first time) at the 15% level, including lattice and ChiPT errors.

In Ref.[6], we found analogous relations between T-violating pion-nucleon couplings and corrections to baryon and meson spectrum, induced by the chiral partner of the qCEDM, the quark chromo-magnetic dipole moment (qCMDM). In work nearing completion, we identified relations that are stable under loop corrections, both in two and three-flavor ChiPT, and are thus suitable for the determination of g0 and g1. Differently from the case of the QCD theta term, the chiral symmetry relations require new, dedicated lattice QCD calculations of the modifications of the baryon and meson spectrum in the presence of a qCMDM. While challenging, these calculations are much simpler than a direct evaluation of the pion-nucleon couplings on the lattice, and preliminary studies are underway.

A necessary step for performing lattice QCD calculations of matrix elements of CP-violating operators, and for combining these results with perturbative calculations of the coefficients of the operators in terms of high-energy couplings, is the establishment of the correct definition of T-violating operators, both in the continuum and on the lattice, and the calculation of the conversion factors between lattice and continuum operators. This seemingly trivial task is complicated by quantum effects: the short distance behavior of loop diagrams causes the appearance of divergences, which need to be subtracted. These divergences cause the mixing of the qCEDM operator with other CP-violating operators of the same or lower dimension, such as the QCD theta term, so that, without the definition of a subtraction scheme ("renormalization scheme"), the definition of an operator is ambiguous.

In Ref. [7] we discussed the renormalization of the qCEDM

operator, both in the continuum and on the lattice. We studied the divergence structure of the operator, and identified all the possible mixings. Then, we defined a renormalization scheme that can be easily implemented in the continuum and on the lattice, and computed the conversion factors between this scheme and the most popular continuum scheme, the "minimal subtraction" scheme, at one loop. Following our work, the first preliminary lattice studies of the nucleon EDM induced by the qCEDM have appeared [8]. An analogous study for gCEDM operator, with an analysis of its divergence structure and the definition of a subtraction scheme, is underway.

Finally, in Ref. [2,3,4] we analyzed the phenomenological implications of EDM bounds. The most important result, so far, of the Large Hadron Collider (LHC) has been the discovery of the last missing piece of the SM, the Higgs boson, with a mass of 125 GeV and interactions close to the SM expectations. In the light of this extraordinary discovery, we asked the question of how much the couplings of the Higgs are constrained by low-energy precision experiments, in particular by EDMs. Secondly, we tried to assess the role of hadronic uncertainties, and the level of accuracy required for EDMs to compete with the LHC.

In Ref. [2], we considered the couplings of the Higgs to quarks and gluons. We once again worked in an Effective Field Theory framework, and added to the SM a complete set of CP-violating operators, constructed with SM fields and respecting the SM gauge symmetry, but with higher canonical dimension, meaning that the operators are suppressed by powers of the high energy scale Λ where T violation arises. We investigated direct and indirect constraints on anomalous CP-violating Higgs couplings to quarks and gluons, by studying their signatures at the LHC and in EDMs. We showed that existing uncertainties in matrix elements have a significant impact on the interpretation of EDM experiments, and we quantified the improvements needed to fully exploit the power of EDM searches.

For example, in Figure 1 we show the limits on the imaginary part of the u and d Yukawa couplings coming from the neutron and mercury EDMs, for different matrix element strategies. If the theoretical uncertainties are not taken into account, the EDMs of the neutron and mercury are very complementary, leading to very strong constraints on both Yukawa couplings. However, once uncertainties are taken into account, severe cancellations are possible, leading to a free direction in the Yu – Yd plane. As shown by the thick dashed line, a modest reduction of the theory errors can close the free direction, and restore strong bounds.

With the current large theoretical uncertainties, the best bounds on the anomalous T-violating Higgs interactions come from a combination of EDM measurements and the data from LHC Run 1. We showed that Higgs production cross section and branching ratios measurements at the LHC Run 2 will not improve the constraints significantly. On the other hand, the bounds on the couplings scale roughly linearly with EDM limits, so that future theoretical and experimental EDM developments can have a major impact in pinning down interactions of the Higgs.

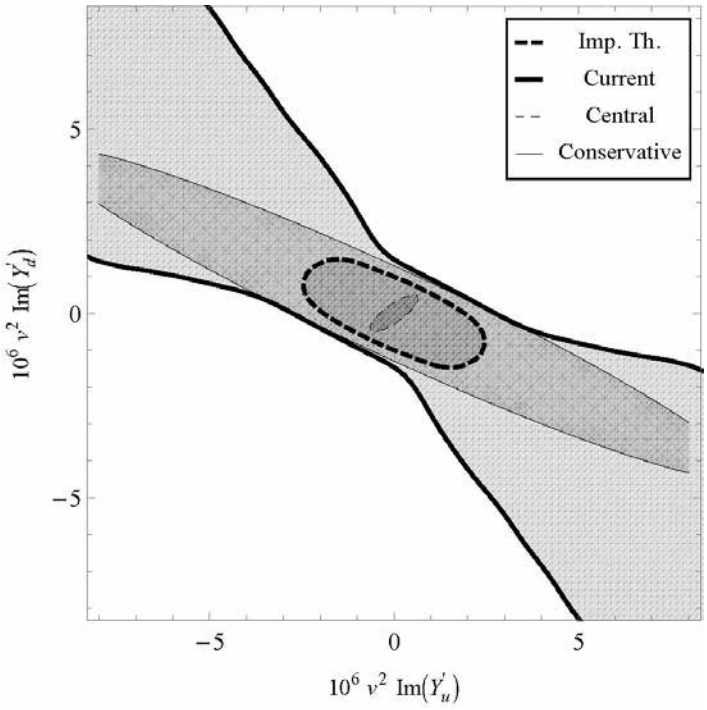

Figure 1. 90% confidence level contours on the imaginary part of the Yukawa couplings of the and quarks to the Higgs, coming from the neutron and mercury EDM bounds. The contours are shown for the three different matrix elements strategies: (thin dashed line), (thin), and (thick). In the strategy no theoretical uncertainty is assigned to the matrix elements. This is the usual method of deriving EDM constraints on BSM physics. The and strategies account for the theoretical uncertainties, the strategy being the most realistic. The thick dashed line denotes the contour that can be achieved with improved matrix elements

In Refs. [3,4], we investigated in more detail the top-Higgs sector, which, in many popular BSM models, is the most affected by new physics. Our analysis included constraints from collider observables, precision electroweak tests, flavor physics, and EDMs. For CP-violating observables, we found that indirect probes are competitive or dominant, even after accounting for uncertainties associated with hadronic and nuclear matrix element. In particular, we found that the electron EDM puts constraints on the electroweak CP-violating dipole moments of the top that are 2 to 3 orders of magnitude stronger than existing limits, putting these couplings out of the LHC reach (see Figure 2).

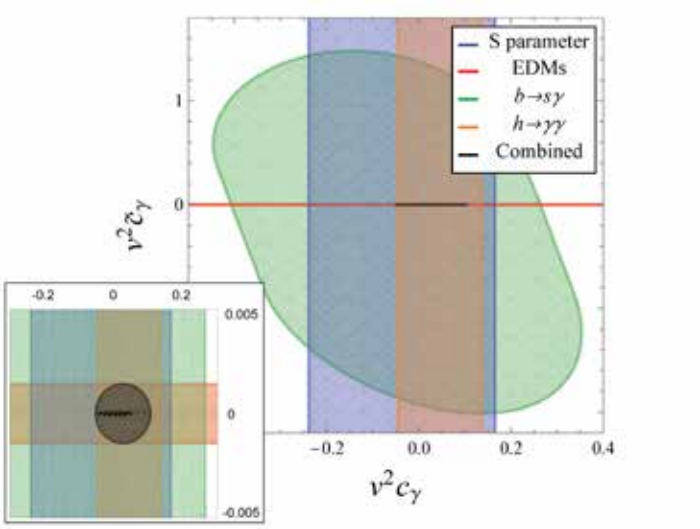

Figure 2. 90% confidence level allowed regions in the plane of top quark magnetic dipole moment (horizontal axis) and electric dipole moment (vertical axis), in unit of 1/v, where v=246 GeV. The couplings are evaluated at the scale L = 1 TeV. The inset zooms into the current combined allowed region, and shows projected future sensitivities. The red band denotes the bound from the electron EDM, which is three orders of magnitude stronger than bounds from other processes considered in previous literature. The green area shows the bounds from rare B meson decays, the blue and orange bands are, respectively, the limits derived from the electroweak precision observables, such as the S parameter, and from the branching ratio for Higgs decays into two photons measured at the Large Hadron Collider.

Impact on National Missions

Understanding the origin of the matter-antimatter asymmetry of the universe is one of the greatest challenges at the interface of nuclear physics, particle physics, and cosmology, and is a top priority for the DOE/SC Offices of Nuclear Physics and High Energy Physics. LANL already plays a leadership role on both the experimental and theoretical aspects of this problem, with considerable DOE/SC investments dedicated to the search of the neutron EDM. In the context of the theory effort, this project has played key role in sharpening the interpretation of null or positive neutron EDM searches in terms of yet undiscovered new interactions originating at very high energy, which may have played a critical role in the evolution of the early universe.

References

1. Engel, J., M. Ramsey-Musolf, and U. van Kolck. Electric Dipole Moments of Nucleons, Nuclei, and Atoms: The Standard Model and Beyond. 2013. Prog. Part. Nucl. Phys.. 71: 21.

2. Chien, Y. T., V. Cirigliano, W. Dekens, et.al. Direct and indirect constraints on CP-violating Higgs-quark and Higgs-gluon interactions. 2016. Journal of High Energy Physics. 16 (02): 11.

3. Cirigliano, V., W. Dekens , E. Mereghetti, and J. de Vries. Is there room for CP violation in the top-Higgs sector?. 2016. Physical Review D . 94 (1): 016002.

4. Cirigliano, V., W. Dekens, et.al. Constraining the top-Higgs sector of the Standard Model Effective Field Theory. 2016. Physical Review D. 94 (3): 034031.

5. Vries, J. de, E. Mereghetti, and A. Walker-Loud. Baryon mass splittings and strong CP violation in SU(3) Chiral Perturbation Theory. 2015. Physical Review C. 92: 4.

6. Mereghetti, E., and U. van Kolck. Effective field theory and time-reversal violation in light nuclei. 2015. Annual Reviews in Nuclear and Particle Physics. 65: 215.

7. Bhattacharya, T., V. Cirigliano, R. Gupta, E. Mereghetti, and B. Yoon. Dimension-5 CP-odd operators: QCD mixing and renormalization. 2016. Physical Review D. 92 (11): 114026.

8. Bhattacharya, T., V. Cirigliano, R. Gupta, E. Mereghetti, and B. Yoon. Neutron electric dipole moment from quark chromo-electric dipole moment. 2016. In Lattice 2015. (Kobe (Japan), 14-18 July 2015). , p. 238. Italy : Proceedings of Science.

Publications

Bhattacharya, T., V. Cirigliano, R. Gupta, et.al. Dimension-5 CP-odd operators: QCD mixing and renormalization. 2016. Physical Review D. 92 (11): 114026.

Chien, Y. T., V. Cirigliano, W. Dekens, et.al. Direct and indirect constraints on CP-violating Higgs-quark and Higgs-gluon interactions. 2016. Journal of High Energy Physics. 16 (02): 11.

Cirigliano, V., W. Dekens , E. Mereghetti, and J. de Vries. Is there room for CP violation in the top-Higgs sector?. 2016. Physical Review D . 94 (1): 016002.

Cirigliano, V., W. Dekens, E. Mereghetti, and J. de Vries. Constraining the top-Higgs sector of the Standard Model Effective Field Theory. 2016. Physical Review D. 94 (3): 034031.

Mereghetti, E., and U. van Kolck. Effective field theory and time-reversal violation in light nuclei. 2015. Annual Reviews in Nuclear and Particle Physics. 65: 215.

Vries, J. de, E. Mereghetti, and A. Walker-Loud. Baryon mass splittings and strong CP violation in SU(3) Chiral Perturbation Theory. 2015. Physical Review C. 92: 4.

Science of Signatures

Chemical Signatures of Detonation Born From Extreme Conditions (U)

David Podlesak
20150050DR

Introduction

The ability to infer information about high explosive (HE) type and design is of high value. Traditional nuclear forensic investigations provide little or no insight into the dynamics of HE detonation. Post-detonation and real-time signatures of explosive test programs and unique materials identifiers are needed, but can only come from a fundamental understanding of the physical processes that lead to their formation and evolution in time. Explosives detonation is an exothermic process whereby metastable, complex molecules are converted to simple, stable molecules and solid carbon, with the type of solid carbon formed depending on the type (composition) of explosive. Recovery studies indicate that several allotropes of solid carbon may form including amorphous graphite, "onion-like" carbon, and detonation nanodiamonds (DND). More recently, carbon graphite-to-diamond ratios have been correlated to explosive type, with high-performance, aromatic-ring based explosives producing the largest quantities of DNDs. We propose to establish an interdisciplinary effort to understand how solid carbon forms and evolves during detonation, develop new models to describe its evolution, and link in situ measurements of signature formation with post-detonation characteristics. A key feature of this effort will be discovery of signature formation in real-time behind the detonation front using in situ time-resolved x-ray scattering at the Advanced Photon Source and U.S. free electron laser beam lines. The formation and evolution of solid carbon (and fluids) will be modeled from formation through chemical equilibrium.

Benefit to National Security Missions

We will establish detonation products as novel chemical signatures of explosive composition, performance, and state. Successful execution of this program will provide models critical to improved weapons simulation and results will be used in DOE/NNSA defense and nuclear nonproliferation programs.

Progress

Task 1: Continue in-house detonation experiments to obtain detonation product samples and use state-of-the-art analytical techniques to determine chemical compositions of detonation products including solids and gases.

We successfully collected detonation products from three high explosives, Composition B, PBX 9501 and PBX 9502. Post det analysis of the soot included Raman, XPS, pXRD analysis, carbon and nitrogen isotopic measurements at multiple scales, as well as static X-ray scattering and TEM imaging. Differences between HE formulations, detonation atmosphere, and peak pressures reached during detonation influenced the quantity, elemental composition, morphology, and isotopic composition of the recovered soot. Unique signatures identified include morphological characteristics directly related to the availability of excess oxygen during detonation. As hypothesized, differences in peak pressures combined with time at high pressures influenced the isotopic composition of the recovered soot. Results have been published and presented at conferences including the Gordon Research Conference on Expanding the Limits of Our Understanding of Energetic Materials Behavior as well as shared with others within the DOE and DOD.
Task 2: Continue to develop x-ray scattering techniques to record evolution of carbon (clustering, morphology, polydispersity) in high explosives in real time to provide a scientific basis of post-detonation signature formation. This builds on ongoing and developing capabilities at the Dynamic Compression Sector (such as vessels, firesets, and x-ray optics).

We continued to collaborate with LLNL, ANL, APS and WSU on enhancing our ability to collect real-time X-ray scattering data on detonating high explosives at The Advanced Photon Source. This collaboration has led to the first collections of these types of data in the United States. The results from these experiments have led to quantification of the carbon cluster size at the 100s of

nanosecond timescale for multiple high explosive formulations. These data and results have been presented at multiple conferences and submitted for publication. As well, the data from these experiments have led to the submission and acceptance of a proposal at the Linac Coherent Light Source (LCLS) at Stanford to study the clustering of carbon in benzene, 6-carbon ring common in many high explosives, at the 10s of nanosecond timescale. These data will be compared to APS data to produce a timeline of carbon clustering from the 10s of nanoseconds to 100s of nanoseconds.

Task 3: Continue development of carbon clustering physics capturing the fluid/solid mixture and carbon surface chemistry. This effort is critical in concert with the x-ray scattering data for defining how detonation products form and evolve; e.g. signature formation.

We continued to improve the modeling of carbon clustering during detonation of high explosives. Current efforts have modeled the clustering of carbon at the 100s of nanoseconds and these models have been compared with empirical data collected from Task 2 as well as other published efforts in this field. These efforts indicate that clustering occurs rapidly behind the detonation front and is relatively fixed in size within a few hundred nanoseconds. Modeling efforts of carbon clustering at the 10s of nanoseconds will be compared to empirical data collected at LCLS.

Task 4: Continue to combine multi-phenomenological data such as the combination of pXRD analysis with XPS analysis of detonation soot to develop a methodology for abductive reasoning from the detonation products to the initial detonation conditions.
Based on recommendations of the external review of the project, this goal has been eliminated from the project.

Future Work

Goal: We will continue to develop the capability to identify the intent/design of a detonation test using detonation products.

Task 1: Continue in-house detonation experiments to obtain detonation product samples and use state-of-the-art analytical techniques to determine chemical compositions of detonation products including solids and gases. This will include collecting products from isotopically-labeled TNT and RDX.

Task 2: Continue to develop x-ray scattering techniques to record evolution of carbon (clustering, morphology, polydispersity) in high explosives in real time to provide a scientific basis of post-detonation signature formation. This builds on ongoing and developing capabilities at the Dynamic Compression Sector (such as vessels, firesets, and x-ray optics). Evaluate data collected on C-clustering of benzene after laser shock experiments at LCLS.

Task 3: Continue development of carbon clustering physics capturing the fluid/solid mixture and carbon surface chemistry. This effort is critical in concert with the x-ray scattering data for defining how detonation products form and evolve; e.g. signature formation.
Conclusion

We will establish detonation products as novel chemical signatures of explosive composition, performance, and state. To this end, we will combine novel methodologies to understand how solid carbon forms and evolves during detonation, develop new models to describe its evolution, and link in situ measurements of signature formation in real time behind the detonation front using time-resolved x-ray scattering at the Advanced Photon Source with state-of-the-art analysis of post-detonation gases and solids.

Publications

Firestone, M. A., D. M. Dattelbaum, D. W. Podlesak, R. L. Gustavsen, R. C. Huber, B. S. Ringstrand, E. Watkins, B. Jensen, T. Wiley, L. Lauderbauch, R. Hodgin, M. Bagge-Hansen, S. Seifert, and T. Graber. Structural evolution of detonation carbon in Composition B-3 by X-ray scattering. To appear in Proceedings of the 19th Biennial APS Conference on Shock Compression of Condensed Matter. (Tampa, FL, 14-19 Jun).

Podlesak, D. W., R. C. Huber, R. S. Amato, D. M. Dattelbaum, M. A. Firestone, R. L. Gustavsen, C. E. Johnson, and J. T. Mang. Characterization of detonation soot produced during steady and overdriven conditions for three high explosive formulations. To appear in Proceedings of the 19th Biennial APS Conference on Shock Compression of Condensed Matter. (Tampa, FL, 14-19 Jun).

Ringstrand, B., S. Seifert, D. Podlesak, and M. Firestone. Self-Assembly directed organization of nanodiamond during ionic liquid crystalline polymer formation. 2016. Macromolular. Rapid Communications. 37: 1155.

Willey, T. M, M. Bagge-Hansen, L. Lauderbach, R. Hodgin, D. Hansen, C. May, T. van Buuren, R. Gustavsen, E. Watkins, M. Firestone, D. Dattelbaum, B. Jensen, T. Graber, S. Bastea, and L. Fried. Measurement of carbon condensates using Small-Angle X-ray Scattering during detonation of high explosives. To appear in Proceedings of the 19th Biennial APS Conference on Shock Compression of Condensed Matter. (Tampa, FL, 14-19 Jun).

Integrated Biosurveillance

Benjamin H. Mcmahon
20150090DR

Introduction

Our study will apply three state of the art diagnostic technologies to a high disease burden population in western Kenya. We will perform multiple types of epidemiological analysis necessary to derive understanding from the novel data. The samples are derived from patients who frequently have co-infections (tuberculosis, Salmonella, Streptococcus, and Staphylococcus) and are associated with a 12 year longitudinal study performed in a pediatric malaria clinic in the Saiya District of Kenya by our collaborator, Prof. DJ Perkins of the University of New Mexico. The three diagnostic technologies are:

Rapid Biomarker Detection: Approaches will be developed to detect proteins, lipids, and carbohydrates from human or animal samples. Reagents for tuberculosis, Staphylococcus, Streptococcus, and Salmonella will be applied and assessed.

Oligonucleotide-based diagnostics for pathogen characterization: This will include 48x or 96x multiplexed, PCR-based nucleic acid assays to species- strain- and antibiotic resistance- type for Streptococcus, Salmonella and Staphylococcus.

Sequencing of non-host RNA: Novel sample preparations will be developed and automated to provide 10 million pathogen RNA sequences from each sample. These data will be analyzed to observe unexpected pathogens, expression level of virulence factors, validity of nucleotide diagnostics from previous task, and strain-type relative database and other samples.

Our epidemiological model will predict outcomes for both individual patients and the population of Siaya (800,000 residents), as a function of investments, treatments, and mitigations. Our focus in the modeling will be to examine how the widespread co-morbidities of HIV, malaria, Salmonella, Streptococcus, Staphylococcus, and tuberculosis combine to cause 1) poor outcome for individuals and the community (30% mortality rate, at age 5), 2) emergence of antibiotic resistant forms, which spread across the globe, and 3) presence of novel pathogens.

This project will lay the foundations to achieve our long-term technical goals of situational awareness for global pathogen circulation and emergence.

Benefit to National Security Missions

This project directly addresses the National Security mission in the area of biological threat reduction by characterizing emerging diseases in the high-disease-burden region where they emerge. Providing this understanding impacts LANL's ability to respond to sponsor requests to predict the course of emerging diseases or bio-terrorism events or understand how climate change and demographic changes impact infectious diseases, which still cause the majority of deaths in developing countries. Furthermore, this project demonstrates how to systematically characterize these diseases as they emerge, in-situ, and how to integrate the resulting biosurveillance data. This capability is essential to accurately predict risk from novel engineered pathogens, as well as the risk to US personnel as they operate in the developing world.

Methodologically, this project integrates signature discovery with measurement in patients, and deployment of assays and models - an important template for the SoS strategy. Biosurveillance has been a key SoS endeavor at LANL, and senior lab leaders organized a biosurveillance deep dive in Sep 2013. At this event, external experts (programmatic, academic, industrial) critically reviewed LANL strategy and investment in BSV, and our proposed concept was extensively appreciated as innovative, challenging and critical. Our effort requires the systematic integration of IS&T and experimental capabilities at LANL (Co-Design), which is not readily achieved in an academic setting. This integration is not limited to

BSV, and can be applied to other threats (nuclear, chemical, environmental) in the future. Similar tools can be applied to nuclear non-proliferation or any other "big data" national security problem.

Progress

Progress occurred in all three aims of our project: Biomarker Discovery, Forward Deployment of Measurement, and Integrative Modeling. Year 2's progress built off of a site visit to the Kenyan Medical Research Institute (KEMRI) and the Siaya County Reference Hospital (SCRH), the two sites where the forward deployment portion of the project is occurring. Representatives for each of the five project capabilities (three diagnostics, modeling, and clinical medicine) were represented, and details of needs, capabilities, and potential solutions were discussed. Upon return to LANL, a morning teleconference of the entire external advisory board was convened, and a detailed plan for Year 2 was articulated. Following this, detailed clinical study plans were articulated in a human subjects research request, which has completed Kenyan approval, and is currently in the UNM approval queue. Additionally, an NIH proposal applying many of this project's components was crafted with a target of understanding how immune-modulation therapies could be developed to combat malaria.

Specific progress in the three aims include:

Biomarker Discovery

- Salmonella Assay: We continued development of this assay, from antigen preparation, antibody selection, and waveguide preparation, and correctly validated 4 positive and one negative clinical Salmonella bacteremia samples. Our expectations is fifteen samples by the end of Year 2.
- Pediatric TB Assay: We continued validation of the pediatric tuberculosis assays (n=8 done, n=30 goal), and associated adults for household contacts). Both archived and newly collected samples were used. The positive validation for pediatric TB is chest X-rays and medical diagnosis as per World Health Organization guidelines. For adults, we will use sputum microscopy and GeneXpert PCR-based assays from sputum (run in Kenya, approved on new IRB). An R21 grant was submitted to the NIH to carry this work forward.
- Staphylococcal Assay: We began optimization of the Staphylococcal biomarker assays in Year 2.
- High throughput characterization of 72 hour bacterial growth curves were performed on two non-typhi Salmonella isolates (one cephalosporin resistant, with the incHI2-type plasmid, one without) and three Staphylococcus isolates (both coagulase positive and coagulase negative strains) was performed, to provide important relevance to the genomic analysis of the isolates.
- Potential difficulties of the analytical sensitivity of RNA seq were identified through preparation, sequencing, and analysis of spiked samples, and potential solutions involving sample fractionation were explored. The sample flow-chart in the previous bullet was articulated, so only unknown samples could be deeply sequenced, where lower sensitivity is acceptable.

Forward Deployment of Measurement

- Bacterial vs. Viral Assay: One need that emerged from the site visit and advisory committee discussions was for procalcitonin and C-Reactive protein assays, to enable rapid differentiation between viral and bacterial pathogens.
- Another need emerging from the site visit was the value of a PCR assay for the identification of non-specific Gram positive or Gram negative bacteria in the blood samples.
- Because of the identified need to detect low copy numbers of bacteria and the limited supply of blood from the highly anemic infants, a sample decision-tree was developed, where step one was measurement by PCR of 200 micro liters of blood and waveguide detection of 50 micro-liters, with 500 micro liters going to blood culture. On the basis of these results, the decision to administer further PCR assays to identify organisms, plasmids, antibiotic resistance elements, or sequence isolates or metagenomic samples with RNA Seq was articulated and demonstrated.
- The need for and form of genomic and phenotypic characterization of bacterial isolates was developed, and exemplified for non-typhi Salmonella, with integration of phylogenetic, plasmid, virulence and antimicrobial resistance elements
- Weekly teleconferences with UNM, KEMRI, and SCRH have occurred throughout Year 2, in part to ensure the data collection fills the needs identified by the analysis tasks.

Integrative Modeling

- Mechanistic Epidemiological Model Development: Continued development of the epidemiological model of co-circulating diseases occurred, guided by both power calculations for our clinical study and development in web-based presentation for other epi-models. The importance of collaborating with the Institute for Health Metrics as a way of extrapolating our work

globally was identified.

- Analysis techniques were developed for cytokine profile analysis and genetic markers, with one manuscript published and two others likely to be submitted before the end of Year 2.

Future Work

Year three will focus on publication of results, collection and analysis of prospective clinical data , informed by a visit to Siaya by McMahon, Mukundan, and Noormohamed, technology development in years 1 and 2 of the project, as well as feedback from the mid-term review. The first two years of the project have greatly clarified the roles of the three diagnostic techniques and modeling so that they can be translated to forward deployment. Additionally, we better understand the necessary collection of samples for continued assay development and validation, in keeping with our original project plan. Although we feel well-prepared for this effort, it will involve considerable logistical complexity, including international human subjects approvals, shipping of infectious disease samples, coordination with academics, clinicians, and government personnel in Kenya, data- and sample-tracking, and communication of results in publications and conference presentations. These logistical issues are formidable barriers to other US Government biosurveillance efforts, and our experience gained here should enable continued development of competitive proposals to several sponsors.

More specifically, our manuscripts to be published are indicative of the most focused technical progress needed in Year 3, and include:

- Cytokine analysis: We have applied state of the art statistical analysis techniques to relate experimentally observed patterns of immune response across ~500 clinical samples to nine separate disease categories
- Description of mechanistic model of co-circulating diseases: Describes how application of diagnostics may reduce the emergence of virulence and drug resistance.
- Non-typhi Salmonella genotype / phenotype characterization: Describes the mechanistic understanding of epidemiological pressures to be derived from genomic and high-throughput phenotypic characterization.
- Pediatric tuberculosis validation and non-typhi Salmonella assay development: Validation of assays for the detection of pathogen biomarkers associated with these diseases in a small cohort of blinded samples.

Conclusion

We will demonstrate integrative biosurveillance in the high disease-burden region of Siaya, Kenya. This will involve biomarker discovery, assay development, and assay deployment of three complementary infectious disease assays on a human population. Direct biomarker detection assays will provide results at the point of care, nucleic acid detection with PCR is a mature technology which will build on established reference laboratory techniques, and RNA sequencing will provide a broad range of genomic information of a variety of pathogens. Overall information integration and process optimization will result from both statistical analysis and development and application of realistic epidemiological models.

Publications

Brown, M., L. Moore, B. McMahon, D. Powell, M. LaBute, J. Hyman, A. Rivas, M. Jankowski, J. Berendzen, J. Loeppky, C. Manore, and J. Fair. Constructing rigourous and broad biosurveillance networks for detecting emereging zoonotic outbreaks. 2015. PLoS ONE. : e0124037.

Davenport, G. C., J. B. Hittner, Otieno, Karim, Mukundan, P. W. Fenimore, N. W. Hengartner, B. H. McMahon, Kempaiah, J. M. Ong'echa, and D. J. Perkins. Reduced Parasite Burden in Children with Falciparum Malaria and Bacteremia Coinfections: Role of Mediators of Inflammation. 2016. MEDIATORS OF INFLAMMATION.

Deshpande, , McMahon, A. R. Daughton, E. L. Abeyta, Hodge, Anderson, and Pillai. SURVEILLANCE FOR EMERGING DISEASES WITH MULTIPLEXED POINT-OF-CARE DIAGNOSTICS. 2016. HEALTH SECURITY. 14 (3): 111.

Doggett, N. A., Mukundan, E. J. Lefkowitz, T. R. Slezak, P. S. Chain, Morse, Anderson, D. R. Hodge, and Pillai. CULTURE-INDEPENDENT DIAGNOSTICS FOR HEALTH SECURITY. 2016. HEALTH SECURITY. 14 (3): 122.

McMahon, B., P. Fenimore, S. Del Valle, N. Hengartner, R. Ribeiro, and J. Hyman. Modeling the impact of spatial heterogeneity, behavior change, and mitigations on the current Ebola epidemic. 2015. LAUR 14-27813.

Stromberg, L. R., N. W. Hengartner, K. L. Swingle, R. A. Moxley, S. W. Graves, G. A. Montano, and Mukundan. Membrane Insertion for the Detection of Lipopolysaccharides: Exploring the Dynamics of Amphiphile-in-Lipid Assays. 2016. PLOS ONE. 11 (5).

Signature Development in LANL's Earth and Space Sciences

Reinhard H. Friedel
20150647DR

Introduction

This DR project expands the scientific understanding of fundamental physical processes that are critical to maintenance of habitat earth homeostasis with the long-term objective of achieving sufficiently detailed knowledge to identify the tipping points that can push habitat earth out of its homeostatic equilibrium. This scientific goal is achieved by promoting and coordinating basic research based on the science of signatures to gain understanding of the structure, and evolution of the earth, the solar system and the Universe in which habitat earth resides, ultimately relevant to understanding future changes as they might perturb habitat Earth homeostasis.

This project will focus on 4 main science disciplines. Within these disciplines, the project emphasizes university collaboration, postdoc and student investment, and emergent ideas.

The project's scientific disciplines are: (1) Geoscience, with the goal of advancing our capabilities to measure and understand significant natural and human-induced changes within their background context using a portfolio of theoretical, modeling, and experimental methods; (2) Climate with the goal of scientific advances that integrate theory, models, simulations, experiments, sensing and observations to push the frontiers of predictability to better prepare for impacts (extreme weather, tipping points, sea level rise), and plan for improved domestic, climate-friendly energy and resilient infrastructures for current and future climate states. (3) Space Science, with the goal of advancing our understanding of the space environment from the Sun to the Earth and beyond – with the particular goal of understanding how the space environment affects space platforms that support security and quality of life in our technological society, (4) Astrophysics and Cosmology, which includes astro-biology, planetary studies, exo-planets, extinction events, other important astrophysical processes. Investment in these areas contributes to the staff pipeline, and builds signature discovery and measurement capability directly relevant to applied missions.

Benefit to National Security Missions

The science of signature and the means to detect and interpret these signatures is directly applicable to the detection needs for nonproliferation and counter proliferation community, space weather and space events, remote sensing and detection of chemical, biological, nuclear, radiologic, or explosive threats, climate impact and treaty verification, and cosmology/astrophysics. Signature discovery and alternate signatures provide the new methods to detect and understand these areas of national need.

Progress

The CSES (formerly IGPPS) has undergone a number of changes that have started to have been implemented in FY16. Since many of these new efforts could not have been anticipated by the original author of this DR, they may not relate much to efforts outlined in the Proposed Work section of last year's data sheet.

The second year of this project has been in effect about 9 months. 20 separate projects are underway in the disciplines of Geophysics, Climate, Space and Astrophysics. In addition, a further 8 projects under CSES's new Emerging Ideas program element have been funded for FY16 that all will finish in FY16.

A Call for Proposals for new task starts in FY17 has been issued with further narrowing of the scientific scope to align more strongly with the Labs strategic direction. This call included several changes and the program elements - student proposals are now only for students coming to LANL with no monies to be subcontracted to external institutions; a new "Emerging Ideas" category was added.

A total of 18 proposals were received and selections

have been made for 8 initial new starts for FY17 with a potential of an additional 5 projects pending funding levels.

Future Work

The scientific goal is to develop signatures or the means to measure signatures that provide insight into changes on earth and space. This goal is achieved by promoting and coordinating basic research on the understanding of the structure, and evolution of the earth, the solar system and relevant to understanding future changes as they might perturb habitat earth. FY17 tasks will be to fund Los Alamos postdoctoral research associates and collaborative research between Los Alamos scientists and university researchers.

Additional related FY17 tasks will be to foster students earlier in their academic careers, and related collaborative research between institutions.

A CSES program change in FY16 added an Emerging Ideas element to the Center. The Emerging Ideas element fosters individual ideas. The FY17 tasks related to Emergent Ideas include idea solicitation, research management and, ultimately, review of milestones and accomplishments.

Conclusion

The impact is the enhancement of University-Laboratory relations by fostering collaborations between academic campus faculty, staff, students, and Los Alamos National Laboratory staff; providing Los Alamos National Laboratory programs with systematic infusion of new ideas, people, and contact with the larger university community; direct support of Los Alamos postdocs; fostering top-quality research at Los Alamos National Laboratory in the more "basic" or "fundamental" aspects of fields that map into existing and/or emerging mission thrust areas of the Laboratory; and harnessing LANL's supercomputing and multi-scale measurements and modeling capabilities.

Publications

Nonlinear elasticity and hysteresis: Fluid-solid coupling in porous media. 2015.

Anthony, R. E., R. C. Aster, Wiens, Nyblade, Anandakrishnan, Huerta, J. P. Winberry, Wilson, and Rowe. The Seismic Noise Environment of Antarctica. 2015. SEISMOLOGICAL RESEARCH LETTERS. 86 (1): 89.

Ferdowsi, , Griffa, R. A. Guyer, P. A. Johnson, Marone, and J. a. n. Carmeliet. Three-dimensional discrete element modeling of triggered slip in sheared granular media. 2014. PHYSICAL REVIEW E. 89 (4).

Grohs, E., G. M. Fuller, C. T. Kishimoto, and M. W. Paris. Probing Neutrino Physics with a Self-consistent Treatment of the Weak Decoupling, Nucleosynthesis, and Photon Decoupling Epochs. . 2015. Journal of Cosmology and Astroparticle Physics. 2015: 1.

Grohs, E., G. M. Fuller, C. T. Kishimoto, and M. W. Paris. Effects of Neutrino Rest Mass on Ionization Equilibrium Freeze-out. 2016. APS Physics. : 1.

Guimond, S., J. Reisner, S. Marras, and F. Giraldo. The Impacts of Dry Dynamic Cores on Asymmetric Hurricane Intensification. To appear in American Meteorological Society.

Haely, C., S. Sayres, J. B. Munster, J. Wilkerson, M. Dubey, and J. G. Anderson. Regional scale methane flux measurements over the Alaskan North Slope using airplane flux observations and in situ measurements of δ13CH4. 2014. In AGU Fall Meeting . (San Francisco, CA, 5-19 Dec 2014). , p. 679. San Francisco, CA: SAO/NASA ADS Physics Abstract Service.

Harding, J. Patrick, C. L. Fryer, and S. Mendel. Explaining TeV Cosmic-Ray Anisotropies with Non-Diffusive Cosmic-Ray Propagation. 2015. High Energy Astrophysical Phenomena. 1: 26.

Healy, C., and M. Dubey. Airborne Flux Measurements of Methane over the Alaskan North Slope. Invited presentation at Institute for Geophysics, and Planetary Physics. (Los Alamos, NM, 14-15, April, 2015).

Healy, C., and M. Dubey. Development of regional-scale airplane flux measurements of CH4, and high spatial resolution, in situ δ13C-CH4 measurements, and their deployment over the N. Slope of Alaska. Invited presentation at WHOI AOPE Seminar. (Woods Hole, MA, 21, May 2014).

Healy, C., and M. Dubey. Observing the Arctic Carbon Feedback: Regional scale methane flux measurements over the Alaskan North Slope using airplane flux observations and in situ measurements of δ13CH4. Invited presentation at American Geophysical Union Fall Meeting. (San Francisco, CA, 14-18 Dec 2015).

Hertzfeld, U. C., E. C. Hunke, B. McDonald, and B. Wallin. Sea ice deformation in Fram Strait— Comparison of CICE simulations with analysis and classification of airborne remote-sensing data. 2015. Cold Regions Science and Technology. 117: 9.

Herzfeld, U. C., S. Williams, J. Heinrichs, S. Sucht, and J. Maslanik. Geostatistical and Statistical Classification of Sea-Ice Properties and Provinces from SAR Data. 2016. Remote Sensing. 8 (8): 616.

Mazzaro, L. J., D. Munoz-Esparza, J. K. Lundquist, and R. R. Linn. Nested Mesoscale-to-LES Modeling of the Atmo-

spheric Boundary Layer in the Presence of Under-Resolved convective Structurers. f Advances in Modeling Earth Systems.

Mazzaro, L. J., D. Munoz-Esparza, J. K. Lundquist, and R. R. Linn. Limitations of Mesoscale-to-LES Grid Nesting in a Convective Atmospheric Boundary Layer . 2016. In American Meteorological society's 32nd Symposium on Boundary Layers and Turbulence. (Salt Lake City, Utah, 20-24 June 2016). , p. 3B.3. Salt Lake City, Utah: AMS.

McDowell, N. G., N. C. Coops, P. S. A. Beck, J. Q. Chambers, Gangodagamage, J. A. Hicke, Huang, Kennedy, D. J. Krofcheck, Litvak, A. J. H. Meddens, Muss, Negron-Juarez, Peng, A. M. Schwantes, J. J. Swenson, L. J. Vernon, A. P. Williams, Xu, Zhao, S. W. Running, and C. D. Allen. Global satellite monitoring of climate-induced vegetation disturbances. 2015. TRENDS IN PLANT SCIENCE. 20 (2): 114.

Pandey, S., and H. Rajaram. Modeling the Influence of Preferential flow on teh Spatial Variability and Time-Dependece of Mineral Weathering Rates. 2016. American Geophysical Union Journal. : 000.

Paris, M. W., E. B. Grohs, G. M. Fuller, and C. Kishimoto. Toward a Unitary and Self-Consistent Treatment of Big Bang Nucleosynthesis. 2015. Los Alamos National Laboratory for public release.

Ranasinghe, N. R., A. C. Gallegos, A. R. Trujillo, A. R. Blanchette, E. A. Sandvol, Ni, T. M. Hearn, Tang, S. P. Grand, Niu, Y. J. Chen, Ning, Kawakatsu, Tanaka, and Obayashi. Lg attenuation in northeast China using NECESSArray data. 2015. GEOPHYSICAL JOURNAL INTERNATIONAL. 200 (1): 67.

Reisner, J. M., and S. R. Guimond. The Impacts of Dry Dynamic Cores on Asymmetric Hurricane Intensification. 2016. Journal of the Atmospheric Sciences (JAS). : 4661.

Vanderwende, B., and J. K. Lundquist. Could Crop Height Impact the Wind Resource at Agriculturally-productive Wind Farm Sites?. 2016. Boundary-Layer Meteorology. 158 (3): 409.

Whitcomb, R. K., J. N. Bassis, L. M. Cathles, W. Lipscomb, M. Hoffman, and S. Price. Implementing damage mechanics in the Community Ice Sheet Model. Invited presentation at Land Ice Working Group Meeting,. (Boulder, CO, Feb 2016).

Whitcomb, R. K., L. M. Cathles, J. N. Bassis, S. Price, and W. Lipscomb. Damage mechanics in the Community Ice Sheet Model. Invited presentation at American Geophysical Union Annual Meeting. (San Francisco, CA, 12-16 Dec. 2016).

Whitcomb, R., J. N. Bassis, L. M. Cathles, S. Price, and W. Lipscomb. A Calving Law for Ice Shelves: Implementing Damage Mechanics into the Community Ice Sheet Model . JGR Earth Surface.

Whitcomb, R., J. N. Bassis, L. M. Cathles, W. Lipscomb, and S. Price. Damage mechanics in the Community Ice Sheet Model. Invited presentation at Los Alamos National Laboratory, Center for Space and Earth Science University Project Seminar. (Los Alamos, NM, 19 Oct. 2016).

Whitcomb, R., L. M Cathles, J. N. Bassis, W. Lipscomb, and S. Price. Implementing damage mechanics in the Community Ice Sheet Model. Invited presentation at CESM Workshop 2016. (Breckenridge, CO, 20-24 June 2016).

Using Extinct Radionuclides for Radiochemical Diagnostics (U)

Hugh D. Selby
20160011DR

Introduction

This project is founded on the concept that old nuclear debris still retains diagnostically useful signatures that were traditionally determined radiometrically. Because these radioactive signatures have long-since decayed away, this concept has been considered impossible to realize. The work therefore represents a paradigm shift from the limits of classical radiochemistry - a shift based on the rapid advancements in mass-spectrometric sensitivity and precision, as well as chemical separations methods developed at Los Alamos National Laboratory (LANL). The proposed measurements themselves are unprecedented in the literature and will move the state-of-the-art for these types of environmental analyses many years forward. The true power of the proposed work will be realized when the measurements are integrated with the Los Alamos performance and statistics simulations teams. This integrated system, the Extinct Radionuclide System (ERS) will take the new measurement data and use it to probe two compelling defense science questions. The ability to answer these questions is enabled not only by the ERS' capability to recreate traditional signatures from aged debris, but also to provide new data that has been previously unavailable. Successful development of the ERS and the demonstration of its ability to address difficult questions in defense science will amount to an entirely new capability for LANL's core defense missions. Specifically, the ERS will reinforce our commitment to Stockpile Stewardship without nuclear testing by providing actual modern measurement data to constrain simulations. More fundamentally, the ERS itself represents a new area of investigation in nuclear phenomenology. Areas of study include fate and transport of radionuclides in the environment, basic nuclear data, heavy-element condensation mechanisms and, as a corollary to the latter, stellar nuclear processes and their measurable elemental signatures.

Benefit to National Security Missions

This work was designed specifically to address known gaps in National Technical Nuclear Forensics (NTNF), Stockpile Stewardship, and Intelligence missions. From a radiochemical standpoint, the critical barrier to progress in any of these missions is the fact that the historic data record is fixed. No further advancements in our understanding is possible because current methods cannot provide new data. Thus, if the historic record is incomplete, the Nation is left with no data-based recourse to answer important questions regarding the Stockpile and other nuclear testing issues. The proposed work directly addresses this problem by providing a system which can provide new data where needed. In addition to directly addressing the data needs in the various programs at LANL, the proposed work focuses specifically on understanding the value of extremely limited sample numbers, concentrations, and dynamic range. This understanding is vital when sampling is constrained in some way or that samples are not of the type optimized for the nuclear testing program. Finally, many of LANL's core mission areas have been forced to adopt quantification of margins and uncertainties (QMU) programs well after the technical work has been executed - often with poorer than ideal accuracy and statistical rigor. The proposed work has an explicit component of QMU built into it, such that the demonstration of principle that LDRD provides can be rolled directly into customer's programs with vetted QMU well in hand.

Progress

The first year (FY2016) Extinct Radionuclide System (ERS) development effort exceeded expectations. As in all research, numerous challenges arose. Some have been addressed and others represent genuine scientific lines of inquiry to be followed in the out-years of this work. Here we briefly summarize the accomplishments and questions that arose this year in terms of the technical foci enumerated in the Proposed Work section.

Measurement
The general concept of the ERS was demonstrated by the evaluation of the first nuclear explosion, the Trinity event. Using samples from the Chemistry Division's Nuclear and Radiochemistry's (C-NR) holdings and public retailers, a complete data set was constructed using entirely ERS-developed measurements. Because Trinity was the first nuclear test, the historic data sets used in the original characterization were crude and incomplete. Even though the ERS data set itself is in the early stages of development, the ERS-derived data set is the only complete example in existence for Trinity. This work culminated in a manuscript submitted and accepted by the Proceedings of the National Academy of Science describing the modern determination of Trinity's yield. In the course of this study, two key fission fragment signatures were developed.

Work was initiated on an underground US test (UGT). An important actinide signature was developed. In both examples (Trinity and the UGT) some distortions of the intra-element actinide data were observed that were not anticipated. Early qualitative assessment suggests these observations are sample size and sample type dependent. A significant portion of the measurement and statistical efforts in the next two years will be aimed at more a quantitative understanding of these observations.

Statistics and Uncertainty
The statistics team members have developed a powerful tool based on Markov-chain Monte Carlo sampling of multiple radiochemical performance models to map out the true multi-dimensional uncertainty in radiochemical performance assessments. Specifically, this tool enables the statistics team to systematically probe each of the fitting parameters in the radiochemical assessment with many thousands of runs and thus develop an uncertainty distribution as a function of each parameter. In addition, this tool allows the team to explore one of the two central defense science questions that the ERS study seeks to probe.

Modeling and Uncertainty
Working in concert with the statistics team, modeling and simulations teammates have begun to explore, using Technical Nuclear Forensics (TNF) tools, the true number of degrees of freedom in the process of "reverse-engineering" an unknown nuclear device in the US TNF scenario. This work is constrained by both historic and ERS derived data for known US tests.

The second defense science question falls under the purview of the simulations teammates working within the Stockpile Stewardship program. Their efforts have resulted in the first models designed specifically to query for radiochemical outputs relevant to the ERS. This work will feed into the uncertainty issues associated with the basic nuclear data employed in modern simulations and will be used to help validate the results of the fully developed ERS as it comes on line.

Future Work
The proposed work has three technical foci: Measurement, Statistics and Uncertainty, and Modeling and Simulation. The tasks and goals for the next fiscal year are listed following these technical themes below.

- Continue development and optimization of the radiochemical separations and measurements of an expanded set of the targeted nuclides listed in the proposal. Emphasis will be on the more challenging nuclides and sample types in FY17.
- Based on the results from FY16 initial validation of the measurements, apply these to more challenging samples, particularly those in modern CNR holdings. These samples represent some of the higher-risk aspects of the proposed work and will require significant experimental effort as well as closer integration of simulation and statistics.
- Plan at least one NNSS surface collection to explore sampling bias issues that arose in FY2016 initial validation. This proposed collection will also further inform basic phenomenological studies that arose in FY16 studies.
- Expand statistical framework for uncertainty estimation and defense science questions
- Expand modeling efforts to explore an NTNF/defense science question. This simulation effort will tightly integrate statistical theory particularly as it pertains to correlated uncertainties.
- Continue simulations to establish specific details about the limitations of basic nuclear data that can be addressed by the new measurements as they become available.

Conclusion
This project will develop a validated suite of measurements that underpin the extinct radionuclide system (ERS). Validation will be realized by comparison to historic radiometric data and assessment using modern simulation tools. A key result will be the understanding of sample requirements and the anticipated limitations of analyte concentrations as a function of sample type. We will also complete up-front integration of statistical theory and uncertainty

modeling of the new ERS, and fold dynamic simulations with ERS data to better understand and implement nuclear physics in simulations.

Publications

Hanson, S. K., A. D. Pollington, C. R. Waidmann, W. S. Kinman, A. M. Wende, J. L. Miller, J. A. Berger, W. J. Oldham, and H. D. Selby. Measurements of extinct fission products in nuclear bomb debris: Determination of the yield of the Trinity nuclear test 70 y later. 2016. In PROCEEDINGS OF THE NATIONAL ACADEMY OF SCIENCES OF THE UNITED STATES OF AMERICA. Vol. 113, 29 Edition, p. 8104.

10 GHz Bandwidth Synthetic Aperture Radar (SAR) Technology Development for Satellite Deployment

Bruce E. Carlsten
20160013DR

Introduction

We will develop a high-frequency (~ 100 GHz), high-bandwidth (~ 10 GHz) RF amplifier with an order of magnitude higher average and peak power. This amplifier will enable a new class of ultra high-resolution imaging radars needed for emerging national security threats. This amplifier will have broad other uses; for example it will also enable a new class of atmospheric gas monitoring tools which can be used for future treaty verification. Additionally, we will demonstrate a novel synthetic aperture radar (SAR) algorithm scheme initially under development by an LDRD ER in FY15.

The project's key innovation is to combine a mode selective photonic-band gap (PBG) RF structure with a sheet electron beam for the RF amplifier. The sheet electron beam can contain an order of magnitude greater power than a conventional round electron beam, but due to its much larger size in one dimension, can couple to unwanted modes in a conventional copper RF structure. However, a PBG structure can be made to be mode selective, thereby eliminating mode competition and allowing use of the wide sheet beam in an amplifier with high bandwidth.

The project's second important innovation is to use the novel SAR algorithm. The higher bandwidth from the novel RF amplifier will provide too much data to be processed by a conventional SAR. We will extend cell-phone CDMA technology to eliminate a processing-intensive step that is used in ordinary SARs and which prevent conventional SAR technology to scale to this high bandwidth.

Benefit to National Security Missions

The project will lead to order-of-magnitude greater power and bandwidth for extremely high frequency RF amplifiers. This improvement in an RF amplifier will lead to new radar (including imaging), communications, and spectroscopy missions. Ultra high resolution, long-range imaging radars is important for future DOD, NASA and intelligence community missions. Ultra high bandwidth communications is important for future DOD, NASA and intelligence community missions (both terrestrial and exo-atmospheric). New spectroscopy missions can be for climate science, space science, and interrogation of potential bio/chem releases and plumes from facilities suspected of producing bio, chem and nuclear weapons.

Progress

We have made significant progress so far in FY16 (through the project's first 8 months) and are on track for all deliverables. In the following, we split the narrative into functional areas: (1) traveling-wave tube (TWT) photonic-band-gap (PBG) structure design and fabrication; (2) beamline development; and (3) W-band synthetic-aperture radar (SAR) development.

TWT PBG structure design and fabrication

Our schedule is to have our first generation PBG structure under high-power test with beam in Q3 of FY17 with our first generation electron beam optics. To facilitate this, we need to have our first generation PBG structure designed by the end of Q3 FY16; fabbed by the end of Q4 FY16; and cold tested (i.e., RF testing without beam) by the end of Q1 FY17. We need to have the PBG couplers designed by the end of Q4 FY16 and fabbed by the end of Q1 FY17. We will then cold test the PBG structure with couplers by the end of Q2 FY17 so it is ready to be installed on the beamline. Currently, we have finished the design of the first generation PBG structure (with about 5 dB/cm gain) and are about 30% complete with the design of the PBG couplers. We developed a simple analytic theory for estimating the gain of the PBG structure and for determining the required transverse electron beam size in it. We have demonstrated machining fabrication tolerances of 3 to 8 microns, with assembly tolerances of 5 microns, more than sufficient for fabricat-

ing the structure. We have performed some particle-in-cell simulations of gain in the PBG structure, but have encountered numerical instabilities in the code. We are working with the code vendor to resolve these instabilities. In Q4 FY17 we will begin work on our second generation PBG structure. We have assembled drafts of two journal papers to be submitted this summer on specifics of the PBG/electron beam interaction and we have a third outlined on the PBG structure itself.

Beamline development

For testing the PBG structure, we need to assemble a 20-kV, 5-A sheet electron beam test line. We are basing this beamline largely on previous sheet beam work, specifically copying our previous architecture of a cylindrical electron gun, an elliptical solenoid to form the sheet beam, and transporting the sheet beam in a focusing wiggler structure. We are planning to reuse a wiggler from the previous work, but are fabbing a new electron gun and elliptical solenoid. Our schedule is to have the beamline running by Q1 FY17 to verify the electron beam size and quality before we insert the PBG structure into it in Q3 FY17. The electron gun has been designed and ordered from Heatwave, the nation's leading electron gun vendor. With the maximum lead time, it should arrive at the start of Q1 FY17. The remaining beam optics, including the elliptical solenoid, are under design right now through the end of Q3 FY16. We will complete the mechanical design, fab all needed parts in local machine shops (i.e., the part for the elliptical solenoid, beam tubes, supports, etc) during Q4 FY16. We are also completing all required modulator work for driving the electron gun in Q3 and Q4 FY16. The major remaining uncertainty we have is how we will image the sheet electron beam. The combination of high current density but low voltage makes the diagnostic particularly complicated. We will downselect our diagnostic scheme by the end of Q3 FY16 and develop the needed hardware by the end of Q4 FY16. Also in Q4 FY16 we will start the design of our second generation beam optics, which will include high-risk (but very high-payoff) electron beam phase-space manipulation.

SAR development

We have successfully developed the SAR image reconstruction algorithm based on a novel approach using range-resolved reflection data. This novel SAR approach eliminates the coherency requirement in conventional SAR algorithms which presents a limitation in high-frequency SAR imaging. We have successfully implemented a 1-GHz SAR demo with a 100-MHz bandwidth to verify the code-division multiple access (CDMA) scheme. We have begun acquiring the needed W-band hardware and are on track to assemble a W-band demo by Q4 FY17.

Future Work

Planned FY17 tasks include

- RF cold test (i.e., without electron beam) the first generation photonic-band gap (PBG) traveling-wave tube (TWT) structure (Q1 FY17)
- Fabricate the PBG couplers (Q1 FY17)
- Assemble the PBG structure and couplers and cold test the entire assembly (Q2 FY17)
- Develop the second generation PBG structure design (Q1-Q2 FY17)
- Demonstrate sheet beam formation and transport with the first generation beam optics hardware (Q1-Q2 FY17)
- Develop the second generation beam optics design using a flat-beam transform (Q1-Q2 FY17)
- Hot test the first generation PBG structure with the sheet electron beam and measure gain (Q3-Q4 FY17)
- Fabricate and assemble the second generation PBG structure (Q3-Q4 FY17)
- Fabricate and assemble the second generation beam optics hardware (Q3-Q4 FY17)
- Assemble the W-band hardware for a W-band SAR imaging demo (Q1-Q2 FY17)
- Experimentally verify the W-band SAR imaging scheme (Q3-Q4 FY17)

Conclusion

RF amplifier technology has a performance limitation at high frequency because sizes shrink, including the size of the electron beam needed for RF amplification. It has been long recognized in the RF amplifier technical community that a sheet electron beam will be needed to bypass this limitation, but previous research has shown that sheet beams with conventional RF structures lead to over-moding. This project proposes to demonstrate a high-frequency RF amplifier using a sheet electron beam and a mode selective photonic-band gap (PBG) RF structure. A PBG structure is a revolutionary architecture change that resolves the issues with conventional RF structures.

Publications

Carlsten, B. E., K. E. Nichols, D. Y. Shchegolkov, and E. I. Simakov. Emittance effects on gain in W-band TWTs. 2016. IEEE Transactions on Electron Devices. 63 (11): 4493.

Simakov, E. I., B. E. Carlsten, F. Fierro, F. L. Krawczyk, K. E. Nichols, J. A. Oertel, D. W. Schmidt, and D. Y. Shchegolkov. Ceramic structures and other test com-

ponents for the 96 GHz mm-wave traveling-wave tube. Presented at 17th International Vacuum Electronics Conference IVEC 2016. (Monterey, CA, 19-21 April, 2016).

Optical and Laser Spectroscopy of Th-229 Electronic and Nuclear Transitions for the Development of Solid State Nuclear Quantum Sensors

Xinxin Zhao
20140011DR

Abstract

The thorium-229 nucleus possesses the lowest-energy nuclear isomeric state with potentially exciting applications in nuclear, atomic and optical physics, including the development of a nuclear clock. Despite decades of search by several groups around the world, the transition wavelength has not been measured directly, and the possible range of the transition wavelength is still too large to begin laser spectroscopy. We have searched the Th-229 nuclear isomer transition by collecting Th-229 recoils following the alpha decay of U-233 into various optical plates and measuring the subsequent light emission using a monochromator. We have observed a spectral feature with a signal-to-noise ratio (S/N) of 7 that is consistent with the Th-229 nuclear isomeric transition, and we determined the wavelength to be 251.1±0.2st±0.3sys nm. Because this result is far out of the currently accepted range of 160±10 nm, additional measurements are ongoing in order to further increase the level of confidence that the spectral feature is indeed the sought-after nuclear isomeric transition. The result so far is very encouraging. If confirmed, this would be a major scientific breakthrough that clears the path for the development of a Th-229 nuclear clock.

In parallel, we have completed time-resolved laser spectroscopy measurement and density function theory calculations to characterize the oxidation state of 229Th implanted in MgF2 crystals. This work confirmed that the solid-state approach is a viable option for creating a nuclear clock. We have also completed the development a new crystal-growth capability at LANL and grown the first LiSAF crystal doped with ultra-pure U-233 isotope. This capability has important spin-off applications in threat reduction for developing radiation detector crystals and has already led to a new multi-million dollar project from the Air Force Office of Scientific Research.

Background and Research Objectives

It has been known for decades that the Th-229 nucleus possesses the lowest-energy nuclear isomeric state in nature. Measurements of the transition energy place it within reach of existing laser capabilities notwithstanding a currently huge uncertainty in the transition wavelength. There is now a growing interest in Th-229 isomer research because of its potential application in nuclear, atomic and optical physics, including the development of an optical clock based on this nuclear transition. The laser-accessible energy and the long lifetime of the isomeric state results in an exploitable quality factor up to 1020 for this nuclear transition which, combined with the well-isolated environment of the nucleus, provides a nuclear probe of unprecedented precision. It would lead to a nuclear clock capable of reaching a stability as remarkable as 10-19. A nuclear clock made from Th-229 is expected to be free from some of the systematic uncertainties that plague modern atomic clocks. For instance, the black body radiation (BBR) shift in modern atomic clocks is a source of uncertainty that must be controlled and calculated at the same level as the stability, or 10-15 as is the case in the current Cs standard. Due to the shielding of electrons around the Th nucleus, a Th nuclear clock would have a suppressed BBR.

The project aims to pin down the wavelength of the nuclear transition to a level that is orders of magnitude better than the current published result, which is a prerequisite for the laser search to succeed.

Scientific Approach and Accomplishments

Despite several key people of this project leaving LANL and a declining budget, the personnel transition and budget adjustment went smoothly and we have made exciting progress in all research areas. One paper has been published, and three papers are submitted or will be submitted in the next couple of months. The highlights of these accomplishments are summarized below:

One potential problem for the solid-state nuclear clock approach is the suitability of the doped environment

for photon emission by the nuclear isomeric state. Specifically, ions in the crystal, particularly Thn<+4, could open non-radiative decay routes for de-excitation and this compete with the photon emission. We have used time-resolved photoluminescence and density function theory (DFT) calculations to characterize MgF2 crystals which have been implanted with Th-229 via alpha decay from a U-233 source. The DFT calculations predicted Th4+ to be the lowest-energy oxidation state and Th3+ to be the next highest in the MgF2 crystal environment. The calculations also show that the Th4+:MgF2 system has a large band gap that suppresses the internal electron conversion decay channel. Experimentally, we found no evidence for thorium ions in oxidation states other than +4 using time-resolved photoluminescence spectroscopy that has a detection limit for Thn<4+ ions several orders of magnitude smaller than the number of implanted Th-229 recoils. This work shows that the solid-state approach is a viable option for a nuclear clock. A paper was submitted to Physical Review Applied [1].

A recent experiment published in Nature claimed the isomeric transition energy to be 6.3 eV to 18 eV. This experiment relied upon imparting a low-energy beam of Th-229 onto a CsI-doped detector where the Th atoms adsorb a few atomic layers deep. They claimed the lower limit of the transition energy based on the ionization potentials of Th atoms in free space. Because this new lower bound reduces the search range if it is indeed correct, we have completed a more realistic analysis of this experiment and calculated the properties of CsI and Th:CsI crystals in the bulk and surface as well as studied the effects of Th doping on the electronic band gap properties. We studied the consequences of a nuclear transition lower bound due to the presence of a conduction band and found a resulting shift of the lower limit of the Th-229 nuclear clock transition to 1.2-1.6 eV from 6.3 eV. This theoretical analysis will be submitted in a few weeks to Physical Review A [2].

Accurate knowledge of the wavelength of the Th-229 isomeric transition is required as a first step towards the construction of a nuclear clock or other sensors. The challenges for optical spectroscopy of the isomeric transition are very low signal count rate and many co-existing "dirty effects" that could be much larger than the signal. We overcame these difficulties and perfected a spectrometer as shown in Figure 1. We have searched for the transition from 146nm to 308nm by collecting Th-229 recoils following the alpha decay of Uranium-233 into either MgF2 (Figure 2) or a fused silica plate (Figure 3). We have observed a spectrally narrow feature with a signal-to-noise ratio of 7 that is consistent with the Th-229 nuclear isomeric transition, and we determined the wavelength to be 251.1±0.2st±0.3sys nm, as shown in Figure 3. Because the signal was very weak and the wavelength was far out of the current widely accepted range of 160±10 nm, there was concern that this spectral feature might be caused by unknown impurities and/or backgrounds instead of the Th-229 nuclear isomeric transition. We have started another set of measurements around the spectrally narrow feature in order to demonstrate reproducibility of the result. The results are very encouraging, with a paper in progress [3].

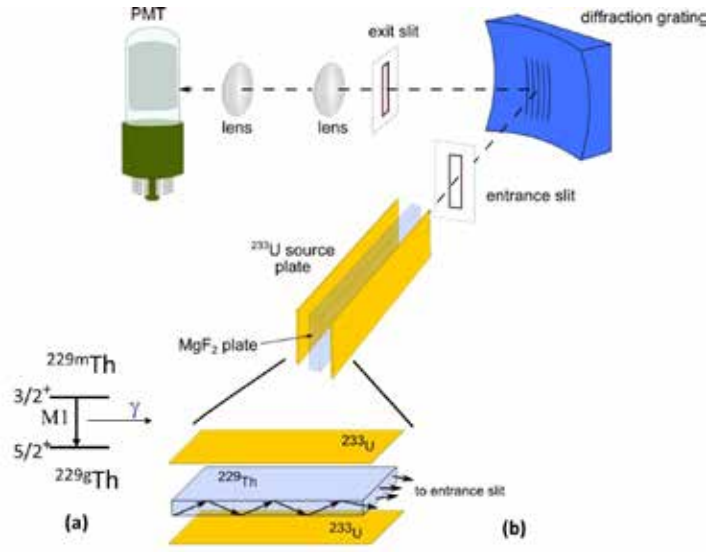

Figure 1. Th-229 nuclear energy levels and experimental details. (a) Ground state and lowest isomeric state of Th-229. (b) Schematic of experimental setup used to measure the gamma-ray emission of the Th-229 isomer: Th-229 recoils from U-233 alpha decay were implanted into MgF or quartz glass optical plate, and the light emission was measured.

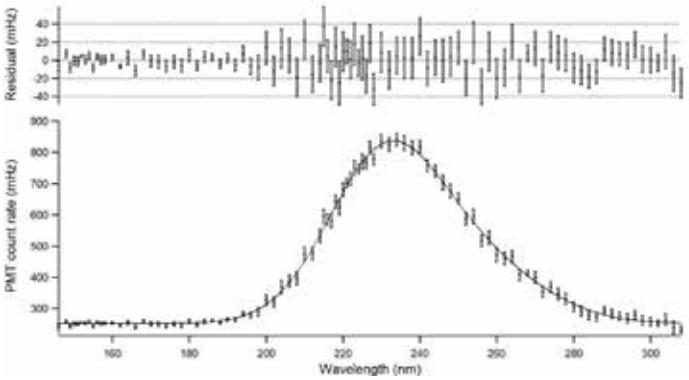

Figure 2. Spectrum of MgF emission after Th-229 isomer implantation. The emission rate after Th-229 isomer implantation (line error bars) is shown as a function of the wavelength. Double Gaussian fit (solid line) yields two color centers at 230.4±2.5 nm and 254±12 nm with a line-width (FWHM) of ~33, 41 nm respectively. There is no statistical significant feature in the residual, but the error bars in the long wavelength (>196 nm) is comparable to the estimated isomer signal.

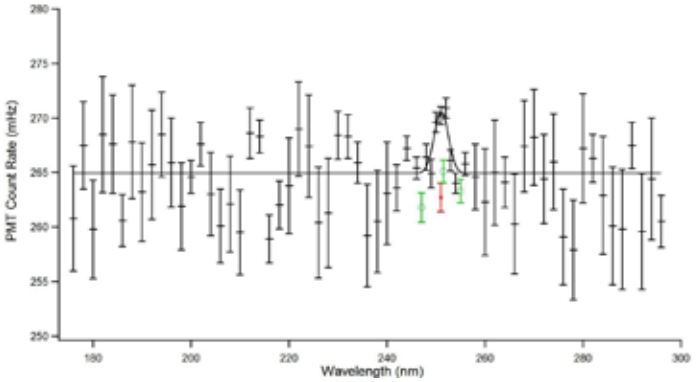

Figure 3. Spectrum of quartz glass emission while Th-229 isomer was implanted continuously. The emission rate (black error bars) is shown as a function of the wavelength. A sharp line was observed at 251.1±0.2±0.3 nm with a peak amplitude of 5.7±0.8 mHz, and a line-width (FWHM) of 3.3±0.6 nm limited by the monochromator. Red dot error bar is the PMT count rate without implantation. Green circle error bars are the PMT count rate with only alpha particle implantation.

We investigated inhomogeneous thermal broadening of the Th-229 nuclear isomeric transition and found that the tiny relative motion of neighboring atoms in a thermally vibrating lattice induces a broadening mechanism that is significant on the scale of the ultra-narrow Th-229 transition. The mechanism becomes especially important for a Thorium ion in the +4 charge state, which necessitates the placement of interstitial ions of negative charge in order to obtain a charge-neutral unit cell via charge compensation. The close proximity of the charges produces a high local electric field, the derivative of which shifts the nuclear energy by virtue of the quadrupole energy shift. In the vibrating lattice, the shift varies in time and gives a randomly time-varying contribution to the autocorrelation function of the transition, broadening the nuclear isomeric transition of Th-229 imbedded in CaF2 to about 10 Hz. This broadening is not significant on the scale of Mossbauer transitions, but it does constitute a significant broadening to a transition having a lifetime on the order of hours.

We have partnered with the University of Pisa (Italy) and completed the development of a new crystal-growth capability at LANL (Figure 4). The system grows crystals by both the micro-pulling-down and the Bridgman methods. The system design and operational basis were implemented such that small amounts of Th-229, U-233, or depleted U-238 can be used as dopants, with the possibility for future expansion to other actinides. This new capability has important spin-off applications in Pu sustainment, threat reduction, and global security, such as the growth of crystals for radiation detectors or solid-state optical refrigerators. Excessive evaporation of LiF was encountered as a limitation for the initial micro-pulling-down approach. The system was thus reconfigured to a Bridgman growth method, which offered better containment and yielded a 1 gram single crystal of undoped LiSAF (inset Figure 4, right). We subsequently succeeded in growing the world's first LiSAF sample doped with ultra-pure U-233 in an effort for an "independent" optical spectroscopy search of the isomeric transition. This sample approach offers exciting prospects for improving the statistics and independently verifying the results of the recoil experiment because (1) the 5 mg of U-233 doped into LiSAF is 12 times that used in the recoil experiment and (2) the doped sample offers a ~100% Th-229 recoil collection efficiency. Our first effort at growing 233U-doped LiSAF was a partial success. The UO2Cl2 precursor was quantitatively dissolved in the LiSAF melt and uniformly incorporated into the resulting LiSAF solid as evidenced by the homogeneous orange color of opaque polycrystalline sample (inset Figure 4, left). However, we suspect that the 0.08 at% oxygen introduced by the UO2Cl2 precursor resulted in the formation of a stable oxyfluoride phase that interfered with the formation of a LiSAF single crystal. Future efforts would explore the use of different precursor compounds and crystal growth process development using less radioactiveTh-232 or depleted U-238. Because this first U-233 doped LiSAF has a poor optical transmission and coupling to the spectrometer, we do not expect a larger isomer signal from this sample, although it might be useful for future optical characterization studies (absorption spectrum, color center emission).

Figure 4. New crystal growth lab at LANL developed under this project. The system is suited for both micro-pulling-down and Bridgman growth of fluoride crystals. The inset shows undoped LiSAF (right) and U-233 doped LiSAF (left) samples grown at LANL using the Bridgman method.

We have extracted and purified 0.8 mg of ultra-pure Th-229 (~ 2×1018 atoms) for the crystal growth and the laser excitation experiment. Starting with approximately 500 mL of an unknown solution containing the legacy 229Th material, the high salt concentration and radiochemical impurities (daughters from the decay of 229Th) had to be removed from the solution, and the 229Th had to be concentrated to a smaller volume. First, the solution containing the 229Th was evaporated to dryness and

reconstituted in 2 liters of 8 M HNO3. This large quantity of HNO3 was necessary in order to lower the salt concentration enough to allow Th-229 absorption on the resin. This solution was then passed through a column containing 20 mL of anion exchange resin (AG-1X8, 200-400 mesh) in several small portions and washed with additional rinses of 8 M HNO3. Under these conditions, maximum sorption of Th-229 onto the resin was obtained, and the salt impurities were removed. Thorium-229 was then stripped from the column with 0.1 M HNO3. The recovery yield of 229Th was 97%. This solution was evaporated to dryness and reconstituted in 5 mL of 8 M HNO3 and passed through a column containing 1 mL of anion exchange resin (AG-1X8, 200-400 mesh) for fine purification to remove residual daughters (Ac-225 and Ra-225) along with remaining salt residues. The thorium was then eluted with 5 mL 0.1 M HNO3 effectively concentrating Th-229 for use in crystal doping experiments. Inductively Coupled Plasma Atomic Emission Spectroscopy (ICP-AES) analysis of the final solution showed no significant chemical impurities or the presence of Th-232, thus verifying that the final product was suitable for small crystal doping.

We have setup a spectrometer system optimized for laser excitation of the isomeric transition experiment. The new system uses a CCD camera with high quantum efficiency. Because we found the transition wavelength to be much longer than initially expected, and diode-based laser systems at the new wavelength are available commercially, we terminated the development effort for 160 nm lasers. The new wavelength can be generated either by doubling a 502 nm diode laser to delivers a few mW at 251 nm or by quadrupling a high-power diode-pumped YAG laser at 1004 nm delivering hundreds of mW output. Such commercial systems cost about $80K-$120k depending on the configuration.

In summary, we have determined a new transition wavelength of the Th-229 nuclear isomer transition and are in the process of confirming this result. The new transition wavelength can be accessed with commercial solid-state laser sources in order to drive the Th-229 transition directly. These experiments will enable exciting advances in laser spectroscopy, quantum manipulation of Th-229 nuclei, and the development of a Th-229 nuclear clock and nuclear quantum sensors.

Impact on National Missions

Once confirmed, advances we achieved under this LDRD project would clear the path for laser excitation of the nuclear isomeric transition that lay the foundation for a nuclear clock. The new crystal growth capability has already led to a multi-million dollar externally funded project and has important spin-off applications in Pu sustainment, threat reduction, and global security. Zhao has submitted a white paper to the National Reconnaissance Office Director's Innovation Initiative program for the laser excitation of the nuclear isomeric transition. We have communicated with future external collaborators for a DARPA proposal. Zhao will give a colloquium at NIST/JILA/University of Colorado to start this process as soon as our discovery is confirmed and accepted, so that two world-leading institutions (one in nuclear and actinide science and the other in atomic clocks) can join forces to compete with the intense European efforts for the development of the first prototype nuclear clock. This technology would result in a wide range of enabling capabilities such as an improved Global Positioning System (GPS), a standalone nuclear clock based navigation system (without GPS) which is especially important for nuclear submarines, and the detection of underground structures through the nuclear clock's sensitivity to gravitational red-shifts.

References

1. Barker, B., E. Meyer, M. Schacht, L. Collins, M. Wilkerson, J. Ellis, R. Martin, and X. Zhao. Oxidation state of Th-229 recoils implanted into MgF2 crystals. Physical Review Applied.

2. Meyer, E., E. Timmermans, J. Kress, L. Collins, and X. Zhao. Thorium doped CsI: implications for the thorium nuclear clock transition. Physical Review A.

3. Zhao, X., Y. De Escobar, A. Roman, E. Bond, R. Rundberg, T. Bredweg, and S. Kozi. Observation of ultra-violet Th-229 nuclear isomeric transition. Physical Review Letters.

Publications

Barker, B., E. Meyer, M. Schacht, L. Collins, M. Wilkerson, J. Ellis, R. Martin, and X. Zhao. Oxidation state of Th-229 recoils implanted into MgF2 crystals. Physical Review Applied.

Ellis, J. K., Wen, and R. L. Martin. Investigation of Thorium Salts As Candidate Materials for Direct Observation of the Th-229m Nuclear Transition. 2014. INORGANIC CHEMISTRY. 53 (13): 6769.

Meyer, E., E. Timmermans, J. Kress, L. Collins, and X. Zhao. Thorium doped CsI: implications for the thorium nuclear clock transition. Physical Review A.

Zhao, X., Y. De Escobar, A. Roman, E. Bond, R. Rundberg, T. Bredweg, and S. Kozimor. Observation (or Search) of ultra-violet Th-229 nuclear isomeric transition. Physical Review Letters.

Remote Raman-LIBS Spectroscopy (RLS) Signature Integration

Samuel M. Clegg
20140033DR

Abstract

This LDRD DR program successfully integrated remote Raman and Laser-Induced Breakdown Spectroscopy (LIBS) for future terrestrial and planetary investigations as well as for national security programs. Raman is sensitive to the sample molecular structure while LIBS is sensitive to the elemental composition. We also successfully added Time-Resolved Fluorescence (TRF) to the technique. The first integrated Raman, LIBS, and TRF spectrometer (RLFS) was constructed on this project. We completed many Raman, LIBS and TRF experiments on geological samples and samples that contain actinides. We produced the first accurate theoretically generated LIBS spectrum of a complex geological sample and developed a method to generate theoretical Raman spectra. Finally, we completed many investigations where multiple experimental and theoretical results were merged into a more complete description of the sample.

Background and Research Objectives

This LDRD DR research program focused on the development and implementation of Raman and Laser-Induced Breakdown Spectroscopy (LIBS) that enables in situ and remote molecular and elemental analysis. Quantitative molecular identification and elemental analysis from a single instrument enables one to distinguish anthropogenic and natural materials, which can rarely be accomplished remotely. LIBS is fundamentally an elemental analysis technique from which one can infer molecular and mineralogical analysis. Raman spectroscopy is fundamentally sensitive to the molecular vibrations of solid, liquid and gas samples from which molecular structure is definitely determined and chemistry can be inferred. Time-Resolved Fluorescence (TRF) spectroscopy was not included in the original proposal but is accomplished using the Raman spectroscopy capabilities. The integration of these synergistic techniques into a single instrument enable the analysis of the same sample location and provides a complete sample characterization. This program completed the following research objectives:

- Remote LIBS analysis of pure chemicals, actinides, and complex geological materials were completed. This included the development of new quantitative analysis techniques.
- Remote Raman analysis of a broad suite of geological materials, some including actinides, biological/organic samples, and pure chemicals.
- Remote TRF was measured to distinguish organic from inorganic samples. This task exceeded the proposed work.
- The first accurate theoretically developed LIBS spectra of a complex geological sample. We were also the first to successfully demonstrate that the oxidation state of a metal could be identified using LIBS.
- A method for the development of theoretical Raman spectra was created.
- The first integrated Raman and LIBS spectrometer (RLS) was constructed and tested. Now that TRF has been incorporated into this instrument, the integrated Raman, LIBS and TRF spectrometer is now referred to as RLFS.

Finally, several external proposals have been submitted and are under development to exploit the results of this program. Most notably, part of the RLFS spectrometer will be integrated into the SuperCam instrument selected for the NASA Mars 2020 rover.

Scientific Approach and Accomplishments

Remote LIBS Analysis

The quantitative elemental analysis of complex geological samples as well as actinides was completed in several studies. The quantitative analysis of LIBS spectra is complicated by chemical matrix effects. These chemical matrix effects are due to the compositional makeup of the sample and can produce non-linear effects [1]. Methods have been developed in this project and elsewhere to understand and predict these matrix effects in an effort to exploit these unique signatures. Judge et al. 2016

completed a study in this program where the emission intensity variations due to samples containing mixtures of Cu and Na or Mg were explored [2]. Experimental observations, supported by theoretical calculations and modeling, show that the neutral Na and Mg emission intensities increase in the presence of copper while the ionized Mg line intensity decreases due to the increase in electron density of the plasma when copper is added.

Barefield et al. 2016 collected LIBS spectra from various uranium containing samples including uranium ores [3]. The uranium LIBS spectrum is typically complex and many observed transitions can be used to quantitatively determine the concentration. Figure 1 contains an excellent calibration curve for several uranium ore samples. The Barefield et al. 2016 paper lists the limits of detection for many of the diagnostic transitions [3].

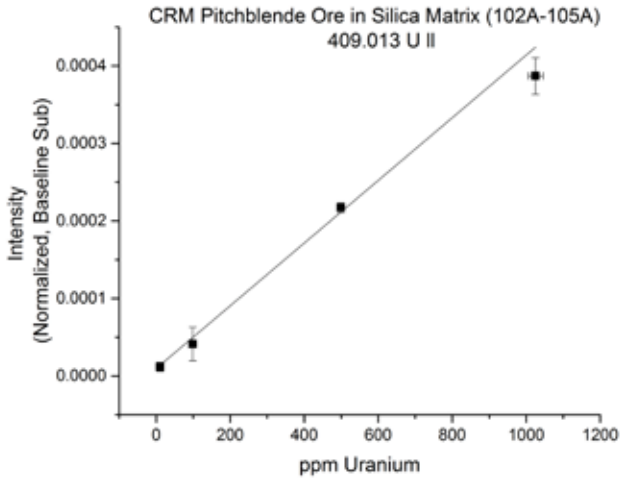

Figure 1. The calibration curve for the 409.013 nm uranium LIBS emission line.

Finally, a series of LIBS elemental spectra were experimentally collected and analyzed by two methods designed to support new quantitative analysis methods in the future. The spectra were collected from chemical simple samples such as Ti metal from which one can easily catalog the transitions due to the element. Henderson has developed an accurate automated method to fit these peaks. With this information, it is expected that one can ultimately distinguish emissions from multiple elements even if the spectral features are unresolved. Finally, theoretical spectra were also generated and were validated against these elemental spectra. These theoretical spectra are essential to the development of quantitative analysis techniques based on the theoretical methods developed in this program. This paper is nearly ready for submission.

Remote Raman Analysis

The RLFS transmission spectrometer was used to collect Raman and TRF spectra from a wide range of geological materials. Figure 2 contains Raman spectra of gypsum (red) and olivine (black). Our requirement was to detect olivine at a 12 m standoff distance, the length of my laboratory, and this was accomplished. We collected the Raman spectra of 32 minerals that Wiens et al. used to develop a method for calculating relative cross sections [4]. These relative cross sections can be used to extract compositions from complex samples in the future. It was very interesting to note that our Raman spectra were capable of identifying several samples that were mislabeled and others that were complex mixtures.

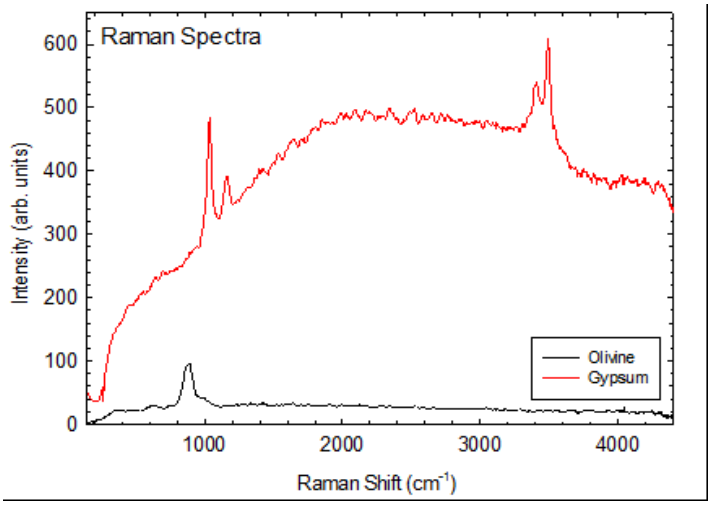

Figure 2. The Raman spectra from gypsum (red) and olivine (black).

The transmission spectrometer is also capable of remote TRF. TRF is capable of distinguishing the short lived fluorescence from organic material from the long lived fluorescence from inorganic material. Figure 3 contains the TRF spectra from the gypsum sample at the top of Figure 2. The fluorescence is gone within 100 ns and is a signature of organic material. Inspection of the sample suggests this organic material is from soil that appears to be embedded in the rock. This task exceeded the proposed work.

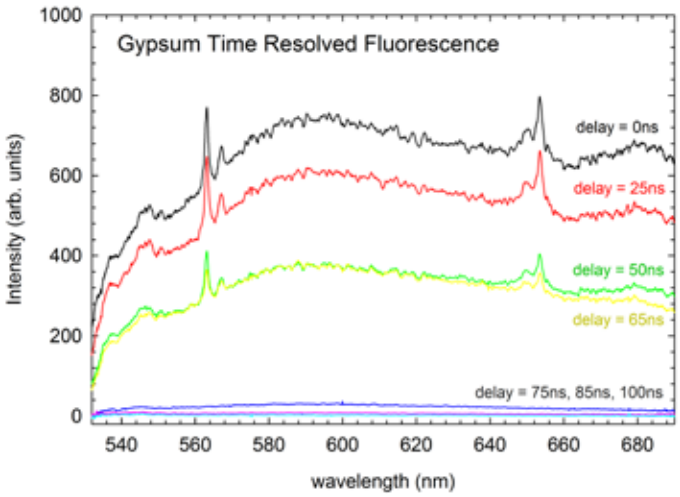

Figure 3. The TRF spectra from the gypsum sample used in Figure 2. Each trace has a different delay from when the laser was fired. The fluorescence decreases as the delay increases from 0 ns (black) through 65 ns (yellow) and completely disappears after about 100 ns.

Remote Raman and LIBS Spectroscopy

Several studies were completed where both Raman and LIBS data were integrated. Clegg et al. discusses the virtues of RLS spectroscopy for planetary exploration on Earth, Mars, Venus, and airless planetary bodies [1]. The paper demonstrates the complementary value of these techniques on the same sample.

Anderson et al. 2015 completed a brief study of remote Raman and LIBS spectra on simple biological samples [5]. Here, the Raman spectra accurately recorded the molecular structure of the biological sample while LIBS accurately determined the elemental composition.

The First Accurate Theoretically-Derived LIBS Model

The success of this task is arguably the most significant product of this program. LIBS spectra are complex phenomena. The team successfully converted and enhanced high temperature plasma codes to model the relatively low temperature plasma environment that produces a LIBS spectrum. We would have been successful had we simply predicted the LIBS plasma from a single element or a relatively simple system such as the Fe spectrum discussed by Colgan et al 2014 [6]. However, Colgan, Kilcrease, and Johns successfully reproduced the LIBS spectrum of a complex geological material as depicted in Figure 4 with all of the observed major elements [7, 8]. Then this team exceeded the goals of the project and successfully distinguished the FeO and Fe2O3 oxidation states, another first in the LIBS community [9]. The theoretical tools used in this program were also used to elucidate the role of radiation transport on the intensity of a LIBS spectrum. It was demonstrated that such physics effects could significantly modify the line intensity from strong emission features in many LIBS measurements.

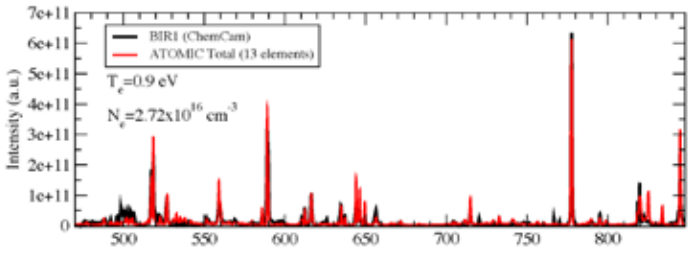

Figure 4. Comparison of the experimental LIBS spectra (black) from a basalt sample (BIR-1A) with the theoretical spectra (red).

The first theoretical models of LIBS spectra containing actinides were developed. Atomic structure calculations for actinides are formidable due to the very complex interactions between multiple open sub-shells. However, tentative atomic structure and collision models were constructed for U and these have been used to distinguish between different oxides of uranium. The predictions of the models agree with new experiments led by Campbell et al., and this work is almost ready for submission for publication.

Theoretical Raman Spectra

While this was the task that matured the least, the theoretical methods for the development Raman spectra was created. In principle, most ab-initio calculations can be used but we found that our implementation of the Gaussian code was more accurate. We used Gaussian to create a mineralogical structure and minimized the structure. Gaussian has a built-in routine that is capable of calculating the Raman active (and infrared active) vibrational modes. This method, in principle, is capable of predicting the vibrational motion and frequency of our geologic samples. This will be a valuable tool in the development of future proposals that include Raman spectroscopy.

The First Integrated Raman and LIBS Spectrometer

Figure 5 contains a picture of the RLFS spectrometer suite. The “UV” and “VIO” spectrometers are only used to collect LIBS signals over the 240 – 340 nm and 380 – 470 nm regions, respectively. The transmission “Trans” spectrometer is used to collect the LIBS spectrum (532 – 900 nm), Raman spectrum (150-4400 cm-1) and TRF (532 – 900 nm). The transmission spectrometer is the prototype for the spectrometer that will be integrated into the SuperCam instrument selected for the NASA Mars 2020 rover. Newell and Peterson completed the optical design and construction of this instrument as well as a very effective software package. Newell will be the first author of the paper that will be submitted to the Reviews of Scientific Instrumentation as soon as possible.

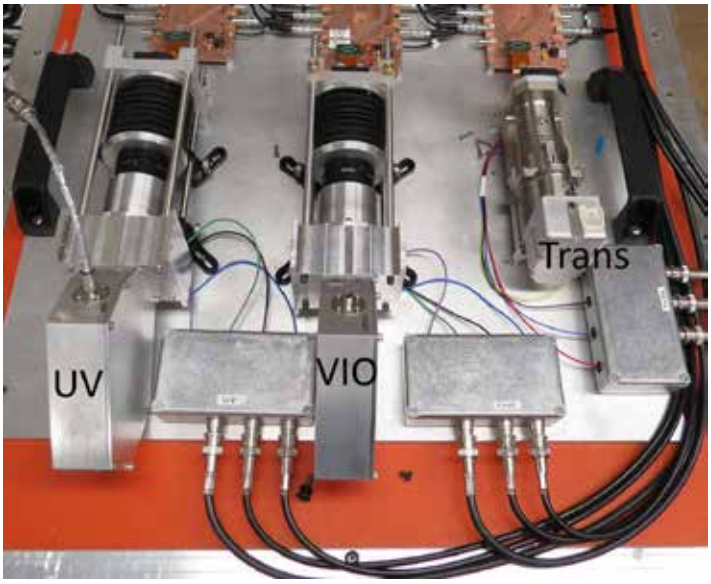

Figure 5. A picture of the RLFS spectrometer suite.

Impact on National Missions

We started program development activities as soon as the program was started in Oct. 2013. Some of the initial scientific investigations in the first year were used in the NASA Mars 2020 proposal that was submitted by the Dec. 23, 2013 deadline. NASA selected the SuperCam proposal on July 31, 2014. The miniature transmission spectrometer that was developed in the first year of this LDRD program became an early prototype of what has become the transmission spectrometer that will fly on SuperCam.

The completed RLS spectrometer suite is now the prototype for a NASA New Frontiers proposal to send the first U.S. landed mission to the Venus surface. This instrument will be capable of collecting thousands of LIBS spectra to measure the Venus surface chemistry and will make the first direct mineralogical analyses from the surface by Raman spectroscopy. According to the draft announcement of opportunity (AO), NASA will release the AO in January 2017 with the proposals due 90 days later.

We just submitted a proposal to the DTRA JSTO-CBD FY17 Service Call to apply the LDRD DR developed RLS architecture to remotely detect chemical and biological weapons.

In collaboration with George Guthrie, we submitted a proposal to use the LDRD DR developed RLS instrument as a prototype for the analysis and detection of Rare Earth Elements within complex geological samples. This proposal was submitted to the DOE FE/NETL program.

References

1. Clegg, S. M., R. Wiens, A. K. Misra, S. K. Sharma, J. Lambert, S. Bender, R. Newell, K. Nowak-Lovato, S. Smrekar, M. D. Dyar, and S. Maurice. Planetary geochemical investigations using Raman and laser-induced breakdown spectroscopy. 2014. Applied Spectroscopy. 68 (9): 925.

2. Judge, E. J., J. Colgan, K. Campbell, J. E. Barefield, H. E. Johns, D. P. Kilcrease, and S. Clegg. Theoretical and experimental investigation of matrix effects observed in emission spectra of binary mixtures of sodium and copper and magnesium and copper pressed powders. 2016. Spectrochimica Acta Part B. 122: 142–148.

3. II, J. E. Barefield, E. J. Judge, K. R. Campbell, J. P. Colgan, D. P. Kilcrease, H. M. Johns, R. C. Wiens, R. E. McInroy, R. K. Martinez, and S. M. Clegg. Analysis of geological materials containing uranium using laser -induced breakdown spectroscopy. 2016. SPECTROCHIMICA ACTA PART B-ATOMIC SPECTROSCOPY. 120: 1.

4. Wiens, R. C., M. Bodine, A. Ollila, R. Newell, R. McInroy, S. K. Sharma, P. Gasda, S. Maurice, and S. M. Clegg. Cross sections of common minerals using pulsed remote Raman spectroscopy. Spectrochim. Acta A.

5. Anderson, A. S., Mukundan, R. E. McInroy, and S. M. Clegg. Combined LIBS-Raman for Remote Detection and Characterization of Biological Samples. 2015. IMAGING, MANIPULATION, AND ANALYSIS OF BIOMOLECULES, CELLS, AND TISSUES XIII. 9328.

6. Colgan, , E. J. Judge, D. P. Kilcrease, and J. E. Barefield II. Ab-initio modeling of an iron laser-induced plasma: Comparison between theoretical and experimental atomic emission spectra. 2014. SPECTROCHIMICA ACTA PART B-ATOMIC SPECTROSCOPY. 97: 65.

7. Colgan, J., E. J. Judge, H. M. Johns, D. P. Kilcrease, J. E. Barefield, R. McInroy, P. Hakel, R. C. Wiens, and S. M. Clegg. Theoretical modeling and analysis of the emission spectra of a ChemCam standard: basalt BIR-1A. 2015. Spectrochimica Acta Part B. 110: 20.

8. Johns, H. M., D. P. Kilcrease, Colgan, E. J. Judge, J. E. Barefield II, R. C. Wiens, and S. M. Clegg. Improved electron collisional line broadening for low-temperature ions and neutrals in plasma modeling. 2015. JOURNAL OF PHYSICS B-ATOMIC MOLECULAR AND OPTICAL PHYSICS. 48 (22).

9. Colgan, , J. E. Barefield II, E. J. Judge, Campbell, H. M. Johns, D. P. Kilcrease, McInroy, and S. M. Clegg. Experimental and theoretical studies of laser-induced breakdown spectroscopy emission from iron oxide: Studies of atmospheric effects. 2016. SPECTROCHIMICA ACTA PART B-ATOMIC SPECTROSCOPY. 122: 85.

Publications

Barker, B. J., J. M. Berg, S. A. Kozimor, N. R. Wozniak, and M. P. Wilkerson. Visible and near-infrared excitation spectra from the neptunyl ion doped into a uranyl tetrachloride lattice. 2016. JOURNAL OF MOLECULAR STRUCTURE. 1108: 594.

Clegg, S. M., Wiens, A. K. Misra, S. K. Sharma, Lambert, Bender, Newell, Nowak-Lovato, S. u. e. Smrekar, M. D. Dyar, and Maurice. Planetary Geochemical Investigations Using Raman and Laser-Induced Breakdown Spectroscopy. 2014. APPLIED SPECTROSCOPY. 68 (9): 925.

Clegg, S. M., Wiens, A. K. Misra, S. K. Sharma, Lambert, Bender, Newell, Nowak-Lovato, S. u. e. Smrekar, M. D. Dyar, and Maurice. Planetary Geochemical Investigations Using Raman and Laser-Induced Breakdown Spectroscopy. 2014. APPLIED SPECTROSCOPY. 68 (9): 925.

Colgan, , E. J. Judge, D. P. Kilcrease, and J. E. Barefield II. Ab-initio modeling of an iron laser-induced plasma: Comparison between theoretical and experimental atomic emission spectra. 2014. SPECTROCHIMICA ACTA PART B-ATOMIC SPECTROSCOPY. 97: 65.

Colgan, , E. J. Judge, H. M. Johns, D. P. Kilcrease, J. E. Liarefield II, McInroy, Hakel, R. C. Wiens, and S. M. Clegg. Theoretical modeling and analysis of the emission spectra of a ChemCam standard: Basalt BIR-1A. 2015. SPECTROCHIMICA ACTA PART B-ATOMIC SPECTROSCOPY. 110: 20.

Colgan, , J. E. Barefield II, E. J. Judge, Campbell, H. M. Johns, D. P. Kilcrease, McInroy, and S. M. Clegg. Experimental and theoretical studies of laser-induced breakdown spectroscopy emission from iron oxide: Studies of atmospheric effects. 2016. SPECTROCHIMICA ACTA PART B-ATOMIC SPECTROSCOPY. 122: 85.

Hartig, K. C., Colgan, D. P. Kilcrease, J. E. Barefield II, and Jovanovic. Laser-induced breakdown spectroscopy using mid-infrared femtosecond pulses. 2015. JOURNAL OF APPLIED PHYSICS. 118 (4).

Hartig, K. C., Colgan, D. P. Kilcrease, J. E. Barefield II, and Jovanovic. Laser-induced breakdown spectroscopy using mid-infrared femtosecond pulses. 2015. JOURNAL OF APPLIED PHYSICS. 118 (4).

II, J. E. Barefield, E. J. Judge, K. R. Campbell, J. P. Colgan, D. P. Kilcrease, H. M. Johns, R. C. Wiens, R. E. McInroy, R. K. Martinez, and S. M. Clegg. Analysis of geological materials containing uranium using laser -induced breakdown spectroscopy. 2016. SPECTROCHIMICA ACTA PART B-ATOMIC SPECTROSCOPY. 120: 1.

Johns, H. M., D. P. Kilcrease, Colgan, E. J. Judge, J. E. Barefield II, R. C. Wiens, and S. M. Clegg. Improved electron collisional line broadening for low-temperature ions and neutrals in plasma modeling. 2015. JOURNAL OF PHYSICS B-ATOMIC MOLECULAR AND OPTICAL PHYSICS. 48 (22).

Judge, E. J., Colgan, Campbell, J. E. Barefield II, H. M. Johns, D. P. Kilcrease, and Clegg. Theoretical and experimental investigation of matrix effects observed in emission spectra of binary mixtures of sodium and copper and magnesium and copper pressed powders. 2016. SPECTROCHIMICA ACTA PART B-ATOMIC SPECTROSCOPY. 122: 142.

Explosives Signatures for Detection: Nonlinear GHz to THz Responses

David S. Moore
20140049DR

Abstract

Our research was intended to fill a major gap in our explosives detection arsenal, by detecting the bulk explosive itself. Serendipitously, the large reflectivity of metals allows metal shielding detection using the same technology. The capability is not intended for use in isolation, but rather as a tool in the toolset – a tool with dramatically improved detection capabilities, specifically penetration through clothing, camouflage, or packaging by using GHz-to-THz frequency radiation, which is a unique electromagnetic spectral region with sparse application to explosives detection. The capability is potentially disruptive to current evasion-of-detection tactics, because it exploits the nonlinear coupling of penetrating GHz-to-THz radiation to explosives and the detection of the alternative signatures that are generated, without exceeding FCC average power exposure limits. We established a theory and modeling framework that clarifies the nature of the microstructural and nonlocal dielectric properties of explosives materials that produce the observable nonlinear signal generation in explosive samples and published two pivotal papers on this framework [1, 2]. We established bounds on the electromagnetic fields (in the 2.5 GHz, 11-17 GHz, and low THz frequency ranges) needed to produce observable nonlinear or thermal effects in explosive samples. The required electromagnetic fields were found to be of the order of the FCC average power exposure limits, which could limit the spheres of application of this technology for explosives detection in field scenarios.

Background and Research Objectives

The detection of explosives is a pressing current problem, both at home and abroad, requiring a suite of technologies to cover the multitude of possible threat scenarios. A serious gap is evident in this suite of technologies – that of detecting the bulk explosive using non-ionizing radiation – the gap that the work described herein is intended to fill.

It is generally believed that the intentional initiation of explosives occurs by a physical concentration of "hot spots" that are, in essence, localized regions of high temperature and pressure within which thermal decomposition chemistry occurs on a rapid time scale. A variety of mechanisms have been proposed for this dynamic localization of energy [3]. Localization of energy under sub-initiation threshold stimulation can potentially generate local temperatures sufficient to release some of the chemical energy stored in explosives, subsequently leading to alternate signatures. These effects were observed in the experiments preliminary to this project.

Our project posits that electromagnetic (EM) fields localize in the microstructure of heterogeneous explosives and are nonlinearly amplified by various mechanisms including chemical processes. The relevant microstructural features observed in tomographic and other images of these materials are of micron to mm size, commensurate with the range of wavelengths in the GHz-to-THz regime. We established a theory and modeling framework to enable the detailed understanding of the nature of the microstructural and nonlocal dielectric properties of these materials under electromagnetic stimulation, underpinned by the metastability of explosives as the unique characteristic that allows their discrimination from inert materials. The models intend to clarify the nonlinear responses of bulk explosives to electromagnetic stimulation in the GHz-to-THz regime [4, 5].

Experimentally, we proceeded by quantifying signatures in relevant and well-defined explosive materials, including their permittivity behavior, EM absorption mechanisms and intrinsic dielectric response as a function of incident frequency, power, and amplitude to determine the effects of EM radiation localized at defects and the subsequent redistribution of that energy followed by generation of emissions detectable at a distance.

Scientific Approach and Accomplishments

Theory and Modeling

We completed first principles simulations of the THz spectrum of an explosives simulant, 1,3-dinitrobenzene. The methodology demonstrated that supercell electronic structure methods are useful for predicting THz spectra in molecular explosives. A paper describing the method and results is in press in European Physics Letters [6]. We found that van der Waals dispersion forces need to be included in the calculations to account for the intermolecular vibrations and to assess and distinguish between the intra- and intermolecular vibrational modes in the THz frequency region. These results were an important first step to establish sufficient theory and modeling methodology at the time and length scales needed for the long-range molecular interactions operative at GHz to THz frequencies.

We formulated micro-CT images of explosives so that they could be utilized in finite element multi-physics software for simulation of the electromagnetic interactions. We translated the 3D micro-CT images of an explosive composed of HMX and HTPB polymer (these have sufficient X-ray contrast to allow segmentation of the images into HMX and binder) into the COMSOL finite element multi-physics code. Simulations were performed with and without inclusion of chemical energy release/thermal feedback and EM emissions. We found strong localization of the RF fields in the smaller (high curvature) sample features, accompanied by concomitant strong localization of the temperature increases (Figure 1).

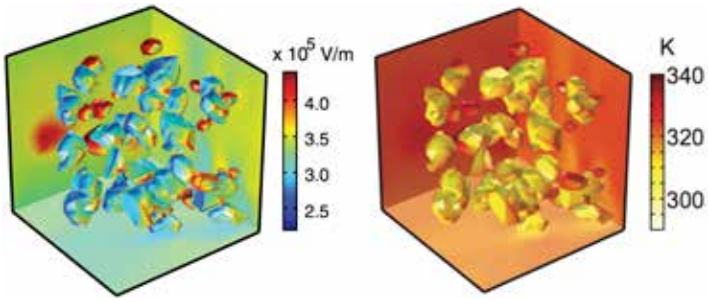

Figure 1. Electric field distribution (left) and temperature distribution (right) for an HMX/Viton A system illuminated from the top by a 13.3 GHz frequency source at 0.22 GW per square meter intensity.

The results were published in Phys. Rev. Applied [1]. We are extending the above numerical FEM simulations to include chemistry in an extremely simplified fashion based on coupled rate equations for the various phase transitions present in HMX. The parameters needed for this simulation can be found in previous publications on electromagnetically induced localized ignition in secondary high explosives [7]. The model allows temporal tracking of the mass fraction of the species generated and consumed during the process, and all the transition probabilities depend on the instantaneous temperature, which itself depends on the energy deposited by the electromagnetic field over the local EM hot spots and whose spatial-temporal evolution is determined by the heat transport equation. We are currently analyzing the impact of phase transitions on the spatio-temporal distribution of the electromagnetic field, the electromagnetic dissipated energy, and the thermal distribution for various combinations of explosives and binders. We are making the drastic assumption that all phases have the same optical response, but their thermal conductivity and heat capacity differ, as given by Table III of the same paper cited above. We also assume heat transfer only by conduction, while it is clear that we must incorporate gas phases produced in combustion and this will require heat convection. How to model in COMSOL these gas phases in our complex heterogeneous explosives, how they also interact with light, and what are their optical and thermal properties, are topics that need a further study.

In order to understand the generation and emission of new GHz to THz frequencies (as observed in Ref. 4), we developed a simulation method for the scattering of electromagnetic waves in anisotropic energetic materials, wherein nonlinear light-matter interactions result in frequency-conversion and polarization changes. Applied electromagnetic fields of moderate intensity can induce these nonlinear effects without triggering chemical decomposition, offering a mechanism for the nonionizing identification of explosives. We leveraged molecular-dynamics simulations and extensions of classical electro-dynamics to predict nonlinear THz emission due to vibrational scattering in PETN and AN. By constraining the simulation geometries and polarizations of the external electric field, our predictions are easily extended to the experimentally relevant far-field measurement. In addition, by using reactive MD simulations we avoided any approximations due to harmonic absorption or emission as well as normal mode descriptions of the molecular vibrations.

While the use of a force field is an approximation of the actual physics of the problem, it does, however, allow for tractable simulations that provide useful and rapid 2D-spectra predictions. We showed the 2D spectra of PETN and ammonium nitrate that differ significantly in the THz frequency range due to changes in the location and intensity of third-harmonic emission of the input light as well as other nonlinear frequency emissions. The calculated output signals are dramatically different in both polarization and frequency from the input electric field pulse, which provides a potential for a THz detection technique with chemical specificity. Further information can be found in Ref. 2. The computed average emission signals for all

output polarizations for incident pulses averaged over all polarizations (the situation that would exist for a powdered or composite sample) are shown in Figure 2.

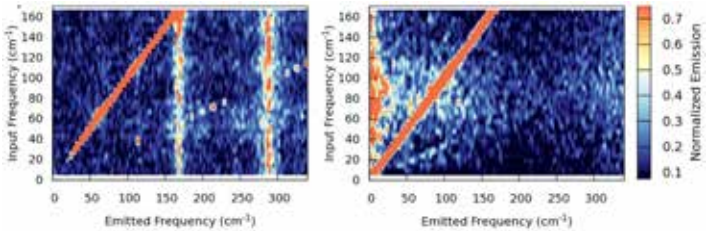

Figure 2. Computed average THz emission signals for all output polarizations for incident pulses averaged over all polarizations for PETN (left) and AN (right).

Experiment

The linear responses of explosives and simulants in the GHz to THz frequency range were measured using a variety of methods, due to the large frequency range. In collaboration with NIST-Boulder, we performed dielectric characterization on a broad range of oxidizers and explosives over the 220-325 GHz frequency range with a millimeter-wave (MMW) free-space scattering measurement system. We used two different methods - explicit and iterative - for determining the complex permittivity of material samples from scattering corrected parameters. Our measurements for the explosives indicate that the real parts of the complex permittivity of the samples are almost non-dispersive in the measurement frequency band, whereas the imaginary parts minimally increase with frequency. Furthermore, we observe that both the real and imaginary parts of the permittivity of the HE samples are fairly constant over 220-325 GHz. The complete results are given in a paper to be submitted to the Journal of Infrared, Millimeter and THz Waves.

We measured linear THz spectra of a large number of explosives, oxidizers, and fuels to establish baselines for the nonlinear THz measurements. In order to establish the baseline for temperature dependence of the linear THz spectra (a possible alternate signature), we measured THz spectra as a function of temperature from liquid Helium temperatures to ambient. One example is shown in Figure 3. All of the THz spectra obtained in this project are being assembled for eventual publication.

In order to understand the physics underlying non-linear processes that generate alternate signatures, we focused on RF time-dependent reflection experiments with careful control of incident RF power and field uniformity. We performed these measurements at 2.45 GHz (see next paragraph) and near 11-17 GHz using a traveling wave tube amplifier from AOT-AE. The experiments at 11-17 GHz (typically 14.5 GHz) were performed using four different waveguide approaches. The first approach measured time dependent reflected power from a 1 mm thick by 6 mm diameter sample placed in the center of a standard 14.5 GHz standard waveguide. The reflectivity was not found to exhibit any nonlinear effects and the samples after exposure (to multiple 1 ms long pulses) were not visibly changed from before exposure.

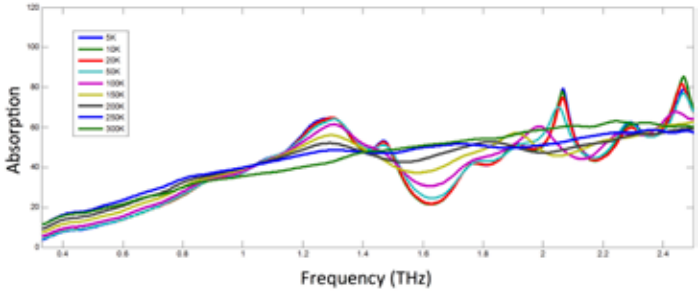

Figure 3. THz spectra of ammonium nitrate versus temperature. There is a phase transition from AN IV to AN V at -18 C.

This result is in opposition to what was found in the preliminary experiments in the circular cavity described below, but the electric field at the sample was lower than that of the circular cavity by nearly a factor of fifty. The second approach implemented a resonant cavity, designed to increase the field at the sample by five times. Again no nonlinear reflectivity effects were observed and the samples were again unchanged. The third approach involved a different resonant cavity design with another factor of two increase in field. Again no nonlinear reflectivity effects were observed and the samples were unchanged from ambient. The final approach utilized a tapered cavity with estimated field at the sample of 0.6 MV/m. The reflectivity measurements for 1 mm thick by 6 mm diameter pressed sugar sample in this cavity showed time dependent reflectivity that increased or decreased during the pulse, depending on whether the drive frequency was above or below (respectively) the cavity resonance frequency, a result that is consistent with a decrease in the sample resonance frequency that could be due to increasing sample temperature during the pulse (see Figure 4). No permanent changes in the sugar samples were observed, however, unlike the results obtained at 1 MV/m fields (c.f., Figure 5). Experiments on explosives samples in this taper cavity are ongoing. While these experiments did not achieve sufficient field strengths to produce sample damage, they did provide a lower bound on the necessary fields for production of non-linear or sample temperature effects on the RF reflectivity. Similarly to the 2.45 GHz experiments described below, these experiments confirm that the field strengths apparently required for observable nonlinear responses are of the order of 0.5 to 1 MV/m for pulses of 1-2 ms duration. Longer duration pulses are not ultimately useful because of potential human effects.

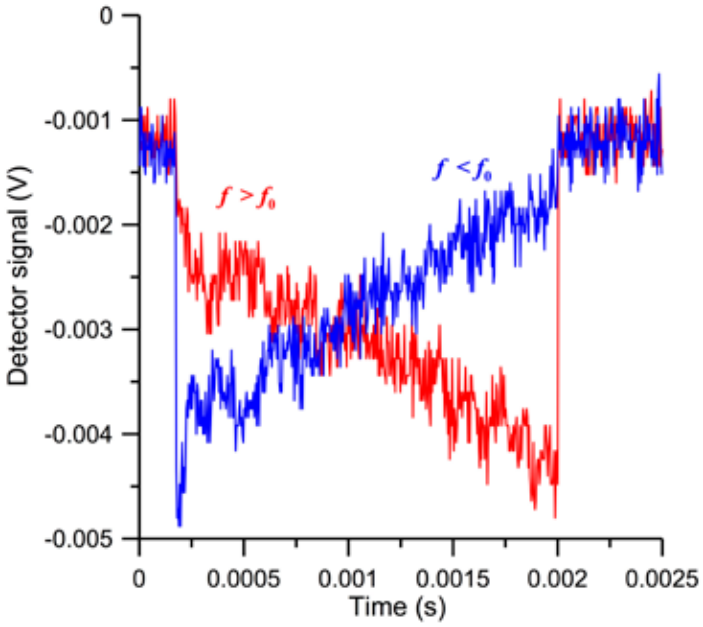

Figure 4. Time dependent RF reflectivity from a pressed sugar sample in the tapered resonant cavity, showing increase in reflectivity for a drive frequency above the sample resonance and decrease in reflectivity for a drive frequency below the sample resonance, consistent with what would be expected for sample heating. Prepulse signal values were recovered after a 10 sec pause, indicating the sample was heated by the pulse and then cooled back to ambient.

At 2.45 GHz, we previously observed a feature in the reflected power signal (see Figure 5) from a sample in a circular resonant cavity, which signifies fast absorption of power by the sample just before ignition occurs. This signature occurred preferentially in the explosives samples and is likely due to enhanced coupling between the 2.45 GHz energy and gas phase ions or radicals released during partial decomposition. In order to avoid having to tune the cavity to each sample to be in resonance with the 2.464 GHz amplifier, as well as more realistically mimic a field use of this technology, we proceeded using a rectangular waveguide, which is much more flexible for ease in performing measurements on many different samples and offers far greater control of the electric field uniformity and consistency, but produces field strengths significantly lower than that of the circular cavity. Repeated experiments with HMX (powdered and hand-packed) showed that the sample heated slightly but the non-linear effect was not observed. A COMSOL simulation of the waveguide and the circular cavity shows that the electric field on the sample in the circular cavity was about 1 MV/m, while the maximum in the waveguide was ca. 0.25 MV/m. We also simulated the heating rate for HMX in the two cavities, finding nearly a factor of 4 slower sample heating in the waveguide than in the circular cavity. We were not able to test longer exposures due to the limits of our current microwave power supply, so did not succeed in recording the characteristic reflected power signal (e.g., like Figure 5) with the waveguide.

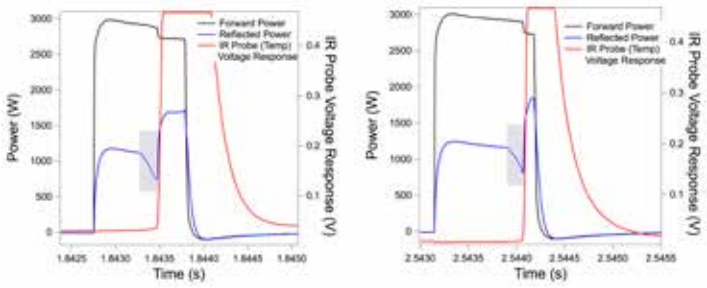

Figure 5. Reflected power signal from an HMX sample in a circular resonant cavity, indicating fast absorption of power by the sample just before ignition (light blue shaded region). Ignition is indicated by the fast rise in the IR probe signal.

We explored nonlinear frequency conversion and other nonlinear THz effects using a high power THz system. The system was found to have too much background THz signal at the third harmonic frequency range to observe expected signatures from single crystal PETN and RDX. We drop cast RDX and HMX samples (polycrystalline 10-50 µm thickness) onto meta-material structures with resonance in the 1-2 THz range. Initial experiments on the THz spectra of these samples did not reveal nonlinear responses beyond the material's normal linear THz spectrum overlying the meta-material resonance. Further experiments with other meta-materials with a variety of THz resonance frequencies are ongoing.

Impact on National Missions

This project represents a transformational approach to bulk explosives detection. The overarching goal of the project directly supports LANL's long-term objective of discovery of the next generation of materials signatures of explosives within its global security mission. The deep fundamental understanding of energy absorption and subsequent responses are applicable to the MaRIE project component "Decadal Challenges for Predicting and Controlling Materials Performance in Extremes" for the design and control of energy release in explosives. Models from this project will aid development of a new framework for a unified description of explosives' hot spots coupled to local mechanical, thermal and electromagnetic signatures. Understanding and controlling the material functionality of defects and crystalline interfaces is important for understanding hot spots and their signatures, underpins research aimed and understanding defects and interfaces, and lays the groundwork for advanced THz and GHz spectroscopies.

References

1. Kort-Kamp, W. J. M., N. L. Cordes, A. Ionita, B. B. Glover, A. L. Higginbotham-Duque, W. L. Perry, B. M. Patterson, D. A. R. Dalvit, and D. S. Moore. Microscale electromagnetic heating in heterogeneous energetic materials based on X-ray computed tomography. 2016. Physical Review Applied. 5: 044008.

2. Wood, M. A., D. A. R. Dalvit, and D. S. Moore. Nonlinear electromagnetic interactions in energetic materials. 2016. Physical Review Applied. 5: 014004.

3. Tokmakoff, A., M. D. Fayer, and D. D. Dlott. Chemical reaction initiation and hot spot formation in shocked energetic molecular materials. 1993. Journal of Physical Chemistry. 97: 1901.

4. Moore, D. S., and R. Oldenborg. Stand-off stimulation of alternate signatures. 2010. Office of Naval Research Sciences Addressing Asymmetric Explosive Threats Program Review.

5. Moore, D. S.. Method and apparatus for detecting explosives. 2011. US Patent 7,939,803.

6. Ahmed, T., A. K. Azad, R. Chellappa, J. X. Zhu, A. Higginbotham-Duque, D. S. Moore, and M. J. Graf. Vibrational signatures in the THz spectrum of 1,3-dinitrobenzene: A first-principles and experimental study. To appear in European Physics Letters.

7. Perry, W. L., J. A. Gunderson, B. B. Glover, and D. M. Dattelbaum. Electromagnetically induced localized ignition in secondary high explosives: Experiments and numerical verification. 2011. Journal of Applied Physics. 110: 034902.

Publications

Ahmed, T., A. K. Azad, R. Chellappa, A. Higginbotham-Duque, D. M. Dattelbaum, Z. Jian-Xin, D. Moore, and M. J. Graf. Vibrational signatures in the THz spectrum of 1,3-DNB: a first-principles and experimental study. 2016. Europhysics Letters. 114 (3): 37010.

Azad, A. K., V. H. Whitley, K. E. Brown, T. Ahmed, C. J. Sorensen, and D. S. Moore. Temperature dependent terahertz properties of energetic materials. 2016. In Terahertz Physics, Devices and Systems X: Advanced Applications in Industry and Defense. (Baltimore, MD, 17-21 April 2016). Vol. 9856, p. 98560W. New York: SPIE.

Boyles, A.. Ticking the dragon: A Los Alamos team teases out differences between hidden explosives and harmless materials. 2016. Stewardship Science: The SSGF Fellowship Magazine.

Brown, K. E., M. T. Greenfield, S. D. McGrane, and D. S. Moore. Advances in explosives analysis: Part I: animal, chemical, ion, and mechanical methods. 2016. Analytical Bioanalytical Chemistry. 408: 35.

Brown, K. E., M. T. Greenfield, S. D. McGrane, and D. S. Moore. Advances in explosives analysis - Part II: photon and neutron methods. 2016. Analytical Bioanalytical Chemistry. 408: 49.

Chowdhury, D. R., X. Su, Y. Zeng, X. Chen, A. J. Taylor, and A. K. Azad. Excitation of dark plasmonic modes in symmetry broken terahertz metamaterials. 2014. Optics Express. 22: 19401.

Kim, S., D. Novotny, A. Higginbotham-Duque, D. S. Moore, and W. L. Perry. Electromagnetic measurements for dielectric properties of explosive materials with millimeter waves. Journal of Infrared, Millimeter, and Terahertz Waves.

Kort-Kamp, W. J., N. L. Cordes, A. Ionita, B. B. Glover, A. L. Duque, W. L. Perry, B. M. Patterson, D. A. Dalvit, and D. S. Moore. Microscale Electromagnetic Heating in Heterogeneous Energetic Materials Based on X-ray Computed Tomography. 2016. PHYSICAL REVIEW APPLIED. 5 (4): 044008.

Moore, D. S., M. A. Wood, and D. A. R. Dalvit. Non-linear terahertz signal generation. 2016. SPIE Newsroom.

Shah, D., D. M. Dattelbaum, B. B. Glover, D. S. Moore, and M. A. Azad. Terahertz Characterization of Dinitrobenzene for Metamaterial Based Sensors. 2014. MPA-CINT: CENTER FOR INTEGRATED NANOTECHNOLOGIES.

Smith, J. E., D. E. Morris, F. L. Taw, D. S. Moore, and R. W. Margevicius. 2016 Science of Signatures Capability Review: Nuclear and Radiological / Chemical and Materials Signatures - Explosives. 2016. Los Alamos Report LA-UR-12-22992.

Sorensen, C. J., and D. S. Moore. Radio frequency electromagnetic emissions from materials under high frequency mechanical excitation. To appear in American Physical Society Topical Conference on Shock Compression of Condensed Matter - 2015. (Tampa, FL, 14-19 June, 2015).

Wood, M. A., D. A. R. Dalvit, and D. S. Moore. Nonlinear electromagnetic interactions in energetic materials. 2016. Physical Review Applied. 5: 014004.

Trojan Horse Drug Development Approach: Targeting Gene Dosage Control to Induce Bacterial Suicide

Sofiya N. Micheva-Viteva
20150664ECR

Introduction

Multi-drug resistant pathogens present an escalating threat to public health. In this project we seek to discover a novel class of antimicrobial therapies that can restrict the evolution of drug resistant pathogenic bacteria. To achieve this goal, we propose to elucidate a poorly understood mechanism for regulation of protein turnover in the bacterial cell. Messenger ribonucleic acids (RNA) translate the genetic information stored on deoxyribonucleic acid (DNA) molecules into amino acid sequence in the proteins. Gene expression is regulated both on transcriptional (DNA) and post-transcriptional (RNA) levels. We will address a fundamental science question of how bacteria use higher order molecular structures within RNA transcripts to control gene expression. Applying biochemical analytical tools and molecular dynamics simulation models we will identify two and three dimensional RNA structures with regulatory role in transcript stability. Furthermore, we will perform a high throughput screen of small molecule libraries to discover compounds that specifically bind to the RNA regulatory structural elements and alter macromolecular dynamics. We aim to identify chemical scaffolds that cause deregulation of protein dosage control. We will exploit a mechanism of gene regulation that is exclusively found in bacteria and lower eukaryotic cells to develop broad-spectrum antimicrobial drugs with minimum toxicity to the human host. Discovery of small molecules that specifically bind to higher order RNA structural elements is the grand challenge of this project.

Benefit to National Security Missions

This research directly supports LANL's mission in national security for biothreat reduction. Discovery of a novel class of antibiotic drugs that can restrict the evolution of drug resistant species directly addresses the "National Strategy for Combating Antibiotic-Resistant Bacteria" and is aligned with the LANL focus area in Complex Natural Systems and the new strategy for development of advanced therapeutics. DoD, DHS, and NIH are interested in discovery of novel antimicrobial therapies.

Progress

The main objective of our research is to decipher evolutionary conserved mechanisms in bacterial cells that regulate gene dosage control on post-transcriptional level through the activity of key regulatory protein RNase E, an endonuclease essential for bacterial cell viability due to its role in the normal rapid decay of many transcripts including maturation of ribonucleic acid (rRNA). Our work has two main streams: (1) identification of structural elements that define the stability of bacterial RNA molecules as substrates of RNaseE, and (2) development of a discovery platform for small molecules that interfere with RNase E activity, that can be used as molecular scaffolds for the development of novel class antimicrobials.

In our model, conserved RNA structures of higher order regulate the activity of RNase E. We performed in vitro biochemical reactions measuring the velocity of E.coli 9S rRNA cleavage to 5S rRNA by RNaseE. We demonstrated that the stem-loop structure located 5 nucleotides (nt) downstream of the RNaseE cleavage site plays the role of a molecular switch that regulates the efficiency of the enzymatic reaction. By reducing the size of the stem-loop structure from 150 nt to 60 nt, we registered 10-fold higher efficiency of RNA processing. In bacterial cells the 5S rRNA is a structural part of the larger (50S) ribosomal subunit. Due to the vital role of ribosomes in protein synthesis inhibition of 5S rRNA maturation process will result in cell death. We developed an assay for high throughput screen (HTS) of inhibitors of 5S rRNA processing by RNaseE. Given the key role of RNaseE in microbial cell life cycle there have been multiple attempts to develop enzyme catalytic inhibitors. Our approach is unique; in contrast to previously published research we are developing a screening procedure with the propensity to identify inhibitors of

enzyme substrate interaction and modulators of substrate (RNA) secondary structure. In previous screening assays a 15 nt long oligonucleotide has been used and the increase in fluorescence intensity has been measured as a reporter of the enzymatic cleavage.

To date, small molecule inhibitors of RNaseE activity have been discovered that show efficiency in the mM concentration range, clearly not suitable for in vivo application as antibiotics. In our assay the RNA substrate is 100 nt and harbors the stem-loop structure naturally found in the RNAse substrates. Initially we attempted to develop a florescence resonance energy transfer (FRET) assay but it showed very poor signal to noise ratio indicating at low index of assay reproducibility for a HTS. Our current assay is based on quantitative analysis of RNA cleavage product measured by capillary electrophoresis using Applied Biosystems® genetic analyzer. Our assay is highly reproducible and informative as we can immediately determine whether an inhibitor targets enzyme catalytic activity or the substrate structure by examining the patterns of the histograms and the fluorescence intensity of the main peaks produced by the cleavage of FITC- tagged RNA substrate.

We are currently performing a screen of small molecule library consisting of 4, 000 compounds with established pharmacological properties and cytotoxicity profiles (supplied by MicroSource Discovery Systems). Each HTS requires a positive control for comparative analysis of the efficiencies of interference of the novel compounds with the enzymatic assay. Since no effective inhibitors of RNaseE activity are currently available on the market we designed synthetic compound consisting of 8 locked nucleic acids (LNA), a bicyclic RNA analogue complementary to the RNAseE cleavage site where the ribose sugar is structurally constrained by a methylene bridge between the 2'-oxygen and the 4'-carbon atoms. The LNA was purchased from Exiqon company and has proven to inhibit the processing of 300 nM RNA by RNaseE with 100% efficiency at 1nM concentration. This synthetic inhibitor has a great application for our assay and at the same time presents a blueprint for the engineering of antibacterial compounds with high selectivity against bacterial species of interest.

Such antimicrobials would have a great potential fighting infectious disease without targeting the normal microfluora. Additionally, we are solving the RNA structure of transcript encoding soluble lytic transglycosylase (SLT) via SHAPE. To date, we have probed only 50% of the RNA sequence due to the technical challenge of in vitro synthesis of a CG rich transcript.

Future Work

During the Fiscal Year 2017 we will validate the role of the ribonucleic acid, RNA, architecture as a molecular switch guiding the interaction with RNase E and regulating endonuclease activity that is crucial for the survival of bacterial cells. We will complete our high throughput screen of small molecules and will identify novel inhibitors of RNaseE endonuclease activity from a pool of 4,000 compounds with established pharmacological properties and cytotoxicity profiles. Our research will focus on the development of novel class anti-bacterial drugs that will inhibit enzymatic activity through changes in substrate secondary architecture, a paradigm shift in enzyme-substrate interaction models where allosteric inhibitors induce changes in enzyme secondary structure. We will perform biochemical assays to evaluate the effect of small molecule inhibitors on the velocity of RNaseE - substrate interaction and the enzymatic cleavage of RNA. These assays will be crafted to determine the changes of key enzyme characteristics including dissociation constants Kd. These assays will identify molecular scaffolds that have affinity to higher order of RNA structure and will serve as templates for the rational design and development of chemical compounds with higher efficiency and specificity as antibacterial drugs.

Conclusion

We will (1) elucidate a key mechanism of microbial cell survival driven by RNA instability, (2) complete a high throughput screen of small molecules in a fluorescence-based assay to find compounds that inhibit RNA degradation, and will (3) validate the small molecule antibiotic activity in live bacterial cells. We will pursue a thus far unexploited strategy for developing of an entirely new class of antibiotics. Discovery of therapeutics that can restrict the emergence of drug resistant pathogenic bacteria will have a high impact on drug development and national security.

Publications

Li, N., S. Hennelly , S. Stubben, S. Micheva-Viteva, B. Hu, Y. Shou, M. Vuyisich, C. Tung, P. Chain, K. Sanbonmatsu, and E. Hong-Geller. Functional and Structural Analysis of a Highly-Expressed Yersinia pestis Small RNA following Infection of Cultured Macrophages. 2016. PLoS One. 11 (12): e0168915.

Stubben, C. J., S. N. Micheva-Viteva, S. K. Buddenborg , J. M. Dunbar , and E. Hong-Geller . Differential expression of small RNAs from Burkholderia thailandensis in response to varying environmental and stress conditions. 2014. BMC Genomics. 19 (15:385): doi: 10.1186/1471.

Hand-held Laser-Ultrasound Two-Dimensional Scanner

Eric B. Flynn
20150673ECR

Introduction

With this project, we will develop and demonstrate a hand-held laser ultrasound scanning device that provides rapid, convenient, stand-off inspection. The form-factor of this device will be similar to that of a hand-held bar-code scanner. The device will be able scan at a rate of up to 250 scan lines per second. In this way, the device will generate a visibly continuous horizontal scan line that the operator can manually sweep over the inspection region.

The proposed hand-held scanner has only become realizable with our recent demonstration of a novel ultrasonic inspection technique based on spatial-frequency response, referred to as acoustic wavenumber spectroscopy (AWS). The premise of the technology is the measurement and analysis of a system's spatially-distributed response to a steady, single-tone excitation.

With AWS, we demonstrated the ability to scan the ultrasonic steady state response of a structure at up to five square meters per minute at a distance of three meters with a scan-line spacing of one mm. This is over 100 times faster than conventional ultrasound and translates to a linear speed of approximately 83 meters per second, which means a 30 mm long scan line can be recorded in 3.6 milliseconds, making a hand-held device possible. AWS relies on the spatial frequencies, or wavenumbers, of the response. In a bounded medium, the wavenumber of a wave at a given frequency is a function of the geometry and material properties of that medium. By making direct estimates of local wavenumber on a pixel by pixel basis for a known excitation frequency, AWS can make estimates of local properties such as thickness or cracking. In AWS, the excitation source is fixed at an arbitrary location, and the location does not affect the imaging. This insensitivity to excitation source is also a key result for the proposed project.

Benefit to National Security Missions

Materials Storage

Rapid, standoff inspection of material storage containers for corrosion, cracking and the presence of material contents such as fluid build-up. A compact scanner could be mounted on robotic inspection systems (aerial or ground) and would enable inspection of hard-to-reach places, such as underground storage and between shielding and encasement layers.

Stockpile Stewardship

Provide a unique ability to detect interlayer disbonds and to map the transmission of acoustic/ultrasonic energy among assembled components. The latter may serve as a form of fingerprinting for identifying when something may have unexpectedly changed as a result of aging or exceeding environment specifications.

Nonproliferation

Ultrasonic fingerprinting (barcoding) of accountable systems and storage containers. In-the-field detection of tampering without the need for tamper evidence devices.

Manufacturing

Non-disruptive, layer-by-layer quality assurance of additive manufacturing processes (3D printing). A sufficiently small and fast scanning system could be built into assembly lines to provide quality control inspection of all manufactured parts (100% QC).

DoD & Aerospace

Maintenance of military air, ground, and naval assets accounts for the majority of system lifecycle cost. New, not well understood, lightweight composite materials magnify this problem. A rapid quick check capability could drastically improve the combat readiness and reduce the maintenance costs of systems utilizing these advanced materials.

Biomedical
Rapid assessment of the elasticity of diseased or burned tissue (far-reaching).

Progress

Several key milestone were met between June 2015 and June 2016. Most importantly, we've designed, built, and tested a completely fiber-optic-based laser-Doppler vibrometer (LDV). In doing so, we bypassed the intermediate objective of building a bread-board system in FY1, and have started meeting the FY2 objective of a completely fiber-optic system.

The vibrometer operates in the 1550 nm range, which means we can increase the laser power up to 50mW while maintaining same laser safety level as the 1mW commercial HeNe system. This will ultimately lead to both a more compact and more sensitive LDV sensor.

We designed and tested a unique method for automatically mapping the scan measurements on to the proper coordinates on the structure being inspected (referred to as coregistration). This method uses a camera mounted with the scan, and a temporary reference target attached to the specimen being scanned. This new method not only maps the scan values appropriately, but it automatically provides information about the distance to the structure, and the relative angle between the scanner and the structure.

We completed a modeling effort that provides a description of the raw LDV output for a given ultrasonic vibration pattern. This model is being used as part of the electronics package to quickly map the LDV measurements back to ultrasonic response, but in a way that is significantly more compact than commercial analog hardware solutions. We have identified commercial, off the shelf solutions that, when combined with a new ultrasonic transducer circuit design, will provide the 50 Watts of ultrasonic power in a sufficiently compact package. We are now looking at in-house designs for providing even more energy with the same form-factor.

Several miscellaneous system components, such the scanning mirror power supply, were made smaller, getting us closer to the hand-held objective.

In support of program development of the technology following the LDRD funding period, several new application areas were demonstrated, including in-situ 3D printing, large-scale infrastructure monitoring, live monitoring of reactions in containers, and inspection of complex aerospace components. The US Airforce and Space Exploration Technologies have both requested on-site demonstrations of the system once the prototype is closer to its final form. USAF and SpaceX both represent applications that support national security.

Future Work

- Design and construct the final packaging solution for the hand-held and shoulder-carried components of the system.
- Finalize and ruggedize the fiber-optic LDV prototype, with an appropriate lens system.
- Optimize the co-registration algorithms, including post-processing of the mapped images according to wave propagation theory.
- Design and test the in-house ultrasound generation unit and compare against COTS solutions in terms of size, cost, and signal quality.
- Develop algorithms for appropriately mapping scans of complex geometries, such as 90 degree welded plate sections.

Conclusion

Develop and demonstrate a scanner that is sufficiently compact to be carried by a person and operated by a single hand. The scanner will provide raw steady-state response measurements with more fidelity and at faster speeds that present commercial off the shelf laser Doppler vibrometry technology. It will seamlessly measure transitions between scanned components in an assembly and automatically map scan lines to physical space.

Enabled technologies would include mobile robotic inspection platforms, "ultrasonic fingerprint" readers, tamper-indicating scanners, inspection of hard-to-reach components, inspection of component assemblies, emergency and quick-check inspections, and in-line manufacturing quality control.

Publications

Flynn, E. B., A. J. Haugh, and S. B. Lopez. Small Defect Detection Through Local Analysis of Acoustic Spatial Wavenumber. 2015. STRUCTURAL HEALTH MONITORING 2015: SYSTEM RELIABILITY FOR VERIFICATION AND IMPLEMENTATION, VOLS. 1 AND 2. : 2623.

Flynn, Eric B., Anthony J. Haugh, and Sheri B. Lopez. Small defect detection through local analysis of acoustic spatial wavenumber. 2015. In International Workshop on Structural Health MOnitoring. (Palo Alto, 1-3 Sep. 2015). , p. 326. Lancaster: DEStech Publications, Inc.

Gannon, Adam M., Elizabeth M. Wheeler, Kyle J. Brown, Eric B. Flynn, and William J. Warren. A high-speed dual-

stage ultrasonic guided wave system for localization and characterization of defects. 2015. In International Modal Analysis Conference. (Orlando, 2-5 Feb. 2015). , p. 123. New York: Springer International Publishing.

Han, , Lee, and E. B. Flynn. Remote Imaging of Local Resonance for Inspection of Honeycomb Sandwich Composite Panels. 2015. 2015 IEEE SENSORS. : 33.

Koskelo, E. C., and E. B. Flynn. Scanning laser ultrasound and wavenumber spectroscopy for in-process inspection of additively manufactured parts. 2016. NONDESTRUCTIVE CHARACTERIZATION AND MONITORING OF ADVANCED MATERIALS, AEROSPACE, AND CIVIL INFRASTRUCTURE 2016. 9804.

Lee, , C. M. Cho, C. Y. Park, Chung Thanh Truong, H. J. Shin, Jeong, and E. B. Flynn. Spar disbond visualization in in-service composite UAV with ultrasonic propagation imager. 2015. AEROSPACE SCIENCE AND TECHNOLOGY. 45: 180.

Discovering Biosignatures in Manganese Deposits on Mars

Nina L. Lanza
20160606ECR

Introduction

The presence of high concentrations of manganese on Mars indicates past episodes of strongly oxidizing conditions within an aqueous environment. On Earth, such simultaneous conditions are almost always both habitable (potentially supportive of life) and inhabited by microbes. Given its close association with life and habitable environments on Earth, manganese has long been considered a principal biosignature for Mars. However, we do not yet understand the unique Mn signatures that can distinguish Mn-rich deposits as biogenic in origin (i.e., produced by life) from altered, abiogenic Mn deposits. By studying trace element abundances and mineralogy, a clearer picture of biosignatures may be obtained.

The goal of this proposal is to identify key chemical and mineralogical signatures that point to a biological origin for Mn-rich materials so that such materials may be identified on Mars should they be encountered by a rover. If these signatures are identified on Mars, they will address one of the highest priority goals of the planetary science community: clear evidence of past or present microbial life in the martian environment. We will examine Mn-rich materials in detail using gold-standard laboratory techniques to elucidate the signatures of these materials with laser-induced breakdown spectroscopy (LIBS), which is currently on the Curiosity Mars rover payload (ChemCam), and Raman spectroscopy, which is part of the Mars 2020 rover payload as SuperCam (combined LIBS-Raman) and SHERLOC (Raman). While initial LIBS experiments on Mn have been completed at Los Alamos, significant work is needed to expand our understanding of how to identify and interpret high-Mn materials observed on Mars by LIBS and Raman spectroscopy.

To aid in the discovery of these signatures in future Mars 2020 datasets, we will also develop and optimize machine learning algorithms to search for biosignatures previously identified in the laboratory in the current ChemCam LIBS Mars dataset.

Benefit to National Security Missions

This work directly supports space science research currently underway at Los Alamos. The currently operating Curiosity Mars rover payload includes the ChemCam instrument, a laser-induced breakdown spectroscopy (LIBS) instrument that was designed and built at Los Alamos. In addition to ChemCam, Los Alamos is also building a new instrument for the upcoming Mars 2020 rover, which will consist of a combined LIBS-Raman instrument. A major goal of the Mars 2020 rover mission is to identify biosignatures should they be present in the martian environment. This project will allow Los Alamos to lead the effort to identify and interpret Mn-bearing materials on Mars during both the current Curiosity mission and the upcoming Mars 2020 mission.

In addition to its relevance for space science at Los Alamos, this work also directly targets the NASA Exobiology program call to examine "the identification of biosignatures for in situ applications." Using "…samples from Earth sites thought to be analogues of other planetary environments that might potentially harbor life," we seek to determine what chemical and mineralogical signatures can uniquely identify these materials as biological in origin. This work also addresses Goal 7 in the NASA Astrobiology Roadmap to "determine how to recognize signatures of life on other worlds." By utilizing analysis techniques included on present and future rover payloads (e.g., LIBS and Raman), the results from this study can be directly applied to currently available Mars mission data sets and will inform near-future rover operations on the martian surface.

Progress

Work on this project commenced in February 2016 after the PI's return from deployment in Antarctica on another project. Thus this report covers the approximately five-month period between the start of the project and now.

Progress on each task is as follows:

1. Select a preliminary sample set of high manganese materials to analyze. PI Lanza has identified seven high-manganese materials to investigate in this fiscal year. Five samples have been obtained from collaborators and are present at Los Alamos; two samples have been prepared by collaborators at another institution and will arrive mid-June; and one sample is in the process of being purchased.
2. Analyze samples with Raman spectroscopy. The laboratory Raman instrument is in the process of being realigned and recalibrated before data acquisition. The current timeframe for the Raman instrument to begin acquiring data for this project is July 2016.
3. Analyze samples with laser-induced breakdown spectroscopy (LIBS). PI Lanza has scheduled time in mid-June to obtain LIBS data on the preliminary sample set selected in Task 0 with the ChemCam engineering model instrument. The five samples already obtained have been prepared for LIBS analysis as rock billets.
4. Validate sample mineralogies and chemistries. Samples for scanning electron microscopy (SEM) analysis are being prepared as thin sections by a commercial vendor. Two days of SEM time at the University of New Mexico has been scheduled for mid-June 2016. Samples for X-ray diffraction (XRD) analysis are being prepared as powders by a commercial vendor. PI Lanza is currently working with the XRD operator at the University of New Mexico to schedule analysis time on the XRD.
5. Determine associations of trace elements and mineral structures in biogenic and abiogenic Mn materials. Progress on this task will commence once data from Tasks 1-3 are obtained. Since LIBS and SEM data acquisition is scheduled for June, analysis of these data sets will begin in July; with Raman data acquisition scheduled for July, analysis of these data will begin in August 2016.
6. Modify current machine learning model to search for evidence of biosignatures identified in tasks 1-4 in LIBS laboratory data. Co-I Oyen has commenced work on modifying the machine learning model to use specific spectral regions of interest for manganese-rich materials as input. Additionally, she has written and submitted a paper on this work, entitled "Interactive Discovery of Chemical Structure in ChemCam Targets Using Gaussian Graphical Models," has been accepted to the BeyondLabeler workshop at the International Joint Conference on Artificial Intelligence, to be held in July.

Future Work

We anticipate making progress on all proposal tasks in the first fiscal year using a preliminary selection of high manganese materials. Tasks in the second fiscal year will be similar to those in the first but will utilize a new selection of samples.

1. Select a preliminary sample set of high manganese materials to analyze. These will include commercially available geological standards and materials from PI Lanza's personal collection.
2. Analyze samples with Raman spectroscopy. Laboratory Raman spectra will be acquired on a range of Mn-bearing geological materials, including whole rock and powdered samples (including physical mixtures).
3. Analyze samples with LIBS. All samples will be analyzed with the ChemCam engineering model LIBS instrument under martian conditions.
4. Validate sample mineralogies and chemistries. The mineralogy and chemistry of laboratory standards will be characterized by X-ray diffraction (XRD) and scanning electron microscopy energy-dispersive spectroscopy (SEM-EDS) to confirm measured LIBS and Raman compositions.
5. Determine associations of trace elements and mineral structures in biogenic and abiogenic Mn materials. LIBS data will be analyzed for the presence of specific and/or noteable minor elements. Raman data will be analyzed for diagnostic Raman shifts to determine mineralogy and organic content. All laboratory data sets will be assessed for chemical and mineralogical trends.
6. Modify current machine learning model to search for evidence of biosignatures identified in tasks 1-4 in LIBS laboratory data. The model will be tested on laboratory LIBS spectra obtained in this project, both to confirm results and also to discover patterns that may not have emerged in Task 4.

Conclusion

The objective of this proposal is to determine what chemical and mineralogical signatures can uniquely identify manganese-rich materials as biological in origin using Mars rover payload instruments. If these signatures are identified on Mars, they will address one of the highest priority goals of the planetary science community: clear evidence of past or present microbial life on Mars.

Publications

Oyen, D., and N. Lanza. Interactive discovery of chemical structure in ChemCam targets using Gaussian graphical models. 2016. In Workshops of the International Joint Conference on Artificial Intelligence (IJCAI). (New York, NY, 10 July 2016).

Imaging the Dome of Santa Maria del Fiore Using Cosmic Rays

Elena Guardincerri
20160629ECR

Introduction

We propose here to develop a muon tracker at LANL to image the inside of The Dome of Florence Cathedral Santa Maria del Fiore. The actual measurement in Florence is outside the scope of this proposal.

The detector should be lightweight, modular and portable, so that it could be easily transported and assembled in-situ on the Dome of the Florence cathedral, and moved in different positions as required by the measurements to be performed.

In particular we plan to design and build two muon trackers made of 1-inch diameter carbon fiber drift tubes. We plan to engineer each tracker so that it can easily be assembled in situ. The most difficult technical challenge here is guarantee that the drift tubes remain leak tight during the transportation, deployment and assembly of the detector.

We will use carbon fiber tube bodies and end-caps made of either aluminum or plastic, neither of which can be welded to the carbon fiber bodies. The design of the end-caps and their coupling to the carbon fiber detector will be subject to extensive R&D.

We will also develop the software to produce tomographic images from multiple views of the same volume taken from different angles.

The same detector and the same imaging technique can be used to radiograph any thick structure and image denser objects inside it. Applications include, but are not limited to, the monitoring of building and civil constructions (e.g. dams, bridges) to assess their structural stability and the imaging of the interior of thick archeological artifacts. The same detectors can also be used to measure the attenuation of the cosmic-muon flux through large structures or geological formations, and this technique can be used to image mountains of volcanoes, tunnels, underground explosion sites, monitor CO2 reservoirs and possibly find water aquifers or oil reservoirs.

Benefit to National Security Missions

The detectors built as part of this project can be used to detect Special Nuclear Material (SNM) as described in the paper NIM A 789 (2015). As such they can be used for both non-proliferation (DoE/NNSA/DHS, Remote Sensing for Nuclear Nonproliferation) and treaty verification (DoD).

The same detectors can be used to image the inside of buildings and structures like bridges and dams (DOT/Commerce and Transportation); they could also be used to find nuclear material hidden inside buildings (Information Collection, Surveillance, and Reconnaissance/Intelligence Agencies).

The detector can also be used to image the inside of casks containing spent nuclear fuel (Energy Security/Nuclear Energy), and a smaller version of the same detectors can be used to monitor CO2 reservoirs (DoE/Climate and Energy Impact) and to image underground explosion sites (UNE) for nuclear forensic purposes.

Progress

This project officially started in the middle of January 2016, therefore I will only describe what was done during the first six months.

We designed a pair of plastic endcaps that will be used to seal a module of 24 drift tubes (the final trackers will each be made of 24 modules). We had the endcaps 3D printed by the Stratasys company and we built a 24 channels module using such endcaps and carbon fiber bodies.

It was also proved that the module is gas tight and that

its drift tubes produce good electronics signals. We verified that the performance of the detector did not change even after a vibration test performed on it.

We placed the orders for the materials needed to build the whole system: all the materials needed to fabricate the detector are already at LANL, the electronics and DAQ have been shipped and are expected in the next weeks.

The support structure for the different modules is currently being designed. The construction of the full detector has started and is in progress.

The framework for the software to produce tomographic images of the object of interest is under development. A prototype of it is currently being used to image shallow geological features using cosmic rays as part of a project funded by the Center for Space and Earth Sciences. The physical quantity that is used in imaging geological features is the fraction of muons absorbed when traversing the object of interest, whereas the quantity to be used to perform the measurement proposed here is the muons multiple scattering angle. New algorithms that use the latter quantity will be developed and used within the same software framework.

Future Work

Task 1: Prototype construction, testing, and design iteration. We will design and build one or more detector prototypes to find the best end cap design that guarantees both performance and drift tube gas-tightness.

Task 2: Support structure design. Design a support to hold the drift tubes in place so that the assembled detector can be safely and easily moved.

Task 3: Purchase the materials to build the actual detector.

Task 4: Procure the electronics and the DAQ system.

Task 5: Assemble the full detector.

Task 6: Test and characterize the detector.

Task 7: Develop the software to produce tomographic images from data.

Conclusion

The tracker will be capable of recording data and tracking muons with a good angular resolution. We will characterize our detectors by measuring the accuracy of the muon tracks reconstructed from the data, and we will leak test the drift tubes periodically and evaluate their long-term performances. The software we develop in parallel will produce tomographic images from multiple views of the same volume taken from different angles. This technology will be applied to image the inside of the Doma of Florence Cathedral, resulting in a high-profile first application of muon tomography to infrastructure monitoring.

Deployment and Installation Technologies for Distributed Measurement Systems in Inconvenient/Hazardous Environments

David D. Mascarenas
20140629ECR

Abstract

In the last 15 years significant effort has been invested in developing unmanned aerial vehicles (UAV). To date the vast majority of this work has focused on using UAVs to collect imagery, and this work has been highly successful. In addition, significant effort has gone into the development of control systems for multirotor vehicles that are robust to disturbances from inputs such as wind and light impacts. The same 15 year period (roughly) saw great advances in the development of wireless sensor network technology. Many advances have been made in small, low-power microcomputers and radios, energy harvesting, new battery technologies, and low-power communications protocols. Interestingly, wireless sensor network research and UAV research has even combined on many occasions. Often this takes the work of a UAV being a node in a wireless sensor network. It has also been proposed to use UAVs to deploy wireless sensor networks. One of the main challenges with wireless sensor networks has been reducing the costs with installing them, particularly in remote and hazardous locations. One solution that has been studied in the literature is to simply drop nodes for a wireless sensor network from a UAV into the desired area. For many applications, however, this is simply not useful. Many applications such as health monitoring of infrastructure require that sensor nodes be placed in very precise locations and be coupled very tightly with their environment. This work focused on making this possible by focusing on the development of a remote sensor placement system that could be deployed from a multirotor to remotely deploy sensor nodes in a precise manner. In addition, because the control systems for these vehicles have improved substantially, effort was also directed towards developing the capability to use UAVs to physically interact with, and collect samples from, the environment. This capability has applications in a wide variety of fields. This work focuses on expanding the capabilities from simply being a platform to collect imagery, to being a tool to interact physically with the environment not only to install sensor nodes, but also to collect samples and make modifications to the environment. In addition, work was done to improve human-machine interfaces for these platforms to better accomplish these objectives.

Background and Research Objectives

A number of global security missions of interest to LANL would benefit from the ability to deploy sensor nodes, collect samples and physically interact with the environment using multirotor unmanned aerial vehicles. These missions include emergency response (deployment of gas sampling sensors after a fire/explosion), nonproliferation (collecting swipe samples from hard-to-reach locations in facilities), and sensor deployment for facility structural integrity monitoring (Hanford tanks). The goal of this early career research project is to develop tools to better address these needs.

The initial plan for this project was to primarily focus on the development of a remote sensor deployment device to emplace wireless sensor nodes quickly with high accuracy at low-cost. Unfortunately it was discovered through the first year of the project that securing the approvals to accomplish this task was going to be much more difficult than originally anticipated. Prior to the beginning of the project safety documents had already been initially created and it was anticipated these were nearly ready to be approved. However it turned out the final approvals were not as easy to acquire as originally anticipated. Alternative testing locations were searched for throughout LANL to facilitate obtaining the approvals, but despite multiple attempts these all resulted in dead ends for finding testing locations. Eventually the PI, David Mascarenas, came to realize he could still make progress on the goal of building tools to improve the ability of unmanned multirotor vehicles to physically interact with the environment if he changed his scope from one focused goal, to a number of broader goals that could be used to try and pursue additional funding in follow-on work. Based on Mascarenas' interaction with LANL pro-

gram managers and staff he identified four research objective areas he could begin to implement proof-of-concept research in that would not require obtaining safety and security approvals while still advancing the goal of enabling multirotors to physically interact with the environment to support global security missions. These topics include:

- High-performance transparent barrier detection using silicon retinas to allow multirotor vehicles to quickly collect samples indoors without colliding into transparent barriers (e.g. windows). (This is a difficult problem even for high performance fliers such as birds and bats.)
- Robotic Inspection and Repair of Nuclear Infrastructure. Specifically developing tap-testing tools that could be deployed from a multirotor vehicle to facilitate the ability of inspectors to quantify the structural integrity of nuclear facilities.
- Extending human proprioception to robotic manipulators for the purpose of high-performance teleoperation of robotic actuators for repair of infrastructure and physical manipulation of the environment (e.g. sample collection).
- Artificial Personality Synthesis for diverse, robust teams of robots that can work together and with humans to physically modify their environment.

These four research objective areas proved to complement the goal of deploying sensor nodes from a multirotor and allowing a multirotor to physically interact with the environment quite well. A number of possible follow-on research activities have been identified as a result of this work and are elaborated below.

Scientific Approach and Accomplishments

Remote Sensor Deployment

The goal of remote sensor placement project was to develop a tool to deploy sensor nodes from a multirotor vehicle in a precise, reliable manner (Figure 1). In order to do this a pneumatically powered remote sensor placement device was developed. The remote sensor placement device was designed to launch sensor packages 25.4 mm in diameter horizontally to attach to vertical surfaces. As mentioned above, there were significant challenges associated with obtaining approval to test and fly the remote sensor placement device on LANL property throughout the life of the project. Despite these obstacles, Mascarenas still demonstrated the remote sensor placement device was capable of deploying a sensor package from a multirotor. For the demonstration, the sensor package was outfitted with a screw tip. The sensor package was launched into a vertical plywood sheet. The screw was successfully embedded into the plywood sheet from the multirotor vehicle from a distance of about 5 meters. During the test the sensor package broke free from the screw, but it is expected this problem can be resolved with some simple improvements to the sensor package design and manufacturing. The current design was built using 3D printing and a very simple hot glue joint to affix the screw to the sensor package. During testing in the benchtop test chamber, this design had no problems with attachment. Based on prior experience the problem most likely is the result of slight misalignments of the plywood board with the remote sensor placement system, and took much power being delivered by the remote sensor placement system. However, getting the screw to embed in the board was the most critical task, and since this was accomplished it is anticipated that the overall package can be made more robust with some straightforward design changes and some testing. It is likely this can be accomplished more easily in the future now that the FAA has released the Part 107 regulatory framework for low-risk commercial unmanned aerial vehicle flight operations.

Figure 1. Remote sensor placement device installed on S100 octorotor for testing

A Multi-modal, Silicon Retina Technique for Detecting the Presence of Reflective and Transparent Barriers

There is currently great interest in enhancing the ability of aerial robots to navigate indoors. Navigating a building under various lighting and environmental conditions would have application in disaster response, infrastructure inspections, as well as a wide variety of commercial applications. In order to achieve this goal, one common feature of indoor environments that must be addressed is the detection of transparent/reflective barriers. The ability to detect and localize transparent barriers will also be important for autonomous navigation. The focus of this work is to develop a multi-modal sensing solution that can

successfully identify transparent/reflective barriers, distinguish between the two, and provide some information on pose and distance to the barrier at human time-scales in order to facilitate navigation of indoor spaces (Figure 2). The sensing solution relies on using an imager to measure the differences in the interactions of actively induced electromagnetic waves with transparent/reflective barriers in the visible and infrared range. A silicon retina imager is used in this work to provide a path to obtaining information on transparent/reflective barriers while requiring very little communications bandwidth.

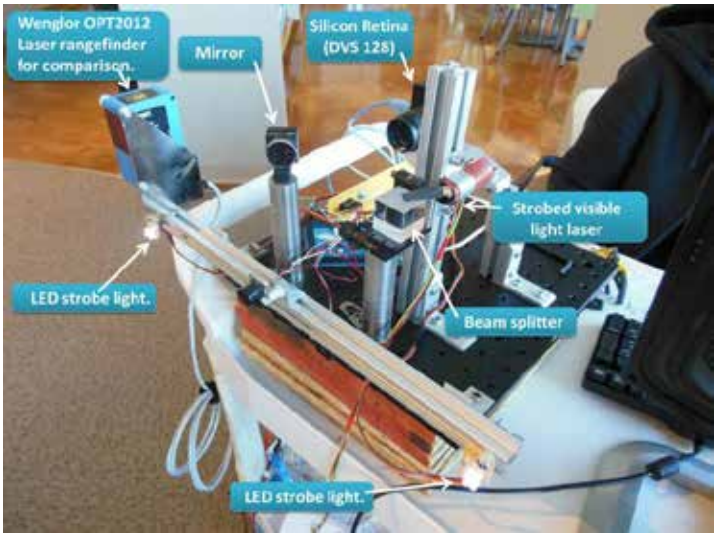

Figure 2. Silicon Retina-based prototype for rapid detection of transparent barriers.

A multirotor-based approach for tap-testing difficult-to-access structures

Despite advances in structural health monitoring (SHM) technology, human-based inspections continue to remain dominant in practice when performing structural assessments. The reasons for this include the high costs associated with installing and maintaining current SHM, confidence decisions makers have in current SHM technology, and the familiarity the structural assessment community has with human-based visual inspection. One of the major challenges and costs associated with human-based visual inspections is that structures are often difficult to access. They may be located high above waterways, requiring an expensive crane or barge to provide the inspectors a platform from which to conduct their inspection. This project began exploring the utility of adding an actuated hammer to a multi-rotor vehicle that can be used to facilitate structural inspections. The system features acoustic microphones and accelerometers that can be used to quantifiably document the results of the tap test (Figure 3).

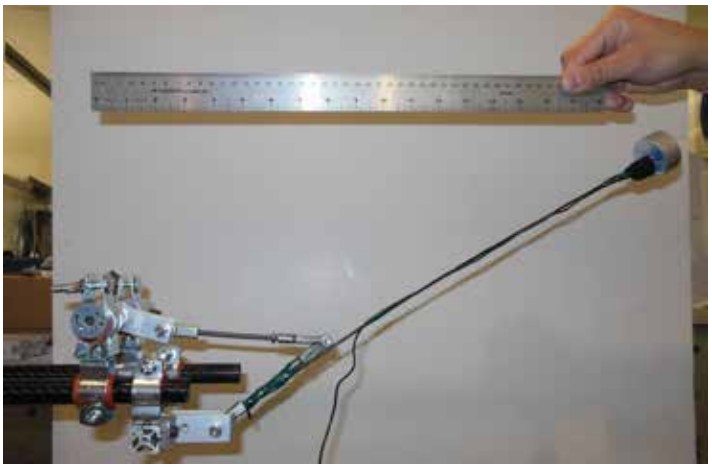

Figure 3. Acoustic microphones and accelerometers quantifiably document results.

Extending Human Proprioception to Cyber-Physical Systems

Humans have a proprioceptive sense that provides us information on how our bodies are distributed in space without having to look directly at our appendages. This work explored employing the phenomena of sensory substitution to build non-invasive, vibro-haptic interfaces that will ultimately allow us to extend the human sense of proprioception to cyber-physical systems (Figure 4). The ultimate goal of this work is to enable high-performance control of cyber-physical systems, particularly robots that physically interact with the environment in demanding ways.

Figure 4. Vibro-haptic sleeve for extending human proprioception to cyber-physical systems.

A Jungian based framework for Artificial Personality Synthesis

In this work an alternative computational personality framework is presented based on the work of Carl Jung. There are two key insights that suggest a Jungian type-based framework is suitable for synthesizing an artificial personality. First, the cognitive functions that form the building blocks of the Jungian personality model can be mapped to classes of algorithms used to emulate cognition. Second, the Jungian framework suggests that at any

given time humans are only using one of the cognitive functions. This suggests that a human personality could be emulated using a state machine with each state implemented using the appropriate class of algorithms (Figure 5).

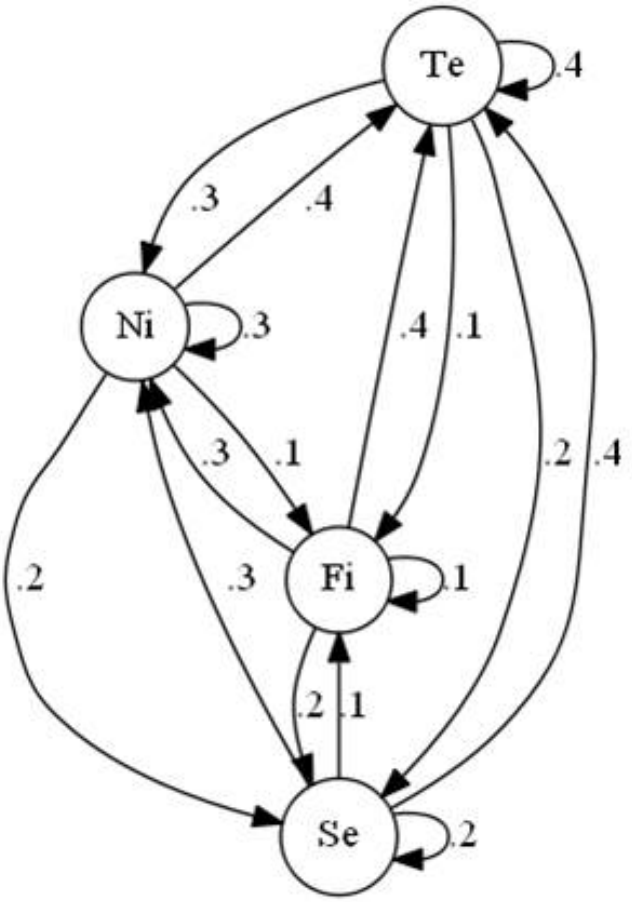

Figure 5. A Markov- chain implementation of a Jungian framework for artificial personality synthesis.

Impact on National Missions

The work that has been completed on this project with regards to giving multirotor vehicles the ability to interact physically with their environment has had an impact on a number of national missions of interest to LANL.

Mascarenas worked with Rollin Lakis of NEN on the development of a mechanism that allows a multirotor vehicle to both deploy and pick up MultiRAE 5 gas analyzers. This capability is of interest to the LANL Emergency Operations Center for responding to emergency situations that involve potentially hazardous gasses. Mascarenas helped Rollin and his staff/students with preparing the octorotor, preparing code for the embedded packages flying on the quadrotor, and preparing for some of the demonstration flights.

The initial work on the haptic interfaces to extend human proprioception to cyber-physical systems such as a robot sparked the interest of Elshan Akodav of A-ARCS. We are now exploring opportunities to use wearables for the LANL cyber security mission.

The development of a Jungian artificial personality synthesis framework has caught the attention of Milton Garces at University of Hawaii. Garces currently focuses on infrasound research for nonproliferation and earth sciences applications. Garces has significant problems with data processing of disparate data that he thinks can be addressed by using the Jungian artificial personality framework as an organizing principle for computation in the cloud. He is currently engaging interest for this idea among his collaborators in industry, government and academia.

Sebastian Zanlongo (DOE Computational Science Graduate Fellow) of Florida International University worked with Mascarenas on artificial personality synthesis in the summer of 2016. Zanlongo is currently exploring options for his PhD that would involve human-machine interfaces to address nuclear cleanup operations at the Hanford site.

Remote sensor deployment and physical interactions with the environment have led to follow-on interest in the area of inspecting the structural integrity of the Hanford tanks. David is currently working under the guidance of Paul Dixon to develop prototype steerable needles built for inspection of infrastructure with access only provided by extremely confined spaces. This prototype will be used to pursue additional work inspecting the structural integrity of the Hanford tanks. In addition it also has potential to provide in-situ measurements of the roots of fuel crops. Characterizing the roots of fuel crops is important for the DOE energy security mission.

Under the direction of Paul Dixon and Amy Larson, Mascarenas is working to detect drips in the Hanford tanks. These drips would typically be captured using video collected by a robot. He has been adapting a technique developed in cooperation with his postdoc Yongchao Yang to address this problem. This is important for finding leaks in the Hanford tanks.

In collaboration with Fernando Moreu of the University of New Mexico, Mascarentas is working to deploy the tap-testing multirotor on infrastructure such as rail. The first paper on using tap-testing to detect damage in the presence of multirotor noise is currently underway. He is also co-mentoring a senior design group at New Mexico Tech with David Grow to continue the work on the use of multirotor vehicles to physically interact with the environment. This endeavor looks at the use of multirotor vehicles to repair damage from lightening to wind turbine blades.

This application is important to the DOE energy security mission.

Mascarenas presented the human-machine interface work at the 2016 Resilience Week. One of the goals of this meeting was to form a coalition of researchers across DOE Labs to strengthen the DOE's ability to perform human-machine interface work.

Lastly, Mascarenas is currently working with Garrett Kenyon and Paul Welch to use event-based silicon retina imagers to monitor the quality of metallic additive manufacturing processes in situ. This is being done by combining silicon retinas with our techniques for automatically extracting structural dynamics from video.

Going forward, Mascarenas will work with Garrett Kenyon on his project using silicon retinas to help unmanned aerial vehicles navigate using silicon retinas and deep learning.

Publications

Ayorinde, E., J. Mason, F. Moreu, C. Farrar, and D. Mascarenas. Remote Railroad Bridge Concrete Tapping using Unmanned Aerial Systems. 2016. Best Poster Award at the 2016 LANL student poster competition in both the Engineering Category as well as the Associate Directorate for Threat Identification and Response (ADTIR) category .

Dickstein, L., K. Keller, E. Robinson, H. Hahn, A. Cattaneo, and D. Mascarenas . Extending Human Proprioception to Cyberphysical Systems. 2016. In SPIE Smart Structures and NDE 2016. (Las Vegas, Nevada, 20-24 March, 2015). , p. 10.1117/12.2219534. Las Vegas: SPIE.

Green, A.. LANL Distinguished Student award for work on Silicon Retina. 2015. Los Alamos National Laboratory.

Green, A., K. Klein, I. Acevedo, D. Kraus, C. Farrar, and D. Mascarenas. A Multi-modal, Silicon Retina Technique for Detecting the Presence of Reflective and Transparent Barriers. To appear in IEEE Sensors Journal.

Green, A., K. Klein, I. Acevedo, D. Kraus, and C. Farrar. A Multi-modal, Silicon Retina Technique for Detecting the Presence of Reflective and Transparent Barriers. To appear in In review at the IEEE Sensors Journal.

Mascarenas, D.. A Jungian based framework for Artificial Personality Synthesis. To appear in 4th Workshop on Emotions and Personality in Personalized Systems (EMPIRE), in conjunction with ACM RecSys. (Boston, 16 September).

Mascarenas, D.. Agile Infrastructure Health Monitoring Solutions to Address Rapid Urbanization, both Domestically and in the Developing World. Invited presentation at Keynote lecture at the International Drone Expo 2016. (Chiba, Japan, 20, April 2016).

Mascarenas, D., A. Green, T. Trombetta, and C. Farrar. A Multirotor-based Approach For Tap-testing Difficult-to-access Structures. 2015. In 10th International Workshop on Structural Health Monitoring. (Stanford, CA, Sept 1-3). , p. 00. Stanford: IWSHM.

Mascarenas, D., A. Green, T. Trombetta, and C. Farrar. A Multirotor-based Approach For Tap-testing Difficult-to-access Structures. 2015. In 10th International Workshop on Structural Health Monitoring. (Stanford, CA, 1-3, Sept, 2015). , p. 1. Lancaster, PA: Destech publications.

Mascarenas, D., L. Ott, A. Curtis, S. Brambilla, A. Larson, S. Brumby, and C. Farrar. Video: remote sensor placement. 2014. In MobiSys '14- Proceedings of the 12th annual international conference on Mobile systems, applications, and services. (Bretton Woods, NH, 16-19 June 2014). , p. NA. Bretton Woods, New Hampshire: ACM.

Mascareñas, D., L. Ott, A. Curtis, S. Brambilla, A. Larson, S. Brumby, and C. Farrar. Demo: A remote sensor placement device for scalable and precise deployment of sensor networks . 2014. In MobiSys '14- Proceedings of the 12th annual international conference on Mobile systems, applications, and services. (Bretton Woods, NH, 16-19 June 2014). , p. NA. Bretton Woods, New Hampshire: NA.

Moreu, F., C. Farrar, E. Ayorinde, J. Mason, and D. Mascarenas. Remote Railroad Bridge Concrete Tapping using Unmanned Aerial Systems. Presented at IMAC XXXV 'Structural Dynamics Challenges in Next Generation Aerospace Systems. (Garden Grove, CA, 2017-01-30 to 2017-02-02).

Yang, Y., A. Cattaneo, and D. Mascarenas. Potential Structural Health Monitoring Tools to Mitigate Corruption in the Construction Industry Associated with Rapid Urbanization. 2015. In 2015 International Conference on Sustainable Development (Winner of Best Paper Award). (New York, Sept 23-24). , p. 00. New York, NY: ICSD.

Yang, Y., C. Dorn, T. Mancini, Z. Talken, G. Kenyon, C. Farrar , and D. Mascarenas. Blind identification of full-field vibration modes from video measurements with phase-based video motion magnification. 2016. Mechanical Systems and Signal Processing. 85 (February): 567.

Laser-Driven Neutron Source for Detection of Nuclear Material

Andrea Favalli
20140580ECR

Abstract

At Los Alamos National Laboratory (LANL), we have recently pioneered a novel, short duration, yet extremely intense, neutron source using a short-pulse laser. At the Trident laser facility, one of the most intense and powerful short-pulse lasers in the world, a laser beam can be concentrated to peak intensity up to 1021 W/cm2. The beam, interacting with an ultra-thin (sub-micron) deuterated plastic foil target, drives a high-energy deuteron beam, which produces neutrons in a beryllium converter. This neutron source features high intensity and directionality, >1010 fast neutrons per sr per shot, peaked in the forward direction, with extremely short neutron pulse duration i.e. on the order of a few nanoseconds. One of the motivations for such a source is the capability to perform nondestructive assay of special nuclear material for nuclear material accountancy, nuclear safeguards, and national security applications in entirely new ways enabled by the unprecedented neutron intensity in a single brief pulse. The detection, characterization and quantification of nuclear materials are an evolving technological challenge being advanced by, for example, non-proliferation and anti-terrorism programs. The detection of shielded special nuclear materials and interdiction of trafficking is a major concern as too is the ability to perform materials analysis and energy resolved neutron radiography. Dedicated experimental campaigns were conducted at LANL to investigate the merits and applicability of such an approach to active interrogation of uranium and plutonium materials. Results of these measurements have provided the first-of-a-kind experimental demonstration of active interrogation using high-intensity laser-driven neutron source, and demonstrated feasibility of interrogation using a single laser-driven neutron pulse. In this summary, we report on the results of laser-driven neutron active interrogation of nuclear material.

Background and Research Objectives

Detecting shielded nuclear material in transport remains a challenging task. The challenges include the need for a fast, movable, and operationally safe neutron source. The neutron source should feature energy tunable and highly directional neutron fluence, thereby overcoming the limitations of present sources, which typically produce isotropic monoenergetic neutrons. Short-pulse laser-driven neutron source possesses these features, allowing for the interrogation of packages with variable shielding conditions and increased signal for the interrogation while improving operational safety. The main research objective of the project was to demonstrate the feasibility of detection of nuclear material using a short-pulse laser-driven neutron interrogation source.

Scientific Approach and Accomplishments

Our scientific approach was based on experimental campaigns, of at least 3 weeks per year, at LANL Trident laser facility. At the present, exploration by direct experiment is the only approach: a theoretical description of the neutron source is not yet established. Only by experimentation can we begin to establish the features and utility of the neutron source for the applications. The project was conducted as multi-division collaboration, mainly Nuclear Engineering and Nonproliferation (NEN) and Physics (P) divisions, including collaboration with other DOE national laboratories, Oak Ridge National Laboratory (ORNL), and an international collaboration with Technical University of Darmstadt, Germany.

Here we describe the main accomplishments of the projects, following the tasks of the project:

Neutron yield and characterization

The short-pulse high-power laser is focused on a target composed of a foil of deuterated plastic, creating an accelerated deuteron beam directed towards a neutron converter. The neutrons produced from various nuclear reactions have an array of energies dependent on the

target/converter configuration. Neutron production from deuterons incident on beryllium was studied using the Monte Carlo N-Particle (MCNP) transport code. Based on such simulations, we designed a flexible, modular beryllium converter, composed of disks of different thickness, surrounded by a tungsten cylinder to enhance neutron production by (n,xn) reactions. These experiments resulted in record neutron production at the LANL Trident facility and very good reproducibility of shot-by-shot neutron yield. The increase in understanding of the ion/neutron production in the laser-driven experiments brought about a novel Science of Signature discovery, i.e. the identification of specific neutrons from the converter (β-delayed neutrons from 9Li decay caused by high energy deuterons incident on beryllium), which provides an important new diagnostic tool for the study of the beam morphology of the deuteron production mechanism in a non-intrusive way. As part of the need of the project, we developed and demonstrated a new neutron detector system (TOTEM) to measure with high accuracy and precision, and without saturation and distortion, the very intense, short duration (~ns) neutron pulse generated by the laser-driven neutron source. Another diagnostic developed in the project is a neutron time of flight prototype for characterization of the neutron energy spectra. Our neutron time of flight prototype diagnostic was developed with LANL custom-made components/devices, and was tested, and used, during our experimental campaigns conducted at Trident. The detector showed very good response linearity, allowing the extraction of neutron energy spectra of the source.

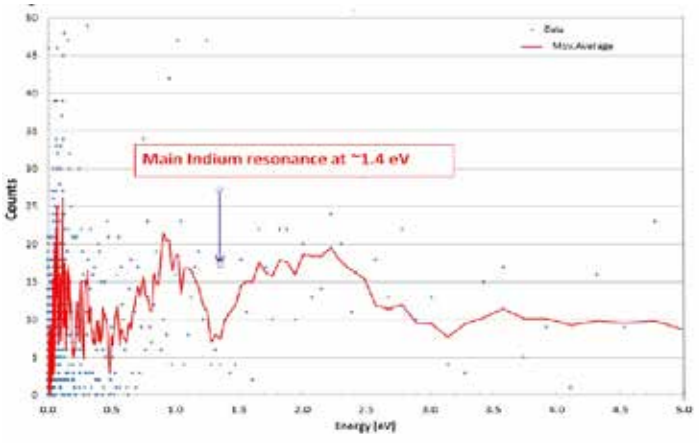

Figure 1. Evidence of the detection of a neutron resonance in a laser-driven neutron experiment

Single Shot Moderated Neutron Pulse and Neutron Resonance. During the experimental campaign in February/ March 2016, a single short-pulse laser moderated bright neutron source was produced. The energy spectral components of the source were fully characterized in each pulse by neutron time-of-flight measurements. The results showed the fast neutron component coming from the initial neutron production, as well as the epithermal, thermal, and cold (few meV) components after the slowdown of the neutrons in the polyethylene neutron moderating material. With this source, we obtained, for the first time, evidence of the detection of a neutron resonance in a laser-driven neutron experiment (Figure1). Such resonance measurements show the potential of laser-driven neutron resonance transmission analysis for isotopic assay of irradiated nuclear fuel and bulk-temperature measurements in shock-driven material experiments.

Active Interrogation of Nuclear Material

One of the motivations behind developing a bright, pulsed neutron source, is the capability to perform an assay of special nuclear materials for nuclear materials accountancy, safeguards and security applications. An intense neutron burst offers (1) the potential of achieving a high signal-to-background ratio in difficult to measure cases (for example materials with high passive neutron emission rate), and (2) the potential of a short assay time, translating to higher throughput. This type of application, also referred to as 'active interrogation', is based on measurements of the neutron signatures to identify/assay nuclear materials during and after an interrogation with an external neutron pulse, such as the laser-driven neutron source we have been developing at Trident, throughout this project. The fission signatures of interest are the prompt- and delayed- fission neutrons, defined here as, (prompt signatures) those produced up to 1 ms after the interrogation of the nuclear materials, and (delayed signatures) those produced later than 1 ms after the stimulation.

Delayed-fission neutron signature

The main fission signature used in the experimental campaign described in this report is the production of β-delayed neutrons: delayed neutrons represent characteristic signature of nuclear material, since very few other processes produce delayed neutrons. Two 3He thermal neutron coincidence well counters were placed outside the chamber; one contained a sample of nuclear material for active interrogation, while the other was kept empty to serve as a reference for background comparison. The counters used were active well coincidence counters (AWCC) composed of 42 3He proportional detectors embedded in polyethylene. In our set up, to assure identical measurement conditions during the interrogation, two counters were located on the equator of the chamber, closely straddling the central beam axis, defined by the laser propagation direction.

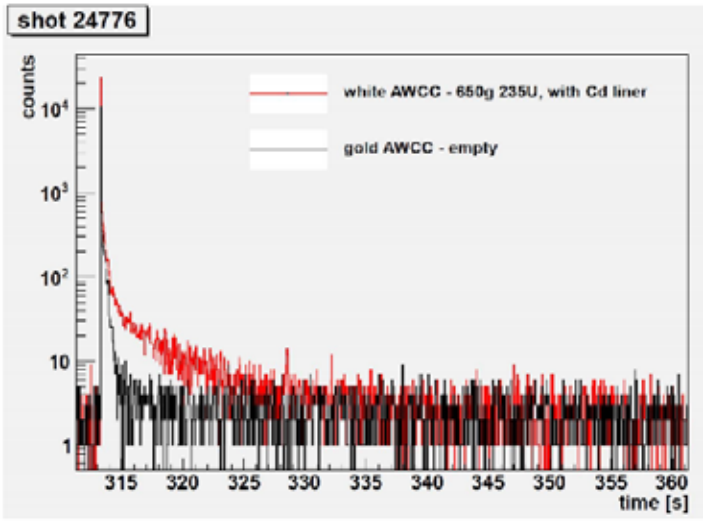

Figure 2. Present the time interval-distributions following interrogation of ~65% high enriched uranium in 'fast mode'. Red line represents results from the master AWCC containing nuclear material, while the time-interval distr butions from the empty, reference AWCC are shown as black line.

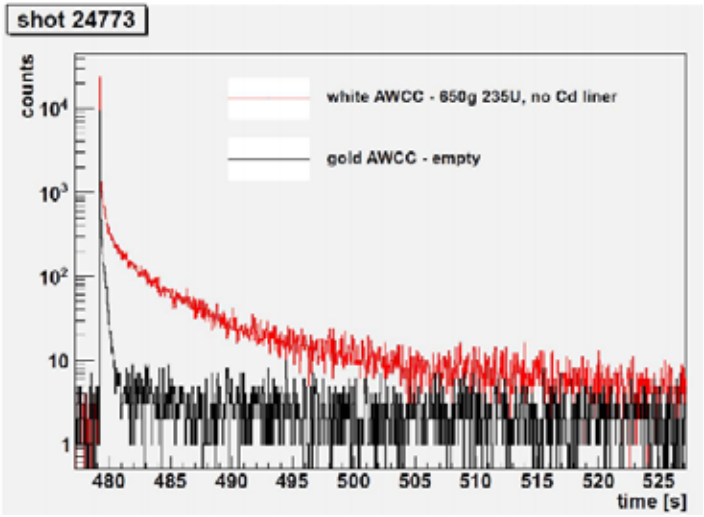

Figure 3. Present the time interval-distributions following interrogation of ~65% high enriched uranium in 'thermal mode'. Red lines represent results from the master AWCC containing nuclear material, while the time-interval distributions from the empty, reference AWCC are shown as black line.

AWCCs are equipped with a thin (~1 mm) Cd sheet that lines the inside of the central well and allows the operation of the counter in two characteristic modes: 'fast mode' with the Cd sheet in place and 'thermal mode' with the Cd sheet removed. In the former case the counter is suitable for interrogation of large quantities of 235U (0.1-20 kg) such as highly enriched uranium materials. In the latter case the sensitivity of the counter is greatly enhanced by increased thermal neutrons in the cavity and in this configuration the counter is more suitable for interrogation of small or low-enriched uranium materials (~0-100 g of 235U). Both modes were investigated in the experimental campaigns. Depleted uranium samples (up to 4.5 kg) and three 900 g enriched uranium samples were used in active interrogation measurements with enrichments of 12%, 38% and 66% in 235U mass. A sample of ~150g of plutonium was also used. Data from the AWCC counters were acquired in the form of time-stamps corresponding to every neutron detection event.

Figures 2 and 3 present the time interval-distributions following interrogation of ~65%high enriched uranium. Figure 2 presents the results in 'fast mode,' and Figure 3 in 'thermal mode.' Red lines in the figures represent results from the master AWCC containing nuclear material, while the time-interval distributions from the empty, reference AWCC are shown as black dotted lines. The sharp peak at the beginning of the time-interval distributions corresponds in time to the interrogating neutron pulse and is followed by a delayed component. A very high increase of the delayed neutron signal (note log scale) with the typical delayed neutron time behavior in the time-interval distribution is visible in the counter with nuclear material compared to the empty reference AWCC. Measurements of the enriched uranium samples, with the same method, with enrichments ranging from 12-65% were used to generate a calibration curve of 235U mass versus counts integrated in a time window of the distributions. It is worth highlighting here that time-distributions, as reported in Figures 2 and 3, represent the first of a kind experimental demonstration of active interrogation of nuclear material using a short-pulse laser-driven neutron source.

Prompt-fission neutron signature

As further challenge in the project, we evaluated if the prompt-fission neutron signal from nuclear fission in the interrogated sample can be exploited for the detection of nuclear material in a one single laser-driven neutron pulse. The prompt-fission signal provides a substantial production of ~2-3 average neutrons per fission, so much higher the delayed neutron signal (~0.01 neutrons/fission), but the signal is difficult to measure and distinguish from the interrogating neutrons. In addition, the prompt-fission neutron signal features the advantage of significantly increasing the single-to-noise ratio in difficult to measurement environments such as conditions with high backgrounds neutron emission rates, as is the situation for active interrogation of plutonium. Based on the results obtained with TOTEM, our neutron developed yield diagnostic (see Neutron yield and characterization chapter in this report), we built, as part of this LDRD project, two modules (BRICKS) each with 6 3He short fast proportional counters: one BRICK-module for nuclear material measurement and one for background determination, in the same fashion as we did for the delayed

neutron signature. BRICK-Modules were connected with LANL developed electronics and the data was collected with a digitizer measuring the currents. BRICK-modules were located in the AWCC counters to collect both prompt- and delayed- neutron signals at each laser-neutron interrogation shot. Figure 4 presents the time distribution of the detector currents following interrogation of ~900g of a 65% enriched uranium item. Blue line in the figure represents the results from the BRICK-module located in the AWCC with nuclear material, while the red line is the time-interval distribution from the BRICK-module located in the empty counter. The time scale now is on the order of a few hundreds of μs, and the results show a net signal from the BRICK detector module seeing prompt-fission neutrons from the interrogated enriched uranium. The approach was applied also to an interrogation of a 170 g sample of plutonium, of which ~150 g is 239Pu: again the results obtained showed a net prompt neutron signal from the interrogated plutonium. During the February and March 2016 campaign, the method was further extended, with success, to measure the prompt-fission signal, from enriched uranium samples, at an early time window (less than ~100 μs after the neutron interrogation) using a modified version of the novel NEN-LANL 6Li glass particle neutron detector.

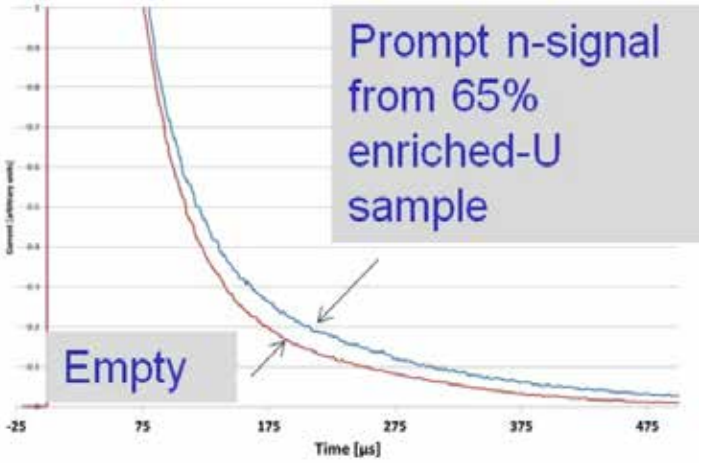

Figure 4. Time distribution of the detector currents following interrogation of ~900g of a 65% enriched uranium item. Blue lines in the figure represent the results from the BRICK-module located in the AWCC with nuclear material, while the red line is the timeinterval distribution from the BRICK-module located in the empty counter.

To summarize, the project achieved the following main results: a record amount of neutron production at Trident laser facility with very good reproducibility of shot-by-shot neutron yield and an unanticipated discovery in the target-neutron converter signature, and a bridge between nuclear physics and the study of relativistic plasmas. The project succeeded in producing a bright moderated neutron shot and showed the first evidence of detection of a neutron resonance (115In) in one laser-driven moderated neutron shot. As laser-driven active interrogation, the results obtained are the following: the first time experimental demonstration of active interrogation of nuclear material, including high enriched uranium, in a short-laser driven neutron source (delayed neutron signature) and the first detection of a prompt-fission neutron signature from enriched uranium and plutonium in active interrogation by single shot from laser-neutron source.

Impact on National Missions

The results of this project provide the first demonstration of feasibility of single-pulse laser-driven neutron interrogation of special nuclear material, so directly supporting the nuclear security mission. An array of national security applications are opened, including high-throughput neutron interrogation of port cargo for detection of nuclear material, explosives and drugs; standoff detection of special nuclear materials, treaty verification (warhead and nuclear material signatures) and stockpile stewardship and certification; spent fuel assay (at storage facility, in cask, for nuclear debris from reactor accidents); neutron therapy and a new generation of nuclear physics experiments (e.g. neutron resonance transmission analysis for isotopic assay of irradiated nuclear material and bulk-temperature measurements in shock-driven material experiments temperature, cross section measurements). Further applications and extensions include, for example, potential alternatives to nuclear reactors used for neutron production at universities.

Publications

E. Timmermans, “Fermion Hole Heating,” Phys. Rev. Lett. 87, 403, (2001).

Eddy Timmermans, Kyoko Furuya, Peter Milonni and Arthur Kerman, “Prospect of Creating a Composite Fermi/Bose Superfluid,” Phys. Lett. A 285, 228 , (2001).

D.J. Berkeland, “Linear Paul trap for strontium ions,” Rev. Sci. Inst., v. 73, pp. 2856-2860 , (2001).

J. Grondalski, D. M. Etlinger and D. F. V. James, “The Fully Entangled Fraction as an Inclusive Measure of Entanglement Applications,” Physics Letters A 300, 569 , (2002).

D.J. Berkeland and M.G. Boshier, “Destabilization of Dark States and Optical Spectroscopy in Zeeman-degenerate Atomic Systems,” Phys. Rev. A 65, 033413 , (2002).

D. F. V. James and P. G. Kwiat, “Atomic vapor-based high efficiency optical detectors with photon number resolution,” Physical Review Letters 89, 183601 , (2002).

P. G. Kwiat and D. F. V. James, “Quantum Optics: Entangle-

ment and Quantum Information," pg. 964, Encyclopedia of Modern Optics (Academic Press). , (2004).

J. Grondalski and D. F. V. James, "Limitations on the Measurement of Spatial Coherence by Near-Field Probes," Optics Letters 28, 1630 (2003).

S. Barraza-Lopez, D. F. V. James and P,. G. Kwiat, "High-visibility Interferometric Measurements of the Phase in Fresnel Diffraction at a Straight Edge," in preparation , (2003).

A. S. Arnold, C. MacCormick, and M. G. Boshier, "Diffraction-limited focusing of Bose-Einstein condensates," submitted to J. Phys. B (early version available as cond-mat/0306188) , (2003).

Tommasini, P; de Passos, EJV; Piza, AFRD; Hussein, MS; Timmermans, E, "Bogoliubov theory for mutually coherent condensates," Physical Review A 67, p.023606-3606 , (2003).

P.W. Milonni, J.H. Carter, C.G. Peterson, and R.J. Hughes, "Effects of propagation in air on photon statistics," SPIE 5111, pp. 7-11 , (2003).

P.W. Milonni, J.H. Carter, C.G. Peterson, and R.J. Hughes, "Effects of propagation in air on photon statistics," J. Opt. B 6, S742 (2004).

P.W. Milonni and R.W. Boyd, "Influence or radiative damping on the optical-frequency susceptibility," Phys Rev A (in press) , (2003).

P.W. Milonni and G.J. Maclay, "Quantized-field description of light in negative-index media," Opt. Commun. (in press). , (2003).

Jinwei Wu, Marc Hausmann, David Vieira and Xinxin Zhao, "Comparison of optical dipole trap and optical lattice with spherical and aspheric lenses," in preparation , (2004).

D.J. Berkeland, D.A. Raymondson, and V.M. Tassin, "Tests for Non-randomness in Quantum Jumps," Phys Rev A, 69, 52103 , (2004).

P.R. Berman and P.W. Milonni, "Microscopic theory of modified spontaneous emission in a dielectric," submitted to Phys. Rev. Lett. , (2004).

P. W. Milonni, J. H. Carter, C. G. Peterson, and R. J. Hughes, "Effects of propagation through atmospheric turbulence on photon statistics," J. Opt. B: Quantum and Semiclassical Optics, 6, S742-S745 , (2004).

M. Hausmann, D.J. Vieira, J. Wu, X. Zhao, M.G. Boulay and A. Hime, "Beta-Asymmetry Studies on Polarized 82Rb Atoms in a TOP Trap," Nucl. Phys. A 746, 669c (2004).

M. Riebe1, H. Haffner1, C. F. Roos, W. Hansel, J. Benhelm, G. P. T. Lancaster, T. W. Korber, C. Becher, F. Schmidt-Kaler, D. F. V. James & R. Blatt, "Deterministic quantum teleportation with atoms," Nature, 429, 734-737 , (2004).

J. L. O'Brien, G. J. Pryde, A. Gilchrist, D. F.V. James, N. K. Langford, T. C. Ralph, and A.G.White, "Quantum Process Tomography of a Controlled-NOT Gate," Phys Rev Lett 93, 080502 , (2004).

J. B. Altepeter, D. F. V. James and P,. G. Kwiat, "Quantum State Tomography," Quantum Estimation of States and Operations Lect. Notes Phys 649, 113 (Matteo Paris, Jarda Rehacek, eds; Springer) , (2004).

Mapping Relativistic Electron Precipitation: Where and When?

Steven K. Morley
20150127ER

Introduction

Earth's upper atmosphere is a major sink for highly energetic electrons in the Van Allen radiation belts. Electron precipitation has been shown to affect telecommunications and atmospheric chemistry, and plays a critical role in determining radiation belt dynamics; it is therefore a key process to understand for space weather modeling. Current detection of electron precipitation into the atmosphere is limited to direct measurements at locations occupied by satellites. A major drawback is that for the large volume of space occupied by the Van Allen radiation belts we only measure this region sparsely and so directly measuring this precipitation is done with satellites at very low altitudes. Most satellite instrumentation on these low altitude missions cannot give sufficient information to describe the changes in the main Van Allen belt electron population, nor do they provide information about the processes driving the precipitation.

We propose a new approach that will allow the first specification of the spatial and temporal extents of electron precipitation from point measurements at high altitude. In essence, we propose to combine measurements from different points on the paths that electrons take when drifting around the Earth in the Van Allen belts (drift orbits) to provide a novel remote-sensing capability. Specifically, we will use the LANL particle instrumentation on the Global Positioning System (GPS) constellation, and at geosynchronous orbit, to identify differences in the electron population along a partial drift orbit, thus "remote sensing" the loss of energetic electrons. By using the measurements of the full electron population, and some modeling of the inner regions of geospace, we will also infer key properties of the waves believed to precipitate the electrons into the atmosphere.

This approach will overcome current sampling limitations to diagnose electron losses and answer the question: Where, and under what conditions, do highly energetic electrons precipitate into the atmosphere?

Benefit to National Security Missions

This project targets understanding where, when and why highly energetic electrons are lost from the Van Allen radiation belts. In order to answer these questions we will develop a new technique for combining point measurements from a constellation of satellites to give a remote sensing capability. From this we will map regions of electron precipitation and infer key properties of the waves driving the electron loss. The specific work proposed will enable future development of models of electron precipitation and electromagnetic ion cyclotron (EMIC) wave activity and properties. Such a capability would directly address the goals of the NASA Living with a Star program: to improve our understanding of how the sun impacts the environment in which satellites operate. While this proposal does not directly address this, these models are known requirements for ongoing Space Weather and Space Situational Awareness modeling efforts. The datasets generated will enable further basic research and applied space weather research.

Progress

Key intervals have been selected for analysis based on data availability, appropriate geomagnetic conditions and the number of satellites in magnetic conjunction. The magnetic ephemeris data for these intervals have been calculated for a simple parameterized magnetic field model. As inaccurate magnetic field modeling is a major source of uncertainty, we have developed a framework for fitting an empirical magnetic field model to satellite observations. A simplified, prototype implementation of this event-fitted magnetic field model is complete, and testing and validation is underway.

The software to find magnetic conjunctions of satellites has been improved and tools have been written to routinely inspect and visualize the conjunction data. Cross-calibrations between the Global Positioning System (GPS) satellites and the Van Allen Probes satellites have

been completed and published. Phase space densities have been calculated for the GPS particle data, using existing empirical magnetic field models, and preliminary analyses of key intervals has begun. Collaborative statistical analysis of electromagnetic ion cyclotron (EMIC) wave properties and the plasma properties observed at times of wave activity has been performed and published, defining typical behavior as a function of geomagnetic activity.

Future Work

The goals for the third fiscal year of this project are: continued development of the phase space differencing software to enable routine analysis; finalizing an event-fitted magnetic field model to improve the accuracy of specifying the data in the adiabatic coordinate system required for this project; analysis of observed precipitation and EMIC waves during selected key intervals; developing fitting code to estimate normalized frequency and wave amplitude of EMIC inferred from particle data; run RAM model to obtain plasma characteristics and predictions of EMIC waves and particle precipitation. Manuscripts on the event-fitted magnetic field model, the phase space density differencing technique and the analysis of the predicted particle losses will be prepared and submitted for publication.

Conclusion

We will develop and test a new approach to locating regions in the Van Allen radiation belts from which electrons are being lost. Our primary objective is to demonstrate that point measurements from a constellation of satellites can be combined to remote sense, and hence map, regions of loss. Our secondary objective is to use these data to infer key properties of a type of electromagnetic wave responsible for driving some of the losses. This will produce new physical understanding, enable scientific studies not previously possible and provide critical inputs for radiation belt models.

Publications

Halford, A. J., B. J. Fraser, S. K. Morley, S. R. Elkington, and A. A. Chan. Dependence of EMIC wave parameters during quiet, geomagnetic storm, and geomagnetic storm phase times. 2016. JOURNAL OF GEOPHYSICAL RESEARCH-SPACE PHYSICS. 121 (7): 6277.

Halford, A. J., B. J. Fraser, and S. K. Morley. EMIC waves and plasmaspheric and plume density: CRRES results. 2015. JOURNAL OF GEOPHYSICAL RESEARCH-SPACE PHYSICS. 120 (3): 1974.

Jordanova, V. K., Tu, Chen, S. K. Morley, A. -. Panaitescu, G. D. Reeves, and C. A. Kletzing. RAM-SCB simulations of electron transport and plasma wave scattering during the October 2012 “double-dip” storm. 2016. JOURNAL OF GEOPHYSICAL RESEARCH-SPACE PHYSICS. 121 (9): 8712.

Morley, S. K., J. P. Sullivan, M. G. Henderson, J. B. Blake, and D. N. Baker. The Global Positioning System constellation as a space weather monitor: Comparison of electron measurements with Van Allen Probes data. 2016. SPACE WEATHER-THE INTERNATIONAL JOURNAL OF RESEARCH AND APPLICATIONS. 14 (2): 76.

Sarno-Smith, L. K., M. W. Liemohn, R. M. Skoug, O. Santolik, S. K. Morley, A. Breneman, B. A. Larsen, G. Reeves, J. R. Wygant, G. Hospodarsky, C. Kletzing, M. B. Moldwin, R. M. Katus, and S. Zou. Hiss or equatorial noise? Ambiguities in analyzing suprathermal ion plasma wave resonance. 2016. Journal of Geophysical Research - Space Physics. 121: 9619.

Exploiting Cross-sensitivity by Bayesian Decoding of Mixed Potential Sensor Arrays

Cortney Kreller
20150236ER

Introduction

Finding specific chemical signatures amongst a background of ordinary substances – a trace explosive signature, an illegal narcotic, a chemical agent intended to kill our soldiers on the battlefield, or civilians in our cities – remains a daunting task. Dogs can seem to handle this proverbial "needle" quite well, but what man's best friend does so well has eluded the sensor industry. Science's best solution to date is devices that use large numbers of inexpensive sensor elements (typically resistive or polymer) in conjunction with pattern recognition methods: commercial instruments based on these principles are available. However, there are significant shortcomings with the performance and capabilities of these sensor constructs, as well as significant limitations to the pattern recognition methods used to extract a meaningful signal from the data because these devices target generic applications requiring significant calibration to obtain qualitative results. The sensors at the heart of these systems are prone to drift and irreversible poisoning, blocking their use in simple, yet harsh, energy-related tasks such as monitoring vehicle emissions or smokestack pollutants. We propose to use a special class of ceramic solid-state electrochemical sensors that are intrinsically inexpensive, durable, and stable. Nobody has ever attempted to create a sensor array using these devices before. Their robustness opens the possibility of detecting a great number of gas chemistries under conditions that would quickly destroy other types of electronic noses. Our highly innovative and original solution to the specificity problem is to create a new gas sensor technology that marries unique sensor design created at LANL with a recently--developed, advanced Bayesian inference treatment of the physical model of relevant sensor-analyte interactions. Our approach is designed to quantitatively decode complex mixtures with fidelity greater than present technology can deliver. Our methods will solve the major shortcomings of the electronic nose concept.

Benefit to National Security Missions

The concept described in this project has the potential to provide low-cost, robust, easily deployable gas-phase quantitative discriminatory sensing capabilities that do not exist today. The broad implications of this work directly support the Revolutionize Measurements aspect of the Science of Signature pillar, and the applications specifically targeted by the proposed work directly address key Energy and National Security concerns. There are presently no low-cost and durable sensors to control and monitor the vehicle emissions systems on today's Selective Catalytic Reduction (SCR) and Exhaust Gas Recirculation (EGR) pollution control technologies comparable to the automotive lambda sensor. Although exact details are understandably kept secret by the pertinent Federal Agencies, the explosives screening technologies employed at critical facilities and used on the battlefield are routinely rendered ineffective because of the presence of complex, natural and human-created background interferences. The proposed research has the ability to create a unique capability at Los Alamos National Laboratory (LANL) by supporting the development of inexpensive and portable systems for use both by civilian first responders and as dedicated screening systems at airports, federal buildings, cargo containers, etc. We will develop the program with collaborators in Materials Physics Applications (MPA-11) and Weapons (WX-9) and also work with Program Managers from Applied Energy (M. Fox) and Global Security- Emerging Threats (P. Knepper) to pursue additional funding from federal agencies interested in Energy Security (Vehicle Technologies (VT)), and explosives (e.g. the Defense Threat Reduction Agency (DTRA) and the Department of Homeland Security (DHS)).

Progress

The capabilities established in year one of the project were utilized in year two to expand the range of sensors tested. In year one we targeted the application of

vehicle emissions monitoring (Energy Security), where analyte species of interest (Nitric Oxide, NO) and background interferents (Nitrogen dioxide, NO2; Ammonia, NH3; and Propane, C3H8) are known and quantifiable. The initial set of experiments utilized two distinct mixed-potential thin film sensors with one having a Lanthanum chromite (LSC) sensing electrode and the second one using gold (Au) as the sensing electrode. Both sensors had a Platinum (Pt) reference electrode and yttria stabilized zirconia (YSZ) electrolyte. These sensors were chosen specifically since prior work had determined that the Au electrode had preferential sensitivity to NH3 while the LSC electrode was selective to either C3H8 or NOx depending on the mode of operation. An extensive data set was collected over a range of mixing ratios (alphas). A non-linear Bayesian inference model was developed by Dr. Morozov at Rutgers University. The preliminary model was able to predict the as within 20% when using just the NO/C3H8 mixtures. However, this data set was insufficient to predict the NO/NO2 ratios with confidence, as well as absolute values of NH3 above a threshold concentration where sensors exhibited saturation in response with increasing concentration.

The feedback from Rutgers indicated the need for additional sensors with varied response characteristics from the initial two sensors tested. Rutgers also advised LANL on modified mixing ratios tailored to each interferent species in order to provide a more robust model training set. In response, we chose to incorporate two additional discreet sensors into our data collection array. Prior work established that not only the sensing electrode material, but also the sensor geometry that controls electrochemical surface area, could be used to tune sensor selectivity and sensitivity. We therefore chose to incorporate sensors using the LSC sensing electrode with geometric surface areas of 0.8, 0.34 and 0.22 mm2 with the Au sensing electrode based device comprising the fourth sensor in the array. Data for binary mixtures of all test gases and ternary mixture of NO/NO2/C3H8 have been collected and supplied to our collaborators at Rutgers. The ternary mixtures using NO/NO2/C3H8/NH3 is currently being evaluated. Rutgers has developed a model based on the well-established Butler-Volmer equation describing electrochemical reaction rates. They have trained this model on the C3H8/NO mixtures, as before, and found an accuracy of 10% in predicting mixtures, a two-fold improvement in the accuracy over the previous work. Rutgers is currently working towards extending the model to other binary and ternary gas mixtures and will present an invited talk on this work at the 2nd International Conference on Sensors Engineering and Electronics Instrumental Advances (SEIA' 2016). This work will also be presented at the 230th Meeting of The Electrochemical Society.

We are currently involved in fabricating Mixed-potential electrochemical sensor (MPES) arrays based on the feedback received from the computational framework of the discreet sensor testing. The testing so far has indicated that using multiple electrodes of the same material but with different geometry provides sufficient fidelity for the computational discrimination of various analyte species. This is highly advantageous from a fabrication standpoint where utilizing many different materials would require consideration of varying substrate/electrode thermal expansion properties, as well as multiple targets and depositions. We are preparing our initial MPES arrays by sputtering LSC working electrodes of varying geometry onto the heater platform. The YSZ electrolyte layer will be electron beam evaporated.

We successfully met the first milestone of establishing a prototype array and predictive algorithm. The computational framework provided feedback on required sensing characteristics and number of sensors that is currently being used in the design and fabrication of the physical MPES array. We will first evaluate the MPES array in the low risk NOx sensing and then extend that work to low concentrations of analyte species belonging to a chemical signature of interest in the presence of large and varying backgrounds. We envision as our end goal a versatile, standalone device that after a single mission-specific calibration in a laboratory setting may be deployed in both remote and harsh conditions to provide quantitative analysis of chemical signatures against large and unknown environmental backgrounds.

Future Work

We will test and validate predictive algorithms for our newly fabricated MPES arrays focusing on concentrations of constituent species relevant to emissions monitoring applications. The feedback from the computational framework has been incorporated into the design of the MPES array to provide optimal individual sensor element response characteristics while minimizing the number of sensor elements required. As with our previous discreet sensor analysis, we will measure the voltage response of each individual sensor element to a wide range of mixing ratios (alphas) of target analytes. The Bayesian model established through our prior work will be used to provide predictive algorithms for monitoring emissions control operations of selective catalyst reduction (SCR) and exhaust gas recirculation (EGR). In parallel, we will explore the lower limits of sensitivity to a target species in the presence of large concentrations of interferents (critical to the detection of HE/EMs with low vapor pressures). Unlike the emissions monitoring application where the analyte species of interest is present at similar levels to background interferents, (al-

pha~1), detection of HE/EM chemical signatures requires sensitivity to low concentrations of target species against a large background (alpha<<1). We will assess the discriminating capability of the MPES array to varying chemical signatures, as well as against background interferents such as humidity, NOx (a common industrial pollutant), or a high nitrogen content fertilizer such as urea. Our initial effort will use the same MPES array for both applications, where subsets of a ranges relevant to each proposed application will be used to train the Bayesian model. Following the methodology established in the first 2 years of this work, Bayesian modeling will be used to identify the combination of sensor attributes that enable the greatest discriminatory capabilities and guide the construct of an MPES array targeted for chemical signature detection.

Conclusion

Proof-of-concept will be demonstrated by fabricating a prototype sensor array and developing/validating predictive algorithms for the quantitative assessment of individual constituent concentrations in a complex gas mixture. After successful demonstration of proof-of-concept we will work closely with our partners at ElectroScience Laboratories (ESL) to fabricate for the very first time Mixed potential Electrochemical Sensor (MPES) array prototypes using their proven High temperature co-fired ceramic (HTCC) manufacturing methods. We will then demonstrate the ability of these sensor arrays and signal processing techniques to analyze individual gas components in two difference applications; viz: 1) vehicle emissions monitoring and high-explosive/energetic-materials detection.

Publications

Javed, U., K. P. Ramaiyan, C. R. Kreller, E. L. Brosha, R. Mukundan, and A. Morozov. A universal experimental and computational framework for decoding complex gas mixtures . To appear in 2nd International Conference on Sensors and Electronic Instrumental Advances . (Spain, 22-23 Sep. 2016).

Kreller, C. R, A. Nadiga, S. C. Brown, J. M. Reynolds, D. Spernjak, F. H. Garzon, E. L. Brosha, A. V. Morozov, and R. Mukundan. Quantitative Decoding of Complex Gas Mixtures for Environmental Monitoring Using Mixed-Potential Sensors. 2015. In 227th ECS Meeting. (Chicago, IL, 24-28 May. 2015). , p. Abstract MA2015. Chicago: ECS Meeting Abstracts.

Ramaiyan, K. P., C. R. Kreller, E. L. Brosha, R. Mukundan, U. Javed, and A. Morozov. Quantitative Decoding of Complex Gas Mixtures Using Mixed-Potential Sensor Arrays . 2016. In 230th Meeting of The Electrochemical Society. (Hawaii, 2-7 Oct. 2016). Vol. 75, 16 Edition, p. 107. New Jersey: ECST.

Reynolds, J. M., S. C. Brown, E. L. Brosha, R. Mukundan, F. H. Garzon, and C. R. Kreller. Electrochemical Characterization of Electrode Materials for Mixed-Potential Sensors. 2015. In 227th ECS Meeting. (Chicago, IL, 24-28 May. 2015). , p. Abstract MA2015. Chicago: ECS Meeting Abstracts.

Ultra-sensitive Parallel Micro-imaging with Atomic Magnetometer

Igor M. Savukov
20150300ER

Introduction

It is widely recognized that the next frontier for magnetometry is biological and neuroscience applications, where impact will result from improvements in both resolution and sensitivity. We propose to meet this need for higher resolution and higher sensitivity magnetometry with a novel approach: combining an ultra-sensitive atomic magnetometer (AM) with flux concentrators (FCs). The technological breakthrough will result from advances in atomic magnetometers and from the novel FC-AM concept. After developing the FC-AM device, we plan to demonstrate its performance by applying it to important problems in science, security, medicine, and industry.

The proposed research program will have two broad research goals. The first goal focuses on technology: (i) demonstrate the FC-AM principle, (ii) characterize its sensitivity and resolution, and (iii) demonstrate that FC-AM can operate in multi-channel configuration. The second goal focuses on applications in bio-security (detection of magnetic nano-particles, neuroscience, detection of bio-magnetic fields of a cluster of neurons), in energy research (fuel cell ion-transport imaging), and in industry (non-destructive evaluation, NDE).

Benefit to National Security Missions

DARPA has issued a call for sensitive magnetometers with high resolution. We will address directly this need.

One class of NIH applications is based on detection of magnetic nano-particles with our micro-magnetometer: applications in detection cancer cells, infections and cancer therapy. The second class on detection of magnetic field of neurons. It is directly relevant to the President Obama brain initiative.

Other federal agencies might be interested in various applications of micro-magnetometry. For example, authentication of micro-chips. Also, The magnetometers can be used for fuel cell diagnostics, which is relevant to reduction in CO2 emission and hence climate impact. Other potential applications include:

- Pathogen detection, based on magnetic nano-particles
- Transportation, such as irport security checks for pathogens
- Commerce, for the authentication of micro-chips
- Fundamental bioscience, in DNA detection and other applications of magnetic nano-particles
- Basic health research, such as brain science, cancer detection and studies

Progress

A single-channel atomic-magnetometer and a flux-concentrator system were constructed. The gradient system was added to compensate gradients from the ferromagnetic material of the flux concentrator. Measured sensitivity of the atomic magnetometer with and without the flux concentrator was found almost equal. The system was experimentally characterized for sensitivity and resolution. Various coils were used as the source of the magnetic field. Numerical simulations with Compsol were performed to obtain the noise of the flux concentrator and its magnetic-field transfer coefficients. The results for resolution and sensitivity were found in agreement with simulations. Simulations were used to find future steps for improving resolution and sensitivity. The results are published in Scientific Reports (6, 24773, 2016). A provisional patent was filed.

Second, we worked on developing an imaging system. A 3D scanning system was built to obtain magnetic images of magnetic micro-particles. A single micro-particle as small as 10 um was detected. Resolution of 200 um was confirmed. One problem was found that 1/f noise was higher than expected, so to improve the sensitivity of

static magnetic field sources, we introduced modulation. The modulation improved the sensitivity by a factor of 10. (In preparation for Appl. Phys. Lett.) In addition to imaging magnetic micro-particles, we also imaged micro-meteorites embedded into a rock sample. We found the micro-meteorites have sufficient magnetization (without applying external field) to be detected. We also found some applications for studies of magnetic contamination important for nEDM experiments.

In addition to constructing the single-sensor scanning magnetic microscope, we constructed a multi-channel atomic magnetometer based on a large Rb cell and multi-photodiode detection. Sensitivity of fT levels was achieved for some channels, but because of the non-uniformity of the intensity distribution across the cell, 16 channels had variation in sensitivity. We are trying to find methods to solve this problem. The single-channel variant of the large-cell system was published.

Future Work

We will continue optimization of the scanning magnetic microscope and develop its applications. In particular, we found that it is capable of detecting small magnetic particles. We would like to implement the detection of nano-particles, which find many biosecurity and medical applications. We are also planning to demonstrate non-destructive tests with sub mm resolution.

Further improvements in the tip sharpness can lead to improved sensitivity to microscopic magnetic sources and increase the resolution. We would like for example to try attach to the existing ferrite tips sharper tips made from mu-metal. It is possible also to use micro-fabrication techniques and magnetic particles themselves as the probes of magnetic field to further improve the resolution to 1-100 um level.

We will continue to optimize the multi-channel system. It accelerates the scan time by 16 times. Also it can enable measurements of dynamic correlations by providing simultaneous measurements in 16 positions.

We also will seek collaborations with other scientists in LANL who can benefit from our technology. For example, nEDM experiment needs characterization of magnetic contamination of materials used in sensitive measurements. In addition, our magnetometers can be useful for axion search. Some simulations were done showing that new limits can be set on various fundamental interactions.

Conclusion

After the FC-AM devices have been tested and characterized, we will work on developing novel applications. We will demonstrate detection of magnetic nano-particles functionalized for specific molecules. Nano-particle applications are relevant to LANL missions in security, energy research, non-prolifiration. In addition, We will test non-destructive evaluation methods. Finally, if time permits, in collaboration we will work on detection of magnetic field of a single neuron or small clusters of neuron. The preliminary data will serve as the basis for proposals, for example within President Obama BRAIN initiative, or DHS (biosecurity), or DOE for fuel cell research.

Publications

Chu, P. H.. Search for exotic spin-dependent interactions with a spin-exchange relaxation-free magnetometer. 2016. Physical Review D. 94: 036002.

Espy, M.. Hardware Developments: Detection using SQUIDs and Atomic Magnetometers, Mobile MRI/ Chapter 7. 2015. In Mobile NMR and MRI: Developments and Applications. Edited by Price, B.. , p. 183. Cambridge, UK: Royal Society of Chemistry.

Karaulanov, T.. Spin-exchange relaxation-free magnetometer with nearly parallel pump and probe beams. 2016. Measurement Science and Technology. 27: 055002.

Savukov, I. M.. Spin Exchange Relaxation Free (SERF) Magnetometers. 2016. In Smart Sensors, Measurements of Instrumentation. Edited by Grosz, A.. , First Edition, p. 451. Cham: Springer International Publishing.

Savukov, Y. J. Kim and I.. Ultra-sensitive Magnetic Microscopy with an Optically Pumped Magnetometer. 2016. Scientific Reports. 6: 24773.

Probing Critical Behavior in Hydraulic Injection Reservoirs and Active Seismic Regions

Paul A. Johnson
20160144ER

Introduction

Earth's crust state of stress controls all elastic-plastic behaviors and plays a fundamental role in energy extraction, fracture propagation, wellbore stability, and earthquake hazard. Global- and regional-scale stresses are well characterized, but our understanding of the state of stress at the reservoir-scale is inadequate. We bring a team of internationally recognized leaders in this field to develop and apply a joint inversion approach using gravity, seismic, and geodetic information to extract the full stress tensor. Imaging the state of stress in reservoirs away from boreholes has never before been accomplished. Our complex systems proposal applies to the complex problem of determining the stress state, in support of national security, energy independence, and civil infrastructure.

Our goal is to develop and test a highly novel approach to measure the stress field. This is important in regions where stress is evolving, in both tectonic environments and regions where fluid pumping is altering the stress field. We are doing so by applying recent advances from laboratory experiments, simulation and seismic observations in earth. We are extending recent progress in data science, uncertainty quantification and algorithm parallelization to maximize our advance. Success will fundamentally change the assessment of seismic hazards, related both to human activities such as energy extraction and waste storage as well as from tectonic activity, and provide the means to image stress-induced changes of all kinds.

Benefit to National Security Missions

Our work has direct impact on an identified mission challenge of DOE/SC in regards to the SubTER Initiative. A major goal of SubTER is determining Earth's state of stress. We will develop the means to determine if faults are in a critical stress state near failure. Additionally, the work has relevance to DOT in terms of potential damaging earthquakes to infrastructure. If we succeed in our work, we will have the means to determine that a fault may be near failure so that mitigative action may be taken regarding infrastructure.

This research has direct relation to Fossil Energy in that we are characterizing faults that may be activated by wastewater injection from unconventional hydrocarbon exploration. Our work can also be applied to hydraulic fracturing during fluid or CO2 injection in reservoirs. The work has important implications for energy impact in that characterizing faults that are critically stressed during fluid injection allows mitigative action to take place. It also has important consequences to nuclear waste in regards to earthquake hazard assessment.

Progress

Our primary goal is to quantify the state of stress in Earth. We have refined the simultaneous joint inversion of seismic and gravity data. We applied the inversion to computer generated data and found the approach works and helped us evaluate errors in the stress calculation. We then applied the inversion to calculate the stress tensor applying known stresses from tectonic boundaries as our baseline by applying a prototype version of this approach in Oklahoma, in the vicinity of the 2011 Prague earthquake. Further work will tell us about the stress difference with time due to injection, and how this relates to seismicity and critically stressed faults. Next year we will report on these findings.

Future Work

- Hone the stress tensor method and work on error analysis.
- Continue laboratory experiments supporting stress calculation.
- Begin numerical simulation of stress and the evolution of stress applying the Element + Discrete Element method.

- We have conducted a preliminary stress study near Prague Oklahoma, where a M>5.0 earthquake took place in 2011. We now intend to apply the stress method at 2 or more time intervals and look at the stress field differential to see where stress was changing at this time and if it can be associated with fluid injection.

Conclusion

Conspicuously, seismicity rates in the mid-west United States have dramatically increased over the last 10 years, corresponding to the rapid growth of unconventional oil and gas production and the associated fluid waste injection. A moderate or large magnitude earthquake located in or near a population center could be potentially catastrophic. If a probe existed for the critical stress state at locations in which earthquakes may occur, preventative action (such as termination of pumping) could be taken. We propose that dynamically triggered microearthquakes can be used as a probe of critical stress state (faults near failure) within injection reservoirs and active tectonic regions, and aim to develop the methodology to quantify the new probe. This work could dramatically advance earthquake hazard analysis for both natural and anthropogenic earthquakes.

Publications

Elst, N. Van der, A. Delorey, D. Shelly, and P. Johnson. Fortnightly modulation of San Andreas tremor and low-frequency earthquakes. 2016. P.N.A.S.. 113: 8601.

Radio Frequency Scintillation Prediction Driven by Direct Measurement of Ionospheric Spatial Irregularities

Max E. Light
20160231ER

Introduction

Scintillation, or distortion and degradation of a radio signal as it passes through the ionospheric plasma, is of particular concern to the space-based nuclear detection mission, specifically at the very high frequency (VHF; 30–300 MHz) radio frequency (RF) spectrum. This scintillation is caused by random structure (plasma depletions and enhancements) in the ionosphere over many scale sizes, from meters to tens of kilometers.

The physics of how this random structure causes signal degradation is well understood. However, the spatial scale spectrum of those irregularities (Irregularity Spectral Density, ISD) required for input into scintillation models is poorly characterized, particularly at the scale lengths important for VHF scintillation prediction. Plasma irregularity sizes scale from less than a meter to tens of kilometers, requiring that the ISD be specified over a wide spatial scale. However, in the absence of a well-specified ISD we cannot know which sizes contribute significantly to scintillation.

We will specify the ISD empirically for the first time using an existing dense network of global position system (GPS) receivers that measure total integrated plasma density in the ionosphere over a local region. An empirically-determined ISD will allow scintillation model predictions to be based on the actual local environmental conditions instead of theoretical best guesses. Due to the fact that such a dense receiver network exists only over Japan, we will explore a proof-of-concept satellite-based technique that uses a wideband VHF beacon on a low-earth-orbiting satellite with a global network of ground receivers. This technique would allow for global specification of the ISD with greater accuracy. We will model this technique through a synthetic study using the emperically-determined ISD as input. We will compare the results to those from the ground-based GPS receiver network to determine which is more accurate and which is globally feasible.

Benefit to National Security Missions

Remote sensing of radio frequency (RF) signatures driven by the electromagnetic pulse (EMP) created by nuclear detonations is one of the cornerstones of the DOE/NNSA Nuclear Nonproliferation program. The broadest coverage for detection of these signatures is achieved through a constellation of satellite-based sensors, which are currently deployed and maintained for the foreseeable future. The frequency bandwidth of these EMP signatures lies in the very high frequency (VHF; 30 - 300 megahertz) range. These signals must traverse the ionosphere before being detected, and can suffer large scintillation distortion. Thus, an understanding of the fundamental drivers behind scintillation, and an accurate modeling capability are vitally important to mission success.

Progress

We used existing GPS infrastructure in Japan and California to provide a direct measurement of the ionospheric irregularity spectral density (ISD) function. Initial results were presented at the 2015 fall meeting of the AGU. This spectrum will be used as input to our existing scintillation model to make the first ever radio frequency scintillation prediction with appropriate empirical inputs. From these two GPS datasets, a two-dimensional map of ionospheric spatial fluctuations was created from which the ISD is calculated. Refinements to the spectral estimation techniques are ongoing and will most likely be published in the next fiscal year.

We have identified additional independent sourced of scintillation measurements taken in other RF bands between 200 MHz and 2 GHz. These will be used to compare and validate modeled scintillation based on GPS measurements.

We have also identified additional dense GPS networks (Honduras, Ecuador, Alaska, Hawaii) that will be used to explore the ISD of differing regions of the ionosphere

(high latitude auroral region, mid-latitude, equatorial).

Future Work

Most spatial spectral estimation techniques rely on a regular grid. The nature of our data sets, however, requires spectral estimation on an irregular grid. While spectral techniques exist for irregularly spaced data, they are not precise enough for our application. We will refine our existing existing techniques for irregularly spaced data to increase the fidelity of our ionospheric spatial spectrum to be used in our scintillation model.

The data sets we have currently analyzed show less scintillation events compared to high latitudes and equatorial regions. This was expected, but we chose to use GPS detectors located at mid latitudes because of the density of detectors required for this research. We have discovered additional dense GPS receiver networks, with existing databases in Honduras, Hawaii, Equador, and Alaska. We will analyzed data from these networks as well.

Our existing multiple phase screen (MPS) scintillation model treats the ionospheric plasma as a unmagnetized, homogeneous medium. This assumption is commonly used in MPS scintillation models. Our research, however, requires a more realistic plasma medium treatment for the ionosphere (magnetized, non-homogeneous plasma). To our knowledge, such a treatment of the ionosphere does not exist. We will extend our MPS scintillation model to include the aforementioned plasma characteristics.

Conclusion

There is currently no global system to measure electron density at the spatio-temporal scales required for scintillation prediction. This project will provide a system architecture and proof-of-concept for such as system. Once implemented, measurements from the proposed system will aid in answering global scintillation questions and could be part of a global scintillation forecasting system. The ability to accurately predict scintillation effects with our model will advance the design of space-based sensors used to detect signals generated from a nuclear detonation.

Time-of-Flight Ion Mass Spectrometer Subsystem for Space and Planetary Missions

Herbert O. Funsten
20160440ER

Introduction

We will grow chemical vapor deposition graphene on Ni and Pd substrates and transfer the graphene to a support grid using a polymer-liftoff/transfer to the mesh via thermal release or solvent dissolution. We will also adapt a commercial magnetron sputterer for physical vapor deposition of TiN or CrOX inside a plastic cylinder. The coating thickness, which increases quadratically with distance down the cylinder, is controlled to obtain <0.5% resistance error. The combination of these technologies will substantially increase performance of space-mass spectrometry and neutral-atom imaging while reducing mass, complexity, and cost.

First, a transformational advance in performance (sensitivity, mass resolution, and measurements at lower energies) will be enabled by development of large area ultrathin, freestanding graphene foils mounted on a high transmission support grid. Second, a factor of ~3 reduction in mass as well as complexity and cost enabled by development of a graded resistance coating in which the resistance varies quadratically with distance in the mass spectrometer drift region, providing a compact, modular energy isochronous reflectron.

Benefit to National Security Missions

Los Alamos uses leadership and participation in NASA missions to (1) develop and validate new technologies and capabilities that can be used in the space Nuclear Detonation Detection program and (2) engage scientists and engineers in cutting edge science and technology. This technology addresses the space environment component of the NDD program as well as space situational awareness. The combination of these two technologies enables future leadership on several NASA missions and portable ground-based mass spectrometers, including:

1. A high sensitivity energetic neutral atom imager for the Interstellar Mapping and Acceleration Probe (IMAP), the highest ranked NASA mission in the National Academy's Heliospheric Decadal Survey. Los Alamos will lead this ~$40M instrument for a mission proposal (~2019) to study the heliosphere (space physics) and interstellar medium (astrophysics)
2. A 2-stage mass spectrometer for measurement of molecular species in gas plumes emitted from airless planetary bodies and Moons. Recently, Los Alamos led a $34 M instrument proposal, and the technology proposed here could be inserted into the flight instrument design in two years.
3. A ground-based, portable gaseous neutral mass spectrometer for national security applications is under current development in ISR Division. This technology would enable volume and mass reduction of the time-of-flight subsystem by ~3.

Progress

Tasks 1 and 2: (1) Chemical vapor deposition growth on Ni and Pd. (2) Suspension on wire mesh support structure

- Analysis performed of conventional carbon foils: analysis completed, foils are not amorphous carbon and have structure similar to diamond-like carbon
- Successful transfer of multi-layer graphene onto a series of commercial transmission electron microscopy (TEM) grids; validation of no pin holes in these foils. These are the thinnest free-standing foils fabricated so far at Los Alamos.
- Testing of graphene foil performance using ion beam facility is ongoing (angular scattering, foil uniformity, secondary electron emission)

Tasks 4 and 5: (4) Develop coating fabrication method. (5) Develop coating characterization method.

- TiN films were successfully fabricated by magnetron sputtering on a glass slide.
- Lehighton Electronics, Inc: LEI-88 Sheet Resistance

System is being procured for precision measurement of coatings (required to be qudratic with distance on cylinder interior with 1% resistance precision). TiN sample has been sent for company to evaluate/demonstrate accuracy and precision of their instrument before order placement.

- Second TiN sample will be measured at DET-2 for evaluation of their capabilities as an alternate to the LEI-88.
- New task: Investigate potential alternate ultrathin foil fabrication using parylene deposited on soluble substrates (e.g., salt, ice).
- Ultrathin parylene sample on Si wafer is being fabricated for secondary electron emission (from incident 10 keV protons) testing and verification of performance for space instruments. Urgency is need for superior foils within time frame of anticipated NASA mission proposal in early 2017.

Future Work

Task 3 (Feb 2017): Optimize: large area, defect free coverage

- Goals: Mount foils in mechanical package, final characterization and validation
- Goals: Optimize carbon precursor, temp profile, transfer technique to suppress defect density
- Task 5 (Jan 2017): Develop coating characterization method. Goals: Perform coating electrical characterization and thickness measurements
- Task 6 (March 2017): Optimize coating fabrication conditions. Goals: Fabricate a set of tubes coated with graded electrically conductive film
- Task 7 (Sept 2017): Demonstrate mass resolution performance of integrated time-of-flight subsystem. Goals: Assemble subsystem with existing channel electron multiplier detectors; Test with incident 0.4-10 keV ion and neutral atom beams of H, He, C, N, O, Ne, and Ar
- ADDED TASK (Feb 2017): Investigate potential alternate ultrathin foil fabrication using parylene deposited on soluble substrates (e.g., salt, ice). Goal: demonstrate utility by Feb 2017 in anticipation of NASA mission proposal.

Conclusion

We will develop and demonstrate two enabling technologies that allow Los Alamos to retain leadership in space mass spectrometry and energetic neutral atom (ENA) imaging. The combination of these two technologies in a mass spectrometer subsystem will enable future leadership on several missions to study Earth, planets, and the Sun's interaction with the interstellar medium. The technologies are also applicable to ground-based and laboratory high mass resolution time-of-flight mass spectrometers. This work has application to mission challenges in the area of space situational awareness.

Narrow Spectrum Gamma-Ray Production Through Inverse Compton Scattering with a Free-Electron Laser

Frank L. Krawczyk
20160459ER

Introduction

There is a need for gamma-ray based detection of special nuclear material (SNM). There are two technology paths to do this: (1) photo-fission by using > 6 MeV gamma rays and (2) very narrow band and selective nuclear resonance fluorescence (NRF) with 1 to 2 MeV gamma rays. Due to the narrow NRF resonances (a few eVs separated by ~ keV), it would be an excellent non-ambiguous interrogation approach if a source of monoenergetic gamma rays is available. However, the leading technology to make narrow spectral gamma rays (through inverse Compton scattering (ICS) of UV photons off relativistic electrons) so far has not produced gamma rays with energy spreads less than a few percent. This is largely because current ICS architectures rely on low repetition rates but with very intense, lasers, and the high intensity of the laser light electric field leads to a nonlinear broadening of the gamma-ray spectrum.

We have recently proposed an ICS architecture that could produce high fluxes of gamma rays with energy spreads of 0.1% and less, where we use a high-repetition rate free electron laser (FEL) to produce the UV photons instead of a low repetition rate intense laser, and we collide the UV photons with electron bunches before they are degraded by the FEL interaction.

This scheme will achieve lower gamma ray spectral widths than ever before and will allow us to probe the fundamental limitations to monoenergetic gamma rays, specifically phenomena like the Fourier transform properties of the UV photon pulses and the electron beam quality. We will study these effects in detail at the JLab UV FEL facility. The project's leave behinds include a demonstration of our novel hybrid ICS/FEL architecture and a validated predictive capability available for designing future SNM detection facilities.

Benefit to National Security Missions

There is a need for gamma-ray based detection of special nuclear material (SNM) which is in the mission areas for NNSA, DTRA, ONR, and DNDO. There are two technology paths to do this: (1) photo-fission by using > 6 MeV gamma rays and (2) very narrow band and selective nuclear resonance fluorescence (NRF) with 1 to 2 MeV gamma rays. Due to the narrow NRF resonances (a few eVs separated by ~ keV), it is an excellent non-ambiguous interrogation approach. However, the leading technology to make narrow spectral gamma rays (through inverse Compton scattering (ICS) of UV photons off relativistic electrons) so far has not produced gamma rays with energy spreads less than a few percent. This is largely because current ICS architectures rely on low repetition rate, but very intense, lasers, and the high intensity of the laser light electric field leads to a nonlinear broadening of the gamma-ray spectrum. We have proposed a new ICS architecture using a high-repetition rate RF linac which produces UV photons through a free-electron laser (FEL) that addresses this issue. This new ICS/FEL architecture should be able to achieve high flux, ~ MeV gamma rays with spectral widths of 0.1% and less. Additionally, this novel gamma-ray generation scheme will enable new nuclear physics studies, specifically with nuclear resonances, nuclear structure, and nuclear astrophysics, relevant to the DOE Office of Science Nuclear Physics mission.

Progress

FY16 work was directed towards the preparation of a successful inverse Compton scattering (ICS) measurement at an existing accelerator in FY18. The purpose of these measurements is to investigate the subtleties and interdependencies of the various physical phenomena leading to ICS gamma ray spectral growth.

We modeled the Jefferson Laboratory (JLab) UV Free Electron Laser (FEL) system and confirmed the suitability

of their beam parameters for lasing and x-ray generation by Inverse Compton Scattering (ICS). Based on the JLab UV FEL parameters with our intracavity ICS design, we estimated the generated gamma photon flux to exceed 1011 photons per second. A concept for a reconfiguration of the interaction region to facilitate the FY18 experiments has been developed. This included electron beam optics and UV light optics that were compatible with the space restrictions from the optical cavity of the oscillator FEL. First configurations have also been developed for the x-ray detector placement that does not suffer from back-ground x-rays from electron beam intercept in the accelerator.

The original plan was to provide about 0.2 FTEs of funding for our JLab collaborators to help with these design tasks. During these negotiation, the funding request by Jlab for the FEL re-commissioning increased up to $500k over the duration of the LDRD. This request significantly exceeded the original amount from prior communication, when we visited JLab before the start of the project. As a result we contacted other accelerator facilities and found strong interest by the accelerator group at LLNL. This group has an electron beamline called ISIS that can be used for a collaborative intra-cavity ICS experiment that meets the proposed work for our LDRD.

The change in location required a minor change in scope, as the ISIS beamline is not yet an FEL facility, and the accelerator is pulsed, not continuous-wave like the JLab facility. FEL simulations showed that an existing brand new wiggler at LANL (available from prior Navy work on a high-power FEL) would be a suitable magnetic device on the LLNL beam-line for converting the ISIS beamline into an IR FEL oscillator and performing inverse Compton scattering with the intracavity IR beam. A big difference between this new oscillator and the JLab UV FEL is the ICS photon energy, which will be 30-40 keV for the LLNL oscillator, instead of the MeV photon energies at the JLab UV FEL. This change in photon energy does not conflict with the desired final deliverables for the LDRD project. Hardware changes in the beam-transport, mainly the bunch compression plus the magnetic lattice to transport the beam through the wiggler, as well as the IR optics for the oscillator FEL are required. The company Advanced Energy Systems (AES) that designed and built the ISIS accelerator is joining the effort and will provide the design simulations for the accelerator configuration itself. The configuration of the electron beam-transport to the wiggler and the oscillator FEL optics will be done internally by the LANL team. The funds that would have supported JLab are sufficient to cover the cost for AES. A statement of work for these simulations is presently under negotiation and will be completed in the second half of June.

For a credibility check of the experimental change to the LANL code, FELEX for FEL interaction was used to perform higher confidence FEL interaction simulations to confirm the suitability of the FEL-ICS interaction with a different set of electron beam-parameters. The FELEX simulations for the desired electron beam parameters are in process. The simulations will be updated, when the simulation results for the actual best performance from AES are available.

This change in scope and location is actually strengthening the relevance of the proposed work. LLNL is willing to contribute their own funds to set up the beam line and as the work fits well in both LANL and LLNL interaction with NA-22 on this topic. LLNL proposed to submit a joint LDRD proposal to complement the LANL focus with their LDRD funds. We are planning to support them in the writing of this proposal to achieve a work plan that matches the needs of both institutions.

Future Work

In FY17 the main tasks will be implementation of the beam-line modifications based on the FY16 simulations, the fabrication and installation of the down-stream section of the accelerator (LANL wiggler, optical cavity and diagnostics), the final design of the FEL oscillator cavity and the development of the experimental plan for FY18.

Task 1 will be performed in collaboration with LLNL and AES. The beam line commissioning at LLNL, based on the simulation results, will implement the modification in beam transport and if needed the addition of a bunch compressor between linac sections 1 and 2. If possible, verification of the beam-transport will be done in FY17.

T

ask 2 includes the transport of the wiggler to LLNL, the fabrication and installation of the beam-transport from the end of the linac to the beam-dump, the installation of optical cavity and x-ray diagnostics. If possible, verification of the beam-transport through the wiggler to the beam-dump will be done in FY17.

Task 3 will provide fine tuning of the FEL oscillator cavity design to produce the high-power intracavity infrared power. The generic design we do at the end FY16 will not use the final optimized electron beam.

Task 4, based on the electron beam properties calculated in tasks 1 and 2 will develop a range of operation scenarios that demonstrate x-ray generation by ICS. The first goal is the prediction of the photon yield and bandwidth for the nominal operation parameters. From a variation of the operation parameters scaling laws for these properties will be developed. The ultimate goal is not to achieve record

performance but to demonstrate that our design approach and tools correctly predict the performance of the ICS-FEL system. This has never before been achieved for any other approach to a narrow band ICS based x-ray source for SNM detection.

Conclusion

The technical goals are to demonstrate a novel inverse Compton scattering/free-electron laser (FEL) hybrid approach to generating MeV gamma rays with spectral widths of 0.1% and less and to develop a validated predictive capability through detailed measurements at the Lawrence Livermore accelerator facility. We will be able to produce high flux gamma rays with an order of magnitude narrower spectral widths than ever before, allowing us to experimentally investigate subtleties and the interdependencies of the various physical phenomena leading to gamma ray spectral broadening.

Publications

Carlsten, B. E., F. L. Krawczyk, J. W. Lewellen, Q. R. Marksteiner, D. C. Nguyen, and N. A. Yampolsky. High repetition-rate inverse Compton scattering x-ray source driven by a free-electron laser. 2014. JOURNAL OF PHYSICS B-ATOMIC MOLECULAR AND OPTICAL PHYSICS. 47 (23).

Range-Resolved Measurement of Atmospheric Greenhouse Gases for Treaty Verification and Climate Science

Brent D. Newman
20160462ER

Introduction

We will investigate the hypothesis that we can do altitude and volume constrained spectroscopy on atmospheric gases in the altitude ranges of 15 to 30 km. The concept is that sulfate aerosols (with densities of 1 to 10 per cubic cm at those altitudes) will provide a large reflection at W-band (nominally 75-110 GHz). We will sweep a transmit signal across rotational resonances of important atmospheric gases (e.g. key greenhouse gases). A receiver will interrogate an intersecting volume and will detect the signal reflected from within that volume. By comparing the received signal just below, at, and just above the resonance will allow us to determine that gas' concentration at the location of that volume.

We are proposing a delicate measurement that will require an engineered system to be done properly. An engineered system for this measurement technique would use a 1-kW average power W-band source and integrate the return signal for 10 minutes. To verify our hypothesis we will use a 100-W W-band source which is currently available. It is unlikely that we will be able to do spectroscopy from aerosol reflections at that lower power, rather we will demonstrate these two phenomena:

1. We will measure ozone concentration at ~ 12 km from a W-band signal scattered off ice crystals in clouds.
2. We will detect Rayleigh scattering from stratospheric sulfate aerosols in a constrained volume.

Together, these measurements will confirm our hypothesis and demonstrate that stratospheric spectroscopy can be done with a properly engineered system.

Benefit to National Security Missions

The technology development is for a novel scheme of broad area surveillance of measuring atmospheric gas concentrations in specific, altitude-constrained, volumes, between nominally 15 and 30 km altitude (i.e. through essentially the entire stratosphere, not just a small fraction of it). These gases include greenhouse gases. Current technology can only do line integration of gas concentrations from the sun to a location on the earth or are based on actual balloon or plane atmospheric sampling and cannot map out large parts of the stratosphere. Both climate science (in particular modeling of greenhouse gases; of interest to NASA and DOE Office of Science) and future greenhouse gas emission treaty verification (of interest to the Department of State) will greatly benefit from this new technology.

Progress

At the start of this project, we modified the project plan to reduce overall project risk. In the proposal, the plan was to assemble outdoor active spectroscopy hardware in FY16 and start making preliminary outdoor measurements. Instead, we decided to start outdoor passive measurements in FY16 with the Fourier Transform Spectrometer to develop a measurement baseline and to quickly demonstrate we could measure greenhouse gas changes in the area we will target with the active W-band spectroscopy. Also, to facilitate the commissioning of our W-band active system, we decided to first do laboratory spectroscopy in a gas cell.

Work to date in FY16 (over the first 8 months) have been in the areas of evaluating chemical species appropriate for W-band spectroscopy including high-resolution modeling; preparing for an indoor active spectroscopy experiment; and preparing for an outdoor passive experiment.

Evaluation of atmospheric chemical species

We have conducted an extensive literature review in millimeter wave passive radiometric systems for atmospheric gases. The purpose of this review was to determine the most feasible system for measuring ozone emission lines in the 75-110 GHz region. We evaluated several software packages for calculating atmospheric trans-

mission and radiance with high resolution. This involved running multiple simulations and interacting with technical support and sales personnel to find a package that fit our needs for modelling W-band atmospheric radiance. Initial calculations indicate the ozone emission lines are weak and this determines the performance specifications for the receiver hardware.

Indoor gas cell experiment

We have identified hardware requirements for a laboratory test-bed with a gas cell as well as outdoor atmospheric measurements. After being purchased, much of the specific hardware has been tested (transmission through windows, etc). The expected power levels have been estimated, and we are comparing those estimates with the capabilities of the hardware. We are developing an IWD to cover the RF/gas cell experimental system.

Outdoors passive measurement

Many pieces required for the passive atmospheric test have been located or specified. We have developed an initial design of a heterodyne spectroscopy receiver system intended to be deployed outdoors, capable of both active and passive measurements. We have done well in terms of making baseline passive spectroscopy measurements with the Fourier Transform Spectroscopy tool from EES division and our efforts to use it to quantify greenhouse gas changes across the boundary layer in the same area that the W-band active spectroscopy will be used. We are on track for the use of the Bandelier VLBA antenna in FY18.

Future Work

In FY17 we plan to begin active W-band spectroscopy using the laboratory gas cell. This will ensure all our W-band equipment is working well for the final outdoor measurement using the VLBA antenna. We will only have limited time with the outdoor antenna so a test bed to commission the hardware is critical. Also, in FY17 we will continue making baseline passive measurements with the Fourier Transform Spectrometer (FTS), identifying the best species for active W-band spectroscopy, and we will continue to make measurements relevant to greenhouse gas dynamics as possible. We will also start passive outdoor W-band measurements, correlating the results with the FTS.

Conclusion

The technical goal of this project is to verify our hypothesis that we can use sulfate aerosols in the stratosphere for volume-constrained spectroscopy of atmospheric gases. Using available hardware, we will separately verify the two key elements in this hypothesis: (1) the Rayleigh reflection of aerosols in the stratosphere between 15 and 30 km altitude at W-band is large enough so a practical spectroscopy instrument can be built, and (2) by measuring the differential absorption of a specific gas rotational resonance at slightly different altitudes, we can determine the gas concentration at that altitude. Both climate science (in particular modeling of greenhouse gases) and future greenhouse gas emission treaty verification will greatly benefit from this new technology.

Novel Antennas Based on Atomic Magnetometers

Malcolm G. Boshier
20160518ER

Introduction

Several Laboratory customers have stated a need for better antennas which are electrically small, i.e., with dimensions small relative to the wavelength of the electromagnetic radiation being detected. This issue is particularly acute in the low frequency regime, where the frequency range 1 – 30 kHz corresponds to wavelengths from 300,000 km to 10 km. The Extremely Low Frequency (ELF) regime below 3000 Hz is important because it can, for example, be used to communicate through hundreds of meters of seawater to submarines, and it should similarly enable communication with submerged sensor arrays. Very Low Frequency (VLF) radiation (3 – 30 kHz) is useful for communicating wider bandwidth signals, such as voice communication, or as a diagnostic of machinery operating in an inaccessible underground facility. Further, while low frequency electric fields are attenuated effectively by grounded conductors, magnetic fields are not, and so low frequency magnetic fields may therefore be used, for example, to communicate through buildings or soil (e.g. mine communications).

We propose to detect ELF and VLF magnetic fields directly using compact high-sensitivity atomic magnetometer technology which has become available in just the past few years. In particular we will use a fieldable, carry-on suitcase-sized atomic magnetometer developed by us. We will characterize this device's performance as an antenna using test facilities available at LANL, and refine the design accordingly. We further propose to add encoded signal characteristics to these tests to demonstrate the power of the combined sensor-signal advantages in ELF and VLF communications. We believe that the marriage between highly sensitive magnetic field detectors and digital encoding techniques is a unique approach that will allow previously unavailable communications between mining operations, underground facilities, very long distance separated terrestrial points, and may be able to provide dramatically improved VLF beacons.

Benefit to National Security Missions

Our goal is to show that atomic magnetometers can be used as compact but highly sensitive receiving antennas for very low frequency magnetic fields and electromagnetic waves. Since this type of radiation penetrates both metals and soil, it can indicate the nature of machinery operating in, for example, an underground facility. Another application concerns beacons using very low frequency electromagnetic waves. Finally, there are a number of applications of interest to the Intelligence Community.

Progress

Our goals in this first year of the project (FY16) are to quantify the performance of our existing atomic magnetometer as an antenna, and then build a new magnetometer dedicated to this project and optimized for it. This will be followed by first steps towards the next project goal, which is demonstrating reception of signals that we broadcast and then characterizing the performance of the magnetometer antenna with these signals.

We have now significantly improved the operation of the original magnetometer. Since our goal is to produce a device that can be used by an untrained operator, we have tried to make the configuration and readout of the magnetometer as automated as possible. For example, noise in the magnetometer output is greatly reduced by taking the difference in the intensities of two laser beams passing through the magnetometer cell in such a way that the signal is doubled while the noise is reduced. Previously this required a manual adjustment with a screwdriver of a potentiometer. We have now successfully replaced that electronic component with a digital version that can be controlled by the small computer that runs the magnetometer. This advance both improves the performance of the device (because the noise cancellation can be continuously adjusted) and makes it much easier to operate. We have also investigated

alternative methods for heating the glass cell containing the atomic vapor that is the heart of the magnetometer. In the current device the cell is heated by absorption of light from a laser, delivered to the cell by optical fiber. While this scheme is free of electrical interference, it is complicated and we have found that it also causes undesirable signal drifts. Accordingly we have investigated heating the cell with electric current passed through a resistive heater. It appears that this can work well as long as the heater is driven with an alternating current at a frequency far from any frequencies of interest.

In the remainder of FY16, we expect to complete construction on the new magnetometer optimized for operation as an antenna and incorporating these improvements. We also expect to perform initial tests of the device's performance as a receiver outside of the laboratory.

Future Work

The broad goal of the project is to apply our atomic magnetometer antenna to two different tasks in the ULF/ELF frequency range: (1) reception of signals transmitted by us, and (2) diagnosis of signals emitted by a remote source. In FY17 we will complete work on the the first task, extending our use of a continuous sine wave to measure the device's signal-to-noise ratio and reception range. We will transmit a digital data stream (e.g. voice or a message) encoded using an appropriate modulation scheme. For the second task, we expect in FY17 to study the spectrum of the magnetic field emanating from a power line supplying rotating machinery, expecting to see characteristic spectral features. We will at the same time investigate techniques for mitigating the effects of ambient magnetic field noise that might interfere with such measurements in a field environment.

Conclusion

The overall technical goal is to show that newly-developed atomic magnetometer technology can realize low-frequency receiving antennas with an unprecedented combination of high sensitivity and compact size. Unclassified applications of these devices include (1) communication underground, through buildings, and under water, (2) receiving signals from low frequency beacons, and (3) remotely diagnosing machinery operating in an underground facility.

Publications

Savukov, I. M., and M. G. Boshier. A high-sensitivity tunable two-beam fiber-coupled high-density magnetometer with laser heating. 2016. Sensors. 16: 1691.

Accumulator for Low-Energy Laser-Cooled Particles

Kevin M. Mertes
20160584ER

Introduction

Our project will form a rare bridge between the two disciplines of high-energy physics (HEP) and low-energy physics (LEP), and their separation by a factor of over one-quadrillion (one-million billion) in the energy of their respective particles. To do this, we will adapt the physics of gathering high-energy particles to the particular circumstance of collecting low-energy particles. In HEP, these "accumulators" are indispensable to the point where many experiments would be inconceivable without them. When extended to low-energy particles in the course of our project, LEP accumulators will open new experimental avenues and eventually be held in the same regard as an essential device. Accumulators, in general, catch and overlap batches of particles into dense packets. In HEP, they are found in storage rings and also synchrotrons in the injection phase. A special rule of physics, however, applies to accumulators and says that the density of the collected packet cannot grow by simple additions of the same particles, as one would add marbles to a box. In the case of HEP accumulators, the "trick" around this rule is to inject particles in one charge state while storing the particles in another, converting between the two within the accumulator. The proton storage ring at Los Alamos National Laboratory, for example, injects into the ring H- atoms—protons cloaked in two electrons that are stripped off following injection. In the context of low-energy particles, particularly laser-cooled neutral atoms and molecules, we will exploit the ability to change not a charge state but a particle's quantum state to make an accumulator. The physical scale of LEP accumulators, whether fashioned into traps or racetracks, would be a diminutive several millimeters compared with their HEP relatives yet would similarly enable a range of basic and applied science that cannot be undertaken in their absence.

Benefit to National Security Missions

New life and ideas are often breathed into scientific fields by uncommon interdisciplinary unions. In our case, we draw on the vast experience of high-energy physics (HEP) to help the field of low-energy physics (LEP) reach unmet goals and desiderata through practical and technically-elegant means. Our successful demonstration of an accumulator for laser-cooled particles would show this technical union to be powerful and would signal those in the field of LEP to consider the application of other extensible concepts from HEP. Accumulators themselves will enhance or create scientific topics that need dense collections of numerous ultracold particles to elicit particular quantum-mechanical phenomena. The foreseen topics would, at first, be academic and include those consistent with Office-of-Science objectives. For example, the dense ensembles that are uniquely possible by accumulators could help the Division of Materials Science and Engineering explore their recent question of how "cold atom research can provide insight into the open questions of [...] condensed-matter systems". The accumulator medium could similarly serve the basic-research objectives declared by the Air Force Office of Scientific Research (AFOSR) in topics concerning ultracold atoms and molecules. With greater familiarity and adoption, accumulators could provide a foundation for applications of ultracold matter in navigation, precision measurement, remote sensing, and chemical detection that are ultimately sought by the AFOSR, the DOE, and other agencies.

Progress

This past year I have completed the design and fabrication of the effusive oven Lithium source. Calculations indicate the source will last several years without need for replenishment. The oven is temperature controlled via a custom built external, two zone, proportional, integral, derivative (PID) controller that governs the high power needed for the oven. The temperature sensor has been integrated directly into the design of the oven.

I have also designed and built an atomic beam collimator. The collimator consists of a hexagonal close packed triangular array of 528 micro-capillary tubes. Each tube is 200 micrometers in diameter and 7 mm long. The micro-capillary tube array is housed in a con-flat flange. The flange is heated to 600 C using the second zone of the PID heater/controller, to prevent the lithium clogging the micro-capillary tubes.

The oven/collimator assembly is attached to a Zeeman slower. The Zeeman slower is a device used to slow the "hot" lithium atoms traveling approximately 500 m/s down to about 30 m/s. The slower consists of a series of magnetic coils arranged along a common axis. In addition, a resonant laser beam is directed along and opposing the direction of the collimated atoms. As lithium atoms travel down the slower, the magnetic field places the atoms in resonance with the laser beam. This light imparts retarding force that slows the atoms. As the atoms slow, the increasing magnetic field of the Zeeman slower keeps the atoms in resonance with the magnetic field. This keeps the atoms in resonance during the entire time in the slower which maximizes the deceleration of the atoms. The slower I am using was inherited from a previous experiment. Unfortunately, it was in need of repair. Three (out of ten) of the current sources failed, and have since been replaced. The magnetic field inside the slower has been carefully measured. This is needed determine the currents needed for each coil in order to maximize the retarding force. I wrote software needed to optimize the magnetic field profile.

I am currently in the process of designing the bending magnetic quadrupole system. After the atoms leave the slower, they need to be directed off the resonant laser beam (otherwise, the laser beam will interfere with the operation of the accumulator). I am also in the process of setting up the optics to measure the phase space density of the lithium atoms just after the collimator and and just after the Zeeman slower. This work is on track and should be completed on time to meet the first milestone described in the proposal.

Future Work

Our main goals over the three-year program are to (1) introduce the accumulator concept and (2) demonstrate its practicality and effectiveness for laser-cooled atoms (and laser-cooled molecules by extension). The two resources needed to attain these goals are a source of laser-cooled atoms and an accumulator, which we will concentrate on developing in the first year. Both resources should be built as simply as possible, for consistency with budgetary limitations but also to establish accumulators as practical devices. We have in our laboratory most, but not all, of the components for producing by a standard technique a stream of cold lithium atoms traveling at 20 meters per second, or 45 mph (were they at room temperature, these atoms would speed about at >2000 mph). By the end of the second year, we plan on completing the fine tuning of the performance of the cold-atom source and to complete construction of magnetic trap and begin measurements of the accumulator's performance.

Conclusion

Accumulators are special tools of high-energy physics (HEP) that catch and overlap batches of particles into dense packets. Accumulator principles, however, are not exclusive to HEP and may be formed for the decidedly low-energy particles of laser-cooled atoms and molecules, as indicated by our calculations. We propose to build an accumulator for cold atoms and demonstrate its capacity for gathering more cold particles than possible by conventional means and concentrating them to very high densities. With greater familiarity and adoption, accumulators could provide a foundation for applications of ultracold matter in navigation, precision measurement, remote sensing, and chemical detection.

Time Resolved Phonon Spectroscopy for Cryogenic Bolometer Readout

John J. Goett III
20140200ER

Abstract

Cryogenic detectors have matured to technological readiness suitable to challenge long-established spectroscopy technologies such as semiconductor radiation detectors, and high-resolution scintillation counters. Time-Resolved Phonon Spectroscopy addressed the first stage in an ambitious research program to close the development gap between our understanding of radiation sensitive cryogenic materials, and applying that understanding to the development of high-resolution, high-bandwidth cryogenic detectors optimized for spectroscopic applications where particle identification capabilities are critical. By applying the theory behind standard techniques from the materials research community (i.e. resonant-ultrasound spectroscopy), we endeavored to produce position sensitive detectors by leveraging the variation in time-of-flight for excitations produced in a crystal lattice by ionizing radiation that passes through it. We produced the tools to study these interactions via detailed Monte Carlo simulation, and applied the results to the design of a prototype radiation detector that has been fabricated and is awaiting deployment in a working cryostat.

Background and Research Objectives

The ability of researchers to discriminate between different types of radiation signatures in a spectroscopic region of interest has been of paramount importance in searches for beyond standard model physics as well as applied fields like actinide science and nuclear forensics. The demand for improvement in these techniques has never been higher. With the requirements for next generation neutrino mass and dark matter searches becoming ever more stringent [1], and assay techniques pioneered by the forensics community not yet satisfying the uncertainty standards to make their findings permissible in a court of law [2], we must continue to innovate to separate the signal from the noise. Unfortunately, it is apparent that innovation on traditional ionization technologies has stagnated as most flagship research programs have switched focus to reducing environmental backgrounds from the natural uranium and thorium decay chains via expensive and time consuming radiopurity programs rather than investing in new detector concepts and methods of optimization.

Over the past 20 years, cryogenic bolometer detectors have evolved to feature unmatched energy resolution, dynamic range, and efficiency, making them ideal complements to traditional ionization detectors optimized for beta or gamma spectroscopy. This becomes more evident as precision measurement campaigns, from XFEL spectrophotometers to astronomical surveys integrate these sensors into their research and development programs. Because the typical carrier energy for a thermal detector is on the order of meV (phonons) as opposed to the few eV (electrons/holes) typical of semiconductor detectors, the number of carriers is substantially higher and their statistical variation smaller for a signal of a given size. The Fano limit and theoretical uncertainty limit is much improved for these devices. Nevertheless, most techniques have settled on resolving changes in material temperature alone, and have not leveraged the mature understanding of energy transport in these systems to attempt the development of time-resolved or tracking detector technologies. Our team is pioneering the design of a novel type of bolometer readout that exploits the facts of anisotropic energy transport mediated via ballistic phonon modes in the absorbing material. We hypothesized the extreme variations in velocity between these modes can be used to reconstruct particle trajectories and vertex information much as one might triangulate the position of a radio-transmitter in space.

Scientific Approach and Accomplishments

We have developed the tools to model this new concept for high-speed bolometers and to determine the optimal crystal dimensions, lattice orientations, and timing requirements to reconstruct particle trajectories and vertex locations; the first ingredients in any particle iden-

tification analysis. First, a material specific parameterized model for phonon propagation in crystals was developed from fundamental theory and constants published in the literature. An example of the slowness surfaces extracted from this code is seen in Figure 1. Using the Geant4 framework for the tracking of particles through matter [3], extended by our software models, we can now generate and track phonons in the crystal lattice for ionizing radiation in crystals relevant to rare-event searches such as TeO2, Ge, diamond and AlO3. Examples of phonon intensities arriving at the crystal surface up to 20 microseconds after a particle interaction are visible in Figure 2. Using this code, we simulated event topologies of interest to the double-beta-decay and dark matter search communities to interrogate the phonon time-of-flight from the point of energy deposit to the location of a thin film bolometer deposited on each of the surfaces of the crystal. A simulated waveform on each face is seen in Figure 3. From the simulated data, we determined that with proper choice in lattice orientation, it is possible to reconstruct a remarkably linear calibration curve relating the time difference in phonon arrival to the position along the axis orthogonal to the two faces. An example of such a curve in TeO2 is visible in Figure 4.

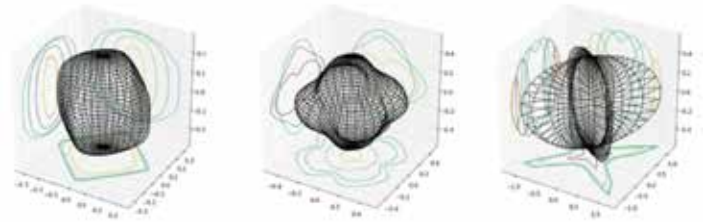

Figure 1. The surfaces of constant frequency in momentum space, and their projections into the <110>, <1-10> and <001> planes in 2 for the (Right) longitudinal, (Middle) fast transverse, (Left) slow transverse phonon as determined by our code. The amplitude of the surface at each point is inversely proportional to the speed of the thermal shock in that direction from the point of origin.

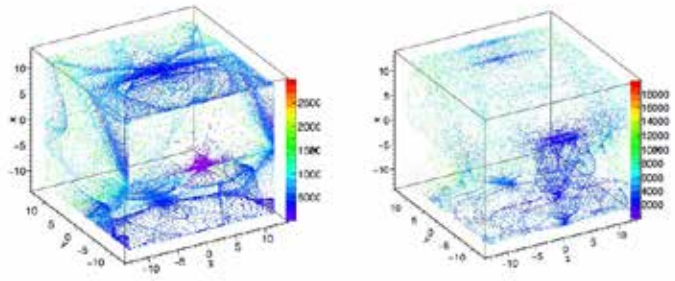

Figure 2. The phonon intensity patterns generated on the surface of mm^3 crystal 18 microseconds after an energy deposition where the primary particle is (Right) an alpha particle generated on the surface, and (Left) a multiple scatter gamma moving through the crystal.

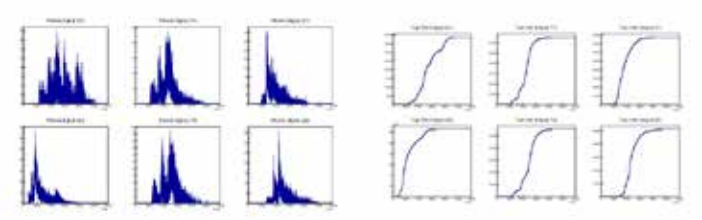

Figure 3. (Right) Simulated waveform corresponding to digitized phonon signal, and (Left) trapezoidal filter output, used to resolve the shock front arrival time for vertex calibration data.

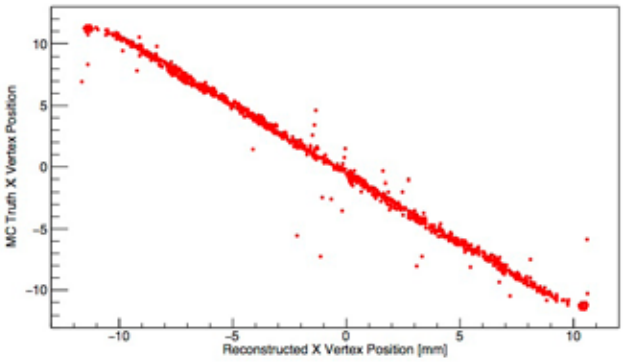

Figure 4. An example of the remarkably linear calibration recovered between the phonon time of flight and the monte-carlo "true" vertex position between the +X and -X faces of a TeO2 crystal.

Preliminary findings show that the timing resolutions necessary to use these effects for particle identification are readily achievable with commercially available, off-the-shelf electronic components below 20 MHz. However, most of the materials of interest for these applications are not standard for use in the semiconductor industry. Reaching out to our colleagues at the National Institute of Standards, Boulder, we were able to adapt an AlMn thin film deposition technique developed for their superconducting transition-edge sensor based polarimeter efforts to produce test samples on Si substrates. [4] Though no photolithography facilities were available here at LANL to test the procedure, we did produce a number of samples via electron-beam vaporization of the AlMn sample. Transitions were seen, but we could not obtain enough time in a working cryostat to fully develop this process.

Many of the most critical elements of a prototype detector have been completed, including cutting crystals orientation, polishing surfaces in preparation for thin film lithography and building and commissioning a high speed SQUID based data acquisition system. A detector array has been fabricated on a cheap, and easily obtained surrogate material (semiconductor grade Si wafers) and assembled for test, (see Figure 5) and is awaiting an open position in a working cryostat to provide a data set to compare to

simulation results. We are currently exploring collaborations with other institutions in order to test a hardware prototype.

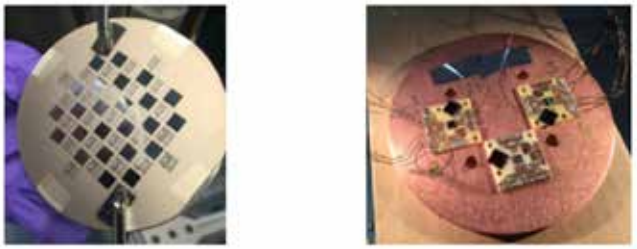

Figure 5. Right) An example of some AlMn thin film devices developed here at LANL using an adaptation of the NIST process, and Left) diced AlMn sensors connected to SQUID devices, ready for testing in a cryostat.

Impact on National Missions

Our simulation results indicate that with adequate timing resolution, we will have the capability to discriminate against alpha, beta and gamma depositions in bulk crystals, a valuable prospect for the development of non-destructive assay techniques on intercepted materials as well as the improvement of uncertainties on key branching ratio measurements needed by the forensics community.

References

1. Abgrall, , I. J. Arnquist, F. T. Avignone III, H. O. Back, A. S. Barabash, F. E. Bertrand, Boswell, A. W. Bradley, Brudanin, Busch, Buuck, Byram, A. S. Caldwell, Y. -. Chan, C. D. Christofferson, P. -. Chu, Cuesta, J. A. Detwiler, J. A. Dunmore, Y. u. Efremenko, Ejiri, S. R. Elliott, Finnerty, Galindo-Uribarri, V. M. Gehman, Gilliss, G. K. Giovanetti, Goett, M. P. Green, Gruszko, I. S. Guinn, V. E. Guiseppe, Henning, E. W. Hoppe, Howard, M. A. Howe, B. R. Jasinski, R. A. Johnson, K. J. Keeter, M. F. Kidd, Kochetov, S. I. Konovalov, R. T. Kouzes, B. D. LaFerriere, Leon, J. C. Loach, MacMullin, MacMullin, R. D. Martin, Massarczyk, Meijer, Mertens, M. L. Miller, J. L. Orrell, O'Shaughnessy, N. R. Overman, A. W. P. Poon, Pushkin, D. C. Radford, Rager, Rielage, R. G. H. Robertson, Romero-Romero, M. C. Ronquest, A. G. Schubert, Shanks, Shirchenko, K. J. Snavely, Snyder, Steele, A. M. Suriano, Tedeschi, J. E. Trimble, R. L. Varner, Vasilyev, Vetter, Vorren, B. R. White, J. F. Wilkerson, Wiseman, Xu, Yakushev, C. -. Yu, Yumatov, and Zhitnikov. The MAJORANA DEMONSTRATOR radioassay program. 2016. NUCLEAR INSTRUMENTS & METHODS IN PHYSICS RESEARCH SECTION A-ACCELERATORS SPECTROMETERS DETECTORS AND ASSOCIATED EQUIPMENT. 828: 22.

2. Pomme, , S. M. Jerome, and Venchiarutti. Uncertainty propagation in nuclear forensics. 2014. APPLIED RADIATION AND ISOTOPES. 89: 58.

3. Allison, J., K. Amako, J. Apostolakis, H. Araujo, P. A. Dubois, M. Asai, G. Barrand, R. Capra, S. Chauvie, R. Chytracek, G. A. P. Cirrone, G. Cooperman, G. Cosmo, G. Cuttone, G. G. Daquino, M. Donszelmann, M. Dressel, G. Folger, F. Foppiano, J. Generowicz, V. Grichine, S. Guatelli, P. Gumplinger, A. Heikkinen, I. Hrivnacova, A. Howard, S. Incerti, V. Ivanchenko, T. Johnson, F. Jones, T. Koi, R. Kokoulin, M. Kossov, H. Kurashige, V. Lara, S. Larsson, F. Lei, O. Link, F. Longo, M. Maire, A. Mantero, B. Mascialino, I. McLaren, P. M. Lorenzo, K. Minamimoto, K. Murakami, P. Nieminen, L. Pandola, S. Parlati, L. Peralta, J. Perl, A. Pfeiffer, M. G. Pia, A. Ribon, P. Rodrigues, G. Russo, S. Sadilov, G. Santin, T. Sasaki, D. Smith, N. Starkov, S. Tanaka, E. Tcherniaev, B. Tome, A. Trindade, P. Truscott, L. Urban, M. Verderi, A. Walkden, J. P. Wellisch, D. C. Williams, D. Wright, and H. Yoshida. Geant4 developments and applications. 2006. IEEE TRANSACTIONS ON NUCLEAR SCIENCE. 53 (1): 270.

4. Schmidt, D. R., H. -. Cho, Hubmayr, Lowell, M. D. Niemack, G. C. O'Neil, J. N. Ullom, K. W. Yoon, K. D. Irwin, W. L. Holzapfel, Lueker, E. M. George, and Shirokoff. Al-Mn Transition Edge Sensors for Cosmic Microwave Background Polarimeters. 2011. IEEE TRANSACTIONS ON APPLIED SUPERCONDUCTIVITY. 21 (3): 196.

Publications

Goett, J., B. Zhu, A. N. Matlashov, J. Ullom, D. Schmidt, and S. R. Elliott. Phonon time of tlight as a tackground mitigation strategy in rare physics searches. 2016. In review for submission to Nuclear Instruments and Methods Section A.

Measuring Winds in the Stratosphere Using Passive Acoustic Sensors

Omar E. Marcillo
20140237ER

Abstract

The objective of this exploratory project was to understand the structure of infrasound acoustic noise, where infrasound refers to sound with frequency below the human threshold (below 20 Hz), and its potential use for probing stratospheric winds. We have found that background, continuous infrasound signals, in particular microbaroms generated by the interaction of the ocean-atmosphere, are comprised not of a single wave-front, but of a superposition of multiple co-incident wave-fronts produced by multiple sources at different locations in space and time and with different life spans. We found through our theoretical work that in order to recover the parameters necessary to perform an atmospheric inversion using microbaroms, it is necessary first to resolve the fine structure in the signal and identify propagation times between locations along consistent propagation paths. We developed a methodology that is able to resolve the fine structure of microbaroms and identify the spatial location of different coexisting sources. This result is fundamental as we are able now to distinguish, characterize, and track sources of microbaroms, often associated with disturbances in the ocean surface, in space and time. Using the global network of infrasound stations we are generating maps of ocean disturbances that have the potential to be used to validate ocean dynamics models and extend research in the ocean-atmosphere interactions.

Background and Research Objectives

The principal component of the acoustic background noise in the infrasonic band (<20Hz) is the microbarom signal. Microbaroms are generated by the interaction of ocean surface waves with the atmosphere. Microbaroms have the potential for long-distances propagation due to the intrinsic low-level of absorption and dispersion of infrasound in the atmosphere. The ozone layer, with a vertical profile between 10-50 km, can provide wind and thermal conditions for the formation of acoustic waveguides that can support propagation of microbaroms to global distances (1000s of km). Because microbaroms propagate in such waveguides, there is active interest in the infrasound community to use microbarom signals to probe the atmospheric conditions of the stratosphere or ozone layer (see for example the Atmospheric dynamics Research InfraStructure in Europe, ARISE Project, http://arise-project.eu).

The objective of this project was to test the feasibility of using continuous infrasonic noise measured at multiple locations on the ground and extract specific parameters from its propagation that contain information about the waveguide produced by the stratospheric winds. In a pilot study we have already demonstrated that an inversion methodology can estimate winds in the stratosphere using transient sources.

Following these results we have identified a fundamental opportunity: to further develop and apply this inversion methodology to the continuous and ubiquitous acoustic background noise would allow us to measure the evolution of stratospheric winds everywhere without the need of an active source. To migrate from a transient to a continuous source for the inversion, we identified three specific research objectives: (1) to refine our data analysis methodology to analyze the much smaller and continuous microbaroms and to identify its coherency at long-distances, (2) to design an experiment to test and formally quantify the uncertainty of our measurements and predicted wind values to validate our inversion results using an independent technique, and (3) to develop and validate a stochastic method based on inverting low frequency acoustic signals from microbaroms, recorded on multiple ground sensors, to continuously track wind in the stratosphere. We will validate our technique by co- locating a specially designed infrasound network with the only LIDAR system capable of reliably recovering wind and temperature from the stratosphere and mesosphere, which is located in Northern Norway.

Scientific Approach and Accomplishments

We 1) developed a theoretical framework to establish the inversion method and to test the sensitivity of its parameters, and 2) designed an experiment to measure the coherency of microbaroms at large distances. The theoretical work led to the development of a general optimized inversion framework for the inversion of the state of the atmosphere using acoustic tomography methods [1]. This framework is very flexible in that it can be extended to other regions of the atmosphere. In particular, this framework can be applied to the troposphere to study the dynamics of the atmospheric boundary layer (up to 1 km above surface) as well as the thermosphere to study the winds associated with the atmospheric tides.

To test the variation in coherency of microbaroms with distance, which was our second main objective, we first designed a linear network and deployed a prototype in central New Mexico. This prototype was designed to provide proof of concept for the analysis algorithms and network operation. We deployed and tested the design, and completed the analysis of the data of this first network. With the data recorded for this prototype, we were able to identify and model infrasound produced by nearby wind farms in Albuquerque, NM. We found that these infrasound signals could propagate up to 90 km and, by modeling its propagation, identify it as energy trapped in the near-ground atmospheric boundary layer (Figure 1).

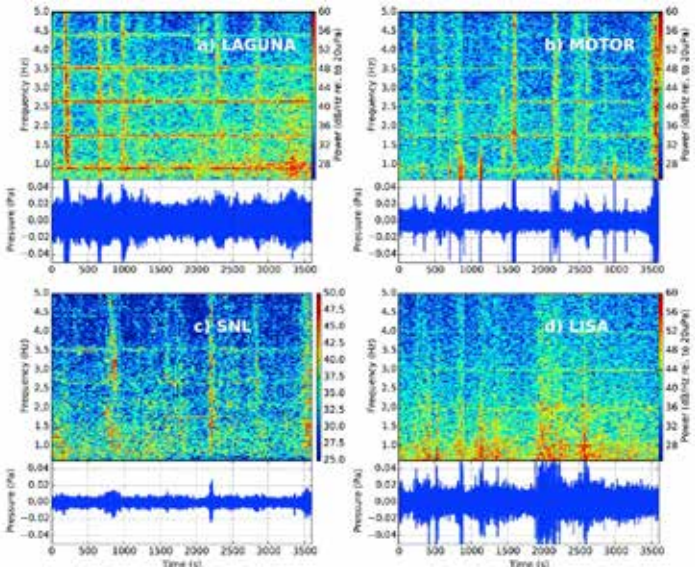

Figure 1. Example of waveforms and spectrograms from the LANL NM Microbarom prototype network. These infrasound waveforms were filtered between 0.6 and 10 Hz with a four-pole zero-phase filter. The spectrograms were constructed with 60 s windows with 50% overlap. (a–c) 4 February 2014 at 04:00 UTC. These spectrograms show energy peaks at a frequency slightly below 0.9 Hz and its harmonics. These energy peaks come from a nearby Wind Farm and can be seen up to station SNL located 90 km East of the wind farm.

This was the first observation of wind farm sound at such large distances. We have written a scientific article now published at the Journal of Geophysical Research Atmospheres on the analysis of this source and its potential to retrieve boundary layer and tropospheric winds and temperature [2]. This result has very important implications for near-surface atmospheric interactions and boundary layer physics.

With the results of the design of our New Mexico prototype, we deployed a second linear array in Northern Norway. Norway was selected for its potential high microbarom activity and the presence of the Alomar Observatory that operates a LIDAR capable of direct measurements of wind in the stratosphere. The LANL NORwegian StratosphErE (NORSE) experiment operated in northern Norway from April 2015 to May 2016 (Figure 2).

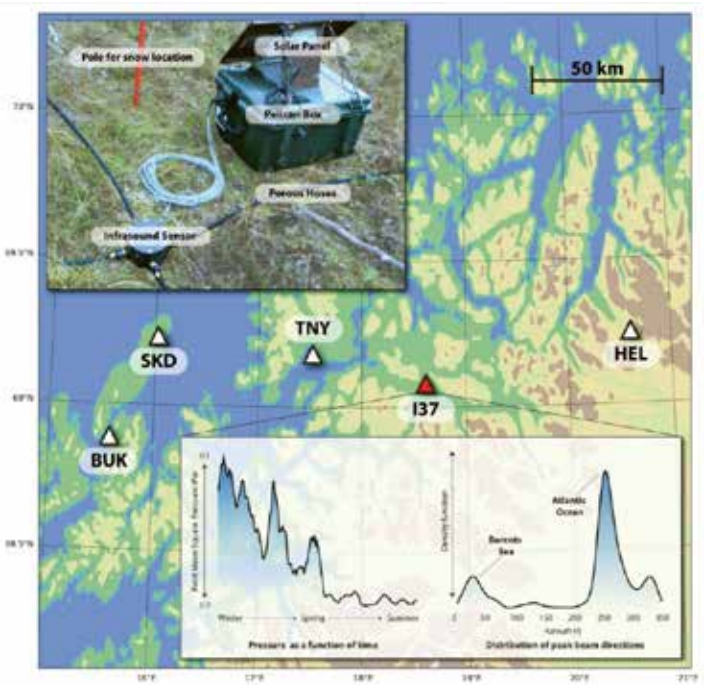

Figure 2. The Norwegian Stratosphere (NORSE) experiment involves the installation of four arrays near the Arctic Lidar Observatory for Middle Atmosphere Research (ALOMAR) and the International Monitoring System (IMS) I37 infrasound array in Norway. The top inset shows a typical station setup. The bottom inset shows microbarom pressure at I37 is strongest during the winter months. Microbarom beam directions from separate sources in the North Atlantic and Barents Sea are prominent peaks in the bearings along the horizontal axis in the graph at right.

This successful deployment involved great logistical efforts from Los Alamos National Laboratory and the Alomar Observatory to install and maintain four infrasound arrays for 12 months in a very harsh environment. Using data obtained during the initial phase of the Norway deployment (2 weeks in November, 2014), we published a paper to the

EOS Transactions AGU Journal focusing on the deployment of the network and its potential for atmospheric studies: "The NORwegian StratospherE (NORSE) experiment: Turning Low-Frequency Coherent Acoustic Noise into Signal" [3]. This article has helped us publicize our efforts so that other institutions (e.g.: NORSAR, the Norwegian seismic center) are aware of our network design and results. Also, using the data from the initial phase of the Norway deployment we were able to identify and study acoustic signals generated by a sounding rocket launched from the Andøya Space Center that is located in close proximity to one of our network nodes. We studied the observed infrasound, modeled its propagation, and submitted a scientific article published at the Journal of Acoustical Society of America Express Letters. The article highlights the potential and implications of obtaining information from rockets (e.g.: trajectory, number of stages and engine characteristics) using acoustic observations as well as some analysis of the efficiency of the aeroacoustic source mechanism of the rocket as it enters the rarefied upper atmosphere: "Analysis and modeling of infrasound from a four-stage rocket launch" [4]. Figure 3 shows results of our processing of the infrasound arrays along with propagation modeling results.

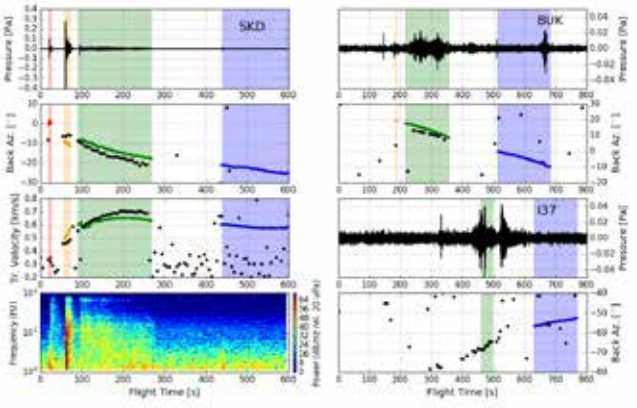

Figure 3. Results of analysis for the infrasonic signals generated by the rocket launch as observed at the NORSE arrays (SKD, BUK, and IMS I37NO). The observed back azimuth and trace velocities (black) are compared with those predicted using eigenray analysis along the rocket trajectory as provided by the GPS tracking that are color-coded for the different stages, i.e, red (first), orange (second), green (third), and blue (forth). The color patches show the time when each stage is active.

In studying the data from the NORSE network, we found no coherency of microbaroms beyond 40 km. We found that our initial observations of coherency of microbarom up to 30 km were related to energy trapped in the troposphere (the lowest 10 km of the atmosphere). Another research group has observed similar coherency for microbarom signals in a tropospheric waveguide at distance of up to 40 km [5]. This low coherency for microbaroms could be related to the complicated nature of the signal as a superposition of multiple co-existing wave-fronts linked to sources located at different locations in space and time and with different life spans rather than single wave-front. These co-existing sources generate microbaroms that arrived at the sensor array with different inclination angles and very similar frequency peaks. We analyzed the signal from the NORSE network and look for frequency characteristics that may be related to different sources but found not evidence of such source specific signatures in the waveforms. A potential direction in further research can be to extend the work of Koper and Burlacu [3] and look for frequency signatures of different sources in long-term records.

We found through our theoretical work that in order to recover the parameters necessary to perform an atmospheric inversion using microbaroms, it is necessary to resolve the fine structure in the signal in order to identify propagation times along unique paths. Thus, we developed a methodology based on a sophisticated array-processing algorithm that is able to resolve the fine structure of microbaroms and identify the spatial location of different coexisting sources even if they are closely separated in space [6]. This methodology is based on the Multiple Signal Classification (MUSIC) algorithm developed by Schmidt [7]. We applied this array processing methodology to the NORSE arrays as well as several stations that are part of the International Monitoring System (IMS) operated by the Comprehensive Test Ban Treaty Organization (CTBTO). Specifically, I37NO in Norway, I18DK in Greenland, I26DE in Germany, and I42PT in the Azores Island were studied and it was found that we are able to identify both persistent and short-lived microbarom sources related to the ocean surface disturbances. This result is important as it demonstrates that we are able to simultaneously distinguish, characterize, and track sources of microbaroms in space and time with high precision. Using the global network of infrasound stations we are generating maps of ocean disturbances that have the potential to be used to validate ocean dynamics models and extend our research in the ocean-atmosphere interactions. Figures 4 and 5 show examples of the back-azimuth (related to the angular location of sources) of our enhanced data analysis applied to background noise. Figure 4 shows histograms of back-azimuth for a three-week period comparing a classic beam-former assuming one source (Panel b) along with our implementation of the MUSIC algorithm assuming three sources (Panel a). The background in the figure is color-coded with the wave height from surface waves ocean models, from Ardhuin and Herbers [8]. Note our histograms are able to separate different sources that are seen as one single source when using the classical Bartlett

beam. Figure 5 shows short-term (6 hours) histograms of back-azimuths. Note again that the algorithm is able to resolve multiple sources as compared to the classical approach. The different panels show different ocean surface parameters: wave height (a and b), wave-wave interaction (c), and peak-frequency of wave interaction (d). As microbaroms are generated by a variety of source conditions (e.g.: near the center of ocean storms, due to the interaction of storm swell and the background wave field, and costal reflections), their source locations are often related to ocean dynamics.

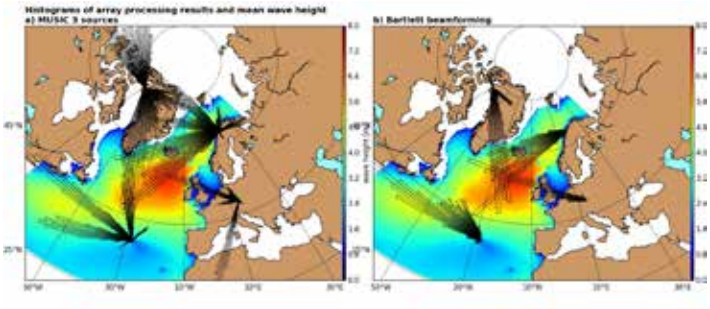

Figure 4. Back-azimuth histograms for IMS stations: I37NO, I18DK, I26DE, and I42PT for MUSIC and Bartlett algorithms, panels a and b, respectively.

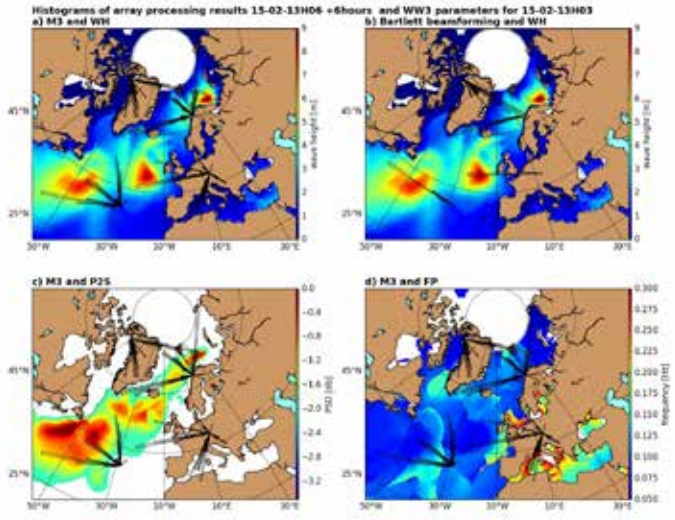

Figure 5. Results of array processing using the MUSIC (Panels a,c,d) and Bartlett (Panel b) algorithms algorithm for IMS stations for 6 hours continuous data. The backgrounds are color-coded with wave height (WH, Panels a and b), and wave-wave interaction coefficient (fp2s)

Impact on National Missions

Our enhanced methodology to study background noise allows characterizing and tracking small ocean disturbances that has the potential for research of the interactions of ocean- atmosphere interactions. This has implications to climate change research as severe ocean weather systems can be remotely tracked and some source characteristics extracted. We are working on disseminating our results with Earth System and Ocean scientists within LANL to find a direct application of our results for validation of Ocean Models. We are in conversations with staff members of the Climate, Ocean, and Sea Ice Modeling (COSIM) project to find venues to provide feedback to the modeling efforts.

We have developed a methodology to resolve the finer noise structure of microbaroms (background acoustic noise), this methodology can provide us with enhanced capabilities to analyze infrasound data and developed improved background noise models for infrasound. We can also extend the methodology to analyze seismic data and couple both phenomenologies. This capability has important implications for Global Security (LANL POC Dale Anderson, EES-17) as they can be used to reduce false alarm rates for geophysical monitoring of chemical and nuclear explosion. We are also disseminating our results and capabilities to Dean Clauter, the Point of Contact for infrasound research at the Air Force Technical Application Center (AFTAC), which is the US National Data Center (US-NDC) for CTBT–IMS data.

Although the optimized parameterization framework developed in this project is not easily applicable to continuous, background infrasonic signals, it is immediately usable for transient signals and provides a significant improvement in methodologies for estimating corrections to atmospheric winds via infrasonic tomography. Optimizing the parameterization to minimize the complexity of the perturbation model improves the computational efficiency of tomography algorithms, reduces the uncertainty in the estimated atmosphere state obtained using infrasound, and makes simultaneous estimation of a source localization and atmosphere state more feasible. This improved knowledge of the atmosphere state is crucial in further analysis and interpretation of transient infrasonic signals and is therefore applicable in detonation detection and similar areas of R&D.

Lastly, the data we collected from the NORSE network is an ideal dataset to test detection algorithms and study infrasonic signals produced by rocket motors and fast moving vehicles. We demonstrated that infrasound could be used to retrieve characteristics of the design and operation of rockets remotely, but a significant amount of additional analysis could be conducted using this dataset.

References

1. Blom, P., and O. Marcillo. An Optimal Parameterization Framework for Infrasonic Tomography of the Stratospheric Winds Using Non-Local Sources. To appear in

Geophysical Journal International.

2. Marcillo, , Arrowsmith, Blom, and Jones. On infrasound generated by wind farms and its propagation in low-altitude tropospheric waveguides. 2015. JOURNAL OF GEOPHYSICAL RESEARCH-ATMOSPHERES. 120 (19).

3. Arrowsmith, M., S. Arrowsmith , and O. Marcillo . The NORwegian StratospherE (NORSE) experiment: Turning Low-Frequency Coherent Acoustic Noise into Signal. 2016. EOS Transactions AGU. 97: 1.

4. Blom, , Marcillo, and Arrowsmith. Analysis and modeling of infrasound from a four-stage rocket launch. 2016. JOURNAL OF THE ACOUSTICAL SOCIETY OF AMERICA. 139 (6): 3134.

5. Fricke, J. T., L. G. Evers, P. S. M. Smets, Wapenaar, and D. G. Simons. Infrasonic interferometry applied to microbaroms observed at the Large Aperture Infrasound Array in the Netherlands. 2014. JOURNAL OF GEOPHYSICAL RESEARCH-ATMOSPHERES. 119 (16): 9654.

6. Marcillo, O., G. Euler, and P. Blom. Resolving the fine structure of microbaroms. Geophysical Research Letters.

7. SCHMIDT, R. O.. MULTIPLE EMITTER LOCATION AND SIGNAL PARAMETER-ESTIMATION. 1986. IEEE TRANSACTIONS ON ANTENNAS AND PROPAGATION. 34 (3): 276.

8. Ardhuin, , and T. H. C. Herbers. Noise generation in the solid Earth, oceans and atmosphere, from nonlinear interacting surface gravity waves in finite depth. 2013. JOURNAL OF FLUID MECHANICS. 716: 316.

Publications

Arrowsmith, M., S. Arrowsmith , and O. Marcillo . The NORwegian StratospherE (NORSE) experiment: Turning Low-Frequency Coherent Acoustic Noise into Signal. 2016. EOS Transactions AGU. 97: 1.

Blom, P., O. Marcillo, and S. Arrowsmith. Analysis and modeling of infrasound from a four-stage rocket launch. 2016. Journal of acoustical society of America Express Letters. 139 (6): 3134.

Blom, P., and O. Marcillo. An Optimal Parameterization Framework for Infrasonic Tomography of the Stratospheric Winds Using Non-Local Sources. To appear in Geophysical Journal International.

Marcillo, O., G. Euler, and P. Blom. Resolving the fine structure of microbaroms. Geophysical Research Letters.

Marcillo, O., S. Arrowsmith, P. Blom, and K. Jones . On infrasound generated by wind farms and its propagation in low-altitude tropospheric waveguides. 2015. Journal of Geophysical Research: Atmospheres. : 1.

Matter Wave Circuits

Changhyun Ryu
20140362ER

Abstract

The goal of this project was to create the de Broglie wave analog of an integrated optical circuit, a device that might be called a matter wave circuit. In this technology, coherent atomic matter waves from an integrated source are guided and manipulated in confining potentials in much the same way that laser light propagation is controlled in a wave-guide photonic circuit. The push to develop matter wave circuits is motivated by several important differences between matter waves and light waves: atomic velocities can be controlled over a wide range; atoms can be brought to rest and trapped; atoms feel gravity and electromagnetic fields; atoms can interact strongly with each other; and atoms can be imaged with high efficiency. These characteristics enable matter wave circuit applications in sensing (particularly interferometry) as well as in quantum information processing, quantum atom optics, and emulation of transport problems in condensed matter systems.

Through this project we successfully realized the first matter wave circuit with several key matter circuit elements: a straight line, a circular bend, and a Y-junction. By combining a line and a bend, we demonstrated coherent transport of matter waves in a closed stadium waveguide. With the use of a Y-junction, we demonstrated a successful coherent splitting of propagating matter waves for the first time. In addition to our experimental work, we also conducted theoretical work to elucidate matter wave circuits. Our theoretical work included the study of excitations of matter wave propagation through a bend and the study of cavity physics with matter waves. As an application of this work, we demonstrated a flexible Bose-Einstein Condensate (BEC) atom interferometer with matter wave circuits. Based on this success, we will pursue the further development of quantum inertial sensor with matter wave circuits.

Background and Research Objectives

Research aimed towards creating matter wave circuits began in earnest not long after the 1995 demonstration of BEC in alkali vapors provided a coherent source for atom optics. Almost all of the initial experimental work in this direction focused on “atom chips”, small magnetic traps and waveguides produced near microfabricated wires on a planar substrate. Trapping the atoms close (less than 1mm) to the wires generated a magnetic field that allowed for strong traps with modest currents and correspondingly low power dissipation; the integrated-circuit like architecture of the atom chip promised easy scalability to complex circuits. Atom chip research has been extremely fruitful: achievements include multi-mode waveguiding, incoherent splitting, a form of Mach-Zehnder interferometry, and splitting of static clouds. However, the original goal of demonstrating single transverse mode matter wave propagation and coherent splitting in a non-trivial geometry had not been accomplished. This appears to be connected to so far insurmountable roughness in the magnetic potential due to fabrication imperfections in the micron scale wires. Many previous attempts in creating matter wave circuits, with the main goal of attaining coherent single-mode propagation and coherent splitting, were unsuccessful [1].

The objective of the project was to confine de Broglie waves from a BEC in waveguides and manipulate them with optical elements all created using our unique “Painted Potential” capability [2]. This technique, explained in detail below, creates arbitrary and dynamic time-averaged optical dipole potentials compatible with the very low energy of a BEC. Our aim here was to carry out the basic science demonstration of the first technology for creating matter wave circuits. Applications will be a topic for later research.

Scientific Approach and Accomplishments

Guiding potentials for matter wave circuits need to have sufficiently high transverse trapping frequencies that the forward motion of matter waves launched into the

ground state of the guide is not coupled into transverse excitations by imperfections in the potential. For the same reason it is important that the potential be as smooth as possible. Our recent work has shown that our "Painted Potential" technique for creating arbitrary and dynamic BEC traps satisfies these requirements. The 87Rb BEC is trapped in a combination of red-detuned (i.e. attractive) optical dipole potentials, namely a horizontal light sheet that confines the atoms tightly in the vertical direction, and a rapidly moving tightly-focused "tweezer" beam which paints the desired potential on top of the light sheet. The atoms experience the time-averaged optical dipole potential because the tweezer beam moves much faster than the atoms can respond to the potential (for a typical time-averaged trap frequency of 500 Hz we paint the potential at a repetition rate of several kHz). Two acousto-optic modulators (AOMs) both move the tweezer beam and control its intensity. A sophisticated computer system changes the RF frequencies going into the AOMs, changing the diffraction angle and hence moving the beam in the focal plane of the lens. In this way we can create and manipulate BECs in any potential which can be drawn on a sheet of paper.

With this technique, we realized several key matter circuit elements [3]. First, a BEC was created in a short linear section and then by turning on a potential gradient, atoms were manipulated through a guide with chosen momentum. After this, several different matter wave circuit elements were turned on to demonstrate coherent propagation of matter waves. By combining a bend and a straight guide, a coherence circulation of matter waves through a stadium wave guide was demonstrated. This is an important waveguide since a propagation of matter waves through a stadium waveguide can be used as a basis for rotation sensor in the future applications. Another important milestone was the coherent splitting of matter waves through a Y-junction. By measuring relative phase of two matter waves after the split, we demonstrated coherence between them for the first time. By demonstrating these several key matter wave circuits experimentally, we achieved the main goal of this project in manipulating matter waves with flexible circuit elements. This will lead to the future research in applications in sensing.

In addition to the experimental work, we conducted theoretical studies to understand the dynamics of matter wave propagation through a bend and a straight line connection [4]. The abrupt change in the curvature creates transverse excitation in matter waves and degrades the performance of interferometer using a stadium waveguide. We discovered several ways to limit this excitation. First, the bend location can be shifted relative to the straight section to eliminate the excitation. Second, the curvature can be changed adiabatically from a straight line to a bend to eliminate excitation. The simulation of the dynamics confirmed these results; future experiments will surely use these modifications to limit excitations. Another topic we studied theoretically is the cavity physics with matter waves. Here we studied various matter wave cavity physics with varying parameters and discovered that the clean demonstration of cavity physics with matter waves can be performed with atoms without interactions.

Toward the goal of realizing a quantum sensor with matter wave circuits, we made a flexible BEC atom interferometer using matter wave circuits. In this experiment, U shape potential was used to connect three BECs. By removing a connector BEC, we could create two coherent BECs for an interferometer. The coherence time was measured to be 9ms consistent with dephasing due to number fluctuation after the split. Also by varying the depth of the trap, the relative phase was varied accordingly, demonstrating the operation as an atom interferometer. Finally, it was shown that two BECs can be moved to enclose an area to be sensitive to rotation without excitation. We simulated movement speed and showed that it is possible to create a large enclosed area rotation sensor. This demonstration shows the possibility of matter wave circuits to be used as quantum sensors.

Impact on National Missions

The atom optical technology that was developed during this project supports Laboratory missions in Sensing, and in Information Science and Technology (IS&T). The atom circuit technology is relevant to rotation sensing in Sensing; matter wave technology, in general, is relevant to quantum information processing in Information Science and Technology (IS&T) mission areas. These applications in sensing and quantum information processing are of interest to many important national security missions relevant to external sponsors in the intelligence and defense communities. The successful proof of principle demonstration of integrated atom optics will be beneficial to the future development of quantum sensor in many important national missions.

References

1. Cronin, A. D., Schmiedmayer, and D. E. Pritchard. Optics and interferometry with atoms and molecules. 2009. REVIEWS OF MODERN PHYSICS. 81 (3): 1051.

2. Henderson, , Ryu, MacCormick, and M. G. Boshier. Experimental demonstration of painting arbitrary and dynamic potentials for Bose-Einstein condensates. 2009. NEW JOURNAL OF PHYSICS. 11.

3. Ryu, , and M. G. Boshier. Integrated coherent matter

wave circuits. 2015. NEW JOURNAL OF PHYSICS. 17.

4. Campo, del, M. G. Boshier, and Saxena. Bent waveguides for matter-waves: supersymmetric potentials and reflectionless geometries. 2014. SCIENTIFIC REPORTS. 4.

5. Publications

6. Campo, A. del, M. G. Boshier, and A. Saxena. Bent waveguides for matter-waves: supersymmetric potentials and reflectionless geometries. 2014. Scientific Reports. 4: 5274.

7. Ryu, C., and M. G. Boshier. Integrated coherent matter wave circuits. 2015. New Journal of Physics. 17 (9): 092002.

Chemical Shift Signatures of Nuclear Material: 235U and 239Pu NMR Spectroscopy

Michael T. Janicke
20140396ER

Abstract

The crux of this research was the development of low frequency DNP-NMR spectroscopy as a tool for detection of U-235 and Pu-239 chemical shift signatures, monitoring the origin, fate and transport of these contaminants, and the bioavailability of such species in the environments. Much of this project focused on instrument development and quantifying the increase in sensitivity with our sights on Pu-239, possibly the easier of the two isotopes. First year results discovered that detection of the spin-½ Pu-239 signal might not be possible at room temperature. This is a result of very short relaxation times that were unknown for these paramagnetic compounds at the start of this project. With this in mind, work shifted towards other relevant elements with some success; however, experimental needs to increase sensitivity became detrimental, which will be quantified in our upcoming publication. However, several new projects (LDRD DR and a DHS program) evolved from our results that will focus on using developments from this project to use zero-field NMR methods and J-coupling spectroscopy to determine unknown chemical threats and chemical agents, as well as the possibility of using DNP-NMR as an additional screening tool for carry-on liquids with a DHS program.

Background and Research Objectives

The driving force for this project was a need for low cost, high sensitivity instruments that can be deployed to assess the speciation of plutonium species for rapid analysis and decision making. Dynamic Nuclear Polarization-Nuclear Magnetic Resonance (DNP-NMR) which results in an amplified Pu-239 NMR signal through a polarization transfer from the electron spins of unpaired electron species of (2,2,6,6-Tetramethylpiperidin-1-yl) oxyl in our case (commonly referred to as TEMPO) is one such technique that can meet this goal and can potentially be adapted for numerous applications. In the area of detecting chemical signatures, knowing the speciation rather than just the concentration will identify the provenance of the nuclear material and improve environmental risk assessments.

The classic DNP method involves cooling a sample to liquid helium temperature in the presence of a stable radical and a strong magnetic field. Under these conditions, the unpaired electrons become strongly polarized and the polarization can be transferred to nearby nuclei using microwave irradiation. The sample is rapidly thawed and conventional NMR spectrum measured with S/N increase expected of greater than 10,000 for H and measured at 44,400 for C-13, and 23,500 for N-15. For Cl-35, As-75, Hg-199, and Pb-207 the measurements would be anticipated to achieve signal enhancement greater than 100,000 based on the higher natural abundance for these elements that play a large role as groundwater contaminants. Our approach was to achieve the polarization transfer at room temperate resulting in only a modest enhancement 2 orders of magnitude lower; however, this would be a huge leap in sensitivity compared to similar systems not using DNP. Higher sensitivity means smaller samples and more dilute quantities can be analyzed.

Scientific Approach and Accomplishments

Simultaneously with the DNP-NMR studies, high field NMR studies were done to determine the location of the chemical shift (frequency) for Pu-239 in solution stable species. To date, only PuO2, a solid diamagnetic sample has had a detectable NMR signal. Unfortunately, no stable diamagnetic samples for solution NMR are available and a paramagnetic system was chosen. The paramagnetic nature of the Pu can cause (a) a shift in frequencies for the signal that might be a strong diagnostic or signature (b) broadening of the signal that can reduce the sensitivity and/or (c) rapid relaxation preventing detection of the signal. The signal essentially decays before it can be measured. For Pu at room temperature it appears that (c) was the case. Shown in Figure 1 is a screen shot for lengthy study into finding the Pu-239

signal from our 9.2 T NMR system. The sample was Pu(III) Cl6(N(CH3)4)2 stabilized with two equivalents of N(CH3)4. Typically the range one might except to find a signal for a specific nuclei will range for 10 kHz to 1-2 MHz. For this sample, the search spread over 20 MHz from 19 to 40 MHz and no signal was detected. Had a signal been found, a peak would be observed in this series. As shown, there are several peaks but they resulted from internal frequencies used by instrument. With this challenge of benchmarking a DNP-NMR system on an isotope that might not be feasible, the project shifted to other nuclei of interest.

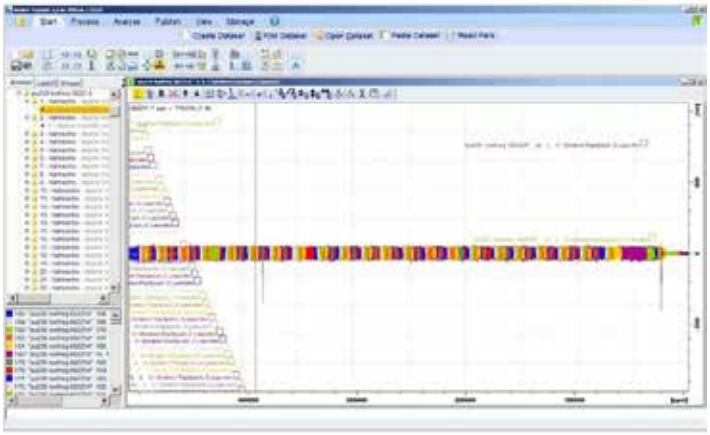

Figure 1. A series of over 400 experiments were conducted to find the Pu-239 frequency. As shown in this screen shot from the instrument, only internal signals were discovered in a range from 19 to 40 MHz.

We designed and built a compact NMR instrument optimized for the analysis of various nuclei in the 0.2 to 4.0 MHz frequency range. This corresponds to magnetic fields of ~ 0.35 T, an attractive range to achieve for DNP enhancement because it was relatively straightforward to produce both a uniform magnetic field at this strength in a compact format, and the RF frequencies for DNP (ca. 10 GHz). The expected S/N increase is > 100. Operating at ultra-low fields (ULF) greatly simplifies the hardware needed for DNP-NMR. Variable DC magnetic fields can be produced with room temperature electromagnets, which allow the magnetic field to be easily tuned for DNP, and generally allow for higher magnetic fields during DNP irradiation. Saturation of the EPR transition can be done with a coil rather than a cavity resonator, allowing a wide range of tunability. NMR hardware is also simplified since, due to the very long characteristic wavelengths of the ULF NMR signals, impedance matching is no longer necessary. As a result retuning merely requires adding or removing capacitance from the detection circuit.

Initially an EPR spectrum was measured with our new instrument to test and demonstrate the electronics for the electron polarization that will be transferred to a given nuclei (such as H) for NMR detection, summarily referred to as DNP-NMR as described earlier. Shown in Figure 2 is the EPR spectrum that was recorded with our spectrometer. These experiments were critical and helped determine the operating space for the instrument.

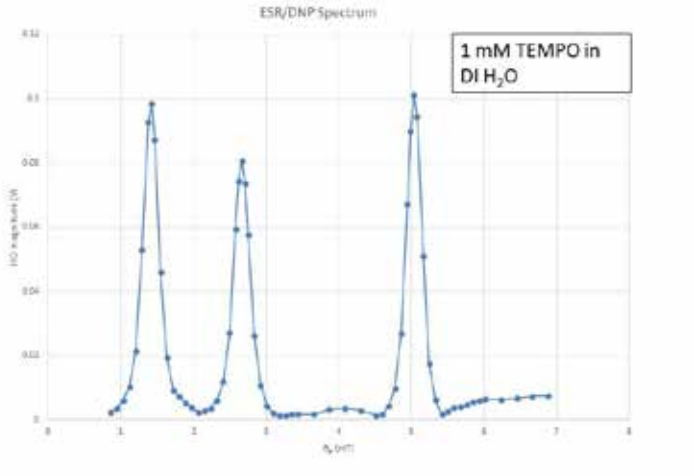

Figure 2. ESR spectrum is largely in agreement with published data at 102 MHz (20W power). Peaks are found at 1.42 mT, 2.67 mT, 5.03 mT.

Having the EPR working, the DNP-NMR was tested with the simplest of solutions, water, to quantify the H NMR signal enhancement. Shown in Figure 3 are our results for the DNP-NMR of water. This example shows nicely the increased signal with the DNP and a 180 degree phase shift that indicates polarization transfer from the electrons of TEMPO molecules to the nearby H2O. With modification and optimization of the system, the enhancement factor increased from 20 to 70, and similar results would be possible for F-19, also considered to be a high frequency nuclei with respect to the other elements on the periodic table.

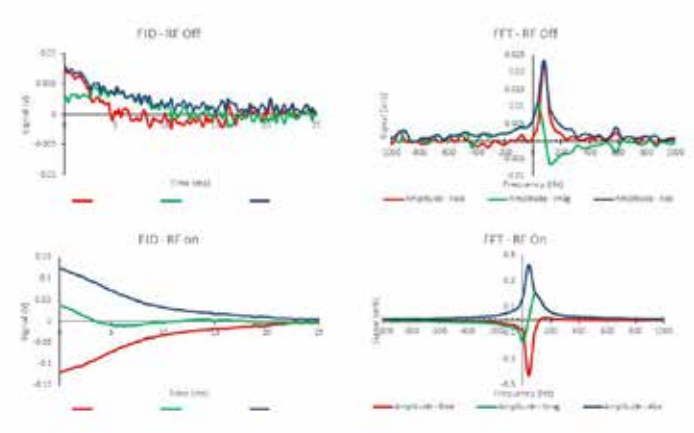

Figure 3. NMR and DNP-NMR results for water observing the 1H NMR signal. With DNP, a 20x increase in NMR signal was measured. Upper left, signal from our instrument without

DNP. Upper right, Fourier transform of signal. Lower left, NMR signal with DNP. Lower right, Fourier transform of DNP-NMR, 180 degrees out of phase with NMR signal consistent with polarization transfer.

To remind the reader, the aim of this project was to have a tool to study low gamma/low frequency nuclei and we successfully detected P-31 and well as H-2. For the example of H-2 from a D2O solution with TEMPO, an enhancement factor of 40 was measured. Recently, the system has since been reconfigured to analyze a more challenging system, Sn-199 in a neat solution of Sn(CH¬3)4. Sn-119 has a lower frequency than H and a lower natural abundance (ca. 8%). To date, at the ULF the team has been unsuccessful in detecting a signal from Sn-119. The challenges will be summarized in our publications. In order to achieve an acceptable enhancement, the amount of TEMPO needs to be increased along with the magnetic field strengths (power to the electromagnets). Increasing these parameters, specifically the TEMPO concentration, dropped the sensitivity of the experiments and no signal from the tin could be measured.

To conclude, in order to achieve large Overhauser-DNP enhancements of NMR signals from low frequency nuclei, large TEMPO concentrations will usually be required. We have seen that, at TEMPO concentrations significantly larger than 20 mM, the EPR magnetic field must be increased substantially beyond the capabilities of the system described here in order to achieve EPR line saturation approaching 50%. Thus, it is nearly impossible to achieve it in a ULF system such as ours for several related reasons. Because our sample volume (4 ml) and diameter (19 mm) is much larger than typical in NMR, the field generation efficiency (power necessary/current) is much lower, and the electric fields much higher. These electric fields are problematic because they create sample losses which reduce the quality factor of the coil and also result in sample heating. The obvious solution to this problem is to reduce sample and coil size, although such an approach has the disadvantage of reducing signal. However, with the known limitation and path forward with corrective actions, we have a solid foundation for follow-on programs.

Impact on National Missions

While we discovered the limitations for ULF DNP-NMR for measuring low frequency nuclei such as Sn-119, U-235, and Pu-239, an unexpected capability emerged that has led to LDRD DR and DHS programs for the team. At these low fields, and more importantly at zero-field or in the earth's magnetic field, J couplings between elements (homo- and hetero-nuclei) can be observed. For a sample of isopropyl methylphosphonate in water, we observed the heteronuclear couplings between H and P-31 using our ULF DNP-NMR (Figure 4). This gives just a glimpse at chemical composition (sample contains hydrogen and phosphorous) and structure (splitting between the J coupling peaks). However, if we decrease the magnetic field strength and use the earth's magnetic field or possibly zero-field for the detection of signals, homonuclear couplings between H's can be measured and this is a potential signature for chemical threat agents.

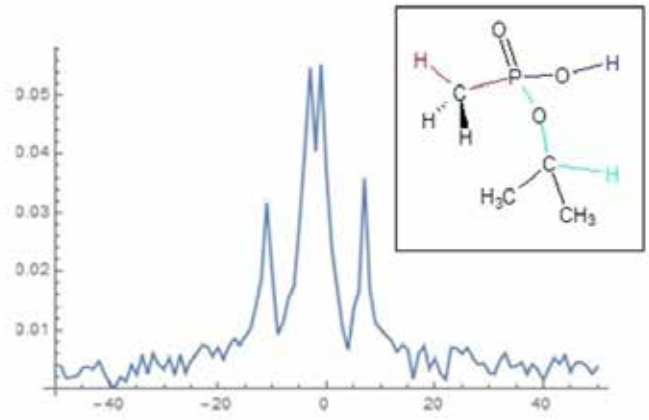

Figure 4. DNP-NMR results for isopropyl methylphosphonate in D2O. Spectrum shows the 31P-1H J couplings spin pairs between the methyl group (red) and 31P and the further away 1H on the isopropyl (blue). Lower magnetic field would allow detection of 1H-1H J couplings. The J coupling signature will allow estimates of chemical composition and structure for unknown compounds.

In follow-on work, our plan is to explore enhancing the intrinsic NMR signal with DNP and using stable, ultra-low magnetic fields, J-coupled spectroscopy (JCS) to directly observe homo and hetero-nuclear J-coupled patterns which are unique and characteristic signatures of threat agents including chemical warfare agents (CWA), their precursors, and CWA production products from any synthetic route allowing positive identification and attribution through database lookup or modeling.

As outlined in our original proposal, NMR is the gold standard for spectroscopic identification of materials, because it can provide non-invasive and detailed analysis of the chemical structure of materials. NMR gives detailed information beyond that available in mass-spectrometry including the atoms present, their relative locations, and the nature of the bonds between them. At LANL we have long been interested in examining NMR at the extreme, the regime of ultra-low magnetic fields (ULMF is typically defined as from earth's magnetic field to mT, as demonstrated by this ER project along with the Battlefield MRI team and MagViz projects). In part this reason stems from the practical desire to be able to locate NMR systems in non-traditional locations and perform screening through packaging. However, there are also numerous

scientific advantages to the ULMF regime. These include very narrow line-widths, very high homogeneity of large magnetic regions, and unique access to both homo- and hetero-nuclear J-coupled spectroscopy (ULMF-NMR-JCS). JCS provides unique insight into chemical bonding and is independent of magnetic field strength. We expect that the JCS signature will be unique for all chemical threat agents (CTA) containing protons, carbons, and other NMR active non-carbon heteroatoms and that a database can be implemented for identification and attribution based on the relative peaks in the spectrum. However, while this is exciting in its own right, a much more exciting aspect of JCS, unique to ULF-NMR, is one of the most intriguing aspects of our future work. This is access to homo-nuclear JCS information that arises from the unique selection rules in play for homo-nuclear J-coupling – a signature that has not been explored for any class of CTAs. This can only happen at ULF because it either requires the proton Larmor frequency to be on the order of the peak splitting or it requires a hetero-atom like F-19 or P-31, and these splittings are often in the Hz to kHz regime. Figure 5 gives an example of the increased information that is available from JCS as the magnetic field is lowered.

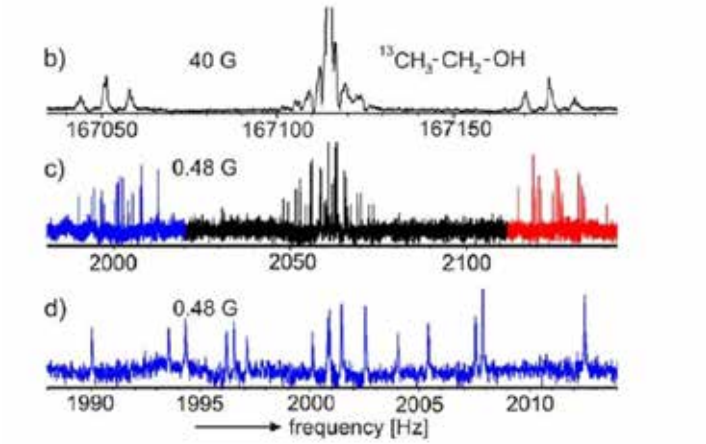

Figure 5. Example of JCS showing (b) 1H NMR spectrum of ethyl-alcohol measured in the intermediate coupling regime at 166 kHz with site-selective 13C enrichment at the methyl group. The 1H resonance is split into a pair of three lines corresponding to the triplet of the 13CH3 group and a pair of four lines corresponding to the quartet of the CH2 group by the indirect homo- and hetero-nuclear couplings. The large central line at 167 kHz is due to the uncoupled OH-proton. (c) Corresponding single-scan earth-field NMR spectrum. In this strong-coupling regime, the 1H resonance is split into highly resolved lines by the indirect homo- and hetero-nuclear couplings. (d) Enhanced view of the left side of (c), showing sixteen resolved lines. Data are from Chemical Physics Letters 477 (2009) 231–240. [1]

The majority of the samples of interest will have F-19 or P-31 instead of C-13, and access to the homo-nuclear couplings will greatly improve the information available. We believe this is the strongest indication for having a unique and robust signature as demonstrated in Figure 5, published results for the arguably very simple molecule of C-13 enriched ethanol.

The obvious downside to the ULF regime, the lower magnetization, can be made up by use of polarization enhancement methods which include pre-polarization and DNP.

References

1. Blumich, B., F. Casanova, and S. Appelt. NMR at low magnetic fields. 2009. Chemical Physics Letters. 477 (4-6): 231.

Publications

Yoder, J., P. E. Magnelind, M. W. Malone, M. Espy, and M. T. Janicke. Understanding Signal Enhancements in DNP-NMR at Ultra-Low Magnetic Fields. To appear in PROGRESS IN NMR SPECTROSCOPY.

Solid-State Gamma-Ray Detectors Based on Quantum Dots

Jeffrey M. Pietryga
20140406ER

Abstract

The threat posed by the proliferation of Special Nuclear Materials (SNM) is especially grave as they carry the potential for disaster in dangerously small packages. Rugged, low-cost gamma-ray detecting devices, and energy-resolving devices in particular, are an invaluable tool for tracking SNM, but limitations in current technologies render wide deployment economically infeasible. In this project, we proposed to develop a new class of solid-state gamma-ray detectors based on cheap, solution-synthesized semiconductor nanocrystals to address the specific needs of the nonproliferation community. The goal was to fabricate relatively simple gamma-sensitive diodes, and probe their response to high-energy radiation, seeking to ultimately achieve performance on a par with common scintillator devices.

Background and Research Objectives

Gamma-rays from SNM have quite high energies (0.1-10 MeV), which make it difficult to shield them inconspicuously, and at the same time translate into massive amounts of potential signal per captured photon. Thus, at the exit portal of a nuclear facility with a known inventory and fixed number of compliant personnel, screening is trivial. This model fails completely when applied to some crucial SNM non-proliferation and homeland security scenarios, such as screening at border crossings, where high throughput of uncontrolled vehicles is required. Such applications raise a unique set of criteria that current technologies have been unable to meet. We propose to develop solid-state gamma-ray detectors based on semiconductor nanocrystals to fill this vital national (and global) security role.

Limitations of current technologies relative to nuclear security

At a shipping portal or a border crossing, there is a premium on throughput, which requires big, sensitive detectors that can discriminate between dangerous and benign materials by providing the energy fingerprint of the gamma rays. The ability of a device to distinguish gammas of different energies is called its "energy resolution." Current technologies offer a range of sizes, sensitivities and resolution; [1] in general the bigger the detector and/or the better the resolution, the higher the cost. To date, no class of gamma detector provides the size and resolution needed for fast screening at anywhere near the cost needed to deploy them around the country.[2]

Nanocrystals to the rescue

Colloidal nanocrystal quantum dots (NQDs) are solution-processible nanometer-sized crystals of semiconductor materials. NQDs offer a means for creating electronic devices by low-cost and highly scalable methods. Moreover, because of quantum size effects, their optical properties (like band gap) are widely tunable by control over particle size, shape and composition, offering further advantages over conventional semiconductors. [3] In one example particularly relevant to detecting high-energy radiation, NQDs have exhibited a phenomenon known as carrier multiplication (CM), in which ultraviolet photons produce more excited charges in an NQD than low energy photons.[4] This suggests that NQD films should be highly efficient at transducing even higher energy photons (like gamma-rays) into current; indeed, the basis for this was confirmed in a previous LDRD project. [5] In the current project, we sought to create charge-collecting gamma-ray detectors, wherein gamma-rays are converted directly into pulses of electrical current, based on conductive films of NQDs. Such devices could potentially be scaled to portal-relevant sizes with excellent energy resolution at low cost.

Preliminary studies and remaining challenges

To detect gamma-rays, it is necessary to first "stop" (or absorb) them; simple calculations showed that films of lead chalcogenide NQDs (PbE, where E = S, Se or Te) can be better at stopping gamma-rays than either Ge or cadmium zinc telluride, the materials most commonly

used in charge-collecting detectors. Having already established that NQDs are good at turning gamma-rays into electrical charges [5], the next open question was whether the conductivity of NQD films can be high enough to allow all the charges can be captured and counted. Once again, previous studies of PbS NQDs in optical field-effect transistors (OFETs) [6], and in solar cells [7] ,have shown that the multiple charges created by high energy photons can actually be collected as current in an efficient manner. However, all previous studies focused on relatively thin films (~50-500 nm); the most important remaining challenge was to accomplish the same efficient charge collection in a film 100-1000 times thicker.

Scientific Approach and Accomplishments

For optimal gamma-ray absorption, we focused on high Z (atomic number) PbE NQDs. Because of quantum confinement effects, PbE NQDs exhibit tunable band gaps as high as 1.4 eV, which should reduce dark current issues at room temperature that made bulk PbE detectors impossible, and have very good CM efficiencies.[4] In the initial plan, the work was described in three tasks: 1) Establish new solution-based methods for creating very thick, conductive nanocrystal quantum dot (NQD) films; 2) Demonstrate and quantify sensitivity to high-energy radiation; and 3) Optimize the devices to ultimately enable high resolution, non-cryogenic-temperature performance.

Fabrication and Electrical Characterization of Thick NQD films

The first, enabling activity of this project was to achieve devices with NQD film thicknesses suitable for gamma-ray detection. We proved early in the project that previous, iterative methods for producing crack-free, highly conductive films were unsuitable for thicknesses >1µm (Figure 1). As an alternative, we desired a one-step deposition of NQD films in which all of the chemistry necessary to achieve high conductivity is performed on the NQDs while they are still in solution. This allows the possibility of using advanced methods like spray-coating, electrophoretic deposition or doctor-blading through which much larger thicknesses can be achieved. Accordingly, we developed a universal protocol for fast, in-solution NQD conductivity treatment for PbS, PbSe and PbTe NQDs. [8] The key proved to be (step one) the use of an amine-based NQD synthesis, combined with (step two) the use of very particular, highly-polar solvents for the conductivity treatment chemistry (Figure 2). After treatment, the NQDs form remarkably stable dispersions in polar solvents, and fully retain their optical properties, indicating that NQD surfaces were not damaged or altered during the process. In addition to constituting a fascinating system for fundamental study of the effect of surface structure on static and dynamical properties of PbE NQDs in polar solution (which has never been possible before), the dispersions proved to be ideal for direct casting of thick, conductive NQD films. A single deposition step by spin-coating from concentrated PbE NQD solutions has produced films as thick as 3-4 µm, with a mirror smooth finish (Figure 1) and without the instability plaguing the films produced by the laborious layer-by-layer method. Finally, the conductivity of the NQD films was verified by studying them in devices called field-effect transistors (FETs); record-high charge carrier mobility (which determines conductivity) was observed.[8]

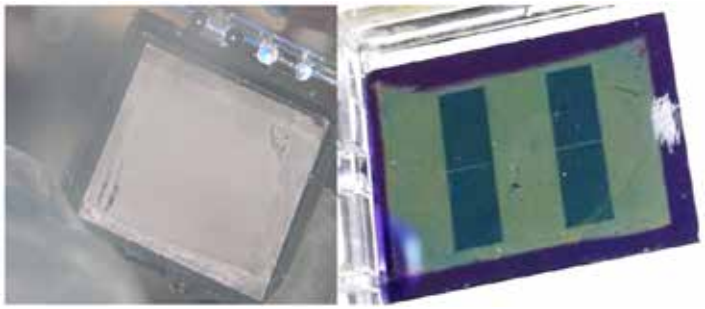

Figure 1. A 3µm-thick film deposited by conventional layer-by-layer deposition (left) is visibly rough and physically unstable, as compared to the 3µm-thick film deposited in a single deposition after in-solution conductivity treatment (right), which is mirror smooth and physically robust.

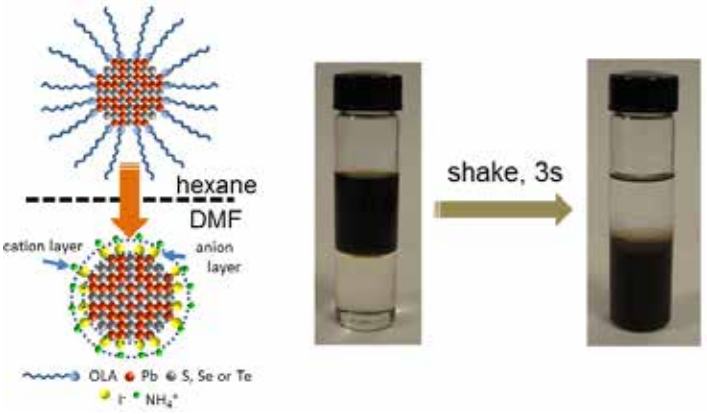

Figure 2. A cartoon depiction (left) of the chemistry that happens during in-solution conductivity treatment, in which non-polar-soluble NQDs exchange their long-chain surfactants (present from the synthesis) for small ionic surface coverage. After exchange, NQDs are soluble in polar solvents. This is a very fast process; the sudden change in solubility of the NQDs after exchange treatment can be seen in the photographs (right) of PbSe NQDs moving from a hexane phase (top) to a N,N-dimethylformamide (DMF) phase (bottom) upon treatment with NH4I.

As expected, in-solution conductivity treatments opened the door to alternative deposition methods. The first we tried was electrophoretic deposition, wherein an electrical bias is applied between a desired substrate and a counter-

electrode, both of which are immersed in a solution of NQDs. In our case, using NQDs in polar solvent, we struggled with side-reactions, as even modest electrical bias applied across our solutions resulted in substantial current, and deposition of products involving both charged NQDs and oxidized stabilizing ionic species. These difficulties will have to be resolved in future efforts using this exchange method. To get really thick films, we also tried simple evaporative methods, in which large drops of concentrated NQD solution were placed on a substrate and left to evaporate slowly, or a substrate was immersed in solution while the solvent was allowed to evaporate. In both cases, extensive cracking was an issue, which we attributed to too much solvent trapped within the film as it solidified from the outer surface inward. Finally, we were successful in using doctor-blading, a technique previously used only for NQD composites, to create films of ~5 µm thickness.

Nanoparticle Shape Control

As mentioned above, both size and shape control can be used to tune the properties of quantum-confined nanomaterials. An original part of this project involved developing and using shape-controlled PbE nanomaterials in radiation-sensing devices. By elongating nanoparticles in one or two dimensions, it is possible to achieve superior charge transport in nanoparticle films if the particles can be properly aligned. Building on previous work on PbSe nanorods, we developed a new synthesis of PbSe nanoplatelets [9], and of PbTe nanorods and nanorings (Figure 3; a manuscript describing the synthesis and characterization of these latter materials has been prepared, but not yet submitted). However, shape-controlled particles required using different organic surfactants than PbE NQDs, requiring a retooling of the surfactant exchange chemistry. Moreover, the deposition of even thin ordered films proved to be difficult to achieve by any method. When the project budget was reduced, we decided the potential benefits of continuing the shape control work were not commensurate with the effort they would require, so this avenue was dropped, to be hopefully continued in a future related project.

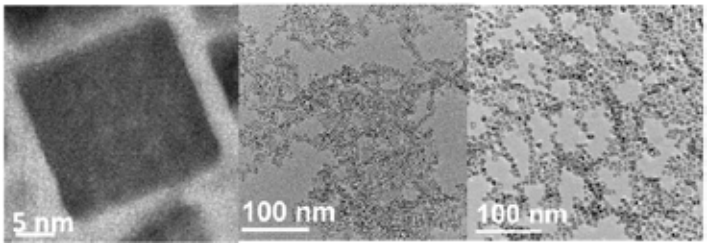

Figure 3. Transmission electron microscope (TEM) images of PbSe nanoplatelets (left), PbTe nanorods (middle), and PbTe nanorings (right), all developed as part of our early interest in using shape-controlled PbE nanoparticles to gain enhanced conductivity in films.

Light and Radiation Sensing NQD Devices

Due to availability, the first radiation testing was performed on an FET-geometry device. The film in this study was only 100 nm thick, prepared in a standard iterative approach using 1,2-ethanedithiol for conductivity treatment. Due to the low thickness and unknown sensitivity of the device, the radiation source was an X-ray tube. Although even for the X-rays the film was only modestly attenuating, under only modest applied voltage, more current was observed under X-ray illumination than without. After this "sanity-check", radiation testing was paused while the new film deposition technique described above was developed.

Once it was established that smooth, high-quality films of 5-10 µm could be regularly prepared, radiation testing was resumed. Taking simple photodetectors as our guide, we adopted a sandwich-type geometry, with our active NQD film deposited directly on a substrate-bound bottom contact, and a top contact evaporatively deposited onto the NQD layer through a custom designed mask (Figure 4). Studies focused on PbSe NQD films with iodide ion conductivity treatment. While a symmetrical device (e.g., Au-NQDs-Au) might be the simplest device, we elected to use ITO-coated glass as the bottom contact, as it would allow us to prove the function of a device using photo-excitation (through the bottom contact) before performing the somewhat more complicated radiation tests with elemental sources (through the top contact, typically 150 nm of Au). Examples of photo-excitation response studies are shown in Figure 5.

Figure 4. At right, the custom masks for thermally evaporating the metallic top contact of sandwich-type radiation detection devices. Three different device areas can be used (2, 5 and 10 mm diameters); the rectangular tab allows electrical contact to be made using a probe without "shadowing" the active device area. At right, actual devices: simple ITO/NQD/Au sandwich device (top); ITO/NQD/Ag device (middle); and ITO/CuSCN/NQD/ZnO/Al device (bottom).

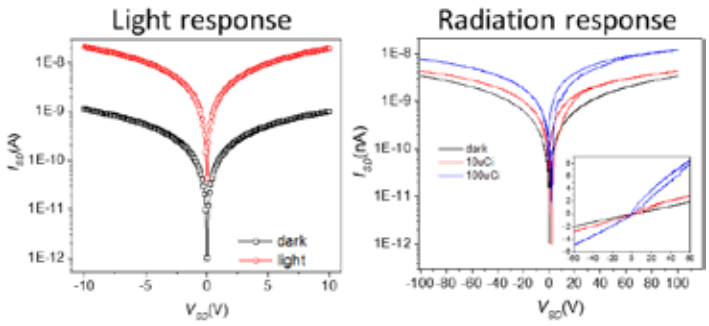

Figure 5. Typical photoresponse and radiation response curves for a sandwich-type device, plotted on a log scale. Studies used a white-light LED and two Am elemental sources of differing activity, respectively. Both devices feature a 2 µm-thick PbSe NQD film treated with iodide ion and Au top contact. In the radiation response studies, overall higher current and greater hysteresis [i.e., splitting between measured current at the same voltage while scanning in the positive direction (upper curve) vs. the return sweep in the negative direction (lower) is observed under positive bias, as seen more clearly in the inset, which shows the same data on a linear scale.

Identification of a radiation testing protocol was, at the outset, hampered by the question of whether such tests could be performed under ambient conditions. Without fully knowing the effect simultaneous exposure to air and ionizing radiation might have on the experimental films, it was decided that all initial studies should be air-free (as the photo-excitation studies had been). This presented complications, as our radiation detector testing collaborators lacked facilities for inert-atmosphere testing, and the NQD collaborators had no radiation sources in their facilities. After some deliberation, it was proposed to bring low-hazard sources into the NQD lab space to perform the radiation tests under as ideal conditions as possible. For this purpose, the best answer was to use 241Am sealed sources, alpha-emitting sources that could be introduced into the NQD lab without disrupting any other activities. As a side effect of the resolution to use alpha instead of gamma-rays, we were able to start radiation testing before fully reaching our target minimal film thickness of 100 µm, which despite the breakthrough technique described above, still required significant further refinement.

Thus, with our custom device architecture with NQD films ranging from 2 – 20 µm in thickness and NQDs of bandgap ranging from 0.8 – 1.1 eV, we performed numerous parallel studies of photo- and radiation-response, using a 2 W white-light LED as our light source, and a series of 241Am sealed sources (activities ranging from 0.1 – 100 µCi). Examples of alpha response curves are shown in Figure 5; responses were definitive for the 10 and 100 µCi sources, but were difficult to discriminate for the lower activity sources. Interestingly, responses often showed asymmetry in respect to the direction of the applied voltage (positive or negative, relative to the ITO electrode), and some degree of hysteresis in the current as the voltage was swept first toward the positive, and then in the negative direction (see Figure 5 inset). To investigate this further, we fabricated and studied devices using top contacts of Ag, which is similar in work function to ITO, and therefore should result in more symmetrical performance from the device. Analysis of this data is not yet complete at the time of this report. Hysteresis was also interpreted as a potential sign of charge build up within the film, possibly due to charge trapping that could ultimately lead to degradation of performance; however, repeated cycles produced essentially identical I-V traces, rather than showing any accumulation of changes. Moreover, long-term "soaking" of the device using overnight exposure to the 100 µCi alpha source had only a minor effect on response (<10%).

A consistent issue found in these studies was the problem of excessive dark current, which dramatically reduced our ability to discriminate radiation- (or light)-induced current from background signal, particularly at high voltages at which we would hope to have the highest efficiencies. In an attempt to reduce dark current, additional layers were added into the device architecture in an attempt to selectively block carriers from either electrode. For instance, first a ZnO layer was introduced between the NQD layer and the Au top contact, which would prevent holes from being collected at the Au electrode. Next, a layer of CuSCN was introduced between the bottom ITO contact and the NQD layer, for the purpose of blocking electrons from reaching the ITO contact. In order not to interfere with desired device operation, the layers were kept relatively thin (~25 nm). To date, the effect of these layers appears to have been minimal, but further data analysis is required before a final accounting can be made. It seems likely that high dark current is a product of relatively high intrinsic (i.e., not-photon generated) concentrations of mobile charges within the film. Preliminary studies of film capacitance seem to bear this out. Efforts to modify these concentrations by changing the NQD structure and the conductivity treatment were attempted, but more data analysis is required before we can determine if there was any effect. A manuscript describing these first known tests of the response of NQD-based diodes to elemental radiation sources is currently in preparation.

In summary, we applied our advanced understanding of NQD surface chemistry to develop a new conductivity treatment protocol for PbE NQDs that allows for the single-step deposition of conductive NQD films of unprecedented thicknesses. We then used this technique to prepare simple prototype radiation detector devices of a custom

architecture, and tested their responses to light and alpha radiation. The methods used here are capable of being extrapolated to thicknesses that will make gamma-ray detection feasible without any further fundamental advances. However, a concerted effort at reducing dark current, at the time of the end of the project, is still needed to bring the sensitivities of these devices into a practical range, and eventually into the range in which single alpha or gamma-ray events can be detected and quantified using pulse-height analysis.

Impact on National Missions

The original goal we chose for this work is to make gamma-radiation detectors that are comparable to gamma scintillators in energy-resolving performance, but much cheaper and easy to scale to portal-relevant detector sizes. This research was motivated by the needs of entities involved in nuclear non-proliferation, [2] as well as defense, intelligence and law-enforcement agencies interested in detecting the presence of illicit nuclear materials. The flexibility of our new detector class would also eventually make them adaptable to needs in nuclear reactor/facility monitoring, and radioactivity-related environmental remediation efforts.

We also note that some collaborators in this project have suggested that solid-state detection of neutrons might be equally or even more interesting for many of these potential uses. For such purpose, we have identified several options that would sensitize our devices to neutrons by addition of elements with high neutron absorption cross-sections, including: the use of CdE NQDs; the use of BH4- or Li+ ionic surfactant exchange for the preparation of NQD films (both of which have been demonstrated); and the infilling of NQD films with Gd2O3. Beyond uses related to nuclear materials, it is quite likely that specific needs of space science (gamma spectroscopy) and satellite surveillance could ultimately be met by this class of detectors. Such sensors could also be of interest to materials scientists for use in various types of radiography, and to the medical field as cheap, superior replacements for current detectors used in x-ray, nuclear, and positron emission tomography (PET) imaging techniques.

References

1. Radiation detection and measurement. 2000.

2. Spafford, T.. Special nuclear materials movement and detection portfolio: Technology Roadmap. 2007. Office of Nonproliferation Research and Development, National Nuclear Security Administration.

3. Pietryga, J. M., Y. S. Park, J. Lim, A. F. Fidler, W. K. Bae, S. Brovelli, and V. I. Klimov. Spectroscopic and device aspects of nanocrystal quantum dots . 2016. Chemical Reviews. 116 (18): 10513.

4. Schaller, R. D., and V. I. Klimov. High efficiency carrier multiplication in PbSe nanocrystals: Implications for solar energy conversion. 2004. PHYSICAL REVIEW LETTERS. 92 (18).

5. Padilha, L. A., W. K. Bae, V. I. Klimov, J. M. Pietryga, and R. D. Schaller. Response of Semiconductor Nanocrystals to Extremely Energetic Excitation. 2013. NANO LETTERS. 13 (3): 925.

6. Nagpal, , and V. I. Klimov. Role of mid-gap states in charge transport and photoconductivity in semiconductor nanocrystal films. 2011. NATURE COMMUNICATIONS. 2.

7. Semonin, O. E., J. M. Luther, Choi, Chen, Gao, A. J. Nozik, and M. C. Beard. Peak External Photocurrent Quantum Efficiency Exceeding 100% via MEG in a Quantum Dot Solar Cell. 2011. SCIENCE. 334 (6062): 1530.

8. Lin, Q., H. J. Yun, W. Liu, H. J. Song, N. S. Makarov, O. Isaienko, T. Nakotte, G. Chen, H. Luo, V. I. Klimov, and J. M. Pietryga. A one-step method for fabricating highly conductive lead chalcogenide quantum dot films. Journal of the American Chemical Society.

9. Koh, W. K., A. F. Fidler, N. Dandu, S. V. Kilina, V. I. Klimov, and J. M. Pietryga. Thickness-controlled quasi-two dimensional colloidal PbSe nanoplatelets. Journal of the American Chemical Society.

Publications

Koh, W. K., A. F. Fidler, N. Dandu, S. V. Kilina, V. I. Klimov, and J. M. Pietryga. Thickness-controlled quasi-two dimensional colloidal PbSe nanoplatelets. Journal of the American Chemical Society.

Lin, Q., H. J. Yun, W. Liu, H. J. Song, N. S. Makarov, O. Isaienko, T. Nakotte, G. Chen, H. Luo, V. I. Klimov, and J. M. Pietryga. A one-step method for fabricating highly conductive lead chalcogenide quantum dot films. Journal of the American Chemical Society.

Makarov, N. S., J. Lim, Q. Lin, J. W. Lewellen, N. A. Moody, I. Robel, and J. M. Pietryga. Quantum dot thin-films as rugged, high-performance photocathodes. Nano Letters.

Signatures of Reactor Operations from Plutonium Production Samples (U)

Anna C. Hayes-Sterbenz
20140433ER

Abstract

In this project we derived novel algorithms for deducing nuclear reactor operations from spent fuel isotopics. To validate the algorithm we analyzed the isotopic content of several uranium samples that had been irradiated in a nuclear reactor. These isotopics included U, Pu, Cs, Ru, Rh, Pd, Eu, Kr and Xe. We found that the algorithm could be used to accurately deduce the total neutron fluence to which the samples had been irradiated, as well as the time since discharge from the reactor.

Background and Research Objectives

The main aim of the project was to quantify a novel scheme for using both uranium isotopics and fission product ratios to determine detailed reactor operations used to irradiate nuclear material. Our goal was to show how uranium isotopics and fission product ratios in spent fuel might be used to determine the reactor fluence, possible number of shutdowns, and the time since discharge. As detailed below, the key ratios of interest are the uranium ratios 235U/238U and 236U/235U, as well as several fission fragment isotopic ratios. The samples in question had been placed in a reactor at various locations and irradiated for time periods ranging from 5 hours to several weeks. Because the neutron flux (n/cm2/sec) is generally not flat across a reactor, different samples experienced different neutron fluxes. An additional complication involved the fact that the reactor in question was repeatedly shut down and restarted over the course of the irradiation periods. All of the samples were about 20 years old, and so the algorithm also needed to be capable of deducing this cooling time

Scientific Approach and Accomplishments

The short irradiation times involved meant that the concentration of the isotopes of interest in the samples was quite low, and this presented a challenge for the radiochemical measurements. The archived samples, which were either uranium metal or UO3, were analyzed for their U and Pu isotopics, as well as the activities of several fission fragments. The actinides were separated and measured as described in [1]. Each sample was dissolved in HNO3, then loaded and separated on anion exchange columns to achieve separation of Pu from U. For many of the isotopes we used extraction chromatography methods followed by inductively coupled plasma mass spectrometry (ICP-MS) and thermal ionization mass spectrometry (TIMS) analysis, in order to characterized isotope concentrations. Fission fragment concentrations were measured by gamma spectrometry.

The isotopics were determined for U, Pu, Cs, Sb, Ru, Rh, Pd, Eu, Kr, and Xe.

The 235U concentration in all of the samples examined was determined to be close to natural uranium, and this was consistent with the declared enrichment. The first reactor operations parameter that we examined was the total neutron fluence (n/cm2) to which the samples had been exposed. Our emphasis on the fluence is because this parameter determines a large number of characteristics of spent fuel, such as the total burnup, i.e., the total energy produced from fission per in-going metric ton or uranium. The relationship between any isotopic observable and the neutron fluence can, in principle, be derived analytically, although in some cases it is sufficiently complicated that it becomes useful to make approximations that simplify the formulae. Any two observables can be related to one another through their respective dependence on the fluence. For example, if we wish to derive expressions relating 236U/U-total to Pu/MTU, we can first derived an expression for each in terms of the neutron fluence Φ. We note that for some observables, there is a dependence on both the fluence and the neutron flux (n/cm2/sec).

Two very useful determinations of the fluence are the 236U/235U ratio and the 235U/238U ratio. We derived analytic expressions for these relations and compared

them to full reactor simulations. The two methods agreed very well. In Figure 1, we graph the relation between the 236U/235U ratio and the fluence. For all short irradiation times, this relationship is linear. The same is true for the relationship between the 235U/238U ratio and the fluence.

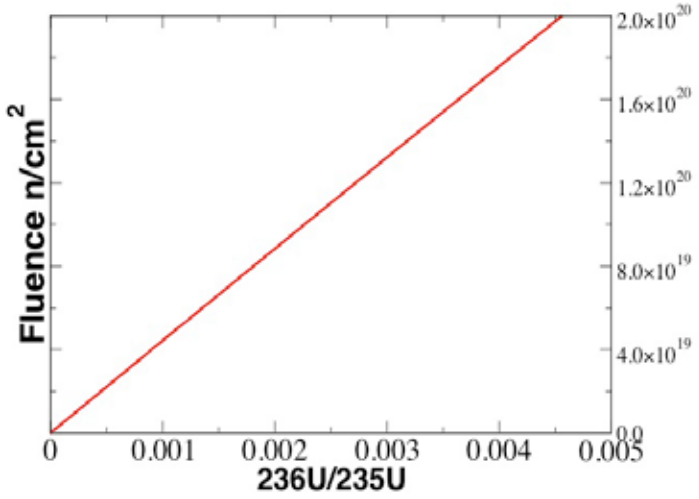

Figure 1. The relation between the 236U/235U ratio in a sample and the total neutron fluence to which the sample was exposed is linear, for all short irradiation times considered in this project.

In Figure 2, we show the fluence deduced from each of these diagnostics. For fluences higher than about 1019 n/cm2 the two diagnostics agree well. However, for lower fluences, the concentration of 236U in the sample was too low to obtain good measurements.

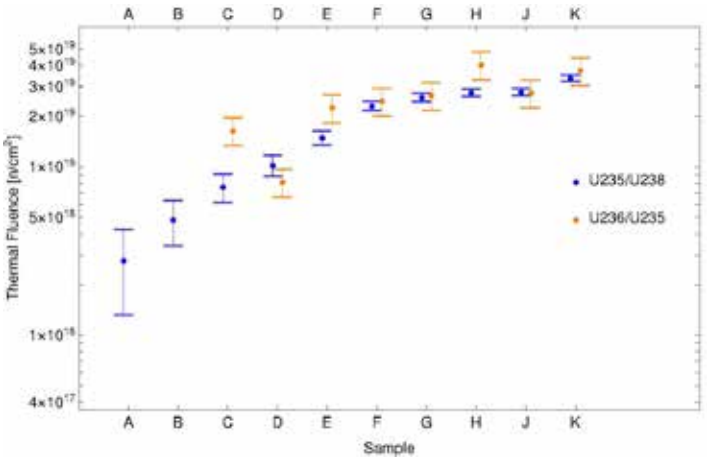

Figure 2. The neutron fluence deduced from the 235U/238U and 236U/235U ratios. For higher fluences (>1E19 n/cm2) the two diagnostics agreed. But below this fluence the concentration of 236U in the sample was too low to obtain an accurate determination of the 236U/235U ratio.

The neutron flux can be determined [2] from a measurement of the 135Cs/137Cs isotopic ratio. If the flux is known, the cesium ratio can be used to determine the number of reactor shutdowns that took place of the irradiation history of the sample. For some of the samples, the position in the reactor was declared, and hence the neutron flux was know. In such cases, we found [1] that the number of shutdowns was clearly discernable fom the 135Cs/137Cs ratio.

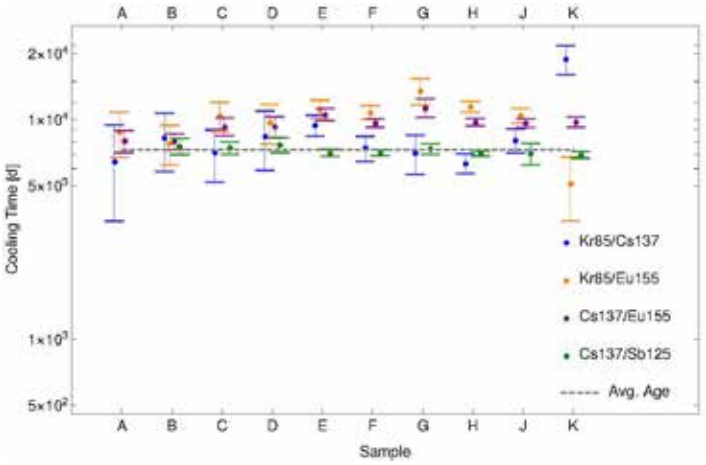

Figure 3. The cooling time as deduced from ratios of long-lived fission fragments. The average cooling time of 20 years can be deduced approximately. But the fact that the deduced cooling time for each varied, depending on the isotopic ratio considered, suggests that fractionation took place.

To determine the cooling time, we examined the ratio of fission produts with long halflives, and no dependence on the neutron flux except through a dependence on the total fluence. The results are shown in Figure 3. On average the cooling time could be reasonably well determined. However, different isotopic ratios did not agree with in the accuracy of the measurements. This tends to suggest that some chemical fractonation may have occurred. For this reason we concluded that only ratios withing the same atomic species could be uses as diagnostics.

Impact on National Missions

This project directly addressed issues relevant to LANL's and DOE's nuclear non-proliferation program. The diagnostics and tests that were developed can be directly applied to other national security programs, including nuclear forensics and nuclear safeguards.

References

1. Byerly, B., L. Tandon, A. Hayes-Sterbenz, and P. Martinez . Determination of Initial Fuel State and Number of Reactor Shutdowns in Archived low burn-up uranium targets. 2016. Journal of Radioanalysis and Nuclear Chemistry. 307: 1871.

2. Hayes, A. C., and G. Jungman. Determiningreactor-fluxfromxenon-136andcesium-135inspentfuel. 2012. Nuclear Instruments and Methods in Physics Research. A690: 68.

Publications

Byerly, B., L. Tandon, and A. Hayes. Determination of initial fuel state and number of reactor shutdowns in archived low-burnup uranium targets. 2016. Journal of Radioanalysis and Nuclear Chemistry . : 1871.

Measurement of Extinct Radionuclides in Historic Nuclear Debris (U)

Warren J. Oldham
20150298ER

Abstract

Debris from historic nuclear weapons test rests on the ground surface and within tunnels and underground cavities at all nuclear testing sites across the globe. This material could be used to determine device design and performance but is currently of limited diagnostic value because the short-lived fission products and key nuclear activation species have long decayed away. The goal of this project is to develop new measurement and assessment techniques necessary to reconstruct the diagnostic information still present in solid debris as the stable decay end-members. The original presence of short-lived radionuclides alters the ultimate isotopic composition measured in historic nuclear debris in a pattern that can be interpreted for detailed forensic and diagnostic evaluation. The success of the proposed effort will be a critical step towards a new capability with direct impact on nuclear forensics and on science based stockpile stewardship. The duration of this Exploratory Research project was one year. Based on the success of this initial "measurements focused" effort, a larger scale Directed Research project was begun under the leadership of Hugh D. Selby in 2016. The title of the follow-on project (20160011DR) is "Using extinct radionuclides for radiochemical diagnostics."

Background and Research Objectives

A nuclear explosion produces an intense burst of energy and associated radiation driven by the violent assembly of a critical mass of fissioning nuclear material. Details of the nuclear event have traditionally been inferred from measurements made during and immediately after the detonation. In the case of radiochemical measurements, many of the nuclear products that have been shown to be of most diagnostic value exist for but a moment in time, typically on timescales of hours to weeks. The key innovation of this proposal is the realization that short-lived fission products and key nuclear activation products that form the basis of modern technical evaluation can in fact be indirectly measured over vastly longer timescales from years to decades, and indeed centuries, after the detonation. We borrow a key insight in how to accomplish this task from similar approaches that have been successfully used in the field of cosmochemistry to measure extinct radionuclides in extraterrestrial samples like meteorites. Chemical fractionation between Pu and U that is known to occur during a nuclear event will cause systematic isotopic perturbation in 237Np and 239, 240Pu concentrations resulting from decay of short-lived U isotopes 237, 239, 240U. The proposed sampling and measurement techniques will be used to determine diagnostically sensitive and now extinct 237, 239, 240U isotopes in historic debris samples. A significant challenge of the proposed research will be to develop indirect methods to measure peak-yield fission products to determine total fissions in a given sample. In order to reconstruct this information we propose to measure perturbations in stable element isotopic composition to infer the original presence of short-lived fission products. This idea depends on the presence of stable multi-isotope elements for which one isotope is the end-point of a fission decay chain and another is blocked from fission decay by a different stable element.

Scientific Approach and Accomplishments

This research aims to develop analytical techniques to characterize the details of a nuclear detonation based on chemical analysis of aged nuclear debris. The analytes of interest are short-lived radionuclides that have decayed beyond detection, but leave signatures of their original presence in the isotopic composition in archived debris samples. We term these signatures, extinct radionuclides. The goals of the project are to recover two types of information, (1) short-lived uranium isotopes (237, 239, 240U) and (2) fissions. For each of these goals good progress has been accomplished. In order to determine the short-lived uranium isotopes, a collection of samples must span a suitable range of volatility as measured by sample specific 236U/238Pu ratios. Although only one unfractionated 236U/238Pu value is actually "true" of

the device, chemical distortion that occurs during debris condensation serves to generate a range of samples that can be relatively enriched (volatile) or depleted (refractory) in uranium compared to a reference 238Pu isotope. The proposed regression technique requires that 236U/238Pu span a sufficient range within the sample set to allow a robust linear fit. In the case of analyses of Trinitite, eight individual samples from archived LANL collections have been completed. The expected trends are observed, however the goodness of fit over a limited range in 236U/238Pu is not sufficient to obtain a high-quality measure of 237, 239, 240U. A new set of Trinitite samples obtained from a commercial rock and gem supplier has been procured. These samples appear as light green vesicular samples, distinctly different from the black glass found in the LANL collection. It is hypothesized that the light green vesicular samples will be more volatile compared to the black glass samples and will provide the range in 236U/238Pu that is needed. Initial analyses of archived core samples from an underground nuclear test have also been completed. For this test, archived samples that transit seven locations through the underground environment are available for analytical study. Duplicate analyses of the first two locations have been completed. Five more duplicate analyses will provide data to assess the 236U/238Pu volatility index and the feasibility of the technique to measure 237, 239, 240U in underground debris samples. Two independent approaches are being pursued to determine fissions in historical debris samples. These include direct measurements of 99Tc and indirect measurements of 95Zr and 97Zr through isotopic perturbation of stable molybdenum isotopic ratios (e.g. 95Mo/96Mo and 97Mo/96Mo). Each of these analytes is a peak yield fission product that can, in principle, be used to determine total fissions in the sample. The first phase of this project has focused on development of chemical methods used to isolate pure 99Tc and molybdenum concentrates that can be assayed using both single and multi-collector ICP-MS instrumentation. In the case of 99Tc determination, a method has been developed during the first year of this project to analyze for 99Tc in aged debris samples. Technetium is purified in high yields (80-100%) using extraction chromatography (TEVA resin) with good decontamination from both Mo and Ru. This decontamination is crucial to the success of the analysis because of potential isobaric interference from 98MoH+ and 99Ru. Standard addition experiments with solutions of Peruvian soil (NIST SRM 4355) and dissolved Trinitite suggest that accurate determinations of 99Tc can be obtained. The associated measurement uncertainty (20-30%) is higher than ideal and reflects inconsistencies in observed instrument count rates that are not yet fully understood. Additional work is needed to identify the source of the variation and improve measurement precision. In the case of 95, 97Zr determination, a novel technique using high precision isotopic measurements of stable molybdenum is being pursued. A sequential two-column ion-exchange protocol was developed and optimized. Purified Mo concentrates have been isolated with good decontamination against potential interferences from Zr, Ru, Cr, Mn, and Fe. The purification protocol performed well in an initial Mo analysis of a dissolved debris sample, which revealed significant deviation from the natural isotopic composition. An optimized measurement routine using the Neptune Plus multicollector ICP-MS is currently being developed. These high precision measurements will be used to quantitatively determine perturbations in 95Mo/96Mo and 97Mo/96Mo isotopic ratios. Future analyses using an isotopically enriched 96Mo spike will be interpreted for absolute fission concentration.

Impact on National Missions

A major limitation of current radiochemical diagnostics is the need to determine the concentration of key signature radionuclides with short half-lives. Within a month after a nuclear detonation, these radionuclides are largely extinct. If successful, the proposed work will be a critical step towards a new capability to extract this crucial information from nuclear debris at later times. Such a capability would have direct and lasting impact on two key DOE/NNSA missions: stockpile stewardship and post detonation nuclear forensics. A demonstrated capability to reanalyze archived debris samples from historic nuclear tests will improve the technical foundation that supports Stockpile Stewardship and will strengthen our Nation's commitment to deterrence without nuclear testing for decades to come. The limitations of historical measurements impacts nuclear forensics as well. Many of our earliest tests used simple designs that could be credibly replicated in a potential terrorist nuclear attack. Because many of these test were fielded in the late 1940's and early 1950's, the radiochemical data for these events is very sparse and/or of low quality. This leads to large uncertainties in evaluation of performance and yield, which in turn prevents proper calibration of LANL's computational design tools. A capability to obtain a complete radiochemical data set for early U.S. tests would significantly improve modeling and forensic capability envisioned for post-detonation nuclear forensics.

Publications

Hanson, S. K., C. R. Waidmann, J. L. Miller, H. D. Selby, and W. J. Oldham. Modern radiochemical measurement and evaluation of 1950's era debris from the Nevada Test Site (U). To appear in Defense Research Review.

Practical Antennas from Disruptive Technology

John Singleton
20150337ER

Abstract

This project designed and constructed two practical, optimized and economical antennas based on a new and disruptive technology: the superluminal polarization current antennas (SPCA). This technology is a radio-wave analog of the "sonic boom" in acoustics; it involves the source of radio waves (a polarization current within an insulator such as alumina) traveling faster than the speed of light and, in some applications, accelerating. This leads to unusual effects such as focusing and efficient long-range signal propagation. In the course of optimizing the two antennas, a new means of sending information securely without encryption was derived, and the scalability of SPCAs was established. The discovery and characterization of a new dielectric metamaterial suggested several new applications for the technology.

Background and Research Objectives

SPCAs have been realized at LANL since 2003 [1-11]. In contrast to conventional antennas, which employ surface currents of free electrons on localized elements such as dipoles to produce radiation, SPCAs use superluminal (faster than light in vacuo) polarization currents (the time derivative of the electric polarization, $\partial P/\partial t$) that are animated within a dielectric solid [2-8]. In practice, this is achieved by placing a series of electrodes on either side of a strip of dielectric (polarizable medium) [2-8,10]. The application of voltages to the electrodes creates a polarized region within the dielectric, which can be moved by varying the voltages on the electrodes in sequence. It is important to note that the emitted radiation is not created by the electrodes, which merely act to apply a voltage across the dielectric, but by the polarization current itself [8]. In consequence, SPCAs are distinct from phased arrays in that they are true volume sources, whose radiation characteristics are entirely dependent on the speed and acceleration of the moving polarization as well as the shape of the dielectric that contains it [2-9].

Indoor and outdoor experiments as well as numerical simulations have established the correlation between polarization current and radiation pattern [6-9]: by controlling the phase difference between the electrodes, the current can be animated at will, directing the emission as desired. The dielectric shape accounts for the beam width, height of the side lobes and the position of nulls, whereas the dielectric constant, εr, determines the optimal operation frequency [1,8,10]. Adding acceleration produces a radio-wave analog of the "sonic boom" in acoustics; this gives emitted radio waves that can either be focused at a distance or used to transmit low-power signals over very long ranges. Prototype general-purpose active SPCAs have already demonstrated advantages over conventional technology for path lengths of up to 50 miles [7], showing that, with further optimization, the technology could translate to industry and defense applications.

SPCA emission cannot be calculated using commercial electromagnetic packages; these neglect contributions to the emitted fields that, that though very small in conventional antennas, can become large in SPCAs because they are true volume sources and waves from multiple retarded times can arrive simultaneously at an observation point [8,11]. However, LANL achievements mean that this technology is now ripe for more widespread exploitation. First, passive SPCAs (i.e. without active electronic control) have been demonstrated [7]. Second, several theoretical and computing challenges have been overcome so that for the first time, it is possible to model the radiation from a SPCA successfully [1,8].

This project therefore sought to optimize SPCA designs to produce practical antennas that can be used for specialized applications in the field and that are economical to produce. The optimization followed three thrusts. (i) Thus far, SPCAs have been built up from individual elements that contain the electrode pairs that are used to produce and animate the polarization within

the dielectric [5-7,8,10]. Each element also contains the feed from the signal/control electronics, providing impedance matching and transforming the signal into the form required to produce the desired polarization current. A considerable optimization effort was therefore applied to making the elements as compact and efficient as possible. (ii) The polarization current itself can also be optimized for desired emission via its motion/time dependence and the geometry of the dielectric within which it flows. (iii) Finally, as the project unearthed several more potential future applications for SPCAs, the underlying antenna design was optimized for economy and ease of production.

Scientific Approach and Accomplishments

Antenna element and feed optimization

The first generation of SPCAs performed well, but the individual antenna elements were complicated to build (Figure 1a) and required individual "tuning" before they were incorporated into the complete antenna [2,10]. This design employed a vertical coaxial feed; the impedance matching and mode transformation (from coax TEM to linearly polarized electric field across the dielectric) employed small features sensitive to positioning [2]. Shielding of electric gaps in the electrode separations was also required, and each individual array element had to be assembled separately. A primary optimization task was therefore development of concepts to remove many of these issues. The most important change was to use stripline feeds for the signals, rather than coaxial lines. This adds ruggedness and, due to a flat foot-print, allows surface mount applications that would have been difficult to achieve with the original design. Figures 1b and 1c show a single element based on the final improved design. Further simplicity in the new design results from the coupling mechanism from the antenna patch at the end of the stripline radiating into the stepped cut-out of the element body (Figures 1b and 1c). This concept does not need any further impedance matching beyond the increasing steps of the cut-out.

The first iteration of this new configuration still required separate fabrication of each individual antenna element. This requirement was driven solely by the use of metallic shielding strips separating neighboring striplines. Further design optimization removed the need for the metallic shielding; decoupling of strips is instead achieved by adding a pin that provides a return path for the surface currents in the metallized body of each antenna element. Figures 1c and 1d show the pin locations; Figure 1d also shows the surface current flow.

Another noteworthy design feature is the short in the stub at the end of the stripline and antenna patch (Figure 1c). The introduction of a break in the antenna element metallic surfaces would have required complex shielding. We learned from the first iterations that this adds significant complexity. It turns out that the stub, where the antenna signal connects to the electrode is highly impedance mismatched and shorting does not affect the performance (Figure 1c). This significantly simplified the design.

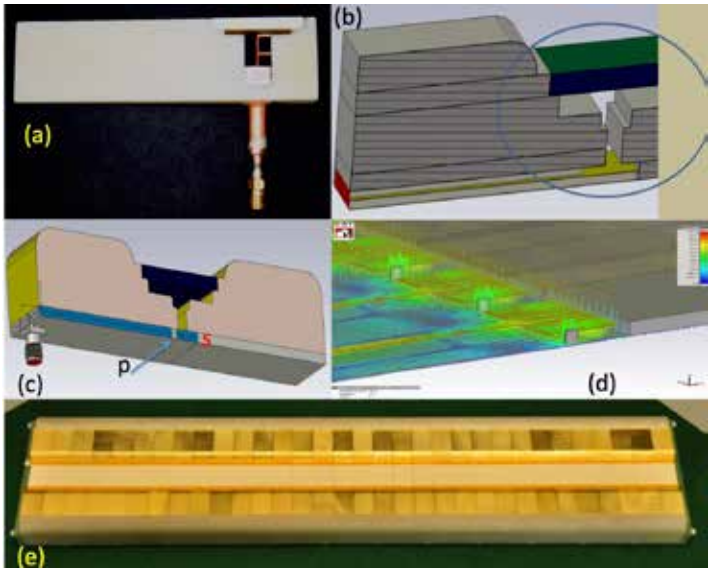

Figure 1. (a) First-generation SPCA element. This was the result of an earlier LDRD-DR project. The signal comes in through the coaxial feed at the bottom. The signal voltage is transformed into the correct geometry to induce polarization in the alumina slab (white block) at the top by the arrangement of small copper parts underneath. (b) New design of SPCA element; the signal is fed through a flat stripline (end shaded red, sides gold) to the stepped cut-out in the element. This transforms the signal into the correct geometry to induce polarization in the dielectric (green). (c) Perspective view of new design showing the shielding pin (labeled p) and the short (labeled s in red). The metal that coats the top surface of the plastic body is shown in gold. (d) Computer model of the shielding effect of the pins; colored lines show the strength of the electric field. (e) Photograph of the completed antenna, consisting of 32 elements.

Based on these developments and a dielectric size determined from the calculations below, a fully functioning antenna was built from 32 individual elements and tested (Figures 1e and 2a). Compared to conventional antennas and previous SPCAs, the design is exceptionally flat and compact. As it is likely that most future mass-produced SPCAs would be based on such a concept, it was patented [12] (see also amendment to [4]). In addition to having several advantages over a similar-sized phased array (Figure 2b), this SPCA's exceptionally flat geometry has led to a suggestion for future antennas built into ceramic tank armor; the ceramics proposed for the armor could be workable dielectrics that would function as part of an SPCA. Integrated armor/antenna applications will form the basis of a future proposal, possibly in collaboration with TARDEC

(The United States Army Tank Automotive Research, Development and Engineering Center).

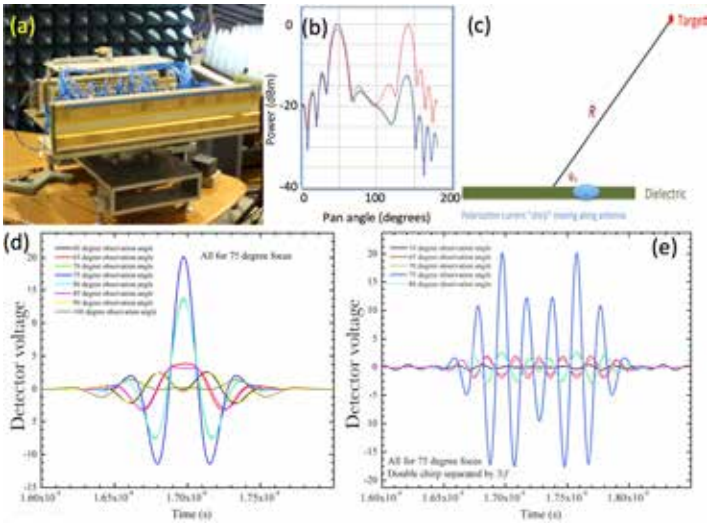

Figure 2. (a) Antenna 1 on a turntable being prepared for tests in the LANL TA-35 anechoic chamber. (b) Angle dependence of power from a 32 element SPCA (blue), a 16 element SPCA (green) and a phased array of the same length (red). The SPCAs show better efficiency (more power in the desired direction) and superior suppression of both sidelobes and the extra peak due to aliasing in the phased array. (c) Geometry of the secure communication models and experiments; the signal from the moving polarization-current chirp (light blue) is targeted at a point a distance and angle ψ relative to the antenna (dark green). (d) The signal received versus time for various angles of transmission (shown in inset key); the antenna used in the model is similar to that in (a). At the desired target angle (75), the chirp is reproduced exactly. As one moves away from the target angle, the chirp is distorted and eventually becomes unrecognizable (even the frequency content changes). (e) Reception of double chirp; the proper shape of the signal is reproduced at the target angle (see inset key for line colors), but nowhere else: information is only understandable at desired location. This gives the possibility to send information securely without encryption.

Optimization of the polarization current

As mentioned above, there are several unique features of SPCAs as sources of electromagnetic radiation [5,7,8]. (1) They are true volume sources; the signal to be transmitted exists over the entire volume of the antenna, rather than at a series of lines and points (as in a phased array). (2) If the polarization current is accelerated, there is no longer a simple correspondence between reception time and retarded time. (3) The acceleration of the polarization current gives the possibility of focusing the signal at large distances. Bearing all of these factors in mind, the time structure, spatial extent/volume and acceleration of the polarization current are all suitable subjects for optimization.

During the course of this phase of the project, it was found that the exceptional long-range performance of the prototype SPCAs is likely due to short-timescale variations of the signal [1], so pulsed or "chirped" polarization-current patterns were examined. It became apparent that such patterns could be used to transmit a signal that is only understandable over a small region near a target, and scrambled elsewhere. The extended volume of the polarization current (attribute (1) above) means that there are destructive and constructive interference mechanisms possible in SPCAs that do not exist in phased arrays. Along with attribute (2), this forms the basis of information scrambling. A new acceleration scheme was invented, whereby the component of a polarization current chirp's velocity in the direction of the target point is always the speed of light, c. This means that all temporal information in the chirp collapses to a single arrival time at the target, i.e., information carried by the chirp's shape is reproduced there, and only there [9].

Figure 2c illustrates the geometry of the effect, whilst Figure 2d shows the reception of a chirp signal; at the desired target angle (in this case 75o, set by the parameters of the acceleration), the chirp is reproduced exactly. As one moves away from the target angle, the chirp is distorted and eventually becomes unrecognizable (Figure 2d; even the frequency content changes). To examine how this would affect a modulated signal, two closely-spaced chirps were used. Figure 2e shows that the modulation is observable at target angle, but lost quickly as one moves away. Hence it is possible to transmit information securely without the need for encryption; only the location of the recipient is needed. This is the subject of a patent application [9].

Turning to the three-dimensional shape of the dielectric that hosts the polarization current, initially, it was hoped that level-set topology optimization [13] would prove a suitable tool for optimizing the detailed shape of the dielectric. However, the method, developed for mechanical components in aircraft, proved difficult to constrain sufficiently in electromagnetic applications. A solution for this was found to be possible, but time-consuming and beyond the resources of the present project. Therefore, within the time constraints of the project, and so as not to delay the production of the second antenna, a simpler "geometrical" optimization routine was adapted [1], producing several useful outcomes. First, this computational work and its experimental validation showed that dielectric layers can have a dramatic (and previously ignored) focusing effect on emitted radiation, even when they are much smaller than the wavelength λ [1,7]. Second, the numerical models showed that SPCA technology is scalable, and that SPCAs can be produced in a wide range of configurations and ge-

ometries. Third, it was shown that one of the roles of the dielectric in an SPCA is to increase its apparent electrical size [1,7]. All of this suggests that in future, since dielectrics and metamaterials can easily be cut, shaped or cast, novel topologies can be created using multivariate material and topological optimization methods, approaches which have, so far, hardly been pursued in antenna design, primarily due to the challenges associated with the fabrication of inhomogeneous materials, the limited access to analysis tools and, frankly, in traditional antennas, the absence of a topology to be optimized. The optimized product can be cut or printed in three dimensions, using, for example, additive manufacturing. This idea will form the basis of a future proposal.

As an example, a pilot study of possible uses of very large-scale SPCAs (and related technologies) was carried out, motivated by our characterization of a foam-based metamaterial with dielectric constant $\varepsilon r \approx 4$ and density ~ 0.1 g/cm3 (Figure 3(a)). Because this dielectric is much less dense than, say, alumina, and potentially available in large quantities, it means that very large dielectric-based antennas are now feasible for the first time. A possible application is in VLF (very low frequency) antennas [15]. These use frequencies from 3 to 30 kHz (λ = 100-10 km); the technology is old and "state of the art" stations date from the 1960s. Since VLF penetrates ~40 m of saltwater, it is the means of communication with nuclear-deterrent submarines. Other strategic uses include military navigation systems employed during/after global disaster or nuclear war. VLF propagation demands vertical polarization; unfortunately, the large λs mean that conventional $\lambda/2$ dipoles or $\lambda/4$ monopoles are 2.5-50 km high [15]! Hence, practical VLF transmitters, though 200-300 m high (Figures 3b and c), are a tiny fraction of λ. Besides their height, VLF transmitters are often >1 km across (Figure 3c); a central monopole is linked to surrounding masts by a network of cables serving as a capacitive load to increase efficiency [15]. A lower network of cables reduces power dissipated in the ground. Despite this complexity (and vast cost), VLF transmitters are inefficient, radiating only 10 to 50% of transmitter power (MW) [15]. Their size and visibility (Figures 3b and 3c) makes them impossible to hide and vulnerable to attack. Using techniques derived from our modeling of SPCAs plus the cheap metamaterial we considered whether an economical structure with the size and engineering properties of a large industrial chimney, or a two-floor parking structure or even a convoy of vehicles, each serving as the element of a SPCA, be more efficient than current VLF transmitters. Our pilot study suggests that this is indeed feasible (see Figure 3c); it will be the subject of a future proposal.

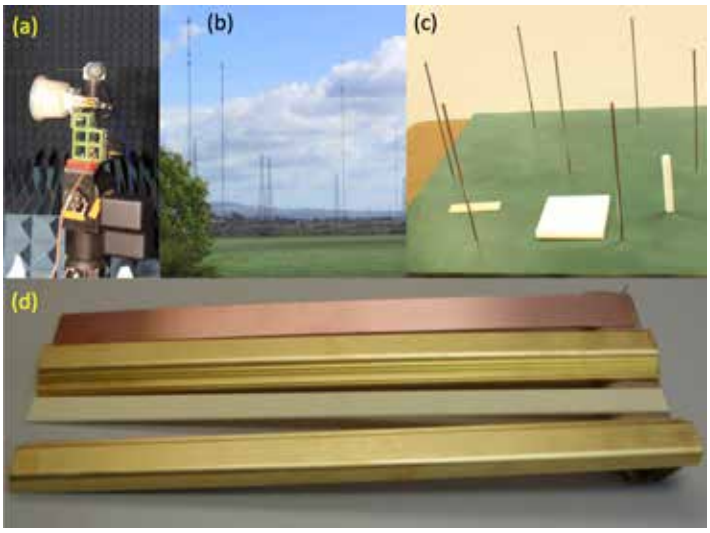

Figure 3. (a) Metamaterial dielectric under test in the LANL TA-35 anechoic chamber. The metamaterial (pale pink) is in a transparent pot surrounding a test antenna on a pan/tilt mount in the foreground; the detector (gray) for the emitted radio waves can be seen in the background. (b) Part of a Navy VLF antenna array. (c) 1:1200 scale model of a typical VLF antenna (metal poles, each of which is about 300 m high). The white cylinder, white square and light-green rectangle show possible replacement antennas based on SPCA technology to the same scale. (d) Monolithic parts of antenna 2, prior to assembly. The copper slab is the base plate; the gold pieces are the two halves of the stepped housing and the white item is the dielectric (c.f. Figure 1). Each component can be made using a few simple cuts of a CNC mill.

Production optimization

A final goal was flexibility and ease of fabrication that could be used to optimize an antenna for a particular application without a complete redesign and development of new tooling fixtures. Rather than employing separate elements, a monolithic configuration of the plated antenna body and polarization dielectric was used; this could be achieved with a minimum of simple cuts using a CNC mill. To achieve flexibility sufficient for a variety of future applications, this was combined with a variable layout of striplines on a single PCB with separations defined by the shielding pins. Thus a fast polarization current with a small phase advance per element can be synthesized with a small number of elements; slower (close to the speed of light) operation (for an end-fire antenna) works best with narrow spacing that decreases the otherwise large phase advance from element to element. Either SPCA can be achieved by a simple change in the stripline circuit board. The monolithic components of the second antenna, constructed according to these principles, are shown prior to assembly in Figure 3d.

Impact on National Missions

Work on the SPCA antennas has led to IP relevant to global security, remote sensing and communications, pivotal to LANL core missions, representing a potential high-payoff quantum leap in multi-role antenna design and fabrication. We maintain working relationships with Mike Everhart-Erickson (FCI- interface to commercial sponsors); Jay Kucko (XTD-PRI/USAAF); Jon Schoonover (GS-ET/Joint Chiefs of Staff); Steve Girrens (ADE-ES); and Bob Shirey (GS-IDC) to ensure appropriate dissemination of results. This work could help to give back to the US a lead in antenna technology, reducing dependence on imported components from e.g. China. Briefings on the technology are given to SPAWAR, the Air War College, TARDEC, DIA and other interested government agencies, to ensure appropriate and effective use of these ideas.

References

1. Schmidt, A. C., and J. Singleton. Quantitative numerical calculations of the emission of accelerated, superluminal polarization currents in a variety of antenna topologies. 2016. Internal report (LANL) intended for publication after protection of IP.

2. Singleton, J., F. L. Krawczyck, L. Earley, and Q. Marksteiner. Superluminal Antenna. 2013. US Patent 20130201073.

3. Singleton, J., H. Ardavan, and A. Ardavan. Apparatus and method for phase fronts based on superluminal polarization current. 2010. US Patent 20100039324.

4. Singleton, J., F. Krawczyk, K. Linehan, and A. C. Schmidt. Feed network and electromagnetic radiation source. 2015. US Patent 20150325914.

5. Singleton, J., A. Ardavan, H. Ardavan, J. Fopma, D. Halliday, and W. Hayes. Experimental demonstration of emission from a superluminal polarization current- a new class of solid-state source for MHz-THz and beyond. 2004. IEEE Digest. 04EX857: 591.

6. Singleton, J., A. C. Schmidt-Zweifel, and J. Wigger. Tests of the Linear Superluminal Antenna done for and in collaboration with CommScope. 2013. CRADA report (2013), IP and commercially sensitive, available on request..

7. Singleton, J., A. C. Schmidt-Zweifel, F. Krawczyk, H. Lu, C. B. Bailey, and J. Wigger. A report on the current status of antennas employing accelerated superluminal polarization currents. 2016. Internal report (LANL) intended for publication after protection of IP. Commercially sensitive..

8. Schmidt-Zweifel, A. C.. “Terrestrial and extraterrestrial radiation sources that move faster than light”. Master of Science Thesis. 2012.

9. Schmidt-Zweifel, A. C., and J. Singleton. Radio transmission of information in a specific direction and nowhere else. 2016. LANL IDEAS 1500121 (2015) and US Patent, submitted (April 2016)..

10. Singleton, J.. Eighteen-Month Report on LDRD 20080085 DR: Construction and Use of Superluminal Emission Technology Demonstrators with Applications in Radar, Astrophysics, and Secure Communications. 2010. Internal report (LANL) available on request.

11. Ardavan, H., A. Ardavan, J. Singleton, J. Fasel, and A. Schmidt. Inadequacies in the conventional treatment of the radiation field of moving sources. 2009. J. Math. Phys.. 50: 103510.

12. Krawczyk, F., J. Singleton, and A. C. Schmidt. Optimized Antenna Elements for Communication Applications of Superluminal Sources. 2016. LANL IDEAS 1500061 (2015), US Patent submitted (2016).

13. Dunning, P. D., and H. A. Kim. Introducing the Sequential Linear Programming Level-set Method for Topology Optimization. 2014. Struct. Multidisc. Optim. . 51 (3): 631.

14. Ultralightweight cylindrical lenses used to triple the capacity of cell base-station antennas. 2015. CommScope press release.

15. Folkestad, K.. Ionospheric Radio Communications. 2013.

Publications

Schmidt, A. C., and J. Singleton. Quantitative numerical calculations of the emission of accelerated superluminal polarization currents in a variety of antenna topologies. 2016. Internal report (LANL) intended for publication after protection of IP.

Singleton, J., A. C. Schmidt-Zweifel, F. Krawczyk, H. Lu, C. B. Bailey, and J. Wigger. A report on the current status of antennas employing accelerated superluminal polarization currents. 2016. Internal report (LANL) intended for journal publication after protection of IP.

Traynor, D. S.. Application of Superlumial Radar to maintain air superiority in 2035. 2016. White paper, Air War College, Air University (USAAF).

Improved Micro-Mirror Arrays for MEMS-Based Adaptive Hyperspectral Imaging (MAHI) Sensor Validation

David L. Graff
20160663ER

Abstract

The pairing of cognitive sensing and spectral imaging presents a number of intriguing opportunities to address outstanding national security needs. Through the use of a highly adaptable spectral imaging sensor, cognitive sensing approaches could be used to learn about the spectral characteristics of an environment, adapt the sensing strategy of the sensor to the environment, and optimally monitor the environment with real-time data products (e.g. full motion video). The Micro Electro-Mechanical Systems (MEMS) -based Adaptive Hyperspectral Imaging (MAHI) sensor, developed by Los Alamos National Laboratory, has demonstrated a "learn – adapt – monitor" approach to applications such as detecting methane leaks and tracking targets in dynamic scenes. The enabling technology of the MAHI sensor is a MEMS micro mirror array (MMA) that provides the user with complete control over the spectral content of the images that are formed by the sensor's camera. Previous work with commercially available MMAs has successfully demonstrated this "learn – adapt – monitor" approach, but featured poor image quality and increased system complexity attributable to MMA design characteristics. This work investigates the feasibility of using a new MMA design that has the potential to greatly simplify the MAHI sensor design, lead to improved image quality, and enable miniaturization efforts for future handheld and Unmanned Aerial Vehicle (UAV) applications.

Background and Research Objectives

The MAHI sensor was developed at Los Alamos National Laboratory through funding from the Laboratory Directed Research and Development (LDRD) program. This sensor is unique in the spectral imaging community in that the spectral response of the sensor is rapidly reconfigurable in real time through the use of MMA technology. This enables the MAHI sensor to take advantage of new cognitive sensing approaches that require highly agile sensors to learn, adapt, and monitor a scene. We have successfully demonstrated some of these approaches in a laboratory setting with versions of our MAHI sensor.

The MMA technology used in previous MAHI prototype sensors is commercially available and packaged as a kit with software and control electronics for easy integration with research prototypes. While highly successful at demonstrating the underlying sensing concepts, these arrays only operate in the visible (vis), near-infrared (NIR), and shortwave infrared (SWIR) spectral regions and were found to introduce unacceptable artifacts into the image that required significant optical engineering efforts (and a second, identical MMA) to ameliorate. This ultimately limits the achievable image quality and size of the sensor.

With this work, we are testing the hypothesis that an alternative MMA design, one in which individual mirrors can be laid "flat," or in the plane of the device, will not introduce these artifacts and will enable both simpler and smaller optical designs for use in handheld or UAV applications. Previously, we were able to identify a commercially available MMA that would satisfy both our "flat state" requirement, and our desire that the individual mirrors be large enough for operation at longer wavelengths in the mid-wave infrared (MWIR) and the long-wave infrared (LWIR). Here we describe the results of our four-month effort to integrate, test, and demonstrate this new array to validate its use for future MAHI designs.

Scientific Approach and Accomplishments

The vendor that provided the MMA was unable to provide either control electronics or software that provide the high voltage signals required to drive the array. Thus, our first task was to fabricate a fixture that would hold the MMA and establish the required electrical connections to individually control the mirrors of the array. The fixture is shown in the left panel of Figure 1 and features three headers arrayed about the MEMS chip to provide

connections to three, 32-channel high voltage controllers and provide nominal control over 96 individual mirrors. The MEMS chip itself was integrated into a ceramic chip carrier and hermetically sealed (right panel of Figure 1). Part testing during this task detected the loss of three connections due to a design oversight and reduced our total number of controllable mirrors to 93.

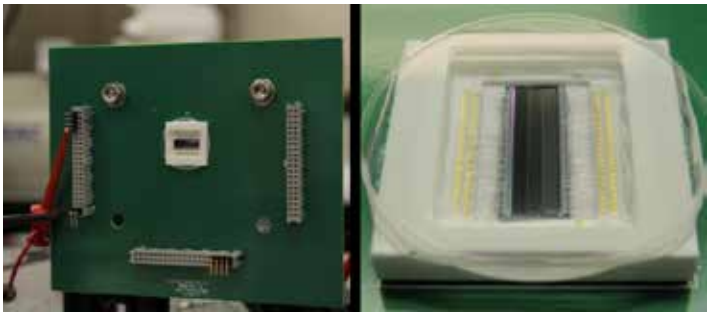

Figure 1. Photograph of the fixture as fabricated with leads for part testing (left) and a close-up photo of the MMA as integrated into a hermetically sealed environment (right).

The second task of this work was to test the array and ensure that each mirror is individually controllable. The procedure was to measure the current drawn by the circuit when a small amount of voltage was applied to the header pin connected to each mirror. Because these are capacitive devices, a functioning mirror should draw no current once fully charged. While the majority of mirrors in the array successfully passed, a small number of mirrors (12 of 93) presented leakage currents up to 0.1 μA at 10 V and failed testing. Consultations with the vendor and inspection under a high-power microscope suggest that small particles of dust may be contaminating the electrical characteristics of the mirror's control surfaces. We were advised not to apply high voltage to these mirrors due to the risk of damage to the array. Follow-up with the vendor may lead to a solution to this issue, or a replacement chip. We were able to test one of the functioning mirrors at high voltage. We found that the mirror performed as described in the vendor's documentation, producing observable deflections of a laser beam, increasing with voltage up to 150 V.

The third task of this work was to assemble a breadboard optical system based on a MAHI design and test our hypothesis that a "flat-state" MMA would not introduce the artifacts observed with previous MMAs. While ultimately successful, this task was hampered by two factors. First, the 12 dead mirrors that were identified above were irregularly distributed and we were unable to find a contiguous section of the array that would support the acquisition of spectrally modified images. Second, the software that was delivered with the high-voltage controllers did not work and we were unable to develop a custom solution to independently control individual mirrors in the array within the time and budget of a four-month project. As a result, we were not able to repeat previous demonstrations of MAHI-style spectral imaging. However, we were able to obtain images with the array in the "flat state" and validate our key hypothesis.

The optical system that was used to test the imaging effects of the array is shown in the left panel of Figure 2. It includes collection optics that forms an image of the scene on the grating (located on the translation stage), a lens pair that projects the spectral content of the scene across the MMA, and a commercial camera that reimages the scene. The right panel of Figure 2 shows the MMA as viewed by the camera under illumination by a fluorescent light bulb. The colored stripes in the center of the array are characteristic of the mercury vapor emission spectrum that dominates the output of fluorescent lighting. The resulting optical system is significantly smaller than our previous prototypes, and requires fewer optical elements. The volume could be reduced further with folding mirrors or new, novel optical designs that leverage the new MMA design.

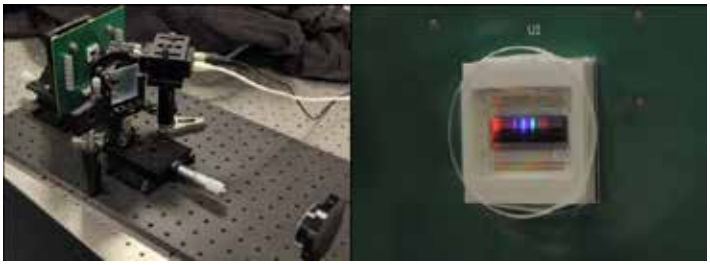

Figure 2. Photographs of the optical system used to demonstrate the achievable image quality with the new-style MMA (left) and the MMA illuminated by a fluorescent light source in a MAHI optical system (right). The clearly defined lines in the center of the array are characteristic of the mercury emission spectrum that dominates the fluorescent lamp output.

Measurements of image quality were made with the MMA in its "flat-state" to test the hypothesis that image quality is greatly improved by the new-style MMA. Previous MAHI sensors produced images of poor quality due to artifacts introduced into the image by the old-style MMAs. These images featured multiple, in-focus images at different wavelengths with slight spatial offsets, which gave the overall appearance of being out of focus. We found that the images acquired with the new-style MMA (left panel of Figure 3) also display small amounts of blurriness due to the sensor's depth of field, but do not display the multiple image blurriness due to MMA artifacts indicating that our hypothesis about the new-MMAs is correct.

Figure 3. Sample images acquired with the optical system showing typical imaging performance of an extended object (left), a standard spiral-type compact fluorescent bulb with an unsaturated sensor (center) and strongly saturated sensor (left). Images of extended objects reveals small issues with focus across the object, but does not exhibit the mis-alignment of otherwise in-focus images typical of the old-style MMAs. Saturation images show two kinds of artifacts due to critical design parameters of the new-style MEMS array and their relative power to the core image. The near field ghosts are more than 10x times less intense than the core image and will impact the diffraction-limited performance of the sensor.

MAHI sensors based on the new-style MMAs are not wholly free of artifacts, as these MMAs still behave like diffraction gratings and will cause ghost images to appear in the sensor's field of view. The relevant questions are: where are the ghost images, and how bright are they relative to the core image. The right two panels of Figure 3 demonstrate these effects by saturating the core image and revealing the cascading ghost images to the left and right. Here a standard spiral-type compact fluorescent bulb is imaged under non-saturating conditions in the center and saturating conditions on the right. Using laser sources we have determined that these artifacts are indeed quite small relative to the core image (less than x10), but as we move forward, it will be critical to understand how design parameters of the MMA (i.e., mirror pitch, mirror height, etc.) impact these important artifacts.

Impact on National Missions

The MAHI sensor has generated significant interest from sponsors interested in agile spectral imaging sensors for handheld and UAV application. Maturing the MAHI technology will require a new kind of MMA than was used in previous efforts. This effort has provided a critical demonstration of the impact of a "flat-state" MMA that eliminates the need for additional optical elements to compensate for MMA artifacts in the optical system. These new micro-mirror designs will eliminate significant optical challenges to MAHI miniaturization and greatly improve image quality and sensor performance. Additionally, this effort has provided important data and knowledge for our conversations with MMA fabrication partners to guide new designs optimized for miniaturized MAHI sensors.

Exploring Advanced Diagnostics with hiRX

Kathryn G. Mcintosh
20160665ER

Abstract

Plutonium (Pu) accountancy is an important aspect of safeguards operations at nuclear fuel reprocessing facilities. High resolution X-ray (hiRX) is a novel X-ray fluorescence spectrometry (XRF)-based approach that has been proven effective for rapid measurement of Pu content in process solutions. In this study, the feasibility of using hiRX to make real-time flow measurements in nuclear material reprocessing plant environments was evaluated. Prototype flow cells were produced and performance characteristics such as ease of use, precision, and accuracy were assessed using a breadboard hiRX instrument. The use of a flow cell improved repeatability relative to the existing approach relying on disposable sample microcells. Linear calibrations were demonstrated with various flow modes, and real-time data on small volumes of flowing sample were successfully collected in the laboratory. The potential for using a flow cell for sample presentation was successfully demonstrated and the results provide a basis for design and execution of a fixed geometry flow system in the hiRX prototype instrument. This expansion in capability will help to improve the accuracy and reduce the uncertainty in nuclear materials accountancy and will allow hiRX technology to meet a wider range of safeguards needs.

Background and Research Objectives

Safeguards operations at nuclear fuel reprocessing facilities require accurate Pu accountancy in order to prevent inventory difference or diversion of materials. While there are several nondestructive and conventional approaches available to accomplish this, including hybrid K-edge densitometry, alpha spectroscopy, and isotope dilution mass spectrometry, each requires either the use of significant modeling and assumptions or complex sample preparation. hiRX is a new XRF technology for the direct, rapid, accurate, and nondestructive determination of Pu in spent fuel dissolver solution and related matrices. hiRX is based on monochromatic wavelength dispersive X-ray fluorescence (MWDXRF) in which two novel doubly curved crystal optics (DCC) provide selective detection of actinides. Because of its unique characteristics, hiRX offers the ability to make more frequent measurements at more key measurement points, thus decreasing the uncertainty in the Pu inventory.

The analytical performance of a prototype benchtop hiRX instrument was recently evaluated in a reprocessing facility. The results of the study showed hiRX to be accurate and sensitive for determination of Pu and uranium (U) in process solutions [1]. Advantages identified that set hiRX apart from other Pu quantification approaches include rapid results without significant sample preparation (<10 min/sample) and enhanced safety with reduced waste (7 µL sample volume). Potential application areas including material control and accountability, waste monitoring, and product specification were identified. The use of a disposable microcell for sample presentation was identified as a source of measurement uncertainty, and it was hypothesized that a fixed geometry flow cell would enhance performance of the hiRX prototype. Further, development of a flow-based system would expand the capabilities of the hiRX technology beyond the laboratory to applications in on-line monitoring, which would be of interest in a reprocessing facility. Figure 1 depicts the hiRX benchtop prototype with the sample microcell in the inset.

The aim of this effort was to explore the feasibility of using hiRX to make real-time flow measurements in nuclear material reprocessing plant environments. Specific objectives included: production and testing of a microfluidic flow cell for characteristics such as ease of use, prevalence of bubble formation, and resistance to acidic matrices; assessment of analytical performance metrics including accuracy, precision, and sensitivity; and modifications to hiRX software to allow real-time data collection for transient signal.

Figure 1. hiRX benchtop prototype instrument and sample microcell in mounting apparatus (inset)

Scientific Approach and Accomplishments

This project leveraged existing capabilities and expertise in the use of hiRX technology for Pu and U determination, including a breadboard hiRX instrument. The breadboard hiRX offers flexibility in both sample positioning and data collection, thus it was well suited to use in this feasibility study. Strontium (Sr) was used as a surrogate analyte for Pu in order to eliminate the hazard and difficulty of working with radioactive solutions. This was possible due to the nearly coincident characteristic X-ray lines for Sr (14.164 keV) and Pu (14.279 keV). For the metrics studied, Sr performance is representative of that expected for Pu.

Two types of flow cells were prototyped for evaluation, one designed for aqueous sample solutions only (type 1) and one which uses an oil carrier along with aqueous samples (type 2). The devices were produced at LANL using a rapid prototyping approach which has been previously described [2]. A laser cutter was used to pattern features such as a chamber and channels into the layers of material including polycarbonate and adhesive that make up the cell. The devices were designed to dimensions similar to the hiRX microcell so that the two sample presentation methods could be compared, and so that the flow cell could in the future be evaluated in the prototype hiRX without significant modification to the instrument. The produced cells are approximately 4 x 3 cm in size with a 5 x 3 mm sample chamber. With a depth of 1 mm, the chamber holds approximately 15 µL of sample. The type 1 device has two ports to serve as sample input and output, while the type 2 device has an additional port for oil carrier input. Commercially available Tygon and silicone tubing and a three-channel Ismatec peristaltic pump were used with the flow cells. Novec hydrofluoroether (HFE) 7500 fluid was used as the oil carrier in the type 2 device.

Initial evaluation efforts focused on suitability and functionality of the flow cells. A type 1 device was demonstrated to be sufficiently resistant to acid based on filling the chamber with 2M HNO3 and monitoring for leaks over 24 hours. This is a relevant consideration for flow cell development as fuel dissolver solution is a highly acidic matrix. Sample flow rates were evaluated and found to play a significant role in the prevalence of bubble formation. It is imperative that bubbles not impinge upon the analysis region (a spot of approximately 200 µm diameter for the breadboard instrument) as this will reduce signal intensity and may impact both accuracy and precision. Flow rates greater than 15 µL/s were associated with the formation of large bubbles in type 1 devices. In type 2 devices, high sample flow rates and extended use produced a heterogeneous oil carrier and sample mixture in the analysis chamber. Lower flow rates of 1-5 µL/s were optimal for type 1 and were consistently used without observation of bubbles. Figure 2 shows a type 1 device with an inset depicting bubble formation and Figure 3 shows a type 2 device. Ease of use considerations were found to favor the type 1 device over type 2 in this feasibility study. This is due to the need to optimize two flow rates (one for the sample, one for the oil carrier) and to the generation of a mixed waste stream for type 2. This approach offers the advantage of automatically generating drops of sample in a repeatable fashion, and was expected to have a lower incidence of bubbles due to elimination of air in the input line and flow cell. In practice, bubbles were observed more frequently in this system than in type 1, so it was not selected as the primary focus of this study.

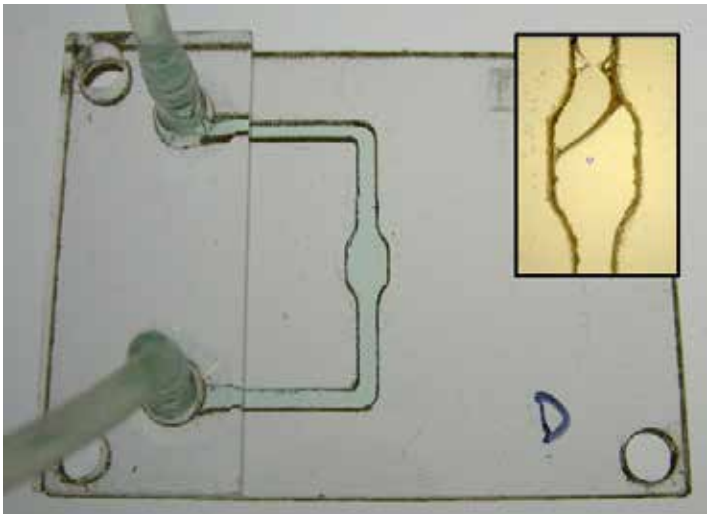

Figure 2. Flow cell prototype (Type 1) filled with blue colored aqueous sample and bubble captured in analytical chamber (inset)

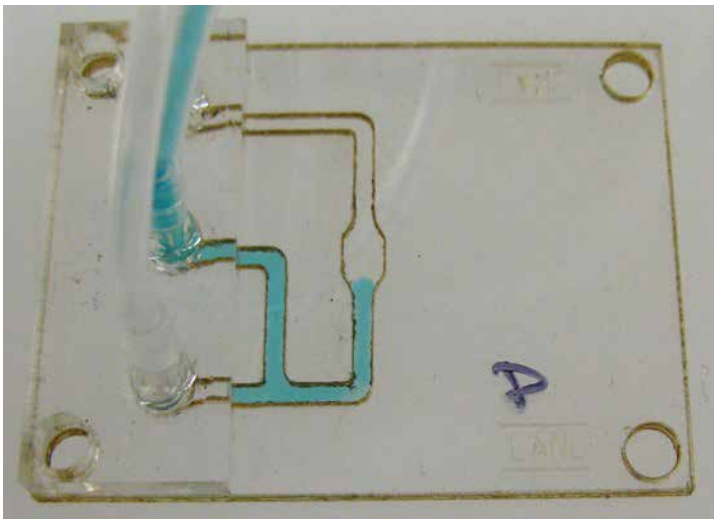

Figure 3. Flow cell prototype (Type 2) filled with blue colored aqueous sample and clear oil carrier

An important aspect in evaluation of the type 1 device was characterizing performance in calibration. Three variations on sample flow were tested in triplicate 100 s measurements, including static, flowing at 5 µL/s, and refreshed (static during measurement but fresh solution flowed into chamber prior to each measurement). The results are shown in Figure 4. All modes produce a linear response, with the static approach having only a slightly higher count rate, and average precision is similar between 2.7 and 3.2% relative standard deviation (RSD). The limit of detection (LOD), which is a measure of sensitivity, is approximately 6 mg/L for a static sample. Accuracy was assessed using additional standard solutions, and is marginally better for flowing (-3% bias) than refreshed (-5% bias) samples. A possible diversion event was simulated by measuring a series of aliquots of 1000 mg/L and 940 mg/L Sr. Results showed that this 6% decrease in concentration was detectable as a 2-4% reduction in signal intensity.

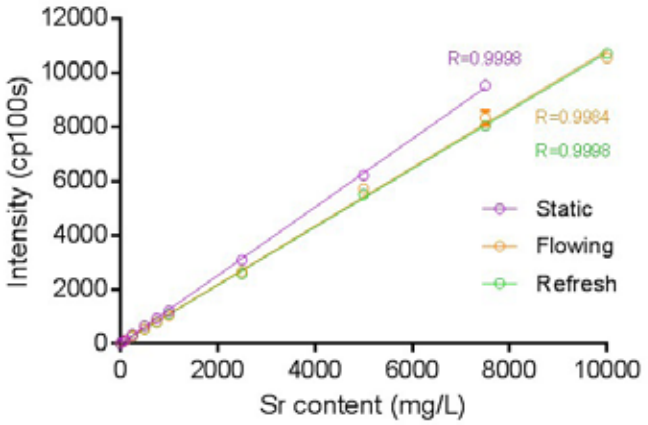

Figure 4. Calibration results for various flow modes (Mean +/- Standard Deviation, n=3)

As part of this effort, the hiRX LabVIEW-based software user interface was enhanced to allow the continuous collection of real time flow data in a chromatogram format (time on X axis and signal on Y axis). Figure 5 shows data collected in this manner for a series of 50 µL standard aliquots flowing at approximately 5 µL/s. A linear calibration (R2=0.99) was also attained using this approach. The fact that the signals are transient makes optimization of introduction and flow parameters as well as signal processing crucial for quantification. The accuracy of the injected sample volume impacts the peak width and thus integrated count rate significantly, while sample volume is less important when constant signal is measured.

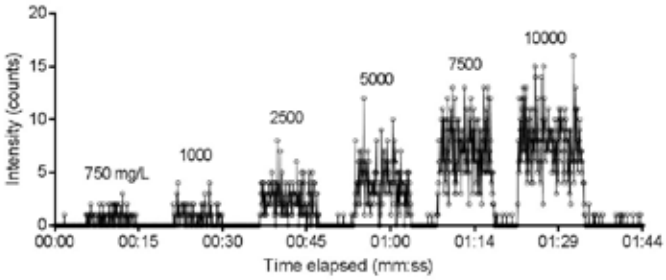

Figure 5. Real time flow data for Sr standard solutions from 750 to 10000 mg/L (50 µL each flowing at 5 µL/s)

The main benefit of a flow cell was expected to be better repeatability as compared with use of disposable microcells. This is because small differences in filling with a pipette, microcell dimensions (even with strict manufacturing tolerances), and positioning can lead to variability in measured Sr intensity, while the use of a fixed geometry flow cell eliminates these considerations. Comparison between triplicate measurements of 1000 mg/L Sr in four hiRX microcells and as four aliquots of sample introduced into the type 1 flow cell shows a substantial improvement from 9% to 2% RSD.

This study demonstrates the feasibility of using a flow cell for sample presentation and suggests that real-time flow measurements could be made with hiRX in a reprocessing environment. Testing of the prototype cells produced excellent results for instrument calibration and repeatability, and showed improvement over existing methods. These data were highlighted in a presentation on hiRX at the Advances in Nuclear Nonproliferation Technology and Policy Conference (ANTPC) sponsored by the American Nuclear Society in Santa Fe on September 26, 2016.

Impact on National Missions

The success of this effort provides a foundation for design and execution of a fixed geometry flow system in the hiRX prototype. These results will direct future efforts on hiRX

project development towards specific hardware and software improvements that can be expected to significantly enhance performance and thus improve the accuracy and reduce the uncertainty in nuclear materials accountancy. Implementation of a flow cell approach will have a transformative impact in improving bias and precision in this type of laboratory analysis, extending the breadth of application spaces for the technology. Further, this expands characterization capabilities beyond the laboratory and provides opportunities for program development in on-line or at-line measurements. This demonstration of XRF-based elemental analysis with a microfluidic flow cell also provides a basis for future exploration of small scale sample processing and separations.

References

1. McIntosh, K., G. Havrilla, R. Gilmore, Jr, and M. Holland. hiRX performance testing at SRNL using spent nuclear fuel. 2016. Los Alamos National Laboratory Report (LA-UR-16-20357 Version 3).

2. Nath, P., D. Fung, Y. Kunde, A. Zeytun, B. Branch, and G. Goddard. Rapid prototyping of robust and versatile microfluidic components using adhesive transfer tapes. 2010. Lab on a Chip. 10: 2286.

Publications

McIntosh, K., G. Havrilla, R. Gilmore, and M. Holland. Hi Resolution X-ray: New Instrument for Non-Destructive Assay. Invited presentation at Advances in Nuclear Nonproliferation Technology and Policy Conference (ANTPC). (Santa Fe, NM, 26 Sept 2016).

A Discrete Element Method Sea-Ice Model for Global Climate Simulation

Adrian K. Turner
20160668ER

Abstract

We have made significant progress with developing a new discrete element sea-ice model suited for high-resolution coupled climate simulations. The currently used model makes assumptions that are questionable at these high resolutions. The new model will allow a more realistic representation of brittle fracturing of sea ice and a better representation of deformation scaling properties. Capability has been developed to perform realistic Arctic basin scale simulations, including implementation of the full sea-ice momentum equations, realistic initial floe distribution and floe contact model.

Background and Research Objectives

Sea ice, the frozen surface of the ocean at high latitudes, is important for Earth's climate system. It blocks the transfer of heat, momentum and mass between the atmosphere and ocean, and it features in a number of critical climate feedback processes, such as when a decrease in high-albedo sea ice increases solar absorption into the ocean and further melts the ice. The recent reduction in sea-ice cover has been implicated in mid-latitude weather changes, including over North America [1]. Wind and ocean currents drive sea-ice motion and determine its location; understanding this motion is essential to accurate climate predictions. Sea ice is composed of rigid plates called floes, and contact forces generated between these floes heavily influence its motion. Traditional sea-ice models, such as the Los Alamos CICE model, make several assumptions that have been questioned by sea-ice observations. Firstly, they assume each model cell has a sufficient number of randomly orientated cracks that the sea ice may be assumed to be an isotropic continuous material. In reality, cracks between ice floes are aligned on kilometer scales, and this anisotropy greatly influences the sea-ice motion. Strong alignment of cracks and a corresponding anisotropy of sea-ice strength was found using Synthetic Aperture Radar (SAR) imagery of deforming sea ice [2]. A multi-fractal analysis of RADARSAT imagery [3] and an analysis of Arctic sea-ice buoy dispersion [4] found sea-ice deformation to be highly heterogeneous and scale free, further conflicting with the homogeneous assumptions used in these models. Secondly, sea-ice models typically assume the ice flows viscously before it fails plastically. Analysis of in-situ stresses and satellite derived strain rates [5] show that stress states are rate- and scale-dependent and that there is no correlation between stress and strains, contrary to the assumption of viscous flow. Although traditional sea-ice models produce reasonable simulation results on length scales of 10-100 km, the issues cited above will become problematic at the high resolutions to be used in the near future.

An alternative approach to continuum models that corrects for these deficiencies is the Discrete Element Method (DEM) [6], in which individual floes are explicitly represented in a Lagrangian framework and contact forces are determined and integrated in time for each floe. The contact force can easily be made as complex as needed, whereas continuum models are restricted in the processes they can represent. Although DEM-based sea-ice models have been developed previously [e.g. 7,8,9], their use has been limited in space and time due to their high computational expense. Our objectives in this project were to develop a discrete element sea-ice model and use this model to assess two potential avenues for improved computational efficiency: increasing the maximum allowable time step and designing the code for efficient use on graphics processing units (GPUs). The maximum allowable time step would be increased by artificially decreasing the elastic stiffness of the floes, since the elastic stiffness determines the elastic "bounce" time of interacting floes and so the allowable time step. It was planned that the physical fidelity of simulations with decreased stiffness would be assessed to determine how much the stiffness could be reduced without unduly affected the results. For designing the code to run on GPUs, we planned to assess what changes to the code layout and data structure were needed that would give

the best performance on GPUs.

Scientific Approach and Accomplishments

Our approach to investigating improved performance of a discrete element sea ice model was first to develop a discrete element sea ice model dynamical core capable of realistic short-term simulations. We have succeeded in developing such a dynamical core: in total 28,000 lines of code have been written. The dynamical core is capable of performing fully realistic Arctic basin scale simulations. All the force terms in the sea ice momentum equation are included (i.e. floe contact forces, wind and ocean current drag, sea-surface tilt and Coriolis forces), as are a realistic representation of land boundaries and realistic atmospheric and oceanic forcing. Several high-resolution Arctic basin scale simulations have been performed demonstrating this ability using 25km floes. The dynamical core has also been parallelized through domain decomposition with MPI to allow it to run on multiple processors to reduce simulation times.

Initialization of the initial floe distribution has been a challenging part of this project. Ideally the initial distribution of floes would be to have floes as tightly packed as possible but without significant overlap. Discrete element models typically produce such initial distributions by simulating an initially non-compact random distribution of elements with a gradually shrinking domain. After the domain has fully shrunk to its final size, the elements are tightly packed together. Initial attempts to use this technique failed because of the complicated shape of the Arctic domain. Ultimately, the initial floe distribution was calculated with a square domain and then that distribution culled to the realistic Arctic domain. This necessitated a significant change in how boundaries were implemented with some of the elements becoming fixed and forming the boundary. Also, the floes in the final distribution would overlap significantly, so a algorithm was developed that removed these overlaps while still keeping as tightly packed distribution as possible. Finally, elements were culled according to observational sea-ice concentration data and ice and snow thickness observations added to create an initial condition for the realistic Arctic basin simulations. Figure 1 shows an example initial condition showing the location of floes and their ice thickness.

Initially a simplified floe contact force model was used for development. This model was sufficient for the development of the dynamical core framework. However, for realistic sea-ice simulations a more complex model was needed that includes the effects of fracturing of bonds between floes. The contact model of [7] was chosen since this model has demonstrated many of the properties desired in a sea ice dynamical model. This model, however, was implemented with polygonal floes initialized with a Voronoi tessellation. To maximize computational efficiency the new sea-ice model has been implemented with circular floes instead of polygonal ones. This necessitated a modification of this contact force law to adapt it for circular elements. Several test cases used by [7] to validate their model were implemented in the new model and used to validate the implementation of the force model with circular elements. Significant differences between the two models were found and a significant amount of investigation was performed to determine why. Ultimately, it was determined that a less simplified model of shear fracturing was needed to generate realistic fracturing of the ice pack. An improved shear fracture model compatible with the circular elements has been implemented and is partly tested.

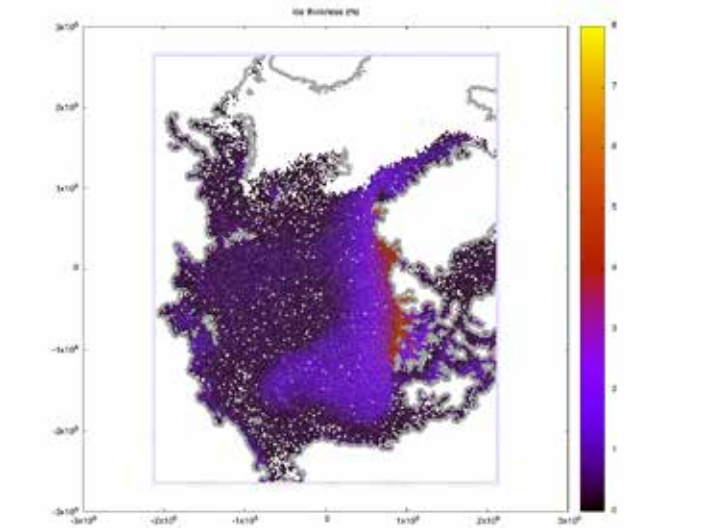

Figure 1. Initial distribution of elements for realistic basin scale simulations. Elements ice thickness is shown as the color. Grey elements are fixed and represent land boundaries.

Several test cases have been developed to aid development and testing of the code. These include simple test cases with two interacting elements to directly test floe contact models, idealized test cases (see Figure 2 for an example) for use with an automated test suite, and whole Arctic basin realistic simulations. These are all kept under revision control in the same repository as the code.

Since one of the goals of the project was to assess how the physical fidelity of the model output would be affected by attempts to improve computational efficiency, it was necessary to develop metrics that access this. To this end, we developed a metric that calculated the distribution of deformation in the sea-ice pack and averages this deformation over various length scales to determine how that deformation scales with length scale. This metric follows the method of [3] closely and uses a line integration of floe

velocities around a Delauney triangulation of the floe positions to determine the deformation field (see Figure 3 for an example deformation field).

Figure 2. Initial distribution of elements in an idealized test case with a vortex wind field (green). Simulation after 2 days. Simulation after 4 days.

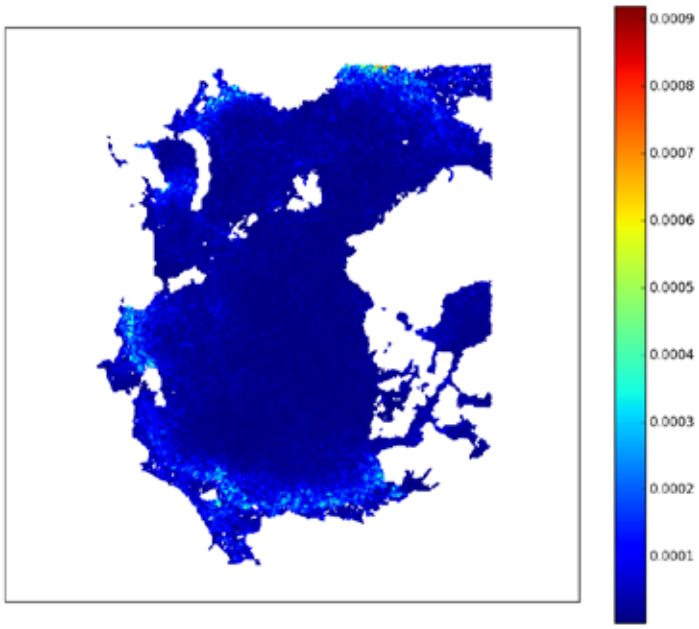

Figure 3. Deformation field for elements undergoing compression from the domain boundaries in a realistic Arctic basin configuration.

We expect significant modifications to code layout and data structures will be needed to make the model computationally efficient on GPUs. We have accessed what changes are needed and these are documented in a short report. The first major recommendation is that the traditional domain decomposition used to parallelize the code be changed to a grid-less system where contiguous groups of floes are stored on each processor. Such a system would allow almost perfect load balancing. Current sea-ice models using traditional domain decomposition suffer from poor load balancing since sea ice only covers a small fraction of the domain. The second recommendation is to split the calculations during each time step up into independent units that would allow greater task parallelization.

In summary, excellent progress has been made developing a numerically efficient discrete element sea ice model. Issues with initialization and shear fracturing were encountered but solutions have been developed.

Impact on National Missions

Recently, the Office of Science's Office of Biological and Environmental Research has started a new ~$20million/year climate modeling project called the Accelerated Climate Modeling for Energy (ACME) project. This project aims to create a high-resolution fully coupled earth system model tailored to address DoE mission critical climate science questions. This model uses the LANL MPAS-Seaice model, whose dynamical core is heavily based on that of CICE. As such this model suffers from the issues at high resolution discussed in the introduction. The discrete element sea-ice model developed during this project represents a possible solution to these issues. Successful development of the model will lead to a next generation sea ice model suitable for the high-resolution climate simulations to be performed by DoE.

References

1. Overland, , J. A. Francis, Hall, Hanna, Kim, and Vihma. The Melting Arctic and Midlatitude Weather Patterns: Are They Connected?. 2015. JOURNAL OF CLIMATE. 28 (20): 7917.

2. Coon, M. a. x., R. o. n. Kwok, G. a. d. Levy, Pruis, Schreyer, and Sulsky. Arctic ice dynamics joint experiment (AIDJEX) assumptions revisited and found inadequate. 2007. JOURNAL OF GEOPHYSICAL RESEARCH-OCEANS. 112 (C11).

3. Marsan, D., H. Stern, R. Lindsay, and J. Weiss. Scale dependence and localization of the deformation of Arctic sea ice. 2004. PHYSICAL REVIEW LETTERS. 93 (17).

4. Rampal, , Weiss, Marsan, Lindsay, and Stern. Scaling properties of sea ice deformation from buoy dispersion analysis. 2008. JOURNAL OF GEOPHYSICAL RESEARCH-OCEANS. 113 (C3).

5. Weiss, , E. M. Schulson, and H. L. Stem. Sea ice rheology from in-situ, satellite and laboratory observations: Fracture and friction. 2007. EARTH AND PLANETARY SCIENCE LETTERS. 255 (1-2): 1.

6. CUNDALL, P. A., and O. D. L. STRACK. DISCRETE NUMERICAL-MODEL FOR GRANULAR ASSEMBLIES. 1979. GEOTECHNIQUE. 29 (1): 47.

7. Hopkins, M. A.. A discrete element Lagrangian sea ice model. 2004. ENGINEERING COMPUTATIONS. 21 (2-4): 409.

8. Baohui, Li, Li Hai, Liu Yu, Wang Anliang, and Ji Shuny-

ing. A modified discrete element model for sea ice dynamics. 2014. ACTA OCEANOLOGICA SINICA. 33 (1): 56.

9. Herman, . Influence of ice concentration and floe-size distribution on cluster formation in sea-ice floes. 2012. CENTRAL EUROPEAN JOURNAL OF PHYSICS. 10 (3): 715.

Ultra-Sensitive Micro-Magnetic Imaging Endoscope

Igor M. Savukov
20150701PRD1

Introduction

We propose to fabricate, test, and use devices capable of magnetic micro-imaging with high sensitivity. They will be based on the technology of micro-mechanical resonators and atomic magnetometry. There are many potential applications. We plan to explore applications based on detection of magnetic nano-particles. These include bio-security applications, such as detection of pathogens, and medical applications, such as cancer detection. Direct micro-magnetic imaging can be used in neuroscience to map functional connections in neurons. This direction is relevant to President Obama's BRAIN initiative. In addition, the devices can be used for micro-current imaging to validate for example authenticity of micro-chips. The micro-magnetic imaging can be used in material science. Apart from magnetic sensing, the micro-resonators can be used for multiple sensing functions: temperature measurements, electro-magnetic power measurements, trace detection of contaminants in the environment.

Benefit to National Security Missions

Tagged magnetic nanoparticle detection with the proposed technology will be of interest to biosecurity applications (pathogen detection) and medical diagnostics (cancer detection). Direct detection of the fields at microscale will be important for neuroscience, President Obama's BRAIN initiative, DARPA, NIH, and NSF. There is some relevance to MaRIE concerning imaging of materials. Micro-magnetic imaging in general will be an important method for basic science research. This is essentially a new, unexplored field.

Progress

The setup for experimental work with whispering mode resonators (WGM) was constructed and experiments testing WGMs were started. Various samples were prepared. High quality factors were demonstrated. One direction for this research was to explore WGM made of liquid. Liquid WGMs are not as much studied as micro-fabricated WGMs, but they are quite promising due to simplicity of construction and modifications. Very high Q factor was achieved, but this unexpectedly brought some issues with noises. Earlier, liquid resonator with low Q operated as expected but sensitivity was low. Some trade off exists and the work is aimed now at finding the best parameters. In terms of magnetic field sensitivity, we demonstrate competitive sensitivity to WGM magnetic sensors based on magnetostriction. Now that the setup is working, we expect to make fast progress in experimental work. We expect to publish some results in the near future: 1) Magnetic sensors based on liquid-state WGMs; 2) Polymer-based WGM sensors; 3) Characterization of 3D printed WGMs.

Future Work

In FY17, we will continue to design and fabricate micocavities with optimized magnetic and mechanical properties and build a system to characterize them. The PI's group has the necessary equipment and expertise to greatly accelerate and enhance the proposed research. We recently found various ways to implement micro-resonators: using liquid droplets and using 3D printing technology. The liquid resonators showed very high quality factors, but there were some noise fluctuations due to this high quality factors. Some compromise will be searched. Constructing micro-resonators with 3D printing technology can be real breakthrough allowing modifications of the resonators on the fly and incorporating various materials. Apart from using micro-resonators as magnetic sensors, we would like to explore some other sensor possibilities, including temperature, heat, mechanical/acoustical, etc.

The research will result in construction and characterization of novel micro-magnetic sensors that will enable many revolutionary applications, including those relevant to LANL mission areas: in ultra-low-field MRI – the

construction of portable scanners for widespread medical diagnostics, in neuroimaging – the unprecedented functional imaging at the single/few neuron level to address the challenge of the President Obama brain initiative; in magnetic nano/microparticle imaging – to enable cancer detection and characterization, to study of antibody-protein binding, and to enable single pathogen detection for biosecurity.

Conclusion

We expect to demonstrate magnetic sensing with micromechanical resonators. In addition, sensing based on atomic spins will be explored. Imaging, either with scanning method or with multi-channel readout, will be tested. After initial demonstrations, we will focus on applications. We will demonstrate the detection of magnetic micro or nano-particles. Then we will try to demonstrate the measurement of neuronal activity.

Development of Radiation Detector Simulation Framework and Safeguards Instrumentation

Edward A. Mckigney
20150705PRD2

Introduction

This work will advance International Safeguards in two ways. The calibration and testing of a Safeguards instrument (the improved Spent Fuel Rod Counter) will be performed, and a coherent framework for coupling radiation transport simulation to radiation detector modeling will be created. The detector modeling framework will allow for the design and optimization of radiation detector systems for a variety of applications. The application this work will focus on is a spent nuclear fuel measurement system for characterization of fuel that has been used in a reactor. The system will be simulated as well as characterized experimentally. The results will be compared and the validated simulation is then available for predicting performance when used in ways that cannot be directly characterized through measurements.

Benefit to National Security Missions

This work is relevant to the DOE missions of nuclear nonproliferation and energy security. It will provide a coherent framework for coupling radiation transport simulation to radiation detector modeling. This set of tools allows for the design and optimization of radiation detector systems for a variety of applications, including nonproliferation. The application this framework will focus on for this project is a spent nuclear fuel measurement system for characterization of fuel that has been used in a reactor. The system will be simulated as well as characterized experimentally. The results will be compared and the validated simulation is then available for predicting performance when used in ways that cannot be directly characterized through measurements.

Progress

During the past year, Madison has extended and validated the detector simulation tool she is developing, called DRiFT(Detector Response Function Toolkit). This toolkit provides a framework for users to couple transport code calculations, such as those performed with MCNP, to radiation detector response functions. The work last year included extensive validation of DRiFT simulations with liquid scintillator data. This resulted in a refereed publication in Nuclear Instruments and Methods. The comparisons included both full spectrum calculations of neutron and gamma-ray energy spectra and time domain pulse shape comparisons for both neutrons and gamma-rays. DRiFT matches data well. Properly simulating both the energy spectra and pulse shapes is important in the design of instruments using liquid scintillator, since the pulse shape is used to discriminate neutrons and gamma-rays, and the energy spectra provide information about the emitting source and moderator between the source and the detector.

In addition, the spent fuel monitoring system has been completed to the point where characterization of the system can begin. This characterization will begin this month, and continue for several months. The characterization data will provide another source of benchmarking data for the DRiFT software.

Future Work

This work will provide a coherent framework for coupling radiation transport simulation to radiation detector modeling. This set of tools allows for the design and optimization of radiation detector systems for a variety of applications. The application this framework will focus on for this project is a spent nuclear fuel measurement system for characterization of fuel that has been used in a reactor. The system will be simulated as well as characterized experimentally. The results will be compared and the validated simulation is then available for predicting performance when used in ways that cannot be directly characterized through measurements.

For the first task, instrument characterization data will be compared with DRiFT models of the instrument.

For the second task, gas detector response functions based on Garfield simulations will be incorporated into DRiFT, for comparison with the calibration data taken for the first task.

Conclusion

The resulting coherent stand-alone tool for detector simulation will be designed to be coupled to the Los Alamos National Laboratory radiation transport simulation software MCNP. The tool will provide a framework for implementation of detector simulations for a wide variety of radiation detector types. The tool will be validated using data from measurements taken with the safeguards instrument.

Publications

Andrews, M. T.. DRiFT - A Detector Response Function Toolkit. 2016. XCP-3: MONTE CARLO CODES.

Andrews, M. T.. DRiFT - A Detector Response Function Toolkit. 2016. XCP-3: MONTE CARLO CODES.

Andrews, M. T., C. J. Solomon, M. E. Rising, C. R. Bates, and G. E. McMath. Demonstrating MCNP6 Correlated Fission Capabilities and MCNP Associated Packages: Intrinsic Source Constructor, MCNPTools, and DRiFT (Detector Response Function Toolkit). 2016. XCP-3: MONTE CARLO CODES.

Andrews, M. T., C. R. Bates, E. A. McKigney, C. J. Solomon, and A. Sood. Organic scintillator detector response simulations with DRiFT. 2016. Nuclear Instruments and Methods in Physics Research, Section A: Accelerators, Spectrometers, Detectors and Associated Equipment. 830: 466.

Andrews, M. T., C. R. Bates, E. A. Mckigney, A. Sood, and C. J. Solomon. DRiFT â A Detector Response Function Toolkit for MCNPÂ® Output. 2016. XCP-3: MONTE CARLO CODES.

Andrews, M. T., C. R. Bates, E. A. Mckigney, A. Sood, and C. J. Solomon. Development of a Scintillator Detector Response Post Processing Tool for MCNP Output. 2016. XCP-3: MONTE CARLO CODES.

Andrews, M. T., C. R. Bates, E. A. Mckigney, C. J. Solomon, and A. Sood. Organic Scintillator Detector Response Simulations with DRiFT. 2016. XCP-3: MONTE CARLO CODES.

Andrews, M. T., C. R. Bates, E. A. Mckigney, C. J. Solomon, and A. Sood. Development of a Scintillator Detector Response Processing Tool for MCNP Output. 2016. XCP-3: MONTE CARLO CODES.

Andrews, M. T., C. R. Bates, E. A. Mckigney, C. J. Solomon, and A. Sood. DRiFT - A Detector Response Function Toolkit. 2016. XCP-3: MONTE CARLO CODES.

Andrews, M. T., C. R. Bates, E. A. Mckigney, C. J. Solomon, and A. Sood. Organic Scintillator Detector Response Simulations with DRiFT. 2016. XCP-3: MONTE CARLO CODES.

Andrews, M. T., C. R. Bates, E. A. Mckigney, and A. Sood. Recent Developments in DRiFT - A Detector Response Function Toolkit for MCNP Output. 2016. XCP-3: MONTE CARLO CODES.

Andrews, M. T., E. A. Mckigney, and C. R. Bates. Extending DRiFT Scintillator Simulation Capabilities. 2016. XCP-3: MONTE CARLO CODES.

Andrews, M. T., K. A. Miller, C. D. Rael, M. T. Swinhoe, and J. B. Marlow. Benchmarking Measurements and MCNP6 Simulations of a Reactor Gate Discharge Monitor. 2016. XCP-3: MONTE CARLO CODES.

Andrews, M. T., K. A. Miller, C. D. Rael, M. T. Swinhoe, and J. B. Marlow. Benchmarking Measurements and MCNP6 Simulations of a Reactor Gate Discharge Monitor. 2016. XCP-3: MONTE CARLO CODES.

Andrews, M. T., K. A. Miller, C. D. Rael, M. T. Swinhoe, and J. B. Marlow. Benchmarking Measurements and MCNP6 Simulations of a Reactor Gate Discharge Monitor. 2016. XCP-3: MONTE CARLO CODES.

Andrews, M. T., M. E. Rising, C. J. Solomon, C. R. Bates, and G. E. McMath. Demonstrating MCNP6 Correlated Fission Capabilities and the MCNP Associated Packages: Intrinsic Source Calculator, MCNPTools, and DRiFT (Detector Response Function Toolkit). 2016. XCP-3: MONTE CARLO CODES.

Andrews, M. T., and A. Sood. Demonstrating MCNP Correlated Fission Capabilities and MCNP Associated Packages: Intrinsic Source Constructor, MCNPTools, and DRiFT (Detector Response Function Toolkit). 2016. XCP-3: MONTE CARLO CODES.

Bates, C. R., M. T. Andrews, E. A. Mckigney, A. Sood, and C. J. Solomon. DRiFT - An Extensible Toolkit for Detector Response Modeling in MCNP. 2016. XCP-3: MONTE CARLO CODES.

Mckigney, E. A., and Q. Pei. Synthesis of conjugated polymer nanocomposites for radiation scintillation. 2012. XCP-7.

Low-cost High-resolution Sensing and Health Monitoring of Urban Infrastructure

David D. Mascarenas
20150708PRD2

Introduction

Yongchao will develop the signal processing tools and techniques needed to enable the use of imagers to perform structural inspections. The impact on the field of structural health monitoring has the potential to be quite large. As of right now the wireless sensor networks the structural health monitoring community uses to collect measurements have high installation costs, are difficult to supply energy to consistently over long periods of time, and suffer from problems associated with noise in communications channels. If Yongchao's work is successful it has the potential to remove most of these problems because in a number of cases a few imagers may be able to collect data that is roughly analogous to the data collected by a dense sensor network consisting of accelerometers and strain gauges.

The results of this work extend beyond structural health monitoring and experimental mechanics. The original application Yongchao suggests is to use this technology to extend Structural Health Monitoring measurements from the individual building scale to the city scale. However, these techniques could also be applied at very small scales as well. For instance, we imagine that these techniques could be applied to microscopy. One particularly exciting possibility is enabling the ability to perform an experimental modal analysis of a single cell. Single cell biology is currently an area of great interest to the life sciences community. Characterizing the dynamics of a single cell could lead to breakthroughs in medicine and drug delivery. Ultrasonic Neuromodulation is also an area of great interest for treating Parkinson's disease. At this time the reason why ultrasonic neuromodulation is therapeutic is not well understood. Having the ability to perform an experimental modal analysis of a single cell could help shed light on this question.

Benefit to National Security Missions

Yongchao's work is relevant to a number of laboratory missions, in particular monitoring transportation networks such as bridges and dams. Yongchao's work could help us characterize the dynamics of bridges and dams in order to perform global structural inspections rapidly and at low cost. This is primarily a data processing project, and thus will directly impact IS&T.

Yongchao's work is essentially the development of a general technique for making experimental dynamics/mechanics measurements. This has application in a wide variety of fields of interest to the Laboratory including monitoring energy infrastructure and transportation networks. It could also be applied to a wide variety of vibration testing in which the Laboratory currently engages. We envision that this work will directly support the science of signatures pillar. By making it possible to collect information on structural dynamics rapidly and at low cost we will be uncovering new signatures that indicate phenomena of interest are occurring.
An area we are interested in applying these techniques is the measurement of the dynamics of fluids. This could could have wide applications in areas such as bubble dynamics, in-process monitoring of additive manufacturing, It could also be applied to verification and validation of fluids models. This would be of great interest to the laboratory's national security mission.

Progress

The accomplishments on this project for FY2016 have been quite impressive. First, a technique was developed to blindly, and automatically extract high-resolution mode shapes of a structure using only video. This technique is able to work quite quickly and only requires about 1 min of runtime on a desktop computer. The technique has been tested on a variety of applicable structures including our 3-story structure, a cryocooler, and a cantilever beam. There is currently one journal paper under review with regards to this technology.

Next, a technique has been developed to take the natural frequencies, damping ratios, and mode shapes and make a model in the video space from this information. The natural frequencies, damping ratios, and mode shapes can be used in conjunction with standard structural dynamics theory to make a model. This model can be exposed to arbitrary excitation and a photo-realistic video of the anticipated structure exposed to the arbitrary excitation can be produced. There is currently one journal paper under review that covers this work.

Also, a technique was developed to extract mode shapes from video whose natural frequencies are high than the sampling rate needed to capture the mode shape at the Nyquist frequency rate. This is a theoretical breakthrough because it has long been assumed that it was necessary to sample at or above the Nyquist rate in order to measure dynamics without suffering from aliasing. In order to do this some observations were made that helped make the final result possible. One observation was that while sampling the system at a rate below Nyquist frequency results in a aliasing, it does not impact the amplitude of the Fourier components. This is because the structural dynamics equations are separable with respect to time and space. Mode shapes are typically extracted using only amplitude so the time ambiguity can be ignored. However, if the frequency must be known it is possible to estimate it by solving a minimization problem for a system of 2 equations that describe how the natural frequency changes for different sampling rates, There is currently one journal paper under review that discusses this work.

Finally the technique has been built upon to enable the detection of very small losses of stiffness in structures for damage detection applications. This work leverages the fact that the technique being developed in this work inherently extracts high-resolution mode shapes of structures from video. The fact that these mode shapes are high-resolution opens the door to being able to apply fractal dimension analysis techniques directly to the mode shapes in order to detect the presence of small damage. This is a big step forward for the structural health monitoring research field. The smallest loss in stiffness we have detected so far is 3%. To put this in context, the state-of-the-art prior to this work was 25%. So the technique described here enables the detection of damage almost an order of magnitude smaller than prior work. There is currently one journal paper under review that discusses this work.

Currently we are looking at seeing if this technique can be applied to the problem of load estimation. Yongchao Yang and David Mascarenas are mentoring a summer-school project group on this topic right now (summer 2016). Thus far FY 2016 has been a very productive year for the project.

Future Work

In the 2017 fiscal year Yongchao will continue the development of signal processing techniques for extracting structural dynamics, and experimental mechanics information from video. Specifically, one of the topic areas that is of particular interest is trying to develop techniques for extracting dynamic loads on structures straight from the video. This would be a fundamentally useful capability for a wide range of applications including structural dynamics, experimental mechanics, biomechanics, and in-process monitoring of manufacturing.

Yongchao may also do some work on extending his techniques to silicon retina imagers. A Silicon retina imagers only collect data when the value of a pixel changes. As a result, these imagers can capture events occurring at very high frequencies. If these techniques can be extended to these imagers, there is hope that we will be able to do real-time control of fast dynamics such as those that occur during manufacturing.

Other areas that I anticipate this work going into is the automatic generation of hybrid models, and the development of structural control systems that make use of the measurements provided by the techniques Yongchao is developing.

In addition, as we go through this work we routinely encounter new areas of interest that we had not considered, we will identify very high impact research topics as we move forward and act on them.
In addition Yongchao will also mentor undergraduate/ graduate students who visit the Engineering Institute as appropriate. Yongchao will document his work by publishing his results in peer-reviewed journals and presenting his work at technical conferences.

Conclusion

This project aims to develop the signal processing tools and techniques needed to enable the use of imagers to perform structural inspections. If successful, the work has potential to remove the energy, bandwidths and installation problems associated with conventional structural health monitoring measurement networks because in a number of cases a few imagers may be able to collect data that is roughly analogous to the data collected by a dense sensor network consisting of accelerometers and strain gauges. This would be a great step toward the widespread adoption of structural health monitoring.

Publications

Dorn, C., T. Mancini, Z. Talken, Y. Yang, G. Kenyon, C. Farrar, and D. Mascarenas. Automated Extraction of Mode Shapes Using Motion Magnified Video and Blind Source Separation. 2016. In Proceedings of the 34th International Modal Analysis Conference. (Orlando, Florida, 25-28 January 2016). , p. 355. Ag, Switzerland: Springer .

Yang, Y., A. Cattaneo, and D. Mascarenas. Potential structural health monitoring tools to mitigate corruption in the construction industry associated with rapid urbanization. Presented at 2015 International Conference on Sustainable Development (Winner Best Paper Award). (New York, Sept 23-24).

Yang, Y., C. Dorn, T. Mancini, Z. Talken, G. Kenyon, C. Farrar, and D. Mascareñas. Blind identification of full-field vibration modes from video measurements with phase-based video motion magnification. 16. Mechanical Systems and Signal Processing. 85 (15): 590.

Yang, Y., C. Dorn, T. Mancini, Z. Talken, S. Nagarajaiah, G. Kenyon, C. Farrar, and D. Mascareñas. Output-only modal identification with uniformly-sampled, possibly temporally-aliased, full field video measurements. 2016. Journal of Sound and Vibration. : NA.

Laboratory Directed Research & Development
Los Alamos National Laboratory
PO Box 1663, MS M708
Los Alamos, NM 87545
505-667-1235 (phone)